

**Advances in Palladium-Catalyzed Benzylolation, Propargylation, and 1,3-Dienylation of
Enolates**

By

Mary Lorraine Maliszewski

Submitted to the graduate degree program in Chemistry and the Graduate Faculty of the
University of Kansas in partial fulfillment of the requirements for the degree of Doctor of
Philosophy.

Chairperson, Jon A. Tunge

Paul R. Hanson

Michael Rubin

Helena C. Malinakova

Zarko Boskovic

Date Defended: 8 July 2021

The Dissertation Committee for Mary L. Maliszewski
certifies that this is the approved version of the following dissertation:

**Advances in Palladium-Catalyzed Benzoylation, Propargylation, and 1,3-Dienylation of
Enolates**

Dr. Jon A. Tunge

Date Approved: 13 July 2021

Abstract

Mary Lorraine Maliszewski and Jon A. Tunge

Department of Chemistry, July 2021

University of Kansas

Presented herein is the development and application of several methods for the palladium-catalyzed decarboxylative benzylation, propargylation, and 1,3-dienylation of various enolate nucleophiles. In chapter 1 and 2, a brief review of many previously reported methods for benzylation and propargylation is presented, with an emphasis on decarboxylative coupling strategies. These chapters review these previously developed methodologies, as well as discuss any shortfalls inherent. In contrast, chapters 3 and 4 focuses on the presentation of the reaction methods developed in the Tunge group over the last several years.

In chapter 3, we present a palladium-catalyzed decarboxylative coupling of enol carbonates with diarylmethyl electrophiles that are derived from secondary benzylic alcohols, allowing for the generation of a variety of β -diaryl ketones with high yields and enantioselectivities. Further, extensive experimentation is described that allowed us to propose a mechanistic pathway that involves a rare intramolecular decarboxylative coupling.

In chapter 4, we present a palladium-catalyzed decarboxylative propargylation and 1,3-dienylation of both 1,3-dicarbonyl compounds and benzoyl acetonitrile derivatives. The dienylated 1,3-dicarbonyl products were further utilized in Diels-Alder coupling reactions, which allows us to illustrate the usefulness of these coupling reactions. Further, timed reactions and deuterium labeling studies allowed us to probe the mechanism of these reactions.

Dedicated to:

My parents, for carrying me when I could not walk and supporting me always;

My siblings, for filling my childhood with love and laughter;

My educators, for guiding me along my quest for knowledge;

My soulmate, for healing all my broken edges.

Table of Contents

Chapter 1. Background of Palladium-Catalyzed Benzylation Reactions

<i>1.1 Introduction to Palladium-Catalyzed Benzylation Methods</i>	1
<i>1.2 Reactivity of η^3-Palladium Benzylic Complexes</i>	3
<i>1.3 Decarboxylative Benzylation (DcB)Reactions</i>	7
<i>1.4 Conclusion</i>	19
<i>1.5 References for Chapter 1</i>	20

Chapter 2. Background of Palladium-Catalyzed Propargylation Reactions

<i>2.1 Introduction</i>	25
<i>2.2 Acid-Catalyzed Propargylation Reactions</i>	26
<i>2.3 Metal-Catalyzed Propargylation Reactions</i>	33
<i>2.4 Reactivity of Propargylpalladium Complexes</i>	47
<i>2.5 Palladium-Catalyzed Propargylations Reactions with Propargylic Electrophiles</i>	50
<i>2.6 Conclusion</i>	55
<i>2.7 References for Chapter 2</i>	55

Chapter 3. Stereospecific Palladium-Catalyzed Decarboxylative Benzylation of Enolates

<i>3.1 Introduction</i>	63
<i>3.2 Asymmetric Benzylation Strategies</i>	65

<i>3.3 Development of Stereospecific Decarboxylative Benzylolation of Enolates</i>	78
<i>3.4 Conclusion</i>	87
<i>3.5 References for Chapter 3</i>	88
Chapter 3 Appendix: Experimental Methods and Spectral Analysis for Ch. 3 Compounds	94

Chapter 4. Palladium-Catalyzed Decarboxylative Propargylation and 1,3-Dienylation of Enolates

<i>4.1 Introduction</i>	228
<i>4.2 Synthetic Methods for the Formation of 1,3-Butadiene Motifs</i>	230
<i>4.3 Decarboxylative Propargylation and Dienylation from Propargylic Electrophiles</i>	237
<i>4.4 Development of Decarboxylative Propargylation and 1,3-Dienylation of 1,3-Dicarbonyl Compounds</i>	249
<i>4.5 Development of Decarboxylative Propargylation and 1,3-Dienylation of Benzoyl Acetonitrile Derivatives</i>	268
<i>4.6 Efforts Towards Asymmetric Dienylation and Propargylation</i>	276
<i>4.7 Conclusion</i>	279
<i>4.8 References for Chapter 4</i>	279
Chapter 4 Appendix: Experimental Methods and Spectral Analysis for Ch. 4 Compounds	288

Abbreviations

°C	degrees Celsius
1°	primary
2°	secondary
3°	tertiary
Ac	acetyl
Aq.	aqueous
Ar	aryl
BDE	bond dissociation energy
BINAP	2,2'- <i>bis</i> (diphenylphosphino) 1,1'-binaphthylbenzyl
Bn	benzyl
Boc	<i>di-tert</i> -butyl decarbonate
BOX	<i>bis</i> (oxazoline)
BPPD	<i>bis</i> (2-pyridylmethyl)-1,3-diaminopropane diacetate
BSA	<i>bis</i> (trimethylsilyl)acetamide
Bu	butyl
<i>c</i>	cyclo
Cat.	catalytic
Cbz	carboxybenzyl
Cee	conserved enantiomeric excess
cm ⁻¹	inverse centimeter
COD	1,5-cyclooctadiene
Cp	cyclopentadiene

Cy	cyclohexyl
d	doublet (NMR)
DavePhos	2-dicyclohexylphosphino-2'-(<i>N,N</i> -dimethylamino)biphenyl
dba	dibenzylideneacetone
DcA	decarboxylative allylation
DcB	decarboxylative benzylation
DCE	dichloroethane
DCM	dichloromethane
dfppe	1,2- <i>bis</i> (dipentafluorophenylphosphino)ethane
dmdba	dimethoxydibenzylideneacetone
DME	dimethylethane
DMF	dimethylformamide
DMSO	dimethyl sulfoxide
DPEPhos	<i>bis</i> [(2-diphenylphosphino)phenyl]
dpp-benzene	1,2- <i>bis</i> (diphenylphosphino)benzene
dppe	1,2- <i>bis</i> (diphenylphosphino)ethane
dppf	1,1'-ferrocenediyl- <i>bis</i> (diphenylphosphine)
dppp	1,3- <i>bis</i> (diphenylphosphino)propane
dr	diastereomeric ratio
DUPHOS	1,2- <i>bis</i> [(2 <i>S</i> ,5 <i>S</i>)-2,5-dimethylphospholano]benzene
EDG	electron donating group
ee	enantiomeric excess
equiv.	equivalent

er	enantiomeric ratio
Et	ethyl
EtOH	ethanol
EWG	electron withdrawing group
g	gram
GC	gas chromatography
h	hour
HRMS	high resolution mass spectrometry
Hz	Hertz
<i>i</i>	<i>iso</i>
<i>i</i> Pr-PHOX	(4 <i>S</i>)-2,2-(diphenylphosphino)phenyl-4,5-dihydro-5,5-dimethyl-4-(1-methylethyl)-oxazole
IR	infrared spectroscopy
Kcal	kilocalorie
L	ligand
LED	light emitting diode
LG	leaving group
LIC-KOR	Schlosser's base
<i>m</i>	meta
M	Mols per liter
m	multiplet (NMR)
Me	methyl
MeCN	acetonitrile
MeOH	methanol

MePhos	2-methyl-2'-dicyclohexylphosphinobiphenyl
Min	minute
mL	milliliter
NBA	nitrobenzoic acid
<i>n</i> BuLi	<i>n</i> -butyllithium
NMR	nuclear magnetic resonance
Np	naphthyl
Nu	nucleophile
<i>o</i>	ortho
OMe	methoxide
<i>p</i>	para
PG	protecting group
Ph	phenyl
PhCN	benzotrile
Pr	propyl
PTSA	<i>p</i> -toluenesulfonic acid
Py	pyridyl
q	quartet (NMR)
rt	room temperature
s	singlet (NMR)
SEGPPOS	5,5'- <i>bis</i> (diphenylphosphino)-4,4'- <i>bi</i> -1,3-benzodioxole
<i>t</i>	<i>tert</i>
t	triplet (NMR)

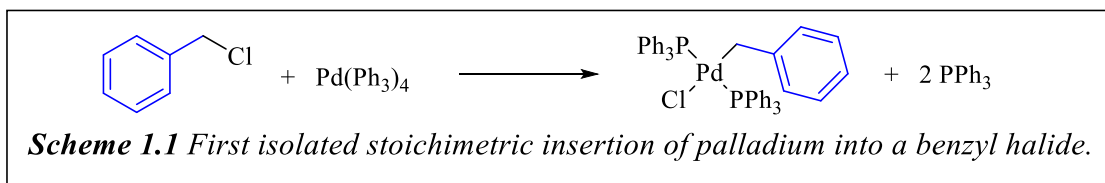
TBAF	tetrabutylammonium fluoride
TBDPS	<i>tert</i> -butyldiphenyl silyl
<i>t</i> Bu-DavePhos	2- <i>di-tert</i> -butylphosphino-2'-(<i>N,N</i> -dimethylamino)biphenyl
<i>t</i> Bu-PHOX	2,2'-isopropylidenebis(4 <i>S</i>)-4- <i>tert</i> -butyl-2-oxazoline
TEA	triethyl amine
TES	triethylsilane
Tf	triflyl
THF	tetrahydrofuran
TLC	thin-layer chromatography
TMS	trimethylsilane
tolyl-PHOX	(<i>S</i>)-2-2- <i>bis</i> (2-tolyl)phosphinophenyl-4- <i>tert</i> -butyl-2-oxazoline
Ts	tosyl
XantPhos	4,5- <i>bis</i> (diphenylphosphino)-9,9-dimethylxanthene
XPhos	2-dicyclohexylphosphino-2',4',6'-triisopropylbiphenyl

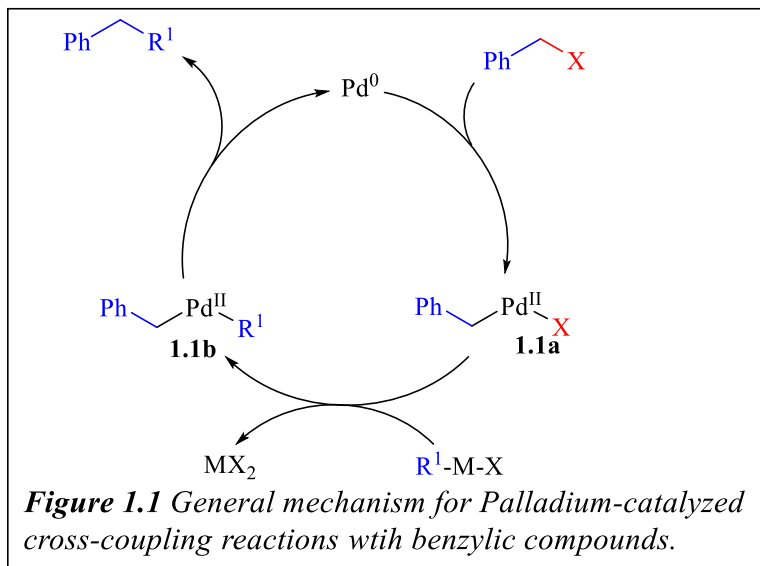
Chapter 1. Background of Palladium-Catalyzed Benzylations

1.1 Introduction to Palladium-Catalyzed Benzylation Methods

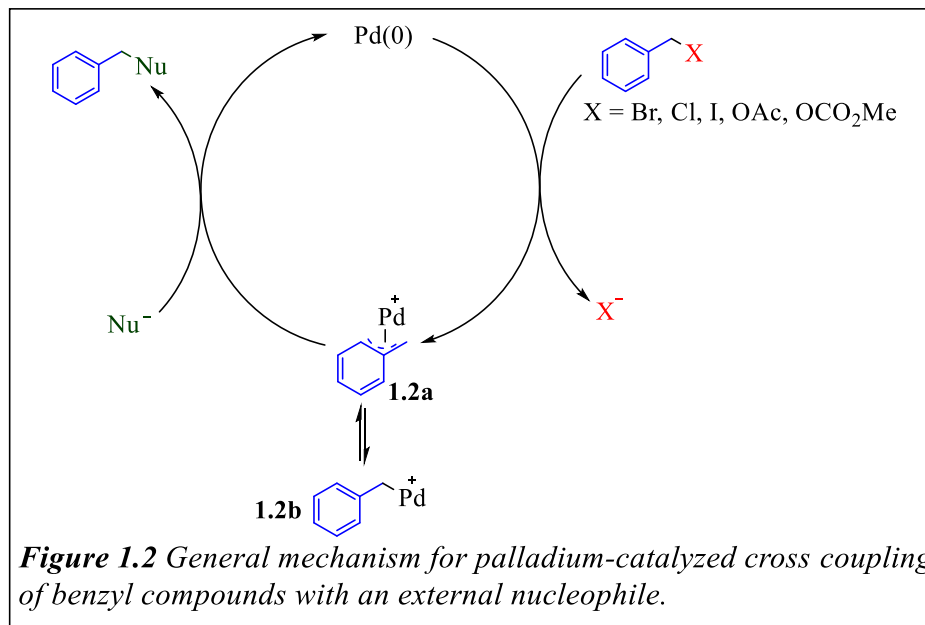
Facile carbon-carbon bond formation is vital in organic synthesis because of the prevalence of C-C bonds throughout most organic molecules. However, these reactions are hindered by carbon's relatively low reactivity and high C-C bond dissociation energy (BDE),¹ often forcing the use of wasteful amounts of precious metals, extremely strong bases, or pre-functionalized starting materials. The ability to form carbon-carbon bonds catalytically and under mild conditions is a powerful addition to the synthetic chemist's toolbox. Furthermore, the ability to directly form carbon-carbon bonds that contain benzylic functionality is extremely desirable due to both the presence of these moieties in many biologically active chemicals and their potential for further reactivity.

While there are reports for the use of other late transition metals to catalyze benzylic cross-coupling reactions, palladium and nickel are most commonly used,² palladium is used particularly often due to its incredible reactivity when paired with many different benzyl substrates.³ While the couplings of moieties other than CH₂Ph are technically aryl methylations, this work will use the term "benzylation" to refer to all aryl methylation reactions for the duration of this dissertation. In 1969, Fitton and coworkers first isolated a benzylpalladium (Bn-Pd) complex through the stoichiometric insertion of palladium into a benzylic chloride bond (Scheme 1.1).⁴ Use of palladium in benzylic coupling reactions has since skyrocketed due to its ability to easily insert into many types of benzylic bonds, including benzyl halides,⁵ acetates,⁶ and carbonates.⁷ Several



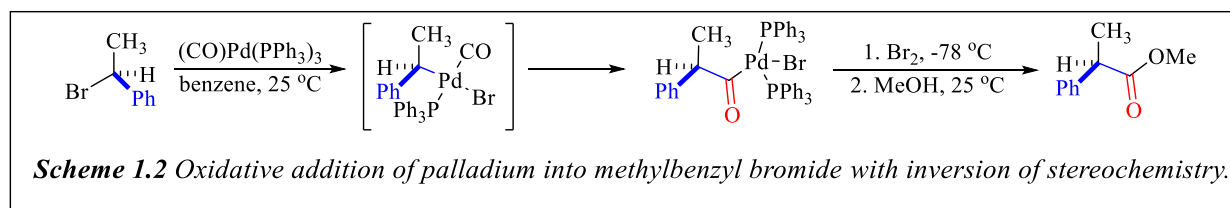


of the named reaction taught in undergraduate organic chemistry course, including the Suzuki,⁸ Stille,⁹ and Negishi¹⁰ cross-coupling reactions, can be used to form new benzylic-carbon bonds. These reactions all follow a general mechanistic pathway, shown in Figure 1.1.¹¹ First, palladium undergoes oxidative addition into benzylic-X (leaving group) bond to generate a Bn-Pd intermediate **1.1a**. This intermediate then reacts with a pre-made organometallic reagent in a transmetalation step to form intermediate **1.1b**. Reductive elimination leads to both the substituted benzylic product and the regeneration of the palladium catalyst. Alternatively, in the presence of an external nucleophile, the nucleophile can directly attack the benzylic position of the benzylpalladium intermediate, releasing the functionalized benzyl product and regenerating the palladium catalyst (Figure 1.2).¹¹ The ability of this reaction to successfully form the final benzylated product depends on many factors shown in the above cycle, including the leaving group used, the substituents present on the benzylic starting material, and the choice of nucleophile.



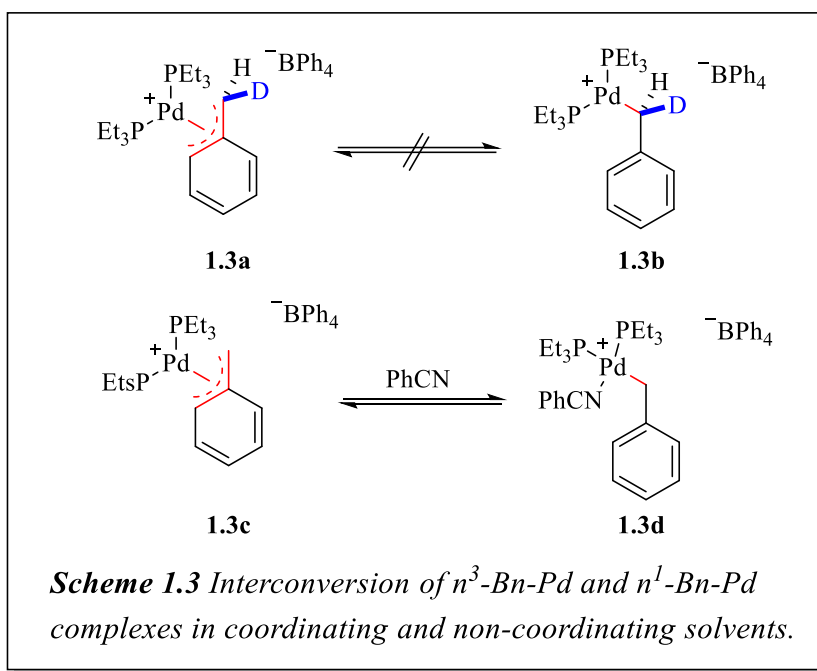
1.2 Reactivity of η^3 -Palladium Benzylic Complexes

While the Bn-Pd intermediate is most commonly depicted as an η^3 -intermediate (Figure **1.2a**) in which the Pd binds into three carbons, it can also exist as the η^1 -Bn-Pd complex **1.2b** shown in Figure 1.2, in which the Pd is bound only to the benzylic position. It was initially reported that formation of the η^1 -Bn-Pd complex is more thermodynamically stable than the η^3 -Bn-Pd complex, due to the loss of aromatization during the formation of the latter;¹² however, the η^3 -Bn-Pd complex can be favored with the addition of sodium, potassium, or silver salts.¹³ Mechanistic studies on the oxidative addition of benzyl halides by palladium were conducted by the Stille group in 1976 (Scheme 1.2).¹⁴ In this reaction, oxidative addition is followed by migratory insertion of



the carbonyl group to form an acyl-palladium intermediate, which is converted to acyl bromide and isolated as a methyl ester. Optical rotation studies determined that the stereochemistry at the α -carbon had been inverted, and, as migratory insertion occurs with retention, it was determined that the oxidative addition of palladium led to inversion of the stereochemistry.

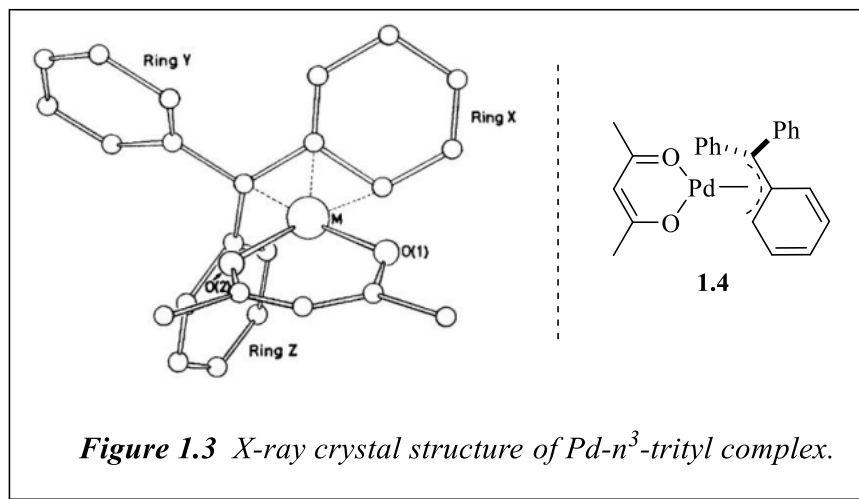
The Stille group then did NMR spectroscopic analysis on the behavior of Bn-Pd complexes in non-coordinating and coordinating solvents at ambient temperatures (Scheme 1.3).¹⁵ In non-



coordinating solvents, a chiral, deuterated η^3 -Bn-Pd complex 1.3a did not undergo any racemization, and the corresponding η^1 -Bn-Pd 1.3b was never detected via NMR. Yet, in benzonitrile (PhCN), a solvent that can readily act as a ligand and coordinate to palladium, NMR analysis showed both the η^3 -Bn-Pd 1.3c and η^1 -Bn-Pd 1.3d complexes as two distinct species. As the temperature was gradually increased, the peaks of the two complexes would coalesce. These observations indicate that in non-coordinating solvents, the η^3 -Bn-Pd is more favored; however,

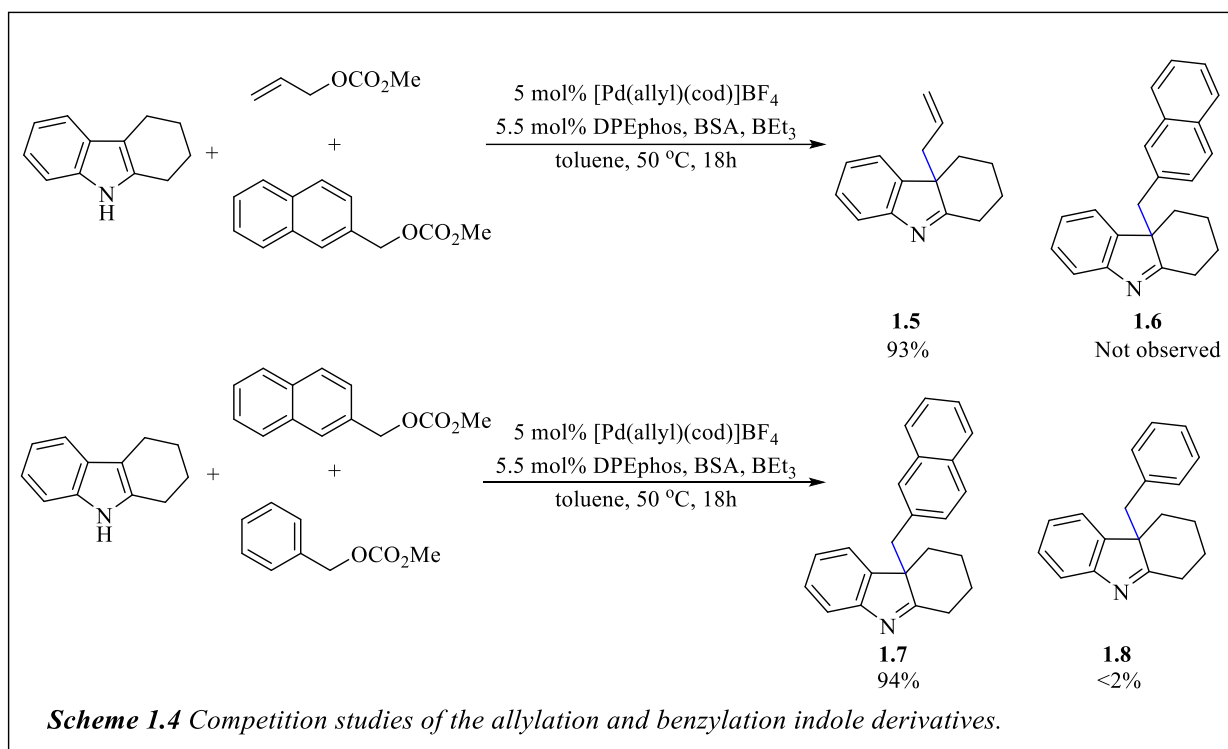
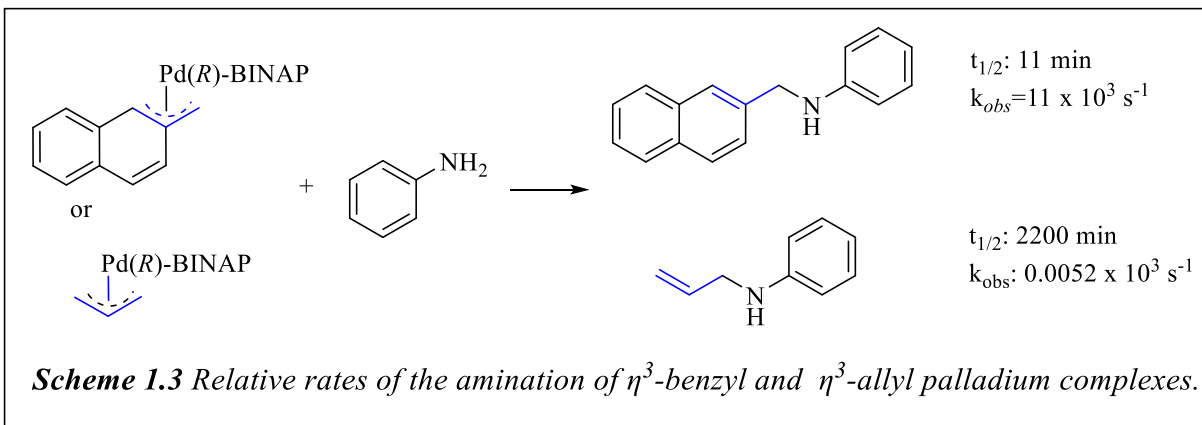
in the presence of an exogenous ligand able to stabilize the 16-electron σ -Bn Pd, the η^1 -Bn-Pd complex dominates.

In 1978, the Maitis group reported the first x-ray crystal structure of an η^3 -Bn-Pd complex, which was synthesized through oxidative addition of palladium into trityl chloride.¹⁶ X-ray crystallographic study of this complex (Figure 1.3) showed that it was square-planar and that the



palladium was bound to both the benzylic (C1) and ortho (C3) carbons. They were then able to determine that Pd-C1 and Pd-C3 bond lengths were 2.105 and 2.20 Å. This indicates that the benzylic position is more electrophilic than the ortho position of the η^3 -Bn-Pd complex, meaning nucleophilic additions would be more likely to occur at the benzylic position.

Hartwig and coworkers ran studies of the relative rates of the amination of η^3 -Bn-Pd and η^3 -allyl-Pd complexes.¹⁷ A selection of these experiments (Scheme 1.3) show that the rate of benzylic amination is significantly faster than the rate of allylic amination, indicating that the η^3 -Bn-Pd complex is more electrophilic relative to the η^3 -allyl-Pd complex. This hypothesis was further strengthened by APT (atomic polar tensor) charge calculations, which indicated that the η^3 -Bn-Pd electrophilic site had a greater amount of positive charge than the electrophilic site of the η^3 -allyl-

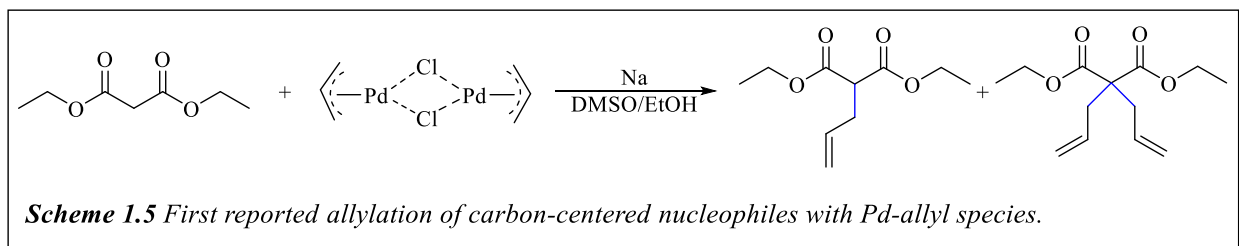


Pd complex, which were 0.113 and 0.343 for the η^3 -allyl-Pd and η^3 -Bn-Pd complexes, respectively. Several years later, Rawal and Zhu reported the results of a series of competition experiments comparing the allylation and benzylation of indole derivatives, which are shown in Scheme 1.4.¹⁸ In the first of these reactions, equal amounts of benzyl and allyl carbonate were reacted with an indole derivative. This reaction yielded an almost quantitative amount of the allylated product **1.5**; however, none of the benzylated product **1.6** was observed. In addition, a

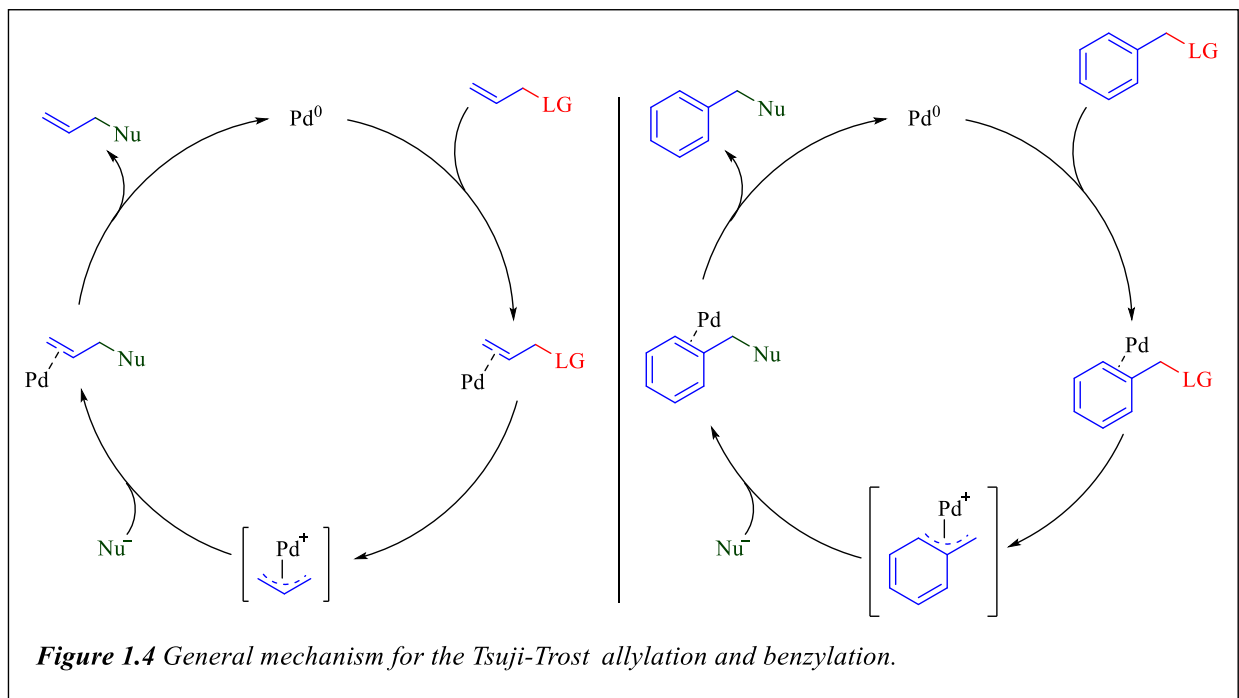
reaction run with equal amounts of benzyl and 2-naphthyl (2-Np) carbonates in the presence of the same indole derivative yielded almost quantitative amounts of the naphthylated product **1.7** and only trace amounts of the benzylated product **1.8**. These observations, when taken with those from the Hartwig groups, indicate that while the formation of the η^3 -Bn-Pd complex is less kinetically favorable than the η^3 -allyl-Pd complex, once it is formed, the η^3 -Bn-Pd complex reacts much faster. In addition, the greater rate with which the 2-Np carbonate reacted when compared to the simple benzyl carbonate illustrates that the stability of the Pd π -complex is key.

1.3 Decarboxylative Benzylation (DcB Reactions)

The ability to selectively install allylic groups into compounds has been the subject of extensive scientific study over the last several decades.¹⁹ While these substitutions were typically done with allylic halides, the development of the Tsuji-Trost reaction allowed for the use of more readily available allylic substrates, such as allylic acetates and carbonates. In 1965, Tsuji and coworkers presented the first Pd-catalyzed allylation of a carbon-centered nucleophile (Scheme 1.5). This reaction required a stoichiometric amount of the palladium dimer and led to a mixture

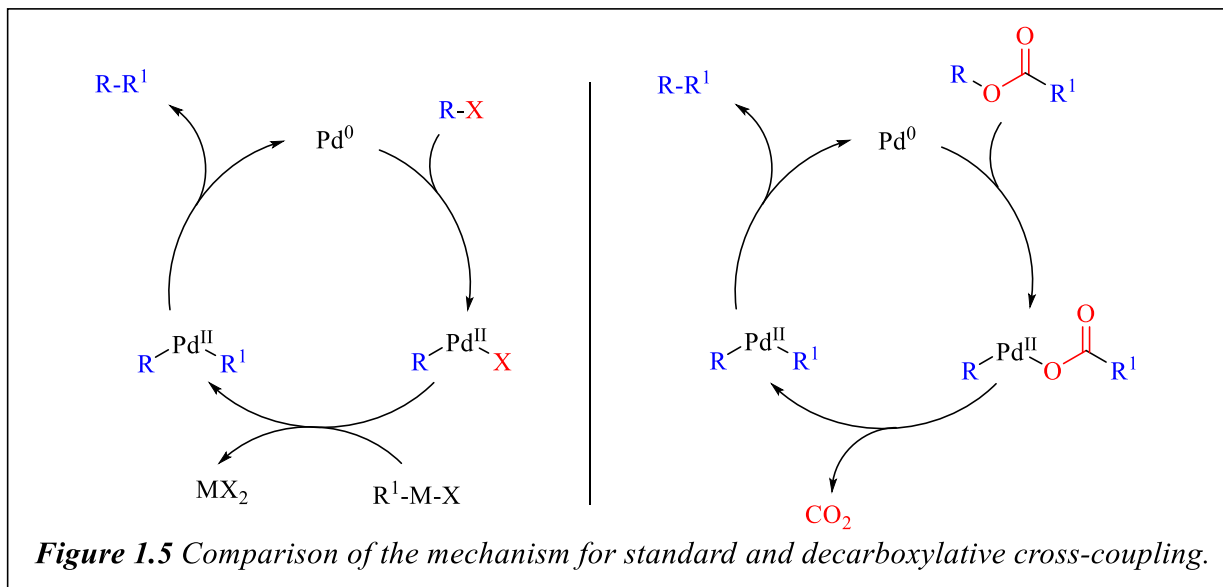


of mono- and diallylated products; however, it was a significant first step in the development of Pd-catalyzed allylation reactions. While the reaction scope expansion was slow initially, in 1973 Trost and coworkers reported that the reaction was greatly improved using phosphine ligands.²⁰ Due to the similar reactivity of η^3 -Bn-Pd complexes with η^3 -allyl-Pd complexes allows for the Tsuji-Trost reaction to also be applied to benzyl compounds, which has greatly increased the scope



Pd-catalyzed benzylations. The mechanism for both the Tsuji-Trost allylation and benzylation is shown in Figure 1.4. Both mechanisms begin with coordination of palladium, followed by oxidative addition to form either a cationic η^3 -Bn-Pd complex or a η^3 -allyl-Pd complex. Lastly, nucleophilic attack at either the allylic or benzylic position generates the expected products and regenerates the active Pd(0) catalyst.

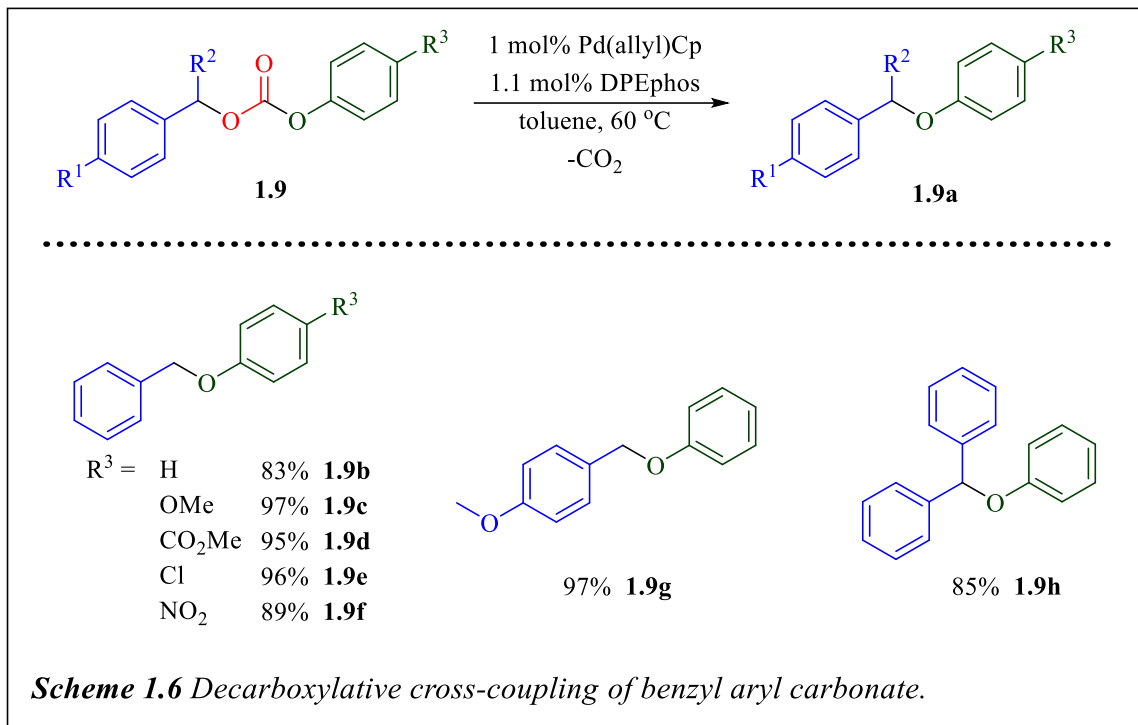
An alternative to many of the previously described methods towards the benzylation of a variety of nucleophilic partners is decarboxylative cross-coupling. While Nesmeyanov reported in 1950 that metal β -keto-carboxylates will undergo decarboxylation under neutral conditions, generating metal enolates,²¹ the full potential of these observations were not realized until decades later. In 1980 when, almost simultaneously, Tsuji²² and Saegusa²³ reported the palladium-catalyzed decarboxylative allylation of β -ketoesters. A direct comparison of the mechanisms for standard and decarboxylative cross-coupling is shown in Figure 1.5. Standard cross-coupling requires the pre-activation of both the electrophilic and nucleophilic components of the reaction,



meaning there will be a stoichiometric amount of metal waste. In comparison, decarboxylative cross-coupling allows for the *in situ* activation of both the electrophile and nucleophile, which allows for the generation of nucleophiles that break the previous pK_a limits and significantly expand the compatibility of different functional groups.²⁴ Furthermore, the decarboxylative coupling allows for the use of more readily available starting materials with only CO_2 as a byproduct. While decarboxylative allylation (DcA) reactions have been studied extensively, decarboxylative benzylation (DcB) is comparatively still in its infancy.

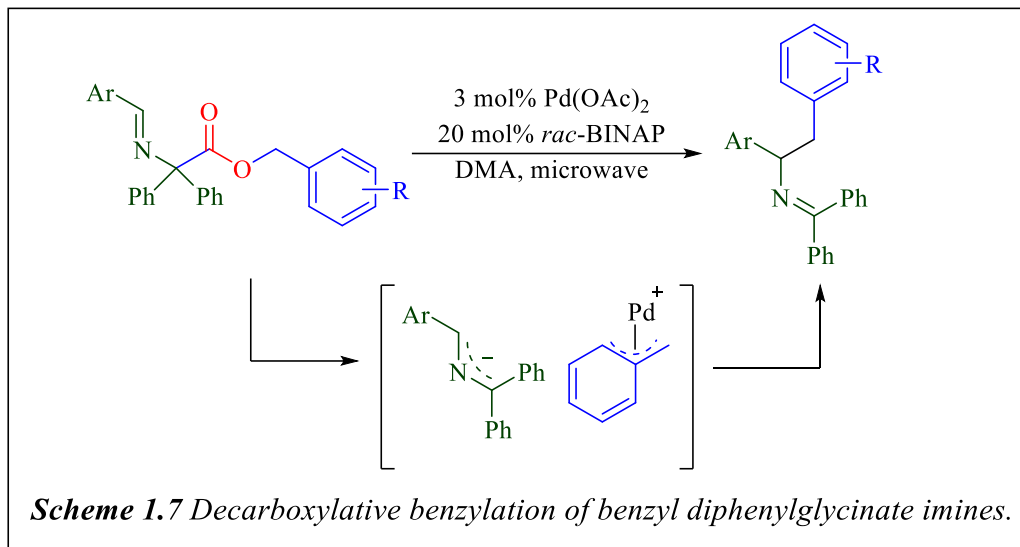
The first reported Pd-catalyzed decarboxylative benzylation was reported by Kuwano and Kusano in 2008.²⁵ They found that in the presence of palladium and DPEPhos, benzyl aryl carbonates would undergo an intramolecular DcB, allowing for the formation of benzyl aryl ethers. A small selection of the scope of this reaction, shown in Scheme 1.6, illustrates the tolerance of these conditions to several different functional groups. The reaction is tolerant to both electron-donating (EDG) (**1.9c**, **1.9g**) and electron-withdrawing groups (EWG) (**1.9d-f**) on both the nucleophilic and electrophilic components. In addition, the reaction proceeded in high yield with a diaryl carbonate, generating diaryl phenyl ether **1.9h**. However, electron-poor substrates did

require either higher catalyst loadings or longer reaction times in comparison to electron-rich substrates.

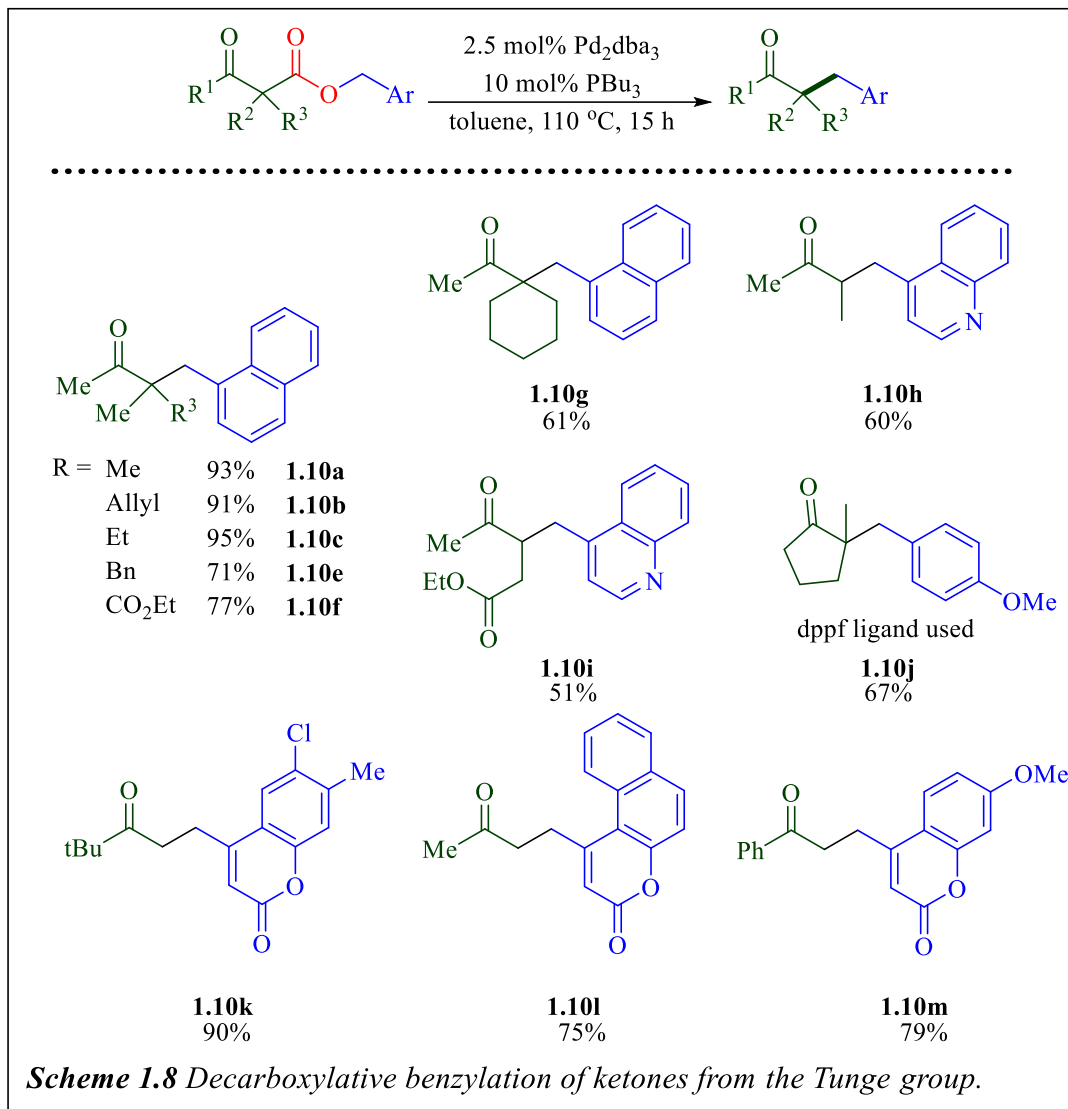


In 2006, the Tunge group disclosed a decarboxylative coupling of amino acid derivatives, allowing for the synthesis of homoallylic amines.²⁶ Shortly after, Chroma and coworkers expanded on this and reported a decarboxylative allylation of allyl diphenylglycinate imines.²⁷ They expanded this work in 2010 to the decarboxylative cross-coupling of benzyl diphenyl imines, pairing an *in situ* generated 2-azaallyl anion and benzylic carbocation (Scheme 1.7).²⁸ This reaction proceeded with a high degree of regioselectivity, providing the product with benzylation at the less hindered position of the 2-azaallyl anion. The reaction worked best with EDGs on the phenyl group of the benzylic carbocation and an electron-withdrawing nitrile substituent on the aryl ring of the 2-azaallyl anion. In addition, an EWG on the phenyl ring led to diminished yields and long reaction

times. These observations highlight the importance of the stabilization of the benzylic carbocation through the use of EDGs and the azaallyl anion with EWGs.

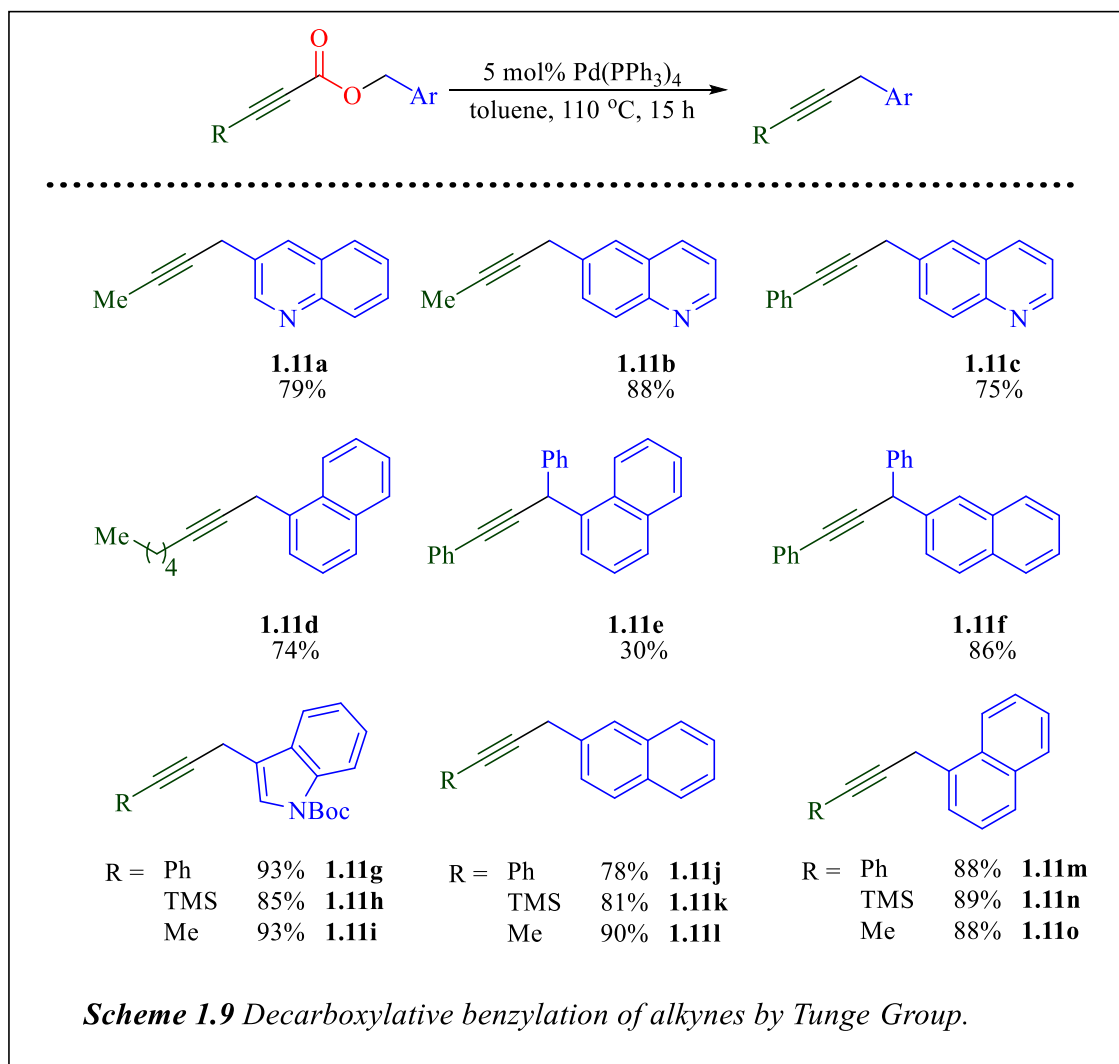


Prompted by recent successes with decarboxylative allylations, the Tunge group began exploration of DcB reactions with the benzylation of ketones and alkynes.²⁹ Catalytic benzylations had typically required highly stabilized nucleophiles, such as stabilized enolates, phenols, and arene sulfonates.³⁰ Our lab, and others, had found success in the early 2000s with the allylation of non-stabilized nucleophiles through the application of decarboxylative coupling methods.³¹ Therefore, we believed that we could expand the scope of Pd-catalyzed benzylations to non-stabilized nucleophiles with the use to decarboxylative protocols. Our first reported DcB reaction, developed by Robert Torregrosa and published in 2010, utilized benzyl β -ketoesters in the presence of Pd_2dba_3 and monodentate ligand PBU_3 , furnishing benzylated ketones in moderate to good yields.³² A selection of compounds from the published reaction scope is shown in Scheme 1.8. The reaction was successful with both linear and cyclic (**1.10j**) enolate nucleophiles. Furthermore, when there were multiple enolizable carbonyls present (**1.10f, i**), no products from enolate isomerization were observed, indicating this reaction proceeds with high regioselectivity.



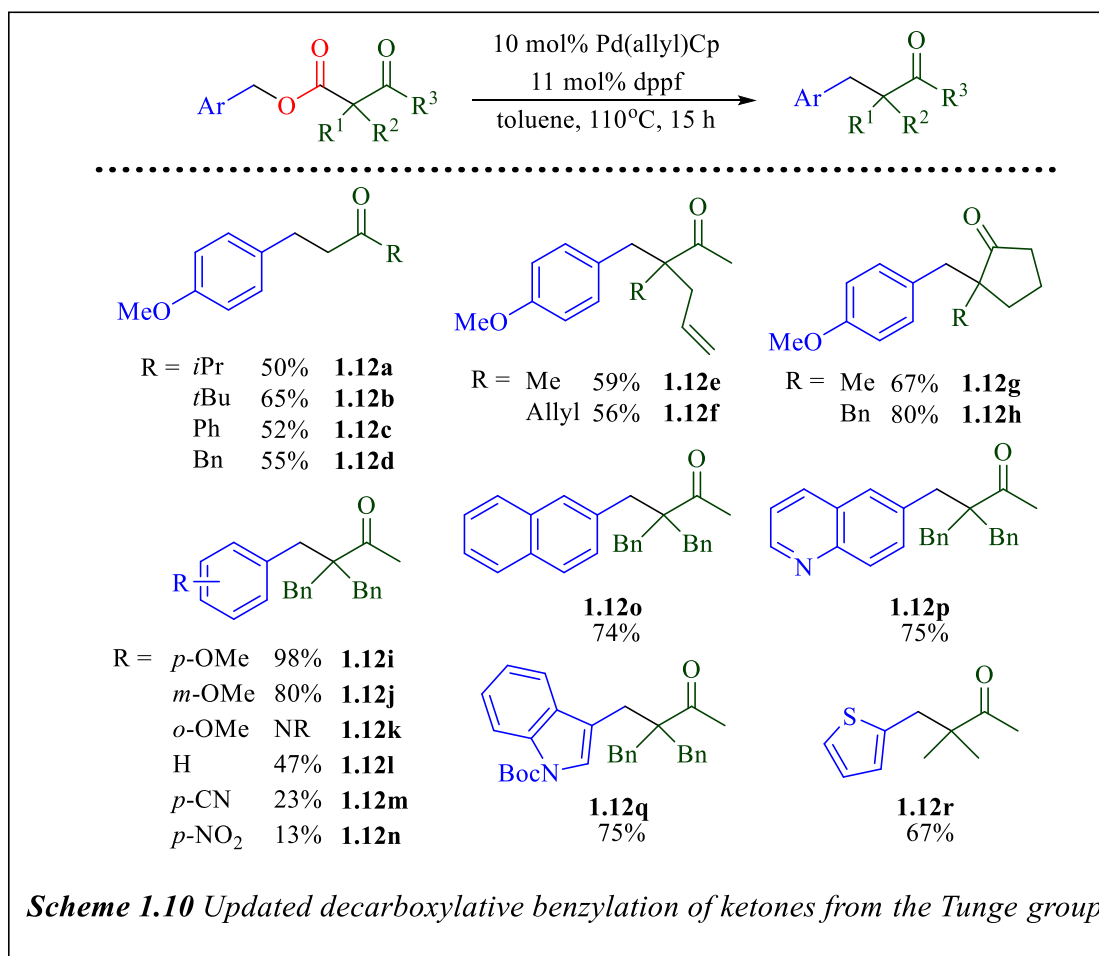
While the nucleophilic component of this reaction could be relatively non-stabilized, as compared to previous examples, it did require a highly stabilized benzylic partner that could stabilize the higher energy benzylic carbocation, either through π -system with extended conjugation or the addition of an electron-donating methoxy substituent on the benzyl ring. Furthermore, the reaction with a simple benzyl group (**1.10j**) required a switch in ligand from PBU_3 to dppf.

Torregrosa also explored decarboxylative coupling reactions using aryl propiolate derivatives to synthesize benzyl alkynes in good yields. A decarboxylative coupling strategy would avoid the need for stoichiometric amounts of base, which often cause isomerization of alkyne substrates to



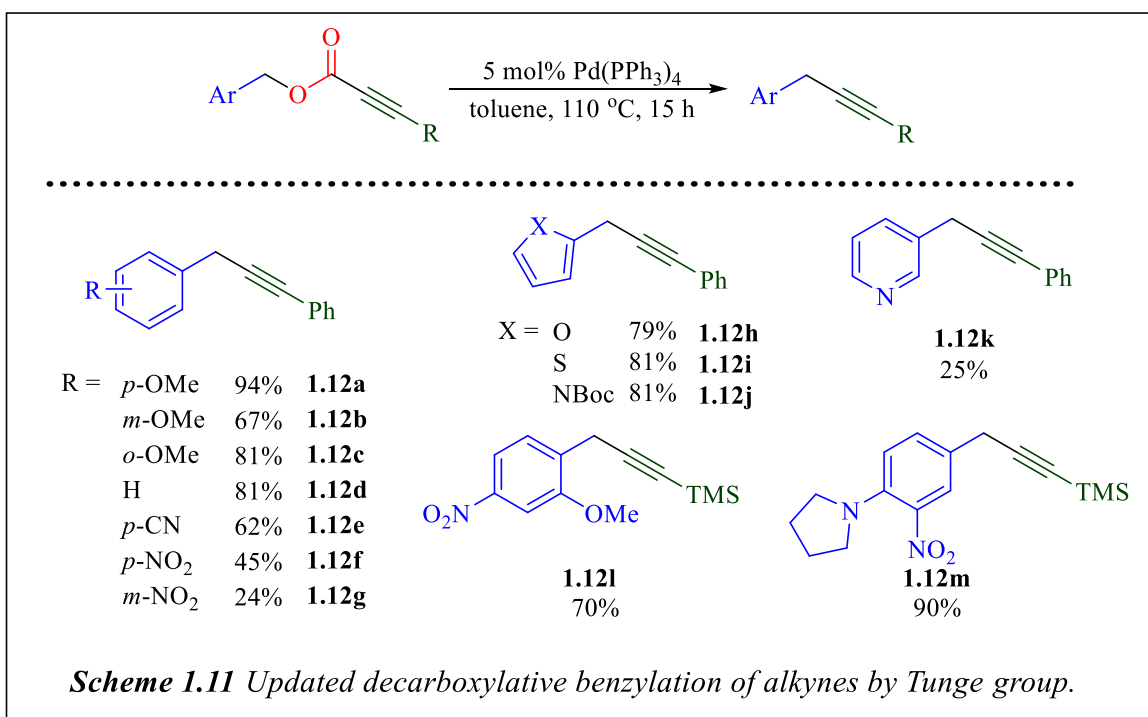
allenes.³³ A selection of substrates from the reaction scope (Scheme 1.9) illustrates the utility of the reaction. The reaction was successful with several different fused benzene systems, including various quinolines (**1.11a-c**), Boc-protected indole (**1.11g-i**), and naphthalene (**1.11e, f, j-l, m-o**). Both aliphatic (**1.11a-b, d, i, l, o**) and aromatic (**1.11c, e, f, g, j, m**) substituted alkynes could be utilized in the reaction with good yields. While terminal alkynes were not suitable for the reaction, alkynes with a terminal TMS substituent (**1.11 h, k, n**) successfully generated the desired product, and this product could be deprotected to furnish the terminal alkyne. Lastly, just as with the DcB of ketones, this reaction required the stabilizing effects of an extended conjugated system.

This work on DcB of enolates and alkynes was revisited by our group in 2018 to better understand and improve the scope and limitations of these decarboxylative reactions.³⁴ Torregrosa noted that in our previous work the only successful example of DcB with simple benzyl substrates required the use of dppf as the ligand; therefore, we developed reaction conditions that centered on using dppf. We found that when paired with Pd(allyl)Cp, this combination was able to facilitate DcB with a wide array of benzyl esters (Scheme 1.10). The new conditions allowed the scope to



be expanded to a wider array of simple benzyl esters, including α -unsubstituted and α,α -disubstituted β -ketoesters. The reaction was also amenable to β -ketoesters that contained several different heterocycles, providing the ketone products in good yields. Finally, the impact of electronics on the electrophilic benzylic component was examined by altering the substituent of

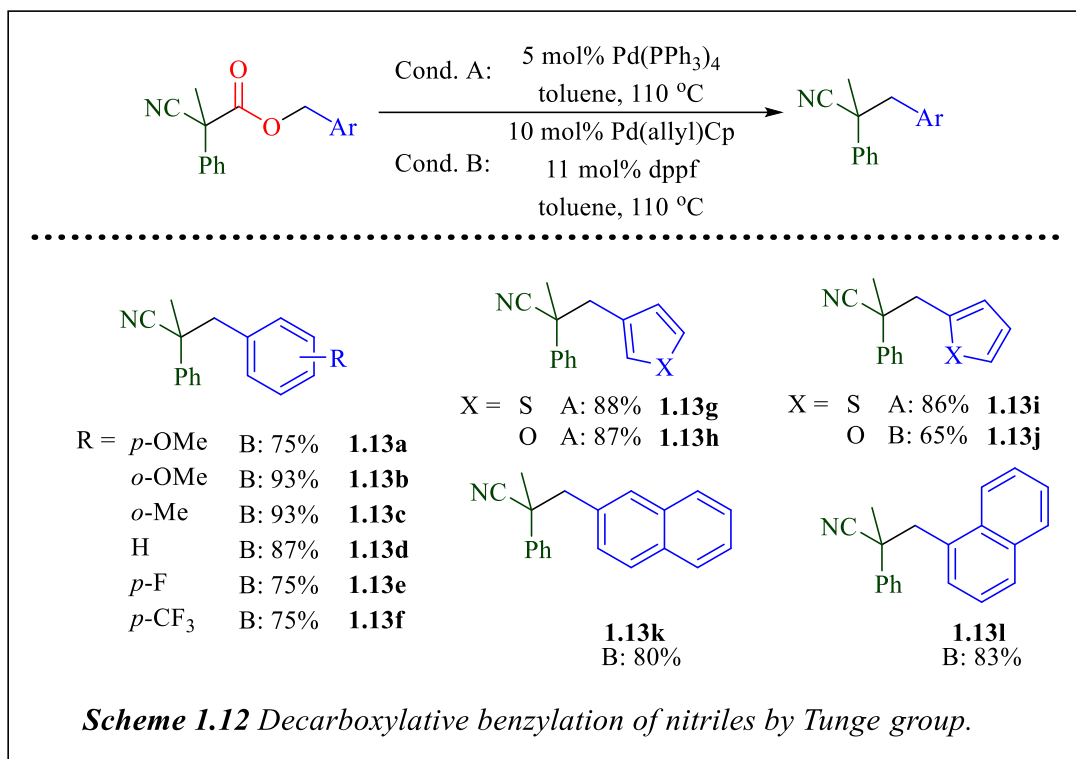
the benzyl ring. Overall, it seems that EDGs on the ring lead to improved yields (**1.12i-j**), and as the ring becomes increasingly electron-poor the yield of the reaction decreases (**1.12l-n**). Of note, substitution at the ortho-position leads to no conversion to the product, possibly due to negative steric interactions preventing coordination or oxidative addition.



While dppf ligand allowed the expansion of DcB of enolates to more simple benzylic substrates without extended conjugation, it did not provide the same results when applied to the DcB of acetylide nucleophiles. However, by switching to a more electron-rich Buchwald ligand, XPhos, the group was able to successfully react a series of simple benzyl propiolates (Scheme 1.11). Just as with the DcB of enolates, electron-rich simple benzyl propiolates with EDGs on the aromatic ring (**1.12a-c**) performed better than their electron-poor counterparts (**1.12d-g**). While furan (**1.12h**), thiophene (**1.12i**), and Boc-protected pyrrole (**1.12j**) propiolates were able to successfully undergo DcB in good yields, the coupling of a 3-pyridyl propiolate (**1.12k**) was relatively low

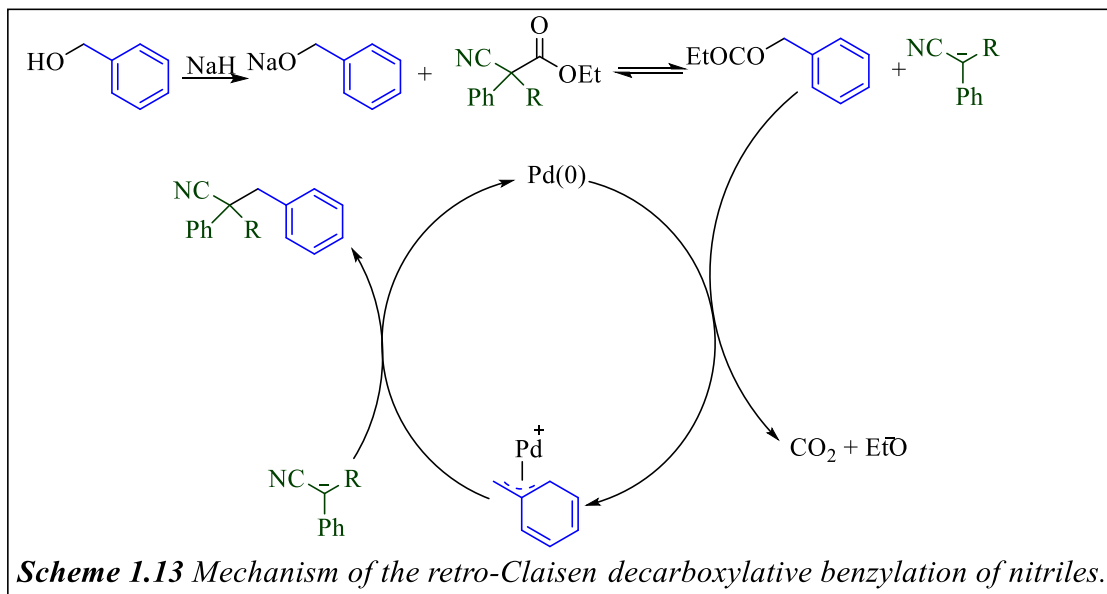
yielding. While EWGs on the aromatic ring typically led to lower yields, the presence of a second electron-donating substituent could overcome this downfall and increase the yields (**1.12l-m**).

In the early to mid-2010s, other Tunge group members worked on the DcB of nitrile compounds. In 2012, Antonio Recio III reported the successful DcB of benzyl cyanoacetates to generate α -benzylated nitriles (Scheme 1.12).³⁵ Use of catalytic Pd(PPh₃)₄ in the presence of



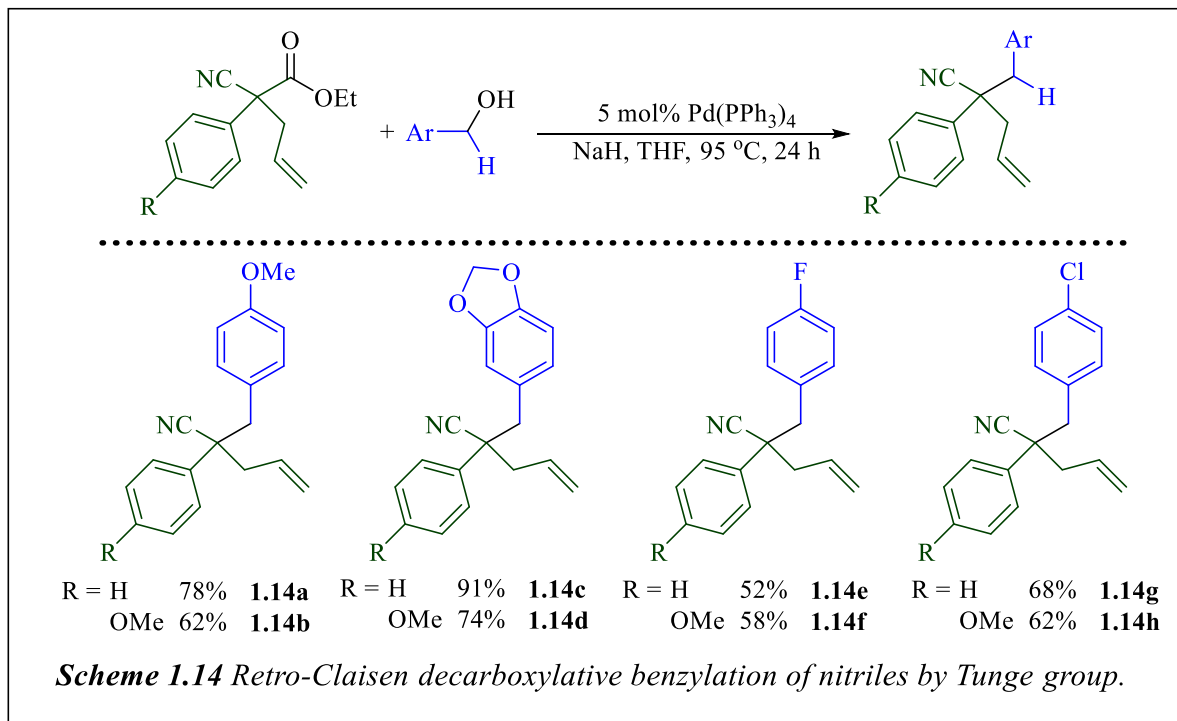
several heteroaromatic nitriles allowed the formation of the desired methyl arylated nitrile compounds (**1.13g-i**). However, 2-methyl furanyl (**1.13j**) and benzyl cyanoacetate (**1.13a-f**) required a switch of conditions to Pd(allyl)Cp and dppf ligand to successfully generate the desired products. In addition, a test of the electronic impact of substituents on the electrophilic benzylic component showed that EDGs lead to increased yields (**1.13a-c**). However, this impact was not as significant as it was with our previous reports, as EWGs only decreased yields by around 12% (**1.13e-f**), while EWGs caused much larger yield decreases with the benzylation of alkynes (Schemes **1.8** and **1.10**)^{29,32} and ketones (Schemes **1.7** and **1.9**).^{32,34}

In 2014, Tapan Maji reported a decarboxylative benzylation to allow for the direct coupling of benzyl alcohols with phenylacetonitrile compounds.³⁶ The mechanism of this transformation, shown in Scheme 1.13, hinges on an initial retro-Claisen activation of a cyanoacetate, which

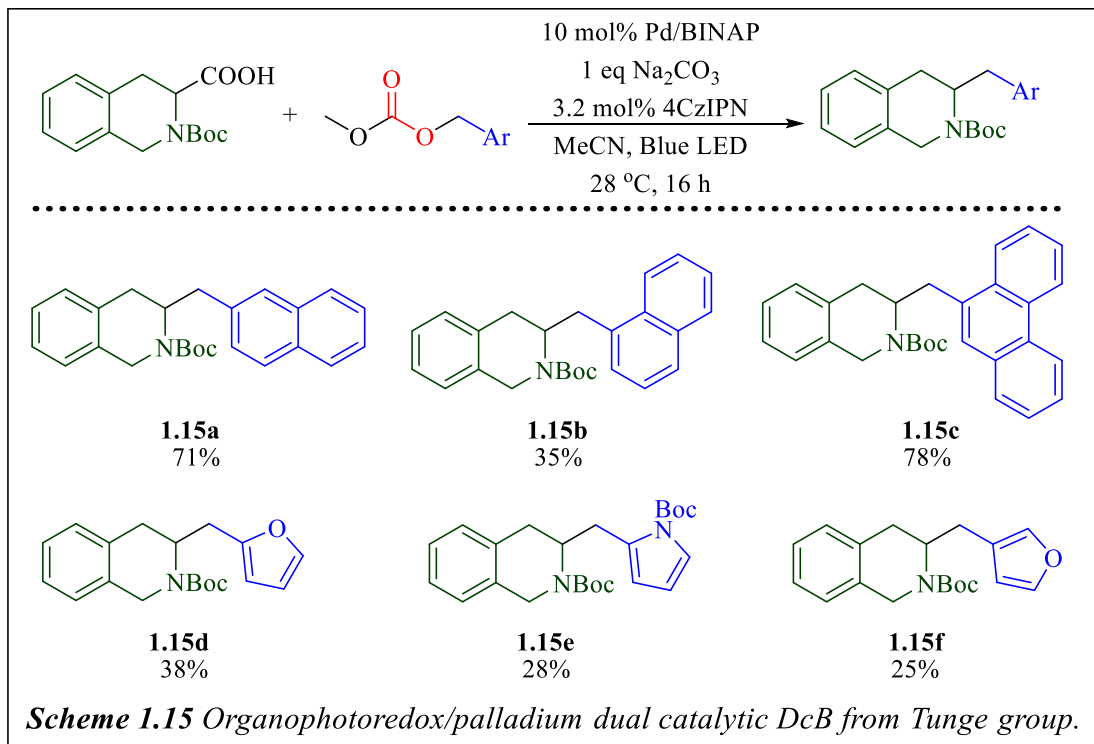


generates a carbanionic nucleophile and benzylic ester. This benzylic ester is then able to undergo oxidative addition to palladium, forming an η^3 -Bn-Pd intermediate that will be attacked by the previously generated nucleophiles, releasing an α -benzylated nitriles. Scheme 1.14 illustrates that this retro-Claisen DcB allowed for the formation of a range of α -benzylated nitriles from easily obtained benzyl nitriles that contain both electron-donating (**1.14a-d**) and withdrawing groups (**1.14e-h**). Furthermore, it was tolerant to the presence of halogen substituents, which could allow for further functionalization of the products.

Over the last several years several members of the Tunge group have explored the application of organophotoredox/palladium dual catalysis to decarboxylative coupling reactions. While much of this research has focused on DcA coupling reactions, a recent publication from 2020 by Kaitie



Cartwright also illustrated the potential for this system for DcB.³⁷ While being a powerful transformation, anionic decarboxylation requires substrates with sufficient stabilization of the generated carbanion, which creates a pKa limit on the nucleophiles that can be generated and thus limits viable compounds that can be produced.³⁸ A photoredox/palladium dual-catalytic cycle would allow for the use of nucleophiles with much higher pKa values. A system of Pd/BINAP, Na₂CO₃, and photocatalyst 4CzIPN was able to generate a series of DcB products when exposed to blue LED light (Scheme 1.15). The highest yielding benzylation reactions were those with 2-naphthyl and phenanthryl carbonates (**1.15a,c**). However, 3-naphthyl carbonate, while able to undergo DcB, formed product in only a 35% yield (**1.15b**) and was accompanied by a 46% yield of the bibenzyl dimerization product. In addition, while heteroaromatic carbonates were able to undergo the DcB reaction, they only provided low yields (**1.15d-f**).



1.4 Conclusion

Throughout chapter 1, several methods for the palladium-catalyzed cross-coupling of benzylic compounds have been presented. In addition, as the reactivity of these benzylation reactions often hinge on the stability of the η^3 -Bn-Pd complex that is formed, research analyzing the reactivity of the η^3 -Bn-Pd complex was reported. Finally, the Pd-catalyzed DcB reaction was described, including the benefits of this reaction over standard cross-coupling reactions and some of the work towards the development and understanding of this useful reaction. However, despite this previous work, in comparison to related allylation reactions, the DcB is still quite limited, particularly in the realm of asymmetric catalysis. In Chapter 3, I will present some previous methods that have been developed for the asymmetric benzylation of various substrates. In addition, I will present research that I have worked on during my tenure in the Tunge group towards the stereospecific benzylation of enolates.

1.5 References for Chapter 1

1. (a) Alkorta, I.; Elguero, I. "The carbon-carbon bond dissociation energy as a function of the chain length." *Chem. Phys. Lett.* **2006**, *425*, 221-224. (b) Lup, Y. R. "Handbook of Bond Dissociation Energies in Organic Compounds." CRC Press, Boca Raton, **2003**.
2. (a) Liegault, B.; Renaud, J.-L.; Bruneu, C. "Activation and Functionalization of Benzylic Derivatives by Palladium Catalysts." *Chem. Soc. Rev.*, **2008**, *37*, 290-299. (b) Swift, E. C.; Jarvo, E. R. "Asymmetric Transition Metal-Catalyzed Cross-Coupling Reactions for the Construction of Tertiary Stereocenters." *Tetrahedron*, **2013**, *69*, 5799-5817.
3. Negishi, E.-I.; Lao, B. "Coupling of Allyl, Benzyl, or Propargyl with Unsaturated Groups" in *Handbook of Organopalladium Chemistry for Organic Synthesis*; Negishi, E.-I.; de Meijere, A.; Eds.; John Wiley & Sons, Inc.; New York, **2002**; pp. 573-579.
4. Fitton, P.; McKeon, J. E.; Ream, B. C. "Preparation of Benzylpalladium(II) Derivatives and their Reactions with Metal Acetates in Acetic Acid." *J. Chem. Soc. D.*, **1969**, *7*, 370-371.
5. (a) Heck, R. F.; Nolley, J. P., Jr. "Palladium-catalyzed vinylic hydrogen substitution reactions with aryl, benzyl, and styryl halides." *J. Org. Chem.*, **1972**, *37*, 2320-2322. (b) Hu, Y.; Zhou, J.; Lian, H.; Zhu, C.; Pan, Y. "Palladium-catalyzed cascade cyclization of benzyl halides with diethyl-diallylmalonate." *Synthesis*, **2003**, *8*, 1177-1180.
6. (a) Nakao, Y.; Ebata, S.; Chen, J.; Imanaka, H.; Hiyama, T. "Cross-coupling reaction of allylic and benzylic carbonates with organo [2-(hydroxymethyl)phenyl]dimethylsilanes." *Chem. Lett.*, **2007**, *36*, 606-607. (b) Ohsumi, M.; Kuwano, R. "Palladium-catalyzed cross-coupling of benzylic carbonates with organostannanes." *Chem. Lett.*, **2008**, *37*, 796-797.
7. (a) Narahashi, H.; Yamamoto, A.; Shimizu, I. "Heck-type benzylation of olefins with benzyl trifluoroacetate." *Chem. Lett.*, **2004**, *33*, 348-349. (b) Kuwano, R.; Yokogi, M.

-
- “Cross-coupling of benzylic acetates with arylboronic acids: one pot transformation of benzylic alcohols to diarylmethanes.” *Chem. Commun.*, **2005**, 5899-5901.
8. Miyaura, N.; Yamada, K.; Suzuki, A. “A New Stereospecific Cross-Coupling by the Palladium-Catalyzed Reaction of 1-Alkenylboranes with 1-Alkenyl or 1-Alkynyl Halides.” *Tetrahedron Lett.*, **1979**, *20*, 3437-3440.
 9. Stille, J. K. “The Palladium-Catalyzed Cross-Coupling Reactions of Organotin Reagents with Organic Electrophiles.” **1986**, *25*, 508-524.
 10. King, A.O.; Okukado, N.; Negishi, E.-I. “Highly General Stereo-, Regio-, and Chemo-Selective Synthesis of Terminal and Internal Conjugated Enynes by the Pd-Catalyzed Reaction of Alkynylzinc Reagents with Alkenyl Halides.” *J. Chem. Soc., Chem. Commun.*, **1977**, *19*, 683-684.
 11. Le Bras, J.; Muzart, J. "Production of Csp³-Csp³ Bond through Palladium-Catalyzed Tsuji-Trost-Type Reactions of (Hetero)Benzylic Substrates." *Eur. J. Org. Chem.*, **2016**, *15*, 2565-2593.
 12. Kuwano, R. “Catalytic Transformations of Benzylic Carboxylates and Carbonates.” *Synthesis*, **2009**, *7*, 1049-1061.
 13. (a) Narahashi, H.; Shimizu, I.; Yamamoto, A. “Synthesis of Benzylpalladium Complexes Through C-O Bond Cleavage of Benzylic Carboxylates: Development of a Novel Palladium-Catalyzed Benzylation of Olefins.” *J. Organomet. Chem.*, **2008**, *693*, 283-296.
(b) Rizzi, G. A.; Morandini, F.; Turco, A.; Bergamin, F. "Synthesis and Characterization of [M(X)(CH₂CH₃)(PR₃)₂] Complexes (M=Pd, Pt; R=cyclo-C₆H₁₁; X=Cl, Br)" *Gazz. Chim. Ital.*, **1993**, *123*, 359-364.

-
14. Lau, K. S. Y.; Wong, K. P.; Stille, J. K. "Oxidative Addition of Benzyl Halides to Zero-valent Palladium Complexes, Inversion of Configuration at Carbon." *J. Am. Chem. Soc.*, **1976**, *98*, 5832-5840.
 15. Becker, Y.; Stille, J. K. "The dynamic η^1 - and η^3 -benzylbis(triethylphosphine)palladium(II) cations. Mechanisms of interconversion" *J. Am. Chem. Soc.*, 1978, *100*, 845–850.
 16. Sonoda, A.; Bailey, P. M.; Maitlis, P. M. "Crystal and molecular structures of pentane-2,4-dionato-(α , 1,2- η -tri-phenylmethyl)-palladium and -platinum." *J. Chem. Soc., Dalton Trans.* **1979**, 346-350.
 17. Johns, A. M.; Tye, J. M.; Hartwig, J. F. "Relative rates for the amination of η^3 -allyl and η^3 -benzyl complexes of palladium." *J. Am. Chem. Soc.* **2006**, *128*, 16010–16011.
 18. Zhu, Y.; Rawal, V. H. "Palladium-catalyzed C3 benzylation of indoles" *J. Am. Chem. Soc.*, **2012**, *134*, 111–114.
 19. (a) Tsuji, J.; Takahashi, H.; Morikawa, M. "Organic synthesis by means of noble metal compounds. XVII. Reaction of π -allylpalladium chloride with nucleophiles" *Tetrahedron Lett.* **1965**, *6*, 4387–4388. (b) Atkins, K. E.; Walker, W. E.; Manyik, R. M. "Palladium catalyzed transfer of allylic groups" *Tetrahedron Lett.* **1970**, 3821–3824.
 20. Trost, B. M.; Fullerton, T. J. "New Synthetic Reactions. Allylic Alkylation." *J. Am. Chem. Soc.*, **1973**, *95*, 292-294.
 21. Nesmeyanov, A. N.; Lutsenko, I. F.; Ananchenko, S. N. *Org. Khim.* **1950**, *132*, 136.
 22. (a) Shimizu, I.; Yamada, T.; Tsuji, J. "Palladium-Catalyzed Rearrangement of Allylic Esters of Acetoacetic Acid to give Unsaturated Methyl Ketones." *Tetrahedron Lett.*, **1980**, *21*, 3199.

-
23. Tsuda, T.; Chujo, Y.; Nishi, S.; Tawara, K.; Saegusa, T. "Facile Generation of a Reactive Palladium(II) Enolate Intermediate by the Decarboxylation of Palladium(II) β -Ketocarboxylate and Its Utilization in Allylic Acylation." *J. Am. Chem. Soc.*, **1980**, *102*, 6381-6384.
24. Weaver, J. D.; Recio (III), A.; Grenning, A. J.; Tunge, J. A. "Transition Metal-Catalyzed Decarboxylative Allylation and Benzylolation Reactions." *Chem. Rev.* **2011**, *111*, 1846-1913.
25. Kuwano, R.; Kusano, H. "Benzyl Protection of Phenols under Neutral Conditions: Palladium-Catalyzed Benzylolation of Phenols." *Org. Lett.*, **2008**, *10*, 1979-1982.
26. Yeagley, A. A.; Churma, J. J. "C-C Bond-Forming Reactions via Pd-Mediated Decarboxylative α -Imino Anion Generation." *Org. Lett.*, **2007**, *9*, 2879-2882.
27. Yeagley, A. A.; Churma, J. J. "C-C Bond-Forming Reactions via Pd-Mediated Decarboxylative α -Imino Anion Generation." *Org. Lett.*, **2007**, *8*, 2879-2882.
29. Fields, W. H.; Churma, J. J. "Palladium-Catalyzed Decarboxylative Benzylolation of Diphenylglycinate Imines." *Org. Lett.* **2010**, *12*, 316-319.
29. Torregrosa, R. R. P.; Ariyaratna, Y.; Chattopadhyay, Tunge, J. A. "Decarboxylative Benzylations of Alkynes and Ketones." *J. Am. Chem. Soc.*, **2010**, *132*, 9280-9282.
30. (a) Kuwano, R.; Kondo, Y.; Shirahama, T. "Transformation of carbonates into sulfones at the benzylic position via palladium-catalyzed benzylic substitution" *Org. Lett.*, **2005**, *7*, 2973– 2975. (b) Kuwano, R.; Kondo, Y.; Matsuyama, Y. "Palladium-catalyzed nucleophilic benzylic substitutions of benzylic esters." *J. Am. Chem. Soc.*, **2003**, *125*, 12104–12105. (c) Mukai, T.; Hirano, K.; Satoh, T.; Miura, M. "Palladium-catalyzed direct benzylolation of azoles with benzyl carbonates." *Org. Lett.*, **2010**, *12*, 1360–1363.

-
31. (a) Burger, E. C.; Tunge, J. A. "Asymmetric Allylic Alkylation of Ketone Enolates: An Asymmetric Claisen Surrogate." *Org. Lett.*, **2004**, *6*, 4113-4115. (b) Tunge, J. A.; Burger E. C. "Transition Metal Catalyzed Decarboxylative Additions of Enolates." *Eur. J. Org. Chem.*, **2005**, 1715-1726. (c) Sherden, N. H.; Behenna, D. C.; Virgil, S. C.; Stoltz, B. M. "Unusual Allylpalladium Carboxylate Complexes: Identification of the Resting State of Catalytic Enantioselective Decarboxylative Allylic Alkylation Reactions of Ketones." *Angew. Chem. Int. Ed.*, **2009**, *48*, 6840-6843.
32. Torregrosa, R. R. P.; Ariyaranthna, Y.; Chattopadhyay, K.; Tunge, J. A. "Decarboxylative Benzylations of Alkynes and Ketones." *J. Am. Chem. Soc.*, **2010**, *132*, 9280-9282.
33. Larsen, C. H.; Anderson, K. W.; Tundel, R. E.; Buchwald, S. L. "Palladium-catalyzed Heck alkynylation of benzyl chlorides" *Synlett*, **2006**, *18*, 2941-2946.
34. Torregrosa, R. R. P.; Mendis, S. N.; Davies, A.; Tunge, J. A. "Palladium-Catalyzed Decarboxylative Benzylation of Acetylides and Enolates." *Synthesis*, **2018**, *50*, 3205-3216.
35. Recio (III), A.; Heinzman, J. D.; Tunge, J. A. "Decarboxylative Benzylation and Arylation of Nitriles." *Chem. Commun.* **2012**, 142-144.
36. Maji, T.; Ramakuma, K.; Tunge, J. A. "Retro-Claisen Benzylation : Direct use of Benzyl Alcohols in Pd-Catalyzed Couplings with Nitriles." *Chem. Commun.* **2014**, 14045-14048.
37. Cartwright, K. C.; Davies, A. M.; Tunge, J. A. "Cobaloxime-catalyzed Hydrogen Evolution in Photoredox-facilitated Small Molecule Functionalization." *Eur. J. Org. Chem.*, **2020**, 1186.
38. Tunge, J. A. "The Evolution of Decarboxylative Allylation: Overcoming pKa Limitations." *Isr. J. Chem.*, **2020**.

Chapter 2. Background of Palladium-Catalyzed Propargylation Reactions

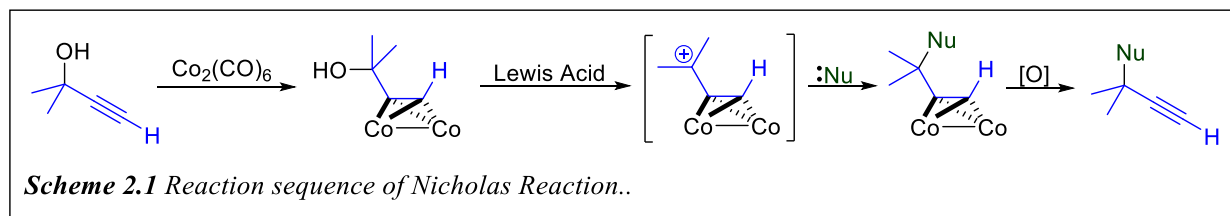
2.1 Introduction to Propargylation Methods

The alkyne functional group serves as a precursor for many useful transformations in organic synthesis.¹ They are extremely useful as reactive intermediates in the synthetic routes for many biologically active compounds. In addition, the alkyne moiety is present in many natural products and pharmaceuticals.² Due to this chemical significance, protocols that would install alkyne groups are extremely useful in synthetic chemistry.

Many synthetic methods that allow for the incorporation of alkyne functional groups to molecular scaffolds utilize propargylic electrophiles. While the simplicity of direct nucleophilic substitution of a propargyl electrophile, such as a propargyl halide,³ is attractive, there are mechanistic drawbacks to this reaction.^{3,4} For example, propargyl halides have limited availability and are relatively toxic. Use of more readily available and less reactive substrates, such as propargyl alcohols and carbonates, can help to mitigate some of those drawbacks. However, regioselectivity when using propargyl electrophiles still poses a possible roadblock, a nucleophilic attack can occur at both the alpha and gamma positions of the propargyl electrophile. This can contribute to a relatively low regioselectivity, especially when compared to allylic electrophiles.⁵ In addition, when paired with palladium and other metal catalysts, propargyl electrophiles can form several different metal-bound intermediates, which causes the control of the reaction selectivity to be quite difficult.⁴

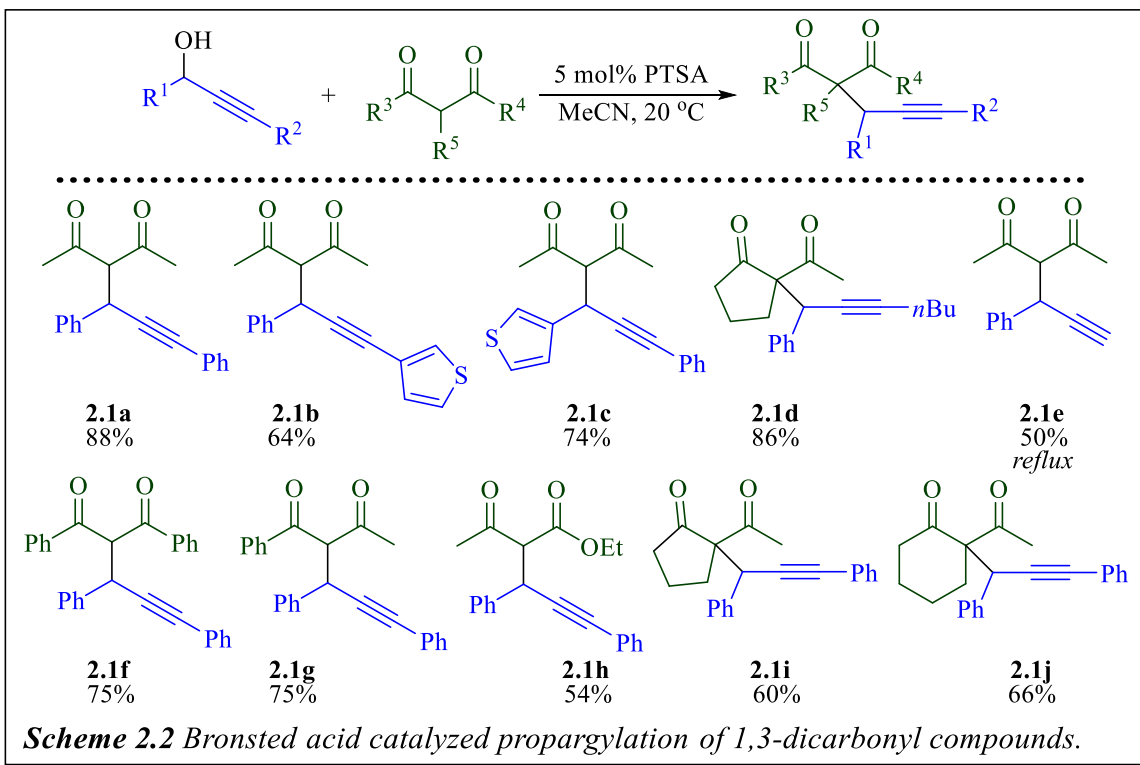
One classically reliable method for propargylation has been the Nicholas reaction, developed in 1987 by its namesake, Kenneth M. Nicholas.⁶ This reaction allows for the regioselective addition of a nucleophile to the α -carbon of propargyl alcohols (Scheme 2.1). While this reaction is compatible with a wide range of nucleophiles, including ketones, amines, and thiols,⁷ it suffers

from the requirement for stoichiometric amounts of cobalt, leading to the production of large amounts of metal waste, and low step and atom economy. For these and other reasons, the development of more efficient propargylation reactions would be extremely useful.

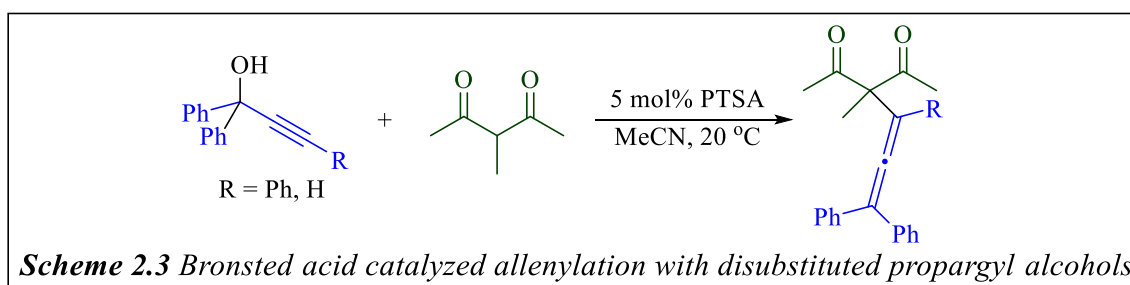


2.2 Acid-Catalyzed Propargylation Reactions

The use of acid catalysis to activate propargyl alcohols for nucleophilic substitution has been the subject of exploration over the last few decades as a more environmentally and cost friendly alternative. During the late 2000's, Sanz and coworkers explored Brønsted acid-catalyzed propargylation reactions, starting with the reaction of 1,3-dicarbonyl compounds with propargyl

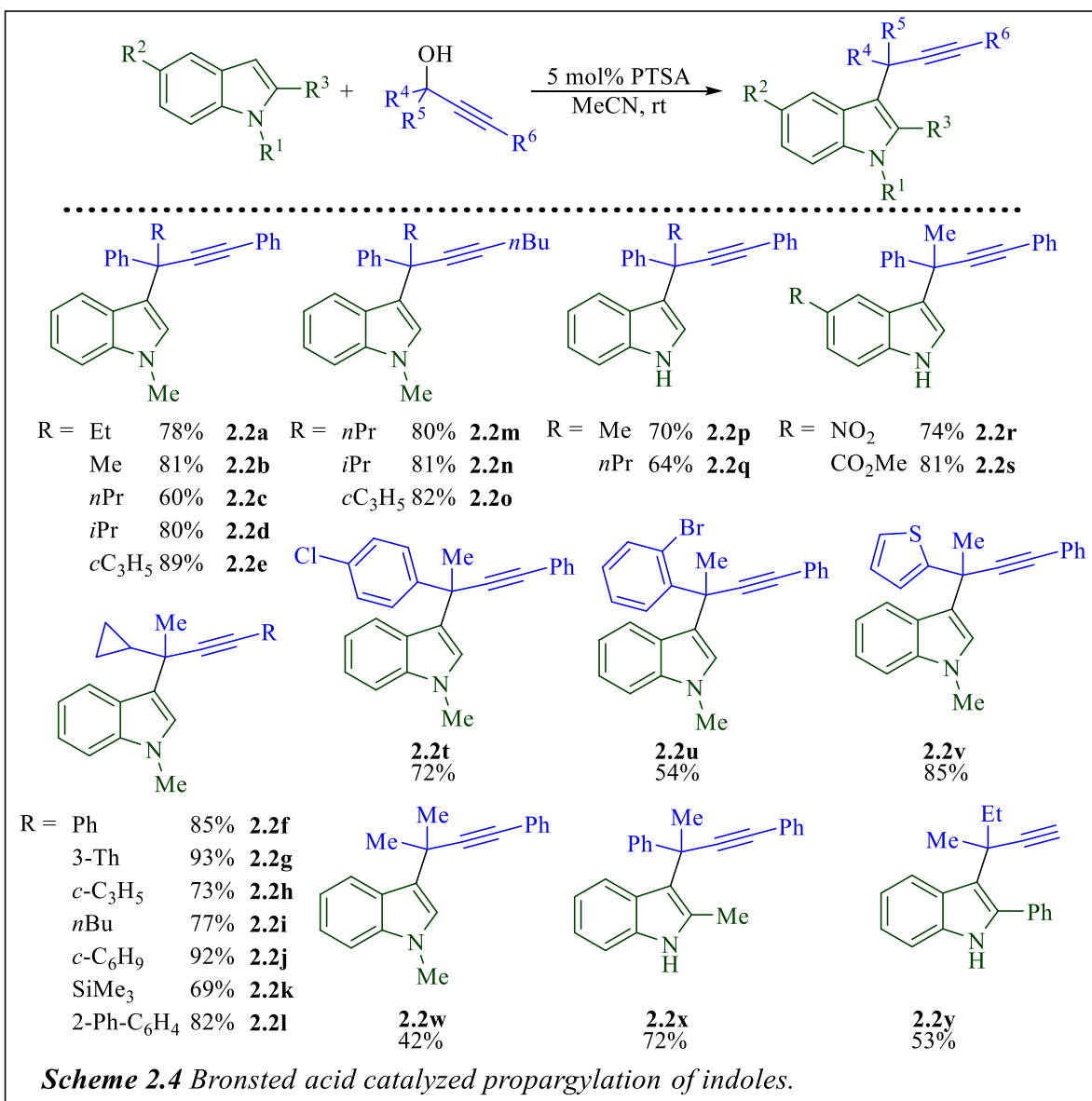


alcohols with water being the only resultant byproduct (Scheme 2.2).⁸ Using *p*-toluenesulfonic acid (PTSA) in acetonitrile (MeCN), they were successfully able to react acyclic β -diketone nucleophiles at room temperature with several internal propargyl alcohols in mild to good yields (**2.1a-c, f-g**). However, there was a slight yield decrease when cyclic β -diketone or β -ketoesters were utilized as the nucleophile (**2.1h-j**). Furthermore, the reaction of 1,3-dicarbonyls with a terminal propargyl alcohol, refluxing reaction conditions were required (**2.1e**). In addition, di-substitution at the propargylic position of the starting alcohols were not tolerated in this reaction, forming only allenylated products due to the increase in steric interaction (Scheme 2.3).

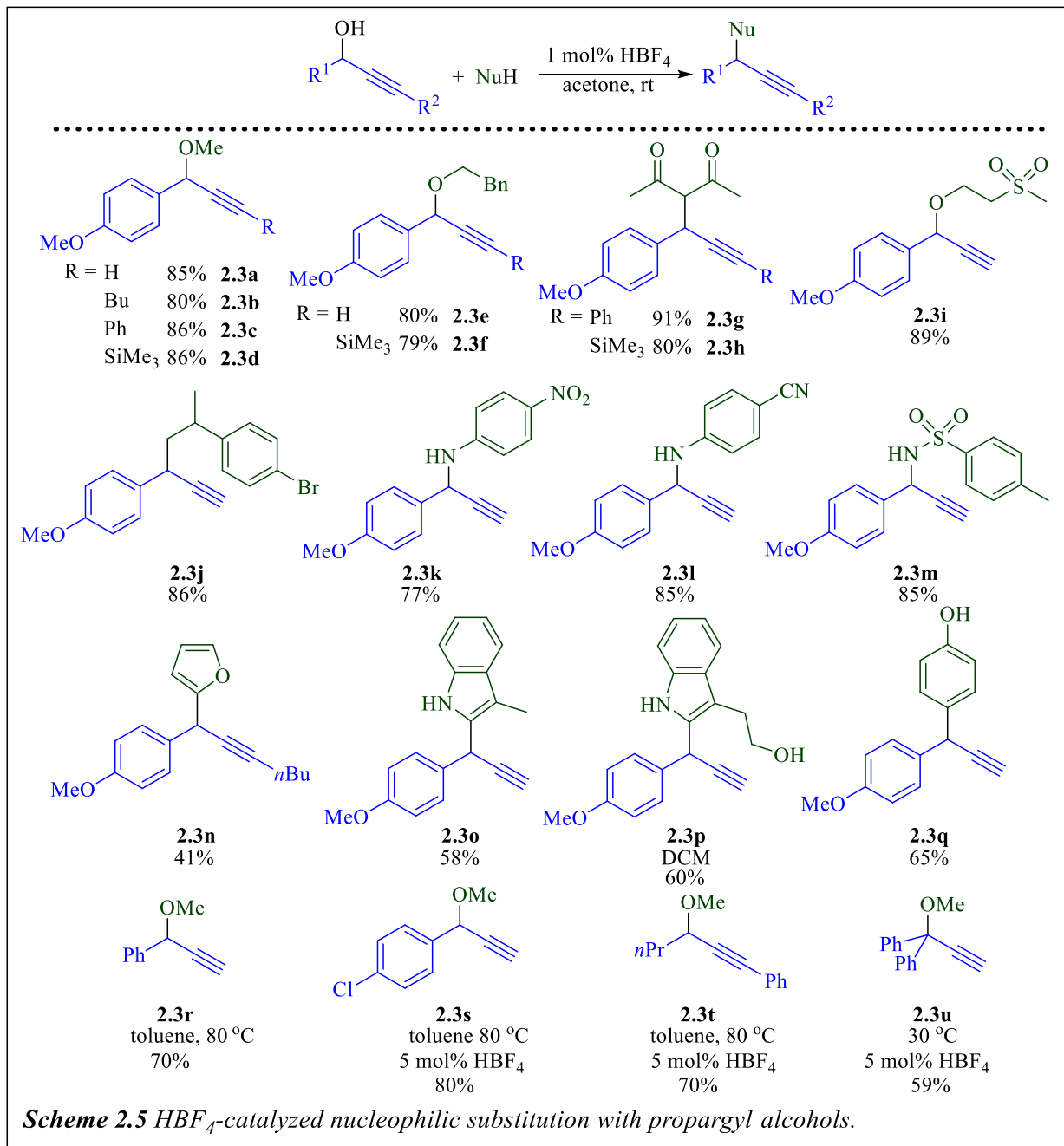


A few years later in 2010, the Sanz group expanded their Brønsted acid protocol to allow for the propargylation of indole derivatives (Scheme 2.4).⁹ While their previous propargylation of 1,3-dicarbonyl compounds was intolerant towards tertiary alkynols, this reaction was well-suited for them, successfully producing a wide-range of 3-propargylated indoles with quaternary centers at the propargylic position. *N*-methylated indole was able to be successfully coupled with several benzylic propargyl alcohols that contained various alkyl groups at the propargylic position in good yields (**2.2a-e**). In addition, propargyl alcohols with two alkyl groups at the propargylic position (**2.2f-l**) or those with substituted benzyl and heteroaromatic groups (**2.2t-v**) could undergo this reaction as well. Furthermore, while previous protocols have been intolerant towards unprotected amines, unsubstituted indole was also able to be successfully employed in this reaction (**2.2p-r**), albeit with a slight reduction of yield. Lastly, both TMS protected and free terminal alkynes

provided their corresponding propargylated products, although with slightly lower yields, 66% and 53% respectively (**2.2k**, **y**).

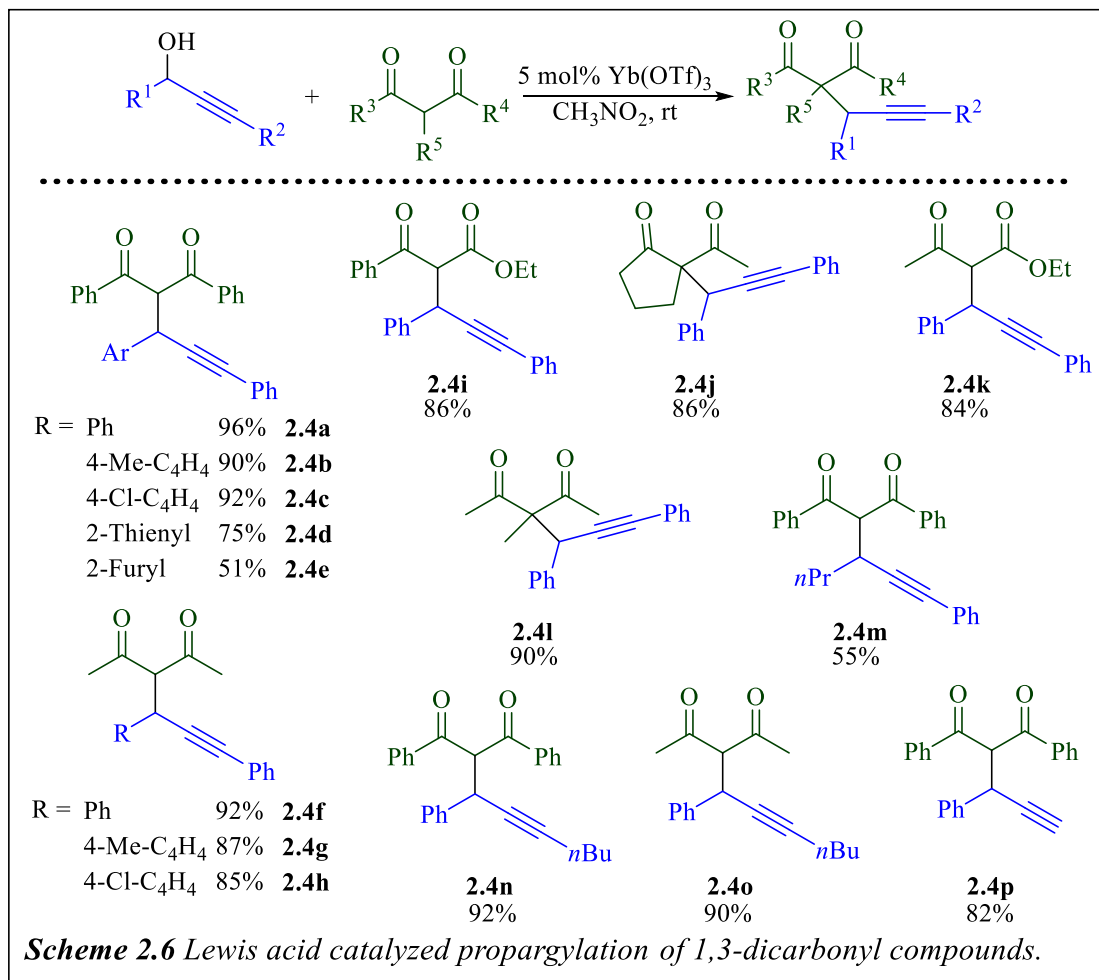


The last example of Brønsted acid-catalyzed propargylation that will be discussed was reported by Díez-González and coworkers in 2015 (Scheme 2.5).¹⁰ They disclosed the use of an inorganic acid HBF₄ to couple propargyl alcohols with oxygen (**2.3a-f**, **i**, **r-u**), nitrogen (**2.3k-m**), and carbon



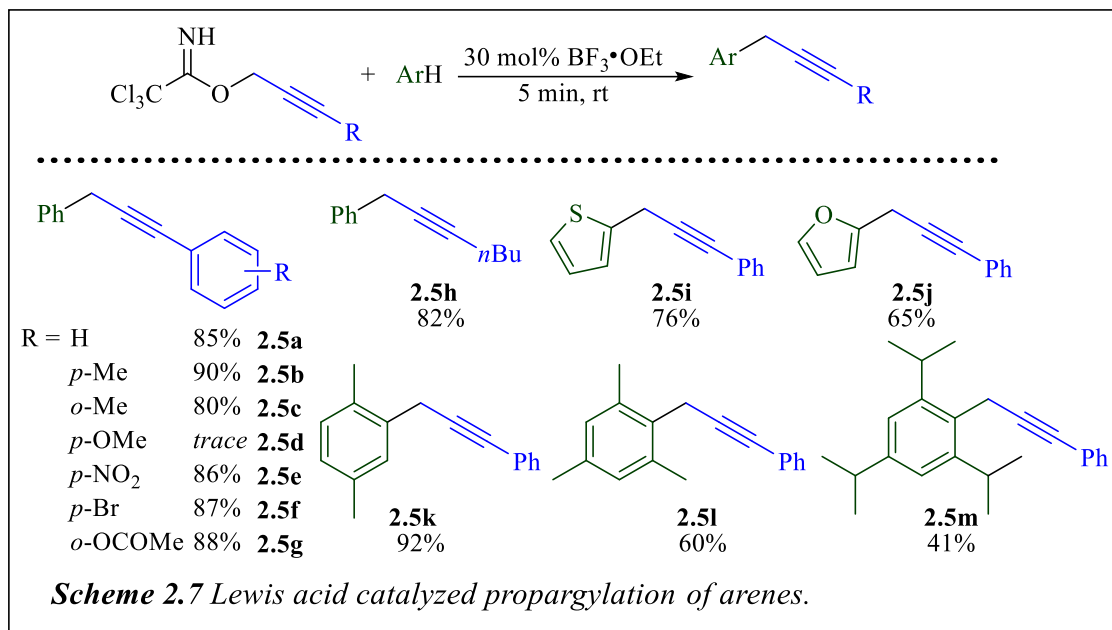
(**2.3g-h, j, n-q**) nucleophiles at room temperature. The reaction was tolerant of several different functional groups, including silyl (**2.3d, h**), sulfonyl (**2.3i, m**), nitro (**2.3k**), cyano (**2.3l**), and unprotected amines (**2.3k-m, o-p**) and alcohol (**2.3q**). In addition, both internal and terminal propargylic alcohols were suitable for this reaction. However, despite the wide scope of the nucleophilic partner, the method was initially restricted to electron-rich 1-aryl propargyl alcohols.

That said, an increase the temperature and catalyst loading, and in some cases a change in solvent, allowed for the substrate scope to be expanded to propargyl alcohols with alkyl substituents. In addition, an increase in the reaction temperature and catalyst loading also allowed for the coupling of di-substituted propargyl alcohols (**2.3u**). Finally, the carbon nucleophile scope also allowed for a Friedel-Crafts type substitution with heteroaromatic compounds (**2.3n-q**).



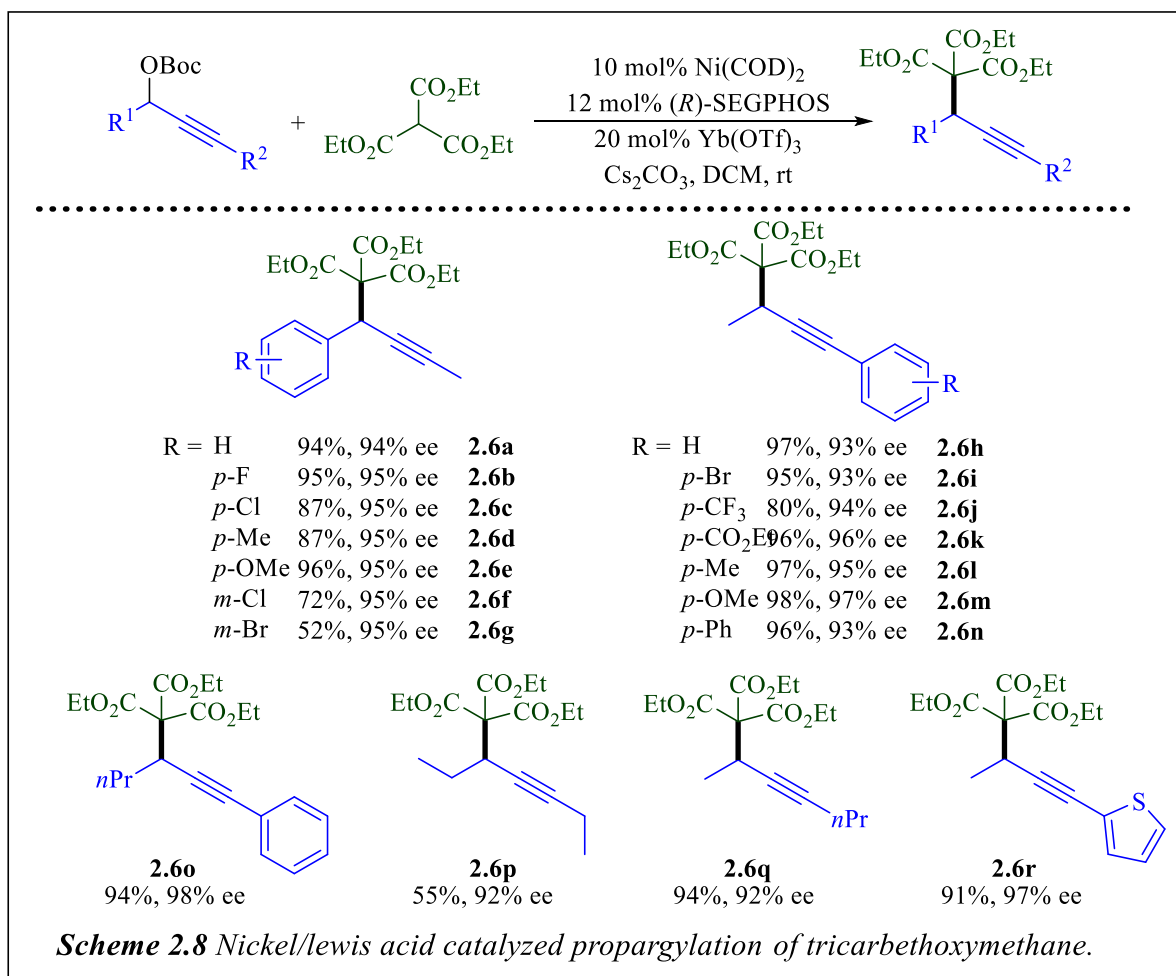
Alternatively, other groups have explored the use of Lewis acids to catalyze the propargylation of various nucleophiles. Soon after the 2007 report from the Sanz group, Zhou and coworkers reported a similar propargylation of 1,3-dicarbonyl compounds that utilized catalytic amounts of Yb(OTf)₃ (Scheme 2.6).¹¹ Unlike the Sanz methods, this reaction was able to tolerate both cyclic β-diketones, β-ketoesters, and terminal propargyl alcohols without the previously observed

significant decrease in yield. However, just as Sanz had observed, di-substituted propargyl alcohols only formed the corresponding allenyl product. Furthermore, while alkyl substituents could be tolerated at either the internal or terminal propargylic position, at least one of them had to have an aromatic substituent, most likely to facilitate the formation of the carbocation with the lose of water.



Also in 2007, Wang and coworkers reported a $\text{BF}_3 \cdot \text{OEt}_2$ -catalyzed Friedel-Crafts propargylation of aromatic compounds with *O*-propargyl trichloroacetimidates (Scheme 2.7).¹² This reaction had fairly good substrate tolerance on the alkyne moiety, reacting favorably with terminal phenyl groups that contain both weak and strong EWGs (**2.5e-g**) and weak EDGs (**2.5a-c**). However, the strongly electron-donating -OMe groups only led to trace amounts of the propargyl product, most likely because the increased stabilization of this group makes the allenyl cation more favorable than the propargyl cation. While this method is able to successfully propargylate both phenyl derivatives and heteroaromatic compounds, the sterics on the aromatic nucleophile had a big impact on the yield of the reaction. A comparison of the yields of products

2.5 k-m illustrates the impact of sterics on the reaction; as the steric bulk on the nucleophile increases the yield of the corresponding propargylated product decreases.



Recently, in 2020, Guo and coworkers reported a nickel/Lewis acid dual catalytic asymmetric propargylation of triesters (Scheme 2.8).¹³ The reaction conditions were tolerant of propargyl carbonates with a diverse array of functional groups on the propargylic benzene ring, including EWGs (**2.6b-c, f-g, i-k**) and EDGs (**2.6d-e, l-n**). In addition, alkyl groups were tolerated at the internal, terminal, and both internal and terminal propargylic positions; however, having an alkyl group at both positions did lead to a decrease in yield (**2.6p**). Most notably, this reaction was able to take racemic propargyl carbonates and produce single enantiomers with high ee values. The value of this method was emphasized by allowing the streamlining of a scale production of several

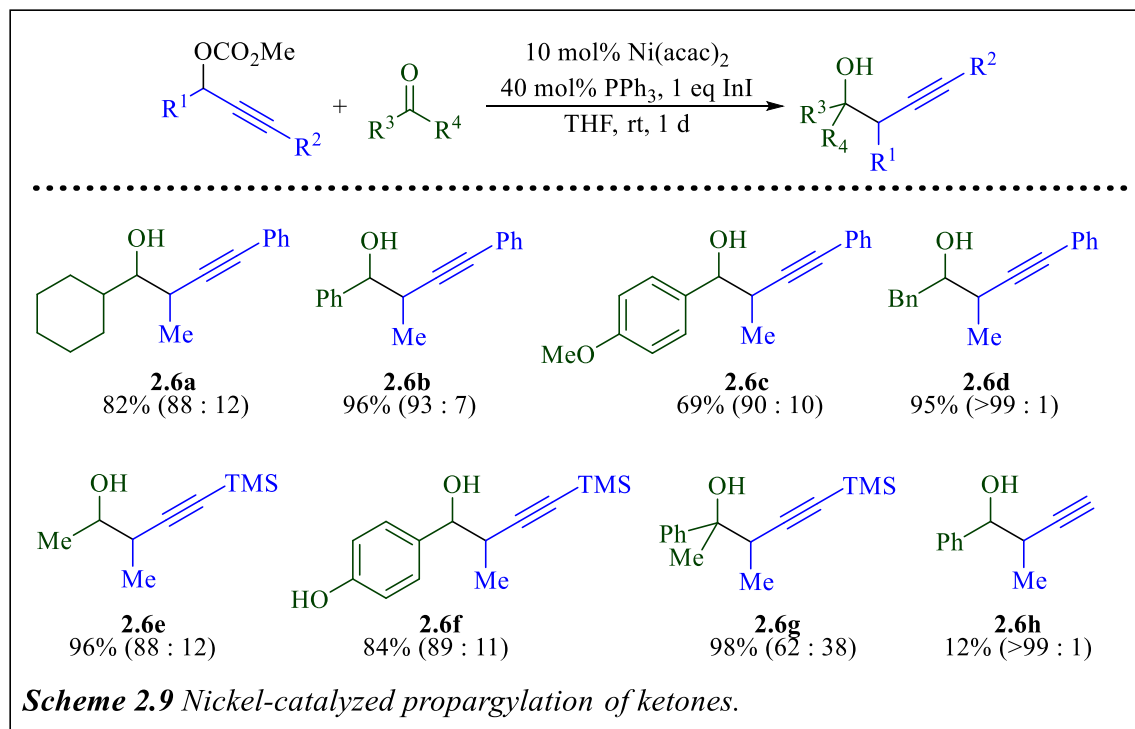
biologically active compounds. Mechanistic studies conducted by the Guo group suggest that the high catalytic activity observed with this system is due to the cooperation between $\text{Yb}(\text{OTf})_3$ and nickel.

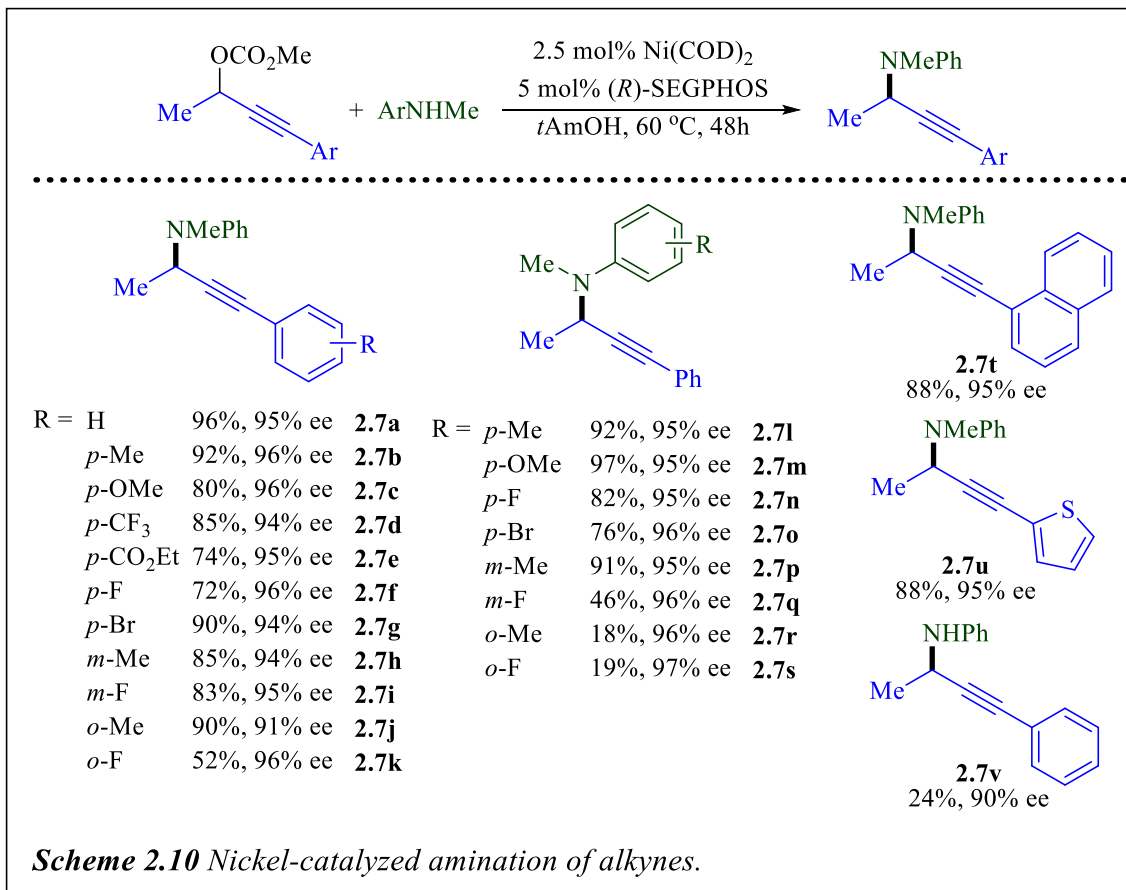
While this section has illustrated that the use of both Brønsted and Lewis acid-catalysis can be extremely effective in the propargylation of several classes of nucleophiles, these methods are not without their faults. Many of the methods are quite reliant on the steric and electronic environment of the starting materials, which greatly limits the utility and scope of these reactions. Furthermore, these methods are intolerant of acid-sensitive functionalities, and applications to more complex systems often face issues of chemoselectivity, further limiting the reaction utility.¹⁴ In addition, as many of these methods occur through an $\text{S}_{\text{N}}1$ -type mechanism, development of an asymmetric protocol is extremely difficult, and overcoming this obstacle typically requires the addition of a metal catalyst, as shown in the last example. Therefore, other methods that use transition-metals to catalyze these propargylation reactions have been developed in order to expand the scope and utility of these reactions. The next section will discuss how several different transition metals have been used to more efficiently synthesize propargylated products.

2.3 Metal-Catalyzed Propargylation Reactions

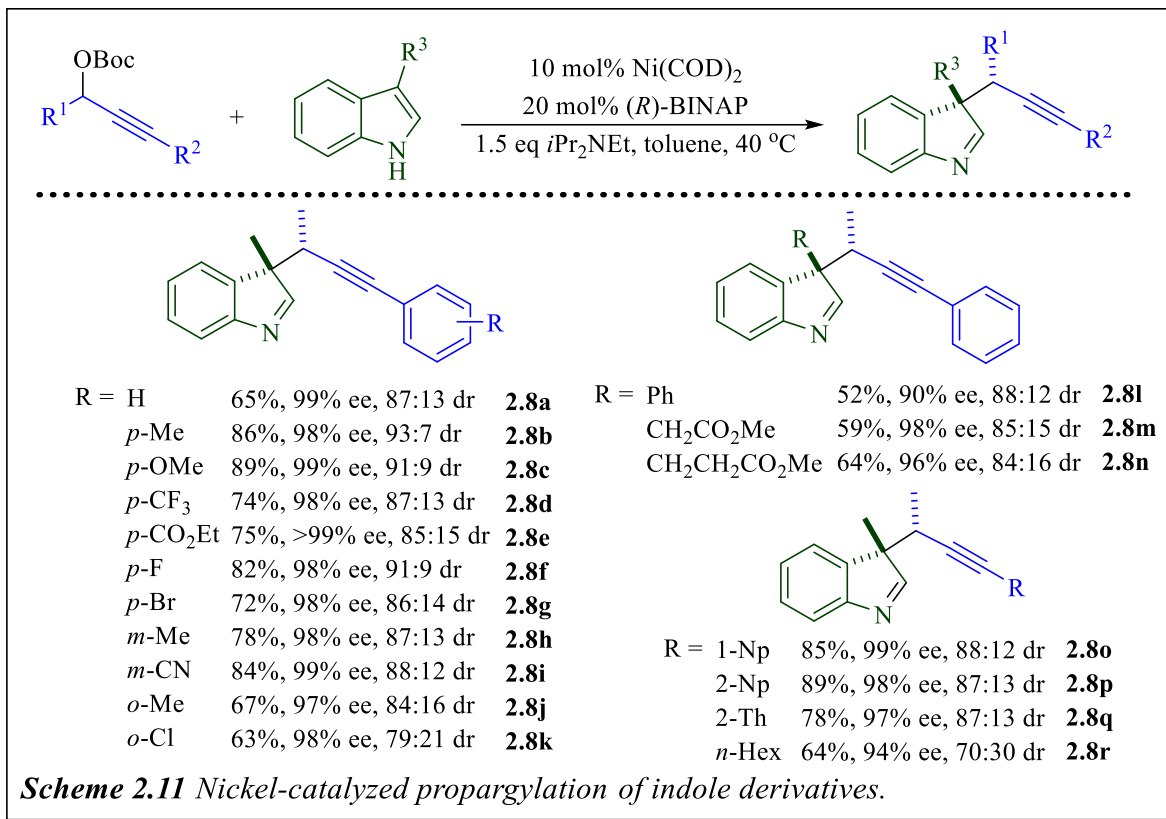
As mentioned in the previous section, transition metal-catalyzed propargylation methods have been developed to further expand the scope of these reactions to increase their overall utility.¹⁵ Methods utilizing several different transition metals have been explored; however, this section is going to focus on the use of nickel and copper. While the asymmetric propargylation reported by the Guo group, as discussed in the last section, illustrates the ability of nickel to work synergistically with a Lewis acid to promote propargylation, nickel is highly reactive towards

propargyl electrophiles and able to catalyze these reaction in its own. In 2012, Hirashita and coworkers reported an indium-mediated, Ni-catalyzed nucleophilic propargylation of aldehydes, which produced propargyl alcohols with high *syn* selectivity (Scheme 2.9).¹⁶ They found that this reaction was successful with both aliphatic (**2.6a, e**) and aromatic (**2.6b-d, f-h**) aldehydes. In addition, this reaction was tolerant of both a free alcohol (**2.6f**) and a TMS-protected terminal alkyne (**2.6g**). However, while the reaction with a free terminal alkyne proceeds with high *syn* selectivity, it led to a low yield (**2.6h**). While reactions with aldehydes produced high *syn* selectivity, a reaction with a ketone (**2.6g**) had a relatively low selectivity, albeit with a high yield. While the overall high selectivity of this method is quite useful, particularly when considering that previous In-mediated propargylations have typically yielded *anti* products,¹⁷ it is worth noting that the reported scope lacked a wide breadth of functional groups.



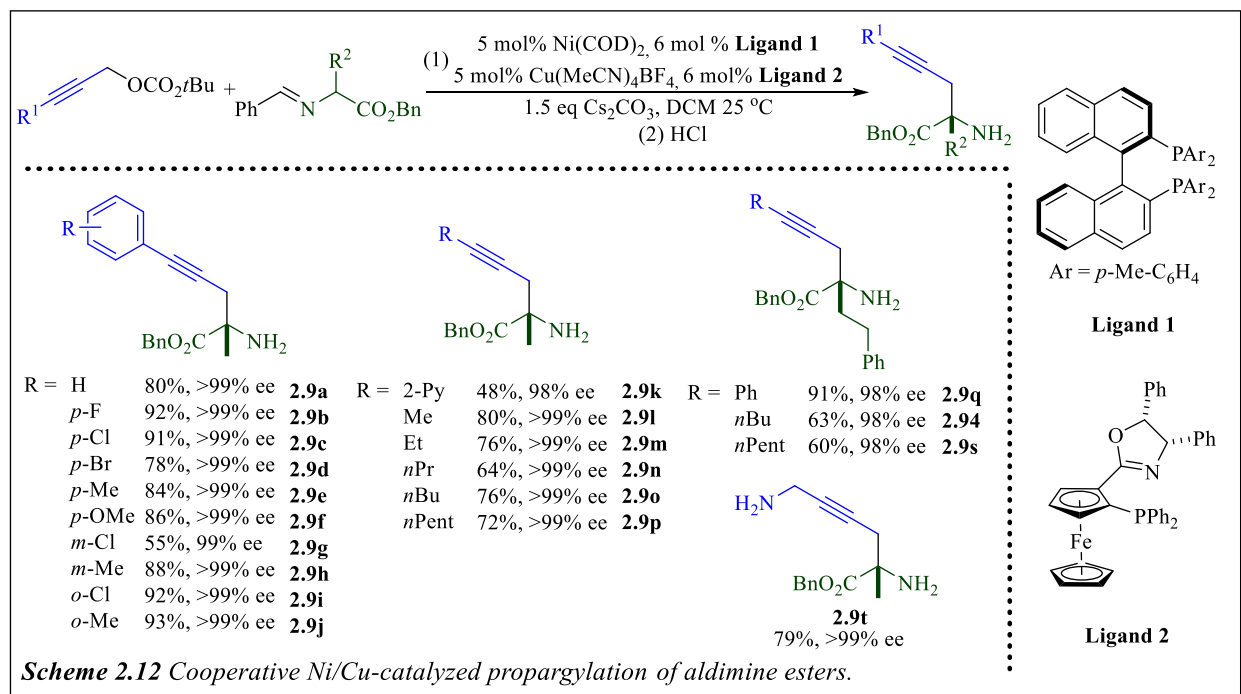


Later in 2018, Kawatsura, Tsuji, and coworkers disclosed a Ni-catalyzed asymmetric propargylic amination that produced propargyl amines with high yields and ee's (Scheme 2.10).¹⁸ This reaction was tolerant of both EWGs and EDGs on the aromatic moiety of both the propargyl carbonate and the amine (**2.7a-s**); however, having a fluorine at the ortho position of the propargylic phenyl led to a reduced yield (**2.7i**). In addition, the presence of an *m*-F (**2.7q**), *o*-F (**2.7s**), or *o*-Me (**2.7r**) on the aromatic group of the amine led to a significant decrease in the yield of the reaction; however, despite these low yields, the reaction still maintained an extremely high level of enantioselectivity. In addition, the reaction was successful with a secondary amine, although it did lead to a significant decrease in the yield (**2.7v**). It is also worth noting that other than a methyl group, no other substitutions at the internal propargylic position were reported, which severely limits the scope of the reaction, greatly decreasing the generality of the method.



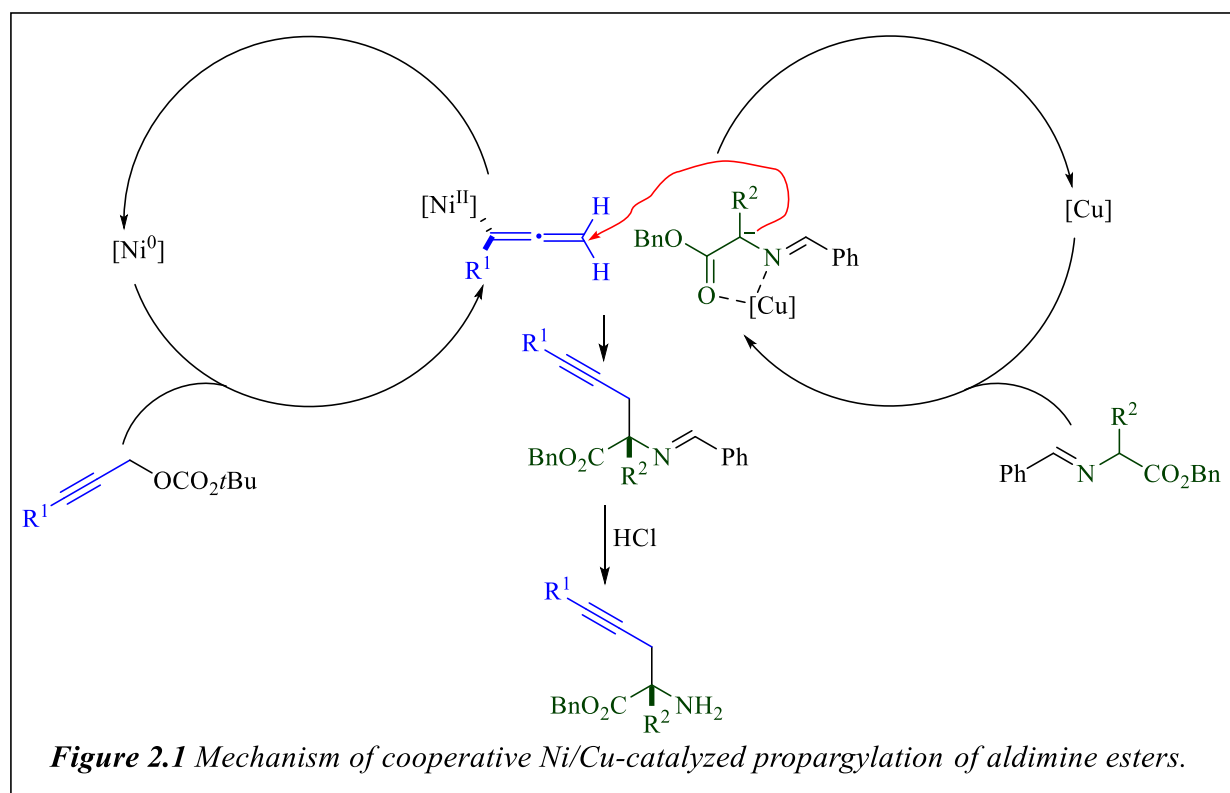
A few years later, the same group reported a Ni-catalyzed asymmetric Friedel-Crafts propargylation of 3-substituted indoles with propargylic carbonates (Scheme 2.11).¹⁹ The synthesis of indolenine **2.8a** could be done on a gram scale without a loss of yield or selectivity. The reaction was compatible with many different functionalities substituted on the terminal aromatic group of the propargyl carbonate, including both EWGs (**2.8c-g, i, k**) and EDGs (**2.8b-c, h, j**); however, substitution at the ortho position did cause a slight decrease in yield. In addition, the reaction was tolerant to other aromatic moieties, including 1- and 2-naphthyl and thiophenyl groups. While the reaction could also proceed with an alkyl group at the terminal propargylic position (**2.8r**), there was a slight decrease in both the yield and diastereoselectivity. It should also be mentioned that the synthesis of substrates **2.8l-n**, with larger substituents at the 3-position of the indolenine compounds, required a slight increase in catalyst and ligand loadings, to 15% and

30% respectively. Furthermore, this reaction required a stoichiometric amount of base, which greatly decreases the overall attractiveness of the method.



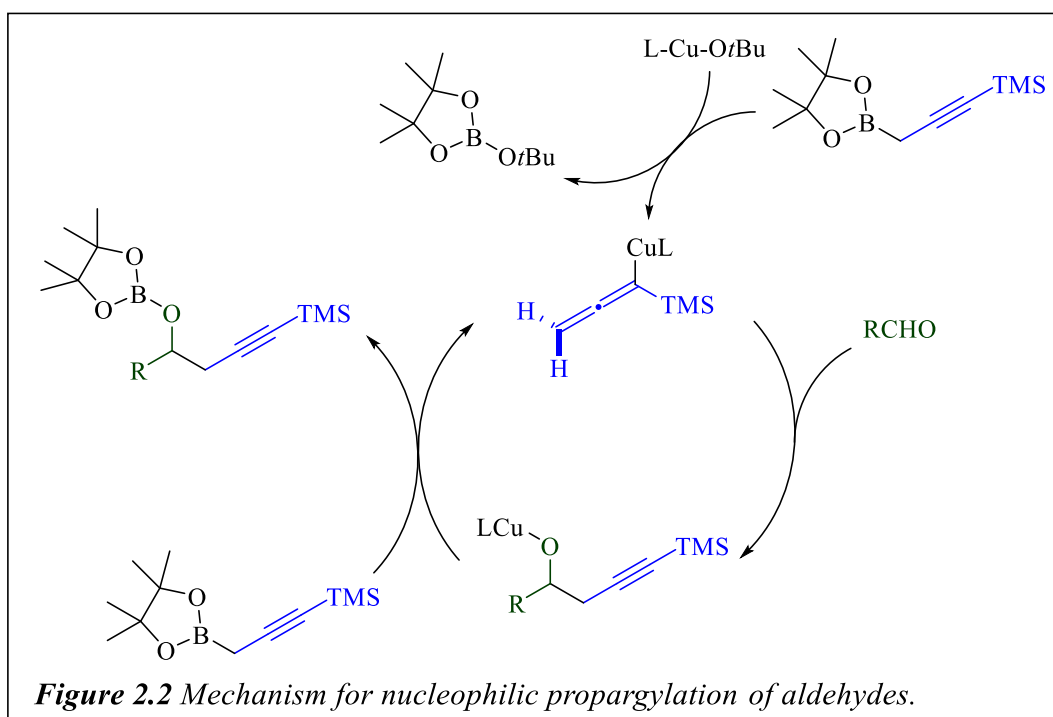
In a previous example from the Guo group nickel acted as a co-catalyst with the Lewis acid Yb(OTf)₂, allowing for the asymmetric propargylation of triesters.¹³ Over the recent years, methods utilizing cooperative catalysis have been developed to promote several different enantioselective transformations,²⁰ including propargylation reactions.²¹ One recent example of dual-catalytic propargylation, also reported by the Guo group, demonstrated a cooperative Ni/Cu-catalyzed enantioselective propargylation of aldimine esters that proceeds in high regio- and stereochemistry (Scheme 2.12).²² This reaction was tolerant of propargyl carbonates bearing a terminal phenyl with both EDG (**2.9f, h, j**) and EWGs (**2.9b-d, g-h, i**) at the ortho-, meta-, or para positions, with most yields being between 80-90% and ee's greater than 99%. In addition, the reaction was also compatible with both terminal alkyl groups (**2.9k-p**), albeit with a noticeable drop in yield, and an unprotected terminal amine (**2.9t**). Control experiments verified that both

catalysts were necessary, as the neither could catalyze the reaction independently. Furthermore, they observed that both catalysts interact cooperatively to control the overall stereochemistry of the products. Their proposed mechanism for this transformation is depicted in Figure 2.1. The reaction begins with a nickel-mediated substitution of the propargyl carbonate, forming an allenyl-nickel complex, while simultaneously copper coordinated with the aldimine ester, allowing for the formation an enolate intermediate. The ylide intermediate then nucleophilically attacks the allenyl-nickel complex. Subsequent acid hydrolysis of the propargylated compound leads to the propargylated amino ester. While the scope of this reaction is fairly extensive, the method does require a stoichiometric amount of base, which does limit its overall usefulness somewhat.

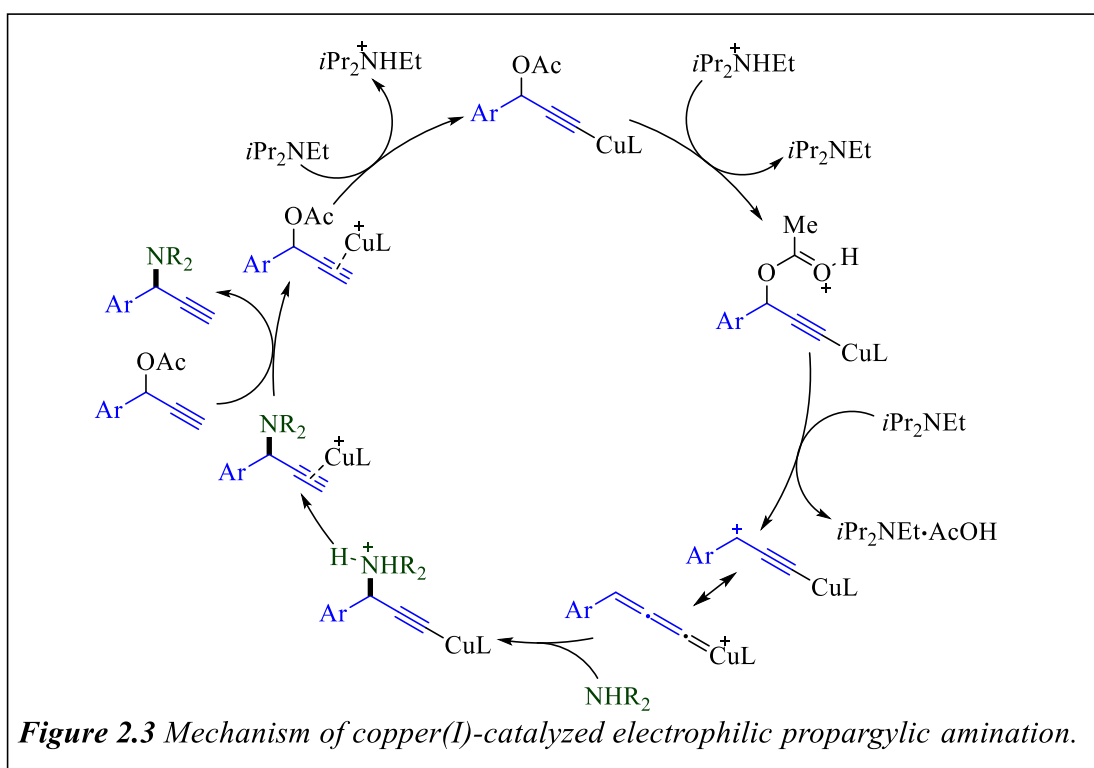
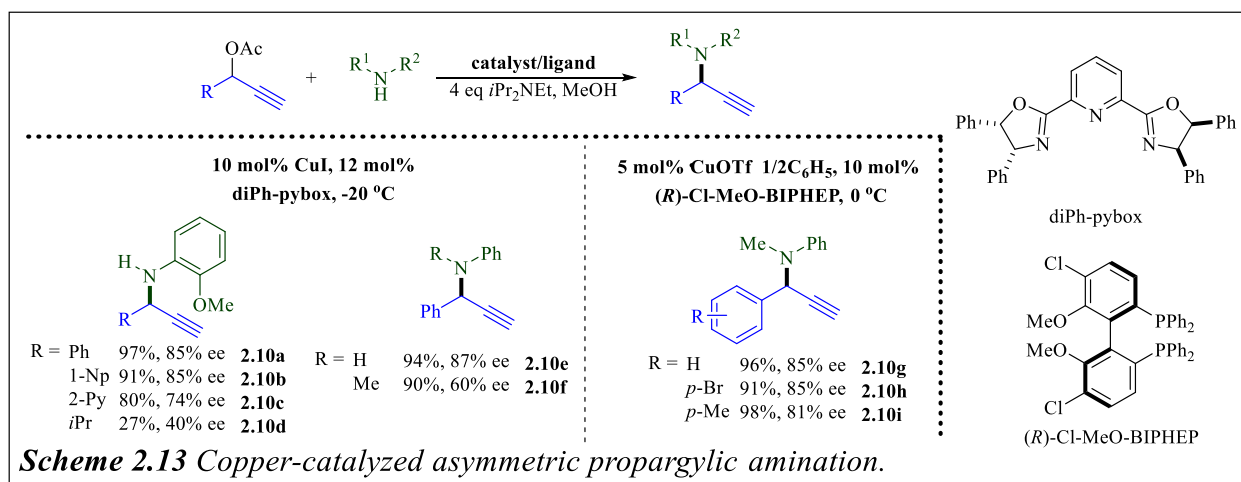


Several late transition metals, including both copper, zinc, silver, and gold are frequently used as catalysts in propargylation reactions; however, they are often used to catalyze nucleophilic propargylations, where the nucleophilic component of the reaction is the propargyl moiety.²³ A

sample mechanism for one of these nucleophilic propargylation reactions, a propargylation of aldehydes, is depicted in Figure 2.2. In this reaction, there is a copper-alkoxide mediated boron/copper exchange with a propargyl borolate, forming an allenyl-copper intermediate. This allenyl-Cu intermediate would undergo an addition to an aldehyde, followed by a subsequent boron/copper exchange with a second propargyl borolate. While this mode of reactivity is frequently used to couple nucleophilic propargyl compounds with various electrophiles, this dissertation will continue to primarily focus on reactions with propargyl electrophiles, and copper is also frequently used as a catalyst in these reactions.²⁴

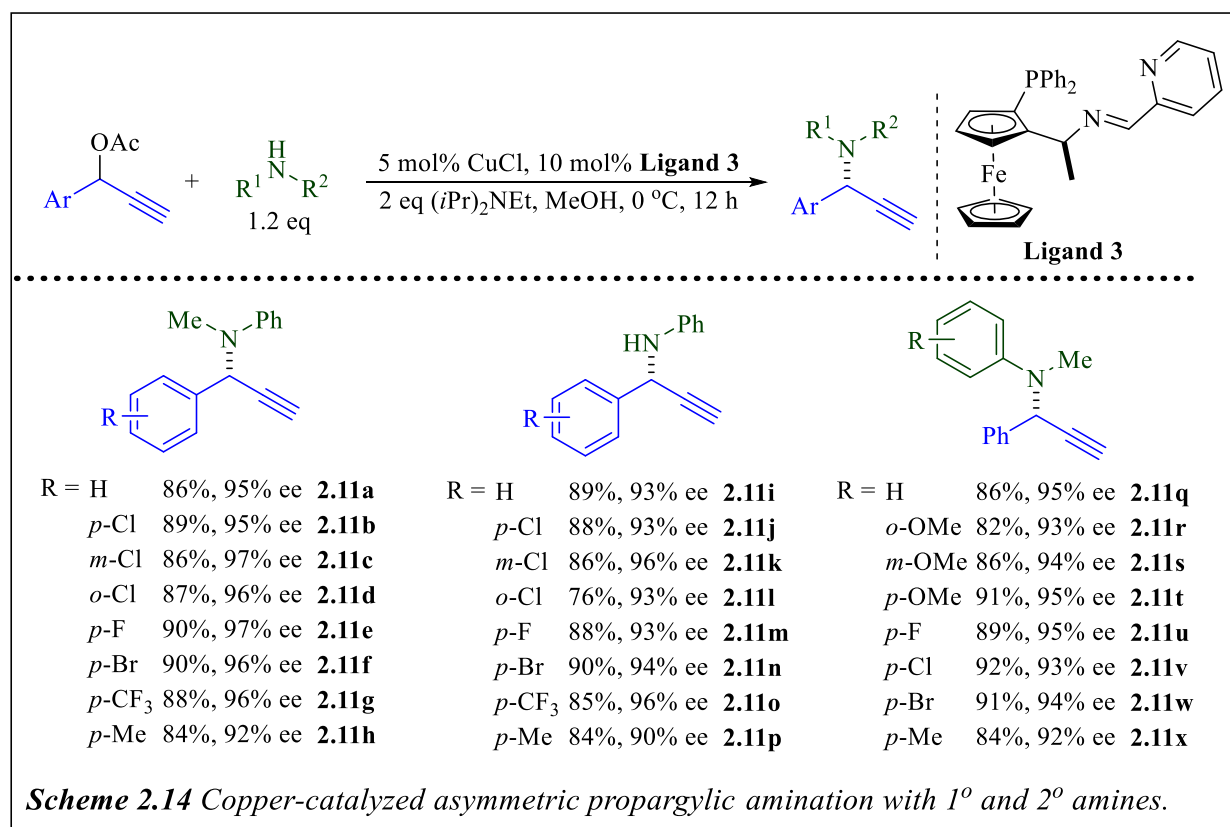


There have been many reported examples of the use of copper(I) to catalyze electrophilic propargylation, which are proposed to proceed via the formation of a copper allenylidene intermediate. One example of this, reported simultaneously in 2008 by van Marseveen²⁵ and Nishibayashi,²⁶ is a Cu-catalyzed asymmetric propargylic amination coupling propargylic acetates with amines, affording propargyl amines in high yields and enantioselectivities (Scheme 2.13).



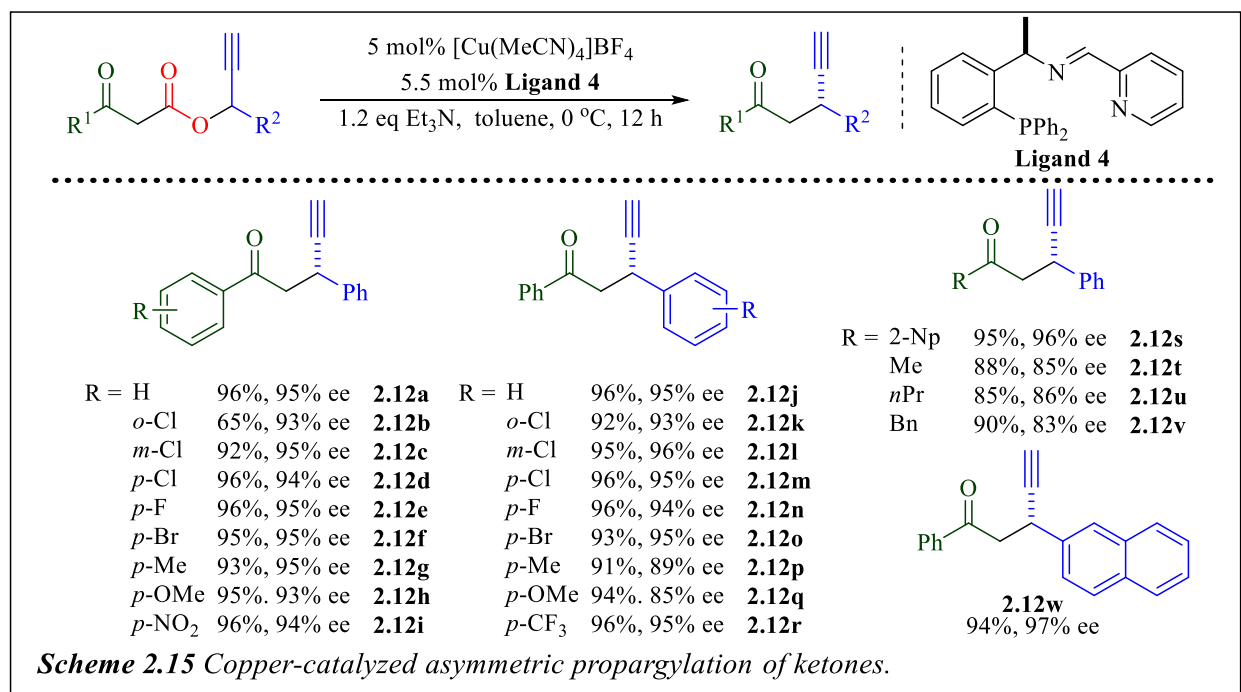
Their two methods differ in their choice of ligand and copper catalyst, with van Maarseveen's protocol using catalytic CuI and a tridentate ligand, diPh-pybox. While primary amines (**2.10a-e**) were typically best suited for this reaction, a single example of a secondary amine (**2.10f**) was also successful. On the other hand, Nishibayashi used CuOTf·1/2C₆H₅ and an atropisomeric ligand, Cl-MeO-BIPHEP, and with this protocol, Nishibayashi found that only secondary amines were

tolerated. The proposed mechanism of these reactions, shown in Figure 2.3, relies on the formation of, and subsequent nucleophilic attack on, a copper-allenyldene complex. DFT calculations reported by Nishibayashi and coworkers support the formation of this Cu-allenyldene intermediate. The formation of a metal-allenyldene complex is a key step in catalytic propargylation reactions that utilize other metals as well, with Ruthenium being the most typical example.²⁷ However, unlike with ruthenium-catalyzed propargylations, these Cu(I)-catalyzed reactions require stoichiometric or super stoichiometric amounts of base to first deprotonate the alkyne. Therefore, these methods are limited to terminal propargylic electrophiles, significantly impacting the utility of the reaction.



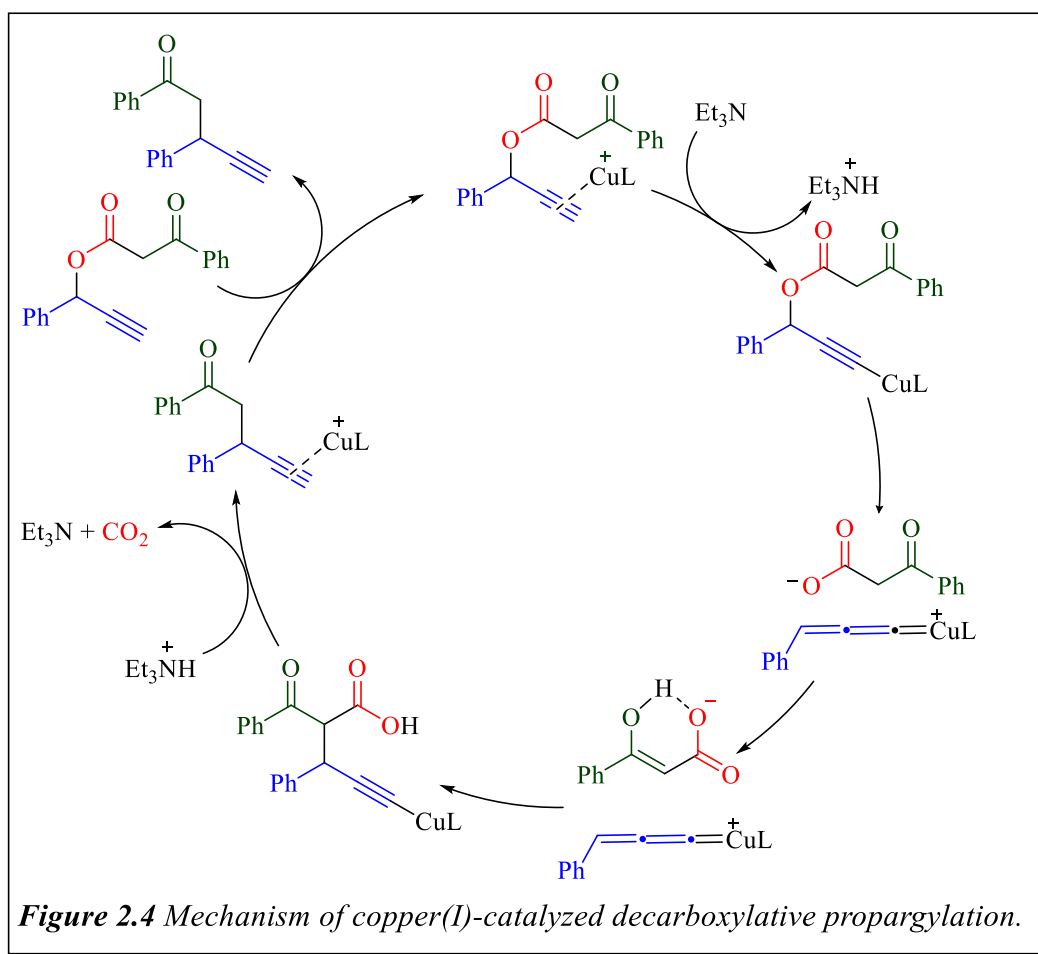
In 2012, Hu and coworkers reported their own method for the Cu-catalyzed asymmetric propargylic amination, affording propargyl amines in high yields and enantioselectivities (Scheme 2.14).²⁸ This reaction was successful at coupling propargyl acetates with both 1° aromatic and 2°

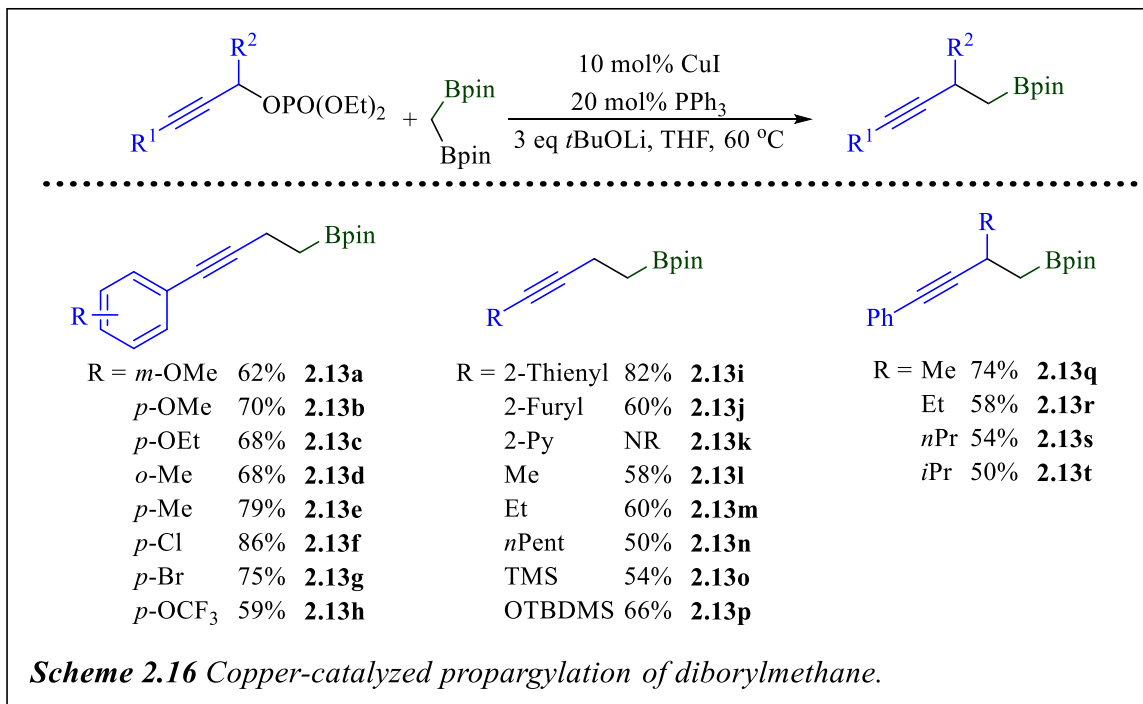
amines, forming the corresponding propargyl amines in high yields and enantioselectivities. This reaction was tolerant of aromatic groups bearing both EDGs (**2.11 h, p, r-t, x**) and EWGs (**2.11b-g, j-o, u-w**). It is also worth noting that this is the first reported protocol that was able to successfully couple both primary and secondary amines without a noticeable drop in either yield or enantioselectivity. However, as with the other Cu(I)-catalyzed propargylations, this protocol was limited to only terminal propargyl acetates.



Later, in 2014, Hu and coworkers developed a method for the Cu(I)-catalyzed intramolecular enantioselective decarboxylative propargylation of ketones (Scheme 2.15).²⁹ This reaction was tolerant of aromatic groups with a wide range of electronic demand. In addition, it was compatible with several different functional groups, including halogens (**2.12b-f, k-o**), methoxy- (**2.12h, q**), and nitro- (**2.12i, r**). In addition, this reaction was also successfully able to propargylate alkyl substituted ketones (**2.12t-u**). The mechanism of this reaction, shown in Figure 2.4, starts with coordination of copper to the terminal alkyne, which is followed by deprotonation to generate the

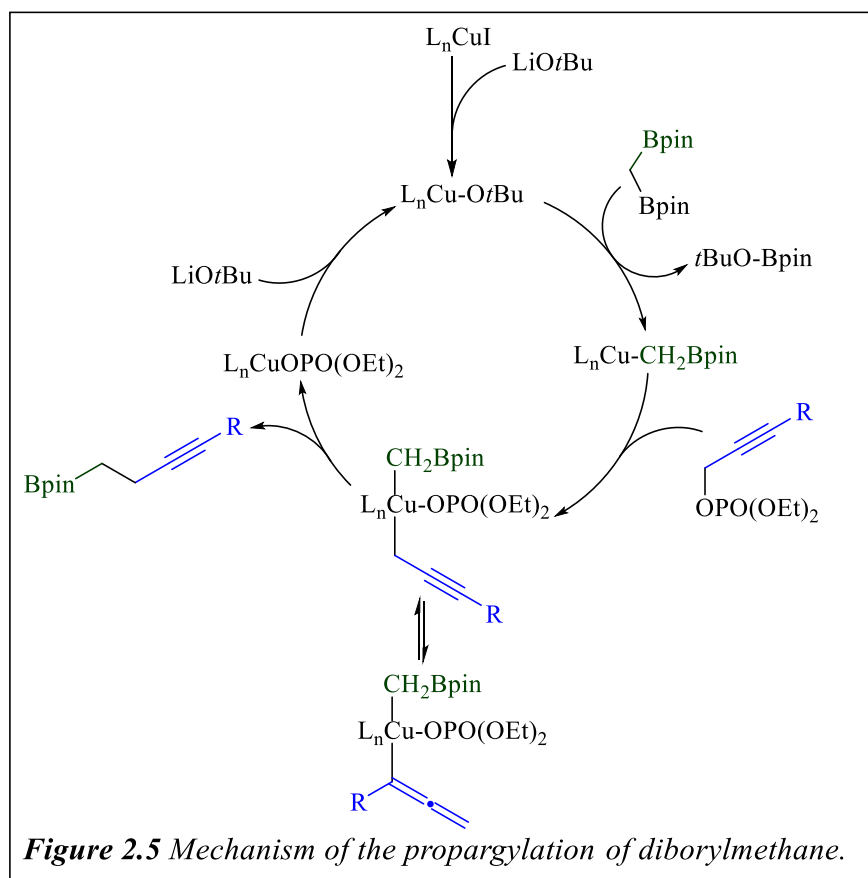
Cu-acetylide complex. This complex undergoes a dissociation, which allows for the formation of a Cu-allenylidene complex. After an isomerization of the carboxylate ion, there is a nucleophilic attack by the enolate on the Cu-allenylidene complex, forming a second Cu-acetylide complex. Decarboxylation and protonation lead to the formation of the propargylated product and the turnover of the active catalyst. By utilizing a decarboxylative mechanism, the authors removed the requirement for preformation of the enolate nucleophile prior to the start of the reaction; however, stoichiometric amounts of base were still required to deprotonate the terminal alkyne to form the Cu-acetylide complex. In addition, as the formation of a Cu-allenylidene is required, this method is also limited to terminal alkynes.



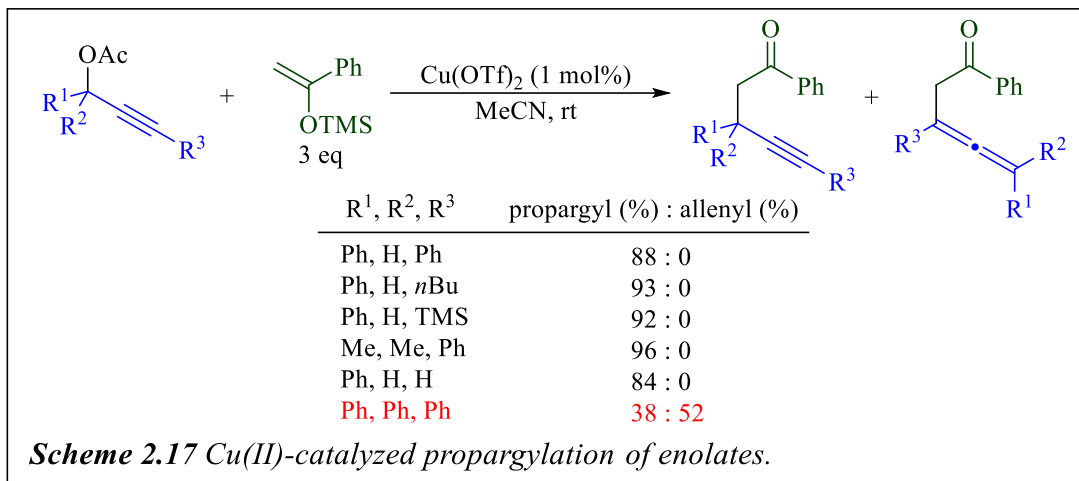


While the previous examples of Cu-catalyzed propargylations were all limited to terminal alkynes, there have been methods developed to allow for reaction of internal alkynes.³⁰ In 2017, Xiao, Fu, and coworkers reported a Suzuki-Miyaura coupling between propargyl electrophiles and *gem*-diborylmethane (Scheme 2.16).³¹ This reaction was compatible with a series of primary aromatic propargyl phosphates that contain a range of functional groups, including EDGs (**2.13a-e**) and EWGs (**2.13f-g**). The reaction was also successful with alkyl propargyl phosphates (**2.13l-n**), a protected alcohol (**2.13p**), and a silyl group (**2.13o**). While it was tolerant of a thienyl (**2.13i**) and furyl (**2.13j**) heteroaromatic group, a pyridyl group led to no reaction. In addition, while the reaction could proceed with secondary propargyl phosphates, as the sterics of the groups at the internal propargylic position increased, the yield of the reaction decreased (**2.13q-t**). Their proposed mechanism starts with an anion exchange between CuI and lithium *t*-butoxide to generate an alkoxide-Cu complex (Figure 2.5). This alkoxide-Cu complex reacts with diborylmethane to form an alkyl-Cu intermediate, which will undergo oxidative addition with the propargyl

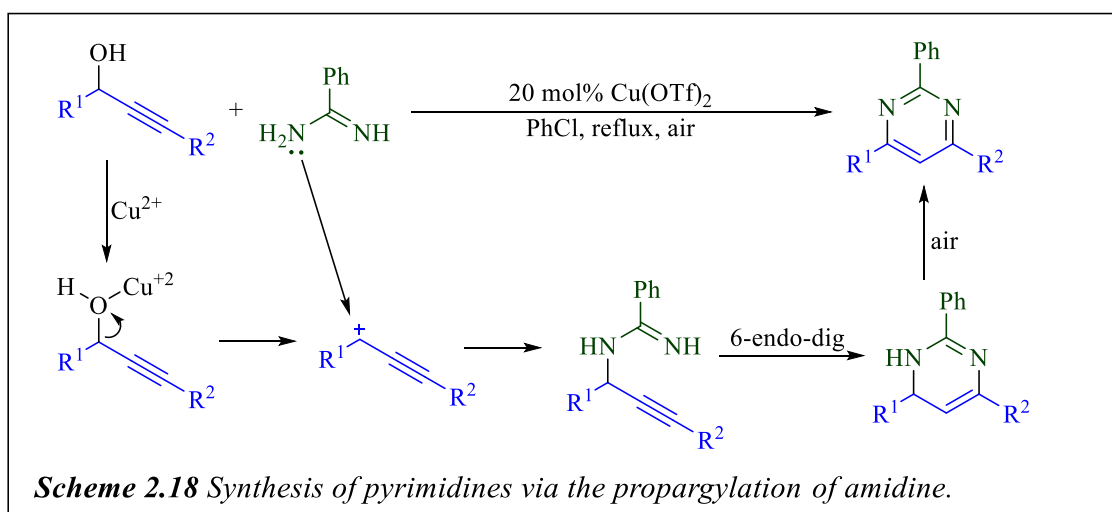
phosphate to form a propargyl-Cu complex. Reductive elimination of this propargyl-Cu complex will release the propargylated product. Subsequent reaction between the copper complex and lithium *t*-butoxide will regenerate the alkoxide-Cu complex. While the expansion of the reaction scope to include internal alkynes is useful, the overall scope of this method was limited, and many of the yields were low to moderate. In addition, the reaction required super-stoichiometric quantities of lithium *t*-butoxide, which decreases the attractiveness of the methodology.



As an alternative to the Cu(I) catalysts of the previous examples, some groups have explored the use of Cu(II) catalysts to expand the scope of these propargylations to also include internal alkynes. While Cu(I) catalysts rely on the formation of Cu- allenylidene or Cu-acetylide, necessitating the use of terminal alkynes, Cu(II) catalysts react through an S_N1 substitution pathway, allowing for both internal and terminal alkynes. In 2007, Zhan and coworkers reported

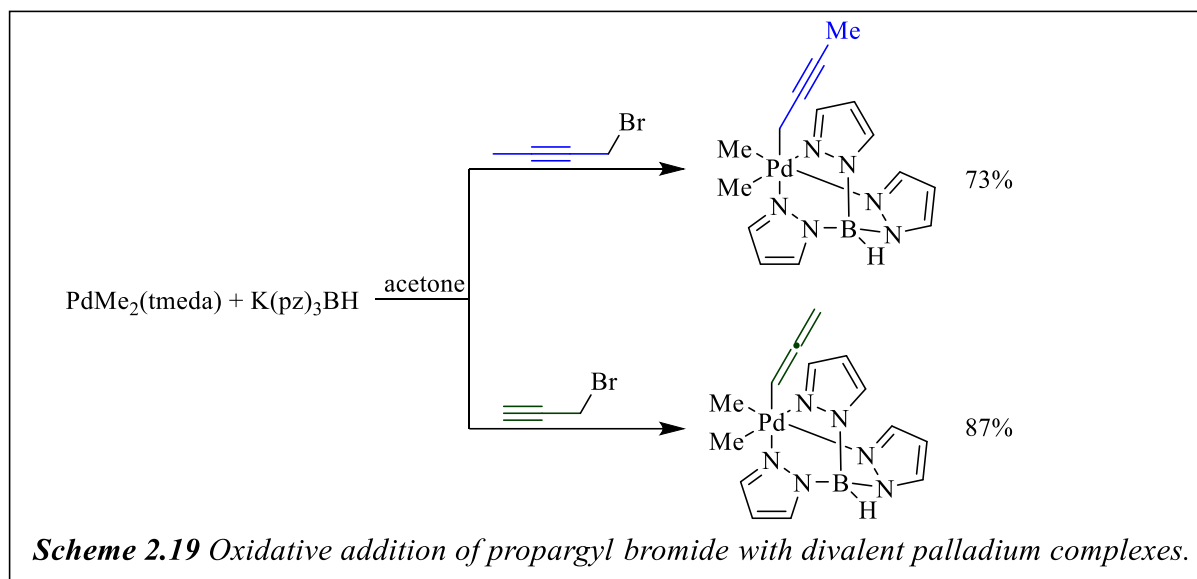


the use of Cu(OTf)₂ to catalyze the nucleophilic substitution of propargylic acetates with silyl enol ether nucleophiles (Scheme 2.17).³² As this reaction proceeds through the formation of a carbocation at the propargylic position, stabilization through either a phenyl group or two methyl groups is required. However, with the more sterically hindered 1,1-diaryl substituted alcohol, the allenyl product is formed preferentially. Zhan and coworkers also used Cu(OTf)₂ to catalyze a propargylic coupling of propargyl alcohols and amidine in their synthesis of pyrimidine derivatives (Scheme 2.18).³³ In these reactions, the copper catalyst facilitates in the formation of a carbocation, which is then attacked by the nucleophile. In the case of the reaction with amidine, the product of propargylation undergoes a cyclization, followed by an aromatization.



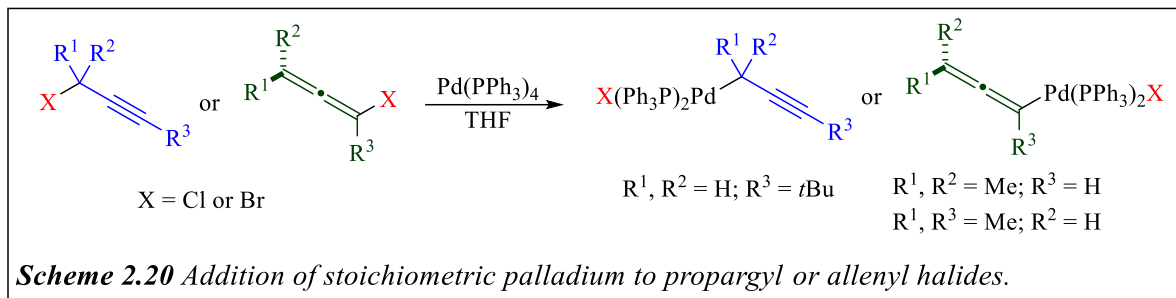
2.4 Reactivity of Propargylpalladium Complexes

While the last few sections have illustrated some of the many contributions to develop catalyzed propargylation reactions by Lewis and Brønsted acids and other metals, palladium-catalyzed propargylations are of some considerable interest due to the ability to yield several different types of products. Both allenyl and propargylic palladium complexes have been prepared and characterized.³⁴ In 1999, Canty and coworkers reported that the oxidative addition of propargyl bromide with divalent palladium complexes (Scheme 2.19).^{34c} Whether these

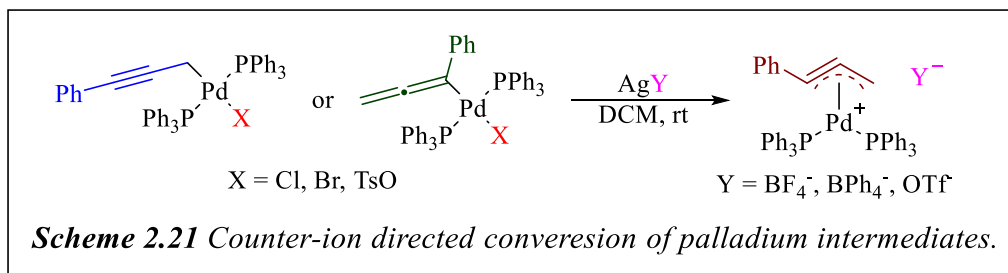


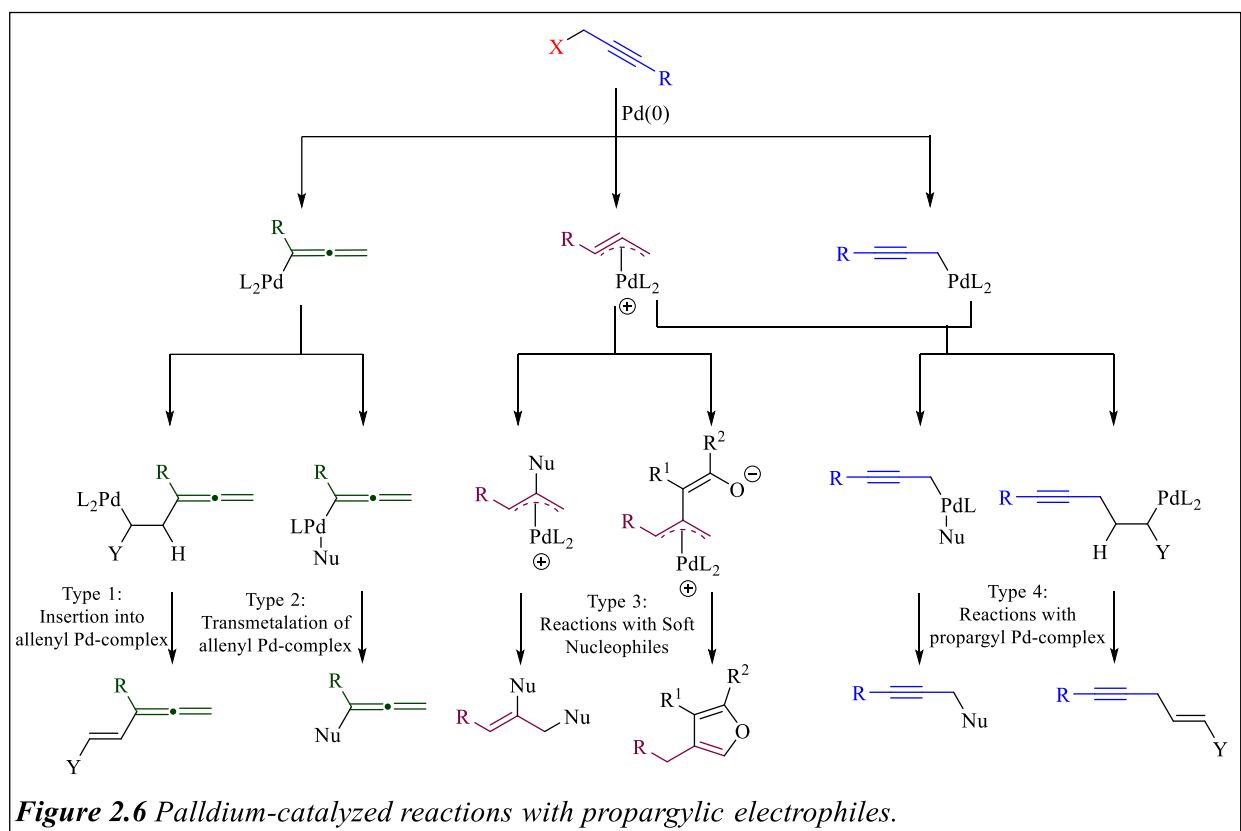
reactions would form the η^1 -allenyl or η^1 -propargyl depended on the structure of the propargylic bromide, with 2-butyne-1-yl bromide forming exclusively the η^1 -propargylic Pd complex and 2-propyne-1-yl bromide forming exclusively the η^1 -allenyl Pd complex.

In the mid to late 1990s, Kurosawa and coworkers conducted thorough mechanistic and reactivity tests on several palladium complexes that are formed from the reaction of propargylic halides with $\text{Pd}(\text{PPh}_3)_4$.³⁵ They reported that when either a propargyl halide or allenyl halide was



reacted with a stoichiometric amount of $\text{Pd}(\text{PPh}_3)_4$, either the η^1 -allenyl Pd complex or the η^1 -propargylic Pd complex could form (Scheme 2.20). Preference for the formation of one over the other was dependent on the steric hindrance at either the internal or terminal position of the starting material, with increased steric interactions at the internal propargylic position leading to the formation of the η^1 -allenyl Pd complex. However, whether the starting material was allenyl or propargyl, the same palladium-bound intermediate will be generated. Kurosawa and coworkers also observed the importance of the counterion for the selectivity of one palladium-bound intermediate over the other (Scheme 2.21) Treatment of neutral η^1 -allenyl or η^1 -propargylic palladium halides or tosylates with AgBF_4 , AgBPh_4 , or AgOTf led to the exclusive formation of the cationic η^3 -propargylpalladium complex. However, while non-coordinating counterions favor the formation of η^3 -propargylpalladium complex, non-coordinating, non-polar solvents favor the η^1 -allenylpalladium complex and polar, coordinating solvents favor the η^3 -propargylpalladium complex. It has also been reported that the η^3 -propargylpalladium complex is favored when in the presence of bidentate phosphine ligands.³⁶





While reactions between propargylpalladium intermediates and many types of nucleophiles have been studied, this work will be limited to reactions with carbon nucleophiles. A brief overview of palladium-catalyzed additions to propargylic electrophiles is illustrated in Figure 2.6.⁴ After reacting a propargyl electrophile with palladium, three possible intermediates could form, η^1 -allenyl, η^3 -propargyl, or η^1 -propargyl. Reactions with the η^1 -allenylpalladium complexes can undergo an insertion (Type I) with an alkene or transmetalation with a hard nucleophile (Type II). Both pathways result in the formation of an allenyl product. While hard nucleophiles are known to react with the η^1 -allenylpropargyl complex, soft nucleophiles selectively attack at the central position of the η^3 -propargyl complex³⁷ (Type III). These reactions will either undergo a second nucleophilic attack, either intermolecularly, yielding an alkene, or intramolecularly, yielding a cyclized product. The last category of reactions (Type IV) is much more rare than the others and

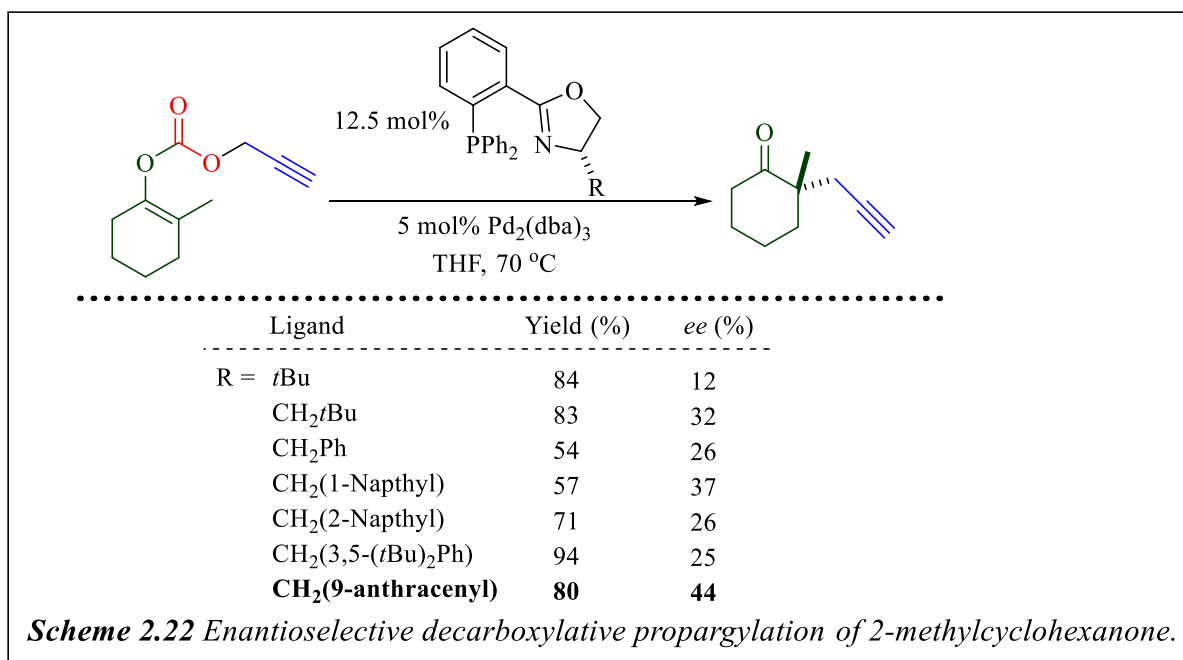
arises from reactions with the η^1 -propargylpalladium complex. Once the complex is formed, it can then undergo nucleophilic attack or insertion with an alkene.

In 2003, Delbecq, Sinou, and coworkers reported that the η^3 -propargylpalladium complex is bound to the palladium atom at both of the terminal carbons; however, the bond distances are not equal.³⁸ The bond distance between palladium and the terminal carbon is slightly shorter than the bond distance between palladium and the substituted carbon. DFT calculations indicate that the central carbon is positively charged and that the terminal propargyl carbons are negatively charged, which would explain why nucleophilic attack occurs exclusively at the central carbon. In addition, Anderson, Paton, and coworkers reported that bidentate ligands with larger bite angles lower the LUMO orbitals of the terminal carbons, favoring attack at the terminal carbon over the center carbon; however, bidentate ligands with smaller bite angles favor nucleophilic attack at the central carbon of the η^3 -propargylpalladium complex.³⁹ The reactivity of propargylpalladium complexes will be revisited in chapters 4 and 5.

2.5 Palladium-Catalyzed Propargylation Reactions with Propargylic Electrophiles

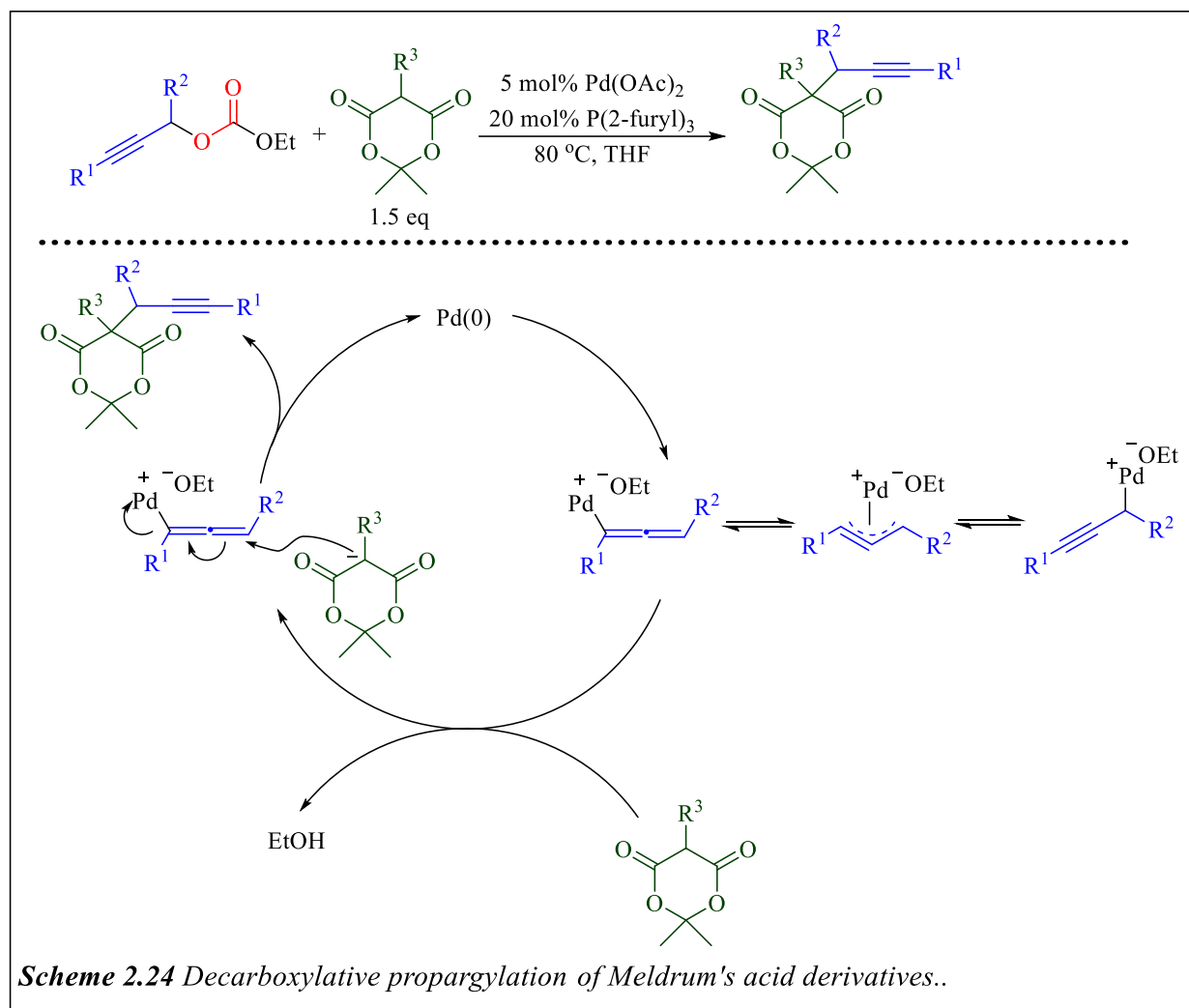
As this chapter has discussed, many of the current methods of the propargylation of various nucleophiles suffer from poor atom-economy, reagent toxicity, lack of selectivity, or a limited reaction scope. In addition, despite the potential advantages of the use of palladium with propargyl electrophiles, the last section illustrated that reactions with palladium and propargyl electrophiles have regioselectivity issues due to the several possible palladium-bound intermediates. In addition, palladium-catalyzed reactions that selectively form the propargylated product are still quite rare; although, some examples of these reactions do exist.

Stoltz and coworkers did a lot of work developing the asymmetric allylation of enol carbonates.⁴⁰ During this research, they explored the asymmetric propargylation of enol carbonates (Scheme 2.22).⁴¹ They found that the propargylation reactions required higher temperatures than were required for the allylation. While their *ee* values never rose above 44%, these preliminary results are still highly promising.



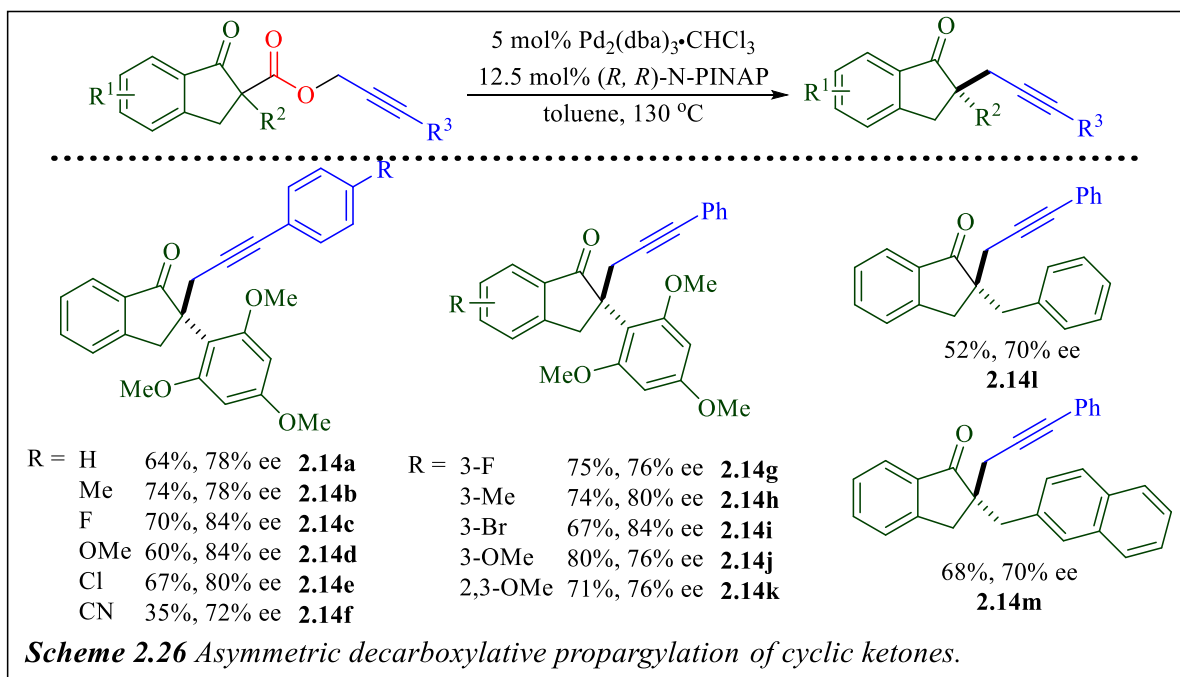
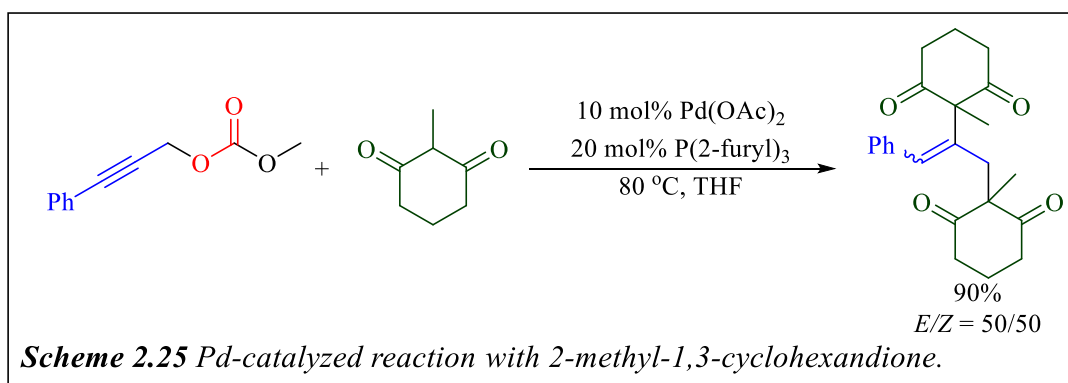
Around this same time, Cuerva and coworkers reported a dual-catalytic titanium/palladium-mediated regioselective nucleophilic propargylation of ketones (Scheme 2.23).⁴² This reaction was able to successfully couple both terminal and internal propargyl carbonates with cyclic and linear ketones, generating the propargyl alcohol in moderate to good yields. However, while this reaction does allow for the coupling of propargyl carbonates with several different substitution patterns, the method requires a super-stoichiometric amount of Cp₂TiCl₂ and Mn. The mechanism (Figure 2.7) begins with the oxidative addition of an electrophilic propargyl carbonate with the Pd(0) catalyst, yielding a Pd(II)-intermediate. This is followed by single-

the ketone. Subsequent acid work up generates the homopropargylic alcohol and closes the second catalytic cycle.



A few years after this work in 2015, Iazzetti and coworkers reported a palladium-catalyzed propargylation of Meldrum's acid derivatives (Scheme 2.24) The reaction was tolerant towards both alkyl and aryl substitution at both the internal and terminal position of the propargyl carbonate.⁴³ The reaction begins with an S_N2 -type displacement of the ethyl carbonate group Pd(0), forming an η^1 -allenylpalladium intermediate, which is in equilibrium with η^3/η^1 -propargylpalladium intermediates. The generated ethoxide anion is then able to deprotonate the Meldrum's acid derivative, which attacks the η^1 -allenylpalladium intermediate, generating the

propargylated product. The Meldrum's acid derivatives could be both alkyl, phenyl, or benzyl groups; however, the reaction did not work with less stabilized nucleophiles. When the reaction run with 2-methyl-1,3-cyclohexandione, Iazzetti and coworkers saw exclusive formation of the bis-addition product (Scheme 2.25).



In 2019, O'Broin and Guiry reported an asymmetric decarboxylative propargylation of cyclic ketones, allowing for the formation of quaternary stereocenters (Scheme 2.26).⁴⁴ The reaction was successful towards a variety of substituents on the terminal propargyl ring, including both EDGs (**2.14a-b, d**) and EWGs (**2.14c, e-f**). It was also tolerant towards both electron-rich (**2.14h, j-k**)

and electron-deficient (**2.14g, i**) indanone rings, and the tri-methoxyphenyl ring could be successfully replaced with both a benzyl (**2.14l**) or methylene-naphthyl (**2.14m**) group.

2.6 Conclusion

In chapter 2, several different methods for the propargylation of various nucleophiles were presented, including the Nicholas reaction, Lewis and Brønsted acid catalysis, and transition metal catalysis. However, many of these methods suffered from one or more drawbacks, including reagent toxicity, low atom-economy, and limited substrate scope. Furthermore, regarding palladium-catalyzed reactions with propargyl electrophiles, the possibility of several different regioisomers makes selective propargylation a major challenge of these reactions. There have only been a few reported methods that have been able to favor the propargyl product over the more largely favored allenyl isomer. Therefore, more methods that can expand the scope of these reactions would amount to a large advancement in the chemistry of propargyl electrophiles. This topic will be revisited throughout later chapters 4 and 5.

2.7 References for Chapter 2

-
1. Trost, B. M.; Li, C-J. "Modern Alkyne Chemistry: Catalytic and Atom-Economic Transformations." New York: John Wiley & Sons, Inc. 2016.
 2. (a) Thompason, A. S.; Corley, E. G.; Huntington, M. F.; Grabowski, E. J. J. "Use of an Ephedrine Alkoxide to Mediate Enantioselective Addition of an Acetylide to a Prochiral Ketone: Asymmetric synthesis of the Reverse Transcriptase Inhibitor L-743,726." *Tetrahedron Lett.*, **1995**, *36*, 8937. (b) Wright, J. L.; Gregory, T. F.; Kesten, S. R.; Boxer,

-
- P. A.; Serpa, K. A.; Meltzer, L. T.; Wise, L. D.; Espitia, S. A.; Konkoy, C. S.; Whittenmore, E. R.; Woodward, R. M. "Subtype-Selective *N*-Methyl-D-Aspartate Receptor Antagonists: Synthesis and Biological Evaluation of 1-(Heteroarylalkynyl)-4-benzylpiperidines." *J. Med. Chem.*, **2000**, *43*, 3408-3419.
3. Florio, S.; Granio, C.; Ingrosso, G.; Troisi, L. "Wittig Rearrangements of (Heteroaryl)alkyl Propargyl Ethers, Synthesis of Allenylic and Propargylic Alcohols." *Eur. J. Org. Chem.*, **2002**, 3465-3472.
 4. Tsuji, J. "Overview of the Palladium-Catalyzed Carbon-Carbon Bond Formation via π -Allylpalladium and Propargylpalladium Intermediates." Ed. Ei-ichi Negishi. New York: John Wiley & Sons, Inc. 2002. 1669-1686. Online
 5. (a) Tsuji, J.; Minami, I. "New Synthetic Reactions of Allyl Alkyl Carbonates, Allyl β -Ketocarboxylates, and Allyl Vinylic Carbonates Catalyzed by Palladium Complexes." *Acc. Chem. Res.*, **1987**, *20*, 140-145. (b) M. Riemer. "Allyl Alkyl Carbonates." *Synlett*, **2014**, *25*, 1041-1042.
 6. Nicholas, K.M. "Chemistry and Synthetic Utility of Cobalt-Complexed Propargylic Cations." *Acc. Chem. Res.* **1987**, *20*, 207-241.
 7. Teobald, B. J. "The Nicholas Reaction: the Use of Dicobalt Hexacarbonyl-Stabilized Propargylic Cations in Synthesis." *Tetrahedron*, **2002**, *58*, 4133-4170.
 8. Sanz, R.; Miguel, D.; Martínez, A.; Álvarez-Gutiérrez, J. M.; Rodríguez, F. "Brønsted Acid Catalyzed Propargylation of 1,3-Dicarbonyl Derivatives. Synthesis of Tetrasubstituted Furans." *Org. Lett.*, **2007**, *9*, 727-730.
 9. Sanz, R.; Miguel, D.; Martínez, A.; Gohain, M.; García-García, P.; Fernández-Rodríguez, M. A.; Álvarez, E.; Rodríguez, F. "Brønsted Acid Catalyzed Alkylation of Indoles with

-
- Tertiary Propargylic Alcohols: Scope and Limitations.” *Eur. J. Org. Chem.*, **2010**, 36, 7027-7039.
10. Barreiro, E.; Sanz-Vidal, A.; Tan, E.; Lau, S-H.; Sheppard, T. D.; Díez-González, S. “ HBF_4 - Catalyzed Nucleophilic Substitutions of Propargylic Alcohols.” *Eur. J. Org. Chem.*, **2015**, 7544-7549.
 11. Huang, W.; Wang, J.; Shen, Q.; Zhou, X. “ $\text{Yb}(\text{OTf})_3$ -catalyzed propargylation and allenylation of 1,3-dicarbonyl derivatives with propargylic alcohols: one-pot synthesis of multi-substituted furocoumarin.” *Tetrahedron*. **2007**, 63, 11636-11643.
 12. Li, C.; Wang, J. “Lewis Acid Catalyzed Propargylation of Arenes with *O*-Propargyl Trichloroacetimidates: Synthesis of 1,3-Diarylpropynes.” *J. Org. Chem.*, **2007**, 72, 7431-7434.
 13. Chang, X.; Zhang, J.; Peng, L.; Guo, C. “Collective Synthesis of Acetylenic Pharmaceuticals via Enantioselective Nickel/Lewis Acid-Catalyzed Propargylic Alkylation.” *Nat. Commun.* **2021**, 12, 299.
 14. Bauer, E. B. “Transition Metal Catalyzed Functionalization of Propargylic Alcohols and Their Derivatives”, *Synthesis*, **2012**, 44, 1131
 15. Nihibayashi, Y. "Transition Metal-Catalyzed Enantioselective Propargylic Substitution Reactions of Propargylic Alcohol Derivatives with Nucleophiles." *Synthesis*, **2012**, 44, 489-503.
 16. Hirashita, T.; Suzuki, Y.; Tsuji, H.; Sato, Y.; Naito, K.; Araki, S. “Nickel-Catalyzed Indium(I)-Mediated *syn*-Selective Propargylation of Aldehydes.” *Eur. J. Org. Chem.*, **2012**, 5668-5672.

-
17. Marshal, J. A.; Grant, C. M. "Formation of Transient Chiral Allenylindium Reagents from Enantioenriched Propargylic Mesylates through Oxidative Transmetallation. Applications to the Synthesis of Enantioenriched Homopropargylic Alcohols." *J. Org. Chem.*, **1999**, *64*, 696– 697.
18. Watanabe, K.; Miyazaki, Y.; Okubo, M.; Zhou, B.; Tsuji, H.; Kawatsura, M. "Nickel-Catalyzed Asymmetric Propargylic Amination of Propargylic Carbonates Bearing an Internal Alkyne Group." *Org. Lett.*, **2018**, *20*, 5448-5451.
19. Miyazaki, Y.; Zhou, B.; Tsuji, H.; Kawatsura, M. "Nickel-Catalyzed Asymmetric Friedel-Crafts Propargylation of 3-Substituted Indoles with Propargylic Carbonates Bearing an Internal Alkyne Group." *Org. Lett.*, **2020**, *22*, 2049-2053.
20. (a) Shao, Z.; Zhang, H. "Combining Transition Metal Catalysis and Organocatalysis: A Broad New Concept for Catalysis." *Chem. Soc. Rev.*, **2009**, *38*, 2745-2755. (b) Allen, A. E.; MacMillan, D. W. C. "Synergistic Catalysis: A Powerful Synthetic Strategy for New Reaction Development." *Chem. Sci.*, **2012**, *3*, 633-658. (c) Shi, X.; Zhong, C. "When Organocatalysis Meets Transition-Metal Catalysis." *J. Org. Chem.*, **2010**, *16*, 2999-1325. (d) Krautwald, S.; Sarlah, D.; Schafroth, M. A.; Carreira, E. M. "Enantio- and Diastereodivergent Dual Catalysis: α -Allylation of Branched Aldehydes." *Science*, **2013**, *340*, 1065-1068. (e) Chen, D-F; Han, Z-Y; Zhou, X-L; Gong, L-Z. "Asymmetric Organocatalysis Combined with Metal Catalysis: Concept, Proof of Concept, and Beyond." *Acc. Chem. Res.*, **2014**, *47*, 2365-2377.
21. (a) Fu, Z.; Deng, N.; Su, S-N; Li, H.; Li, R-Z; Zhang, X.; Liu, J.; Niu, D. "Diastereo- and Enantioselective Propargylation of 5*H*-Thiazol-4-ones and 5*H*-Oxazol-4-ones as Enabled by Cu/Zn and Cu/Ti Catalysis." *Angew. Chem.*, **2018**, *130*, 15437-15441.; (b) Li, R-Z; Tang, H.; Yang, K. R.; Wan, L-Q; Zhang, X.; Liu, J.; Fu, Z.; Niu, D. "Enantioselective Propargylation of Polyols and Desymmetrization of *meso* 1,2-Diols by Copper/Borinic Acid Dual Catalysis." *Angew. Chem.*, **2017**, *129*, 7319-7323.; (c) Huang, H-M; Bellotti,

-
- P.; Daniliuc, C. G.; Glorius, F. "Radical Carbonyl Propargylation by Dual Catalysis." *Angew. Chem.*, **2021**, *133*, 2494-2501.
22. Peng, L.; He, Z.; Xu, X.; Guo, C. "Cooperative Ni/Cu-Catalyzed Asymmetric Propargylic Alkylation of Aldimine Esters." *Angew. Chem.*, **2020**, *132*, 14376-14380.
23. For select examples of nucleophilic propargylation: (a) Huang, G.; Yin, Z.; Zhang, X. "Construction of Optically Active Quaternary Propargyl Amines by Highly Enantioselective Zinc/BINOL-Catalyzed Alkynylation of Ketoimines." *Chem. Eur. J.*, **2013**, *19*, 11992-11998.; (b) Fandrick, D. R.; Fandrick, F. R.; Reeves, J. R.; Tan, Z.; Tang, W.; Capacci, A. G.; Rodriguez, S.; Song, J. J.; Lee, H.; Yee, N. K.; Senanayake, C. H. "Copper-Catalyzed Asymmetric Propargylation of Aldehydes." *J. Am. Chem. Soc.*, **2010**, *132*, 7600-7601.; (c) Osborne, C. A.; Endean, T. B. D.; Jarvo, E. R. "Silver-Catalyzed Enantioselective Propargylation Reactions of *N*-Sulfonylketimines." *Org. Lett.*, **2015**, *17*, 5340-5343.
24. Zhang, D-Y; Hu, X-P "Recent Advances in Copper-Catalyzed Propargylic Substitution." *Tetrahedron Lett.*, **2015**, *56*, 283-295.
25. Detz, R. J.; Delville, M. M. E.; Hiemstra, H.; van Maarseveen, J. H. "Enantioselective Copper-Catalyzed Propargylic Amination." *Angew. Chem., Int. Ed.* **2008**, *47*, 3777-3780.
26. Hattori, G.; Matsuzawa, H.; Miyake, Y.; Nishibayashi, Y. "Copper-Catalyzed Asymmetric Propargylic Substitution Reactions of Propargylic Acetates with Amines." *Angew. Chem., Int. Ed.* **2008**, *47*, 3781.
27. For select examples of Ruthenium-catalyzed propargylations: (a) Nishibayashi, Y.; Yoshikawa, M.; Inada, Y.; Hidai, M.; Uemura, S. "Ruthenium-Catalyzed Propargylation of Aromatic Compounds with Propargylic Alcohols." *J. Am. Chem. Soc.*, **2002**, *124*, 11846-11847. (b) Kondo, T.; Kanda, Y.; Baba, A.; Fukuda, K.; Nakamura, A.; Wada, K.; Morisaki, Y.; Mitsudo, T-a "Ruthenium-Catalyzed *S*-Propargylation of Thiols Enables the

-
- Rapid Synthesis of Propargylic Sulfides.” *J. Am. Chem. Soc.*, **2002**, *124*, 12960-12961.; (c) Kanao, K.; Miyake, Y.; Nishibayashi, Y. “Ruthenium-Catalyzed Enantioselective Intramolecular Propargylation of Thiophenes with Propargylic Alcohols.” *Organometallics*, **2009**, *28*, 2920-2926.
28. Zhang, C.; Wang, Y-H ; Hu, X-H; Zhen, Z.; Xu, J.; Hu, X-P “Chiral Tridentate P,N,N-Ligands for Highly Enantioselective Copper-Catalyzed Propargylic Amination with both Primary and Secondary Amines as Nucleophiles.” *Adv. Synth. Catal.*, **2012**, *354*, 2854-2858.
29. Zhu, F-L; Zou, Y.; Zhang, D-Y ; Wang, Y-H ; Hu, X-H ; Chen, S.; Xu, J.; Hu, X-P. “Enantioselective Copper-Catalyzed Decarboxylative Propargylic Alkylation of Propargyl β -Ketoesters with a Chiral Ketimine P,N,N-Ligand.” *Angew. Chem.*, **2014**, *126*, 1434-1438.
30. Ambler, B. R.; Peddi, S.; Altman, R. A. “Copper-Catalyzed Decarboxylative Trifluoromethylation of Propargyl Bromodifluoroacetates.” *Synthesis*, **2014**, *46*, 1938-1946.
31. Li, F.; Zhang, Z-Q; Lu, X.; Xiao, B.; Fu, Y. “Copper-Catalyzed Propargylation of Diborylmethane.” *Chem. Commun.*, **2017**, *53*, 3551-3554.
32. Zhan, Z.-P.; Wang, S.-P.; Cai, X.-B.; Liu, H.-J.; Yu, J.-L.; Cui, Y.-Y. “Copper(II) Triflate-Catalyzed Nucleophilic Substitution of Propargylic Acetates with Epoxysilanes. A Straightforward Synthetic Route to Polysubstituted Furans.” *Adv. Synth. Catal.*, **2007**, *349*, 2097-2102.
33. Lin, M.; Chen, Q.-Z.; Zhu, Y.; Chen, X.-L.; Cai, J.-J.; Pan, Y.-M.; Zhan, Z.-P. “Copper(II)-Catalyzed Synthesis of Pyrimidines from Propargylic Alcohols and Amidine: A Propargylation-Cyclization-Oxidation Tandem Reaction.” *Synlett*, **2011**, *8*, 1179-1183.

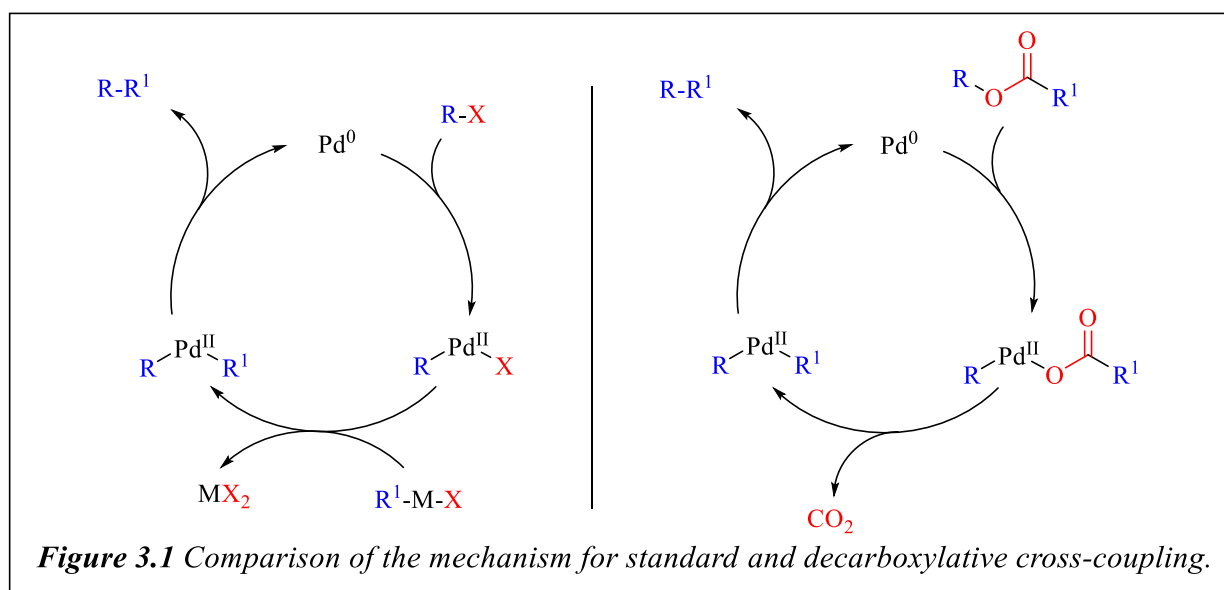
-
34. (a) Elsevier, C. J.; Kleijn, H.; Boersma, J.; Vermeer, P. "Synthesis, structure and reactivity of some (σ -allenyl)- and (σ -prop-2-ynyl)palladium(II) complexes." *Organometallics*, **1986**, *5*, 716-720. (b) Wouters, J. M. A.; Klein, R. A.; Elsevier, C. J.; Haming, L.; Stam, L. "Synthesis of trans-(σ -allenyl)platinum(II) and -palladium(II) compounds. X-ray crystal structure of trans-[PtBr{C(H):C:CM₂}(PPh₃)₂] and highly diastereoselective trans-cis isomerization of (σ -allenyl)palladium(II) bromides." *Organometallics*, **1994**, *13*, 4586-4593. (c) Canty, A. J.; Jin, H.; Penny, J. D. "Allenyl-propargyl tautomerism at Palladium(IV) and Platinum(IV) Centers." *J. Organomet. Chem.*, **1999**, *573*, 30-35.
35. (a) Ogoshi, S.; Tsutsumi, K.; Kurosawa, H. "Synthesis and Structure of Cationic η^3 -allenyl/propargylpalladium Complexes." *J. Organomet. Chem.*, **1995**, *493*, C19-C21.; (b) Tsutsumi, K.; Kawase, T.; Kakiuchi, K.; Ogoshi, S.; Okada, Y.; Kurosawa, H. "Synthesis and Characterization of Some Cationic η^3 -propargylpalladium Complexes." *Bull. Chem. Soc. Jpn.*, **1999**, *72*, 2687-2692.
36. Tsutsumi, K.; Yabukami, T.; Fujimoto, K.; Kawase, T.; Morimoto, T.; Kakiuchi, K. "Effects of a Bidentate Phosphine Ligand on Palladium-Catalyzed Nucleophilic Substitution Reactions of Propargyl and Allyl Halides with Thiol." *Organometallics*, **2003**, *22*, 2996-2999.
37. Graham, J. P.; Wojcicki, A.; Bursten, B. E. "Molecular Orbital Description of the Bonding and Reactivity of the Platinum η^3 -Propargyl Complex [η^3 -CH₂CCPh)Pt(PPh₃)₂]⁺" *Organometallics*, **1999**, *19*, 837-842.
38. Labrosse, J-R.; Lhoste, P.; Delbecq, F.; Sinou, D. "Palladium-Catalyzed Annulation of Aryl-1,2-Diols and Propargylic Carbonates. Theoretical Study of the Observed Regioselectivities." *Eur. J. Org. Chem.*, **2003**, 2813-2322.
39. (a) Kamer, P. C. J.; Van Leeuwen, P. W. N. M.; Reek, J. N. H. "Wide Bite Angle Diphosphines: Xantphos Ligands in Transition Metal Complexes and Catalysis." *Acc.*

-
- Chem. Res.*, **2001**, *34*, 895-904.; (b) Daniels, D. S. B.; Jones, A. S.; Thompson, A. L.; Paton, R. S.; Anderson, E. A. "Ligand Bite Angle-Dependent Palladium-Catalyzed Cyclization of Propargylic Carbonates to 2-Alkynyl Azacycles or Cyclic Dienamides." *Angew. Chem. Int. Ed.*, **2014**, *53*, 1915-1920.
40. Behanna, D. C.; Mohr, J. T.; Sherden, N. H.; Marinescu, S. C.; Harned, A. M.; Tani, K.; Seto, M.; Ma, S.; Novák, Z.; Krout, M. R.; McFadden, R. M.; Roizen, J. L.; Enquist, J. A.; White, D. E.; Levine, S. R.; Petrova, K. V.; Iwashita, A.; Virgil, S. C.; Stoltz, B. M. "Enantioselective Decarboxylative Alkylation Reactions: Catalyst Development, Substrate Scope, and Mechanistic Studies." *Chem. Eur. J.*, **2011**, *17*, 14199-14223.
41. (a) Mohr, J. T.; Nishimata, T.; Behenna, D. C.; Stoltz, B. M. "Catalytic Enantioselective Decarboxylative Protonation." *J. Am. Chem. Soc.*, **2006**, *128*, 11348-11349. (b) Marinescu, S. C.; Nishimata, T.; Mohr, J. T.; Stoltz, B. M. "Homogeneous Pd-Catalyzed Enantioselective Decarboxylative Protonation." *Org. Lett.*, **2008**, *10*, 1039-1042.
42. Millán, A.; Álvarez de Cienfuegos, L.; Martín-Lasanta, A.; Campaña, A. G.; Cuerva, J. M. "Titanium/Palladium-Mediated Regioselective Propargylation of Ketones using Propargylic Carbonates as Pronucleophiles." *Adv. Synth. Catal.*, **2011**, *353*, 73-78.
43. Ambrogio, I.; Cacchi, S.; Fabrizi, G.; Goggiamani, A.; Iazzetti, A. "Palladium-Catalyzed Nucleophilic Substitution of Propargylic Carbonates and Meldrum's Acid Derivatives." *Eur. J. Org. Chem.*, **2015**, 3147-3151.
44. O'Broin, C. Q.; Guiry, P. J. "Construction of All-Carbon Quaternary Stereocenters by Palladium-Catalyzed Decarboxylative Propargylation." *Org. Lett.*, **2019**, *21*, 5402-5406.

Chapter 3. Stereospecific Palladium-Catalyzed Decarboxylative Benzylation of Enolates

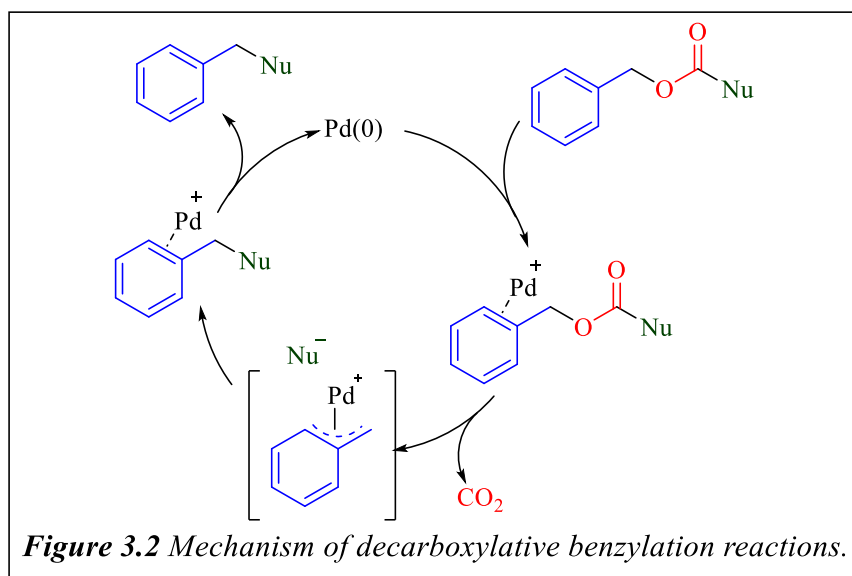
3.1 Introduction

Chapter 1 described the importance of the formation of carbon-carbon bonds due to their prevalence throughout most organic molecules. Furthermore, it went into detail describing the utility of palladium-catalyzed decarboxylative coupling reactions to form new C–C bonds.¹ In addition, chapter 1 detailed the chemical significance of benzylic moieties, as they are present in many biologically active chemicals and have potential for further reactivity. The majority of chapter 1 was a review of many current methods for the palladium-catalyzed benzylations of several different nucleophiles, including ketones, alkynes, and amines, and special focus was given towards the palladium-catalyzed decarboxylative benzylation (DcB).



A direct comparison of standard and decarboxylative coupling is shown in Figure 3.1.² In standard cross-coupling reactions, activation of both the nucleophilic and electrophilic component is required prior to the start of the reaction, which typically occurs with the use of a strong base or a preformed organometallic reagent. Therefore, standard cross-coupling reactions lead to the

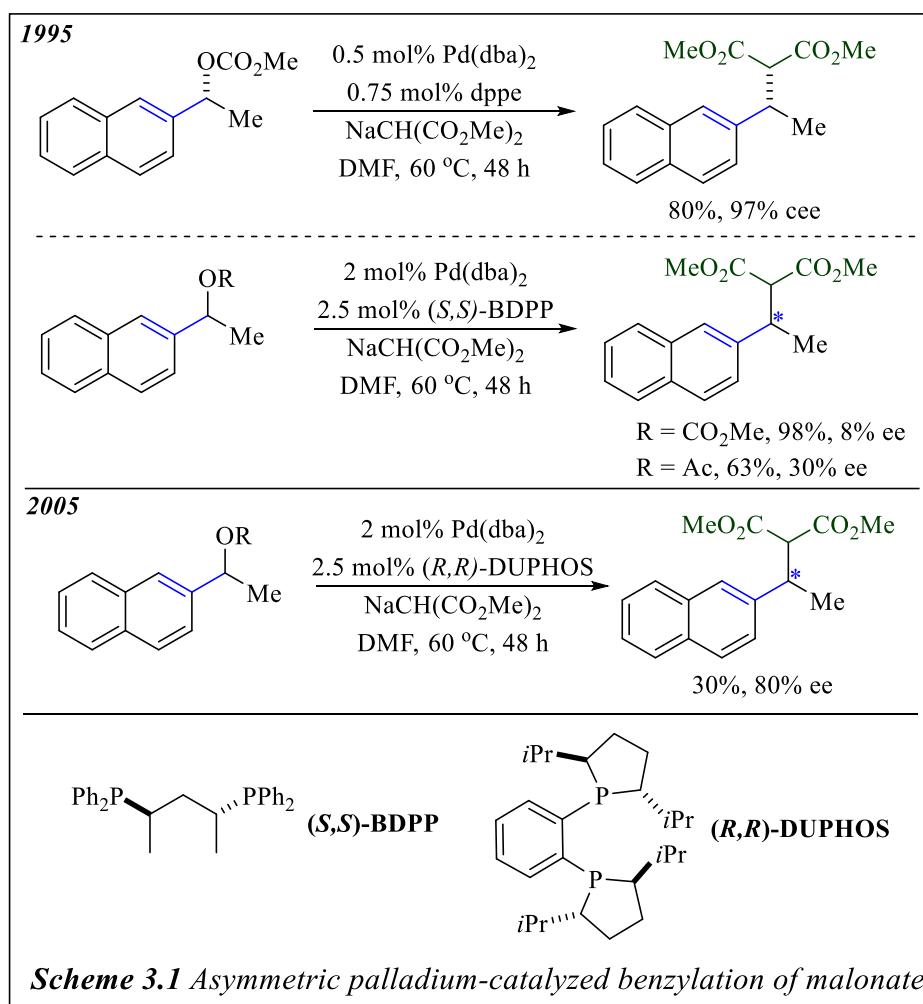
production of a stoichiometric amounts of metal waste. Comparatively, decarboxylative cross-coupling reactions pose several advantages over standard cross-coupling reactions. The starting materials can be easily synthesized from readily available reagents, and the reaction can be driven forward by irreversible decarboxylation, forming CO₂ as the only byproduct. The more specific DcB mechanism, shown in Figure 3.2,¹ leads to the formation of an η³-benzylpalladium (Bn-Pd) intermediate, which undergoes nucleophilic attack at the benzylic position.



Despite the methodologies presented in chapter 1, it was stated that, in comparison to related allylation reactions,^{3,4} the DcB is still quite limited, particularly in the realm of asymmetric catalysis. This chapter will review some previously reported methods developed for the asymmetric benzylation of several different nucleophiles. Furthermore, I will discuss research that I have worked on during my tenure in the Tunge group towards the stereospecific benzylation of enolates through the decarboxylative coupling of benzylic enol carbonates, many of which contain an indole motif present in many biologically active compounds.

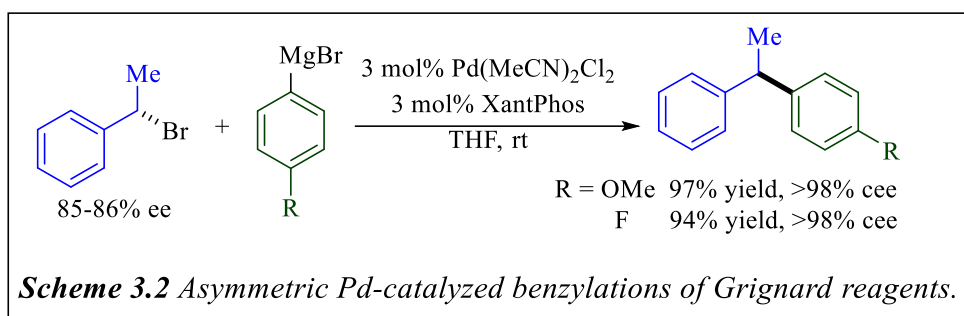
3.2 Asymmetric Benzylation Strategies

While asymmetric decarboxylative benzylation reactions are still quite limited, asymmetric benzylations using secondary benzylic halides have been reported as early as the 1970s.⁵ These reports included extensive mechanistic studies that determined that oxidative addition of palladium into a benzylic bond occurs with inversion of stereochemistry. In the early 1990s, Legros and coworkers released a couple of reports focused on the benzylation of malonate derivatives (Scheme 3.1).⁶ In 1995, they disclosed a reaction between 2-naphthyl methyl carbonate and

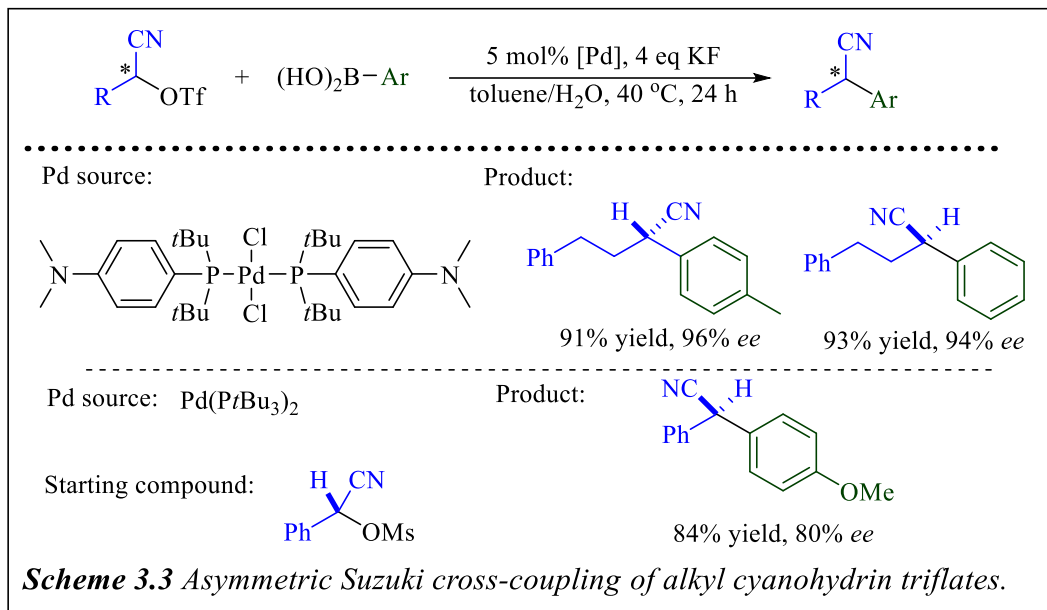


dimethylmalonate in the presence Pd(dba)_2 . They found that when they began with a chiral 2-naphthyl methyl carbonate in the presence of dppe, they were able to form the benzylated dimethyl

malonate product with a high yield and cee, or conserved enantiomeric excess. They next tried to develop an asymmetric variant beginning from an achiral carbonate in the presence of BDPP and found that the nature of the LG played a major role. With a carbonate LG, they determined that they could isolate the desired product in an extremely high yield but with a very low ee. However, when the carbonate LG was replaced with acetate, they saw a slight increase in the ee of the reaction, albeit with a sharp decrease in the overall yield. Years later, Legros and coworkers disclosed that they were able to greatly improve the enantioselectivity of the reaction using the achiral starting material through a kinetic resolution, although this necessitated a greatly decreased isolated yield.⁷

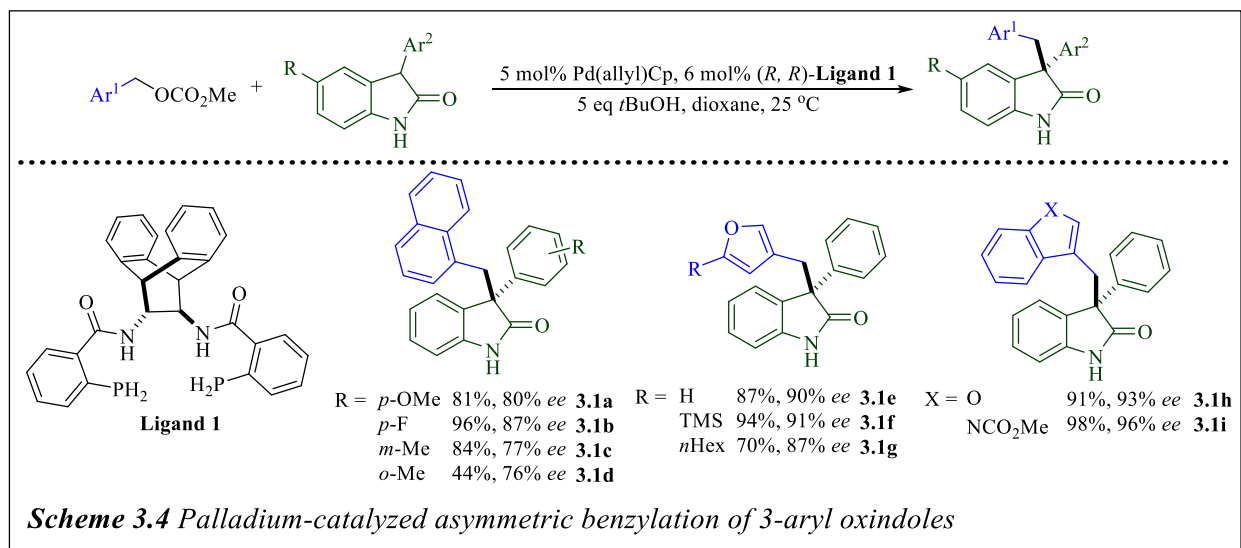


In 2009, Carretero and coworkers reported a mild, palladium catalyzed Kumada-Corriu reaction of secondary benzylic bromides with Grignard reagents in the presence of Xantphos ligand.⁸ Within this report, they examined the stereochemical course of the reaction using two chiral secondary benzylic bromides (Scheme 3.2). Under these conditions they were able to isolate the corresponding benzylated products in high yields with almost complete cee values, which agreed with many other previously reported Pd-catalyzed couplings of enantiopure secondary halides.⁹ While the sample asymmetric reactions proceeded with high yields and enantioselectivities, these were the only asymmetric reactions attempted.

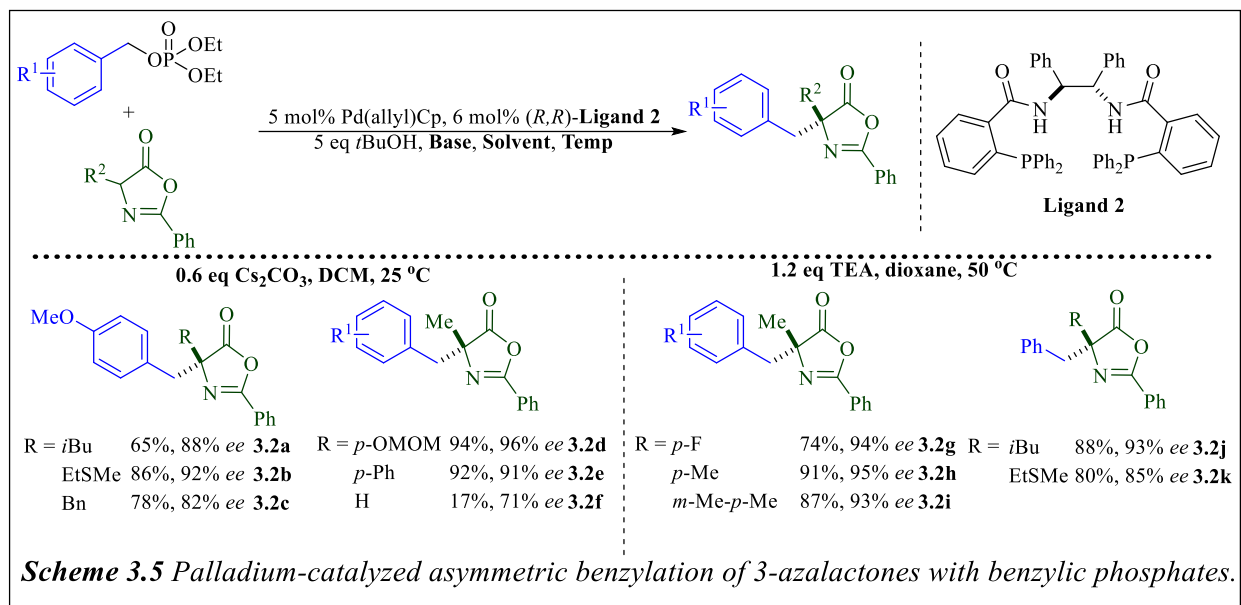


Soon after this report, Flack and He disclosed a stereospecific Suzuki cross-coupling of alkyl α -cyanohydrin triflates with aryl boronic acids (Scheme 3.3).¹⁰ They found that pairing palladium with a bulky, electron-rich ligand eliminated any undesired β -hydride elimination side-reaction and allowed for the selective formation of the cross-coupled product. Flack and He analyzed the stereochemical outcomes of this method by exposing several chiral starting compounds to the reaction conditions. Under these reaction conditions, they were able to isolate the desired benzylated products in both high yield and enantioselectivities, with inversion of stereochemistry. While most aliphatic α -cyanohydrin mesylates decomposed under the reaction conditions, when benzylic α -cyanohydrin mesylate was paired with Pd(*t*Bu₃)₂ it was able to successfully react with 4-methoxyphenylboronic acid in a high yield. While some racemization was observed, they hypothesized that this was due to the lability of the benzylic proton of the product, rather than the reaction process. It is also worth mentioning that the method calls for super-stoichiometric amounts of base, which decreases the overall utility of the reaction.

In the early 2010s, the Trost group released a series of asymmetric benzylation reports. The first of these reports, published in 2010, detailed a palladium-catalyzed asymmetric benzylation of 3-aryl oxindoles using benzylic carbonates in the presence of an anthracenyl bidentate phosphine ligand (Scheme 3.4).¹¹ Unlike the previously described reports, this was the first reported benzylation of an achiral pronucleophile, where the asymmetric induction occurred during the nucleophilic attack. They were able to successfully form the benzylated product with both EDGs (**3.1a,c**) and a fluorine group (**3.1b**) in high yields and ee's; a methyl substituent at the *ortho* position of the indole aromatic group led to a lower yield, most likely due to the steric interaction during the formation of the π -benzylic carbocation. This methodology also tolerated several different heteroaromatic moieties, including furan (**3.1e-g**), benzofuran (**3.1h**), and indole (**3.1i**). Of particular interest, the reaction did not require protection of the amide group, and there was no noticeable formation of the *N*-benzylated product.

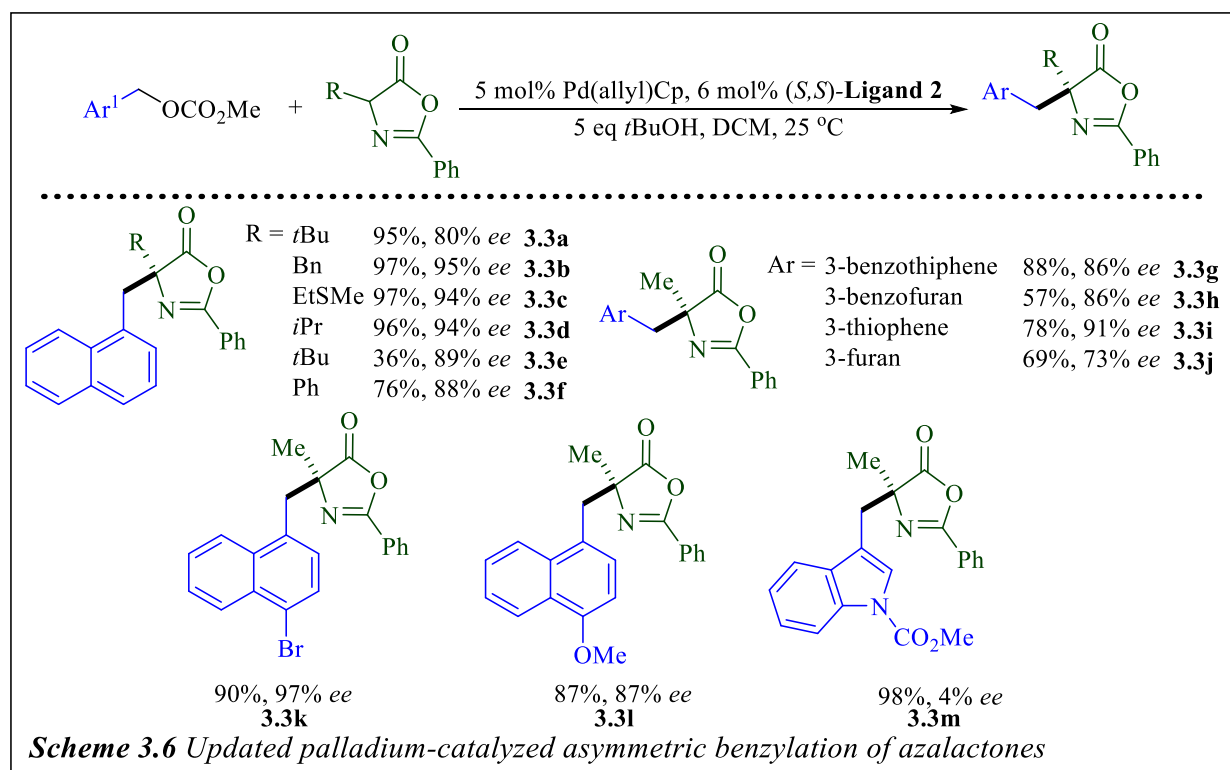


A few years after this first report, in 2012, Trost and Czabaniuk disclosed a Pd-catalyzed benzylation of azalactones using benzylic phosphates in the presence of a chiral dibenzylamino Trost-type ligand (Scheme 3.5).¹² While unreactive in their previous method, this reaction allowed

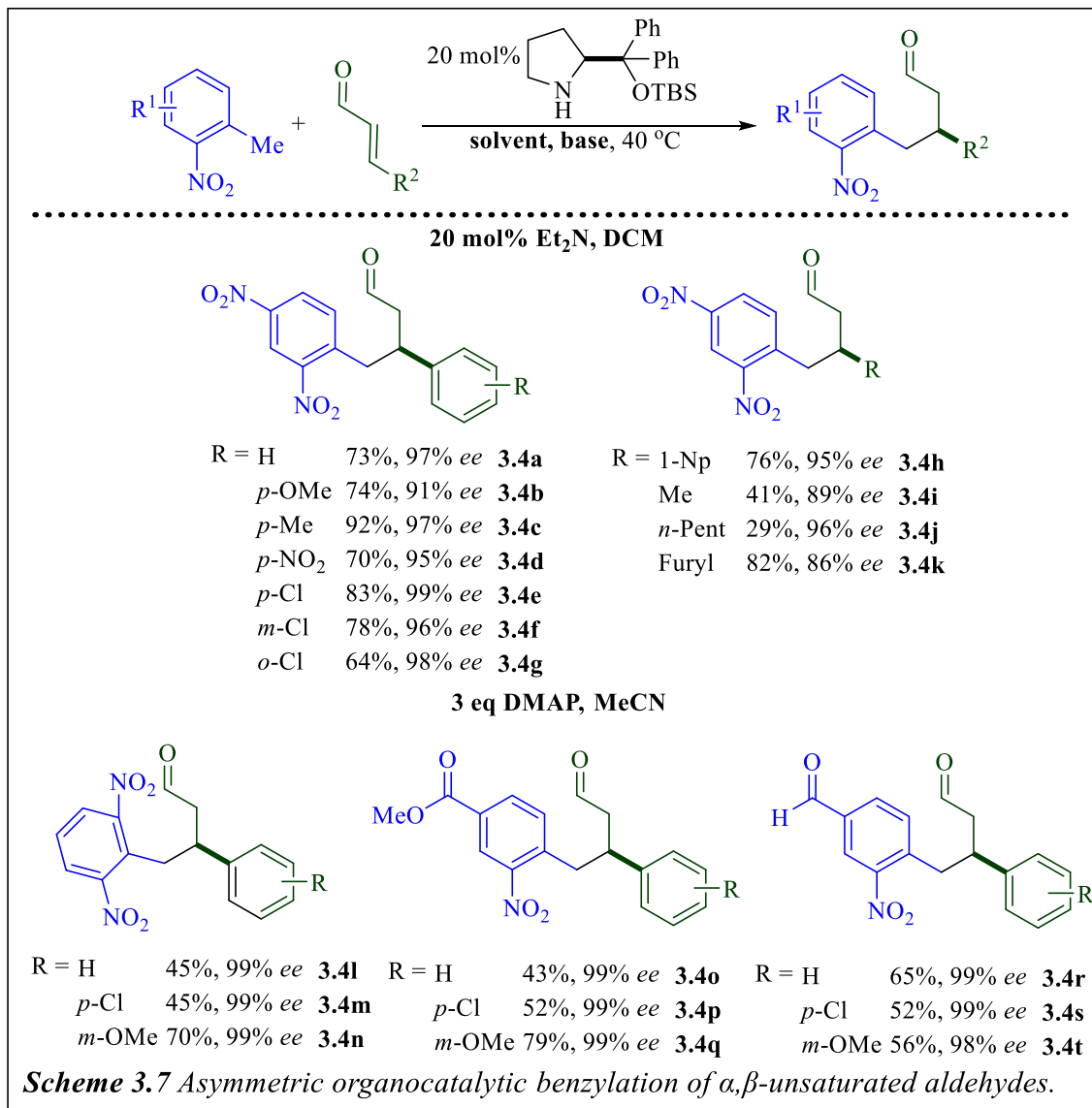


them to expand the reaction scope to include monocyclic benzylic electrophiles. This was the first reported use of monocyclic benzylic electrophiles in an asymmetric benzylation. The low reactivity of the monocyclic benzylic electrophile required the use of more labile leaving groups, causing them to switch from carbonate to phosphate. With the benzylic phosphates, the reaction required the addition of a basic additive, Cs₂CO₃, to deprotonate the nucleophile. The reaction was successful with nucleophiles derived from leucine (**3.2a**), methionine (**3.2b**), and phenylalanine (**3.2c**), forming the corresponding benzylated products in moderate yields with high enantioselectivities. The reaction was also successful with MOM-protected phenol (**3.2d**) and *p*-phenyl (**3.2e**) benzylic electrophiles, leading to the coupled products in both high yields and enantioselectivities. Interestingly, sulfide substituents were well tolerated, providing the benzylated products with both high yields and enantioselectivities (**3.2b,k**). However, an electron-poor unsubstituted benzylic phosphate (**3.2f**) only reacted to give a very low yield, albeit with a moderate enantioselectivity. There were able to expand the scope to some electron-deficient benzylic phosphates by switching the basic additive from Cs₂CO₃ to triethylamine (TEA) (**3.2g-k**).

A year later in 2013 they released another report on the asymmetric benzylation of azlactones, which included an expansion of their previous work to include benzylic carbonates (Scheme 3.6).¹³ Using benzylic carbonates with extended conjugation, they were able to form benzylated azlactones with a range of substituents at the α -position of the lactone, including alkyl (**3.3a-b,d-e**), sulfide (**3.3c**), and phenyl (**3.3f**), and on the benzylic electrophile (**3.3k-l**). The reaction was also tolerant of several different heteroaromatic moieties, forming the benzylated product in mild to high yields and moderate to high enantioselectivities. In addition, the electronic nature of the electrophile played a big role in the enantioselectivity of the reaction, as shown in the almost complete loss of enantioselectivity with the indole-derivative (**3.3m**).

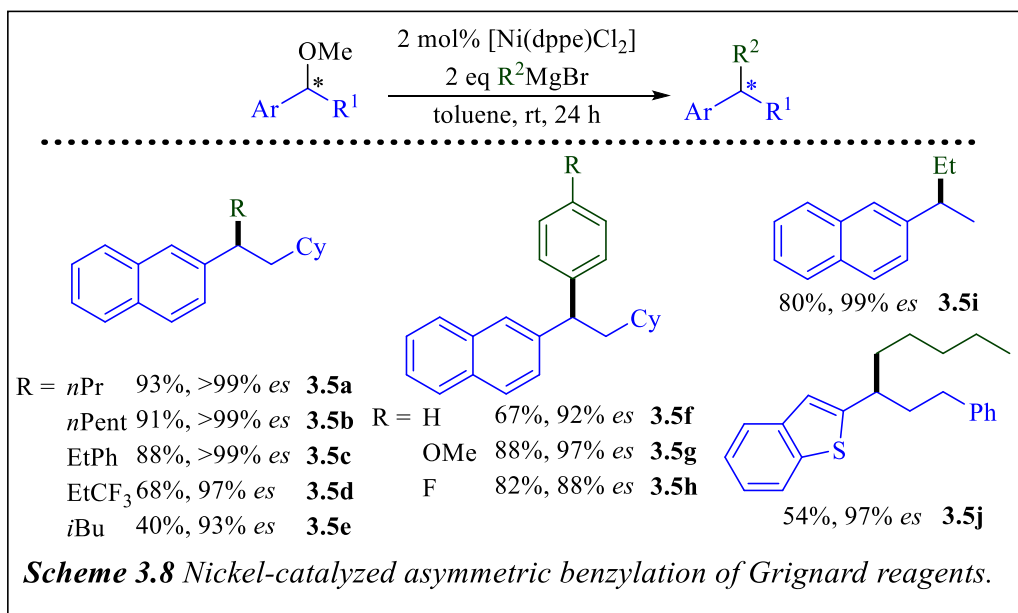
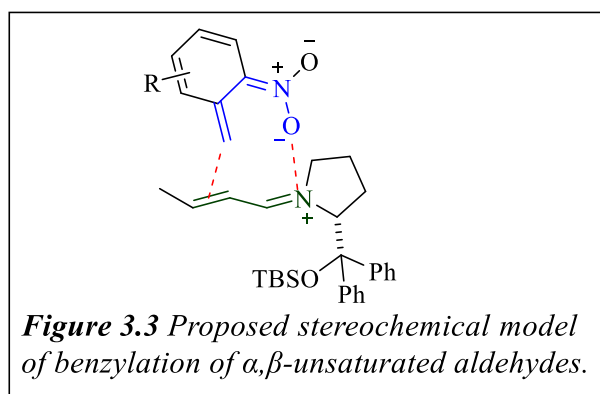


That same year, Jørgensen and coworkers disclosed an enantioselective benzylic addition of toluene derivatives to α,β -unsaturated aldehydes under mild conditions (Scheme 3.7).¹⁴ Using an organocatalyst in the presence of Et₃N, they successfully coupled 2,4-dinitrotoluene with a range



of cinnamaldehyde derivatives with various substituents on the aromatic ring, including EDGs (**3.4a-c**) and EDGs (**3.4d-g**) in moderate to high yields and very high enantioselectivities. A chlorine substituent was tolerated at the *para*, *meta*, and *ortho* positions, albeit with a slight decrease in yield when substituted at the *ortho* position. The α,β -unsaturated aldehyde could also be substituted with a naphthyl (**3.4h**), furyl (**3.4k**) or alkyl (**3.4i-j**) group. Less reactive toluene derivatives required a switch from 20 mol% of Et₃N to 3 equivalents of DMAP. This allowed for them to couple α,β -unsaturated aldehydes with 2,6-nitrotoluene derivatives (**3.4l-n**) and *p*-

carboxaldehyde substituted 2-nitrotoluene derivatives (**3.4o-t**). The authors proposed that the source of chirality stems from a synergistic effect of the organocatalyst and the organic base, shown in Figure 3.3. The positive charge of the *in situ* formed iminium ion would coordinate with the *o*-nitro substituent of the toluene derivative, which would create an electron-sink, facilitating deprotonation of the toluene by the organic base. This interaction would position the toluene derivatives in a manner to direct the attack, allowing for the observed high enantioselectivity.



In 2014, Jarvo and coworkers published a report detailing a stereospecific Ni-catalyzed cross-coupling of alkyl Grignard reagents with benzylic ethers (Scheme 3.8).¹⁵ Starting from a chiral benzylic ether in the presence of 2 mol% [Ni(dppe)Cl₂] and an alkyl Grignard reagent, they were

able to synthesize a range of benzylated compounds. They found that organomagnesium bromides led to much higher enantiospecificities, than the respective chloride and iodide-containing Grignard reagents. Under these reaction conditions, they could successfully couple a range of alkyl Grignard reagents (**3.5a-e**) in moderate to high yields with very high enantiospecificities. The reaction was also tolerant of aryl Grignard reagents, including those with EDGs, (**3.5f-h**) and a benzothiophene moiety (**3.5j**).

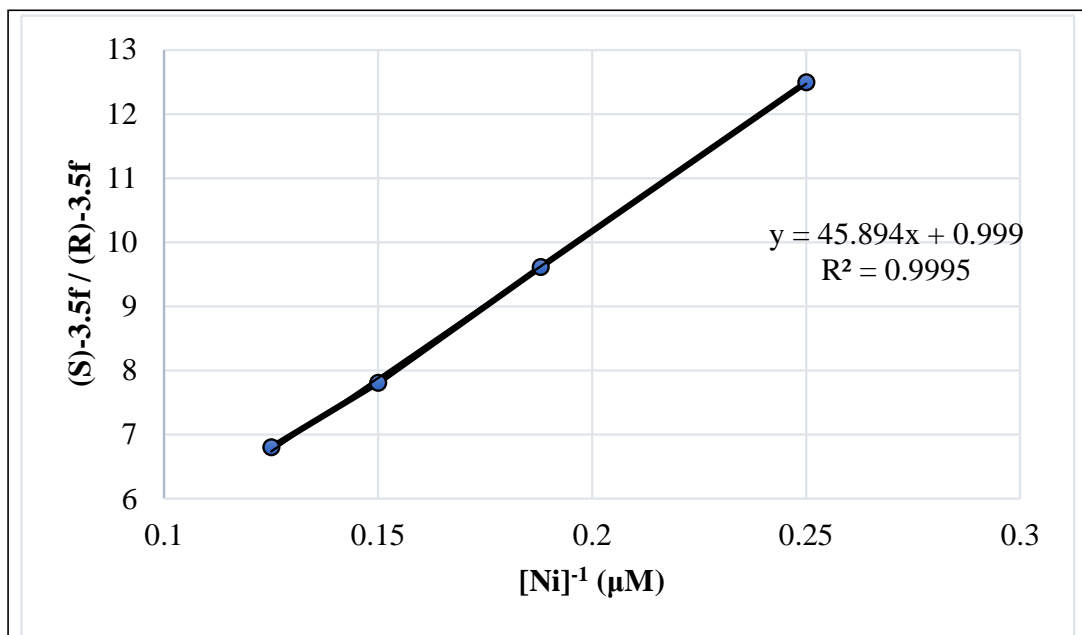
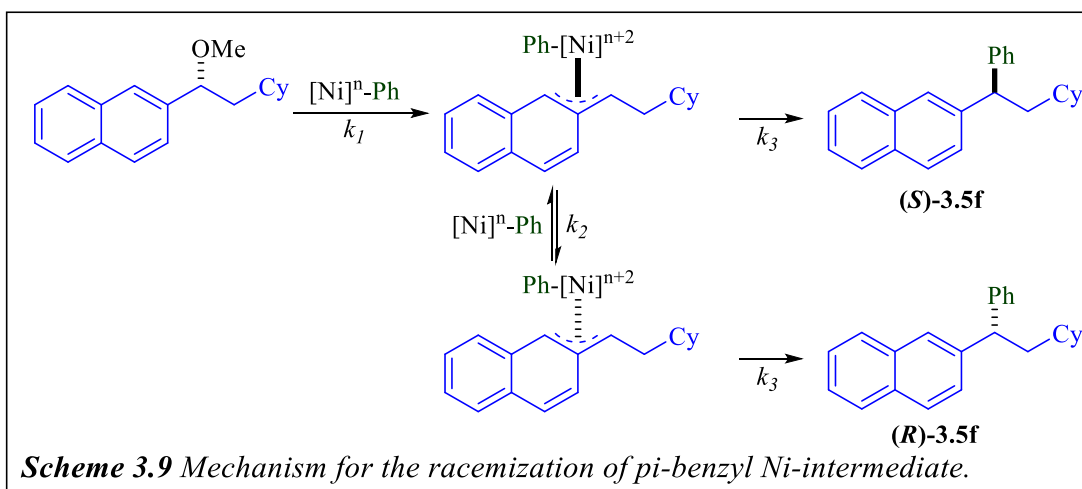
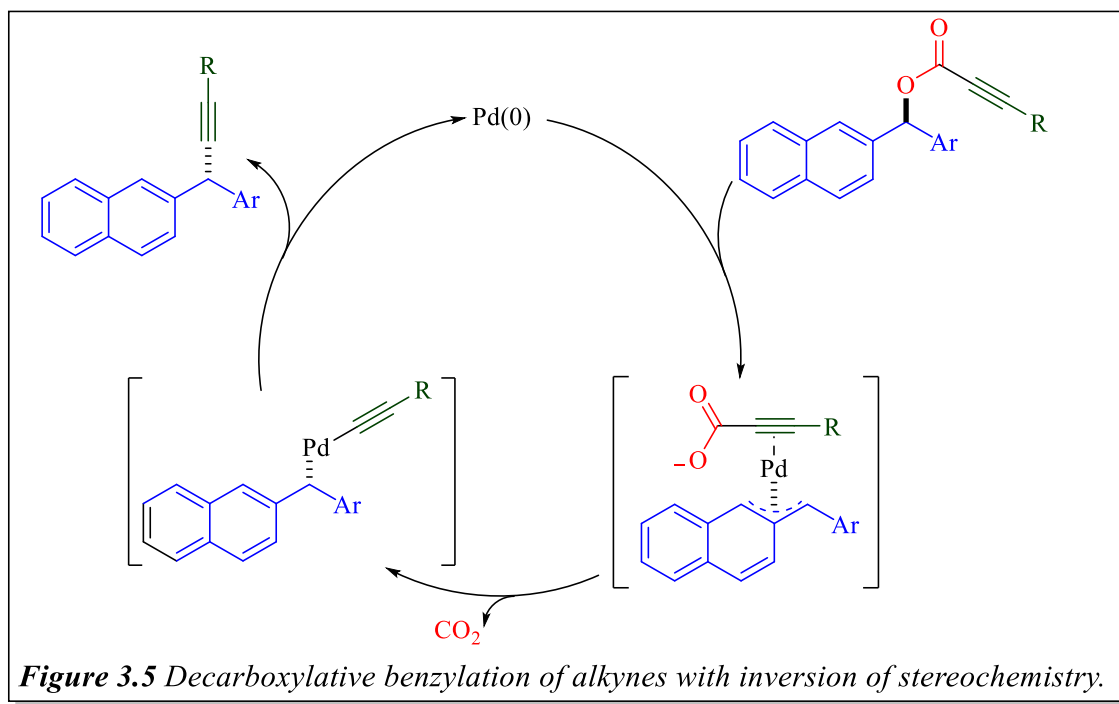
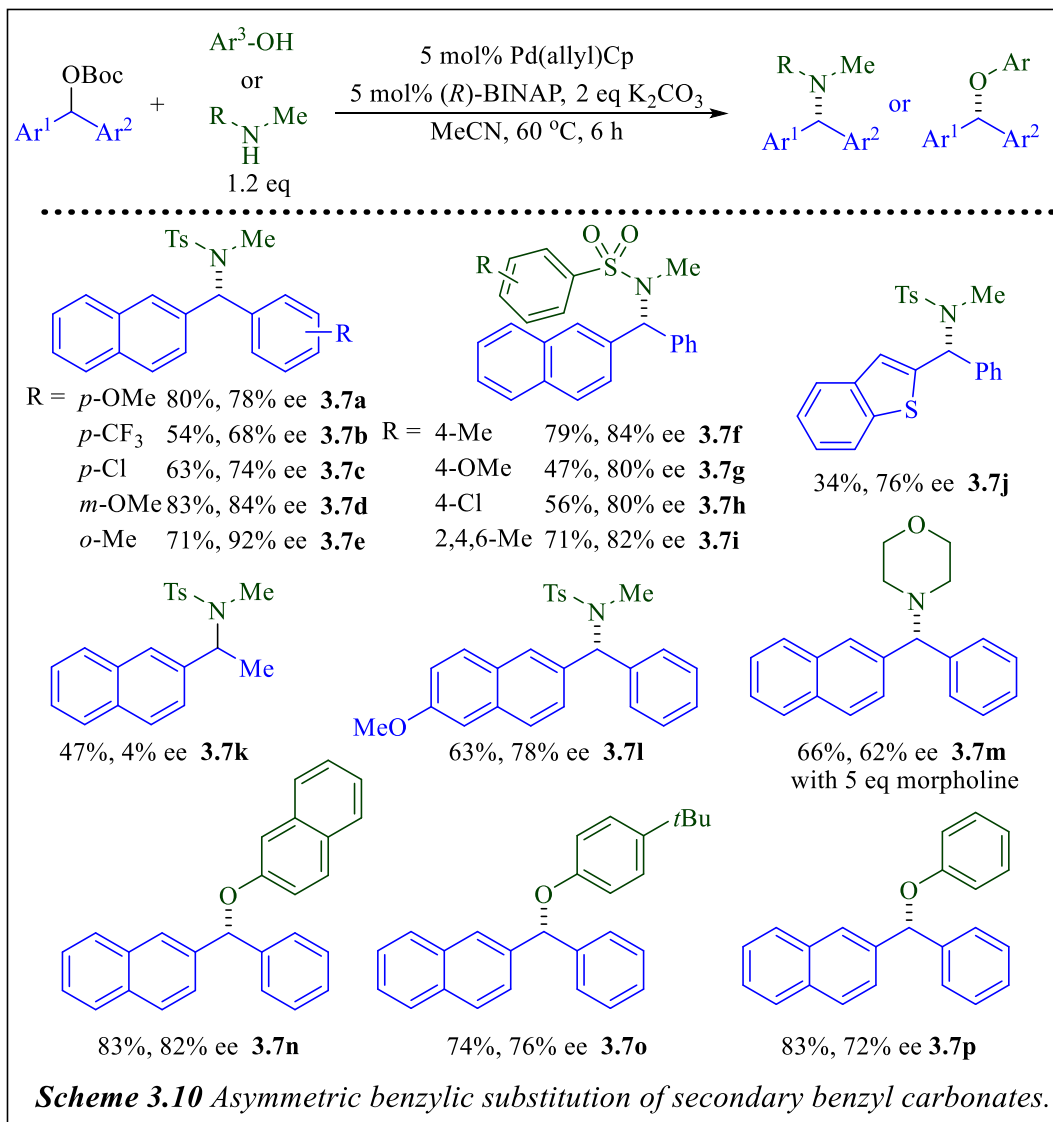


Figure 3.4 Plot of S/R enantiomeric ratio vs $[Ni]^{-1}$.
Graph reproduced from data provided in original paper SI.

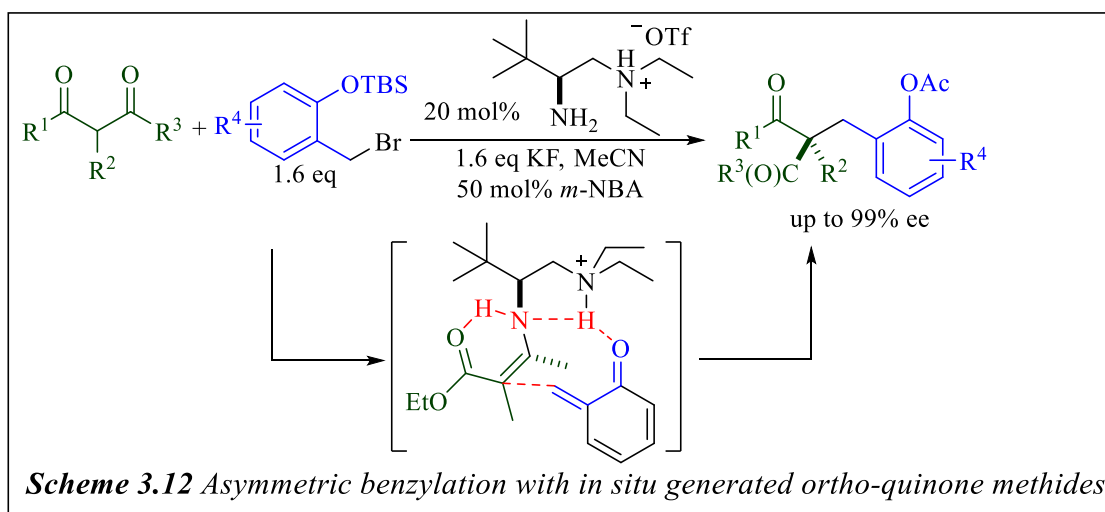
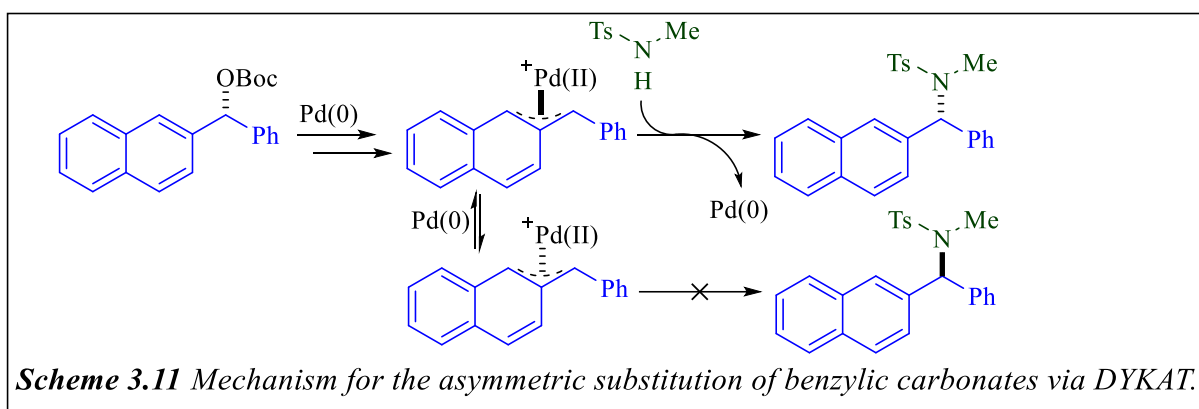
not require basic additives or preformed organometallic reagents. Starting with enantioenriched benzyl esters, they were able to form a range of chiral 1,1-diarylmethanes in mild to high yields with moderate to very high stereospecificity. This methodology was tolerant of many functionalities, including alkyl groups (**3.6a,c,e,g**), methoxy (**3.5h,l,n**), halogen (**3.6b,f**), and sulfur (**3.6d**). The reaction was also successful with other heteroaromatic groups, including a furan (**3.6j**), thiophene (**3.6i**), and Boc-protected indole (**3.6k**). It is worth mentioning that substituents on the *ortho* position of one of the aromatic rings of the benzyl ester would cause a sharp decrease in yield (**3.6l**), presumably due to steric interactions causing oxidative addition to be more disfavored. Due to an overall observed inversion of stereochemistry, it was hypothesized that the mechanism (Figure 3.5), starts with oxidative addition of palladium via an S_N2 -like reaction, which leads to inversion of stereochemistry. Decarboxylative metallation leads to the formation of a Bn-Pd-acetylide intermediate, and reductive elimination with retention of stereochemistry would immediately follow.





In 2017, Miura and coworkers reported a palladium-catalyzed asymmetric benzylation of secondary benzylic carbonates with nitrogen or oxygen nucleophiles through a dynamic kinetic asymmetric transformation (DYKAT) (Scheme 3.10).¹⁷ In the presence of Pd(allyl)Cp and (*R*)-BINAP, benzylic carbonates were successfully coupled with a range of sulfonamide nucleophiles, allowing for the formation of the benzylated products in moderate to high yields and moderate enantioselectivities. The reaction was tolerant towards benzylic carbonates that contained both EDGs (**3.7a,d-e**), EWGs (**3.7b-c**), and benzothiophene (**3.7j**). The reaction conditions also allowed

for the coupling of benzylic carbonates with morpholine (**3.7m**) and several phenol derivatives (**3.7n-p**). Their proposed mechanism (Scheme 3.11) starts with an S_N2 -substitution of the racemic benzylic carbonate with palladium, which would occur with inversion of the stereochemistry. This would be quickly followed by decarboxylation to two diastereomeric π -benzylic intermediates, which would interconvert through an invertive displacement of Pd(0) by S_N2 attack by a second Pd catalyst. Nucleophilic attack on one of these intermediates would occur much faster than attack on the other intermediate, allowing for the DYKAT of a racemic starting material to a single major enantiomer.

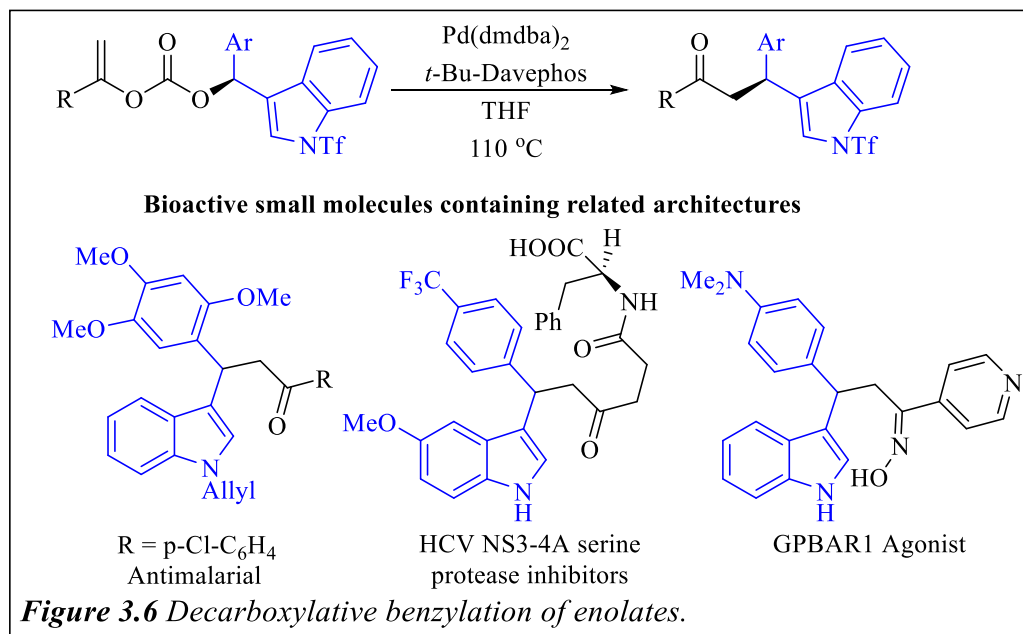


In 2017, Luo and coworkers published the utilization of a dual activation strategy of primary amine catalysis and Lewis base activation to allow for the asymmetric α -benzylation of dicarbonyl

compounds that proceeds via *in-situ* generation of *ortho*-quinone methides (Scheme 3.12).¹⁸ They hypothesized that their observed stereoselectivity occurs through the transition state shown in Scheme 3.12. Hydrogen bonding between the tertiary amine and carbonyl of the *ortho*-quinone methide would hold the two substrates in a specific conformation to allow for a selective *Re*-face attack of the *Z*-enamine, accounting for both the high reactivity and stereoselectivity.

3.3 Development of Stereospecific Decarboxylative Benzylation of Enolates

Despite the methods described in the previous section, benzylation reactions that lead to the formation of enantioenriched products have not been fully developed, especially regarding asymmetric decarboxylative benzylation. Therefore, we hoped to expand these decarboxylative benzylic couplings to allow for the coupling of secondary benzyl esters with enolate nucleophiles, focusing on indole-based diarylmethyl electrophiles, allowing for the formation of chiral tertiary diarylmethanes, which are very common biologically active molecules (Figure 3.6).¹⁹ While there has been some progress made with Ni-catalyzed benzylations with secondary benzylic



electrophiles, including the 2014 example from Jarvo and coworkers described in the previous section,¹⁵ these methods require stoichiometric organometallic reagents.²⁰

Due primarily to the synthetic utility of the indole motif, we began our optimization studies by reacting a secondary 3-indolylcarbinol-derived enol carbonate **3.11a** as the model substrate to determine the optimal conditions for this decarboxylative coupling to occur (Table 3.1). Despite being successful in our previous work with primary benzyl electrophiles, Pd(PPh₃)₄ was not able to effectively catalyze the reaction with secondary benzylic carbonates (entry 1). We next paired Pd₂dba₃CHCl₃ with several different ligands that are common in Pd-catalyzed benzylic coupling reactions (entries 2-4). While P(furyl)₃, dppe, and Xantphos failed to produce the desired product, MePhos, a bulky, monodentate Buchwald ligand,²¹ allowed for the formation of the benzylated product, albeit in only a modest yield (entry 5). Changing the solvent from toluene to dimethyl ether (DME) increased the yield from 47 to 55% (entry 7). We next examined other classes of Buchwald ligands (entries 8-9), finding that XPhos improved the yield slightly and DavePhos increased the yield a further 13% (entry 9, 73%). This yield was further improved when the palladium source was switched to Pd(dmdba)₂ precatalyst (entry 11). Switching the solvent to THF and diluting from 0.1 M to 0.04 M led to slightly better yields and cleaner reactions (entries 12-13). Finally, we increased the steric hinderance of the ligand by switching to the *t*Bu-DavePhos ligand, which furnished the desired benzylated product **3.12a** in the optimal yield (entry 14, 86%).

After establishing the optimal reaction conditions, we sought to test the generality of this method by evaluating the scope of both the electrophilic diarylmethanes and nucleophilic enolate partners (Scheme 3.15). We first tested this reaction using a series of indole-derived diarylmethyl electrophiles and found that many substituted secondary 3-indolylcarbinols were well tolerated as coupling partners. The electronics of the substituents on the aromatic system had a slight impact

Reaction scheme: 3.11a (enol carbonate) $\xrightarrow[\text{solvent}]{\text{Pd source, ligand, 110 }^\circ\text{C}}$ 3.12a (ketone)

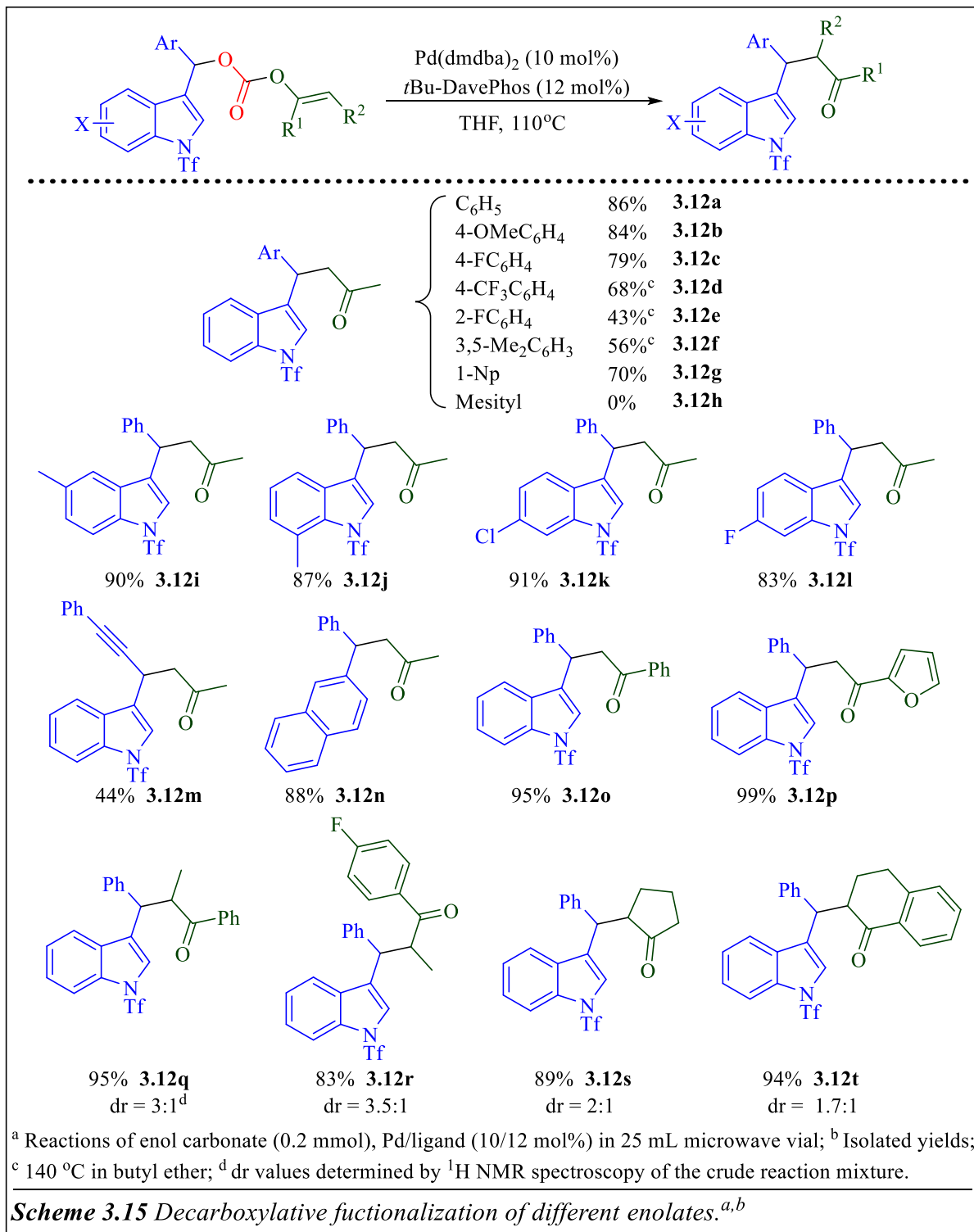
entry	Pd source	ligand	solvent	conc. (M)	yield (%) ^b
1	Pd(PPh ₃) ₄	none	toluene	0.1	trace
2	Pd ₂ dba ₃ CHCl ₃	P(furyl) ₃	toluene	0.1	trace
3	Pd ₂ dba ₃ CHCl ₃	dppe	toluene	0.1	N.R.
4	Pd ₂ dba ₃ CHCl ₃	Xantphos	toluene	0.1	trace
5	Pd ₂ dba ₃ CHCl ₃	MePhos	toluene	0.1	47
6	Pd ₂ dba ₃ CHCl ₃	MePhos	Dioxane	0.1	32
7	Pd ₂ dba ₃ CHCl ₃	MePhos	DME	0.1	55
8	Pd ₂ dba ₃ CHCl ₃	XPhos	DME	0.1	60
9	Pd ₂ dba ₃ CHCl ₃	DavePhos	DME	0.1	73
10	Pd(dba) ₂	DavePhos	DME	0.1	66
11	Pd(dmdba) ₂ ^c	DavePhos	DME	0.1	74
12	Pd(dmdba) ₂	DavePhos	THF	0.1	75
13	Pd(dmdba) ₂	DavePhos	THF	0.04	76
14	Pd(dmdba)₂	<i>t</i>Bu-DavePhos	THF	0.04	86 (86)

XPhos
MePhos
DavePhos
***t*-BuDavePhos**

^aReactions of enol carbonate (0.1 mmol), Pd/ligand (10/12 mol%), 24-48 h.
^bNMR yield (isolated yield in parentheses).
^cdmdba = 3,5,3',5'-(dimethoxydibenzylidene)acetone.

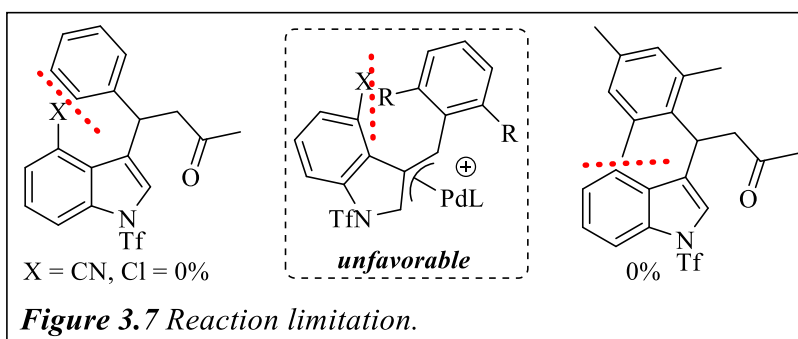
Table 3.1 Optimization of reaction conditions.^{a,b}

on the reaction yields. There was a slight increase in the reaction yield with an electron-donating *p*-methoxy substituent (**3.12b**), when compared to similarly *para*-substituted EWGs, including a F (**3.12c**) and CF₃ (**3.12d**). This increase in reaction yield is most likely due to the electron-donating methoxy group stabilizing the intermediate π -Bn-Pd complex, which would enable to

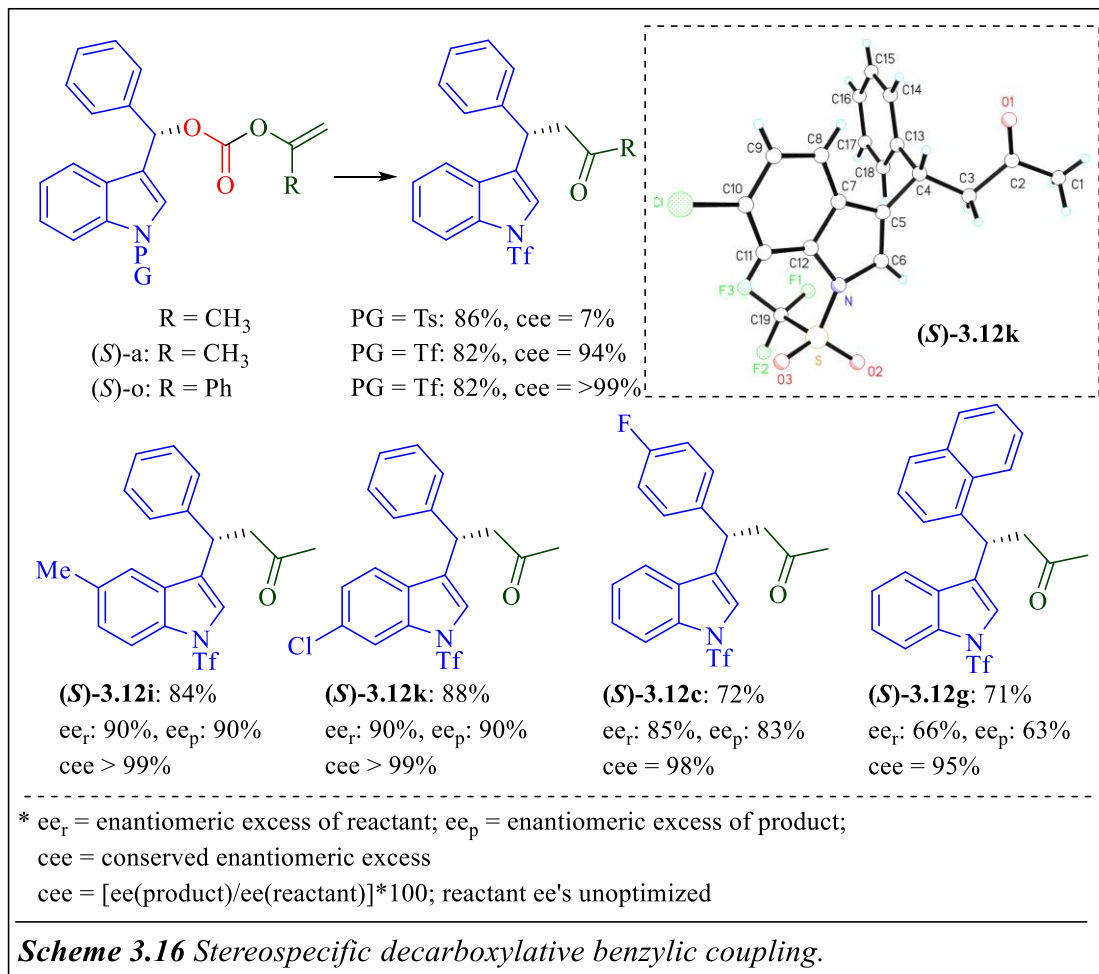


more facile oxidative addition of palladium. While the electronics of the substituents of the aromatic ring had a slight impact the yield, sterics played a much larger role in the reaction, as *o*-

F (**3.12e**) and dimethyl (**3.12f**) substrates gave low yields and a mesityl substrate (**3.12h**) failed to react entirely. Furthermore, any substitution at the 4-position of the indole completely shut down the reaction. We hypothesized that these substrates failed because oxidative addition was prevented due to steric destabilization of the intermediate π -Bn-Pd complex, which is illustrated in Figure 3.7. Substitution at the 5- and 6-position of the indole with methyl groups (**3.12i-j**) and the 6- and 7-positions with halogens (**3.12k-l**) were well tolerated. Lastly, we observed that this coupling did not require both the indole and phenyl moieties, as replacing the phenyl group with an alkynyl group (**3.12m**) and the indole motif with a naphthyl group (**3.12n**) both produced the corresponding benzylated ketones. However, the switch from a phenyl to an alkynyl moiety did lead to a rather sharp decrease in the yield of the reaction to 44%.

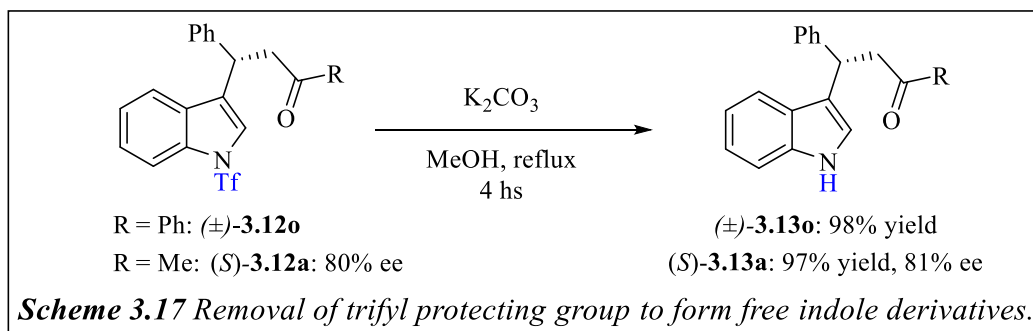
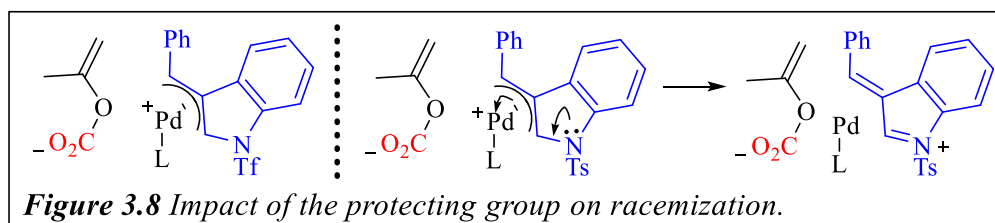


We next found that several enol carbonates derived from a variety of ketones were able to successfully form the α -functionalized ketones in good to excellent yields. The enol carbonate derived from acetophenone provided the benzylated ketone (**3.12o**) in a higher yield than the acetone-derived enol carbonate. Likewise, several other enol carbonates containing aromatic enolates underwent successful decarboxylation to form the benzylated ketones in good to high yields (**3.12p-r,t**). In addition, secondary enolates were also suitable to the reaction conditions, providing the corresponding products in good yields, albeit with low diastereoselectivities (**3.12q-t**).



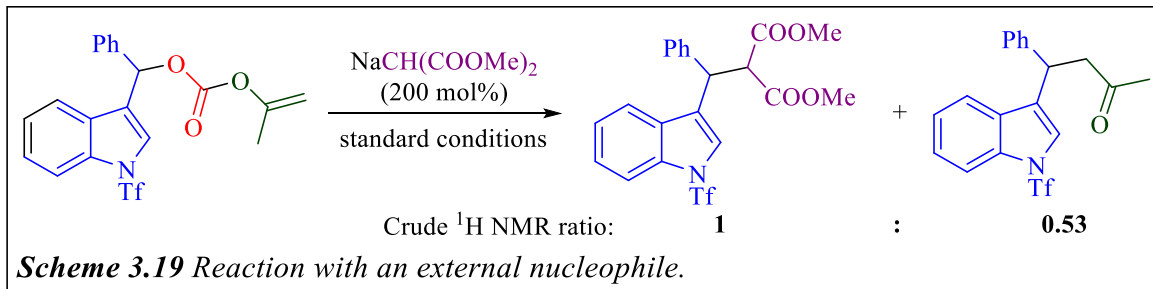
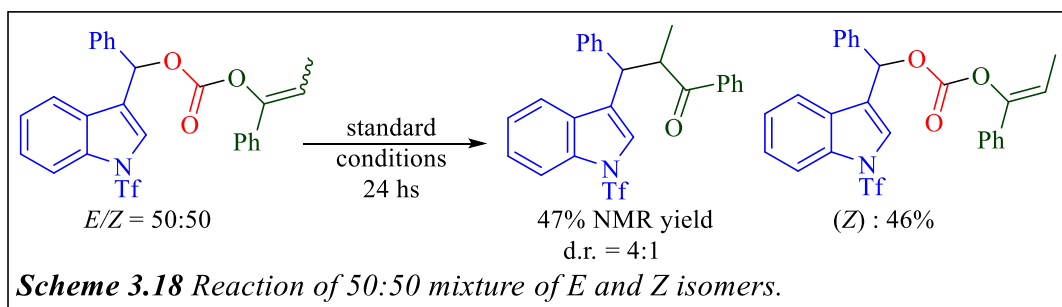
Due to the electron-donating effects of nitrogen, indole-based electrophiles form relatively stable carbocations and, therefore, easily undergo racemization.²² Therefore, we found that the nature of the *N*-protecting was crucial for the enantiospecificity of the decarboxylative coupling (Scheme. 3.16). An enantioenriched enol carbonate with a tosyl protecting group on the indole amide, produced the benzylated ketone with only 7% enantiospecificity. However, when the tosyl protecting group was replaced with the triflate protecting group, the reaction was able to proceed with very high stereospecificity (94%). We tested the enantiospecificity of this reaction on several other enantioenriched enol carbonates with variations on the enolate, indole, or aryl moieties and found that all successfully formed the benzylated ketone products in good yields with high enantiospecificity. We hypothesized that this observed stereochemical fidelity was due to the

triflate protecting group destabilizes the intermediate π -Bn-Pd complex enough to prevent the formation of a free carbocation, thus preventing racemization of the enantioenriched substrates (Figure 3.8). Furthermore, the triflate protecting group undergoes facile deprotection, allowing for the straightforward formation of enantioenriched free indoles using mild conditions (Scheme 3.17). Finally, X-ray crystallography of the product determined that the reaction proceeded with overall retention of stereochemistry.²³ As oxidative addition typically occurs with inversion of stereochemistry; this indicates that the key bond forming step of the reaction is occurring with inversion of configuration.²⁴



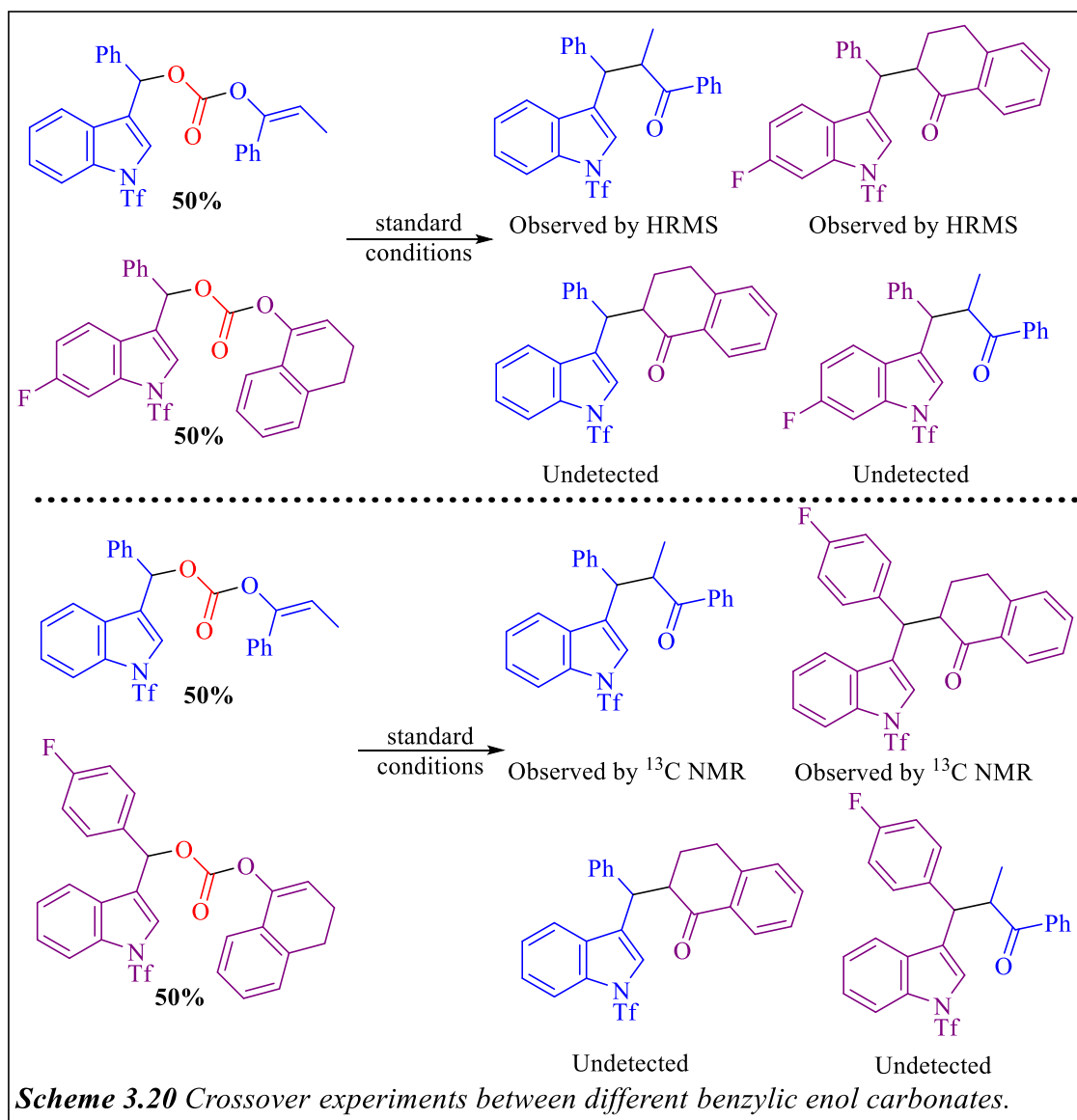
When examining the mechanism of this reaction, we found that, when using a secondary enolate, the geometry of the enolate was critical. Interestingly, when a mixture of *E/Z* isomers of enol carbonate was reacted, the *Z* isomer was completely unreactive to the reaction conditions, and only the *E* isomer produced the desired benzylated ketone (Scheme 3.18). We next probed the mechanistic details of the transformation by running the reaction in the presence of an external malonate nucleophile to test the reactivity of both the π -Bn-Pd complex and *in-situ* generated enolate nucleophile (3.19). When the standard reaction proceeded in the presence of 2 equivalents

of sodium dimethyl malonate, a 2:1 mixture of the malonate substitution and decarboxylative coupling product was produced. This observation agrees with previous reports of catalytic benzylic coupling that suggest that oxidative addition is the rate-limiting step. In addition, despite being the minor product, the reaction with the acetone enolate must be extremely facile because its concentration in solution is much smaller than the malonate nucleophile, as it is only generated *in situ* through oxidative addition with palladium and subsequent decarboxylation, while the malonate nucleophile is performed.



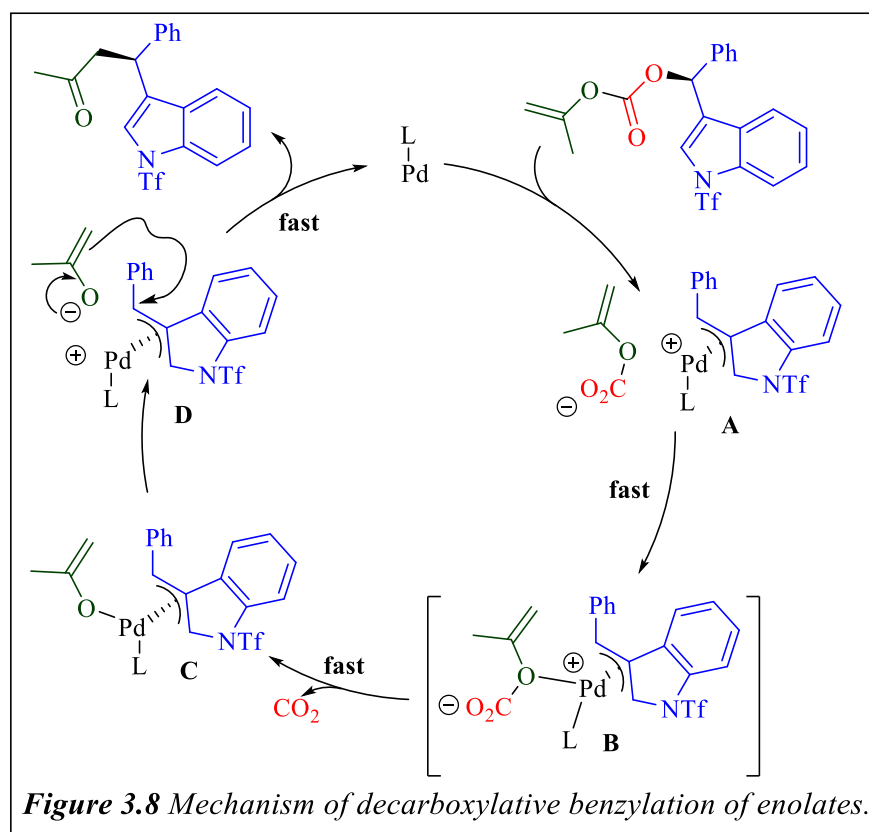
To further investigate the mechanistic details of this reaction, we performed a series of crossover experiments between 50:50 mixtures of equally reactive enol carbonates (Scheme 3.20). These crossover experiments provided key mechanistic information for our transformation. When subjected to our reaction conditions, each 50:50 mixture of two enol carbonates only produced the direct coupling product with no formation of the crossover product detected by either mass spectrometry or NMR spectroscopy. Most decarboxylative cross-coupling reactions lead to extensive formation of crossover products.²⁵ The lack of crossover product formation indicates

that enolate dissociation occurs through short-lived, solvent-caged ion pairs. These ion pairs would then undergo C–C bond formation much faster than diffusion from the solvent cage.



The observed mechanistic data allowed us to produce the following mechanism of decarboxylative benzylation of enolates (Figure 3.8). The reaction proceeds through ionization of the benzylic enol carbonate with inversion of stereochemistry, forming intermediate A. The triflate protecting group destabilizes this intermediate enough to prevent the formation of the free carbocation, which stops racemization from occurring. Coordination and decarboxylation of the

enol carbonate would immediately follow. As steric interference would prohibit coordination of the (*Z*)-enol, this would explain why only the (*E*)-isomer is reactive in our method. The palladium enolate (**C**) could then ionize, forming a solvent-caged ion pair that would quickly collapse via an outer-sphere attack, causing the second inversion of configuration and overall observed retention.



3.4 Conclusion

In conclusion, we developed the first stereospecific decarboxylative benzylation of enolates by utilizing catalytic decarboxylative coupling of secondary benzylic enol carbonates. We observed that choice of protecting group had a profound impact on the overall stereoselectivity of the reaction, with a triflate protecting group allowing for the formation of enantioenriched benzylated ketones that contain biologically useful indole derivatives. In addition, although we found that this reaction proceeds through a fairly standard benzylation mechanism, there was no crossover

product observed, which is highly unusual in these types of reactions. Thus, this protocol allows for the generation of a wide variety of β -diaryl ketones in an efficient and highly stereospecific manner.

3.5 References for Chapter 3

-
1. (a) Rodriguez, N.; Goosen, L. J. "Decarboxylative Coupling Reactions: A Modern Strategy for C-C Bond Formation." *Chem. Soc. Rev.* **2011**, *40*, 5030-5048. (b) Park, J.; Park, E.; Kim, A.; Park, S-A; Lee, Y.; Chi, K-W; Jung, Y. H.; Kim, I. S. "Pd-Catalyzed Decarboxylative Coupling of Propiolic Acids: One-Pot Synthesis of 1,4-Disubstituted 1,3-Diynes via Sonogashira-Homocoupling Sequence." *Sci. China: Chem.* **2011**, *54*, 1670-1687. (c) Dzik, W. I.; Lange, P. P.; Gooßen, L. J. *Chem. Sci.* **2012**, *3*, 2671-2678.
 2. Weaver, J. D.; Recio (III), A.; Grenning, A. J.; Tunge, J. A. "Transition Metal-Catalyzed Decarboxylative Allylation and Benzylation Reactions." *Chem. Rev.*, **2011**, *111*, 1846-1913.
 3. For select examples of decarboxylative allylations: (a) He, H.; Zhang, X-J; Li, Y.; Dai, L-X; You, S-L. "Ir-Catalyzed Regio- and Enantioselective Decarboxylative Allylic Alkylations." *Org. Lett.*, **2007**, *9*, 4339-4341. (b) Weaver, J. D.; Tunge, J. A. "Decarboxylative Allylation using Sulfones as Surrogates of Alkanes." *Org. Lett.*, **2008**, *10*, 4657-4660. (c) Recio (III), A.; Tunge, J. A. "Regiospecific Decarboxylative Allylation of Nitriles." *Org. Lett.* **2009**, *11*, 5630-5633. (d) Grenning, A. J.; Tunge, J. A. "Rapid Decarboxylative Allylation of Nitroalkanes." *Org. Lett.* **2010**, *12*, 740-742. (e) Lang, S. B.; O'Nele, K. M.; Tunge, J. A. "Decarboxylative Allylation of Amino Alkanoic Acids and Esters via Dual Catalysis." *J. Am. Chem. Soc.* **2014**, *136*, 13606-13609.
 4. For select examples of asymmetric decarboxylative allylation: (a) Behenna, D. C.; Stoltz, B. M. "The Enantioselective Tsuji Allylation." *J. Am. Chem. Soc.* **2004**, *126*, 15044-

-
15045. (b) Burger, E. C.; Tunge, J. A. "Ruthenium-catalyzed Stereospecific Decarboxylative Allylation of Non-stabilized Ketone Enolates." *Chem. Commun.* **2005**, 2835-2837. (c) Chattopadhyay, K.; Jana, R.; Day, V. W.; Douglas, J. T.; Tunge, J. A. "Mechanistic Origin of the Stereodivergence in Decarboxylative Allylation." *Org. Lett.* **2010**, *12*, 3042-3045. (d) Weaver, J. D.; Ka, B. J.; Morris, D. K.; Thompson, W.; Tunge, J. A. "Stereospecific Decarboxylative Allylation of Sulfones." *J. Am. Chem. Soc.* **2010**, *132*, 12179-12181. (e) Grenning, A. J.; Van Allen, C. K.; Maji, T.; Lang, S. B.; Tunge, J. A. "Development of Asymmetric Decarboxylative Allylation." *J. Org. Chem.* **2013**, *78*, 7281-7287.
5. (a) Wong, K. P.; Lau, K. S. Y.; Stille, J. K. "Stereochemistry of Oxidative Addition of Benzyl- α - δ Chloride to Tetrakis(triphenylphosphine)palladium(0). Direct Evidence for Configurational Inversion at Carbon via a Nonradical Mechanism." *J. Am. Chem. Soc.* **1974**, *96*, 5956-5957. (b) Lau, K. S. Y.; Wong, K. P.; Stille, J. P. "Oxidative Addition of Benzyl Halides to Zero-Valent Palladium Complexes. Inversion of Configuration at Carbon." *J. Am. Chem. Soc.* **1976**, *98*, 5832-5840. (c) Becker, Y.; Stille, J. K. "The Dynamic η^1 - and η^3 -Benzylbis(triethylphosphine)palladium(II) cations. Mechanisms of Interconversion." *J. Am. Chem. Soc.*, **1978**, *100*, 845-850. (d) Becker, Y.; Stille, J. K. "Stereochemistry of Oxidative Addition of Benzyl- α - δ Chloride and Bromide to tris(triethylphosphine)palladium(0). Direct Observation of Optical Activity in a Carbon-Palladium σ -bonded Complex." *J. Am. Chem. Soc.* **1978**, *100*, 838-844.
6. (a) Legros, J-Y; Fiaud, J-C "Palladium-catalyzed Nucleophilic Substitution of Naphthyl, Methyl, and 1-Naphthylethyl Esters." *Tetrahedron Lett.*, **1992**, *33*, 2509-2510. (b) Legros, J-Y ; Toffano, M. ; Fiaud, J-C "Asymmetric Palladium-Catalyzed Nucleophilic Substitution of Racemic 1-Naphthylethyl Esters." *Tetrahedron: Asymmetry*, **1995**, *6*, 1899-1902. (c) Legros, J-Y; Toffano, M.; Fiaud, J-C "Palladium-Catalyzed Substitution of Esters of Naphthimethanols, 1-Naphthylethanol, and Analogues by Sodium Dimethyl Malonate. Stereoselective Synthesis from Enantiomerically Pure Substrates." *Tetrahedron Lett.*, **1995**, *51*, 3235-3246.

-
7. Assié, M.; Legros, J-Y; Fiaud, J-C “Asymmetric Palladium-Catalyzed Benzylic Nucleophilic Substitution: High Enantioselectivity with the DUPHOS Family Ligands.” *Tetrahedron: Asymmetry*, **2005**, *16*, 1183-1187.
 8. López-Pérez, A.; Adrio, J.; Carretero, J. C. “Palladium-Catalyzed Cross-Coupling Reaction of Secondary Benzylic Bromides with Grignard Reagents.” *Org. Lett.*, **2009**, *11*, 5514-5517.
 9. (a) Sustmann, R.; Lau, J.; Zipp, M. “Alkylation of Aryl Bromides with Tetra Alkyl Tin Compounds in Presence of (2,2’-Bipyridine)fumaronitrile Palladium(0).” *Tetrahedron Lett.*, **1986**, *27*, 5207-5210. (b) Rudolph, A.; Rackelmann, N.; Lautens, M. “Stereochemical and Mechanistic Investigations of a Palladium-Catalyzed Annulation of Secondary Alkyl Iodides.” *Angew. Chem., Int. Ed.*, **2007**, *46*, 1485-1488. (c) Firmansjah, L.; Fu, G. C. “Intramolecular Heck Reactions of Unactivated Alkyl Halides.” *J. Am. Chem. Soc.*, **2007**, *129*, 11340-11341. (d) Netherton, M. R.; Fu, G. C. “Suzuki Cross-Couplings of Alkyl Tosylates that Possess β -Hydrogen Atoms: Synthetic and Mechanistic Studies.” *Angew. Chem., Int. Ed.*, **2002**, *41*, 3910-3912.
 10. He, A.; Flack, J. R. “Stereospecific Suzuki Cross-Coupling of Alkyl α -Cyanohydrin Triflates.” *J. Am. Chem. Soc.*, **2010**, *132*, 2524-2525.
 11. Trost, B. M.; Czabaniuk, L. C. “Palladium-Catalyzed Asymmetric Benzoylation of 3-Aryl Oxindoles.” *J. Am. Chem. Soc.*, **2010**, *132*, 15534-15536.
 12. Trost, B. M.; Czabaniuk, L. C. “Benzylic Phosphates as Electrophiles in the Palladium-Catalyzed Asymmetric Benzoylation of Azlactones.” *J. Am. Chem. Soc.*, **2012**, *134*, 5778-5781.
 13. Trost, B. M.; Czabaniuk, L. C. “Palladium-Catalyzed Asymmetric Benzoylation of Azlactones.” *Chem. Eur. J.*, **2013**, *19*, 15210-15218.

-
14. Dell'Amico, L.; Companyó, X.; Naicker, T.; Bräuer, T. M.; Jørgensen, K. A. "Asymmetric Organocatalytic Benzylolation of α,β -Unsaturated Aldehydes with Toluenes." *Eur. J. Org. Chem.*, **2013**, 5262-5265.
 15. Yonova, I. M.; Johnson, G.; Osborne, C. A.; Moore, C. E.; Morrisette, N. S.; Jarvo, E. R. "Stereospecific Nickel-Catalyzed Cross-Coupling Reactions of Alkyl Grignard Reagents and Identification of Selective Anti-Breast Cancer Agents." *Angew. Chem.*, **2014**, *126*, 2454-2459.
 16. Mendis, S.; Tunge, J. A. "Palladium-catalyzed Stereospecific Decarboxylative Benzylolation of Alkynes." *Org. Lett.*, **2015**, *17*, 5164.
 17. Najib, A.; Hirabon, K. Miura, M. "Palladium-Catalyzed Asymmetric Benzylic Substitution of Secondary Benzyl Carbonates with Nitrogen and Oxygen Nucleophiles." *Org. Lett.*, **2017**, *19*, 2438-2441.
 18. Zhu, Y.; Zhang, W-Z; Zhang, L.; Luo, S. "Chiral Primary Amine Catalyzed Asymmetric α -Benzylolation with In Situ Generated ortho-Quinone Methides." *Chem. Eur. J.*, **2017**, *23*, 1253-1257.
 19. For specific examples of biologically active diarylmethane compounds: (a) Ismail, N. S. M.; El Dine, R. S.; Hattori, M.; Takahashi, K.; Ihara, M. "Computer-based Design, Synthesis, and Biological Evaluation of Novel Indole Derivatives as HCV NS3-4A Serine Protease Inhibitors." *Bioorg. Med. Chem.*, **2008**, *16*, 7877-7887. (b) Hu, Q.; Yin, L.; Jagusch, C.; Hille, U. E.; Hartmann, R. W. "Isopropylidene Substitution Increases Activity and Selectivity of Biphenylmethylene 4-Pyridine Type CYP17 Inhibitors." *J. Med. Chem.*, **2010**, *53*, 5049-5053. (c) El-labbad, E. M.; Ismail, M. A.; Abou Ei Ella, D. A.; Ahmed, M.; Wang, F.; Barakat, K. H.; Abouzid, K. A. "Discovery of Novel Peptidomimetics as Irreversible CHIKV Nsp2 Protease Inhibitors Using Quantum Mechanical-Based Ligand Descriptors." *Chem. Biol. Drug Des.*, **2015**, *86*, 1518-1520.

-
20. For specific examples of Ni-catalyzed cross-couplings of secondary benzylic electrophiles: (a) Taylor, B. L. H.; Harris, M. R.; Jarvo, E. R. "Synthesis of Enantioenriched Triarylmethanes by Stereospecific Cross-Coupling Reactions." *Angew. Chem. Int. Ed.*, **2012**, *51*, 7790-7793. (b) Greene, M. A.; Yonova, I. M.; Williams, F. J.; Jarvo, E. R. "Traceless Directing Group for Stereospecific Nickel-Catalyzed Alkyl-Alkyl Cross-Coupling Reactions." *Org. Lett.*, **2012**, *14*, 4293-4296. (c) Harris, M. R.; Hanna, L. E.; Greene, M. A.; Moore, C. E.; Jarvo, E. R. "Retention or Inversion in Stereospecific Nickel-Catalyzed Cross-Coupling of Benzylic Carbamates with Arylboronic Esters: Control of Absolute Stereochemistry with an Achiral Catalyst." *J. Am. Chem. Soc.*, **2013**, *135*, 3303-3306.
21. (a) Old, D. W.; Wolfe, J. P.; Buchwald, S. L. "A Highly Active Catalyst for Palladium-Catalyzed Cross-Coupling Reactions: Room-Temperature Suzuki Couplings and Aminations of Unactivated Aryl Chlorides." *J. Am. Chem. Soc.*, **1998**, *120*, 9722-9723. (b) Martin, R.; Buchwald, S. L. "Palladium-Catalyzed Suzuki-Miyaura Cross-Coupling Reactions Employing Dialkylbiaryl Phosphine Ligands." *Acc. Chem. Res.*, **2008**, *41*, 1461-1473.
22. Wisniewska, H. M.; Swift, H. M.; Jarvo, E. R. "Functional-Group-Tolerant, Nickel-Catalyzed Cross-Coupling Reactions for Enantioselective Construction of Tertiary Methyl-Bearing Stereocenters." *J. Am. Chem. Soc.*, **2013**, *135*, 9083-9090.
23. Crystallographic data of (S)-3.12k were deposited as the Cambridge Crystallographic Data Centre as supplementary publication No. CCDC 1532316.
24. Marquard S. L.; Hartwig, J. F. "C(sp³)-O Bond-Forming Reductive Elimination of Ethers from Biphosphine-Ligated Benzylpalladium(II) Aryloxy Complexes." *Angew. Chem. Int. Ed.*, **2011**, *50*, 7119-7123.
25. (a) Trost B. M.; Xu, J. "Palladium-Catalyzed Decarboxylative Asymmetric Allylic Alkylation of Enol Carbonates." *J. Am. Chem. Soc.*, **2009**, *131*, 18343-18357. (b) Burger,

E. C.; Tunge, J. A. "Asymmetric Allylic Alkylation of Ketone Enolates: An Asymmetric Claisen Surrogate." *Org. Lett.*, **2004**, *6*, 4113-4115.

Chapter 3. Appendix

Experimental Methods, Spectral Analysis, and Spectra for Chapter 3 Compounds

Reprinted (adapted) with permission from (Li, T-R; Maliszewski, M. L.; Tunge, J. A. “Stereospecific Decarboxylative Benzoylation of Enolates: Development and Mechanistic Insight.” *Org. Lett.*, **2018**, *20*, 1730-1734.) Copyright (2018) American Chemical Society.

Table of Contents

<i>General Information</i>	96
<i>Preparation and Spectral Data of Reactants</i>	96
<i>General Procedure and Spectral Data of Products</i>	111
<i>Crossover Studies</i>	124
<i>References</i>	127
<i>X-Ray Structure of Products (S)-3.12k</i>	127
<i>Copies of ¹H NMR and ¹³C NMR Spectra</i>	128
<i>Copies of HPLC Spectra</i>	215

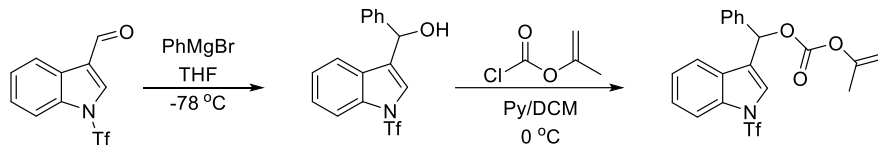
1. General Information

All reactions were run under an argon atmosphere using standard Schlenk techniques or an inert atmosphere glove box. All glassware were oven or flame dried prior to use. Toluene and THF were dried over sodium and distilled in the presence of benzophenone. Dried toluene was taken to the glove box in a Schlenk flask with activated molecular sieves. CH₂Cl₂ was dried over alumina. Other commercially available solvents were used without additional purification. All palladium catalysts and ligands were purchased from Strem and stored in the glove box under an argon atmosphere. Compound purification was effected by flash chromatography using 230x400 mesh, 60 Å porosity silica obtained from Sorbent Technologies.

¹H NMR and ¹³C NMR spectra were obtained on a Bruker Avance 400 or a Bruker Avance 500 DRX spectrometer equipped with a QNP cryoprobe and referenced to residual protio solvent signals. Structural assignments were based on ¹H, ¹³C, DEPT-135, COSY, HSQC. Mass spectrometry was run using EI or ESI techniques. Chiral HPLC analysis was performed by LC-10ATVP Shimadzu HPLC using Chiralpak AD, AS-H, AD-H and Chiralcell OD-H, OD chiral columns (0.46cmØx25cm), eluting with hexane/iso-propanol mixture. All HPLC data are provided in a separate document. Optical rotations were measured on a Autopol® IV automatic polarimeter using a 5 cm cell and sodium D line (589 nm) at ambient temperature in the solvent and concentration indicated.

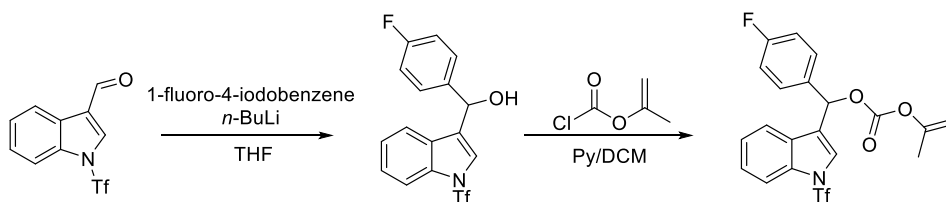
2. Preparation and Spectral Data of Reactants

Substrates were prepared with the procedures shown below. The *N*-Tf indole-3-carboxaldehyde was synthesised via the reported process^[1].



2.1 Standard procedure 1: N-Tf indole-3-carboxaldehyde (832 mg, 3 mmol) was dissolved into THF (15 ml). After the mixture was cooled to $-78\text{ }^{\circ}\text{C}$, phenylmagnesium bromide (1.5 eq, 4.5 mmol) was added dropwise. The mixture was allowed to stir at this temperature for 30 min. Then the reaction was quenched with $\text{NH}_4\text{Cl(aq.)}$ and organic layer was separated. The aqueous layer was extracted with EtOAc 3 times. The combined organic layer was dried by MgSO_4 . The solvent was removed on rotary evaporator, the corresponding secondary benzylic alcohol was purified by column chromatography (978 mg, 92% yield).

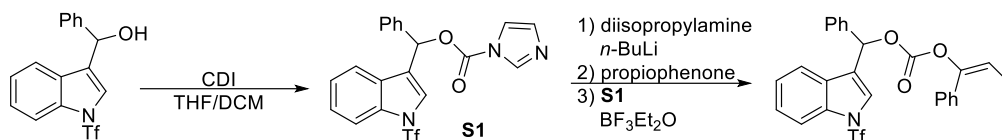
Then product of last step (711 mg, 2 mmol) was re-dissolved into DCM. Pyridine (483 L, 6 mmol) was added and the mixture was cooled to $0\text{ }^{\circ}\text{C}$ in a ice bath. After that, isopropenylchloroformate (289 mg, 2.4 mmol) was added dropwise. The reaction mixture was allowed to warm to room temperature and monitored by TLC. After the starting material completely converted, the product was isolated by column chromatography (705 mg, 80% yield).



2.2 Standard procedure 2: 1-Fluoro-4-iodobenzene (666 mg, 3 mmol) was dissolved into THF (15 ml). After the mixture was cooled to $-78\text{ }^{\circ}\text{C}$, $n\text{-BuLi}$ (1.2 ml, 2.5 N in hexane) was added dropwise. The mixture was allowed to stirring at $-78\text{ }^{\circ}\text{C}$ for 30 min. N-Tf indole-3-carboxaldehyde (554 mg, 2 mmol) was added with 5 ml THF, further stirring for 30 min before quenched with $\text{NH}_4\text{Cl(aq.)}$. Organic layer was separated. The aqueous layer was extracted with EtOAc 3 times.

The combined organic layer was dried by MgSO₄. Removed the solvent on rotary evaporator, the corresponding secondary alcohol could be purified by column chromatography (636 mg, 85% yield).

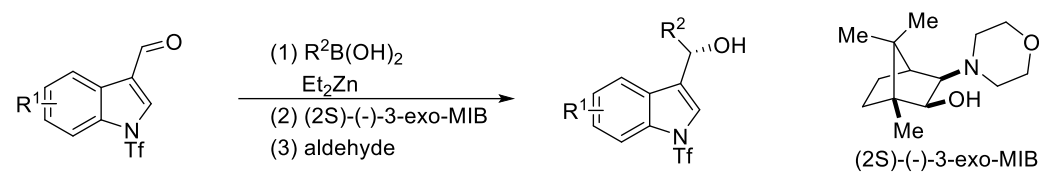
Then procedure of next step was as same as procedure 1.



2.3 Standard procedure 3^[2]: CDI (1.62 g, 10 mmol) was dissolved into THF (20 mL), cooled to 0 °C in a ice bath. Phenyl(1-((trifluoromethyl)sulfonyl)-1H-indol-3-yl)-methanol (1.76 g, 5 mmol) was added slowly dropwise with 20 mL DCM via syringe. After complete addition, the mixture was allowed to warm to room temperature and continuously stirred for 3 hs and monitored by TLC. When the starting material totally disappeared, the solvent was removed via rotary evaporator and the desired product was purified by column chromatography (2.04 g, 90% yield). The 1H-imidazole-1-carboxylate intermediate **S1** was stored at 4 °C for more than 7 days without apparent decomposition.

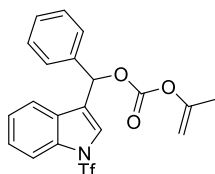
Diisopropylamine (313 uL, 2.2 mmol) was dissolved into THF (5 mL), cooled to -78 °C before n-BuLi (880 uL, 2.2 mmol, 2.5 N in hexane) was added via syringe. The mixture was stirred at this temperature for 10 min, then propiophenone (269 mg, 2 mmol) was added. This mixture was allowed to stir at -78 °C for 30 min. A separate flask was charged with a THF solution of 1H-imidazole-1-carboxylate intermediate **S1** (450 mg, 1 mmol), also cooled to -78 °C followed by the addition of BF₃Et₂O (303 uL, 2.4 mmol). After stirring at this temperature for 15 min, the enolate

mixture was transferred into the solution of 1H-imidazole-1-carboxylate and $\text{BF}_3 \cdot \text{Et}_2\text{O}$ quickly. Then the mixture was further stirred at $-78\text{ }^\circ\text{C}$ for 30 min. After 1H-imidazole-1-carboxylate intermediate totally disappeared, the reaction was quenched by H_2O , extracted with EtOAc 3 times. The combined organic layer was dried by MgSO_4 . The solvent was removed on a rotary evaporator and the corresponding enol carbonate could be purified by column chromatography (388 mg, 76% yield, E/Z = 50:1).



2.4 Standard procedure for the preparation of enantioenriched diarylmethanols^[3]: To a flame dried Schlenk flask was added phenyl boronic acid (731 mg, 6 mmol) and toluene (10 mL). Then diethyl zinc (18 mL, 18 mmol, 1.0 M in hexanes) was added and the solution was heated at $60\text{ }^\circ\text{C}$ for 24 hours in an oil bath. After 24 hours, it was removed from the oil bath and cooled to room temperature. Then a solution of (2S)-(-)-3-exo-MIB (59.8 mg, 0.25 mmol) in toluene (5 mL) was added to the reaction mixture and was allowed to stir for one hour at room temperature before the addition of corresponding N-Tf indole-3-carboxaldehyde (2.5 mmol, 692 mg). Then the reaction mixture was allowed to stir for 12 hours and the resulting mixture was quenched with 1N HCl acid and the product was extracted with EtOAc. The combined organics were washed with brine and dried over MgSO_4 and concentrated in vacuo. The crude product was purified via flash chromatography over silica gel to isolate enantioenriched secondary alcohol in 87% yield.

Phenyl(1-((trifluoromethyl)sulfonyl)-1H-indol-3-yl)methyl prop-1-en-2-yl carbonate (3.11a)



Appearance: White solid, mp. 65-67 °C.

^1H NMR (400 MHz, CDCl_3) δ (ppm) = 7.81 (d, J = 8.4 Hz, 1H), 7.42–7.38 (m, 2H), 7.37–7.34 (m, 1H), 7.34–7.27 (m, 5H), 7.23–7.19 (m, 1H), 6.88 (s, 1H), 4.76–4.72 (m, 1H), 4.63 (dd, J = 1.8, 1.1 Hz, 1H), 1.87 (d, J = 0.6 Hz, 3H).

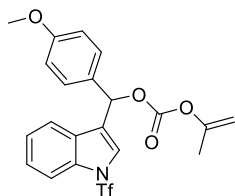
$^{13}\text{C}\{^1\text{H}\}$ NMR (100 MHz, CDCl_3) δ 152.90, 152.12, 136.84, 135.92, 129.12, 128.89, 128.54, 127.27, 126.29, 125.04, 124.35, 124.02, 120.81, 119.50 (q, J = 322.0 Hz), 113.92, 102.04, 74.81, 19.10.

ATR-IR: 1759.14, 1450.52, 1419.66, 1271.13, 1232.55, 1209.41, 1149.61, 1112.96 cm^{-1} .

HRMS for: $\text{C}_{16}\text{H}_{11}\text{F}_3\text{NO}_2\text{S}$ [$\text{M}-\text{C}_4\text{H}_5\text{O}_3$] $^+$: calcd 338.0468, found 338.0504.

The molecular ion peak wasn't found in standard high resolution mass spectrometry, instead the diarylmethane cation was observed.

(4-Methoxyphenyl)(1-((trifluoromethyl)sulfonyl)-1H-indol-3-yl)methyl prop-1-en-2-yl carbonate (3.11b)



Appearance: Yellow oil.

^1H NMR (500 MHz, CDCl_3) δ (ppm) = 7.81 (d, J = 8.3 Hz, 1H), 7.35–7.27 (m, 5H), 7.21 (ddd, J = 8.2, 7.2, 0.9 Hz, 1H), 6.86–6.81 (m, 3H), 4.74–4.61 (m, 2H), 3.73 (s, 3H), 1.87 (d, J = 0.6 Hz, 3H).

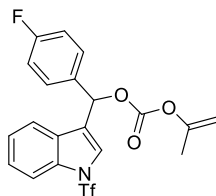
$^{13}\text{C}\{^1\text{H}\}$ NMR (125 MHz, CDCl_3) δ = 160.17, 152.89, 152.12, 135.90, 129.05, 128.82, 128.54, 126.23, 124.99, 124.24, 123.92, 120.81, 119.50 (q, J = 321.3 Hz), 114.21, 113.89, 102.02, 74.80, 55.25, 19.12.

ATR-IR: 1752.00, 1643.41, 1514.17, 1417.73, 1207.48, 1174.69, 1147.68, 991.44, 744.55 cm^{-1} .

HRMS for: $\text{C}_{17}\text{H}_{13}\text{F}_3\text{NO}_3\text{S}$ [$\text{M}-\text{C}_4\text{H}_5\text{O}_3$] $^+$: calcd 368.0563, found 368.0596.

The molecular ion peak wasn't found in standard high resolution mass spectrometry, instead the diarylmethane cation was observed.

(4-Fluorophenyl)(1-((trifluoromethyl)sulfonyl)-1H-indol-3-yl)methyl prop-1-en-2-yl carbonate (3.11c)



Appearance: colorless oil.

^1H NMR (500 MHz, CDCl_3) δ (ppm) = 7.93 (d, J = 8.4 Hz, 1H), 7.51–7.47 (m, 2H), 7.44 (ddd, J = 8.4, 7.3, 1.2 Hz, 1H), 7.39 (d, J = 6.5 Hz, 2H), 7.33 (td, J = 7.6, 0.9 Hz, 1H), 7.14–7.08 (m, 2H), 6.95 (s, 1H), 4.85 (d, J = 1.5 Hz, 1H), 4.75 (dd, J = 1.8, 1.1 Hz, 1H), 1.98 (d, J = 0.6 Hz, 3H).

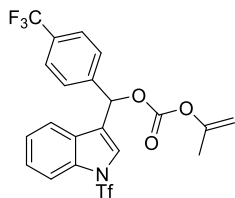
$^{13}\text{C}\{^1\text{H}\}$ NMR (125 MHz, CDCl_3) δ 163.03 (d, J = 247.5 Hz), 152.86, 152.05, 135.93, 132.73 (q, J = 3.8 Hz), 129.40 (q, J = 8.8 Hz), 128.32, 126.40, 125.09, 124.21, 123.72, 120.69, 119.49 (q, J = 322.5 Hz), 116.92 (q, J = 35.0 Hz), 113.99, 102.14, 74.23, 19.11.

ATR-IR: 1759.14, 1676.20, 1606.76, 1510.31, 1450.52, 1421.58, 1273.06, 1234.48, 1209.41, 1149.61, 1112.96, 991.44, 746.48, 611.45 cm^{-1} .

HRMS for: $\text{C}_{16}\text{H}_{10}\text{F}_4\text{NO}_2\text{S}$ [$\text{M}-\text{C}_4\text{H}_5\text{O}_3$] $^+$: calcd 356.0363, found 356.0371.

The molecular ion peak wasn't found in standard high resolution mass spectrometry, instead the diarylmethane cation was observed.

Prop-1-en-2-yl-((4-(trifluoromethyl)phenyl)(1-((trifluoromethyl)sulfonyl)-1H-indol-3-yl)methyl) carbonate (3.11d)



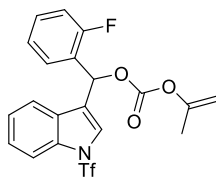
Appearance: White solid, mp. 75-76 $^{\circ}\text{C}$.

^1H NMR (500 MHz, CDCl_3) δ (ppm) = 7.93 (d, J = 8.3 Hz, 1H), 7.69 (d, J = 8.3 Hz, 2H), 7.66–7.61 (m, 2H), 7.47–7.41 (m, 3H), 7.34 (td, J = 7.7, 0.9 Hz, 1H), 4.85 (d, J = 1.6 Hz, 1H), 4.75 (dd, J = 1.8, 1.1 Hz, 1H), 1.98 (d, J = 0.6 Hz, 3H).

$^{13}\text{C}\{^1\text{H}\}$ NMR (125 MHz, CDCl_3) δ 152.88, 152.02, 140.86 (q, J = 2.0 Hz), 135.95, 131.24 (q, J = 32.0 Hz), 128.19, 127.49, 126.53, 125.96 (q, J = 4.0 Hz), 125.20, 124.69, 123.78 (q, J = 270.0 Hz), 123.13, 120.64, 119.49 (q, J = 322.0 Hz), 114.04, 102.16, 73.92, 19.04.

ATR-IR: 1759.14, 1421.58, 1325.14, 1273.06, 1234.48, 1209.41, 1166.97, 1149.61, 1130.32, 1112.96, 1068.60, 989.52, 746.48, 609.53 cm^{-1} .

(2-Fluorophenyl)(1-((trifluoromethyl)sulfonyl)-1H-indol-3-yl)methyl prop-1-en-2-yl carbonate (3.11e)



Appearance: Yellow solid, mp. 58-61 °C.

^1H NMR (500 MHz, CDCl_3) δ (ppm) = 7.81 (d, J = 8.4 Hz, 1H), 7.51–7.48 (m, 1H), 7.44 (td, J = 7.6, 1.7 Hz, 1H), 7.35–7.31 (m, 1H), 7.30–7.24 (m, 3H), 7.17 (s, 1H), 7.12 (td, J = 7.6, 1.0 Hz, 1H), 7.06–7.01 (m, 1H), 4.75 (d, J = 1.5 Hz, 1H), 4.64 (dd, J = 1.8, 1.1 Hz, 1H), 1.88 (d, J = 0.7 Hz, 3H).

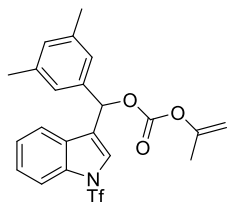
$^{13}\text{C}\{^1\text{H}\}$ NMR (125 MHz, CDCl_3) δ 159.98 (d, J = 247.5 Hz), 152.93, 151.91, 135.87, 130.94 (d, J = 31.0 Hz), 128.45, 128.24 (d, J = 2.5 Hz), 126.42, 125.19, 124.73 (d, J = 3.8 Hz), 124.60 (d, J = 12.5 Hz), 124.28, 123.27, 120.55, 119.51 (q, J = 322.5 Hz), 116.04 (d, J = 21.3 Hz), 113.99, 102.16, 68.73 (q, J = 3.8 Hz), 19.11.

ATR-IR: 1761.07, 1674.27, 1491.02, 1450.52, 1421.58, 1271.13, 1232.55, 1207.48, 1147.68, 1112.96, 989.52, 758.05, 605.67 cm^{-1} .

HRMS for: $\text{C}_{16}\text{H}_{10}\text{F}_4\text{NO}_2\text{S}$ [$\text{M}-\text{C}_4\text{H}_5\text{O}_3$] $^+$: calcd 356.0363, found 356.0368.

The molecular ion peak wasn't found in standard high resolution mass spectrometry, instead the diarylmethane cation was observed.

(3,5-Dimethylphenyl)(1-((trifluoromethyl)sulfonyl)-1H-indol-3-yl)methyl prop-1-en-2-yl carbonate (3.11f)



Appearance: White solid, mp. 63-65 °C.

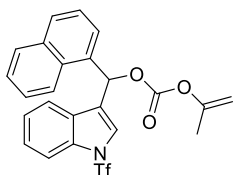
^1H NMR (400 MHz, CDCl_3) δ (ppm) = 7.91 (d, J = 8.4 Hz, 1H), 7.52–7.44 (m, 1H), 7.44–7.38 (m, 1H), 7.38–7.29 (m, 2H), 7.13–7.06 (m, 2H), 7.01 (s, 1H), 6.90 (s, 1H), 4.84 (d, J = 1.4 Hz, 1H), 4.73 (dd, J = 1.7, 1.2 Hz, 1H), 2.33 (s, 6H), 1.98 (d, J = 0.7 Hz, 3H).

$^{13}\text{C}\{^1\text{H}\}$ NMR (100 MHz, CDCl_3) δ 152.92, 152.14, 138.49, 136.67, 135.90, 130.81, 128.65, 126.22, 125.03, 125.00, 124.32, 124.18, 120.83, 119.52 (q, J = 322.0 Hz), 113.89, 102.00, 74.94, 21.29, 19.13.

ATR-IR: 1759.14, 1672.34, 1610.61, 1450.52, 1419.66, 1271.13, 1232.55, 1207.48, 1149.61, 1111.03, 989.52, 839.06, 746.48, 609.53 cm^{-1} .

HRMS for: C₂₂H₂₁F₃NO₅S [M+H]⁺: calcd 468.1093, found 468.1230.

Naphthalen-1-yl(1-((trifluoromethyl)sulfonyl)-1H-indol-3-yl)methyl prop-1-en-2-yl carbonate (3.11g)



Appearance: White oil.

¹H NMR (500 MHz, CDCl₃) δ (ppm) = 8.02–7.96 (m, 1H), 7.78 (dd, *J* = 8.4, 5.1 Hz, 3H), 7.66–7.58 (m, 2H), 7.44–7.36 (m, 4H), 7.28 (dd, *J* = 8.2, 7.5 Hz, 1H), 7.18 (t, *J* = 7.6 Hz, 1H), 7.13 (s, 1H), 4.73 (s, 1H), 4.60 (d, *J* = 0.8 Hz, 1H), 1.84 (s, 3H).

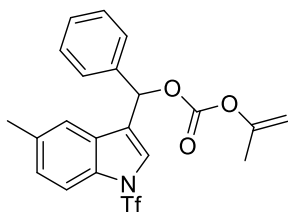
¹³C{¹H} NMR (125 MHz, CDCl₃) δ 151.89, 151.28, 134.85, 132.90, 131.16, 129.43, 128.99, 127.98, 127.80, 125.76, 125.30, 125.05, 124.76, 124.19, 124.11, 123.02, 122.09, 119.68, 118.40 (q, *J* = 321.3 Hz), 112.90, 101.02, 71.36, 18.04.

ATR-IR: 1755.28, 1674.27, 1450.52, 1421.58, 1274.99, 1232.55, 1207.48, 1149.61, 1112.96, 987.59, 779.27, 746.48, 615.31 cm⁻¹.

HRMS for: C₂₀H₁₃F₃NO₂S [M-C₄H₅O₃]⁺: calcd 388.0614, found 388.0637.

The molecular ion peak wasn't found in standard high resolution mass spectrometry, instead the diarylmethane cation was observed.

(5-Methyl-1-((trifluoromethyl)sulfonyl)-1H-indol-3-yl)(phenyl)methyl prop-1-en-2-yl carbonate (3.11i)



Appearance: White solid, mp. 71-73 °C.

¹H NMR (400 MHz, CDCl₃) δ (ppm) = 7.77 (d, *J* = 9.0 Hz, 1H), 7.48 (dd, *J* = 7.6, 1.6 Hz, 2H), 7.45–7.37 (m, 3H), 7.30 (s, 1H), 7.22 (d, *J* = 6.8 Hz, 2H), 6.94 (s, 1H), 4.83 (d, *J* = 1.5 Hz, 2H), 4.72 (s, 1H), 2.39 (s, 3H), 1.97 (s, 3H).

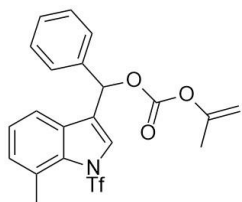
¹³C{¹H} NMR (100 MHz, CDCl₃) δ 152.96, 152.19, 136.92, 134.99, 134.12, 129.12, 128.92, 128.81, 127.68, 127.29, 124.49, 123.88, 120.63, 119.56 (q, *J* = 322.0 Hz), 113.59, 102.06, 74.84, 21.38, 19.15.

ATR-IR: 1759.14, 1417.73, 1273.06, 1232.55, 1203.62, 1153.47, 1141.90, 1111.03, 1089.82, 991.44, 698.25, 624.96, 586.38 cm^{-1} .

HRMS (ESI) for: $\text{C}_{17}\text{H}_{13}\text{F}_3\text{NO}_2\text{S}$ $[\text{M}-\text{C}_4\text{H}_5\text{O}_3]^+$: calcd 352.0614, found 352.0619.

The molecular ion peak wasn't found in standard high resolution mass spectrometry, instead the diarylmethane cation was observed.

(7-Methyl-1-((trifluoromethyl)sulfonyl)-1H-indol-3-yl)(phenyl)methyl prop-1-en-2-yl carbonate (3.11j)



Appearance: Beige solid, mp. 62.1-64.9 $^{\circ}\text{C}$

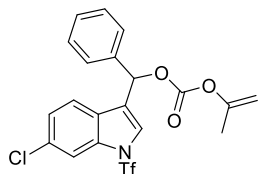
^1H NMR (500 MHz, CDCl_3) δ 7.48 (d, $J = 2.0$ Hz, 1H), 7.46 (d, $J = 1.6$ Hz, 2H), 7.42–7.39 (m, 1H), 7.39–7.35 (m, 2H), 7.28 (t, $J = 4.7$ Hz, 1H), 7.21 (s, 1H), 7.20 (d, $J = 1.1$ Hz, 1H), 6.93 (s, 1H), 4.82 (d, $J = 1.7$ Hz, 1H), 4.72–4.70 (m, 1H), 2.68 (s, 3H), 1.96 (s, 3H).

$^{13}\text{C}\{^1\text{H}\}$ NMR (126 MHz, CDCl_3) δ 152.93, 152.15, 136.80, 135.72, 130.66, 130.53, 129.10, 128.88, 127.34, 125.74, 125.47, 123.84, 118.63, 102.04, 74.80, 21.85 (d, $J = 1.8$ Hz), 19.14.

ATR-IR: 1757.65, 1418.80, 1270.03, 1230.83, 1207.34, 1112.49, 1082.83, 738.64, 723.71 cm^{-1} .

HRMS for: $\text{C}_{21}\text{H}_{18}\text{F}_3\text{NO}_5\text{S}$ $[\text{M}]^+$: calcd 453.0858, found 453.0864.

(6-Chloro-1-((trifluoromethyl)sulfonyl)-1H-indol-3-yl)(phenyl)methyl prop-1-en-2-yl carbonate (3.11k)



Appearance: White solid, mp. 101-103 $^{\circ}\text{C}$.

^1H NMR (500 MHz, CDCl_3) δ (ppm) = 7.93 (d, $J = 1.7$ Hz, 1H), 7.48 (dd, $J = 7.9, 1.5$ Hz, 2H), 7.44–7.38 (m, 4H), 7.36 (d, $J = 8.5$ Hz, 1H), 7.29 (dd, $J = 8.5, 1.8$ Hz, 1H), 6.95 (s, 1H), 4.84 (d, $J = 1.5$ Hz, 1H), 4.74 (dd, $J = 1.8, 1.1$ Hz, 1H), 1.97 (d, $J = 0.7$ Hz, 3H).

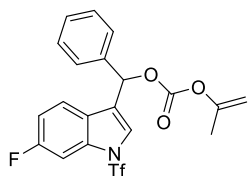
$^{13}\text{C}\{^1\text{H}\}$ NMR (125 MHz, CDCl_3) δ 152.86, 152.04, 136.57, 136.23, 132.55, 129.22, 128.94, 127.19, 127.01, 125.84, 124.80, 123.76, 121.65, 119.38 (q, $J = 321.3$ Hz), 114.21, 102.08, 74.53, 19.06.

ATR-IR: 1759.14, 1421.58, 1269.20, 1232.55, 1209.41, 1151.54, 1120.68, 1074.39, 993.37, 624.96, 601.81 cm^{-1} .

HRMS for: $\text{C}_{16}\text{H}_{10}\text{ClF}_3\text{NO}_2\text{S}$ [$\text{M}-\text{C}_4\text{H}_5\text{O}_3$] $^+$: calcd 372.0073, found 372.0087.

The molecular ion peak wasn't found in standard high resolution mass spectrometry, instead the diarylmethane cation was observed.

(6-Fluoro-1-((trifluoromethyl)sulfonyl)-1H-indol-3-yl)(phenyl)methyl prop-1-en-2-yl carbonate (3.11l)



Appearance: White solid, mp. 72-74 $^{\circ}\text{C}$.

^1H NMR (400 MHz, CDCl_3) δ (ppm) = 7.63 (dd, $J = 9.2, 2.2$ Hz, 1H), 7.50–7.45 (m, 2H), 7.43–7.35 (m, 5H), 7.06 (td, $J = 8.9, 2.3$ Hz, 1H), 6.93 (s, 1H), 4.83 (d, $J = 1.5$ Hz, 1H), 4.73 (dd, $J = 1.7, 1.1$ Hz, 1H), 1.96 (d, $J = 0.6$ Hz, 3H).

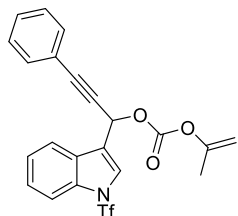
$^{13}\text{C}\{^1\text{H}\}$ NMR (125 MHz, CDCl_3) δ 162.52 (d, $J = 245.0$ Hz), 152.87, 152.09, 136.63, 136.20 (d, $J = 12.5$ Hz), 129.24, 128.96, 127.21, 124.79 (d, $J = 1.3$ Hz), 124.62 (d, $J = 3.8$ Hz), 123.76, 121.87 (d, $J = 8.8$ Hz), 119.42 (q, $J = 321.3$ Hz), 113.66 (d, $J = 25.0$ Hz), 102.12, 101.74 (d, $J = 28.8$ Hz), 74.63, 19.11.

ATR-IR: 1759.14, 1676.20, 1616.40, 1577.82, 1489.10, 1271.13, 1234.48, 1209.41, 1147.68, 1097.53, 1001.09, 904.64 cm^{-1} .

HRMS for $\text{C}_{16}\text{H}_{10}\text{F}_4\text{NO}_2\text{S}$ [$\text{M}-\text{C}_4\text{H}_5\text{O}_3$] $^+$: calcd 356.0363, found 356.0380.

The molecular ion peak wasn't found in standard high resolution mass spectrometry, instead the diarylmethane cation was observed.

3-Phenyl-1-(1-((trifluoromethyl)sulfonyl)-1H-indol-3-yl)prop-2-yn-1-yl prop-1-en-2-yl carbonate (3.11m)



Appearance: Yellowish oil.

^1H NMR (400 MHz, CDCl_3) δ (ppm) = 7.88–7.81 (m, 2H), 7.56 (s, 1H), 7.42–7.33 (m, 4H), 7.28–7.21 (m, 3H), 6.72 (d, $J = 0.7$ Hz, 1H), 4.81–4.77 (m, 1H), 4.66 (dd, $J = 1.8, 1.1$ Hz, 1H), 1.91 (d,

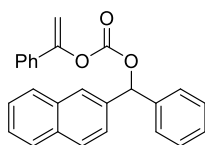
$J = 0.6$ Hz, 3H).

$^{13}\text{C}\{^1\text{H}\}$ NMR (100 MHz, CDCl_3) δ 152.98, 152.02, 136.02, 132.05, 129.37, 128.45, 128.17, 126.56, 125.64, 125.26, 121.37, 120.99, 120.93, 119.51 (q, $J = 322.0$ Hz), 114.01, 102.19, 88.19, 82.77, 63.09, 19.16.

ATR-IR: 1759.14, 1678.13, 1491.02, 1450.52, 1421.58, 1323.21, 1267.27, 1234.48, 1209.41, 1149.61, 1112.96, 756.12, 613.38 cm^{-1} .

HRMS for: $\text{C}_{22}\text{H}_{16}\text{F}_3\text{NNaO}_5\text{S}$ $[\text{M}+\text{Na}]^+$: calcd 486.0593, found 486.0518.

Naphthalen-2-yl(phenyl)methyl (1-phenylvinyl) carbonate (3.11n)



Appearance: White oil.

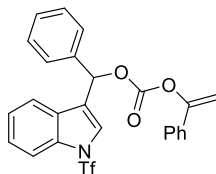
^1H NMR (500 MHz, CDCl_3) δ (ppm) = ^1H NMR (500 MHz, CDCl_3) δ 7.89 (d, $J = 0.5$ Hz, 1H), 7.86–7.80 (m, 3H), 7.52–7.46 (m, 4H), 7.44–7.40 (m, 3H), 7.39–7.35 (m, 2H), 7.35–7.28 (m, 3H), 6.90 (s, 1H), 5.45 (d, $J = 2.5$ Hz, 1H), 5.15 (d, $J = 2.5$ Hz, 1H).

$^{13}\text{C}\{^1\text{H}\}$ NMR (125 MHz, CDCl_3) δ 153.37, 152.48, 139.09, 136.53, 133.78, 133.03, 133.02, 129.09, 128.60, 128.55, 128.51, 128.29, 128.18, 127.66, 127.09, 126.39, 126.37, 126.03, 124.86, 124.62, 101.87, 81.60.

ATR-IR: 1755.28, 1672.34, 1271.13, 1207.48, 1166.97, 1124.54, 1085.96, 935.51, 852.56, 815.92, 698.25 cm^{-1} .

HRMS for: $\text{C}_{26}\text{H}_{20}\text{NaO}_3$ $[\text{M}+\text{Na}]^+$: calcd 403.1305, found 403.1346.

Phenyl(1-((trifluoromethyl)sulfonyl)-1H-indol-3-yl)methyl (1-phenylvinyl) carbonate (3.11o)



Appearance: White solid, mp. 97-100 °C.

^1H NMR (500 MHz, CDCl_3) δ (ppm) = 7.91 (d, $J = 8.3$ Hz, 1H), 7.46 (m, 5H), 7.43–7.39 (m, 4H), 7.35–7.28 (m, 5H), 6.97 (s, 1H), 5.45 (d, $J = 2.6$ Hz, 1H), 5.15 (d, $J = 2.6$ Hz, 1H).

$^{13}\text{C}\{^1\text{H}\}$ NMR (125 MHz, CDCl_3) δ 152.33, 151.32, 135.60, 134.88, 132.58, 128.20, 128.16,

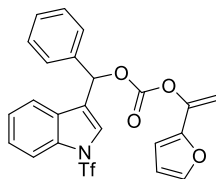
127.88, 127.59, 127.47, 126.27, 125.29, 124.03, 123.77, 123.40, 122.85, 119.79, 118.46 (q, $J = 321.3$ Hz), 112.90, 100.94, 74.21.

ATR-IR: 1764.93, 1417.73, 1278.85, 1228.70, 1147.68, 1111.03, 989.52, 746.48, 698.25, 605.67 cm^{-1} .

HRMS for: $\text{C}_{16}\text{H}_{11}\text{F}_3\text{NO}_2\text{S}$ [$\text{M}-\text{C}_9\text{H}_7\text{O}_3$] $^+$: calcd 338.0463, found 338.0504.

The molecular ion peak wasn't found in standard high resolution mass spectrometry, instead the diarylmethane cation was observed.

1-(Furan-2-yl)vinyl (phenyl(1-((trifluoromethyl)sulfonyl)-1H-indol-3-yl)methyl) carbonate (3.11p)



Appearance: Yellow oil.

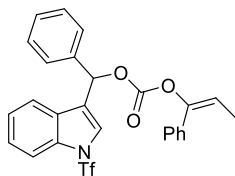
^1H NMR (500 MHz, CDCl_3) δ (ppm) = 7.95 (d, $J = 8.4$ Hz, 1H), 7.56–7.53 (m, 2H), 7.51–7.48 (m, 1H), 7.47–7.38 (m, 6H), 7.33 (td, $J = 7.8, 0.9$ Hz, 1H), 7.05 (s, 1H), 6.37 (dd, $J = 3.4, 1.8$ Hz, 1H), 6.33 (d, $J = 3.4$ Hz, 1H), 5.49 (d, $J = 2.7$ Hz, 1H), 5.10 (d, $J = 2.7$ Hz, 1H).

$^{13}\text{C}\{^1\text{H}\}$ NMR (125 MHz, CDCl_3) δ 152.23, 147.77, 144.72, 143.27, 136.54, 135.88, 129.21, 128.90, 128.44, 127.28, 126.32, 125.04, 124.41, 123.78, 120.79, 119.47 (q, $J = 322.5$ Hz), 113.90, 111.32, 107.77, 100.17, 75.44.

ATR-IR: 1764.93, 1450.52, 1417.73, 1232.55, 1209.41, 1147.68, 1111.03, 989.52, 744.55, 603.74, 578.66 cm^{-1} .

HRMS for: $\text{C}_{23}\text{H}_{16}\text{F}_3\text{NNaO}_6\text{S}$ [$\text{M}+\text{Na}$] $^+$: calcd 514.0593, found 514.0590.

(E)-phenyl(1-((trifluoromethyl)sulfonyl)-1H-indol-3-yl)methyl-(1-phenylprop-1-en-1-yl) carbonate (3.11q)



Appearance: Pale yellow solid, mp. 88-91 $^{\circ}\text{C}$.

^1H NMR (500 MHz, CDCl_3) δ (ppm) = 7.80 (d, $J = 8.4$ Hz, 1H), 7.35 (m, 3H), 7.31–7.25 (m, 6H), 7.22 (s, 1H), 7.20–7.14 (m, 4H), 6.87 (s, 1H), 5.75 (q, $J = 7.0$ Hz, 1H), 1.58 (d, $J = 7.0$ Hz, 3H).

$^{13}\text{C}\{^1\text{H}\}$ NMR (125 MHz, CDCl_3) δ 152.10, 147.44, 136.74, 135.94, 134.46, 129.18, 128.92, 128.60, 128.54, 128.32, 127.26, 126.35, 125.08, 124.39, 124.21, 124.04, 120.84, 119.52 (q, $J =$

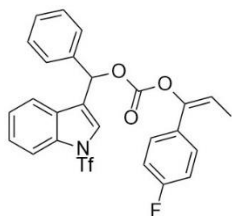
321.3 Hz), 113.95, 112.98, 75.23, 11.22.

ATR-IR: 1763.00, 1450.52, 1417.73, 1147.68, 1111.03, 991.44, 952.87, 746.48, 698.25, 605.67, 578.66 cm^{-1} .

HRMS for: $\text{C}_{16}\text{H}_{11}\text{F}_3\text{NO}_2\text{S}$ $[\text{M}-\text{C}_{10}\text{H}_9\text{O}_3]^+$: calcd 338.0463, found 338.0467.

The molecular ion peak wasn't found in standard high resolution mass spectrometry, instead the diarylmethane cation was observed.

(E)-(4-fluorophenyl)(1-((trifluoromethyl)sulfonyl)-1H-indol-3-yl)methyl-(1-phenylprop-1-en-1-yl) carbonate (3.11r)



Appearance: White solid, mp. 102.4-105.6 $^{\circ}\text{C}$.

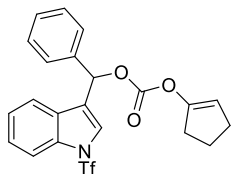
^1H NMR (500 MHz, CDCl_3) δ 7.91 (d, $J = 8.7$ Hz, 1H), 7.49–7.44 (m, 2H), 7.44–7.37 (m, 5H), 7.34–7.27 (m, 4H), 6.99–6.91 (m, 3H), 5.77 (q, $J = 7.0$ Hz, 1H), 1.68 (d, $J = 7.0$ Hz, 3H).

$^{13}\text{C}\{^1\text{H}\}$ NMR (126 MHz, CDCl_3) δ 163.65, 161.67, 152.00, 146.62, 136.66, 135.94, 129.22, 128.92, 128.49, 127.23, 126.37, 126.15, 126.09, 125.06, 124.39, 123.93, 120.77, 115.64, 115.47, 113.97, 112.86 (d, $J = 2.1$ Hz), 75.34, 11.17.

ATR-IR: 1762.37, 1606.88, 1509.55, 1450.62, 1419.57, 1232.89, 1112.31, 991.58, 843.01, 664.70, 452.47 cm^{-1} .

HRMS for $\text{C}_{26}\text{H}_{19}\text{F}_4\text{NO}_5\text{S}$ $[\text{M}+\text{Na}]^+$: calcd 556.0818, found 556.0812.

Cyclopent-1-en-1-yl (phenyl(1-((trifluoromethyl)sulfonyl)-1H-indol-3-yl)methyl) carbonate (3.11s)



Appearance: Colorless oil.

^1H NMR (500 MHz, CDCl_3) δ (ppm) = 7.89 (d, $J = 8.4$ Hz, 1H), 7.48 (dd, $J = 7.7, 1.3$ Hz, 2H), 7.44–7.38 (m, 5H), 7.36 (s, 1H), 7.32–7.28 (m, 1H), 6.95 (s, 1H), 5.48 (d, $J = 1.8$ Hz, 1H), 2.54–2.32 (m, 4H), 1.95 (dt, $J = 14.9, 7.7$ Hz, 2H).

$^{13}\text{C}\{^1\text{H}\}$ NMR (125 MHz, CDCl_3) δ 151.81, 150.77, 136.81, 135.94, 129.19, 128.94, 128.56,

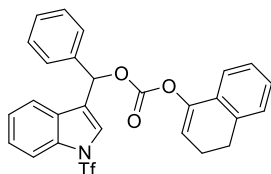
127.37, 126.32, 125.08, 124.43, 123.93, 120.86, 119.52 (q, $J = 322.5$ Hz), 113.95, 112.68, 74.88, 30.60, 28.48, 20.91.

ATR-IR: 1763.00, 1417.73, 1232.55, 1213.27, 1147.68, 1111.03, 744.55, 609.53 cm^{-1} .

HRMS for: $\text{C}_{16}\text{H}_{11}\text{F}_3\text{NO}_2\text{S}$ [$\text{M}-\text{C}_6\text{H}_7\text{O}_3$] $^+$: calcd 338.0463, found 338.0497.

The molecular ion peak wasn't found in standard high resolution mass spectrometry, instead the diarylmethane cation was observed.

3,4-Dihydronaphthalen-1-yl (phenyl(1-((trifluoromethyl)sulfonyl)-1H-indol-3-yl)methyl) carbonate (3.11t)



Appearance: Pale yellow solid, mp. 128-131 $^{\circ}\text{C}$.

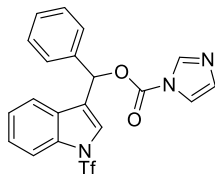
^1H NMR (500 MHz, CDCl_3) δ (ppm) = 7.91 (d, $J = 8.4$ Hz, 1H), 7.53–7.48 (m, 2H), 7.46 (dd, $J = 7.9, 0.8$ Hz, 1H), 7.44–7.39 (m, 4H), 7.35 (s, 1H), 7.33–7.29 (m, 1H), 7.20–7.13 (m, 2H), 7.09 (td, $J = 7.3, 1.8$ Hz, 1H), 7.05–7.00 (m, 1H), 6.99 (s, 1H), 5.81 (t, $J = 4.7$ Hz, 1H), 2.86 (t, $J = 8.1$ Hz, 2H), 2.44 (ddd, $J = 9.2, 7.4, 4.7$ Hz, 2H).

$^{13}\text{C}\{^1\text{H}\}$ NMR (125 MHz, CDCl_3) δ 152.72, 146.19, 136.78, 136.34, 135.96, 129.85, 129.22, 128.96, 128.58, 128.20, 127.66, 127.38, 126.49, 126.36, 125.10, 124.45, 124.00, 120.89, 120.47, 119.53 (q, $J = 322.5$ Hz), 115.37, 113.97, 75.25, 27.32, 21.94.

ATR-IR: 1764.93, 1450.52, 1417.73, 1224.84, 1147.68, 1111.03, 1006.88, 744.55, 619.17 cm^{-1} .

HRMS for: $\text{C}_{27}\text{H}_{20}\text{F}_3\text{NNaO}_5\text{S}$ [$\text{M}+\text{Na}$] $^+$: calcd 550.0906, found 550.0882.

Phenyl(1-((trifluoromethyl)sulfonyl)-1H-indol-3-yl)methyl-1H-imidazole-1-carboxylate



Appearance: Yellowish oil.

^1H NMR (400 MHz, CDCl_3) δ (ppm) = 8.19 (s, 1H), 7.93 (d, $J = 8.4$ Hz, 1H), 7.53–7.40 (m, 8H), 7.34 (t, $J = 7.6$ Hz, 1H), 7.28 (d, $J = 3.1$ Hz, 2H), 7.09 (d, $J = 0.8$ Hz, 1H).

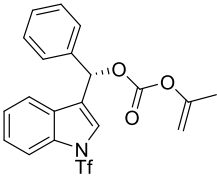
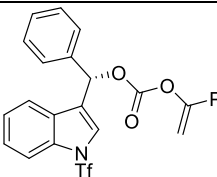
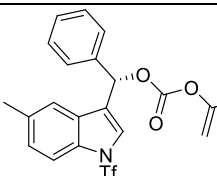
$^{13}\text{C}\{^1\text{H}\}$ NMR (125 MHz, CDCl_3) δ 147.87, 137.11, 135.95, 135.87, 131.04, 129.62, 129.17, 128.38, 127.18, 126.64, 125.32, 125.15, 123.00, 120.60, 119.45 (q, $J = 321.3$ Hz), 118.16, 114.11, 74.80.

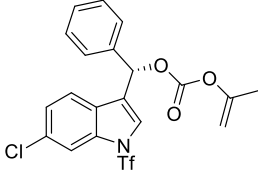
ATR-IR: 1761.07, 1471.74, 1390.72, 1315.50, 1288.49, 1240.27, 1172.76, 1001.09, 763.84, 746.48 cm^{-1} .

HRMS for: $\text{C}_{16}\text{H}_{11}\text{F}_3\text{NO}_2\text{S}$ [$\text{M} - \text{C}_4\text{H}_5\text{O}_3$]: calcd 338.0463, found 338.0469.

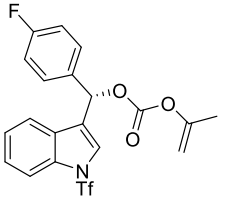
The molecular ion peak wasn't found in standard high resolution mass spectrometry, instead the diarylmethane cation was observed.

2.6 HPLC analysis for enantioenriched materials

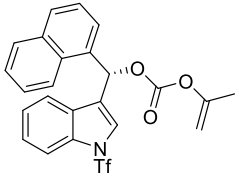
(S)-phenyl(1-((trifluoromethyl)sulfonyl)-1H-indol-3-yl)methyl prop-1-en-2-yl carbonate ((S)-3.11a)	
	HPLC analysis: 85% ee (Chiralcel AD, 99.8:0.2 Hexanes/isopropanol, 0.2 mL/min, 254 nm, major $R_t = 51.6$ min, minor $R_t = 58.9$ min)
(S)-phenyl(1-((trifluoromethyl)sulfonyl)-1H-indol-3-yl)methyl (1-phenylvinyl) carbonate ((S)-3.11o)	
	HPLC analysis: 30% ee (Chiralcel AD-H, 98:2 Hexanes/isopropanol, 0.5 mL/min, 254 nm, major $R_t = 26.0$ min, minor $R_t = 33.4$ min)
(S)-(5-methyl-1-((trifluoromethyl)sulfonyl)-1H-indol-3-yl)(phenyl)methyl prop-1-en-2-yl carbonate ((S)-3.11i)	
	HPLC analysis: 90% ee (Chiralcel AD-H, 99.6:0.4 Hexanes/isopropanol, 0.2 mL/min, 254 nm, major $R_t = 37.9$ min, minor $R_t = 43.4$ min)
(S)-(6-chloro-1-((trifluoromethyl)sulfonyl)-1H-indol-3-yl)(phenyl)methyl prop-1-en-2-yl carbonate ((S)-3.11k)	

	<p>HPLC analysis: 90% ee (Chiralcel AD-H, 99.6:0.4 Hexanes/isopropanol, 0.2 mL/min, 254 nm, major $R_t = 44.1$ min, minor $R_t = 51.6$ min)</p>
---	---

(*S*)-(4-fluorophenyl)(1-((trifluoromethyl)sulfonyl)-1H-indol-3-yl)methyl prop-1-en-2-yl carbonate ((*S*)-3.11c)

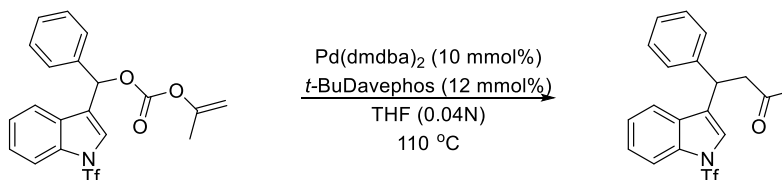
	<p>HPLC analysis: 85% ee (Chiralcel AD-H, 99.6:0.4 Hexanes/isopropanol, 0.2 mL/min, 254 nm, major $R_t = 43.5$ min, minor $R_t = 47.3$ min)</p>
---	---

(*S*)-naphthalen-1-yl(1-((trifluoromethyl)sulfonyl)-1H-indol-3-yl)methyl prop-1-en-2-yl carbonate ((*S*)-3.11g)

	<p>HPLC analysis: 66% ee (Chiralcel AD-H, 99.6:0.4 Hexanes/isopropanol, 0.2 mL/min, 254 nm, major $R_t = 34.3$ min, minor $R_t = 44.2$ min)</p>
--	---

3. General Procedure and Spectral Data of Products

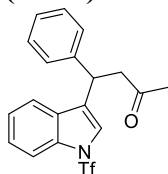
3.1 General Procedure



In a glove box, under an argon atmosphere, a flame dried 25 mL microwave vial with a stir bar was charged with secondary benzylic enol carbonate **3.11a** (88 mg, 0.2 mmol), Pd(dmdba)_2 (10 mmol%, 16.6 mg, 0.02 mmol), $t\text{-BuDavephos}$ (12 mmol%, 8.4 mg, 0.024 mmol) and THF (5 mL, 0.04N). The vial was carefully sealed with a cap and removed from glove box and stirring under 110 °C until the material totally converted. After the solvent was removed under vacuum, the crude product was purified by column chromatography.

3.2 Characterization Data of Products

(3.12a): 4-Phenyl-4-(1-((trifluoromethyl)sulfonyl)-1H-indol-3-yl)butan-2-one



Appearance: Colorless oil, 36 h, 86% yield.

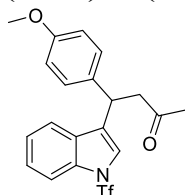
^1H NMR (500 MHz, CDCl_3) δ (ppm) = 7.75 (d, J = 8.4 Hz, 1H), 7.38–7.25 (m, 2H), 7.23–7.20 (m, 1H), 7.19–7.15 (m, 3H), 7.13–7.08 (m, 3H), 4.68 (t, J = 7.2 Hz, 1H), 3.14–3.03 (m, 2H), 1.98 (s, 3H).

$^{13}\text{C}\{^1\text{H}\}$ NMR (125 MHz, CDCl_3) δ (ppm) 205.84, 141.49, 135.94, 130.28, 129.14, 128.91, 127.78, 127.20, 126.10, 124.86, 122.19, 120.81, 119.68 (q, J = 322.5 Hz), 113.86, 49.12, 37.56, 30.68.

ATR-IR: 1718.63, 1450.52, 1415.80, 1359.86, 1282.17, 1230.63, 1205.55, 1147.68, 1112.96, 1022.31, 989.52, 744.55, 702.11, 611.45 cm^{-1} .

HRMS: Calcd for $\text{C}_{19}\text{H}_{16}\text{F}_3\text{NNaO}_3\text{S}$ [$\text{M}+\text{Na}$] $^+$: 418.0695. Found: 418.0690.

(3.12b): 4-(4-methoxyphenyl)-4-(1-((trifluoromethyl)sulfonyl)-1H-indol-3-yl)butan-2-one



Appearance: Colorless oil, 24 h, 84% yield.

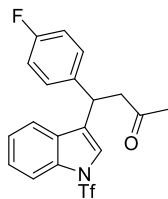
^1H NMR (500 MHz, CDCl_3) δ (ppm) = 7.78 (d, J = 8.3 Hz, 1H), 7.31–7.25 (m, 2H), 7.20–7.16 (m, 1H), 7.14–7.04 (m, 3H), 6.79–6.70 (m, 2H), 4.65 (t, J = 7.0 Hz, 1H), 3.69 (s, 3H), 3.08 (dd, J = 7.3, 2.6 Hz, 2H), 2.03 (s, 3H).

$^{13}\text{C}\{^1\text{H}\}$ NMR (125 MHz, CDCl_3) δ (ppm) = 206.01, 158.52, 135.88, 133.30, 130.18, 128.70, 128.44, 125.99, 124.75, 121.93, 120.76, 119.58 (q, J = 322.5 Hz), 114.17, 113.80, 55.19, 49.20, 36.75, 30.78.

ATR-IR: 1718.63, 1608.69, 1512.24, 1450.52, 1413.87, 1521.84, 1232.55, 1205.55, 1147.68, 1111.03, 1031.95, 748.41, 611.45 cm^{-1} .

HRMS: Calcd for $\text{C}_{20}\text{H}_{18}\text{F}_3\text{NNaO}_4\text{S}$ [$\text{M}+\text{Na}$] $^+$: 448.0801. Found: 448.0807.

(3.12c): 4-(4-fluorophenyl)-4-(1-((trifluoromethyl)sulfonyl)-1H-indol-3-yl)butan-2-one



Appearance: Colorless oil, 48 h, 79% yield.

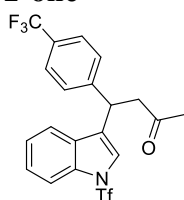
^1H NMR (500 MHz, CDCl_3) δ (ppm) = 7.87 (d, J = 8.4 Hz, 1H), 7.39–7.32 (m, 2H), 7.28–7.22 (m, 3H), 7.18 (s, 1H), 7.04–6.92 (m, 2H), 4.78 (t, J = 7.2 Hz, 1H), 3.18 (qd, J = 16.9, 7.2 Hz, 2H), 2.12 (s, 3H).

$^{13}\text{C}\{^1\text{H}\}$ NMR (125 MHz, CDCl_3) δ 205.52, 161.75 (d, J = 243.8 Hz), 137.13 (d, J = 3.8 Hz), 135.88, 129.97, 129.27 (d, J = 7.5 Hz), 127.95, 126.14, 124.82, 122.04, 120.61, 119.57 (q, J = 321.3 Hz), 115.72 (d, J = 21.3 Hz), 113.86, 49.07, 36.66, 30.71.

ATR-IR: 1718.63, 1604.83, 1508.38, 1450.52, 1415.80, 1282.71, 1232.55, 1205.55, 1147.68, 1112.96, 746.48, 611.45 cm^{-1} .

HRMS: Calcd for $\text{C}_{18}\text{H}_{19}\text{FN}_2\text{O}$ $[\text{M}+\text{NH}_4\text{-Tf}]^+$: 298.1481. Found: 298.1493.

(3.12d): 4-(4-(trifluoromethyl)phenyl)-4-(1-((trifluoromethyl)sulfonyl)-1H-indol-3-yl)butan-2-one



Appearance: Colorless oil, 72 h, 68% yield.

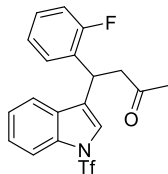
^1H NMR (400 MHz, CDCl_3) δ (ppm) = 7.87 (d, J = 8.4 Hz, 1H), 7.56 (d, J = 8.1 Hz, 2H), 7.42–7.36 (m, 3H), 7.35–7.26 (m, 2H), 7.22 (s, 1H), 4.87 (t, J = 7.1 Hz, 1H), 3.29–3.15 (m, 2H), 2.14 (s, 3H).

$^{13}\text{C}\{^1\text{H}\}$ NMR (125 MHz, CDCl_3) δ 205.02, 145.57, 135.87, 129.80, 129.42 (q, J = 32.5 Hz), 128.18, 127.22, 126.31, 125.85 (q, J = 3.8 Hz), 124.93, 123.95 (q, J = 270.0 Hz), 122.27, 120.45, 119.56 (q, J = 322.5 Hz), 113.94, 48.75, 37.01, 30.62.

ATR-IR: 1720.56, 1618.33, 1450.52, 1415.80, 1325.14, 1232.55, 1207.28, 1165.02, 1149.61, 1112.96, 1068.60, 1018.45, 742.62, 609.53 cm^{-1} .

HRMS : Calcd for $\text{C}_{19}\text{H}_{16}\text{F}_3\text{NNaO}$ $[\text{M}+\text{Na-Tf}]^+$: 354.1082. Found: 354.1849.

(3.12e): 4-(2-fluorophenyl)-4-(1-((trifluoromethyl)sulfonyl)-1H-indol-3-yl)butan-2-one



Appearance: Colorless oil, 72 h, 43% yield.

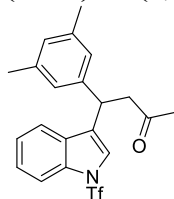
^1H NMR (500 MHz, CDCl_3) δ (ppm) = 7.55 (dd, $J = 9.2, 2.2$ Hz, 1H), 7.28–7.16 (m, 7H), 6.96 (td, $J = 8.9, 2.3$ Hz, 1H), 4.72 (t, $J = 7.2$ Hz, 1H), 3.19–3.10 (m, 2H), 2.08 (s, 3H).

$^{13}\text{C}\{^1\text{H}\}$ NMR (125 MHz, CDCl_3) δ 205.67, 162.47 (d, $J = 6.3$ Hz), 141.26, 136.14 (q, $J = 12.5$ Hz), 128.96, 127.93, 127.69, 127.30, 126.53, 126.51, 122.32, 121.77 (q, $J = 8.8$ Hz), 119.56 (q, $J = 322.5$ Hz), 113.35 (q, $J = 23.8$ Hz), 101.68 (q, $J = 28.7$ Hz), 49.11, 37.47, 30.72.

ATR-IR: 1714.77, 1614.47, 1487.17, 1415.80, 1269.20, 1232.55, 1207.48, 1147.68, 1097.53, 997.23, 900.79, 746.48, 702.11 cm^{-1} .

HRMS: Calcd for $\text{C}_{19}\text{H}_{19}\text{F}_4\text{N}_2\text{O}_3\text{S}$ $[\text{M}+\text{NH}_4]^+$: 431.1047. Found: 431.1043.

(3.12f): 4-(3,5-Dimethylphenyl)-4-(1-((trifluoromethyl)sulfonyl)-1H-indol-3-yl)butan-2-one



Appearance: White foam, 72 h, 56% yield.

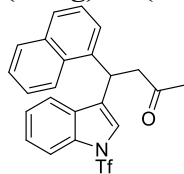
^1H NMR (500 MHz, CDCl_3) δ (ppm) = 7.86 (d, $J = 8.3$ Hz, 1H), 7.43 (d, $J = 7.9$ Hz, 1H), 7.37–7.34 (m, 1H), 7.28 (dd, $J = 10.2, 3.1$ Hz, 1H), 7.18 (s, 1H), 6.87 (s, 2H), 6.85 (s, 1H), 4.70 (t, $J = 7.1$ Hz, 1H), 3.21–3.13 (m, 2H), 2.26 (s, 6H), 2.12 (s, 3H).

$^{13}\text{C}\{^1\text{H}\}$ NMR (125 MHz, CDCl_3) δ 205.91, 141.23, 138.27, 135.83, 130.33, 128.82, 128.36, 125.96, 125.41, 124.78, 121.97, 120.74, 119.56 (q, $J = 321.3$ Hz), 113.76, 49.26, 37.33, 30.66, 21.30.

ATR-IR: 1714.77, 1643.41, 1415.80, 1230.63, 1205.55, 1147.68, 1111.03, 744.55, 646.17, 609.53, 578.66 cm^{-1} .

HRMS: Calcd for $\text{C}_{21}\text{H}_{20}\text{F}_3\text{NNaO}_3\text{S}$ $[\text{M}+\text{Na}]^+$: 446.1014. Found: 446.1001.

(3.12g): 4-(Naphthalen-1-yl)-4-(1-((trifluoromethyl)sulfonyl)-1H-indol-3-yl)butan-2-one



Appearance: Colorless oil, 48 h, 70% yield.

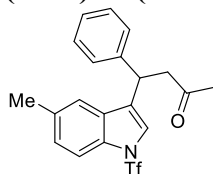
^1H NMR (500 MHz, CDCl_3) δ (ppm) = 8.14 (d, J = 8.4 Hz, 1H), 7.82–7.77 (m, 2H), 7.67 (d, J = 8.2 Hz, 1H), 7.46 (dddd, J = 23.0, 7.9, 6.9, 1.3 Hz, 2H), 7.25 (dt, J = 8.7, 4.3 Hz, 2H), 7.19–7.13 (m, 2H), 7.09 (ddd, J = 8.0, 6.4, 0.9 Hz, 2H), 5.56 (dd, J = 7.9, 6.0 Hz, 1H), 3.21 (ddd, J = 23.1, 17.5, 7.0 Hz, 2H), 2.09 (s, 3H).

$^{13}\text{C}\{^1\text{H}\}$ NMR (125 MHz, CDCl_3) δ 205.76, 137.16, 135.92, 134.14, 130.88, 130.25, 129.18, 128.10, 127.92, 126.64, 126.08, 125.87, 125.41, 124.81, 124.73, 122.92, 122.69, 120.70, 119.57 (q, J = 322.5 Hz), 113.82, 48.81, 32.72, 30.45.

ATR-IR: 1714.77, 1450.52, 1415.80, 1359.86, 1282.71, 1230.63, 1205.55, 1165.04, 1147.68, 1112.96, 1030.02, 792.77, 746.48, 613.38 cm^{-1} .

HRMS: Calcd for $\text{C}_{23}\text{H}_{18}\text{F}_3\text{NNaO}_3\text{S}$ $[\text{M}+\text{Na}]^+$: 468.0852. Found: 468.0871.

(3.12i): 4-(5-Methyl-1-((trifluoromethyl)sulfonyl)-1H-indol-3-yl)-4-phenylbutan-2-one



Appearance: White foam, 36 h, 90% yield.

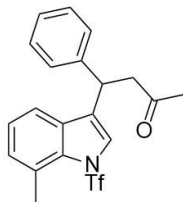
^1H NMR (500 MHz, CDCl_3) δ (ppm) = 7.65 (d, J = 9.0 Hz, 1H), 7.26–7.19 (m, 4H), 7.17–7.13 (m, 1H), 7.08 (dd, J = 11.7, 6.7 Hz, 3H), 4.68 (t, J = 7.0 Hz, 1H), 3.10 (dd, J = 7.3, 2.3 Hz, 2H), 2.29 (s, 3H), 2.03 (s, 3H).

$^{13}\text{C}\{^1\text{H}\}$ NMR (125 MHz, CDCl_3) δ 205.83, 141.38, 134.64, 133.99, 130.37, 128.84, 127.97, 127.65, 127.38, 127.11, 122.19, 120.48, 119.60 (q, J = 322.5 Hz), 113.45, 49.20, 37.40, 30.70, 21.35.

ATR-IR: 1716.70, 1413.87, 1230.63, 1205.55, 1153.47, 1112.96, 700.18, 632.67, 617.24, 584.45 cm^{-1} .

HRMS : Calcd for $\text{C}_{20}\text{H}_{18}\text{F}_3\text{NNaO}_3\text{S}$ $[\text{M}+\text{Na}]^+$: 432.0892. Found: 432.0896.

(3.12j): 4-(7-Methyl-1-((trifluoromethyl)sulfonyl)-1H-indol-3-yl)-4-phenylbutan-2-one



Appearance: Beige solid, mp. 74.3-77.0 $^{\circ}\text{C}$, 48 h, 87% yield.

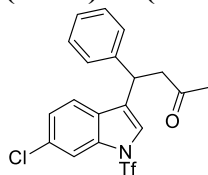
^1H NMR (500 MHz, CDCl_3) δ 7.32–7.24 (m, 6H), 7.22 (s, 1H), 7.18–7.12 (m, 2H), 4.74 (t, J = 7.2 Hz, 1H), 3.24–3.10 (m, 2H), 2.66 (s, 3H), 2.11 (s, 3H).

$^{13}\text{C}\{^1\text{H}\}$ NMR (126 MHz, CDCl_3) δ 205.76, 141.44, 135.67, 132.42, 130.28, 128.84, 127.99, 127.69, 127.10, 125.72, 125.27, 125.15, 118.56, 49.18, 37.40, 30.73, 21.82 (d, J = 1.6 Hz).

ATR-IR: 1718.10, 1414.14, 1230.39, 1203.79, 1144.90, 1109.73, 1083.39, 535.30, 466.68 cm^{-1} .

HRMS: Calcd for $\text{C}_{20}\text{H}_{18}\text{F}_3\text{NNaO}_3\text{S}$ $[\text{M}+\text{Na}]^+$: 432.0857, Found: 432.0868.

(3.12k): 4-(6-Chloro-1-((trifluoromethyl)sulfonyl)-1H-indol-3-yl)-4-phenylbutan-2-one



Appearance: White solid, mp. 139–141 $^\circ\text{C}$, 72 h, 91% yield.

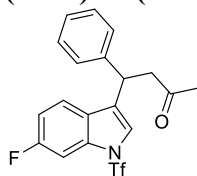
^1H NMR (500 MHz, CDCl_3) δ (ppm) = 7.80 (d, J = 1.6 Hz, 1H), 7.24–7.14 (m, 8H), 7.11 (d, J = 0.5 Hz, 1H), 4.67 (t, J = 6.9 Hz, 1H), 3.10 (dd, J = 7.2, 1.1 Hz, 2H), 2.04 (s, 3H).

$^{13}\text{C}\{^1\text{H}\}$ NMR (125 MHz, CDCl_3) δ 205.56, 141.11, 136.19, 132.27, 128.94, 128.72, 127.86, 127.63, 127.30, 125.57, 122.50, 121.55, 119.78 (q, J = 322.5 Hz), 114.14, 49.03, 37.36, 30.71.

ATR-IR: 1716.70, 1417.73, 1284.63, 1207.48, 1151.54, 1118.75, 1072.46, 991.44, 813.99, 702.11, 626.89, 601.81 cm^{-1} .

HRMS: Calcd for $\text{C}_{18}\text{H}_{20}\text{ClN}_2\text{O}$ $[\text{M}+\text{H}]^+$: 315.1264. Found: 315.1288.

(3.12l): 4-(6-Fluoro-1-((trifluoromethyl)sulfonyl)-1H-indol-3-yl)-4-phenylbutan-2-one



Appearance: Yellowish oil, 72 h, 83% yield.

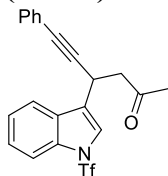
^1H NMR (400 MHz, CDCl_3) δ (ppm) = 7.50 (dd, J = 9.3, 2.2 Hz, 1H), 7.24–7.14 (m, 6H), 7.10 (s, 1H), 6.91 (td, J = 8.9, 2.3 Hz, 1H), 4.66 (t, J = 6.9 Hz, 1H), 3.09 (dd, J = 7.2, 1.9 Hz, 2H), 2.03 (s, 3H).

$^{13}\text{C}\{^1\text{H}\}$ NMR (100 MHz, CDCl_3) δ 205.58, 162.41 (d, J = 244.0 Hz), 141.21, 136.10 (d, J = 12.0 Hz), 128.90, 127.88, 127.63, 127.24, 126.47 (d, J = 1.0 Hz), 122.26 (d, J = 4.1 Hz), 121.70 (d, J = 10.0 Hz), 119.51 (q, J = 322.0 Hz), 113.27 (d, J = 24.0 Hz), 101.64 (d, J = 39.0 Hz), 49.06, 37.43, 30.64.

ATR-IR: 1716.7, 1487.17, 1417.73, 1232.55, 1207.48, 1147.68, 1099.46, 478.36, 464.86, 403.14 cm^{-1} .

HRMS: Calcd for $\text{C}_{19}\text{H}_{19}\text{F}_4\text{N}_2\text{O}_3\text{S}$ $[\text{M}+\text{NH}_4]^+$: 431.1503. Found: 431.1573.

(3.12m): 6-Phenyl-4-(1-((trifluoromethyl)sulfonyl)-1H-indol-3-yl)hex-5-yn-2-one



Appearance: Yellow oil, 48 h, 44% yield.

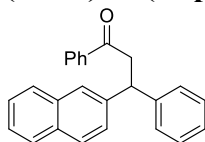
^1H NMR (500 MHz, CDCl_3) δ (ppm) = 7.84 (dd, J = 7.3, 1.3 Hz, 1H), 7.76–7.73 (m, 1H), 7.37–7.31 (m, 5H), 7.25–7.21 (m, 3H), 4.60 (ddd, J = 8.0, 5.8, 0.7 Hz, 1H), 3.10 (dd, J = 16.9, 8.1 Hz, 1H), 2.99 (dd, J = 16.9, 5.8 Hz, 1H), 2.16 (s, 3H).

$^{13}\text{C}\{^1\text{H}\}$ NMR (125 MHz, CDCl_3) δ ^{13}C NMR (126 MHz, CDCl_3) δ 204.91, 136.01, 131.71, 129.15, 128.35, 128.32, 126.16, 124.88, 124.63, 123.27, 122.73, 120.41, 119.56 (q, J = 322.5 Hz), 114.12, 88.13, 83.05, 48.85, 30.63, 24.62.

ATR-IR: 1720.56, 1450.52, 1415.80, 1361.79, 1280.78, 1232.55, 1205.55, 1147.68, 1111.03, 987.56, 758.03, 609.53 cm^{-1} .

HRMS (ESI): Calcd for $\text{C}_{25}\text{H}_{24}\text{LiN}_2\text{O}_2\text{S}$ $[\text{M}+\text{Li}-\text{Tf}]^+$: 293.1186. Found: 293.1147.

(3.12n): 3-(Naphthalen-2-yl)-1,3-diphenylpropan-1-one (4ad) [CAS : 1198215-04-1]



Appearance: Colorless oil, 72 h, 88% yield.

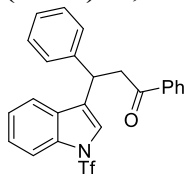
^1H NMR (500 MHz, CDCl_3) δ (ppm) = 8.03–7.91 (m, 2H), 7.83–7.68 (m, 4H), 7.56 (ddd, J = 6.8, 4.0, 1.2 Hz, 1H), 7.48–7.39 (m, 5H), 7.36–7.27 (m, 4H), 7.22–7.17 (m, 1H), 5.02 (t, J = 7.3 Hz, 1H), 3.92–3.80 (m, 2H).

$^{13}\text{C}\{^1\text{H}\}$ NMR (125 MHz, CDCl_3) δ 197.91, 143.96, 141.52, 136.99, 133.42, 133.10, 132.15, 128.61, 128.59, 128.56, 128.25, 128.04, 127.94, 127.74, 127.53, 126.73, 126.43, 125.99, 125.73, 125.51, 45.93, 44.54.

ATR-IR: 1714.77, 1597.11, 1248.60, 1182.40, 1074.39, 1022.31, 599.89 cm^{-1} .

HRMS : Calcd for $\text{C}_{25}\text{H}_{20}\text{NaO}$ $[\text{M}+\text{Na}]^+$: 359.1406. Found: 359.1414.

(3.12o): 1,3-Diphenyl-3-(1-((trifluoromethyl)sulfonyl)-1H-indol-3-yl)propan-1-one



Appearance: White solid, mp. 107-109 °C, 15 h, 95% yield.

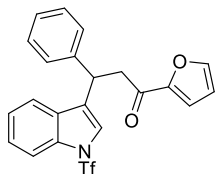
^1H NMR (500 MHz, CDCl_3) δ (ppm) = 7.96–7.91 (m, 2H), 7.87 (d, J = 8.4 Hz, 1H), 7.56 (d, J = 7.4 Hz, 1H), 7.48–7.41 (m, 3H), 7.38–7.26 (m, 6H), 7.24–7.18 (m, 2H), 5.03 (t, J = 7.0 Hz, 1H), 3.74 (d, J = 7.1 Hz, 2H).

$^{13}\text{C}\{^1\text{H}\}$ NMR (125 MHz, CDCl_3) δ (ppm) 197.18, 141.63, 136.67, 135.88, 133.39, 130.31, 128.84, 128.69, 128.30, 128.01, 127.77, 127.10, 126.00, 124.78, 122.22, 120.77, 119.56 (q, J = 322.5 Hz), 113.81, 44.31, 37.59.

ATR-IR: 1685.84, 1450.52, 1413.87, 1282.71, 1230.63, 1205.55, 1147.68, 1111.03, 991.44, 617.24 cm^{-1} .

HRMS: Calcd for $\text{C}_{24}\text{H}_{18}\text{F}_3\text{NNaO}_3\text{S}$ $[\text{M}+\text{Na}]^+$: 480.0857. Found: 480.0865.

(3.12p): 1-(Furan-2-yl)-3-phenyl-3-(1-((trifluoromethyl)sulfonyl)-1H-indol-3-yl)propan-1-one



Appearance: Yellow solid, mp. 127-130 °C, 15 h, 99% yield.

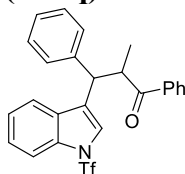
^1H NMR (500 MHz, CDCl_3) δ (ppm) = ^1H NMR (500 MHz, CDCl_3) δ 7.85 (d, J = 8.4 Hz, 1H), 7.57 (dd, J = 1.7, 0.7 Hz, 1H), 7.40 (dd, J = 7.9, 0.7 Hz, 1H), 7.37–7.24 (m, 7H), 7.24–7.19 (m, 1H), 7.17 (dd, J = 3.6, 0.7 Hz, 1H), 6.52 (dd, J = 3.6, 1.7 Hz, 1H), 4.97 (t, J = 7.3 Hz, 1H), 3.59 (ddd, J = 38.9, 16.3, 7.4 Hz, 2H).

$^{13}\text{C}\{^1\text{H}\}$ NMR (125 MHz, CDCl_3) δ (ppm) = 186.47, 152.68, 146.62, 141.39, 135.89, 130.30, 128.86, 128.04, 127.80, 127.18, 126.04, 124.81, 122.38, 120.83, 119.60 (q, J = 322.5 Hz), 117.46, 113.81, 112.54, 43.95, 37.66.

ATR-IR: 1670.41, 1570.11, 1467.88, 1413.87, 1286.56, 1230.63, 1203.62, 1147.68, 1112.96, 700.18, 617.24 cm^{-1} .

HRMS : Calcd for $\text{C}_{22}\text{H}_{16}\text{F}_3\text{NNaO}_4\text{S}$ $[\text{M}+\text{Na}]^+$: 470.0644. Found: 470.0640.

(3.12q): 2-Methyl-1,3-diphenyl-3-(1-((trifluoromethyl)sulfonyl)-1H-indol-3-yl)propan-1-one



Appearance: White solid, mp. 144-146 °C, 15 h, 95% yield, d.r. = 3:1.

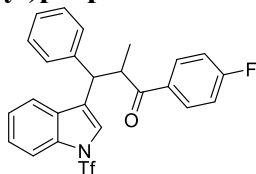
^1H NMR (500 MHz, CDCl_3) δ (ppm) = 7.90 (dd, J = 8.4, 1.2 Hz, 2H, minor), 7.81 (d, J = 8.2 Hz, 1H, major), 7.80–7.74 (m, 2H, major), 7.67 (d, J = 8.2 Hz, 1H, minor), 7.55 (dd, J = 7.2, 0.7 Hz, 1H, major), 7.52 (d, J = 1.3 Hz, 2H, minor), 7.47–7.42 (m, 1H, major+minor), 7.41–7.18 (m, 7H, major+minor), 7.17–7.14 (m, 2H, minor), 7.08–7.03 (m, 2H, major), 7.00–6.93 (m, 1H, major+minor), 4.65 (d, J = 10.8 Hz, 1H, major), 4.60 (d, J = 10.9 Hz, 1H, minor), 4.35 (dq, J = 10.9, 6.9 Hz, 1H, major), 4.15 (dd, J = 10.9, 7.0 Hz, 0H, minor), 1.22 (d, J = 6.9 Hz, 3H, major), 1.05 (d, J = 7.0 Hz, 3H, minor).

$^{13}\text{C}\{^1\text{H}\}$ NMR (125 MHz, CDCl_3) δ (ppm) = 202.69, 202.57, 140.92, 140.13, 136.54, 136.10, 135.62, 135.47, 133.53, 133.11, 130.82, 130.62, 128.93, 128.79, 128.61, 128.54, 128.06, 127.96, 126.95, 126.79, 126.07, 125.98, 124.88, 124.73, 122.55, 121.25, 120.76, 120.52, 119.60 (q, J = 321.3 Hz), 119.35 (q, J = 321.3 Hz), 113.87, 113.52, 45.12, 45.09, 44.85, 44.77, 17.72, 17.65.

ATR-IR: 1683.91, 1676.20, 1448.59, 1413.87, 1282.71, 1230.63, 1205.55, 1147.68, 1111.03, 970.23, 742.62, 700.18 cm^{-1} .

HRMS: Calcd for $\text{C}_{25}\text{H}_{20}\text{F}_3\text{NNaO}_3\text{S}$ [$\text{M}+\text{Na}$] $^+$: 494.1008. Found: 494.1003.

(3.12r): 1-(4-Fluorophenyl)-2-methyl-3-phenyl-3-(1-((trifluoromethyl)sulfonyl)-1H-indol-3-yl)propan-1-one



Appearance: White foam, 24 h, 83% yield, d.r. = 3.5:1.

^1H NMR (500 MHz, CDCl_3) δ (ppm) = 7.92–7.81 (m, 3H), 7.61 (d, J = 7.7 Hz, 1H), 7.42 (s, 1H), 7.39–7.35 (m, 1H), 7.34–7.30 (m, 1H), 7.25 (dd, J = 4.7, 4.1 Hz, 2H), 7.13 (t, J = 7.7 Hz, 2H), 7.09–6.98 (m, 3H), 4.69 (d, J = 10.9 Hz, 1H), 4.37 (dq, J = 11.0, 6.8 Hz, 1H), 1.29 (d, J = 6.8 Hz, 3H).

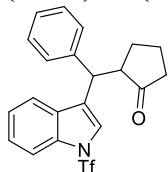
$^{13}\text{C}\{^1\text{H}\}$ NMR (125 MHz, CDCl_3) δ (ppm) = 201.19, 165.71 (d, J = 253.8 Hz), 140.78, 135.62, 132.95 (d, J = 2.5 Hz), 130.79, 130.71 (d, J = 10.0 Hz), 128.57, 127.93, 126.89, 126.81, 126.12, 124.91, 122.49, 120.47, 119.60 (q, J = 322.5 Hz), 115.72 (d, J = 21.3 Hz), 113.88, 45.24, 44.78, 17.62.

ATR-IR: 1683.91, 1676.20, 1448.59, 1413.87, 1282.71, 1230.63, 1205.55, 1147.68, 1111.03,

970.23, 742.62, 700.18 cm^{-1} .

HRMS: Calcd for $\text{C}_{25}\text{H}_{19}\text{F}_4\text{NNaO}_3\text{S}$ $[\text{M}+\text{Na}]^+$: 512.0914. Found: 512.1005.

(3.12s): 2-(Phenyl(1-((trifluoromethyl)sulfonyl)-1H-indol-3-yl)methyl)cyclopentan-1-one



Appearance: Colorless oil, 18 h, 89% yield, d.r. = 2:1.

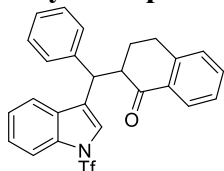
^1H NMR (500 MHz, CDCl_3) δ (ppm) = 7.89 (d, J = 8.4 Hz, 1H), 7.37–7.33 (m, 2H), 7.28–7.23 (m, 3H), 7.19 (td, J = 7.6, 0.9 Hz, 1H), 7.15–7.08 (m, 3H), 4.95–4.90 (m, 1H), 2.94–2.85 (m, 1H), 2.39–2.25 (m, 2H), 1.90–1.77 (m, 3H), 1.73–1.65 (m, 1H).

$^{13}\text{C}\{^1\text{H}\}$ NMR (100 MHz, CDCl_3) δ (ppm) 192.01, 138.88, 135.77, 130.61, 129.13, 128.57, 127.68, 127.23, 125.98, 124.73, 122.55, 121.23, 119.69 (q, J = 322.5 Hz), 113.71, 52.77, 41.27, 38.35, 26.00, 20.60.

ATR-IR: 1714.77, 1415.80, 1267.27, 1230.63, 1205.55, 1153.47, 1112.96, 750.33, 700.18, 659.68, 632.67, 617.24 cm^{-1} .

HRMS: Calcd for $\text{C}_{21}\text{H}_{18}\text{F}_3\text{NNaO}_3\text{S}$ $[\text{M}+\text{Na}]^+$: 444.0852. Found: 444.0865.

(3.12t): 2-(phenyl(1-((trifluoromethyl)sulfonyl)-1H-indol-3-yl)methyl)-3,4-dihydronaphthalen-1(2H)-one



Appearance: Yellow oil, 18 h, 94% yield.

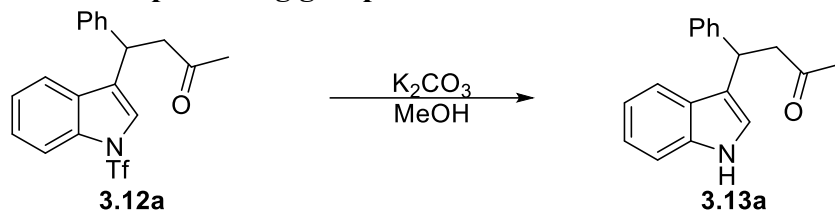
^1H NMR (500 MHz, CDCl_3) δ (ppm) = 7.92 (dd, J = 7.9, 1.2 Hz, 1H), 7.79 (d, J = 8.4 Hz, 1H), 7.38 (td, J = 7.5, 1.4 Hz, 1H), 7.29 (d, J = 0.7 Hz, 1H), 7.27–7.19 (m, 5H), 7.18–7.11 (m, 5H), 5.14 (dd, J = 5.5, 1.1 Hz, 1H), 3.25 (ddd, J = 12.4, 5.5, 4.1 Hz, 1H), 2.97 (ddt, J = 16.9, 8.6, 5.6 Hz, 2H), 2.12 (dq, J = 13.0, 4.2 Hz, 1H), 1.70–1.61 (m, 1H).

$^{13}\text{C}\{^1\text{H}\}$ NMR (125 MHz, CDCl_3) δ (ppm) = 197.54, 143.37, 139.47, 135.69, 133.46, 132.59, 130.84, 129.10, 128.66, 128.51, 127.89, 127.70, 127.06, 126.73, 125.89, 124.67, 122.04, 121.04, 119.64 (q, J = 322.5 Hz), 113.70, 51.62, 40.49, 28.84, 26.43.

ATR-IR: 1685.84, 1599.04, 1450.52, 1413.87, 1278.85, 1230.63, 1205.55, 1147.68, 1112.96, 989.52, 744.55, 704.04, 607.60, 576.74, 526.58 cm^{-1} .

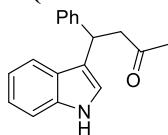
HRMS: Calcd for C₂₆H₂₀F₃NNaO₃S [M+Na]⁺: 506.1008. Found: 506.1025.

3.3 Removal of the Tf protecting group.



Procedure: To an oven-dried 10 mL flask with a stir bar under Ar atmosphere, the ketone product **3.12a** (0.2 mmol), K₂CO₃ (138 mg, 1 mmol), 3 ml MeOH was added. The resulting mixture was stirred at 65 °C until the **3.12a** totally disappeared (about 4 h). The mixture was filtered and washed with EtOAc. The filtrate was concentrated in vacuum and the residue was purified via flash column chromatography (EA:PE = 1:5) to give the product **3.13a** in 97% yield as colorless oil.

4-(1H-indol-3-yl)-4-phenylbutan-2-one (**3.13a**) [CAS : 21909-35-3]



Appearance: Colorless oil, 4 h, 97% yield.

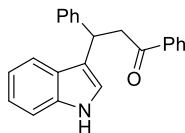
¹H NMR (500 MHz, CDCl₃) δ (ppm) = 8.03–7.97 (b, 1H), 7.39 (dd, *J* = 7.9, 0.7 Hz, 1H), 7.24 (ddd, *J* = 11.2, 8.8, 4.4 Hz, 5H), 7.18–7.06 (m, 2H), 6.99 (ddd, *J* = 8.0, 7.1, 0.9 Hz, 1H), 6.96–6.89 (m, 1H), 4.80 (t, *J* = 7.6 Hz, 1H), 3.17 (ddd, *J* = 44.3, 16.1, 7.6 Hz, 2H), 2.04 (s, 3H).

¹³C{¹H} NMR (125 MHz, CDCl₃) δ = 207.72, 143.89, 136.51, 128.44, 127.65, 126.45, 126.34, 122.13, 121.31, 119.37, 118.73, 111.12, 50.28, 38.32, 30.35.

ATR-IR: 1707.06, 1492.95, 1454.38, 1415.80, 1356.00, 1336.71, 1240.27, 1161.19, 1099.46, 1010.73, 738.76, 700.18, 472.58 cm⁻¹.

HRMS : Calcd for C₁₈H₁₇NNaO [M+Na]⁺: 286.1602. Found: 286.1673.

3-(1H-indol-3-yl)-1,3-diphenylpropan-1-one (**3.13o**) [CAS : 5884-15-1]



Appearance: Colorless oil, 4 h, 98% yield.

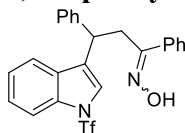
^1H NMR (500 MHz, CDCl_3) δ (ppm) = 7.98 (s, 1H), 7.94 (dd, J = 8.3, 1.2 Hz, 2H), 7.57–7.52 (m, 1H), 7.48–7.41 (m, 3H), 7.38–7.34 (m, 2H), 7.32 (d, J = 8.2 Hz, 1H), 7.28–7.25 (m, 2H), 7.21–7.13 (m, 2H), 7.05–7.00 (m, 1H), 6.99 (d, J = 2.3 Hz, 1H), 5.08 (t, J = 7.2 Hz, 1H), 3.78 (ddd, J = 24.4, 16.7, 7.2 Hz, 2H).

$^{13}\text{C}\{^1\text{H}\}$ NMR (125 MHz, CDCl_3) δ = 198.54, 144.18, 137.06, 136.56, 133.00, 128.55, 128.41, 128.08, 127.80, 126.58, 126.27, 122.12, 121.38, 119.52, 119.37, 119.26, 111.08, 45.16, 38.16.

ATR-IR: 1681.98, 1597.11, 1492.95, 1448.59, 1415.80, 1230.63, 1205.55, 1153.47, 746.48, 700.18 cm^{-1} .

HRMS: Calcd for $\text{C}_{23}\text{H}_{19}\text{NNaO}$ $[\text{M}+\text{Na}]^+$: 348.1364. Found: 348.1384.

1,3-diphenyl-3-(1-((trifluoromethyl)sulfonyl)-1H-indol-3-yl)propan-1-one oxime



Appearance: Colorless oil, 12 h, 90% yield, E/Z = 10:1.

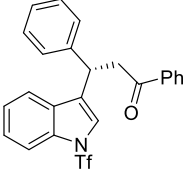
^1H NMR (400 MHz, CDCl_3) δ (ppm) = 9.20–8.80 (b, 1H), 7.75 (d, J = 8.4 Hz, 1H), 7.46 (s, 1H), 7.26–7.19 (m, 6H), 7.16–7.06 (m, 7H), 4.51 (t, J = 7.8 Hz, 1H), 3.73 (dd, J = 13.6, 8.3 Hz, 1H), 3.23 (dd, J = 13.6, 7.5 Hz, 1H).

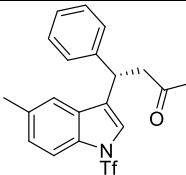
$^{13}\text{C}\{^1\text{H}\}$ NMR (100 MHz, CDCl_3) δ = 157.98, 141.49, 135.84, 135.30, 130.43, 129.25, 128.68, 128.53, 127.66, 127.19, 127.13, 126.49, 125.73, 124.53, 122.80, 120.77, 119.61 (q, J = 322.0), 113.68, 39.45, 32.38.

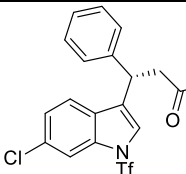
3.4 HPLC analysis for enantioenriched products

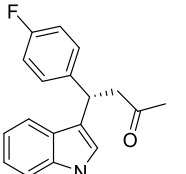
(S)-4-phenyl-4-(1-((trifluoromethyl)sulfonyl)-1H-indol-3-yl)butan-2-one	
	HPLC analysis: 80% ee (Chiralcel OD-H, 98:2 Hexanes/isopropanol, 0.5 mL/min, 254 nm, major R_t = 29.1 min, minor R_t = 49.2 min)

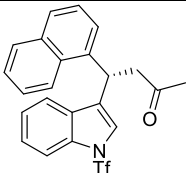
(S)-1,3-diphenyl-3-(1-((trifluoromethyl)sulfonyl)-1H-indol-3-yl)propan-1-one
--

	HPLC analysis: 31% ee (Chiralcel AD-H, 99:1 Hexanes/isopropanol, 0.5 mL/min, 254 nm, major $R_t = 25.2$ min, minor $R_t = 30.0$ min)
---	---

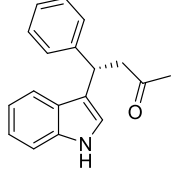
(S)-4-(5-methyl-1-((trifluoromethyl)sulfonyl)-1H-indol-3-yl)-4-phenylbutan-2-one	
	HPLC analysis: 91% ee (Chiralcel AD-H, 98:2 Hexanes/isopropanol, 0.5 mL/min, 254 nm, major $R_t = 24.4$ min, minor $R_t = 31.8$ min)

(S)-4-(6-chloro-1-((trifluoromethyl)sulfonyl)-1H-indol-3-yl)-4-phenylbutan-2-one	
	HPLC analysis: 90% ee (Chiralcel OD, 98:2 Hexanes/isopropanol, 0.5 mL/min, 254 nm, major $R_t = 40.8$ min, minor $R_t = 73.3$ min)

(S)-4-(4-fluorophenyl)-4-(1-((trifluoromethyl)sulfonyl)-1H-indol-3-yl)butan-2-one	
	HPLC analysis: 83% ee (Chiralcel OD, 99:1 Hexanes/isopropanol, 0.2 mL/min, 254 nm, major $R_t = 77.7$ min, minor $R_t = 89.2$ min)

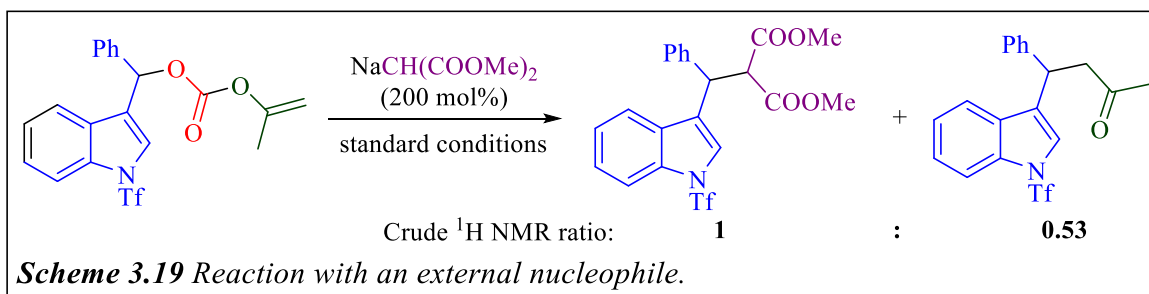
(S)-4-(naphthalen-1-yl)-4-(1-((trifluoromethyl)sulfonyl)-1H-indol-3-yl)butan-2-one	
	HPLC analysis: 63% ee (Chiralcel AD-H, 98:2 Hexanes/isopropanol, 0.2 mL/min, 254 nm, major $R_t = 17.7$ min, minor $R_t = 13.5$ min)

(S)-4-(1H-indol-3-yl)-4-phenylbutan-2-one	
---	--

	<p>HPLC analysis: 81% ee (Chiralcel AD-H, 95:5 Hexanes/isopropanol, 0.5 mL/min, 254 nm, major $R_t = 73.2$ min, minor $R_t = 67.0$ min)</p>
---	---

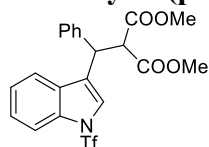
4. Crossover studies

4.1 Nucleophile obstruction experiment:



Procedure: In a glove box, under an argon atmosphere, a flame dried 25 mL microwave vial with a stir bar was charged with dimethyl malonate and 5 mL THF. NaH was added and stirred for 10 min until no more gas generated. After that, secondary benzylic enol carbonate **3.11a** (88 mg, 0.2 mmol), Pd(dmdba)₂ (10 mmol%, 0.02 mmol), *t*-BuDavephos (12 mmol%, 0.024 mmol) was added. The vial was carefully sealed with a cap and removed from glove box and stirring under 110 °C until the material totally disappeared. The conversion and ratio of products determined by ^1H NMR spectroscopy of the crude mixture. After the solvent was removed under vacuum, the malonate substitution product was separated by column chromatography.

Dimethyl 2-(phenyl(1-((trifluoromethyl)sulfonyl)-1H-indol-3-yl)methyl)malonate (**3.14a**)



Appearance: Colorless oil, 6 h, 68% yield.

^1H NMR (500 MHz, CDCl_3) δ (ppm) = 7.85 (d, $J = 8.3$ Hz, 1H), 7.48 (d, $J = 7.8$ Hz, 1H), 7.39 (s, 1H), 7.37–7.32 (m, 3H), 7.30–7.25 (m, 3H), 7.22 (ddd, $J = 7.1, 3.9, 1.4$ Hz, 1H), 5.05–5.01 (m, 1H), 4.25 (d, $J = 11.6$ Hz, 1H), 3.65 (s, 3H), 3.52 (s, 3H).

$^{13}\text{C}\{^1\text{H}\}$ NMR (125 MHz, CDCl_3) δ = 167.71, 167.31, 138.14, 135.55, 130.03, 128.76, 128.17, 127.71, 126.23, 126.04, 124.88, 121.66, 120.52, 119.53 (q, $J = 322.5$ Hz), 113.69, 57.18, 52.80, 52.66, 42.38.

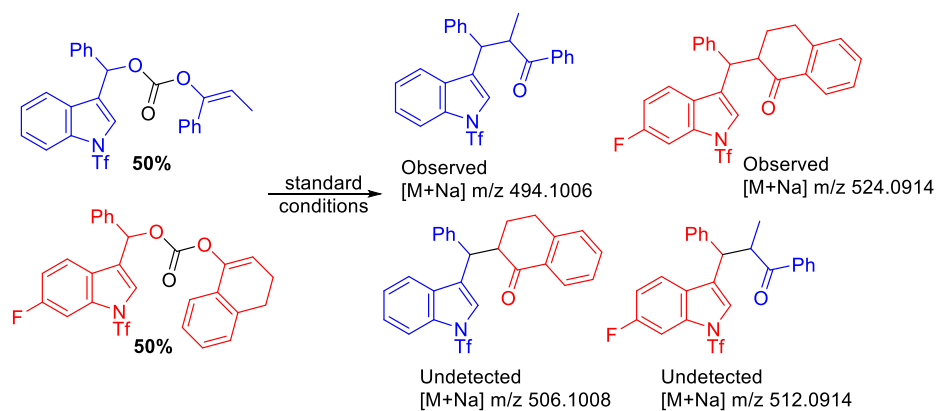
ATR-IR: 1759.14, 1737.92, 1450.52, 1415.80, 1263.42, 1232.55, 1201.69, 1166.97, 1149.61,

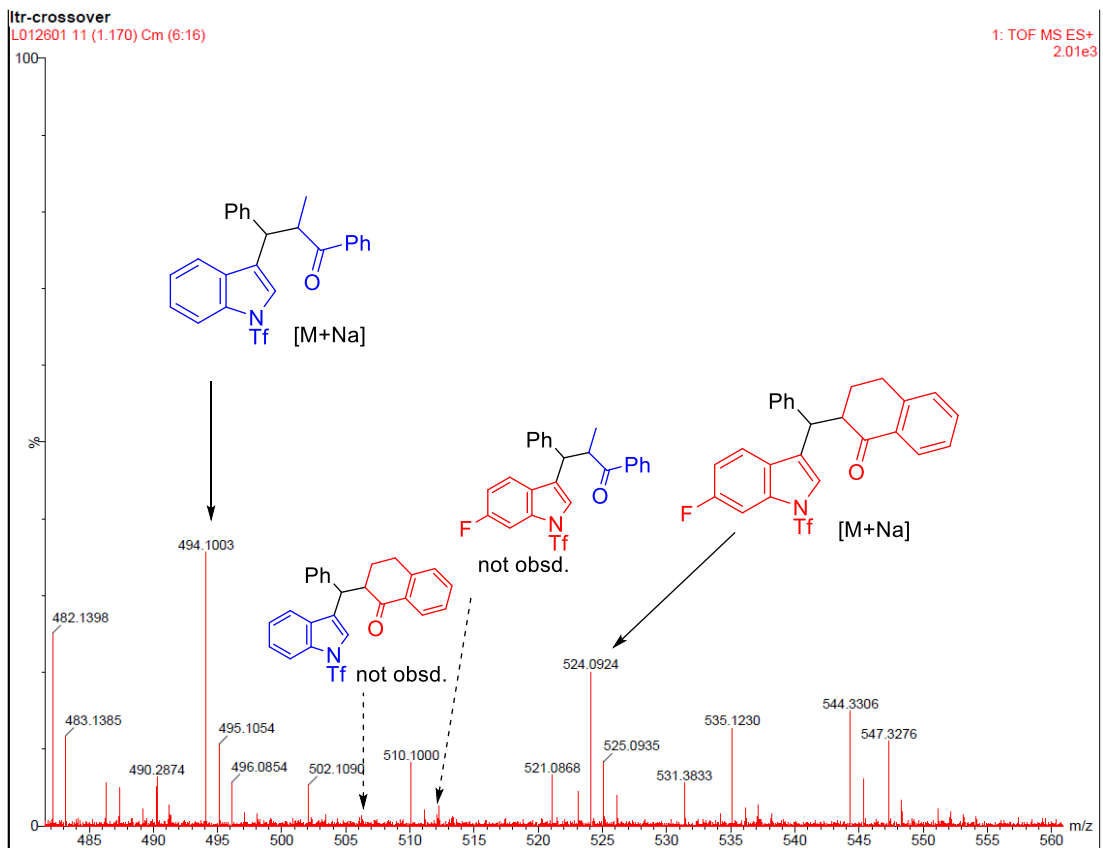
1112.96, 989.52, 755.12, 578.66 cm^{-1} .

HRMS: Calcd for $\text{C}_{21}\text{H}_{18}\text{F}_3\text{KNO}_6\text{S}$ $[\text{M}+\text{K}]^+$: 508.0439. Found: 508.0451.

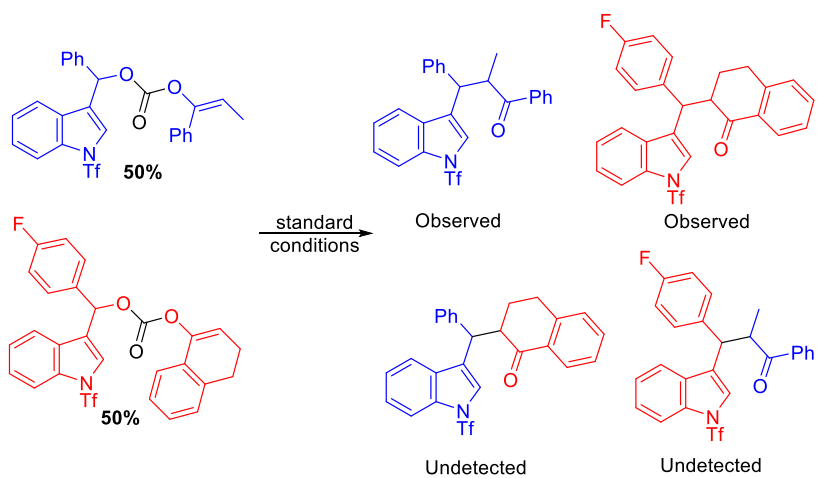
4.2 Crossover experiments:

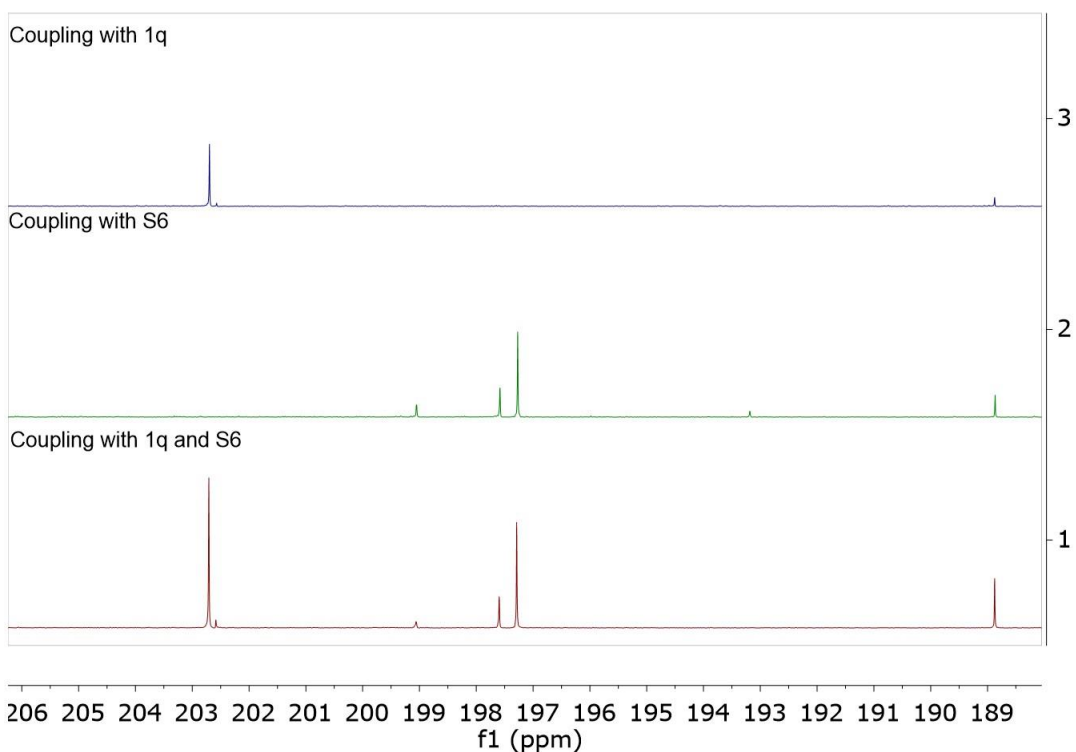
Procedure: In a glove box, under an argon atmosphere, a flame dried 25 mL microwave vial with a stir bar was charged with secondary benzylic enol carbonate **3.11d** (52 mg, 0.1 mmol, 50%), **S5** or **S6** (54 mg, 0.1 mmol, 50%), $\text{Pd}(\text{dmdba})_2$ (10 mmol%, 0.02 mmol, 16.6 mg), *t*-BuDavephos (12 mmol%, 0.024 mmol, 8.4 mg) and THF (5 ml, 0.04N). The vial was carefully sealed with a cap and removed from glove box and stirring under 110 °C until the materials totally converted. The reaction mixture was directly loaded on HRMS.





¹³C NMR Analysis of Crossover:



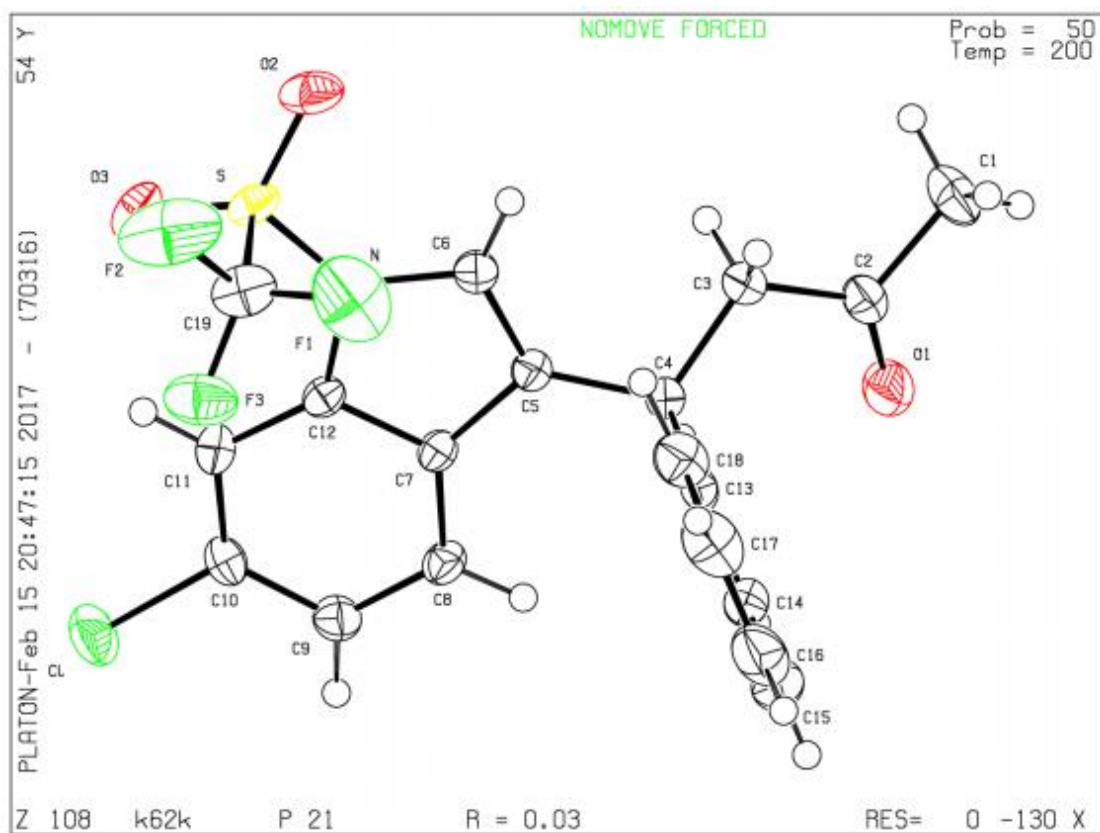


Crude ^{13}C spectra for the coupling of individual enol carbonates and the crossover experiment (bottom). No additional peaks for crossover products are observed.

5. References:

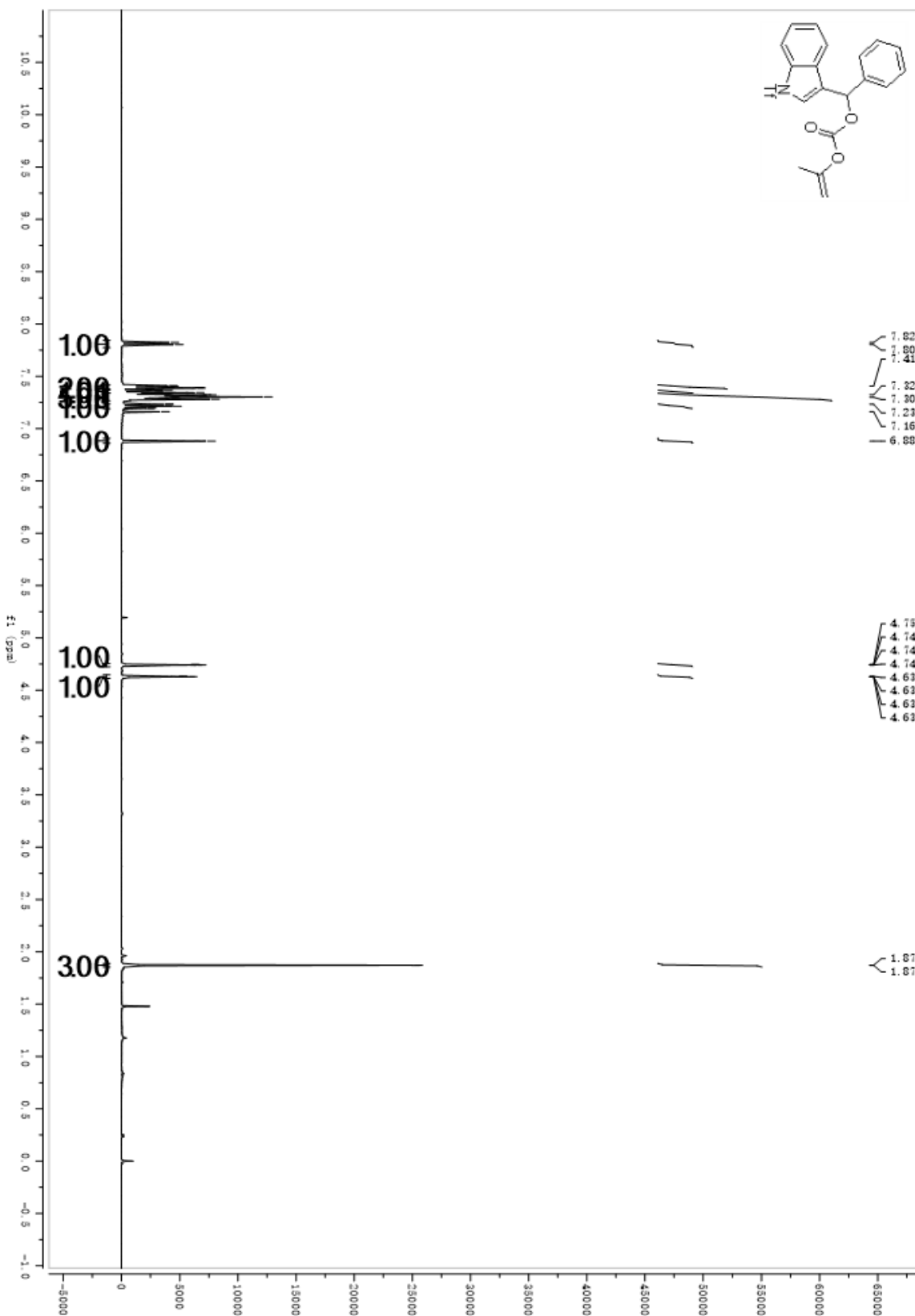
- (1) Chen, X. B.; Fan, H. Q.; Zhang, S. L.; Yu, C. G.; Wang, W. *Chem. Eur. J.* **2016**, *22*, 716.
- (2) Mendis, S. N.; Tunge, J. A. *Chem. Commun.* **2016**, *52*, 7695.
- (3) Mendis, S. N.; Tunge, J. A. *Org. Lett.* **2015**, *17*, 5164.

6. X-Ray Structure of Products (S)-3.12k

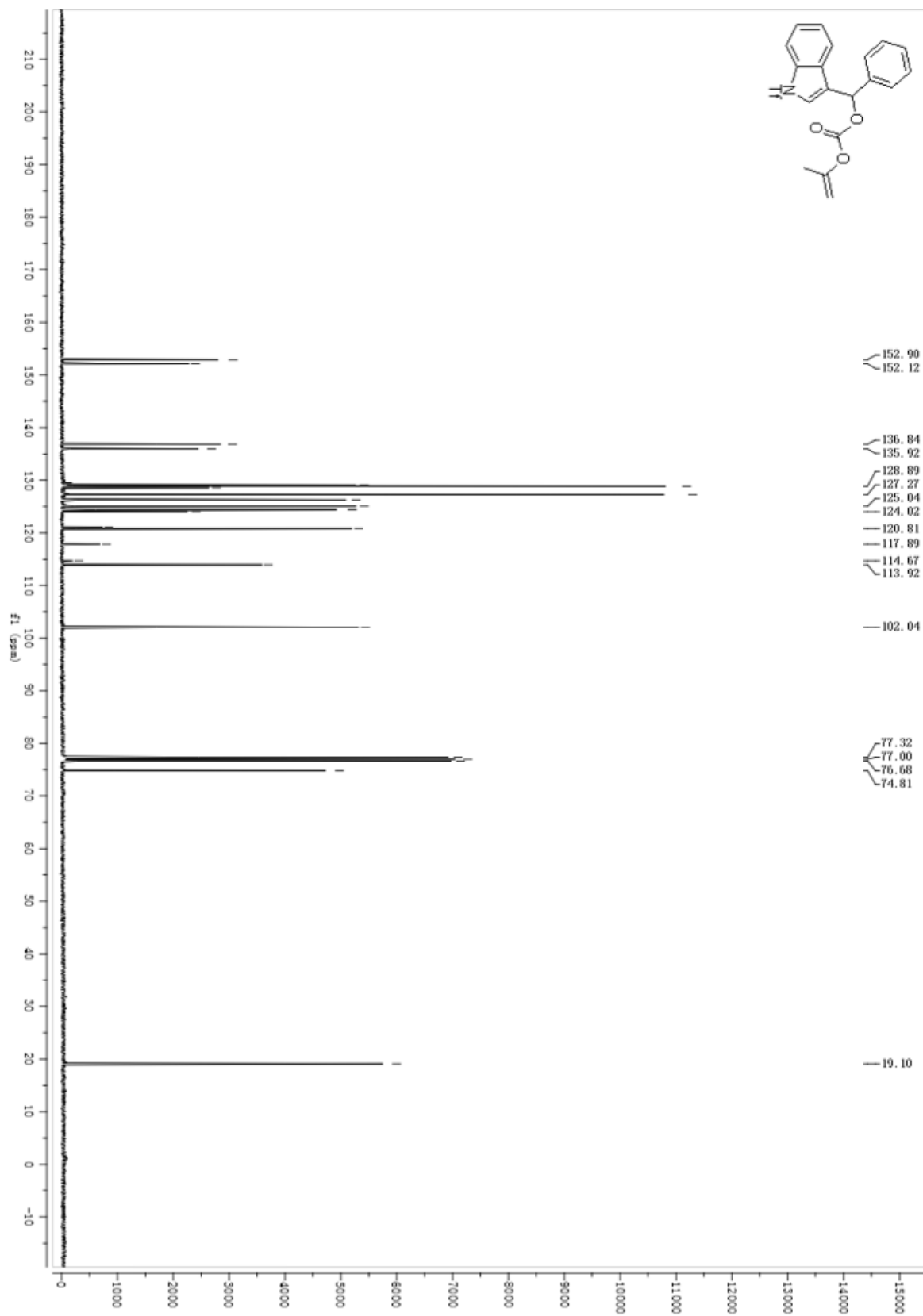


7. Copies of ^1H NMR and ^{13}C NMR Spectra

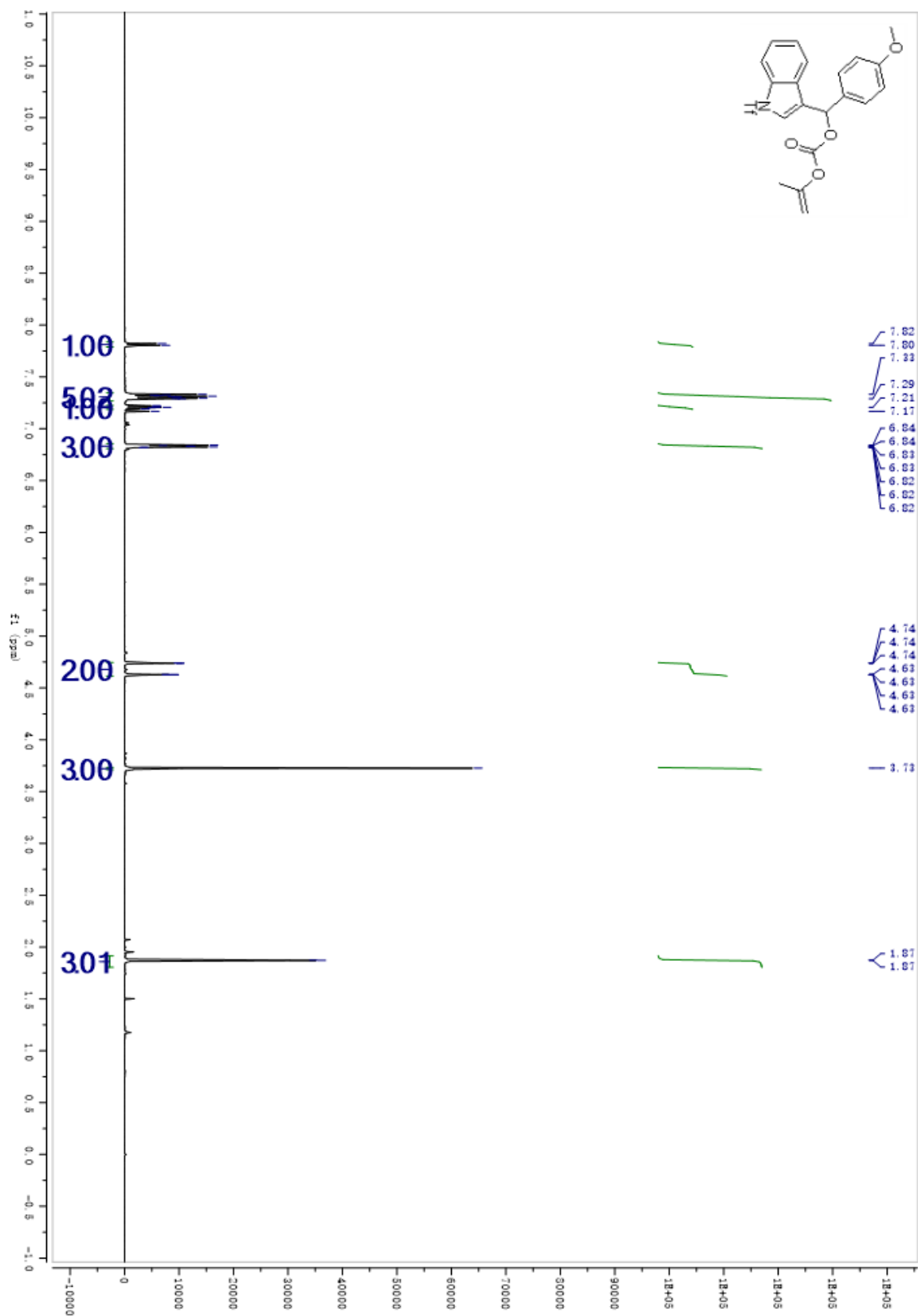
¹H NMR 3.11a



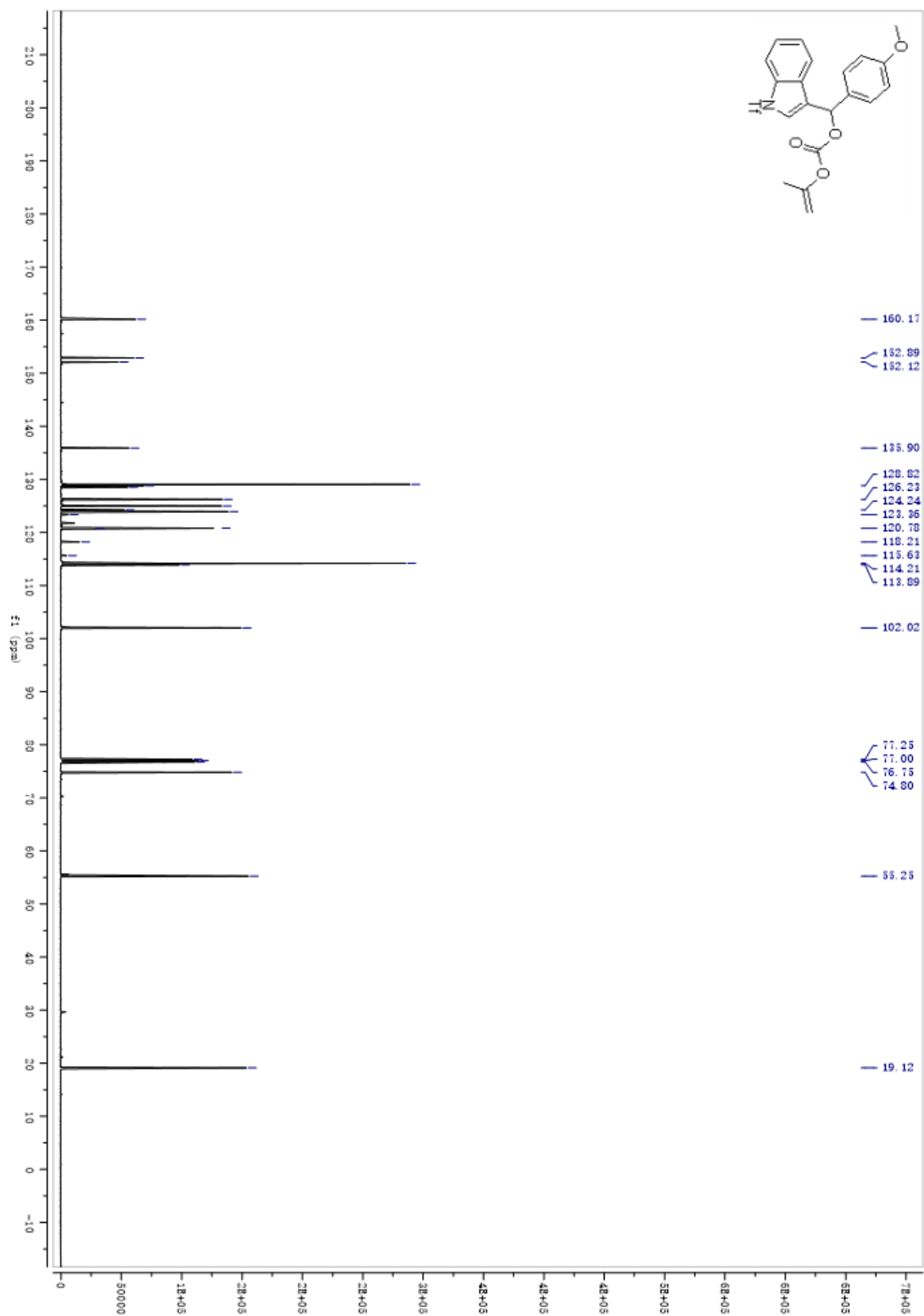
¹³C NMR 3.11a



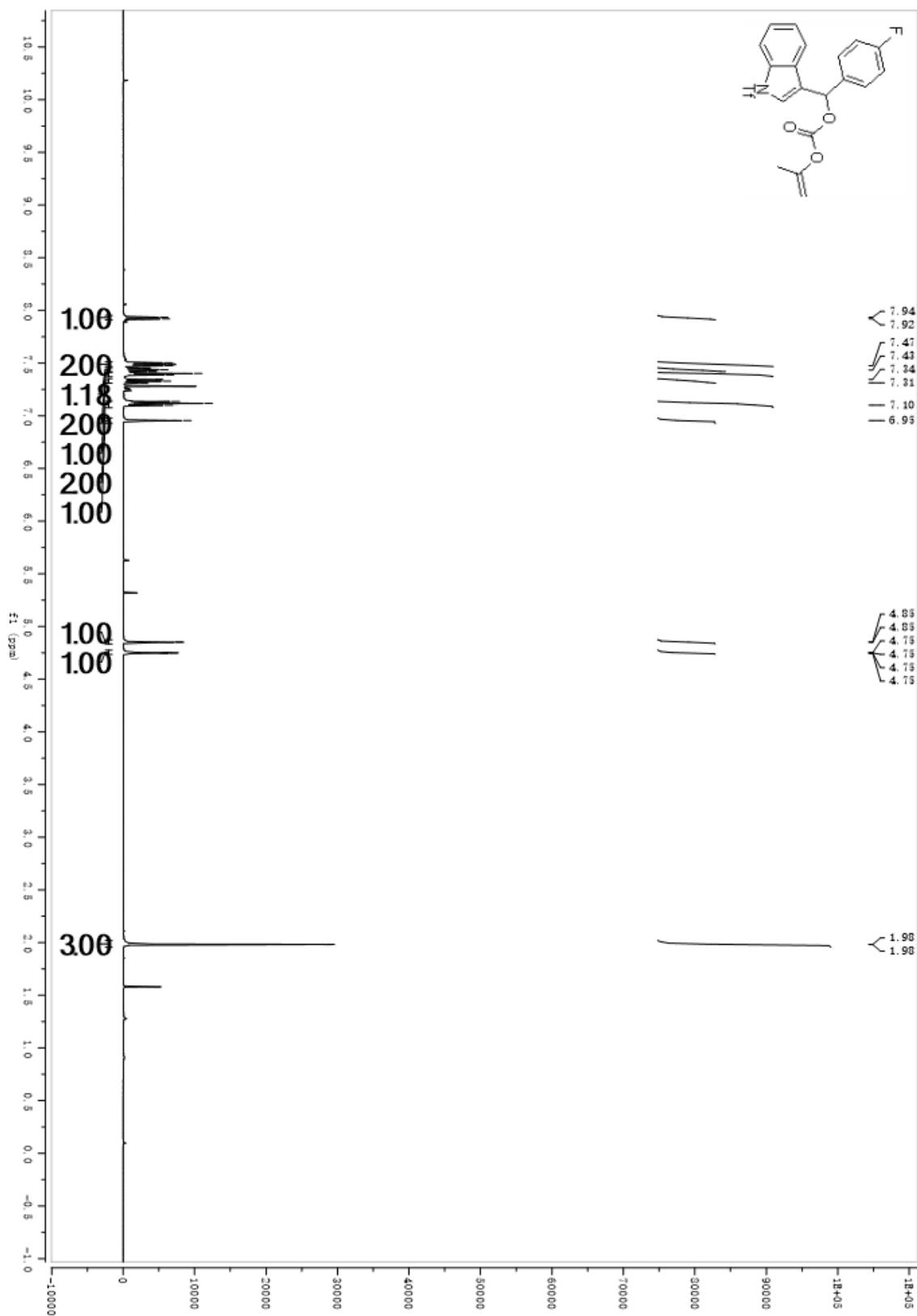
¹H NMR 3.11b



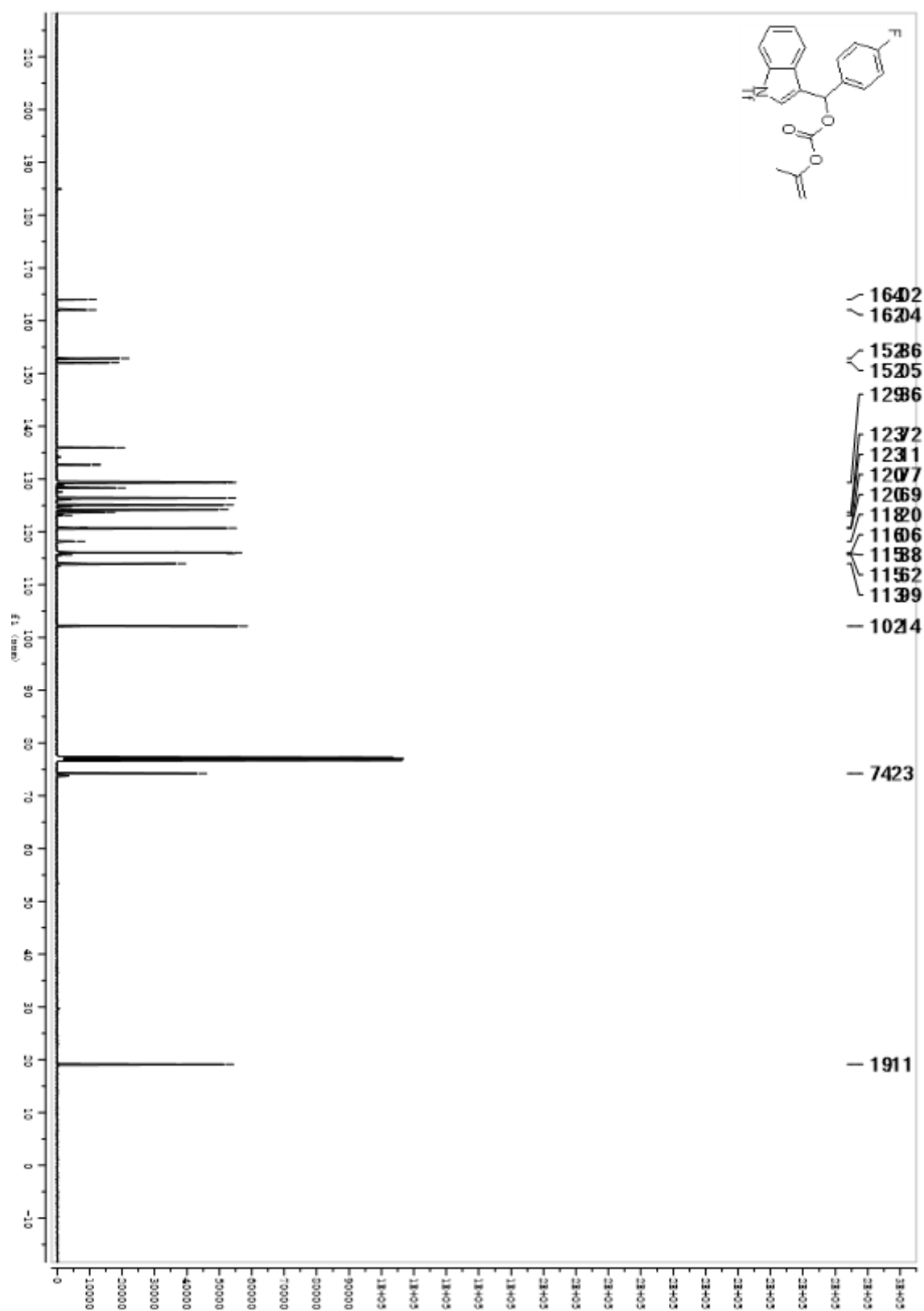
¹³C NMR 3.11b



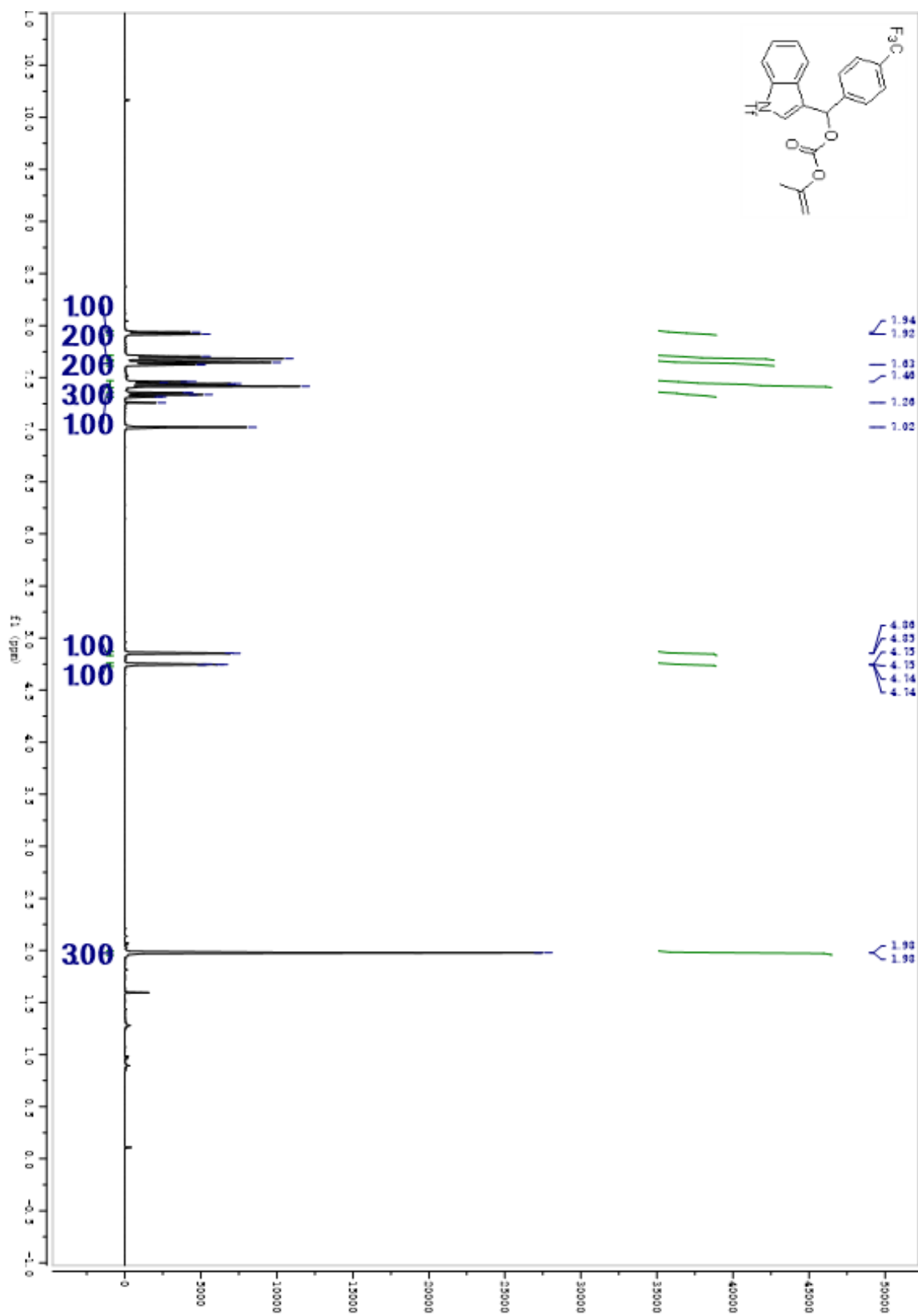
¹H NMR 3.11c



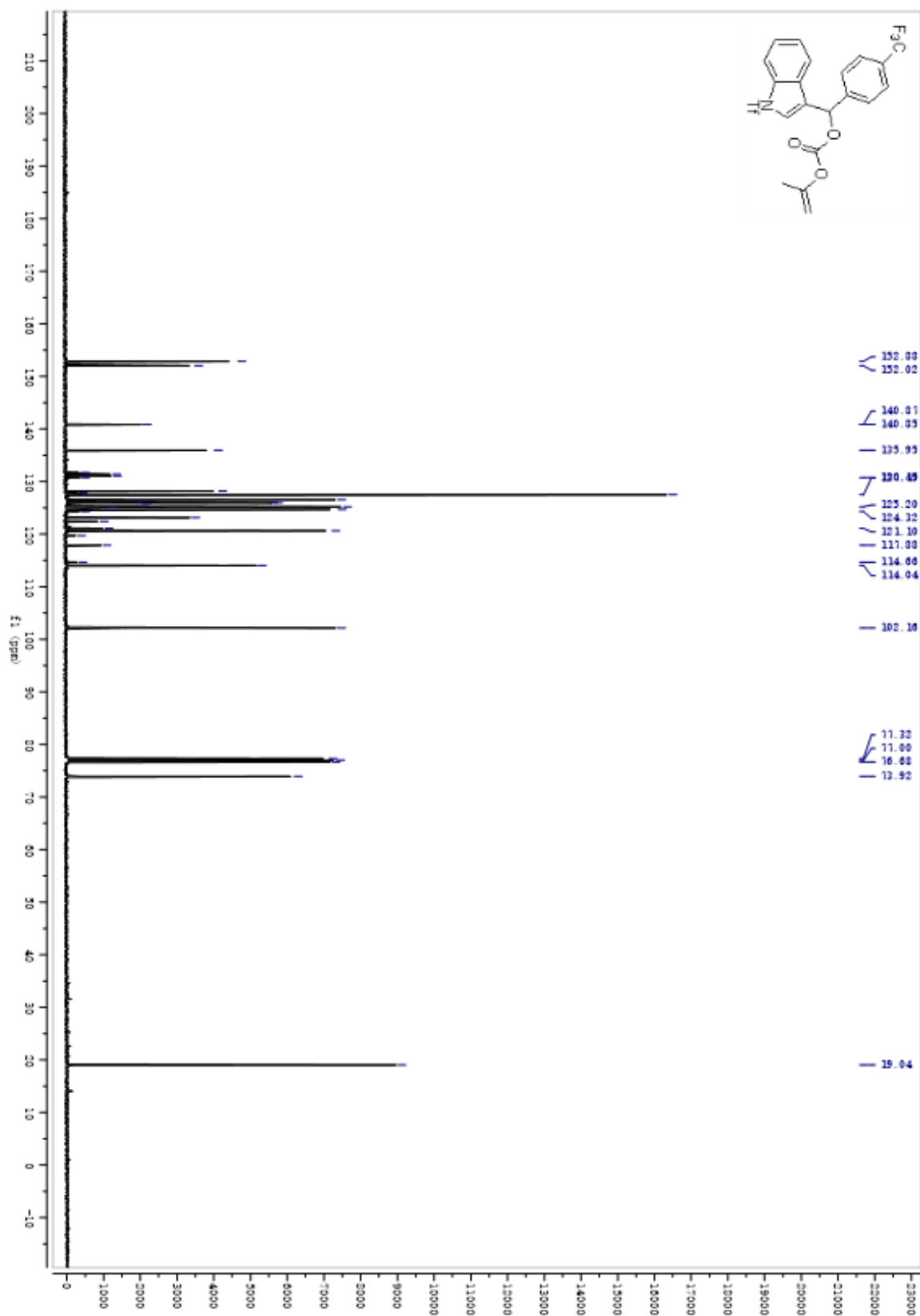
¹³C NMR 3.11c



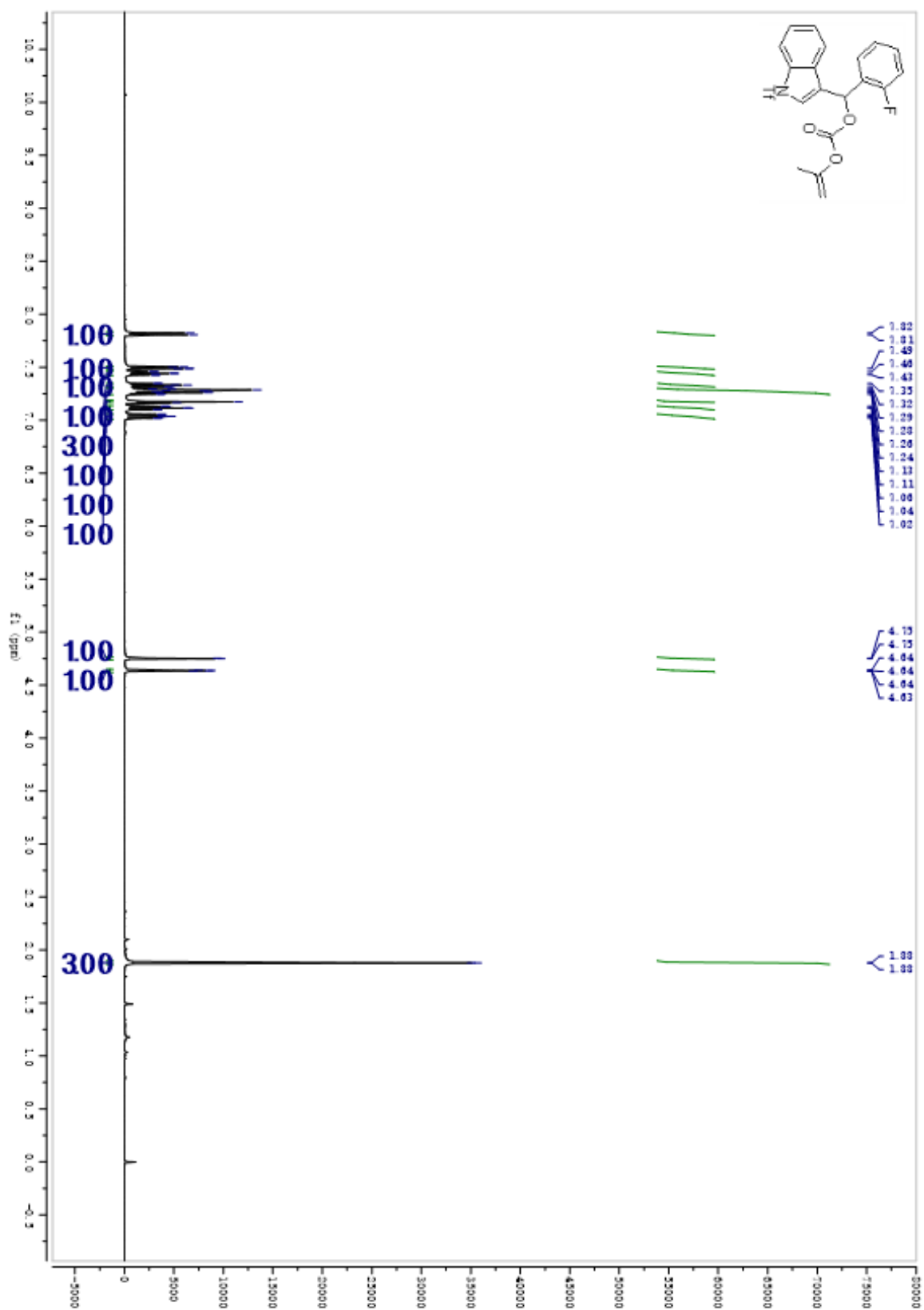
¹H NMR 3.11d



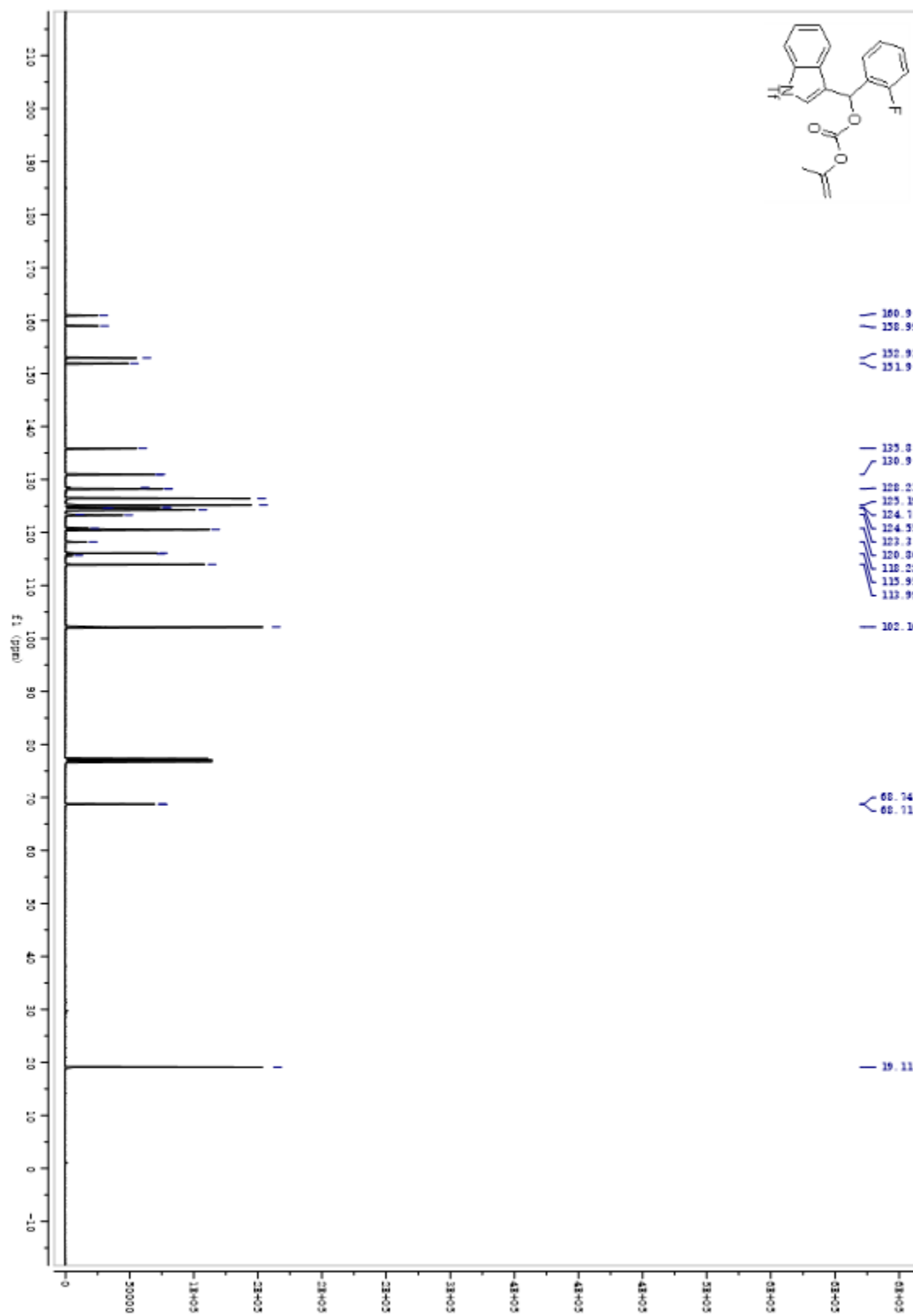
¹³C NMR 3.11d



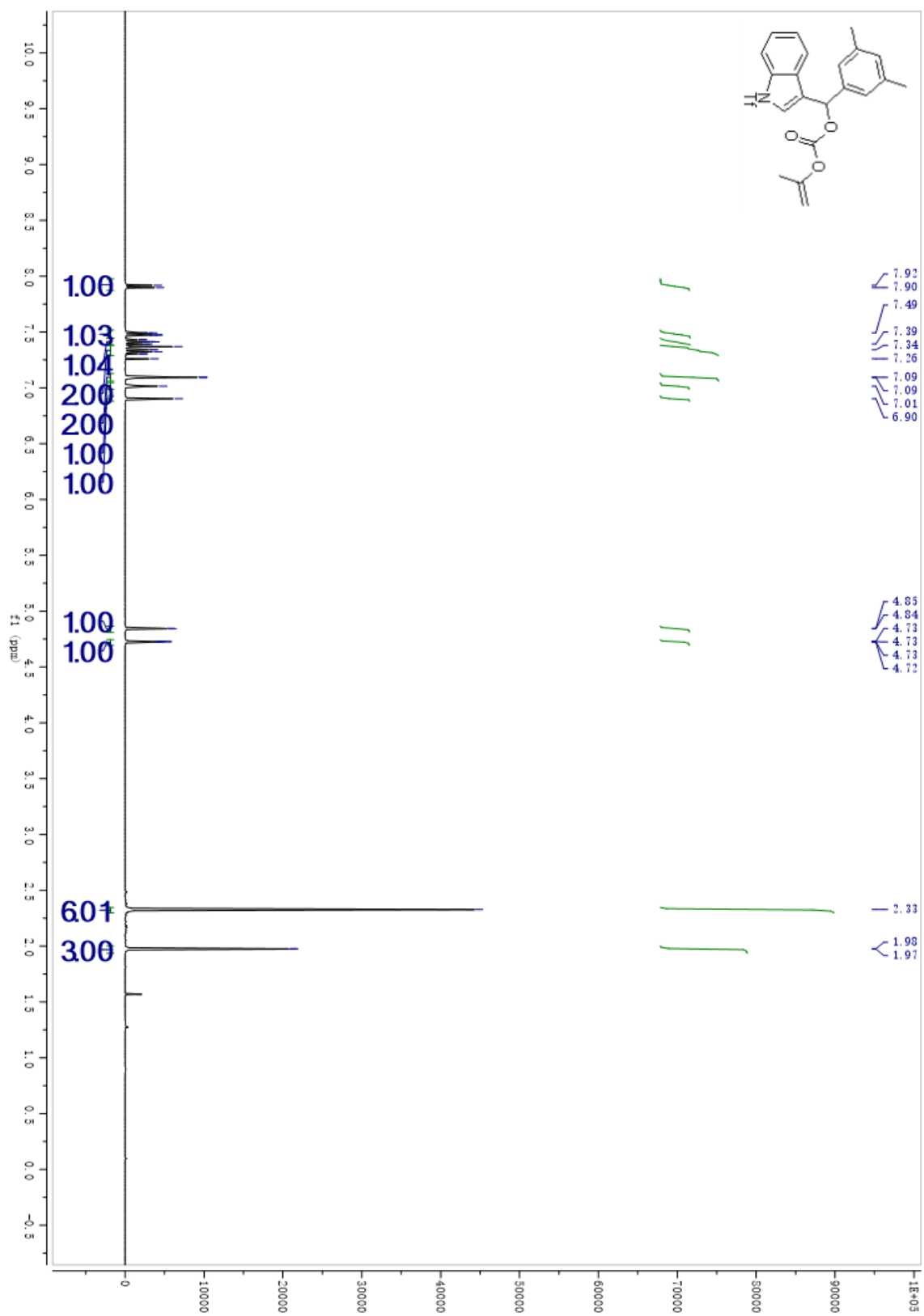
¹H NMR 3.11e



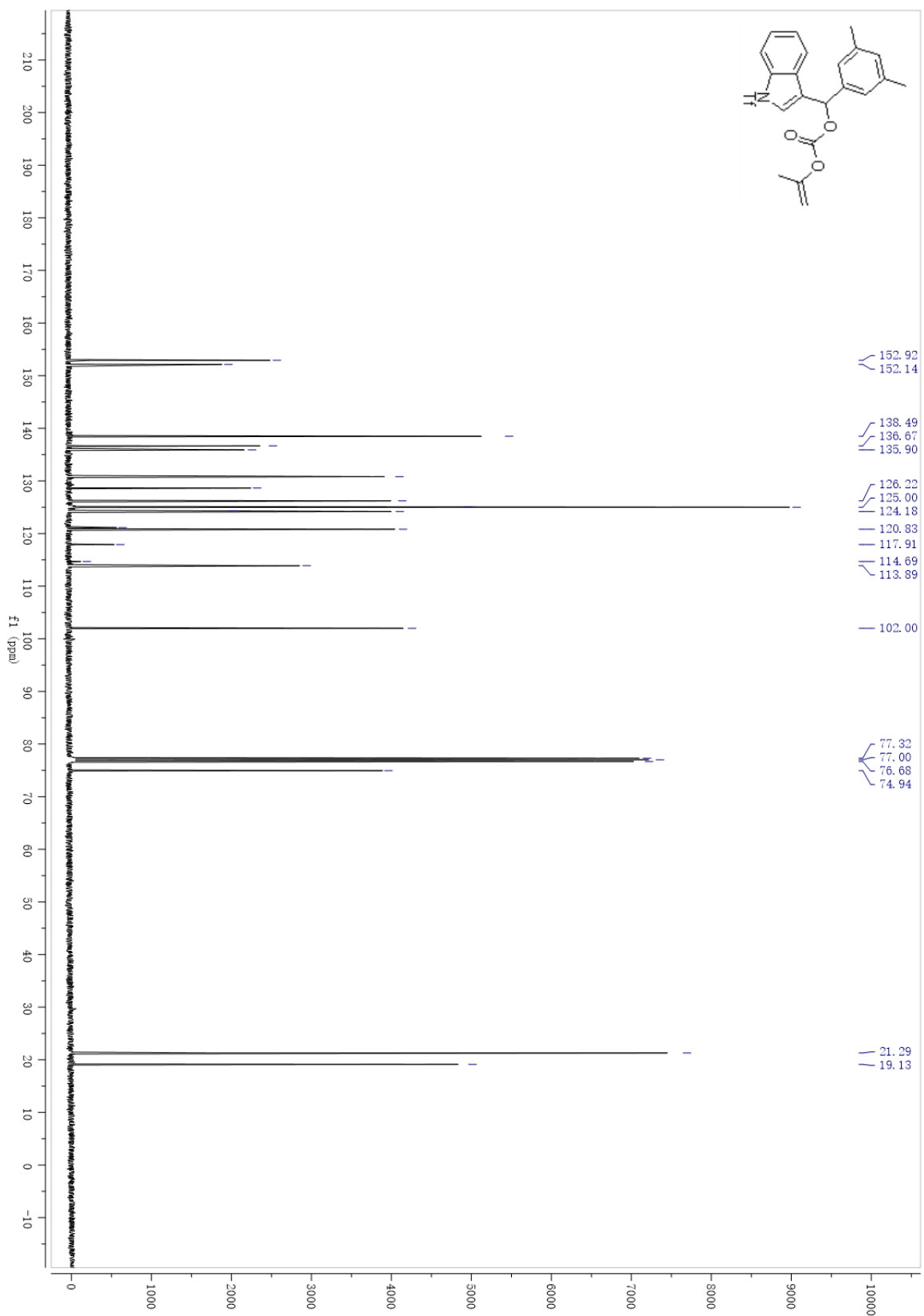
¹³C NMR 3.11e



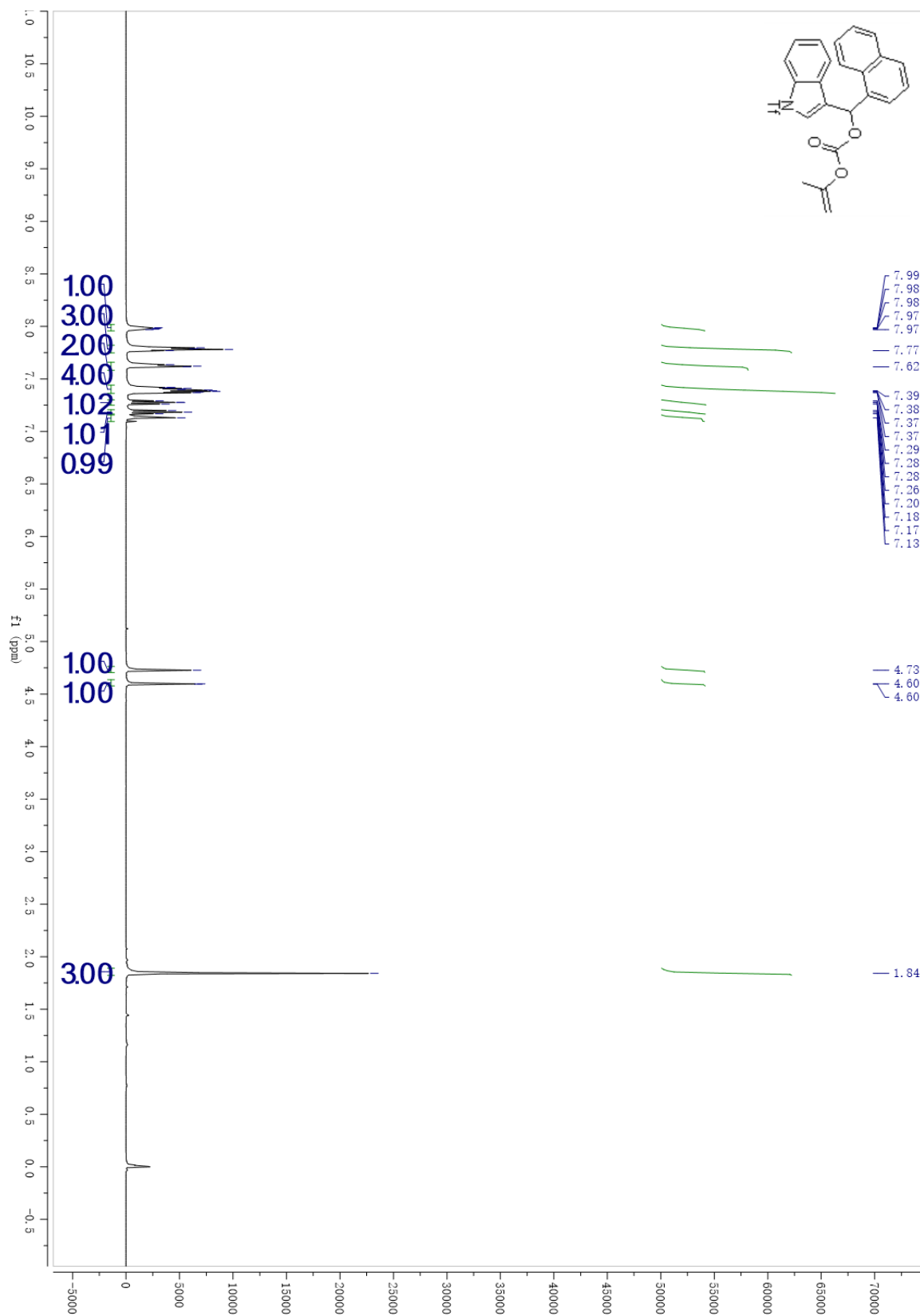
¹H NMR 3.11f



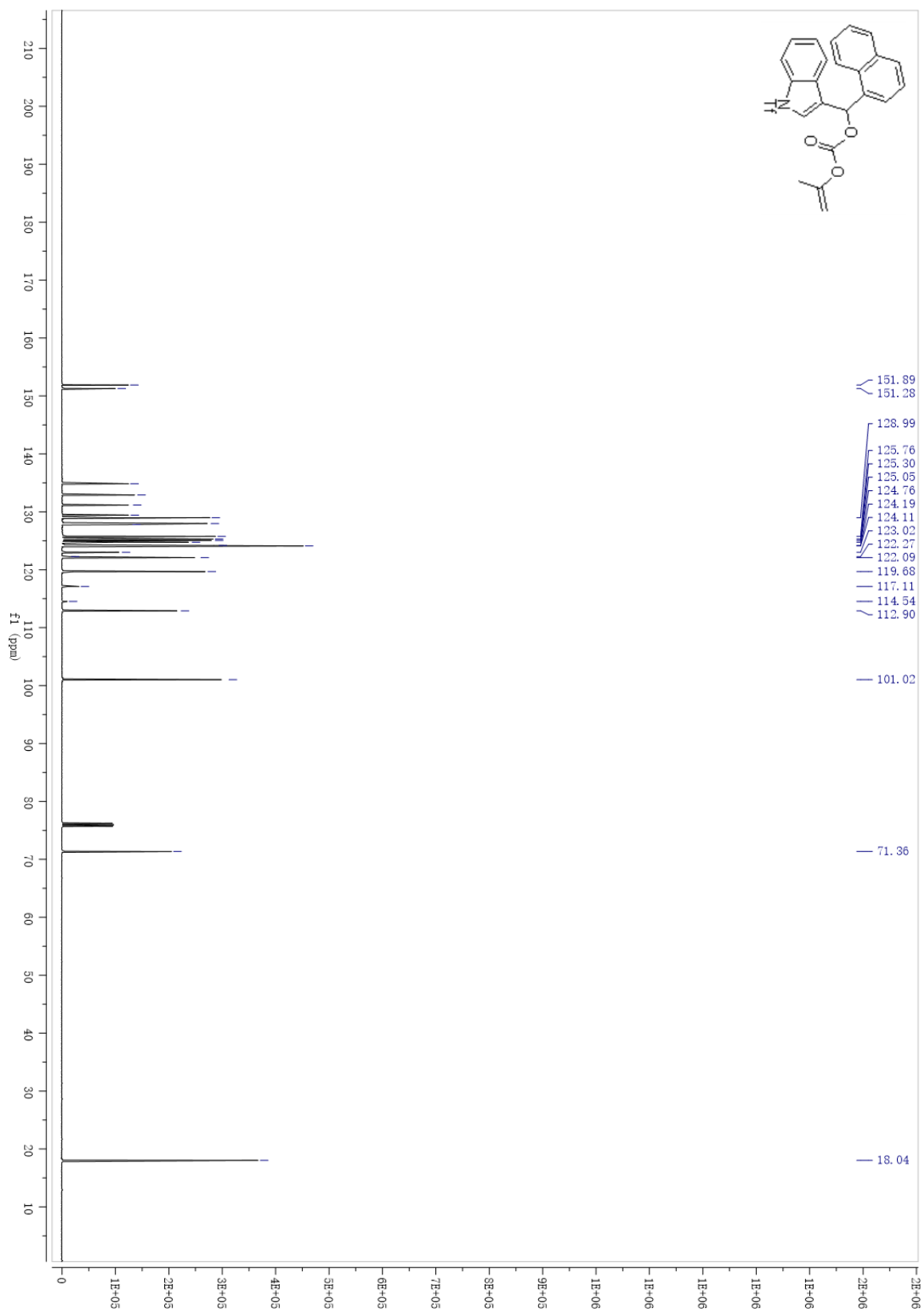
¹³C NMR 3.11f



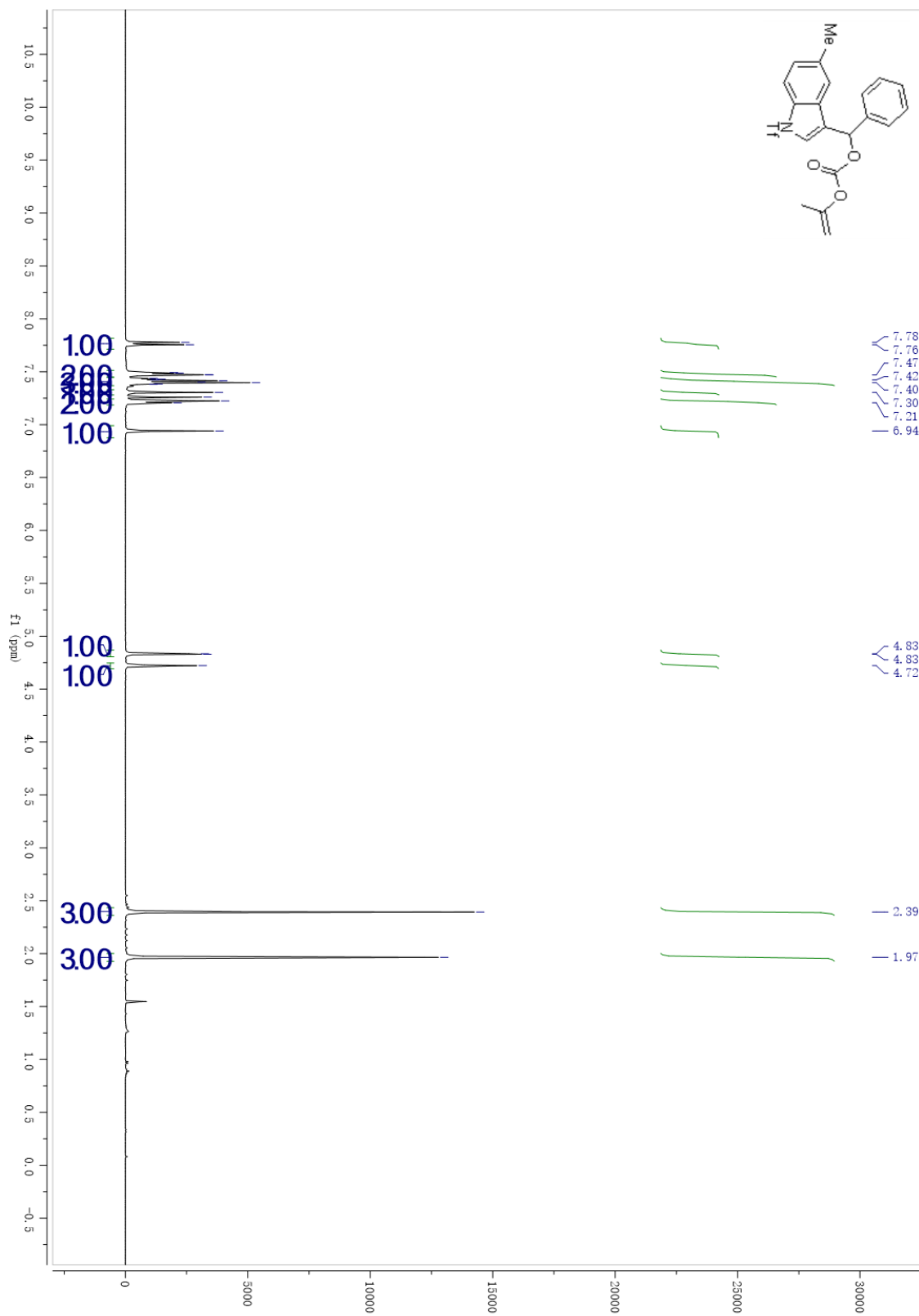
¹H NMR 3.11g



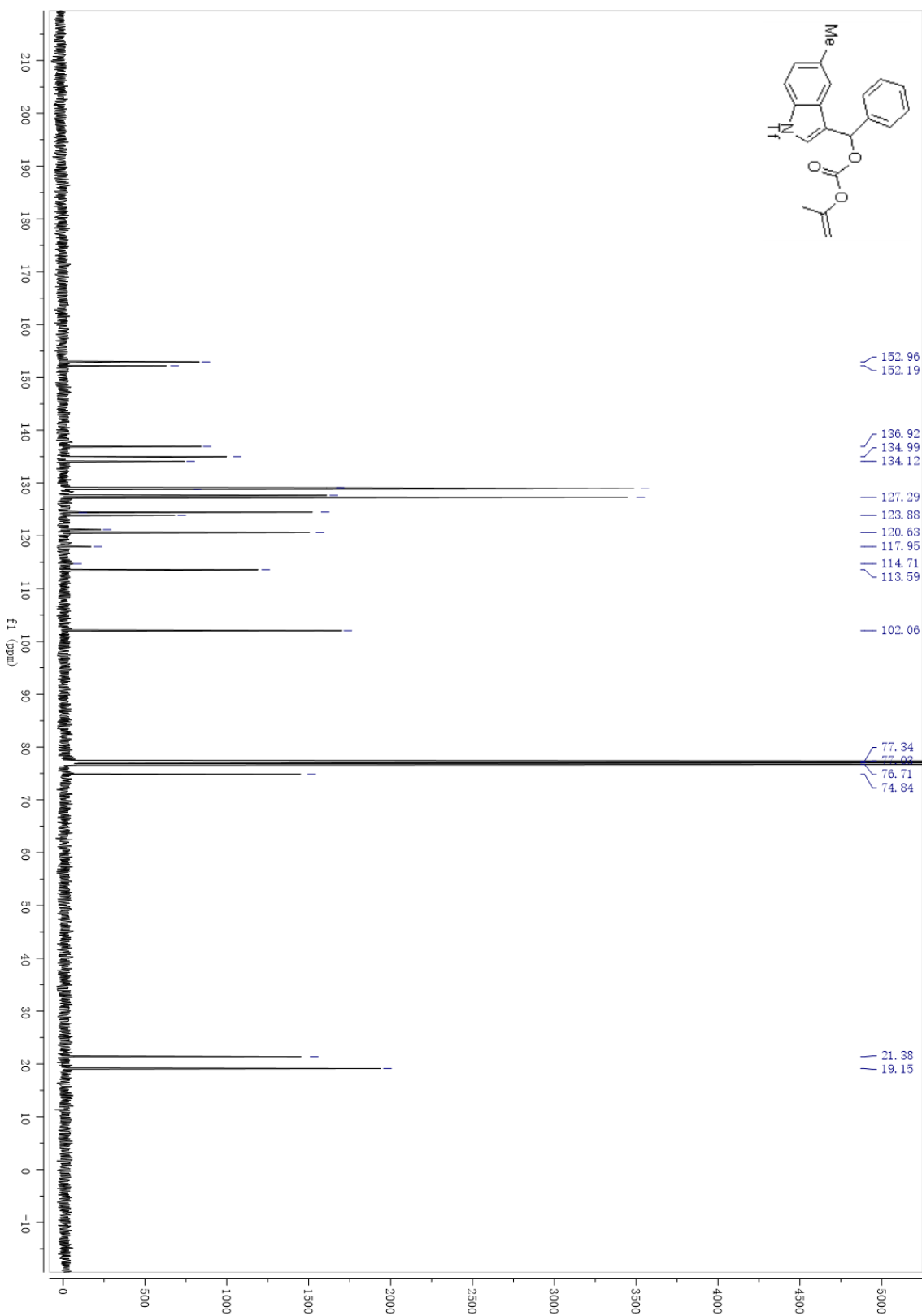
¹³C NMR 3.11g



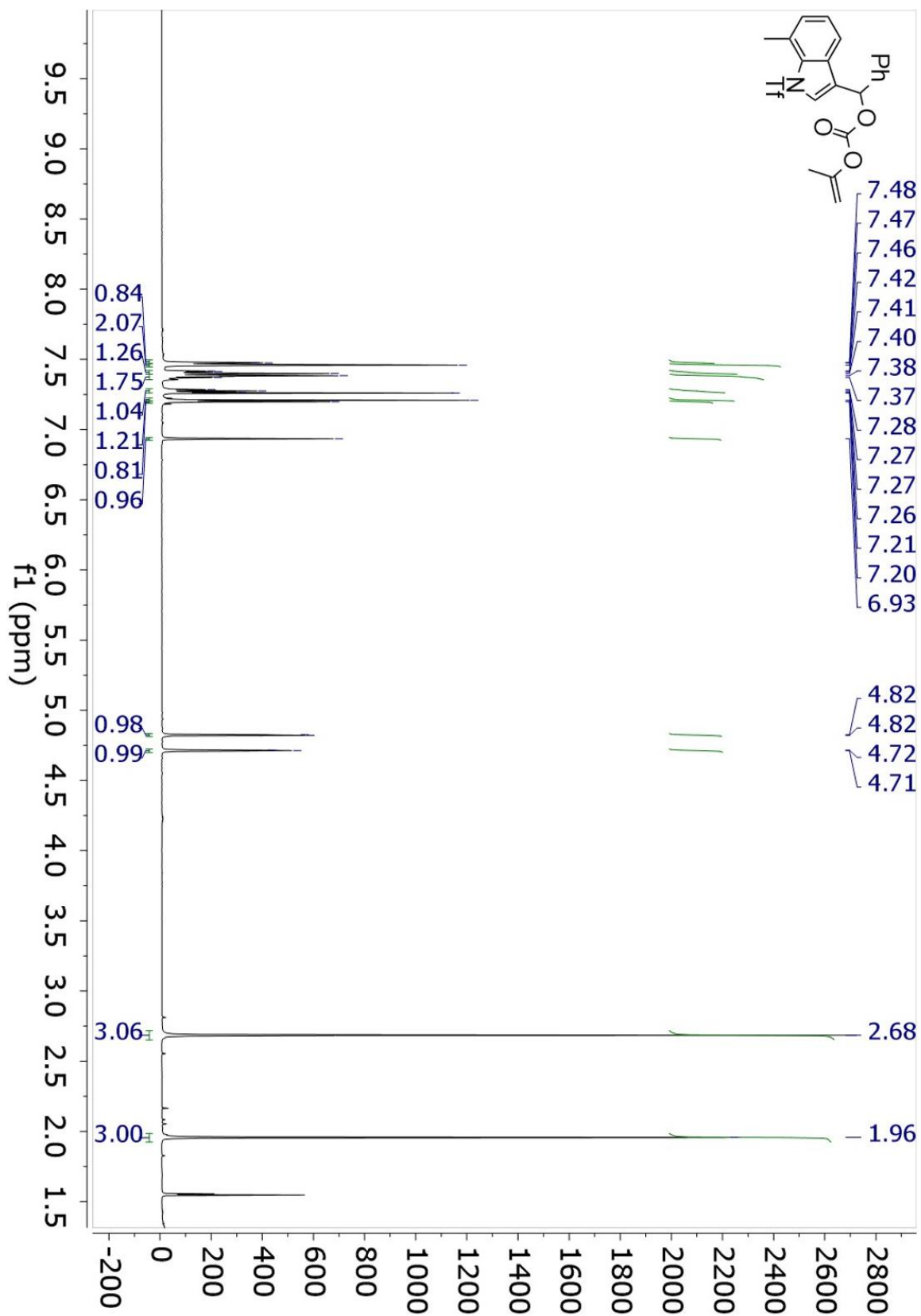
¹H NMR 3.11i



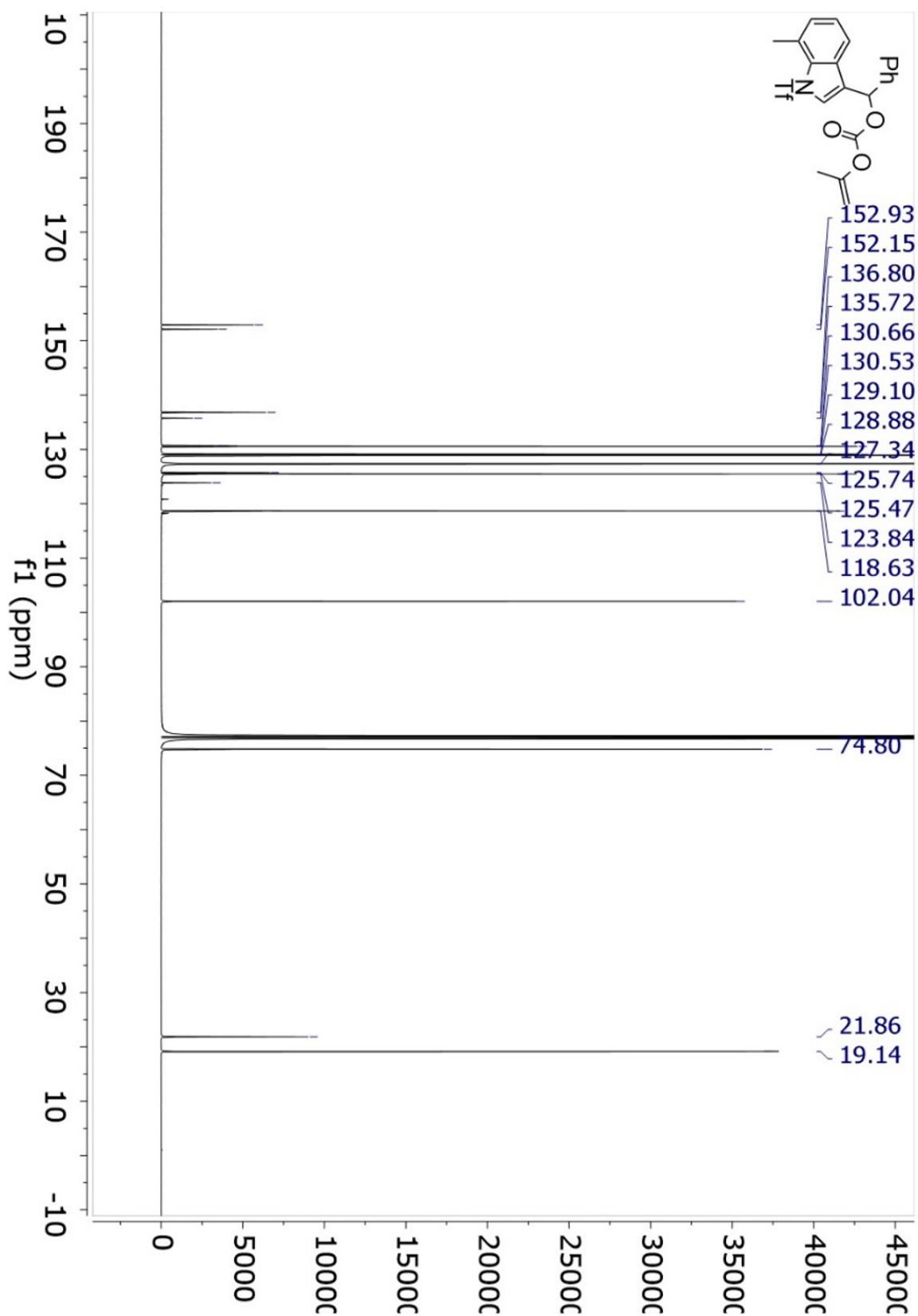
¹³C NMR 3.11i



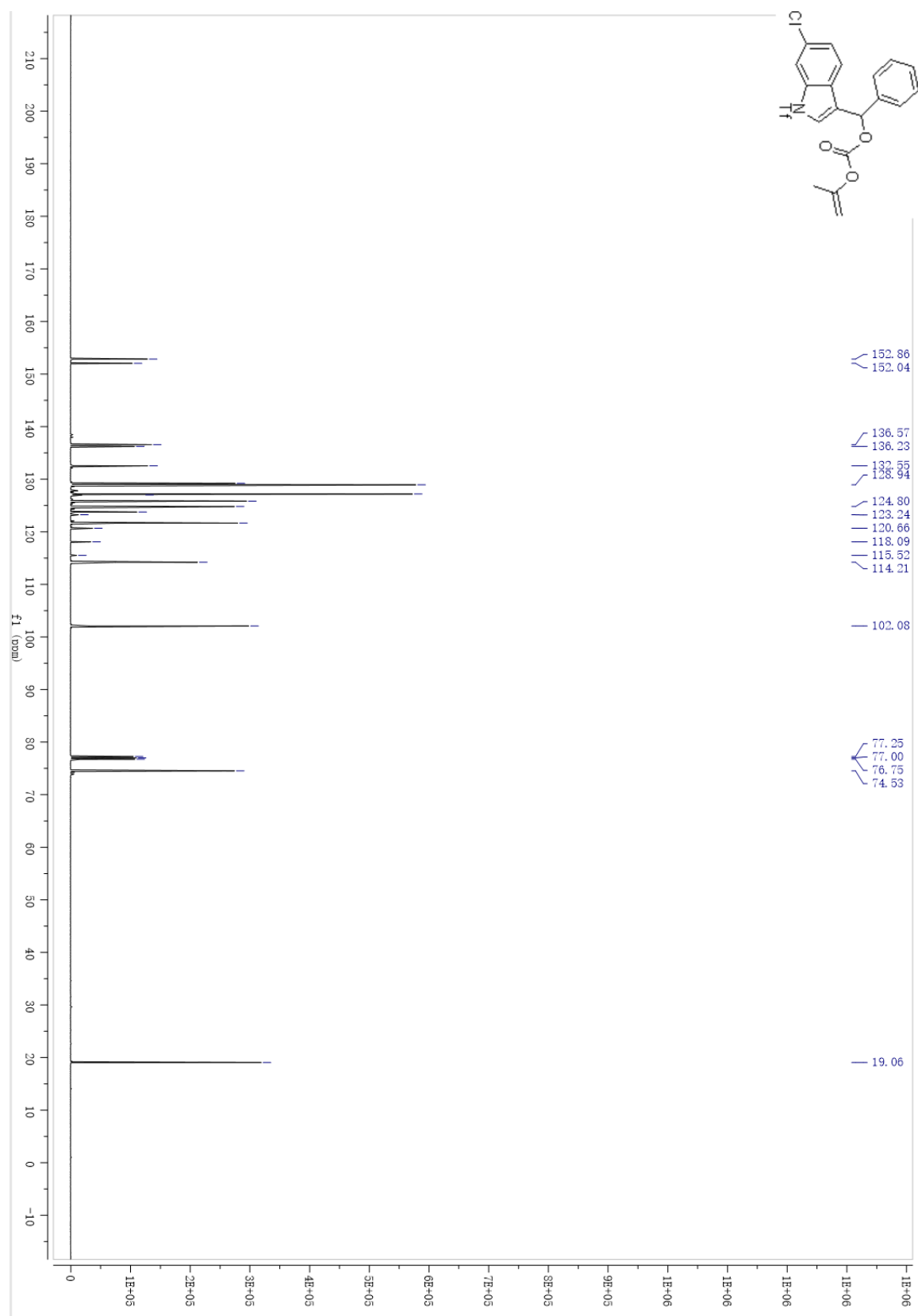
¹H NMR 3.11j



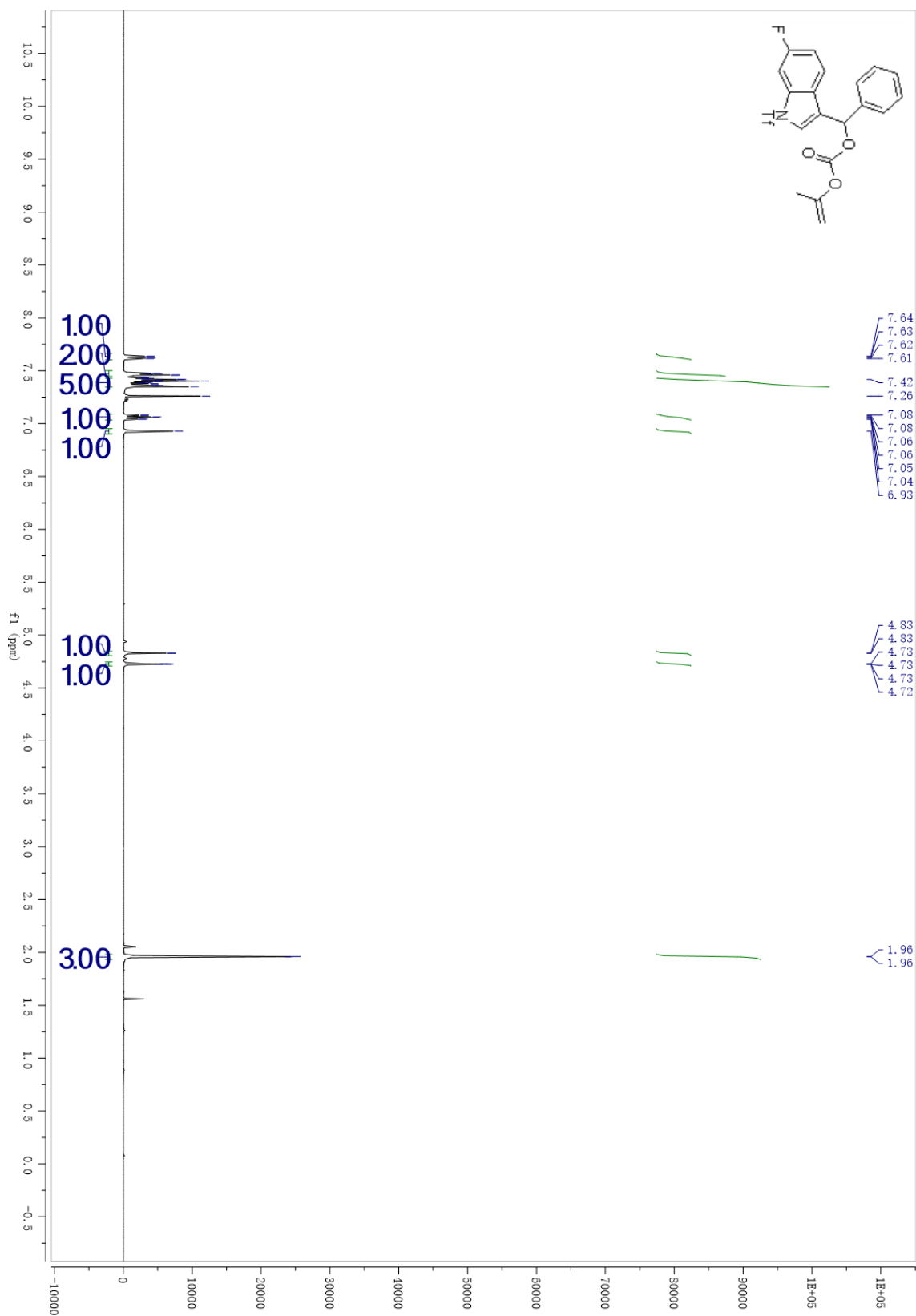
¹³C NMR 3.11j



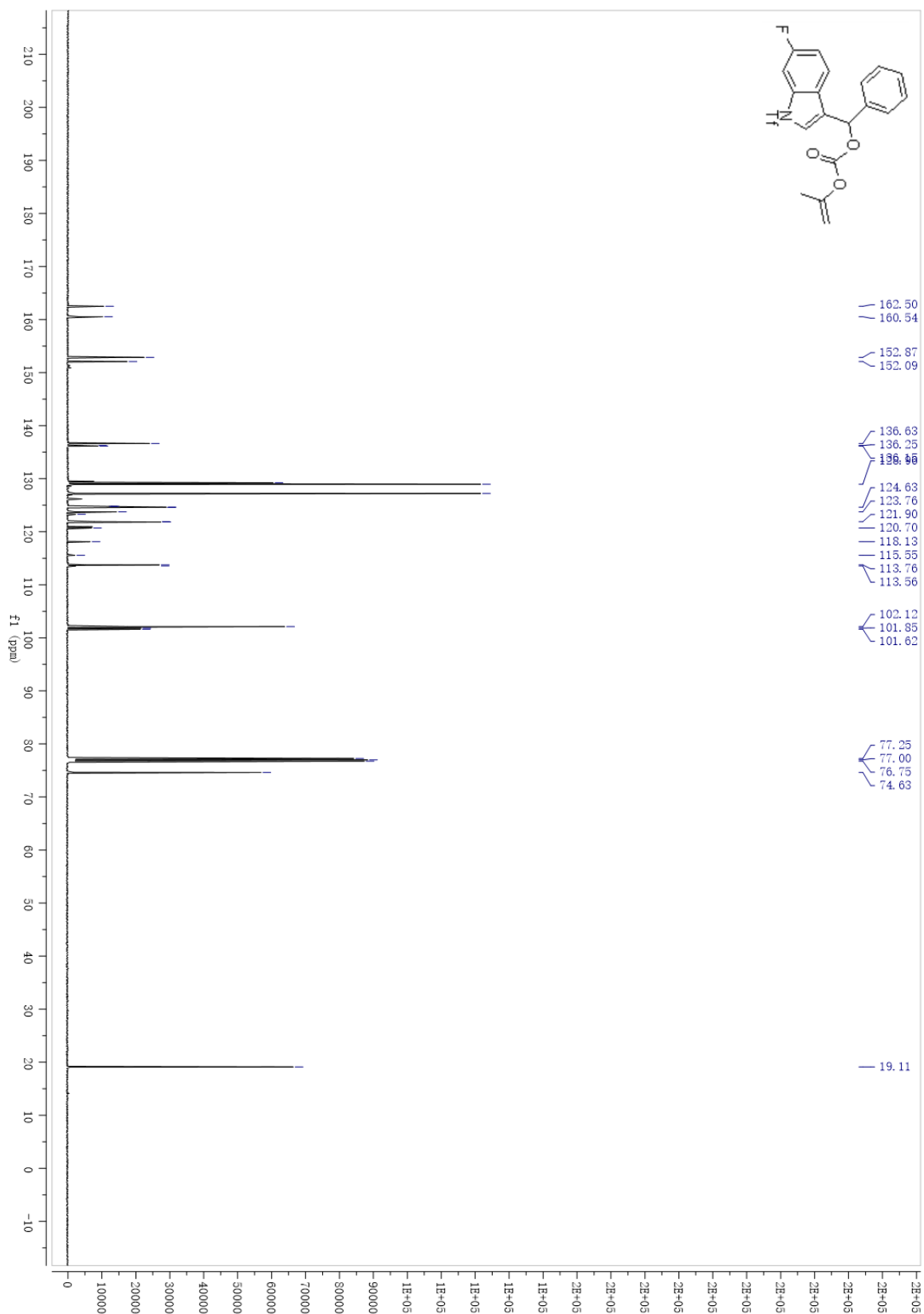
¹³C NMR 3.11k



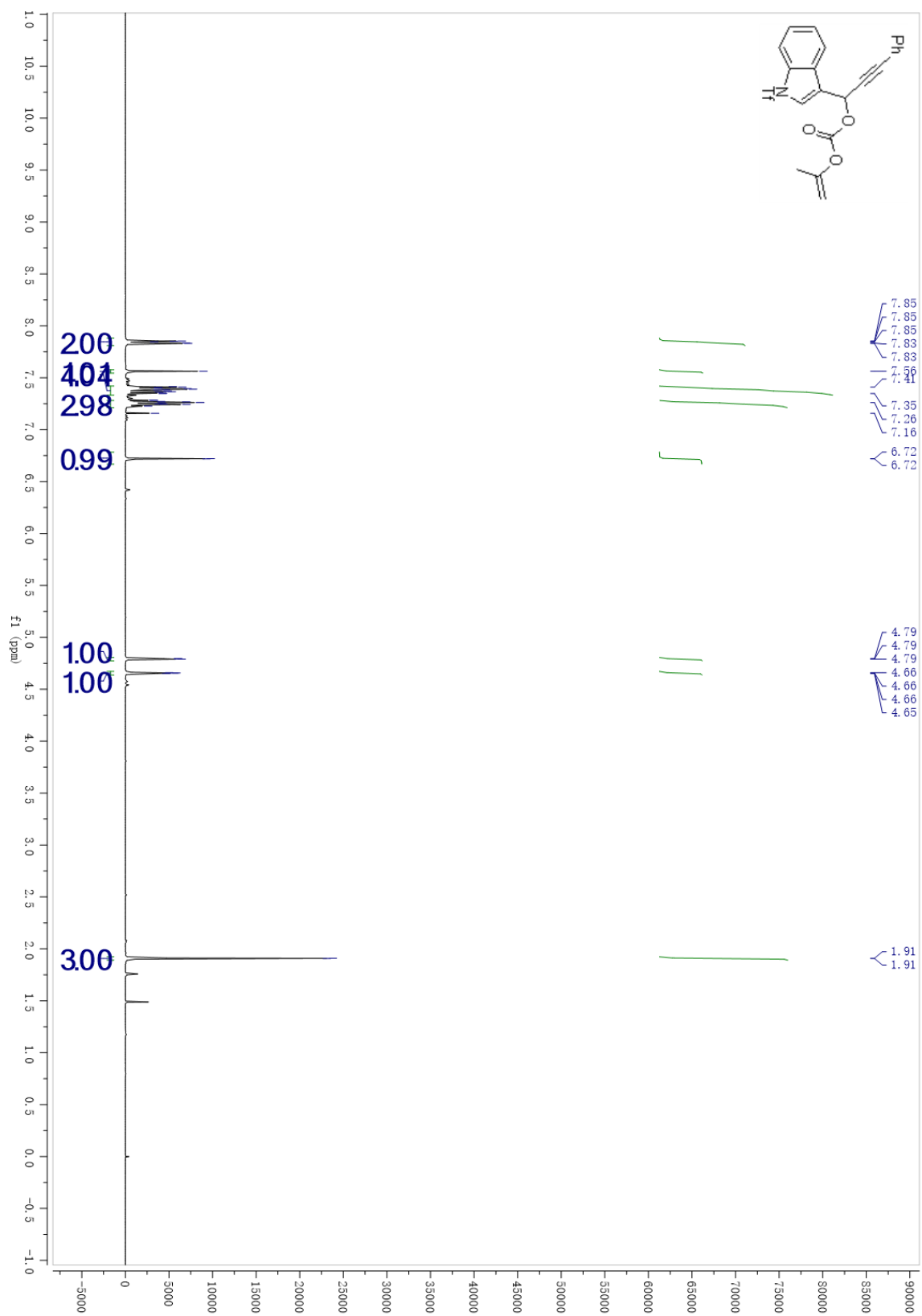
¹H NMR 3.111



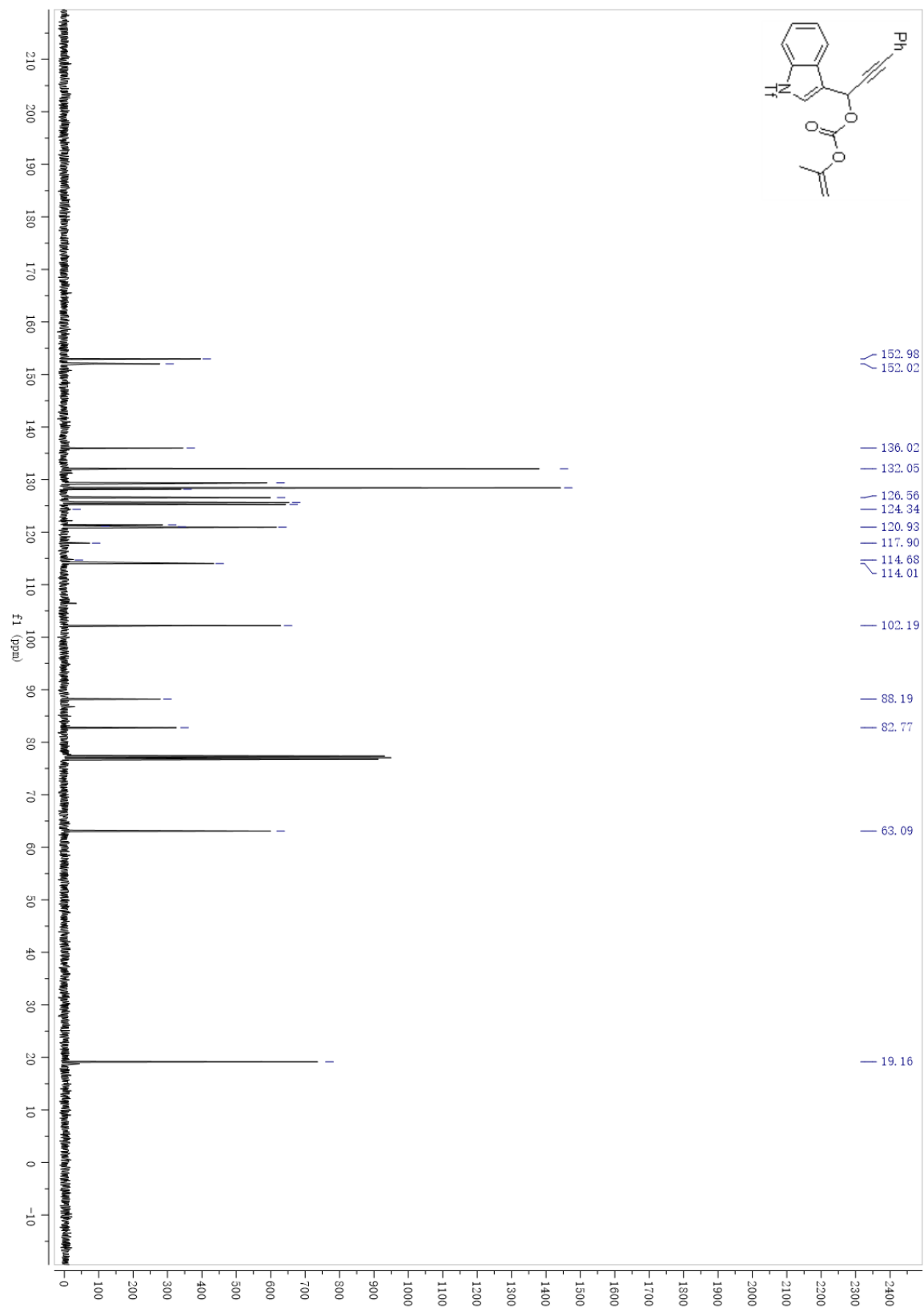
¹³C NMR 3.111



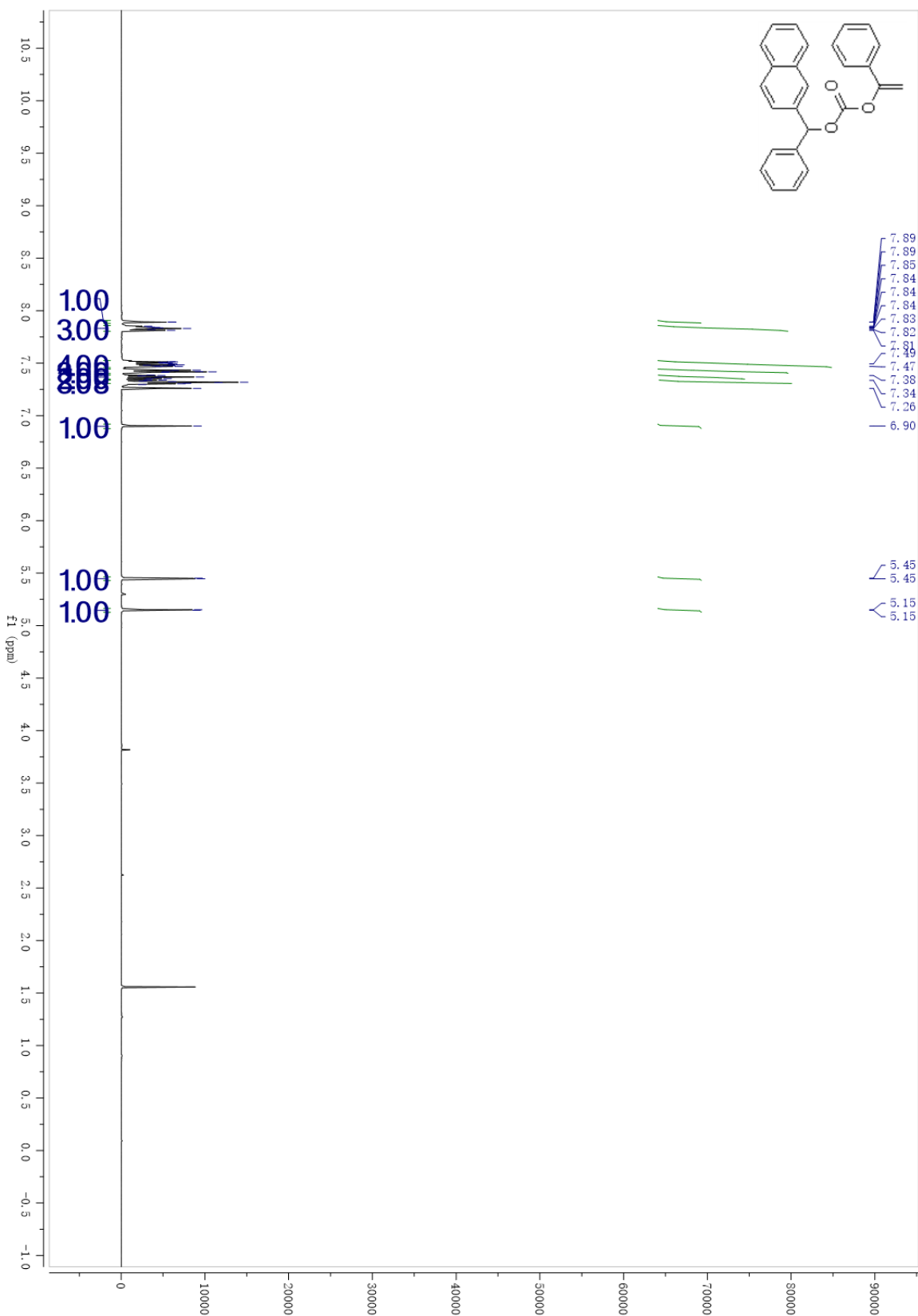
¹H NMR 3.11m



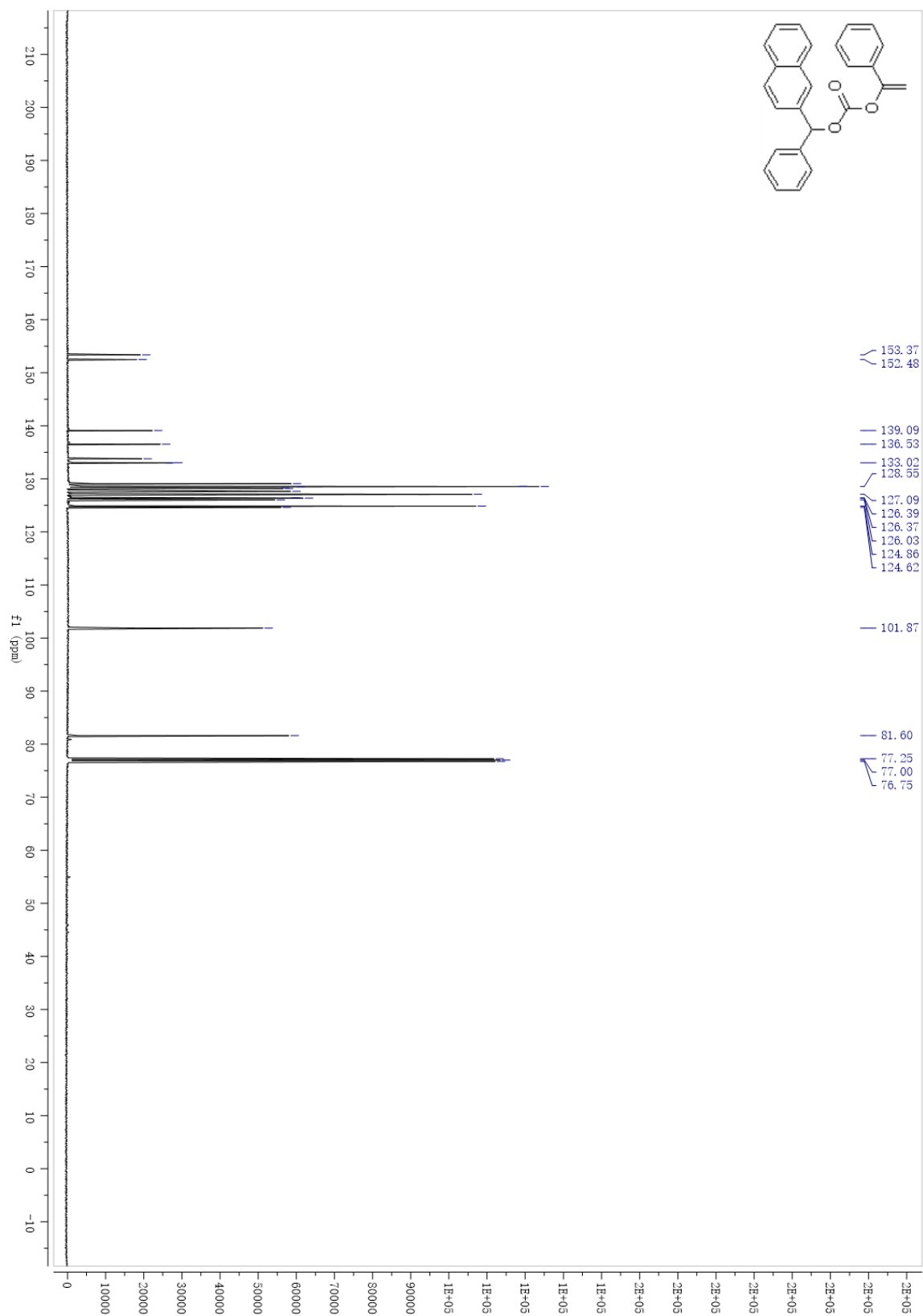
¹³C NMR 3.11m



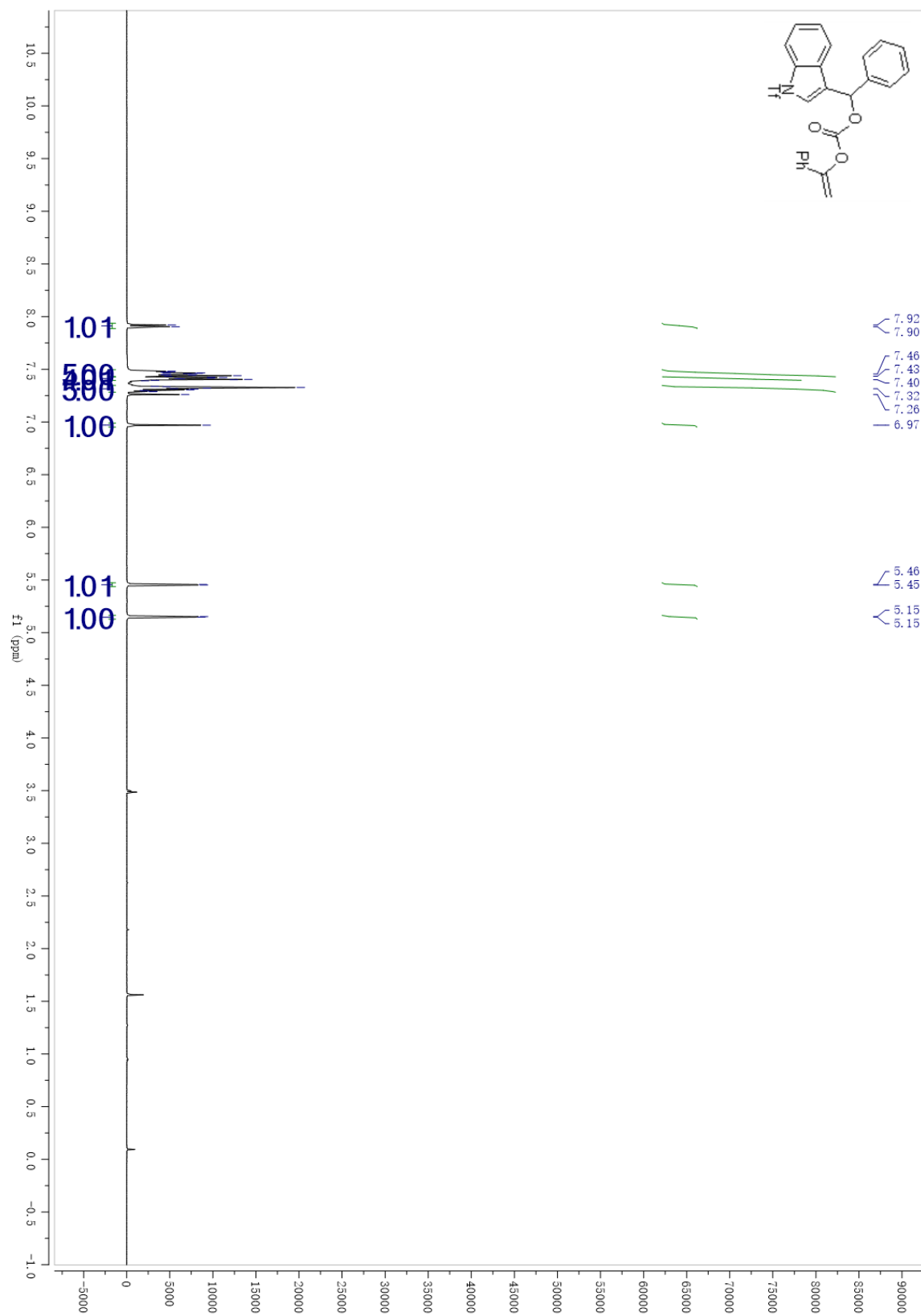
¹H NMR 3.11n



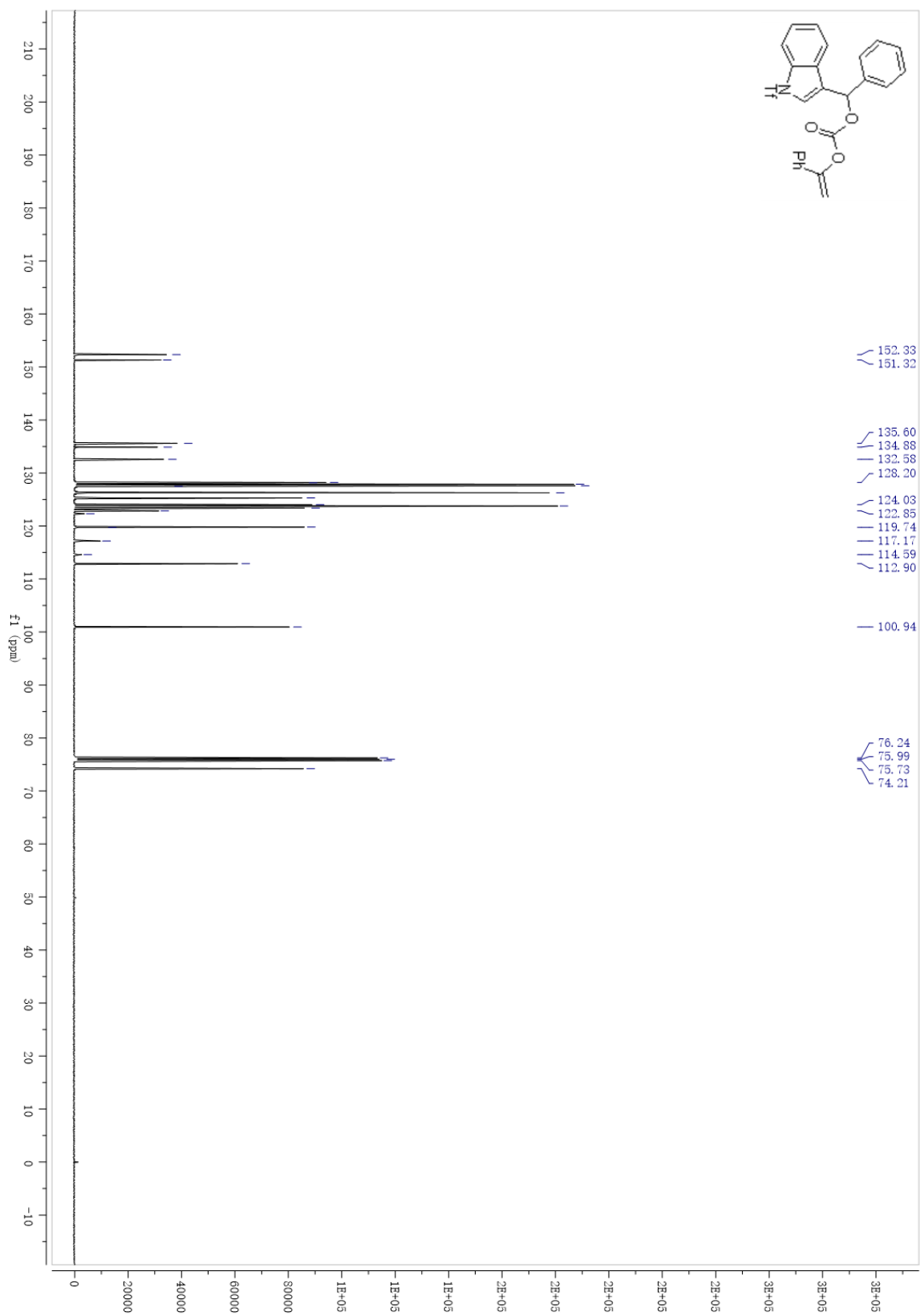
¹³C NMR 3.11n



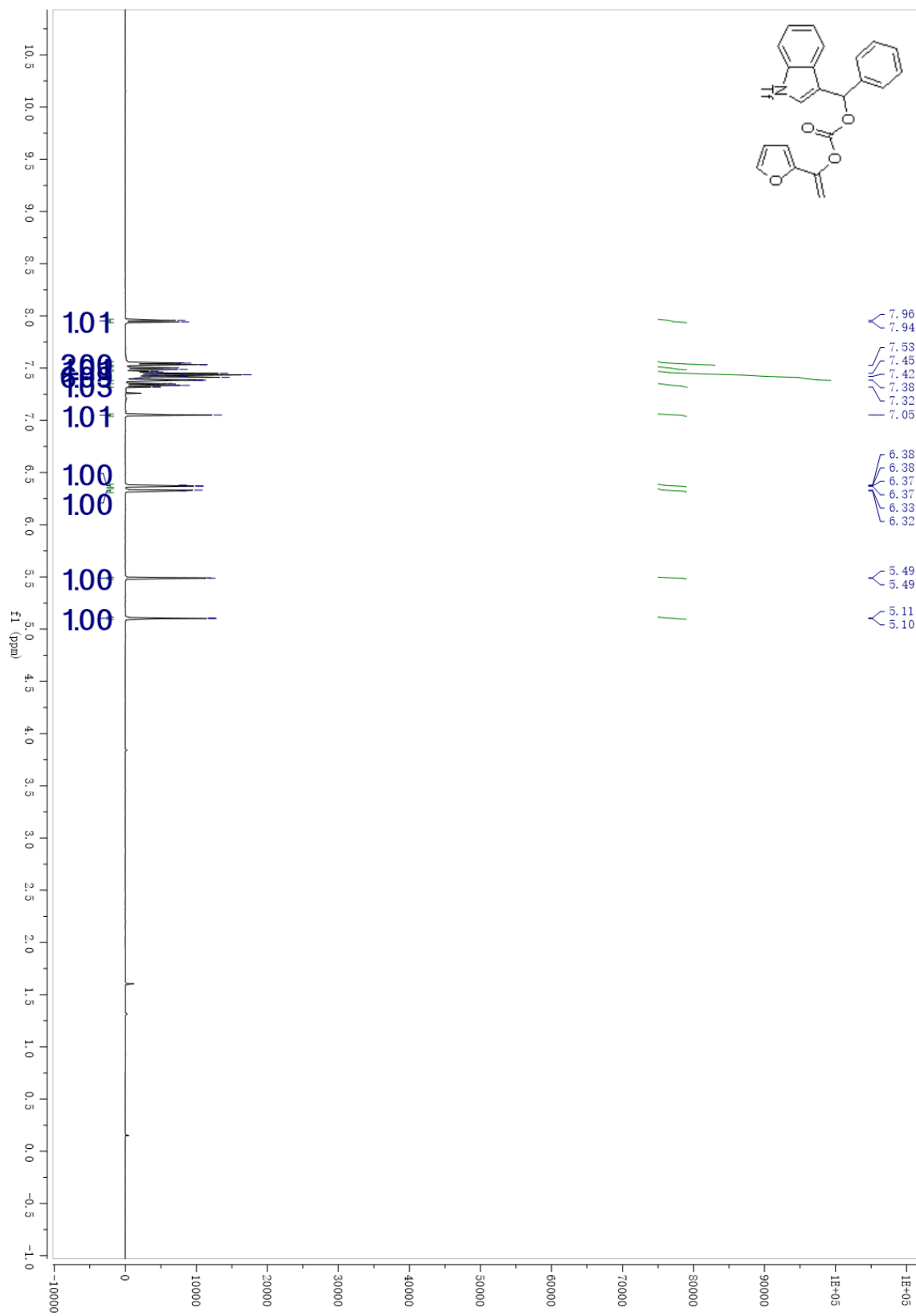
¹H NMR 3.11o



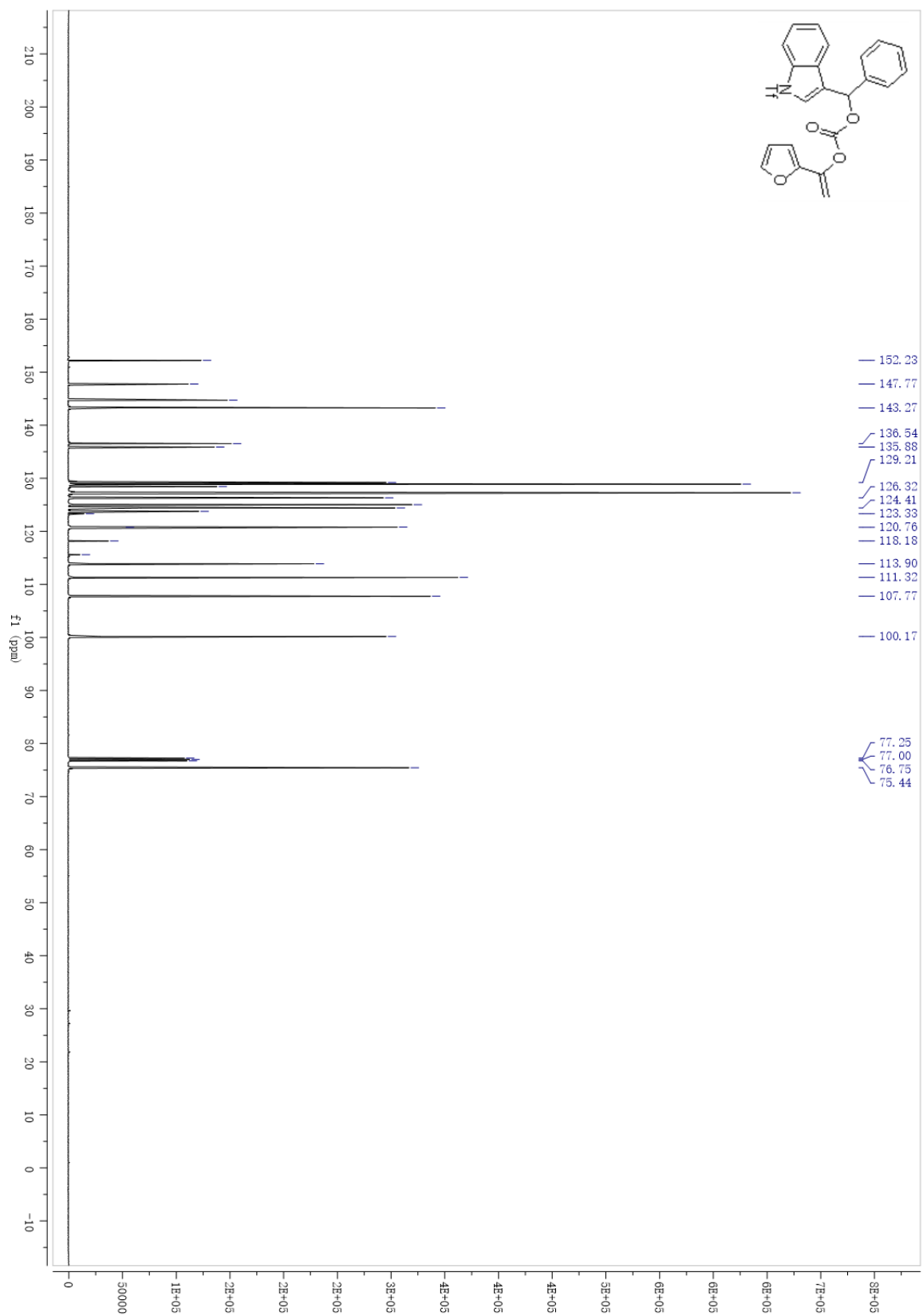
¹³C NMR 3.11o



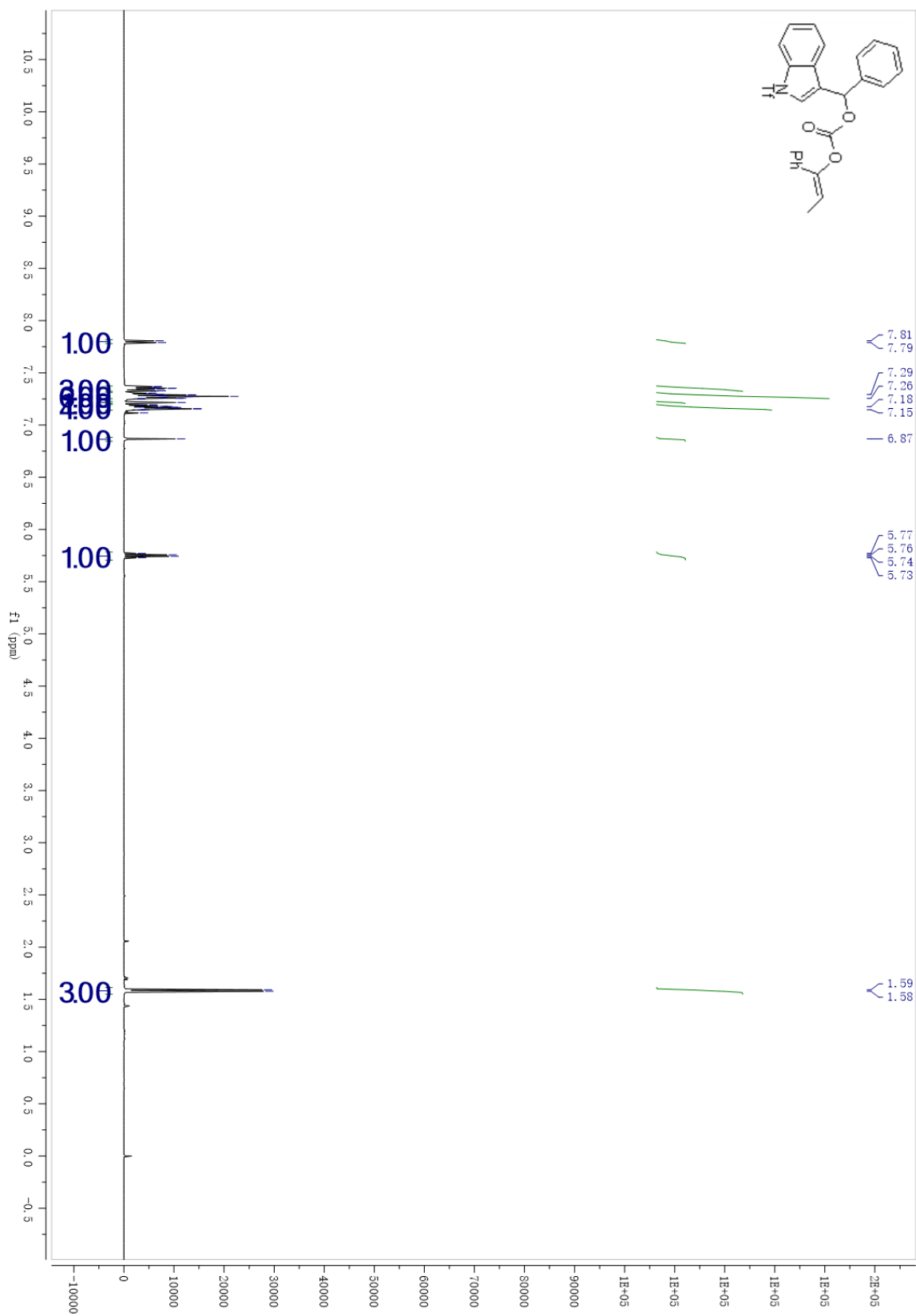
¹H NMR 3.11p



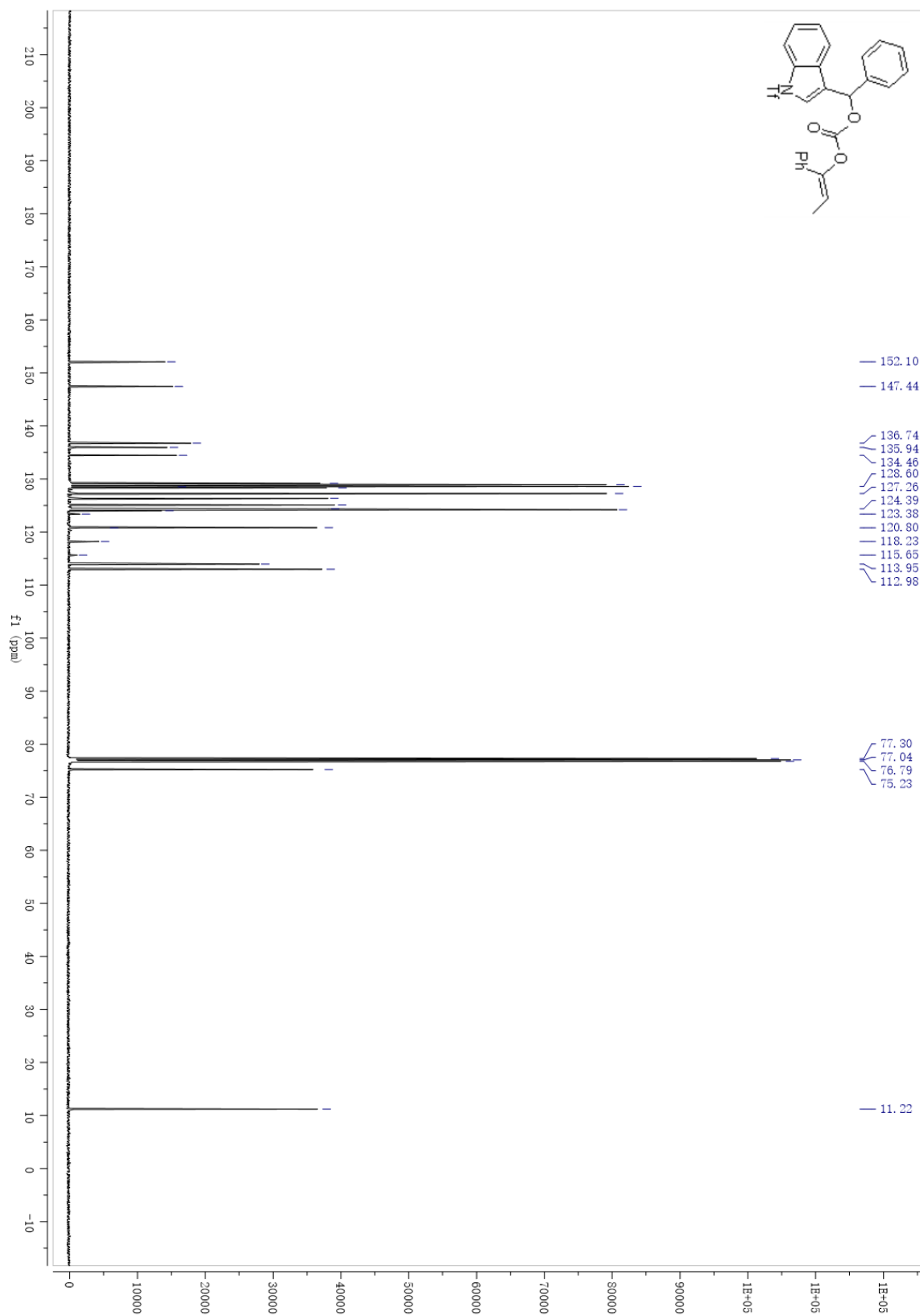
¹³C NMR 3.11p



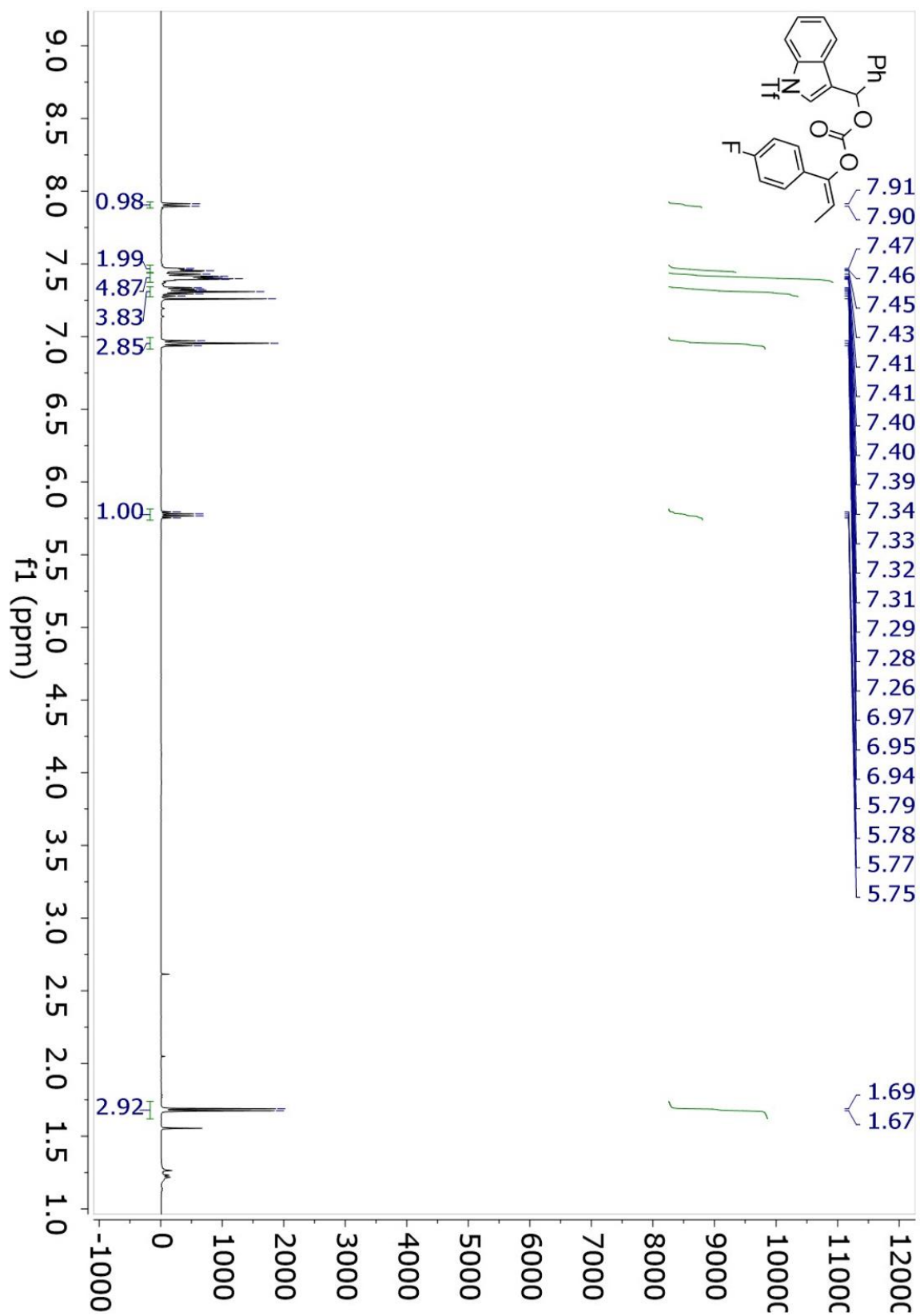
¹H NMR 3.11q



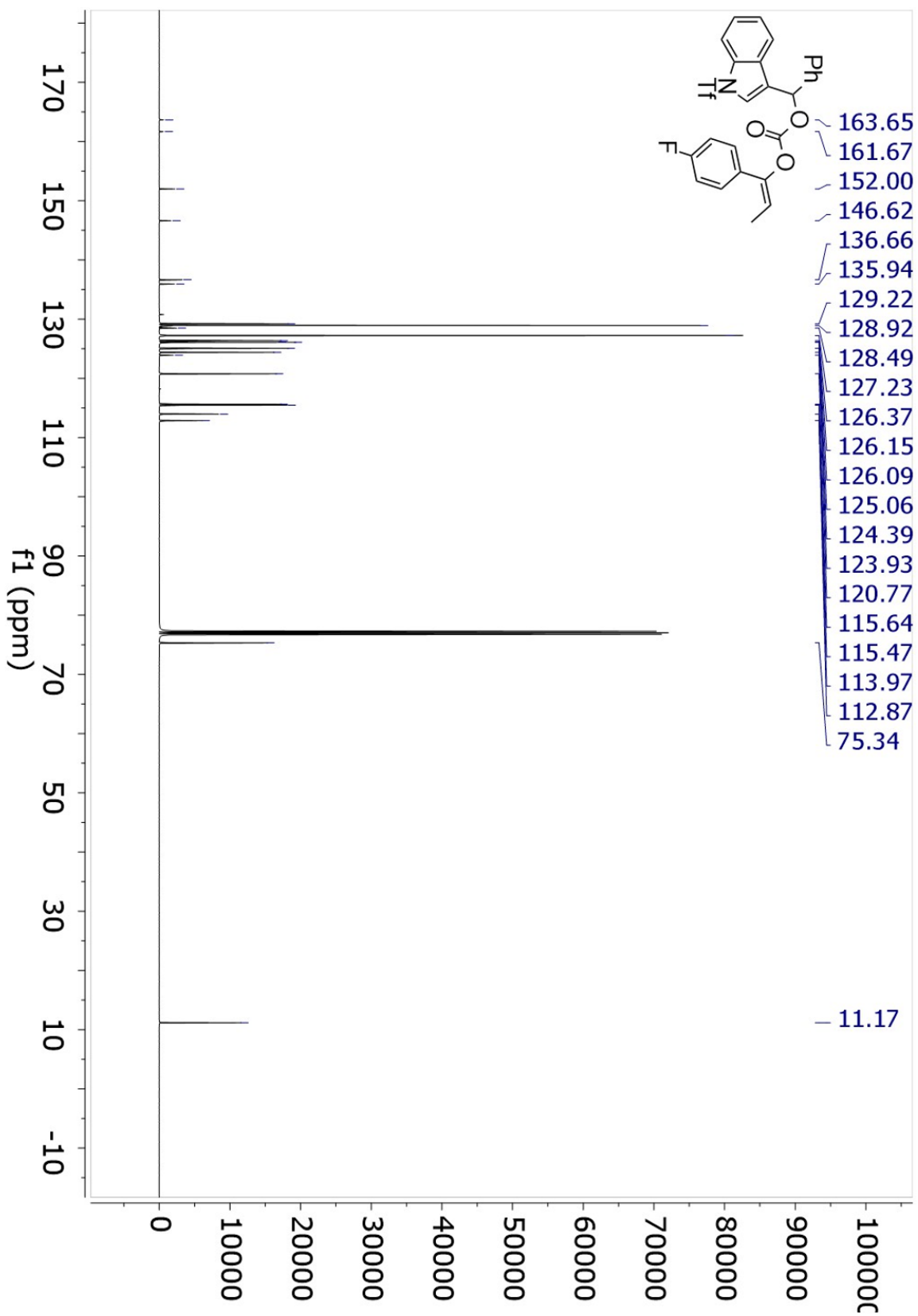
¹³C NMR 3.11q



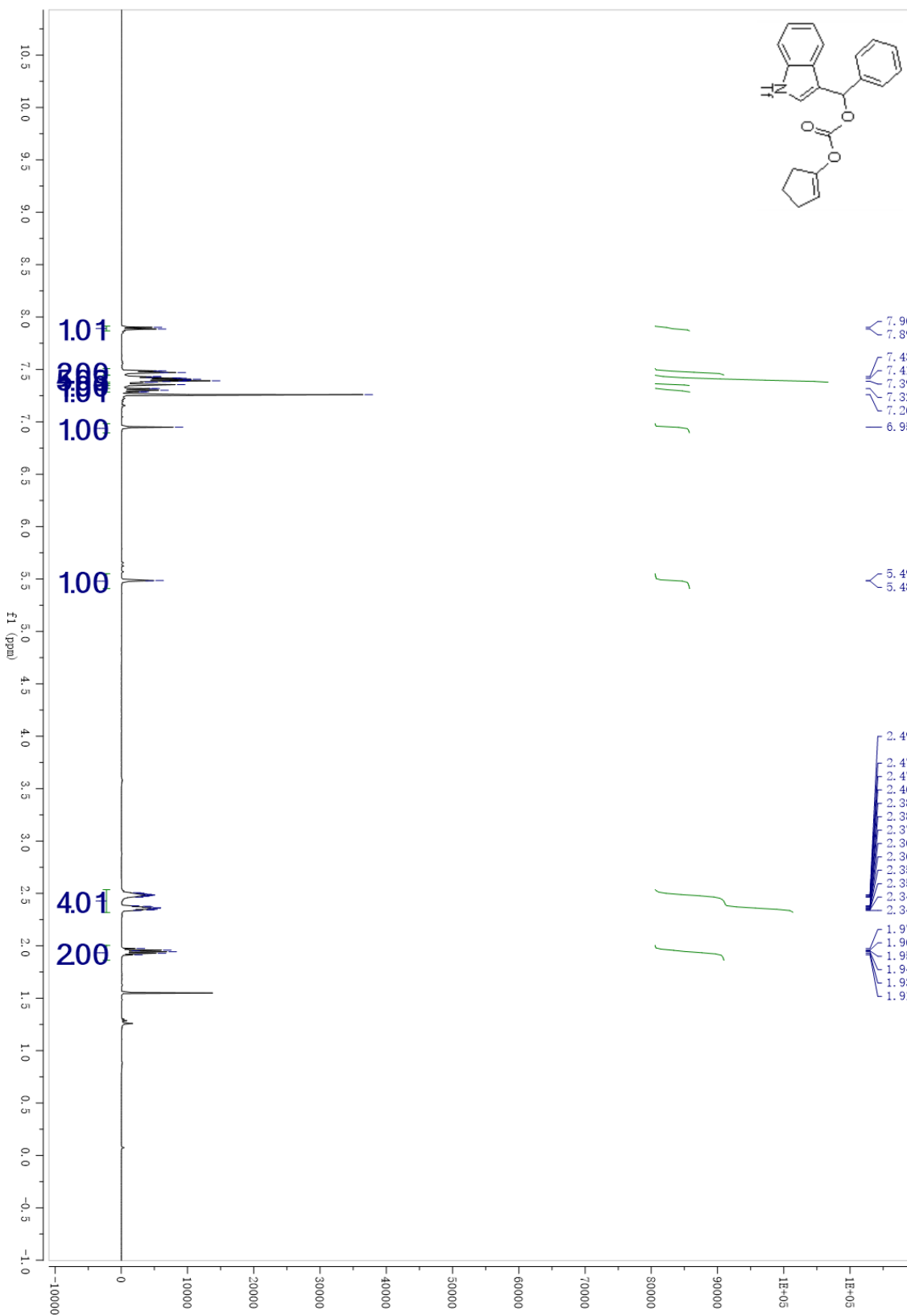
¹H NMR 3.11r



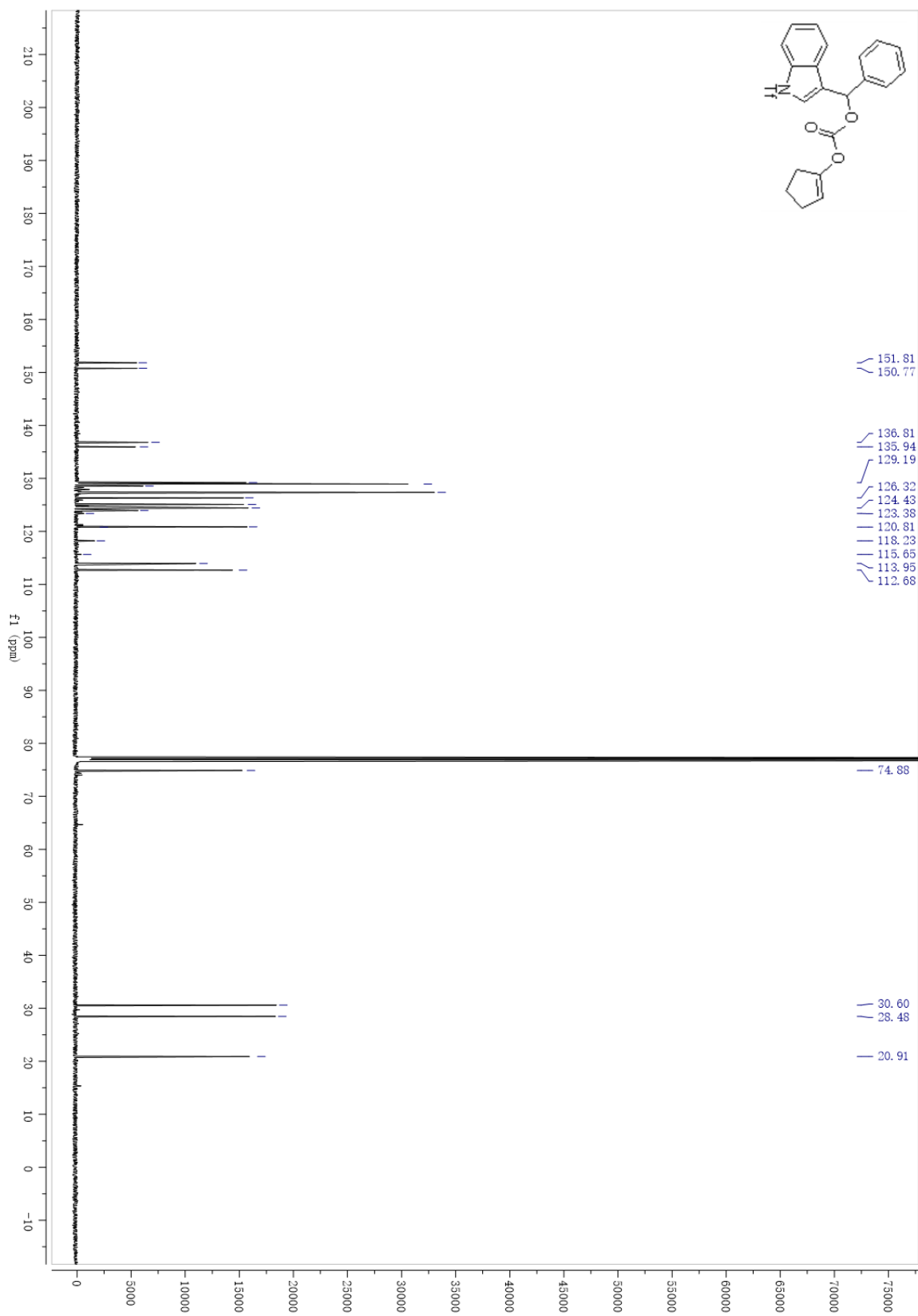
¹³C NMR 3.11r



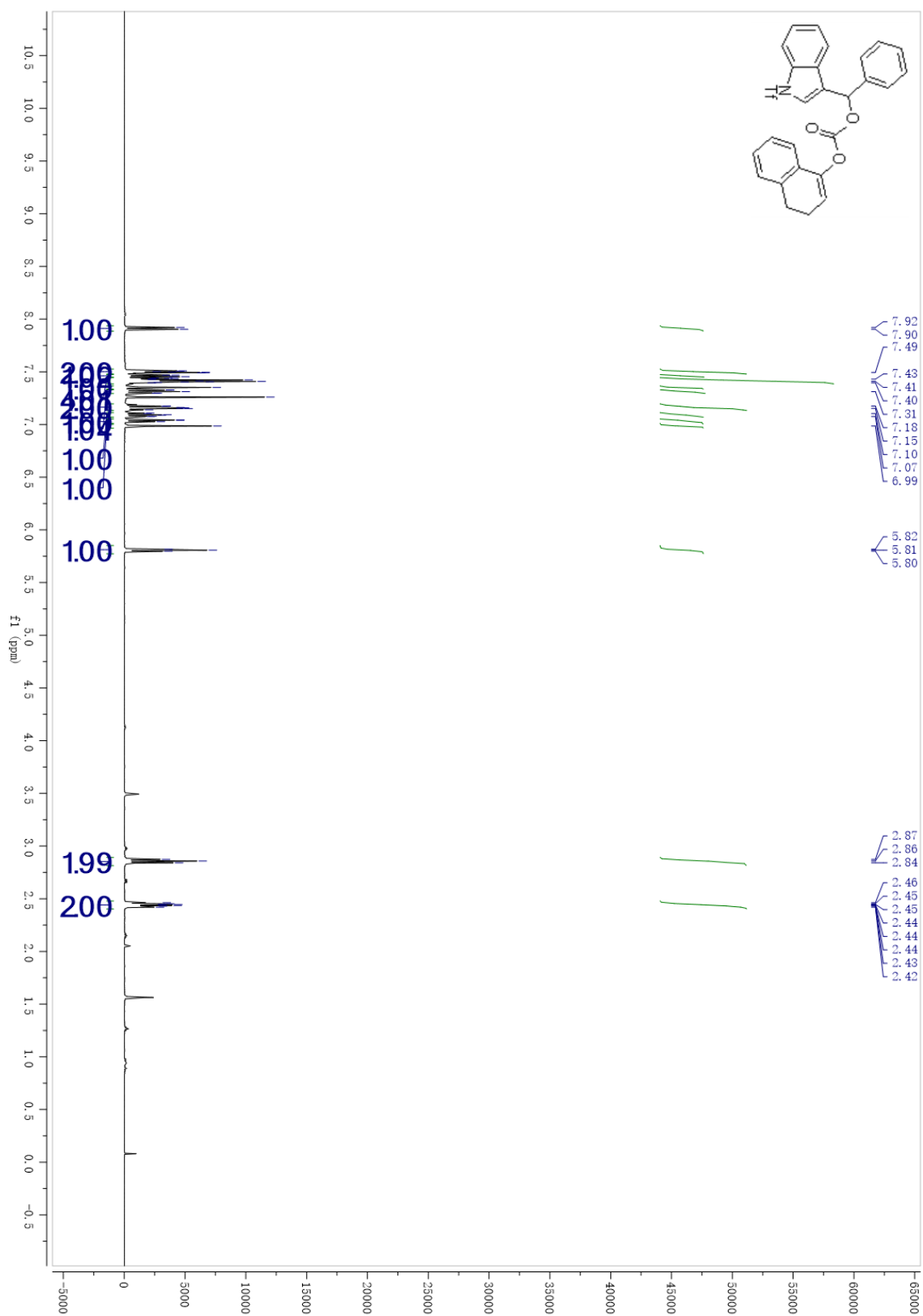
¹H NMR 3.11s



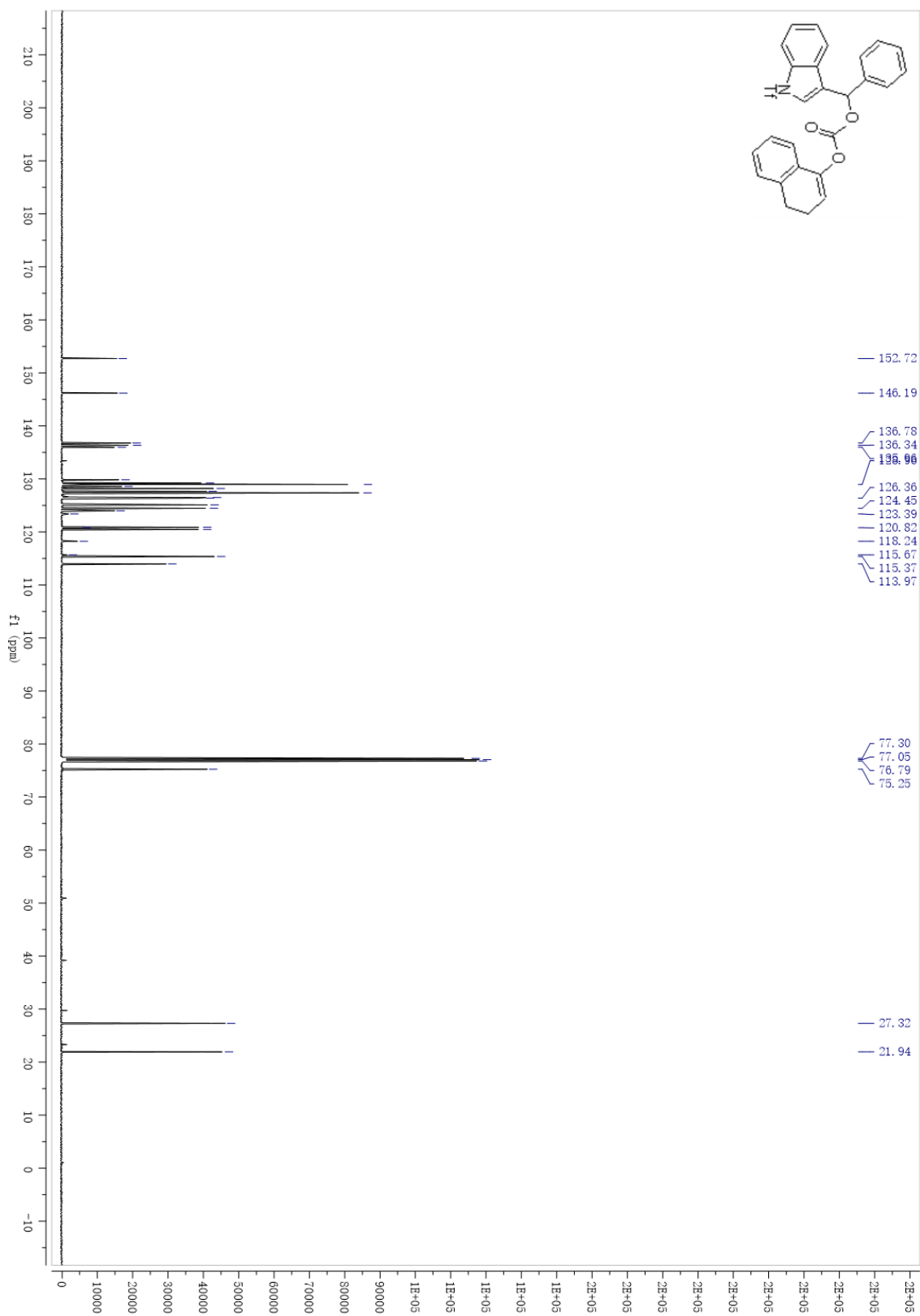
¹³C NMR 3.11s



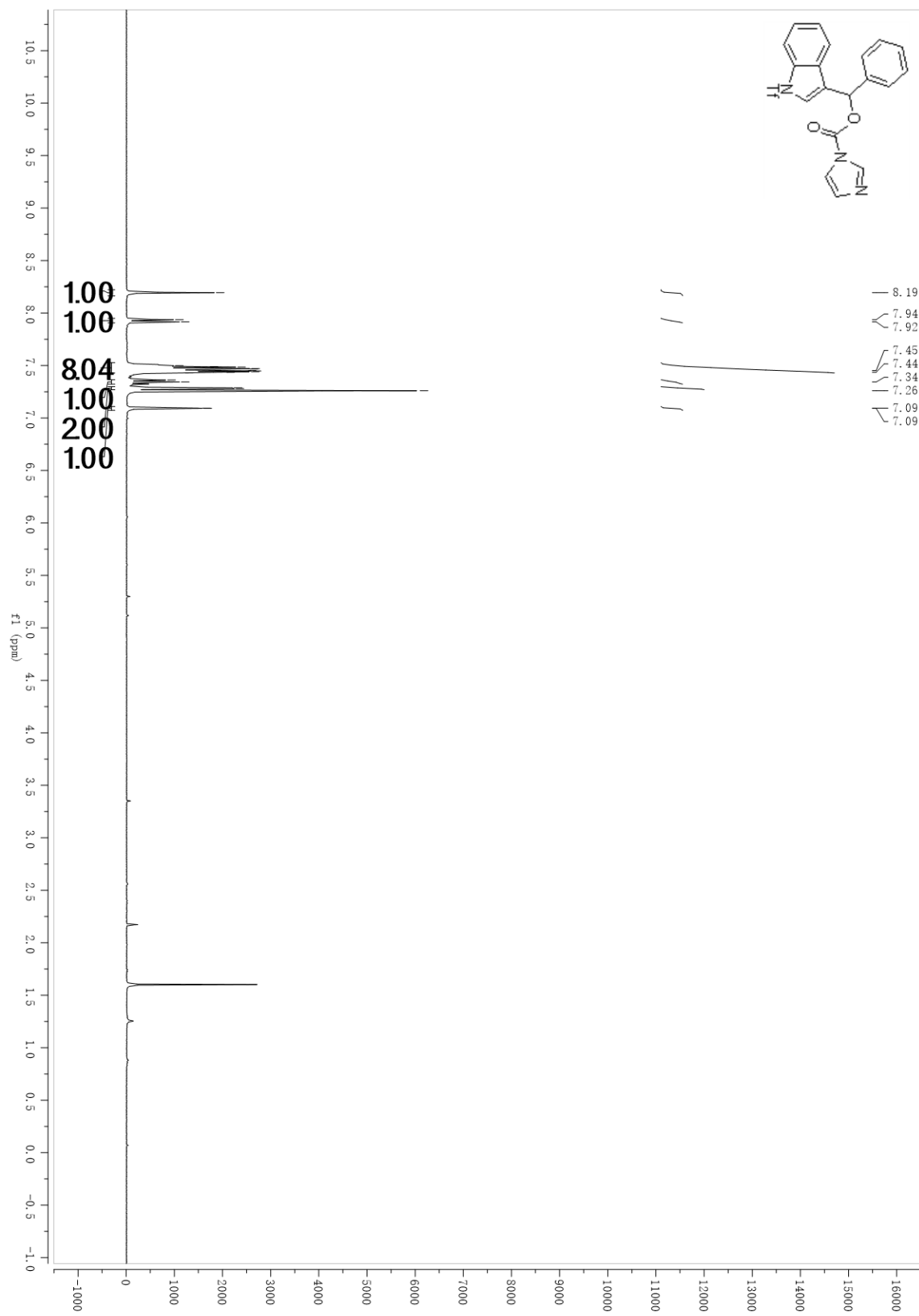
¹H NMR 3.11t



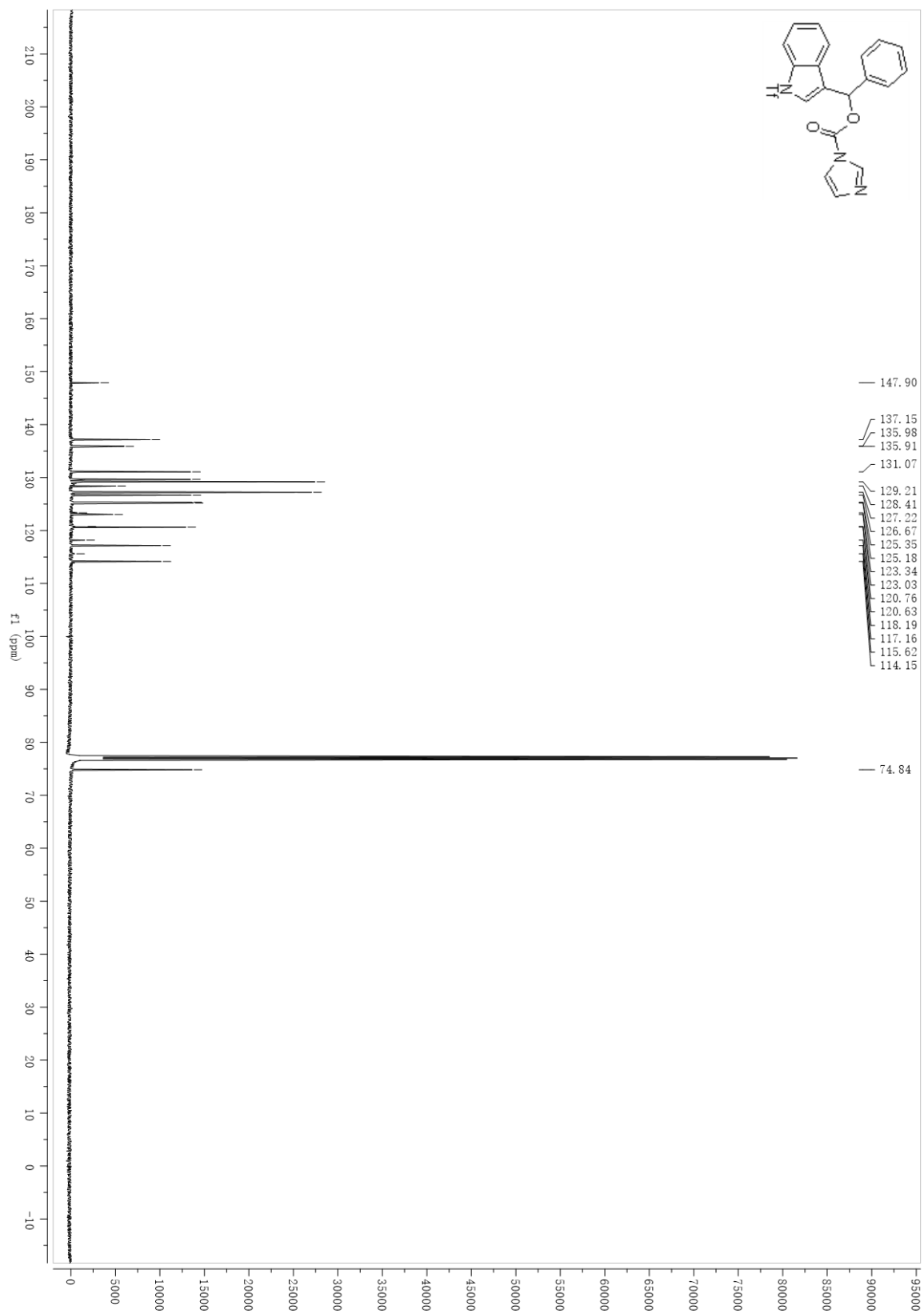
¹³C NMR 3.11t



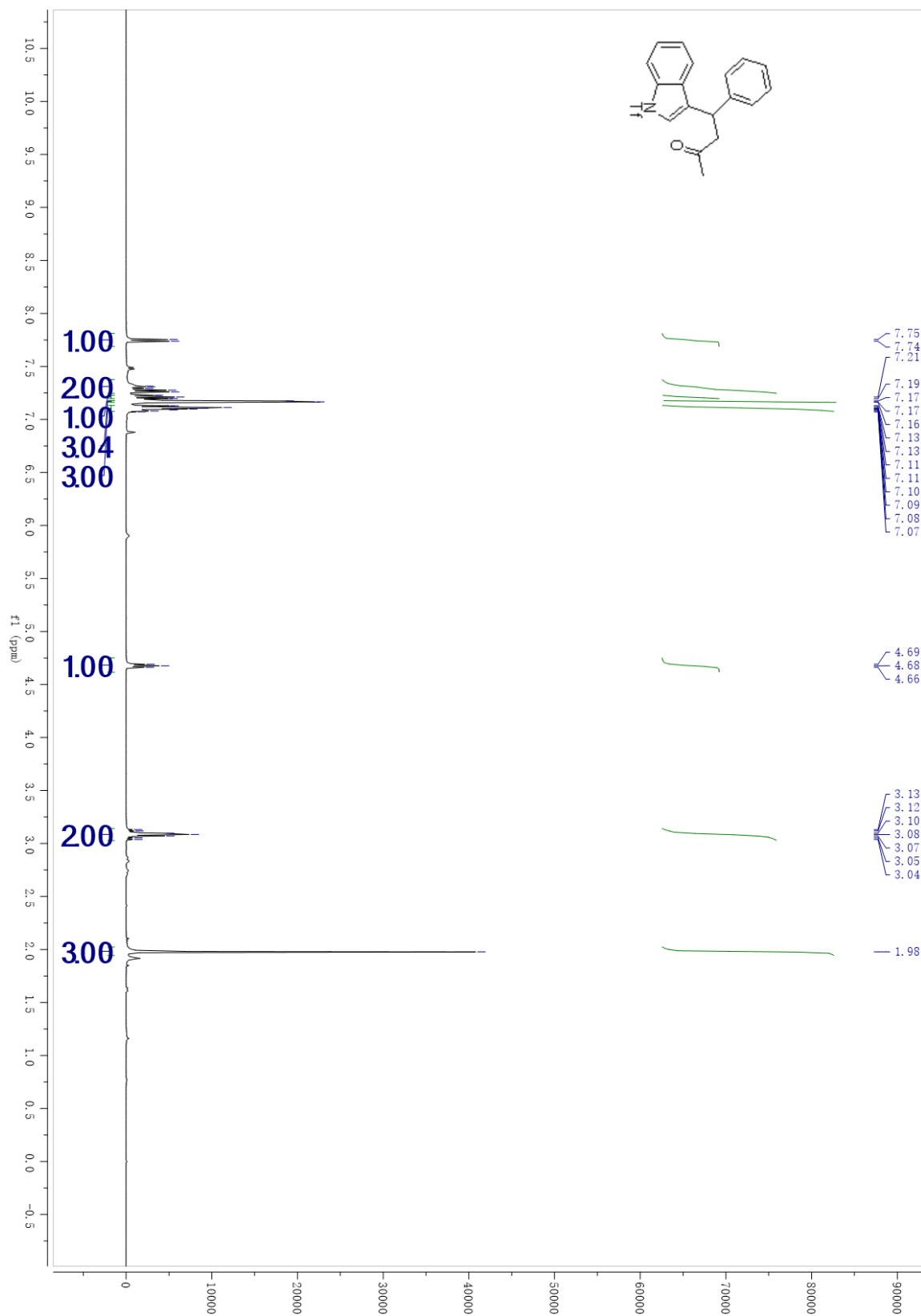
¹H NMR S1



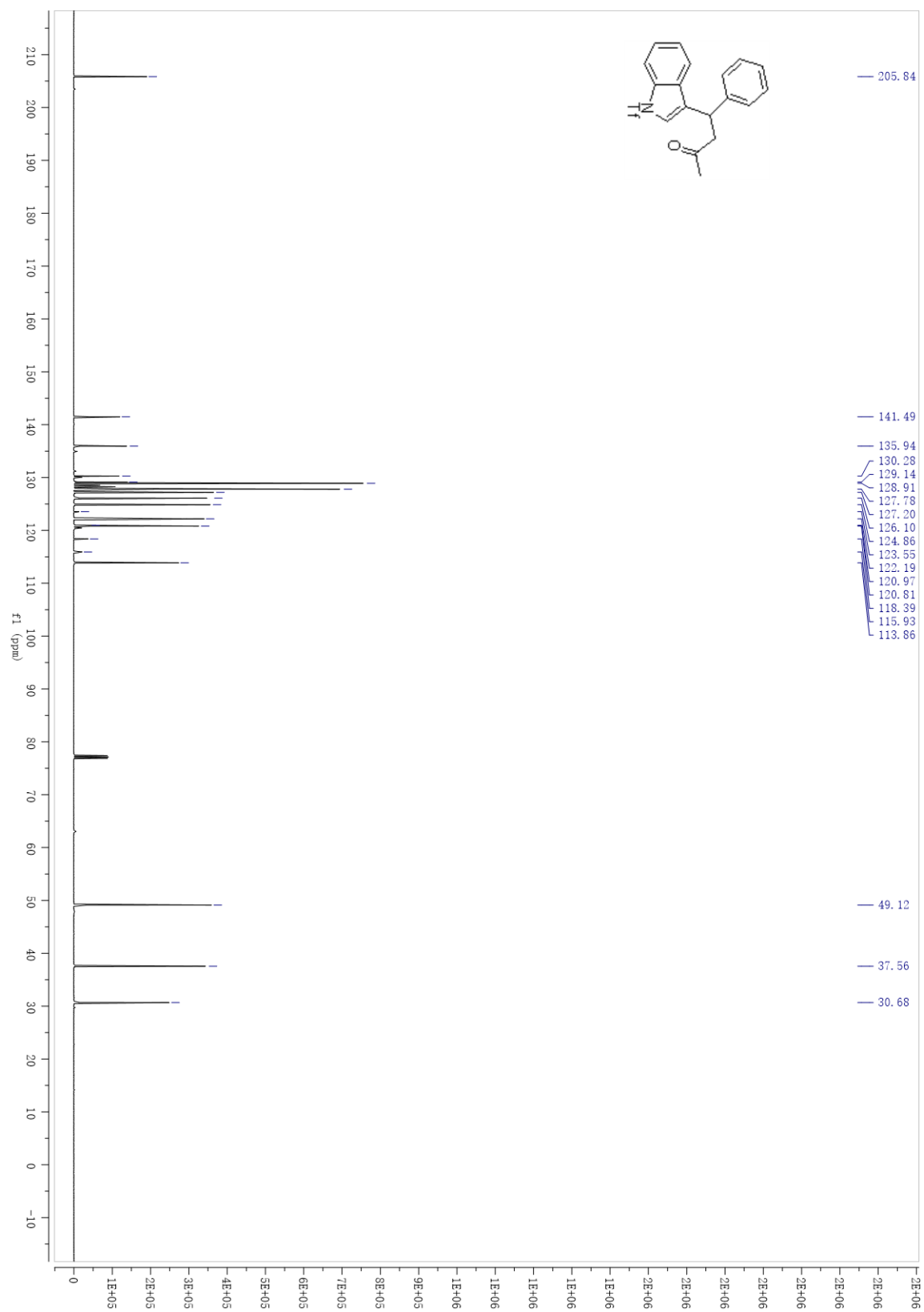
¹³C NMR S1



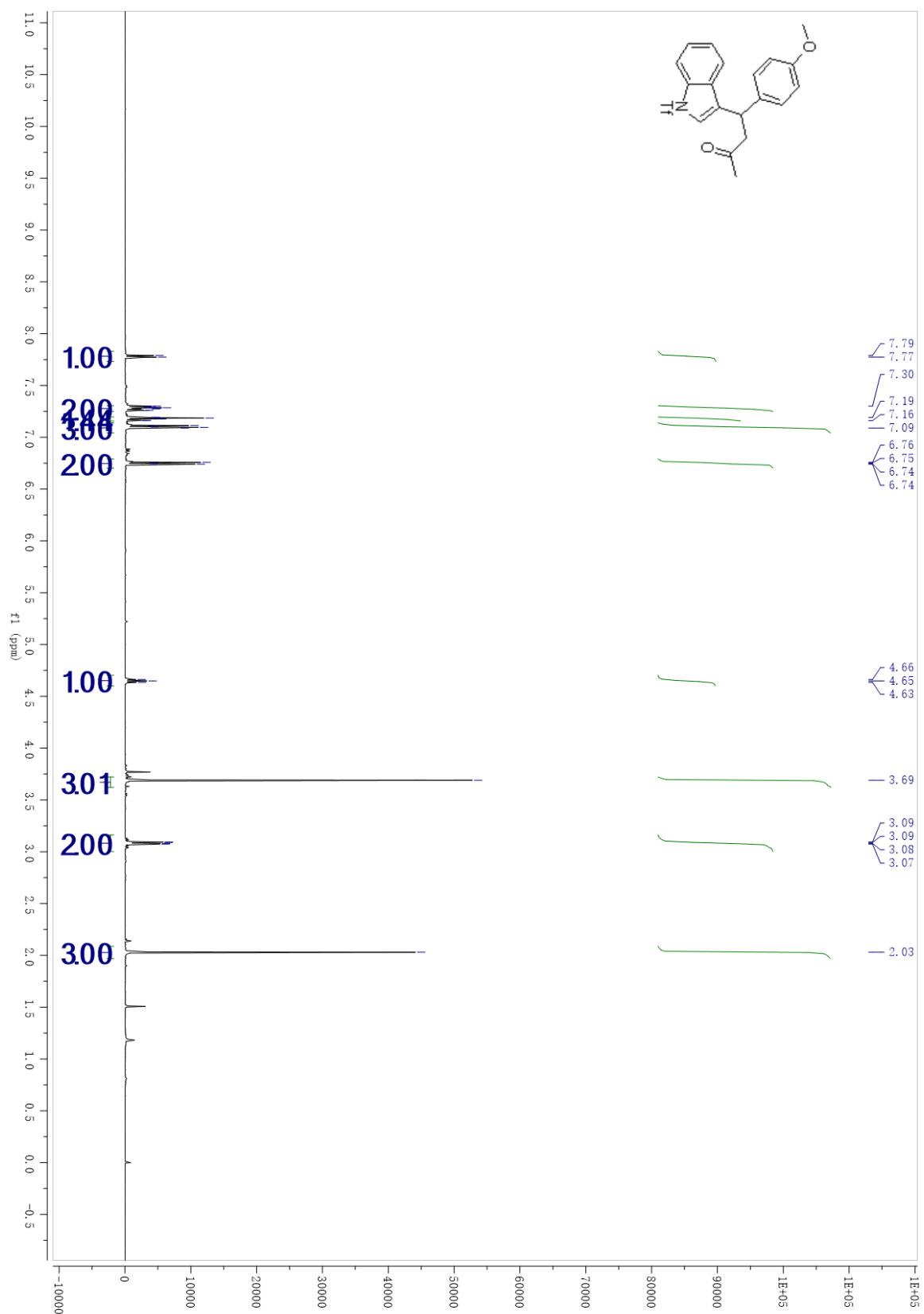
¹H NMR 3.12a



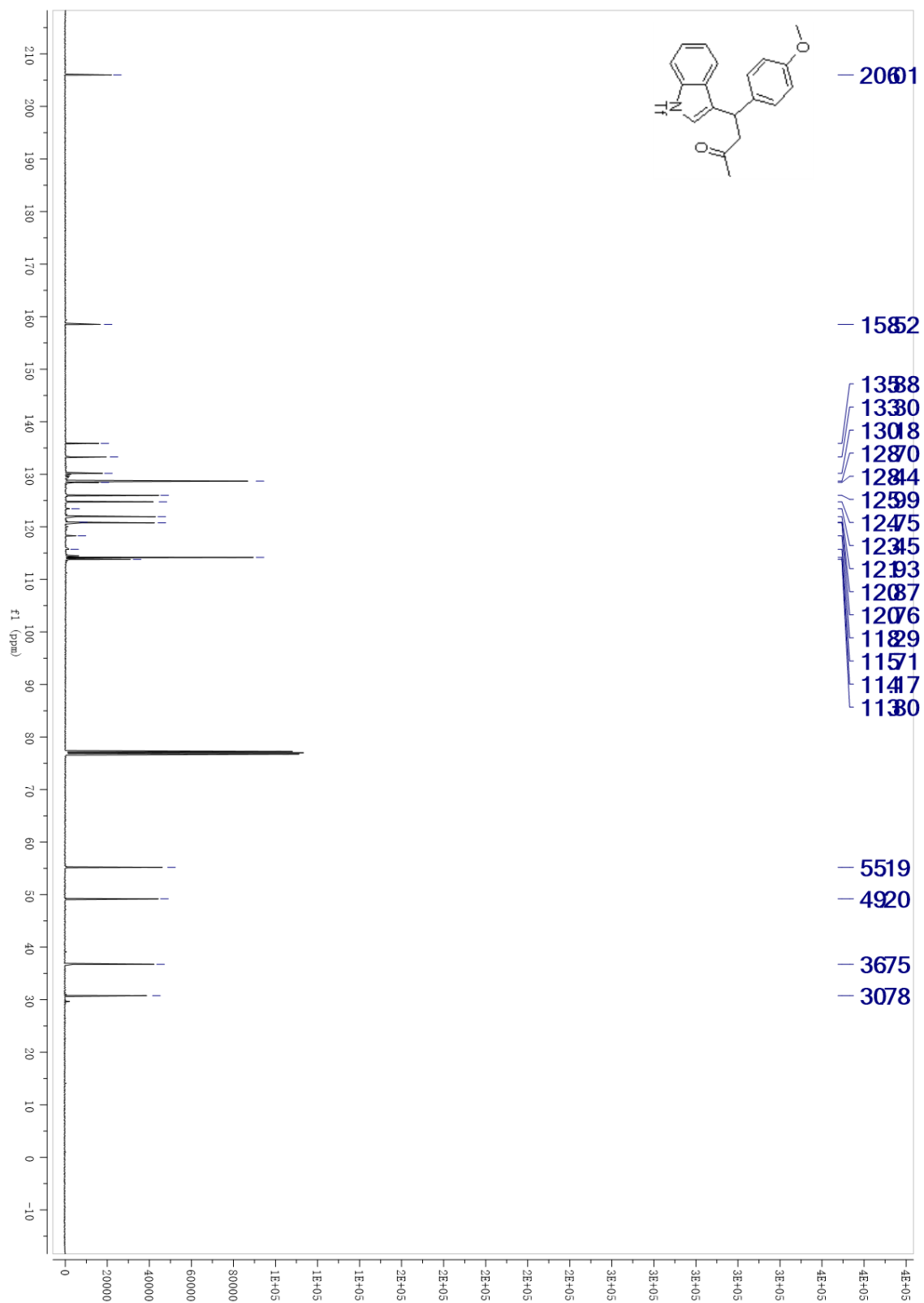
¹³C NMR 3.12a



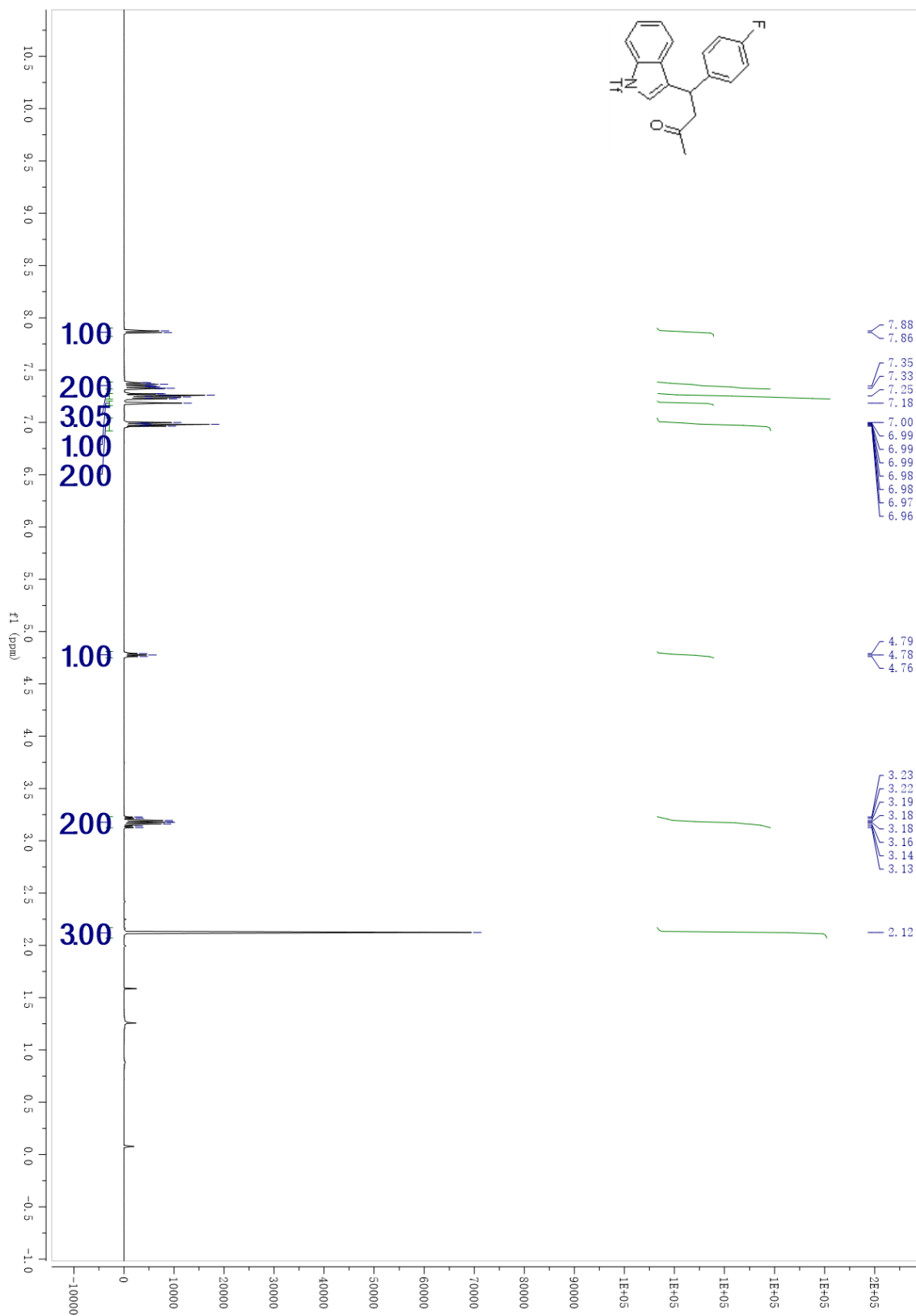
¹H NMR 3.12b



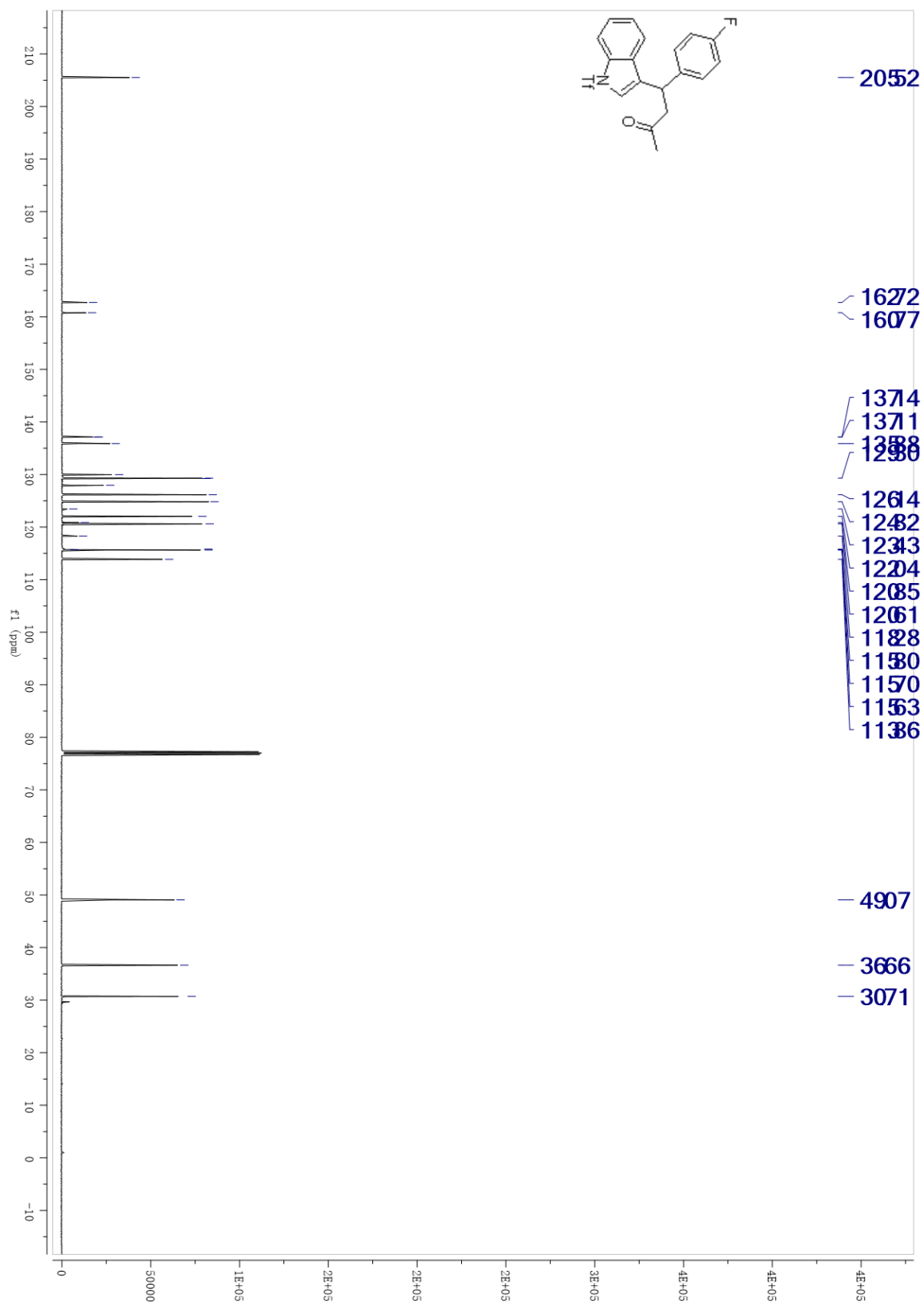
¹³C NMR 3.12b



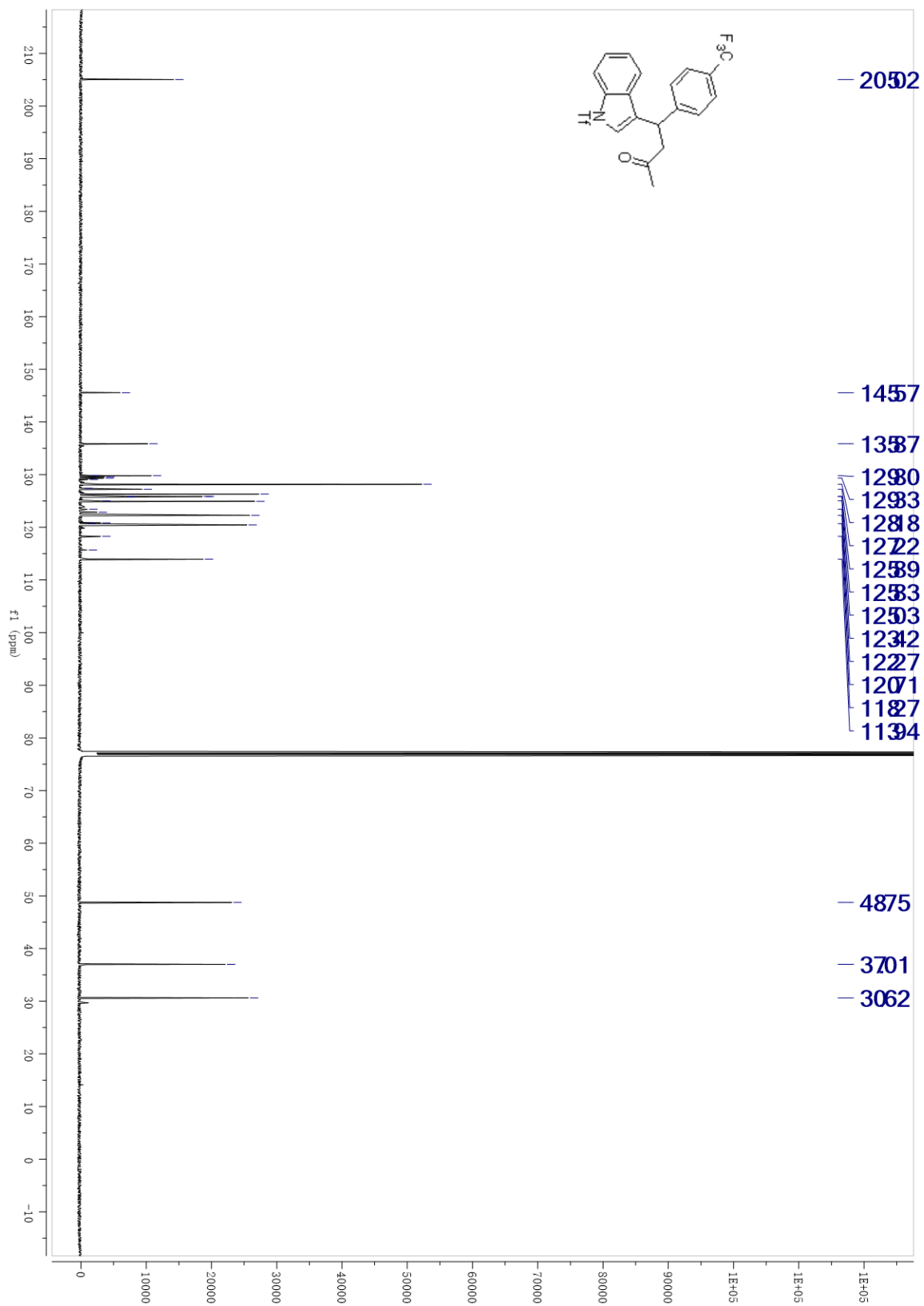
¹H NMR 3.12c



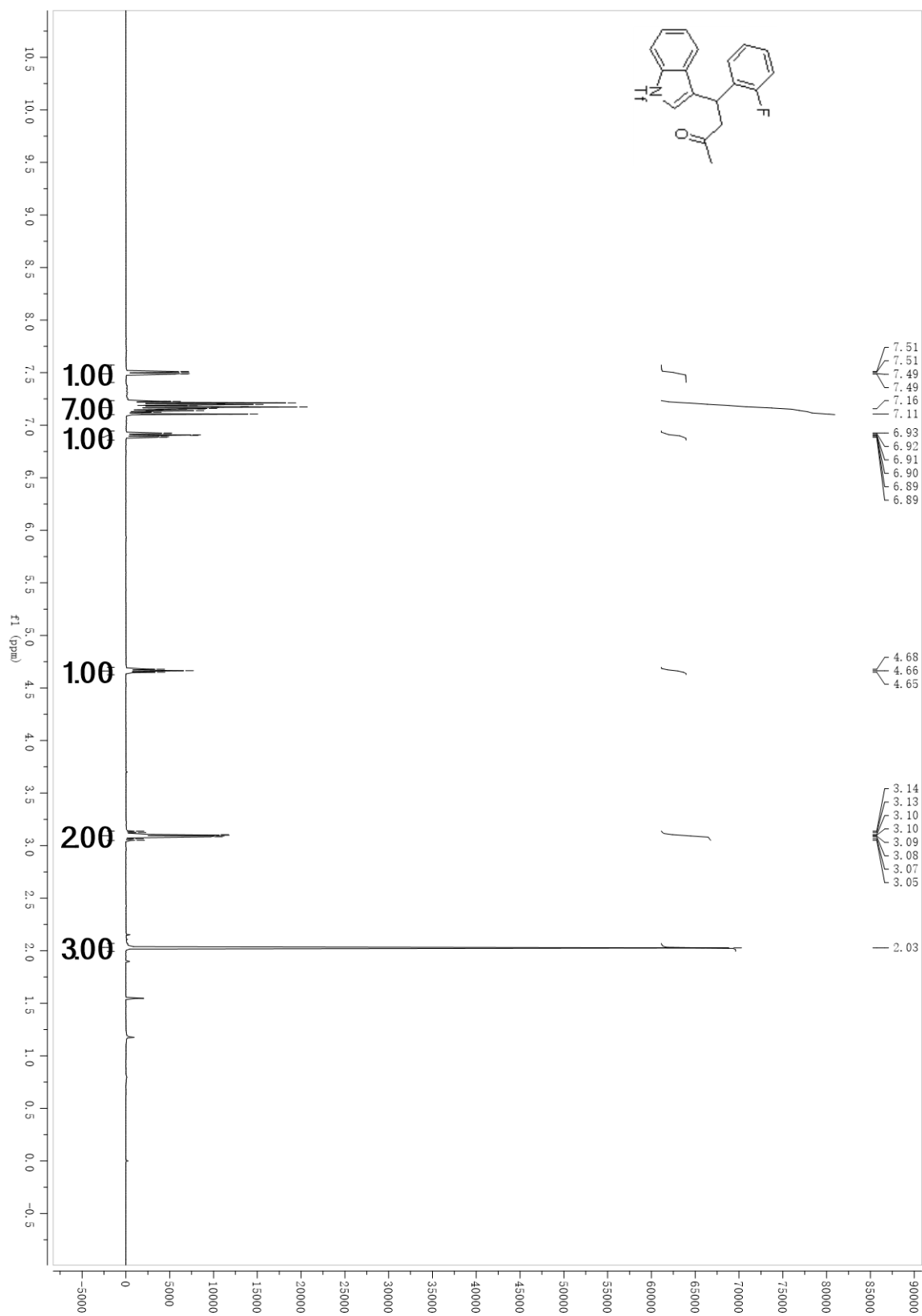
¹³C NMR 3.12c



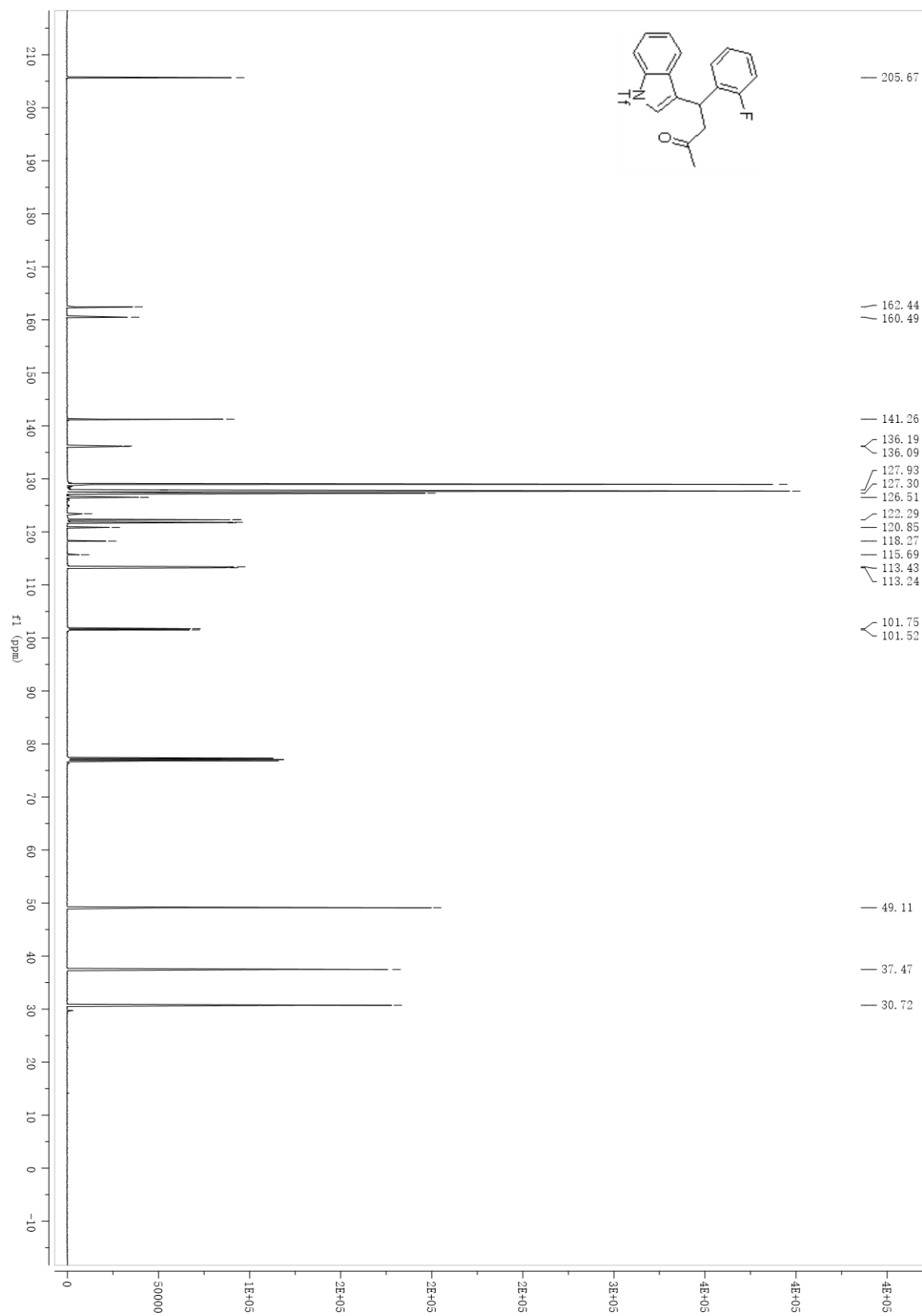
¹³C NMR 3.12d



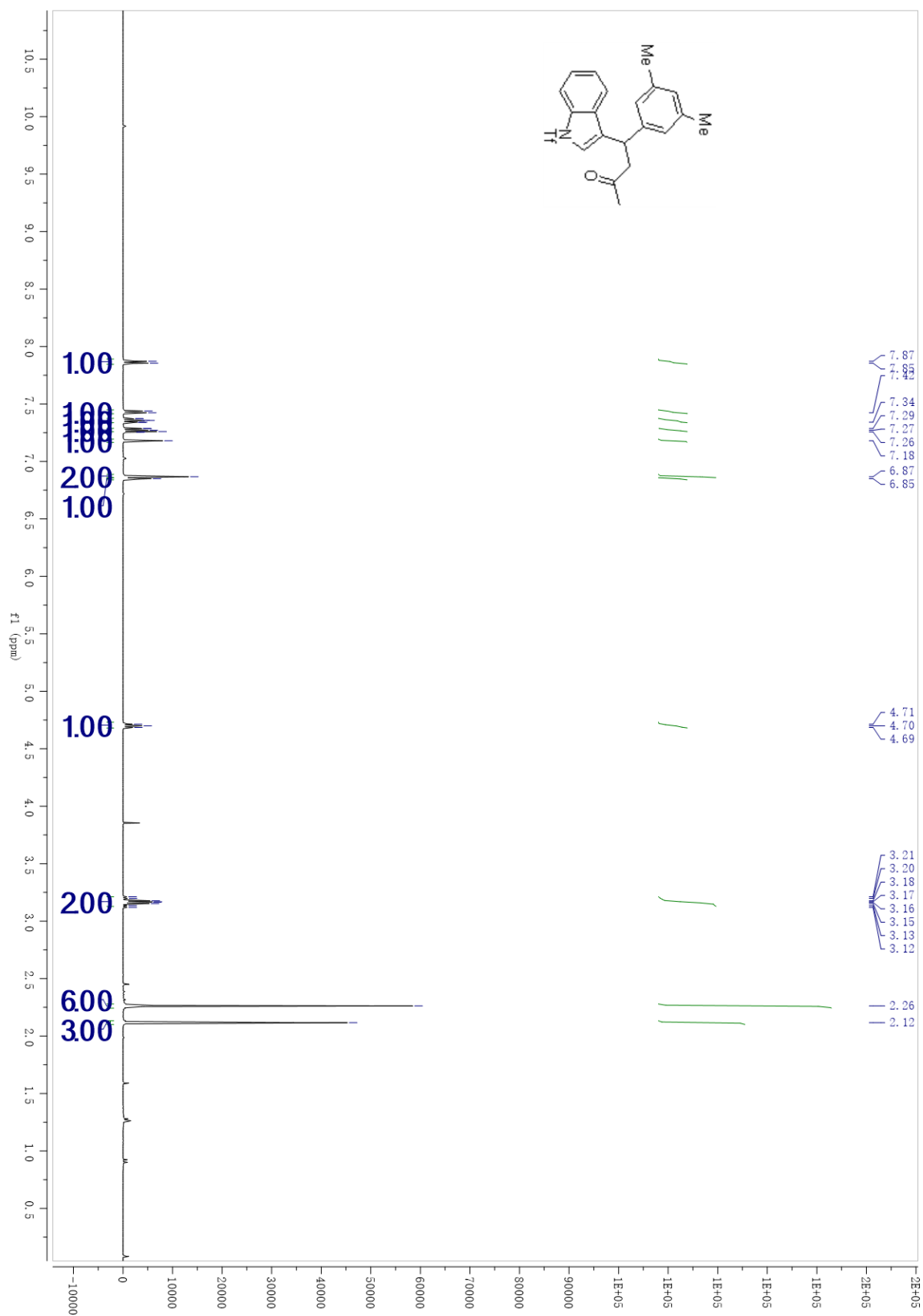
¹H NMR 3.12e



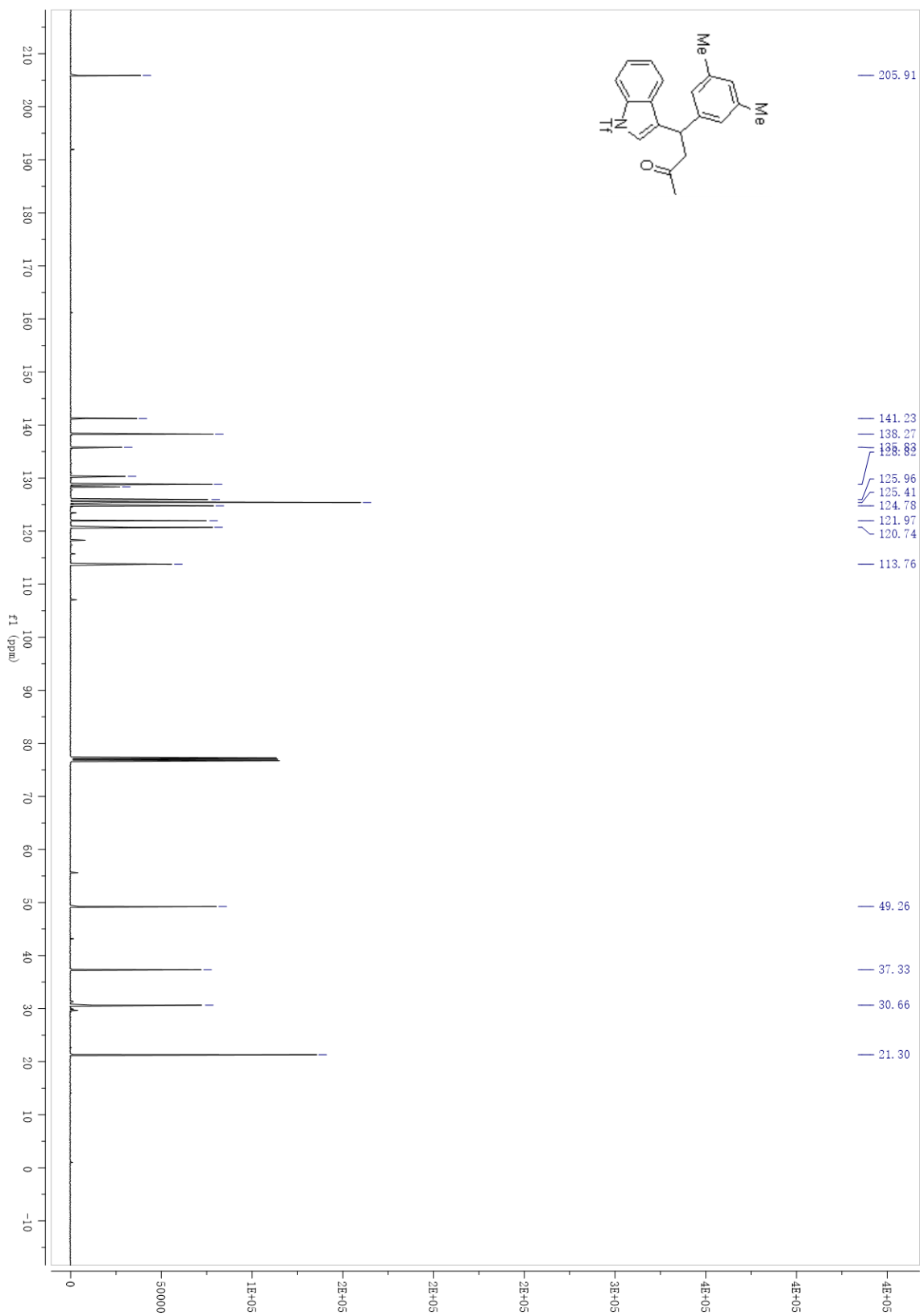
¹³C NMR 3.12e



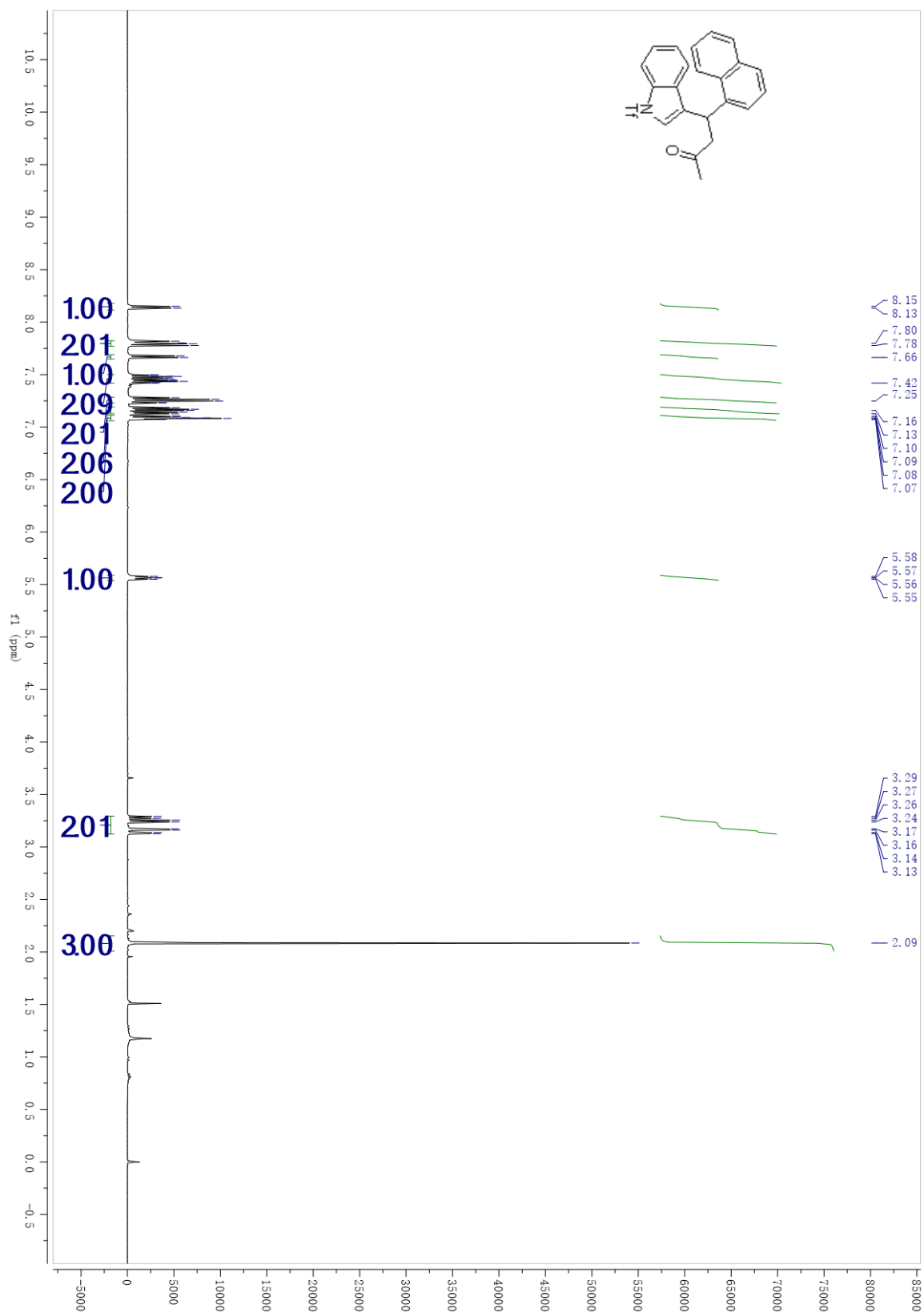
¹H NMR 3.12f



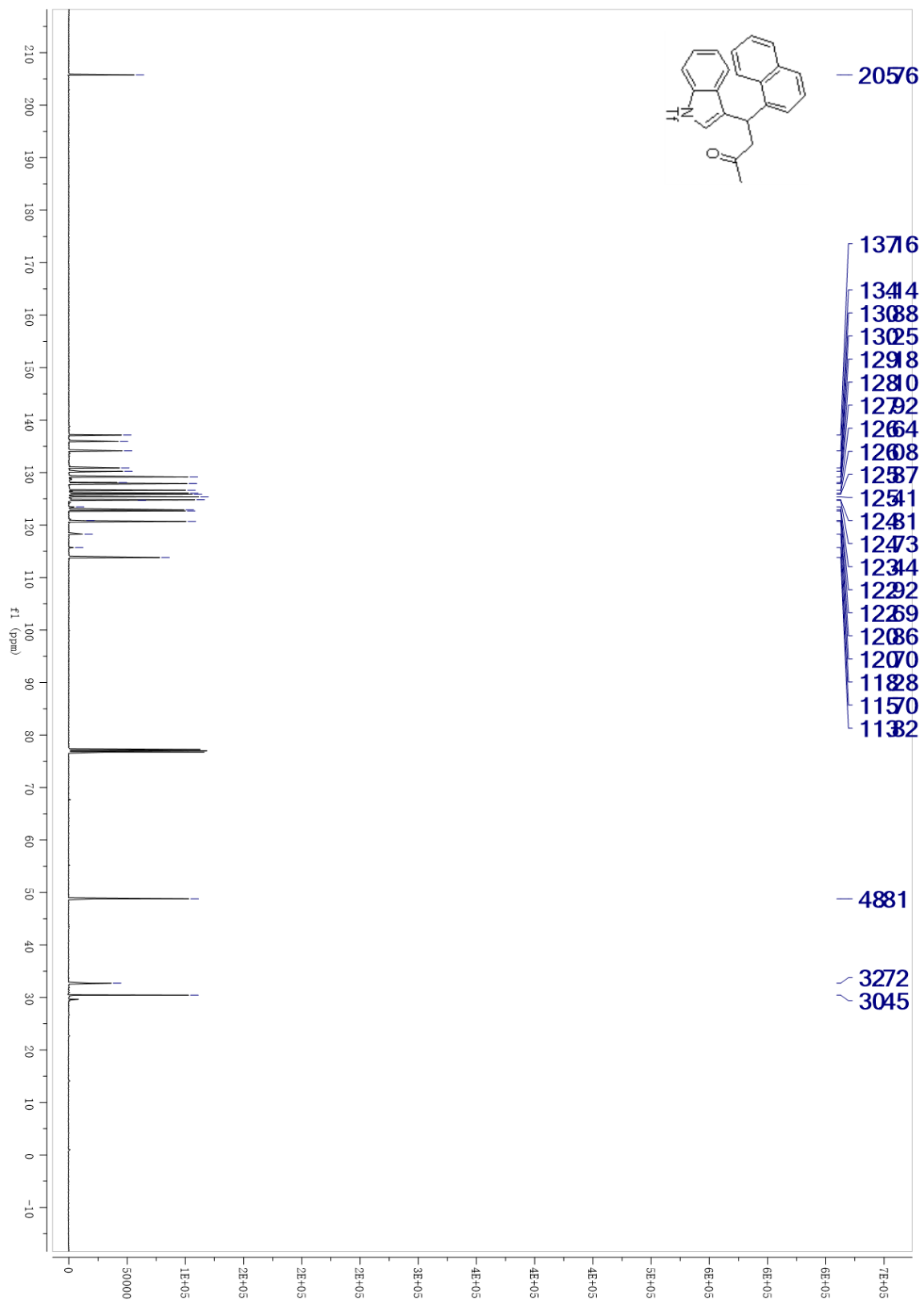
¹³C NMR 3.12f



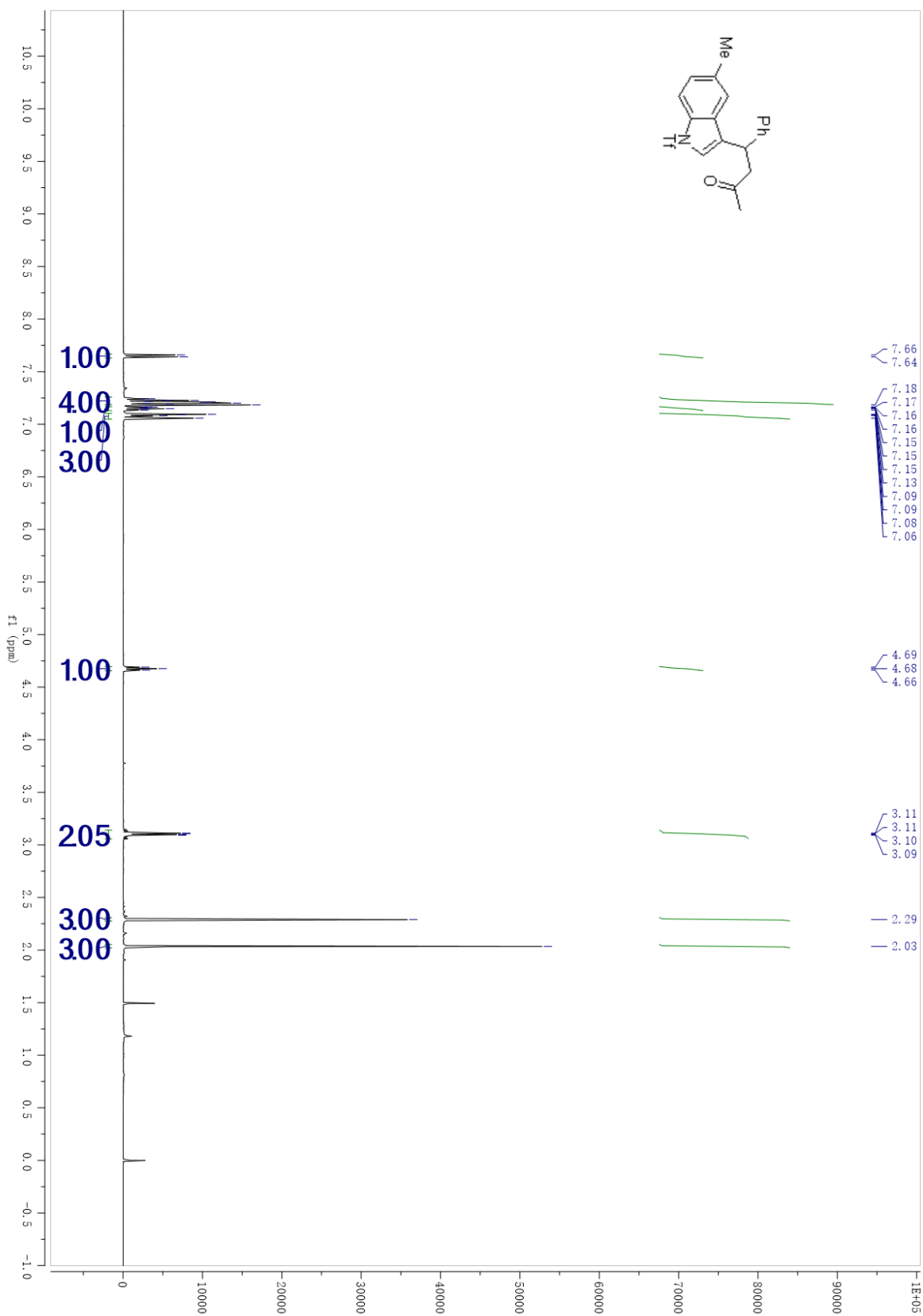
¹H NMR 3.12g



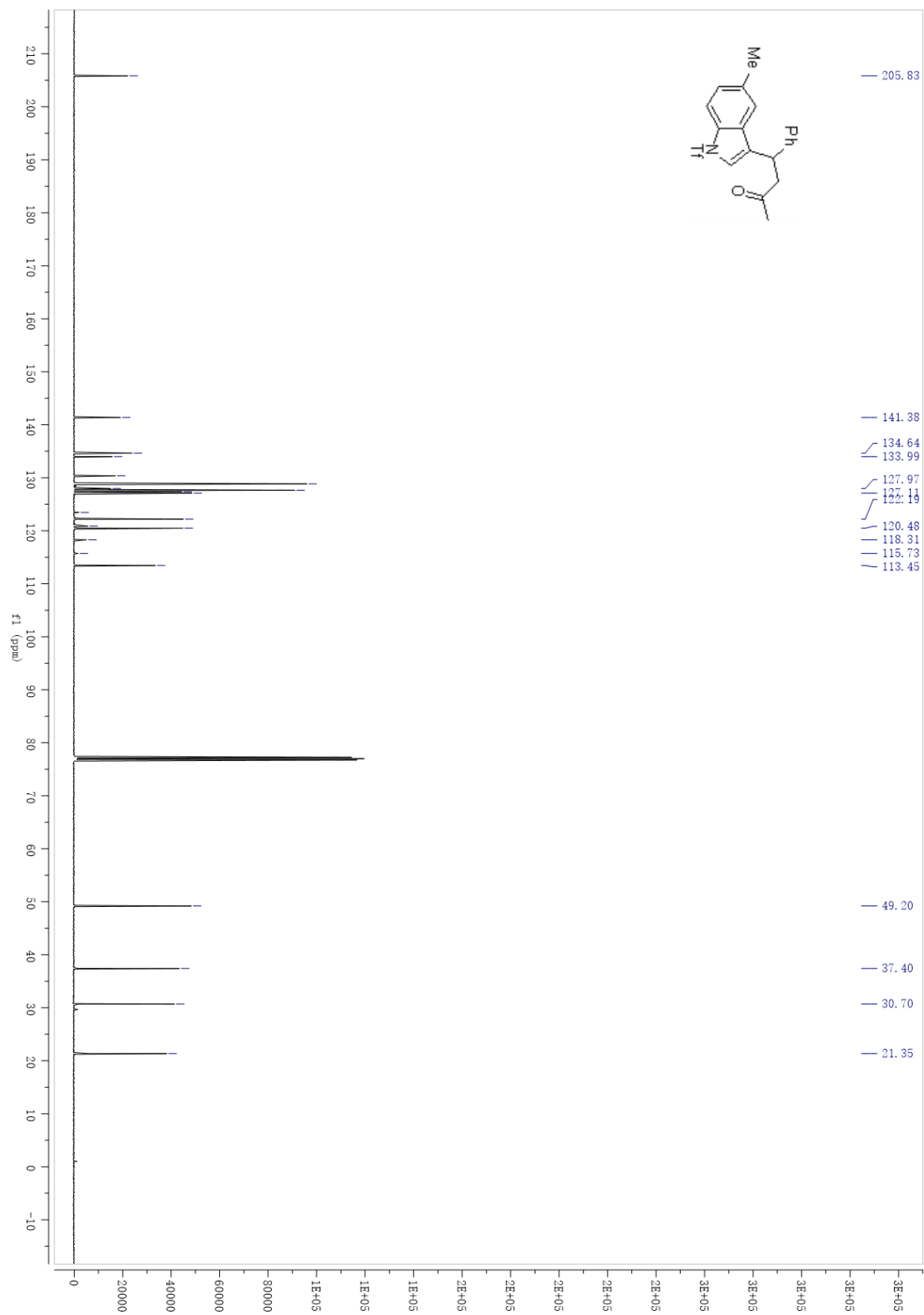
¹³C NMR 3.12g



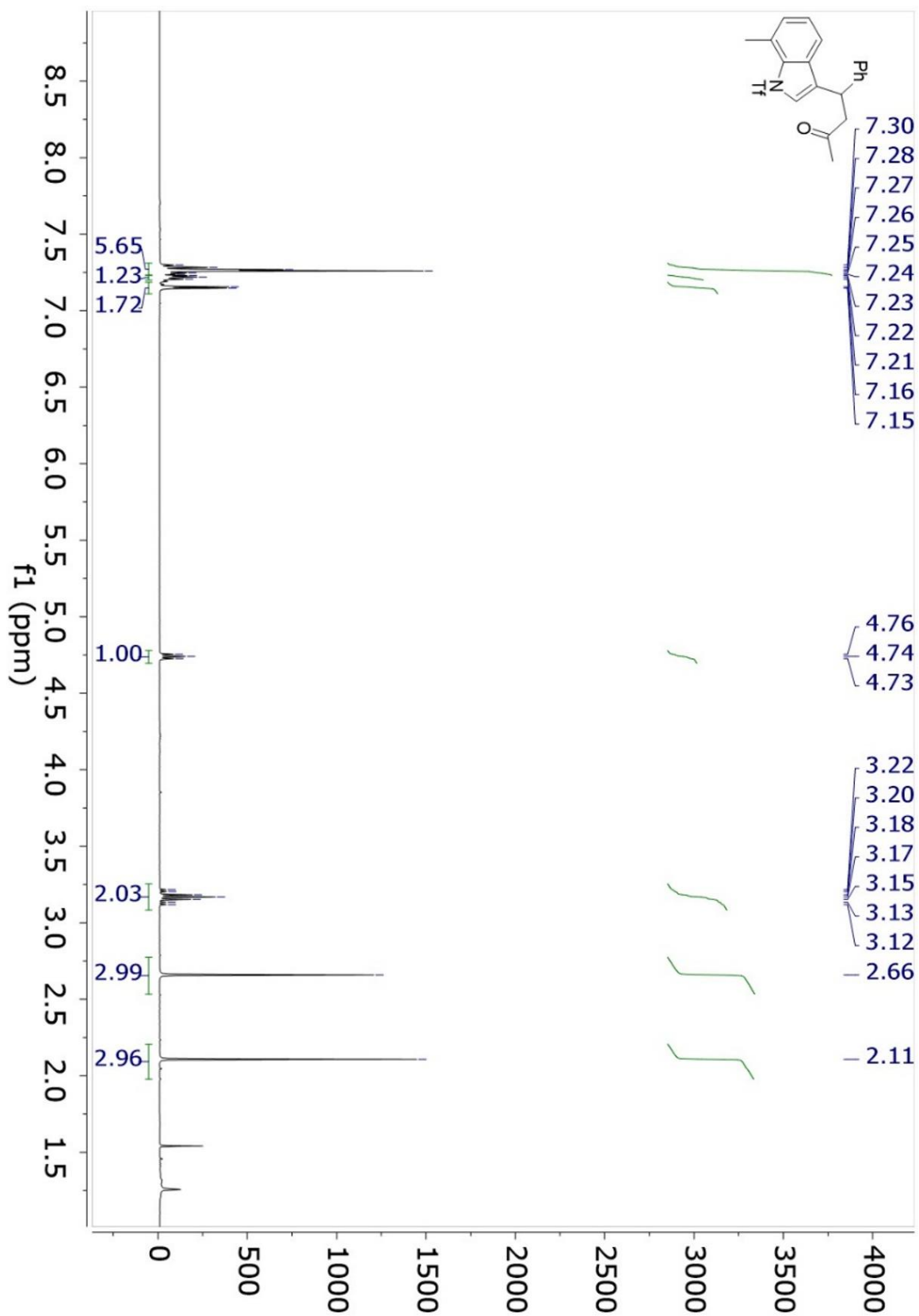
¹H NMR 3.12i



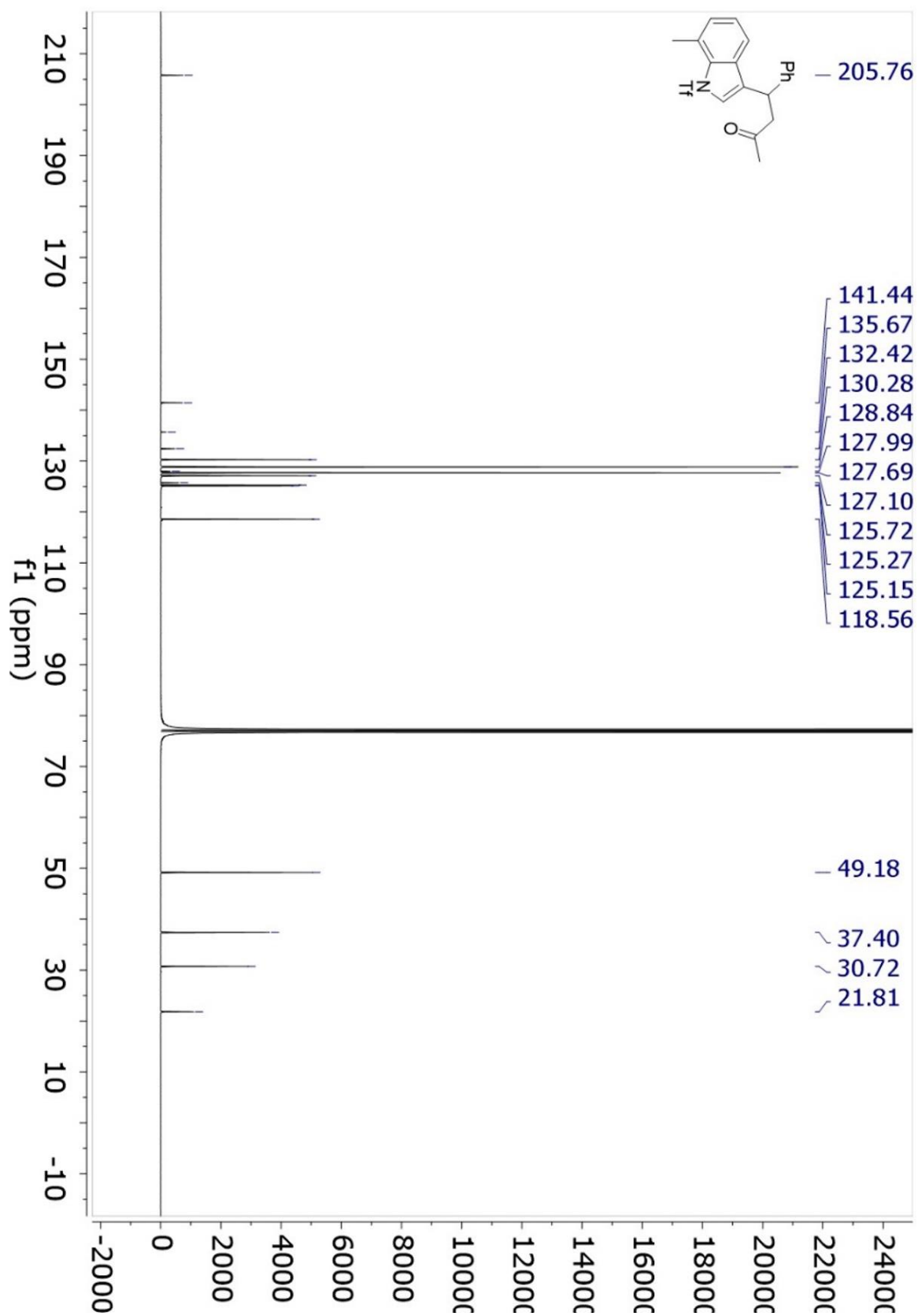
¹³C NMR 3.12i



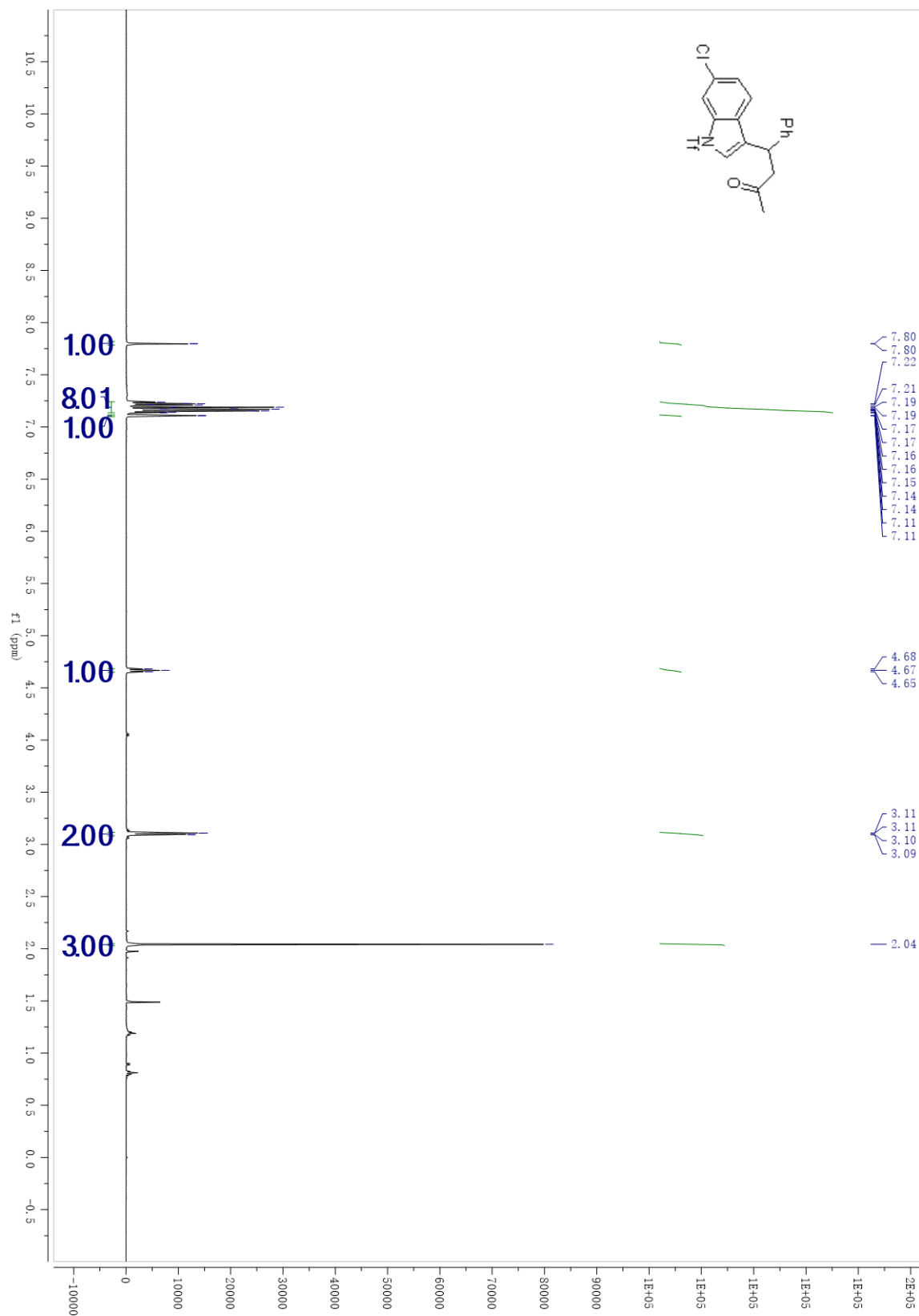
¹H NMR 3.12j



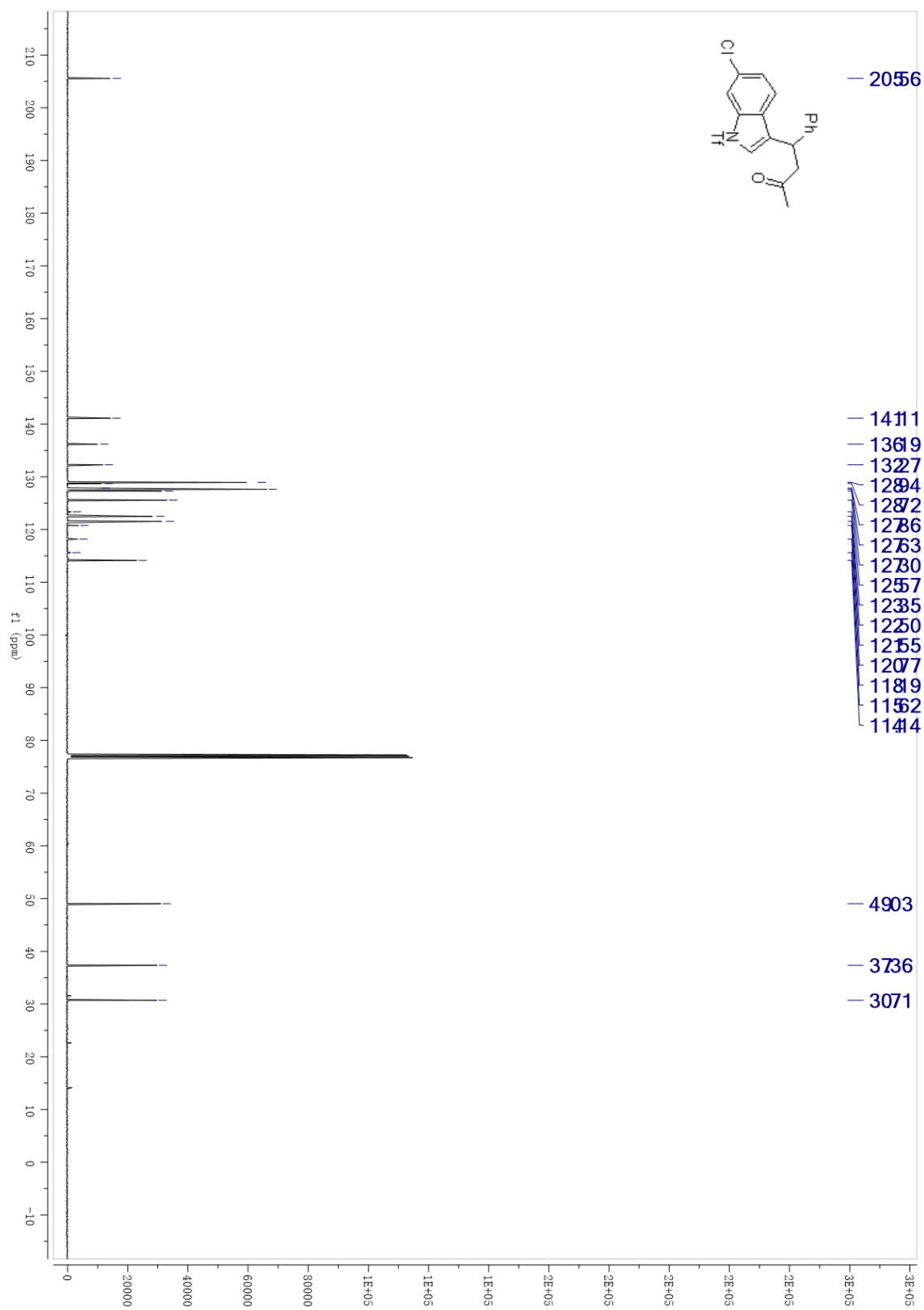
¹³C NMR 3.12j



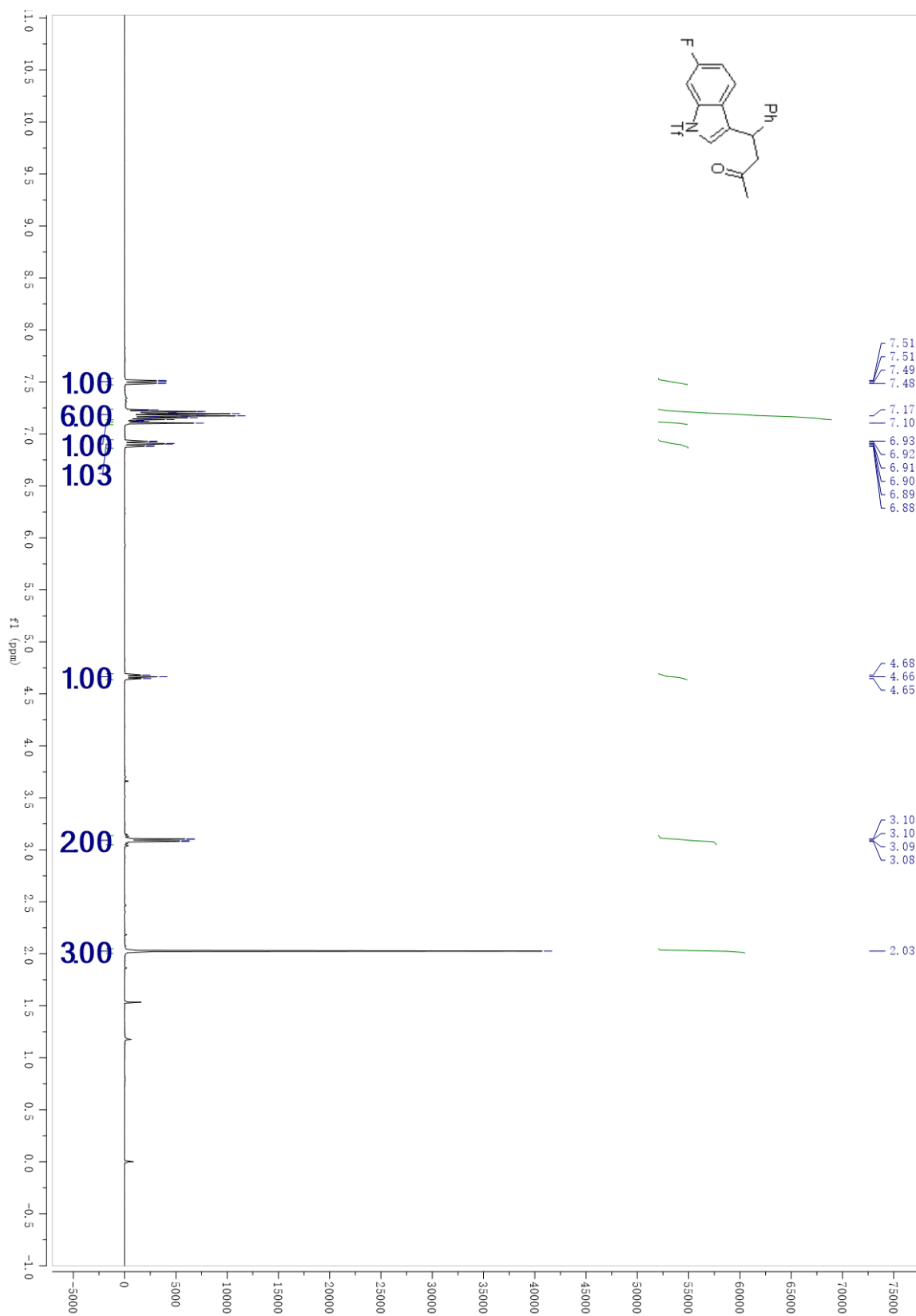
¹H NMR 3.12k



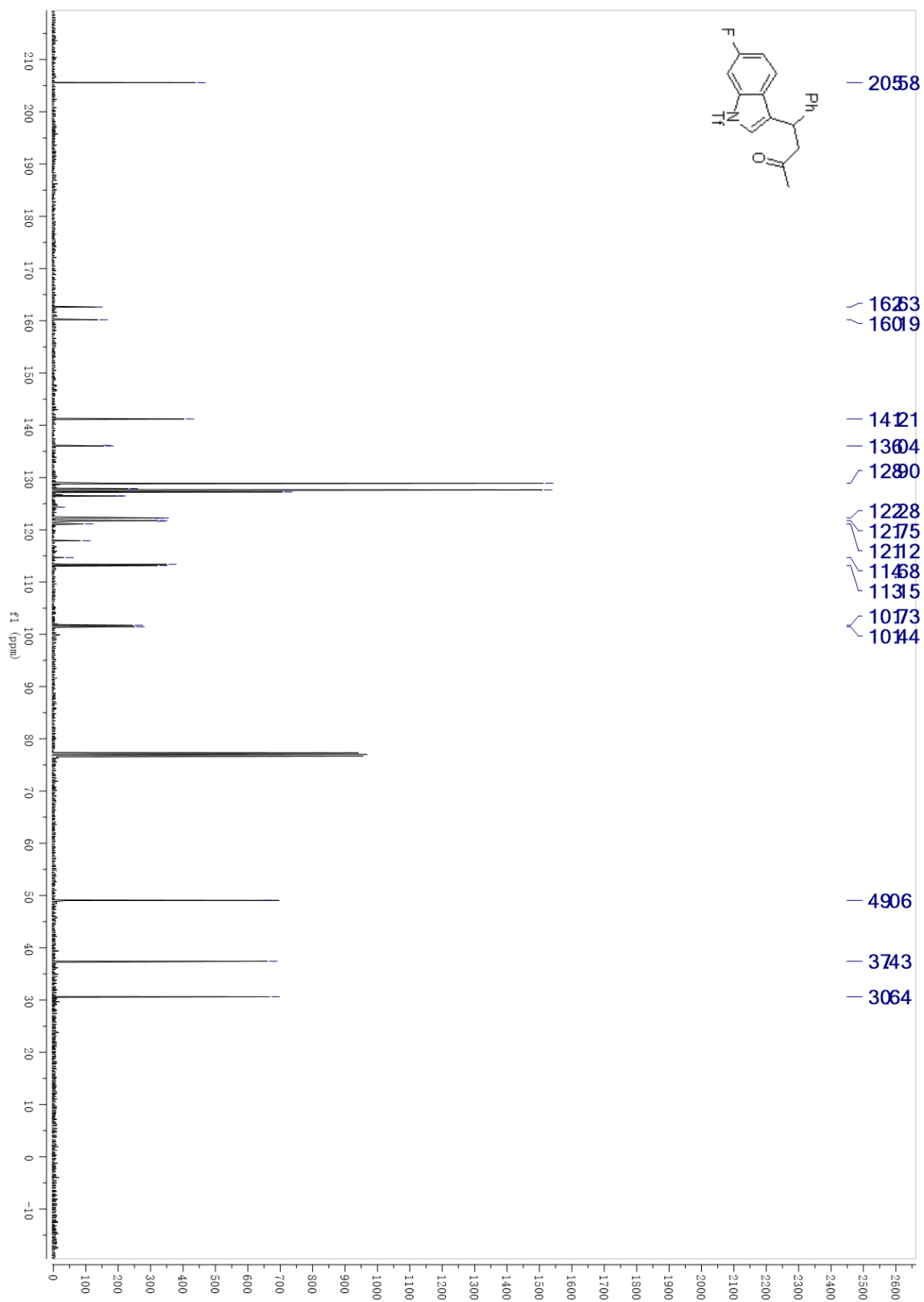
¹³C NMR 3.12k



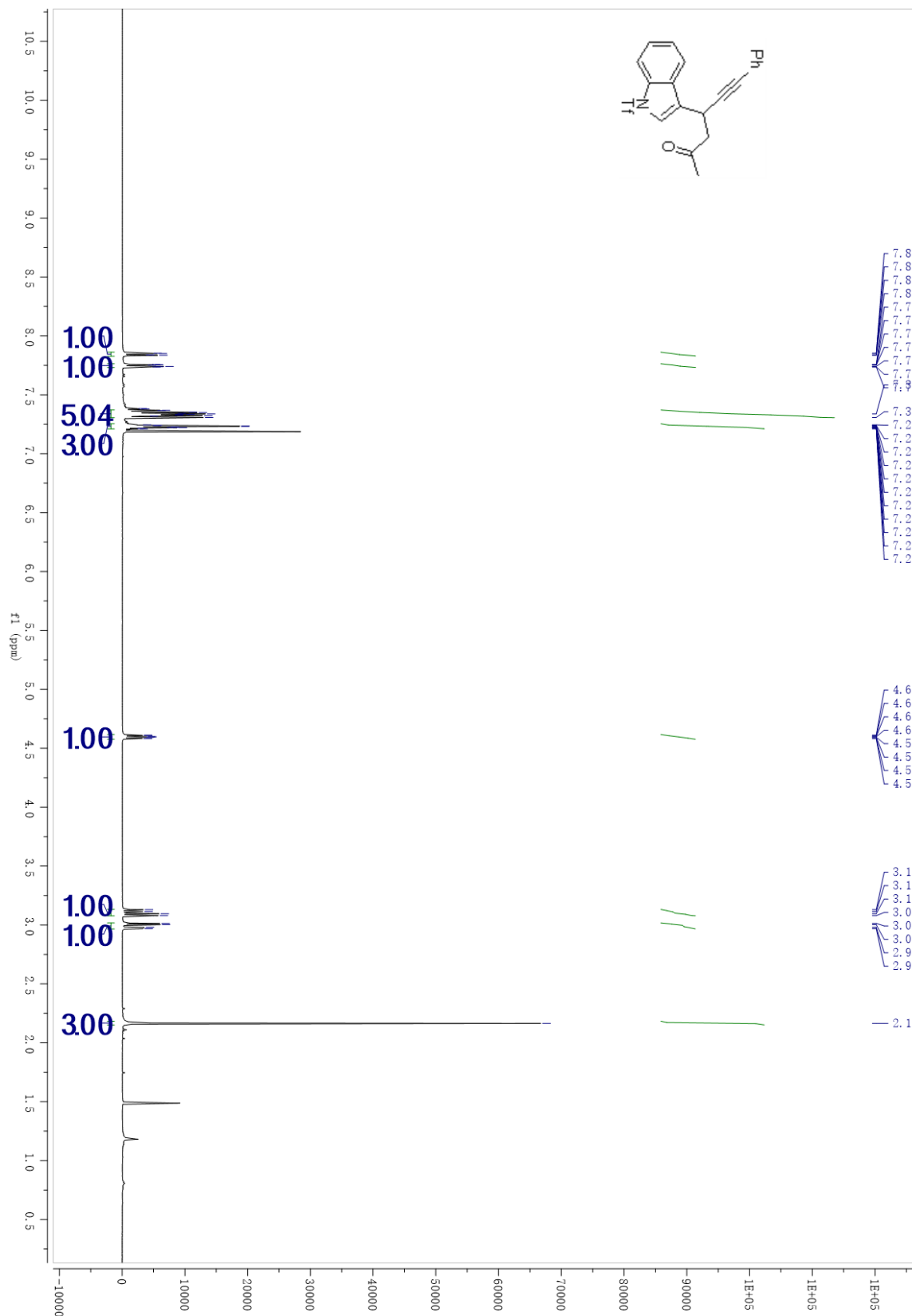
¹H NMR 3.121



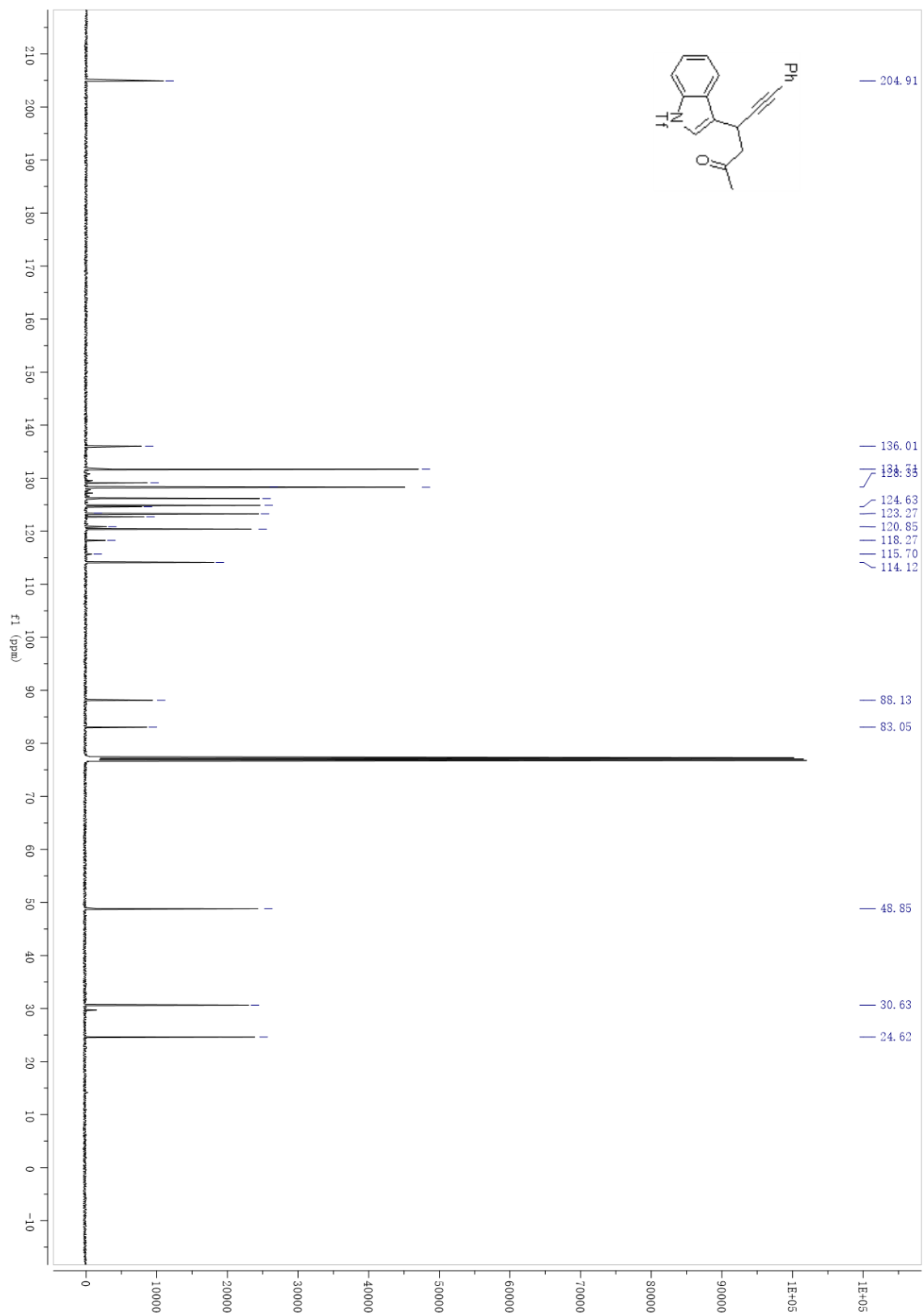
¹³C NMR 3.121



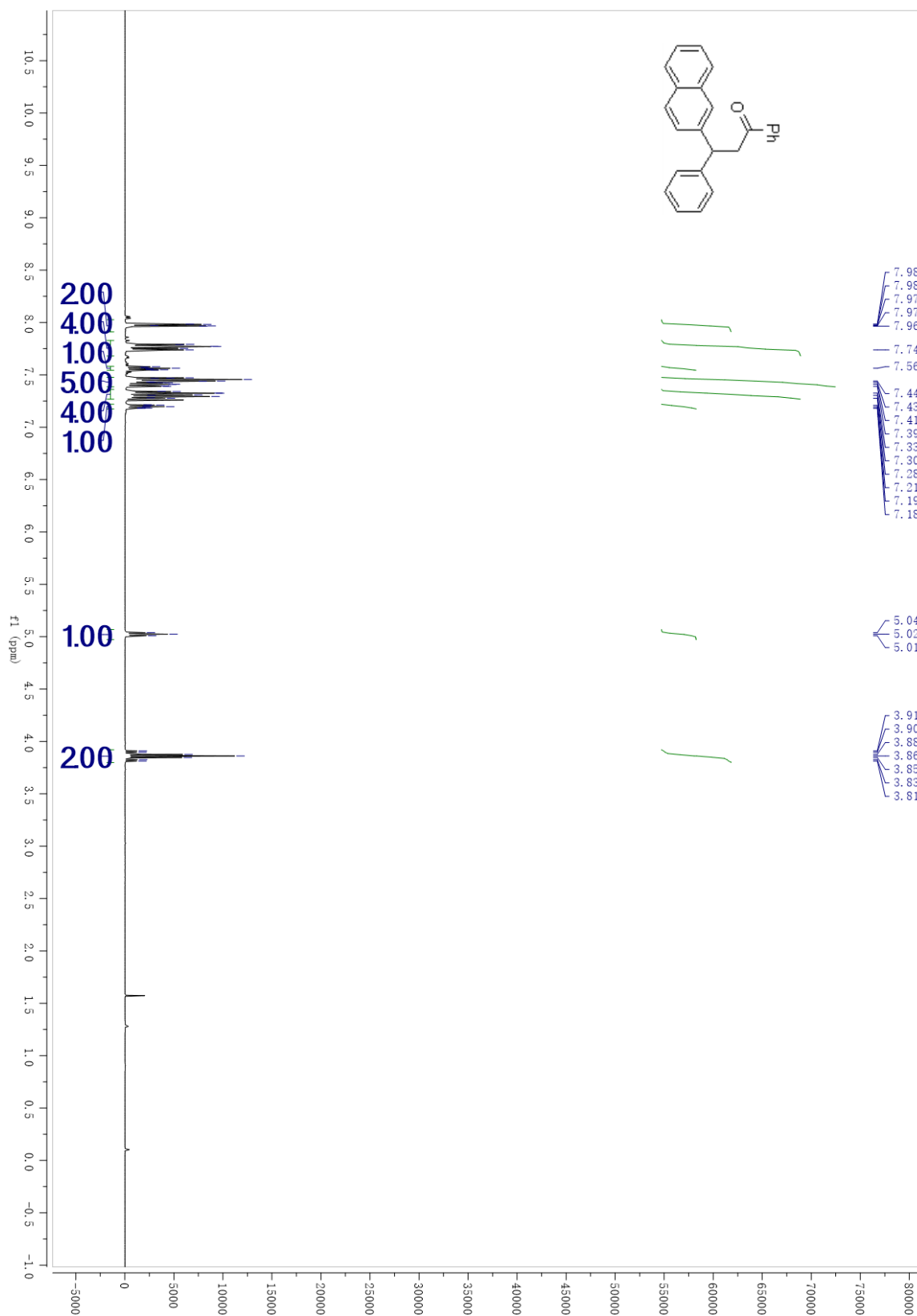
¹H NMR 3.12m



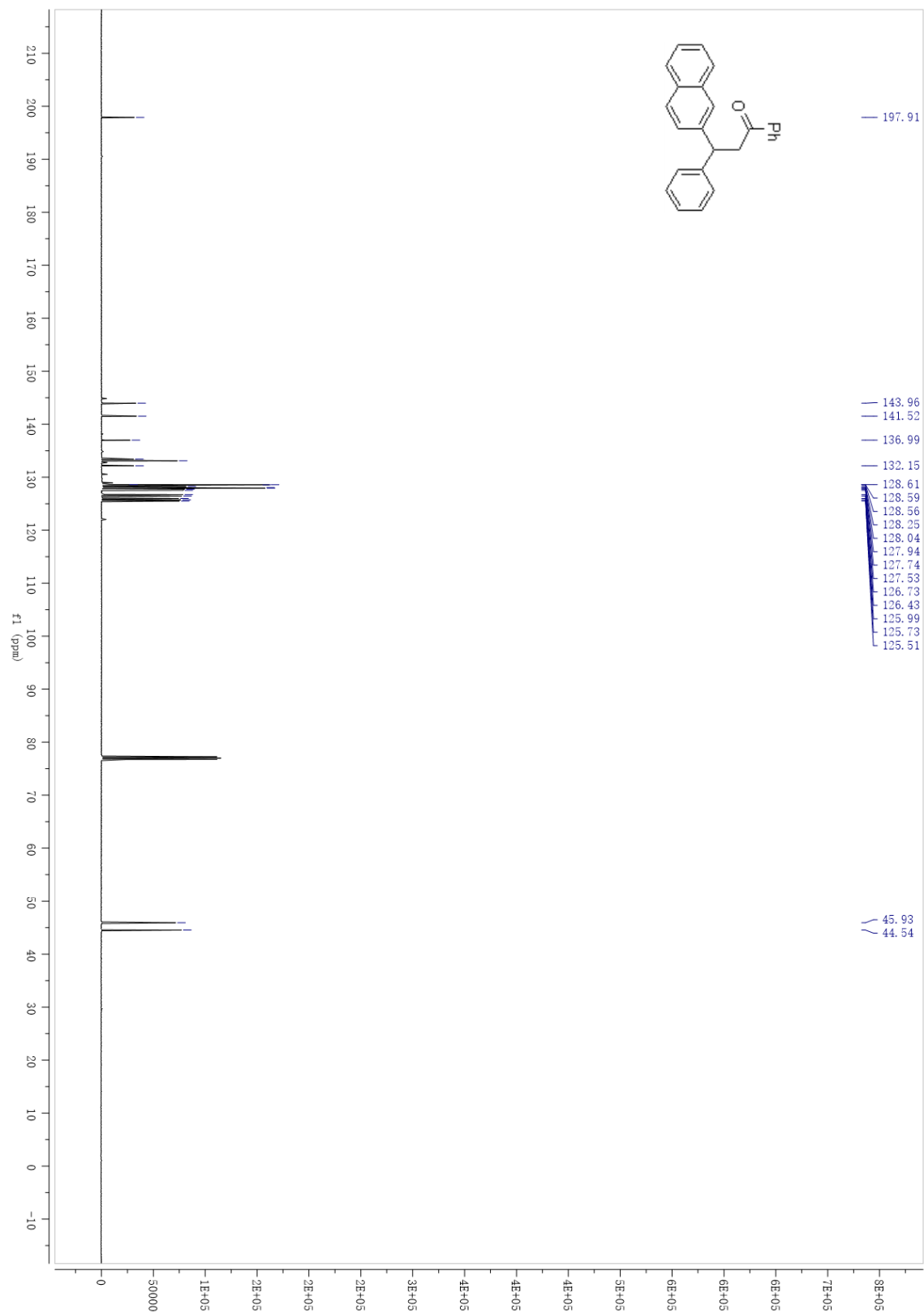
¹³C NMR 3.12m



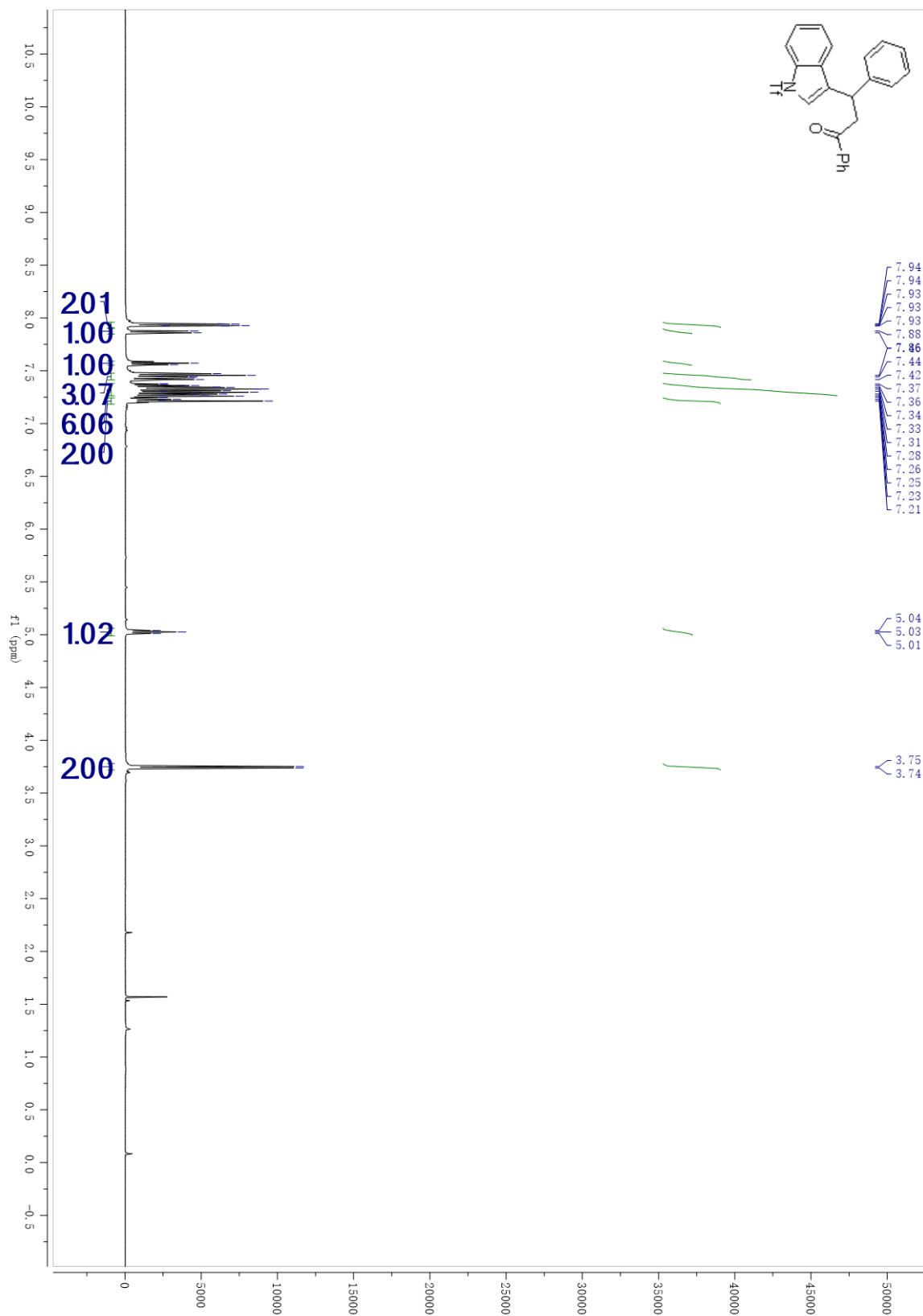
¹H NMR 3.12n



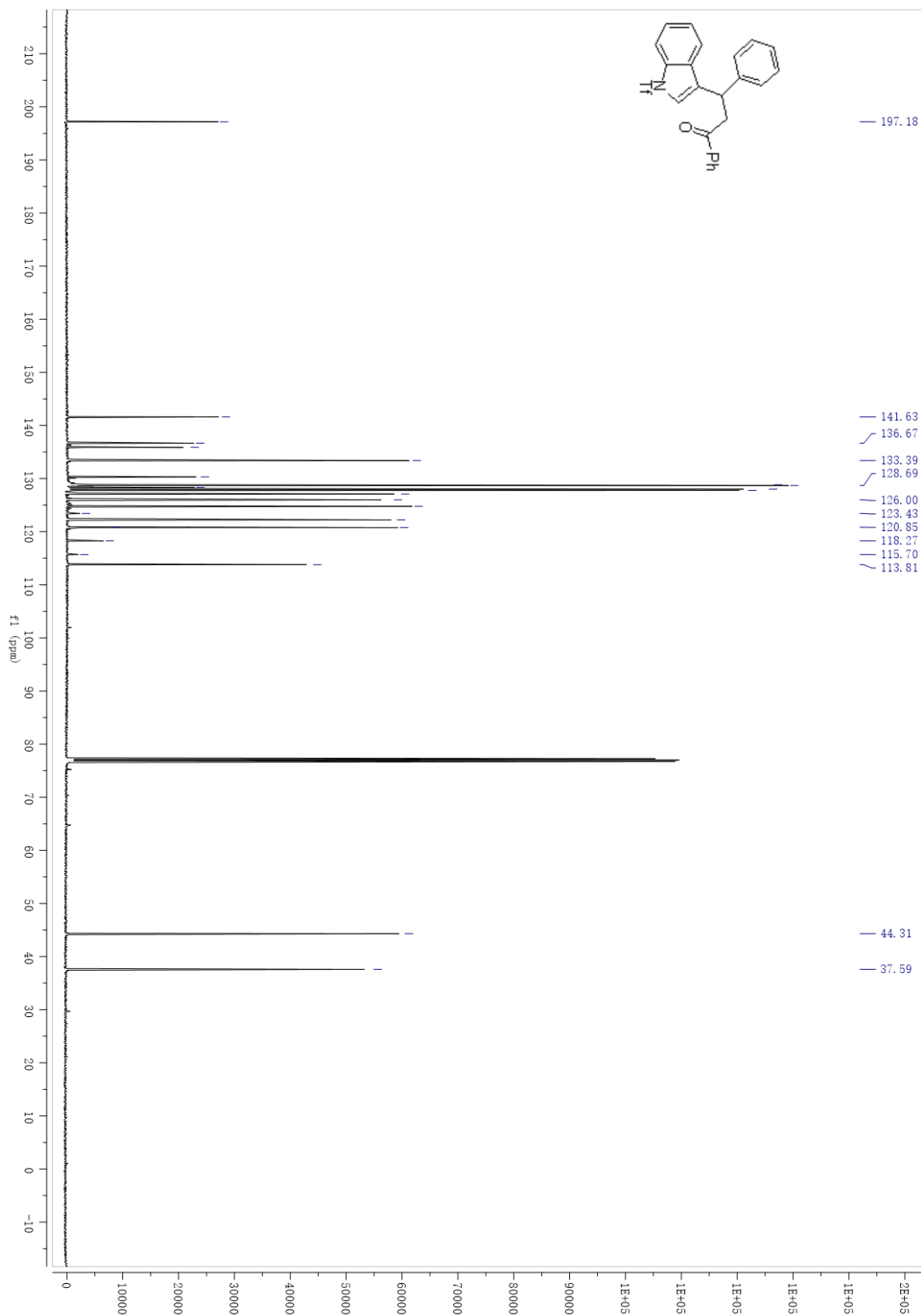
¹³C NMR 3.12n



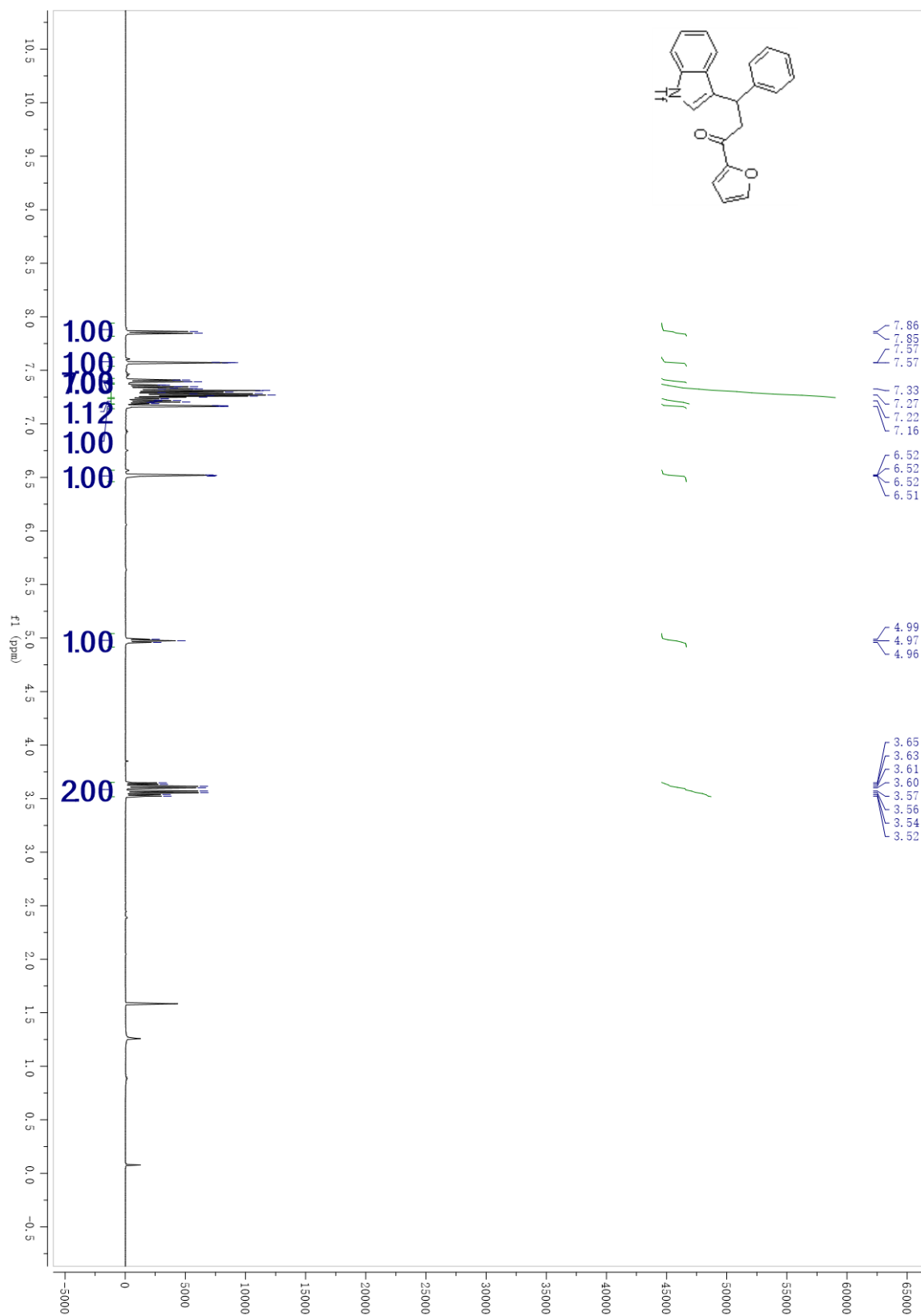
¹H NMR 3.12o



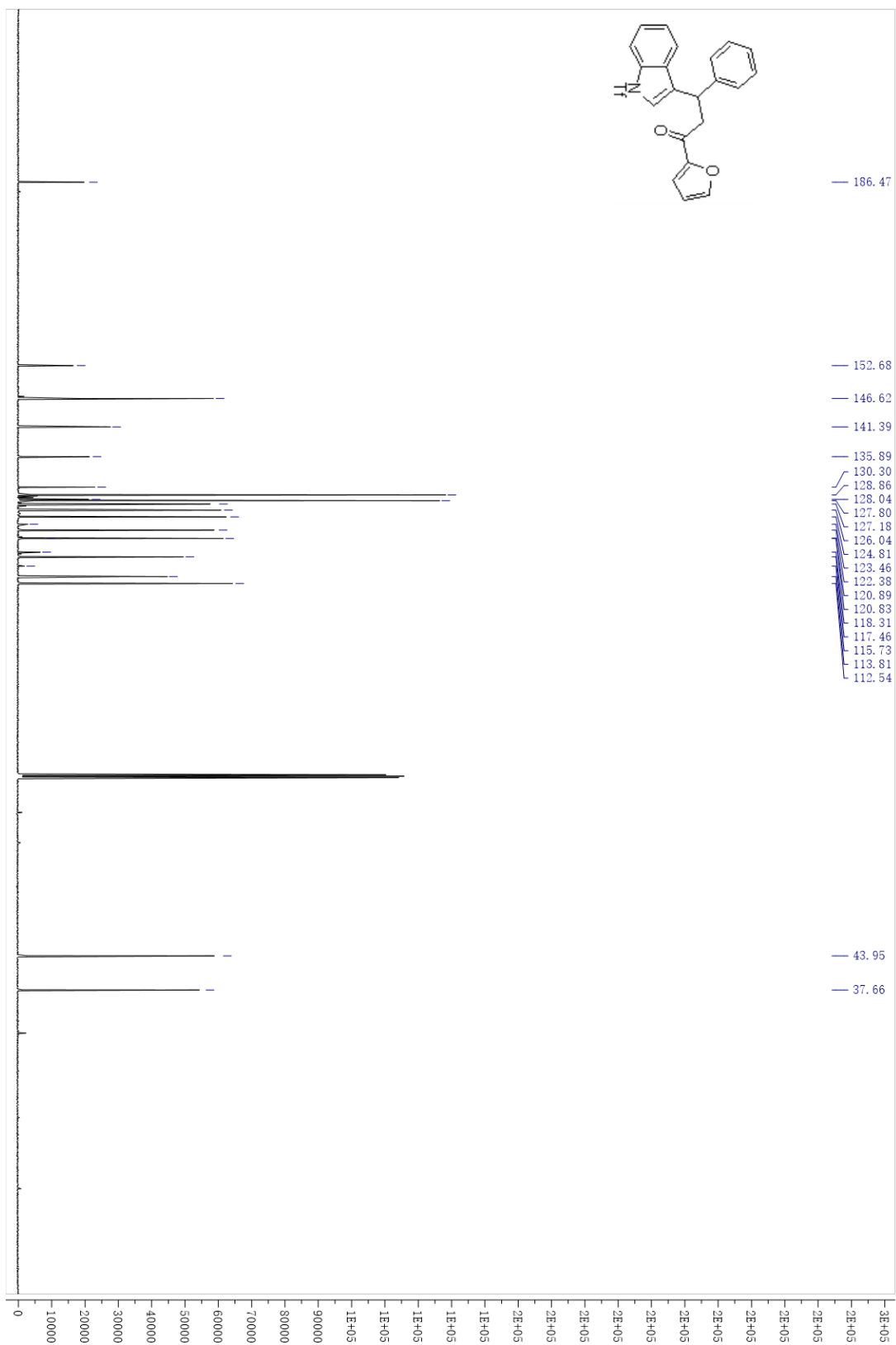
¹³C NMR 3.12o



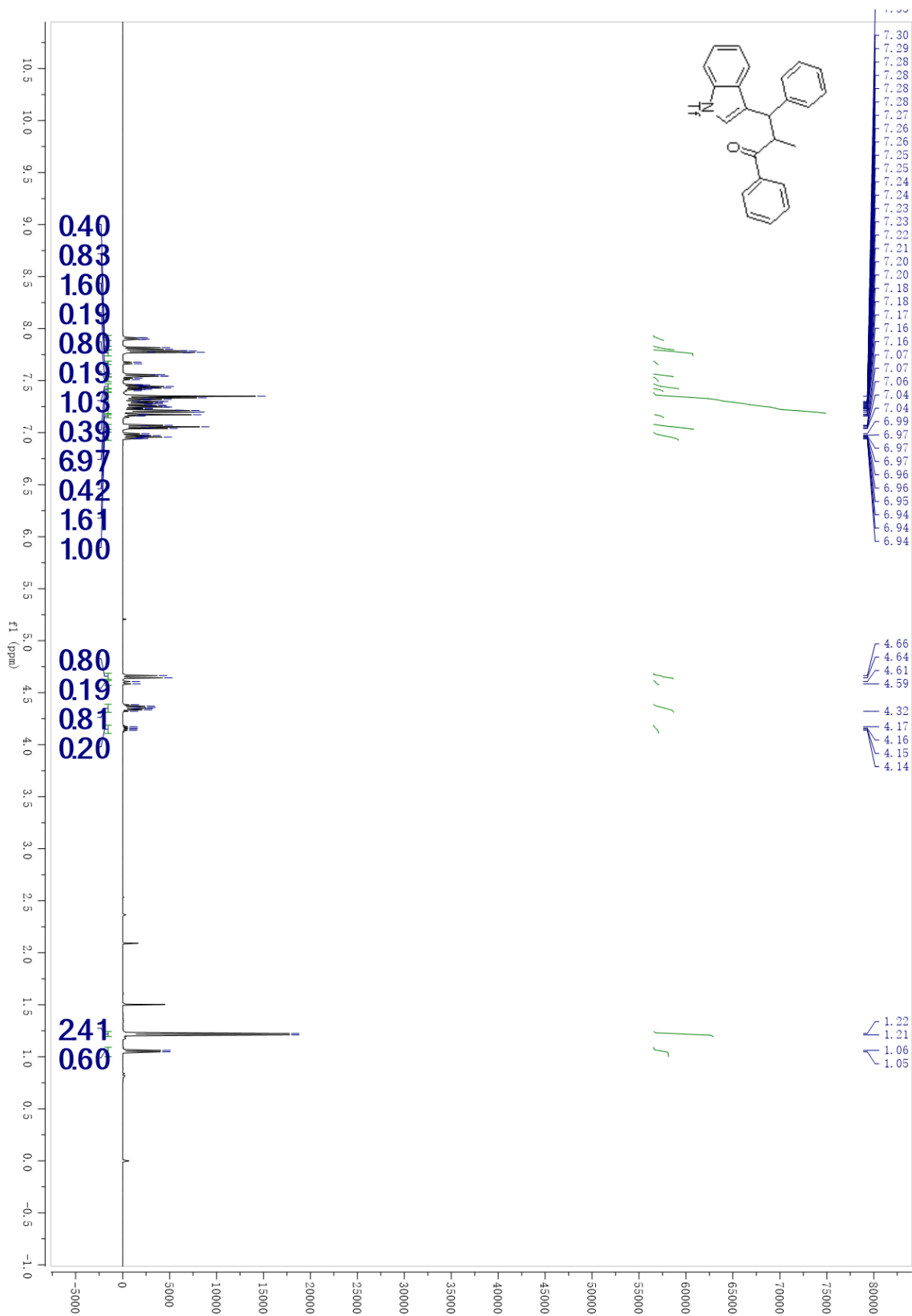
¹H NMR 3.12p



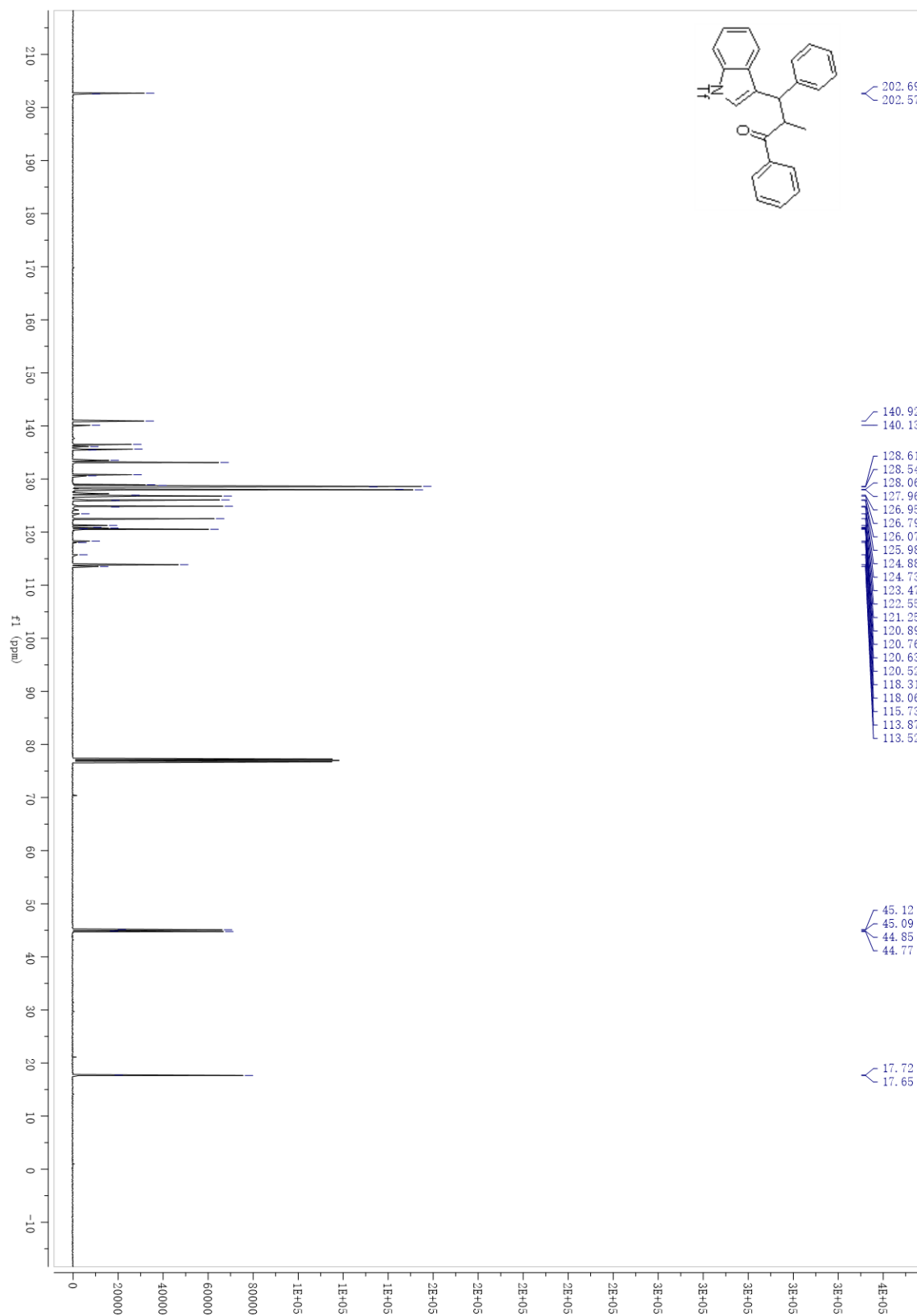
¹³C NMR 3.12p



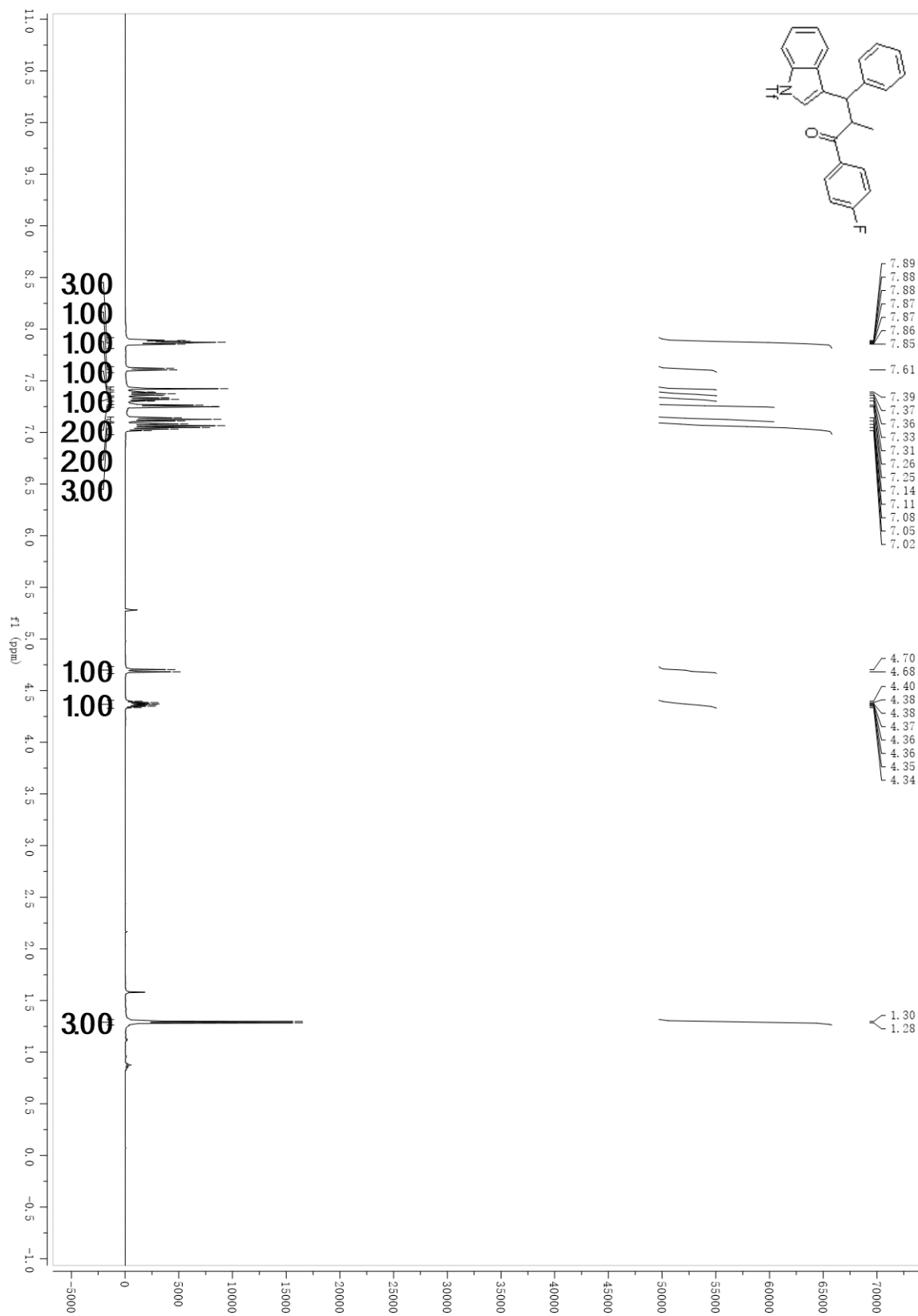
¹H NMR 3.12q



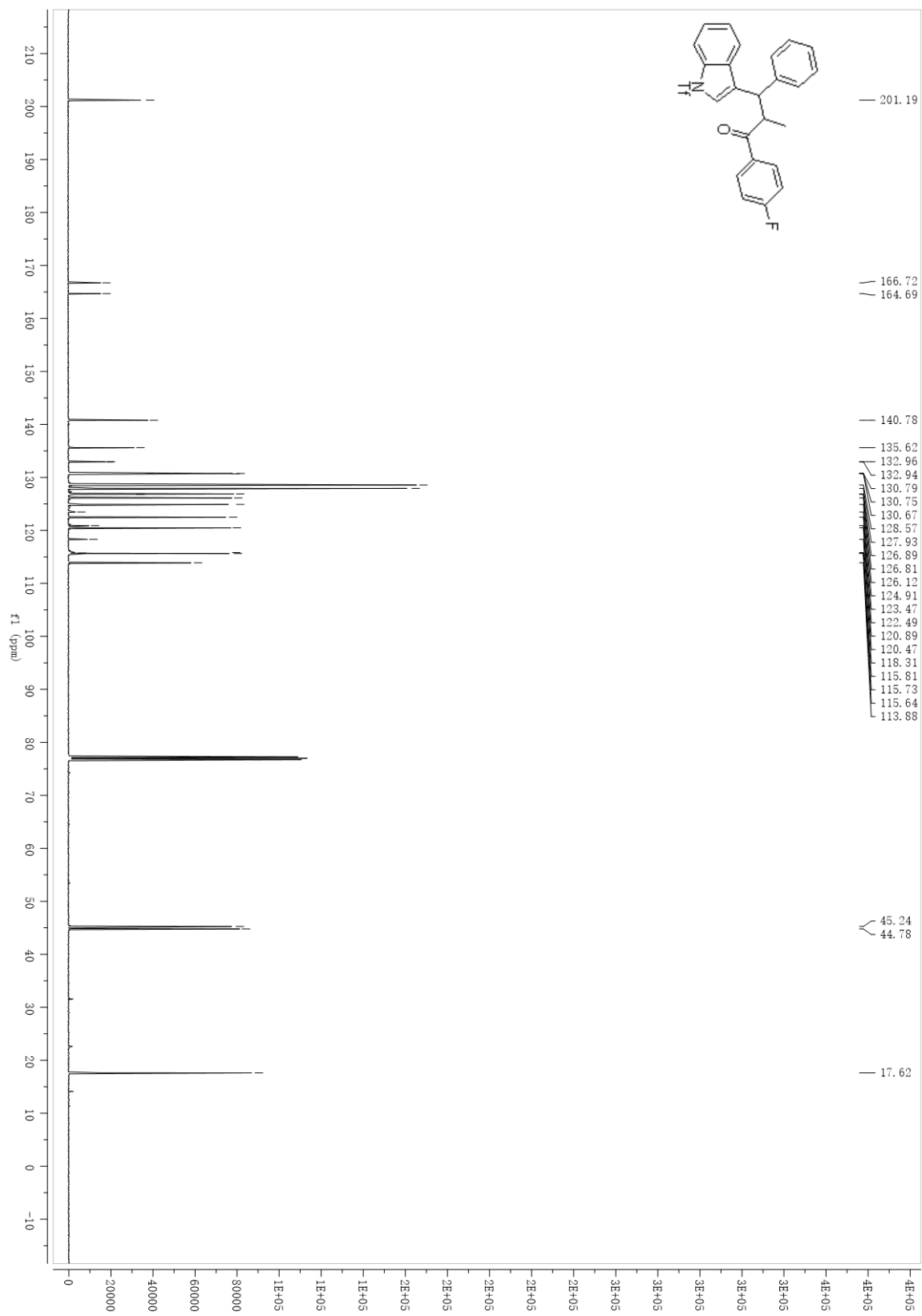
¹³C NMR 3.12q



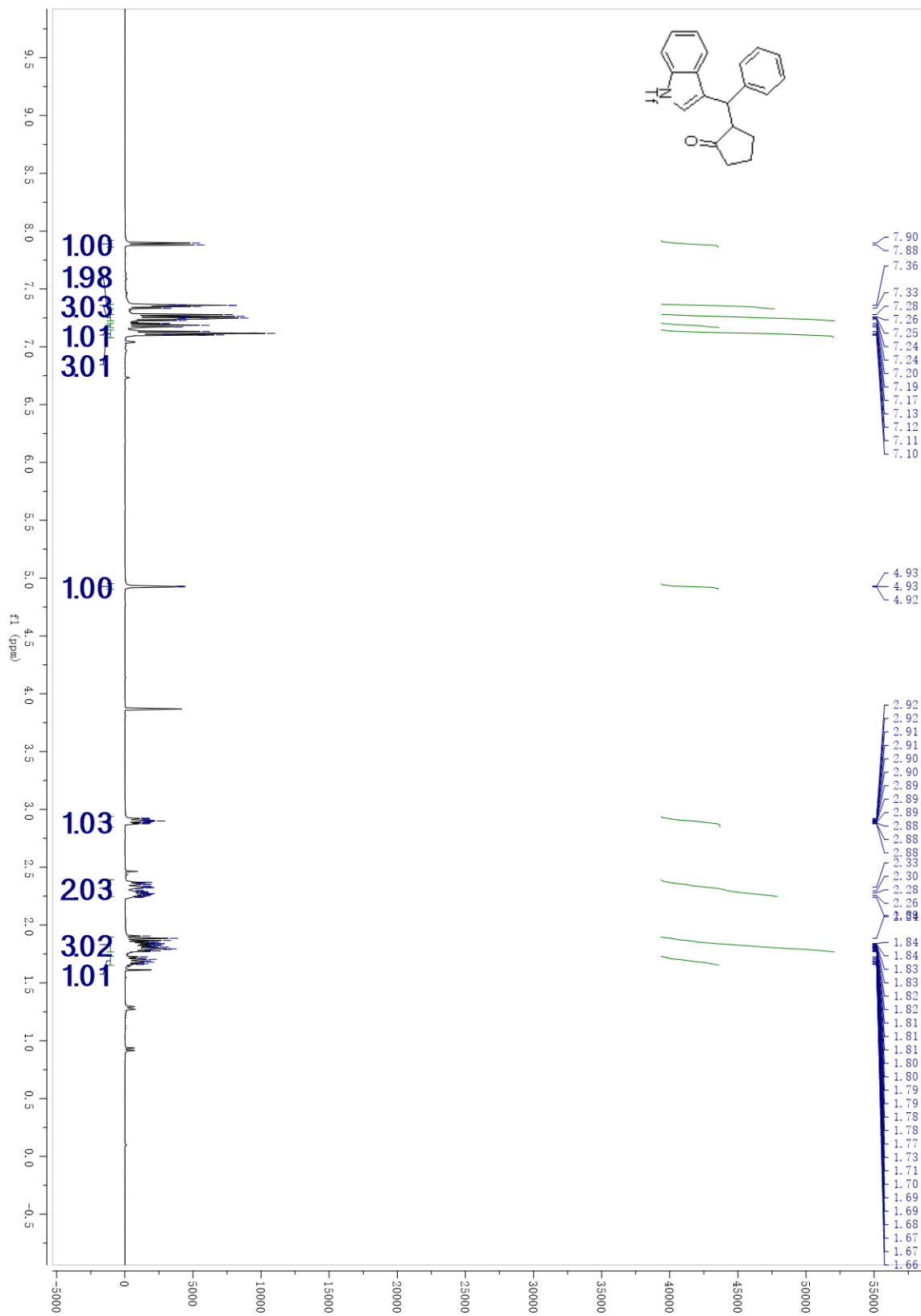
¹H NMR 3.12r



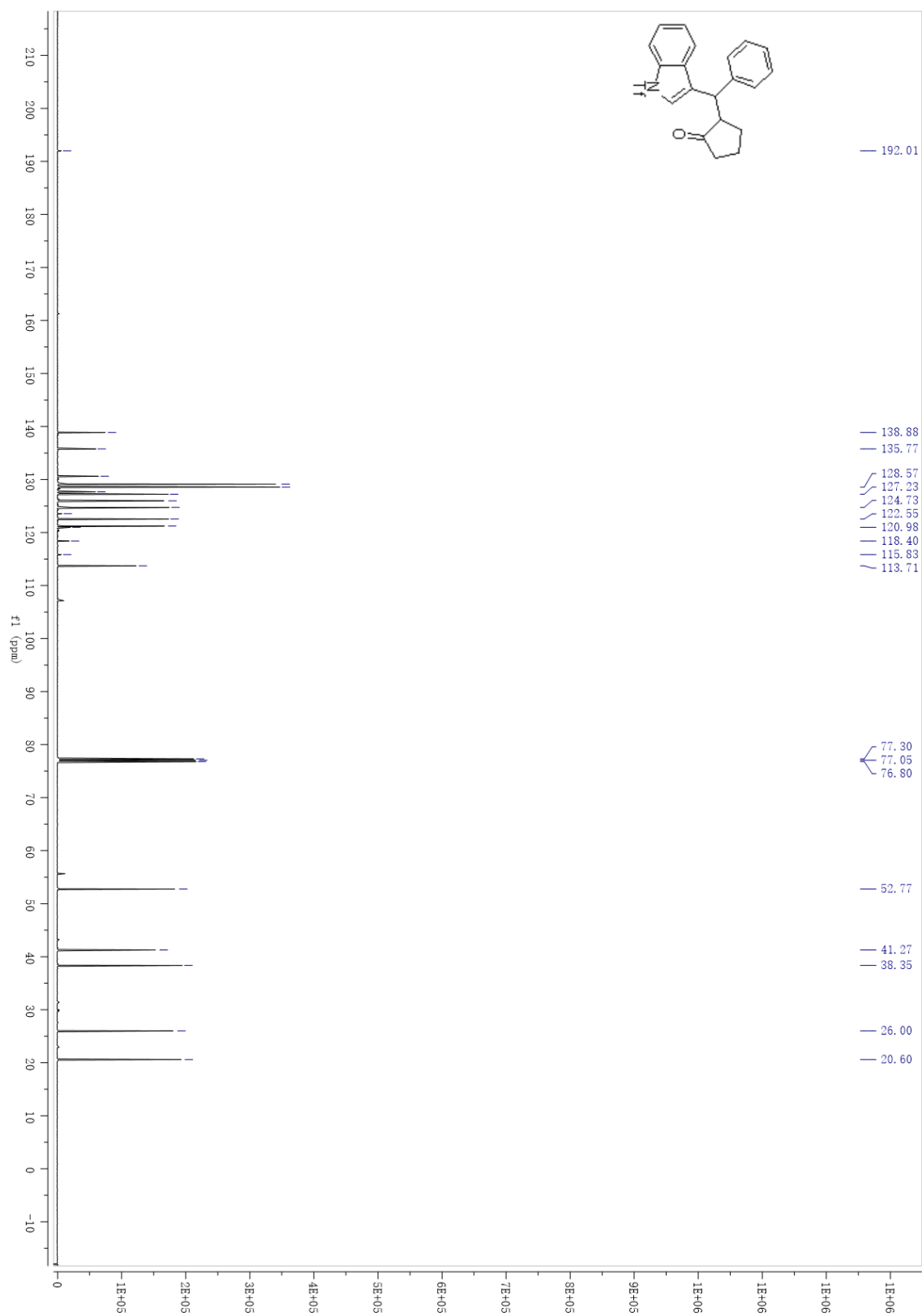
¹³C NMR 3.12r



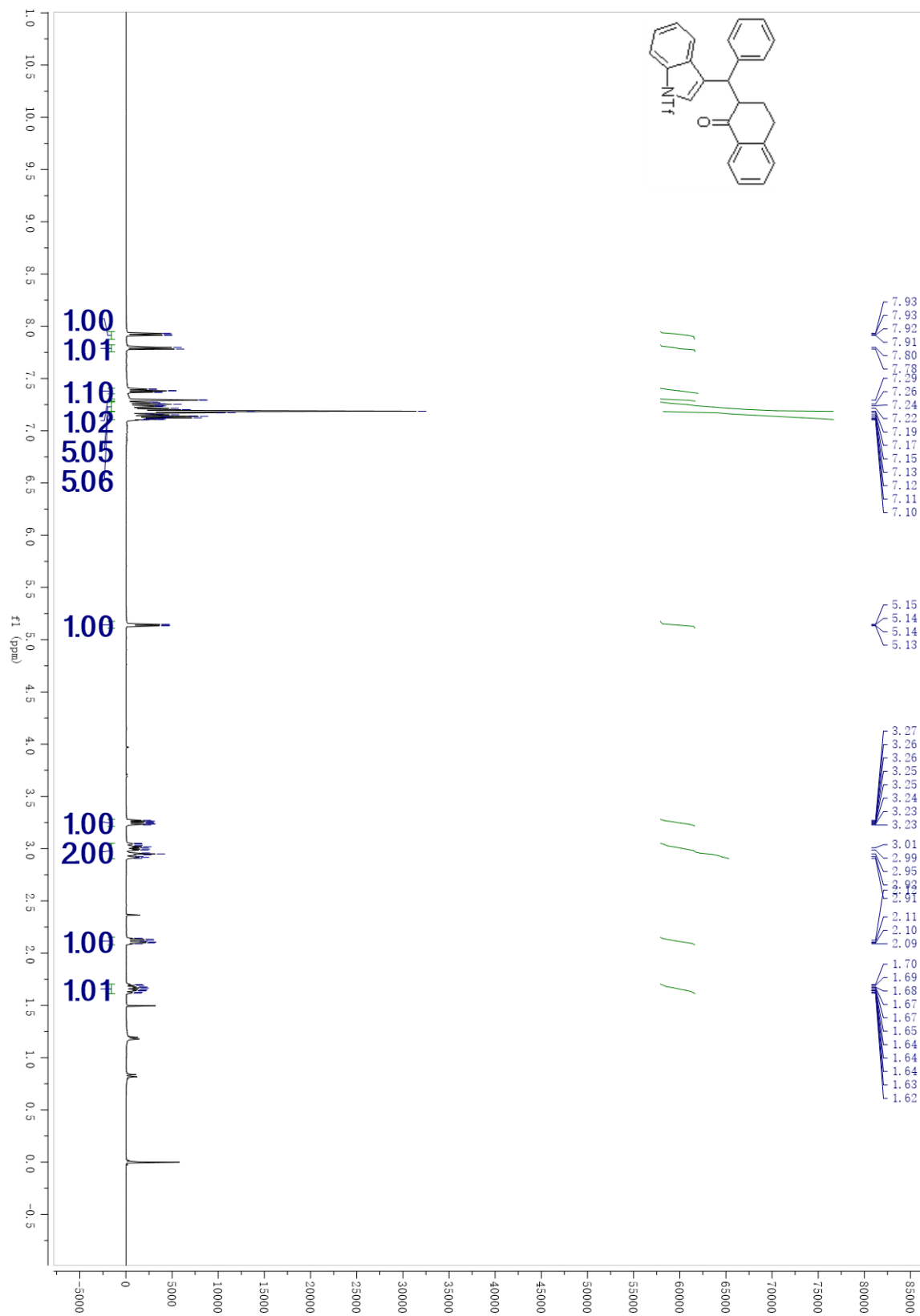
¹H NMR 3.12s



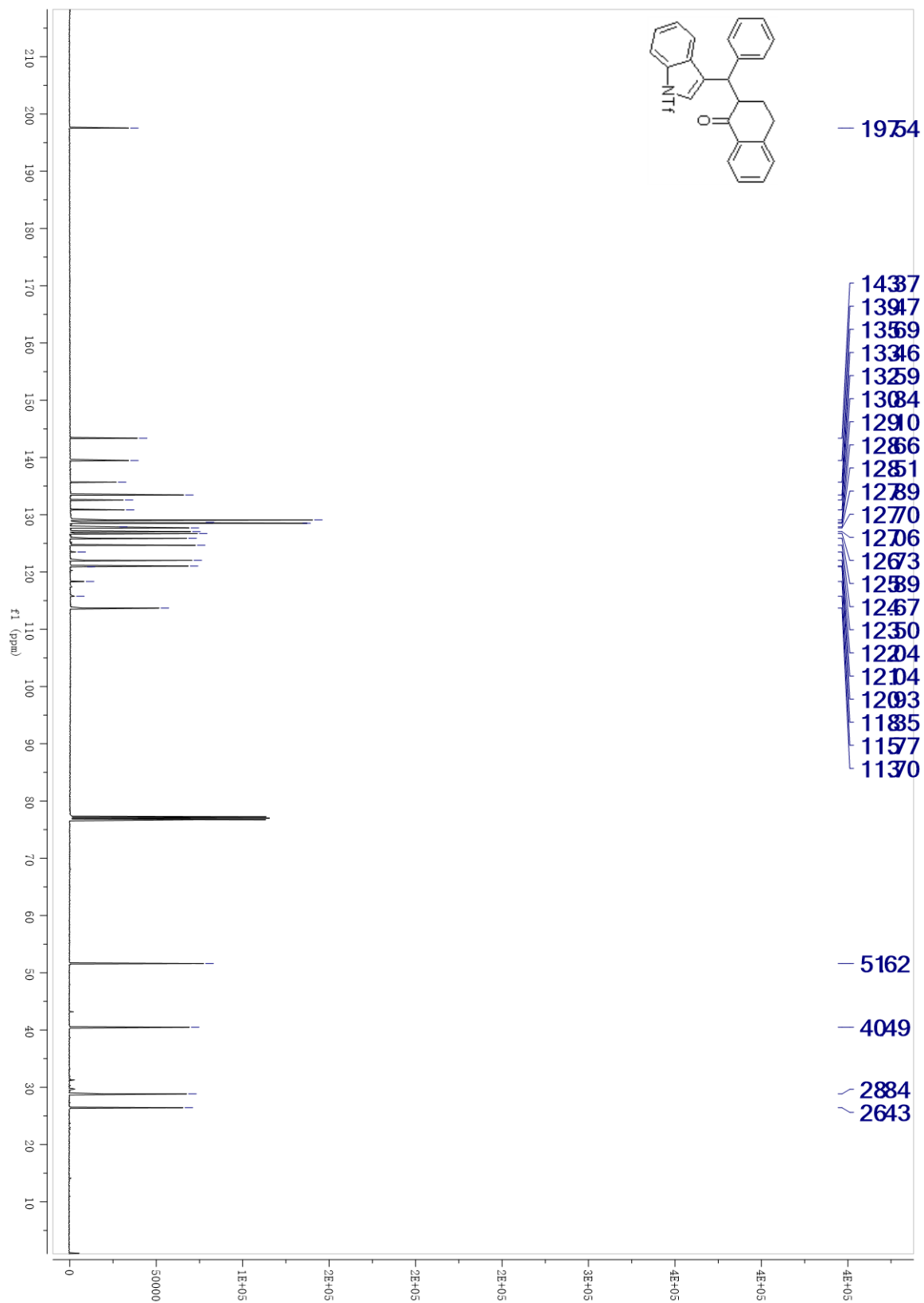
¹³C NMR 3.12s



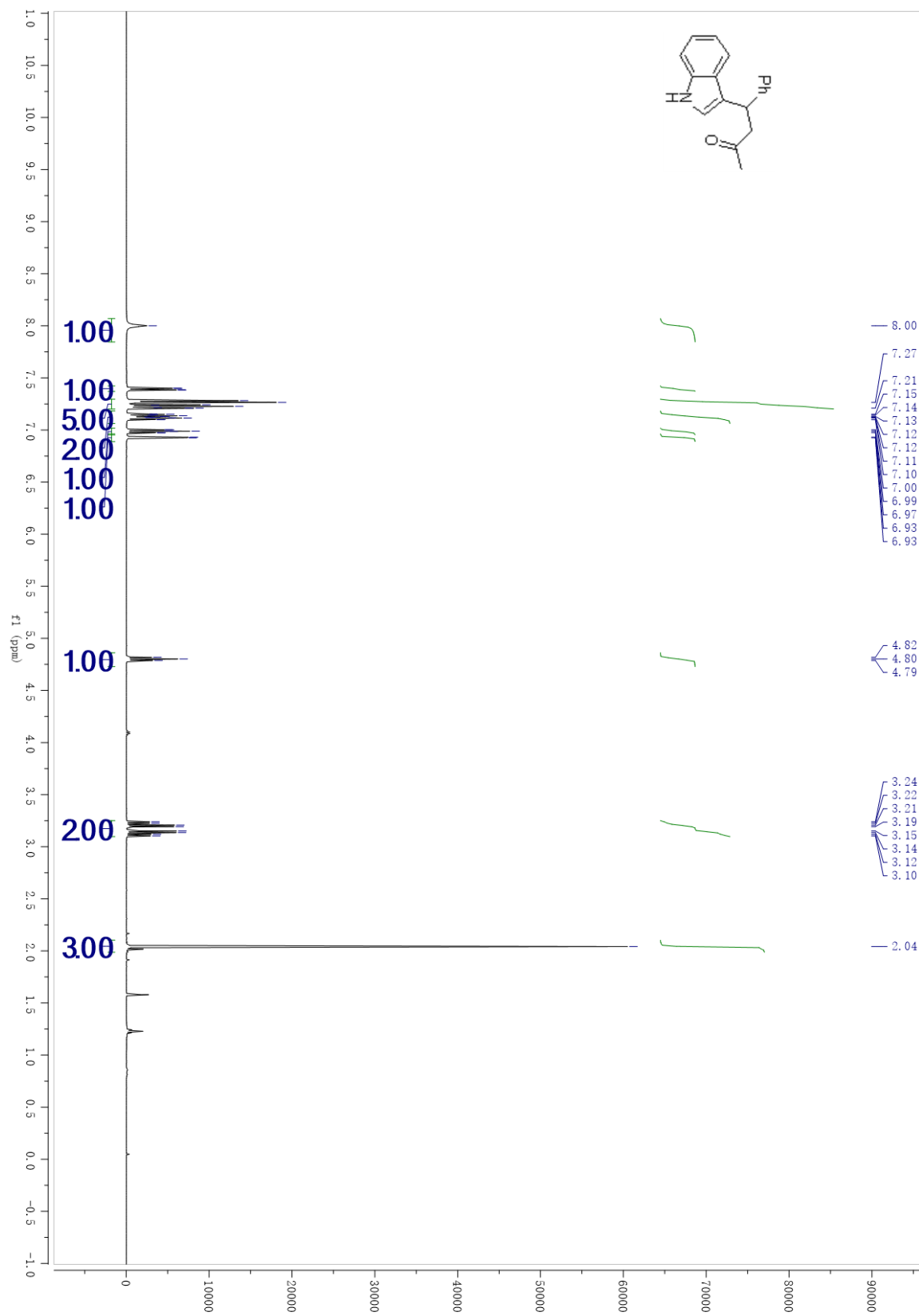
¹H NMR 3.12t



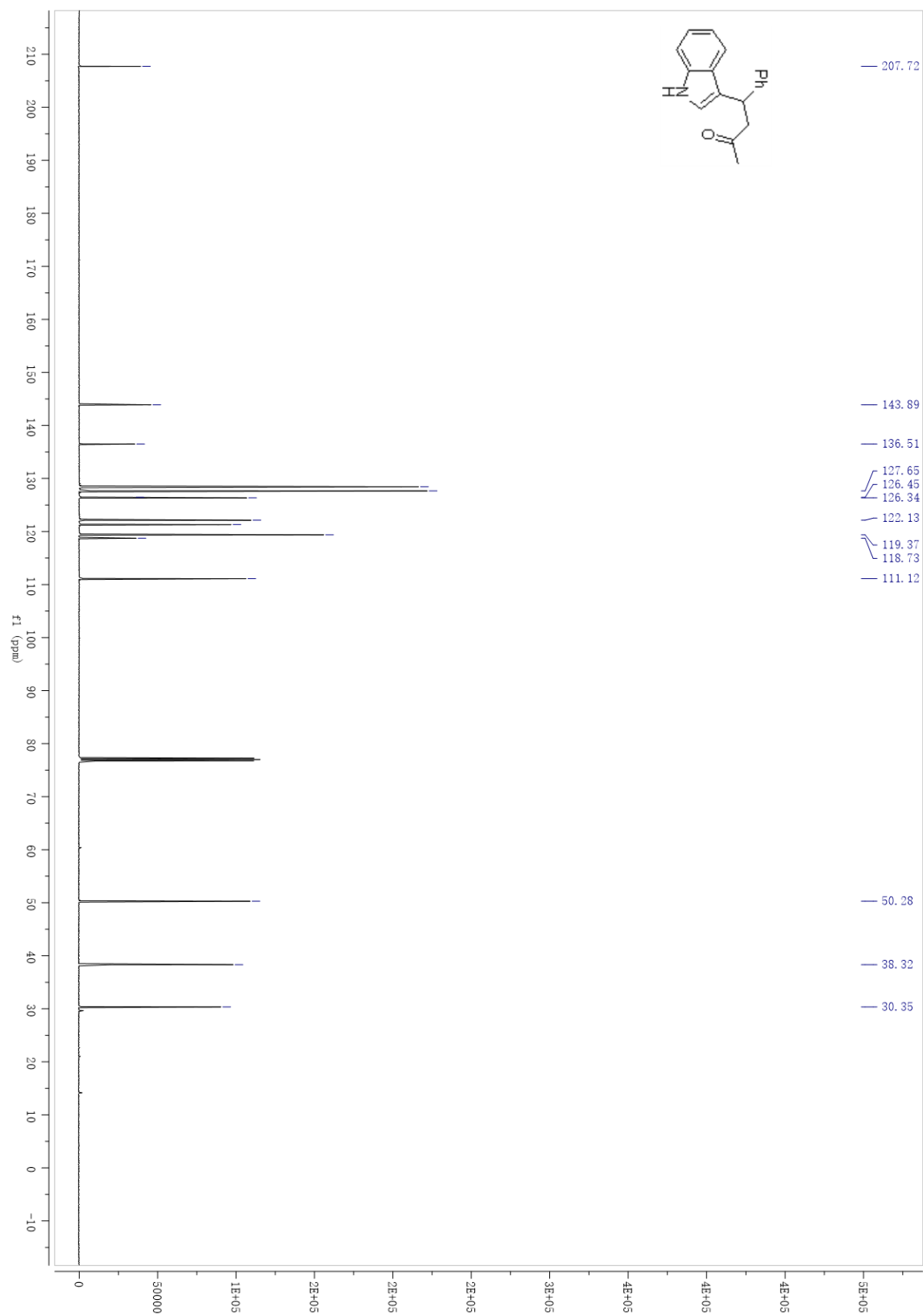
¹³C NMR 3.12t



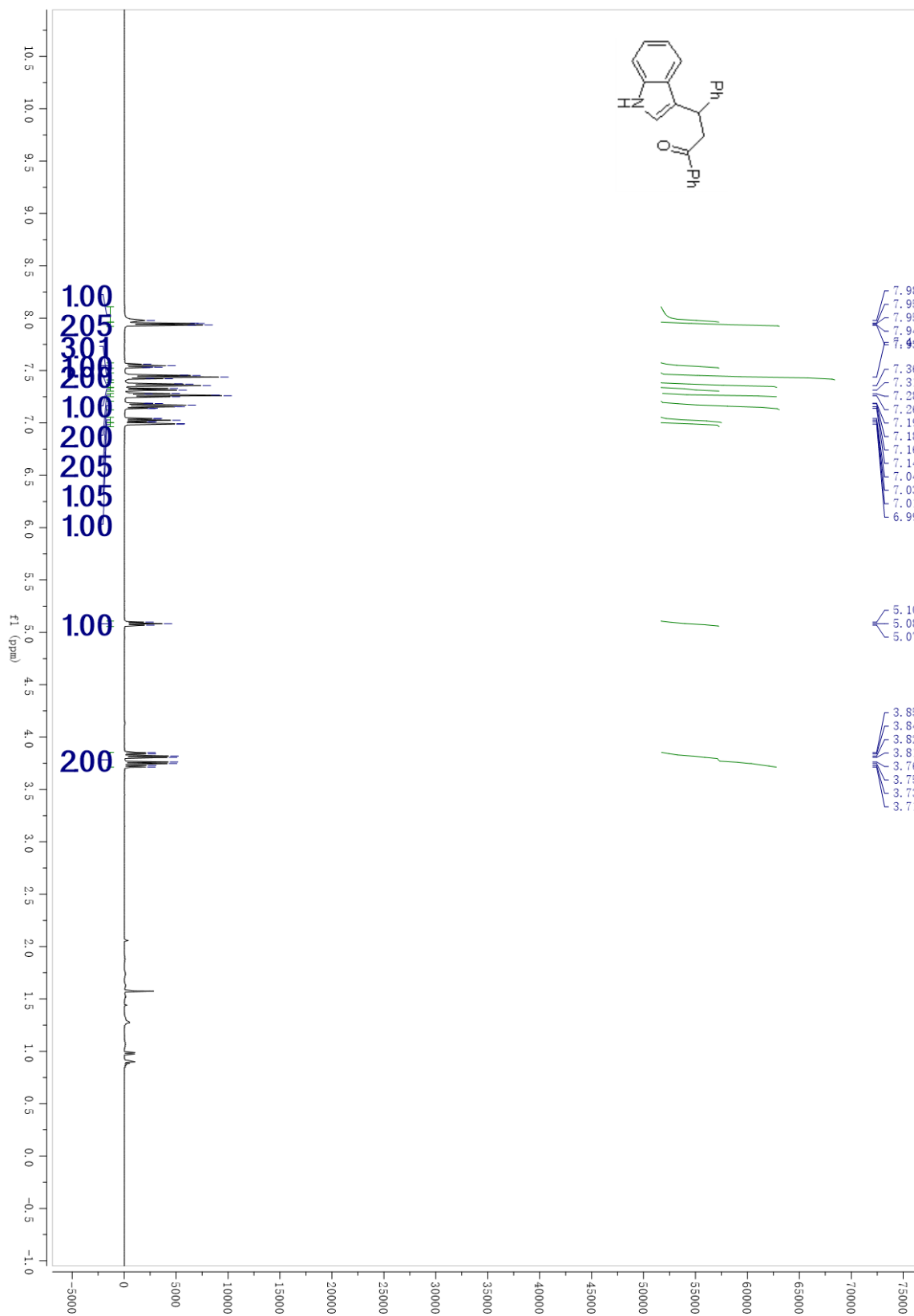
¹H NMR 3.13a



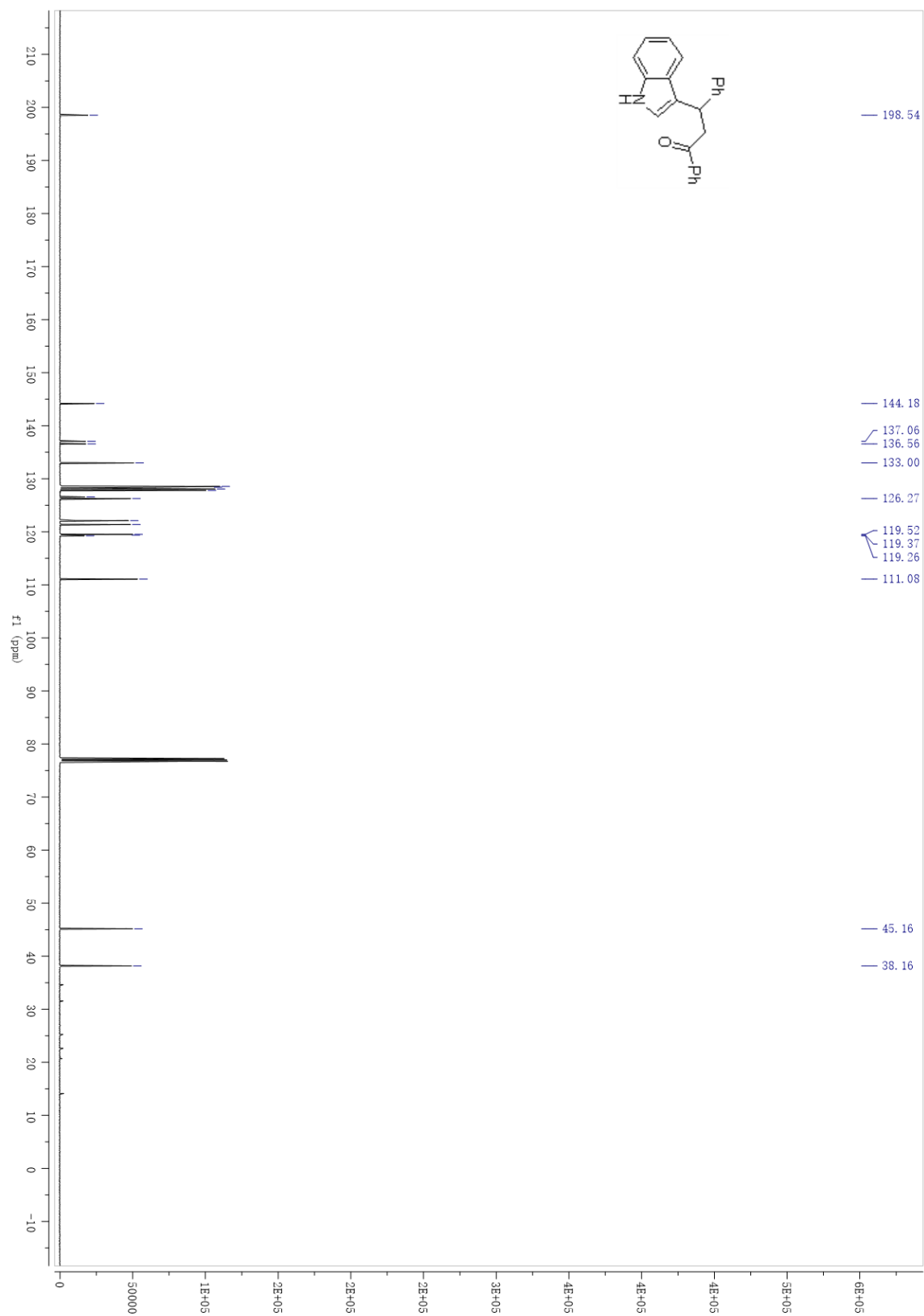
¹³C NMR 3.13a



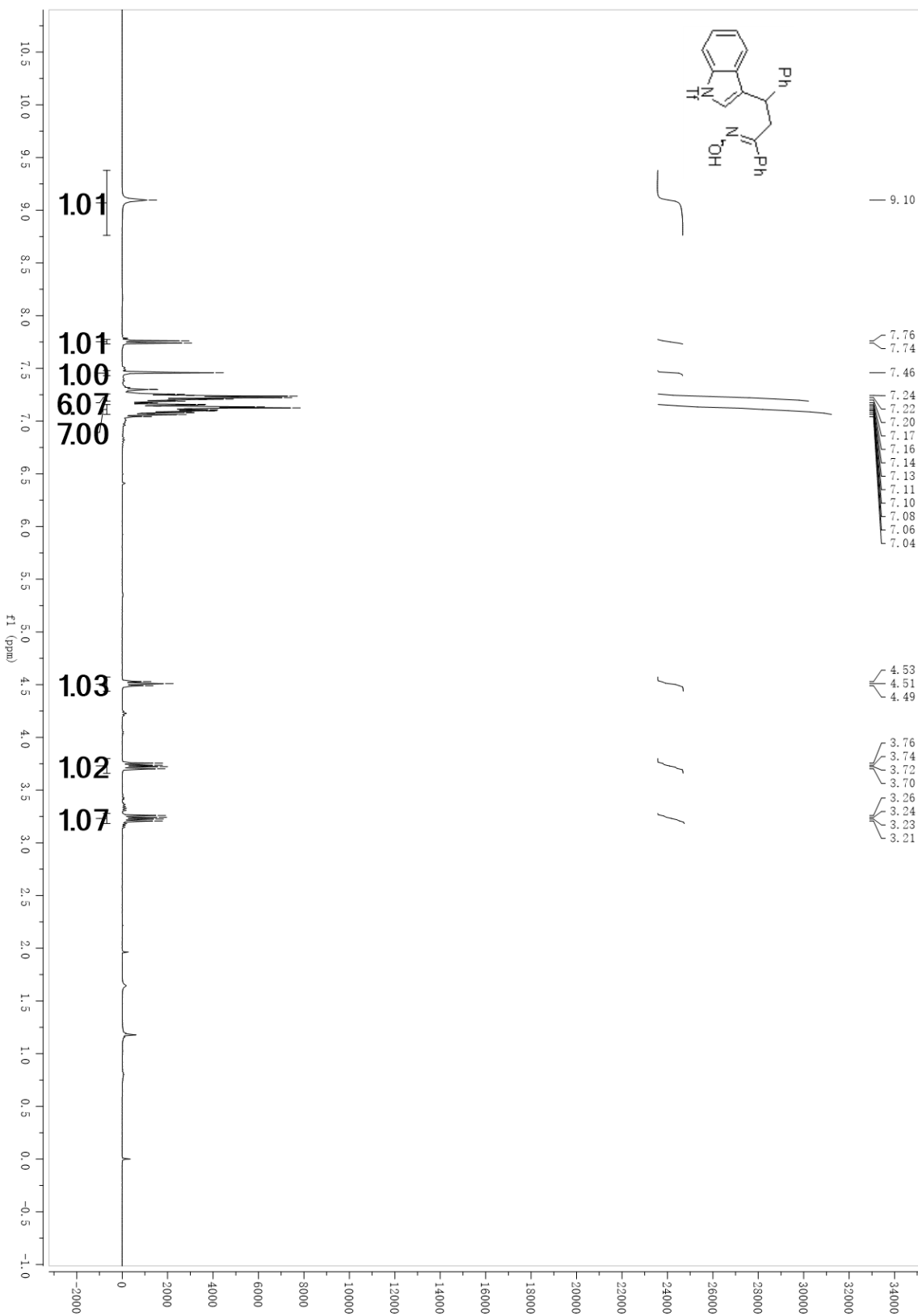
¹H NMR 3.13o



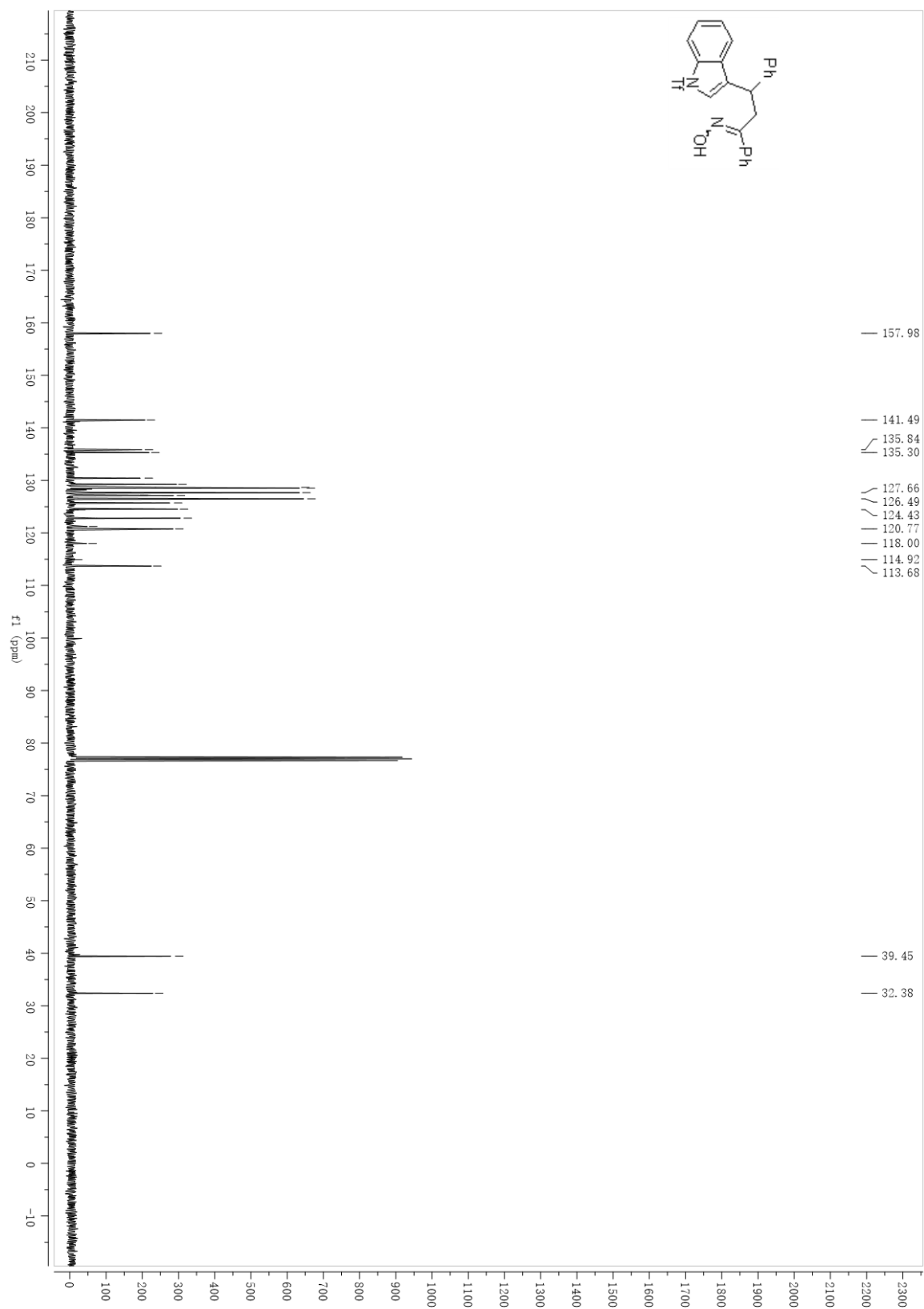
¹³C NMR 3.13o



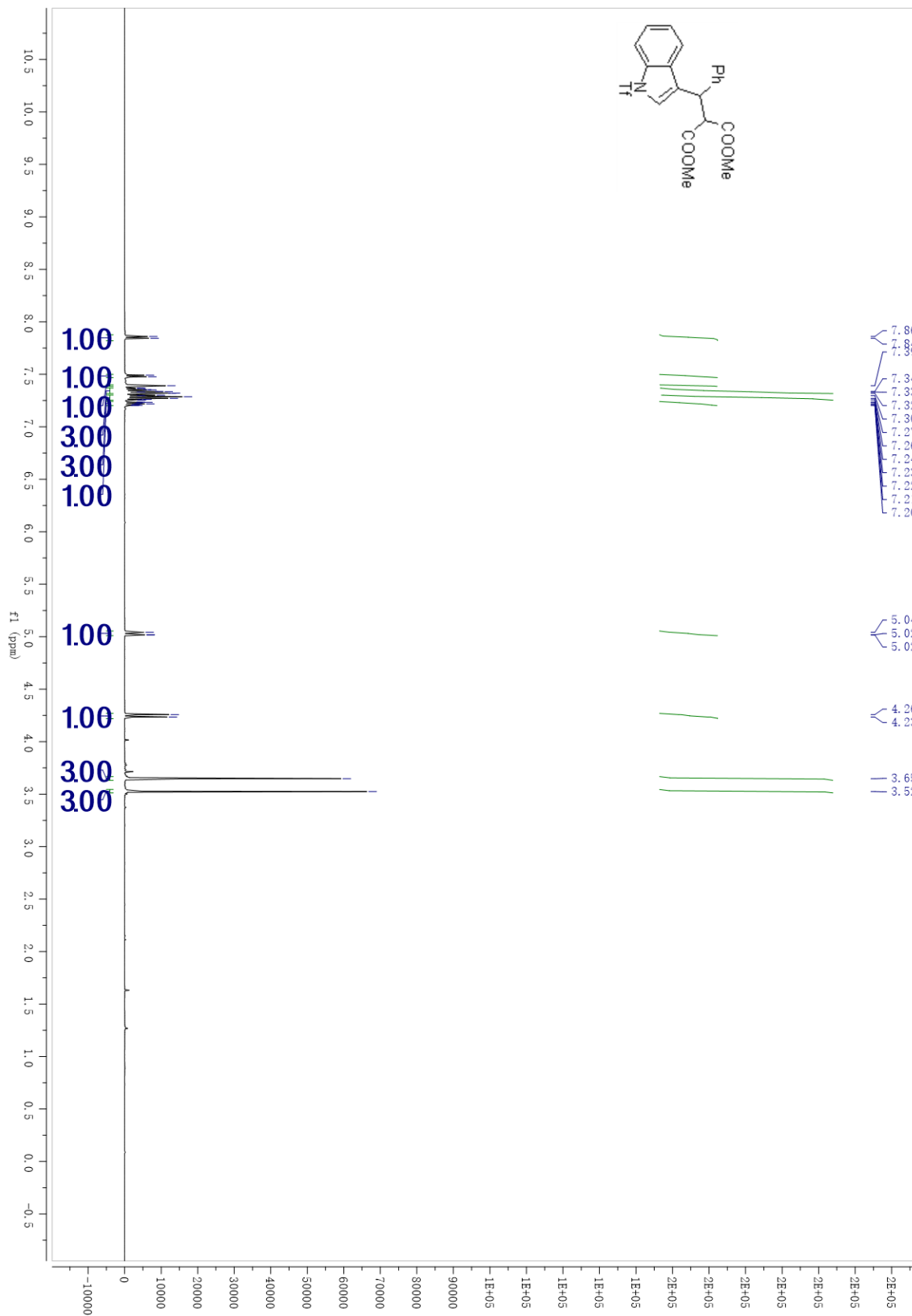
¹H NMR S2



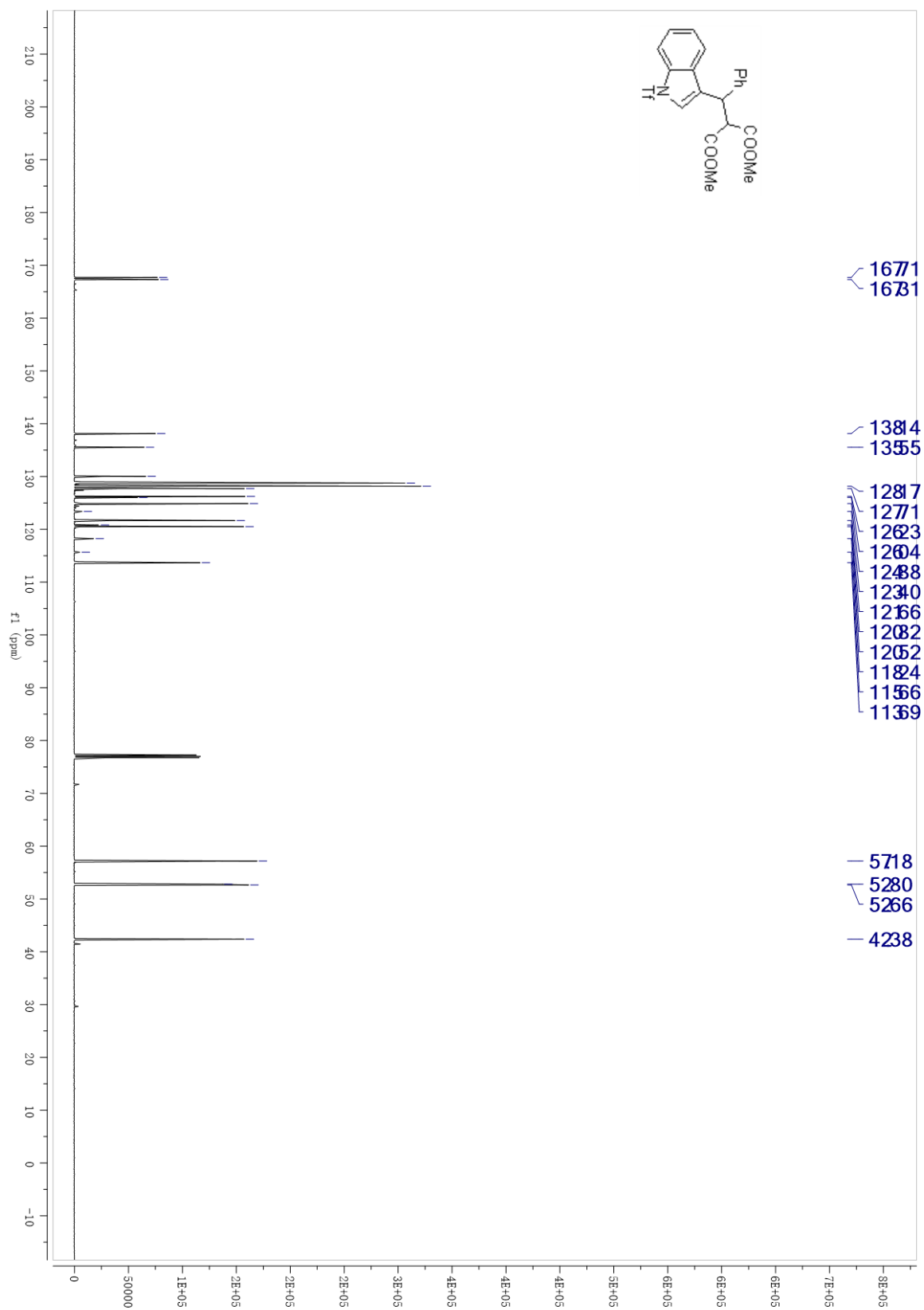
¹³C NMR S2



¹H NMR 3.14a

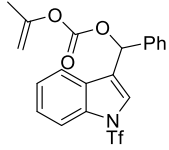


¹³C NMR 3.14a



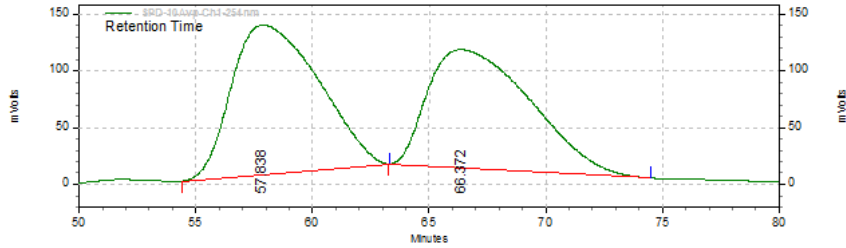
8. Copies of HPLC Spectra

Phenyl(1-((trifluoromethyl)sulfonyl)-1H-indol-3-yl)methyl prop-1-en-2-yl carbonate



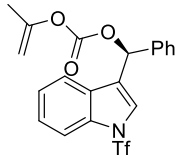
Area % Report

Data File: C:\EZStart\Data\Tian-Ren\LTR-167E AD 99.8-0.2 @0.2 12.13.16.dat
 Method: C:\EZStart\Methods\Shehani\99.8-0.2 at 0.2.met
 Acquired: 12/13/2016 4:09:46 PM
 Printed: 2/14/2017 10:39:07 PM



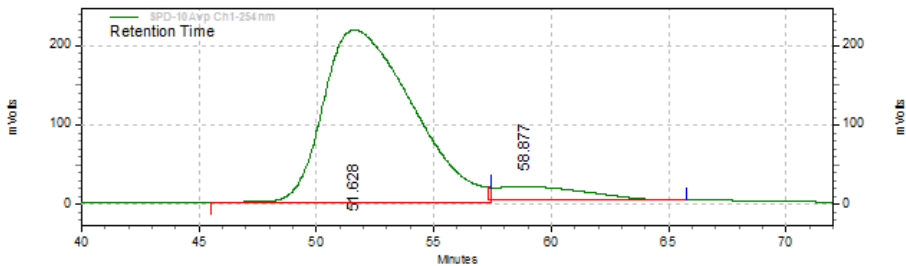
SPD-10Avp Ch1-254nm Results				
Retention Time	Area	Area %	Height	Height %
57.838	34018184	51.46	131673	55.83
66.372	32090597	48.54	104187	44.17
Totals	66108781	100.00	235860	100.00

(S)-phenyl(1-((trifluoromethyl)sulfonyl)-1H-indol-3-yl)methyl prop-1-en-2-yl carbonate



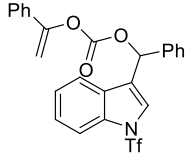
Area % Report

Data File: C:\EZStart\Data\Tian-Ren\LR-235E AD 99.8-0.2 @0.2 12.13.16.dat
 Method: C:\EZStart\Methods\Mary\90-10 @0.8.met
 Acquired: 12/13/2016 5:44:01 PM
 Printed: 2/25/2017 1:02:07 PM



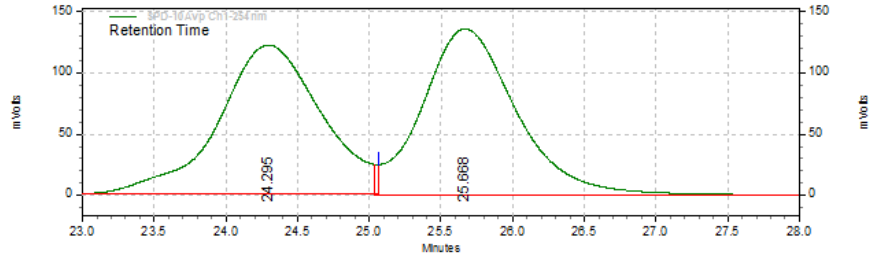
SPD-10Avp Ch1-254nm Results				
Retention Time	Area	Area %	Height	Height %
51.628	57758498	92.59	217954	92.72
58.877	4619501	7.41	17121	7.28
Totals	62377999	100.00	235075	100.00

Phenyl(1-((trifluoromethyl)sulfonyl)-1H-indol-3-yl)methyl (1-phenylvinyl) carbonate



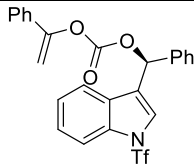
Area % Report

Data File: C:\EZStart\Data\Tian-Ren\ltr323-1 99-1 @0.5 02.23.17.dat
 Method: C:\EZStart\Methods\Shehani\99-1 at 0.5.met
 Acquired: 2/23/2017 4:49:43 PM
 Printed: 2/23/2017 5:22:29 PM



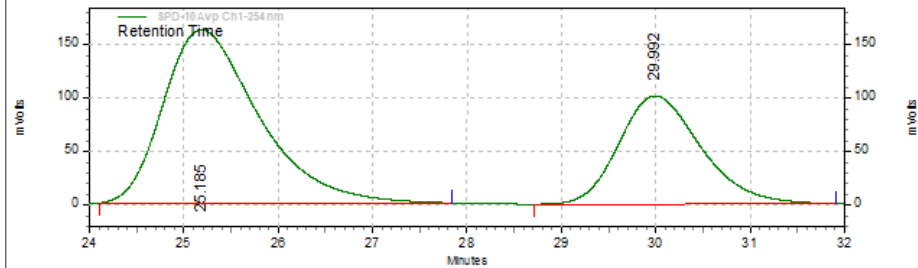
SPD-10Avp Ch1-254nm Results				
Retention Time	Area	Area %	Height	Height %
24.295	6073645	49.46	121499	47.27
25.668	6205754	50.54	135553	52.73
Totals	12279399	100.00	257052	100.00

(S)-phenyl(1-((trifluoromethyl)sulfonyl)-1H-indol-3-yl)methyl (1-phenylvinyl) carbonate



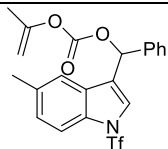
Area % Report

Data File: C:\EZStart\Data\Tian-Ren\ltr-370 99-1 @0.5 02.22.17.dat
 Method: C:\EZStart\Methods\Oid\Methods\10% wash.met
 Acquired: 2/22/2017 10:11:22 PM
 Printed: 2/25/2017 8:51:34 PM



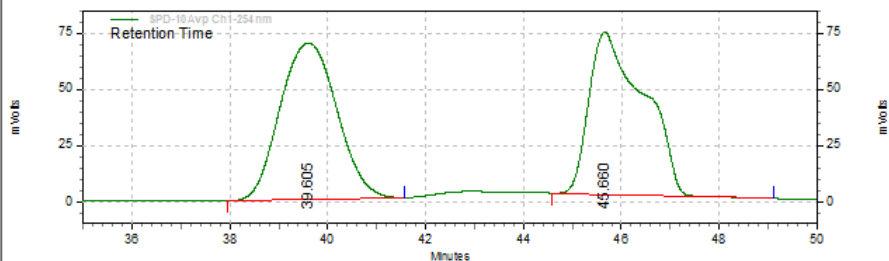
SPD-10Avp Ch1-254nm Results				
Retention Time	Area	Area %	Height	Height %
25.185	11379580	65.09	162058	61.61
29.992	6103613	34.91	100999	38.39
Totals	17483193	100.00	263057	100.00

(5-methyl-1-((trifluoromethyl)sulfonyl)-1H-indol-3-yl)(phenyl)methyl prop-1-en-2-yl carbonate



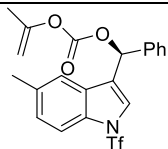
Area % Report

Data File: C:\EZStart\Data\Tian-Ren\tr-239 AD-H 99.6-0.4@0.2 12.31.16.dat
 Method: C:\EZStart\Methods\Mary90-10@0.8.met
 Acquired: 12/31/2016 4:19:42 PM
 Printed: 2/15/2017 12:39:43 PM



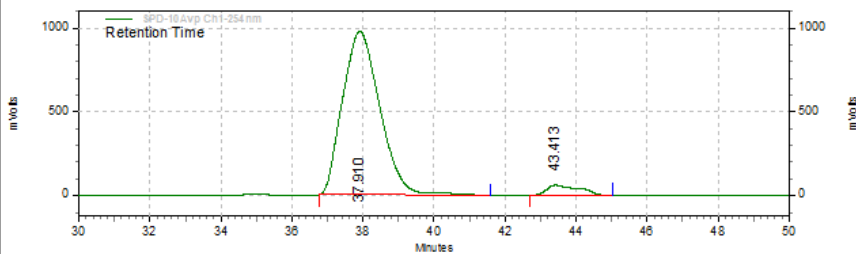
SPD-10Avp Ch1-254nm Results				
Retention Time	Area	Area %	Height	Height %
39.605	5613187	49.96	69487	49.09
45.660	5622225	50.04	72072	50.91
Totals	11235412	100.00	141559	100.00

(S)-(5-methyl-1-((trifluoromethyl)sulfonyl)-1H-indol-3-yl)(phenyl)methyl prop-1-en-2-yl carbonate



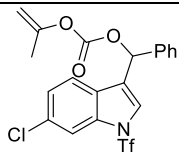
Area % Report

Data File: C:\EZStart\Data\Tian-Ren\tr-284 AD-H 99.6-0.4@0.2 12.31.16.dat
 Method: C:\EZStart\Methods\Mary90-10@0.8.met
 Acquired: 12/31/2016 5:23:05 PM
 Printed: 2/15/2017 12:48:25 PM



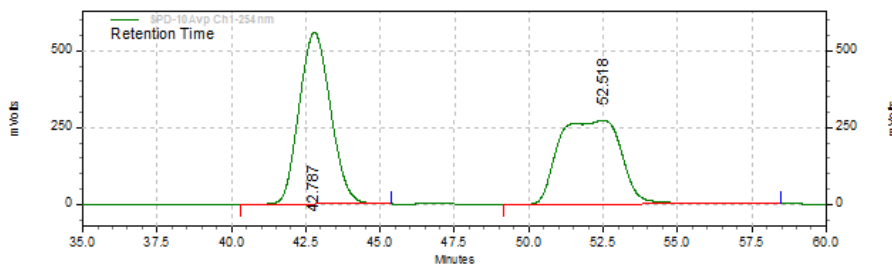
SPD-10Avp Ch1-254nm Results				
Retention Time	Area	Area %	Height	Height %
37.910	71001755	95.09	975134	94.26
43.413	3666503	4.91	59340	5.74
Totals	74668258	100.00	1034474	100.00

(6-chloro-1-((trifluoromethyl)sulfonyl)-1H-indol-3-yl)(phenyl)methyl prop-1-en-2-yl carbonate



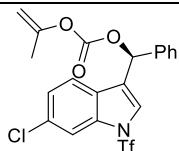
Area % Report

Data File: C:\EZStart\Data\Tian-Ren\tr-250c AD-H 99.6-0.4@0.2 12.31.16.dat
 Method: C:\EZStart\Methods\Mary90-10@0.8.met
 Acquired: 12/31/2016 12:25:14 PM
 Printed: 2/15/2017 12:43:39 PM



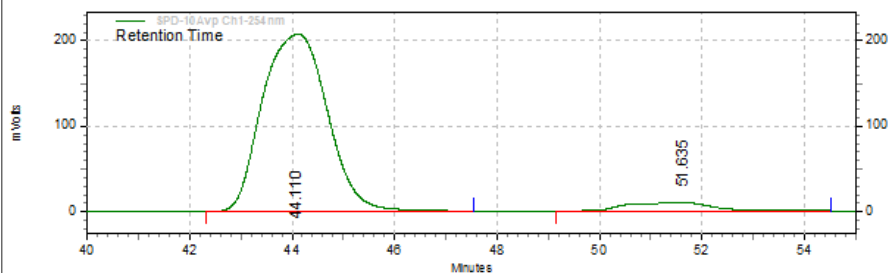
SPD-10Avp Ch1-254nm Results				
Retention Time	Area	Area %	Height	Height %
42.787	41006785	50.64	558236	67.17
52.518	39976282	49.36	272876	32.83
Totals	80983067	100.00	831112	100.00

(S)-(6-chloro-1-((trifluoromethyl)sulfonyl)-1H-indol-3-yl)(phenyl)methyl prop-1-en-2-yl carbonate



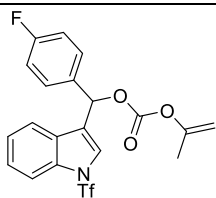
Area % Report

Data File: C:\EZStart\Data\Tian-Ren\tr-283b AD-H 99.6-0.4@0.2 12.31.16.dat
 Method: C:\EZStart\Methods\Mary90-10@0.8.met
 Acquired: 12/31/2016 2:38:13 PM
 Printed: 2/15/2017 12:49:58 PM



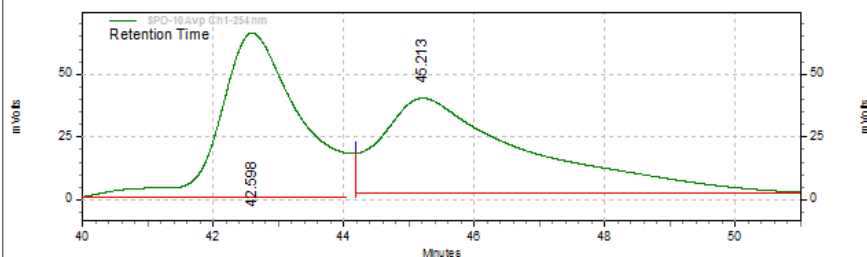
SPD-10Avp Ch1-254nm Results				
Retention Time	Area	Area %	Height	Height %
44.110	18185022	94.21	207062	95.63
51.635	1117307	5.79	9473	4.37
Totals	19302329	100.00	216535	100.00

(4-Fluorophenyl)(1-((trifluoromethyl)sulfonyl)-1H-indol-3-yl)methyl prop-1-en-2-yl carbonate



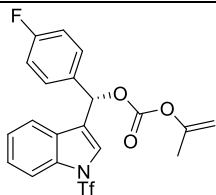
Area % Report

Data File: C:\EZStart\Data\Tian-Ren\ltr-p-f-s AD-H 99.6-0.4@0.2 02.21.17.dat
 Method: C:\EZStart\Methods\Shehani\10% wash.met
 Acquired: 2/22/2017 11:40:36 AM
 Printed: 2/23/2017 10:22:46 AM



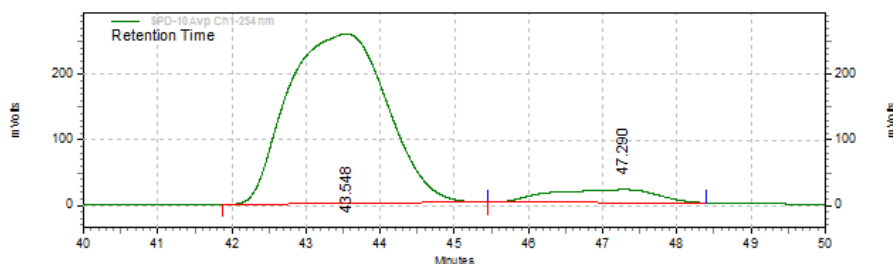
SPD-10Avp Ch1-254nm Results				
Retention Time	Area	Area %	Height	Height %
42.598	5671472	49.44	65663	63.58
45.213	5800829	50.56	37619	36.42
Totals	11472301	100.00	103282	100.00

(S)-(4-fluorophenyl)(1-((trifluoromethyl)sulfonyl)-1H-indol-3-yl)methyl prop-1-en-2-yl carbonate



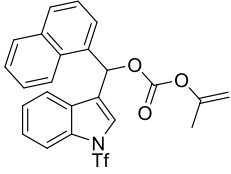
Area % Report

Data File: C:\EZStart\Data\Tian-Ren\ltr-285 AD-H 99.6-0.4@0.2 12.31.16.dat
 Method: C:\EZStart\Methods\Mary90-10@0.8.met
 Acquired: 12/31/2016 9:31:30 PM
 Printed: 2/15/2017 12:46:30 PM



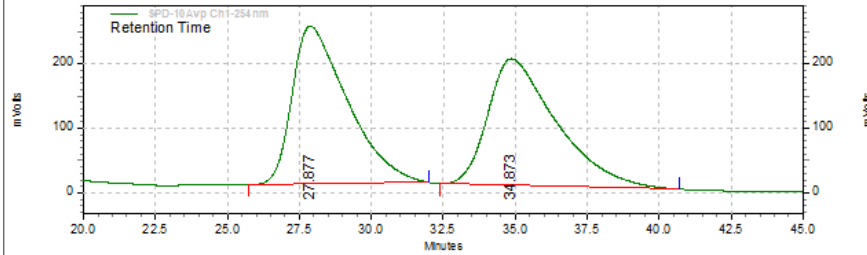
SPD-10Avp Ch1-254nm Results				
Retention Time	Area	Area %	Height	Height %
43.548	23990425	92.16	259049	92.81
47.290	2040752	7.84	20069	7.19
Totals	26031177	100.00	279118	100.00

Naphthalen-1-yl(1-((trifluoromethyl)sulfonyl)-1H-indol-3-yl)methyl prop-1-en-2-yl carbonate



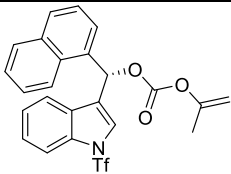
Area % Report

Data File: C:\EZStart\Data\Tian-Ren\ltr-267 AD-H 99.6-0.4@0.2 01.01.17.dat
 Method: C:\EZStart\Methods\Mary90-10@0.8.met
 Acquired: 1/1/2017 1:27:58 PM
 Printed: 2/15/2017 1:10:36 PM



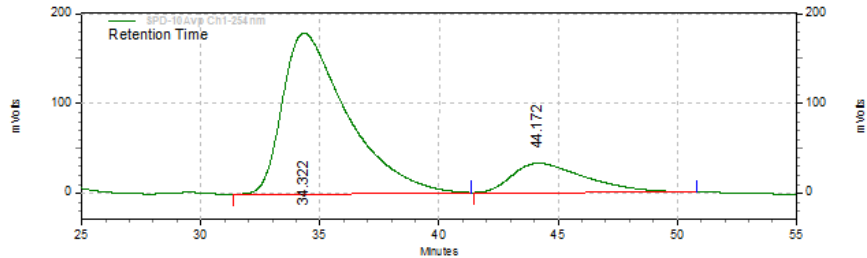
SPD-10Avp Ch1-254nm Results				
Retention Time	Area	Area %	Height	Height %
27.877	32630182	50.10	244350	55.48
34.873	32500148	49.90	196112	44.52
Totals		65130330	440462	100.00

(S)-naphthalen-1-yl(1-((trifluoromethyl)sulfonyl)-1H-indol-3-yl)methyl prop-1-en-2-yl carbonate



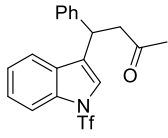
Area % Report

Data File: C:\EZStart\Data\Tian-Ren\ltr-290 AD-H 99.6-0.4@0.2 01.03.17.dat
 Method: C:\EZStart\Methods\Mary90-10@0.8.met
 Acquired: 1/3/2017 11:50:30 AM
 Printed: 2/15/2017 1:11:34 PM



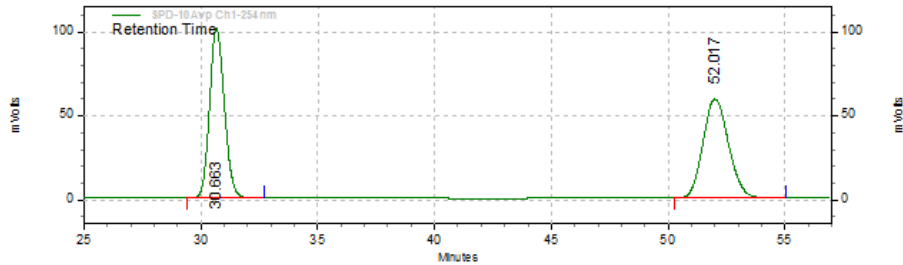
SPD-10Avp Ch1-254nm Results				
Retention Time	Area	Area %	Height	Height %
34.322	33701119	83.16	178769	84.70
44.172	6826720	16.84	32282	15.30
Totals		40527839	211051	100.00

4-Phenyl-4-(1-((trifluoromethyl)sulfonyl)-1H-indol-3-yl)butan-2-one



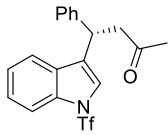
Area % Report

Data File: C:\EZStart\Data\Tian-Ren\LTR-238 OD-H 98-2@0.5 12.11.16.dat
 Method: C:\EZStart-Methods\Mary90-10@0.8.met
 Acquired: 12/11/2016 8:03:07 PM
 Printed: 2/15/2017 12:36:13 PM



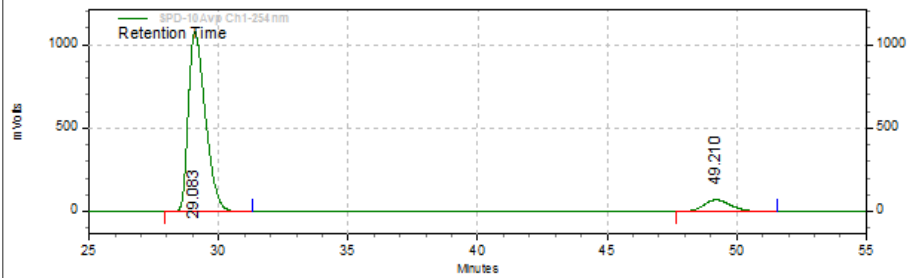
SPD-10Avp Ch1-254nm Results				
Retention Time	Area	Area %	Height	Height %
30.663	4439904	50.02	101140	63.31
52.017	4436261	49.98	58602	36.69
Totals	8876165	100.00	159742	100.00

(S)-4-phenyl-4-(1-((trifluoromethyl)sulfonyl)-1H-indol-3-yl)butan-2-one



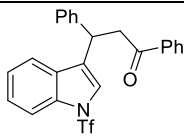
Area % Report

Data File: C:\EZStart\Data\Tian-Ren\LTR-235 OD-H 98-2@0.5 12.11.16.dat
 Method: C:\EZStart-Methods\Mary90-10@0.8.met
 Acquired: 12/11/2016 6:07:41 PM
 Printed: 2/15/2017 12:37:30 PM



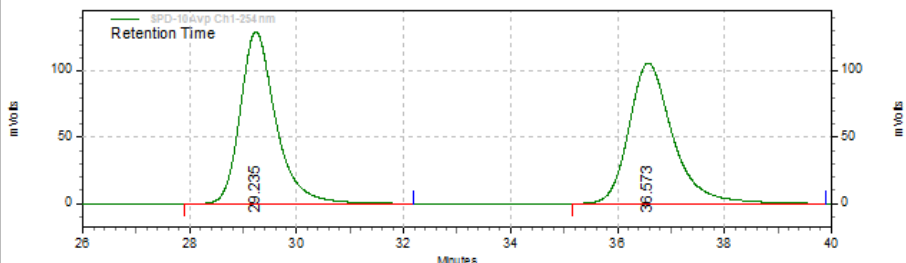
SPD-10Avp Ch1-254nm Results				
Retention Time	Area	Area %	Height	Height %
29.083	49096333	90.76	1077483	93.94
49.210	4999016	9.24	69522	6.06
Totals	54095349	100.00	1147005	100.00

1,3-Diphenyl-3-(1-((trifluoromethyl)sulfonyl)-1H-indol-3-yl)propan-1-one



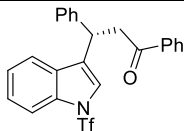
Area % Report

Data File: C:\EZStart\Data\Tian-Ren\ltr309-2 AD-H 98-2@0.5 02.21.17.dat
 Method: C:\EZStart\Methods\Shehani\99-1 at 0.5.met
 Acquired: 2/21/2017 4:26:44 PM
 Printed: 2/23/2017 5:27:40 PM



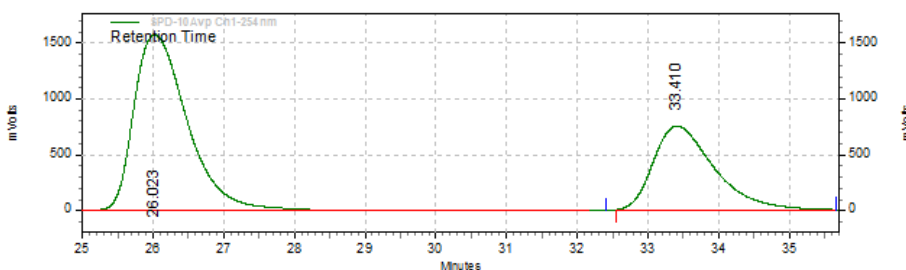
SPD-10Avp Ch1-254nm Results				
Retention Time	Area	Area %	Height	Height %
29.235	6002229	49.90	129729	55.04
36.573	6027119	50.10	105980	44.96
Totals	12029348	100.00	235709	100.00

(S)-1,3-diphenyl-3-(1-((trifluoromethyl)sulfonyl)-1H-indol-3-yl)propan-1-one



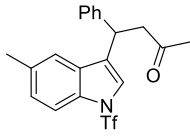
Area % Report

Data File: C:\EZStart\Data\Tian-Ren\ltr367 AD-H 98-2@0.5 02.21.17.dat
 Method: C:\EZStart\Methods\Old Methods\10% wash.met
 Acquired: 2/21/2017 6:03:54 PM
 Printed: 2/25/2017 8:36:13 PM



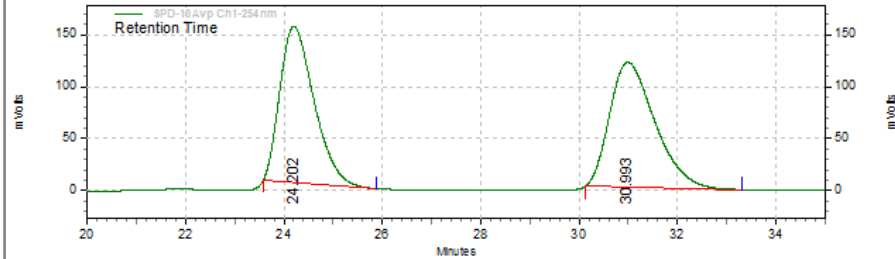
SPD-10Avp Ch1-254nm Results				
Retention Time	Area	Area %	Height	Height %
26.023	82797004	65.08	1571002	67.72
33.410	44418756	34.92	748797	32.28
Totals	127215760	100.00	2319799	100.00

4-(5-Methyl-1-((trifluoromethyl)sulfonyl)-1H-indol-3-yl)-4-phenylbutan-2-one



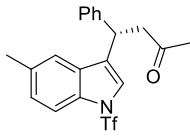
Area % Report

Data File: C:\EZStart\Data\Tian-Ren\Itr-239 OD 98-2@0.5 01.01.17.dat
 Method: C:\EZStart\Methods\Mary90-10@0.8.met
 Acquired: 1/2/2017 9:20:59 PM
 Printed: 2/15/2017 1:34:09 PM



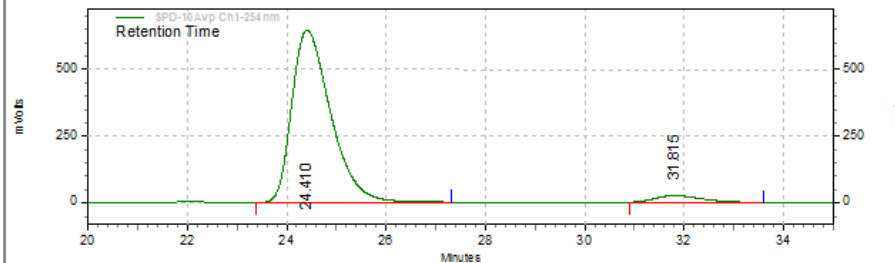
SPD-10Avp Ch1-254nm Results				
Retention Time	Area	Area %	Height	Height %
24.202	7225009	48.41	149867	55.50
30.993	7700151	51.59	120178	44.50
Totals	14925160	100.00	270045	100.00

(S)-4-(5-methyl-1-((trifluoromethyl)sulfonyl)-1H-indol-3-yl)-4-phenylbutan-2-one



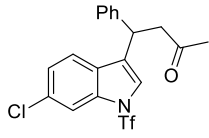
Area % Report

Data File: C:\EZStart\Data\Tian-Ren\Itr-287 AD-H 98-2@0.5 01.03.17.dat
 Method: C:\EZStart\Methods\Mary90-10@0.8.met
 Acquired: 1/3/2017 3:19:42 PM
 Printed: 2/15/2017 1:06:45 PM



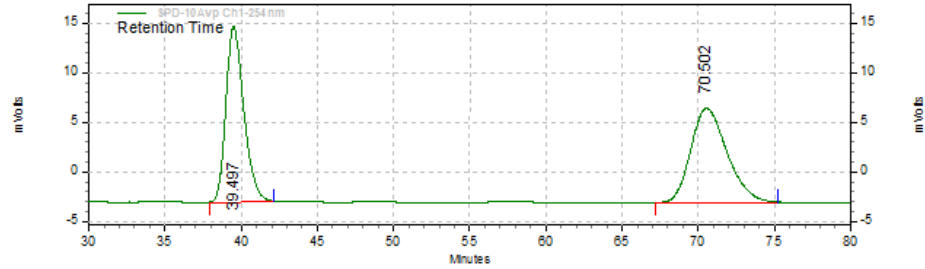
SPD-10Avp Ch1-254nm Results				
Retention Time	Area	Area %	Height	Height %
24.410	35038623	95.53	645471	96.24
31.815	1640145	4.47	25236	3.76
Totals	36678768	100.00	670707	100.00

4-(6-Chloro-1-((trifluoromethyl)sulfonyl)-1H-indol-3-yl)-4-phenylbutan-2-one



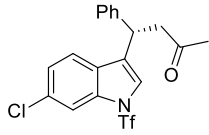
Area % Report

Data File: C:\EZStart\Data\Tian-Ren\ltr-259b OD 98-2@0.5 01.04.17.dat
 Method: C:\EZStart\Methods\Mary90-10@0.8.met
 Acquired: 1/4/2017 4:10:12 PM
 Printed: 2/15/2017 1:40:29 PM



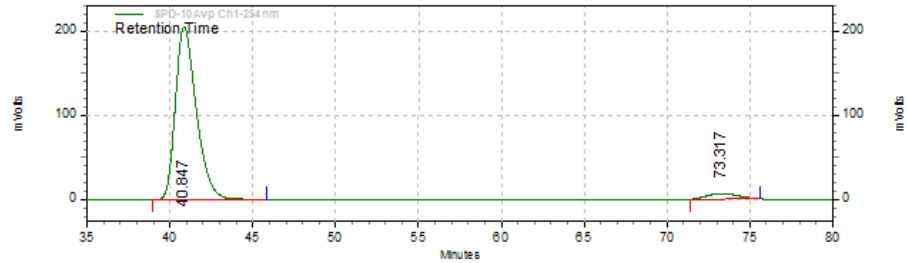
SPD-10Avp Ch1-254nm Results				
Retention Time	Area	Area %	Height	Height %
39.497	1446384	47.95	17750	65.15
70.502	1570001	52.05	9493	34.85
Totals	3016385	100.00	27243	100.00

(S)-4-(6-chloro-1-((trifluoromethyl)sulfonyl)-1H-indol-3-yl)-4-phenylbutan-2-one



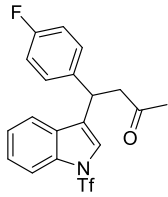
Area % Report

Data File: C:\EZStart\Data\Tian-Ren\ltr-286b OD 98-2@0.5 01.04.17.dat
 Method: C:\EZStart\Methods\Mary90-10@0.8.met
 Acquired: 1/4/2017 5:52:58 PM
 Printed: 2/15/2017 1:42:56 PM



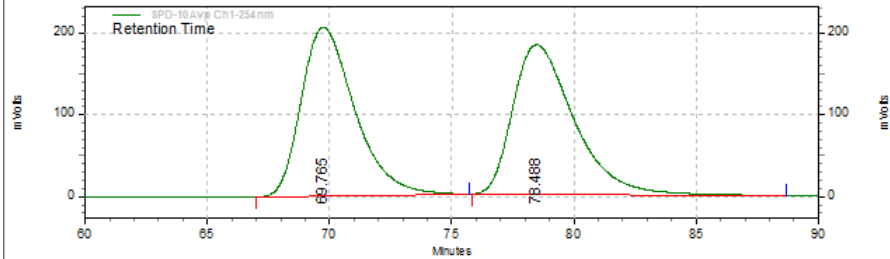
SPD-10Avp Ch1-254nm Results				
Retention Time	Area	Area %	Height	Height %
40.847	18048919	95.27	205147	96.77
73.317	895841	4.73	6837	3.23
Totals	18944760	100.00	211984	100.00

4-(4-Fluorophenyl)-4-(1-((trifluoromethyl)sulfonyl)-1H-indol-3-yl)butan-2-one



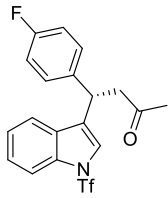
Area % Report

Data File: C:\EZStart\Data\Tian-Ren\Itr-255 A.OD 99-1@0.2 01.06.17.dat
 Method: C:\EZStart\Methods\Mary90-10@0.8.met
 Acquired: 1/6/2017 2:47:08 PM
 Printed: 2/15/2017 12:58:03 PM



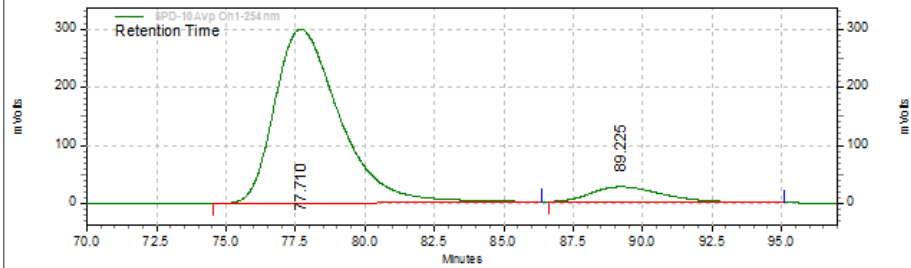
SPD-10Avp Ch1-254nm Results				
Retention Time	Area	Area %	Height	Height %
69.765	31431205	49.76	205957	53.00
78.488	31733810	50.24	182632	47.00
Totals	63165015	100.00	388589	100.00

(S)-4-(4-fluorophenyl)-4-(1-((trifluoromethyl)sulfonyl)-1H-indol-3-yl)butan-2-one



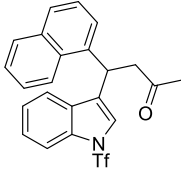
Area % Report

Data File: C:\EZStart\Data\Tian-Ren\Itr-288 OD 99-1@0.2 01.06.17.dat
 Method: C:\EZStart\Methods\Mary90-10@0.8.met
 Acquired: 1/6/2017 4:51:54 PM
 Printed: 2/15/2017 12:54:37 PM



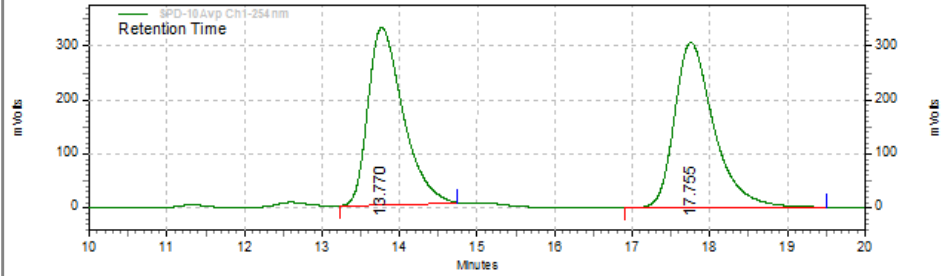
SPD-10Avp Ch1-254nm Results				
Retention Time	Area	Area %	Height	Height %
77.710	48339668	91.31	298552	92.00
89.225	4603338	8.69	25957	8.00
Totals	52943006	100.00	324509	100.00

4-(Naphthalen-1-yl)-4-(1-((trifluoromethyl)sulfonyl)-1H-indol-3-yl)butan-2-one



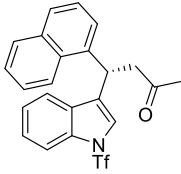
Area % Report

Data File: C:\EZStart\Data\Tian-Ren\ltr-291 AD-H 98-2@0.5 01.06.17.dat
 Method: C:\EZStart\Methods\Mary90-10@0.8.met
 Acquired: 1/6/2017 9:22:07 PM
 Printed: 2/15/2017 1:13:15 PM



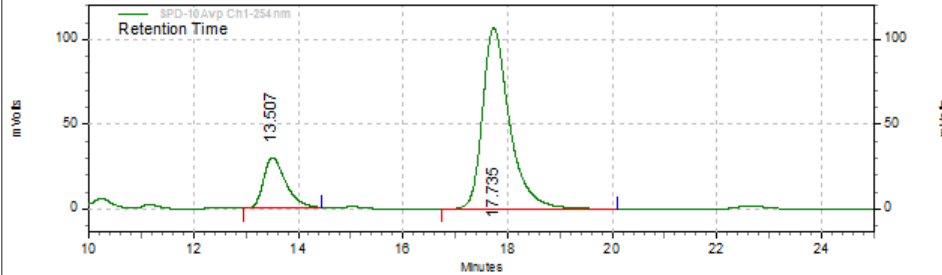
SPD-10Avp Ch1-254nm Results				
Retention Time	Area	Area %	Height	Height %
13.770	10304803	48.90	328815	51.81
17.755	10766673	51.10	305885	48.19
Totals	21071476	100.00	634700	100.00

(S)-4-(naphthalen-1-yl)-4-(1-((trifluoromethyl)sulfonyl)-1H-indol-3-yl)butan-2-one



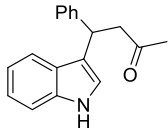
Area % Report

Data File: C:\EZStart\Data\Tian-Ren\ltr-295 AD-H 98-2@0.5 01.06.17.dat
 Method: C:\EZStart\Methods\Mary90-10@0.8.met
 Acquired: 1/6/2017 8:44:19 PM
 Printed: 2/15/2017 1:14:11 PM



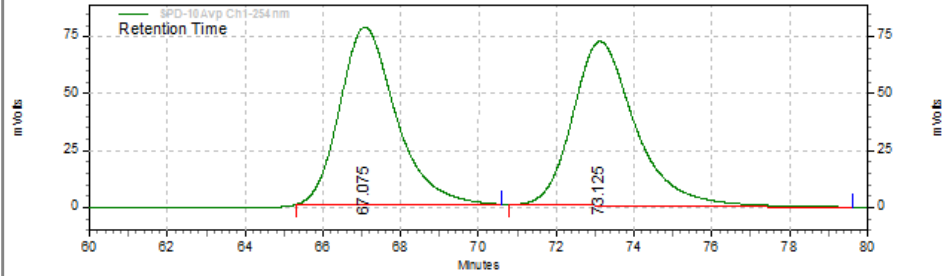
SPD-10Avp Ch1-254nm Results				
Retention Time	Area	Area %	Height	Height %
13.507	873800	18.54	29625	21.66
17.735	3839121	81.46	107128	78.34
Totals	4712921	100.00	136753	100.00

4-(1H-indol-3-yl)-4-phenylbutan-2-one



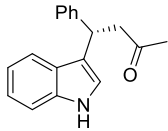
Area % Report

Data File: C:\EZStart\Data\Tian-Ren\LTR-320 AD-H 95-5@0.5 01.12.17.dat
 Method: C:\EZStart\Methods\Mary90-10@0.8.met
 Acquired: 1/12/2017 2:33:26 PM
 Printed: 2/15/2017 1:49:06 PM



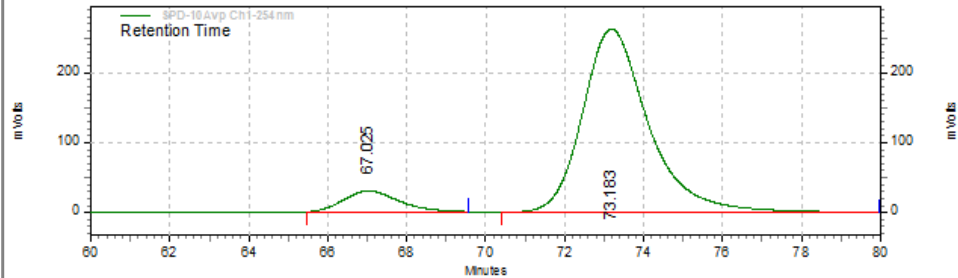
SPD-10Avp Ch1-254nm Results				
Retention Time	Area	Area %	Height	Height %
67.075	7828791	49.33	77842	52.00
73.125	8040514	50.67	71857	48.00
Totals	15869305	100.00	149699	100.00

(S)-4-(1H-indol-3-yl)-4-phenylbutan-2-one



Area % Report

Data File: C:\EZStart\Data\Tian-Ren\LTR-317 AD-H 95-5@0.5 01.12.17.dat
 Method: C:\EZStart\Methods\Mary90-10@0.8.met
 Acquired: 1/12/2017 4:48:06 PM
 Printed: 2/15/2017 1:50:30 PM

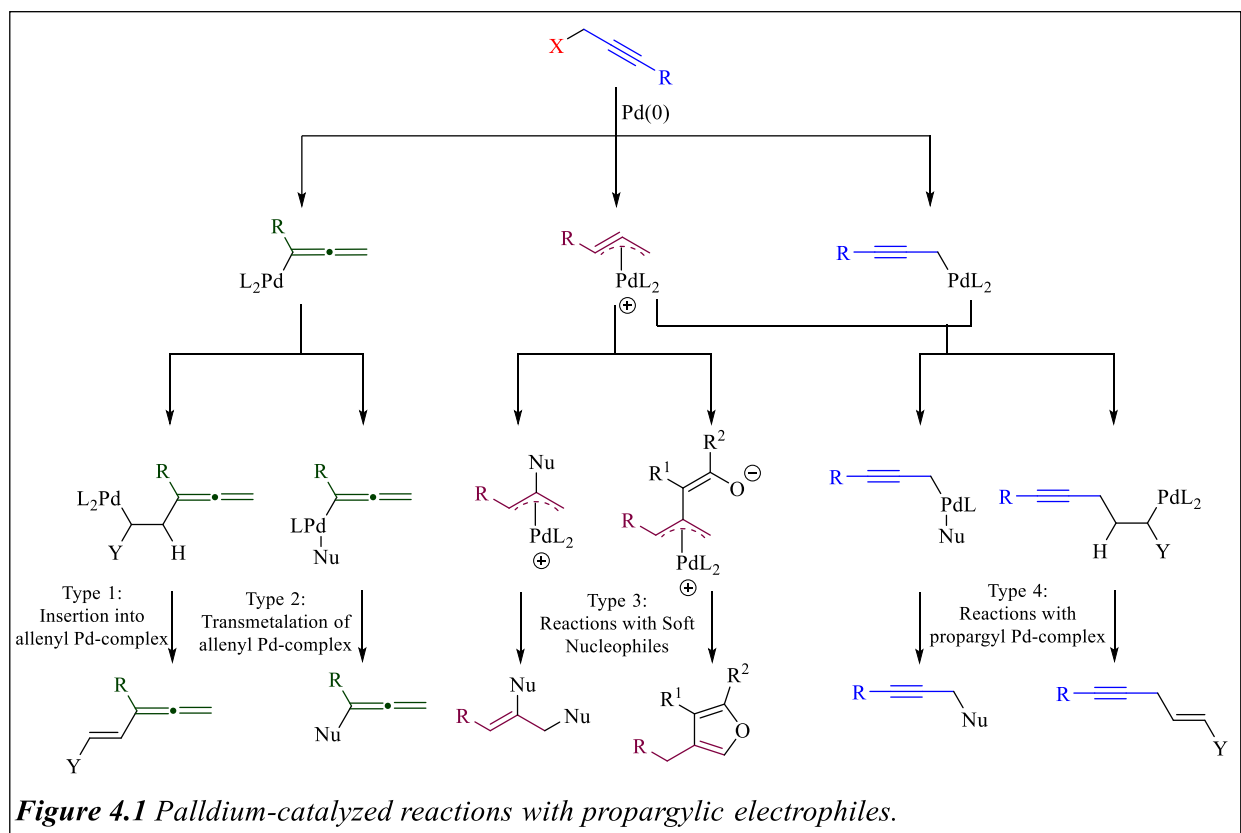


SPD-10Avp Ch1-254nm Results				
Retention Time	Area	Area %	Height	Height %
67.025	2895568	8.69	29949	10.27
73.183	30429588	91.31	261809	89.73
Totals	33325156	100.00	291758	100.00

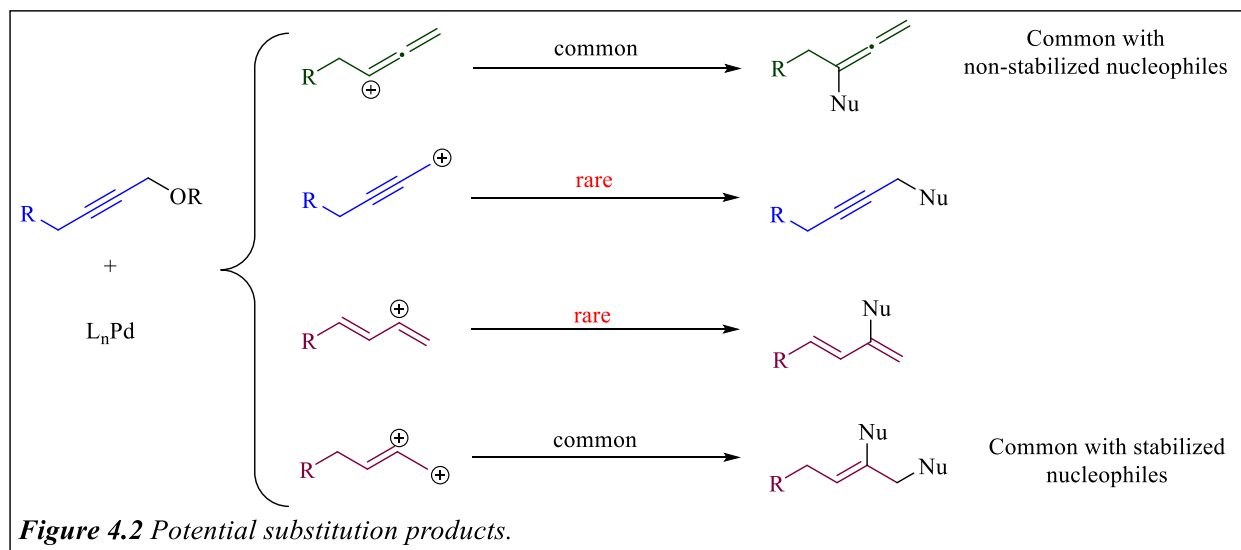
Chapter 4. Palladium-Catalyzed Decarboxylative Propargylation and 1,3-Dienylation of Enolates

4.1 Introduction

Chapter 2 of this dissertation presented a review of many different methods for installing a propargylic moiety onto a variety of compounds, with a focus on electrophilic propargylic substitution. Among these methods were the Nicholas reaction,¹ Lewis or Brønsted-catalyzed propargylations,² and propargylic substitutions that were catalyzed by various transition metals.³ However, many of these methods suffer from either a limited substrate scope, a requirement for superstoichiometric basic additives, or the generation of quantitative toxic waste. Therefore, the development of new methods that both expand the scope and improve the reaction conditions would be extremely useful.



In addition to discussing several of the previously reported propargylation methods, chapter 2 also reviewed the reactivity of palladium with propargylic electrophiles. Figure 4.1, which was also included in chapter 2, illustrates several of the potential mechanistic pathways of propargylpalladium complexes with various nucleophiles.⁴ After reacting with palladium, several, structurally diverse metal-bound intermediates can be generated, including η^1 -propargyl, η^1 -allenyl, or η^3 -propargylpalladium complexes. Therefore, reaction conditions that selectively favor one of the propargylpalladium complexes would allow for the tuning of the reactivity.

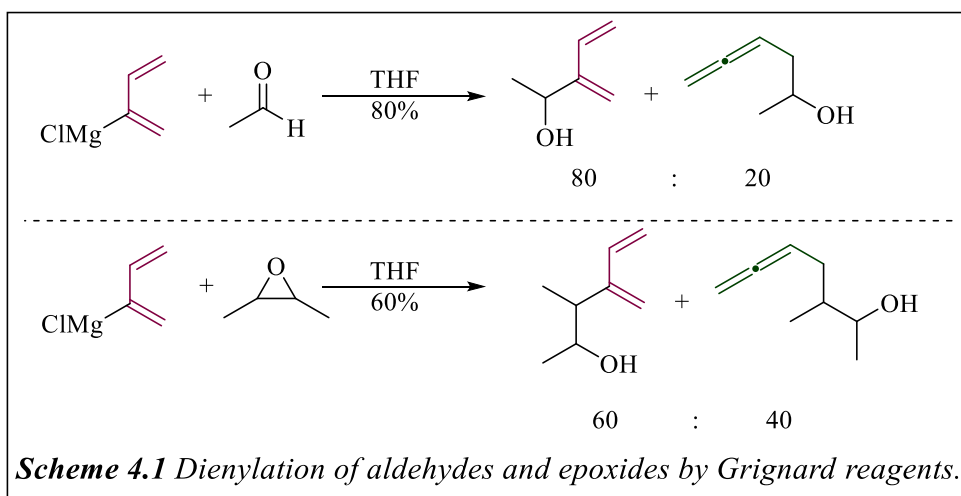


A brief overview of the reaction patterns of Pd-catalyzed propargylations with propargylic electrophiles and carbon-centered nucleophiles is shown in Figure 4.2. Reactions with the η^1 -allenylpalladium complexes can undergo an insertion (Type I) with an alkene or transmetalation with a hard nucleophile (Type II).⁵ Both pathways result in the formation of an allenyl product. While hard nucleophiles are known to react with the η^1 -allenylpropargyl complex, soft nucleophiles selectively attack at the central position of the η^3 -propargyl complex (Type III).⁶ These reactions will either undergo a second nucleophilic attack, either intermolecularly, yielding an alkene,⁷ or intramolecularly, yielding a cyclized product.⁸ The last category of reactions (Type

IV) is much more rare than the others and arises from reactions with the η^1 -propargylpalladium complex.^{24-28,31} Once the complex is formed, it can then undergo nucleophilic attack or insertion with an alkene.

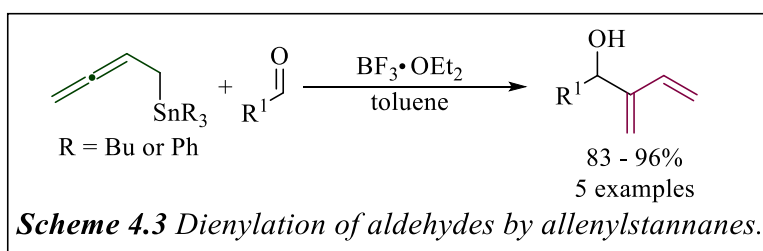
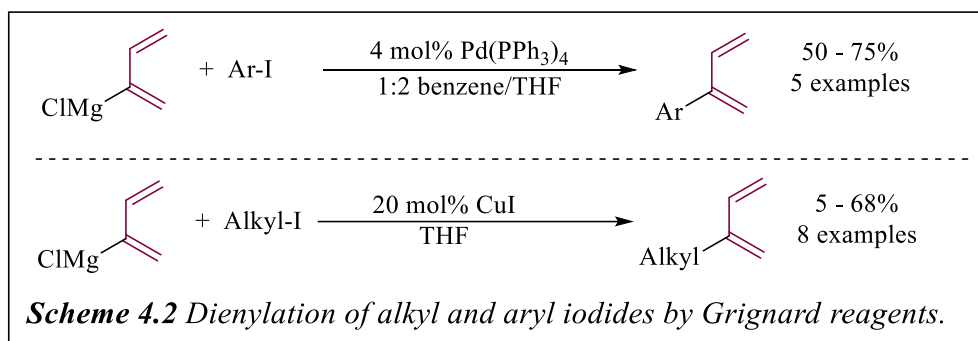
4.2 Synthetic Methods for the Formation of 1,3-Butadiene Motifs

1,3-butadienyl motifs are synthetically valuable targets in organic synthesis for several reasons. They are present in a number of natural products⁹ and biologically active compounds.¹⁰ Furthermore, 1,3-dienyl moieties are commonly used as functional handles in the synthesis of larger, more complex molecular systems,¹¹ as they can undergo many well-known chemical transformations.¹² Therefore, synthetic methods to access 1,3-dienes are extremely important in organic synthesis. This section will give a brief summary of several of the previously reported methodologies for the coupling 1,3-butadienyl motifs.



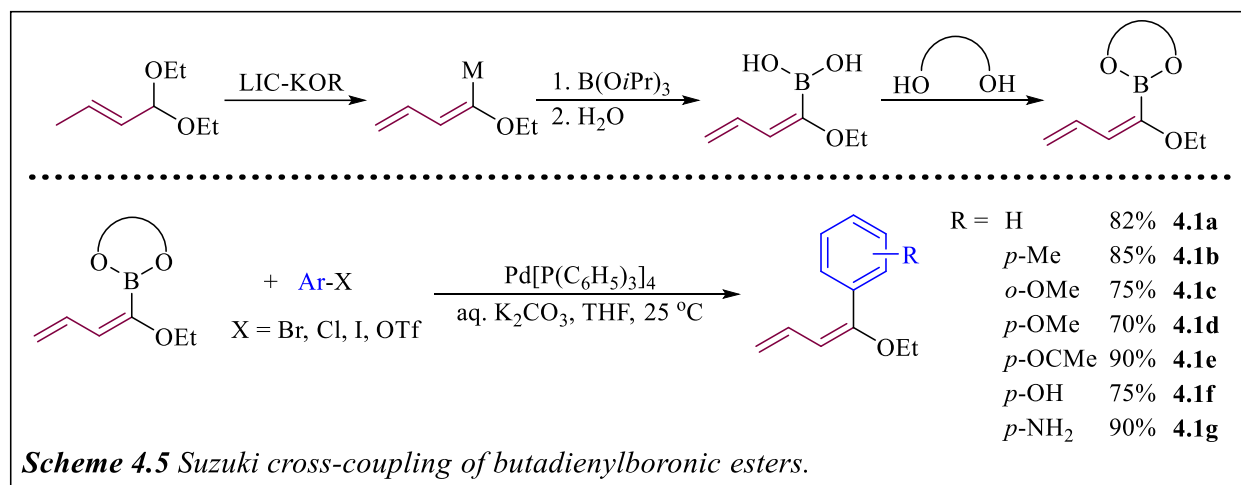
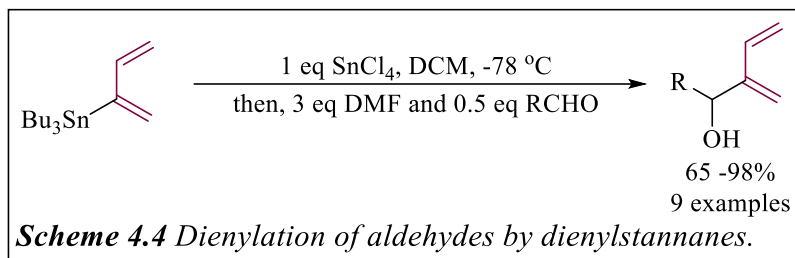
In the late 1970s and early 1980s, Nunomoto and coworkers released a series of publications focused on the coupling of dienyl Grignard reagents with various electrophiles. First, in 1981, they disclosed a method for the dienylation of aldehydes and epoxides using 2-(1,3-butadienyl)magnesium chloride (Figure 4.1).¹³ However, the substrate scope for this reaction was

quite limited, and led to mixtures of both the dienyl and allenyl products. Furthermore, as the steric hinderance increased, the amount of allenyl product also increased. They followed this publication in 1981, expanding the scope of their electrophiles to aryl and alkyl iodides by altering the reaction conditions to include either palladium *tetrakis*(triphenylphosphine) or copper iodide, respectively (Scheme 4.2).¹⁴ While this method did not suffer as much contamination from the allenyl isomer as the previous, it still had an extremely limited reaction scope and the yields were mostly low to moderate. Furthermore, both methods require the pre-formation of 2-(1,3-butadienyl)magnesium chloride, which greatly decreases the utility of the reaction.



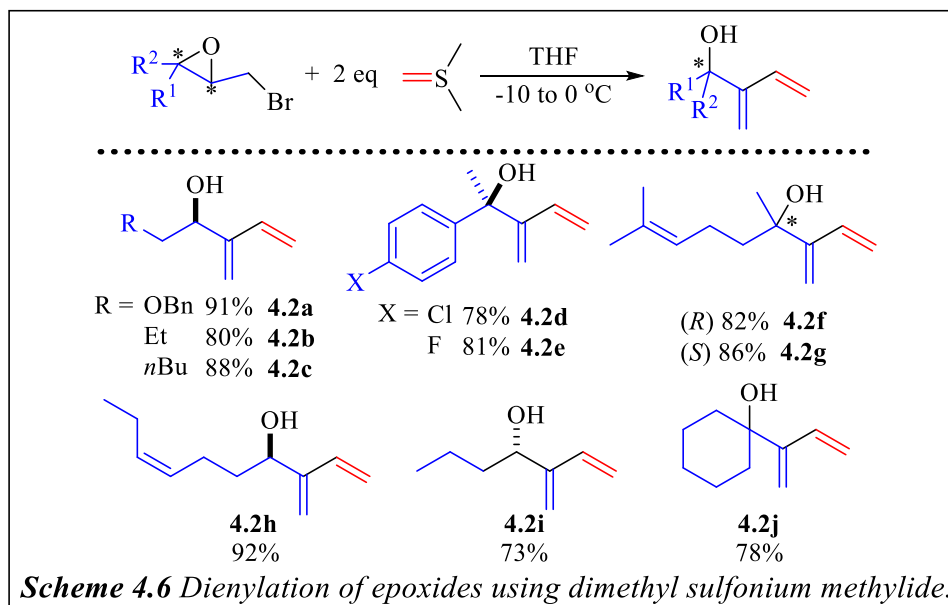
Almost twenty-years later, Hatakeyama and coworkers disclosed a series of reports on the dienylation of aldehydes using tin reagents. In 1998, they published a report describing the Lewis acid-catalyzed 1,3-dienylation of aldehydes with buta-2,3-dienylstannanes, allowing for the formation of 1,3-dienyl alcohols in high yields (Scheme 4.3).¹⁵ However, this method suffered from an extremely limited scope. The following year, they reported the dienylation of aldehydes

using 2-tributylstannylbuta-1,3-diene in the presence of stoichiometric amounts of SnCl₄ (Scheme 4.4).¹⁶ The SnCl₄ allowed for the formation of an homoallenyl tin intermediate, which reacted in a similar fashion to the allenyl tin reagent in Scheme 4.3. While both methods were fairly high yielding and selective, they both suffered from limited scopes and the requirement for stoichiometric amounts of toxic tin reagents.

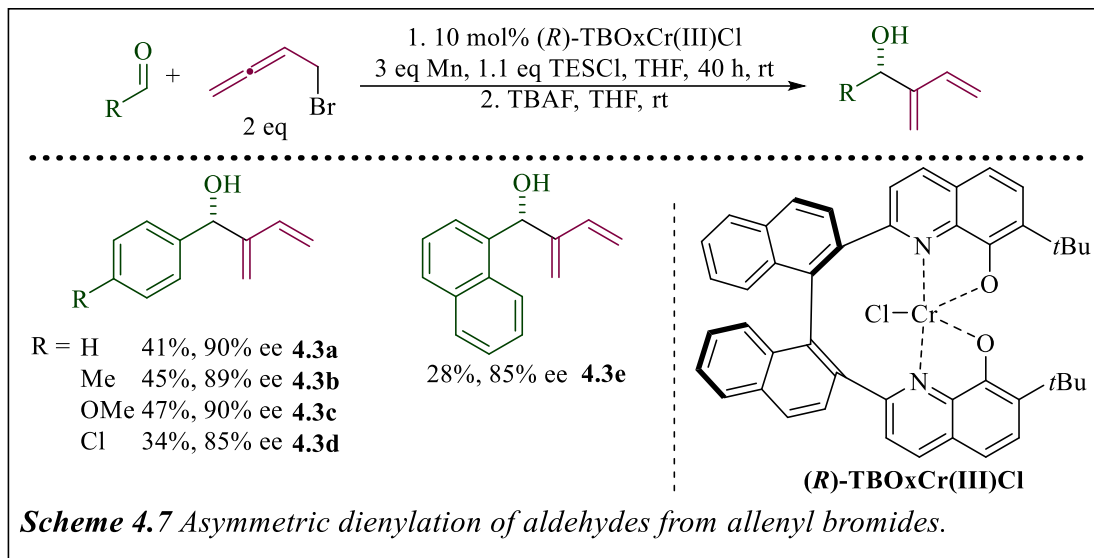


In 2002, Venturello and coworkers disclosed a synthesis of butadienyl- and styrylboronic esters from α,β -unsaturated acetals that were then subsequently used in Suzuki cross-coupling reactions with aryl bromides, chlorides, iodides, and triflates (Scheme 4.5).¹⁷ This method successfully generated several 1,3-dienylated aryl compounds with substituents of varying electronic demands in moderate to high yields, including those containing a free alcohol (**4.1f**) and amine (**4.1g**). However, this method suffers from a limited scope and the need to generate stoichiometric amounts of boronic acid. In addition, the first step of the reaction required superstoichiometric

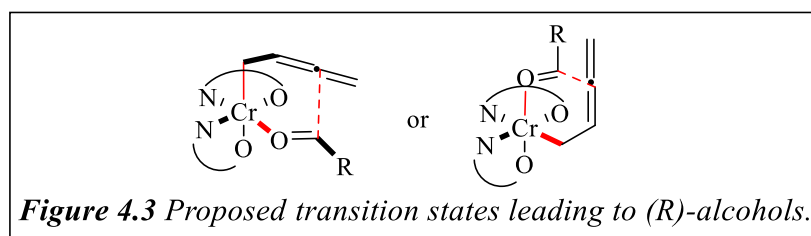
amounts of Schlosser's base (LIC-KOR), which is an equal mixture of *n*BuLi and KO*t*Bu. Furthermore, reactions with aryl chlorides suffered from extremely low yields of the corresponding 1,3-dienylated products.



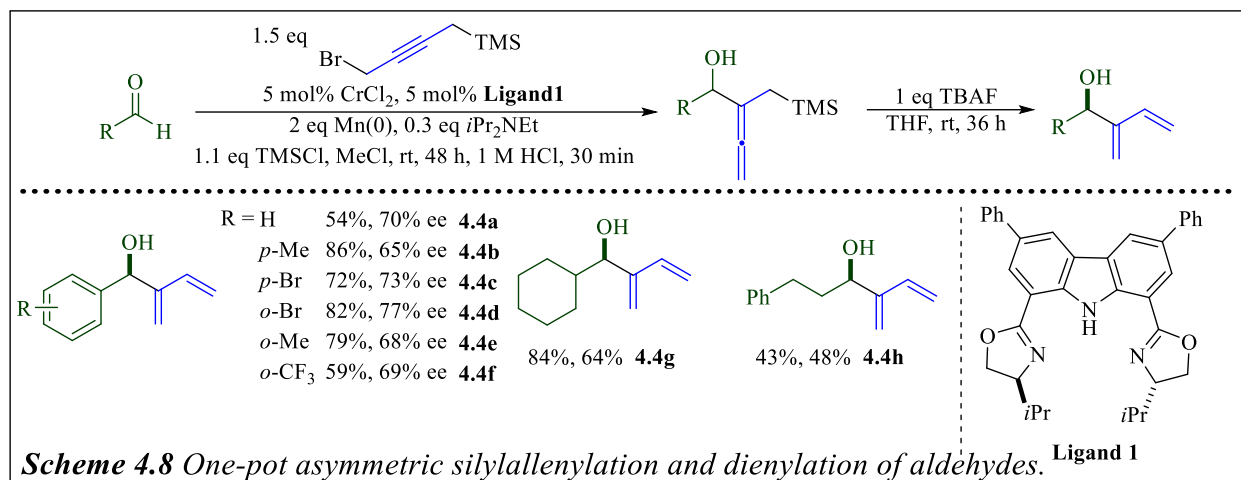
As an alternative approach, a few years later in 2005, Alcaraz and coworkers published a report on the synthesis of 1,3-butadien-2-ylmethanols through a reaction with alkyl bromide epoxides and excess dimethylsulfonium methylide (Scheme 4.6).¹⁸ They had previously shown that dimethyl sulfonium methylide could react with 1,2-disubstituted *cis*-epoxides to generate allylic alcohols.¹⁹ Furthermore, Mioskowski and coworkers had demonstrated that they could react with terminal halides to produce terminal alkenes.²⁰ Therefore, Alcaraz and coworkers combined the two methods in order to synthesize 1,3-dienyl alcohols in good to high yields, including *p*-halogenated benzyl alcohols (**4.2d-e**) and distal alkenes (**4.2h-i**). Further, the reaction was tolerant to tri-substituted epoxides (**4.2j**), forming the corresponding tertiary alcohol in a moderate yield. In addition, the enantiopurity of the starting materials was conserved through the course of the reaction. However, the method requires 6 equivalents of dimethylsulfonium methylide, which greatly decreases the utility of the reaction.



In 2008, Yamamoto and coworkers disclosed an enantioselective coupling of allenyl bromides and aldehydes in the presence of tethered bis(8-quinolinato) chromium complex catalyst (TBOxCr(III)Cl) and stoichiometric manganese (Scheme 4.7).²¹ Under their reaction conditions, they successfully generated several benzyl alcohols with varying electronic demand, albeit in only low to mild yields. An electron-rich substrate with a *para* methoxy group (**4.3c**) had a noticeably higher yield than that of one with an electron-withdrawing chloro- group (**4.3d**). However, despite the lower yields, the observed enantioselectivities for the reactions were fairly high, which they attribute to the chromium complex that forms one of the two transition states shown in Figure 4.3.



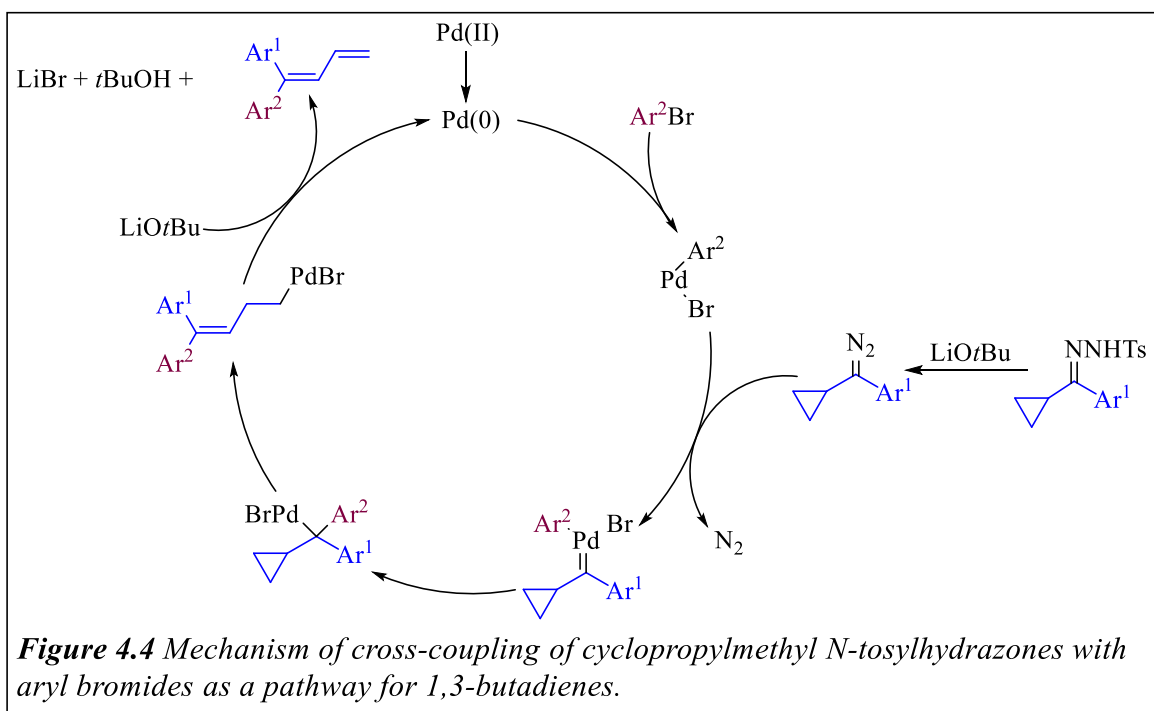
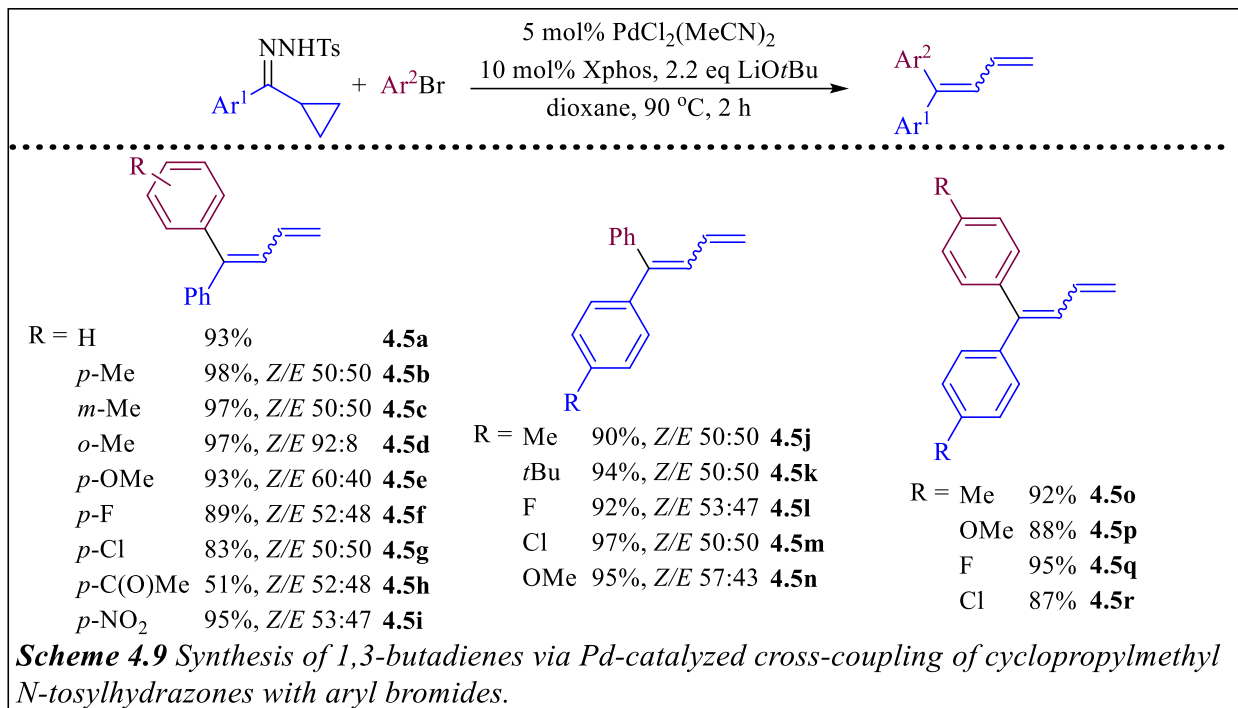
They hypothesized that this complex allowed for them to avoid many of the issues with regioselectivity that are common with these reactions. However, despite the high enantioselectivities, the report had an extremely limited reaction scope, and the requirement for superstoichiometric quantities of manganese is less than ideal.



Scheme 4.8 One-pot asymmetric silyllallenylation and dienylation of aldehydes.

In 2010, Durán-Galván and Connell reported an enantioselective 1,3-dienylation of aldehydes through a reaction of (4-bromobut-2-ynyl)trimethylsilane in the presence of CrCl₂ catalyst and stoichiometric manganese (Scheme 4.8).²² Dienenylation occurs over a two-step process, the first step being a chromium-catalyzed silyllallenylation of the aldehyde in the presence of stoichiometric manganese and other additives. Immediately after this, the allenyl alcohol is converted to the 1,3-dienyl product with the addition of TBAF. This protocol was compatible with benzaldehydes with several different functional groups, including alkyl (**4.4b,e**), bromine (**4.4c-d**), and -CF₃ (**4.4f**). Further, alkyl aldehydes (**4.4g-h**) are also tolerated under the reaction conditions, albeit the linear alkyl group (**4.4h**) delivered a significant decrease in both yield and enantioselectivity. While this method shows some promise, the requirement for stoichiometric amounts of several different additives combined with the limited scope limits its overall utility. Further, the reported scope was limited to only a handful of examples with low to moderate yields and only moderate enantioselectivity.

In 2013, Yu and coworkers disclosed that they could access butadiene motifs with cyclopropylmethyl *N*-tosylhydrazones to generate 1,3-dienyl aryl compounds (Scheme 4.9).²³ In the

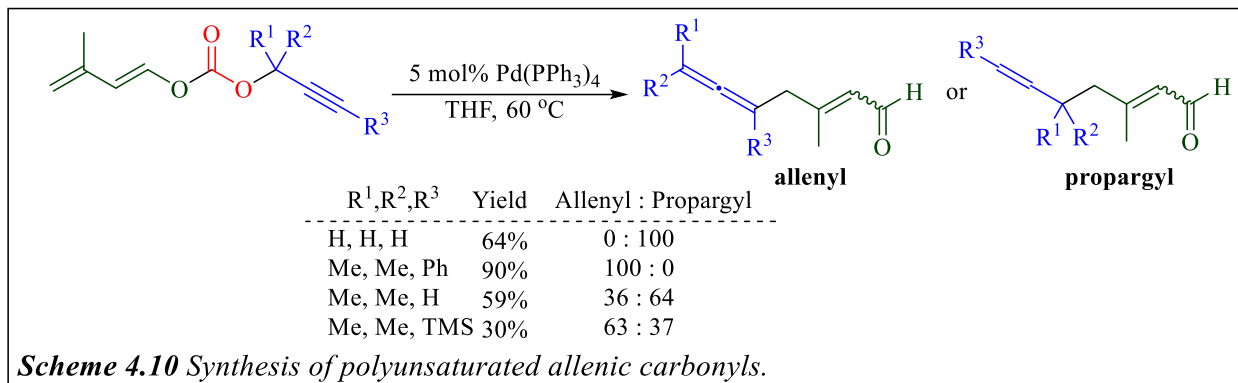


presence of palladium catalyst, Xphos ligand, and LiOtBu, they were able to successfully generate a wide range of 1,3-dienylated aromatic compounds with a range of different substituents on the aromatic system, including EDGs (**4.5b-e,j-l,n,o-p**) and EWGs (**4.5f-i,l-m,q-r**). The mechanism

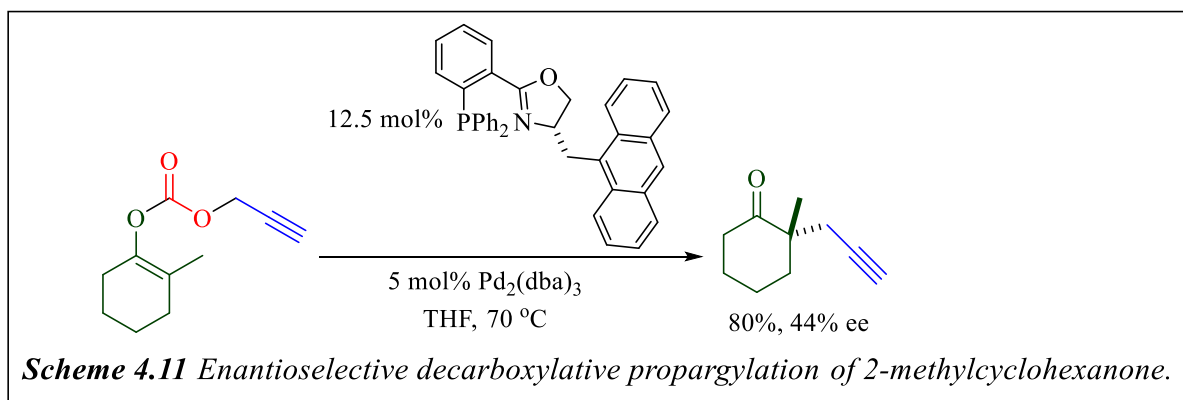
for this reaction, depicted in in Figure 4.4, begins with oxidative addition of the aryl bromide reagent with an *in situ* generate Pd(0) species. This reacts with a diazo intermediate, which was formed from the reaction of *N*-tosylhydrazone with LiOtBu, generating a palladium-carbene intermediate. Migratory insertion of the aryl moiety is followed by β -carbon-Pd elimination, and subsequent reaction with LiOtBu and β -hydride elimination releases the 1,3-dienylated product and regenerates the active Pd(0) catalyst. While this protocol eliminates the need for pre-formed organometallic reagents or stoichiometric metal additives, it does require multiple equivalents of base, and the *E/Z* selectivity was extremely poor.

4.3 Decarboxylative Propargylation and Dienylation from Propargylic Electrophiles

Chapter 2 discussed several methods for the decarboxylative propargylation of a variety of nucleophiles. This section will describe various protocols for the decarboxylation of propargylic electrophiles to generate both propargyl and 1,3-dienyl compounds. In 1994, Bienaymé disclosed that when exposed to catalytic amounts of palladium tetrakis(triphenylphosphine) substituted propargylic carbonates were able to successfully undergo decarboxylative cross-coupling to form both allenyl and propargylic carbonyls (Scheme 4.10).²⁴ They found that the ratio of isomers produced was highly dependent on the substitution pattern of the starting propargyl carbonate. Unsubstituted, terminal propargylic carbonates largely favor the formation of the propargyl product. However, as the steric bulk surrounding the alkyne of the propargyl carbonate increases, the preference for the allenyl product also increases. Furthermore, many of the examples presented suffered from low to moderate yields.

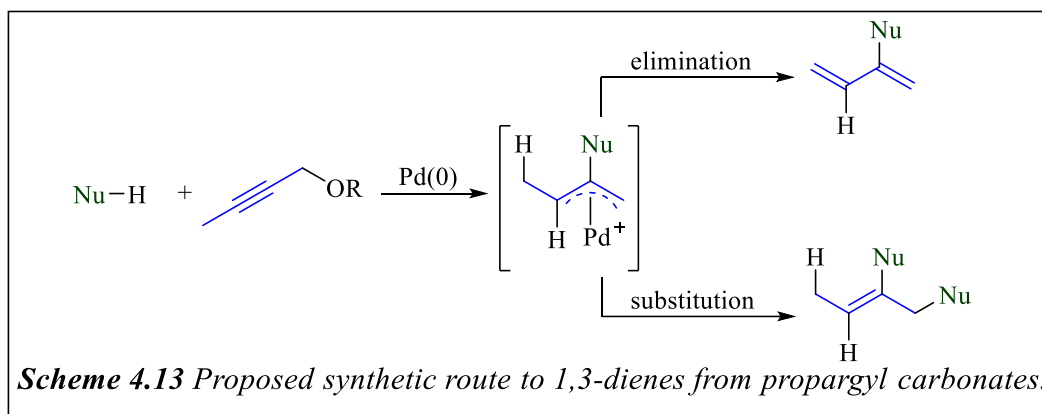
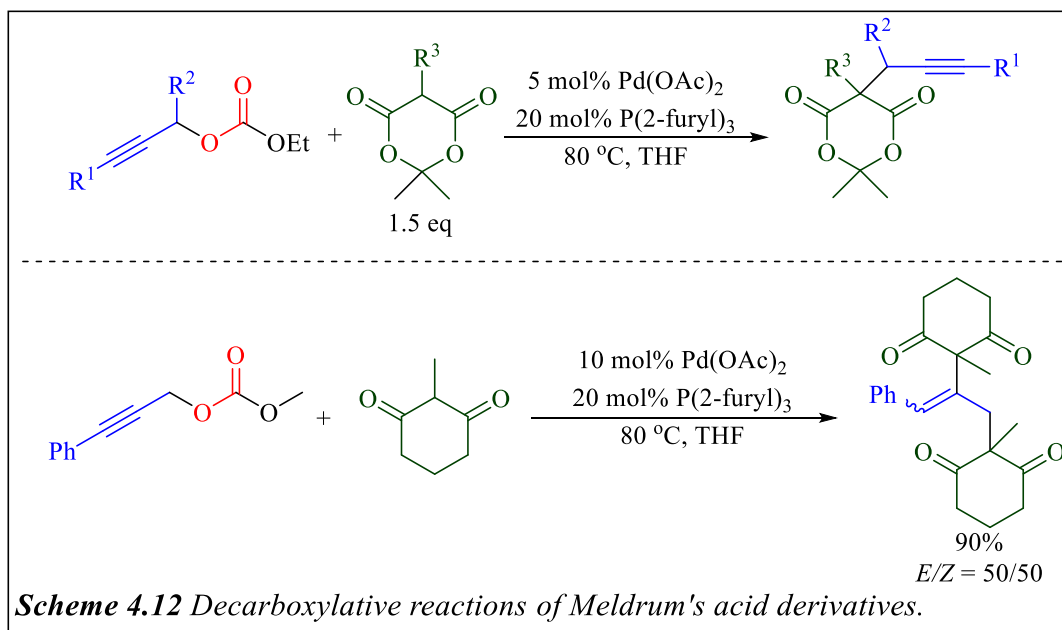


As discussed previously in chapter 2, in 2011 Stoltz and coworkers disclosed much of their work on the development of the asymmetric allylation of enol carbonates. In addition to this work on decarboxylative allylation, they also reported on the asymmetric propargylation of a single cyclohexanone derivative (Scheme 4.11).²⁵ While they were able to isolate the propargylated ketone in an 80% yield, the enantioselectivity was only 44%. However, their method provided insight for further development of asymmetric decarboxylative propargylation.



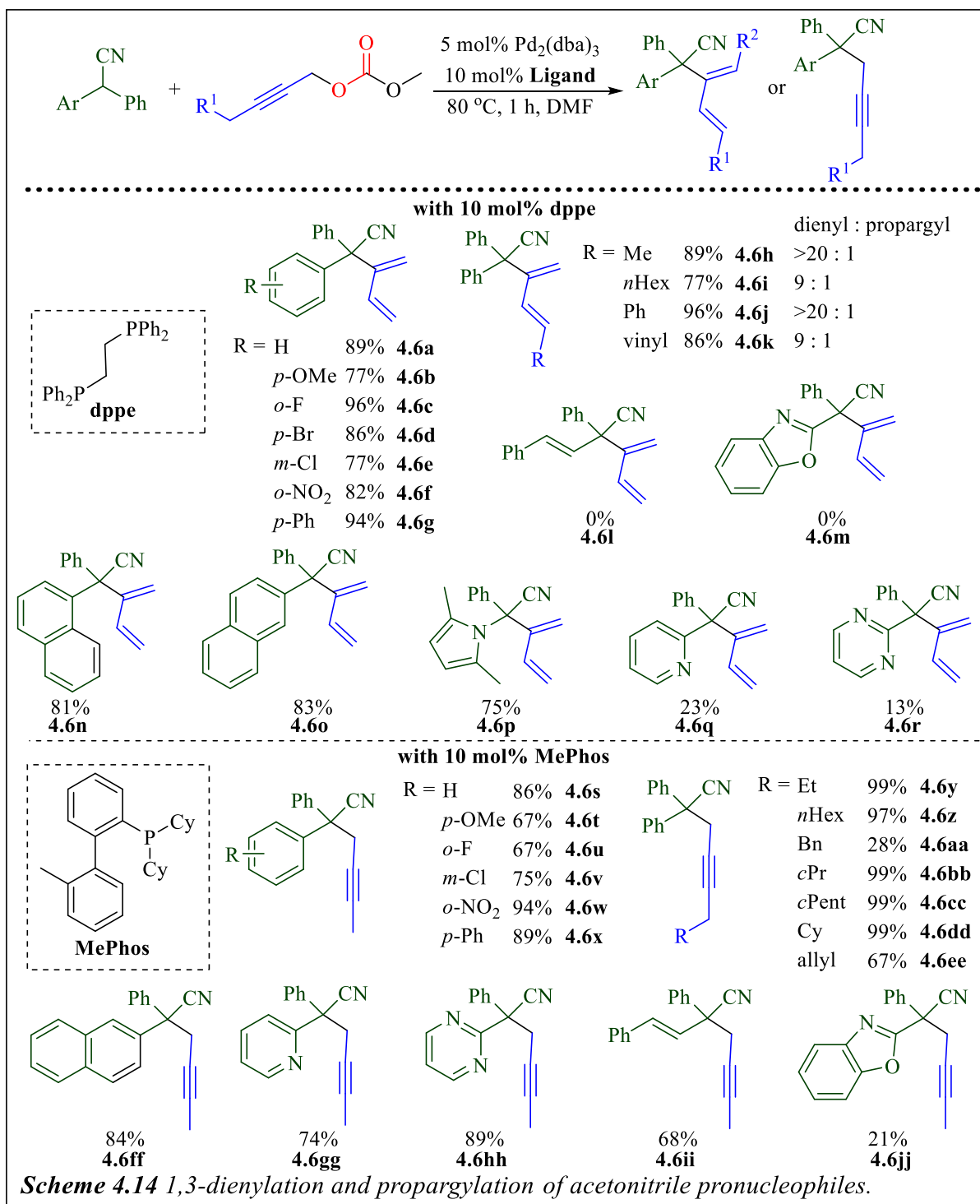
A few years later in 2015, Iazzetti and coworkers reported a decarboxylative propargylation of Meldrum's acid derivatives, which was previously discussed in chapter 2 (Scheme 4.12).²⁶ They found that, while the reaction could tolerate propargyl carbonates with alkyl and aryl substitutions at both the internal and terminal positions, the nucleophiles were limited to mono-substituted Meldrum's acid derivatives. When they attempted to use 2-methylcyclohexandione in their

reaction conditions, the dinucleophilic addition product was exclusively formed with no observed generation of the propargyl product.



With these observations, our lab believed that propargyl carbonates could serve as sources for electrophilic 1,3-butadiene synthons (Scheme 4.13). We proposed that after nucleophilic attack at the central position, there are two possible mechanistic pathways, the more common second nucleophilic attack, generating the bis-addition product, or elimination, producing a 1,3-dienyl product. In 2016, the Tunge group successfully implemented this proposed synthetic protocol

towards the regiodivergent propargylation and 1,3-dienylation of diaryl acetonitrile pronucleophiles (Scheme 4.14).²⁷ We observed that formation of either the propargyl or 1,3-dienyl



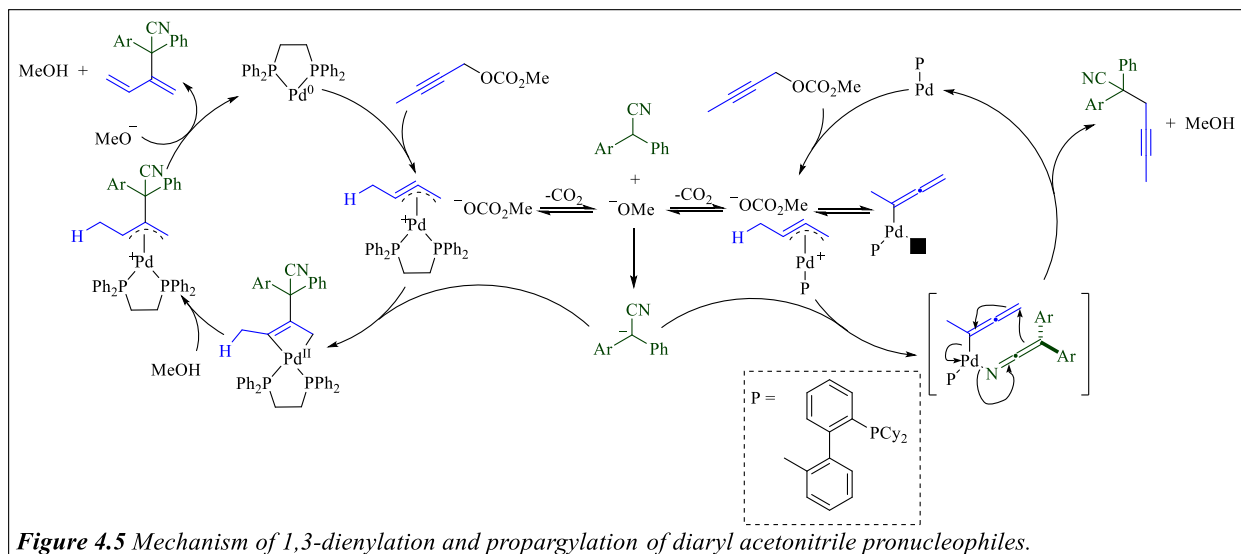
products was dependent on the choice of ligand used in the reaction, with a bidentate ligand, dppe, selectively generating the dienylated product and a monodentate ligand, MePhos, exclusively formed the propargylated product.

In the presence of catalytic Pd₂(dba)₂ and dppe, a range of 1,3-dienylated acetonitrile compounds were generated, containing a variety of functional groups, in good to high yields. Diaryl acetonitrile reactants with both EDGs (**4.6a-b**) and EWGs (**4.6c-f**) were well tolerated, including *para*-bromo (**4.6d**) and *meta*-chloro (**4.6e**) substituted aromatic groups, which have the potential for further coupling reactions. Furthermore, the steric bulk of the terminal position of the propargyl carbonate could be increased, while still generating the dienylated product, albeit with slight formation of the propargyl isomer as well (**4.6h-k**). Lastly, while reactants containing a non-basic heteroaromatic moiety were successful (**4.6p**), compounds containing basic heteroaromatic groups lead to low or no yield (**4.6m,q-r**).

When the bidentate ligand, dppe, was replaced with MePhos, we were able to isolate a variety of propargylated diaryl acetonitrile compounds in mild to high yields. Both electron-rich (**4.6s-t,x**) and electron-poor (**4.6u-w**) diaryl acetonitrile reactants were well-suited to the reaction conditions. Further, heteroaromatic moieties that were mostly unsuccessful in the dienylation reaction were able to successfully generate the propargylated product (**4.6gg-hh,jj**). Finally, propargyl carbonates with several alkyl substituents at the terminal position were tolerated, successfully synthesizing the corresponding propargyl compounds (**4.6y-ee**).

Based on the synthetic scope of these reactions and mechanistic testing, we developed a proposed mechanistic pathway to explain the observed ligand-dependent regioselectivity (Figure 4.5). With both dppe and MePhos, the first step would be oxidative addition and decarboxylation of the propargylic carbonate, which would generate an η^3 -propargyl palladium intermediate.

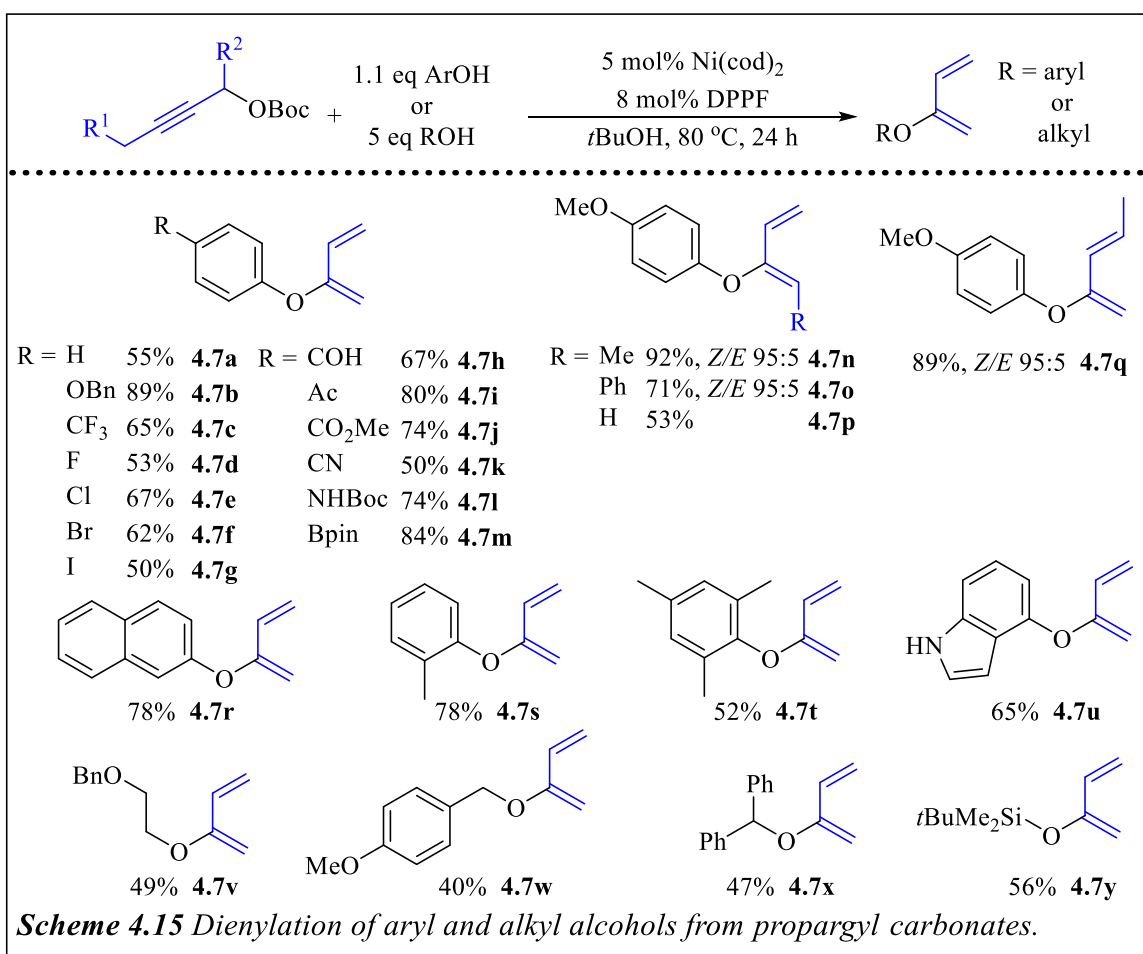
Previous reports have shown that η^3 -propargyl palladium intermediates are favored in the presence of bidentate ligands.²⁸ Nucleophilic attack would then occur at the center carbon, generating a palladacyclobutene intermediate. Protonation from either methanol or the acetonitrile starting material would form a π -allyl palladium intermediate, and base-induced elimination would generate the dienylated product and regenerate that active Pd(0) catalyst.



With MePhos, while initial oxidative addition of the propargyl carbonate would form a cationic η^3 -propargyl palladium intermediate, the open coordination site provided by the monodentate ligand would allow for coordination of the nucleophilic nitrile compounds, which has been known to favor an η^1 -allenyl intermediate.²⁸ Nucleophilic attack at the terminal position of the allenyl carbon would immediately follow, releasing the propargylated product and regenerating the active Pd(0) catalyst.

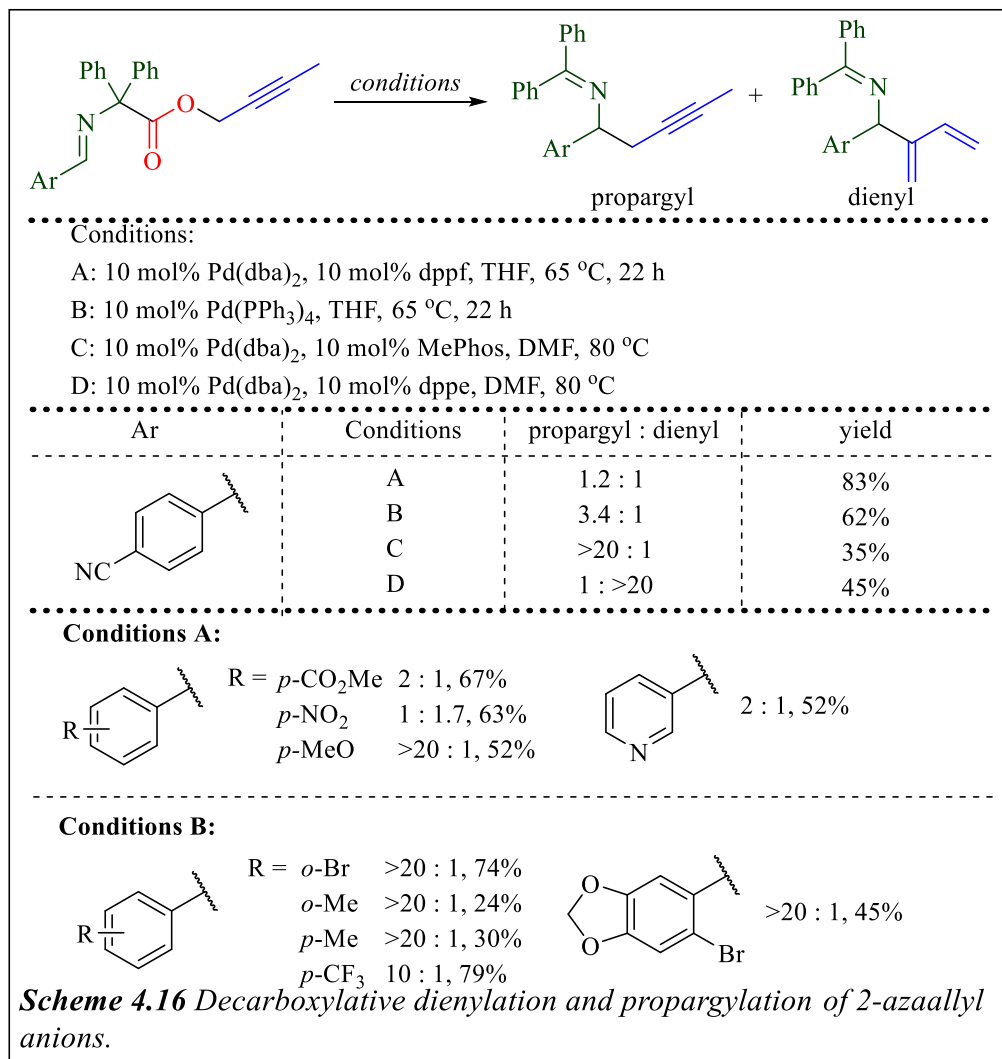
While this 2016 report from our lab was the first example of using a propargyl carbonate as a source for butadienyl electrophiles, other groups have developed their own versions of this reaction as well. In early 2019, Murakami and coworkers disclosed a protocol for the Ni-catalyzed decarboxylative 1,3-dienylation of aryl and alkyl alcohols with propargyl carbonates (Scheme

4.15).²⁹ They found that a diverse scope of *p*-substituted phenol starting compounds were well-suited for this reaction, including an array of halogens (**4.7c-g**), carbonyl (**4.7h-j**), and cyano (**4.7k**), and protected amine (**4.7l**). Furthermore, sterically congested *ortho*-substituted phenols were also successful under these reaction conditions (**4.7s-t**); however, as the steric bulk increased, there was a noticeable decrease in the yield of the reaction. While the dienylation of alkyl and silyl alcohols required five equivalents of the starting alcohols, the corresponding 1,3-dieneylated products could still be produced, albeit in only mild yields (**4.7v-y**).



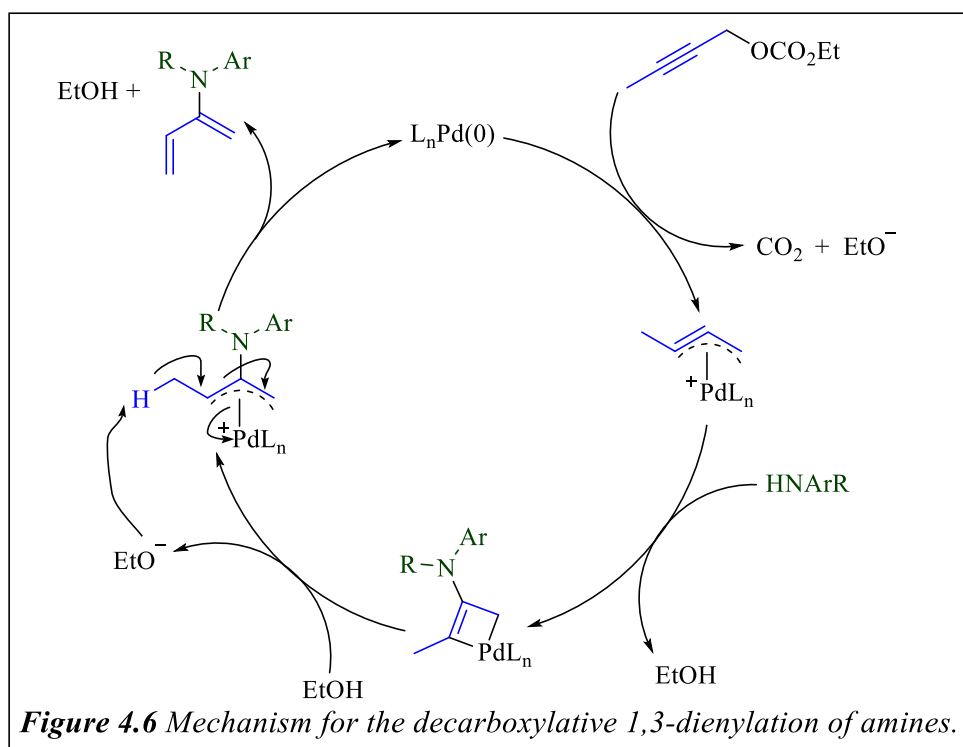
Almost simultaneously, Chroma and coworkers reported a palladium-catalyzed decarboxylative generation and propargylation of 2-azaallyl anions (Scheme 4.16).³⁰ They observed that the catalytic system employed greatly impacted the ratio of the propargyl and dienylation

products generated. While they developed conditions to favor the formation of the propargylated product, they also tested the conditions developed by the Tunge lab in 2016. They observed that same ligand-dependent selectivity as we did, with dppe favoring the formation of the dienyl product and MePhos favoring the formation of the propargyl product. However, despite the high selectivity, the yields using the Tunge conditions were quite low.



As previously discussed in chapter 2, O’Broin and Guiry disclosed an asymmetric decarboxylative propargylation of cyclic ketones, constructing quaternary propargylic stereocenters in high yields and enantioselectivities that same year (Scheme 4.17).³¹ O’Broin and

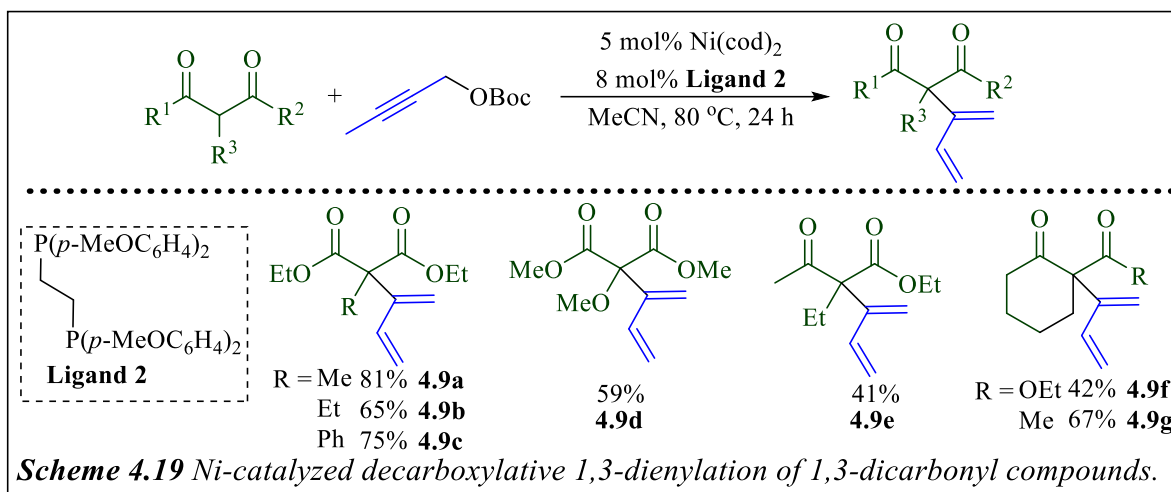
reaction could be used to successfully dienylate a range of indole derivatives of diverse electronic demand, although the yields were only mild to moderate, ranging from 35-68% (**4.8p-x**). Several heteroaromatic compounds (**4.8bb-cc**), carbazole (**4.8aa**), and a quinolinone derivative (**4.8dd**) were well suited for this reaction.



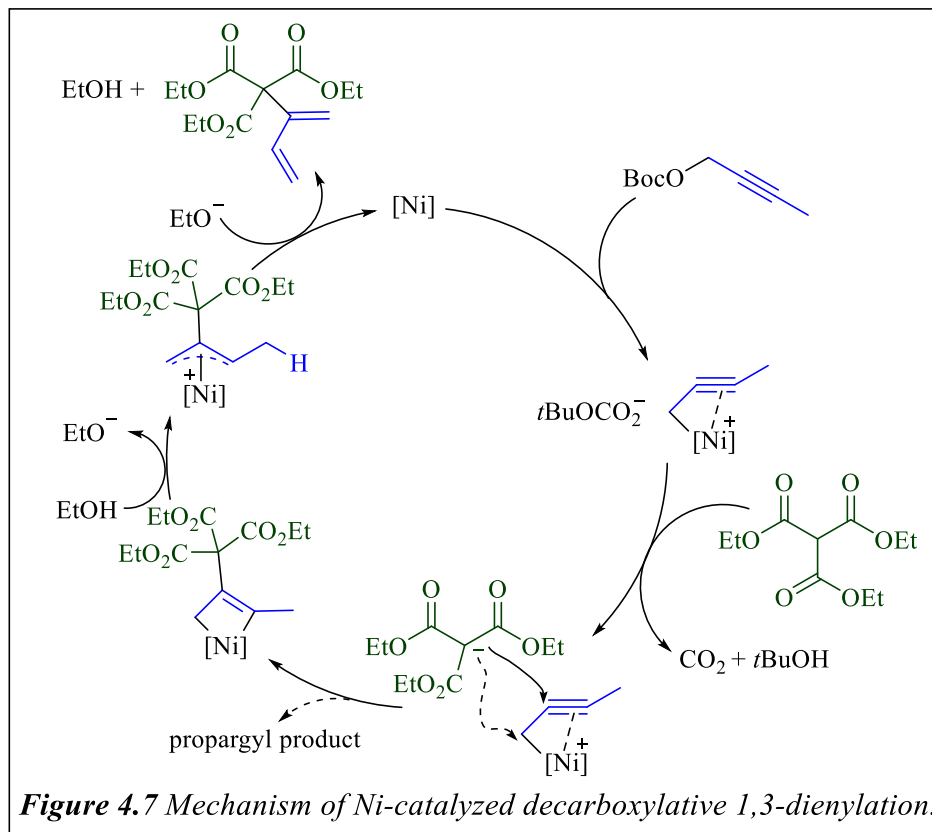
After several mechanistic tests, they proposed a mechanism for the decarboxylative dienylation of amines that was very similar to the one proposed by our group in 2016. Their proposed mechanistic pathway, illustrated in Figure 4.6, begins with oxidative addition of palladium to propargyl carbonate, which is followed by the release of CO_2 and ethoxide, generating a π -propargyl palladium intermediate. Subsequent nucleophilic attack of the amine at the central carbon leads to the formation of a palladacyclobutene intermediate that is protonated by ethanol to give a π -allyl palladium intermediate. Deprotonation of this intermediate would release the 1,3-diene product and re-generate the active catalyst. Their observations and subsequent mechanistic

insight give further support for our initial mechanism for the propargylation and dienylation of diaryl acetonitrile compounds.

In 2020, Murakami and coworkers updated their previous method for the dienylation of alcohols to allow for the nickel-catalyzed decarboxylative 1,3-dienylation of 1,3-dicarbonyl compounds with propargyl carbonates (Scheme 4.19).³³ Malonates containing an *alpha* alkyl (**4.9a-b**), phenyl (**4.9c**) or methoxy (**4.9d**) group were successfully dienylated under their reaction conditions. Further, both β -ketoesters (**4.9e**) and diketones (**4.9f-g**) were able to successfully deliver the corresponding dienylated 1,3-dicarbonyl compounds in mild to moderate yields.



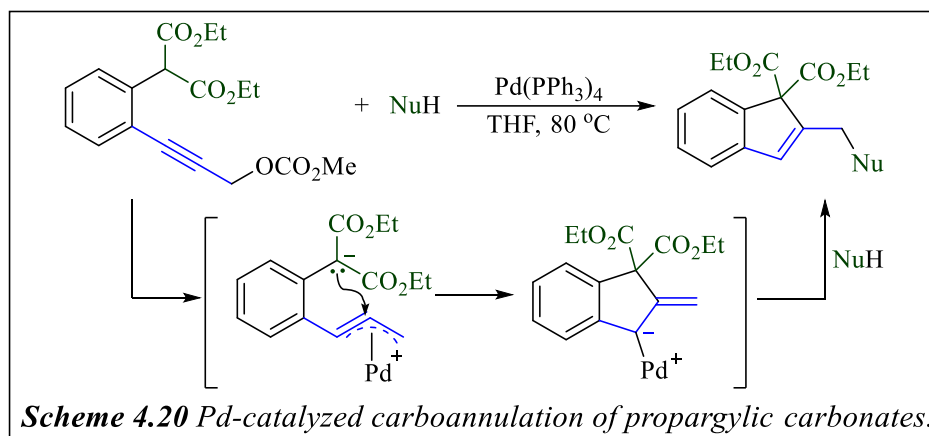
Murakami and coworkers also tested their dienylation of 1,3-dicarbonyl compounds utilizing the reaction conditions developed by our lab for the dienylation of diaryl acetonitrile compounds; however, with 1,3-dicarbonyl compounds the reaction led to a mixture of dienyl, propargyl, and dinucleophilic addition products, indicating that their catalytic system is more efficient and selective when reacting with dicarbonyl compounds. However, their proposed mechanistic pathway was still almost identical to that previously established in our laboratory, simply with nickel instead of palladium. Their proposed mechanism, illustrated in Figure 4.7, starts with the typical oxidative addition of nickel with the propargyl carbonate, followed by a release of carbon



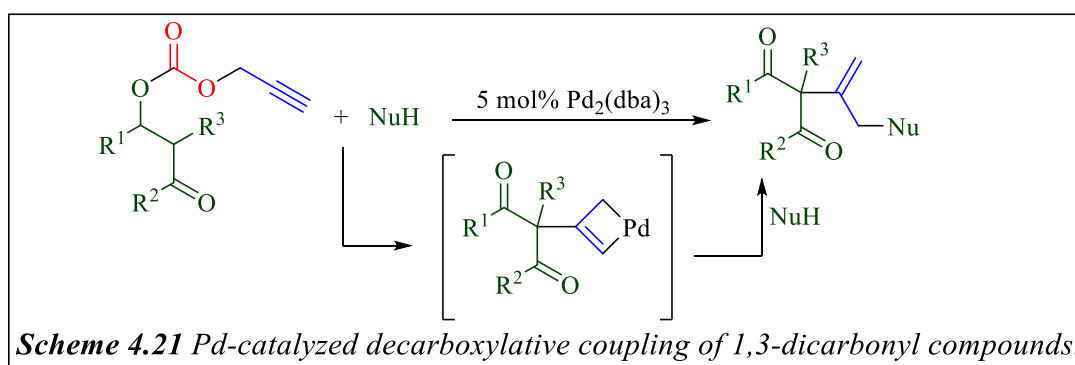
dioxide and nucleophilic attack from the malonate at the central carbon, generating a nickellacyclobutene intermediate. Attack at the internal carbon position would lead to the formation of the propargylated byproduct. Protonation of the nickellacyclobutene intermediate would form a π -allyl nickel intermediate, and subsequent deprotonation would release the dienylated product. While this method is quite promising, the report suffers from a relatively limited scope with only moderate yields. Furthermore, most of the reactions were contaminated with the formation of small amounts of propargyl byproduct. However, we believed that there was potential to develop a method that would allow for both a wider scope of products and higher reaction yields.

4.4 Development of Decarboxylative Propargylation and 1,3-Dienylation of 1,3-Dicarbonyl Compounds

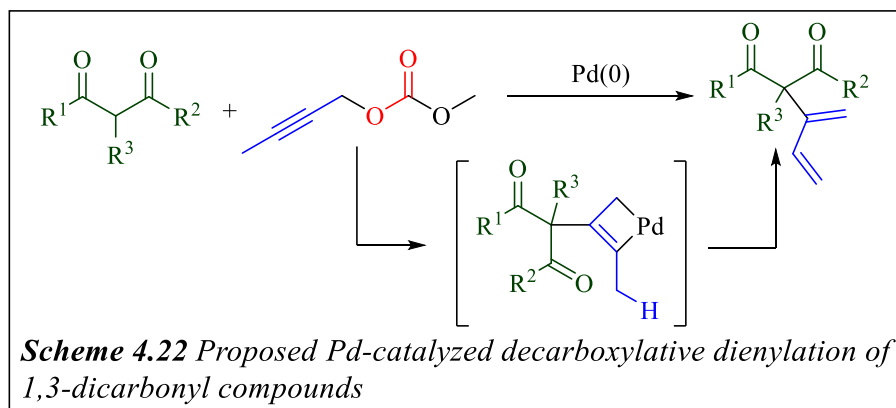
Compounds



In 2007, Liang and coworkers reported a synthesis of 2-substituted indenenes through a palladium-catalyzed carboannulation of propargylic carbonates (Scheme 4.20).³⁴ After oxidative addition of palladium into the propargyl carbonate and subsequent decarboxylation, the *in situ* generated malonate nucleophile attacked at the center position of the η^3 -propargyl palladium intermediate, forming the cyclized intermediate. Attack from a second nucleophile immediately followed, producing the 2-substituted indene product. Building off of this work in the 2010s, the Franckevičius group disclosed a series of reports on the decarboxylative alkenylation of 1,3-dicarbonyl compounds utilizing terminal propargyl carbonates coupled with carbon,³⁵ oxygen,³⁶ and nitrogen nucleophiles³⁷ (Scheme 4.21). Just as with the Liang protocol, their reactions started



with oxidative addition of palladium with the propargyl carbonate, generating an η^3 -propargyl palladium intermediate that is attacked at the center carbon position by the *in situ* generated enolate nucleophile, forming the palladacyclobutene intermediate. At this point, a second nucleophile attacks to generate the alkenylated product. We hoped that using an internal propargyl carbonate, we could develop conditions to favor elimination towards the dienylated product instead (Scheme 4.22).



With those previous examples in mind, we began our optimization experiments by examining the impact of the palladium source, ligand, and solvent on the decarboxylative cross-coupling of 1,3-dicarbonyl **4.10a** and methyl propargyl carbonate **4.11a** (Table 4.1). As Franckevičius and coworkers were able to achieve attack at the central position of a Pd-propargyl intermediate, our first optimization studies utilized their original conditions. NMR analysis of the sample reaction under the Franckevičius conditions indicated that both the dienyl propargyl products formed, albeit in a fairly low yield and selectivity (entry 1). We next analyzed the impact of the ligand on the reaction, starting with MePhos and dppe, which were successful in our ligand-dependent regioselective propargylation and dienylation of diaryl acetonitrile compounds (entries 3-4). Use monodentate ligand MePhos led to extremely low yields of both products (entry 3). Further, while

$\text{4.10a} + \text{4.11a} \xrightarrow[\text{Solvent}]{\text{Pd}^0 \text{ Source, Ligand, } 80 \text{ }^\circ\text{C, 2 h}}$

entry	Pd source	ligand	solvent	Dienyl ^b	Propargyl ^b
1	Pd ₂ (dba) ₃	DPEPhos	Dioxane	22%	27%
2	Pd ₂ (dba) ₃	MePhos	Dioxane	3%	5%
3	Pd ₂ (dba) ₃	dppe	Dioxane	29%	15%
4	Pd₂(dba)₃	dppb	Dioxane	49%	12%
5	Pd ₂ (dba) ₃ ^c	dppb	Dioxane	41%	17%
6	Pd ₂ (dba) ₃	dppb ^d	Dioxane	40%	15%
7	Pd(OAc) ₂	dppb	Dioxane	19%	trace
8	Pd(dmdba)₂	dppb	Dioxane	48% (47%)	12%
9	Pd(dmdba) ₂	XPhos	Dioxane	trace	trace
10	Pd(dmdba) ₂	dpp-benzene	Dioxane	16%	10%
11	Pd(dmdba) ₂	dppe	Dioxane	30%	12%
12	Pd(dmdba) ₂	dfppe	Dioxane	trace	trace
13	Pd(dmdba) ₂	dppb	MeOH	trace	trace
14	Pd(dmdba) ₂	dppb	Toluene	3%	4%

$\text{Ar} = 3,5\text{-OMe-C}_6\text{H}_3$

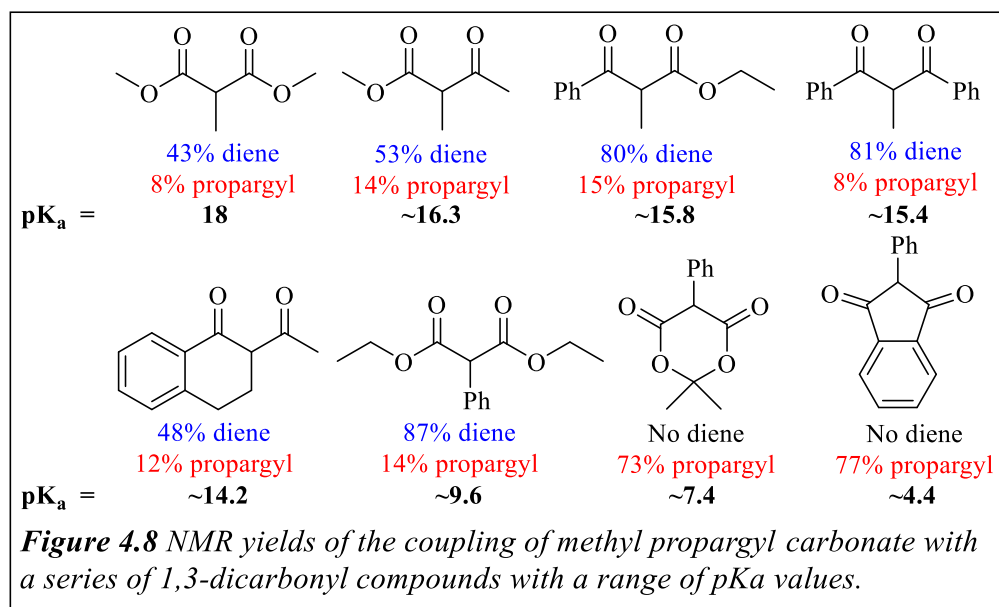
^a Reactions of diketone 4.10a (0.24 mmol), propargyl carbonate 4.12a (0.24 mmol), Pd/ligand (10 mol%), 1.6 mL solvent. ^b NMR yield (isolated yield in parentheses). ^c Pd₂(dba)₃ (10 mol %). ^d dppb (20 mol%).

Table 4.1 Optimization of reaction conditions for the dienylation of 1,3-dicarbonyl compounds.

the bidentate ligand dppe increased the selectivity of the reaction to better favor the formation of the dienyated product, the yield was still quite low (entry 4). While previous reports have shown that ligands with smaller bite angles tend to favor nucleophilic attack at the central carbon and those with larger bite angles typically attack at the terminal position,³⁸ the reports from the Franckevičius group showed that when using 1,3-dicarbonyl compounds they had better success with ligands with larger bite angles when selecting for attack at the central carbon position. Therefore, we attempted the reaction with dppb, a bidentate ligand with a larger bite angle than dppe, which led to a large increase in the yield of the dieny product to 49% (entry 4). Increasing the amount of catalyst or ligand caused the yield to slightly decrease without any further improvement of the selectivity (entries 5-6). When attempting to isolate compounds while optimizing the reaction conditions, we found that the dba ligands on the Pd₂(dba)₃ precatalyst had an extremely similar retention factor to that of the products, which made purification difficult. Switching from Pd₂(dba)₃ to Pd(dmdba)₂ allowed for much more facile isolation of the coupled products without a significant decrease in yield. After switching catalysts, we next examined a series of ligands; however, all led to a sharp decrease in product yield (entries 9-12). Further, switching to either a polar protic or non-polar solvent led to only trace amounts of either the dieny or propargyl products (entries 13-14).

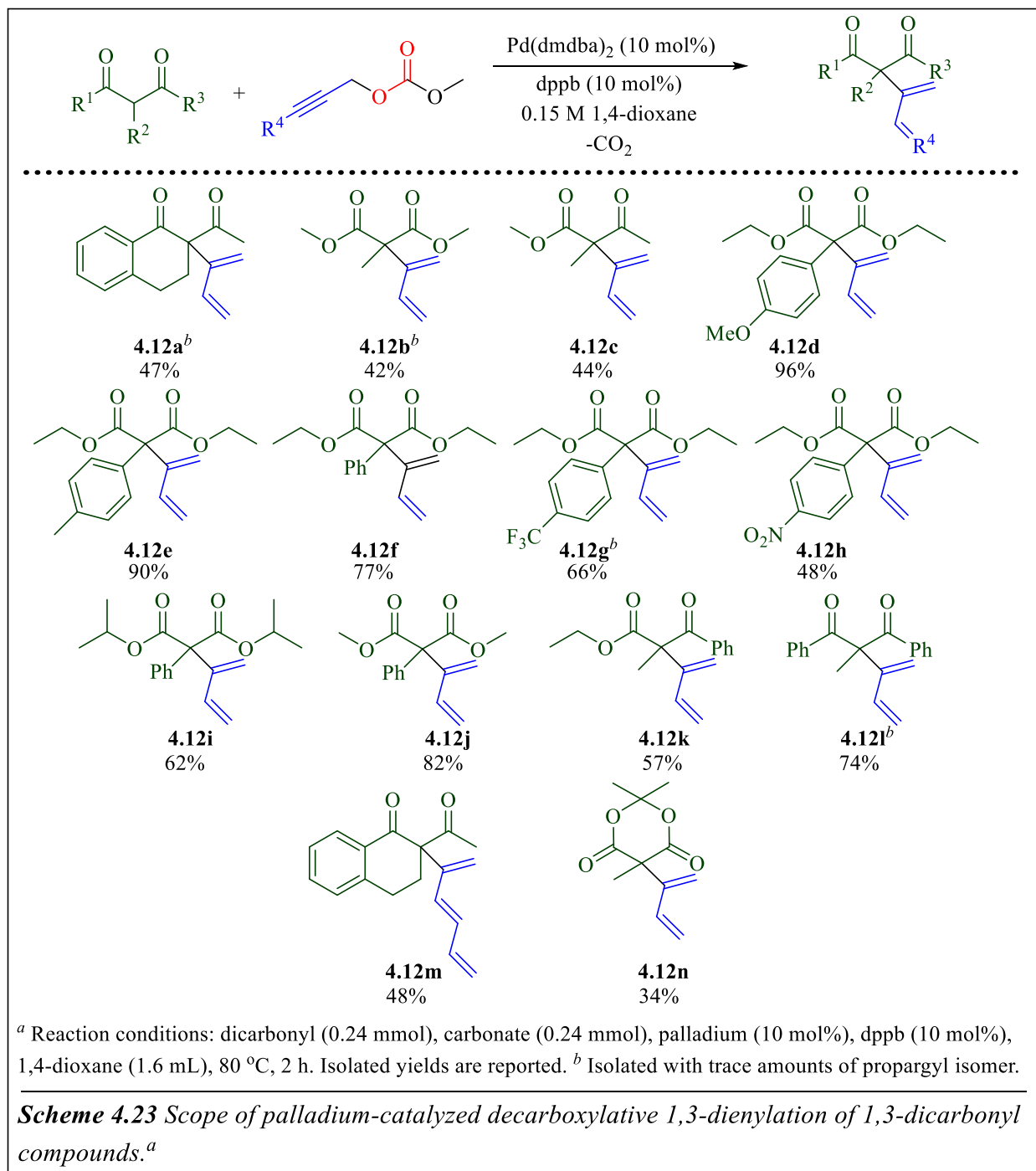
While the best developed conditions still only led to a fairly low yield, we decided to apply these conditions to a series of 1,3-dicarbonyl hoping that a change in substrate might lead to an improvement in the reaction yield. Interestingly, when 1,3-dicarbonyl compounds with a wide range of pK_a values were subjected to the reaction conditions, an interesting trend emerged that indicated that the reaction performance had a strong dependence on the pK_a value of the 1,3-dicarbonyl compound (Figure 4.8).³⁹ Starting with dimethyl methylmalonate, the yield of the

dienylated product was 43%, and the propargylated product had a yield of only 8%. Then, as the pK_a of the 1,3-dicarbonyl compound decreased, initially there was a large increase in the yield of the 1,3-dienyl product, with the yield of the propargyl product staying quite low, until the diene product yield peaked at 87% with diethyl phenylmalonate. After this point, the yield of the dienyl product began to decrease until the selectivity switched to exclusively favor the propargylated product at low pK_a values. Based on this trend, the optimal range pK_a for dienylation appears to be between 16 and 9, with yields sharply dropping at values much higher and selectivity switching towards the propargyl product at values much lower. Our original dicarbonyl **4.10a** and alpha-methyl methyl acetoacetate both reacted with low yields that fell outside of the overall trend. This observation is most likely due to a side decomposition of the starting dicarbonyl, possibly due to deacylation reaction.



With those observations in mind, we expanded our screening to include a larger range of 1,3-dicarbonyl compounds and successfully isolated a series of dienylated 1,3-dicarbonyl compound products in mild to high yields (Scheme 4.23). Various phenylmalonate compounds were tested and successfully provided the 1,3-dienylated products in moderate to high yields (**4.12d-j**). Sterics

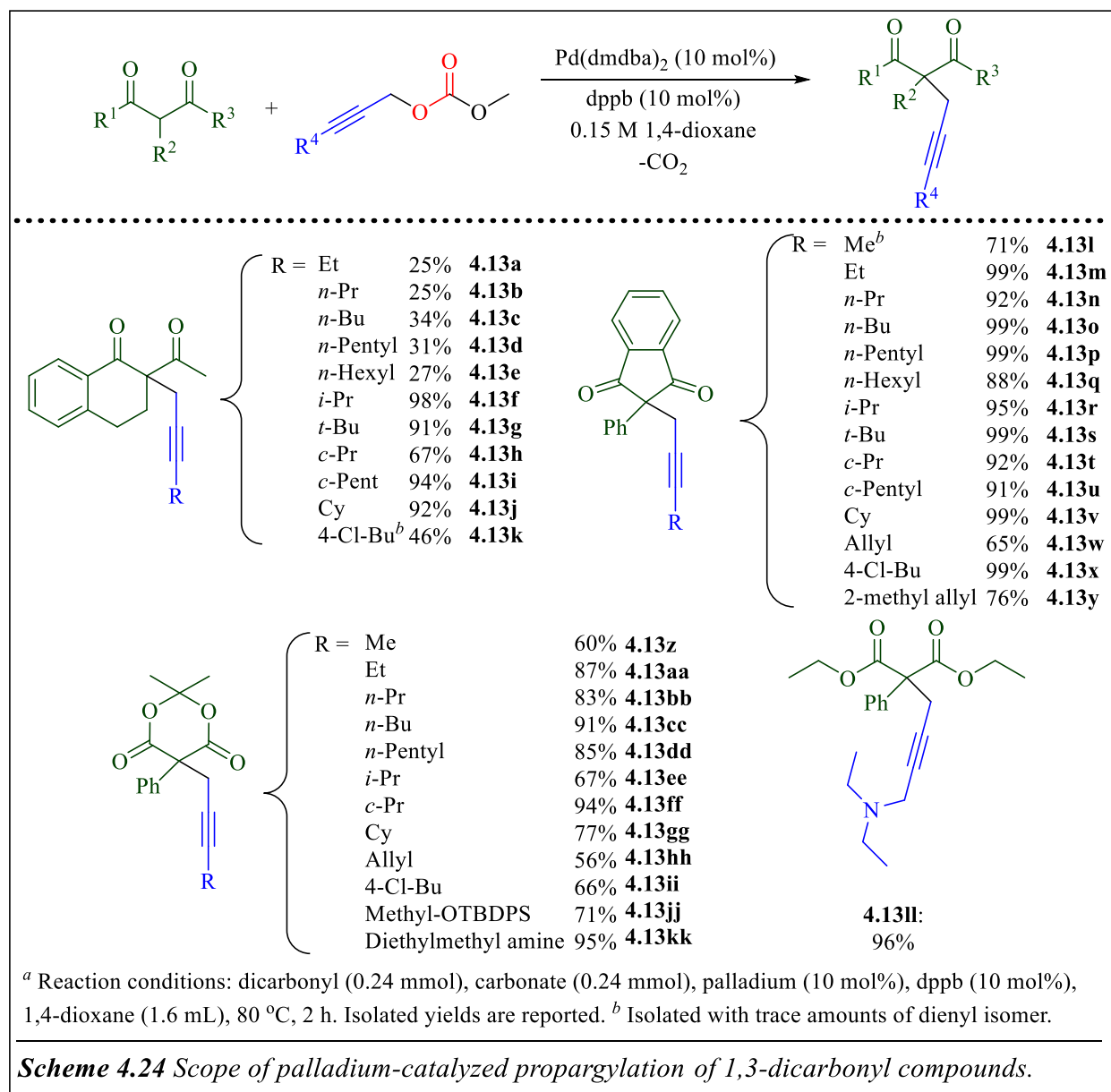
on the dicarbonyl compound seemed to have a slight impact in the yield of the reaction, as the dimethyl phenylmalonate (**4.12j**) led to a slightly higher yield than the diethyl phenylmalonate (**4.12f**), which had an even higher yield than the diisopropyl phenylmalonate (**4.12i**). However,



electronics appears to contribute to the reaction in a much more significant manner, as evident when comparing the yields of the various phenyl-substituted dicarbonyl compounds to those of the methyl-substituted dicarbonyl compounds. Dicarbonyl compounds with an α -methyl group (**4.12b-c,k-l,n**) led to a diminished yield of the dienylated product as compared to the phenyl-substituted dicarbonyl compounds. Furthermore, changing the substituents at the *para* position of diethyl phenylmalonate greatly impacted the yield of the reaction. Compounds with an electron-donating methyl- (**4.12e**) or methoxy- (**4.12d**) substituent provided the corresponding 1,3-dienylated product in yields significantly higher than that of the reaction with unsubstituted diethyl phenylmalonate (**4.12f**). In contrast, compounds with an electron-withdrawing group, such as a trifluoromethyl- (**4.12g**) or nitro- (**4.12h**) substituent at the *para* position, caused the yield of the reaction to decrease substantially. For the optimization of a dienylation reaction in this system, there seems to be a precise balance between the need to lower the pK_a of the dicarbonyl enough to enable adequate formation of the enolate with the necessary nucleophilicity of the formed enolate to enable the necessary nucleophilic attack. As the stability of the generated enolate increases, the nucleophilic attack becomes increasingly reversible, which allows for the selectivity of the reaction to switch from the dienylated product

The sterics surrounding the propargyl carbonate played a large role in the overall performance of the reaction. When the terminal position on the propargyl carbonate is an alkyl chain consisting of two or more carbon atoms, the selectivity of the reaction is reversed, favoring the propargyl product, even with 1,3-dicarbonyl compounds with higher pK_a values. In many of the previously reported dienylation reactions that utilize propargyl carbonates, including our protocol for the 1,3-dienylation of diaryl acetonitrile compounds, the proposed mechanisms for the formation of the dienylated products includes a deprotonation at the position corresponding to the terminal

propargylic carbon. Therefore, it would logically follow that steric hinderance at this position would negatively impact the yield of the dienylated product. However, when the propargyl carbonate is substituted at the terminal position with an allylic group, formation of the dienylated product creates an extended conjugated triene. The resonance stabilization of the formation of this triene system can overcome the steric hinderance, reverting the selectivity of the reaction back to the dienyl product (**4.12m**).



We then moved on to explore the scope of the propargylation reaction with several 1,3-dicarbonyl compounds (Scheme 4.24). We were able to react the original dicarbonyl **4.10a** with a range of propargyl carbonates, generating the propargylated 1,3-dicarbonyl compound in mild to high yields. While a propargyl carbonate with a terminal alkyl chain substituent (**4.13a-e**) led to the propargyl products in fairly low yields, propargyl carbonates that were di- and trisubstituted at the terminal position (**4.13f-j**) led to the propargylated products in moderate to high yields, with most being over 90%. Cyclic dicarbonyl compounds, which have much lower pK_a values, reacted with mono-, di-, and trialkyl terminally substituted propargyl carbonates, furnishing the corresponding propargyl products in moderate to high yields (**4.13l-v,z-gg**). While the reaction between dicarbonyl **4.10a** and an allyl substituted propargyl carbonate led to the majority formation of the dienyl product (**4.12m**), when the pK_a of the dicarbonyl was much lower, the propargyl product was still favored in moderate yield (**4.13w,y,hh**). The propargylation reaction tolerated propargyl carbonates substituted with 4-chlorobutyl (**4.13k,x,ii**) with moderate to high yields. The reaction was also successful when reacted with a propargyl carbonate containing an -OTBS protected alcohol (**4.13jj**) or diethylamine (**4.13kk-ll**), forming the propargylated 1,3-dicarbonyl products in moderate to high yields.

We next sought to determine the mechanistic pathways of both the 1,3-dienylation and the propargylation reactions. Just as with our past experiments with the dienylation of diaryl acetonitrile pronucleophiles, we believed that this dienylation could occur via two potential reaction pathways, which are shown in Figure 4.9. First, oxidative addition of palladium into the propargyl carbonate would generate an η^3 -propargyl palladium intermediate **A** and a carboxylate anion. This carboxylate anion would undergo decarboxylation, forming a methoxide anion, which would deprotonate the dicarbonyl compound to generate the enolate nucleophile. Nucleophilic attack

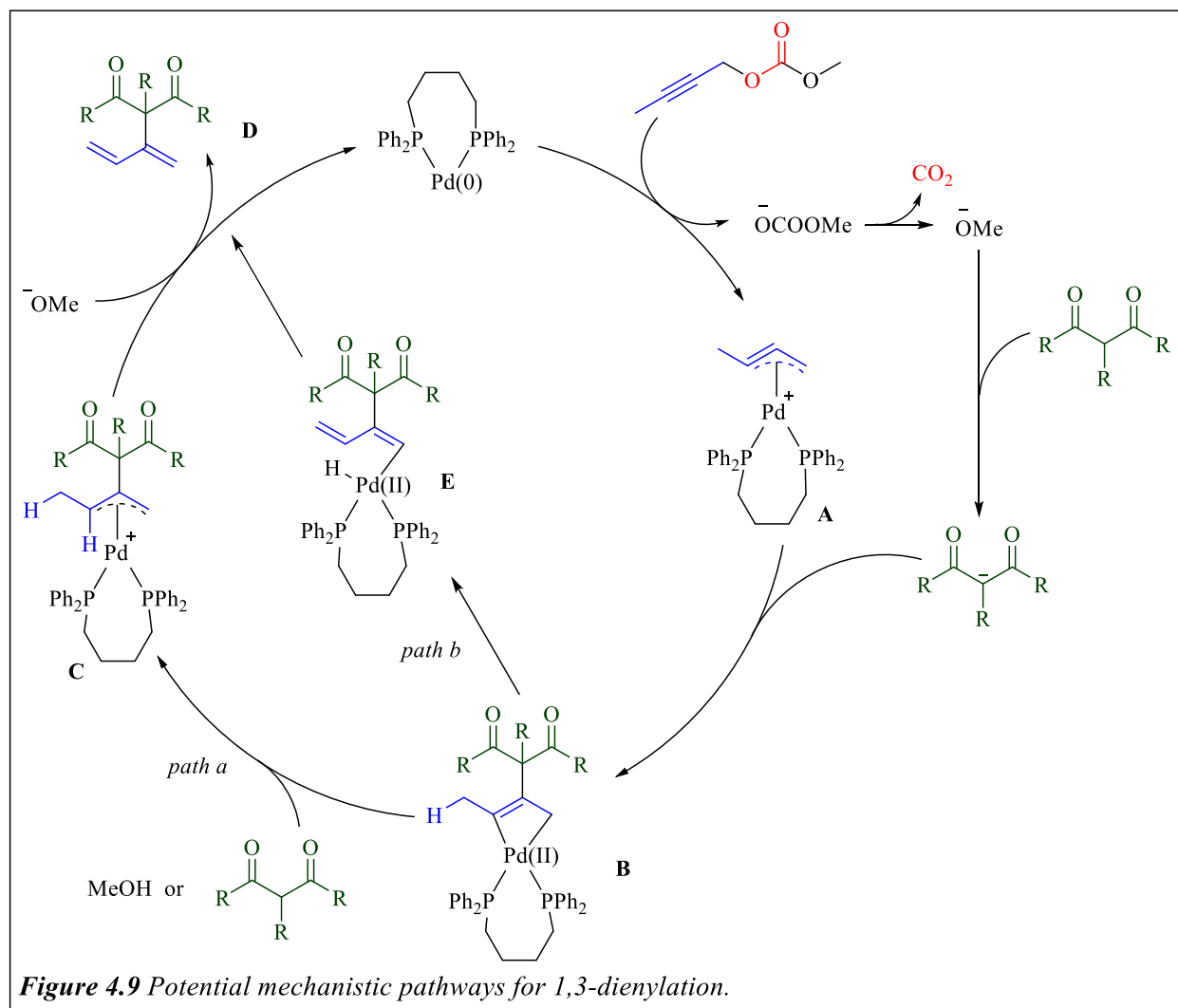
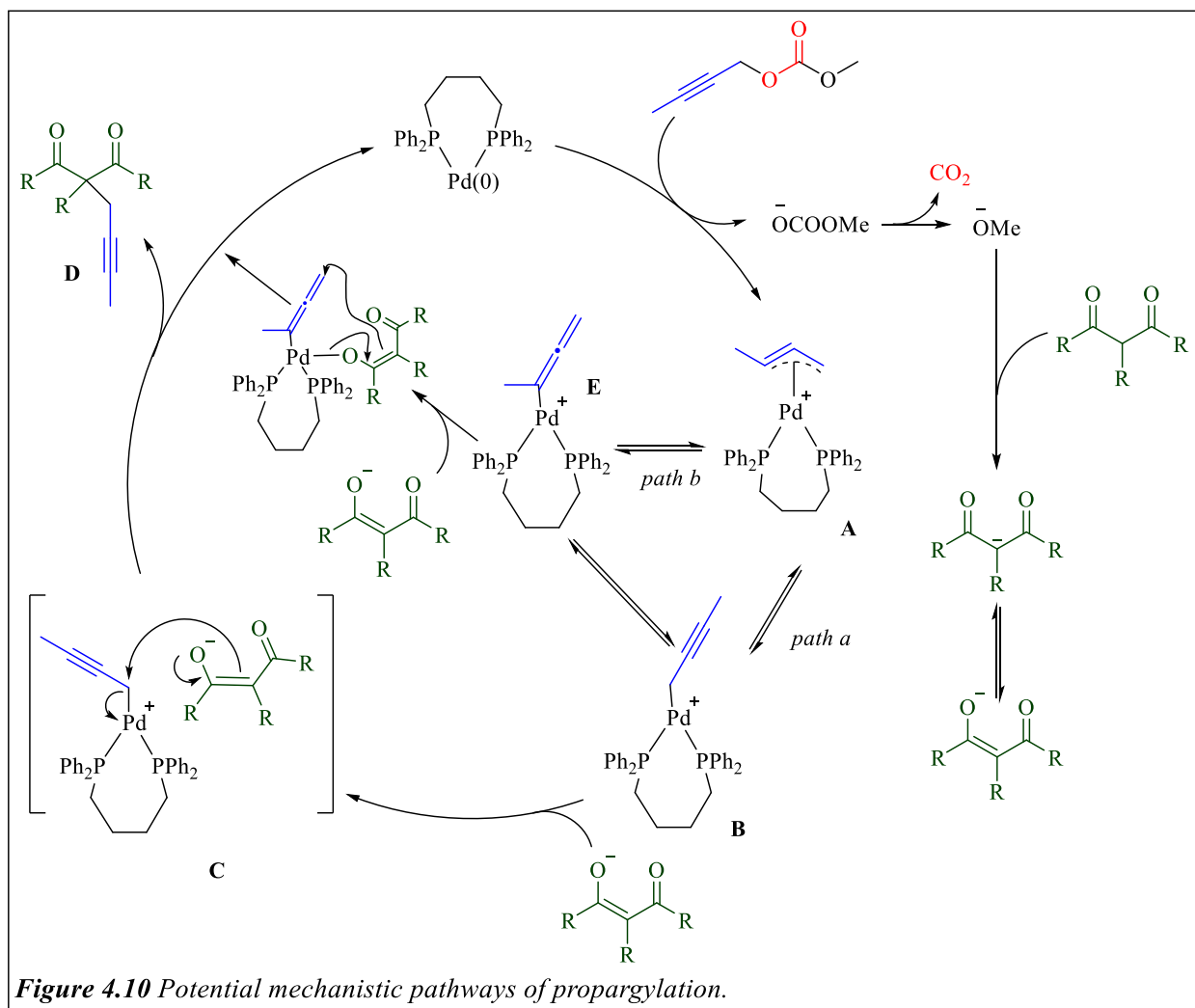


Figure 4.9 Potential mechanistic pathways for 1,3-dienylation.

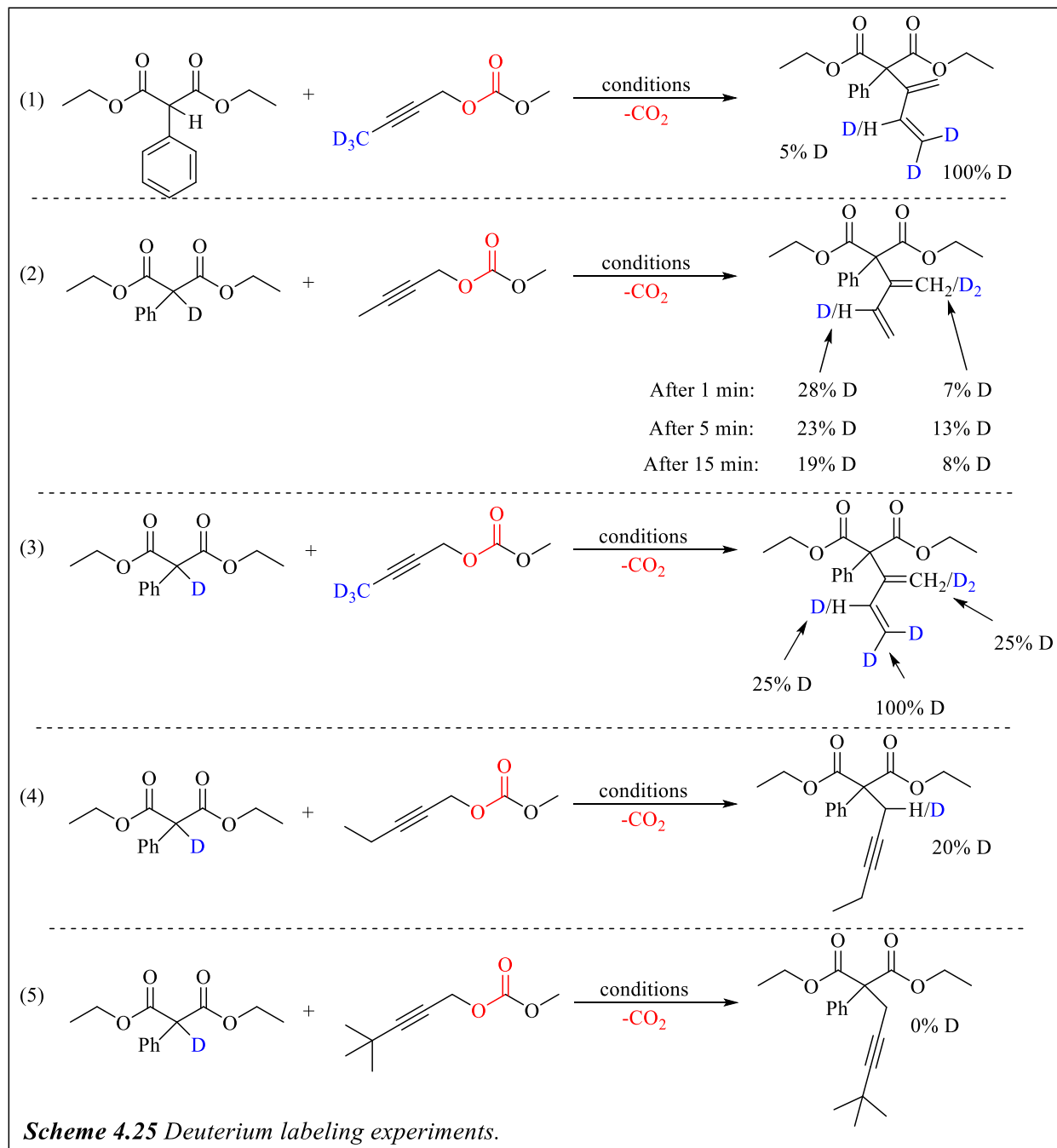
from this enolate on intermediate **A** would occur through an outer-sphere attack at the center carbon of the η³-propargyl palladium complex, forming palladacyclobutene **B**. At this point, the two proposed mechanistic pathways diverge. With *path a*, palladacyclobutene **B** would undergo protonation, either from another molecule of dicarbonyl starting material or methanol, forming π-allyl palladium intermediate **C**. Elimination of a hydrogen from this intermediate with methoxide anion would produce the dienyl product **D** and regenerate the active Pd(0) catalyst. However, if the mechanism follows *path b*, formation of palladacyclobutene **B** would be followed by β-hydride

elimination and reductive elimination, which would also release the same dienylated product and turnover the catalyst.

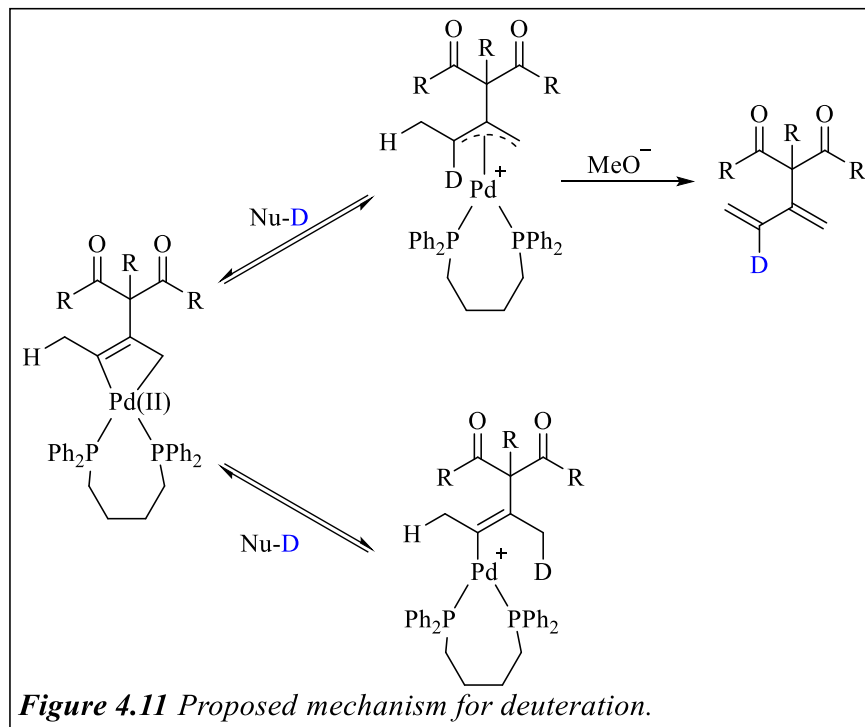


Regarding the mechanism of the propargylation of the 1,3-dicarbonyl compounds, we believed there were two possible pathways as well (Figure 4.10.) The initial oxidative addition of the propargyl carbonate with palladium would be the same as with the 1,3-dienylation mechanism, generating an η^3 -propargyl palladium intermediate and a carboxylate anion, which would undergo decarboxylation leaving behind a methoxide anion that can deprotonate the 1,3-dicarbonyl compound. The original η^3 -propargyl palladium intermediate **A** is in equilibrium with either an η^1 -propargyl palladium intermediate **B**, labeled *path a*, or an η^1 -allenyl palladium intermediate **E**,

labeled *path b*. From intermediate **B**, the enolate nucleophile would undergo an outer-sphere attack at the internal propargylic carbon, producing the propargylated product and regenerating the active palladium catalyst. In *path b*, the enolate would instead attack the η^1 -allenyl palladium intermediate **E** at the terminal position, possibly by first coordinating with the catalyst, forming the propargylated product via an inner-sphere nucleophilic attack.



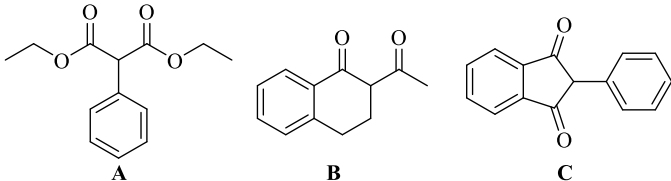
To differentiate between the two pathways for dienylation, we ran a series of deuterium labeling experiments (Scheme 4.25). First, a terminally deuterated propargyl carbonate was reacted with diethyl phenyl malonate under our usual reaction conditions (Scheme 4.25, equation 1). If the mechanism followed *path b*, we would expect to see 100% and 50% deuterium at the C4 and C1 positions of the diene, respectively. However, while there was 100% deuterium at the C4 position, there was no deuterium detected at the C1 terminal position and trace amounts of deuterium at the internal C3 position of the diene. A second deuterium labeling experiment reacted deuterated diethyl phenylmalonate with non-deuterated propargyl carbonate (Scheme 4.25, equation 2). If the reaction favors *path b*, we would expect to see no incorporation of deuterium into the 1,3-dienylated product. However, after one minute of reaction, there was noticeable deuteration at both the terminal C1 and internal C3 positions. Over time, the amount of deuterium incorporated at the C3 position steadily declined, while the amount of deuterium at the terminal C1 position first slightly increased and then began to decline. While these results are inconsistent with the *path b* mechanism, they are consistent with the protonation and deprotonation mechanism of *path a*. To further confirm these observations, we ran a third deuterium labeling experiment with both a deuterated diethyl phenyl malonate and a terminally deuterated propargyl carbonate (Scheme 4.25, equation 3). This reaction also showed incorporation of deuterium at both the terminal C1 and internal C3 position of the formed diene, providing more evidence for the protonation/deprotonation mechanism of dienylation. To explain the incorporation of deuterium at both the C1 and C3 positions, we propose the mechanism depicted in Figure 4.11. From the palladacyclobutene intermediate that was generated from nucleophilic attack the central carbon of the η^3 -propargyl palladium complex, a reversible protonation can occur at either the C1 or C3



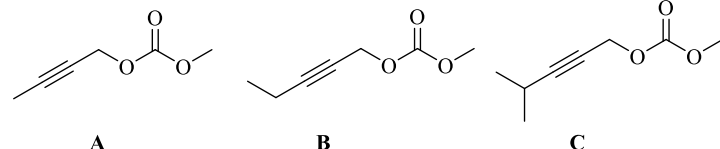
positions. Protonation at the C3 position would be followed by deprotonation at the terminal C4 position, leading to the 1,3-dienylated product. However, protonation at the C1 position would be unable to move forward, but deprotonation at the C1 position would reform the palladacyclobutene intermediate that could then undergo protonation at the C3 position. To further probe this proposed mechanism of deuteration, we two more deuterium labeling experiments between diethyl phenylmalonate and ethyl propargyl carbonate (Scheme 4.25, equation 4) and *t*-butyl propargyl carbonate (Scheme 4.25 equation 5), which both favor formation of the propargylated product. We saw that the reaction with ethyl propargyl carbonate led to incorporation of deuterium at the internal propargyl position. In contrast, the reaction with *t*-butyl propargyl carbonate did not see any incorporation of deuterium into the propargyl product. As the additional sterics at the terminal position of the *t*-butyl propargyl carbonate would prevent nucleophilic attack at the central position of the η^3 -propargyl palladium intermediate, the subsequent protonation of the palladacyclobutene

would not be able to occur. Therefore, these observations further support the hypothesis that deuteration occurs through a reversible protonation of the C1 position.

1,3-Dicarbonyl compounds:



Propargyl carbonates:



Standard Conditions^a → Dienyl Product and/or Propargyl Product

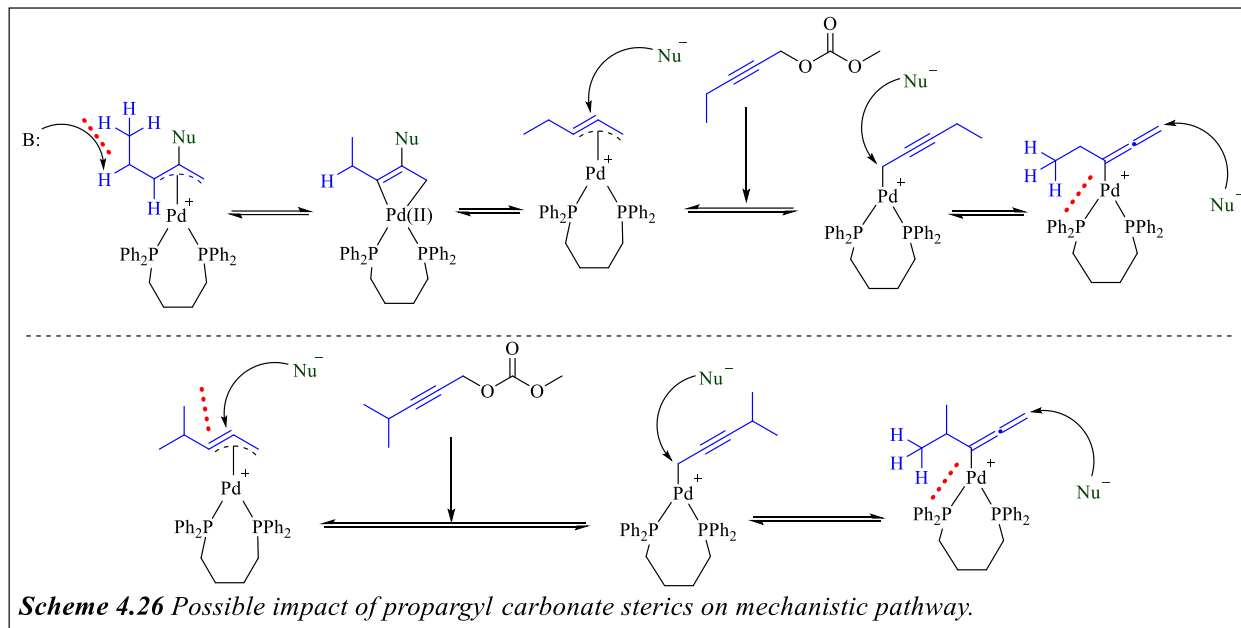
Dicarbonyl	Propargyl carbonate	10 minutes	15 minutes	30 minutes	45 minutes	1 hour
A	A	62% dienyl	77% dienyl 15% propargyl	87% dienyl 13% propargyl	86% dienyl 14% propargyl	87% dienyl 13% propargyl
	B	29% dienyl 69% propargyl	29% dienyl 70% propargyl	complete		
	C	100% propargyl	complete			
B	A	26% dienyl	36% dienyl	35% dienyl	40% dienyl	50% dienyl 14% propargyl
	B	4% dienyl 16% propargyl	6% dienyl 28% propargyl	9% dienyl 28% propargyl	12% dienyl 32% propargyl	12% dienyl 43% propargyl
	C	100% propargyl	complete			
C	A	1% dienyl 8% propargyl	2% dienyl 15% propargyl	2% dienyl 25% propargyl	2% dienyl 50% propargyl	3% dienyl 61% propargyl
	B	85% propargyl	85% propargyl	100% propargyl	complete	
	C	100% propargyl	complete			

^a Reaction conditions: dicarbonyl (0.24 mmol), carbonate (0.24 mmol), palladium (10 mol%), dppb (10 mol%), 1,4-dioxane (1.6 mL), 80 °C, 2 h. NMR yields are reported.

Table 4.2 Timed experiments of various 1,3-dicarbonyl compounds with propargyl carbonates with increasing steric bulk.

To further probe the mechanism of both the dienylation propargylation pathways, we conducted a series of timed reactions, the results of which are shown in Table 4.2. With methyl propargyl carbonate, the reactions proceeded much more slowly, taking far longer to reach

completion as compared to the bulkier propargyl carbonates. As the steric bulk on the terminal position of the propargyl carbonate grew, the reaction rate increased, as did the selectivity for the propargylated product. Since propargyl carbonates with bulky terminal groups favor formation of the propargyl product, this indicates that the reactive intermediate of propargylation is most likely the η^1 -propargyl palladium species (Scheme 4.26). The η^1 -allenyl palladium intermediate would

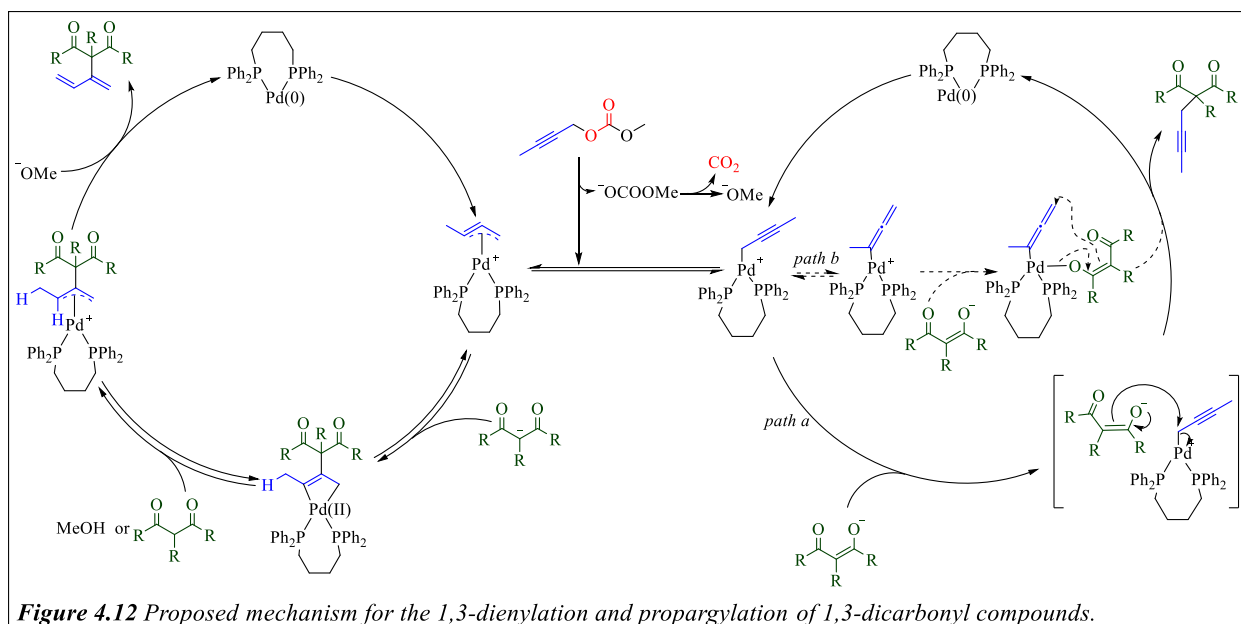


require coordination of palladium to the internal allenyl position, which would force it into close proximity with substituents. Additionally, the slower reaction times of the methyl propargyl carbonates, as compared to propargyl carbonates with bulkier terminal substituents, suggests the reaction first progresses through the dienylation pathway. However, when the carbonate is substituted with a group larger than a methyl at the terminal position, the final deprotonation is sterically hindered, forcing the reaction to reverse back to the initial η^3 -propargyl palladium intermediate that can then rearrange into either the η^1 -propargyl palladium intermediate or the η^1 -allenyl palladium intermediate. As the sterics of the group at this terminal position grows, the initial attack at the central carbon of the η^3 -propargyl palladium intermediate becomes increasingly

sterically hindered, giving the intermediate time to rearrange to either the η^1 -allenyl or propargyl intermediate. As the substrate would not first go through the dienyl pathway, the reaction would progress much faster, leading to the propargyl product in much less time, which is exactly what was observed with the timed experiments.

Previous reports have shown that anionic nucleophiles favor binding to an η^1 -allenyl species,⁴⁰ which would mean the bound enol would then undergo an inner-sphere nucleophilic attack at the terminal position of the allenyl complex. However, it has been shown previously that bidentate ligands tend to favor outer-sphere nucleophilic processes.²⁸ While at this point we are unable to determine with absolute certainty which route is most favored in propargylation, the impact of sterics on the propargyl carbonate does seem to favor *path a* as the more likely mechanistic pathway for the formation of the propargylated product. Further, dicarbonyl compounds with lower pK_a values would provide highly stabilized enolates that would be able to survive in solution long enough for the η^3 -propargyl palladium intermediate to rearrange, which would account for the selectivity differences between higher and lower pK_a dicarbonyl compounds. In addition, the higher stability of the *in-situ* generated enolates of the dicarbonyl compounds with lower pK_a values would increase the reversibility of the nucleophilic attack, which could improve the yield of the propargylated product.

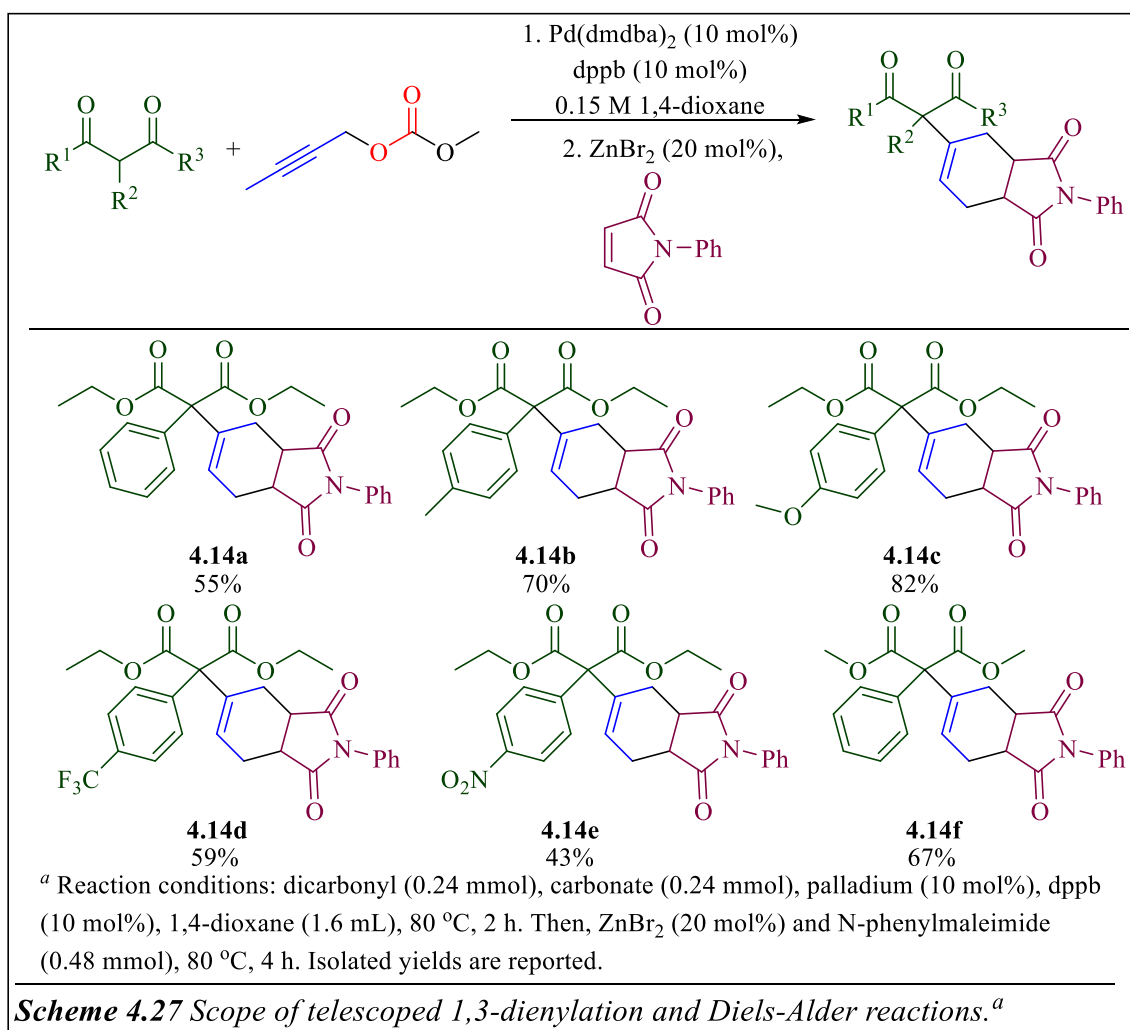
These observations, along with the results of our deuterium labeling experiments, we allowed us to propose the following mechanistic pathways for 1,3-dienylation and propargylation of 1,3-dicarbonyl compounds (Figure 4.12). With both dienylation and propargylation, initial oxidative addition of the propargylic carbonate and subsequent loss of CO_2 would generate an η^3 -propargyl palladium intermediate and a methoxide anion that will deprotonate the 1,3-dicarbonyl compound to form the enolate nucleophile. Nucleophilic attack from the enolate onto the η^3 -propargyl



palladium intermediate would occur exclusively at the central carbon, forming a palladacyclobutene intermediate. Protonation from either another 1,3-dicarbonyl molecule or methanol would generate a π -allyl complex, and subsequent deprotonation would release the diene product and regenerate the active Pd(0) catalyst. However, when the sterics at the terminal position are larger than methyl, deprotonation is too sterically hindered, forcing the reaction to reverse back through to the initial η^3 -propargyl palladium intermediate. Additionally, if the sterics at the terminal position are larger than a single alkyl chain, the initial attack at the central carbon would be too sterically cumbersome to occur. At this point, the η^3 -propargyl palladium complex would rearrange to either a η^1 -propargyl or allenyl intermediate. From the η^1 -propargyl palladium complex, nucleophilic attack from the *in situ* generated enolate would occur at the internal propargyl carbon, releasing the propargyl product. On the other hand, from the η^1 -allenyl complex, the enolate would coordinate with palladium, and attack at the terminal position of the allenyl intermediate through an inner-sphere process, generating the same propargylated product. While

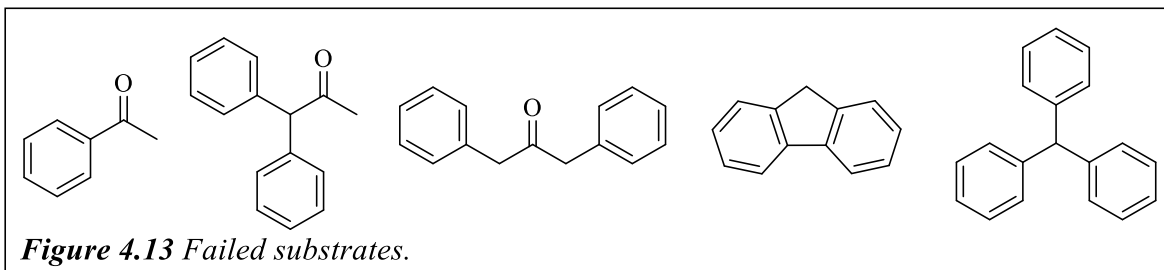
we are unable to determine which of these propargylation routes is correct, the observations from the timed experiments favor *path a*.

To further test the utility of this reaction, we attempted a Diels-Alder reaction on some of our generated 1,3-dienylated products (Scheme 4.27). We reacted several phenylmalonate compounds with methyl propargyl carbonate under our optimized reaction conditions. After diene formation, 2 equivalents of *N*-phenylmaleimide and 20 mol% ZnBr₂ were added to the crude reaction mixture. We were pleased to find that through this telescoped reaction method, we were able to generate several Diels-Alder products in mild to high yields over two steps (**4.14a-f**).



4.5 Development of Decarboxylative Propargylation and 1,3-Dienylation of Benzoyl Acetonitrile

Derivatives



After developing our decarboxylative 1,3-dienylation and propargylation of 1,3-dicarbonyl compounds, we attempted to expand this reaction to other substrate classes. Our initial attempts towards the 1,3-dienylation or propargylation of compounds with much higher pK_a values than our previous reports were unsuccessful (Figure 4.13). These substrates were typically entirely unreactive in our reaction conditions, so we decided to focus our attentions towards substrates with pK_a values closer to our successful examples, starting with a benzoyl acetonitrile derivative with an alpha benzyl substituent (**4.15a**). Gratifyingly, when we reacted compound **4.15a** with methyl propargyl carbonate **4.11a** under the conditions we optimized for the reaction with 1,3-dicarbonyl compounds, we saw selective formation of the dienylated product in a moderate yield of 73% (Table 4.3, entry 1). Attempting the reaction with other ligands and solvents led to significant decreases in the yield of the reaction (entries 2-13). Further, the only condition that led to any formation of the propargyl product only formed it in a 15% yield with a significant amount of the dienylated product formed as well. Therefore, we decided to use the original conditions when developing the reaction scope.

With the optimized reaction conditions in hand, we reacted the benzoyl acetonitrile **4.15a** with a series of propargyl carbonate compounds that had been successful in our reactions with 1,3-

dicarbonyl compounds (Scheme 4.28). With the reactions with 1,3-dicarbonyl compounds, we observed that having substituents larger than a methyl at the terminal position of the propargyl carbonate led to exclusive formation of the propargyl product, apart from allyl substituents that allowed for the formation of triene products. We saw a similar observation with the reaction with benzoyl acetonitrile derivatives, with methyl and allyl substituted propargyl carbonates forming

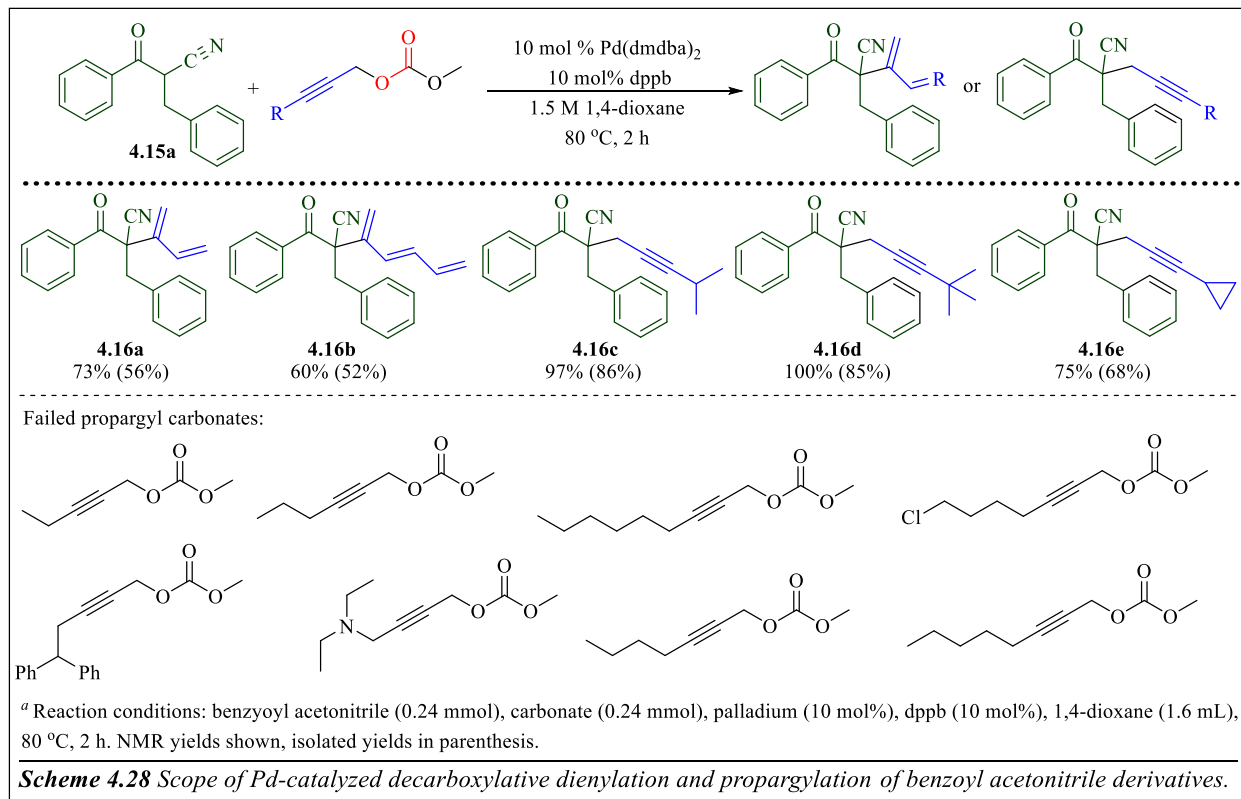
Reaction scheme: 4.15a + 4.11a $\xrightarrow[\text{Solvent}]{\text{Pd}^0 \text{ Source, Ligand, } 80^\circ\text{C, 2 h}}$ Dienyl or Propargyl

entry	Pd source	ligand	solvent	Dienyl ^b	Propargyl ^b
1	Pd(dmdba)₂	dppb	dioxane	73%	-
2	Pd(dmdba) ₂	MePhos	dioxane	8%	-
3	Pd ₂ (dba) ₃	dppe	DMF	-	-
4	Pd(dmdba) ₂	dppe	dioxane	48%	-
5	Pd(dmdba) ₂	dppb	toluene	37%	-
6	Pd(dmdba) ₂	dppb	THF	27%	-
7	Pd(dmdba) ₂	dppb	pentane	16%	-
8	Pd(dmdba) ₂	dppb	DMSO	24%	-
9	Pd(dmdba) ₂	dppe	dioxane	54%	-
10	Pd(dmdba) ₂	dppp	dioxane	57%	-
11	Pd(dmdba) ₂	DPEPhos	dioxane	43%	15%
12	Pd(dmdba) ₂	DavePhos	dioxane	26%	-
13	Pd(dmdba) ₂	<i>t</i> Bu-Davephos	dioxane	3%	-

^a Reactions of benzyol acetonitrile 4.15a (0.24 mmol), propargyl carbonate 4.16a (0.24 mmol), Pd/ligand (10 mol%), 1.6 mL solvent. ^b NMR yield (isolated yield in parentheses).

Table 4.3 Optimization of reaction conditions for the dienylation and propargylation of benzyol acetonitrile derivatives.

the corresponding diene (**4.16a**) and triene (**4.16b**) product, and di- and trisubstituted propargyl carbonates exclusively forming the propargylated products (**4.16c-d**). However, while propargyl carbonates that were monosubstituted at the terminal position led to the generation of the propargylated product when reacted with 1,3-dicarbonyl compounds, they failed to react with compound **4.15a** entirely, even when the reaction temperature was increased to 120 °C.



We next attempted the reaction with a benzoyl acetonitrile derivative with an alpha phenyl substituent, and, under the previous conditions the yield of the diene was fairly low. As this substrate contained a similar benzyl cyanide moiety as the diaryl acetonitrile compounds from our previously developed dienylation and propargylation report, we thought that conditions closer to those used previously might get better results. Therefore, we decided to re-optimize the reaction conditions to see if we would get better results when reacting benzoyl acetonitrile derivative **4.17a**

with the original methyl propargyl carbonate (Table 4.4). When we tested the reaction using the ligands that were successful with our ligand-dependent propargylation and 1,3-dienylation of

Reaction scheme: $\text{Ph-CO-CH(Ph)-CN} + \text{4.11a} \xrightarrow[\text{Solvent}]{\text{Pd}^0 \text{ Source, Ligand, } 80^\circ\text{C, 2 h}}$ Dienyl or Propargyl

entry	Pd source	ligand	solvent	Dienyl ^b	Propargyl ^b
1	Pd(dmdba) ₂	dppb	dioxane	47%	-
2	Pd(dmdba) ₂	MePhos	dioxane	2%	45%
3	Pd(dmdba)₂	dppe	dioxane	65%	-
4	Pd(dmdba)₂	<i>t</i>Bu-DavePhos	dioxane	-	54%
5	Pd(dmdba)	DPEPhos	dioxane	34%	30%
6	Pd(dmdba) ₂	XPhos	dioxane	14%	30%
7	Pd(dmdba) ₂	dppp	dioxane	44%	-
8	Pd(dmdba) ₂	DavePhos	dioxane	20%	43%

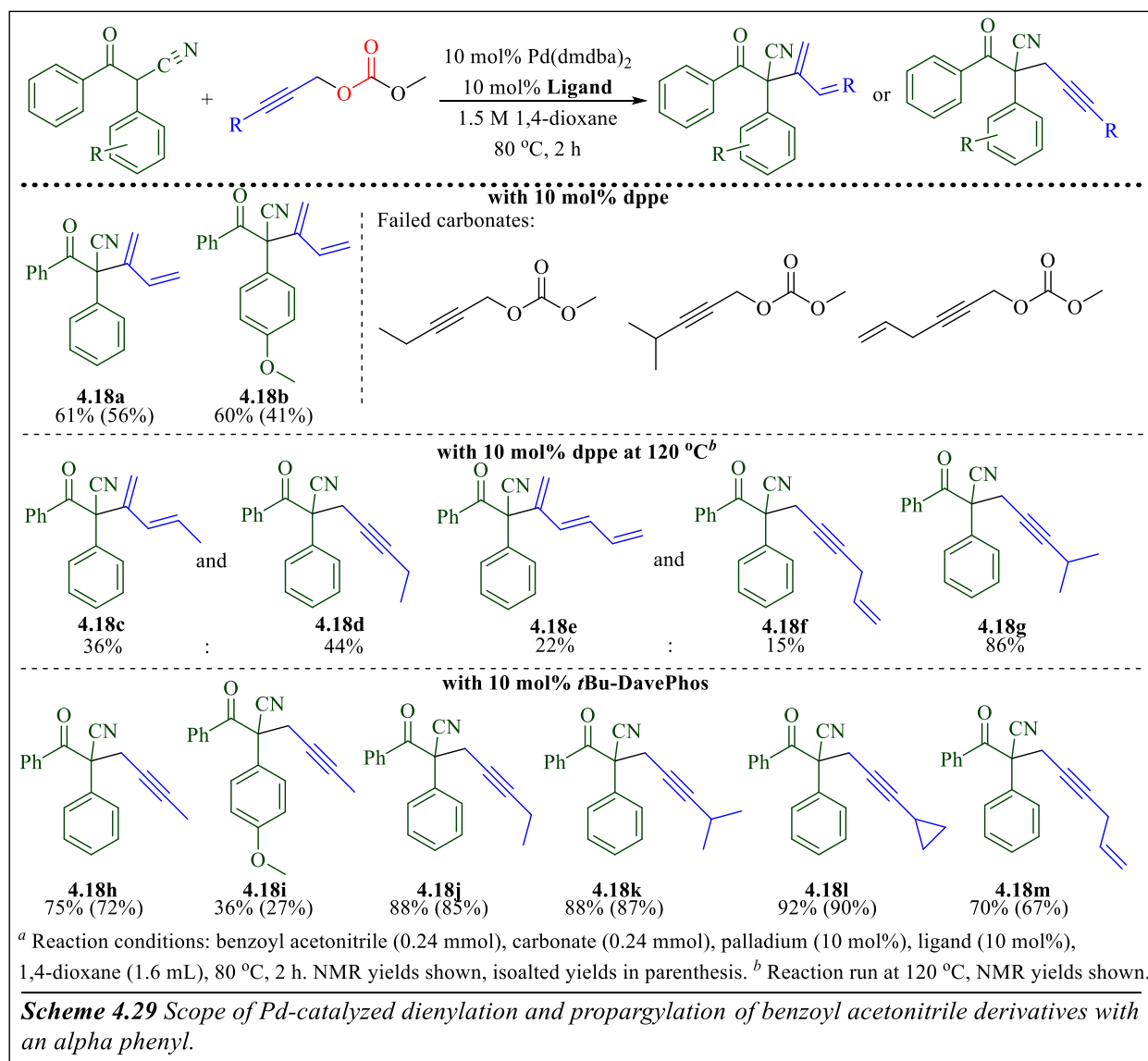
Structures shown: DPEPhos, dppe, *t*Bu-DavePhos, and Pd(dmdba)₂ (Ar = 3,5-OMe-C₆H₃).

^a Reactions of benzoyl acetonitrile 4.15a (0.24 mmol), propargyl carbonate 4.16a (0.24 mmol), Pd/ligand (10 mol%), 1.6 mL solvent. ^b NMR yield (isolated yield in parentheses).

Table 4.4 Optimization of reaction conditions for the dienylation and propargylation of benzoyl acetonitrile derivatives with an alpha phenyl.

diaryl acetonitrile compounds we saw the same divergent selectivity, with MePhos (entry 2) leading to the formation of the propargylated product and dppe (entry 3) to the 1,3-dienylated product. Further, the use of dppe ligand improved the yield of the reaction by almost 20% as compared to the yield with dppb (entry 1). In addition, switching from MePhos to *t*Bu-DavePhos

(entry 4) ligand increased the yield of the propargylated product by almost 10%. However, further testing with other ligands caused significant decreases in both the yield and selectivity of the reaction (entries 5-8). We next took the conditions from entries 3 and 4 for the development of a reaction scope with these compounds (Scheme 4.29).

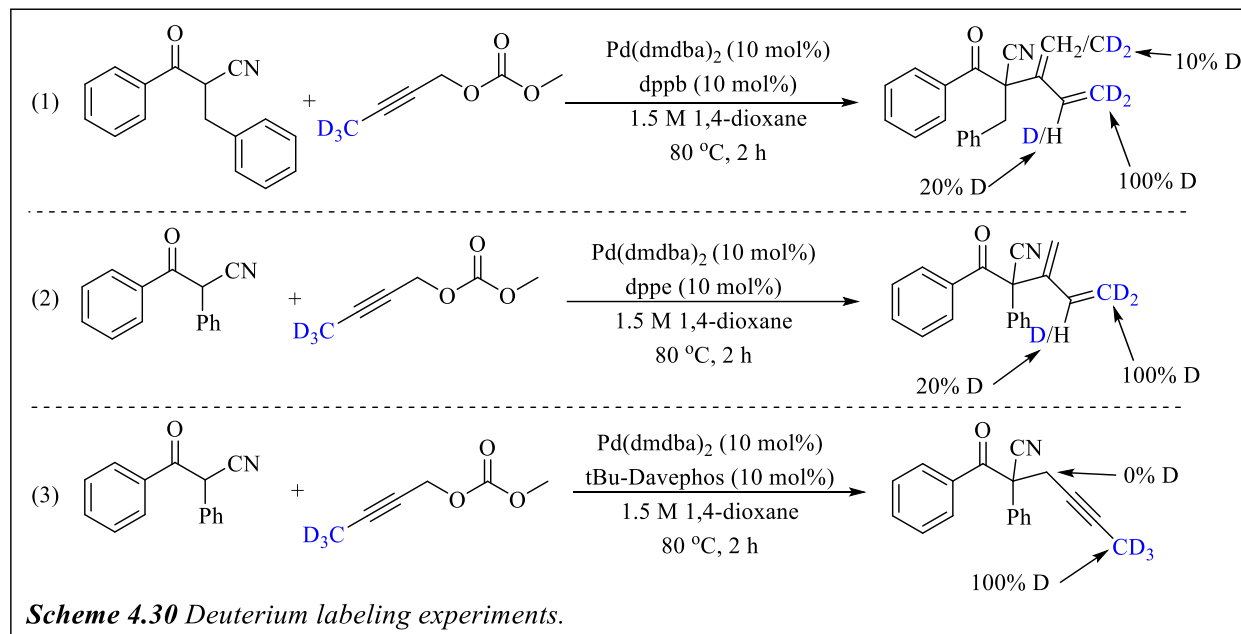


When using the bidentate ligand dppe, we found that the reaction was only successful with the most simple methyl substituted propargyl carbonate, forming the 1,3-dienylated product with both

the simple alpha phenyl benzoyl acetonitrile (**4.18a**) and one with a *para* methoxy substituent (**4.18b**) in moderate yields. Like with the previous benzoyl acetonitrile derivatives, reactions with propargyl carbonates that were monosubstituted at the terminal position were completely unreactive. Unlike with the previous examples, these benzoyl acetonitrile derivatives were also unreactive with propargyl carbonates that were di- or trisubstituted or substituted with an allyl group. However, when these compounds were subjected to the reaction conditions at 120 °C, the reaction could be forced, albeit in much lower yields and selectivities (**4.18c-g**). When the ligand was switched from dppe to *t*Bu-DavePhos, we were able to isolate a range of propargylated compounds. Unlike with dppe, the reaction with the monodentate *t*Bu-DavePhos was successful with mono- and disubstituted propargyl carbonates (**4.18h-m**). Further, while reactions with allyl substituted propargyl carbonate previously led to the generation of the triene product, when in the presence of *t*Bu-DavePhos it led to the formation of the propargylated product (**4.18m**).

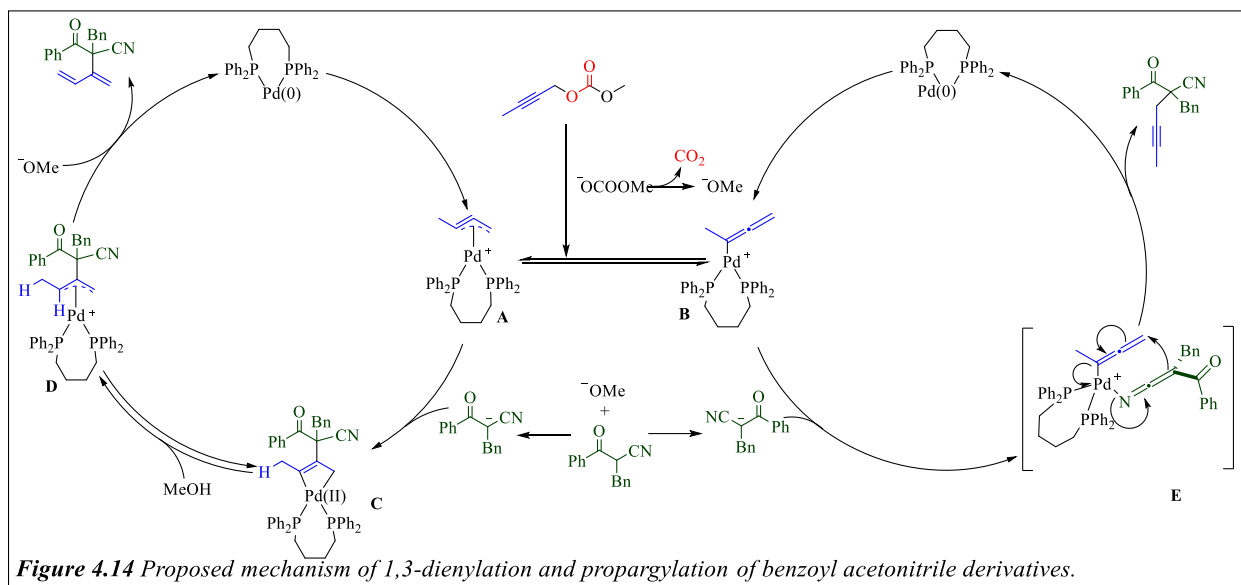
To get a better sense of the mechanistic pathways that could cause the differences in reactivities of these two classes of benzoyl acetonitrile derivatives, we ran a series of deuterium labeling experiments (Scheme 4.30). The first deuterium labeling experiment reacted the first benzoyl acetonitrile with an alpha benzyl substituent with a terminally deuterated propargyl carbonate, which generated results very similar to that of our deuterium labeling experiments with 1,3-dicarbonyl compounds (Scheme 4.30, equation 1). There was 100% deuterium at the terminal C4 position of the diene product that corresponded to the deuterated position of the starting propargyl carbonate. Further, there was 20% and 10% deuterium incorporation at the internal C3 and terminal C1 positions of the diene respectively. The second two labeling experiments reacted the benzoyl acetonitrile derivative with an alpha phenyl substituent using the regiodivergent conditions. First, we reacted compound **4.17a** with deuterated propargyl carbonate using bidentate

ligand dppe, generating the dienylated compound. Interestingly, while the dienylated product had 100% deuterium at the terminal C4 and 20% deuterium at the internal C3 position, there was no deuterium at the terminal C1 position. Further, when the reaction was run in the presence of *t*Bu-DavePhos, the propargylated product formed only had deuterium at the terminal position with no deuterium incorporated at the internal position.



From the results of our deuterium labeling experiments and the observed reactivity patterns while developing the scope of our reaction, we were able to propose the following mechanistic pathways for the two compound derivatives. For the benzoyl acetonitrile derivatives bearing an α -benzyl substituent, initial oxidative addition of the propargyl carbonate with $\text{Pd}(0)$ would generate an η^3 -propargyl palladium complex and a carboxylate anion that would then undergo decarboxylation leaving behind a methoxide anion (Figure 4.14). This methoxide anion would deprotonate the benzoyl acetonitrile compound to form the enolate nucleophile that would then attack at the center carbon of the η^3 -propargyl palladium complex, leading to the palladacyclobutene intermediate. Protonation from either methanol or another molecule of starting

material would form a π -allyl intermediate, and subsequent deprotonation would synthesize the 1,3-dienylated product. Results from the deuterium labeling studies indicate that the protonation step is reversible. Further, lack of reactivity of monosubstituted propargyl carbonates as compared to disubstituted propargyl carbonates indicates that nucleophilic addition occurs irreversibly.



Propargyl carbonates that are di- or trisubstituted at the terminal position of the propargyl carbonate would be too sterically hindered to undergo nucleophilic attack at the central position of the η^3 -propargyl palladium complex, allowing it time to rearrange to the η^1 -allenyl palladium complex. While rearrangement to the η^1 -propargyl palladium complex is possible, binding of anionic nitrile compounds has been previously proposed to favor the η^1 -allenyl complex, forming a bound nitrile intermediate.⁴¹ Inner-sphere nucleophilic attack at the terminal position of the η^1 -allenyl palladium complex would provide the propargylated product.

The mechanism of benzoyl acetonitrile derivatives that bear an alpha phenyl substituent begins identically with oxidative addition of the propargyl carbonate with palladium to generate an η^3 -propargyl palladium complex and carboxylate ion (Figure 4.15). With the bidentate ligand dppe, nucleophilic attack from the *in-situ* generated enolate occurs at the central position of the η^3 -

propargyl palladium intermediate, forming the palladacyclobutene intermediate. Protonation at the C3 position of this intermediate would lead to a π -allyl intermediate and deprotonation would generate the 1,3-dienylated product. Observations from the reactivity of the various propargyl carbonates and the results of the deuterium labeling studies indicate the both the nucleophilic addition and protonation steps are irreversible. In contrast, when using the monodentate ligand *t*Bu-DavePhos, there is an open coordination site that better allows for binding of the anionic ligand, which allows for a greater preference for the η^1 -allenyl palladium complex. Finally, nucleophilic attack at the terminal carbon of the allenyl intermediate would product the propargylated product.

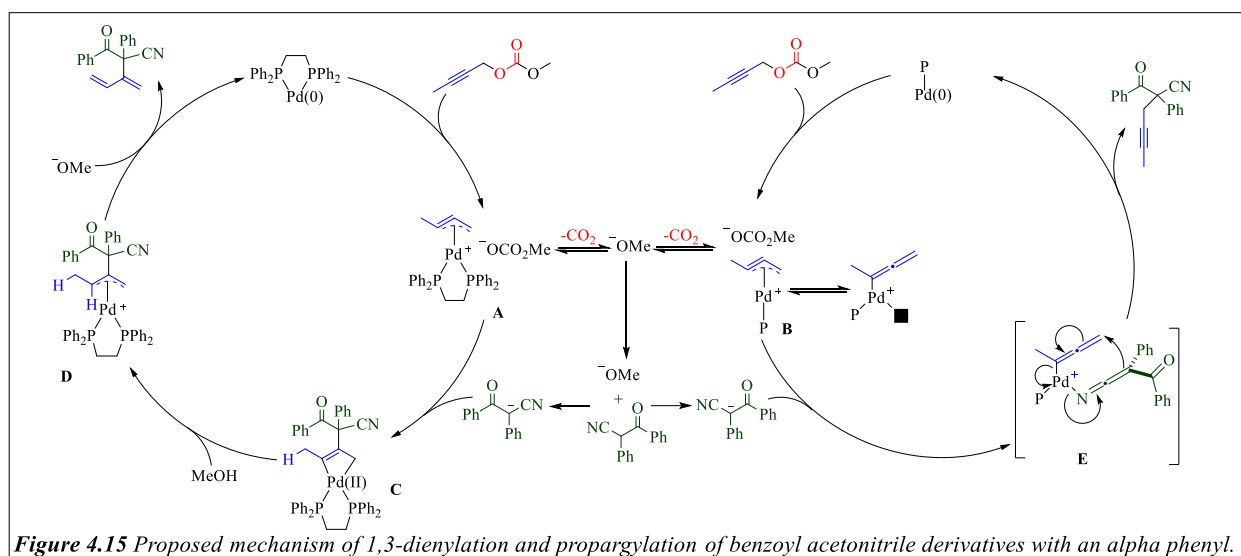
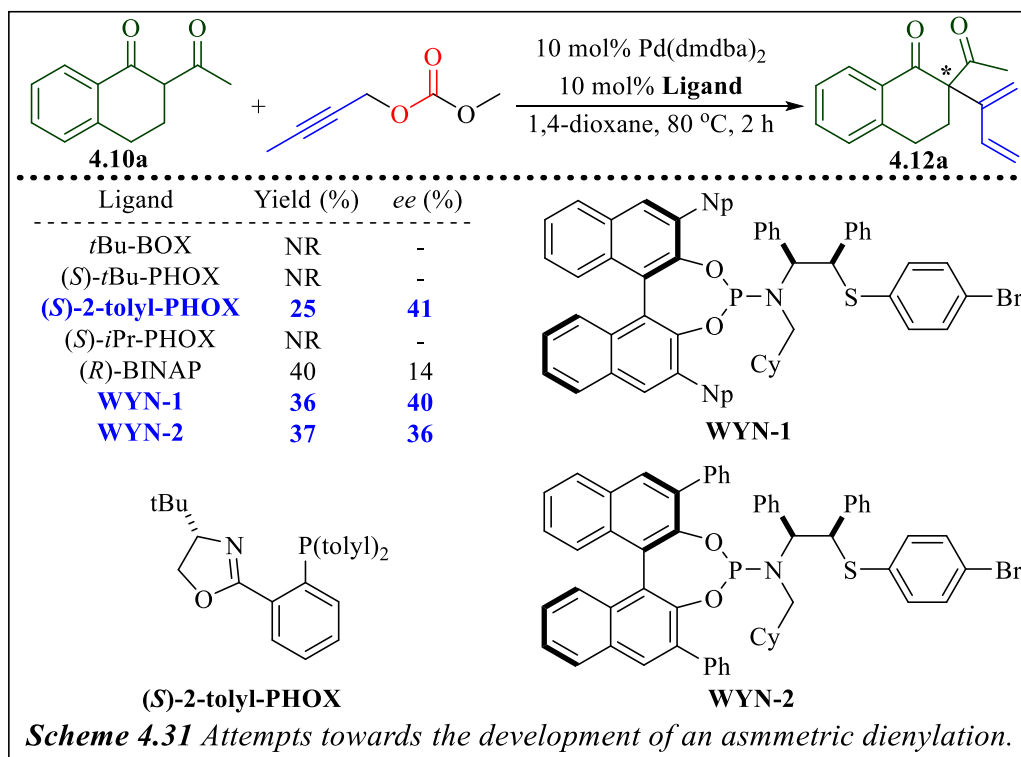


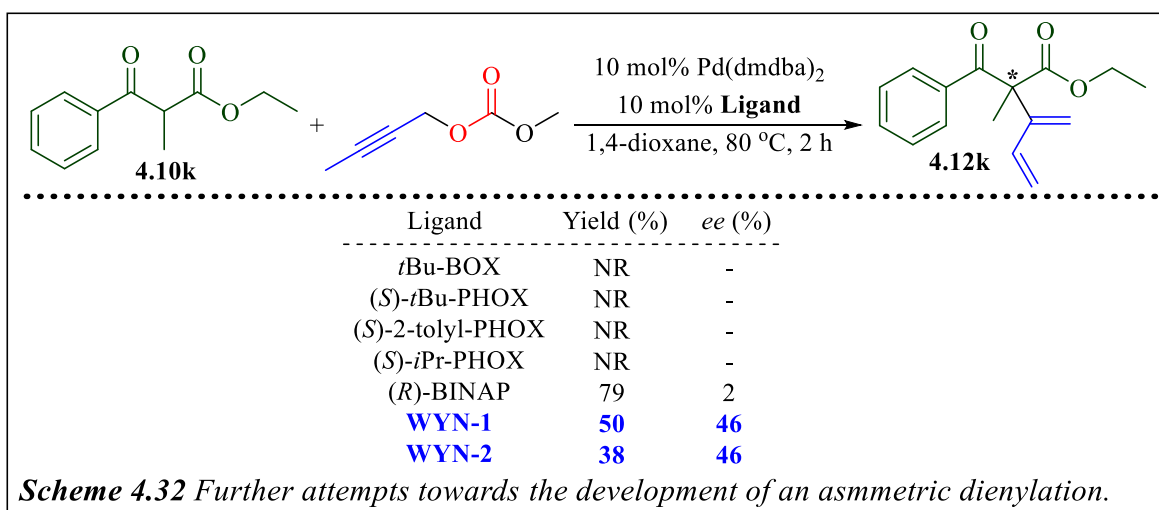
Figure 4.15 Proposed mechanism of 1,3-dienylation and propargylation of benzoyl acetonitrile derivatives with an alpha phenyl.

4.6 Efforts Towards Asymmetric Dienylation

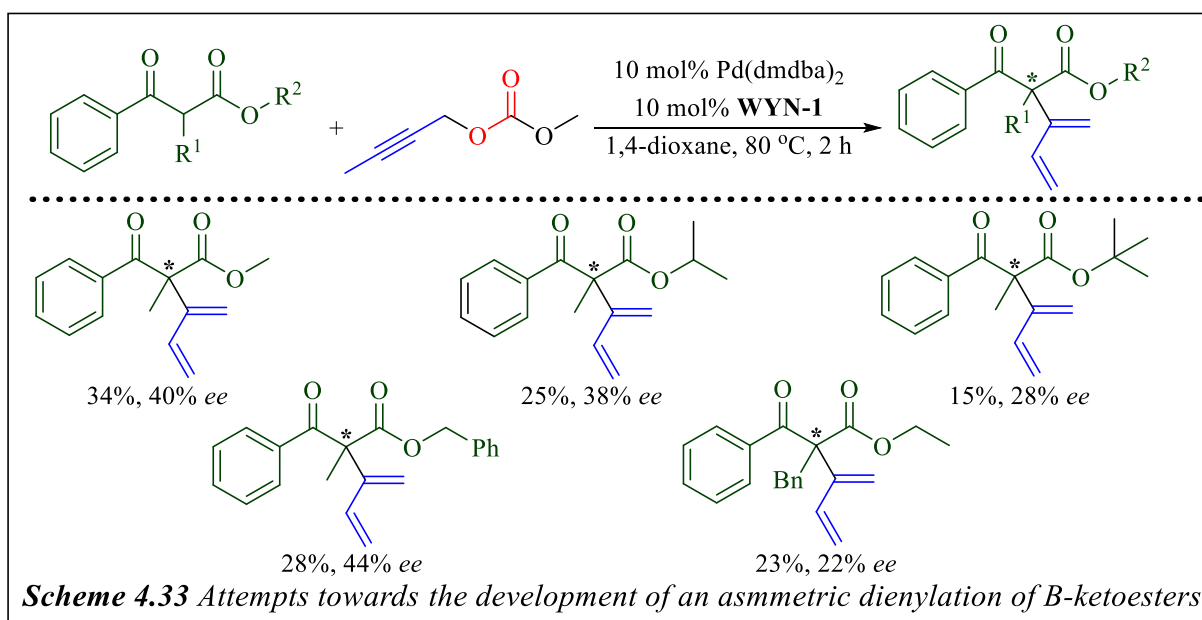
During the development of our methods for the dienylation and propargylation of enolate nucleophiles, we made attempts to develop an enantioselective version of our methodology. Starting with our initial 1,3-dicarbonyl **4.10a**, we reacted it with methyl propargyl carbonate in the presence of a series of chiral ligands and analyzed the resulting 1,3-dienylated product on a chiral HPLC to determine the enantioselectivity of the reaction (Scheme 4.31). While several BOX and



PHOX ligands led to no reaction occurring, a single PHOX ligand, (*S*)-2-tolyl-PHOS was able to form the desired product in with a 41% ee. Two other P,N ligands developed by the Xiao group,⁴² WYN-1 and WYN-2 were used in attempts to provide higher enantioselectivity, providing the dienylated product with 40% ee and 36% ee respectively. While these results were promising, the lower yields of the reactions made analysis of the products difficult.



Therefore, we decided to switch our focus towards 1,3-dicarbonyl **4.10k**, a compound that had led to much higher yields for us in the past. When we ran the reaction with **4.10k** in the presence of the same series of chiral ligands, we found that the PHOX ligand that worked previously was no longer successful (Scheme 4.32). However, the other two ligands, WYN-1 and WYN-2 both provided the dienylated product with an enantioselectivity of 46%, albeit WYN-1 led to a slightly higher yield. As switching the 1,3-dicarbonyl compound had led to such a noticeable difference in the selectivity of the reaction, we decided to react a series of 1,3-dicarbonyl compounds with WYN-1, the best performing ligand thus far, in our typical reaction conditions (Scheme 4.33).



We observed that while an ethyl substituent on the ester improved the ee (46%) as compared to a methyl substituent (40%), as the sterics at that position grew larger there was a gradual decrease in the enantioselectivity of the reaction. Further, when the substituent at the alpha position of the 1,3-dicarbonyl was switched from a methyl to a benzyl group, the enantioselectivity was more than halved. While the current results are still far from perfect, they are quite promising as they are still in their elementary stages. Work is still underway to further improve the enantioselectivity of the dienylation of enolate compounds.

4.7 Conclusion

In conclusion, we have developed a series of methods for the propargylation and 1,3-dienylation of various enolate nucleophiles. We presented a protocol for the dienylation and propargylation of 1,3-dicarbonyl compounds that was highly dependent on the pK_a of the starting compound, with the optimal pK_a for dienylation being between the values of 16 and 9. Values higher than 16 led to low yields of either isomer, and values lower than 9 led to a switch in selectivity to instead favor the propargyl product. Additionally, the sterics present on the propargyl carbonate had a large impact on both the yield and selectivity of the reaction. Further, we showed a similar method for the dienylation and propargylation of benzoyl acetonitrile compounds that bear an alpha benzyl group. This method contrasted with a third method for the propargylation and 1,3-dienylation of benzoyl acetonitrile compounds that contain an α phenyl substituent. Interestingly, changing the α -substituent from an benzyl group to a phenyl altered the reactivity of the compounds, allowing for a ligand-dependent regiodivergent methodology. Finally, we started work on the development of an enantioselective dienylation of 1,3-dicarbonyl compounds, and the initial results are quite promising.

4.8 References for Chapter 4

-
1. Nicholas, K.M. "Chemistry and Synthetic Utility of Cobalt-Complexed Propargylic Cations." *Acc. Chem. Res.* **1987**, *20*, 207-241.
 2. (a) Sanz, R.; Miguel, D.; Martínez, A.; Álvarez-Gutiérrez, J. M.; Rodríguez, F. "Brønsted Acid Catalyzed Propargylation of 1,3-Dicarbonyl Derivatives. Synthesis of Tetrasubstituted Furans." *Org. Lett.*, **2007**, *9*, 727-730. (b) Sanz, R.; Miguel, D.; Martínez, A.; Gohain, M.; García-García, P.; Fernández-Rodríguez, M. A.; Álvarez, E.; Rodríguez,

-
- F. “Brønsted Acid Catalyzed Alkylation of Indoles with Tertiary Propargylic Alcohols: Scope and Limitations.” *Eur. J. Org. Chem.*, **2010**, *36*, 7027-7039 (c) Barreiro, E.; Sanz-Vidal, A.; Tan, E.; Lau, S-H.; Sheppard, T. D.; Díez-González, S. “HBF₄- Catalyzed Nucleophilic Substitutions of Propargylic Alcohols.” *Eur. J. Org. Chem.*, **2015**, 7544-7549. (d) Huang, W.; Wang, J.; Shen, Q.; Zhou, X. “Yb(OTf)₃-catalyzed propargylation and allenylation of 1,3-dicarbonyl derivatives with propargylic alcohols: one-pot synthesis of multi-substituted furocoumarin.” *Tetrahedron*. **2007**, *63*, 11636-11643. (e) Li, C.; Wang, J. “Lewis Acid Catalyzed Propargylation of Arenes with *O*-Propargyl Trichloroacetimidates: Synthesis of 1,3-Diarylpropynes.” *J. Org. Chem.*, **2007**, *72*, 7431-7434. (f) Chang, X.; Zhang, J.; Peng, L.; Guo, C. “Collective Synthesis of Acetylenic Pharmaceuticals via Enantioselective Nickel/Lewis Acid-Catalyzed Propargylic Alkylation.” *Nat. Commun.* **2021**, *12*, 299.
3. (a) Bauer, E. B. “Transition Metal Catalyzed Functionalization of Propargylic Alcohols and Their Derivatives”, *Synthesis*, **2012**, *44*, 1131. (b) Nihibayashi, Y. "Transition Metal-Catalyzed Enantioselective Propargylic Substitution Reactions of Propargylic Alcohol Derivatives with Nucleophiles." *Synthesis*, **2012**, *44*, 489-503. (c) Hirashita, T.; Suzuki, Y.; Tsuji, H.; Sato, Y.; Naito, K.; Araki, S. “Nickel-Catalyzed Indium(I)-Mediated *syn*-Selective Propargylation of Aldehydes.” *Eur. J. Org. Chem.*, **2012**, 5668-5672. (d) Detz, R. J.; Delville, M. M. E.; Hiemstra, H.; van Maarseveen, J. H. “Enantioselective Copper-Catalyzed Propargylic Amination.” *Angew. Chem., Int. Ed.* **2008**, *47*, 3777-3780. (e) Hattori, G.; Matsuzawa, H.; Miyake, Y.; Nishibayashi, Y. “Copper-Catalyzed Asymmetric Propargylic Substitution Reactions of Propargylic Acetates with Amines.” *Angew. Chem., Int. Ed.* **2008**, *47*, 3781.
4. Tsuji, J. “*Overview of the Palladium-Catalyzed Carbon-Carbon Bond Formation via π -Allylpalladium and Propargylpalladium Intermediates.*” Ed. Ei-ichi Negishi. New York: John Wiley & Sons, Inc. 2002. 1669-1686. Online.
5. For select examples of allene synthesis from Pd-catalyzed reactions with propargyl carbonates: (a) Ye, J.; Ma, S. “Palladium-Catalyzed Cyclization Reactions of Allenes in

-
- the Presence of the Unsaturated Carbon-Carbon Bonds.” *Acc. Chem. Res.*, **2014**, *47*, 989-1000. (b) Yoshida, M.; Ohno, S; Namba, K. “Synthesis of Substituted Tetrahydricyclobuta[*b*]benzofurans by Palladium-Catalyzed Substitution/[2+2] Cycloadditions of Propargylic Carbonates with 2-Vinylphenols.” *Angew. Chem. Int. Ed.* **2013**, *52*, 13597-13600. (c) Kalek, M.; Johansson, T.; Jezowska, M.; Stawinski, J. “Palladium-Catalyzed Propargylic Substitution with Phosphorus Nucleophiles: Efficient, Stereoselective Synthesis of Allenylphosphonates, and Related Compounds.” *Org. Lett.*, **2010**, *12*, 4702-4704. (d) Shu, W.; Jia, G.; Ma, S. “Palladium-Catalyzed Regioselective Cyclopropanating Allenylation of (2,3-Butadienyl)malonates with Propargylic Carbonates and Their Application to Synthesize Cyclopentenones.” *Org. Lett.*, **2009**, *11*, 117-120.
6. Graham, J. P. ; Wojcicki, A.; Bursten, B. E. “Molecular Orbital Description of the Bonding and Reactivity of the Platinum η^3 -Propargyl Complex $[\eta^3\text{-CH}_2\text{CCPh)Pt(PPh}_3)_2]^+$ ” *Organometallics*, **1999**, *19*, 837-842.
7. For select examples of dinucleophilic substitution: (a) Bi, H-P; Guo, L-N; Gou, F-R; Duan, X-H; Liu, X-Y; Liang, Y-M. “Highly Regio- and Stereoselective Synthesis of Indene and Benzo[*b*]furan Derivatives via a Pd-Catalyzed Carboannulation of Propargyl Carbonates with Nucleophiles.” *J. Org. Chem.*, **2008**, *73*, 4713-4716. (b) Ren, Z-H; Guan, Z-H; Liang, Y-M. *J. Org. Chem.* **2009**, *74*, 3145-3147. (c) Yoshida, M.; Nakagawa, T.; Kinoshita, K.; Shishido, K. “Regiocontrolled Construction of Furo[3,2-*c*]pyran-4-one Derivatives by Palladium-Catalyzed Cyclization of Propargylic Carbonates with 4-Hydroxy-2-pyrones.” *J. Org. Chem.*, **2013**, *78*, 1687-1692.
8. (a) Kozawa, Y.; Mori, M. “Novel Synthesis of Carbapenam by Intramolecular Attack of Lactam Nitrogen toward η^1 -Allenyl and η^3 -Propargylpalladium Complex.” *J. Org. Chem.*, **2003**, *68*, 8068-8074. (b) Ambrogio, I.; Cacchi, S.; Gabrizi, F.; Prastaro, A. “3-(*o*-Trifluoroacetamidoryl)-1-propargylic Esters: Common Intermediates for the Palladium-Catalyzed Synthesis of 2-Aminomethyl-, 2-Vinyllic, and 2-Alkylindoles.” *Tetrahedron*, **2009**, *65*, 8916-8929.

-
9. (a) Vidadala, S. R.; Walman, H. "One-Pot Synthesis of a Natural Product Inspired Pyrrolocoumarin Compound Collection by Means of An Intramolecular 1,3-dipolar Cycloaddition as a Key Step." *Tetrahedron Lett.*, **2015**, *56*, 3358-3360. (b) Asai, T.; Yamamoto, T.; Oshima, Y. "Histone Deacetylase Inhibitor Induced the Production of Three Novel Prenylated Tryptophan Analogs in the Entomopathogenic Fungus, *Torrubiella luteostrata*." *Tetrahedron Lett.*, **2011**, *52*, 7042-7045.
10. (a) Zheng, R.; Li, S.; Zhang, X.; Zhao, C. "Biological Activities of Some New Secondary Metabolites Isolated from Endophytic Fungi: A Review Study." *Int. J. Mol. Sci.*, **2021**, *22*, 959. (b) Trost, B. M.; Cregg, J. J.; Hohn, C.; Bai, W-J.; Zhang, G.; Tracy, J. S. "Ruthenium-Catalyzed Multicomponent Synthesis of the 1,3-dienyl-6-oxy Polyketide Motif." *Nature Chem.*, **2020**, *12*, 629-637.
11. (a) Fujii, T.; Oki, Y.; Nakada, M. "Research on Liebeskind-Strogl Coupling/Intramolecular Diels-Alder Reaction Cascade." *Tetrahedron Lett.*, **2018**, *59*, 882-886. (b) Zhao, P.; Beaudry, C. M. "Total Synthesis of (+)-Cavicularin: The Pyrone Diels-Alder Reaction in Enantioselective Cyclophane Synthesis." *SynLett*, **2015**, *26*, 1923-1929.
12. Select examples of Diels-Alder reactions: (a) Aragonès, A.; Haworth, N. L.; Darwish; Ciampi, S.; Bloomfield, N. J.; Wallace, G. G.; Diez-Perez, I.; Coote, M. L. "Electrostatic catalysis of a Diels-Alder reaction." *Nature*, **2016**, *531*, 88-91. (b) Son, J-H; Cheung, A.; Zhu, J. S. ; Haddadin, M. J.; Kurth, M. J. "Davis-Beirut Reaction Inspired Nitroso Diels-Alder Reaction." *Tetrahedron Lett.*, **2021**, *69*, 152951. Select examples of epoxidations: (a) Jat, J. L.; De, S. R.; Kumar, G.; Adebesein, A. M.; Gandham, S. K.; Falck, J. R. "Regio- and Enantioselective Catalytic Monoepoxidation of Conjugated Dienes: Synthesis of Chiral Allylic cis-Epoxides." *Org. Lett.*, **2015**, *17*, 1058-1061. (b) De, S. R.; Kumar, G.; Jat, J. L. ; Birudaraju, S.; Lu, Biao ; Manne, R. ; Puli, N. ; Adebesein, A. M. ; Falck, J. R. "Regio- and Stereoselective Monoepoxidation of Dienes using Methyltrioxorhenium: Synthesis of Allylic Epoxides." *J. Org. Chem.*, **2014**, *79*, 103230-10333. Select examples of hydrogenation reactions: (a) Luza, L.; Gual, A.; Dupont, J. "The Partial Hydrogenation of 1,3-Dienes Catalyzed by Soluble Transition-Metal Nanoparticles." *ChemCatChem*,

-
- 2014**, *6*, 702-710. (b) Stephenson, C. J.; Hupp, J. T.; Farha, O. K. "Pt@ZIF-8 Composite for the Regioselective Hydrogenation of Terminal Unsaturation in 1,3-Dienes and Alkynes." *Inorg. Chem. Front.*, **2015**, *2*, 448-452.
13. Nunomoto, S.; Yamashita, Y. "Reaction of 2-(1,3-Butadienyl)magnesium Chloride with Carbonyl Compounds and Epoxides. A Regioselectivity Study." *J. Org. Chem.*, **1979**, *44*, 4788-4791.
14. Nunomoto, S.; Kawakami, Y.; Yamashita, Y. "Synthesis of 2-Substituted 1,3-Butadienes by Cross-Coupling Reaction of 2-(1,3-Butadienyl)magnesium Chloride with Alkyl or Aryl Iodides." *Bull. Chem. Soc. Jpn.*, **1981**, *54*, 2831-2832.
15. Luo, M.; Iwabuchi, Y.; Hatakeyama, S. "Buta-2,3-dienylstannanes, Effective Reagents for Regioselective Buta-1,3-Dienylation of Aldehydes and Acetals." *Chem. Commun.*, **1999**, 267-268.
16. Luo, M.; Iwabuchi, Y.; Hatakeyama, S. "Regioselective Buta-1,3-Dienylation of Aldehydes via Transmetalation of 2-Tributylstannylbuta-1,3-diene." *Synlett*, **1999**, *7*, 1109-1111.
17. Tivola, P. B.; Deagostino, A.; Prandi, C.; Venturello, P. "A New Synthesis of Butadienyl- and Styrylboronic Esters: Highly Reactive Intermediates for Suzuki Cross-Coupling." *Org. Lett.*, **2002**, *4*, 1275-1277.
18. Alcaraz, L.; Cox, K.; Cridland, A. P.; Kinchin, E.; Morris, J.; Thompson, S. P. "Novel Enantioselective Synthesis of 1,3-Butadien-2-ylmethanols via Tandem Alkylbromide-epoxide Vinylations Using Dimethylsulfonium Methylide" *Org. Lett.*, **2005**, *7*, 1399-1401.
19. Alcaraz, L.; Cridland, A.; Kinchin, E. "Novel Conversion of 1,2-Disubstituted *cis*-Epoxides to One-Carbon Homologated Allylic Alcohols Using Dimethylsulfonium Methylide." *Org. Lett.*, **2001**, *3*, 4051-4053.

-
20. Alcaraz, L.; Harnett, J. J.; Mioskowski, C.; Martel, J. P.; Le Gall, T.; Shin, D-S; Falck, J-R "Sulfur Ylide Vinylation of Halides and Mesylates." *Tetrahedron Lett.*, **1994**, *35*, 5453-5456.
21. Naodovic, M.; Xia, G.; Yamamota, H. "TBOxCrIII Cl-Catalyzed Enantioselective Synthesis of 1,3-Butadien-2-ylcarbinols." *Org. Lett.*, **2008**, *10*, 4053-4055.
22. Durán-Galván, M.; Connell, B. T. "Asymmetric Synthesis of (1,3-Butadien-2-yl)methanols from Aldehydes via [1-(Silylmethyl)allenyl]methanols." *Eur. J. Org.*, **2010**, 2445-2448.
23. Yang, Q.; Chai, H.; Liu, T.; Yu, Z. "Palladium-catalyzed Cross-coupling of Cyclopropylmethyl *N*-tosylhydrazones with Aromatic Bromides: An Easy Access to Multisubstituted 1,3-Butadienes." *Tetrahedron Lett.*, **2013**, *54*, 6485-6489.
24. Bienaymé, H. "A New Synthesis of Polyunsaturated Allenic Carbonyls." *Tetrahedron Lett.*, **1994**, *35*, 7387-7390.
25. Behanna, D. C.; Mohr, J. T.; Sherden, N. H.; Marinescu, S. C.; Harned, A. M.; Tani, K.; Seto, M.; Ma, S.; Novák, Z.; Krout, M. R.; McFadden, R. M.; Roizen, J. L.; Enquist, J. A.; White, D. E.; Levine, S. R.; Petrova, K. V.; Iwashita, A.; Virgil, S. C.; Stoltz, B. M. "Enantioselective Decarboxylative Alkylation Reactions: Catalyst Development, Substrate Scope, and Mechanistic Studies." *Chem. Eur. J.*, **2011**, *17*, 14199-14223.
26. Ambrogio, I.; Cacchi, S.; Fabrizi, G.; Goggiamani, A.; Iazzetti, A. "Palladium-Catalyzed Nucleophilic Substitution of Propargylic Carbonates and Meldrum's Acid Derivatives." *Eur. J. Org. Chem.*, **2015**, 3147-3151.
27. Locascio, T.; Tunge, J. A. "Palladium-Catalyzed Regiodivergent Substitution of Propargylic Carbonates." *Chem. Eur. J.*, **2016**, *22*, 18140-18146.

-
28. Tsutsumi, K.; Yabukami, T.; Fujimoto, K.; Kawase, T.; Morimoto, T.; Kakiuchi, K. "Effects of a Bidentate Phosphine Ligand on Palladium-Catalyzed Nucleophilic Substitution Reactions of Propargyl and Allyl Halides with Thiol." *Organometallics*, **2003**, *22*, 2996-2999.
29. Ishida, N.; Hori, Y.; Okumura, S.; Murakami, M. "Synthesis of 2-Aryloxy-1,3-Dienes from Phenols and Propargyl Carbonates." *J. Am. Chem. Soc.*, **2019**, *141*, 84-88.
30. Tang, S.; Wei, W.; Yin, D.; Poznik, M. Chruma, J. J. "Palladium-Catalyzed Decarboxylative Generation and Propargylation of 2-Azaallyl Anions." *J. Org. Chem.*, **2019**, 3964-3978.
31. O'Broin, C. Q.; Guiry, P. J. "Construction of All-Carbon Quaternary Stereocenters by Palladium-Catalyzed Decarboxylative Propargylation." *Org. Lett.*, **2019**, *21*, 5402-5406.
32. O'Broin, C. Q.; Guiry, P. J. "Synthesis of 2-Amino-1,3-Dienes from Propargyl Carbonates via Palladium-Catalyzed Carbon-Nitrogen Bond Formation." *Org. Lett.*, **2020**, *22*, 879-883.
33. Ishida, N.; Kamino, Y.; Murakami, M. "Nickel-Catalyzed 1,3-Dienylation of 1,3-Dicarbonyl Compounds with Propargylic Carbonates." *Synlett*, **2020**, *31*, A-D.
34. Guo, L-N; Duan, X-H; Bi, H-P; Liu, X-Y; Liang, Y-M. "Palladium-Catalyzed Carboannulation of Propargylic Carbonates and Nucleophiles to 2-Substituted Indenes." *J. Org. Chem.*, **2007**, *72*, 1538-1540.
35. Kenny, M.; Christensen, J.; Coles, S. J.; Franckevičius, V. "Regioswitchable Palladium-Catalyzed Decarboxylative Coupling of 1,3-Dicarbonyl Compounds." *Org. Lett.*, **2015**, *17*, 3926-3929.

-
36. Schröder, S. P.; Taylor, N. J.; Jackson, P.; Franckevičius, V. "Catalytic Decarboxylative Alkenylation of Enolates." *Org. Lett.*, **2013**, *15*, 3778-3781.
37. Kenny, M.; Kitson, D. J.; Franckevičius, V. "Catalytic Chemo- and Regioselective Coupling of 1,3-Dicarbonyls with *N*-Heterocyclic Nucleophiles." *J. Org. Chem.*, **2016**, *81*, 5162-5172.
38. (a) Kozawa, Y.; Mori, M. "Novel Synthesis of Carbapenam by Intramolecular Attack of Lactam Nitrogen Toward η^1 -Allenyl and η^3 -Propargylpalladium Complex." *J. Org. Chem.*, **2003**, *68*, 8068-8074. (b) Daniels, D. S. B.; Jones, A. S.; Thompson, A. L.; Paton, R. S.; Anderson, E. A. "Ligand Bite Angle-Dependent Palladium-Catalyzed Cyclization of Propargylic Carbonates to 2-Alkynyl Azacycles or Cyclic Dienamides." *Angew. Chem. Int. Ed.*, **2014**, *53*, 1915-1920.
39. For the source of pKa values see: (a) Olmstead, W. N.; Bordwel, F. G. "Ion-Pair Association Constants in Dimethyl Sulfoxide." *J. Org. Chem.*, **1980**, *45*, 3299-3305. (b) Arnett, E. M.; Maroldo, S. G.; Schilling, S. L.; Harrelson, J. A. "Ion Pairing and Reactivity of Enolate Anions. 5. Thermodynamics of Ionizations of Beta-Di- and Tricarbonyl Compounds in Dimethyl Sulfoxide Solution and Ion Pairing of Their Alkali Salts." *J. Am. Chem. Soc.*, **1984**, *106*, 6759-6767. (c) Zhang, X. M.; Bordwell, F. G.; Van Der Puy, M.; Fried, H. E. "Equilibrium acidities and homolytic bond dissociation energies of the acidic carbon-hydrogen bonds in *N*-substituted trimethylammonium and pyridinium cations." *J. Org. Chem.*, **1993**, *58*, 3060-3066.
40. Kalek, M.; Stawinski, J. "Novel, Stereoselective, and Stereospecific Synthesis of Allenylphosphonates and Related Compounds *via* Palladium-Catalyzed Propargylic Substitution." *Adv. Synth. Catal.*, **2011**, *353*, 1741-1755.
41. (a) Recio III, A.; Heinzman, J. D.; Tunge, J. A. "Decarboxylative Benzylation and Arylation of Nitriles." *Chem. Commun.*, **2012**, *48*, 142-144. (b) Recio III, A.; Tunge, J.

-
- A. "Regiospecific Decarboxylative Allylation of Nitriles." *Org. Lett.*, **2009**, *11*, 5630-5633.
42. Wang, Y-N; Xiong, Q.; Lu, L-Q; Zhang, Q-L; Wang, Y.; Lan, Y.; Xiao, W-J. "Inverse-Electron-Demand Palladium-Catalyzed Asymmetric [4+2] Cycloadditions Enabled by Chiral P,S-Ligand and Hydrogen Bonding." *Angew. Chem., Int. Ed.*, **2019**, *58*, 11013-11017.

Chapter 4. Appendix

Experimental Methods, Spectral Analysis, and Spectra for Chapter 4 Compounds

Table of Contents

<i>General Information</i>	290
<i>Preparation and Spectral Data of Starting 1,3-Dicarbonyl Compounds:</i>	291
<i>Preparation and Spectral Data of Starting Propargyl Carbonate Compounds:</i>	300
<i>General Procedure and Spectral Data of Dienyl and Propargyl Products: Project 1</i>	307
<i>General Procedure and Spectral Data of Diels-Alder Products:</i>	334
<i>Preparation and Spectral Data of Starting Benzoyl Acetonitrile Compounds</i>	338
<i>General Procedure and Spectral Data of Dienyl and Propargyl Products: Project 2</i>	341
<i>References:</i>	348
<i>Copies of HPLC Spectra</i>	348
<i>Copies of ¹H NMR and ¹³C NMR Spectra</i>	359

1. General Information:

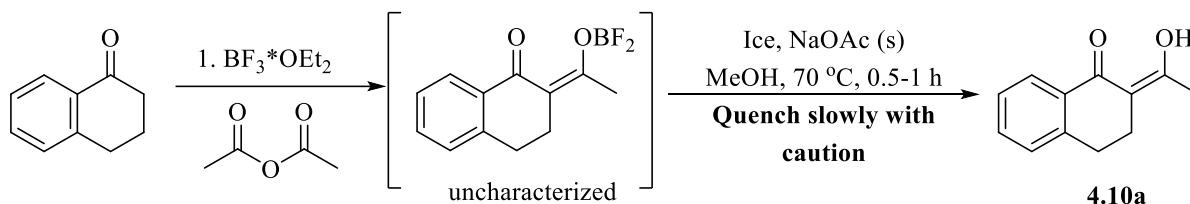
Compounds, unless otherwise specified, were purified via flash column chromatography with 60 Å porosity, 230 x 400 mesh standard silica gel from Sorbent Technologies. TLC analysis on obtained compounds was conducted using silica gel HL TLC plates with UV254 from Sorbent Technologies. A Shimadzu GCMS-QP2010 SE was used to obtain gas chromatography/mass spectrometry data, and NMR spectra were generated using a Bruker Advance 400 or Bruker Advance 500 DRX equipped with a QNP cryoprobe. All generated ^1H and ^{13}C spectra were normalized using any residual undeuterated CDCl_3 solvent signals, 7.26 ppm for ^1H and 77.36 ppm for ^{13}C .¹ Structural assignments were determined using ^1H and ^{13}C NMR. HRMS data was obtained via ESI mass spectrometry. Chiral HPLC analysis was performed by Agilent Technologies 1220 Infinity LC HPLC using Chiralpak IA, IB, IC, and ID chiral columns (0.46cmØx25cm), eluting with hexane/iso-propanol mixture.

All reactions were run either under nitrogen with standard Schlenk techniques or under argon through an inert atmosphere glovebox. 1,4-dioxane was purchased from Sigma Aldrich. Dichloromethane (DCM) and tetrahydrofuran (THF) were purified by an Innovative Technology Pure Solv solvent purification system. Bis(3,5,3',5'-dimethoxydibenzylideneacetone) palladium(0) ($\text{Pd}(\text{dmdba})_2$), 1,4-bis (diphenylphosphino) butane (dppb), ethylenebis (diphenylphosphine) (dppe), and 2-dicyclohexylphosphino-2'-methylbiphenyl (MePhos) were all purchased from Alfa Aesar and stored in a glovebox. Diethyl phenyl malonate was purchased from Alfa Aesar; 2-phenyl-1,3-indandione was purchased from TCI Chemicals; and 2,2,5-trimethyl-1,3-dioxane-4,6-dione was purchased from Sigma Aldrich. These three chemicals were used as starting materials without further purification.

2. Preparation and Spectral Data of Starting 1,3-Dicarbonyl Compounds:

Diketone 4.10a: (Z)-2-(1-hydroxyethylidene)-3,4-dihydronaphthalen-1(2H)-one

Synthesis of diketone 1a modified from known procedure²:



α -Tetralone (14 mmol) is dissolved in 25 mL of acetic acid anhydride in a flame-dried 500 ml Schlenk flask, equipped with a stir bar and attached to a Schlenk-argon line. The reaction is stirred, 7.5 mL of $\text{BF}_3 \cdot \text{OEt}_2$ is added dropwise over 1 minute, and the reaction is capped and stirred an additional 2 hours. After two hours, a medium sized scoop of ice is added piece by piece in order to quench the reaction. This is done with great caution due to the exothermic nature of the quenching process. Once quenched, 40 mL of MeOH and NaOAc (366 mmol) is added to the ice slurry, and the reaction mixture is heated to 70°C for 45 minutes.

The reaction mixture is added to a separatory funnel, and the reaction flask is washed with 300 mL of EtOAc. The organic layer is extracted with 100 mL of 1 N HCl three times and 50 mL of brine one time. The organic layer is dried over anhydrous MgSO_4 , filtered, and concentrated by rotary evaporation. An azeotrope formed with toluene is used to remove any residual acetic acid. The crude material is purified via column chromatography using an eluent of 20% EtOAc in hexanes.

Appearance: red-orange solid, 2.2 g, 11.7 mmol, 84% yield.

^1H NMR Spectra (500 MHz, CDCl_3): δ 7.96 (ddd, $J = 12.3, 7.6, 1.4$ Hz, 1H), 7.42 (td, $J = 7.5, 1.5$ Hz, 1H), 7.34 (td, $J = 7.6, 1.3$ Hz, 1H), 7.22 (dd, $J = 7.7, 1.3$ Hz, 1H), 2.90 (dd, $J = 8.4, 6.3$ Hz, 2H), 2.65 (dd, $J = 8.3, 6.5$ Hz, 2H), 2.26 (s, 3H).

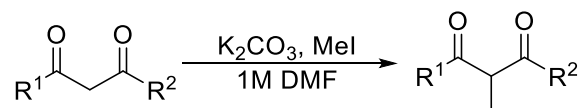
$^{13}\text{C}\{^1\text{H}\}$ NMR Spectra (126 MHz, CDCl_3): δ 194.16, 177.26, 141.13, 132.20, 131.46, 127.88, 127.18, 126.18, 106.30, 28.55, 24.25, 23.09.

HRMS: m/z $[\text{M}+\text{Li}]^+$ calcd for $\text{C}_{12}\text{H}_{12}\text{O}_2$: 195.0997. Found: 195.0993.

IR: 3069, 2953, 2842, 1694, 1614, 1429, 1302, 1212, 1155, 976, 904, 791, 739 cm^{-1} .

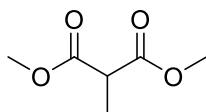
1,3-Dicarbonyl Compounds 4.10b, 4.10c, 4.10k, and 4.10l

General procedure for methylation of 1,3-dicarbonyls in the synthesis of α -methyl 1,3-dicarbonyls 4.10b, 4.10c, 4.10k, and 4.10l³:



A flame-dried 100 mL Schlenk flask equipped with a stir bar was attached to a Schlenk-nitrogen line and charged with N_2 . A 1,3-dicarbonyl compound (30 mmol), iodomethane (33 mmol), and K_2CO_3 (45 mmol) were added to the flask and dissolved in 30 mL of dry DMF. The reaction mixture is heated to 60 $^\circ\text{C}$ and stirred for five hours. After five hours, the mixture was cooled to room temperature and quenched with 50 mL of H_2O . The reaction mixture was extracted with 120 mL of EtOAc three times, and the combined organic layers was washed with 100 mL of brine one time. The organic layer was dried over anhydrous Na_2SO_4 , and it was filtered and concentrated by rotary evaporation. The crude material was purified via flash column chromatography using an eluent of 10% EtOAc in Hexanes.

4.10b: dimethyl 2-methyl malonate



Appearance: yellow liquid, 2.86 g, 19.6 mmol, 65% yield.

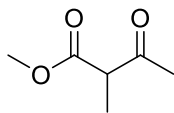
^1H NMR Spectra (500 MHz, CDCl_3): δ 3.74 (d, $J = 0.9$ Hz, 6H), 3.46 (q, $J = 7.3$ Hz, 1H), 1.43 (d, $J = 7.2$ Hz, 3H)

$^{13}\text{C}\{^1\text{H}\}$ NMR Spectra (126 MHz, CDCl_3): δ 170.86, 52.88, 46.18, 14.00.

HRMS: m/z $[\text{M}]^+$ calcd for $\text{C}_6\text{H}_{10}\text{O}_4$: 146.0479. Found: 146.0579.

IR: 2999, 2956, 2848, 1739, 1456, 1436, 1380, 1336, 1200, 1159, 1098, 1083, 1045, 986, 961 cm^{-1} .

4.10c: methyl 2-methyl-3-oxobutanoate



Appearance: clear liquid, 1.72 g, 13.2 mmol, 44% yield.

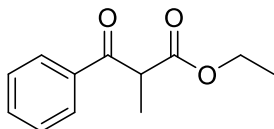
^1H NMR Spectra (500 MHz, CDCl_3): δ 3.77 (s, 3H), 3.54 (q, $J = 7.1$ Hz, 1H), 2.26 (s, 3H), 1.37 (d, $J = 7.2$ Hz, 3H)

$^{13}\text{C}\{^1\text{H}\}$ NMR Spectra (126 MHz, CDCl_3): δ 203.58, 170.98, 53.44, 52.43, 28.44, 12.78.

HRMS: m/z $[\text{M}]^+$ calcd for $\text{C}_6\text{H}_{10}\text{O}_3$: 130.0630. Found: 130.0633.

IR: 2999, 2956, 2848, 1739, 1456, 1436, 1380, 1336, 1200, 1159, 1098, 1083, 1045, 986, 961 cm^{-1} .

4.10k: ethyl 2-methyl-3-oxo-3-phenylpropanoate



Appearance: yellow liquid, 2.95 g, 14.3 mmol, 48% yield.

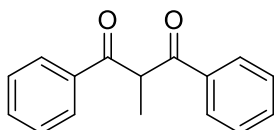
^1H NMR Spectra (500 MHz, CDCl_3): δ 7.98 (dd, $J = 8.1, 1.4$ Hz, 2H), 7.58 (t, $J = 7.5$ Hz, 1H), 7.48 (t, $J = 7.6$ Hz, 2H), 4.37 (q, $J = 7.1$ Hz, 1H), 4.15 (q, $J = 7.1$ Hz, 2H), 1.50 (d, $J = 7.1$ Hz, 3H), 1.17 (t, $J = 7.1$ Hz, 3H).

$^{13}\text{C}\{^1\text{H}\}$ NMR Spectra (126 MHz, CDCl_3): δ 195.88, 170.88, 135.89, 133.43, 128.71, 128.58, 61.37, 48.39, 13.97, 13.75.

HRMS: m/z $[\text{M}+\text{H}]^+$ calcd for $\text{C}_{12}\text{H}_{14}\text{O}_3$: 207.1021. Found: 207.1013.

IR: 2983, 2940, 2362, 1736, 1684, 1597, 1449, 1216, 1186, 1155, 971, 958, 689 cm^{-1} .

4.10l: 2-methyl-1,3-diphenylpropane-1,3-dione



Appearance: white solid, 1.04 g, 4.36 mmol, 87% yield.

^1H NMR Spectra (500 MHz, CDCl_3): δ 7.89 (d, $J = 7.1$ Hz, 4H), 7.50 (t, $J = 7.4$ Hz, 2H), 7.43–7.36 (m, 4H), 5.20 (q, $J = 7.1$ Hz, 1H), 1.54 (d, $J = 7.0$ Hz, 3H)

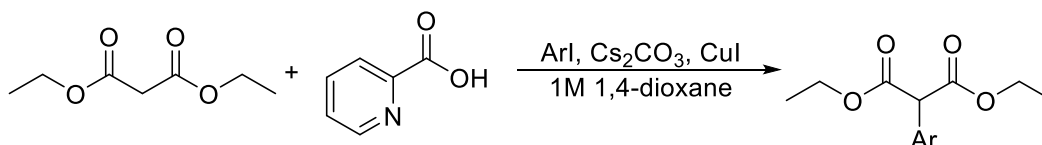
$^{13}\text{C}\{^1\text{H}\}$ NMR Spectra (126 MHz, CDCl_3): δ 197.17, 136.65, 133.48, 128.89, 128.55, 51.08, 14.38.

HRMS: m/z $[\text{M}+\text{H}]^+$ calcd for $\text{C}_{16}\text{H}_{14}\text{O}_2$: 239.1072. Found: 239.1067.

IR: 2941, 1687, 1663, 1594, 1449, 1343, 1232, 1203, 1179, 1153, 973, 694 cm^{-1}

1,3-Dicarbonyl Compounds 4.10d, 4.10e, 4.10g, and 4.10h

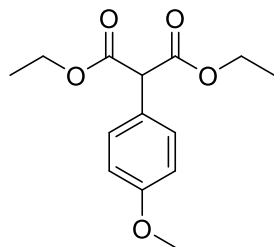
General procedure for the arylation of diethyl malonate compounds in the synthesis of α -aryl diethyl malonate 4.10d, 4.10e, 4.10g, and 4.10h:⁴



CuI (0.5 mmol), Cs_2CO_3 (30 mmol), picolinic acid (1 mmol), and ArI , if solid, (10 mmol) were added to a flame dried 50 mL Schlenk flask equipped with a stir bar. The reaction vessel was attached to a Schlenk-nitrogen line and was evacuated and backfilled with nitrogen three times. 10 mL of 1,4-dioxane, diethyl malonate (20 mmol), and ArI , if liquid, were added to the reaction vessel. The reaction flask was then sealed and stirred at room temperature for 20 hours.

After 20 hours, the reaction mixture was partitioned by adding 20 mL of EtOAc and 10 mL of saturated aqueous NH_4Cl . The mixture was extracted three times with 20 mL of EtOAc , and the combined organic layers were dried over anhydrous MgSO_4 . The dried organic layer was filtered and concentrated by rotary evaporation. The crude material was purified via flash column chromatography with an eluent of 20% EtOAc in Hexanes.

4.10d: diethyl-2-(4-methoxyphenyl)malonate



Appearance: clear oil, 0.319 g, 1.2 mmol, 60% yield.

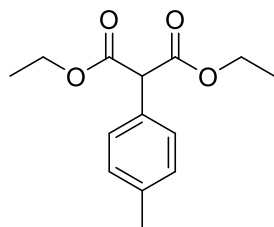
^1H NMR Spectra (500 MHz, CDCl_3): δ 7.33 (d, $J = 8.7$ Hz, 2H), 6.89 (d, $J = 8.7$ Hz, 2H), 4.28–4.13 (m, 4H), 3.80 (d, $J = 0.6$ Hz, 3H), 1.26 (td, $J = 7.2, 0.6$ Hz, 6H)

$^{13}\text{C}\{^1\text{H}\}$ NMR Spectra (126 MHz, CDCl_3): δ 168.68, 159.72, 130.63, 125.18, 114.26, 61.98, 57.40, 55.51, 14.28

HRMS: m/z $[\text{M}+\text{NH}_4]^+$ calcd for $\text{C}_{14}\text{H}_{18}\text{O}_5$: 284.1498. Found: 284.1502.

IR: 3037, 2983, 2839, 1731, 1613, 1514, 1465, 1367, 1305, 1252, 1219, 1179, 1150, 1033, 836, 794, 752, 555, 530 cm^{-1}

4.10e: diethyl-2-(*p*-tolyl)malonate



Appearance: Clear oil, 0.469 g, 1.86 mmol, 93% yield.

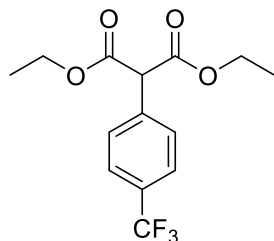
^1H NMR Spectra (500 MHz, CDCl_3): δ 7.31 (d, $J = 8.1$ Hz, 2H), 7.19 (d, $J = 7.9$ Hz, 2H), 4.59 (s, 1H), 4.28–4.19 (m, 4H), 2.37 (s, 3H), 1.28 (t, $J = 7.1$ Hz, 6H).

$^{13}\text{C}\{^1\text{H}\}$ NMR Spectra (126 MHz, CDCl_3): δ 168.33, 137.98, 129.83, 129.31, 129.09, 61.74, 57.63, 21.16, 14.03.

HRMS: m/z $[\text{M}+\text{H}]^+$ calcd for $\text{C}_{14}\text{H}_{18}\text{O}_4$: 251.1283. Found: 251.1276.

IR: 3028, 2983, 2939, 1757, 1736, 1465, 1446, 1417, 1390, 1367, 1332, 1306, 1268, 1220, 1209, 1186, 1146, 1096, 1034, 865, 819, 748, 680, 601, 508 cm^{-1} .

4.10g: diethyl-2-(4-(trifluoromethyl)phenyl)malonate



Appearance: Yellow solid, 3.4 g, 11.2 mmol, 56% yield.

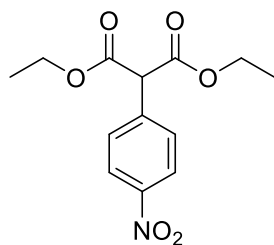
^1H NMR Spectra (500 MHz, CDCl_3): δ 7.63 (d, $J = 8.1$ Hz, 2H), 7.54 (d, $J = 8.1$ Hz, 2H), 4.67 (s, 1H), 4.30–4.16 (m, 4H), 1.27 (t, $J = 7.1$ Hz, 6H).

$^{13}\text{C}\{^1\text{H}\}$ NMR Spectra (126 MHz, CDCl_3): δ 167.47, 136.60, 130.61, 130.35, 129.78, 125.51, 62.14, 57.69, 13.99.

HRMS: m/z $[\text{M}+\text{H}]^+$ calcd for $\text{C}_{14}\text{H}_{15}\text{F}_3\text{O}_4$: 305.1001. Found: 305.1010.

IR: 2985, 2942, 1736, 1620, 1423, 1369, 1327, 1206, 1175, 1150, 1128, 1069, 1021, 849, 759, 719, 600 cm^{-1} .

4.10h: diethyl-2-(4-nitrophenyl)malonate



Appearance: White solid, 0.458 g, 1.62 mmol, 81% yield.

^1H NMR Spectra (500 MHz, CDCl_3): δ 8.23 (d, $J = 8.7$ Hz, 2H), 7.61 (d, $J = 8.8$ Hz, 2H), 4.72 (s, 1H), 4.37–4.10 (m, 4H), 1.28 (t, $J = 7.1$ Hz, 6H)

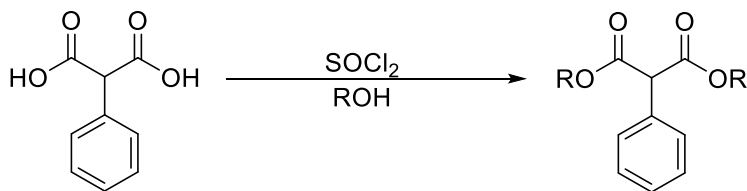
$^{13}\text{C}\{^1\text{H}\}$ NMR Spectra (126 MHz, CDCl_3): δ 167.25, 148.08, 139.90, 130.70, 123.95, 62.63, 57.83, 14.23.

HRMS: m/z $[\text{M}+\text{H}]^+$ calcd for $\text{C}_{13}\text{H}_{15}\text{NO}_6$: 282.0978. Found: 282.0985.

IR: 3115, 3083, 2985, 2940, 1733, 1609, 1523, 1496, 1466, 1446, 1369, 1350, 1300, 1220, 1152, 1112, 1096, 1030, 858, 734, 718, 595 cm^{-1} .

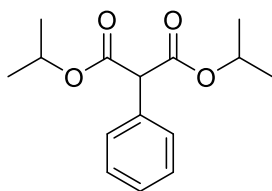
1,3-Dicarbonyl Compounds 4.10i and 4.10j

General procedure for the synthesis of α -aryl diethyl malonates 4.10i and 4.10j:⁵



A 250 mL Schlenk flask was flame dried and equipped with a magnetic stir bar. Phenylmalonic acid (20 mmol) was dissolved in the chosen alcohol to create a 0.33 M solution at 0 °C. While stirring at 0 °C, SOCl₂ (50 mmol) was added dropwise, and the reaction was allowed to warm to room temperature. The reaction mixture was stirred at room temperature for 26 hours. The solvent was then removed under vacuum, and the residual solid was washed with hexane and dried under vacuum.

4.10i: diisopropyl 2-phenylmalonate



Appearance: Clear liquid, 3.22 g, 12.16 mmol, 61% yield.

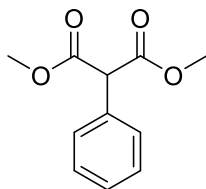
¹H NMR Spectra (500 MHz, CDCl₃): δ 7.42–7.29 (m, 5H), 5.07 (hept, *J* = 6.3 Hz, 2H), 4.54 (s, 1H), (dd, *J* = 14.0, 6.3 Hz, 12H)

¹³C{¹H} NMR Spectra (126 MHz, CDCl₃): δ 167.93, 133.25, 129.54, 128.72, 128.29, 69.57, 58.67, 21.80.

HRMS: *m/z* [M]⁺ calcd for C₁₅H₂₀O₄: 264.1362. Found: 264.1359.

IR: 3092, 3066, 3033, 2981, 2937, 2880, 1967, 1736, 1499, 1467, 1456, 1387, 1303, 1266, 1220, 1155, 1101, 1033, 999, 969, 918, 901, 728, 708, 697, 581 cm⁻¹.

4.10j: dimethyl 2-phenyl malonate



Appearance: Beige solid, 4.1 g, 19.7 mmol, 99% yield.

^1H NMR Spectra (500 MHz, CDCl_3): δ 7.46–7.29 (m, 5H), 4.65 (s, 1H), 3.76 (s, 6H).

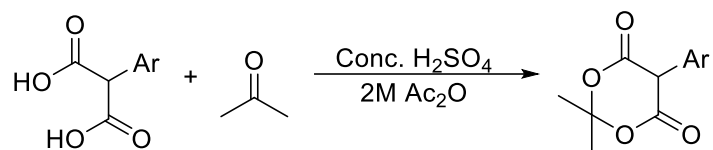
$^{13}\text{C}\{^1\text{H}\}$ NMR Spectra (126 MHz, CDCl_3): δ 168.81, 132.81, 129.58, 128.93, 128.59, 57.84, 53.12.

HRMS: m/z $[\text{M}+\text{H}]^+$ calcd for $\text{C}_{11}\text{H}_{12}\text{O}_4$: 209.0814. Found: 209.0812.

IR: 3063, 3035, 2956, 1960, 1749, 1734, 1500, 1436, 1349, 1302, 1278, 1179, 1150, 1075, 1021, 1008, 936, 912, 731, 705, 697, 598 cm^{-1} .

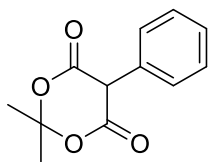
1,3-Dicarbonyl Compounds 1m and S1

General procedure for the synthesis of Meldrum's Acid derivatives 1m and S1⁶



A 50 mL Schlenk flask was flame-dried and equipped with a stir bar. An aryl malonic acid (25 mmol) was dissolved in 12.5 mL Ac₂O at room temperature. Concentrated H₂SO₄ (10 mmol) was added dropwise, and the solid was given time to dissolve. After complete dissolution of the solid material, acetone was added, and the reaction was allowed to stir at room temperature for 12 hours. After 12 hours, the reaction was cooled and filtered, and the precipitate was washed with ice-cold water (10 mL) and dissolved in dichloromethane (10 mL). The solution was washed with brine (15 mL) and dried with MgSO₄. The dried reaction mixture was filtered and concentrated by rotary evaporation. The crude solid was purified by trituration in a 7/3 mixture of hexanes and EtOAc, and the pure precipitate was collected via filtration.

4.10m: 2,2-dimethyl-5-phenyl-1,3-dioxane-4,6-dione



Appearance: Beige solid, 3.47 g, 15.8 mmol, 63% yield.

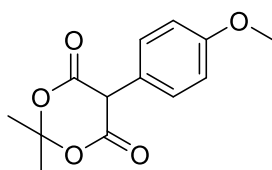
^1H NMR Spectra (500 MHz, CDCl_3): δ 7.45–7.38 (m, 3H), 7.32–7.28 (m, 2H), 4.77 (s, 1H), 1.88 (s, 3H), 1.75 (s, 3H).

$^{13}\text{C}\{^1\text{H}\}$ NMR Spectra (126 MHz, CDCl_3): δ 164.93, 130.77, 129.44, 129.28, 129.10, 105.99, 52.99, 28.82, 27.85.

HRMS: m/z $[\text{M}+\text{H}]^+$ calcd for $\text{C}_{12}\text{H}_{12}\text{O}_4$: 221.0814. Found: 221.0807.

IR: 3003, 2889, 2359, 1781, 1739, 1457, 1320, 1208, 1152, 1068, 1013, 886, 751, 699, 662, 554 cm^{-1} .

S1: 5-(4-methoxyphenyl)-2,2-dimethyl-1,3-dioxane-4,6-dione



Appearance: Yellow-Orange solid, 0.35 g, 1.4 mmol, 45% yield.

^1H NMR Spectra (500 MHz, CDCl_3): δ 7.24–7.17 (m, 2H), 6.97–6.90 (m, 2H), 4.72 (s, 1H), 3.82 (s, 3H), 1.87 (s, 3H), 1.75 (s, 3H).

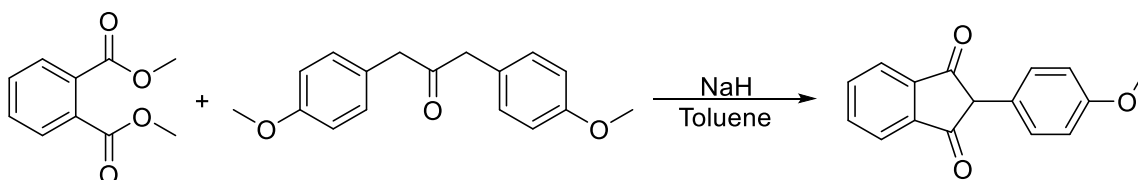
$^{13}\text{C}\{^1\text{H}\}$ NMR Spectra (126 MHz, CDCl_3): δ 165.22, 130.48, 122.57, 114.88, 105.87, 55.58, 52.34, 28.80, 27.77.

HRMS: m/z $[\text{M}+\text{H}]^+$ calcd for $\text{C}_{13}\text{H}_{14}\text{O}_5$: 251.0920. Found: 251.0911.

IR: 3002, 2889, 2359, 1781, 1743, 1616, 1589, 1519, 1395, 1385, 1343, 1317, 1302, 1253, 1218, 1180, 1156, 1070, 1016, 895, 819, 654, 530 cm^{-1} .

1,3-Dicarbonyl Compound S2: 2-(4-methoxyphenyl)-1H-indene-1,3(2H)-dione

General Procedure for the synthesis of diketone S2:



A 250 mL Shlenk flask was flame dried and equipped with a magnetic stir bar. A 0.5M solution of NaH (39 mmol) in dry toluene was made and dimethyl phthalate was added. Then, a 0.5 M solution of 1,3-bis(4-methoxyphenyl)propan-2-one (36 mmol) in dry toluene was added, and the

reaction mixture was heated to a reflux overnight. The residue was filtered, washed with 70 mL toluene and dissolved in water. This aqueous mixture was washed with 70 mL dichloromethane and 70 mL diethyl ether and then acidified dropwise with a 35% solution of HCl. The precipitate was filtered and washed with 50 mL 1M HCl and 50 mL water. This solid was dissolved in dichloromethane and dried with MgSO₄. The dried solution was filtered, concentrated via rotary evaporation, and purified with hot 90% ethanol.

Appearance: red-orange solid, 1.95 g, 7.83 mmol, 22% yield.

¹H NMR Spectra (500 MHz, CDCl₃): δ 8.07 (dd, *J* = 5.7, 3.1 Hz, 2H), 7.90 (dd, *J* = 5.7, 3.0 Hz, 2H), 7.16–7.08 (m, 2H), 6.92–6.84 (m, 2H), 4.21 (s, 1H), 3.79 (s, 3H)

¹³C{¹H} NMR Spectra (126 MHz, CDCl₃): δ 198.64, 159.24, 142.59, 135.95, 129.84, 125.16, 123.74, 114.52, 59.12, 55.30.

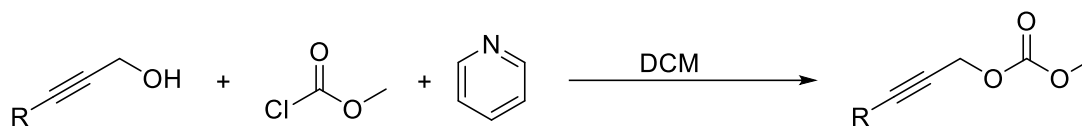
HRMS: *m/z* [M]⁺ calcd for C₁₆H₁₂O₃: 252.0786. Found: 252.0788.

IR: 2966, 2359, 2340, 1746, 1706, 1613, 1586, 1519, 1306, 1259, 1208, 1152, 1068, 1029, 811, 758, 668, 554 cm⁻¹.

3. Preparation and Spectral Data of Starting Propargyl Carbonate Compounds:

Propargyl Carbonates Compounds 4.11a-l:

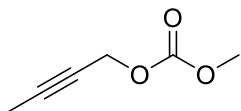
General procedure for the synthesis of propargyl carbonates 4.11a-l:



A 100 mL Schlenk flask was flame dried and equipped with a magnetic stir bar. A propargyl alcohol (10 mmol) was dissolved in dichloromethane (50 mL) and stirred 5 minutes. Pyridine (20 mmol) was added, and the mixture was stirred at room temperature for 10 minutes. The reaction mixture was then cooled to 0 °C, and methyl chloroformate (20 mmol) was added dropwise. The reaction was stirred at 0 °C for one hour and then allowed to warm to room temperature. The

reaction was quenched with 50 mL aqueous saturated NH_4Cl , extracted two times with 50 mL DCM, and washed one time with 50 mL of water and one time with 50 mL of brine. The combined organic layers were dried with MgSO_4 . The dried solution was filtered and concentrated via rotary evaporation. The crude material was purified via flash column chromatography with an eluent of 10% EtOAc in hexanes.

4.11a: but-2-yn-1-yl methyl carbonate



Appearance: Clear liquid, 1.1 g, 8.59 mmol, 86% yield.

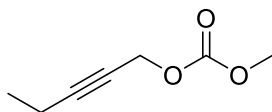
^1H NMR Spectra (500 MHz, CDCl_3): δ 4.70 (q, $J = 2.4$ Hz, 2H), 3.80 (s, 3H), 1.86 (t, $J = 2.4$ Hz, 3H).

$^{13}\text{C}\{^1\text{H}\}$ NMR Spectra (126 MHz, CDCl_3): δ 155.34, 84.04, 72.59, 56.20, 55.02, 3.66.

HRMS: m/z $[\text{M}+\text{NH}_4]^+$ calcd for $\text{C}_6\text{H}_8\text{O}_3$: 146.0187. Found: 146.0182.

IR: 3012, 2959, 2858, 2361, 2340, 2238, 1754, 1446, 1375, 1263, 1209, 1153, 1019, 948, 901, 794 cm^{-1} .

4.11b: methyl pent-2-yn-1-yl carbonate



Appearance: Clear liquid, 0.68 g, 4.78 mmol, 96% yield.

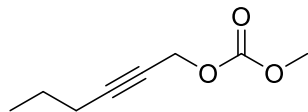
^1H NMR Spectra (500 MHz, CDCl_3): δ 4.72 (t, $J = 2.2$ Hz, 2H), 3.80 (s, 3H), 2.23 (qt, $J = 7.5, 2.2$ Hz, 2H), 1.13 (t, $J = 7.5$ Hz, 3H)

$^{13}\text{C}\{^1\text{H}\}$ NMR Spectra (126 MHz, CDCl_3): δ 155.56, 89.99, 72.95, 56.48, 55.23, 13.70, 12.68.

HRMS: m/z $[\text{M}]^+$ calcd for $\text{C}_7\text{H}_{10}\text{O}_3$: 142.0630. Found: 142.0628.

IR: 2980, 2959, 2882, 2308, 2238, 1754, 1586, 1446, 1376, 1320, 1262, 1150, 1105, 1021, 963, 944 cm^{-1} .

4.11c: hex-2-yn-1-yl methyl carbonate



Appearance: Clear liquid, 0.67 g, 4.29 mmol, 86% yield.

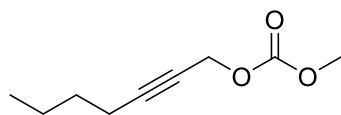
^1H NMR Spectra (500 MHz, CDCl_3): δ 4.72 (t, $J = 2.2$ Hz, 2H), 3.80 (s, 3H), 2.19 (tt, $J = 7.1, 2.2$ Hz, 2H), 1.53 (h, $J = 7.2$ Hz, 2H), 0.97 (t, $J = 7.4$ Hz, 3H)

$^{13}\text{C}\{^1\text{H}\}$ NMR Spectra (126 MHz, CDCl_3): δ 155.56, 88.62, 73.73, 56.51, 55.23, 22.02, 20.96, 13.67.

HRMS: m/z $[\text{M}+\text{H}]^+$ calcd for $\text{C}_{18}\text{H}_{12}\text{O}_3$: 157.0865. Found: 157.0859.

IR: 2963, 2938, 2875, 2237, 1754, 1683, 1584, 1446, 1376, 1339, 1329, 1270, 1150, 1105, 1073, 1031, 1021, 949 cm^{-1} .

4.11d: hept-2-yn-1-yl methyl carbonate



Appearance: Clear liquid, 0.605 g, 3.55 mmol, 71% yield.

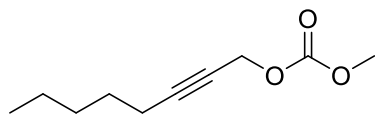
^1H NMR Spectra (500 MHz, CDCl_3): δ 4.72 (t, $J = 2.2$ Hz, 2H), 3.80 (s, 3H), 2.22 (tt, $J = 7.1, 2.2$ Hz, 2H), 1.53–1.46 (m, 2H), 1.46–1.34 (m, 2H), 0.90 (t, $J = 7.3$, 3H)

$^{13}\text{C}\{^1\text{H}\}$ NMR Spectra (126 MHz, CDCl_3): δ 155.32, 88.54, 73.31, 56.29, 55.00, 30.38, 21.89, 18.43, 13.55.

HRMS: m/z $[\text{M}]^+$ calcd for $\text{C}_9\text{H}_{14}\text{O}_3$: 170.0943. Found: 170.0941.

IR: 3490, 2959, 2936, 2873, 2308, 2235, 1754, 1586, 1445, 1376, 1263, 1155, 1106, 1055, 1021, 998, 983, 949 cm^{-1} .

4.11e: methyl oct-2-yn-1-yl carbonate



Appearance: Clear liquid, 0.902 g, 4.9 mmol, 98% yield.

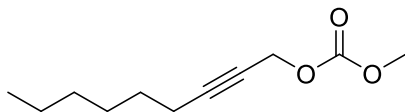
^1H NMR Spectra (500 MHz, CDCl_3): δ 4.72 (t, $J = 2.2$ Hz, 2H), 3.80 (s, 3H), 2.21 (tt, $J = 7.2, 2.2$ Hz, 2H), 1.57–1.46 (m, 2H), 1.40–1.23 (m, 4H), 0.89 (t, $J = 7.1$ Hz, 3H).

$^{13}\text{C}\{^1\text{H}\}$ NMR Spectra (126 MHz, CDCl_3): δ 155.57, 88.86, 73.56, 56.55, 55.24, 31.24, 28.27, 22.41, 18.97, 14.19.

HRMS: m/z $[\text{M}]^+$ calcd for $\text{C}_{10}\text{H}_{16}\text{O}_3$: 184.1099. Found: 184.1094.

IR: 2958, 2935, 2862, 2733, 2655, 2308, 2235, 2158, 1754, 1584, 1445, 1376, 1329, 1269, 1155, 1106, 1064, 1021, 951 cm^{-1} .

4.11f: methyl non-2-yn-1-yl carbonate



Appearance: Clear liquid, 0.925 g, 4.67 mmol, 93% yield.

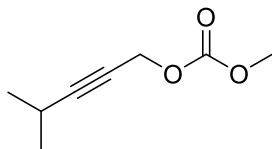
^1H NMR Spectra (500 MHz, CDCl_3): δ 4.72 (t, $J = 2.2$ Hz, 2H), 3.80 (s, 3H), 2.21 (tt, $J = 7.2, 2.2$ Hz, 2H), 1.49 (q, $J = 7.3$ Hz, 2H), 1.40–1.33 (m, 2H), 1.32–1.23 (m, 4H), 0.88 (t, $J = 7.0$ Hz, 3H).

$^{13}\text{C}\{^1\text{H}\}$ NMR Spectra (126 MHz, CDCl_3): δ 155.32, 88.61, 73.31, 56.30, 54.99, 31.29, 28.49, 28.29, 22.52, 18.75, 14.03.

HRMS: m/z $[\text{M}+\text{Na}]^+$ calcd for $\text{C}_{11}\text{H}_{18}\text{O}_3$: 221.1154. Found: 221.1150.

IR: 3587, 2956, 2932, 2859, 2658, 2308, 2235, 2045, 1756, 1586, 1445, 1376, 1262, 1155, 1108, 1021, 948 cm^{-1} .

4.11g: methyl (4-methylpent-2-yn-1-yl) carbonate



Appearance: Clear liquid, 1.15 g, 7.26 mmol, 88% yield.

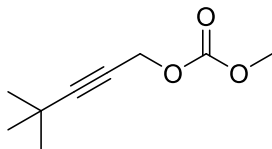
^1H NMR Spectra (500 MHz, CDCl_3): δ 4.72 (d, $J = 2.1$ Hz, 2H), 3.80 (s, 3H), 2.72–2.46 (m, 1H), 1.16 (d, $J = 6.9$ Hz, 6H).

$^{13}\text{C}\{^1\text{H}\}$ NMR Spectra (126 MHz, CDCl_3): δ 155.54, 94.00, 72.78, 56.51, 55.22, 22.85, 20.76.

HRMS: m/z $[\text{M}+\text{Na}]^+$ calcd for $\text{C}_8\text{H}_{12}\text{O}_3$: 179.0684. Found: 179.0679.

IR: 3439, 2973, 2875, 2657, 2568, 2374, 2321, 2261, 2231, 2181, 2047, 1756, 1586, 1445, 1377, 1322, 1189, 1156, 1130, 1108, 1058, 1019, 946 cm^{-1} .

4.11h: 4,4-dimethylpent-2-yn-1-yl methyl carbonate



Appearance: Clear liquid, 0.682 g, 4.00 mmol, 80% yield.

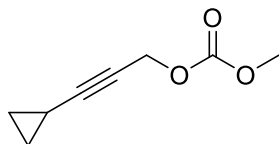
^1H NMR Spectra (500 MHz, CDCl_3): δ 4.72 (s, 2H), 3.80 (s, 3H), 1.22 (s, 9H).

$^{13}\text{C}\{^1\text{H}\}$ NMR Spectra (126 MHz, CDCl_3): δ 155.51, 96.73, 72.07, 56.57, 55.21, 30.93, 27.68.

HRMS: m/z $[\text{M}+\text{H}]^+$ calcd for $\text{C}_9\text{H}_{14}\text{O}_3$: 171.1021. Found: 171.1025.

IR: 2970, 2933, 2903, 2869, 2247, 1756, 1583, 1477, 1446, 1375, 1365, 1260, 1208, 1155, 1112, 1019, 949 cm^{-1} .

4.11i: 3-cyclopropylprop-2-yn-1-yl methyl carbonate



Appearance: Clear liquid, 1.025 g, 6.65 mmol, 83% yield.

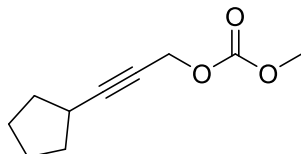
^1H NMR Spectra (500 MHz, CDCl_3): δ 4.68 (d, $J = 2.1$ Hz, 2H), 3.79 (s, 3H), 1.33–1.18 (m, 1H), 0.85–0.74 (m, 2H), 0.74–0.59 (m, 2H).

$^{13}\text{C}\{^1\text{H}\}$ NMR Spectra (126 MHz, CDCl_3): δ 155.53, 91.82, 68.91, 56.53, 55.22, 8.50, -0.33.

HRMS: m/z $[\text{M}]^+$ calcd for $\text{C}_8\text{H}_{10}\text{O}_3$: 154.0630. Found: 154.0628.

IR: 3096, 3012, 2959, 2858, 2367, 2260, 2237, 1751, 1584, 1559, 1445, 1376, 1357, 1259, 1163, 1106, 1055, 1029, 1017, 944 cm^{-1} .

4.11j: 3-cyclopentylprop-2-yn-1-yl methyl carbonate



Appearance: Clear liquid, 0.91 g, 4.99 mmol, 100% yield.

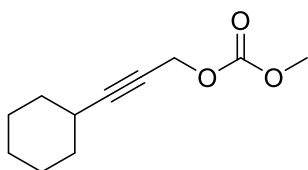
^1H NMR Spectra (500 MHz, CDCl_3): δ 4.73 (d, $J = 2.0$ Hz, 2H), 3.80 (s, 3H), 2.63 (ddt, $J = 9.7, 7.6, 3.8$ Hz, 1H), 1.90 (dttd, $J = 10.1, 5.1, 3.8, 2.0$ Hz, 2H), 1.70 (qdd, $J = 9.3, 4.9, 2.9$ Hz, 2H), 1.65–1.48 (m, 4H)

$^{13}\text{C}\{^1\text{H}\}$ NMR Spectra (126 MHz, CDCl_3): δ 155.65, 93.02, 73.16, 56.74, 55.32, 33.86, 30.41, 25.32.

HRMS: m/z $[\text{M}]^+$ calcd for $\text{C}_{10}\text{H}_{14}\text{O}_3$: 182.0943. Found: 182.0949.

IR: 2959, 2872, 2359, 2240, 1756, 1559, 1445, 1376, 1340, 1212, 1155, 1113, 1021, 952 904 cm^{-1} .

4.11k: 3-cyclohexylprop-2-yn-1-yl methyl carbonate



Appearance: Clear liquid, 0.954 g, 4.86 mmol, 97% yield.

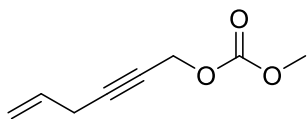
^1H NMR Spectra (500 MHz, CDCl_3): δ 4.74 (d, $J = 2.1$ Hz, 2H), 3.80 (s, 3H), 2.45–2.35 (m, 1H), 1.85–1.75 (m, 2H), 1.69 (ddt, $J = 8.2, 6.0, 3.5$ Hz, 2H), 1.48–1.37 (m, 2H), 1.28 (ddd, $J = 12.1, 7.5, 2.7$ Hz, 2H).

$^{13}\text{C}\{^1\text{H}\}$ NMR Spectra (126 MHz, CDCl_3): δ 155.30, 92.48, 73.22, 56.37, 54.98, 32.31, 29.05, 25.80, 24.80.

HRMS: m/z $[\text{M}+\text{H}]^+$ calcd for $\text{C}_{11}\text{H}_{16}\text{O}_3$: 197.1178. Found: 197.1172.

IR: 3003, 2932, 2856, 2237, 1756, 1716, 1704, 1699, 1694, 1683, 1446, 1376, 1266, 1156, 949, 791, 612 cm^{-1} .

4.11l: hex-5-en-2-yn-1-yl methyl carbonate



Appearance: Yellow liquid, 3.2 g, 20.8 mmol, 83% yield.

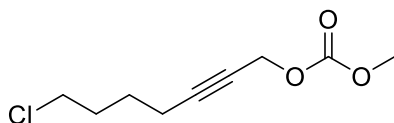
^1H NMR Spectra (500 MHz, CDCl_3): δ 5.79 (ddt, $J = 17.0, 10.3, 5.3$ Hz, 1H), 5.31 (dq, $J = 16.9, 1.8$ Hz, 1H), 5.12 (dq, $J = 9.9, 1.6$ Hz, 1H), 4.76 (t, $J = 2.2$ Hz, 2H), 3.81 (s, 3H), 3.01 (dp, $J = 5.9, 2.0$ Hz, 2H).

$^{13}\text{C}\{^1\text{H}\}$ NMR Spectra (126 MHz, CDCl_3): δ 155.64, 132.04, 116.87, 85.22, 76.10, 56.44, 55.40, 23.39.

HRMS: m/z $[\text{M}+\text{H}]^+$ calcd for $\text{C}_8\text{H}_{10}\text{O}_3$: 155.0708. Found: 155.0702.

IR: 3086, 3016, 2959, 2308, 2242, 1754, 1643, 1446, 1375, 1263, 1153, 1108, 1051, 1019, 992, 949 cm^{-1} .

4.11m: 7-chlorohept-2-yn-1-yl methyl carbonate



Appearance: Yellow liquid, 1.67 g, 8.16 mmol, 81% yield.

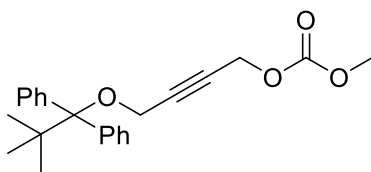
^1H NMR Spectra (500 MHz, CDCl_3): δ 4.72 (t, $J = 2.2$ Hz, 2H), 3.81 (s, 3H), 3.56 (t, $J = 6.5$ Hz, 2H), 2.28 (tt, $J = 7.0, 2.4$ Hz, 2H), 1.88 (p, $J = 6.7$ Hz, 2H), 1.74–1.61 (m, 2H).

$^{13}\text{C}\{^1\text{H}\}$ NMR Spectra (126 MHz, CDCl_3): δ 155.63, 87.81, 74.45, 56.47, 55.40, 44.79, 31.79, 25.79, 18.41.

HRMS: m/z $[\text{M}+\text{Na}]^+$ calcd for $\text{C}_9\text{H}_{13}\text{ClO}_3$: 227.0451. Found: 227.0458.

IR: 3002, 2956, 2868, 2359, 2235, 1759, 1584, 1445, 1376, 1278, 1155, 1105, 1021, 949, 901, 791, 739, 651, 597, 554, 507 cm^{-1} .

4.11n: 4-((tert-butyl)diphenylsilyloxy)but-2-yn-1-yl methyl carbonate



Appearance: Orange liquid, 2.2 g, 5.75 mmol, 88% yield.

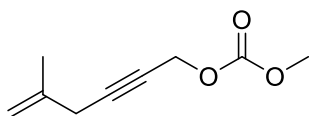
^1H NMR Spectra (500 MHz, CDCl_3): δ 7.75–7.65 (m, 4H), 7.47–7.33 (m, 6H), 4.72 (t, $J = 1.9$ Hz, 2H), 4.34 (t, $J = 1.8$ Hz, 2H), 3.81 (s, 3H), 1.06 (s, 9H).

$^{13}\text{C}\{^1\text{H}\}$ NMR Spectra (126 MHz, CDCl_3): δ 155.22, 135.54, 132.88, 129.91, 127.73, 85.95, 78.49, 55.82, 55.18, 52.47, 26.68, 19.27, -14.74.

HRMS: m/z $[\text{M}+\text{Na}]^+$ calcd for $\text{C}_{23}\text{H}_{26}\text{O}_4$: 389.1729. Found: 389.1739.

IR: 3030, 2958, 2932, 2859, 2362, 1756, 1445, 1429, 1375, 1266, 1210, 1152, 1113, 1078, 998, 955, 824, 791, 739, 702, 614, 504 cm^{-1} .

4.11o: methyl (5-methylhex-5-en-2-yn-1-yl) carbonate



Appearance: Yellow liquid, 0.68 g, 4.04 mmol, 81% yield.

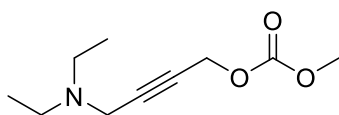
^1H NMR Spectra (500 MHz, CDCl_3): δ 5.00–4.96 (m, 1H), 4.84 (p, $J = 1.6$ Hz, 1H), 4.76 (t, $J = 2.2$ Hz, 2H), 3.81 (s, 3H), 2.94 (t, $J = 1.8$ Hz, 2H), 1.78 (s, 3H).

$^{13}\text{C}\{^1\text{H}\}$ NMR Spectra (126 MHz, CDCl_3): δ 155.65, 140.15, 112.37, 85.66, 76.04, 56.48, 55.39, 27.84, 22.39.

HRMS: m/z $[\text{M}+\text{Li}]^+$ calcd for $\text{C}_9\text{H}_{12}\text{O}_3$: 175.0947. Found: 175.0948.

IR: 3083, 2958, 2888, 2858, 2732, 2655, 2305, 2235, 2047, 1756, 1657, 1584, 1445, 1375, 1259, 1150, 1105, 1021, 948 cm^{-1} .

4.11p: 4-(diethylamino)but-2-yn-1-yl methyl carbonate



Appearance: Yellow liquid, 0.939 g, 4.7 mmol, 47% yield.

^1H NMR Spectra (500 MHz, CDCl_3): δ 4.76 (t, $J = 1.9$ Hz, 2H), 3.81 (s, 3H), 3.45 (t, $J = 2.0$ Hz, 2H), 2.53 (q, $J = 7.2$ Hz, 4H), 1.05 (t, $J = 7.2$ Hz, 6H).

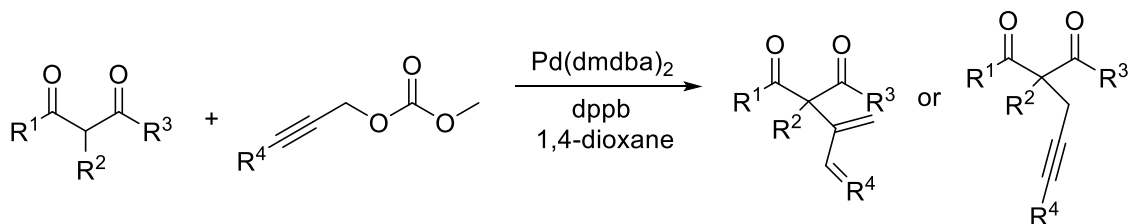
$^{13}\text{C}\{^1\text{H}\}$ NMR Spectra (126 MHz, CDCl_3): δ 155.58, 83.16, 78.27, 56.26, 55.41, 47.55, 41.25, 12.94.

HRMS: m/z $[\text{M}]^+$ calcd for $\text{C}_{10}\text{H}_{17}\text{NO}_3$: 199.1208. Found: 199.1203.

IR: 2971, 2821, 1756, 1446, 1375, 1263, 1209, 1155, 1122, 1091, 1061, 1021, 952, 901, 791, 619, 504 cm^{-1} .

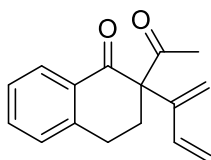
4. General Procedure and Spectral Data of Dienylated and Propargylated Products (Project 1)

General Procedure for the Dienylation and Propargylation of 1,3-Dicarbonyl Compounds 4.12a-n and 4.13a-ll



A Biotage microwave reaction vial (part no. 354624) was flame dried, equipped with a magnetic stir bar, and brought into a glovebox under an argon atmosphere. Inside of the glovebox, catalyst (10 mol% Pd(dmdba)₂), ligand (10 mol% dppb), a 1,3-dicarbonyl compound (0.24 mmol), and a propargyl carbonate (0.24 mmol) were added to the reaction vial and dissolved in 1.5 mL 1,4-dioxane. The reaction vial was sealed, removed from the glovebox, and placed in an oil bath heated to 80 °C. The reaction vial was stirred at 80 °C for 2 hours, after which the vial was unsealed. The solvent was removed via rotary evaporation, and the crude product was purified and isolated via column chromatography using an eluant of 10% EtOAc in hexanes.

4.12a: 2-acetyl-2-(buta-1,3-dien-2-yl)-3,4-dihydronaphthalen-1(2H)-one



Appearance: Yellow oil, 0.027 g, 0.112 mmol, 47% yield.

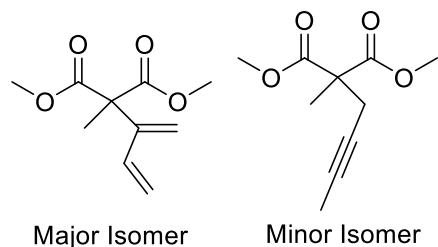
¹H NMR Spectra (500 MHz, CDCl₃): δ 8.03 (dd, *J* = 7.9, 1.3 Hz, 1H), 7.47 (td, *J* = 7.5, 1.4 Hz, 1H), 7.31 (t, *J* = 7.3 Hz, 1H), 7.19 (d, *J* = 7.6 Hz, 1H), 6.26–6.15 (m, 1H), 5.46 (s, 1H), 5.35 (d, *J* = 17.4 Hz, 1H), 5.16 (d, *J* = 11.1 Hz, 1H), 4.86 (s, 1H), 2.90–2.78 (m, 2H), 2.62 (ddd, *J* = 14.2, 10.4, 5.8 Hz, 1H), 2.44–2.30 (m, 4H).

¹³C{¹H} NMR Spectra (126 MHz, CDCl₃): δ 207.88, 197.21, 143.74, 143.55, 136.01, 134.01, 132.69, 129.04, 128.03, 127.15, 118.96, 117.31, 68.24, 29.56, 29.15, 25.83.

HRMS: *m/z* [M+H]⁺ calcd for C₁₆H₁₆O₂: 241.1229. Found: 241.1223.

IR: 3090, 2928, 2853, 2359, 2344, 1713, 1676, 1599, 1455, 1430, 1352, 1296, 1206, 1152, 992, 912, 898, 784, 764, 738, 659 cm⁻¹.

4.12b: dimethyl-2-(buta-1,3-dien-2-yl)-2-methylmalonate



Isolated as a mixture of isomers:

Appearance: Clear oil, 0.02 g, 0.101 mmol, 42% yield.

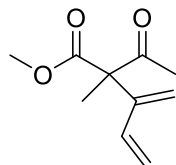
^1H NMR Spectra (500 MHz, CDCl_3) *major isomer*: δ 6.28 (dd, $J = 17.4, 11.0$ Hz, 1H), 5.42 (s, 1H), 5.37 (dd, $J = 17.2, 1.2$ Hz, 1H), 5.10 (dd, $J = 11.0, 1.1$ Hz, 1H), 5.00 (s, 1H), 3.74 (d, $J = 9.8$ Hz, 6H), 1.65 (s, 3H).

$^{13}\text{C}\{^1\text{H}\}$ NMR Spectra (126 MHz, CDCl_3): δ 171.72, 145.19, 136.16, 116.20, 114.62, 59.15, 53.10, 21.54.

HRMS: m/z $[\text{M}]^+$ calcd for $\text{C}_{10}\text{H}_{14}\text{O}_4$: 198.0892. Found: 198.0889.

IR: 2999, 2953, 2853, 2337, 1733, 1456, 1436, 1260, 1206, 1152, 1115, 554 cm^{-1} .

4.12c: methyl-2-acetyl-2-methyl-3-methylenepent-4-enoate



Appearance: Clear oil, 0.019 g, 0.104 mmol, 44% yield.

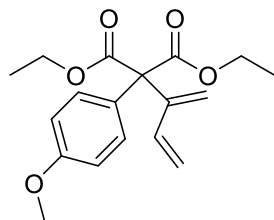
^1H NMR Spectra (500 MHz, CDCl_3): δ 6.22 (dd, $J = 17.4, 11.1$ Hz, 1H), 5.46 (s, 1H), 5.35 (dd, $J = 17.3, 1.1$ Hz, 1H), 5.11 (d, $J = 11.0$ Hz, 1H), 5.04 (s, 1H), 3.75 (d, $J = 0.8$ Hz, 3H), 2.23 (d, $J = 1.0$ Hz, 3H), 1.56 (d, $J = 1.0$ Hz, 3H).

$^{13}\text{C}\{^1\text{H}\}$ NMR Spectra (126 MHz, CDCl_3): δ 205.47, 172.29, 145.60, 136.17, 116.73, 115.81, 64.89, 52.84, 27.48, 20.38.

HRMS: m/z $[\text{M}]^+$ calcd for $\text{C}_{10}\text{H}_{14}\text{O}_3$: 182.0943. Found: 182.0942.

IR: 3090, 2996, 2952, 2925, 2369, 2314, 1734, 1716, 1456, 1435, 1356, 1259, 1206, 1152, 1123, 1096, 985, 914 cm^{-1} .

4.12d: diethyl 2-(buta-1,3-dien-2-yl)-2-(4-methoxyphenyl)malonate



Appearance: Clear oil, 0.75 g, 0.23 mmol, 96% yield.

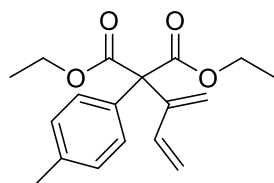
^1H NMR Spectra (500 MHz, CDCl_3): δ 7.45–7.33 (m, 2H), 6.88–6.82 (m, 2H), 6.16 (dd, $J = 17.4$, 11.1 Hz, 1H), 5.64 (s, 1H), 5.32 (s, 1H), 5.25 (dd, $J = 17.4$, 0.9 Hz, 1H), 4.99 (d, $J = 11.0$ Hz, 1H), 4.25 (qd, $J = 7.1$, 0.8 Hz, 4H), 3.80 (d, $J = 0.8$ Hz, 3H), 1.26 (td, $J = 7.1$, 0.8 Hz, 6H).

$^{13}\text{C}\{^1\text{H}\}$ NMR Spectra (126 MHz, CDCl_3): δ 169.81, 159.23, 144.26, 136.92, 130.89, 129.73, 128.46, 117.46, 115.75, 113.62, 62.12, 55.54, 14.26.

HRMS: m/z $[\text{M}]^+$ calcd for $\text{C}_{18}\text{H}_{22}\text{O}_5$: 318.1467. Found: 318.1475.

IR: 3060, 2980, 2936, 2839, 1731, 1653, 1610, 1577, 1513, 1464, 1366, 1299, 1252, 1186, 1158, 1095, 1035, 924, 861, 836, 796, 767, 701, 554, 535 cm^{-1} .

4.12e: diethyl-2-(buta-1,3-dien-2-yl)-2-(*p*-tolyl)malonate



Appearance: Clear oil, 0.066 g, 0.216 mmol, 90% yield.

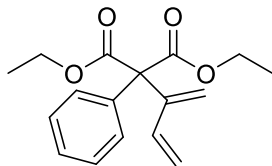
^1H NMR Spectra (500 MHz, CDCl_3): δ 7.40–7.31 (m, 2H), 7.13 (d, $J = 8.1$ Hz, 2H), 6.16 (dd, $J = 17.4$, 11.0 Hz, 1H), 5.64 (s, 1H), 5.30 (s, 1H), 5.26 (dd, $J = 17.4$, 1.0 Hz, 1H), 4.98 (dd, $J = 11.0$, 1.0 Hz, 1H), 4.25 (q, $J = 7.1$ Hz, 4H), 2.33 (s, 3H), 1.26 (t, $J = 7.1$ Hz, 6H).

$^{13}\text{C}\{^1\text{H}\}$ NMR Spectra (126 MHz, CDCl_3): δ 169.74, 144.29, 137.74, 136.96, 133.48, 129.52, 129.00, 117.42, 115.67, 77.56, 62.13, 21.38, 14.27.

HRMS: m/z $[\text{M}]^+$ calcd for $\text{C}_{18}\text{H}_{22}\text{O}_4$: 302.1518. Found: 302.1526.

IR: 3028, 2982, 2936, 1733, 1514, 1446, 1366, 1248, 1208, 1153, 1095, 1039, 1021, 861, 806, 764, 554 cm^{-1} .

4.12f: diethyl-2-(buta-1,3-dien-2-yl)-2-phenylmalonate



Appearance: Clear oil, 0.053 g, 0.185 mmol, 77% yield.

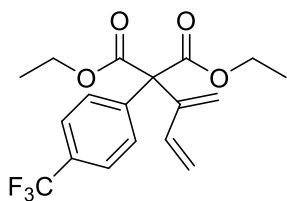
^1H NMR Spectra (500 MHz, CDCl_3): δ 7.47 (dd, $J = 7.2, 2.0$ Hz, 2H), 7.37–7.27 (m, 3H), 6.17 (dd, $J = 17.4, 11.0$ Hz, 1H), 5.65 (s, 1H), 5.30 (s, 1H), 5.25 (dd, $J = 17.5, 1.0$ Hz, 1H), 4.99 (d, $J = 11.2$ Hz, 1H), 4.26 (q, $J = 7.1$ Hz, 4H), 1.26 (t, $J = 7.1$ Hz, 6H).

$^{13}\text{C}\{^1\text{H}\}$ NMR Spectra (126 MHz, CDCl_3): δ 169.61, 144.20, 136.91, 136.49, 129.68, 128.25, 128.00, 117.64, 115.80, 77.56, 62.19, 14.25.

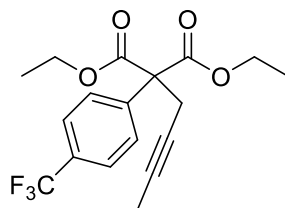
HRMS: m/z $[\text{M}+\text{H}]^+$ calcd for $\text{C}_{17}\text{H}_{20}\text{O}_4$: 289.1440. Found: 289.1446.

IR: 3060, 2982, 2938, 2905, 2359, 1731, 1497, 1447, 1389, 1366, 1298, 1243, 1156, 1095, 1043, 1031, 861, 754, 727, 698, 611 cm^{-1} .

4.12g: diethyl-2-(buta-1,3-dien-2-yl)-2-(4-(trifluoromethyl)phenyl)malonate



Major Isomer



Minor Isomer

Isolated as mixture of isomers.

Appearance: Yellow oil, 0.056 g, 0.157 mmol, 66% yield.

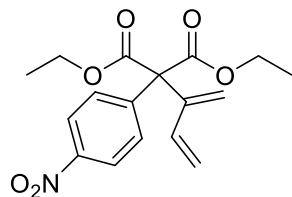
^1H NMR Spectra (500 MHz, CDCl_3) *Major isomer*: δ 7.64 (d, $J = 8.3$ Hz, 2H), 7.58 (d, $J = 8.4$ Hz, 2H), 6.15 (dd, $J = 17.4, 11.1$ Hz, 1H), 5.69 (s, 1H), 5.37 (s, 1H), 5.19 (d, $J = 17.4$ Hz, 1H), 5.01 (d, $J = 11.2$ Hz, 1H), 4.31–4.22 (m, 4H), 1.26 (td, $J = 7.1, 0.9$ Hz, 6H).

$^{13}\text{C}\{^1\text{H}\}$ NMR Spectra (126 MHz, CDCl_3) *Major isomer*: δ 169.08, 143.40, 140.44, 136.52, 130.25, 129.15, 125.13, 125.07, 118.56, 116.51, 77.56, 62.36, 14.22.

HRMS: m/z $[\text{M}]^+$ calcd for $\text{C}_{18}\text{H}_{19}\text{O}_3$: 356.1235. Found: 356.1225.

IR: 3481, 2985, 2940, 2908, 2359, 1736, 1620, 1466, 1447, 1413, 1390, 1367, 1327, 1300, 1247, 1208, 1169, 1123, 1096, 1071, 1039, 1019, 859, 846, 767, 715, 668, 602, 508 cm^{-1} .

4.12h: diethyl-2-(buta-1,3-dien-2-yl)-2-(4-nitrophenyl)malonate



Appearance: Clear oil, 0.038 g, 0.114 mmol, 48% yield.

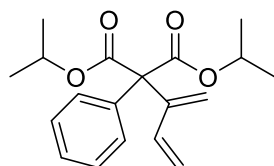
^1H NMR Spectra (500 MHz, CDCl_3): δ 8.19–8.15 (m, 2H), 7.78–7.68 (m, 2H), 6.15 (dd, $J = 17.5$, 11.1 Hz, 1H), 5.71 (s, 1H), 5.40 (s, 1H), 5.13 (d, $J = 17.5$ Hz, 1H), 5.01 (d, $J = 11.1$ Hz, 1H), 4.27 (q, $J = 7.2$ Hz, 4H), 1.26 (t, $J = 7.1$ Hz, 6H).

$^{13}\text{C}\{^1\text{H}\}$ NMR Spectra (126 MHz, CDCl_3): δ 168.70, 147.55, 143.66, 142.98, 136.33, 130.99, 130.81, 123.23, 119.18, 116.93, 62.76, 14.20.

HRMS: m/z $[\text{M}+\text{Na}]^+$ calcd for $\text{C}_{17}\text{H}_{19}\text{O}_6$: 356.1110. Found: 356.1101.

IR: 3083, 2982, 2939, 2364, 1734, 1607, 1597, 1523, 1496, 1350, 1298, 1249, 1208, 1153, 1112, 1096, 1035, 858, 751, 734, 699, 554 cm^{-1} .

4.12i: diisopropyl-2-(buta-1,3-dien-2-yl)-2-phenylmalonate



Appearance: Yellow oil, 0.047 g, 0.0149 mmol, 62% yield.

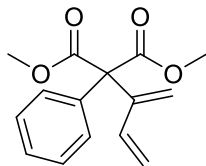
^1H NMR Spectra (500 MHz, CDCl_3): δ 7.50–7.46 (m, 2H), 7.34–7.27 (m, 3H), 6.17 (dd, $J = 17.4$, 11.0 Hz, 1H), 5.65 (s, 1H), 5.35 (s, 1H), 5.25 (dt, $J = 17.4$, 0.9 Hz, 1H), 5.11 (dq, $J = 12.6$, 6.3 Hz, 2H), 4.97 (d, $J = 11.1$ Hz, 1H), 1.24 (d, $J = 6.4$ Hz, 12H).

$^{13}\text{C}\{^1\text{H}\}$ NMR Spectra (126 MHz, CDCl_3): δ 169.07, 144.23, 137.05, 136.74, 129.77, 128.12, 127.86, 117.59, 115.63, 77.56, 69.86, 21.79.

HRMS: m/z $[\text{M}+\text{H}]^+$ calcd for $\text{C}_{19}\text{H}_{24}\text{O}_4$: 317.1753. Found: 317.1747.

IR: 3060, 2982, 2936, 2880, 1787, 1729, 1497, 1466, 1449, 1387, 1375, 1255, 1212, 1182, 1155, 1105, 1035, 975, 905, 697 cm^{-1} .

4.12j: dimethyl-2-(buta-1,3-dien-2-yl)-2-phenylmalonate



Appearance: Clear oil, 0.051 g, 0.197 mmol, 82% yield.

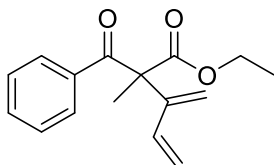
^1H NMR Spectra (500 MHz, CDCl_3): δ 7.49–7.40 (m, 2H), 7.38–7.27 (m, 3H), 6.22–6.13 (m, 1H), 5.66 (d, $J = 0.8$ Hz, 1H), 5.26 (s, 1H), 5.23 (dd, $J = 17.5, 0.9$ Hz, 1H), 5.00 (d, $J = 11.1$ Hz, 1H), 3.79 (s, 6H).

$^{13}\text{C}\{^1\text{H}\}$ NMR Spectra (126 MHz, CDCl_3): δ 170.13, 143.99, 136.79, 136.22, 129.57, 128.35, 128.12, 118.02, 115.98, 53.24, 31.27.

HRMS: m/z $[\text{M}+\text{NH}_4]^+$ calcd for $\text{C}_{15}\text{H}_{16}\text{O}_4$: 278.1392. Found: 278.1389.

IR: 3060, 3003, 2953, 2849, 1736, 1597, 1493, 1447, 1433, 1250, 1209, 1153, 1088, 1045, 1006, 921, 755, 728, 699 cm^{-1} .

4.12k: ethyl-2-benzoyl-2-methyl-3-methylenepent-4-enoate



Appearance: Clear oil, 0.035 g, 0.135 mmol, 57% yield.

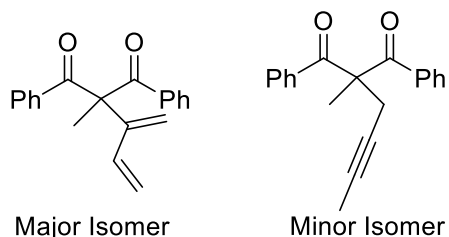
^1H NMR Spectra (500 MHz, CDCl_3): δ 7.96–7.83 (m, 2H), 7.57–7.45 (m, 1H), 7.37 (t, $J = 7.7$ Hz, 2H), 6.35 (dd, $J = 5, 17.2, 10.9$ Hz, 1H), 5.51 (s, 1H), 5.40 (dd, $J = 17.3, 1.2$ Hz, 1H), 5.19 (s, 1H), 5.05 (dd, $J = 10.9, 1.3$ Hz, 1H), 4.20–4.02 (m, 2H), 1.73 (d, $J = 0.9$ Hz, 3H), 1.07 (td, $J = 7.2, 0.8$ Hz, 3H).

$^{13}\text{C}\{^1\text{H}\}$ NMR Spectra (126 MHz, CDCl_3): δ 197.65, 172.22, 147.12, 136.56, 136.36, 132.92, 129.59, 128.45, 116.43, 114.86, 62.94, 61.78, 23.33, 14.03.

HRMS: m/z $[\text{M}+\text{H}]^+$ calcd for $\text{C}_{16}\text{H}_{18}\text{O}_3$: 259.1334. Found: 259.1339.

IR: 3089, 2982, 2936, 2364, 2345, 1736, 1686, 1597, 1449, 1375, 1262, 1208, 1153, 1109, 1018, 966, 914, 692, 554 cm^{-1} .

4.12l: 2-(buta-1,3-dien-2-yl)-2-methyl-1,3-diphenylpropane-1,3-dione



Isolated as mixture of isomers.

Appearance: Yellow oil, 0.052 g, 0.178 mmol, 74% yield.

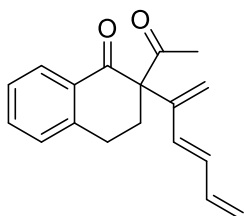
^1H NMR Spectra (500 MHz, CDCl_3) *Major isomer*: δ 7.82 (dd, $J = 8.1, 1.5$ Hz, 4H), 7.47–7.42 (m, 2H), 7.34 (dd, $J = 9.5, 6.0$ Hz, 4H), 6.41 (dd, $J = 17.1, 10.8$ Hz, 1H), 5.60 (d, $J = 0.9$ Hz, 1H), 5.46 (dd, $J = 17.2, 1.4$ Hz, 1H), 5.11 (dd, $J = 10.8, 1.4$ Hz, 1H), 5.03 (s, 1H), 1.84 (s, 3H).

$^{13}\text{C}\{^1\text{H}\}$ NMR Spectra (126 MHz, CDCl_3) *Minor isomer*: δ 200.44, 148.77, 137.06, 132.88, 129.87, 129.32, 128.99, 128.59, 116.34, 115.72, 24.32.

HRMS: m/z $[\text{M}+\text{H}]^+$ calcd for $\text{C}_{20}\text{H}_{18}\text{O}_2$: 291.1385. Found: 291.1375.

IR: 3062, 2929, 2358, 1721, 1683, 1667, 1596, 1580, 1447, 1377, 1317, 1263, 1209, 1153, 1071, 1026, 1002, 962, 769, 704, 617 cm^{-1} .

4.12m: (*E*)-2-acetyl-2-(hexa-1,3,5-trien-2-yl)-3,4-dihydronaphthalen-1(2*H*)-one



Appearance: Yellow oil, 0.31 g, 0.115 mmol, 48% yield.

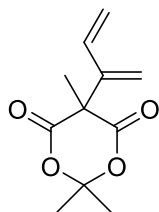
^1H NMR Spectra (500 MHz, CDCl_3): δ 8.03 (d, $J = 8.0$ Hz, 1H), 7.47 (td, $J = 7.5, 1.3$ Hz, 1H), 7.31 (t, $J = 7.6$ Hz, 1H), 7.19 (d, $J = 7.6$ Hz, 1H), 6.42–6.28 (m, 2H), 6.05 (d, $J = 14.6$ Hz, 1H), 5.48 (s, 1H), 5.31–5.25 (m, 1H), 5.20–5.14 (m, 1H), 4.86 (s, 1H), 2.89–2.80 (m, 2H), 2.63 (ddd, $J = 14.2, 10.5, 5.7$ Hz, 1H), 2.39 (s, 4H).

$^{13}\text{C}\{^1\text{H}\}$ NMR Spectra (126 MHz, CDCl_3): δ 208.06, 197.21, 143.75, 142.78, 136.92, 134.03, 132.74, 132.57, 131.38, 129.04, 128.04, 127.18, 119.48, 118.62, 68.42, 29.61, 29.29, 25.89.

HRMS: m/z $[\text{M}+\text{H}]^+$ calcd for $\text{C}_{18}\text{H}_{18}\text{O}_2$: 266.1385. Found: 266.1385.

IR: 3056, 2925, 2359, 1709, 1673, 1599, 1556, 1486, 1453, 1430, 1353, 1295, 1208, 1153, 1033, 971, 898, 741, 622 cm^{-1} .

4.12n: 5-(buta-1,3-dien-2-yl)-2,2,5-trimethyl-1,3-dioxane-4,6-dione



Appearance: Clear oil, 0.017 g, 0.082 mmol, 34% yield.

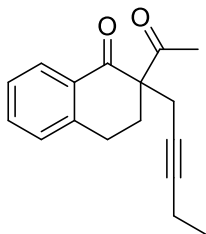
^1H NMR Spectra (500 MHz, CDCl_3): δ 6.34 (dd, $J = 17.1, 10.9$ Hz, 1H), 5.53 (s, 1H), 5.48 (dd, $J = 17.1, 1.0$ Hz, 1H), 5.27–5.20 (m, 2H), 1.76 (d, $J = 3.5$ Hz, 9H).

$^{13}\text{C}\{^1\text{H}\}$ NMR Spectra (126 MHz, CDCl_3): δ 167.49, 144.44, 133.41, 118.80, 115.81, 105.96, 54.99, 29.82, 28.16, 23.68.

HRMS: m/z $[\text{M}]^+$ calcd for $\text{C}_{11}\text{H}_{14}\text{O}_4$: 210.0892. Found: 210.0886.

IR: 2999, 2925, 2855, 2361, 1777, 1743, 1457, 1393, 1380, 1292, 1205, 1153, 1066, 976 cm^{-1} .

4.13a: 2-acetyl-2-(pent-2-yn-1-yl)-3,4-dihydronaphthalen-1(2H)-one



Appearance: Yellow oil, 0.015 g, 0.06 mmol, 25% yield.

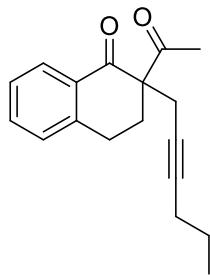
^1H NMR Spectra (500 MHz, CDCl_3): δ 8.03 (dd, $J = 7.9, 1.3$ Hz, 1H), 7.49 (td, $J = 7.5, 1.4$ Hz, 1H), 7.31 (t, $J = 7.6$ Hz, 1H), 7.22 (d, $J = 7.7$ Hz, 1H), 3.17 (ddd, $J = 17.5, 10.4, 4.9$ Hz, 1H), 2.99–2.91 (m, 2H), 2.75 (dt, $J = 13.7, 4.9$ Hz, 1H), 2.68 (dt, $J = 17.0, 2.5$ Hz, 1H), 2.22–2.14 (m, 4H), 2.11 (qt, $J = 7.5, 2.4$ Hz, 2H), 1.06 (t, $J = 7.5$ Hz, 3H).

$^{13}\text{C}\{^1\text{H}\}$ NMR Spectra (126 MHz, CDCl_3): δ 205.00, 196.70, 144.29, 134.34, 132.07, 129.29, 128.26, 127.08, 85.77, 74.36, 63.43, 29.72, 27.34, 26.13, 25.46, 14.40, 12.74.

HRMS: m/z $[\text{M}+\text{H}]^+$ calcd for $\text{C}_{17}\text{H}_{18}\text{O}_2$: 255.1385. Found: 255.1378.

IR: 3066, 2975, 2935, 2361, 1713, 1676, 1600, 1455, 1356, 1319, 1209, 1155, 962, 929, 901, 769, 739, 608 cm^{-1} .

4.13b: 2-acetyl-2-(hex-2-yn-1-yl)-3,4-dihydronaphthalen-1(2H)-one



Appearance: Yellow oil, 0.016 g, 0.06 mmol, 25% yield.

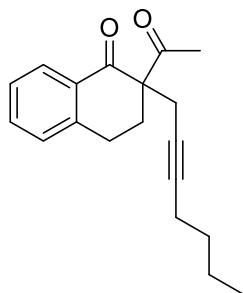
^1H NMR Spectra (500 MHz, CDCl_3): δ 8.03 (dd, $J = 8.0, 1.3$ Hz, 1H), 7.48 (td, $J = 7.5, 1.4$ Hz, 1H), 7.30 (t, $J = 7.6$ Hz, 1H), 7.24–7.20 (m, 1H), 3.17 (ddd, $J = 17.7, 10.4, 4.9$ Hz, 1H), 3.00–2.91 (m, 2H), 2.75 (dt, $J = 13.7, 4.9$ Hz, 1H), 2.68 (dt, $J = 16.8, 2.5$ Hz, 1H), 2.25–2.13 (m, 4H), 2.08 (tt, $J = 7.1, 2.5$ Hz, 2H), 1.45 (h, $J = 7.2$ Hz, 2H), 0.91 (dd, $J = 7.7, 7.1$ Hz, 3H).

$^{13}\text{C}\{^1\text{H}\}$ NMR Spectra (126 MHz, CDCl_3): δ 204.99, 196.69, 144.29, 134.33, 132.04, 129.29, 128.26, 127.07, 84.28, 75.11, 63.45, 29.72, 27.33, 26.13, 25.53, 22.61, 21.05, 13.75.

HRMS: m/z $[\text{M}]^+$ calcd for $\text{C}_{18}\text{H}_{20}\text{O}_2$: 268.1463. Found: 268.1458.

IR: 3025, 2960, 2932, 2872, 2359, 2344, 1713, 1676, 1600, 1456, 1356, 1310, 1208, 1153, 904, 739 cm^{-1} .

4.13c: 2-acetyl-2-(hept-2-yn-1-yl)-3,4-dihydronaphthalen-1(2H)-one



Appearance: Yellow oil, 0.023 g, 0.082 mmol, 34% yield.

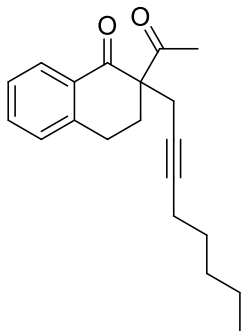
^1H NMR Spectra (500 MHz, CDCl_3): δ 8.03 (dd, $J = 7.9, 1.3$ Hz, 1H), 7.48 (td, $J = 7.5, 1.4$ Hz, 1H), 7.30 (t, $J = 7.6$ Hz, 1H), 7.22 (d, $J = 7.7$ Hz, 1H), 3.16 (ddd, $J = 17.2, 10.4, 4.9$ Hz, 1H), 2.95 (ddd, $J = 17.4, 4.9, 2.3$ Hz, 2H), 2.79–2.65 (m, 2H), 2.25–2.14 (m, 4H), 2.10 (tt, $J = 7.1, 2.5$ Hz, 2H), 1.44–1.36 (m, 2H), 1.36–1.29 (m, 2H), 0.86 (t, $J = 7.2$ Hz, 3H).

$^{13}\text{C}\{^1\text{H}\}$ NMR Spectra (126 MHz, CDCl_3): δ 205.00, 196.68, 144.27, 134.31, 132.05, 129.27, 128.24, 127.06, 84.38, 74.94, 63.45, 31.23, 29.73, 27.33, 26.12, 25.53, 22.19, 18.71, 13.90.

HRMS: m/z $[\text{M}+\text{Na}]^+$ calcd for $\text{C}_{19}\text{H}_{22}\text{O}_2$: 305.1518. Found: 305.1517.

IR: 2956, 2929, 2857, 1713, 1674, 1533, 1520, 1456, 1436, 1356, 1310, 1292, 1208, 1155, 902, 751, 739, 668, 552, 502 cm^{-1} .

4.13d: 2-acetyl-2-(oct-2-yn-1-yl)-3,4-dihydronaphthalen-1(2H)-one



Appearance: Yellow oil, 0.022 g, 0.074 mmol, 31% yield.

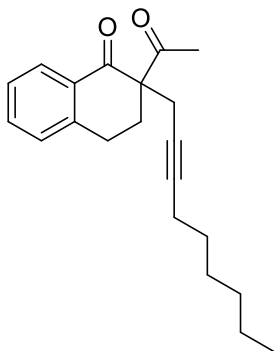
^1H NMR Spectra (500 MHz, CDCl_3): δ 8.03 (dd, $J = 7.9, 1.4$ Hz, 1H), 7.48 (td, $J = 7.5, 1.3$ Hz, 1H), 7.30 (t, $J = 7.6$ Hz, 1H), 7.22 (s, 1H), 3.16 (ddd, $J = 17.5, 10.4, 4.9$ Hz, 1H), 2.99–2.91 (m, 2H), 2.78–2.66 (m, 2H), 2.25–2.12 (m, 4H), 2.10 (td, $J = 7.0, 3.3$ Hz, 2H), 1.41 (q, $J = 6.8, 6.4$ Hz, 2H), 1.30–1.25 (m, 4H), 0.86 (td, $J = 7.0, 1.3$ Hz, 3H).

$^{13}\text{C}\{^1\text{H}\}$ NMR Spectra (126 MHz, CDCl_3): δ 205.02, 196.69, 144.28, 134.32, 132.06, 129.28, 128.26, 127.07, 84.45, 74.97, 63.47, 31.31, 29.74, 28.84, 27.35, 26.13, 25.54, 22.49, 19.00, 14.31.

HRMS: m/z $[\text{M}]^+$ calcd for $\text{C}_{20}\text{H}_{24}\text{O}_2$: 296.1776. Found: 296.1783.

IR: 2929, 2858, 2337, 1713, 1677, 1206, 1152, 902, 554 cm^{-1} .

4.13e: 2-acetyl-2-(non-2-yn-1-yl)-3,4-dihydronaphthalen-1(2H)-one



Appearance: Yellow oil, 0.020 g, 0.065 mmol, 27% yield.

^1H NMR Spectra (500 MHz, CDCl_3): δ 8.03 (dd, $J = 7.9, 1.4$ Hz, 1H), 7.48 (td, $J = 7.5, 1.4$ Hz, 1H), 7.30 (t, $J = 7.6$ Hz, 1H), 3.16 (ddd, $J = 17.1, 10.4, 4.9$ Hz, 1H), 3.00–2.88 (m, 2H), 2.80–2.66

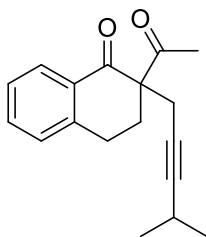
(m, 2H), 2.26–2.14 (m, 4H), 2.09 (tt, $J = 7.0, 2.3$ Hz, 2H), 1.40 (q, $J = 7.2$ Hz, 2H), 1.33–1.21 (m, 6H).

$^{13}\text{C}\{^1\text{H}\}$ NMR Spectra (126 MHz, CDCl_3): δ 204.66, 196.35, 143.93, 133.97, 131.71, 128.93, 127.91, 126.73, 84.11, 74.63, 63.13, 31.30, 29.39, 28.78, 28.46, 27.00, 25.79, 25.19, 22.54, 18.69, 14.05.

HRMS: m/z $[\text{M}+\text{H}]^+$ calcd for $\text{C}_{21}\text{H}_{26}\text{O}_2$: 311.2011. Found: 311.2000.

IR: 2929, 2856, 2344, 1713, 1676, 1600, 1455, 1436, 1356, 1310, 1292, 1209, 1155, 934, 902, 739, 554 cm^{-1} .

4.13f: 2-acetyl-2-(4-methylpent-2-yn-1-yl)-3,4-dihydronaphthalen-1(2H)-one



Appearance: Yellow oil, 0.063 g, 0.235 mmol, 98% yield.

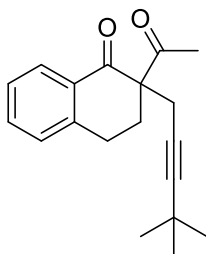
^1H NMR Spectra (500 MHz, CDCl_3): δ 8.03 (d, $J = 7.8$ Hz, 1H), 7.48 (tt, $J = 7.6, 1.0$ Hz, 1H), 7.30 (t, $J = 7.6$ Hz, 1H), 7.22 (d, $J = 7.7$ Hz, 1H), 3.17 (ddd, $J = 17.5, 10.3, 4.9$ Hz, 1H), 3.00–2.92 (m, 2H), 2.75 (dt, $J = 13.8, 4.9$ Hz, 1H), 2.65 (dd, $J = 16.9, 2.3$ Hz, 1H), 2.50–2.43 (m, 1H), 2.22–2.11 (m, 4H), 1.08 (ddd, $J = 6.9, 2.4, 0.8$ Hz, 6H).

$^{13}\text{C}\{^1\text{H}\}$ NMR Spectra (126 MHz, CDCl_3): δ 204.95, 196.69, 144.31, 134.32, 132.09, 129.28, 128.24, 127.07, 90.14, 74.28, 63.43, 29.73, 27.33, 26.15, 25.46, 23.45, 20.83.

HRMS: m/z $[\text{M}+\text{H}]^+$ calcd for $\text{C}_{18}\text{H}_{20}\text{O}_2$: 269.1542. Found: 269.1543.

IR: 2967, 2930, 1713, 1674, 1600, 1455, 1357, 1320, 1292, 1208, 1153, 934, 904, 785, 762, 739, 554 cm^{-1} .

4.13g: 2-acetyl-2-(4,4-dimethylpent-2-yn-1-yl)-3,4-dihydronaphthalen-1(2H)-one



Appearance: Yellow oil, 0.062 g, 0.218 mmol, 91% yield.

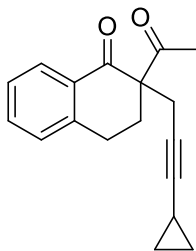
^1H NMR Spectra (500 MHz, CDCl_3): δ 8.03 (dd, $J = 7.9, 1.3$ Hz, 1H), 7.48 (td, $J = 7.5, 1.4$ Hz, 1H), 7.30 (t, $J = 7.5$ Hz, 1H), 7.23 (d, $J = 7.7$ Hz, 1H), 3.17 (ddd, $J = 17.4, 10.1, 4.9$ Hz, 1H), 3.02–2.94 (m, 2H), 2.75 (dt, $J = 13.8, 5.0$ Hz, 1H), 2.63 (d, $J = 17.0$ Hz, 1H), 2.19 (s, 3H), 2.14 (ddd, $J = 13.8, 10.1, 5.0$ Hz, 1H), 1.13 (s, 9H).

$^{13}\text{C}\{^1\text{H}\}$ NMR Spectra (126 MHz, CDCl_3): δ 204.91, 196.68, 144.34, 134.33, 132.12, 129.26, 128.27, 127.06, 93.05, 73.62, 63.45, 31.41, 31.32, 29.82, 29.70, 27.31, 25.48.

HRMS: m/z $[\text{M}+\text{Na}]^+$ calcd for $\text{C}_{19}\text{H}_{22}\text{O}_2$: 305.1518. Found: 305.1519.

IR: 3067, 3026, 2968, 2929, 2866, 2359, 2240, 1713, 1676, 1600, 1455, 1390, 1360, 1310, 1266, 1222, 1156, 1059, 962, 935, 902, 785, 758, 738, 668, 618, 554 cm^{-1} .

4.13h: 2-acetyl-2-(3-cyclopropylprop-2-yn-1-yl)-3,4-dihydronaphthalen-1(2H)-one



Appearance: Yellow oil, 0.043 g, 0.162 mmol, 67% yield.

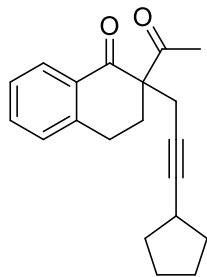
^1H NMR Spectra (500 MHz, CDCl_3): δ 8.03 (dd, $J = 8.0, 1.4$ Hz, 1H), 7.49 (td, $J = 7.5, 1.4$ Hz, 1H), 7.31 (t, $J = 7.6$ Hz, 1H), 7.22 (d, $J = 7.7$ Hz, 1H), 3.16 (ddd, $J = 16.1, 10.4, 4.9$ Hz, 1H), 2.98–2.91 (m, 2H), 2.73 (ddd, $J = 13.6, 5.4, 4.3$ Hz, 1H), 2.65 (dd, $J = 17.0, 1.7$ Hz, 1H), 2.17 (d, $J = 1.2$ Hz, 4H), 1.15 (ttt, $J = 8.3, 4.8, 1.8$ Hz, 1H), 0.72–0.64 (m, 2H), 0.60–0.52 (m, 2H).

$^{13}\text{C}\{^1\text{H}\}$ NMR Spectra (126 MHz, CDCl_3): δ 204.90, 196.64, 144.28, 134.35, 132.05, 129.30, 128.25, 127.09, 87.46, 70.28, 63.44, 29.75, 27.32, 26.13, 25.50, 8.46, -0.14.

HRMS: m/z $[\text{M}]^+$ calcd for $\text{C}_{18}\text{H}_{18}\text{O}_2$: 266.1307. Found: 266.1296.

IR: 3009, 2929, 1713, 1674, 1599, 1557, 1506, 1484, 1454, 1356, 1309, 1292, 1205, 1153, 1052, 1033, 932, 905, 885, 812, 785, 759, 738, 624, 554 cm^{-1} .

4.13i: 2-acetyl-2-(3-cyclopentylprop-2-yn-1-yl)-3,4-dihydronaphthalen-1(2H)-one



Appearance: Yellow oil, 0.067 g, 0.227 mmol, 94% yield.

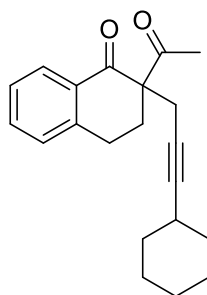
^1H NMR Spectra (500 MHz, CDCl_3): δ 8.03 (dd, $J = 8.0, 1.3$ Hz, 1H), 7.48 (td, $J = 7.5, 1.4$ Hz, 1H), 7.30 (t, $J = 7.6$ Hz, 1H), 7.22 (d, $J = 7.7$ Hz, 1H), 3.17 (ddd, $J = 17.3, 10.3, 4.9$ Hz, 1H), 3.01–2.91 (m, 2H), 2.75 (dt, $J = 13.8, 5.0$ Hz, 1H), 2.66 (dd, $J = 17.0, 2.2$ Hz, 1H), 2.56–2.50 (m, 1H), 2.19 (s, 4H), 1.87–1.77 (m, 2H), 1.55–1.41 (m, 4H).

$^{13}\text{C}\{^1\text{H}\}$ NMR Spectra (126 MHz, CDCl_3): δ 204.97, 196.70, 144.31, 134.31, 132.08, 129.28, 128.24, 127.07, 88.86, 74.58, 63.48, 34.25, 30.53, 29.75, 27.33, 26.16, 25.60, 25.14.

HRMS: m/z $[\text{M}+\text{H}]^+$ calcd for $\text{C}_{20}\text{H}_{22}\text{O}_2$: 295.1698. Found: 295.1697.

IR: 3416, 3066, 2958, 2869, 2358, 2235, 1713, 1674, 1600, 1455, 1356, 1310, 1292, 1268, 1233, 1223, 1156, 1125, 962, 936, 895, 785, 754, 739, 631, 565 cm^{-1} .

4.13j: 2-acetyl-2-(3-cyclohexylprop-2-yn-1-yl)-3,4-dihydronaphthalen-1(2H)-one



Appearance: Yellow oil, 0.068 g, 0.221 mmol, 92% yield.

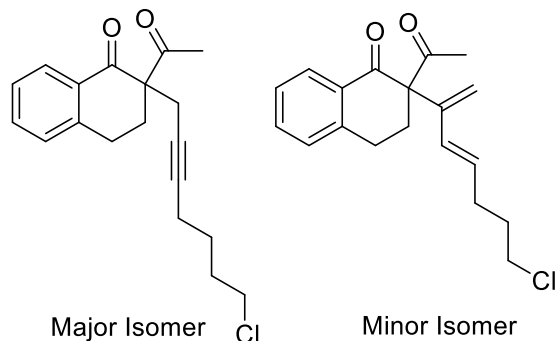
^1H NMR Spectra (500 MHz, CDCl_3): δ 8.03 (dd, $J = 7.9, 1.3$ Hz, 1H), 7.52–7.46 (m, 1H), 7.31 (t, $J = 7.6$ Hz, 1H), 7.22 (d, $J = 7.7$ Hz, 1H), 3.21–3.13 (m, 1H), 3.03–2.92 (m, 2H), 2.76 (dt, $J = 13.8, 4.9$ Hz, 1H), 2.67 (dd, $J = 17.0, 2.2$ Hz, 1H), 2.31 (d, $J = 11.0$ Hz, 1H), 2.25–2.09 (m, 4H), 1.76–1.66 (m, 2H), 1.62 (ddt, $J = 12.6, 6.3, 3.3$ Hz, 2H), 1.45 (s, 2H), 1.34 (dt, $J = 12.6, 9.5$ Hz, 2H), 1.25 (t, $J = 10.4$ Hz, 3H).

$^{13}\text{C}\{^1\text{H}\}$ NMR Spectra (126 MHz, CDCl_3): δ 204.96, 196.69, 144.32, 134.31, 132.08, 129.28, 128.25, 127.06, 100.34, 88.74, 63.50, 33.10, 29.74, 29.32, 27.35, 26.23, 26.17, 25.59, 25.07.

HRMS: m/z $[\text{M}+\text{H}]^+$ calcd for $\text{C}_{21}\text{H}_{24}\text{O}_2$: 309.1855. Found: 309.1858.

IR: 3413, 3066, 2929, 2852, 2361, 2324, 1713, 1676, 1600, 1445, 1356, 1309, 1292, 1268, 1205, 1176, 1152, 1123, 1008, 962, 934, 904, 785, 748, 657, 632, 607, 565, 554 cm^{-1} .

4.13k: 2-acetyl-2-(7-chlorohept-2-yn-1-yl)-3,4-dihydronaphthalen-1(2H)-one



Isolated as a mixture of isomers.

Appearance: Yellow oil, 0.035 g, 0.11 mmol, 46% yield.

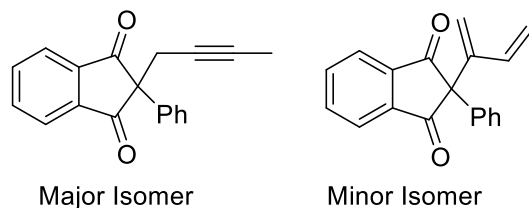
^1H NMR Spectra (500 MHz, CDCl_3) *Major isomer*: δ 8.04 (dd, $J = 7.9, 1.3$ Hz, 1H), 7.49 (td, $J = 7.5, 1.4$ Hz, 1H), 7.31 (t, $J = 7.6$ Hz, 1H), 7.23 (d, $J = 7.7$ Hz, 1H), 3.51 (t, $J = 6.5$ Hz, 2H), 3.16 (ddd, $J = 17.6, 10.5, 4.9$ Hz, 1H), 2.99–2.90 (m, 2H), 2.75–2.67 (m, 2H), 2.26–2.10 (m, 6H), 1.81 (dt, $J = 14.8, 6.7$ Hz, 2H), 1.60–1.55 (m, 2H).

$^{13}\text{C}\{^1\text{H}\}$ NMR Spectra (126 MHz, CDCl_3) *Major isomer*: δ 204.85, 196.63, 144.25, 134.39, 132.05, 129.31, 128.25, 127.12, 83.36, 75.84, 63.45, 44.90, 31.76, 29.84, 27.32, 26.23, 26.12, 25.53, 18.33.

HRMS: m/z $[\text{M}+\text{H}]^+$ calcd for $\text{C}_{19}\text{H}_{21}\text{ClO}_2$: 317.1308. Found: 317.1311.

IR: 2930, 2859, 2362, 1713, 1676, 1600, 1453, 1356, 1312, 1293, 1210, 1155, 971, 934, 902, 739, 628, 554, 504 cm^{-1} .

4.13l: 2-(but-2-yn-1-yl)-2-phenyl-1H-indene-1,3(2H)-dione



Isolated as a mixture of isomers.

Appearance: White solid, 0.047 g, 0.171 mmol, 71% yield.

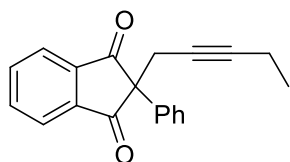
^1H NMR Spectra (500 MHz, CDCl_3) *Major isomer*: δ 8.06 (tt, $J = 5.2, 2.3$ Hz, 2H), 7.87 (dd, $J = 5.7, 3.1$ Hz, 2H), 7.41–7.37 (m, 2H), 7.36–7.26 (m, 3H), 3.09 (q, $J = 2.5$ Hz, 2H), 1.44 (t, $J = 2.5$ Hz, 3H).

$^{13}\text{C}\{^1\text{H}\}$ NMR Spectra (126 MHz, CDCl_3) *Major isomer*: δ ^{13}C NMR (126 MHz, CDCl_3) δ 200.88, 142.69, 136.16, 129.23, 128.35, 127.10, 123.94, 79.13, 77.56, 74.03, 61.72, 25.67, 3.56.

HRMS: m/z $[\text{M}]^+$ calcd for $\text{C}_{19}\text{H}_{14}\text{O}_2$: 274.0994. Found: 274.0998.

IR: 3060, 3033, 2919, 2853, 2231, 1746, 1713, 1596, 1496, 1447, 1350, 1332, 1252, 1155, 1036, 982, 965, 918, 889, 775, 755, 715, 699, 687, 581, 520 cm^{-1} .

4.13m: 2-(pent-2-yn-1-yl)-2-phenyl-1H-indene-1,3(2H)-dione



Appearance: Yellow oil, 0.069 g, 0.238 mmol, 99% yield.

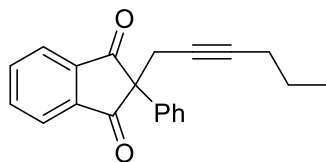
^1H NMR Spectra (500 MHz, CDCl_3): δ 8.06 (dt, $J = 6.9, 3.6$ Hz, 2H), 7.87 (dd, $J = 5.7, 3.0$ Hz, 2H), 7.44–7.35 (m, 2H), 7.36–7.26 (m, 3H), 3.10 (t, $J = 2.4$ Hz, 2H), 1.79 (qt, $J = 7.5, 2.4$ Hz, 2H), 0.63 (dd, $J = 8.2, 7.0$ Hz, 3H).

$^{13}\text{C}\{^1\text{H}\}$ NMR Spectra (126 MHz, CDCl_3): δ 201.07, 142.88, 136.15, 129.21, 128.33, 127.15, 123.85, 85.55, 74.43, 61.62, 25.78, 13.79, 12.34.

HRMS: m/z $[\text{M}+\text{H}]^+$ calcd for $\text{C}_{20}\text{H}_{16}\text{O}_2$: 289.1229. Found: 289.1235.

IR: 3062, 2976, 2936, 2916, 2876, 1744, 1709, 1596, 1497, 1447, 1422, 1350, 1332, 1250, 1158, 1036, 885, 784, 758, 715, 698, 591 cm^{-1} .

4.13n: 2-(hex-2-yn-1-yl)-2-phenyl-1H-indene-1,3(2H)-dione



Appearance: Yellow solid, 0.067 g, 0.222 mmol, 92% yield.

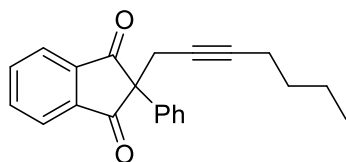
^1H NMR Spectra (500 MHz, CDCl_3): δ 8.06 (dt, $J = 6.8, 3.5$ Hz, 1H), 7.87 (dd, $J = 5.7, 3.1$ Hz, 1H), 7.40 (dt, $J = 8.2, 1.1$ Hz, 1H), 7.37–7.22 (m, 2H), 3.11 (t, $J = 2.4$ Hz, 1H), 1.78 (td, $J = 6.9, 3.4$ Hz, 1H), 1.03 (h, $J = 7.2$ Hz, 1H), 0.57 (dd, $J = 7.8, 6.9$ Hz, 1H).

$^{13}\text{C}\{^1\text{H}\}$ NMR Spectra (126 MHz, CDCl_3): δ 200.70, 142.51, 135.79, 135.71, 128.87, 127.98, 126.80, 123.55, 83.58, 74.78, 61.27, 25.50, 21.75, 20.30, 12.99.

HRMS: m/z $[\text{M}]^+$ calcd for $\text{C}_{11}\text{H}_{14}\text{O}_4$: 210.0892. Found: 210.0886.

IR: 3065, 2965, 2928, 2869, 1747, 1709, 1594, 1497, 1457, 1446, 1416, 1380, 1352, 1332, 1315, 1252, 1209, 1155, 1082, 1033, 981, 968, 916, 888, 782, 755, 718, 699, 590 cm^{-1} .

4.13o: 2-(hept-2-yn-1-yl)-2-phenyl-1H-indene-1,3(2H)-dione



Appearance: Yellow oil, 0.76 g, 0.24 mmol, 100% yield.

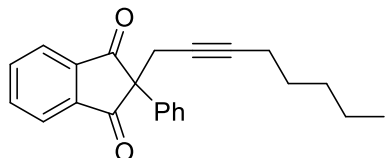
^1H NMR Spectra (500 MHz, CDCl_3): δ 8.06 (dt, $J = 7.8, 3.8$ Hz, 2H), 7.87 (dq, $J = 6.8, 3.7$ Hz, 2H), 7.39 (dd, $J = 7.5, 2.0$ Hz, 2H), 7.29 (q, $J = 8.5, 7.8$ Hz, 3H), 3.11 (t, $J = 2.5$ Hz, 2H), 1.81 (tt, $J = 6.7, 2.5$ Hz, 2H), 0.96 (qd, $J = 7.8, 6.9, 4.1$ Hz, 4H), 0.64 (t, $J = 6.9$ Hz, 3H).

$^{13}\text{C}\{^1\text{H}\}$ NMR Spectra (126 MHz, CDCl_3): δ 201.04, 142.87, 136.13, 136.06, 129.22, 128.32, 127.14, 123.88, 83.98, 75.00, 61.64, 30.70, 25.85, 21.73, 18.30, 13.83.

HRMS: m/z $[\text{M}]^+$ calcd for $\text{C}_{22}\text{H}_{20}\text{O}_2$: 316.1463. Found: 316.1466.

IR: 3060, 2956, 2930, 2870, 2359, 1746, 1713, 1596, 1350, 1332, 1307, 1252, 1210, 1155, 1083, 1036, 981, 963, 918, 891, 781, 754, 717, 698, 591, 574, 508 cm^{-1} .

4.13p: 2-(oct-2-yn-1-yl)-2-phenyl-1H-indene-1,3(2H)-dione



Appearance: Yellow oil, 0.078 g, 0.238 mmol, 99% yield.

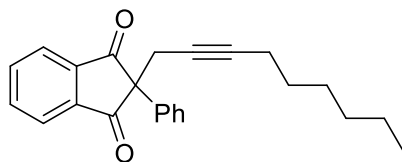
^1H NMR Spectra (500 MHz, CDCl_3): δ 8.06 (ddt, $J = 7.2, 4.9, 2.4$ Hz, 2H), 7.89–7.84 (m, 2H), 7.42–7.37 (m, 2H), 7.29 (qd, $J = 8.5, 7.8, 1.3$ Hz, 3H), 3.11 (q, $J = 2.4, 1.8$ Hz, 2H), 1.82–1.76 (m, 2H), 1.06 (q, $J = 7.2$ Hz, 2H), 1.02–0.97 (m, 2H), 0.96–0.90 (m, 2H), 0.77 (td, $J = 7.3, 1.2$ Hz, 3H).

$^{13}\text{C}\{^1\text{H}\}$ NMR Spectra (126 MHz, CDCl_3): δ 200.66, 142.50, 135.78, 135.71, 128.87, 127.98, 126.79, 123.53, 83.74, 74.63, 61.31, 30.53, 28.02, 25.49, 22.04, 18.26, 13.87.

HRMS: m/z $[\text{M}]^+$ calcd for $\text{C}_{23}\text{H}_{22}\text{O}_2$: 330.1620. Found: 330.1615.

IR: 3439, 3060, 3035, 2956, 2930, 2858, 2228, 1746, 1709, 1596, 1496, 1447, 1330, 1250, 1156, 1036, 981, 963, 886, 779, 754, 717, 698, 591, 574, 515 cm^{-1} .

4.13q: 2-(non-2-yn-1-yl)-2-phenyl-1*H*-indene-1,3(2*H*)-dione



Appearance: Yellow oil, 0.073 g, 0.2112 mmol, 88% yield.

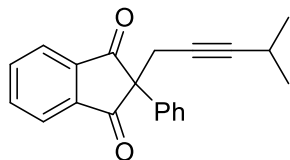
^1H NMR Spectra (500 MHz, CDCl_3): δ ^1H NMR (500 MHz, Chloroform-*d*) δ 8.08–8.04 (m, 2H), 7.87 (dd, $J = 5.7, 3.1$ Hz, 2H), 7.40–7.37 (m, 2H), 7.33–7.26 (m, 3H), 3.11 (t, $J = 2.4$ Hz, 2H), 1.79 (dq, $J = 4.7, 3.2, 2.5$ Hz, 2H), 1.16 (p, $J = 7.3$ Hz, 2H), 1.04–0.94 (m, 6H), 0.83 (t, $J = 7.3$ Hz, 3H).

$^{13}\text{C}\{^1\text{H}\}$ NMR Spectra (126 MHz, CDCl_3): δ 201.01, 142.85, 136.11, 136.06, 129.21, 128.32, 127.14, 123.88, 84.10, 74.98, 61.67, 31.58, 28.67, 28.44, 25.85, 22.78, 18.65, 14.41.

HRMS: m/z $[\text{M}]^+$ calcd for $\text{C}_{24}\text{H}_{24}\text{O}_2$: 344.1776. Found: 344.1771.

IR: 3060, 3035, 2955, 2929, 2858, 2359, 2230, 1747, 1709, 1596, 1496, 1447, 1419, 1377, 1349, 1332, 1252, 1212, 1155, 1036, 982, 963, 918, 886, 778, 755, 717, 698, 591, 575, 517 cm^{-1} .

4.13r: 2-(4-methylpent-2-yn-1-yl)-2-phenyl-1*H*-indene-1,3(2*H*)-dione



Appearance: Yellow oil, 0.068 g, 0.227 mmol, 95% yield.

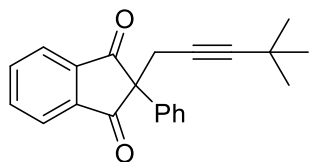
^1H NMR Spectra (500 MHz, CDCl_3): δ 8.06 (dd, $J = 5.6, 3.1$ Hz, 2H), 7.87 (dt, $J = 5.7, 3.3$ Hz, 2H), 7.39 (d, $J = 7.7$ Hz, 2H), 7.36–7.25 (m, 5H), 3.11 (t, $J = 2.3$ Hz, 2H), 1.79 (dt, $J = 6.5, 4.1$ Hz, 2H), 1.16 (dq, $J = 14.9, 7.5$ Hz, 2H), 0.99 (tdd, $J = 13.8, 12.0, 10.9, 5.2$ Hz, 6H), 0.83 (d, $J = 14.7$ Hz, 3H).

$^{13}\text{C}\{^1\text{H}\}$ NMR Spectra (126 MHz, CDCl_3): δ 201.01, 142.85, 136.11, 136.06, 129.21, 128.32, 127.14, 123.88, 84.10, 74.98, 61.67, 31.58, 28.67, 28.44, 25.85, 22.78, 18.65, 14.41.

HRMS: m/z $[\text{M}]^+$ calcd for $\text{C}_{21}\text{H}_{18}\text{O}_2$: 302.1307. Found: 302.1304.

IR: 3437, 3060, 2969, 2930, 2870, 1744, 1709, 1596, 1496, 1447, 1350, 1332, 1307, 1250, 1209, 1155, 1036, 981, 918, 889, 874, 782, 758, 699, 594, 508 cm^{-1} .

4.13s: 2-(4,4-dimethylpent-2-yn-1-yl)-2-phenyl-1H-indene-1,3(2H)-dione



Appearance: White solid, 0.075 g, 0.238 mmol, 99% yield.

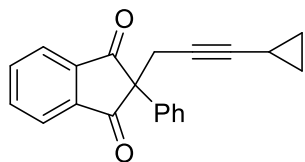
^1H NMR Spectra (500 MHz, CDCl_3): δ 8.09–8.05 (m, 2H), 7.90–7.86 (m, 2H), 7.41–7.37 (m, 2H), 7.33–7.28 (m, 2H), 3.09 (s, 2H), 0.75 (s, 9H).

$^{13}\text{C}\{^1\text{H}\}$ NMR Spectra (126 MHz, CDCl_3): δ 201.24, 143.09, 136.13, 136.03, 129.18, 128.28, 127.22, 123.75, 93.03, 73.71, 61.49, 30.76, 27.26, 25.85.

HRMS: m/z $[\text{M}]^+$ calcd for $\text{C}_{22}\text{H}_{20}\text{O}_2$: 316.1463. Found: 316.1474.

IR: 3062, 2968, 2928, 2866, 2238, 1746, 1713, 1596, 1494, 1446, 1362, 1350, 1332, 1306, 1266, 1249, 1208, 1156, 1036, 981, 918, 884, 834, 781, 757, 719, 699, 590, 511 cm^{-1} .

4.13t: 2-(3-cyclopropylprop-2-yn-1-yl)-2-phenyl-1H-indene-1,3(2H)-dione



Appearance: Yellow oil, 0.066 g, 0.22 mmol, 92% yield.

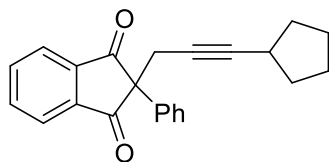
^1H NMR Spectra (500 MHz, CDCl_3): δ 8.06 (dt, $J = 6.7, 3.4$ Hz, 2H), 7.93–7.85 (m, 2H), 7.41–7.35 (m, 2H), 7.35–7.26 (m, 3H), 3.07 (d, $J = 1.9$ Hz, 2H), 0.84 (dddd, $J = 10.1, 8.3, 6.8, 4.4, 1.9$ Hz, 1H), 0.45–0.38 (m, 2H).

$^{13}\text{C}\{^1\text{H}\}$ NMR Spectra (126 MHz, CDCl_3): δ 201.00, 142.82, 136.19, 135.97, 129.20, 128.33, 127.15, 123.82, 87.44, 70.20, 61.58, 25.85, 8.10, -0.56.

HRMS: m/z $[\text{M}]^+$ calcd for $\text{C}_{21}\text{H}_{16}\text{O}_2$: 300.1150. Found: 300.1158.

IR: 2923, 2853, 2351, 1743, 1710, 1651, 1594, 1206, 1153, 1033, 875, 782, 757, 699 cm^{-1} .

4.13u: 2-(3-cyclopentylprop-2-yn-1-yl)-2-phenyl-1H-indene-1,3(2H)-dione



Appearance: Yellow oil, 0.072 g, 0.218 mmol, 91% yield.

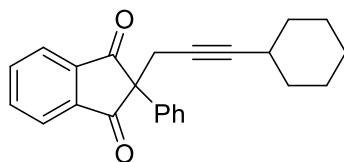
^1H NMR Spectra (500 MHz, CDCl_3): δ 8.07 (dd, $J = 5.7, 3.1$ Hz, 2H), 7.88 (dd, $J = 5.7, 3.1$ Hz, 2H), 7.39 (dd, $J = 7.4, 1.8$ Hz, 2H), 7.35–7.26 (m, 3H), 3.10 (d, $J = 2.2$ Hz, 2H), 2.27–2.20 (m, 1H), 1.49–1.42 (m, 2H), 1.29 (dddd, $J = 12.9, 9.3, 6.1, 2.8$ Hz, 4H), 1.00 (dt, $J = 11.2, 6.7$ Hz, 2H).

$^{13}\text{C}\{^1\text{H}\}$ NMR Spectra (126 MHz, CDCl_3): δ 201.18, 142.96, 136.14, 136.03, 129.19, 128.30, 127.18, 123.81, 88.86, 74.62, 61.57, 33.70, 30.03, 25.95, 24.89.

HRMS: m/z $[\text{M}+\text{NH}_4]^+$ calcd for $\text{C}_{23}\text{H}_{20}\text{O}_2$: 346.1807. Found: 346.1803.

IR: 3449, 3060, 2959, 2869, 2235, 1744, 1710, 1596, 1499, 1447, 1420, 1349, 1332, 1306, 1250, 1209, 1155, 1036, 982, 885, 781, 755, 718, 699, 597 cm^{-1} .

4.13v: 2-(3-cyclohexylprop-2-yn-1-yl)-2-phenyl-1H-indene-1,3(2H)-dione



Appearance: White solid, 0.082 g, 0.24 mmol, 100% yield.

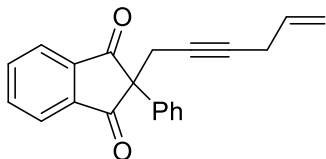
^1H NMR Spectra (500 MHz, CDCl_3): δ 8.07 (dd, $J = 5.6, 3.1$ Hz, 2H), 7.87 (dd, $J = 5.7, 3.1$ Hz, 2H), 7.44–7.36 (m, 2H), 7.35–7.27 (m, 3H), 3.12 (d, $J = 2.1$ Hz, 2H), 2.07–2.01 (m, 1H), 1.27 (t, $J = 7.9$ Hz, 4H), 1.15–0.96 (m, 4H), 0.93 (t, $J = 10.0$ Hz, 2H).

$^{13}\text{C}\{^1\text{H}\}$ NMR Spectra (126 MHz, CDCl_3): δ 201.14, 143.00, 136.12, 136.07, 129.20, 128.30, 127.18, 123.86, 86.06, 75.13, 74.68, 32.38, 28.70, 26.11, 25.93, 24.48.

HRMS: m/z $[\text{M}]^+$ calcd for $\text{C}_{24}\text{H}_{22}\text{O}_2$: 342.1620. Found: 342.1625.

IR: 3085, 3055, 2929, 2852, 2345, 1743, 1710, 1654, 1589, 1492, 1466, 1446, 1413, 1359, 1337, 1303, 1255, 1212, 1182, 1156, 1083, 971, 921, 889, 791, 768, 749, 718, 697, 591, 572 cm^{-1} .

4.13w: 2-(hex-5-en-2-yn-1-yl)-2-phenyl-1H-indene-1,3(2H)-dione



Appearance: White solid, 0.047 g, 0.156 mmol, 65% yield.

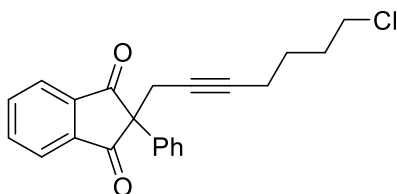
^1H NMR Spectra (500 MHz, CDCl_3): δ 8.11–8.00 (m, 2H), 7.87 (dd, $J = 5.8, 3.1$ Hz, 2H), 7.46–7.36 (m, 2H), 7.36–7.26 (m, 3H), 5.40 (dddd, $J = 15.1, 11.3, 5.8, 4.5$ Hz, 1H), 4.87–4.74 (m, 2H), 3.16 (q, $J = 2.4, 1.9$ Hz, 2H), 2.60 (dp, $J = 4.3, 1.9$ Hz, 2H).

$^{13}\text{C}\{^1\text{H}\}$ NMR Spectra (126 MHz, CDCl_3): δ 200.86, 142.77, 136.19, 135.99, 132.40, 129.25, 128.38, 127.13, 123.97, 115.86, 80.30, 77.56, 61.54, 25.77, 22.98.

HRMS: m/z $[\text{M}]^+$ calcd for $\text{C}_{21}\text{H}_{16}\text{O}_2$: 300.1150. Found: 300.1146.

IR: 3062, 2919, 1744, 1709, 1683, 1596, 1496, 1446, 1417, 1332, 1252, 1209, 1153, 1036, 991, 778, 754, 717, 698, 577 cm^{-1} .

4.13x: 2-(7-chlorohept-2-yn-1-yl)-2-phenyl-1H-indene-1,3(2H)-dione



Appearance: Yellow oil, 0.083 g, 0.238 mmol, 99% yield.

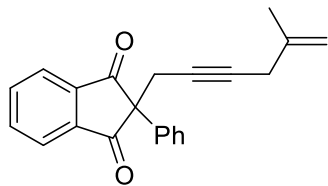
^1H NMR Spectra (500 MHz, CDCl_3): δ 8.07 (dd, $J = 5.7, 3.1$ Hz, 2H), 7.89 (dd, $J = 5.7, 3.1$ Hz, 2H), 7.41–7.36 (m, 2H), 7.34–7.27 (m, 3H), 3.28 (t, $J = 6.5$ Hz, 2H), 3.11 (t, $J = 2.4$ Hz, 2H), 1.87 (tt, $J = 6.9, 2.5$ Hz, 2H), 1.47–1.40 (m, 2H), 1.19 (p, $J = 7.0$ Hz, 2H).

$^{13}\text{C}\{^1\text{H}\}$ NMR Spectra (126 MHz, CDCl_3): δ 200.87, 155.53, 142.75, 136.29, 135.93, 129.25, 128.39, 127.11, 123.93, 82.89, 75.83, 61.59, 44.71, 31.29, 25.75, 17.91.

HRMS: m/z $[\text{M}]^+$ calcd for $\text{C}_{22}\text{H}_{19}\text{ClO}_2$: 350.1074. Found: 350.1075.

IR: 3060, 2929, 2863, 2359, 1744, 1709, 1596, 1496, 1446, 1350, 1332, 1309, 1250, 1209, 1152, 1036, 985, 886, 779, 755, 718, 698, 651, 592, 507 cm^{-1} .

4.13y: 2-(5-methylhex-en-2-yn-1-yl)-2-phenyl-1H-indene-1,3(2H)-dione



Appearance: Clear oil, 0.057 g, 0.182 mmol, 76% yield.

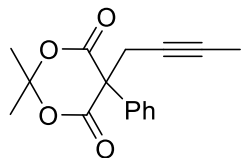
^1H NMR Spectra (500 MHz, CDCl_3): δ 8.08–8.01 (m, 2H), 7.86 (dd, $J = 5.7, 3.1$ Hz, 2H), 7.44–7.38 (m, 2H), 7.37–7.26 (m, 3H), 4.49 (dt, $J = 3.3, 1.6$ Hz, 2H), 3.15 (t, $J = 2.4$ Hz, 2H), 2.54 (t, $J = 1.9$ Hz, 2H), 1.44 (s, 3H).

$^{13}\text{C}\{^1\text{H}\}$ NMR Spectra (126 MHz, CDCl_3): δ 200.85, 142.75, 140.54, 136.18, 136.02, 129.24, 128.37, 127.12, 123.98, 111.48, 80.74, 61.53, 27.52, 25.78, 21.99.

HRMS: m/z $[\text{M}]^+$ calcd for $\text{C}_{22}\text{H}_{18}\text{O}_2$: 314.1307. Found: 314.1296.

IR: 2972, 2916, 2359, 1746, 1710, 1596, 1496, 1446, 1350, 1332, 1309, 1252, 1209, 1153, 1036, 982, 892, 778, 754, 717, 698, 668, 595, 571, 505 cm^{-1} .

4.13z: 5-(but-2-yn-1-yl)-2,2-dimethyl-5-phenyl-1,3-dioxane-4,6-dione



Appearance: White solid, 0.039 g, 0.144 mmol, 60% yield.

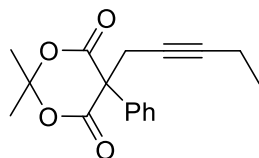
^1H NMR Spectra (500 MHz, CDCl_3): δ 7.47 (dq, $J = 7.6, 1.4$ Hz, 2H), 7.39 (tdt, $J = 7.0, 5.5, 1.4$ Hz, 3H), 3.11 (q, $J = 2.4$ Hz, 2H), 1.82–1.74 (m, 6H), 1.37 (s, 3H).

$^{13}\text{C}\{^1\text{H}\}$ NMR Spectra (126 MHz, CDCl_3): δ 166.56, 134.70, 130.01, 129.58, 126.57, 106.03, 79.17, 74.38, 61.03, 31.33, 29.67, 28.31, 3.93.

HRMS: m/z $[\text{M}]^+$ calcd for $\text{C}_{16}\text{H}_{16}\text{O}_4$: 272.1049. Found: 272.1054.

IR: 3066, 3000, 2923, 2359, 2342, 1780, 1744, 1496, 1449, 1395, 1382, 1325, 1280, 1208, 1153, 1076, 1043, 954, 954, 892, 759, 719, 697, 668, 554, 537 cm^{-1} .

4.13aa: 2,2-dimethyl-5-(pent-2-yn-1-yl)-5-phenyl-1,3-dioxane-4,6-dione



Appearance: White solid, 0.06 g, 0.209 mmol, 87% yield.

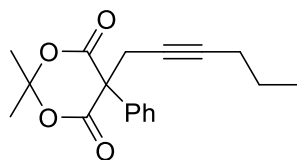
^1H NMR Spectra (500 MHz, CDCl_3): δ ^1H NMR (500 MHz, Chloroform-*d*) δ 7.52–7.44 (m, 2H), 7.45–7.34 (m, 3H), 3.13 (q, $J = 1.9$ Hz, 2H), 2.14 (qt, $J = 7.5, 2.2$ Hz, 2H), 1.77 (s, 3H), 1.38 (s, 3H), 1.10 (td, $J = 7.5, 1.1$ Hz, 3H).

$^{13}\text{C}\{^1\text{H}\}$ NMR Spectra (126 MHz, CDCl_3): δ 166.60, 134.66, 129.98, 129.55, 126.65, 105.94, 85.32, 74.71, 61.16, 31.47, 29.67, 28.41, 14.27, 12.70.

HRMS: m/z $[\text{M}+\text{H}]^+$ calcd for $\text{C}_{17}\text{H}_{18}\text{O}_4$: 287.1283. Found: 287.1290.

IR: 3065, 2975, 2923, 2880, 2235, 1779, 1747, 1494, 1449, 1422, 1393, 1380, 1319, 1280, 1249, 1208, 1155, 1099, 1076, 1045, 996, 954, 768, 719, 697, 538 cm^{-1} .

4.13bb: 5-(hex-2-yn-1-yl)-2,2-dimethyl-5-phenyl-1,3-dioxane-4,6-dione



Appearance: Clear oil, 0.060 g, 0.199 mmol, 83% yield.

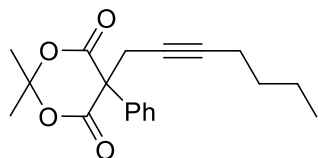
^1H NMR Spectra (500 MHz, CDCl_3): δ 7.53–7.45 (m, 2H), 7.44–7.34 (m, 3H), 3.13 (t, $J = 2.3$ Hz, 2H), 2.11 (ddt, $J = 7.0, 4.6, 2.3$ Hz, 2H), 1.76 (s, 3H), 1.49 (q, $J = 7.2$ Hz, 2H), 1.37 (s, 3H), 0.96 (t, $J = 7.3$ Hz, 3H).

$^{13}\text{C}\{^1\text{H}\}$ NMR Spectra (126 MHz, CDCl_3): δ 166.57, 134.63, 129.98, 129.54, 126.64, 105.90, 83.78, 75.54, 61.21, 31.63, 29.58, 28.41, 22.43, 20.95, 13.71.

HRMS: m/z $[\text{M}+\text{H}]^+$ calcd for $\text{C}_{18}\text{H}_{20}\text{O}_4$: 301.1440. Found: 301.1445.

IR: 3000, 2963, 2934, 2873, 1780, 1743, 1496, 1449, 1416, 1393, 1382, 1317, 1278, 1206, 1155, 1102, 1076, 1043, 954, 764, 697, 535 cm^{-1} .

4.13cc: 5-(hept-2-yn-1-yl)-2,2-dimethyl-5-phenyl-1,3-dioxane-4,6-dione



Appearance: Clear oil, 0.068 g, 0.218 mmol, 91% yield.

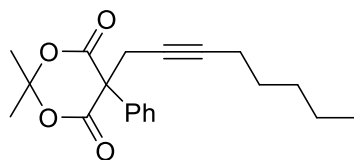
^1H NMR Spectra (500 MHz, CDCl_3): δ 7.51–7.47 (m, 2H), 7.42–7.36 (m, 3H), 3.13 (t, $J = 2.3$ Hz, 2H), 2.13 (tt, $J = 6.9, 2.3$ Hz, 2H), 1.76 (s, 3H), 1.51–1.38 (m, 4H), 1.37 (s, 3H), 0.90 (t, $J = 7.2$ Hz, 3H).

$^{13}\text{C}\{^1\text{H}\}$ NMR Spectra (126 MHz, CDCl_3): δ 166.56, 134.65, 129.98, 129.54, 126.63, 105.88, 83.90, 75.36, 61.21, 31.63, 31.06, 29.57, 28.40, 22.11, 18.63, 13.93.

HRMS: m/z $[\text{M}]^+$ calcd for $\text{C}_{19}\text{H}_{22}\text{O}_4$: 314.1518. Found: 314.1522.

IR: 3000, 2958, 2933, 2872, 2258, 1781, 1743, 1599, 1496, 1449, 1416, 1393, 1382, 1316, 1278, 1205, 1155, 1102, 1076, 1043, 995, 954, 757, 721, 697, 535 cm^{-1} .

4.13dd: 2,2-dimethyl-5-(oct-2-yn-1-yl)-5-phenyl-1,3-dioxane-4,6-dione



Appearance: Clear oil, 0.067 g, 0.204 mmol, 85% yield.

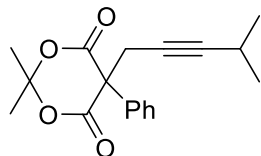
^1H NMR Spectra (500 MHz, CDCl_3): δ 7.52–7.46 (m, 2H), 7.44–7.36 (m, 3H), 3.13 (t, $J = 2.4$ Hz, 2H), 2.12 (tt, $J = 7.1, 2.4$ Hz, 2H), 1.77 (s, 3H), 1.77 (s, 3H), 1.46 (q, $J = 7.2$ Hz, 2H), 1.36–1.26 (m, 4H), 0.90 (t, $J = 6.9$ Hz, 3H).

$^{13}\text{C}\{^1\text{H}\}$ NMR Spectra (126 MHz, CDCl_3): δ 166.55, 134.66, 129.98, 129.53, 126.63, 105.88, 83.96, 75.35, 61.20, 31.61, 31.21, 29.60, 28.71, 28.39, 22.53, 18.93, 14.31.

HRMS: m/z $[\text{M}]^+$ calcd for $\text{C}_{20}\text{H}_{24}\text{O}_4$: 328.1675. Found: 328.1670.

IR: 3065, 2956, 2932, 2859, 2234, 1781, 1747, 1496, 1449, 1393, 1380, 1316, 1278, 1206, 1155, 1102, 1076, 1043, 993, 954, 764, 697, 535 cm^{-1} .

4.13ee: 2,2-dimethyl-5-(4-methylpent-2-yn-1-yl)-5-phenyl-1,3-dioxane-4,6-dione



Appearance: Yellow oil, 0.048 g, 0.161 mmol, 67% yield.

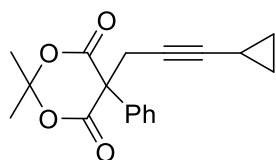
^1H NMR Spectra (500 MHz, CDCl_3): δ 7.50 (dt, $J = 8.1, 1.3$ Hz, 2H), 7.44–7.36 (m, 3H), 3.15–3.09 (m, 2H), 2.53–2.46 (m, 1H), 1.77 (s, 3H), 1.39 (s, 3H), 1.12 (dd, $J = 6.9, 1.1$ Hz, 6H).

$^{13}\text{C}\{^1\text{H}\}$ NMR Spectra (126 MHz, CDCl_3): δ 166.62, 134.60, 129.94, 129.51, 126.71, 105.83, 89.70, 74.67, 61.26, 31.61, 29.65, 28.50, 23.33, 20.76.

HRMS: m/z $[\text{M}+\text{H}]^+$ calcd for $\text{C}_{18}\text{H}_{20}\text{O}_4$: 301.1440. Found: 301.1443.

IR: 3063, 2970, 2933, 2872, 2342, 1781, 1747, 1496, 1449, 1416, 1393, 1382, 1322, 1278, 1206, 1155, 1102, 1076, 1043, 954, 764, 697, 540 cm^{-1} .

4.13ff: 5-(3-cyclopropylprop-2-yn-1-yl)-2,2-dimethyl-5-phenyl-1,3-dioxane-4,6-dione



Appearance: Clear oil, 0.068 g, 0.227 mmol, 94% yield.

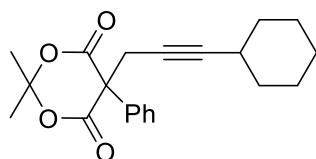
^1H NMR Spectra (500 MHz, CDCl_3): δ 7.51–7.44 (m, 2H), 7.45–7.31 (m, 3H), 3.10 (d, $J = 1.9$ Hz, 2H), 1.78 (s, 3H), 1.38 (s, 3H), 1.17 (tt, $J = 8.1, 5.2$ Hz, 1H), 0.70 (dt, $J = 8.1, 3.3$ Hz, 2H), 0.65–0.56 (m, 2H).

$^{13}\text{C}\{^1\text{H}\}$ NMR Spectra (126 MHz, CDCl_3): δ 166.57, 134.62, 129.95, 129.53, 126.64, 105.94, 87.16, 70.52, 61.14, 31.45, 29.70, 28.43, 8.54, -0.20.

HRMS: m/z $[\text{M}+\text{H}]^+$ calcd for $\text{C}_{18}\text{H}_{18}\text{O}_4$: 299.1283. Found: 299.1294.

IR: 3066, 3004, 2930, 2252, 1779, 1740, 1494, 1450, 1420, 1395, 1380, 1323, 1282, 1248, 1208, 1155, 1099, 1076, 1058, 1042, 954, 879, 762, 699, 538 cm^{-1} .

4.13gg: 5-(3-cyclohexylprop-2-yn-1-yl)-2,2-dimethyl-5-phenyl-1,3-dioxane-4,6-dione



Appearance: Clear oil, 0.063 g, 0.185 mmol, 77% yield.

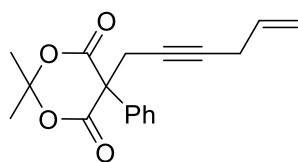
^1H NMR Spectra (500 MHz, CDCl_3): δ 7.55–7.47 (m, 2H), 7.44–7.34 (m, 3H), 3.14 (d, $J = 2.0$ Hz, 2H), 2.36 (s, 1H), 1.74–1.61 (m, 4H), 1.48–1.25 (m, 9H).

$^{13}\text{C}\{^1\text{H}\}$ NMR Spectra (126 MHz, CDCl_3): δ 166.59, 134.60, 129.96, 129.51, 126.69, 105.79, 88.14, 75.60, 61.36, 32.84, 31.81, 29.56, 29.05, 28.48, 26.26, 24.84.

HRMS: m/z $[\text{M}+\text{Na}]^+$ calcd for $\text{C}_{21}\text{H}_{24}\text{O}_4$: 363.1572. Found: 363.1582.

IR: 3063, 3000, 2930, 2853, 2232, 1781, 1747, 1496, 1449, 1416, 1393, 1382, 1316, 1278, 1205, 1246, 1102, 1078, 1043, 992, 954, 889, 767, 755, 722, 698, 535 cm^{-1} .

4.13hh: 5-(hex-5-en-2-yn-1-yl)-2,2-dimethyl-5-phenyl-1,3-dioxane-4,6-dione



Appearance: White solid, 0.40 g, 0.135 mmol, 56% yield.

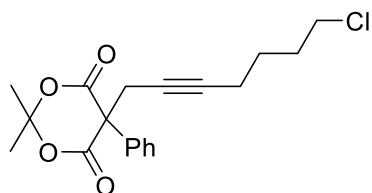
^1H NMR Spectra (500 MHz, CDCl_3): δ 7.49 (dt, $J = 8.1, 1.4$ Hz, 2H), 7.45–7.32 (m, 3H), 5.80–5.73 (m, 1H), 5.29 (dq, $J = 17.0, 1.7$ Hz, 1H), 5.10 (dq, $J = 10.1, 1.6$ Hz, 1H), 3.18 (t, $J = 2.0$ Hz, 2H), 2.92 (dp, $J = 5.7, 1.9$ Hz, 2H), 1.76 (s, 3H), 1.49 (s, 2H), 1.37 (s, 3H).

$^{13}\text{C}\{^1\text{H}\}$ NMR Spectra (126 MHz, CDCl_3): δ 166.49, 134.58, 132.62, 130.03, 129.61, 126.63, 116.40, 106.03, 80.22, 78.00, 61.06, 31.48, 29.60, 28.35, 23.26.

HRMS: m/z $[\text{M}+\text{Na}]^+$ calcd for $\text{C}_{18}\text{H}_{18}\text{O}_4$: 321.1103. Found: 321.1098.

IR: 3085, 3002, 2933, 2330, 1780, 1744, 1642, 1496, 1449, 1416, 1393, 1317, 1280, 1206, 1155, 1078, 1045, 993, 954, 757, 698, 535 cm^{-1} .

4.13ii: 5-(7-chlorohept-2-yn-1-yl)-2,2-dimethyl-5-phenyl-1,3-dioxane-4,5-dione



Appearance: yellow oil, 0.055 g, 0.158 mmol, 66% yield.

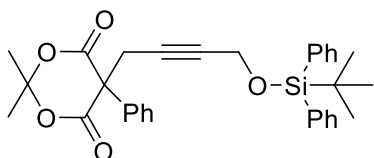
^1H NMR Spectra (500 MHz, CDCl_3): δ 7.52–7.44 (m, 2H), 7.44–7.34 (m, 3H), 3.55 (t, $J = 6.5$ Hz, 2H), 3.12 (t, $J = 2.3$ Hz, 2H), 2.19 (tt, $J = 7.0, 2.4$ Hz, 2H), 1.90–1.82 (m, 2H), 1.77 (s, 3H), 1.63 (q, $J = 7.2$ Hz, 2H), 1.35 (s, 3H).

$^{13}\text{C}\{^1\text{H}\}$ NMR Spectra (126 MHz, CDCl_3): δ 166.46, 134.54, 130.04, 129.61, 126.58, 105.96, 82.83, 76.19, 61.15, 44.91, 31.66, 31.56, 29.63, 28.31, 26.11, 18.24.

HRMS: m/z $[\text{M}+\text{H}]^+$ calcd for $\text{C}_{19}\text{H}_{21}\text{ClO}_4$: 349.1207. Found: 349.1208.

IR: 3063, 3000, 2935, 2866, 2359, 1780, 1744, 1496, 1449, 1393, 1382, 1316, 1279, 1206, 1153, 1102, 1076, 1043, 993, 954, 892, 761, 721, 697, 668, 649, 535 cm^{-1} .

4.13jj: 5-(4-((*tert*-butyldiphenylsilyl)oxy)but-2-yn-1-yl)-2,2-dimethyl-5-phenyl-1,3-dioxane-4,6-dione



Appearance: yellow oil, 0.09 g, 0.171 mmol, 71% yield.

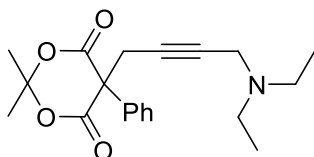
^1H NMR Spectra (500 MHz, CDCl_3): δ 7.76–7.63 (m, 5H), 7.50–7.47 (m, 2H), 7.43–7.38 (m, 8H), 4.26 (t, $J = 2.1$ Hz, 2H), 3.18 (t, $J = 2.1$ Hz, 2H), 1.70 (s, 3H), 1.34 (s, 3H), 1.05 (s, 9H).

$^{13}\text{C}\{^1\text{H}\}$ NMR Spectra (126 MHz, CDCl_3): δ 166.19, 135.91, 133.45, 130.07, 129.66, 128.10, 126.57, 106.11, 81.53, 80.37, 60.65, 53.08, 31.10, 29.67, 28.23, 27.03, 19.51.

HRMS: m/z $[\text{M}]^+$ calcd for $\text{C}_{32}\text{H}_{34}\text{O}_5\text{Si}$: 526.2176. Found: 526.2192.

IR: 3070, 2930, 2858, 2359, 1781, 1746, 1494, 1472, 1449, 1427, 1393, 1317, 1280, 1208, 1153, 1112, 1076, 1045, 996, 952, 824, 741, 701, 614, 537, 504 cm^{-1} .

4.13kk: 5-(4-(diethylamino)but-2-yn-1-yl)-2,2-dimethyl-5-phenyl-1,3-dioxane-4,6-dione



Appearance: yellow oil, 0.080 g, 0.233 mmol, 96% yield.

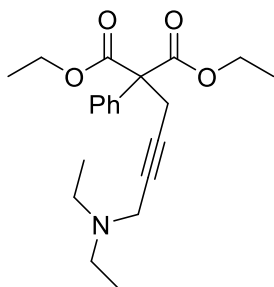
^1H NMR Spectra (500 MHz, CDCl_3): δ 7.52–7.46 (m, 2H), 7.44–7.36 (m, 3H), 3.41 (t, $J = 2.1$ Hz, 2H), 3.16 (t, $J = 2.1$ Hz, 2H), 2.50 (q, $J = 7.2$ Hz, 4H), 1.75 (s, 3H), 1.33 (s, 3H), 1.06 (t, $J = 7.2$ Hz, 6H).

$^{13}\text{C}\{^1\text{H}\}$ NMR Spectra (126 MHz, CDCl_3): δ 166.28, 134.45, 130.11, 129.67, 126.56, 105.91, 77.56, 61.20, 47.56, 40.79, 31.68, 29.49, 28.27, 13.16.

HRMS: m/z $[\text{M}]^+$ calcd for $\text{C}_{20}\text{H}_{25}\text{NO}_4$: 343.1784. Found: 343.1778.

IR: 2970, 2935, 2822, 2359, 1781, 1746, 1395, 1316, 1278, 1208, 1153, 1118, 1076, 1043, 954, 755, 698, 618, 554, 535, 502 cm^{-1} .

4.13ll: diethyl 2-(4-(diethylamino)but-2-yn-1-yl)-2-phenylmalonate



Appearance: Yellow oil, 0.068 g, 0.189 mmol, 79% yield.

^1H NMR Spectra (500 MHz, CDCl_3): δ 7.58–7.45 (m, 2H), 7.41–7.27 (m, 3H), 4.25 (qd, $J = 7.1$, 4.6 Hz, 4H), 3.33 (t, $J = 2.1$ Hz, 2H), 3.22 (t, $J = 2.1$ Hz, 2H), 2.39 (q, $J = 7.2$ Hz, 4H), 1.26 (t, $J = 7.1$ Hz, 6H), 0.98 (t, $J = 7.2$ Hz, 6H).

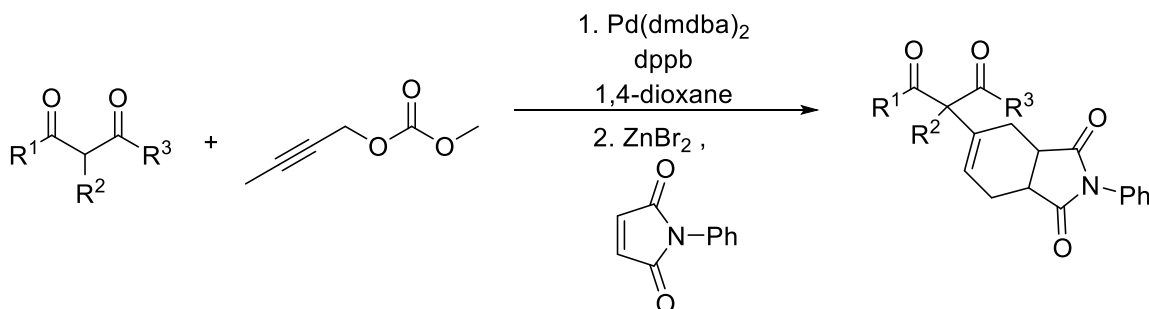
$^{13}\text{C}\{^1\text{H}\}$ NMR Spectra (126 MHz, CDCl_3): δ 169.87, 136.19, 128.53, 128.28, 128.11, 80.29, 78.39, 62.51, 62.23, 47.42, 40.92, 26.82, 14.33, 12.99.

HRMS: m/z $[\text{M}]^+$ calcd for $\text{C}_{21}\text{H}_{29}\text{NO}_4$: 359.2097. Found: 359.2107.

IR: 2970, 2935, 2821, 2358, 1734, 1500, 1456, 1386, 1366, 1317, 1290, 1208, 1153, 1092, 1066, 1038, 1025, 859, 755, 697, 617, 505 cm^{-1} .

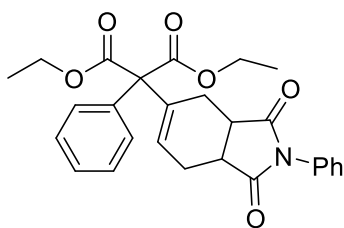
5. General Procedure and Spectral Data of Diels-Alder Products 4.14a-d:

General Procedure for the Diels-Alder Reaction of Dienylated Products:



A Biotage microwave reaction vial (part no. 354624) was flame dried, equipped with a magnetic stir bar, and brought into a glovebox under an argon atmosphere. Inside of the glovebox, catalyst (10 mol% Pd(dmdba)₂), ligand (10 mol% dppb), a 1,3-dicarbonyl compound (0.24 mmol), and a propargyl carbonate (0.24 mmol) were added to the reaction vial and dissolved in 1.5 mL 1,4-dioxane. The reaction vial was sealed, removed from the glovebox, and placed in an oil bath heated to 80 °C. The reaction vial was stirred at 80 °C for 2 hours, after which the vial was removed from the oil bath and returned to the glovebox. Inside of the glovebox, the vial was unsealed, and ZnBr₂ (20 mol%) and N-phenylmaleimide (0.48 mmol) were added. The vial was resealed, removed from the glovebox, and returned to the oil bath heated to 80 °C. The reaction vial was stirred at 80 °C for 4 hours and then removed from the oil bath and unsealed. The solvent was removed via rotary evaporation, and the crude product was purified and isolated via column chromatography using an eluant of 20-40% EtOAc in hexanes.

4.14a: diethyl 2-(1,3-dioxo-2-phenyl-2,3,3a,4,7,7a-hexahydro-1H-isoindol-5-yl)-2-phenylmalonate



Appearance: Yellow solid, 0.061 g, 0.132 mmol, 55% yield.

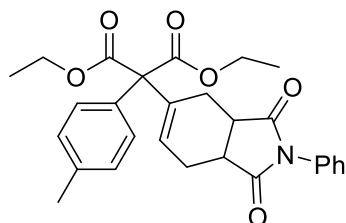
¹H NMR Spectra (500 MHz, CDCl₃): δ ¹H NMR (500 MHz, Chloroform-*d*) δ 7.46 (t, *J* = 7.7 Hz, 2H), 7.40–7.36 (m, 1H), 7.35–7.25 (m, 7H), 5.75 (dd, *J* = 6.2, 4.4 Hz, 1H), 4.27 (qd, *J* = 7.1, 1.8 Hz, 4H), 3.27–3.12 (m, 2H), 2.66 (ddd, *J* = 15.3, 6.3, 4.0 Hz, 1H), 2.51 (t, *J* = 5.2 Hz, 2H), 2.42 (ddd, *J* = 15.3, 6.8, 4.5 Hz, 1H), 1.26 (td, *J* = 7.1, 1.0 Hz, 6H).

¹³C{¹H} NMR Spectra (126 MHz, CDCl₃): δ 179.02, 178.24, 169.55, 169.32, 139.41, 135.87, 132.50, 129.32, 129.19, 128.74, 128.44, 128.08, 126.86, 126.72, 70.19, 67.43, 62.39, 62.26, 40.28, 39.68, 28.34, 24.48, 14.30.

HRMS: *m/z* [M+H]⁺ calcd for C₂₇H₂₇NO₆: 462.1917. Found: 462.1913.

IR: 3062, 2980, 2872, 2359, 1731, 1599, 1500, 1447, 1383, 1246, 1206, 1186, 1155, 1025, 859, 755, 695, 622, 582, 507 cm^{-1} .

4.14b: diethyl 2-(1,3-dioxo-2-phenyl-2,3,3a,4,7,7a-hexahydro-1H-isoindol-5-yl)-2-(*p*-tolyl)malonate



Appearance: Yellow oil, 0.080 g, 0.168 mmol, 70% yield.

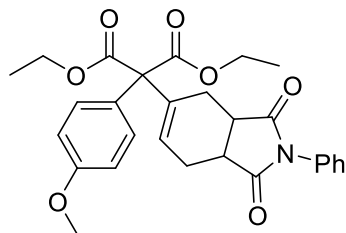
^1H NMR Spectra (500 MHz, CDCl_3): δ 7.46 (dd, $J = 8.4, 7.1$ Hz, 2H), 7.40–7.36 (m, 1H), 7.32 (dd, $J = 8.2, 1.3$ Hz, 2H), 7.21–7.12 (m, 2H), 7.07 (d, $J = 8.1$ Hz, 2H), 5.74 (t, $J = 5.3$ Hz, 1H), 4.25 (q, $J = 7.1$ Hz, 4H), 3.23–3.14 (m, 2H), 2.64 (ddd, $J = 15.4, 6.2, 4.2$ Hz, 1H), 2.55–2.46 (m, 2H), 2.43 (ddd, $J = 15.3, 6.7, 4.5$ Hz, 1H), 2.30 (s, 3H), 1.26 (t, $J = 7.1$ Hz, 6H).

$^{13}\text{C}\{^1\text{H}\}$ NMR Spectra (126 MHz, CDCl_3): δ 179.05, 178.29, 169.70, 169.46, 139.54, 137.85, 132.86, 132.54, 129.31, 129.18, 129.05, 128.73, 126.87, 126.56, 100.33, 69.91, 62.34, 62.21, 40.33, 39.74, 28.39, 24.50, 21.34, 14.30.

HRMS: m/z $[\text{M}+\text{Na}]^+$ calcd for $\text{C}_{28}\text{H}_{29}\text{NO}_6$: 498.1893. Found: 498.1902.

IR: 2980, 2929, 2851, 2361, 1713, 1599, 1500, 1446, 1383, 1248, 1208, 1153, 1035, 859, 755, 694, 621, 585, 504 cm^{-1} .

4.14c: diethyl 2-(1,3-dioxo-2-phenyl-2,3,3a,4,7,7a-hexahydro-1H-isoindol-5-yl)-2-(4-methoxyphenyl)malonate



Appearance: orange solid, 0.097 g, 0.197 mmol, 92% yield.

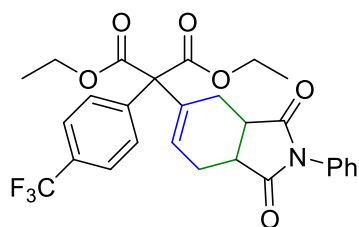
^1H NMR Spectra (500 MHz, CDCl_3): δ 7.46 (t, $J = 7.7$ Hz, 2H), 7.40–7.36 (m, 1H), 7.35–7.27 (m, 2H), 7.24–7.16 (m, 2H), 6.77 (d, $J = 8.7$ Hz, 2H), 5.75 (dd, $J = 6.1, 4.5$ Hz, 1H), 4.33–4.17 (m, 4H), 3.74 (d, $J = 0.9$ Hz, 3H), 3.23–3.14 (m, 2H), 2.66 (ddd, $J = 15.3, 6.3, 3.9$ Hz, 1H), 2.51 (t, $J = 4.9$ Hz, 2H), 2.42 (dd, $J = 15.3, 5.1$ Hz, 1H), 1.26 (t, $J = 7.1$ Hz, 6H).

$^{13}\text{C}\{^1\text{H}\}$ NMR Spectra (126 MHz, CDCl_3): δ 179.05, 178.24, 169.74, 169.54, 159.25, 139.68, 132.55, 130.39, 129.32, 128.73, 127.85, 126.86, 126.40, 113.86, 69.54, 62.35, 62.22, 55.55, 40.31, 39.73, 28.31, 24.50, 14.31.

HRMS: m/z $[\text{M}+\text{Na}]^+$ calcd for $\text{C}_{28}\text{H}_{29}\text{NO}_7$: 514.1842. Found: 514.1840.

IR: 3063, 2979, 2935, 1727, 1711, 1610, 1512, 1502, 1443, 1383, 1299, 1253, 1206, 1186, 1153, 1032, 838, 768, 694, 621, 585, 554 cm^{-1} .

4.14d: diethyl 2-(1,3-dioxo-2-phenyl-2,3,3a,4,7,7a-hexahydro-1H-isoindol-5-yl)-2-(4-(trifluoromethyl)phenyl)malonate



Appearance: Yellow oil, 0.075 g, 0.142 mmol, 59% yield.

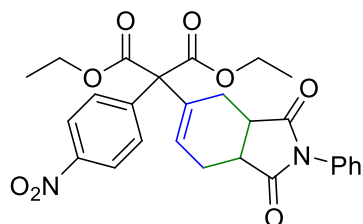
^1H NMR Spectra (500 MHz, CDCl_3): δ 7.59–7.41 (m, 6H), 7.41–7.37 (m, 1H), 7.31 (dt, $J = 8.3, 1.1$ Hz, 2H), 5.75 (dd, $J = 6.5, 3.9$ Hz, 1H), 4.34–4.18 (m, 4H), 3.25–3.17 (m, 2H), 2.71 (ddd, $J = 15.4, 6.6, 3.6$ Hz, 1H), 2.53 (td, $J = 17.0, 16.3, 5.2$ Hz, 2H), 2.42 (ddd, $J = 15.3, 6.8, 4.1$ Hz, 1H), 1.32–1.17 (m, 6H).

$^{13}\text{C}\{^1\text{H}\}$ NMR Spectra (126 MHz, CDCl_3): δ 178.87, 178.03, 169.00, 168.78, 139.86, 138.89, 132.43, 129.74, 129.35, 128.80, 127.35, 126.70, 125.42, 125.38, 125.35, 125.32, 69.95, 62.75, 40.17, 39.54, 28.22, 24.54, 14.28.

HRMS: m/z $[\text{M}+\text{H}]^+$ calcd for $\text{C}_{28}\text{H}_{26}\text{F}_3\text{NO}_6$: 530.1790. Found: 530.1768.

IR: 2982, 2938, 2361, 1734, 1713, 1383, 1329, 1255, 1208, 1153, 1123, 1072, 1018, 848, 769, 754, 692, 502 cm^{-1} .

4.14e: diethyl 2-(1,3-dioxo-2-phenyl-2,3,3a,4,7,7a-hexahydro-1H-isoindol-5-yl)-2-(4-nitrophenyl)malonate



Appearance: Yellow solid, 0.053 g, 0.103 mmol, 43% yield.

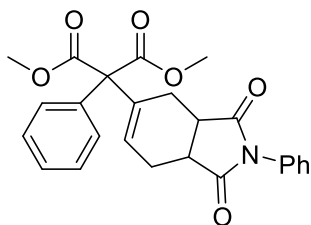
^1H NMR Spectra (500 MHz, CDCl_3): δ 8.10–8.02 (m, 2H), 7.56–7.43 (m, 4H), 7.42–7.38 (m, 1H), 7.34–7.27 (m, 2H), 5.77 (ddd, $J = 6.2, 4.1, 1.5$ Hz, 1H), 4.28 (dq, $J = 14.2, 7.1, 2.1$ Hz, 4H), 3.26–3.18 (m, 2H), 2.77–2.72 (m, 1H), 2.57–2.47 (m, 2H), 2.44–2.39 (m, 1H), 1.27 (dt, $J = 9.6, 7.1$ Hz, 6H).

$^{13}\text{C}\{^1\text{H}\}$ NMR Spectra (126 MHz, CDCl_3): δ 178.77, 177.91, 168.62, 168.44, 147.52, 143.00, 138.56, 132.35, 130.42, 129.40, 128.90, 127.68, 126.58, 123.49, 69.92, 62.97, 62.82, 40.09, 39.40, 28.12, 24.61, 14.26.

HRMS: m/z $[\text{M}+\text{H}]^+$ calcd for $\text{C}_{27}\text{H}_{26}\text{N}_2\text{O}_8$: 507.1767. Found: 507.1767.

IR: 3056, 2980, 2936, 2361, 2344, 1740, 1714, 1559, 1522, 1208, 1153, 858, 771, 554, 501 cm^{-1} .

4.14f: dimethyl 2-(1,3-dioxo-2-phenyl-2,3,3a,4,7,7a-hexahydro-1H-isoindol-5-yl)-2-phenylmalonate



Appearance: Yellow oil, 0.070 g, 0.161 mmol, 67% yield.

^1H NMR Spectra (500 MHz, CDCl_3): δ 7.47 (dd, $J = 8.4, 7.1$ Hz, 2H), 7.40–7.36 (m, 1H), 7.35–7.26 (m, 7H), 5.72 (ddd, $J = 6.1, 3.9, 1.6$ Hz, 1H), 3.74 (d, $J = 1.7$ Hz, 6H), 3.22 (dddd, $J = 16.4, 13.4, 9.7, 3.9$ Hz, 2H), 2.71 (ddd, $J = 15.5, 6.6, 3.7$ Hz, 1H), 2.57–2.46 (m, 2H), 2.43–2.36 (m, 1H).

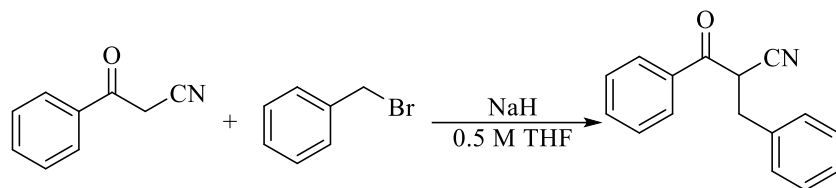
$^{13}\text{C}\{^1\text{H}\}$ NMR Spectra (126 MHz, CDCl_3): δ 179.03, 178.30, 170.12, 169.78, 139.04, 135.69, 132.49, 129.38, 129.11, 128.82, 128.58, 128.25, 127.13, 126.88, 70.33, 53.41, 53.29, 40.22, 39.63, 28.43, 24.50.

HRMS: m/z $[\text{M}]^+$ calcd for $\text{C}_{25}\text{H}_{23}\text{NO}_6$: 433.1525. Found: 433.1530.

IR: 3062, 3003, 2953, 2848, 1732, 1709, 1597, 1497, 1447, 1435, 1385, 1315, 1255, 1210, 1156, 1089, 1031, 1012, 956, 757, 695, 622, 582 cm^{-1} .

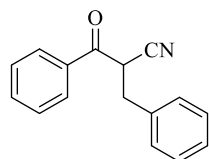
6. Preparation and Spectral Data of Benzoyl Acetonitrile Compounds

General procedure for the synthesis of benzoyl acetonitrile derivative 4.15a



A flame-dried 100 mL Schlenk flask equipped with a stir bar was attached to a Schlenk-nitrogen line and charged with N₂. Sodium hydride (30 mmol) was dissolved in THF (40 mL). Benzoyl acetonitrile (20 mmol) was added slowly and stirred at room temperature for 10 minutes. Then benzyl bromide (20 mmol) was added dropwise. The reaction mixture was stirred at room temperature for 16 h. Then, the reaction was quenched with saturated NH₄Cl (aq) and extracted with EtOAc (3 x 100 mL). The organic layers were combined and dried over MgSO₄. The crude material was purified via flash column chromatography using an eluent of 20% EtOAc in Hexanes.

4.15a: 2-benzyl-3-oxo-3-phenylpropanenitrile



Appearance: White solid.

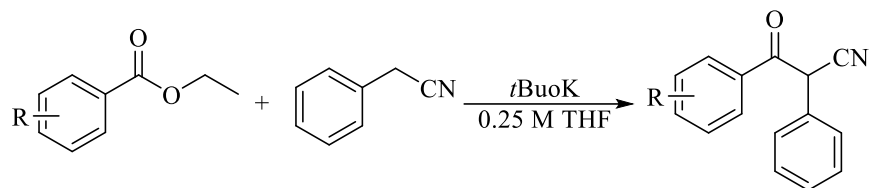
¹H NMR Spectra (500 MHz, CDCl₃): δ 7.96 (d, *J* = 7.8 Hz, 2H), 7.66 (t, *J* = 7.4 Hz, 1H), 7.52 (t, *J* = 7.7 Hz, 2H), 7.40–7.27 (m, 5H), 4.53 (dd, *J* = 8.9, 5.7 Hz, 1H), 3.37 (dd, *J* = 14.0, 5.7 Hz, 1H), 3.25 (dd, *J* = 14.0, 8.9 Hz, 1H).

¹³C{¹H} NMR Spectra (126 MHz, CDCl₃): δ 189.96, 135.93, 134.64, 134.03, 129.17, 129.06, 128.98, 128.85, 127.71, 116.99, 41.84, 35.48.

HRMS: *m/z* [M+Na]⁺ calcd for C₁₆H₁₃NO: 258.0895. Found: 258.0892.

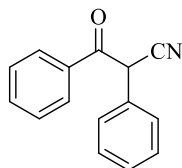
IR: 3040, 2360, 2340, 1700, 1684, 1670, 1653, 1636, 1617, 1559, 1540, 1219, 1154, 772, 668, 504 cm⁻¹.

General procedure for the synthesis of benzoyl acetonitrile derivatives 4.17a-b⁷



A flame-dried 100 mL Schlenk flask equipped with a stir bar was attached to a Schlenk-nitrogen line and charged with N₂. *t*BuOK (22 mmol) was dissolved in THF (40 mL). Ethyl benzoate derivatives (10 mmol) were then added slowly and stirred at room temperature for 10 minutes. Then benzyl cyanide (10 mmol) was added dropwise. The reaction mixture was stirred at room temperature for 16 h. Then, the reaction was quenched with water and diluted with EtOAc (20 mL). The mixture was extracted with EtOAc (2 x 30 mL) and washed with NaHCO₃ (aq) (25 ml) and brine (25 ml). The organic layers were combined and dried over anhydrous Na₂SO₄. The crude mixture was purified via flash column chromatography using an eluent of 20% EtOAc in Hexanes.

4.17a: 3-oxo-2,3-diphenylpropanenitrile



Appearance: White solid.

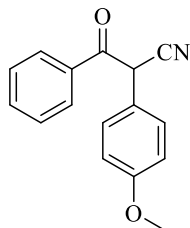
¹H NMR Spectra (500 MHz, CDCl₃): δ 7.95 (dd, *J* = 8.4, 1.3 Hz, 2H), 7.63–7.57 (m, 1H), 7.51–7.33 (m, 7H), 5.59 (s, 1H).

¹³C{¹H} NMR Spectra (126 MHz, CDCl₃): δ 188.84, 134.44, 130.21, 129.68, 129.29, 129.16, 129.04, 128.51, 128.25, 116.50, 46.70.

HRMS: *m/z* [M+H]⁺ calcd for C₁₅H₁₁NO: 222.0919. Found: 222.0915.

IR: 3028, 2360, 2340, 1733, 1699, 1684, 1655, 1559, 1540, 1507, 1457, 1219, 1153, 1045, 911, 770, 668 cm⁻¹.

4.17b: 2-(4-methoxyphenyl)-3-oxo-3-phenylpropanenitrile



Appearance: Beige solid.

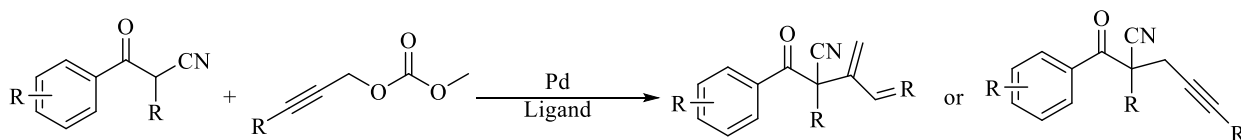
^1H NMR Spectra (500 MHz, CDCl_3): δ 8.01–7.92 (m, 2H), 7.64–7.59 (m, 1H), 7.51–7.44 (m, 2H), 7.41–7.34 (m, 2H), 6.97–6.89 (m, 2H), 5.57 (s, 1H), 3.81 (s, 3H).

$^{13}\text{C}\{^1\text{H}\}$ NMR Spectra (126 MHz, CDCl_3): δ 189.05, 160.11, 134.37, 133.61, 129.51, 129.21, 129.02, 122.10, 116.76, 115.09, 55.38, 45.93.

HRMS: m/z $[\text{M}]^+$ calcd for $\text{C}_{16}\text{H}_{13}\text{NO}_2$: 251.0946. Found: 251.0952.

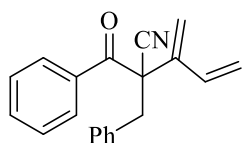
IR: 3040, 2360, 2340, 1717, 1684, 1653, 1616, 1559, 1540, 1510, 1457, 1448, 1306, 1219, 1181, 1153, 1032, 773, 668, 639, 505 cm^{-1} .

7. General Procedure and Spectral Data of Dienyl and Propargyl Products (Project 2)



A Biotage microwave reaction vial (part no. 354624) was flame dried, equipped with a magnetic stir bar, and brought into a glovebox under an argon atmosphere. Inside of the glovebox, catalyst (10 mol% $\text{Pd}(\text{dmdba})_2$), ligand (10 mol% dppb, dppe, or *t*Bu-DavePhos), a benzoyl acetonitrile derivative (0.24 mmol), and a propargyl carbonate (0.24 mmol) were added to the reaction vial and dissolved in 1.5 mL 1,4-dioxane. The reaction vial was sealed, removed from the glovebox, and placed in an oil bath heated to 80 °C. The reaction vial was stirred at 80 °C for 2 hours, after which the vial was unsealed. The solvent was removed via rotary evaporation, and the crude product was purified and isolated via column chromatography using an eluant of 10% EtOAc in hexanes.

4.16a: 2-benzoyl-2-benzyl-3-methylenepent-4-enitrile



Appearance: Yellow oil, 0.039 g, 0.134 mmol, 56% yield.

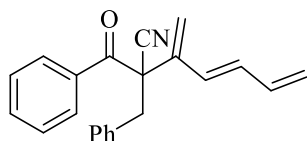
^1H NMR Spectra (500 MHz, CDCl_3): δ 8.13–8.01 (m, 2H), 7.60–7.53 (m, 1H), 7.48–7.35 (m, 2H), 7.33–7.26 (m, 5H), 6.08 (dd, $J = 17.3, 11.1$ Hz, 1H), 5.54 (s, 1H), 5.48 (d, $J = 17.3$ Hz, 1H), 5.30 (d, $J = 1.6$ Hz, 1H), 5.19 (d, $J = 11.1$ Hz, 1H), 3.55–3.49 (m, 1H), 3.35 (d, $J = 13.8$ Hz, 1H).

$^{13}\text{C}\{^1\text{H}\}$ NMR Spectra (126 MHz, CDCl_3): δ 167.31, 153.15, 144.77, 134.02, 132.76, 130.88, 129.72, 128.47, 128.12, 127.51, 123.78, 118.93, 117.99, 104.37, 92.36, 40.73.

HRMS: m/z $[\text{M}+]^+$ calcd for $\text{C}_{20}\text{H}_{17}\text{NO}$: 287.1310. Found: 287.1314.

IR: 3005, 2360, 2340, 1700, 1684, 1653, 1646, 1559, 1540, 1219, 1155, 772, 668 cm^{-1} .

4.16b: (E)-2-benzoyl-2-benzyl-3-methylenehepta-4,6-dienitrile



Appearance: Yellow oil, 0.015 g, 0.048 mmol, 48% yield, isolated with some leftover starting benzoyl acetonitrile compound.

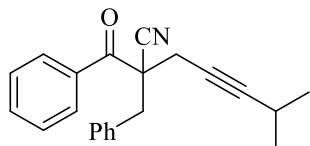
^1H NMR Spectra (500 MHz, CDCl_3): δ 8.06–7.93 (m, 2H), 7.48 (dd, $J = 7.9, 6.6$ Hz, 1H), 7.34 (td, $J = 7.4, 4.5$ Hz, 2H), 7.25–7.19 (m, 5H), 6.42 (dd, $J = 15.4, 10.5$ Hz, 1H), 6.21 (dt, $J = 16.8, 10.3$ Hz, 1H), 5.84 (d, $J = 15.4$ Hz, 1H), 5.49 (s, 1H), 5.25–5.17 (m, 2H), 5.12 (d, $J = 10.0$ Hz, 1H), 3.45 (d, $J = 13.9$ Hz, 1H), 3.27 (d, $J = 13.8$ Hz, 1H).

$^{13}\text{C}\{^1\text{H}\}$ NMR Spectra (126 MHz, CDCl_3): δ 191.22, 140.24, 136.31, 133.99, 133.96, 130.90, 130.41, 129.72, 128.97, 128.69, 128.50, 128.43, 128.10, 127.55, 127.51, 120.03, 116.87, 41.00.

HRMS: m/z $[\text{M}+\text{H}]^+$ calcd for $\text{C}_{22}\text{H}_{19}\text{NO}$: 314.1545. Found: 314.1548.

IR: 3019, 2840, 2360, 2340, 1717, 1684, 1653, 1576, 1559, 1540, 1507, 1457, 1220, 1153, 913, 772 cm^{-1} .

4.16c: 2-benzoyl-2-benzyl-6-methylhept-4-ynitrile



Appearance: Clear oil, 0.028 g, 0.086 mmol, 86% yield.

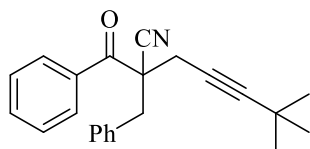
^1H NMR Spectra (500 MHz, CDCl_3): δ 7.87–7.81 (m, 2H), 7.57–7.52 (m, 1H), 7.44–7.36 (m, 2H), 7.28 (ddt, $J = 7.2, 4.4, 2.0$ Hz, 5H), 3.45 (d, $J = 13.5$ Hz, 1H), 3.33 (d, $J = 13.6$ Hz, 1H), 2.91 (dd, $J = 16.5, 2.2$ Hz, 1H), 2.81 (dd, $J = 16.5, 2.2$ Hz, 1H), 2.52 (ddt, $J = 13.7, 6.9, 2.2$ Hz, 1H), 1.12 (dd, $J = 6.9, 2.4$ Hz, 6H).

$^{13}\text{C}\{^1\text{H}\}$ NMR Spectra (126 MHz, CDCl_3): δ 194.47, 135.84, 133.92, 133.24, 130.41, 128.95, 128.65, 128.37, 127.89, 120.25, 91.73, 72.40, 53.02, 41.81, 27.95, 22.90, 20.41.

HRMS: m/z $[\text{M}]^+$ calcd for $\text{C}_{22}\text{H}_{21}\text{NO}$: 315.1623. Found: 315.1624.

IR: 2839, 2360, 2340, 2235, 1695, 1608, 1511, 1457, 1301, 1256, 1223, 1184, 1154, 1032, 821, 759, 699, 668 cm^{-1} .

4.16d: 2-benzoyl-2-benzyl-6,6-dimethylhept-4-ynenitrile



Appearance: Clear oil, 0.028 g, 0.085 mmol, 85% yield.

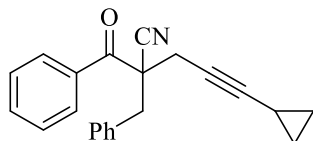
^1H NMR Spectra (500 MHz, CDCl_3): δ 7.85 (dd, $J = 8.3, 1.4$ Hz, 2H), 7.57–7.52 (m, 1H), 7.41 (t, $J = 7.8$ Hz, 2H), 7.32–7.25 (m, 5H), 3.45 (d, $J = 13.5$ Hz, 1H), 3.33 (d, $J = 13.6$ Hz, 1H), 2.90 (d, $J = 16.5$ Hz, 1H), 2.81 (d, $J = 16.5$ Hz, 1H), 1.18 (s, 9H).

$^{13}\text{C}\{^1\text{H}\}$ NMR Spectra (126 MHz, CDCl_3): δ 194.34, 135.84, 134.02, 133.27, 130.42, 128.96, 128.65, 128.30, 127.82, 120.30, 94.61, 71.87, 52.70, 41.68, 30.77, 27.44, 27.29.

HRMS: m/z $[\text{M}+\text{Na}]^+$ calcd for $\text{C}_{23}\text{H}_{23}\text{NO}$: 352. 1677. Found: 352.1692.

IR: 2968, 2360, 2340, 1695, 1684, 1653, 1559, 1540, 1457, 1219, 1152, 913, 772, 744, 668, 638, 504 cm^{-1} .

4.16e: 2-benzoyl-2-benzyl-5-cyclopropylpent-4-ynenitrile



Appearance: Yellow oil, 0.021 g, 0.068 mmol, 68% yield.

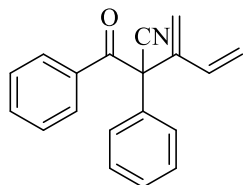
^1H NMR Spectra (500 MHz, CDCl_3): δ 7.83 (dd, $J = 8.3, 1.4$ Hz, 2H), 7.57–7.53 (m, 1H), 7.41 (t, $J = 7.8$ Hz, 2H), 7.32–7.25 (m, 5H), 3.44 (d, $J = 13.5$ Hz, 1H), 3.31 (d, $J = 13.6$ Hz, 1H), 2.89 (dd, $J = 16.6, 2.0$ Hz, 1H), 2.79 (dd, $J = 16.6, 2.0$ Hz, 1H), 1.21 (dddd, $J = 13.3, 6.4, 5.0, 2.8$ Hz, 1H), 0.72 (dt, $J = 8.2, 3.2$ Hz, 2H), 0.64–0.55 (m, 2H).

$^{13}\text{C}\{^1\text{H}\}$ NMR Spectra (126 MHz, CDCl_3): δ 194.90, 136.24, 134.42, 133.82, 130.91, 129.40, 129.12, 128.90, 128.42, 120.82, 89.63, 68.95, 53.24, 42.45, 28.45, 8.77, -0.09.

HRMS: m/z $[\text{M}]^+$ calcd for $\text{C}_{22}\text{H}_{19}\text{NO}$: 313.1467. Found: 313.1465.

IR: 2970, 2360, 2340, 1717, 1695, 1684, 1653, 1576, 1559, 1540, 1457, 1212, 1151, 913, 772, 635 cm^{-1} .

4.18a: 2-benzoyl-3-methylene-2-phenylpent-4-enitrile



Appearance: Yellow oil, 0.037 g, 0.134 mmol, 56% yield.

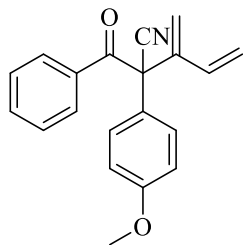
^1H NMR Spectra (500 MHz, CDCl_3): δ 7.96–7.85 (m, 2H), 7.63–7.32 (m, 8H), 6.39 (dd, $J = 17.5, 11.2$ Hz, 1H), 5.65 (s, 1H), 5.43 (d, $J = 17.6$ Hz, 1H), 5.28 (d, $J = 11.1$ Hz, 1H), 4.79 (s, 1H).

$^{13}\text{C}\{^1\text{H}\}$ NMR Spectra (126 MHz, CDCl_3): δ 190.90, 143.60, 134.54, 134.01, 133.88, 133.20, 130.15, 129.40, 129.16, 128.50, 128.22, 121.20, 121.18, 119.40, 117.85.

HRMS: m/z $[\text{M}+\text{Li}]^+$ calcd for $\text{C}_{19}\text{H}_{15}\text{NO}$: 280.1314. Found: 280.1327.

IR: 2986, 2360, 2340, 1770, 1751, 1717, 1700, 1653, 1374, 1220, 1153, 1045, 847, 770, 668, 637, 608, 504 cm^{-1} .

4.18b: 2-benzoyl-2-(4-methoxyphenyl)-3-methylenepent-4-enitrile



Appearance: Yellow oil, 0.030 g, 0.098 mmol, 41% yield.

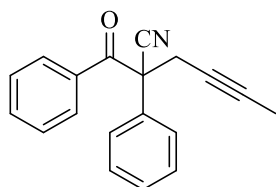
^1H NMR Spectra (500 MHz, CDCl_3): δ 7.98–7.83 (m, 2H), 7.62–7.49 (m, 1H), 7.47–7.32 (m, 4H), 6.39 (dd, $J = 17.6, 11.2$ Hz, 1H), 5.64 (s, 1H), 5.41 (d, $J = 17.6$ Hz, 1H), 5.27 (d, $J = 11.2$ Hz, 1H), 4.81 (s, 1H), 3.84 (s, 3H).

$^{13}\text{C}\{^1\text{H}\}$ NMR Spectra (126 MHz, CDCl_3): δ 191.11, 159.97, 143.87, 134.58, 134.14, 133.88, 130.12, 129.51, 128.49, 124.83, 121.13, 121.07, 119.63, 117.72, 114.75, 55.54.

HRMS: m/z $[\text{M}+\text{Na}]^+$ calcd for $\text{C}_{20}\text{H}_{17}\text{NO}_2$: 326.1157. Found: 326.1160.

IR: 2839, 2360, 2340, 1695, 1607, 1511, 1447, 1223, 1185, 1032, 759, 699, 669 cm^{-1} .

4.18h: 2-benzoyl-2-phenylhex-4-ynenitrile



Appearance: Yellow oil, 0.021 g, 0.078 mmol, 78% yield, collected with a small amount of diene isomer.

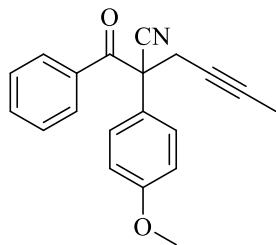
^1H NMR Spectra (500 MHz, CDCl_3): δ 7.88–7.81 (m, 2H), 7.52–7.46 (m, 3H), 7.44–7.33 (m, 5H), 3.25 (dq, $J = 16.5, 2.5$ Hz, 1H), 2.93 (dq, $J = 16.6, 2.5$ Hz, 1H), 1.76 (t, $J = 2.5$ Hz, 3H).

$^{13}\text{C}\{^1\text{H}\}$ NMR Spectra (126 MHz, CDCl_3): δ 190.07, 134.80, 133.83, 133.49, 130.15, 129.59, 129.00, 128.50, 126.08, 119.14, 80.40, 72.73, 56.83, 30.85, 3.64.

HRMS: m/z $[\text{M}+\text{H}]^+$ calcd for $\text{C}_{19}\text{H}_{15}\text{NO}$: 274.1232. Found: 274.1229.

IR: 3019, 2400, 2360, 2339, 2253, 1695, 1653, 1635, 1449, 1220, 1153, 913, 773, 701, 668, 638, 505 cm^{-1} .

4.18i: 2-benzoyl-2-(4-methoxyphenyl)hex-4-ynenitrile



Appearance: Yellow oil, 0.0197 g, 0.068 mmol, 27% yield.

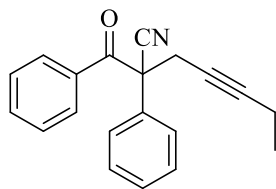
^1H NMR Spectra (500 MHz, CDCl_3): δ 7.90–7.82 (m, 2H), 7.50 (t, $J = 7.4$ Hz, 1H), 7.43–7.31 (m, 4H), 6.97–6.89 (m, 2H), 3.80 (s, 3H), 3.21 (dq, $J = 16.5, 2.5$ Hz, 1H), 2.89 (dq, $J = 16.6, 2.5$ Hz, 1H), 1.76 (t, $J = 2.5$ Hz, 3H).

$^{13}\text{C}\{^1\text{H}\}$ NMR Spectra (126 MHz, CDCl_3): δ 190.42, 159.86, 133.78, 133.54, 130.15, 128.49, 127.38, 126.58, 119.37, 114.92, 80.43, 72.99, 56.11, 55.53, 31.07, 3.64.

HRMS: m/z $[\text{M}]^+$ calcd for $\text{C}_{20}\text{H}_{17}\text{NO}_2$: 303.1259. Found: 303.1257.

IR: 2839, 2360, 2340, 2235, 1695, 1653, 1608, 1511, 1301, 1256, 1223, 1184, 1032, 759, 699, 669 cm^{-1} .

4.18j: 2-benzoyl-2-phenylhept-4-ynenitrile



Appearance: Yellow oil, 0.025 g, 0.204 mmol, 85% yield, collected with a small amount of diene isomer.

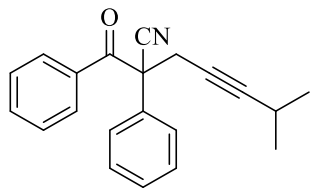
^1H NMR Spectra (500 MHz, CDCl_3): δ 7.90–7.80 (m, 2H), 7.53–7.46 (m, 3H), 7.45–7.40 (m, 2H), 7.40–7.33 (m, 3H), 3.24 (dt, $J = 16.6, 2.3$ Hz, 1H), 2.96 (dt, $J = 16.6, 2.4$ Hz, 1H), 2.16–2.07 (m, 2H), 1.06 (t, $J = 7.5$ Hz, 3H).

$^{13}\text{C}\{^1\text{H}\}$ NMR Spectra (126 MHz, CDCl_3): δ 190.24, 134.79, 133.81, 133.53, 130.13, 129.52, 128.97, 128.49, 126.16, 119.05, 86.62, 73.15, 56.81, 30.90, 14.05, 12.42.

HRMS: m/z $[\text{M}+\text{H}]^+$ calcd for $\text{C}_{20}\text{H}_{17}\text{NO}$: 288.1388. Found: 288.1389.

IR: 3019, 2360, 2340, 1699, 1684, 1653, 1559, 1540, 1219, 1153, 776, 668, 638, 504 cm^{-1} .

4.18k: 2-benzoyl-6-methyl-2-phenylhept-4-ynenitrile



Appearance: Yellow oil, 0.026 g, 0.087 mmol, 87% yield.

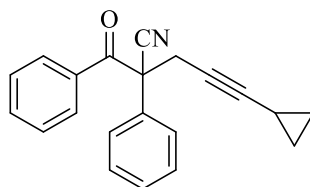
^1H NMR Spectra (500 MHz, CDCl_3): δ 7.87–7.83 (m, 2H), 7.53–7.47 (m, 3H), 7.45–7.40 (m, 2H), 7.40–7.33 (m, 3H), 3.22 (dd, $J = 16.6, 2.1$ Hz, 1H), 2.97 (dd, $J = 16.6, 2.3$ Hz, 1H), 2.47 (dtdd, $J = 9.1, 6.9, 4.5, 2.2$ Hz, 1H), 1.08 (t, $J = 7.0$ Hz, 6H).

$^{13}\text{C}\{^1\text{H}\}$ NMR Spectra (126 MHz, CDCl_3): δ 190.28, 134.78, 133.79, 133.57, 130.11, 129.46, 128.93, 128.49, 126.23, 118.98, 90.96, 72.98, 56.91, 30.75, 22.91, 20.50.

HRMS: m/z $[\text{M}]^+$ calcd for $\text{C}_{21}\text{H}_{19}\text{NO}$: 301.1467. Found: 301.1458.

IR: 3020, 2840, 2360, 2340, 1770, 1751, 1734, 1717, 1684, 1653, 1559, 1374, 1239, 1152, 1049, 913, 771, 668 cm^{-1} .

4.18l: 2-benzoyl-5-cyclopropyl-2-phenylpent-4-ynenitrile



Appearance: Yellow oil, 0.027 g, 0.09 mmol, 90% yield.

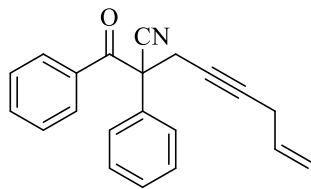
^1H NMR Spectra (500 MHz, CDCl_3): δ 7.89–7.78 (m, 2H), 7.53–7.45 (m, 3H), 7.45–7.40 (m, 2H), 7.40–7.33 (m, 3H), 3.21 (dd, $J = 16.6, 2.0$ Hz, 1H), 2.94 (dd, $J = 16.6, 1.9$ Hz, 1H), 1.15 (dddd, $J = 10.1, 8.6, 4.9, 2.5$ Hz, 1H), 0.73–0.63 (m, 2H), 0.56 (ttd, $J = 9.0, 5.6, 2.6$ Hz, 2H).

$^{13}\text{C}\{^1\text{H}\}$ NMR Spectra (126 MHz, CDCl_3): δ 190.62, 135.29, 134.33, 134.01, 130.64, 130.03, 129.49, 129.01, 126.65, 119.50, 88.92, 69.25, 57.48, 31.32, 8.65, 0.05.

HRMS: m/z $[\text{M}+\text{H}]^+$ calcd for $\text{C}_{21}\text{H}_{17}\text{NO}$: 300.1388. Found: 300.1392.

IR: 3020, 2924, 2360, 2340, 1717, 1695, 1684, 1653, 1576, 1559, 1448, 1226, 1154, 758, 704, 668, 638, 507 cm^{-1} .

4.18m: 2-benzoyl-2-phenyloct-7-en-4-ynenitrile



Appearance: Yellow oil, 0.020 g, 0.067 mmol, 67% yield.

^1H NMR Spectra (500 MHz, CDCl_3): δ 7.92–7.80 (m, 2H), 7.50 (dtt, $J = 5.6, 2.6, 1.7$ Hz, 3H), 7.46–7.40 (m, 2H), 7.36 (dtd, $J = 14.0, 6.7, 1.6$ Hz, 3H), 5.73 (dtd, $J = 17.0, 10.2, 5.1$ Hz, 1H), 5.21 (dq, $J = 17.0, 1.8$ Hz, 1H), 5.05 (dq, $J = 10.0, 1.7$ Hz, 1H), 3.30 (dt, $J = 16.6, 2.3$ Hz, 1H), 3.02 (dt, $J = 16.6, 2.4$ Hz, 1H), 2.97–2.82 (m, 2H).

$^{13}\text{C}\{^1\text{H}\}$ NMR Spectra (126 MHz, CDCl_3): δ 190.25, 134.68, 133.85, 133.47, 132.27, 130.14, 129.61, 129.03, 128.50, 126.15, 118.86, 115.99, 81.51, 56.92, 30.79, 22.88.

HRMS: m/z $[\text{M}+]^+$ calcd for $\text{C}_{22}\text{H}_{19}\text{NO}$: 315.1467. Found: 315.1455

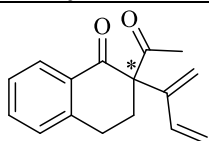
IR: 3019, 2400, 2360, 2339, 2253, 1695, 1653, 1449, 1220, 1153, 913, 773, 701, 668, 638, 505 cm^{-1} .

8. References:

- Gottlieb, H. E.; Kotlyar, V.; Nudelman, A. *J. Org. Chem.* **1997**, *62*, 7512.
- Minuti, Lucio; Taticchi, Aldo; Marrocchi, Assunta; Gacs-Baitz, Eszter. *Syn. Commun.*, **1998**, *28*, 2181.
- He, Z.; Li, H.; Li, Z. *J. Org. Chem.*, **2010**, *75*, 4636.
- Yip, S. F.; Cheung, H. Y.; Zhou, Z.; Kwong, F. Y. *Org. Lett.*, **2007**, *9*, 3469.
- Shintani, R.; Murakami, M.; Hayashi, T. *J. Am. Chem. Soc.*, **2007**, *129*, 12356.
- Capaccio, V.; Sicignano, M.; Rodríguez, R. I.; Salla, G. D.; Alemán, J. *Org. Lett.*, **2020**, *22*, 219.
- Wang, F.; Yang, T.; Wu, T.; Zheng, L-S; Yin, C.; Shi, Y.; Ye, X-Y; Chen, G-Q; Zhang, X. *J. Am. Chem. Soc.*, **2021**, *143*, 2477-2483.

9. Copies of HPLC Spectra

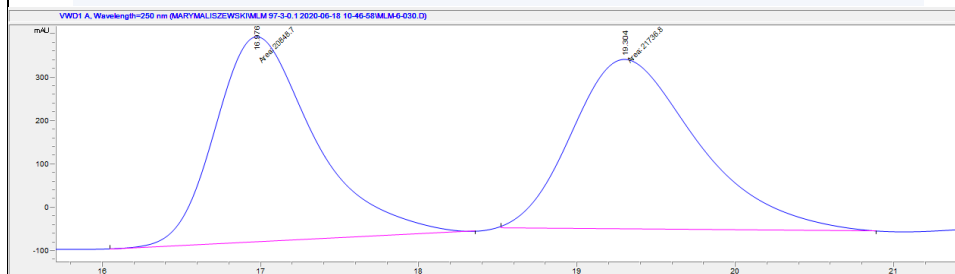
2-acetyl-2-(buta-1,3-dien-2-yl)-3,4-dihydronaphthalen-1(2H)-one



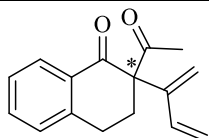
with dppe

File Information

LC-File	MLM-6-030.D
File Path	C:\CHEM32\1\DATA\MARYMALISZEWSKI\MLM 97-3-0.1 2020-06-18
Date	18-Jun-20, 11:05:30
Sample	MLM-6-030
Sample Info	
Barcode	
Operator	SYSTEM
Method	MLM_IB_IPA99-1-40MIN-FR0.3-250NM.M
Reference	
Analysis Time	39.997 min
Sampling Rate	0.0033 min (0.198 sec), 12000 datapoints



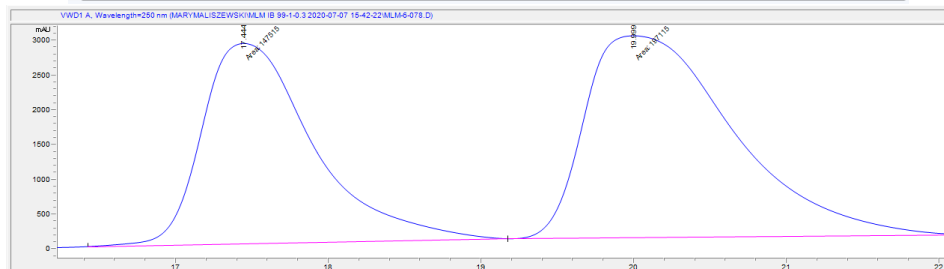
#	Time	Area	Height	Width	Area%	Symmetry
1	16.976	20848.7	473.2	0.7343	48.957	0.707
2	19.304	21736.8	391.2	0.9261	51.043	0.695



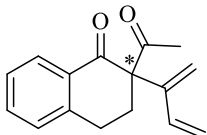
with (R)-BINAP

File Information

LC-File	MLM-6-078.D
File Path	C:\CHEM32\1\DATA\MARYMALISZEWSKI\MLM IB 99-1-0.3 2020-07-
Date	07-Jul-20, 15:59:51
Sample	MLM-6-078
Sample Info	
Barcode	
Operator	SYSTEM
Method	MLM_IB_IPA99-1-40MIN-FR0.3-250NM.M
Reference	
Analysis Time	29.997 min
Sampling Rate	0.0033 min (0.198 sec), 9000 datapoints



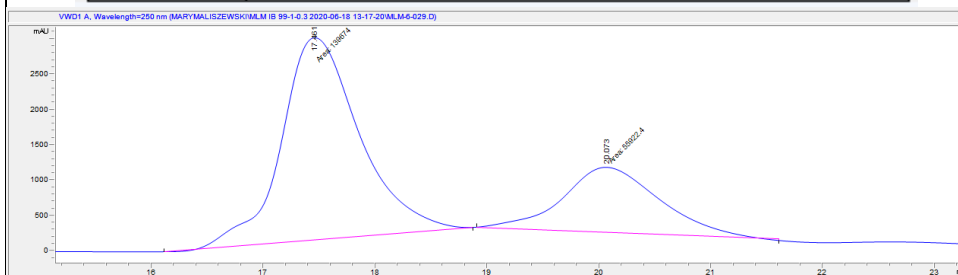
#	Time	Area	Height	Width	Area%	Symmetry
1	17.444	147514.8	2883.1	0.8527	42.804	0.591
2	19.999	197115.2	2902.7	1.1318	57.196	0.478



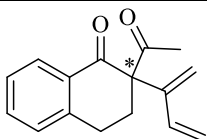
with (S)-2-tolyl-
PHOX

File Information

LC-File	MLM-6-029.D
File Path	C:\CHEM32\1\DATA\MARYMALISZEWSKI\MLM IB 99-1-0.3 2020-06-
Date	18-Jun-20, 13:34:49
Sample	MLM-6-029
Sample Info	
Barcode	
Operator	SYSTEM
Method	MLM_IB_IPA99-1-40MIN-FRO.3-250NM.M
Reference	
Analysis Time	39.997 min
Sampling Rate	0.0033 min (0.198 sec), 12000 datapoints



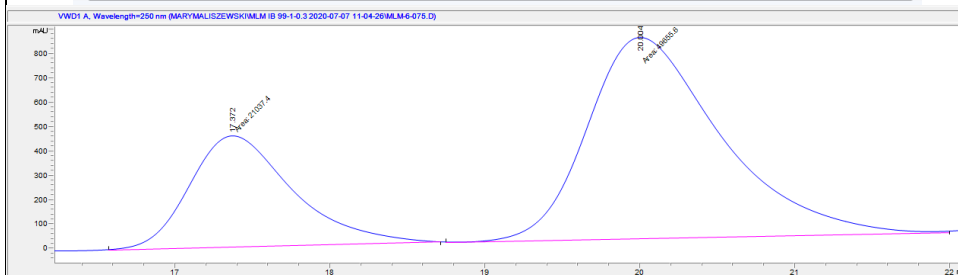
#	Time	Area	Height	Width	Area%	Symmetry
1	17.461	139673.7	2862.3	0.8133	71.409	0.751
2	20.073	55922.4	922.4	1.0104	28.591	0.784



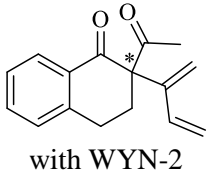
with WYN-1

File Information

LC-File	MLM-6-075.D
File Path	C:\CHEM32\1\DATA\MARYMALISZEWSKI\MLM IB 99-1-0.3 2020-07-
Date	07-Jul-20, 11:21:48
Sample	MLM-6-075
Sample Info	
Barcode	
Operator	SYSTEM
Method	MLM_IB_IPA99-1-40MIN-FRO.3-250NM.M
Reference	
Analysis Time	40 min
Sampling Rate	0.0033 min (0.198 sec), 12001 datapoints

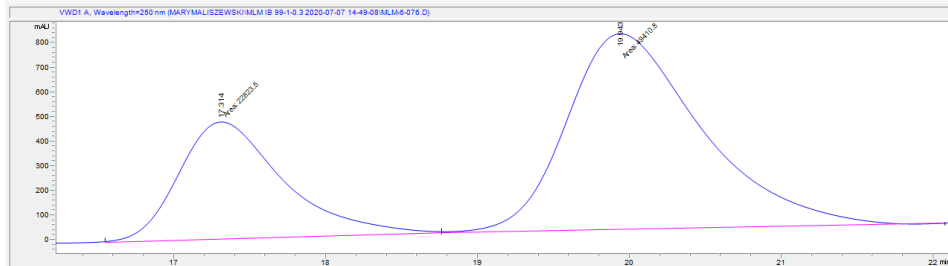


#	Time	Area	Height	Width	Area%	Symmetry
1	17.372	21037.4	455.9	0.7691	29.759	0.711
2	20.004	49655.6	825.1	1.003	70.241	0.645



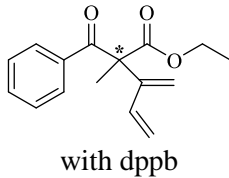
File Information

LC-File	MLM-6-076.D
File Path	C:\CHEM32\1\DATA\MARYMALISZEWSKI\MLM IB 99-1-0.3 2020-07-
Date	07-Jul-20, 15:07:40
Sample	MLM-6-076
Sample Info	
Barcode	
Operator	SYSTEM
Method	MLM_IB_IPA99-1-40MIN-FR0.3-250NM.M
Reference	
Analysis Time	29.997 min
Sampling Rate	0.0033 min (0.198 sec), 9000 datapoints



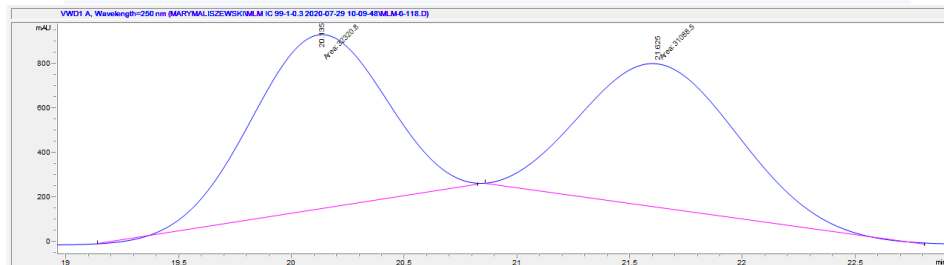
#	Time	Area	Height	Width	Area%	Symmetry
1	17.314	22823.5	476.9	0.7976	31.596	0.676
2	19.943	49410.8	797.3	1.0329	68.404	0.651

ethyl 2-benzoyl-2-methyl-3-methylenepent-4-enoate

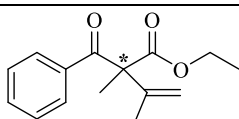


File Information

LC-File	MLM-6-118.D
File Path	C:\CHEM32\1\DATA\MARYMALISZEWSKI\MLM IC 99-1-0.3 2020-07-
Date	29-Jul-20, 10:28:19
Sample	MLM-6-118
Sample Info	
Barcode	
Operator	SYSTEM
Method	MLM_IC_IPA99-1-40MIN-FR0.3-250NM.M
Reference	
Analysis Time	39.997 min
Sampling Rate	0.0033 min (0.198 sec), 12000 datapoints



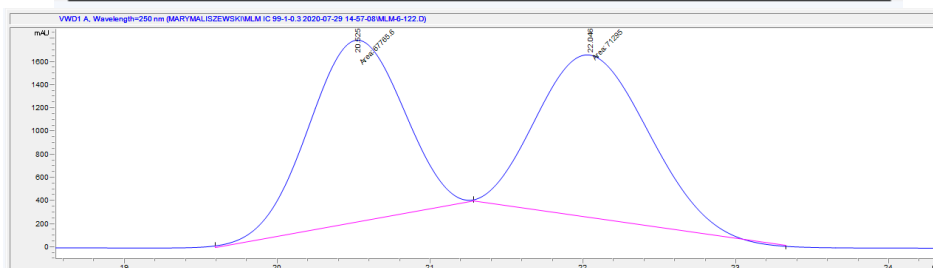
#	Time	Area	Height	Width	Area%	Symmetry
1	20.135	32320.8	783.3	0.6877	50.972	1.109
2	21.625	31088.5	645.6	0.8026	49.028	0.82



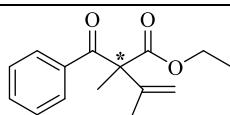
with (R)-BINAP

File Information

LC-File	MLM-6-122.D
File Path	C:\CHEM32\1\DATA\MARYMALISZEWSKI\MLM IC 99-1-0.3 2020-07
Date	29-Jul-20, 15:14:33
Sample	MLM-6-122
Sample Info	
Barcode	
Operator	SYSTEM
Method	MLM_IC_IPA99-1-40MIN-FR0.3-250NM.M
Reference	
Analysis Time	39.997 min
Sampling Rate	0.0033 min (0.198 sec), 12000 datapoints



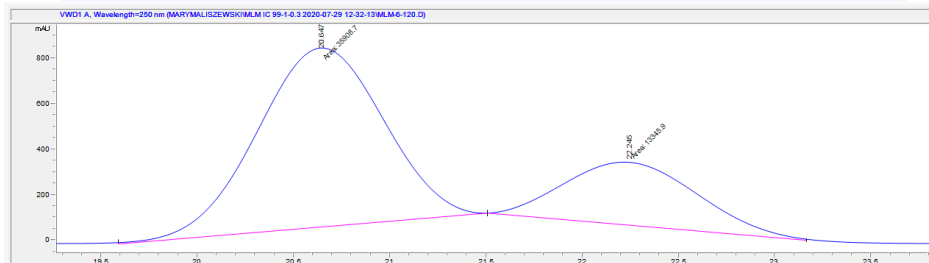
#	Time	Area	Height	Width	Area%	Symmetry
1	20.525	67765.6	1574.2	0.7174	48.731	1.076
2	22.046	71295	1409.5	0.843	51.269	0.797



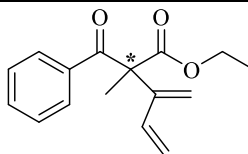
with WYN-1

File Information

LC-File	MLM-6-120.D
File Path	C:\CHEM32\1\DATA\MARYMALISZEWSKI\MLM IC 99-1-0.3 2020-07
Date	29-Jul-20, 12:50:43
Sample	MLM-6-120
Sample Info	
Barcode	
Operator	SYSTEM
Method	MLM_IC_IPA99-1-40MIN-FR0.3-250NM.M
Reference	
Analysis Time	39.997 min
Sampling Rate	0.0033 min (0.198 sec), 12000 datapoints



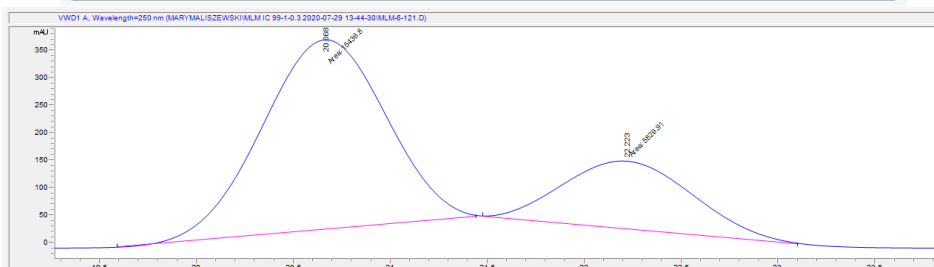
#	Time	Area	Height	Width	Area%	Symmetry
1	20.647	35908.7	786.7	0.7607	72.904	1.051
2	22.245	13345.9	277.1	0.8026	27.096	0.788



with WYN-2

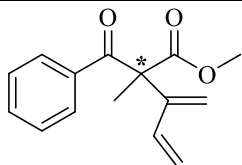
File Information

LC-File	MLM-6-121.D
File Path	C:\CHEM32\1\DATA\MARYMALISZEWSKI\MLM IC 99-1-0.3 2020-07
Date	29-Jul-20, 14:01:53
Sample	MLM-6-121
Sample Info	
Barcode	
Operator	SYSTEM
Method	MLM_IC_IPA99-1-40MIN-FR0.3-250NM.M
Reference	
Analysis Time	39.997 min
Sampling Rate	0.0033 min (0.198 sec), 12000 datapoints



#	Time	Area	Height	Width	Area%	Symmetry
1	20.668	15436.8	347.2	0.741	72.587	1.066
2	22.223	5829.9	124.7	0.7793	27.413	0.818

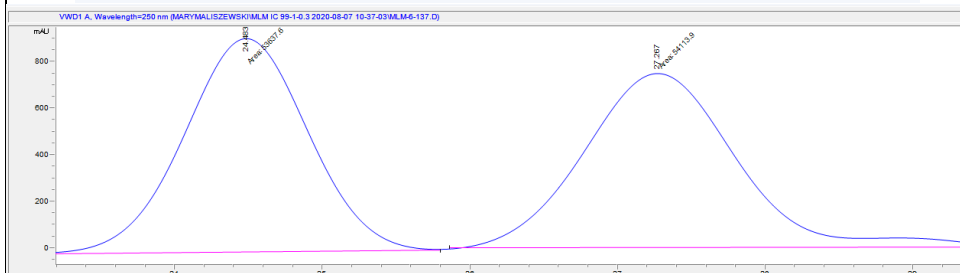
methyl 2-benzoyl-2-methyl-3-methylenepent-4-enoate



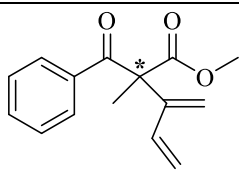
with dppb

File Information

LC-File	MLM-6-137.D
File Path	C:\CHEM32\1\DATA\MARYMALISZEWSKI\MLM IC 99-1-0.3 2020-08
Date	07-Aug-20, 10:55:39
Sample	MLM-6-137
Sample Info	
Barcode	
Operator	SYSTEM
Method	MLM_IC_IPA99-1-40MIN-FR0.3-250NM.M
Reference	
Analysis Time	39.997 min
Sampling Rate	0.0033 min (0.198 sec), 12000 datapoints



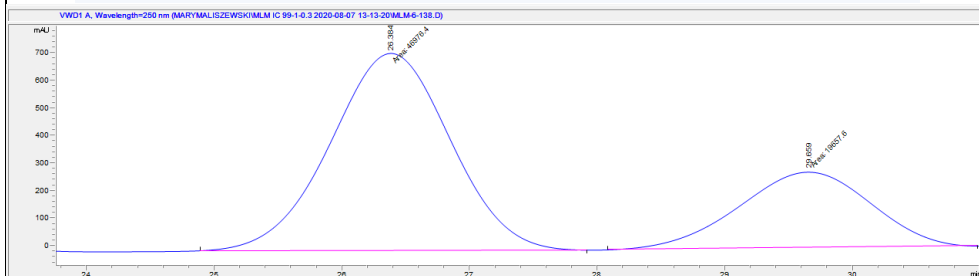
#	Time	Area	Height	Width	Area%	Symmetry
1	24.483	53637.6	917.4	0.9745	49.779	0.999
2	27.267	54113.9	751.3	1.2004	50.221	0.907



with WYN-1

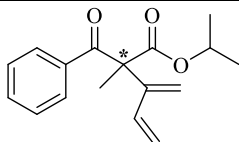
File Information

LC-File	MLM-6-137.D
File Path	C:\CHEM32\1\DATA\MARYMALISZEWSKI\MLM IC 99-1-0.3 2020-08
Date	07-Aug-20, 10:55:39
Sample	MLM-6-137
Sample Info	
Barcode	
Operator	SYSTEM
Method	MLM_IC_IPA99-1-40MIN-FR0.3-250NM.M
Reference	
Analysis Time	39.997 min
Sampling Rate	0.0033 min (0.198 sec), 12000 datapoints



#	Time	Area	Height	Width	Area%	Symmetry
1	26.384	46976.4	717.3	1.0916	70.499	1.008
2	29.659	19657.6	274.4	1.1939	29.501	1.101

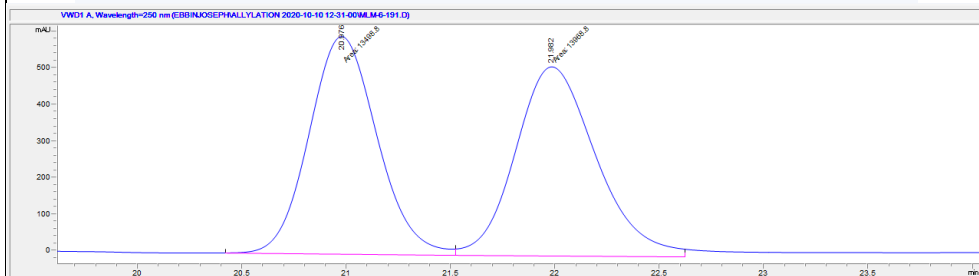
isopropyl 2-benzoyl-2-methyl-3-methylenepent-4-enoate



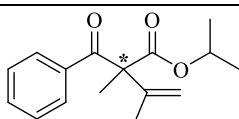
with dppb

File Information

LC-File	MLM-6-191.D
File Path	C:\CHEM32\1\DATA\EBBINJOSEPH\ALLYLATION 2020-10-10 12-31-
Date	10-Oct-20, 13:04:29
Sample	MLM-6-191
Sample Info	
Barcode	
Operator	SYSTEM
Method	MLM_ID_IPA99-1-40MIN-FR0.3-250NM.M
Reference	
Analysis Time	29.997 min
Sampling Rate	0.0033 min (0.198 sec), 9000 datapoints



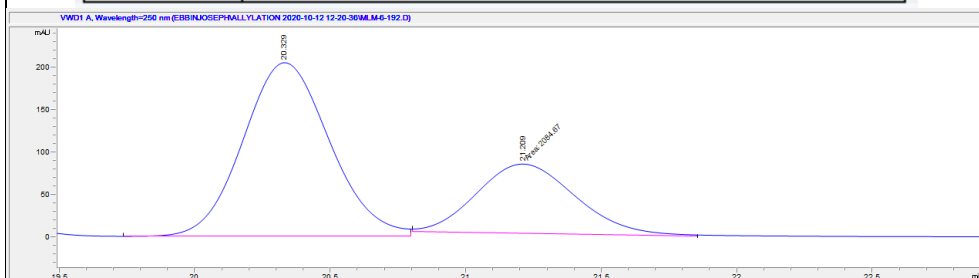
#	Time	Area	Height	Width	Area%	Symmetry
1	20.976	13498.8	595.6	0.3778	49.144	0.89
2	21.982	13968.8	518.3	0.4492	50.856	0.797



with WYN-1

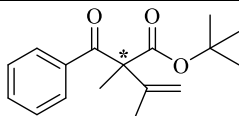
File Information

LC-File	MLM-6-191.D
File Path	C:\CHEM32\1\DATA\EBBINJOSEPH\ALLYLATION 2020-10-10 12-31-
Date	10-Oct-20, 13:04:29
Sample	MLM-6-191
Sample Info	
Barcode	
Operator	SYSTEM
Method	MLM_ID_IPA99-1-40MIN-FR0.3-250NM.M
Reference	
Analysis Time	29.997 min
Sampling Rate	0.0033 min (0.198 sec), 9000 datapoints



#	Time	Area	Height	Width	Area%	Symmetry
1	20.329	4547.1	203.9	0.3462	68.565	0.893
2	21.209	2084.7	81.4	0.4266	31.435	0.834

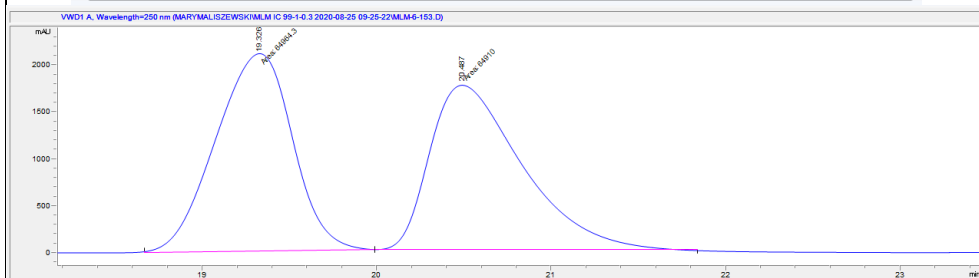
tert-butyl 2-benzoyl-2-methyl-3-methylenepent-4-enoate



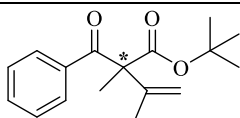
with dppb

File Information

LC-File	MLM-6-153.D
File Path	C:\CHEM32\1\DATA\MARYMALISZEWSKI\MLM IC 99-1-0.3 2020-08
Date	25-Aug-20, 09:57:46
Sample	MLM-6-153
Sample Info	
Barcode	
Operator	SYSTEM
Method	MLM_ID_IPA99-1-40MIN-FR0.3-250NM.M
Reference	
Analysis Time	29.997 min
Sampling Rate	0.0033 min (0.198 sec), 9000 datapoints



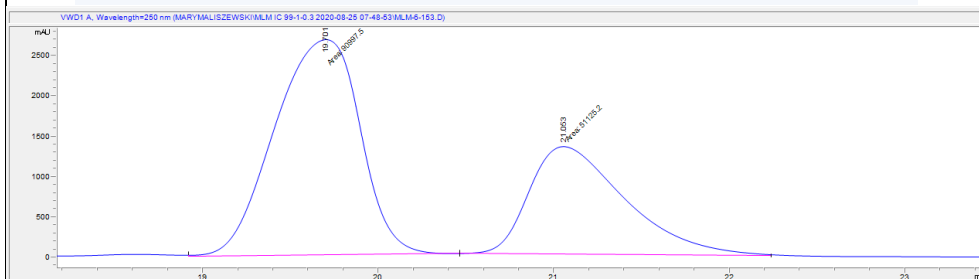
#	Time	Area	Height	Width	Area%	Symmetry
1	19.326	64964.3	2114.4	0.5121	50.021	1.28
2	20.487	64910	1761.6	0.6141	49.979	0.53



with WYN-1

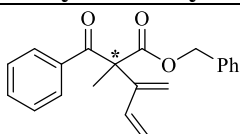
File Information

LC-File	MLM-6-153.D
File Path	C:\CHEM32\1\DATA\MARYMALISZEWSKI\MLM IC 99-1-0.3 2020-08
Date	25-Aug-20, 08:22:21
Sample	MLM-6-153
Sample Info	
Barcode	
Operator	SYSTEM
Method	MLM_ID_IPA99-1-40MIN-FR0.3-250NM.M
Reference	
Analysis Time	30 min
Sampling Rate	0.0033 min (0.198 sec), 9001 datapoints



#	Time	Area	Height	Width	Area%	Symmetry
1	19.701	90997.5	2680.6	0.5658	64.027	1.449
2	21.053	51125.2	1341.4	0.6352	35.973	0.542

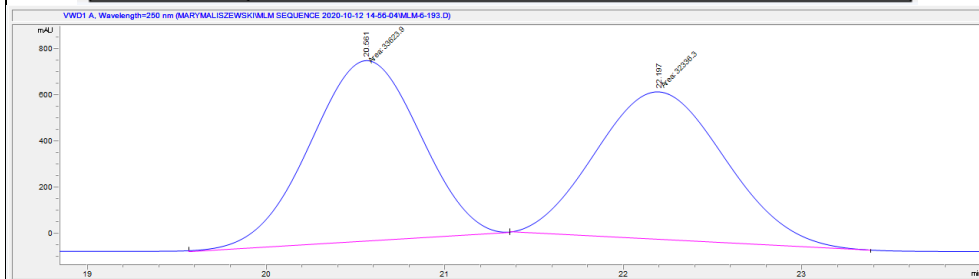
benzyl 2-benzoyl-2-methyl-3-methylenepent-4-enoate



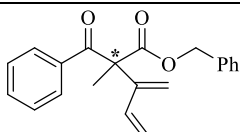
with dppb

File Information

LC-File	MLM-6-193.D
File Path	C:\CHEM32\1\DATA\MARYMALISZEWSKI\MLM SEQUENCE 2020-10-
Date	12-Oct-20, 15:13:29
Sample	MLM-6-193
Sample Info	
Barcode	
Operator	SYSTEM
Method	MLM_IC_IPA99-1-40MIN-FR0.3-250NM.M
Reference	
Analysis Time	39.997 min
Sampling Rate	0.0033 min (0.198 sec), 12000 datapoints



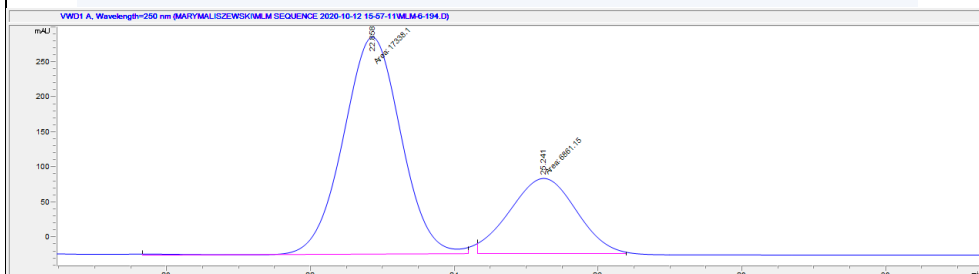
#	Time	Area	Height	Width	Area%	Symmetry
1	20.561	33623.9	783.6	0.7151	50.976	1.056
2	22.197	32336.3	640.9	0.8409	49.024	0.881



with WYN-1

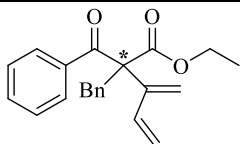
File Information

LC-File	MLM-6-194.D
File Path	C:\CHEM32\1\DATA\MARYMALISZEWSKI\MLM SEQUENCE 2020-10-
Date	12-Oct-20, 16:14:38
Sample	MLM-6-194
Sample Info	
Barcode	
Operator	SYSTEM
Method	MLM_IC_IPA99-1-40MIN-FR0.3-250NM.M
Reference	
Analysis Time	39.997 min
Sampling Rate	0.0033 min (0.198 sec), 12000 datapoints



#	Time	Area	Height	Width	Area%	Symmetry
1	22.858	17338.1	309.2	0.9345	71.647	0.999
2	25.241	6861.1	106.9	1.0698	28.353	1.015

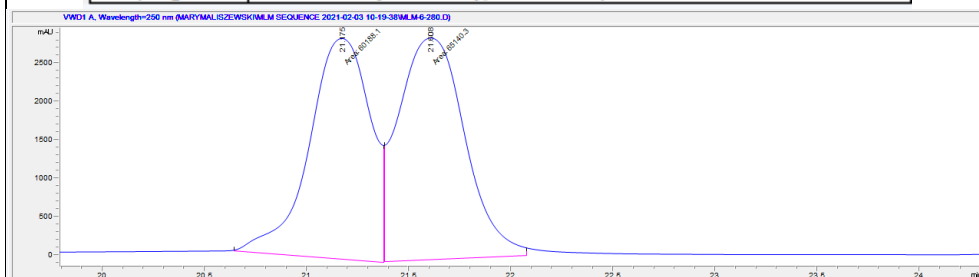
ethyl 2-benzoyl-2-benzyl-3-methylenepent-4-enoate



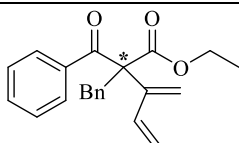
with dppb

File Information

LC-File	MLM-6-280.D
File Path	C:\CHEM32\1\DATA\MARYMALISZEWSKI\MLM SEQUENCE 2021-02-
Date	03-Feb-21, 10:53:06
Sample	MLM-6-280
Sample Info	
Barcode	
Operator	SYSTEM
Method	MLM_ID_IPA99-1-40MIN-FR0.3-250NM.M
Reference	
Analysis Time	29.997 min
Sampling Rate	0.0033 min (0.198 sec), 9000 datapoints



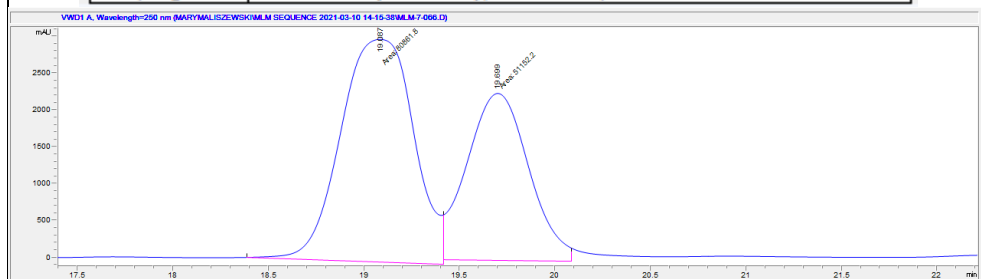
#	Time	Area	Height	Width	Area%	Symmetry
1	21.175	60188.1	2877.3	0.3486	48.024	1.13
2	21.608	65140.3	2886.4	0.3761	51.976	0.897



with WYN-1

File Information

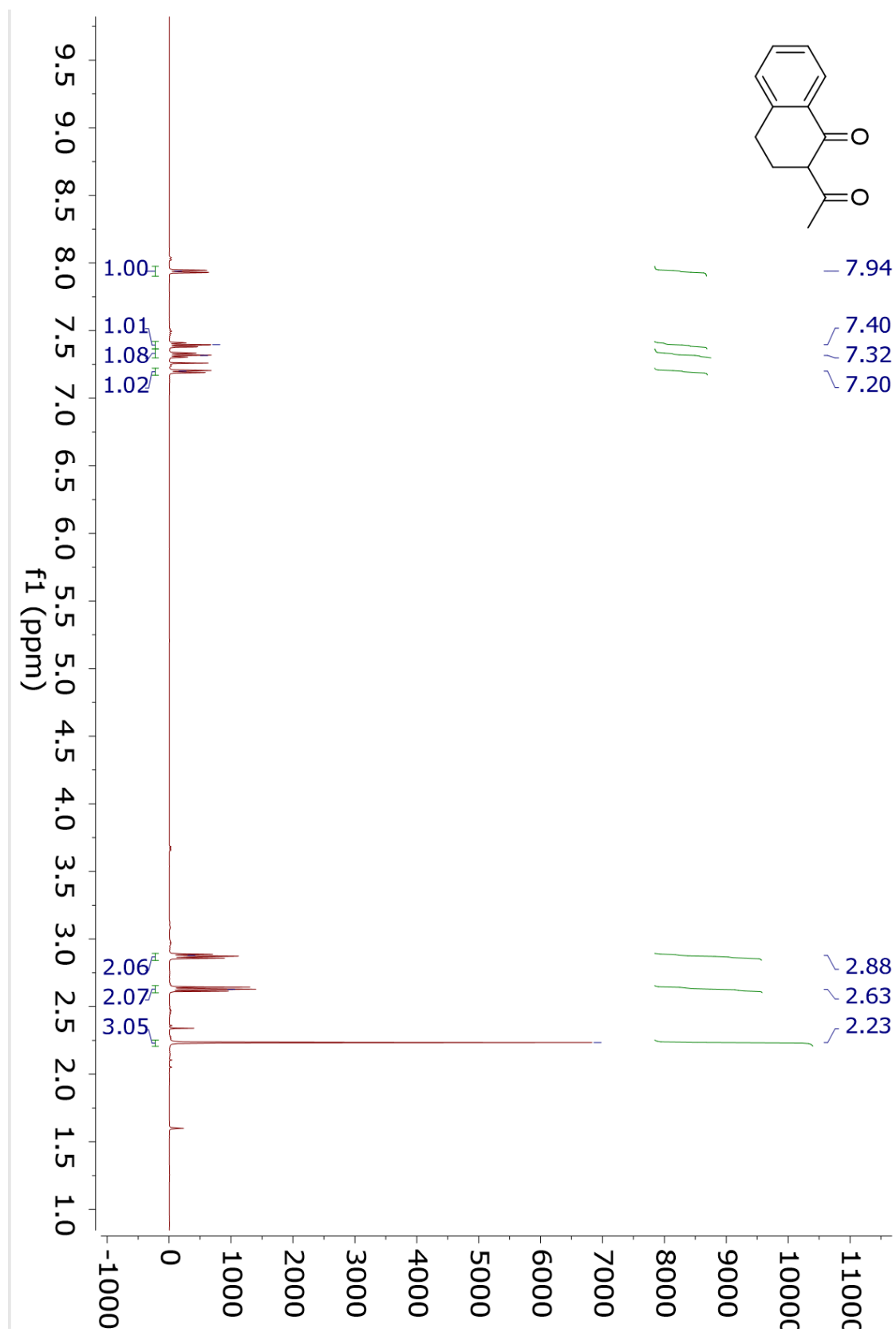
LC-File	MLM-7-066.D
File Path	C:\CHEM32\1\DATA\MARYMALISZEWSKI\MLM SEQUENCE 2021-03-
Date	10-Mar-21, 14:48:51
Sample	MLM-7-066
Sample Info	
Barcode	
Operator	SYSTEM
Method	MLM_ID_IPA99-1-40MIN-FR0.3-250NM.M
Reference	
Analysis Time	30 min
Sampling Rate	0.0033 min (0.198 sec), 9001 datapoints



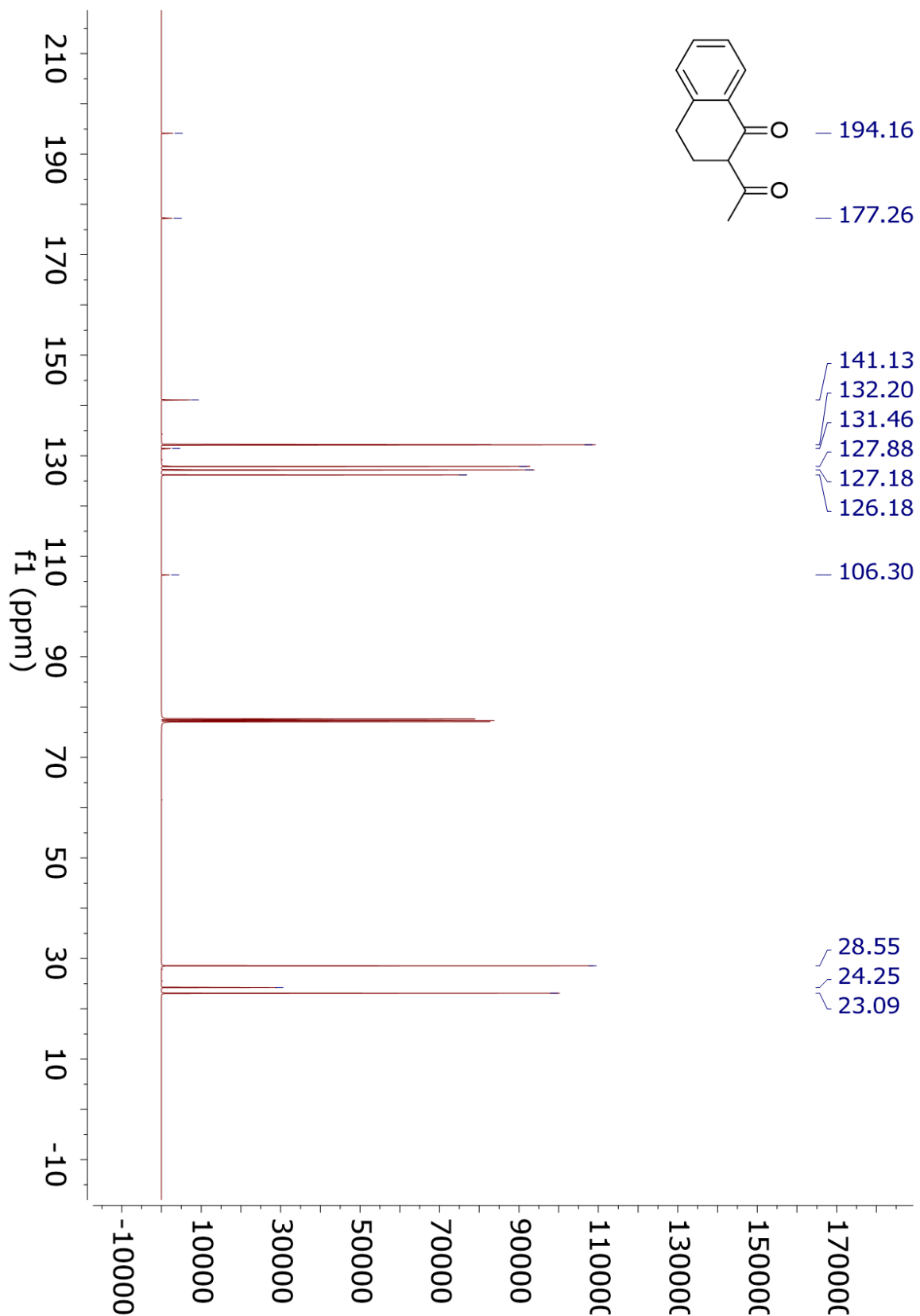
#	Time	Area	Height	Width	Area%	Symmetry
1	19.087	80861.8	3029.4	0.4449	61.252	1.124
2	19.699	51152.2	2274	0.3749	38.748	0.958

10. Copies of ^1H and ^{13}C NMR Spectra

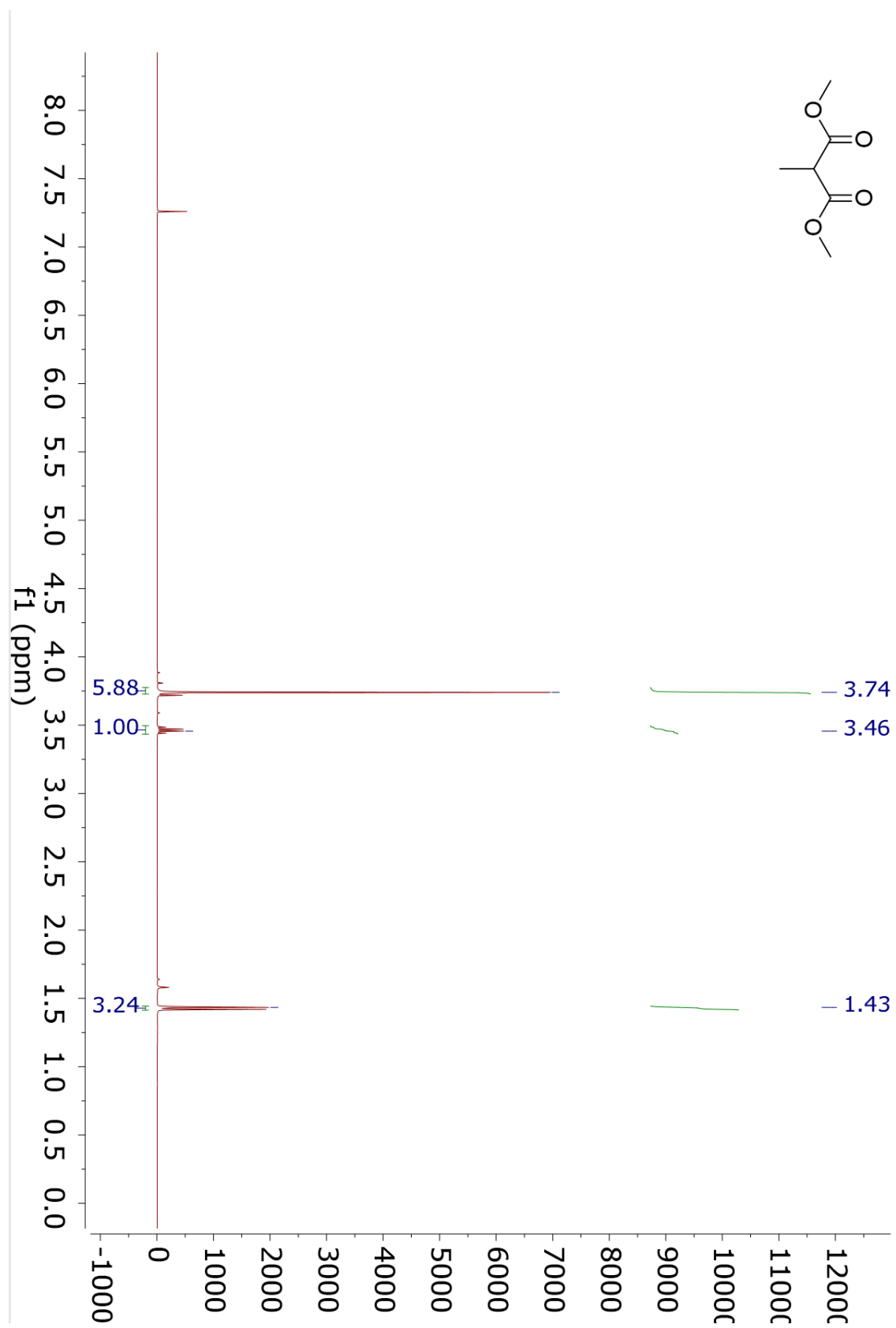
¹H NMR 4.10a



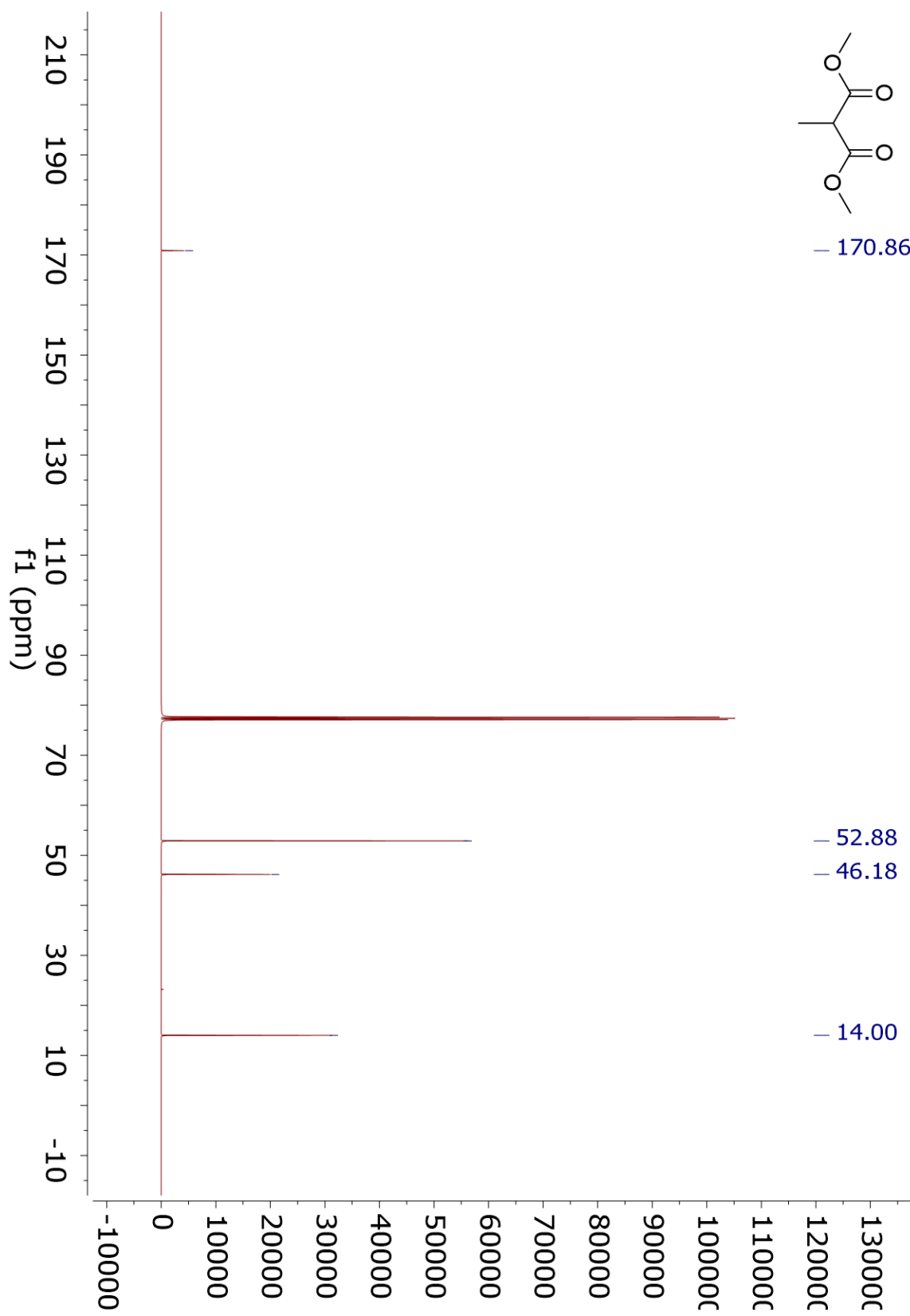
¹³C NMR 4.10a



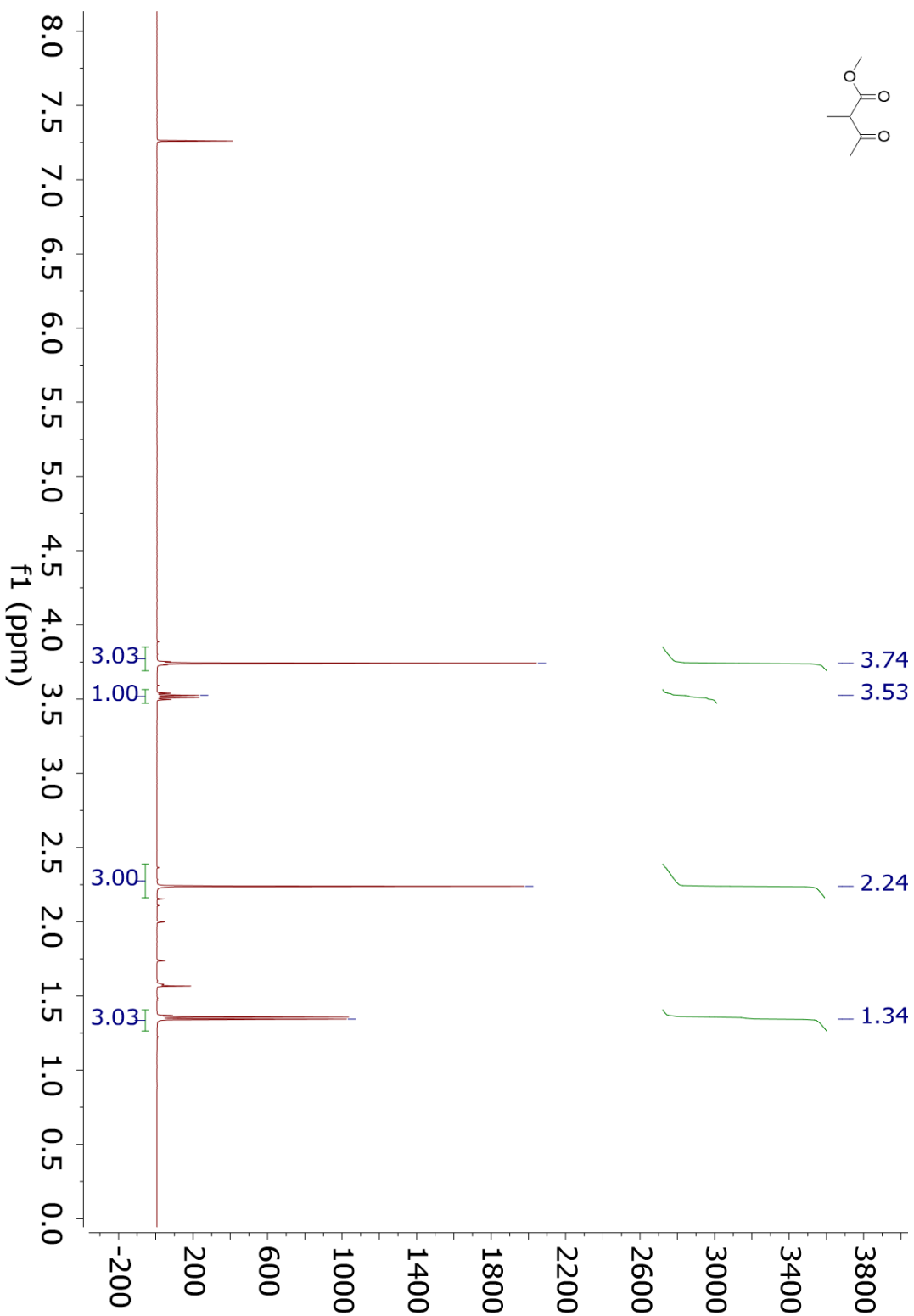
¹H NMR 4.10b



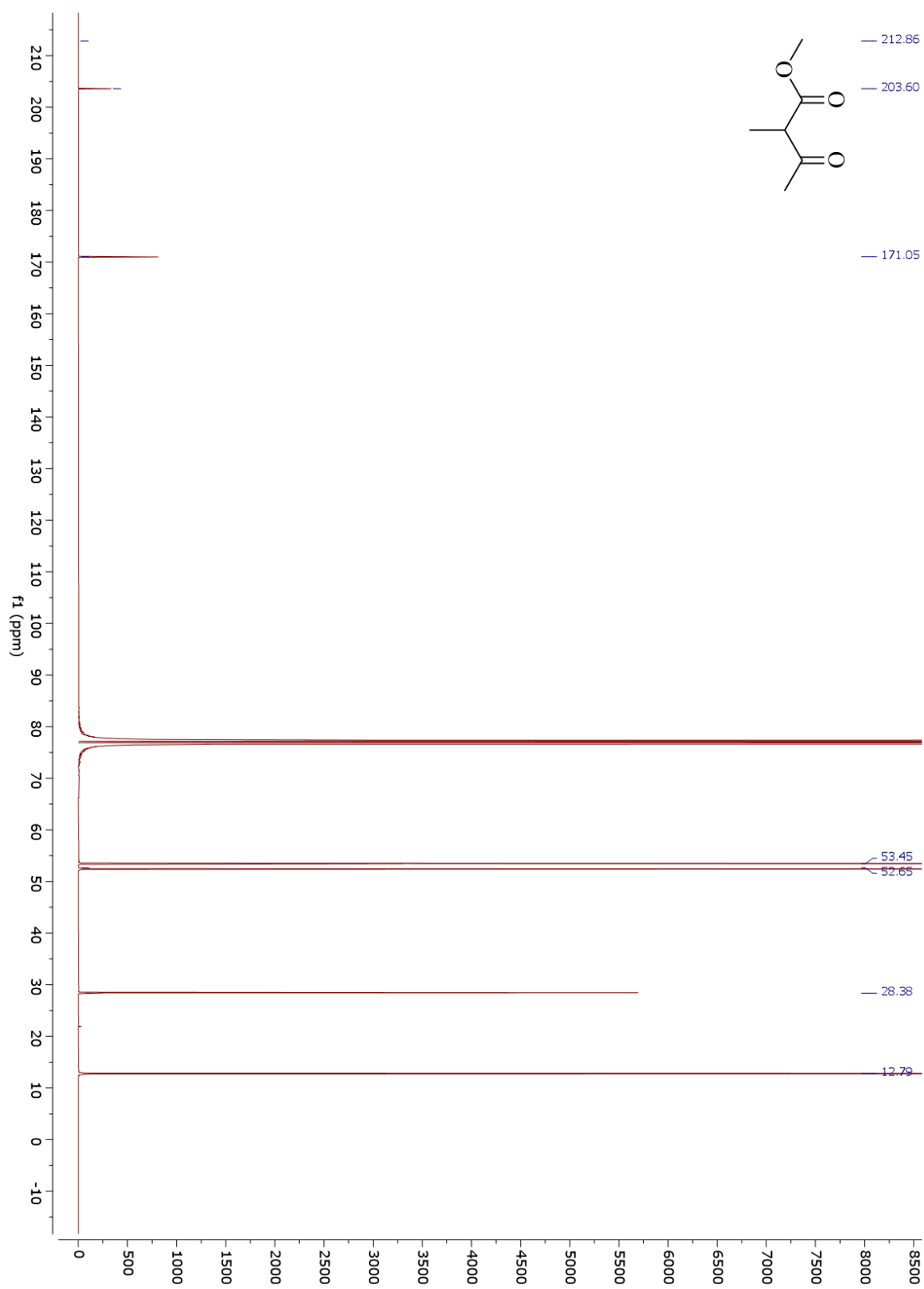
¹³C NMR 4.10b



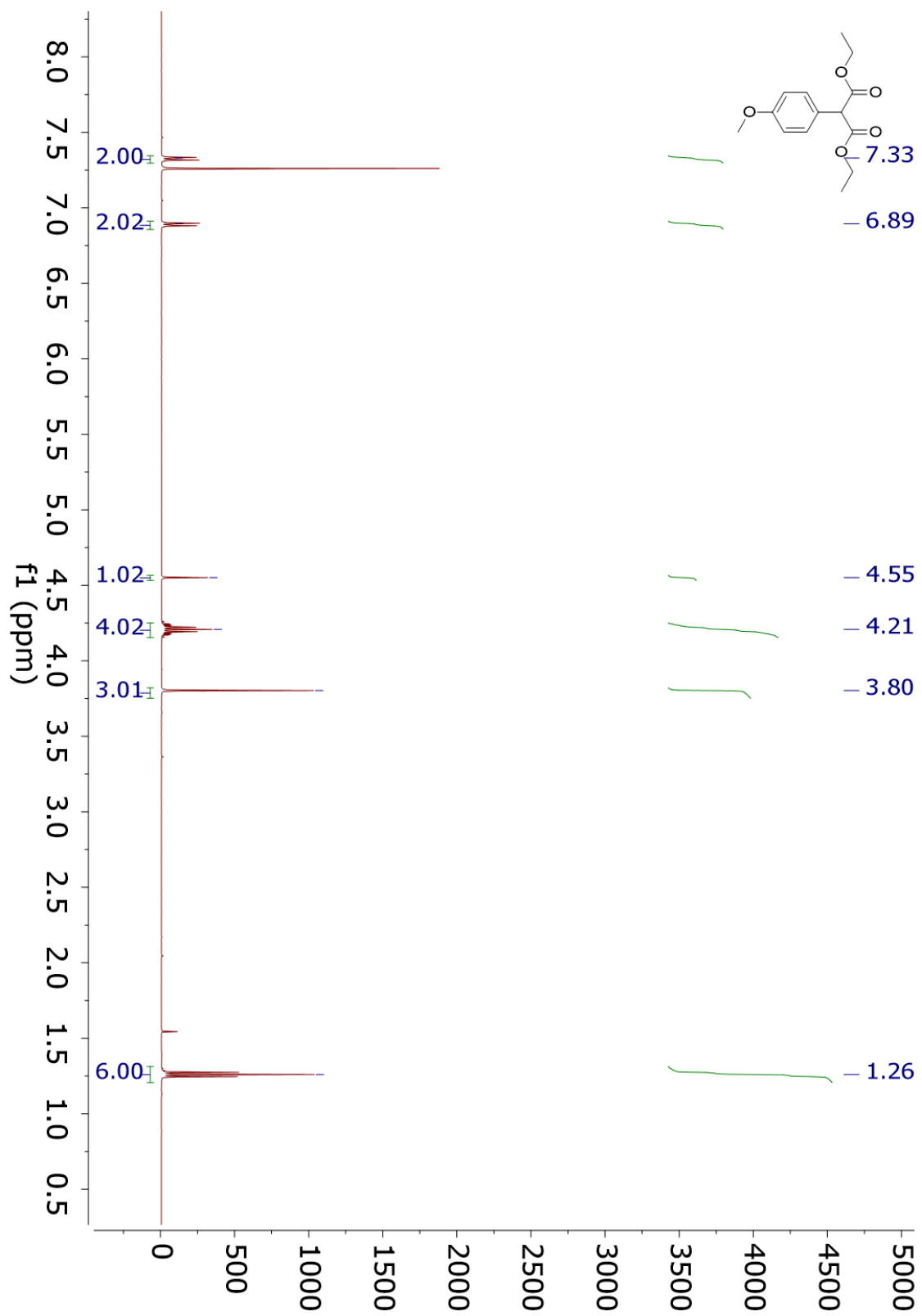
¹H NMR 4.10c



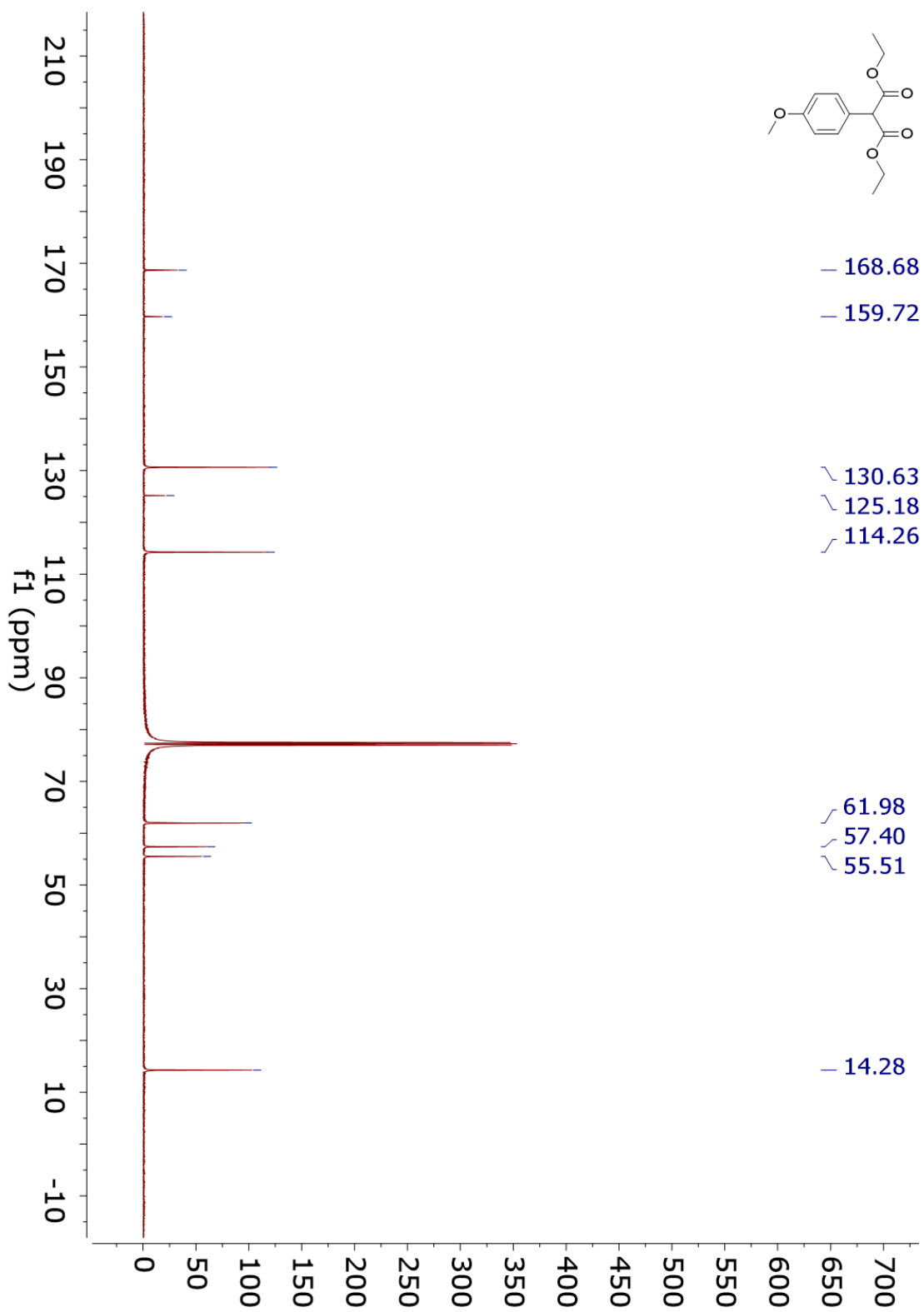
¹³C NMR 4.10c



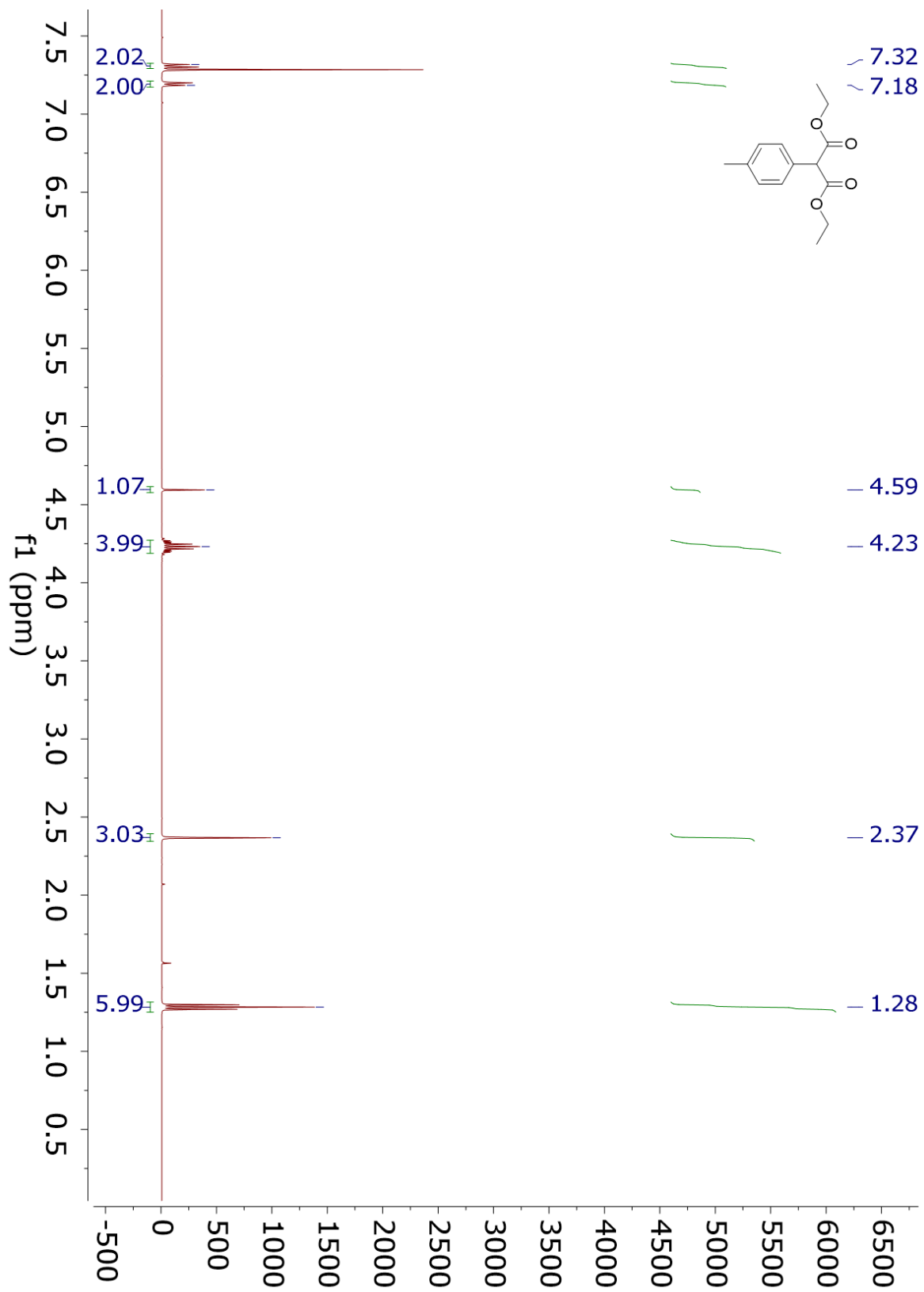
¹H NMR 4.10d



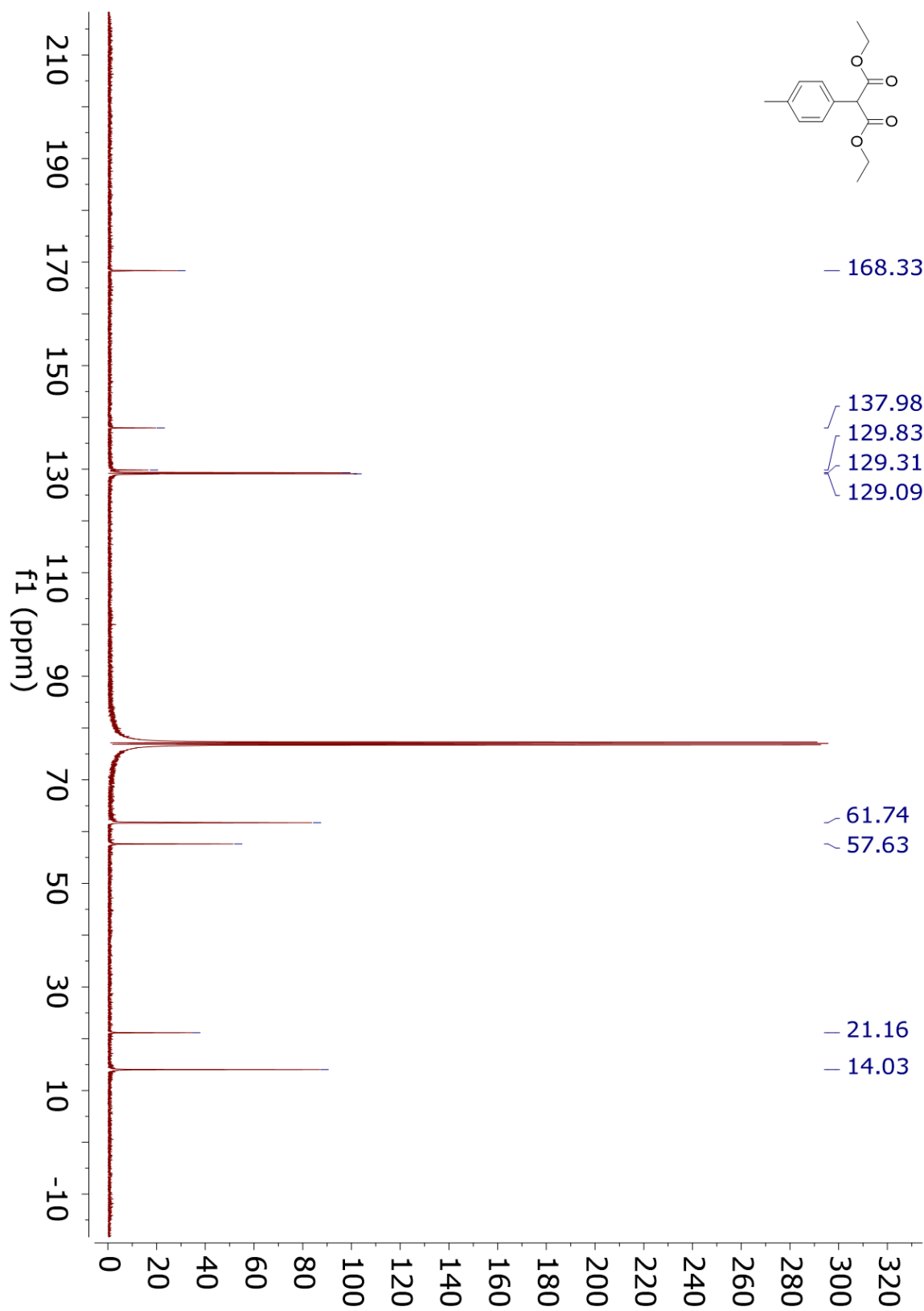
¹³C NMR 4.10d



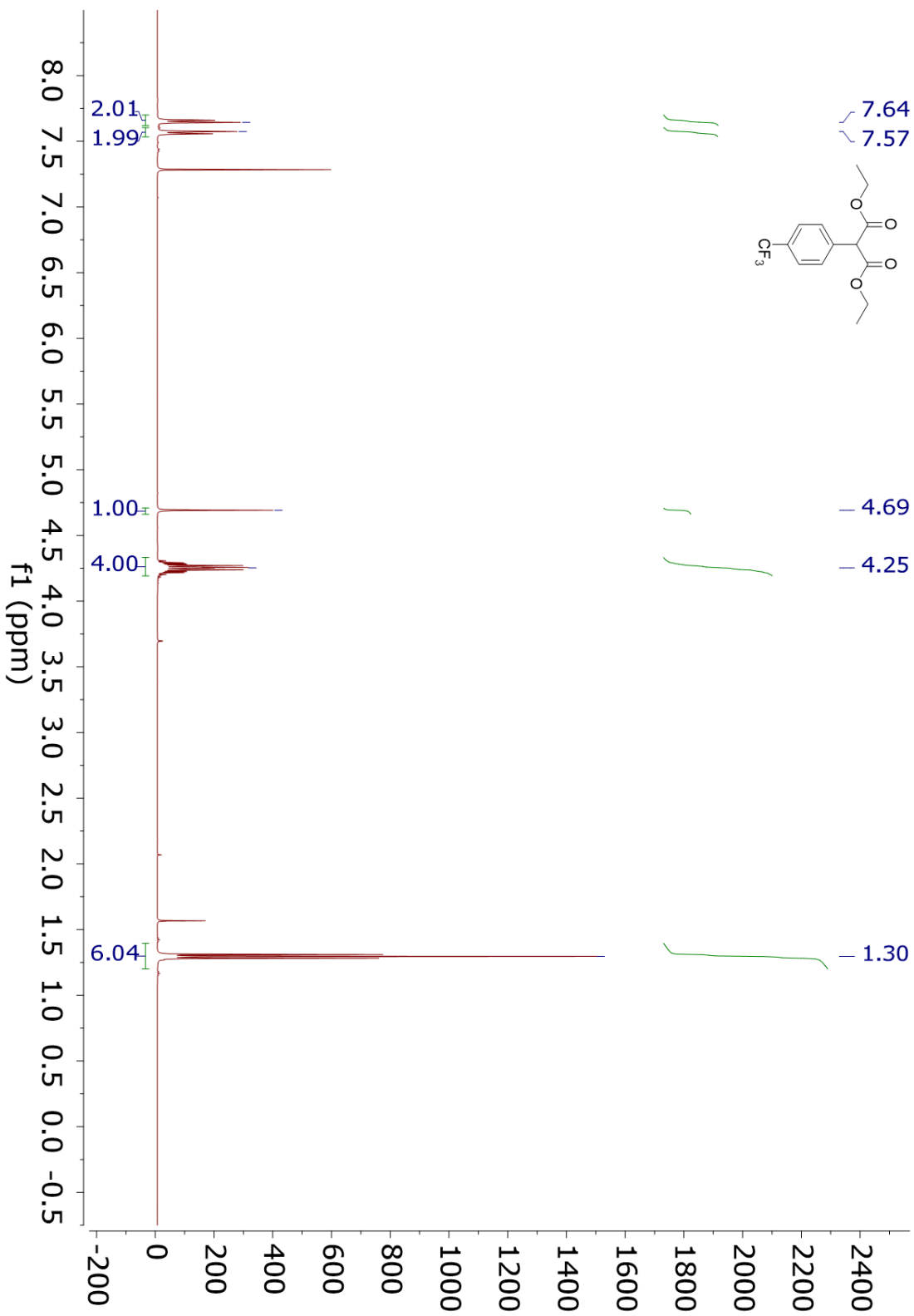
¹H NMR 4.10e



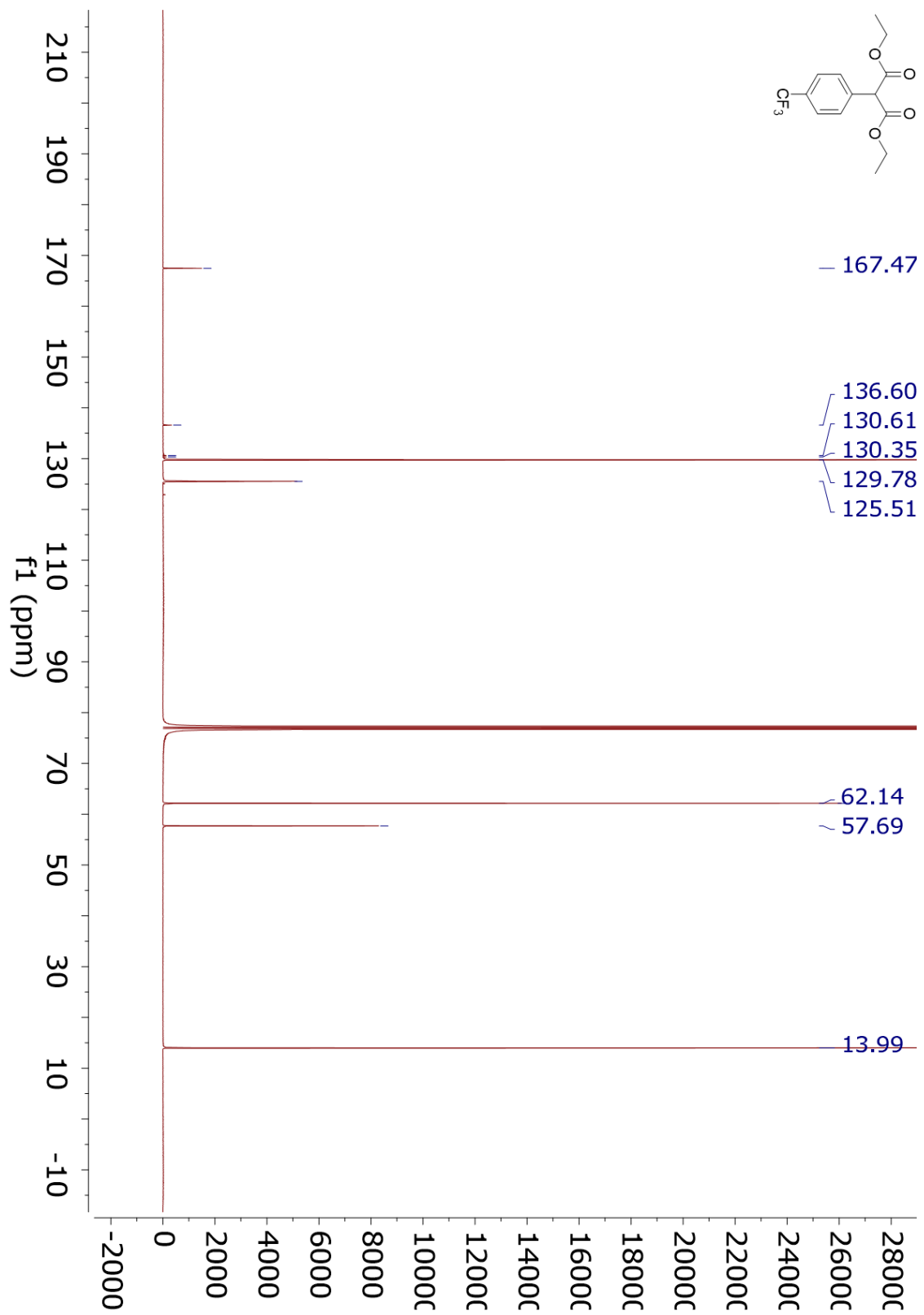
¹³C NMR 4.10e



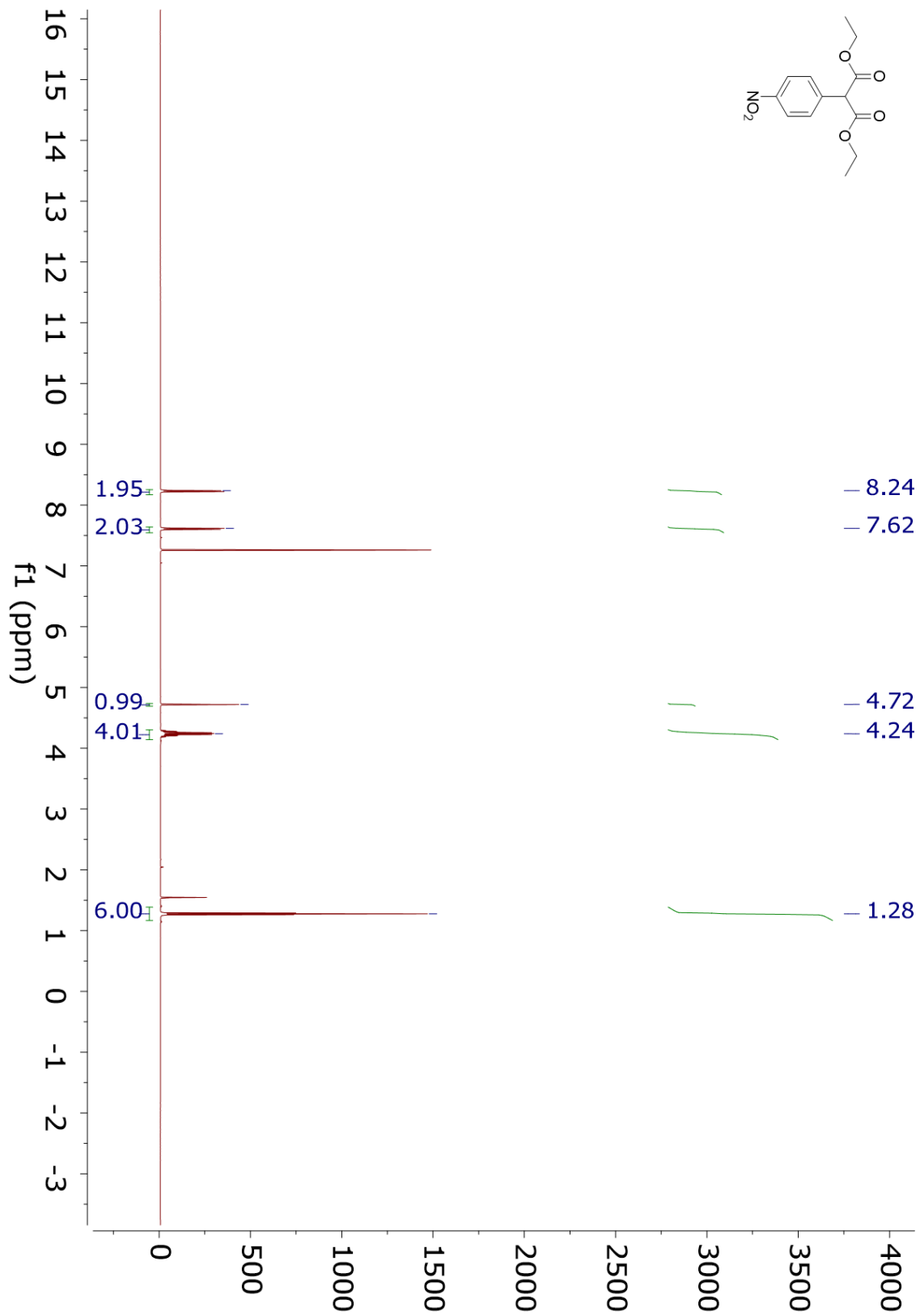
¹H NMR 4.10g



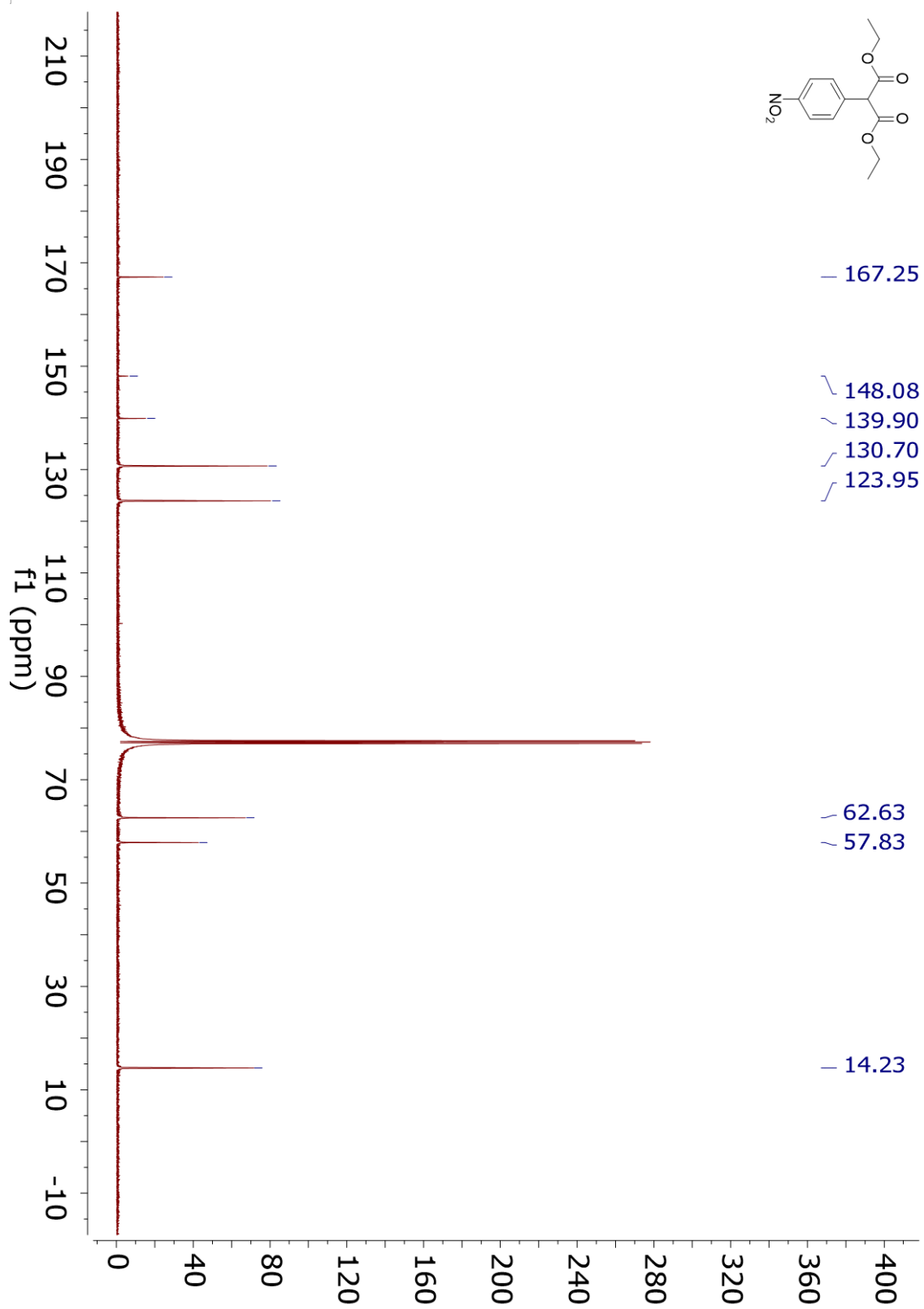
¹³C NMR 4.10g



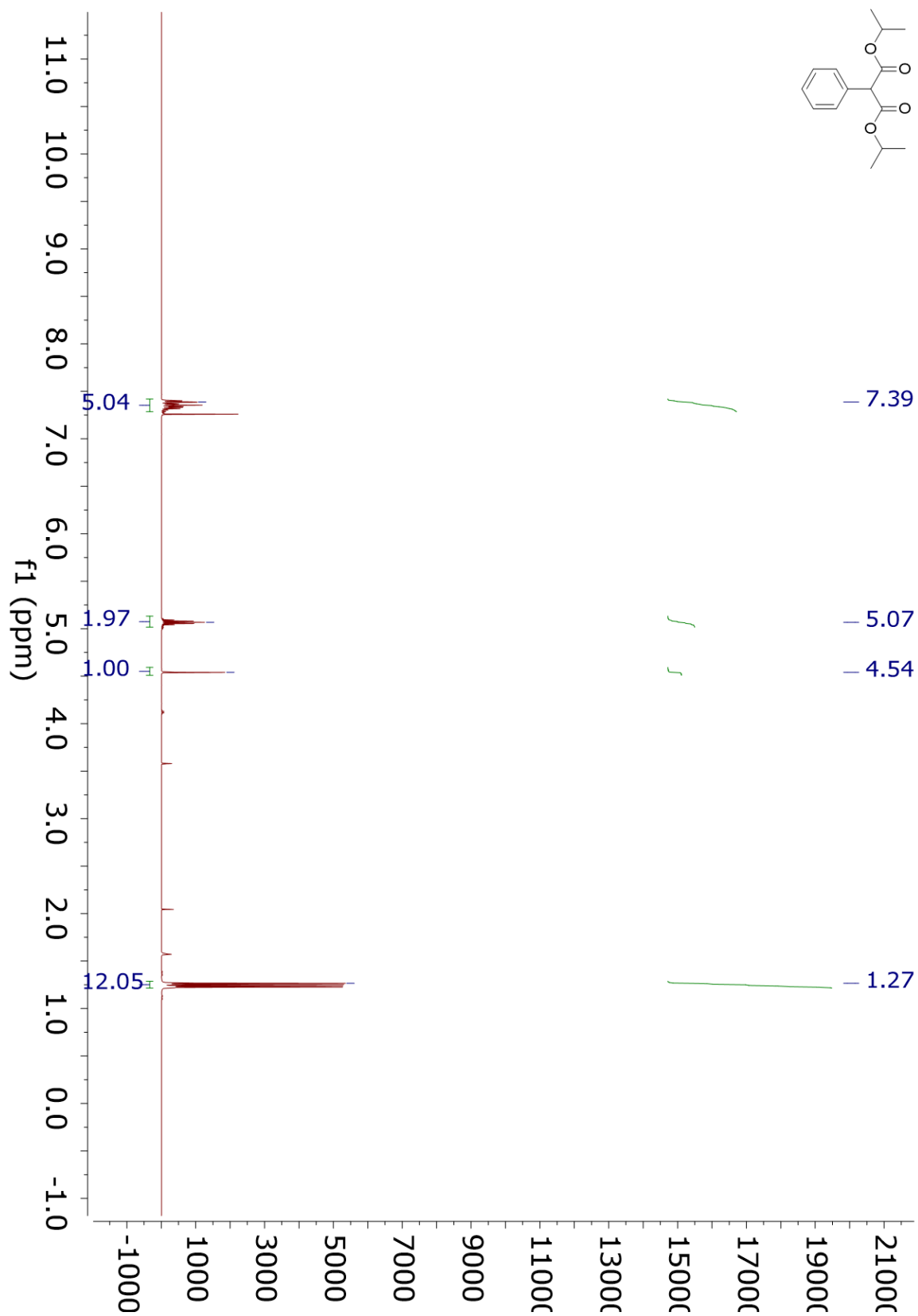
¹H NMR 4.10h



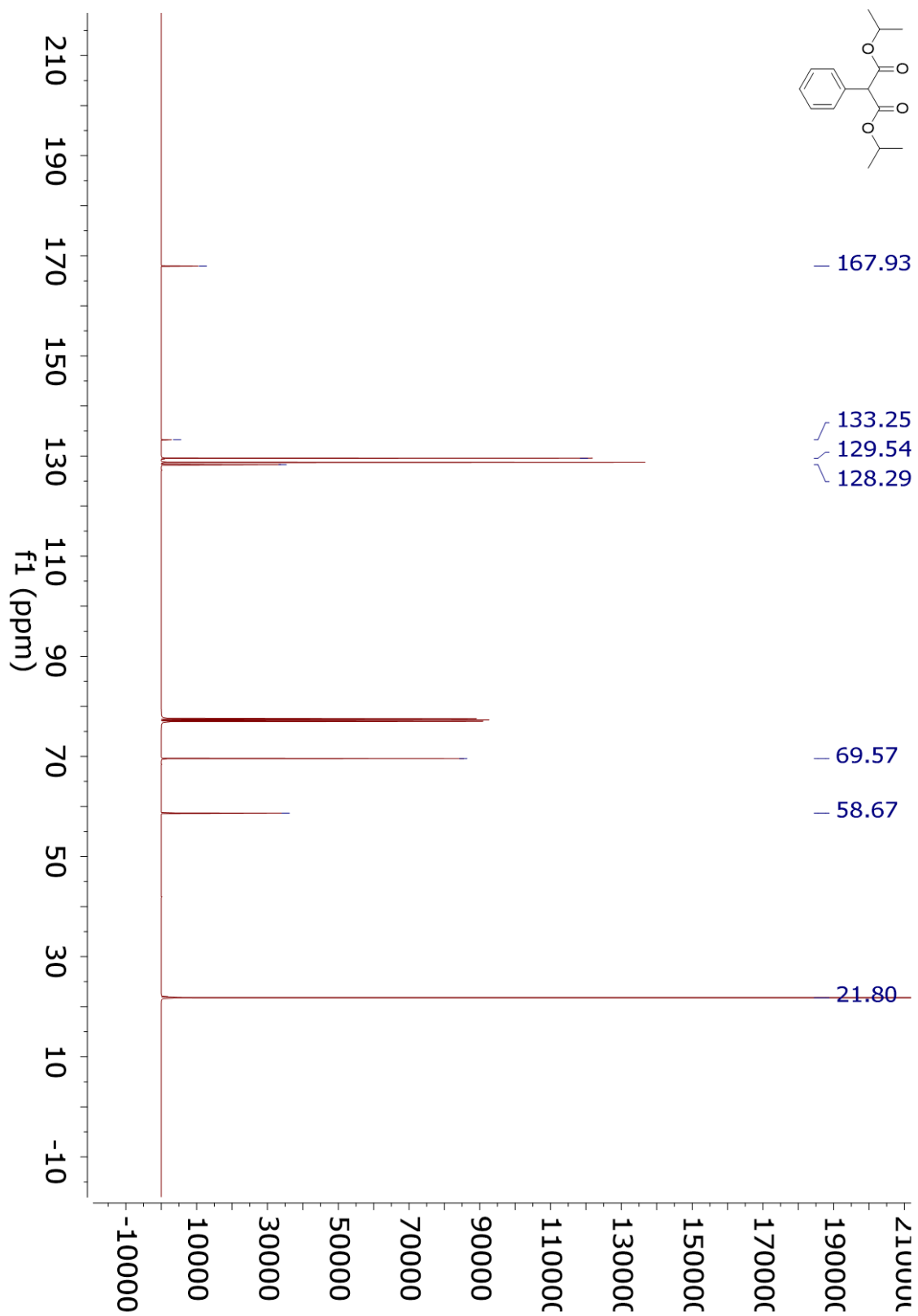
¹³C NMR 4.10h



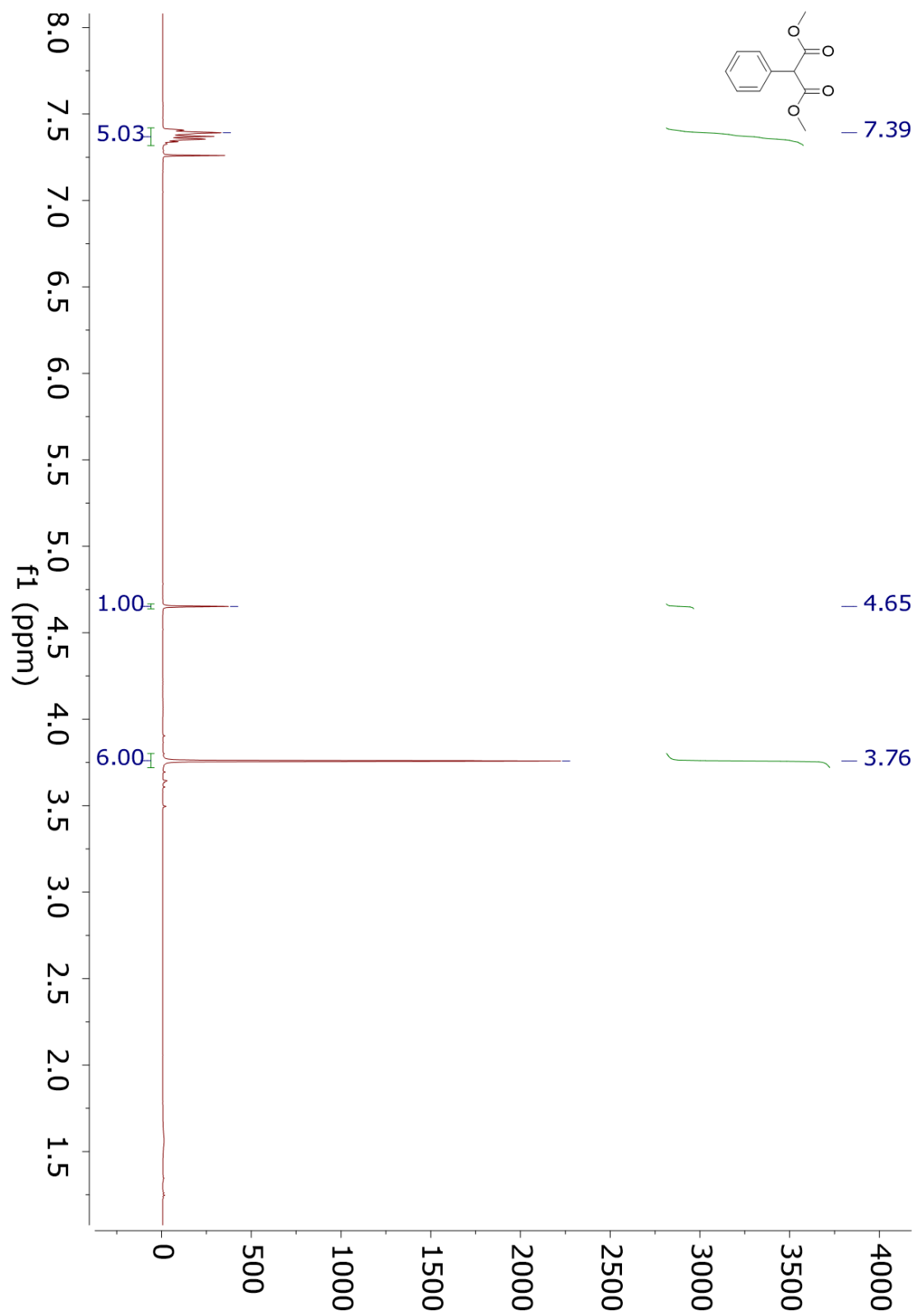
¹H NMR 4.10i



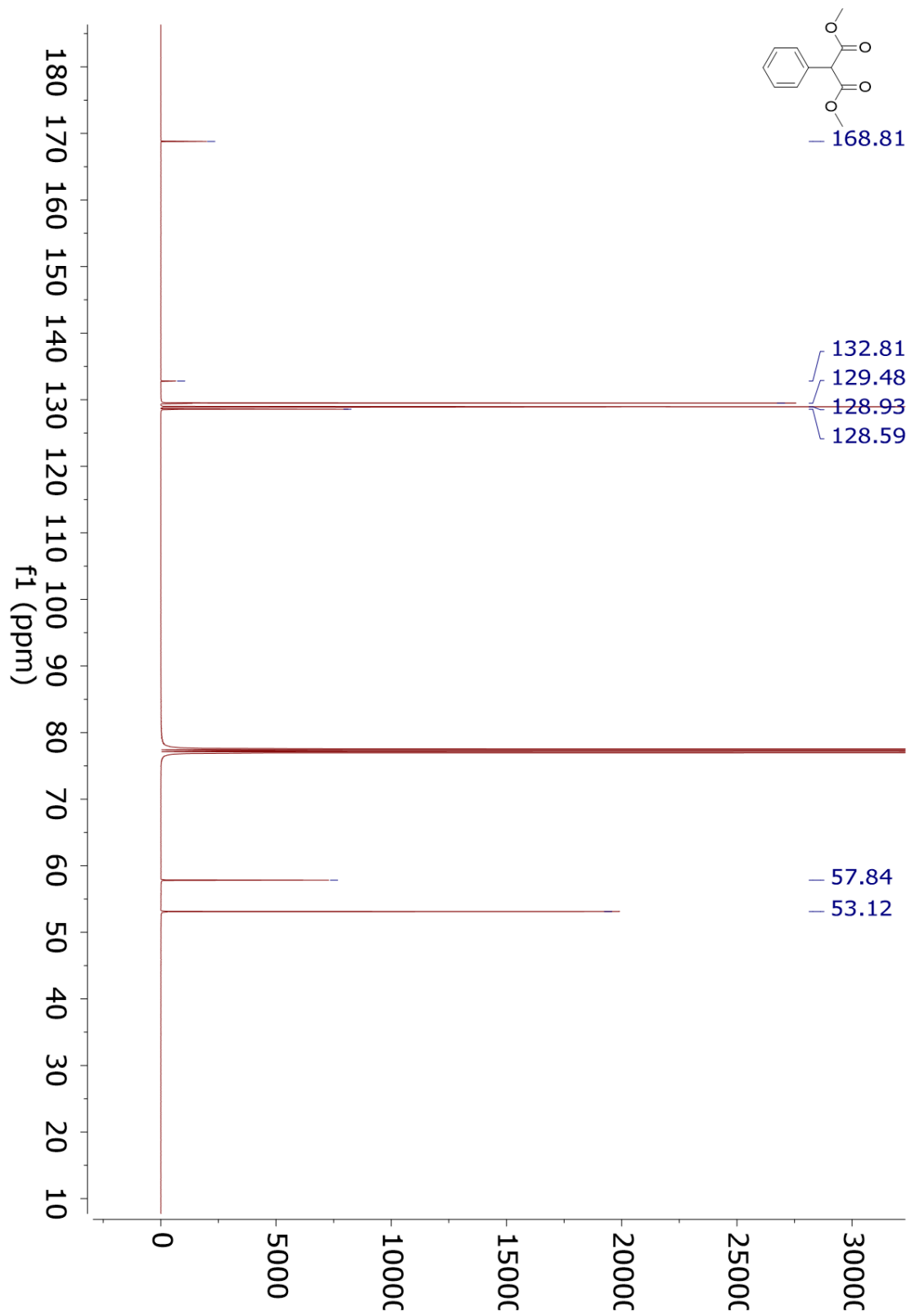
¹³C NMR 4.10i



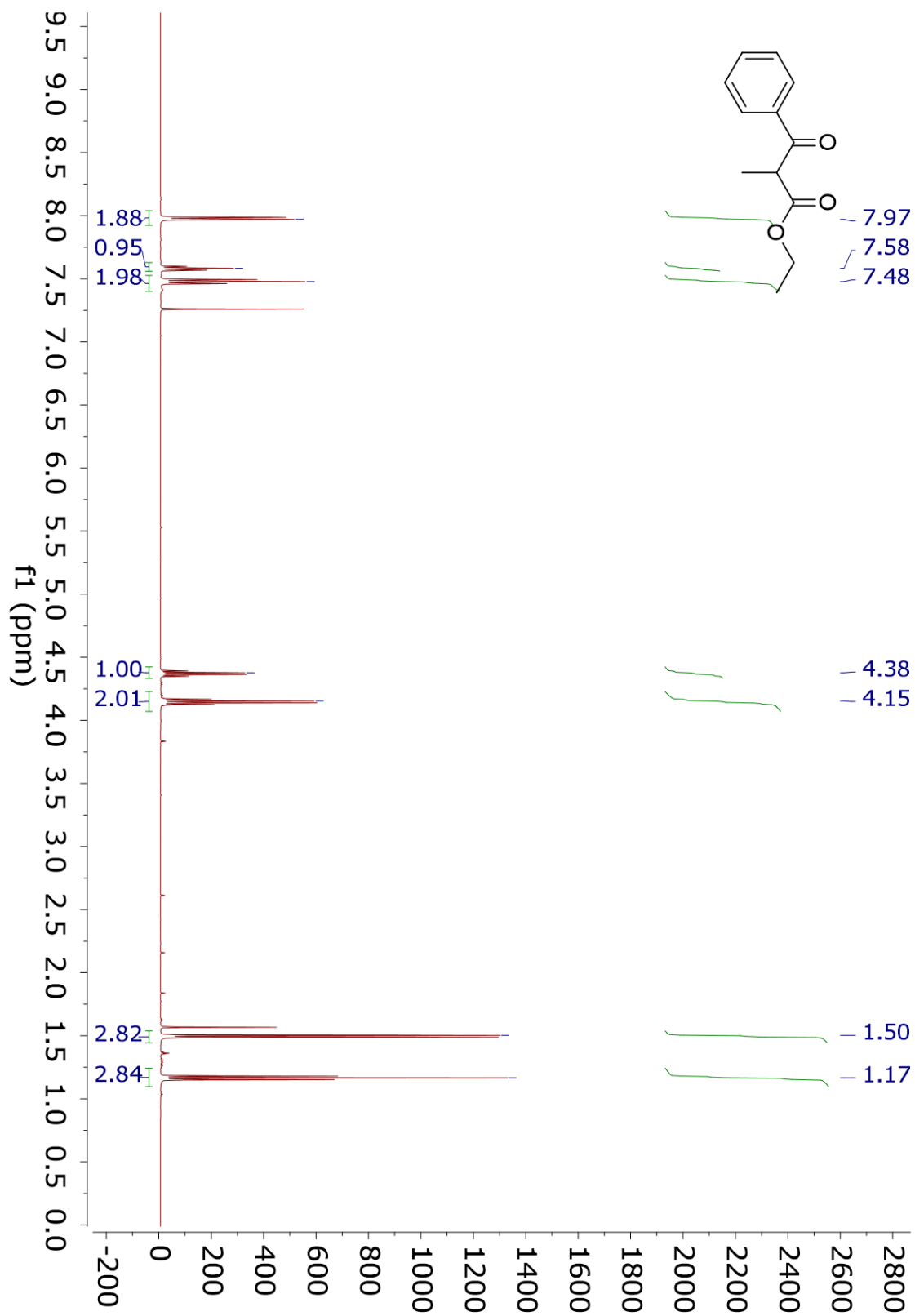
¹H NMR 4.10j



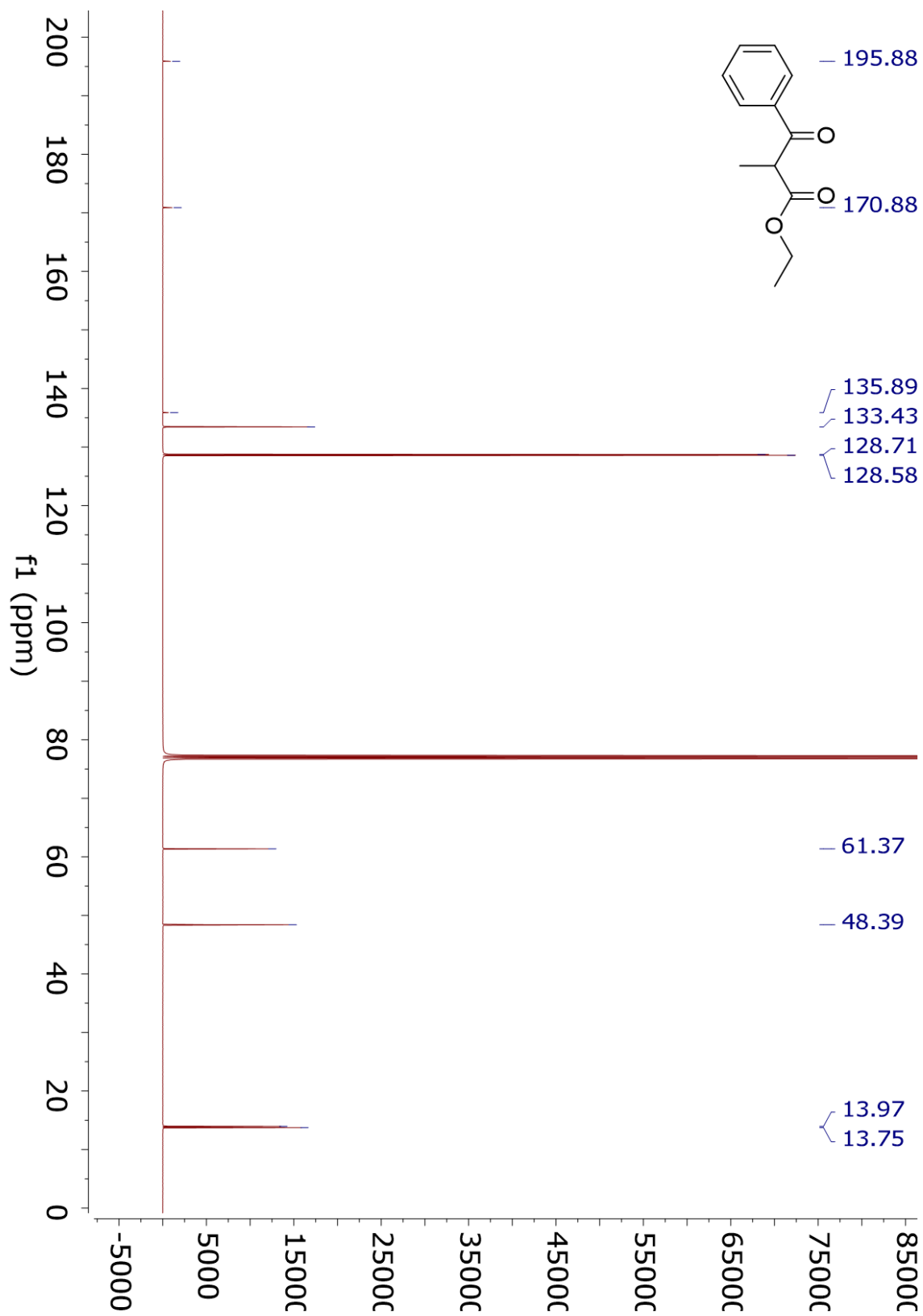
¹³C NMR 4.10j



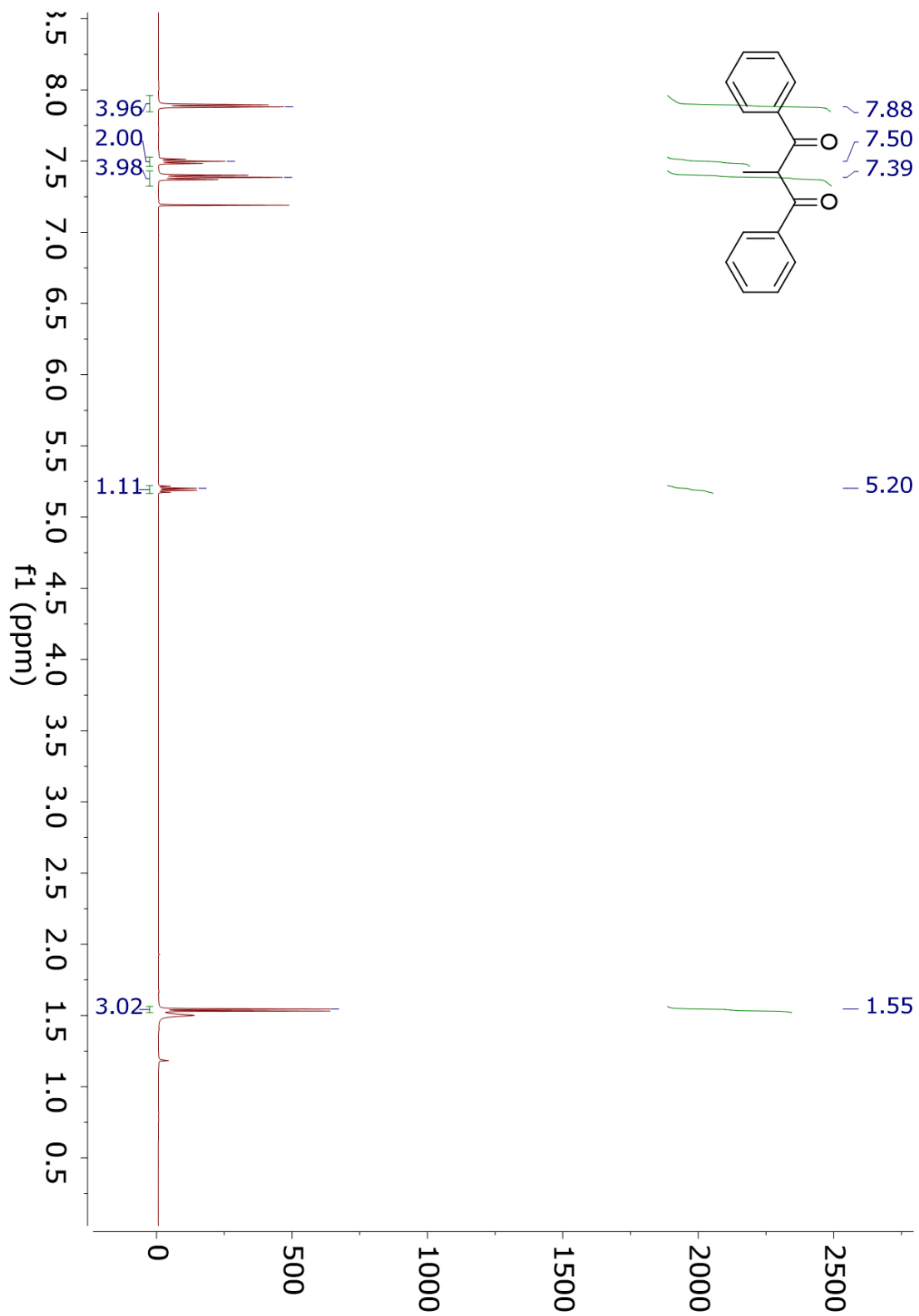
¹H NMR 4.10k



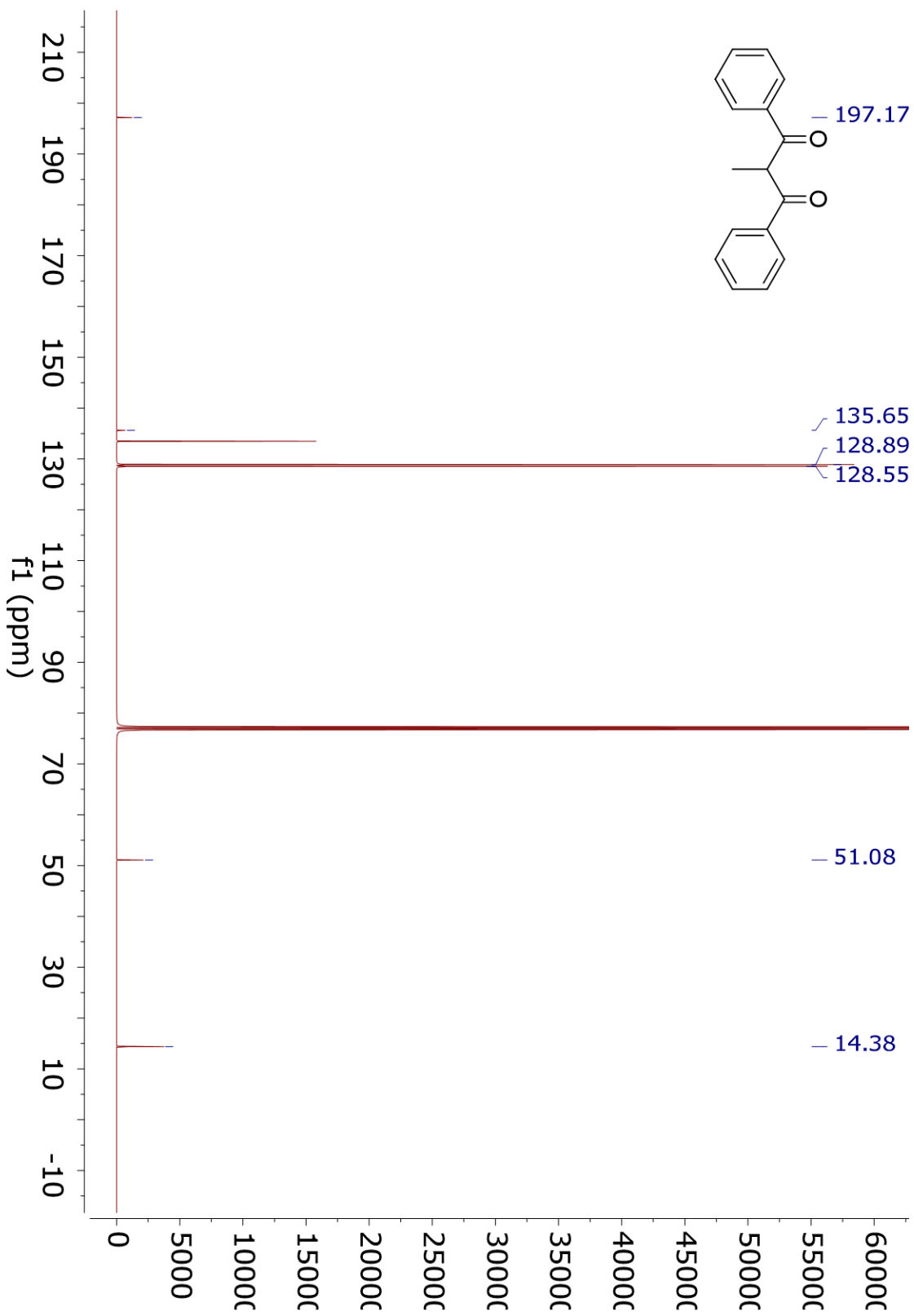
¹³C NMR 4.10k



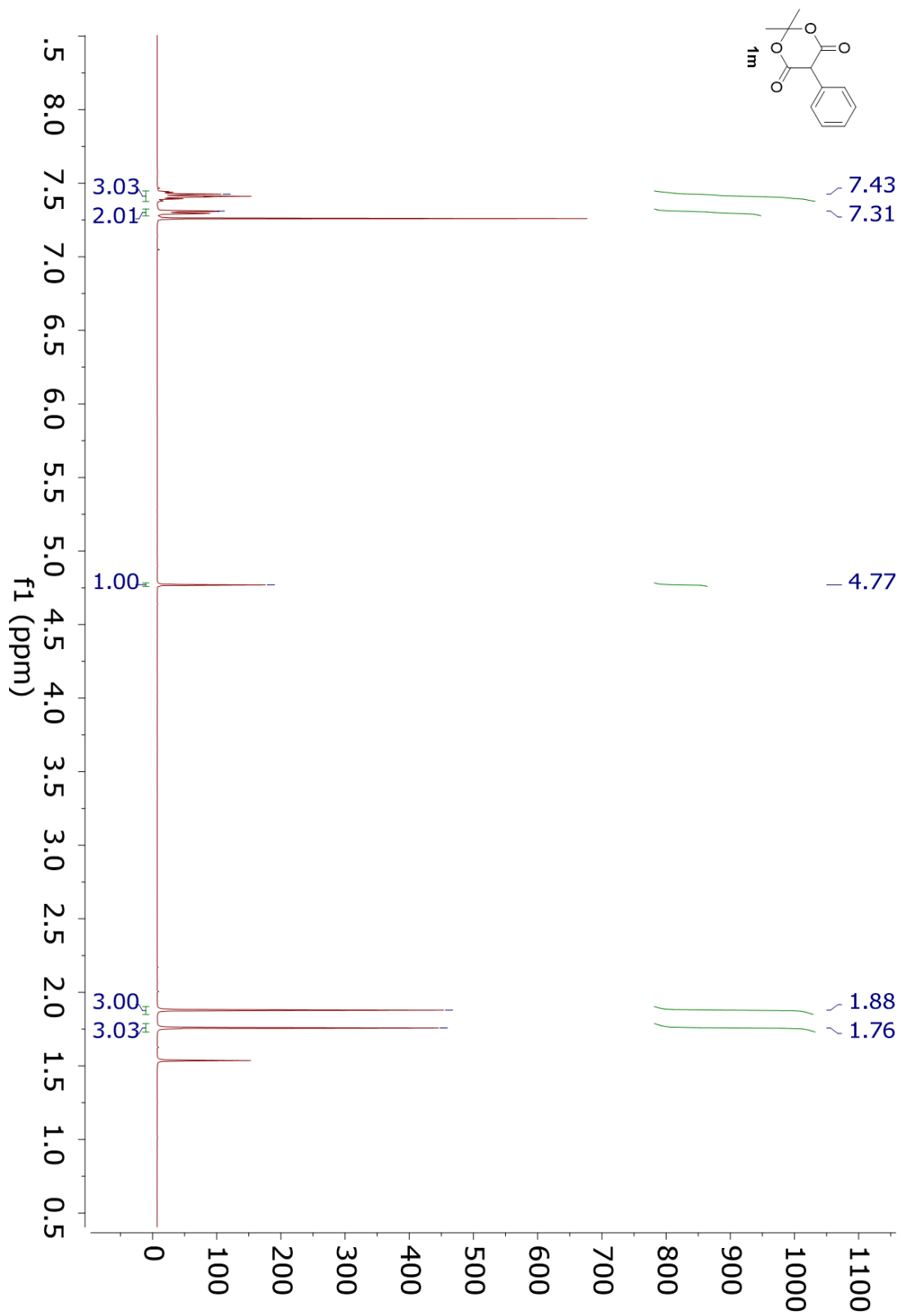
¹H NMR 4.101



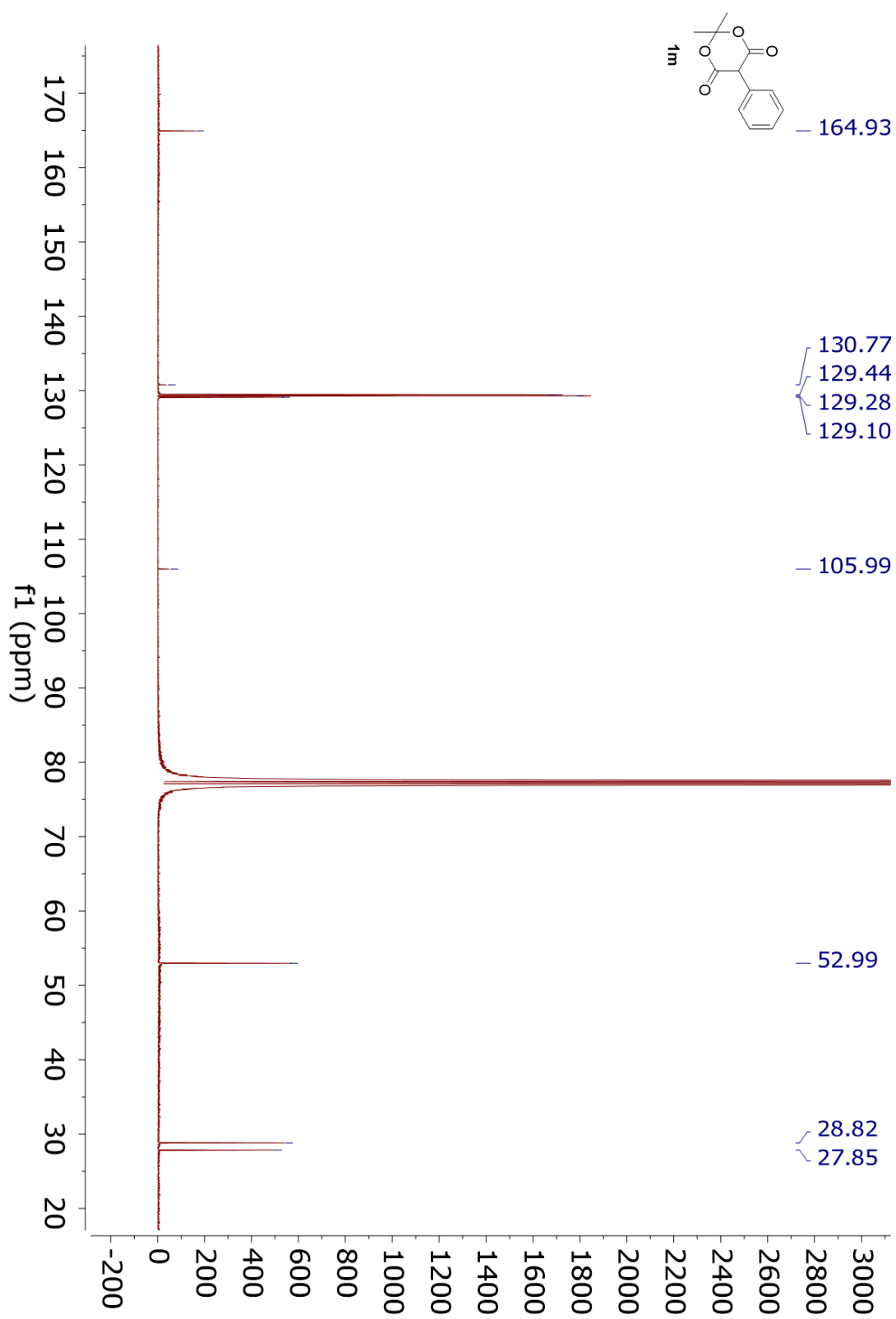
¹³C NMR 4.101



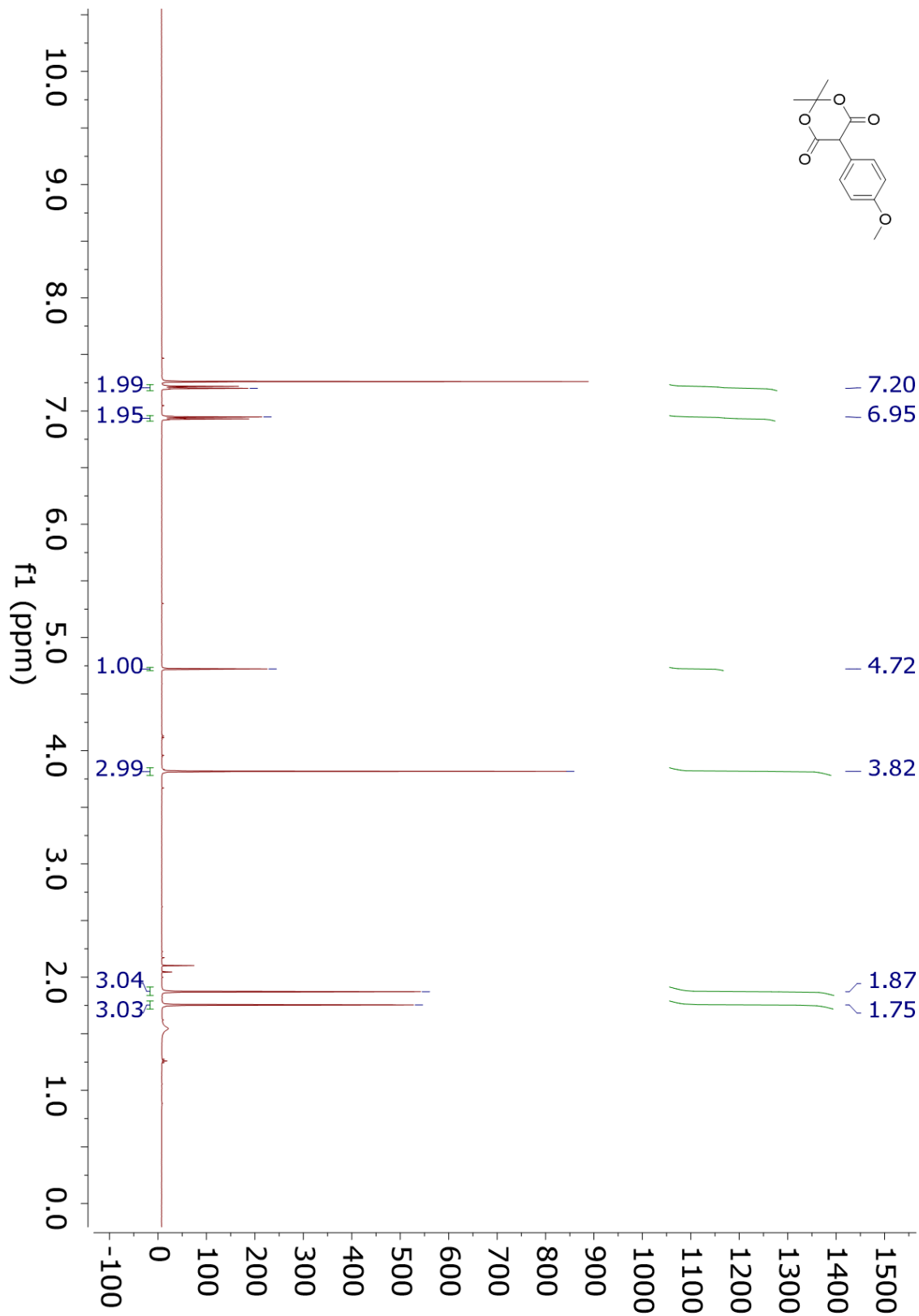
¹H NMR 4.10m



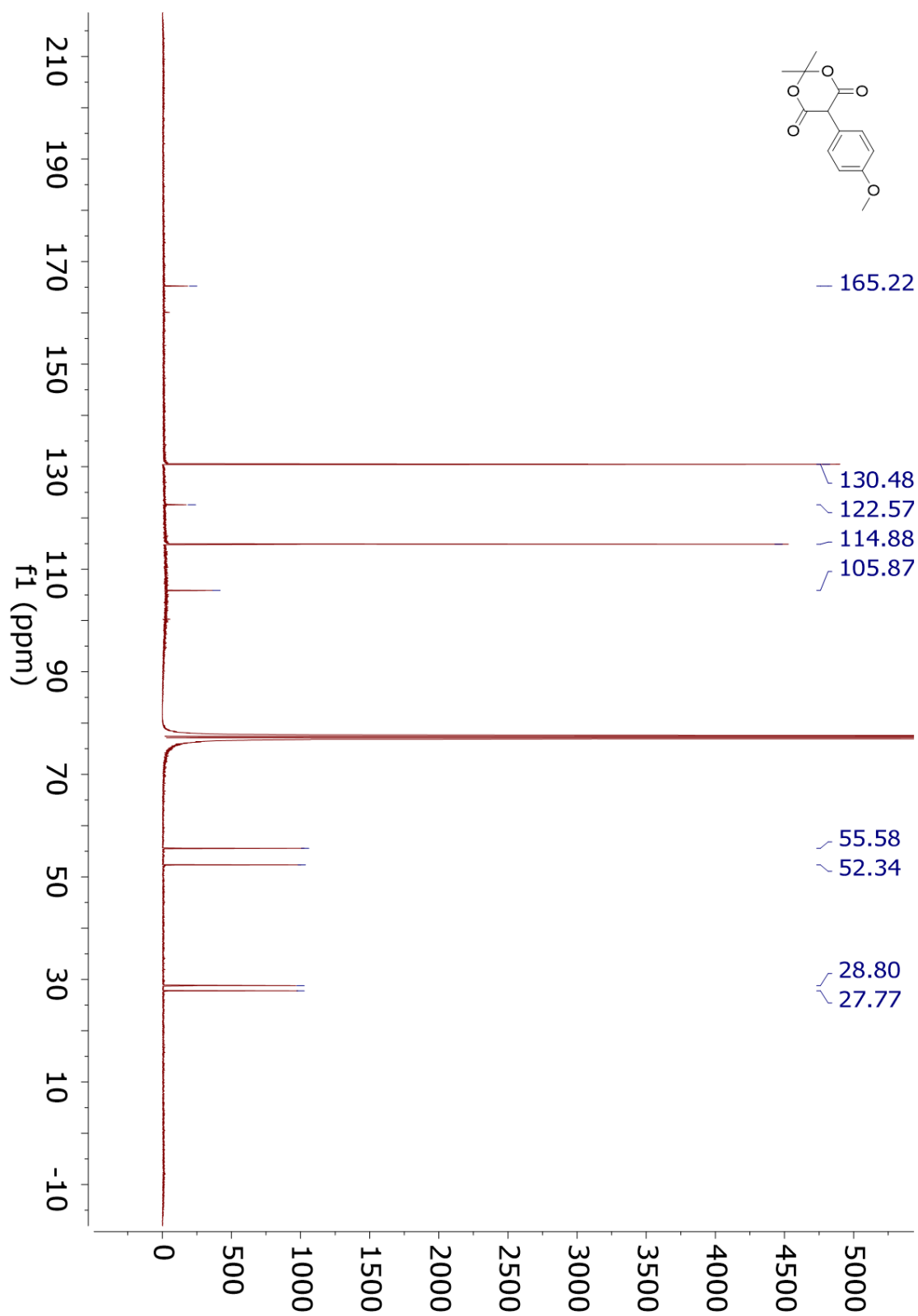
¹³C NMR 4.10m



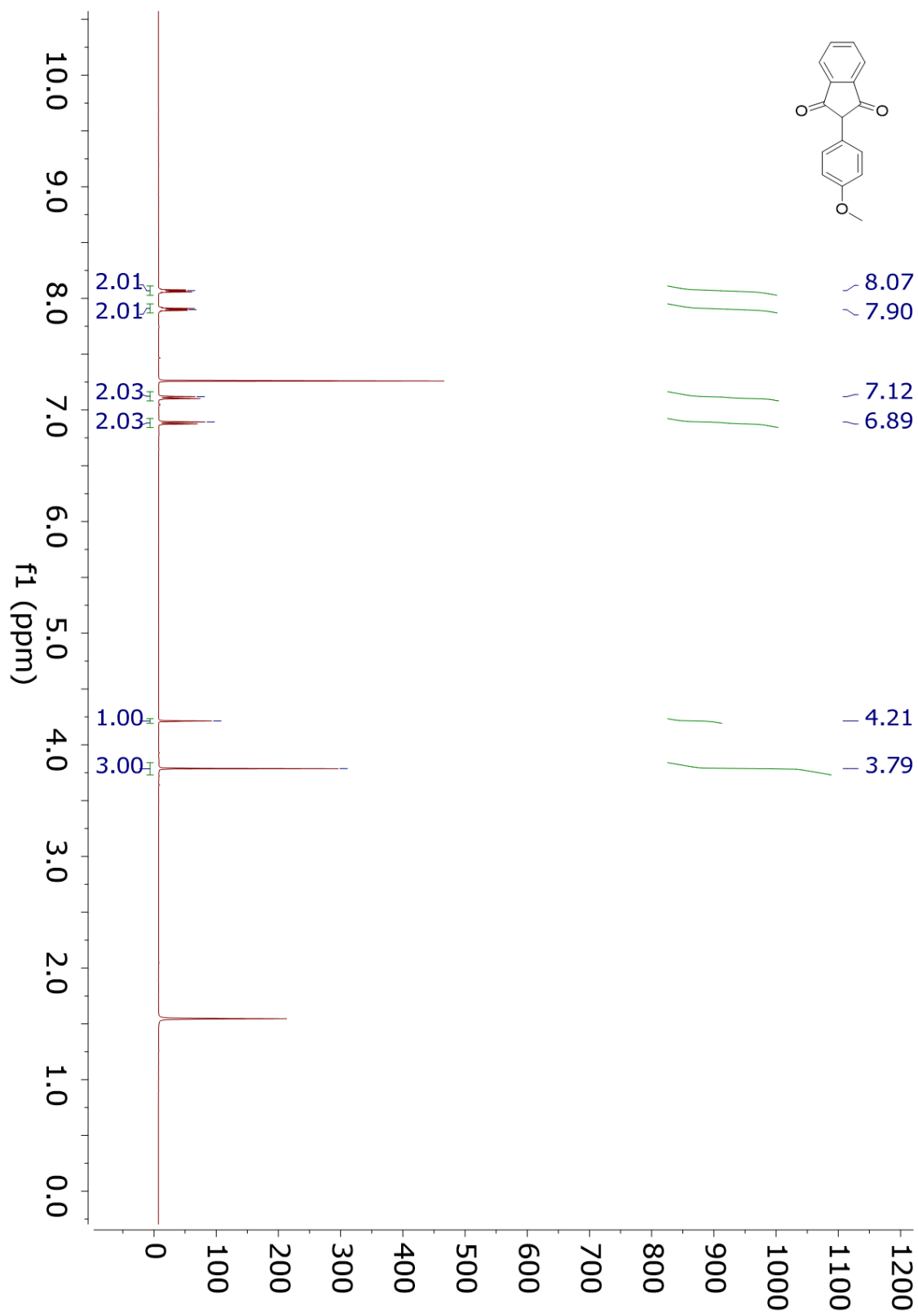
¹H NMR S1



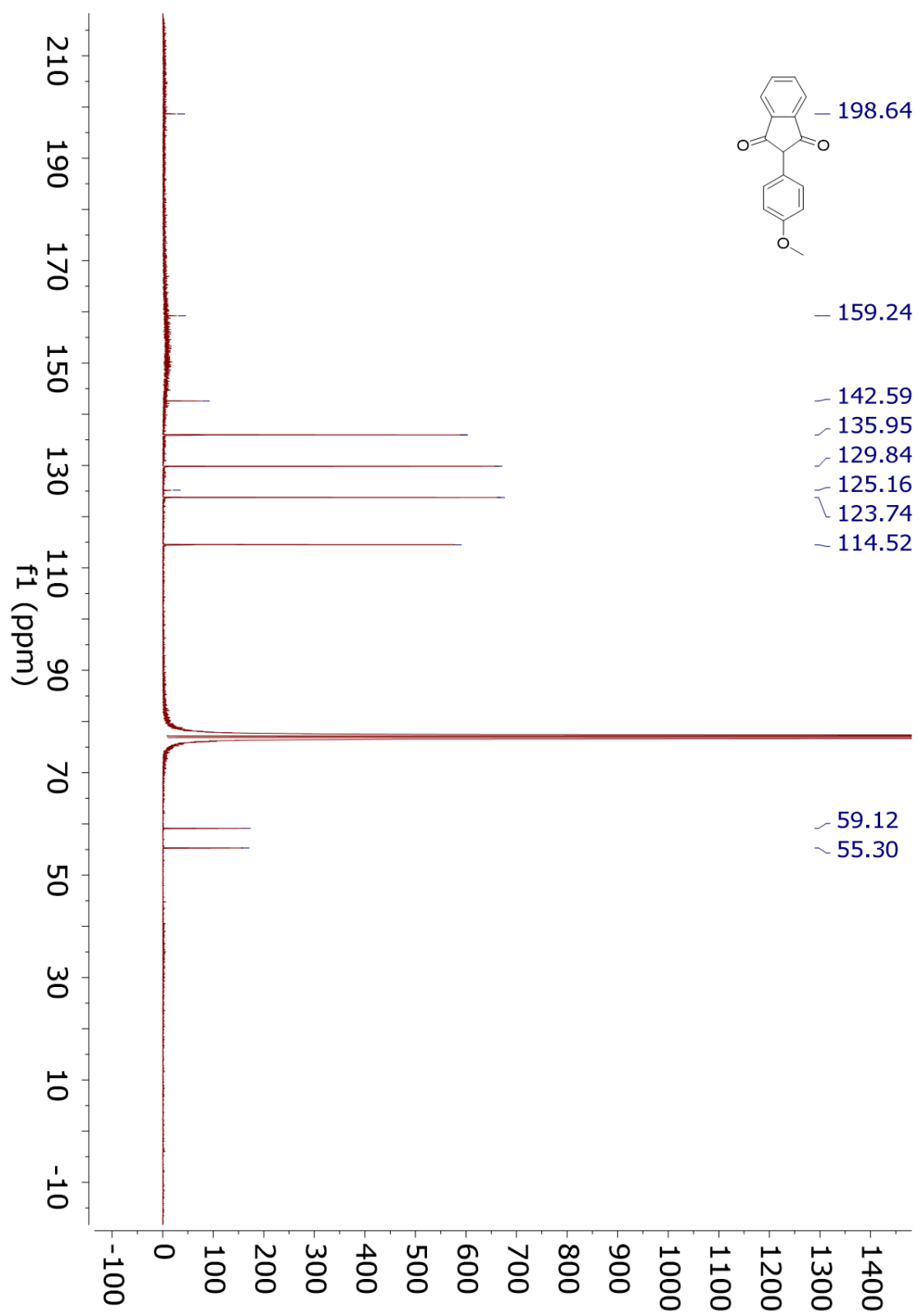
¹³C NMR S1



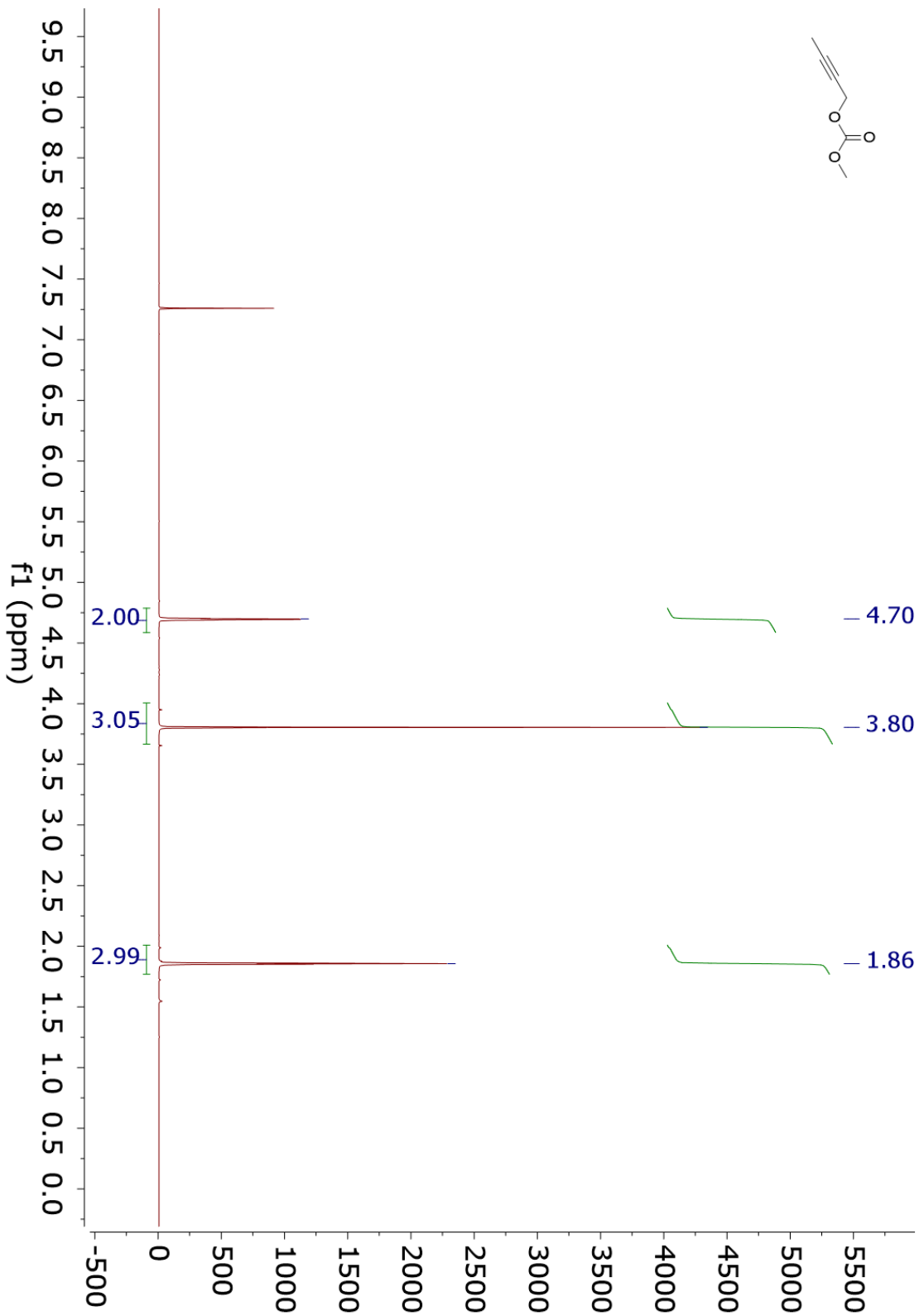
¹H NMR S2



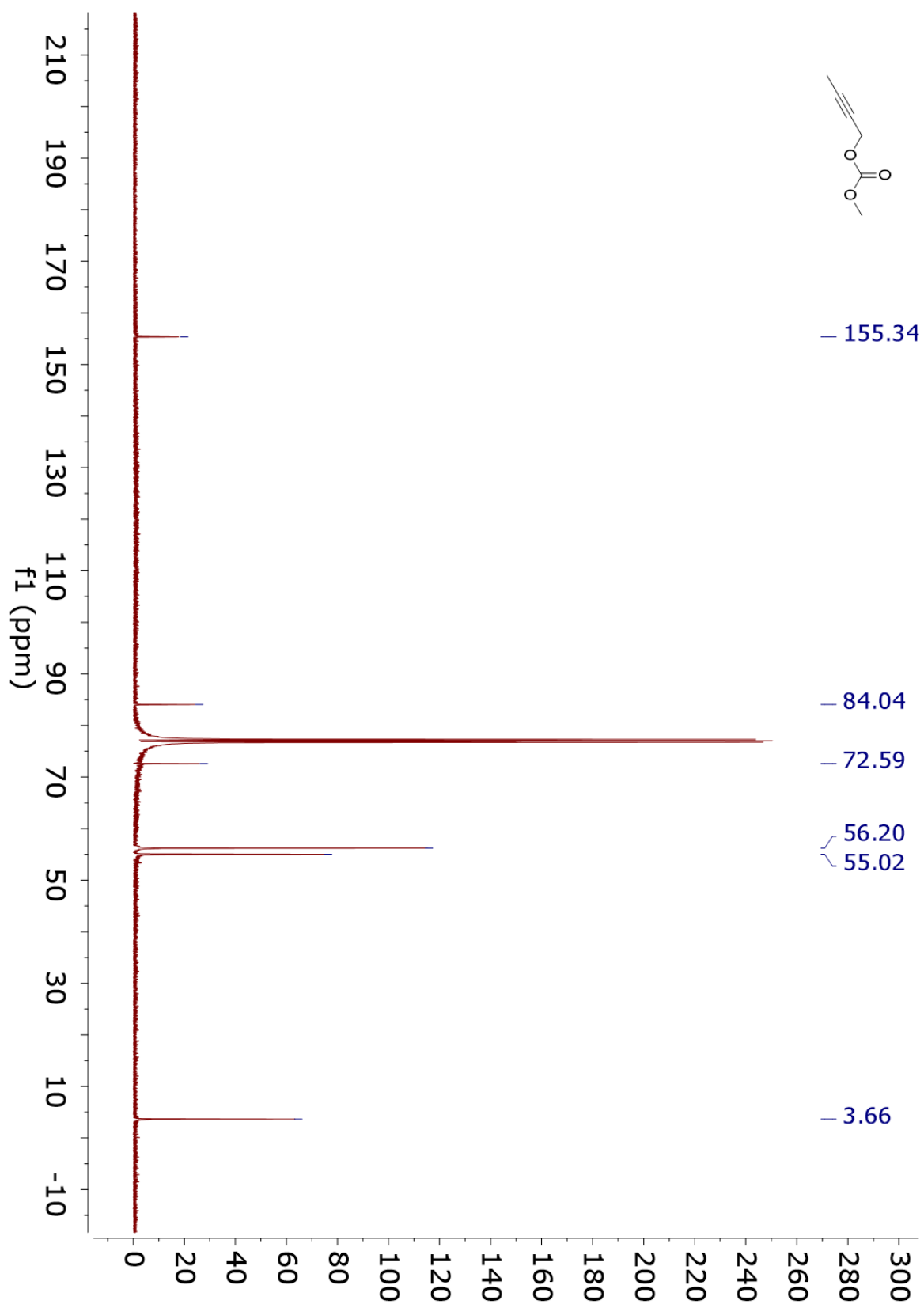
¹³C NMR S2



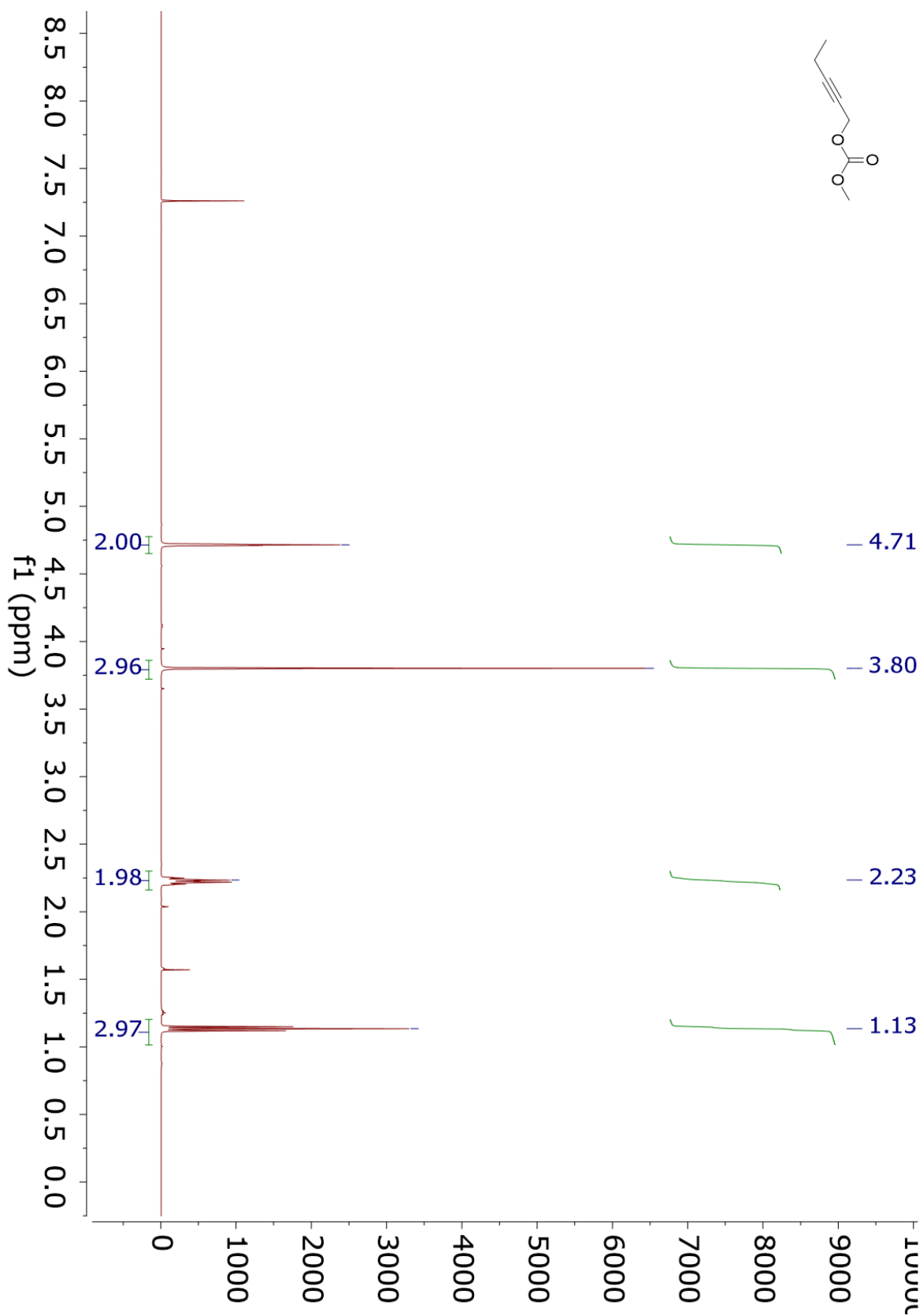
¹H NMR 4.11a



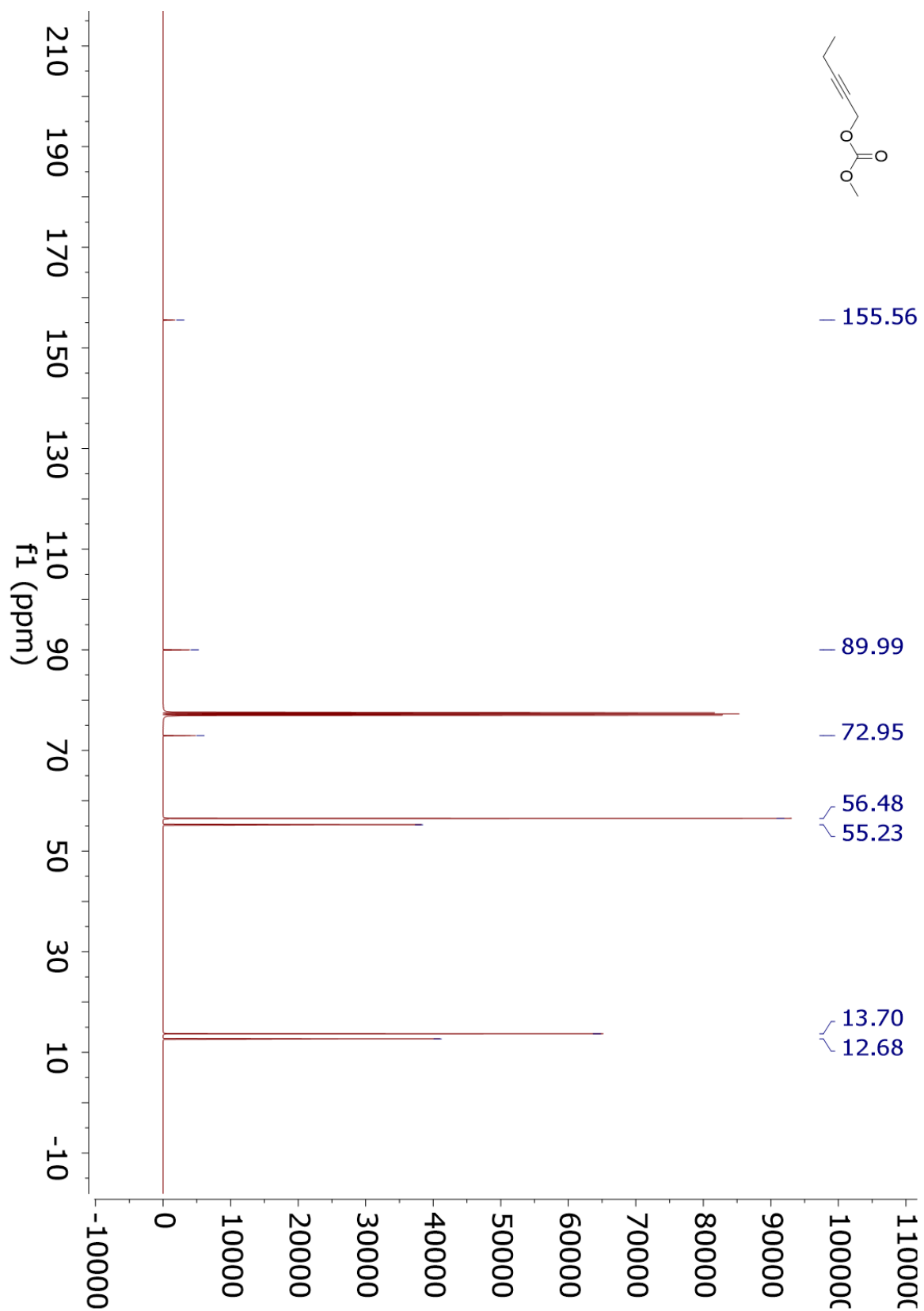
¹³C NMR 4.11a



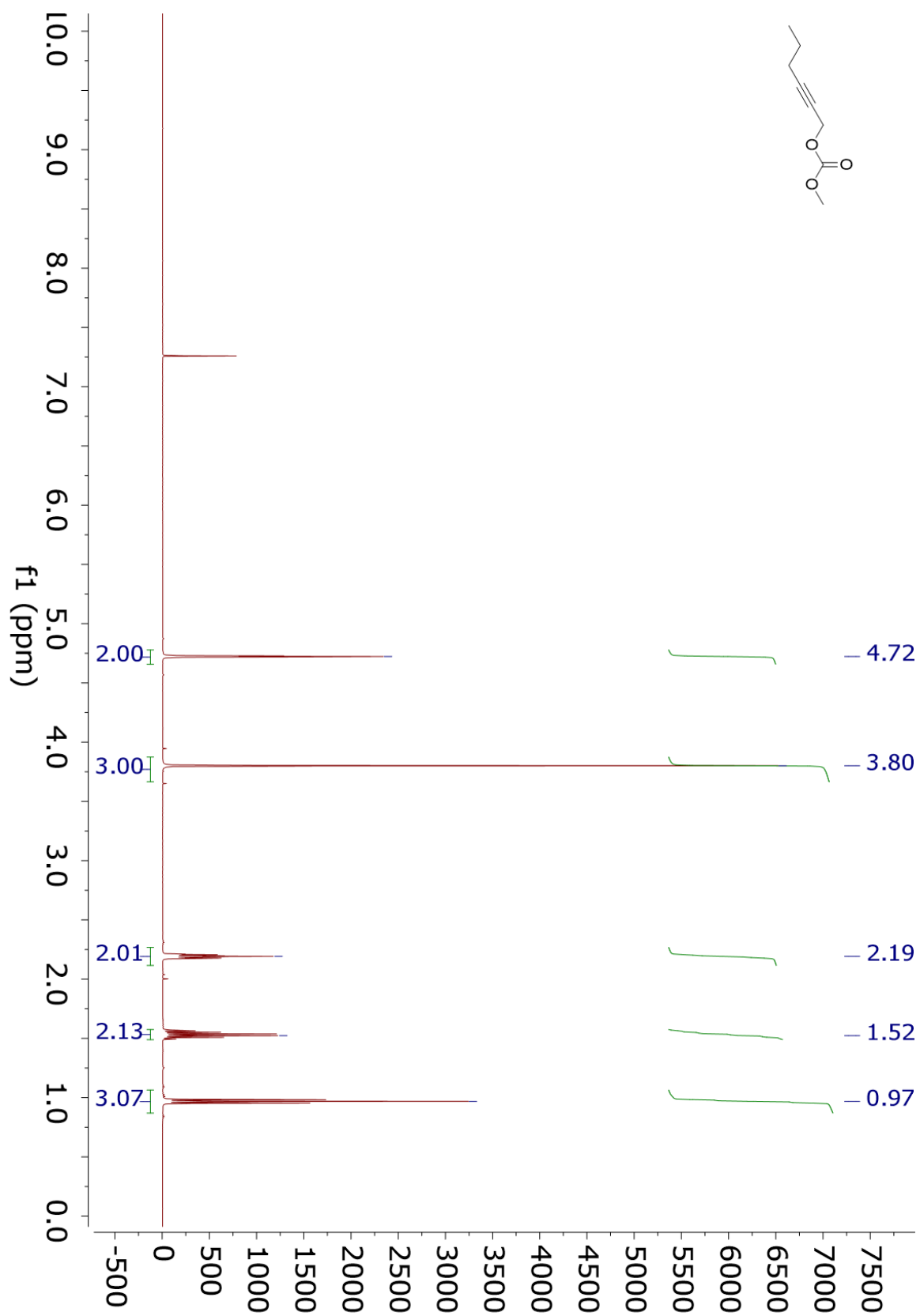
¹H NMR 4.11b



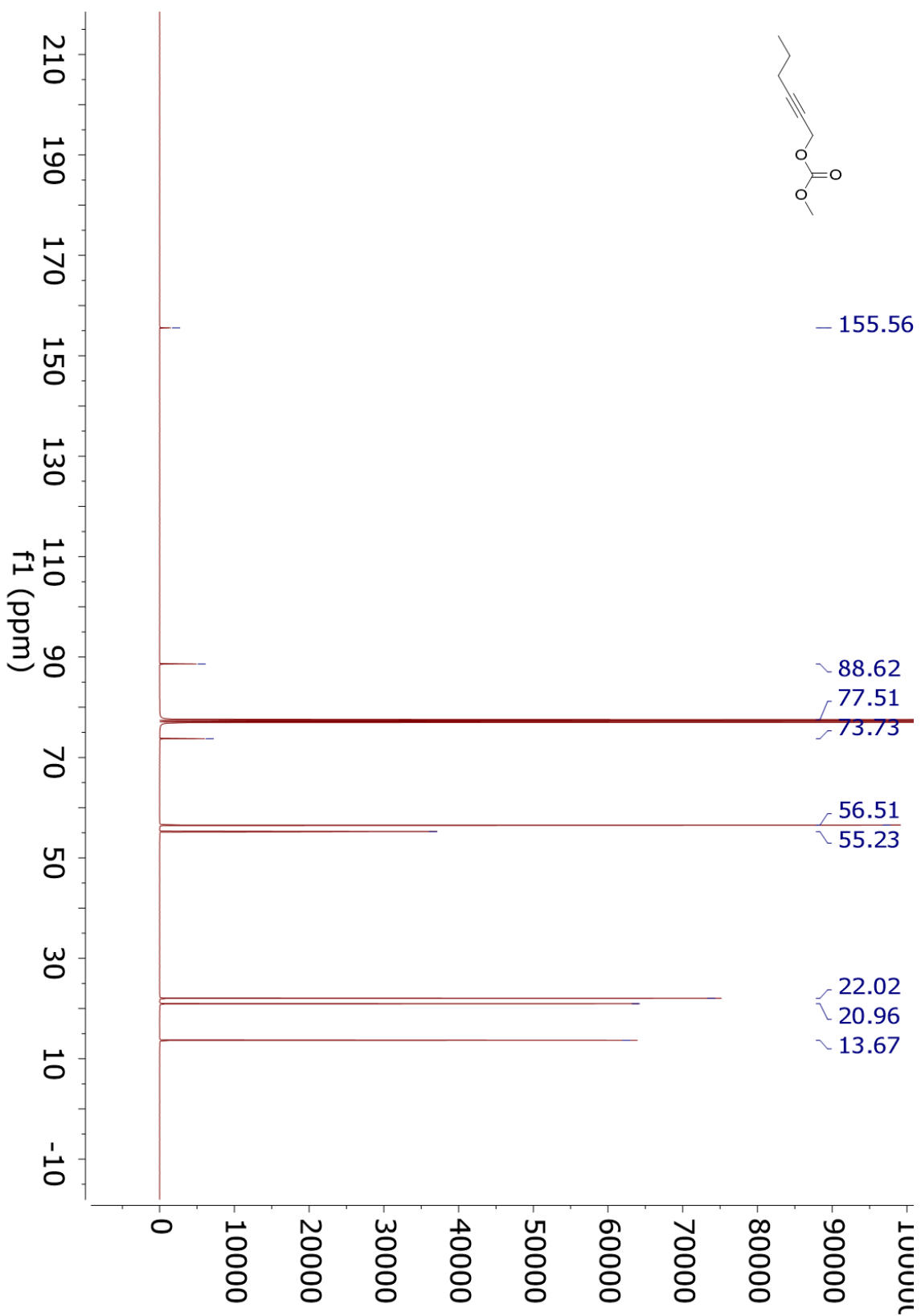
¹³C NMR 4.11b



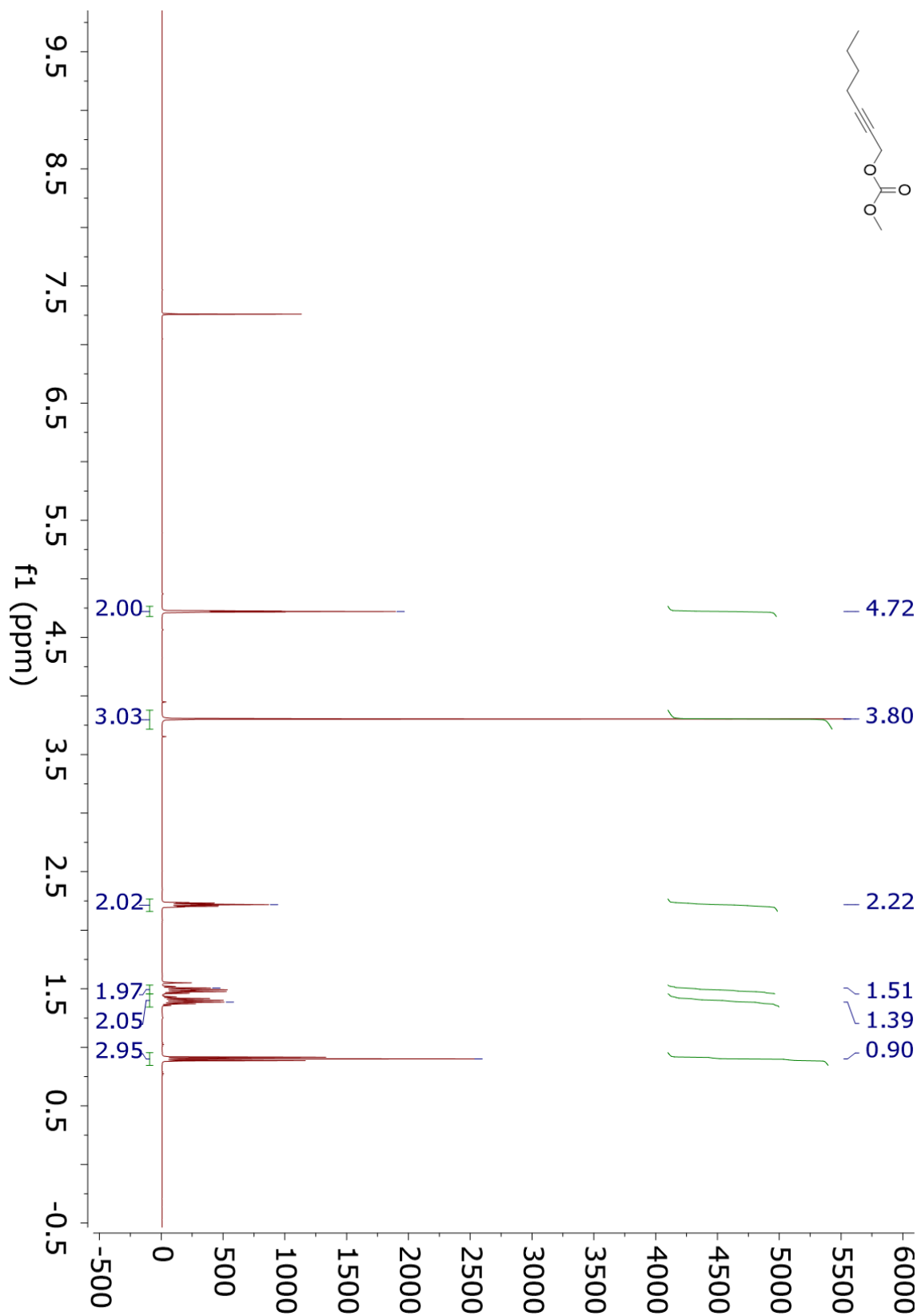
¹H NMR 4.11c



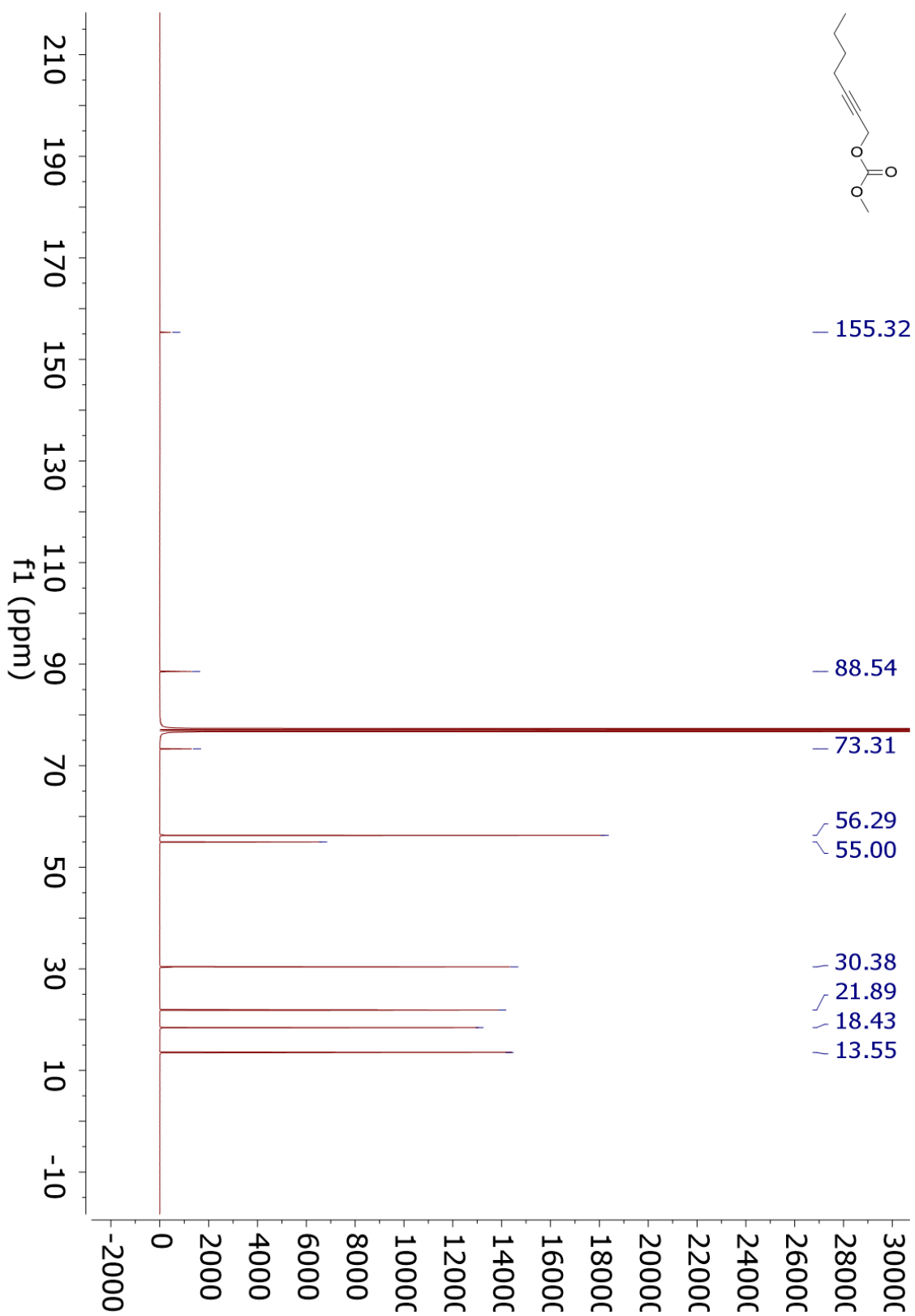
¹³C NMR 4.11c



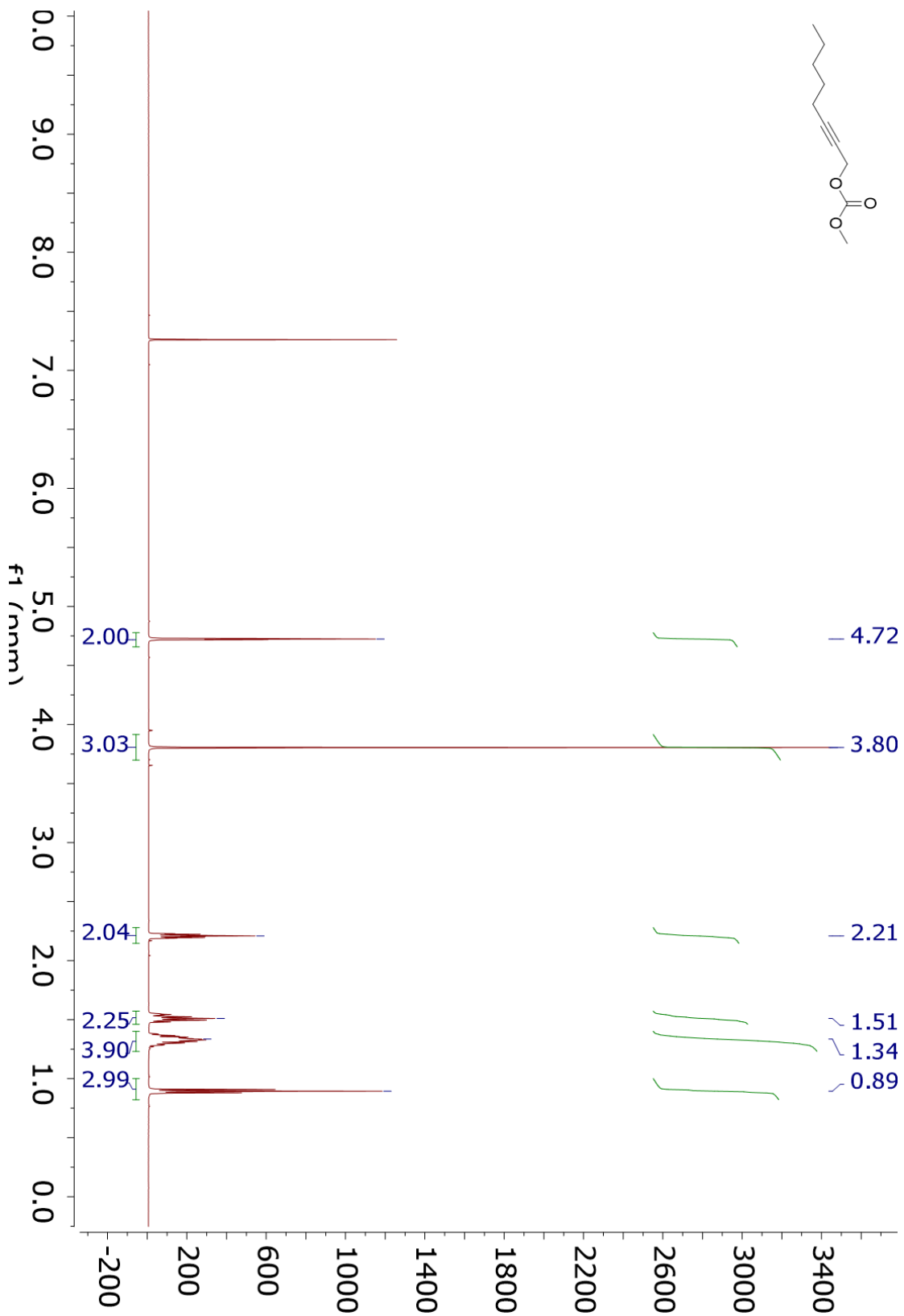
¹H NMR 4.11d



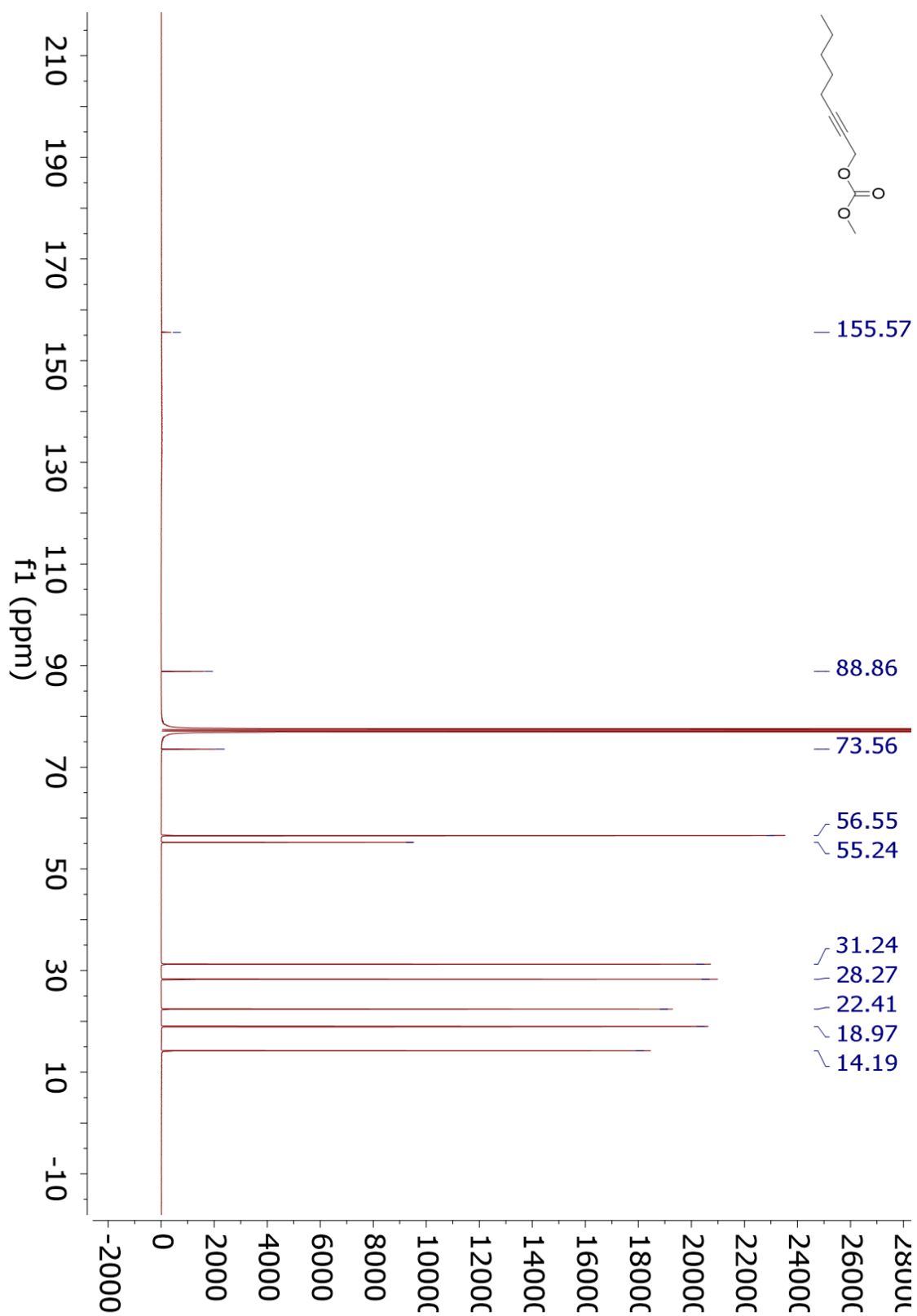
¹³C NMR 4.11d



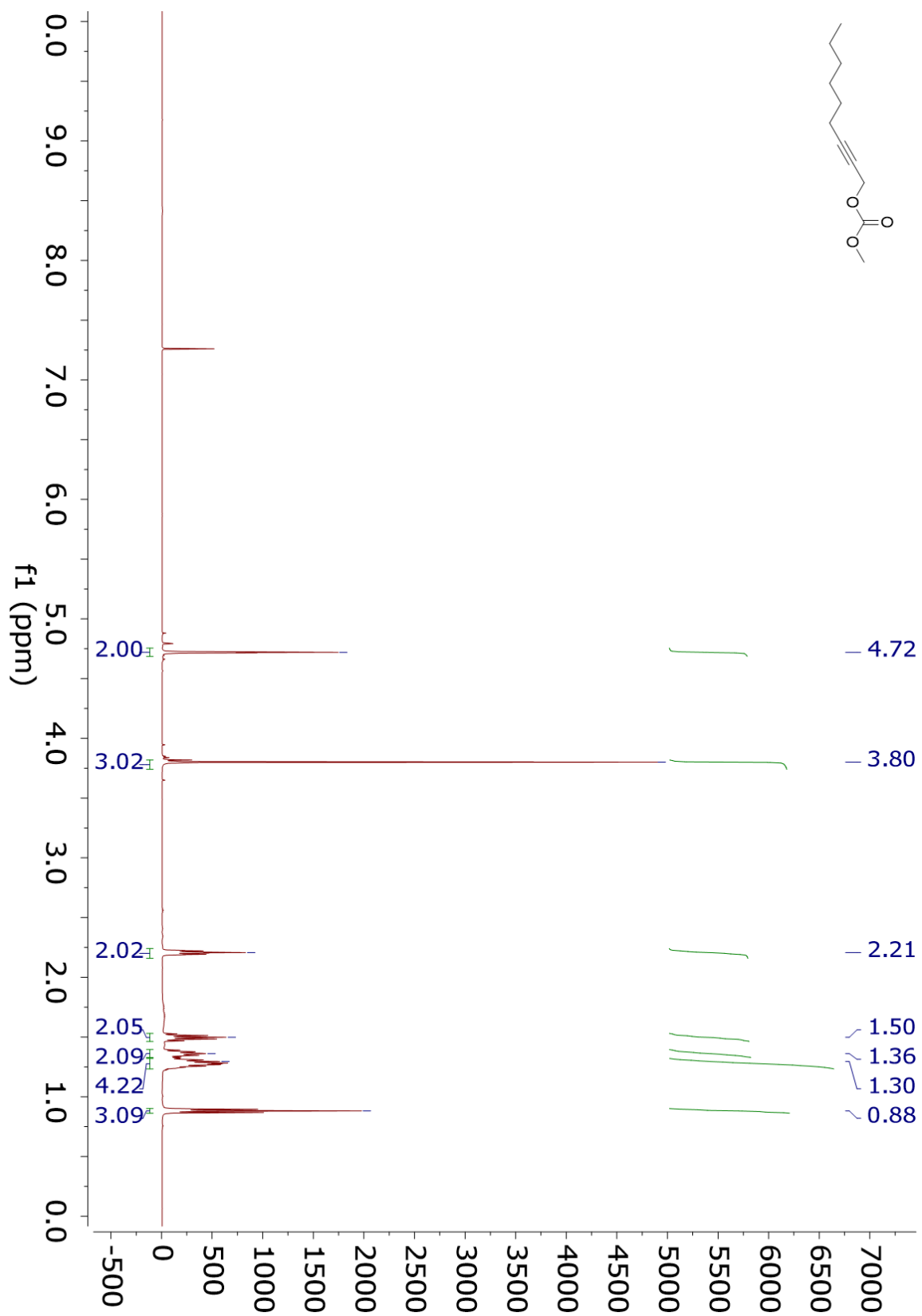
¹H NMR 4.11e



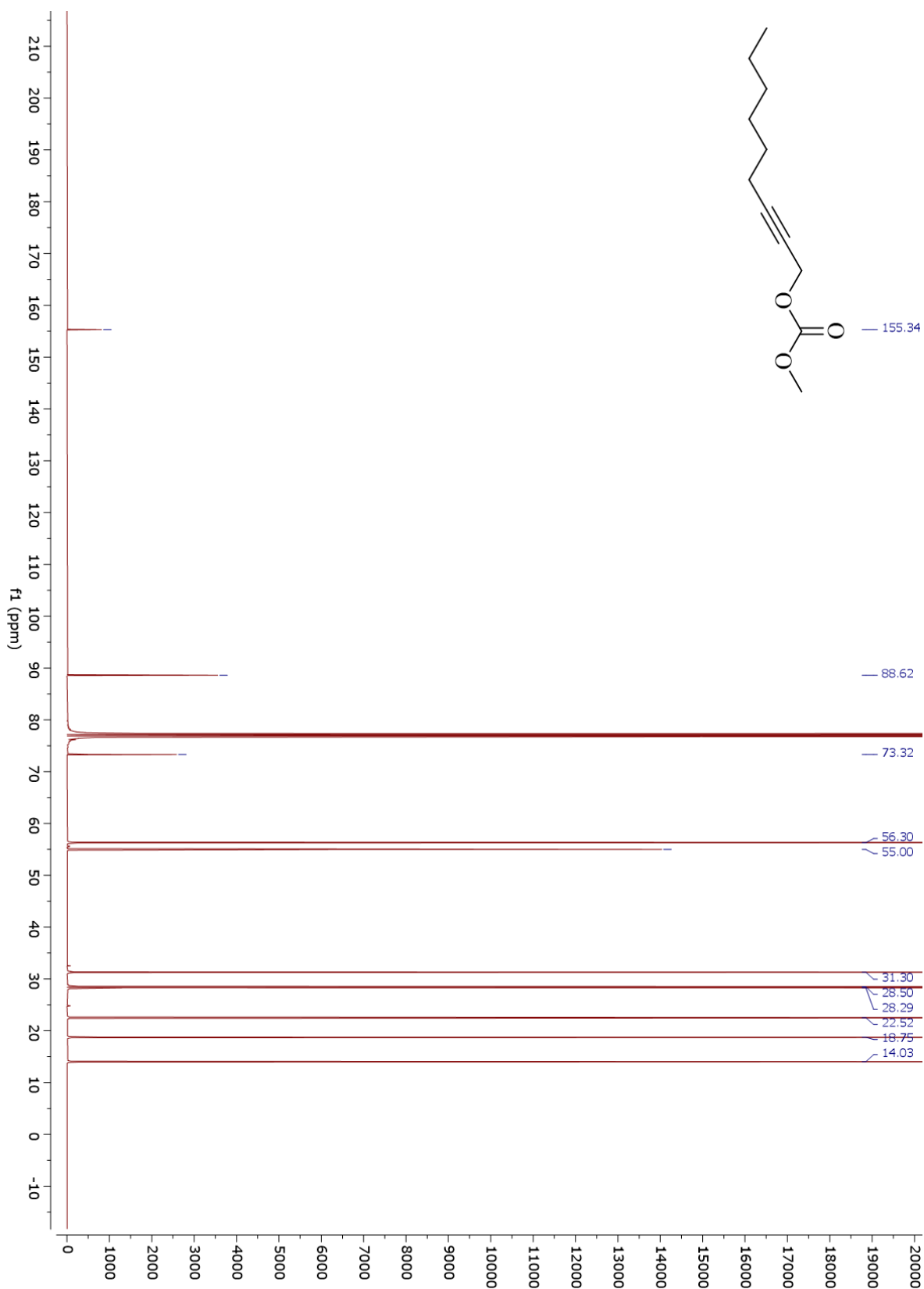
¹³C NMR 4.11e



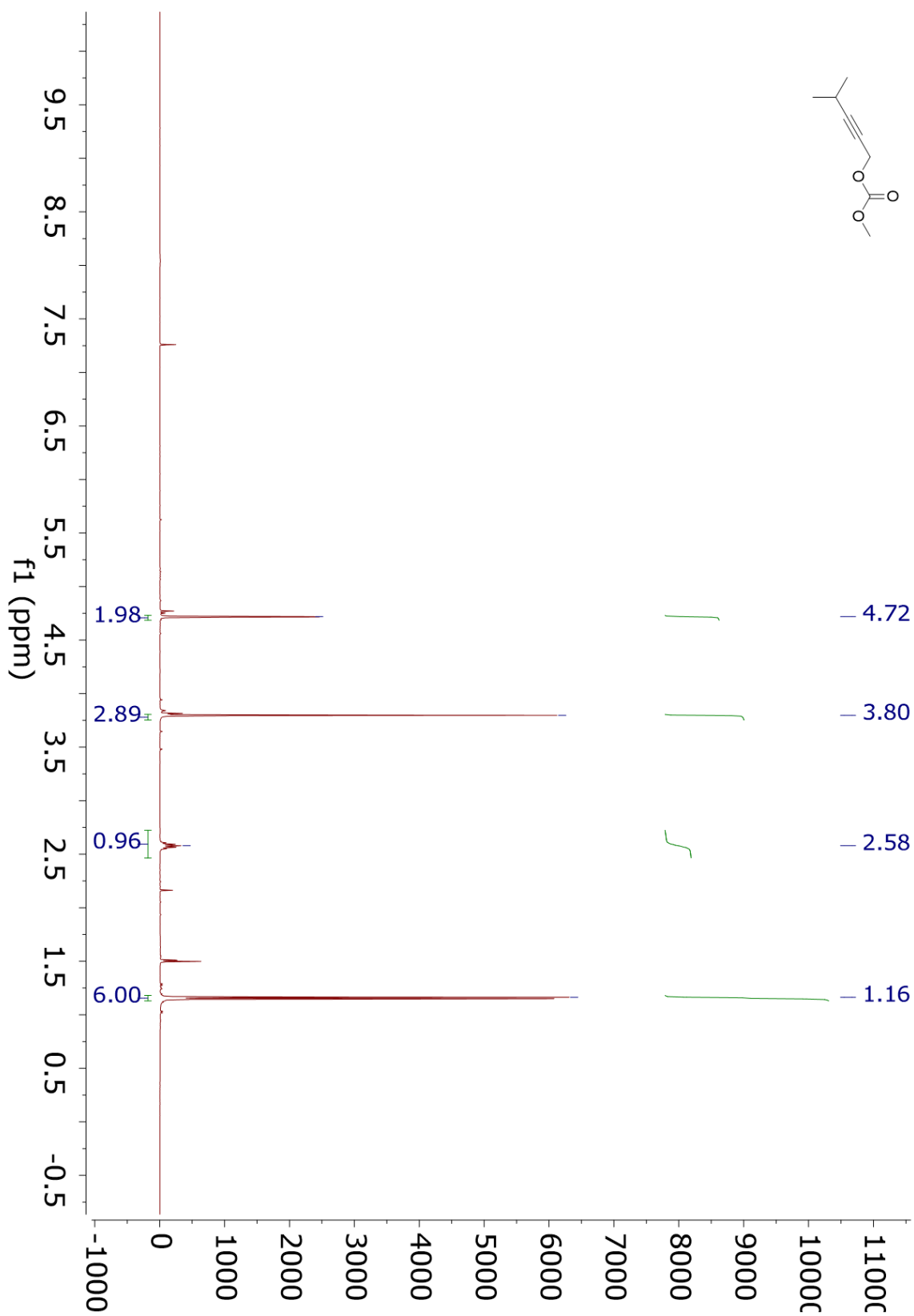
¹H NMR 4.11f



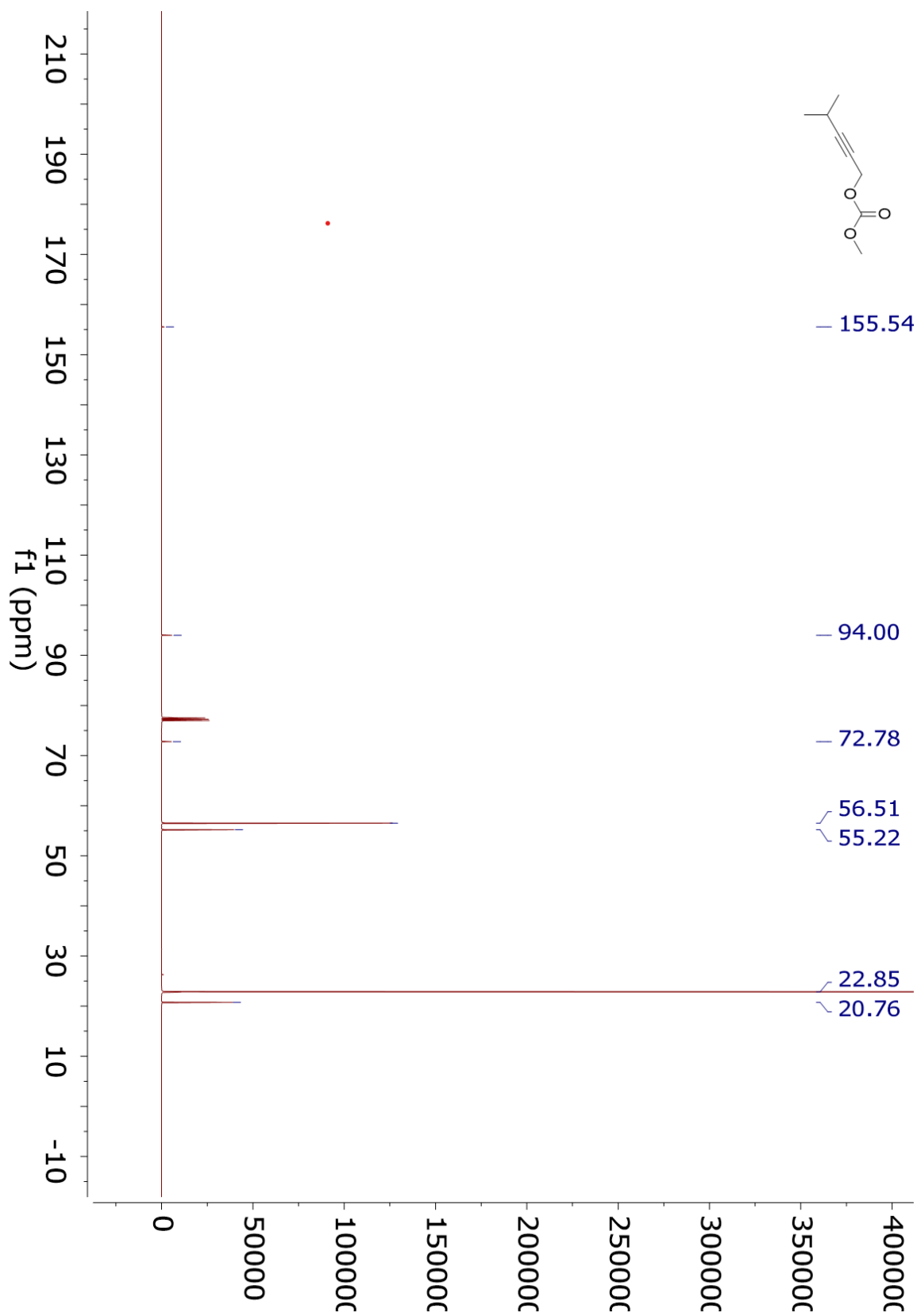
¹³C NMR 4.11f



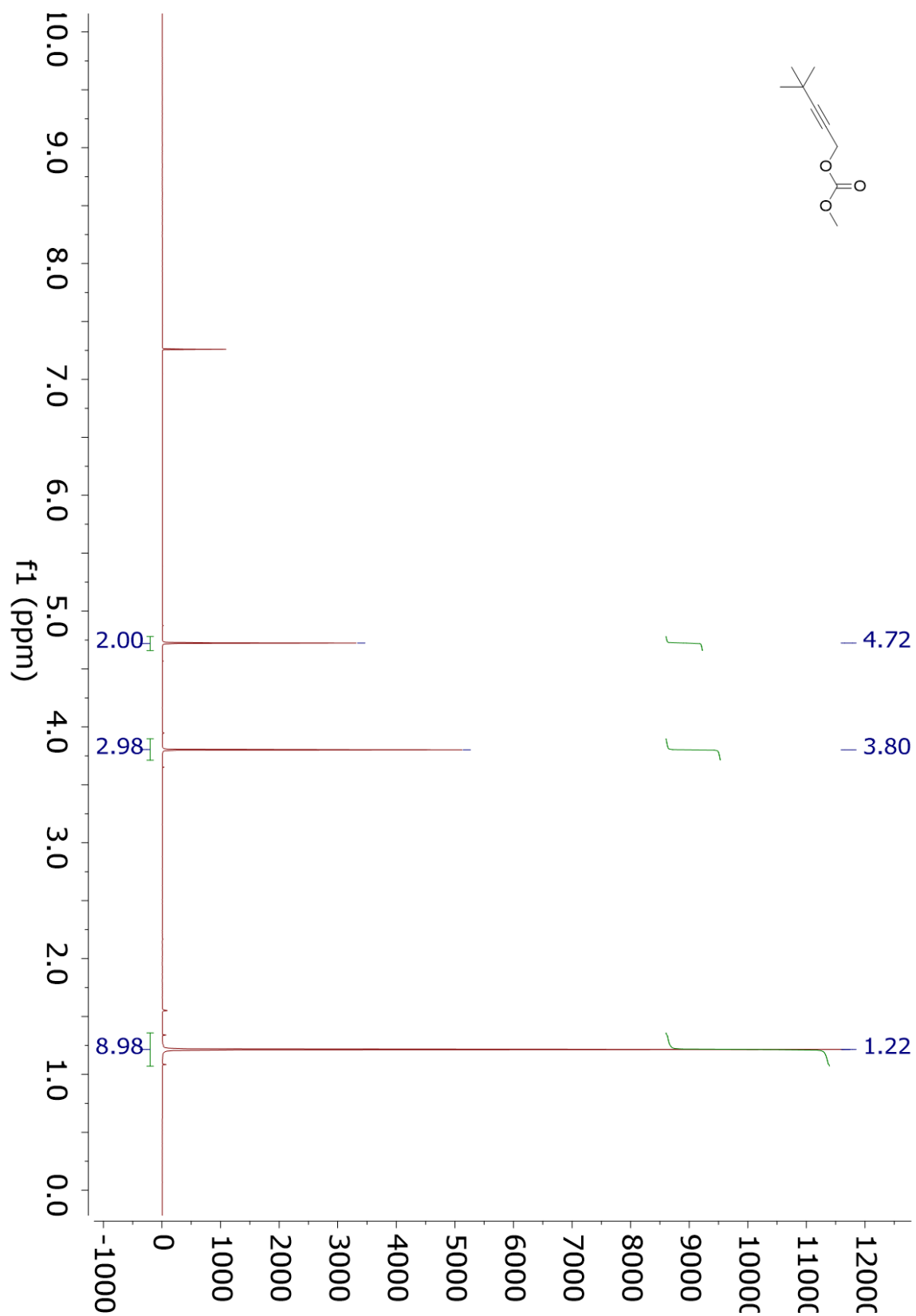
¹H NMR 4.11g



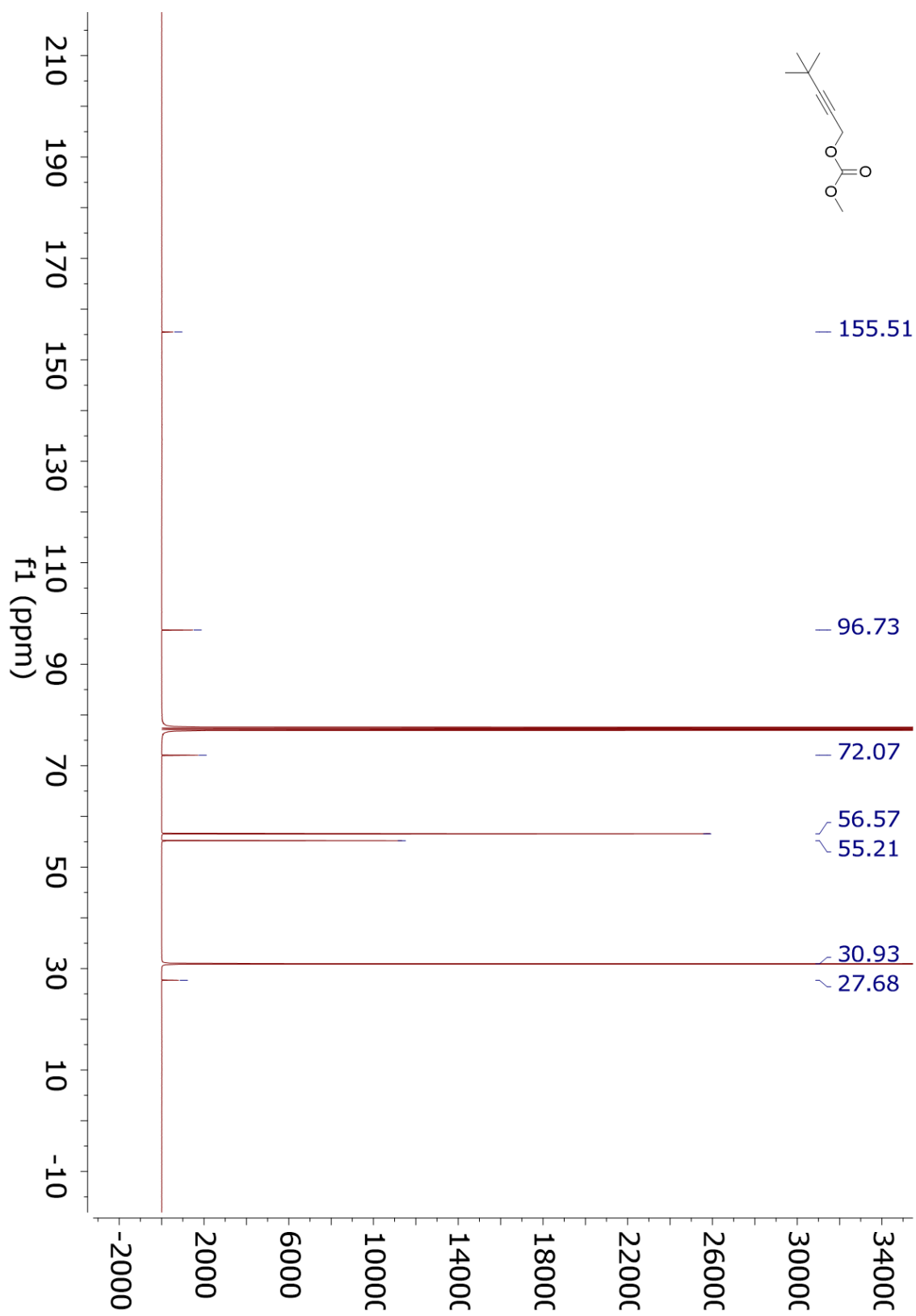
¹³C NMR 4.11g



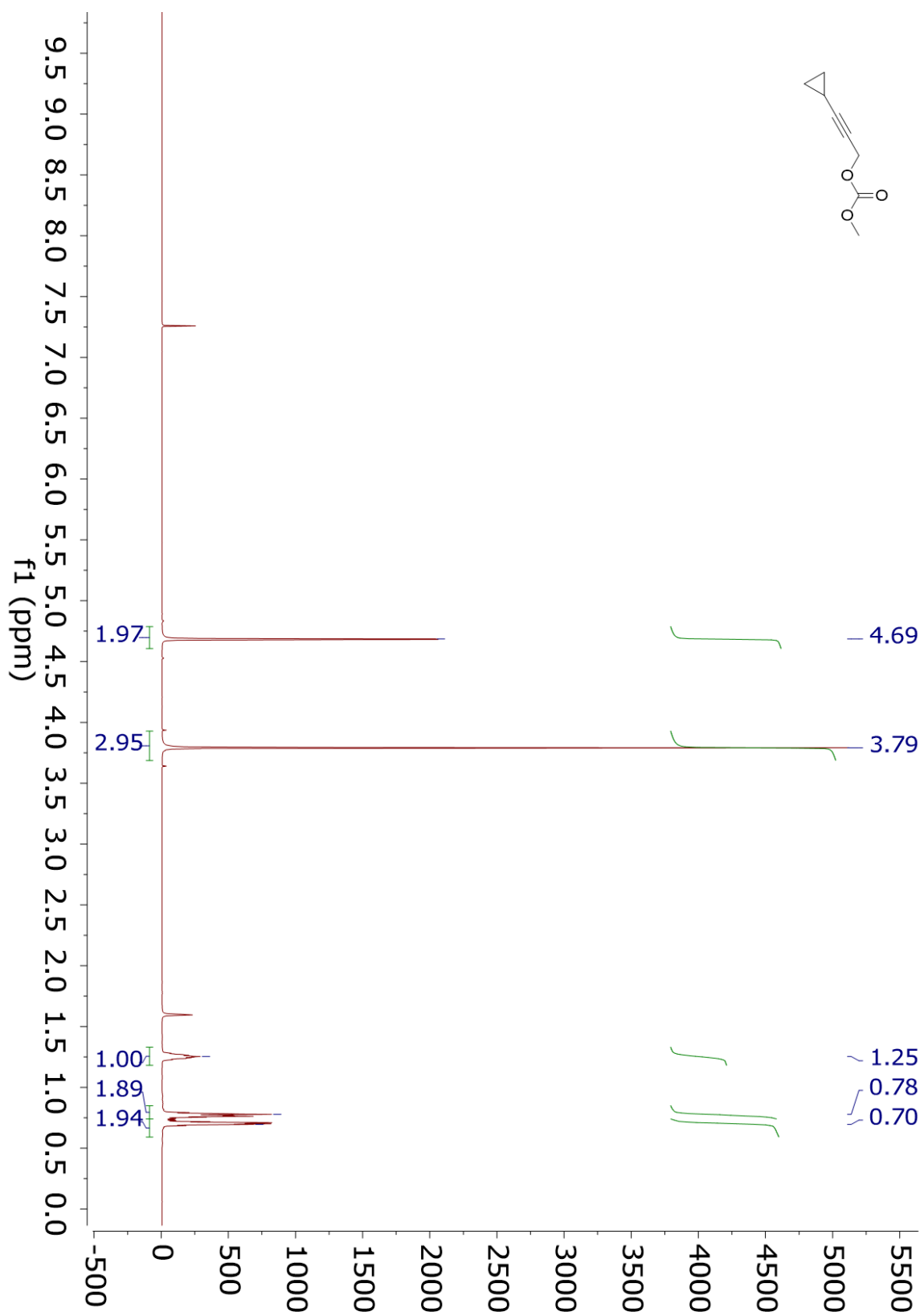
¹H NMR 4.11h



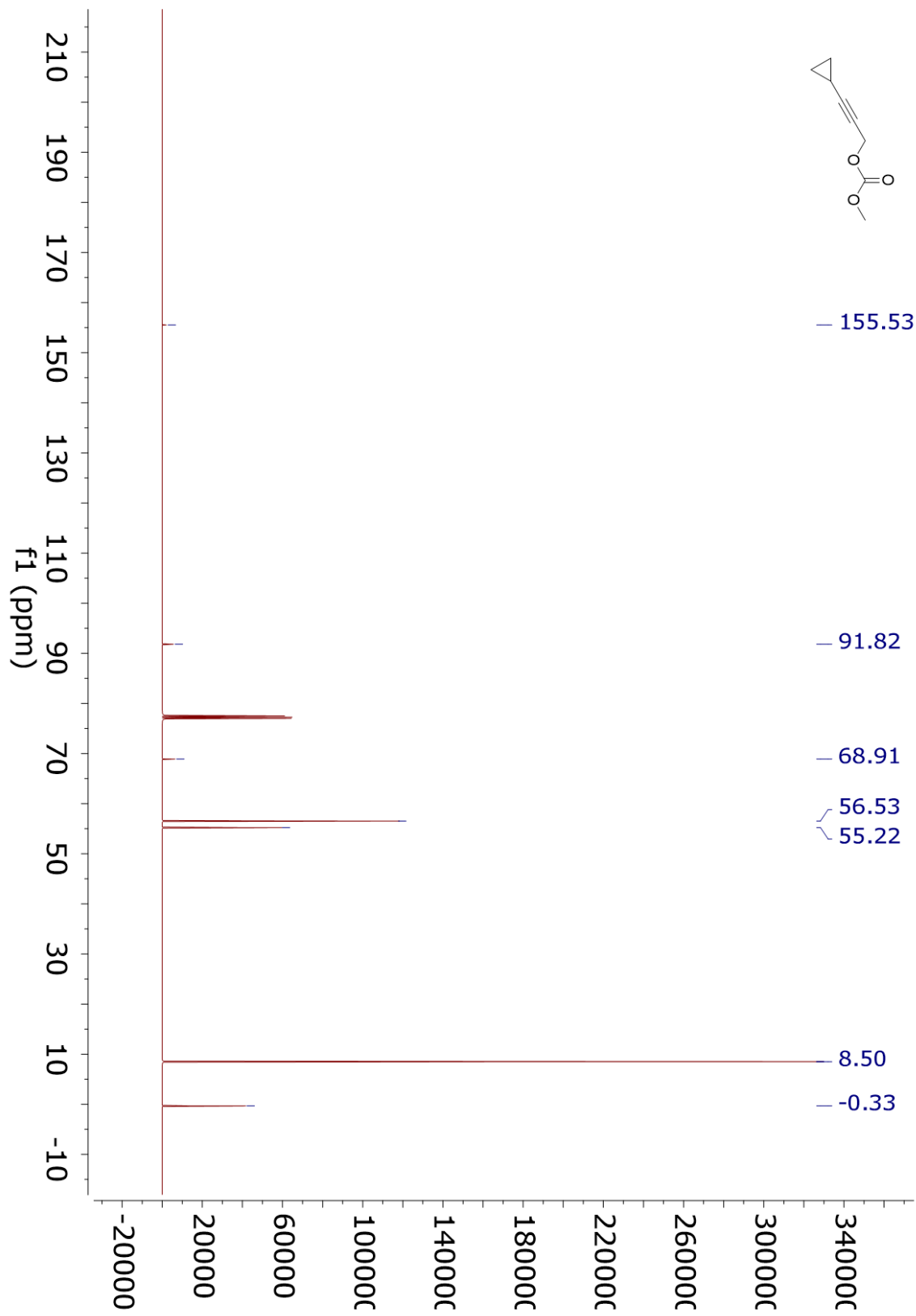
¹³C NMR 4.11h



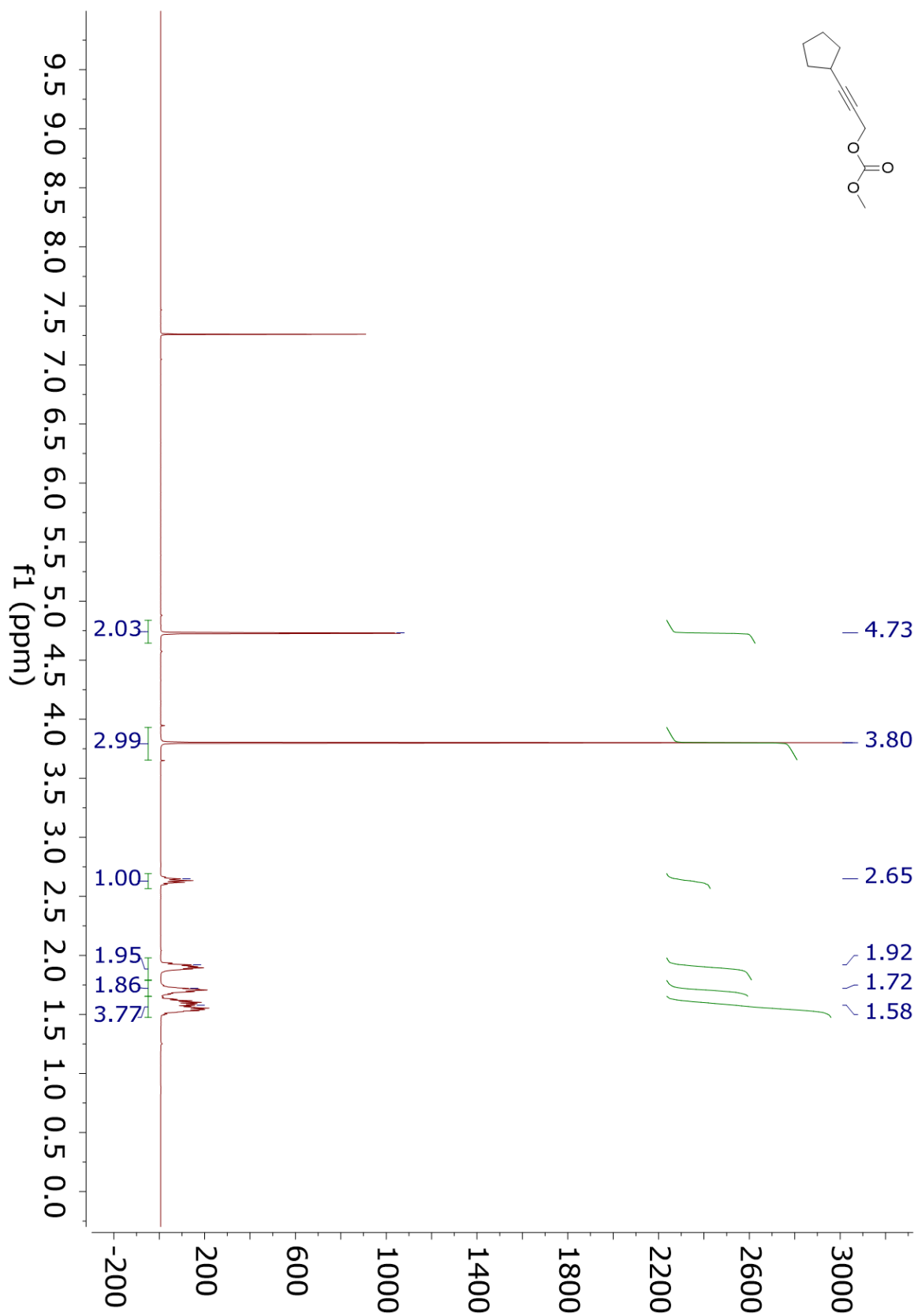
¹H NMR 4.11i



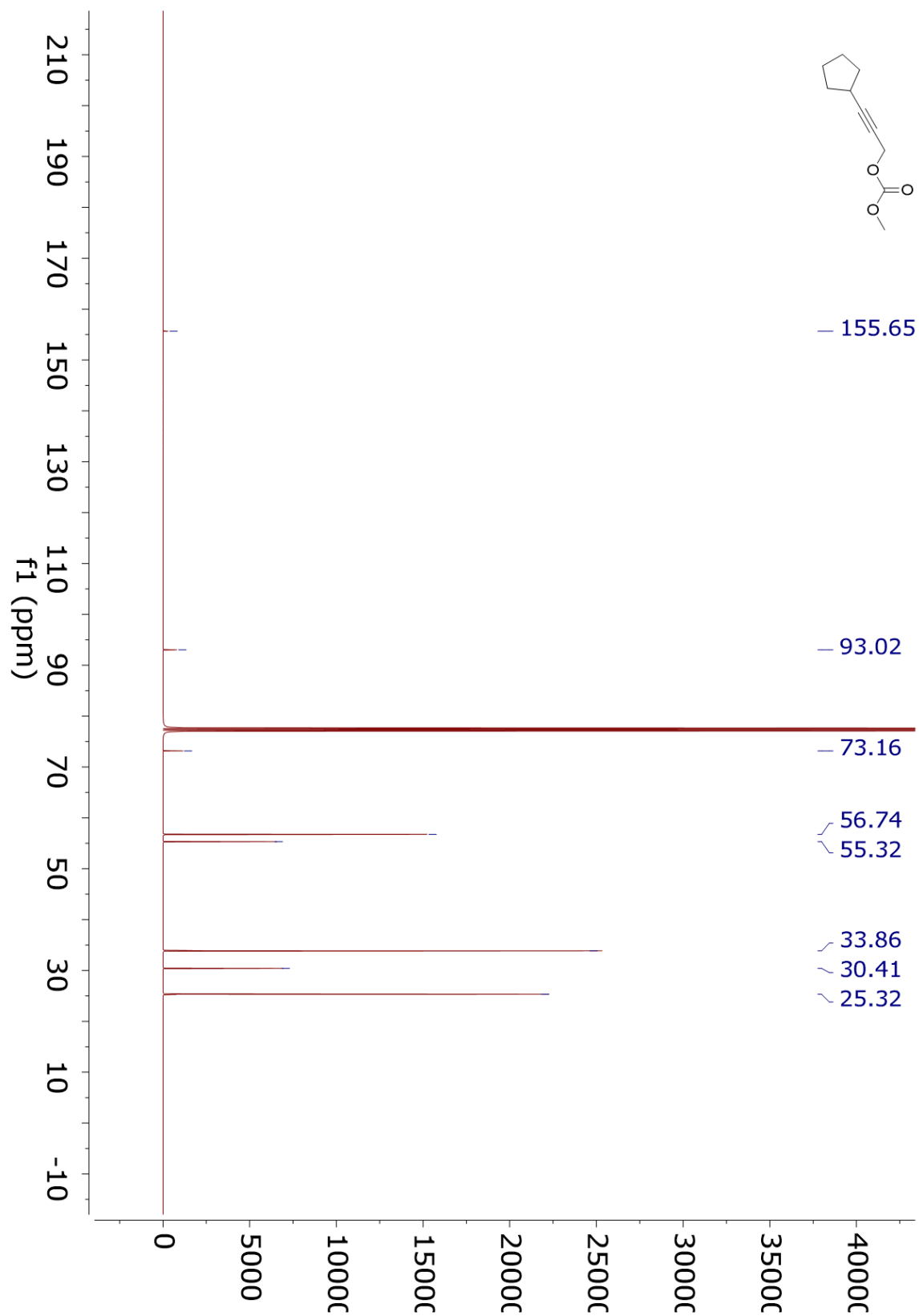
¹³C NMR 4.11i



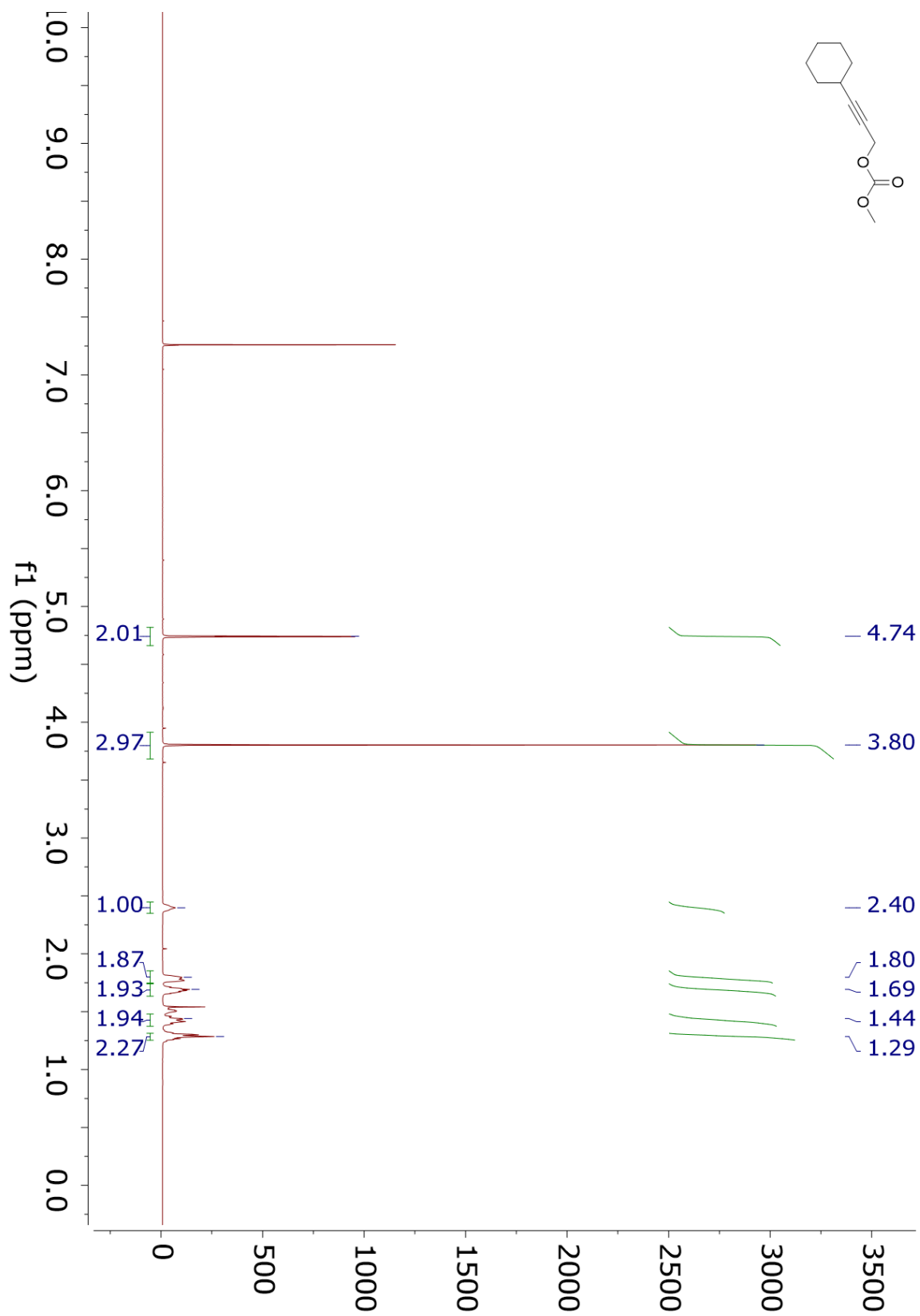
¹H NMR 4.11j



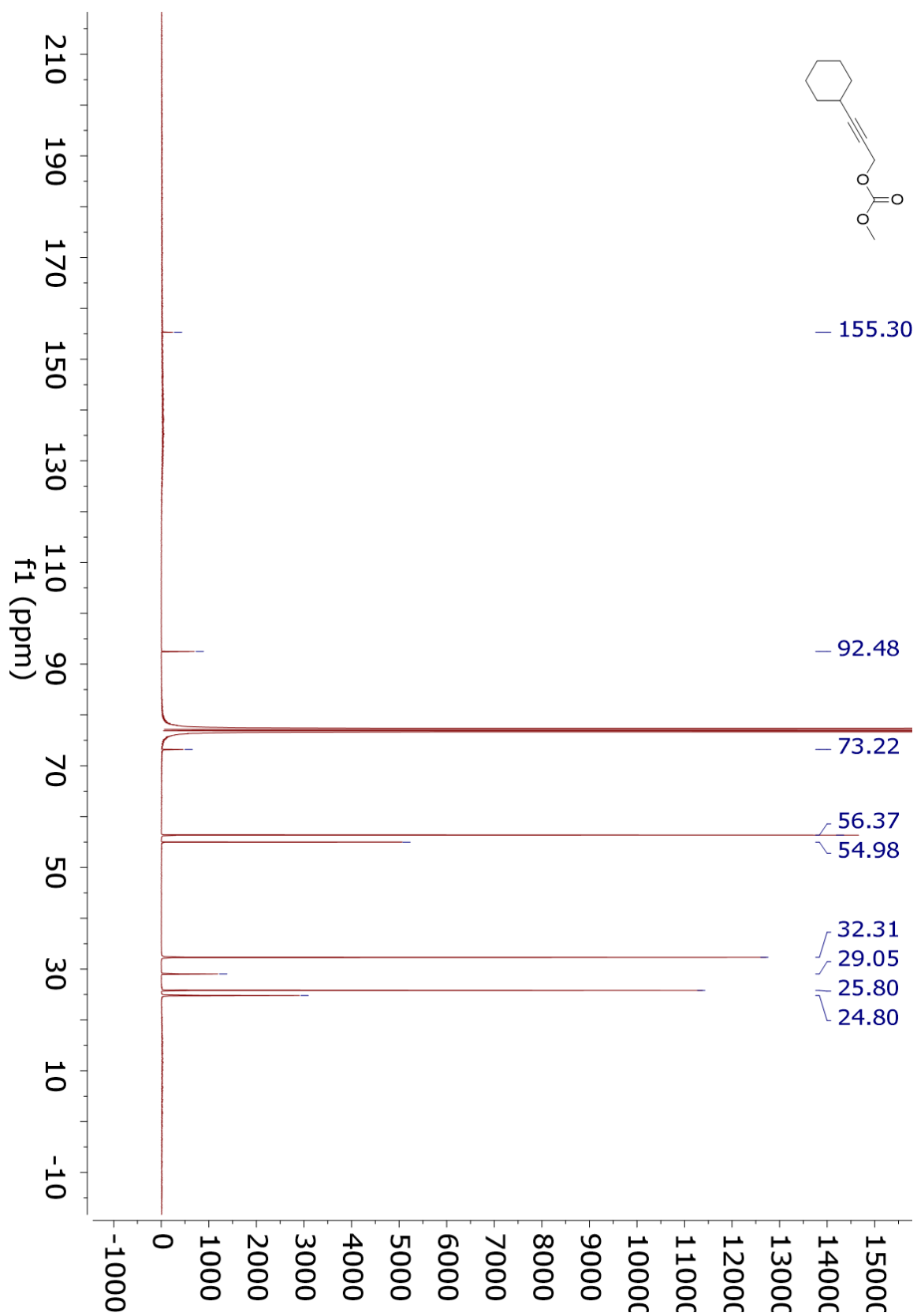
¹³C NMR 4.11j



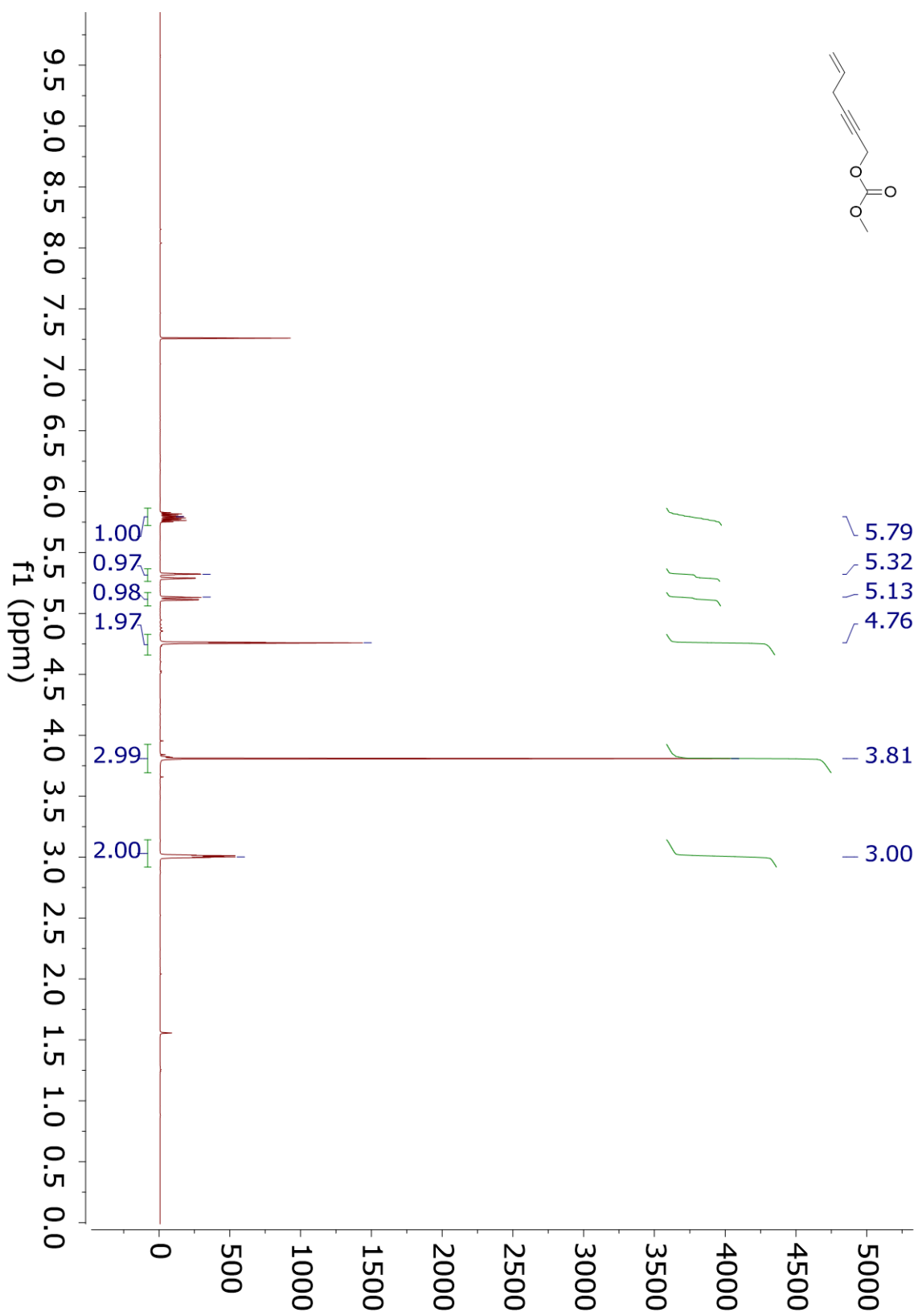
¹H NMR 4.11k



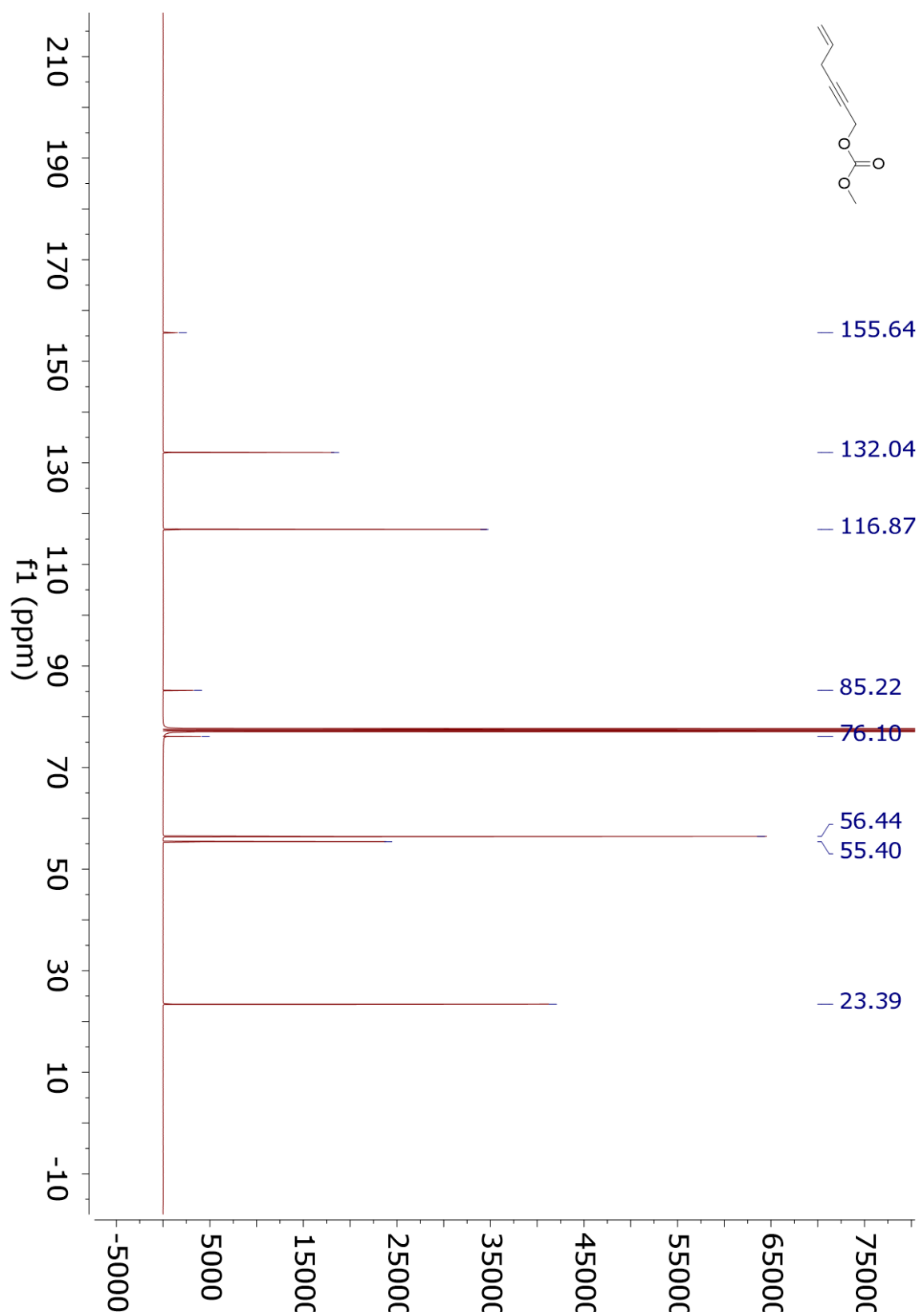
¹³C NMR 4.11k



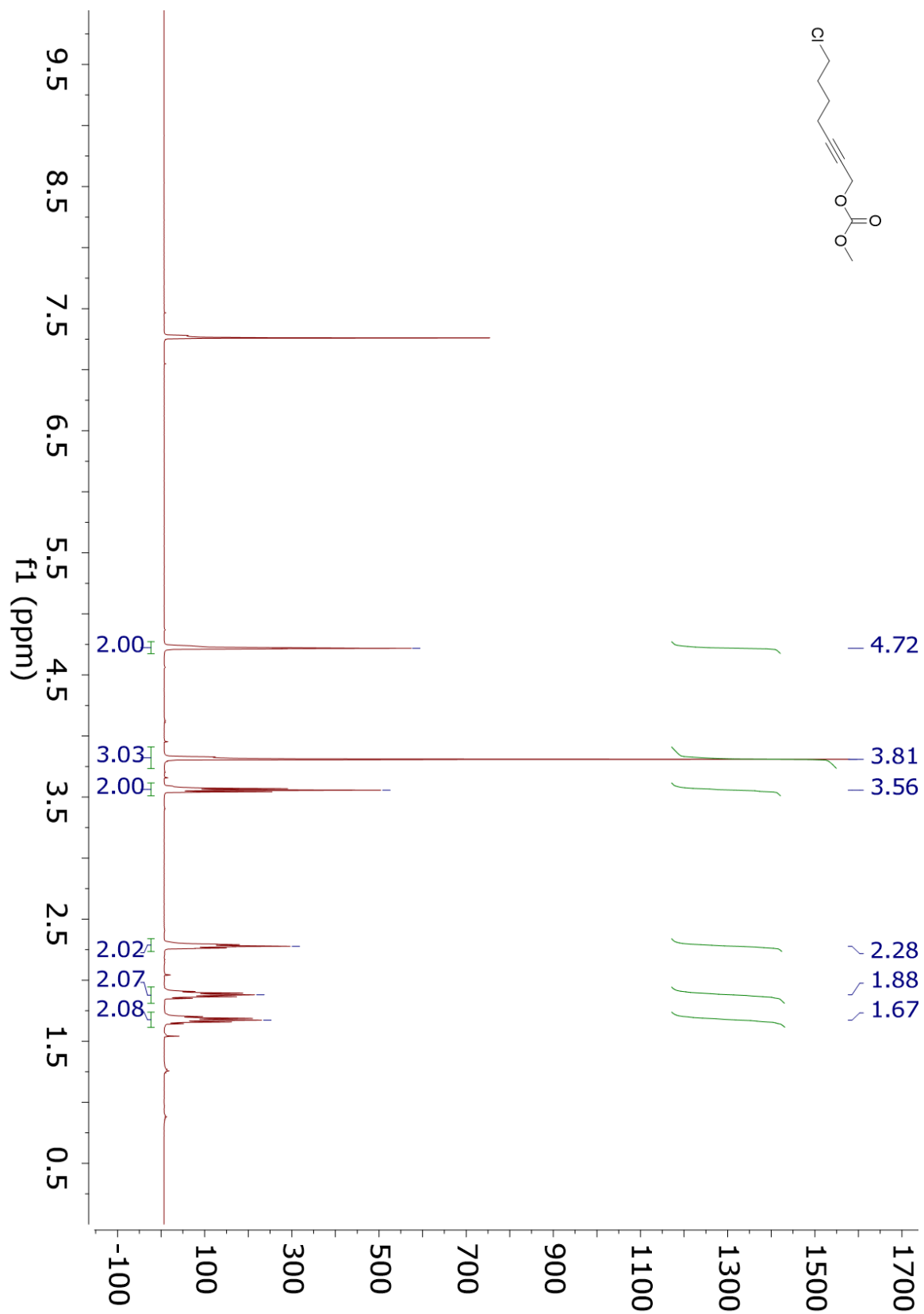
¹H NMR 4.111



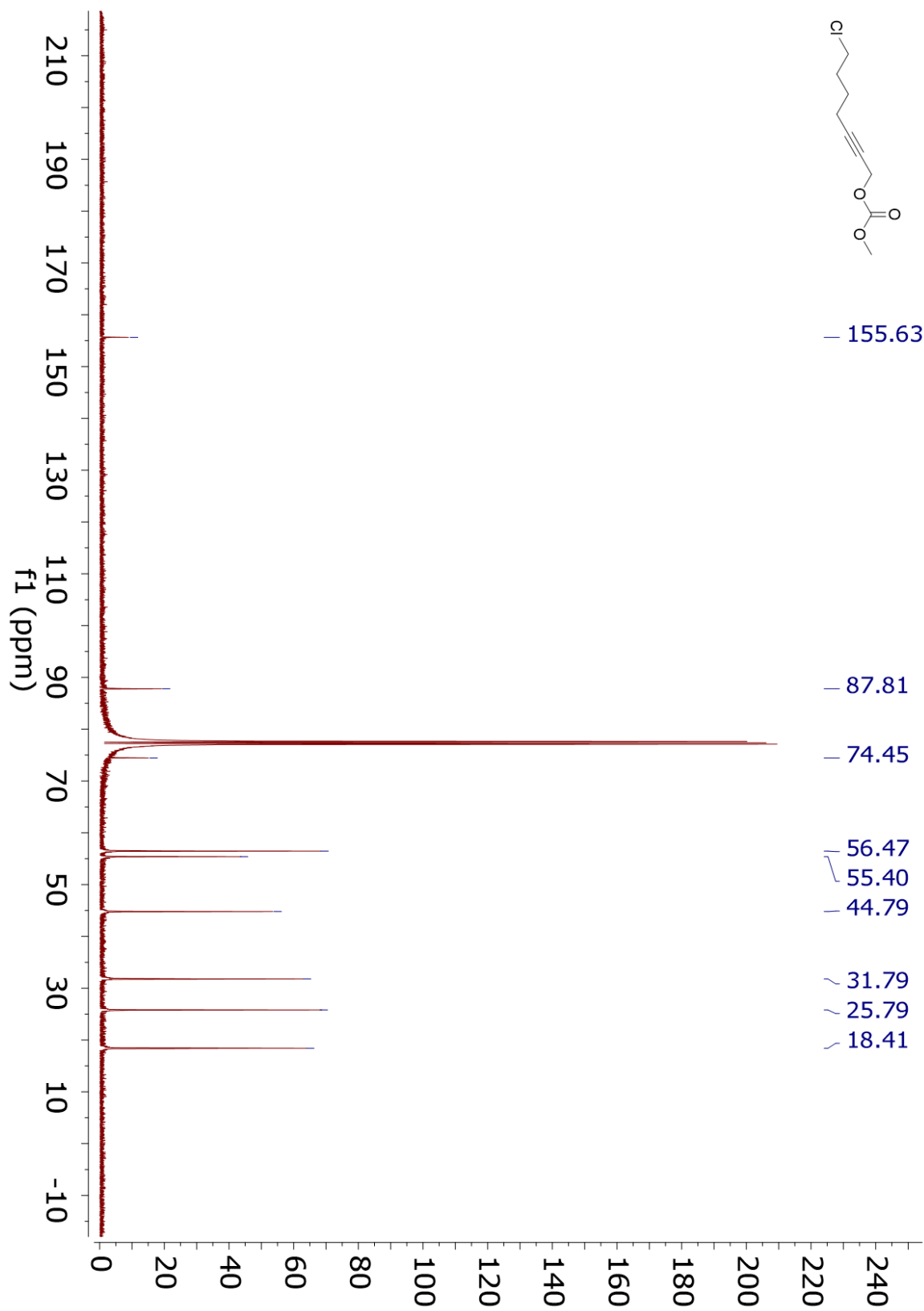
¹³C NMR 4.111



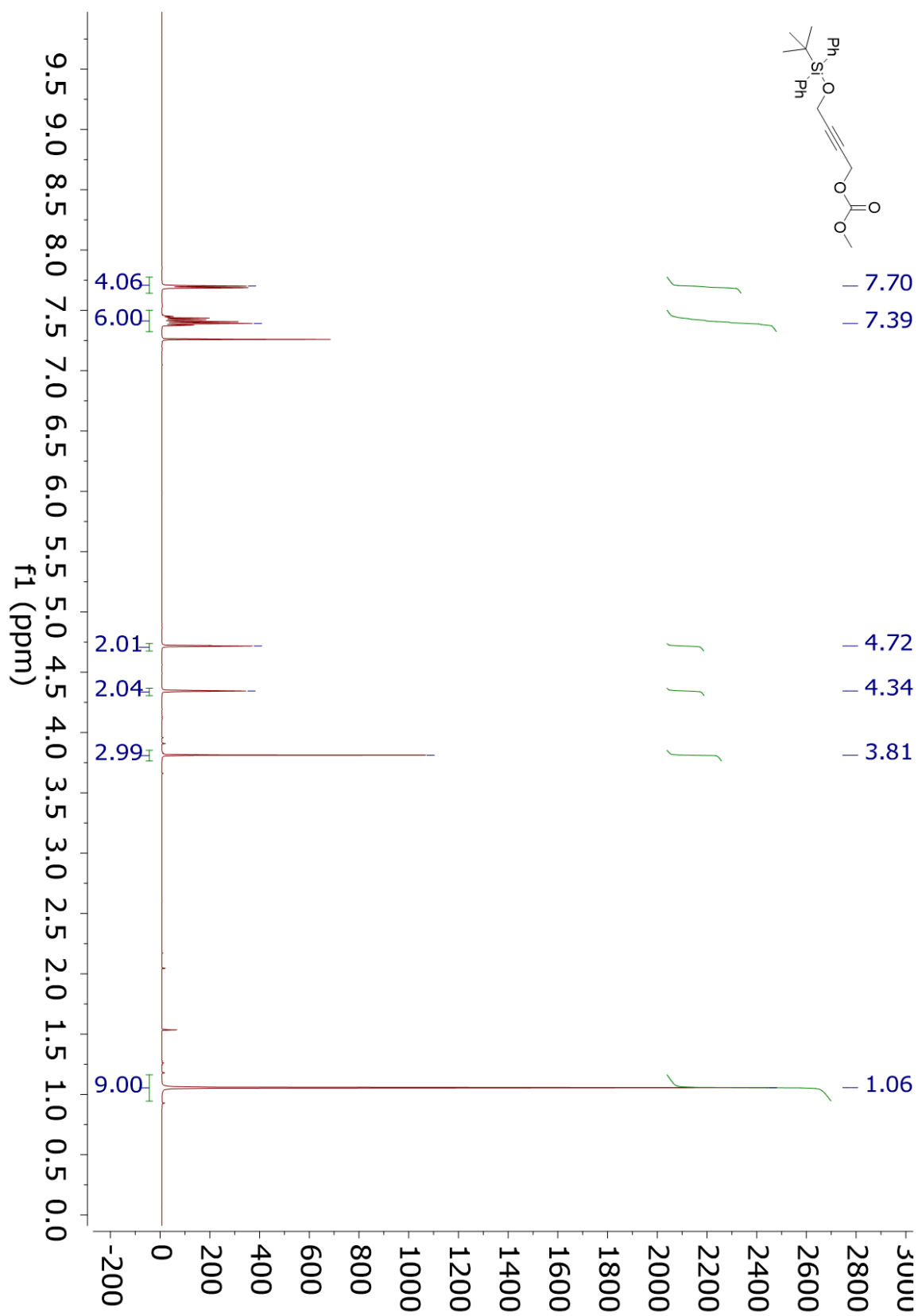
¹H NMR 4.11m



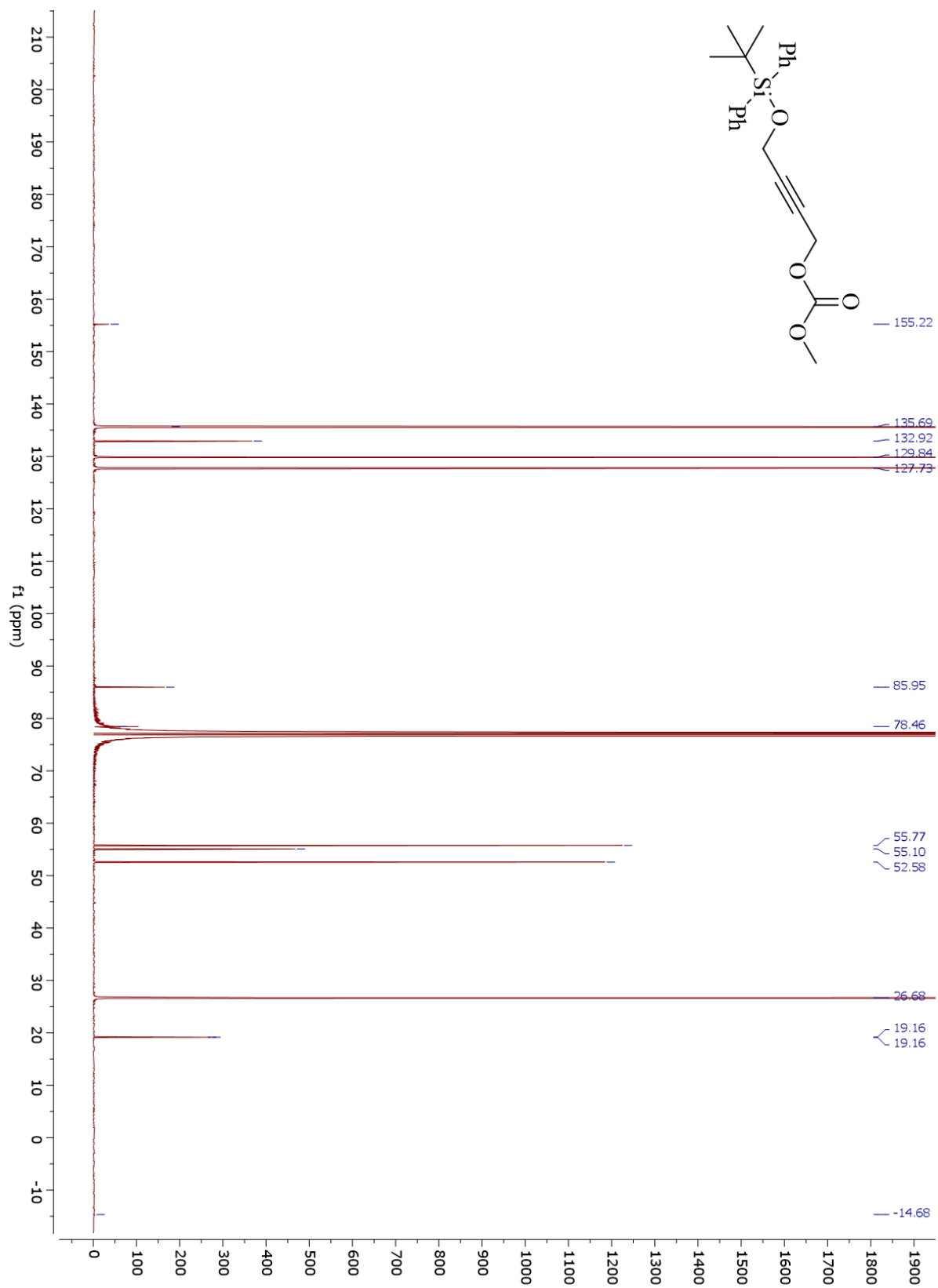
¹³C NMR 4.11m



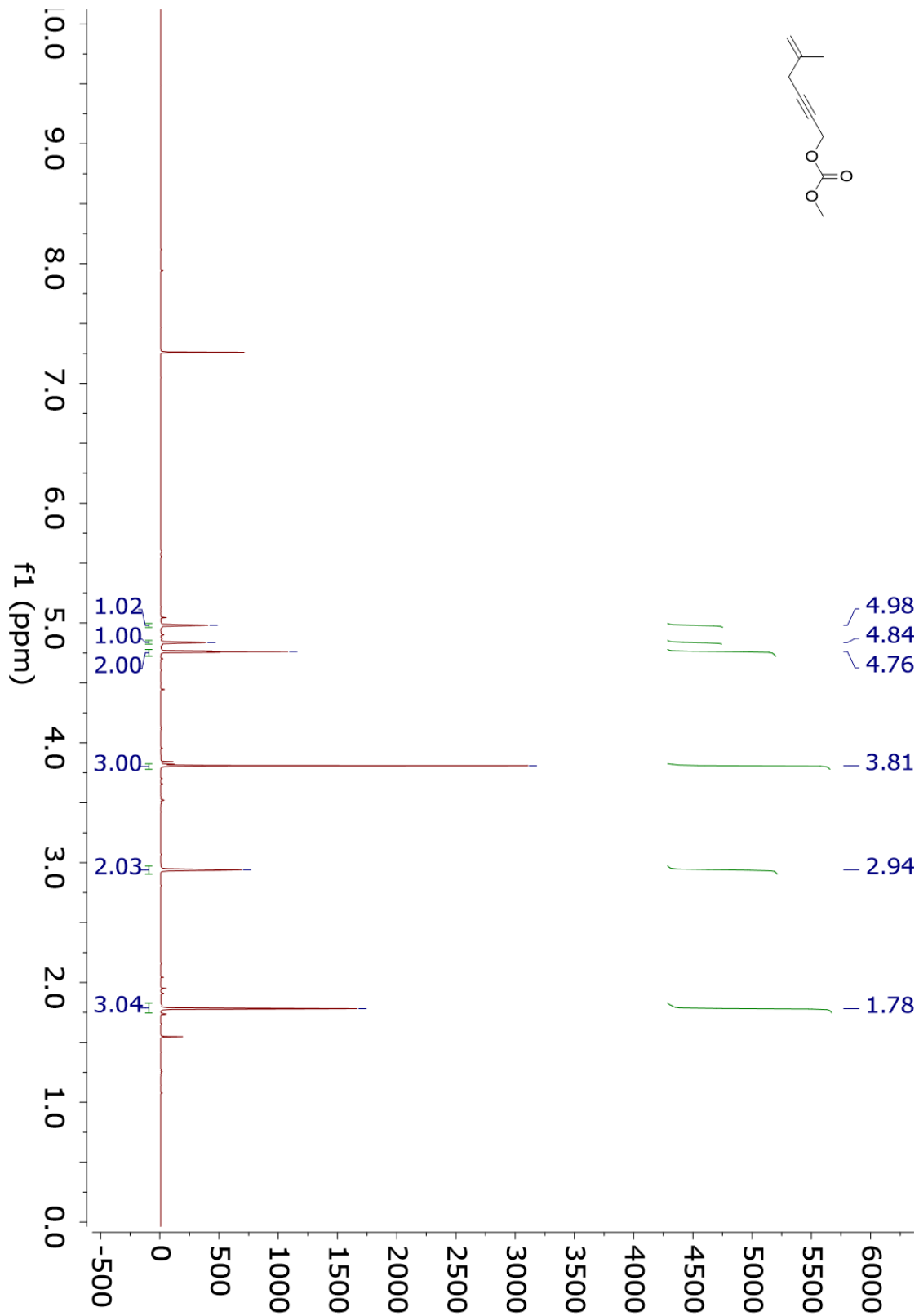
¹H NMR 4.11n



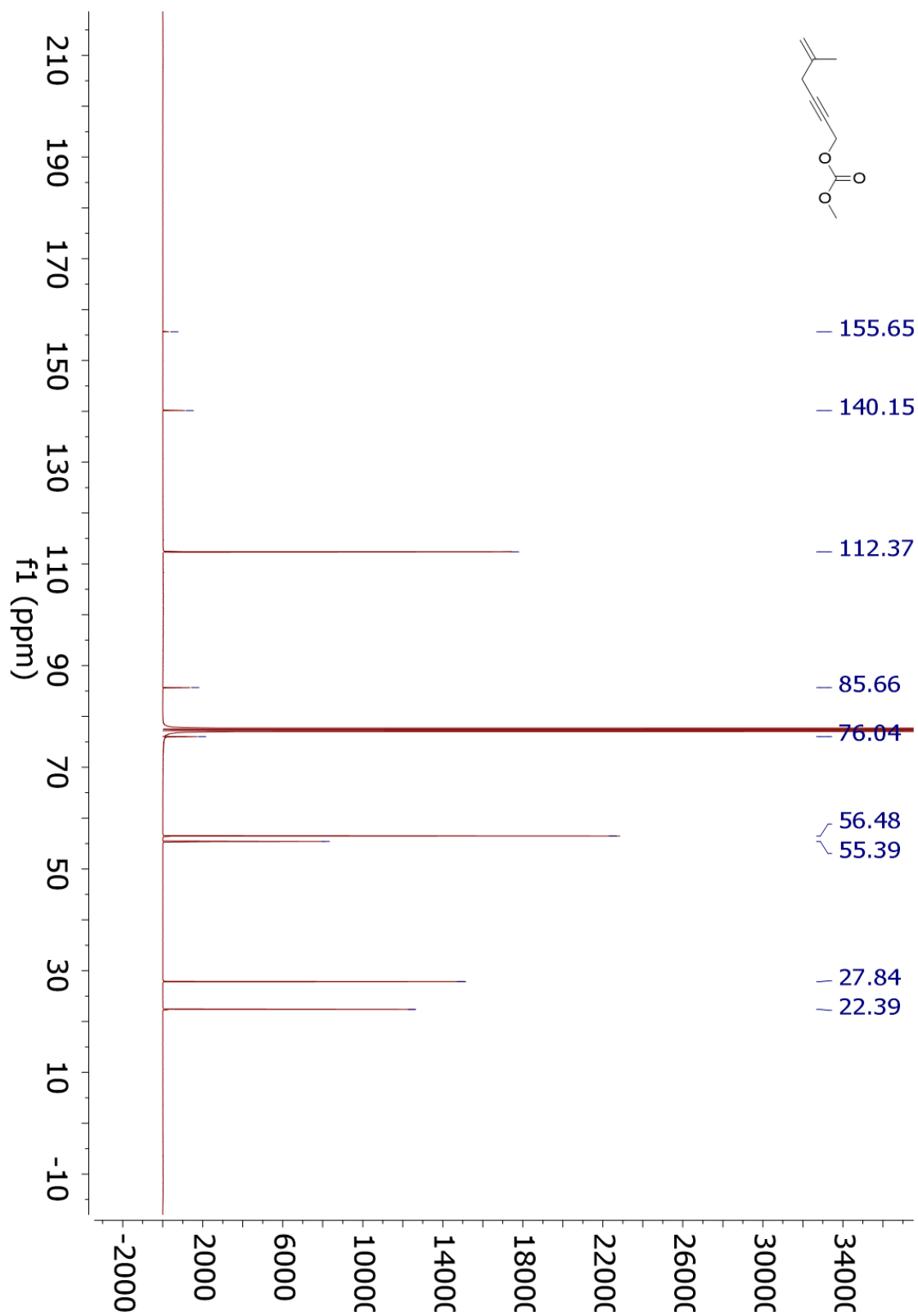
¹³C NMR 4.11n



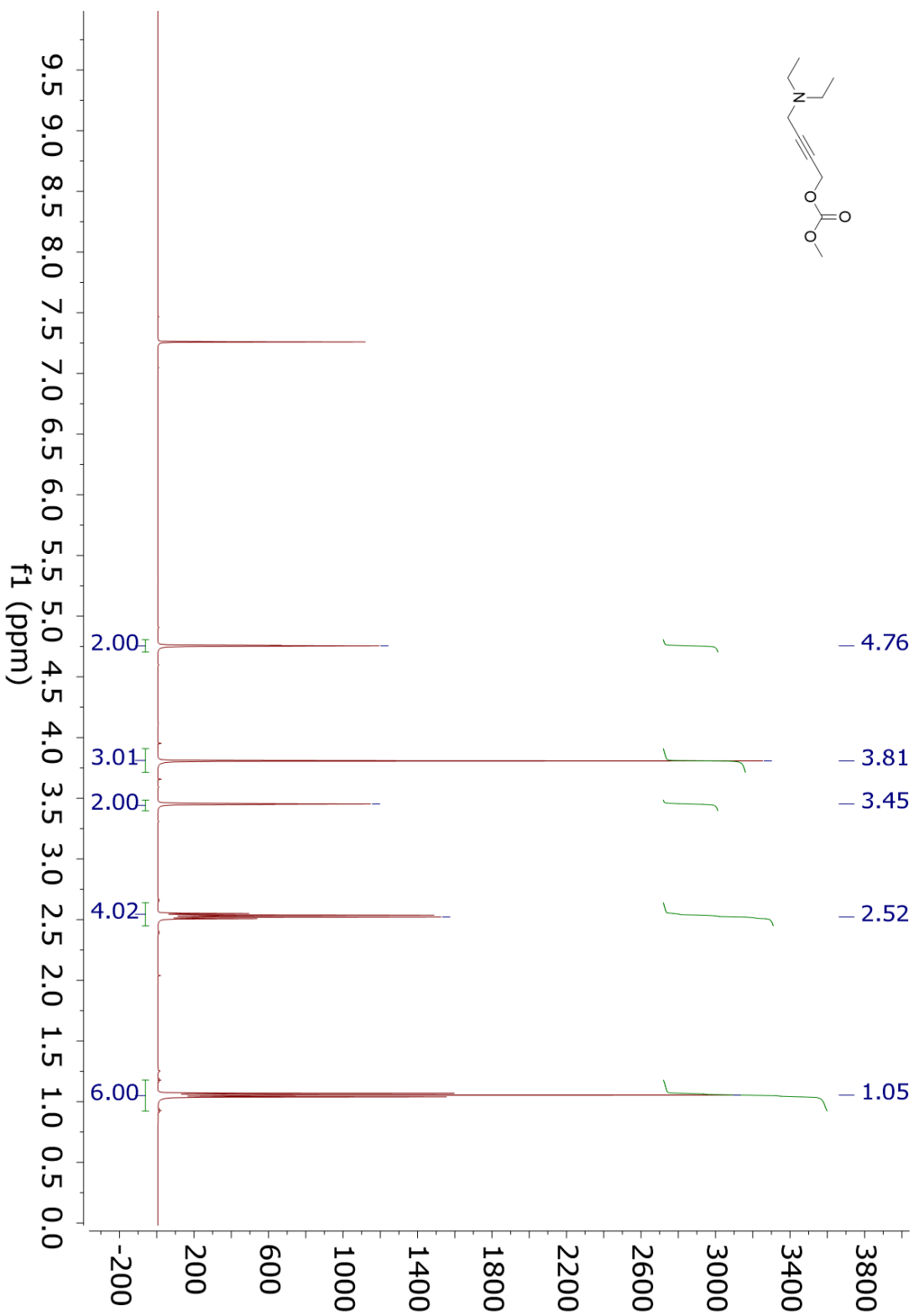
¹H NMR 4.11o



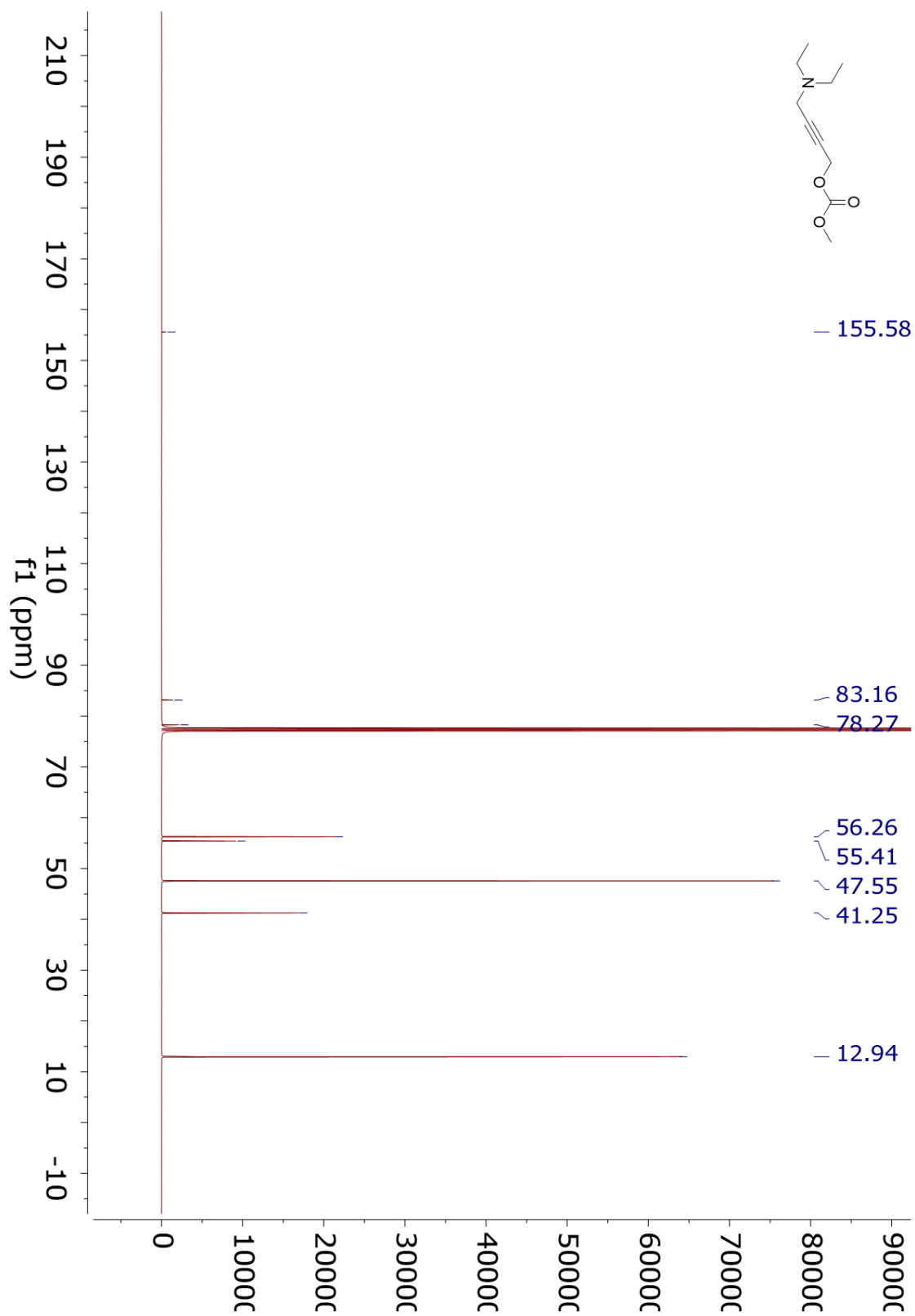
¹³C NMR 4.11o



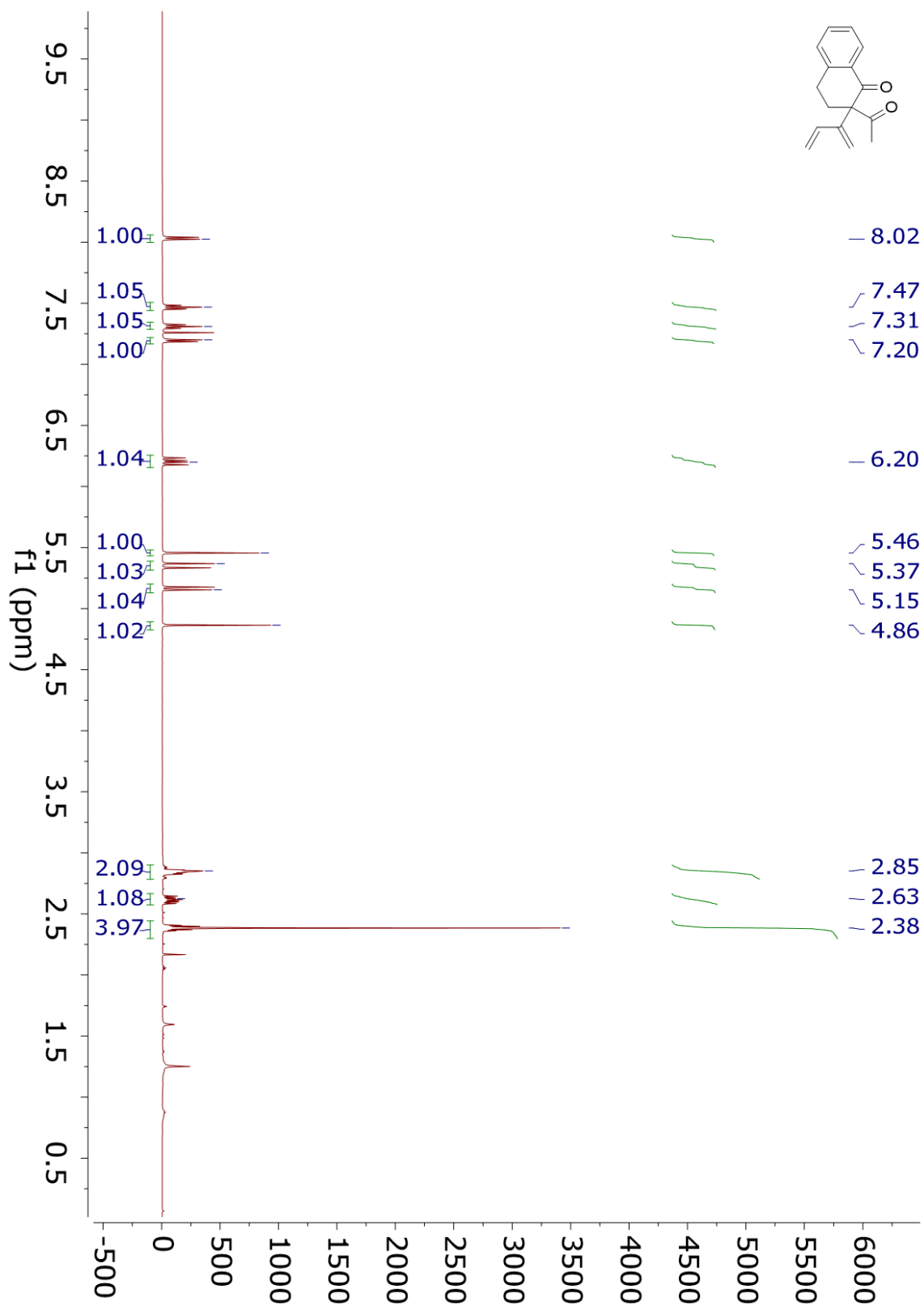
¹H NMR 4.11p



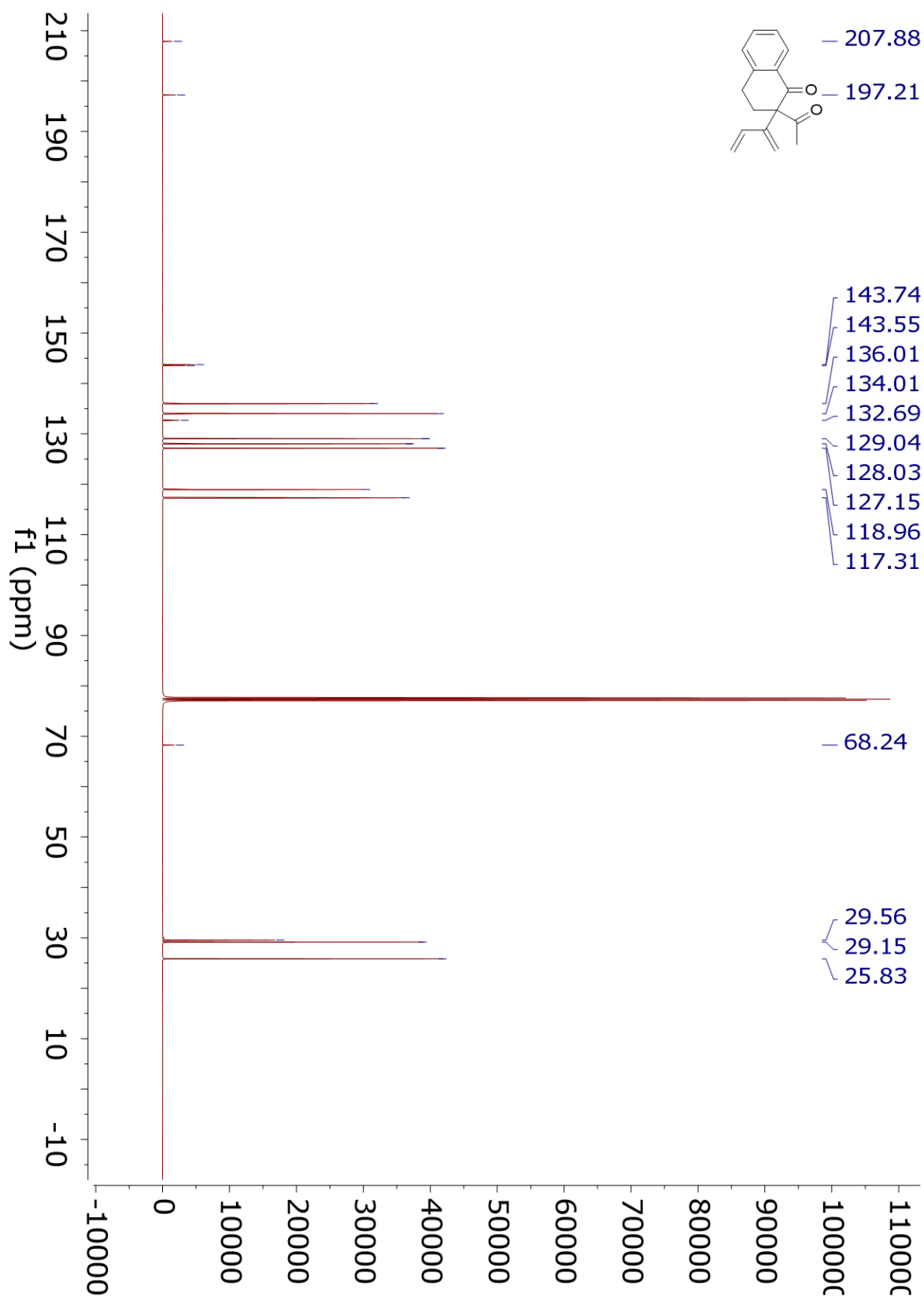
¹³C NMR 4.11p



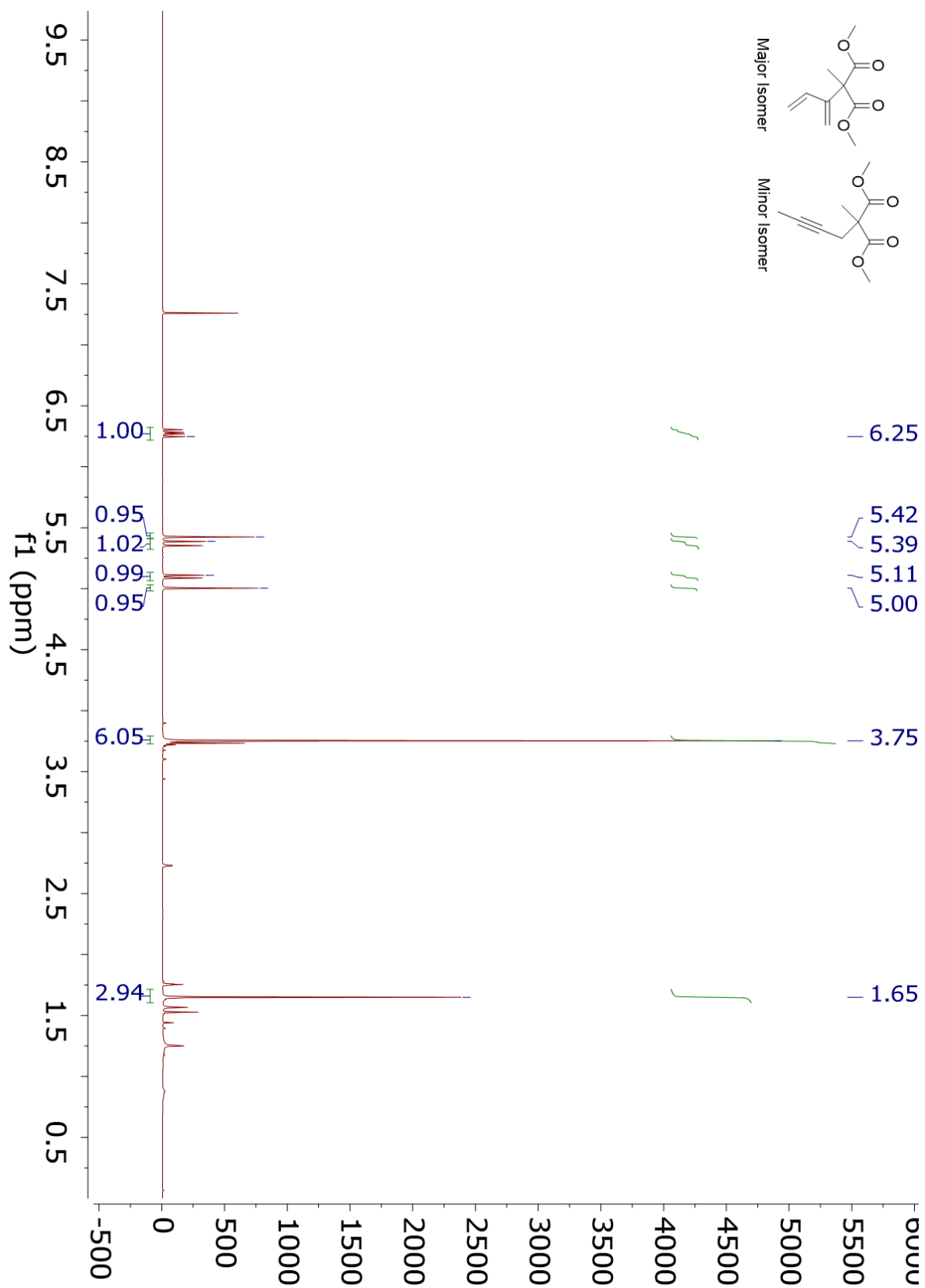
¹H NMR 4.12a



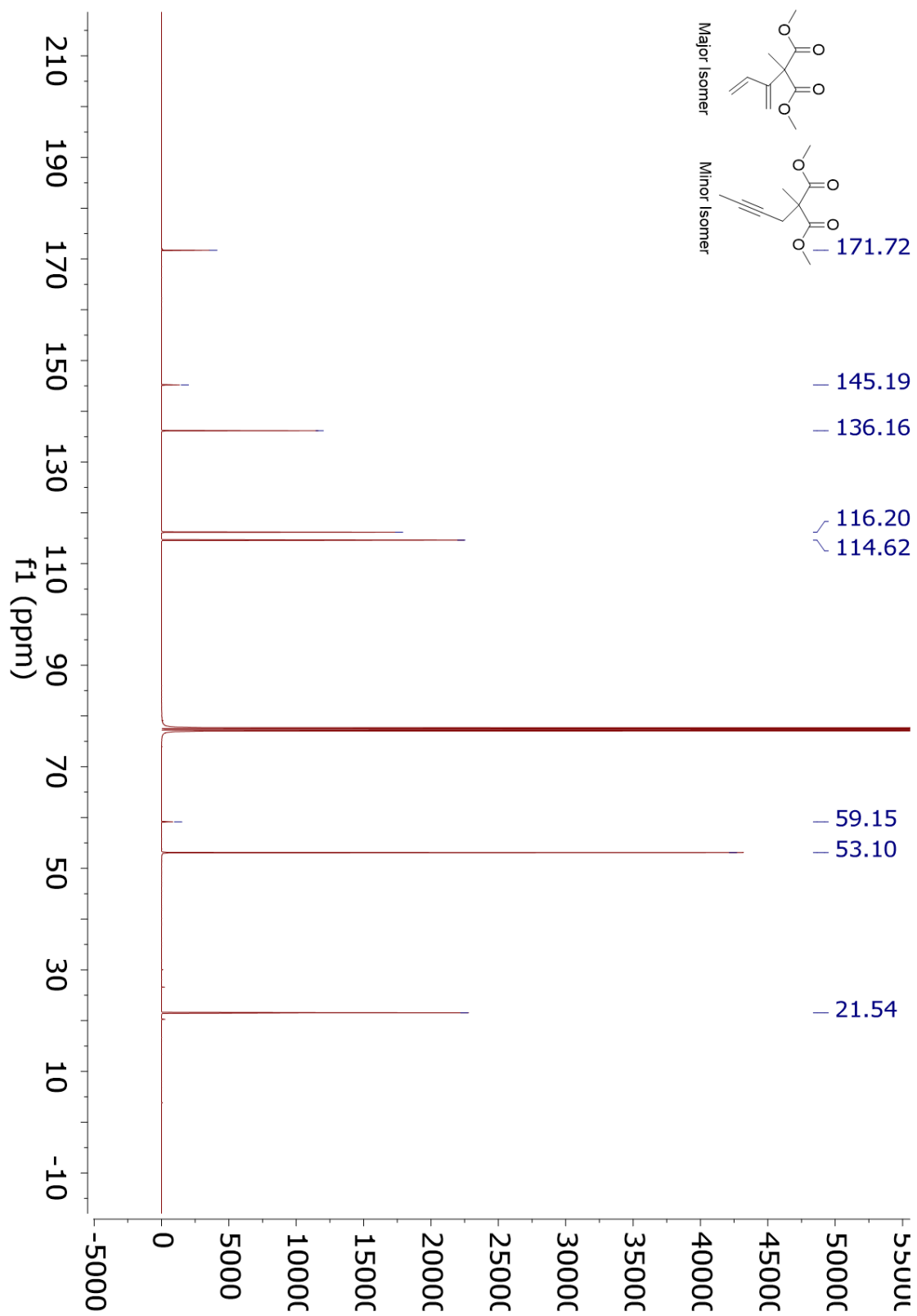
¹³C NMR 4.12a



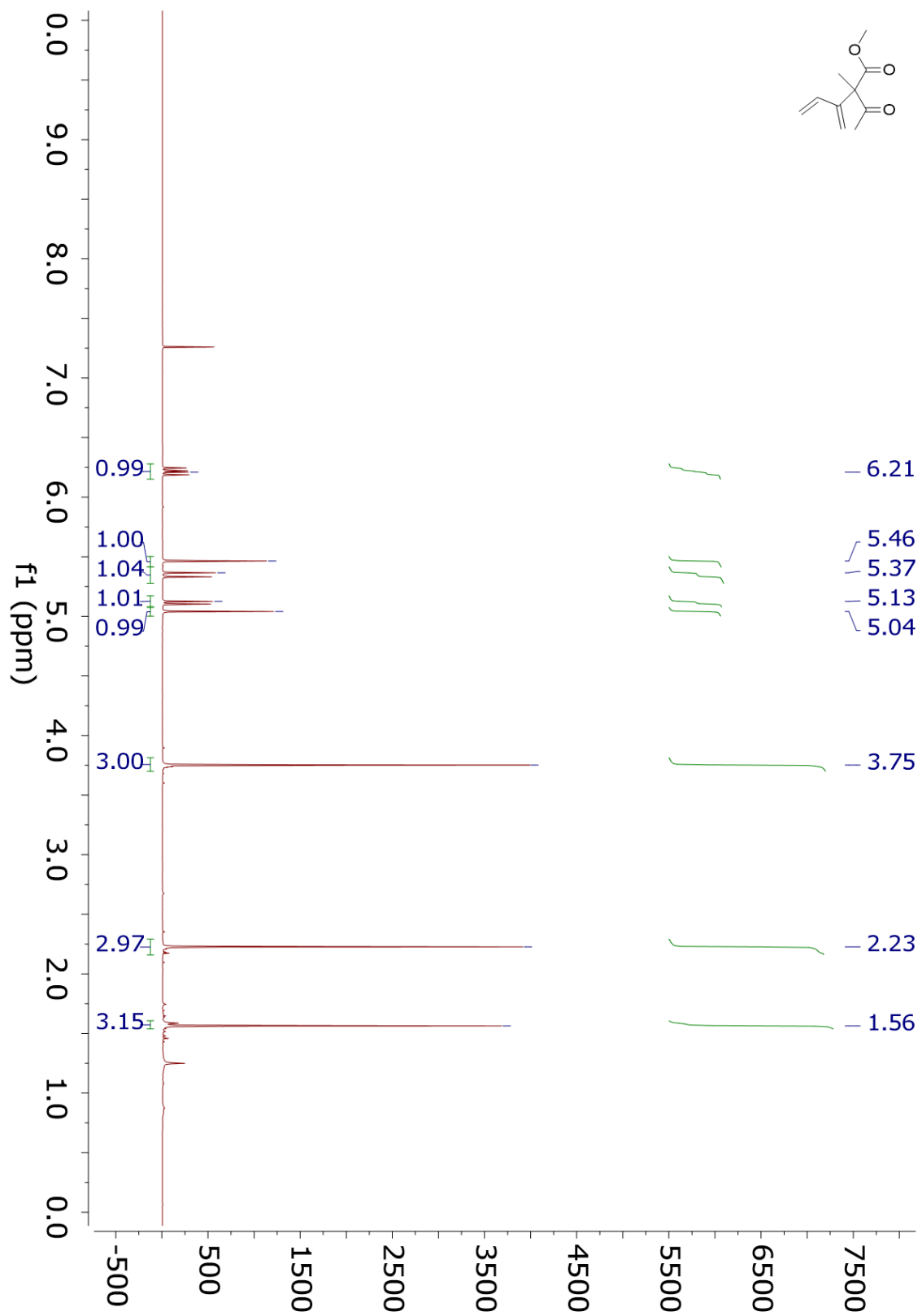
¹H NMR 4.12b



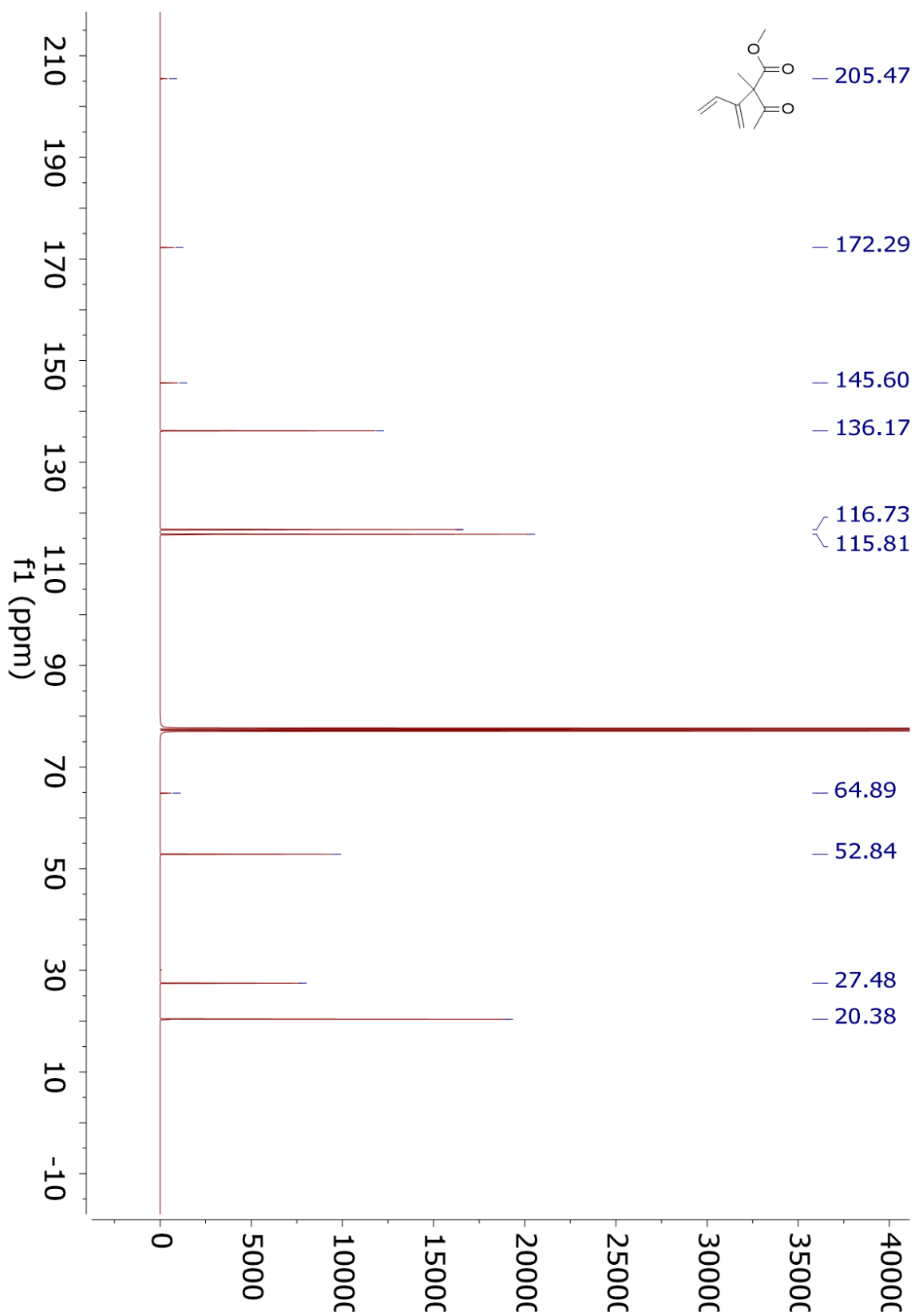
¹³C NMR 4.12b



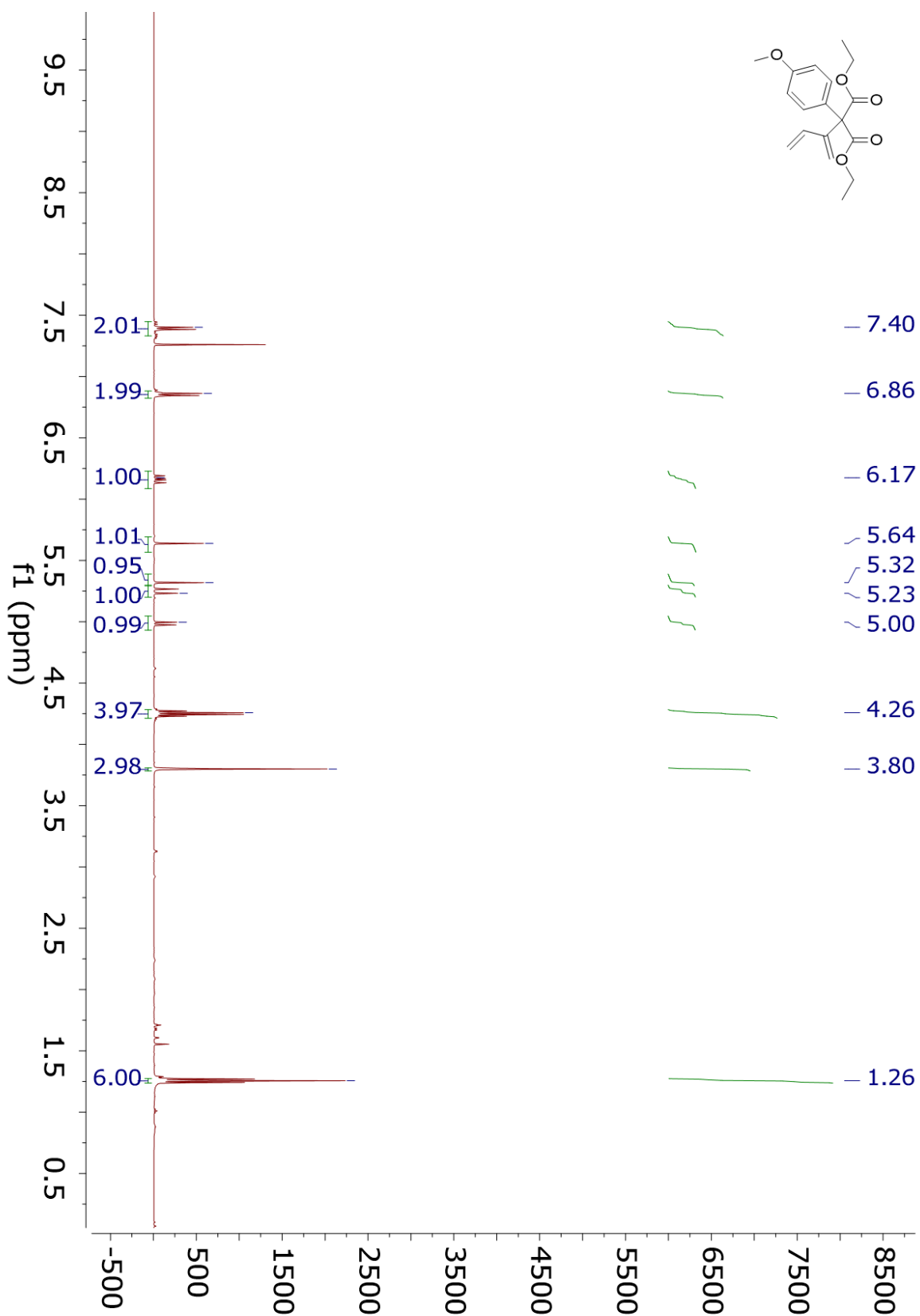
¹H NMR 4.12c



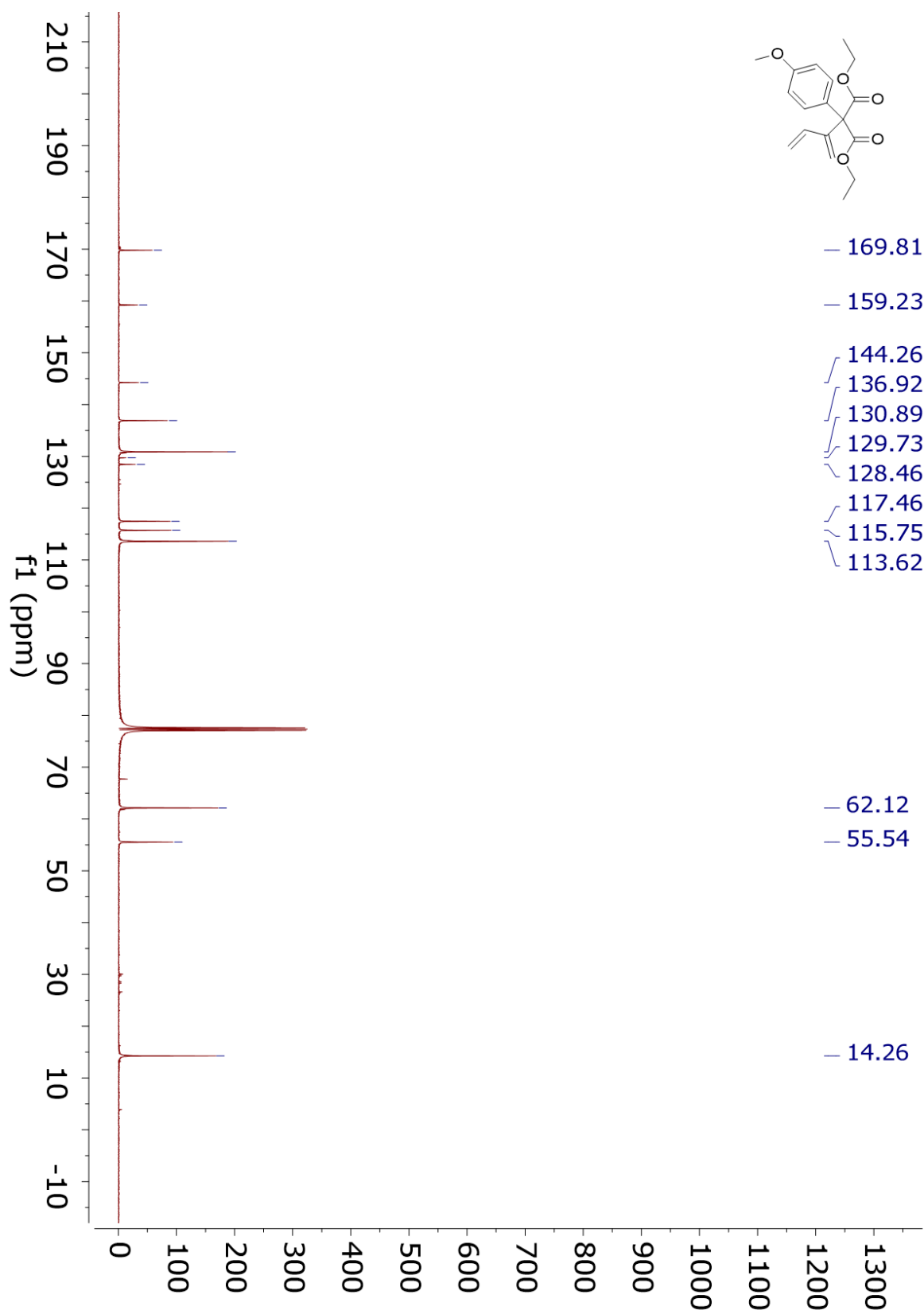
¹³C NMR 4.12c



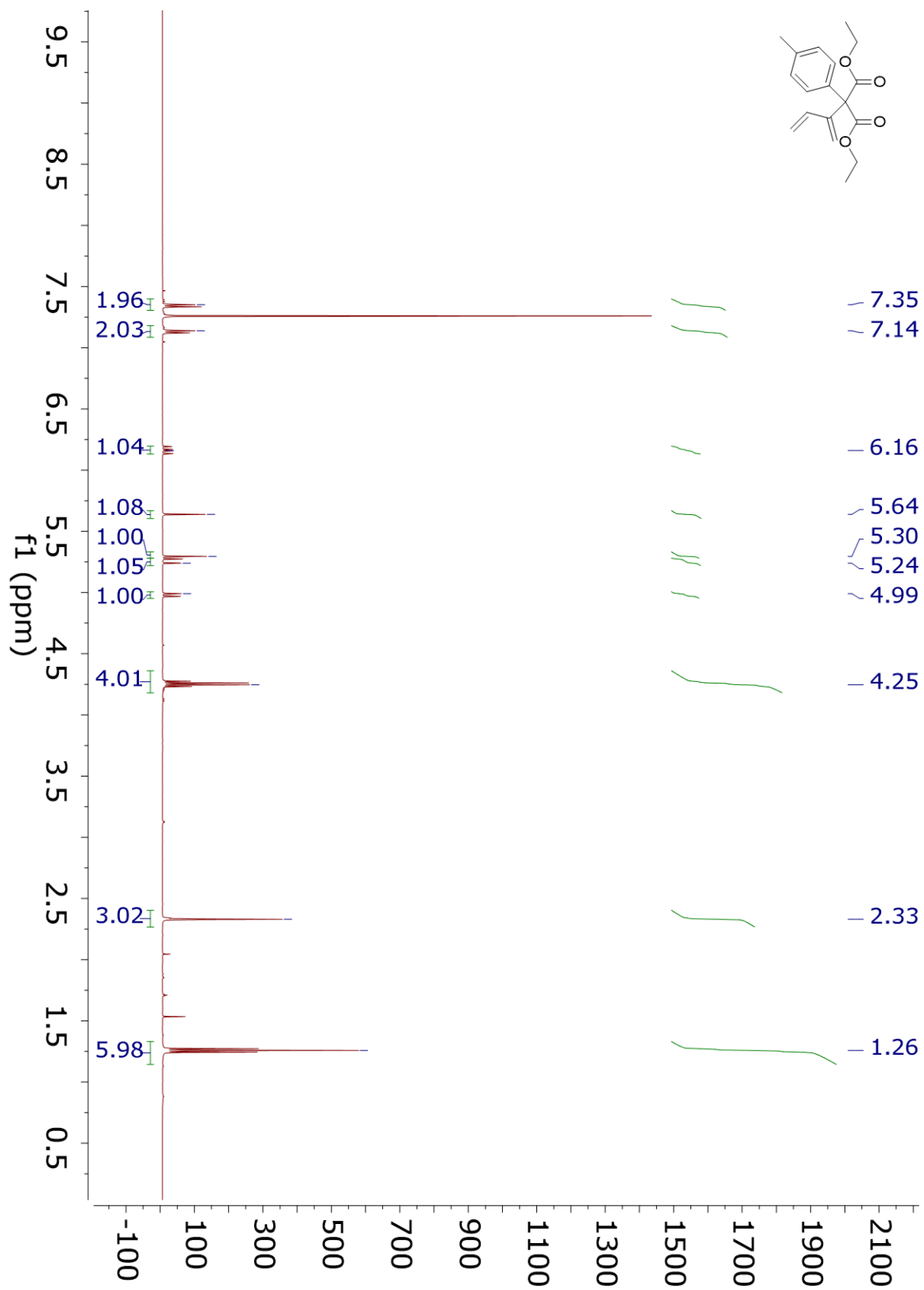
¹H NMR 4.12d



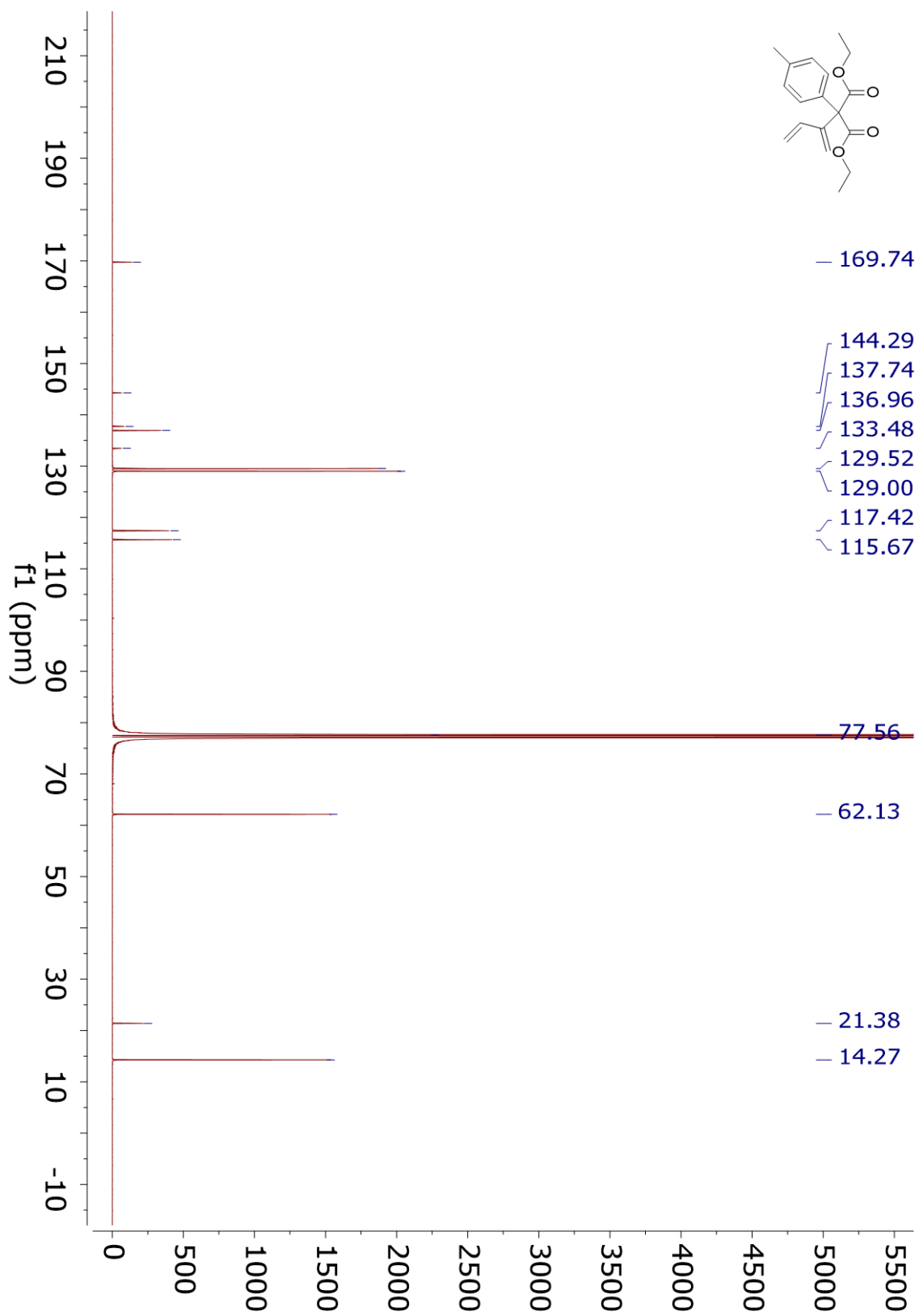
¹³C NMR 4.12d



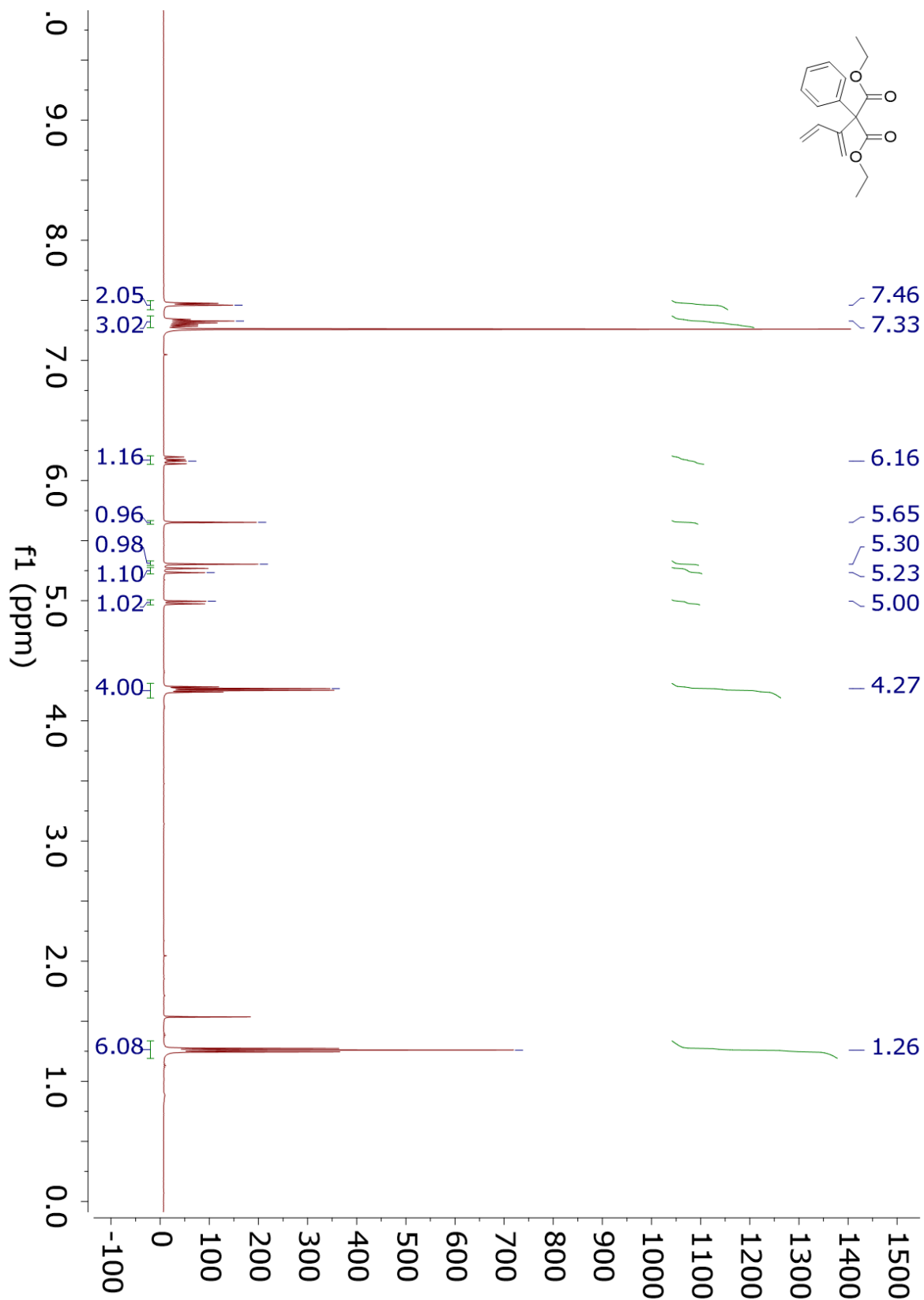
¹H NMR 4.12e



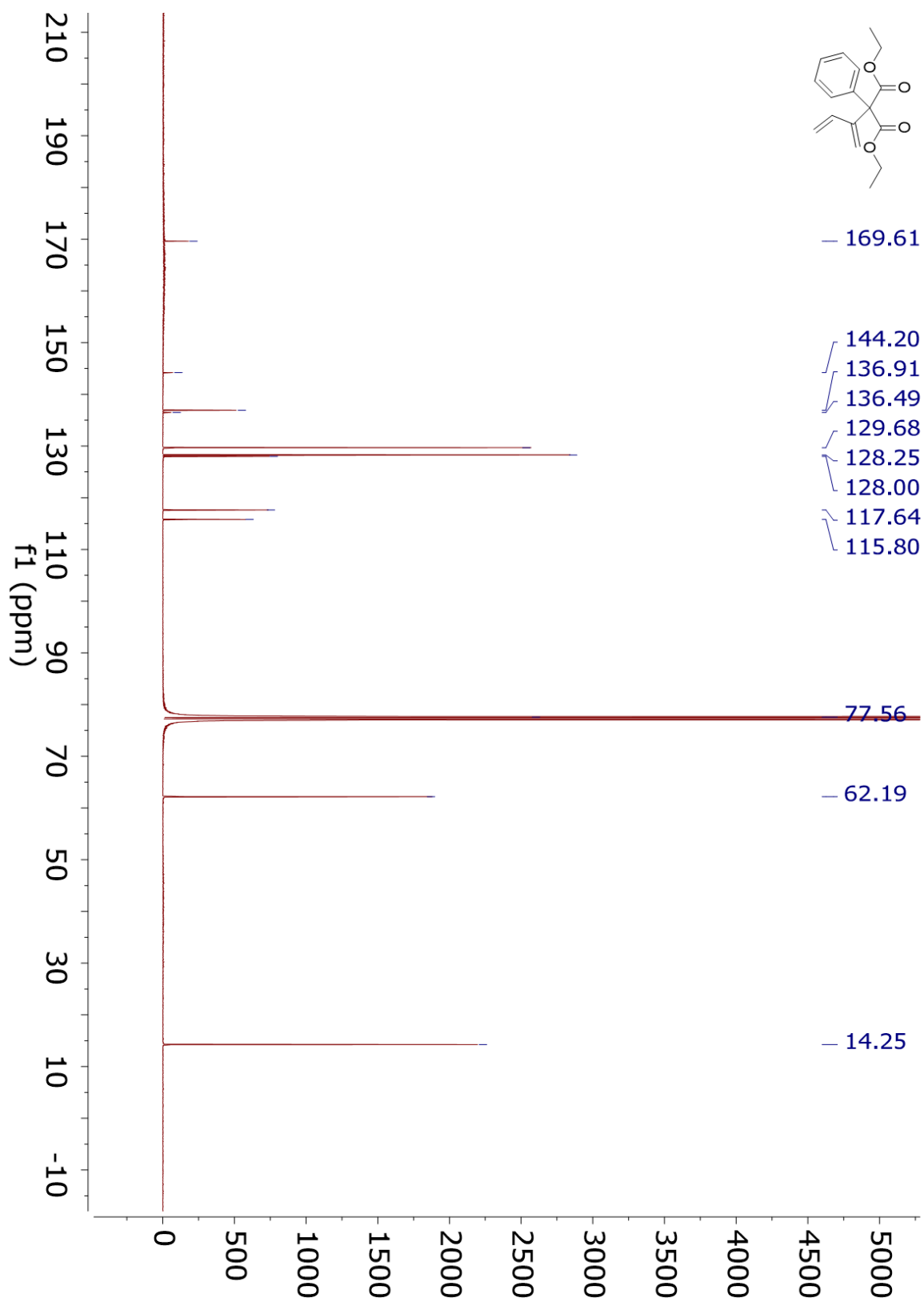
¹³C NMR 4.12e



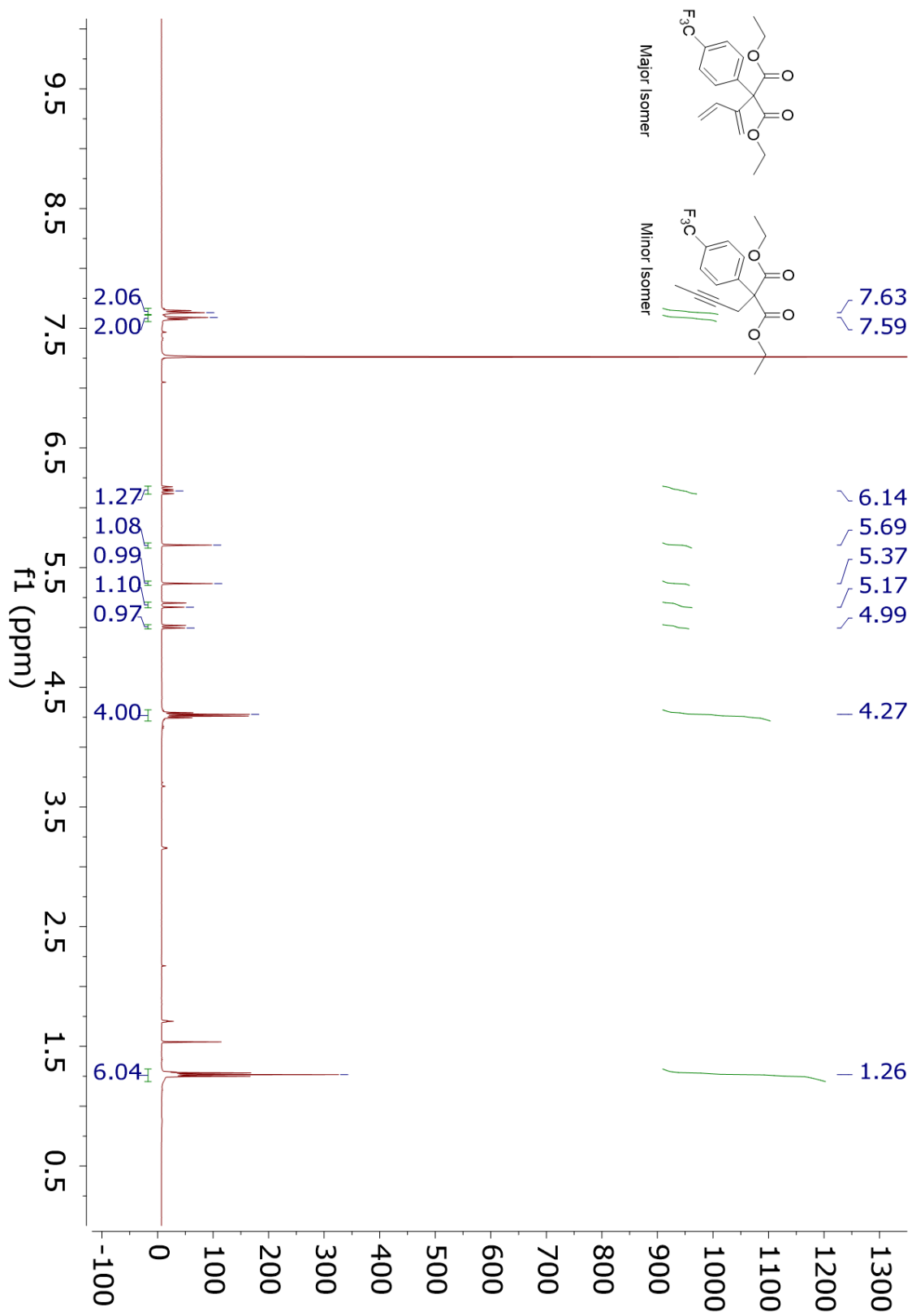
¹H NMR 4.12f



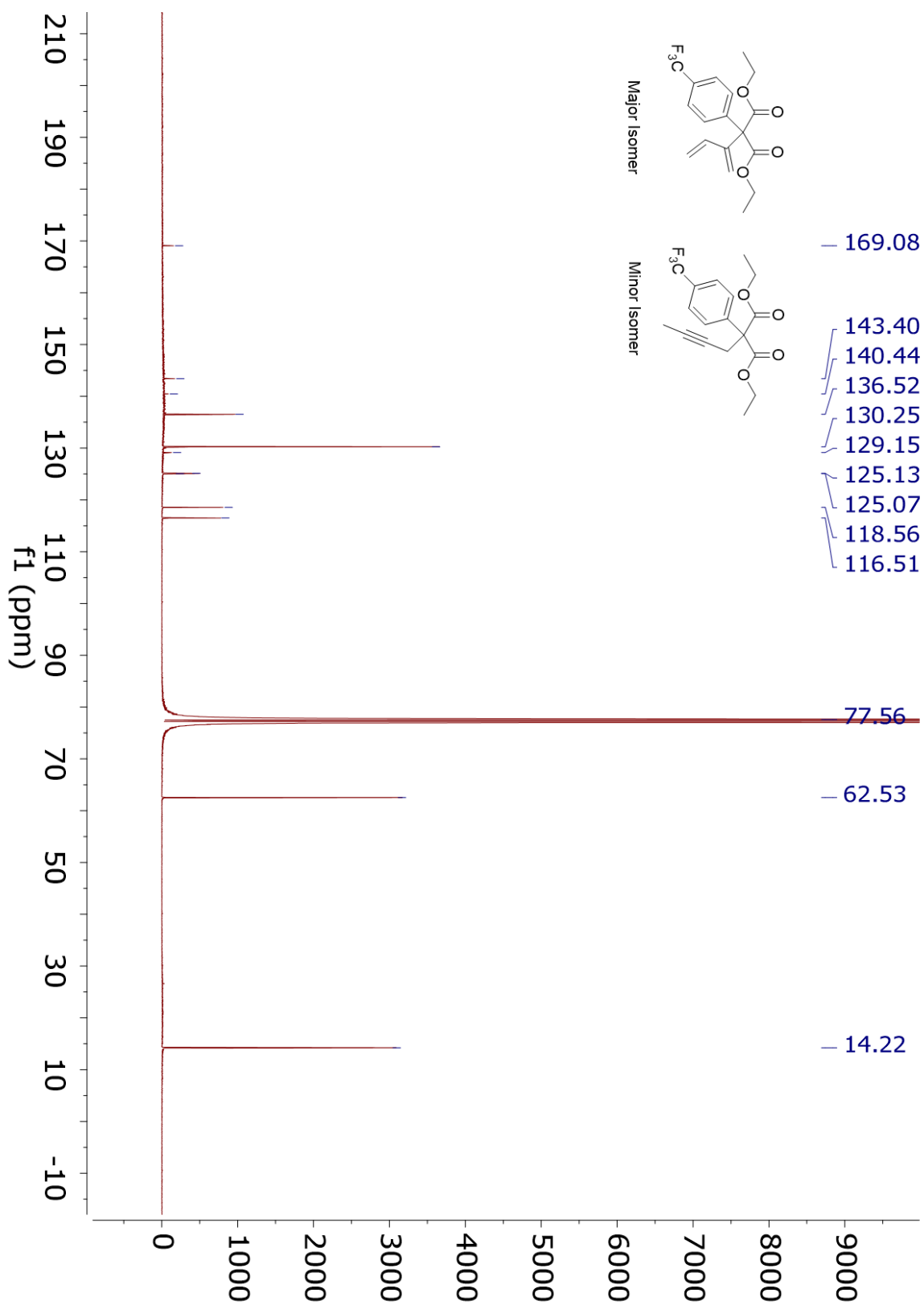
¹³C NMR 4.12f



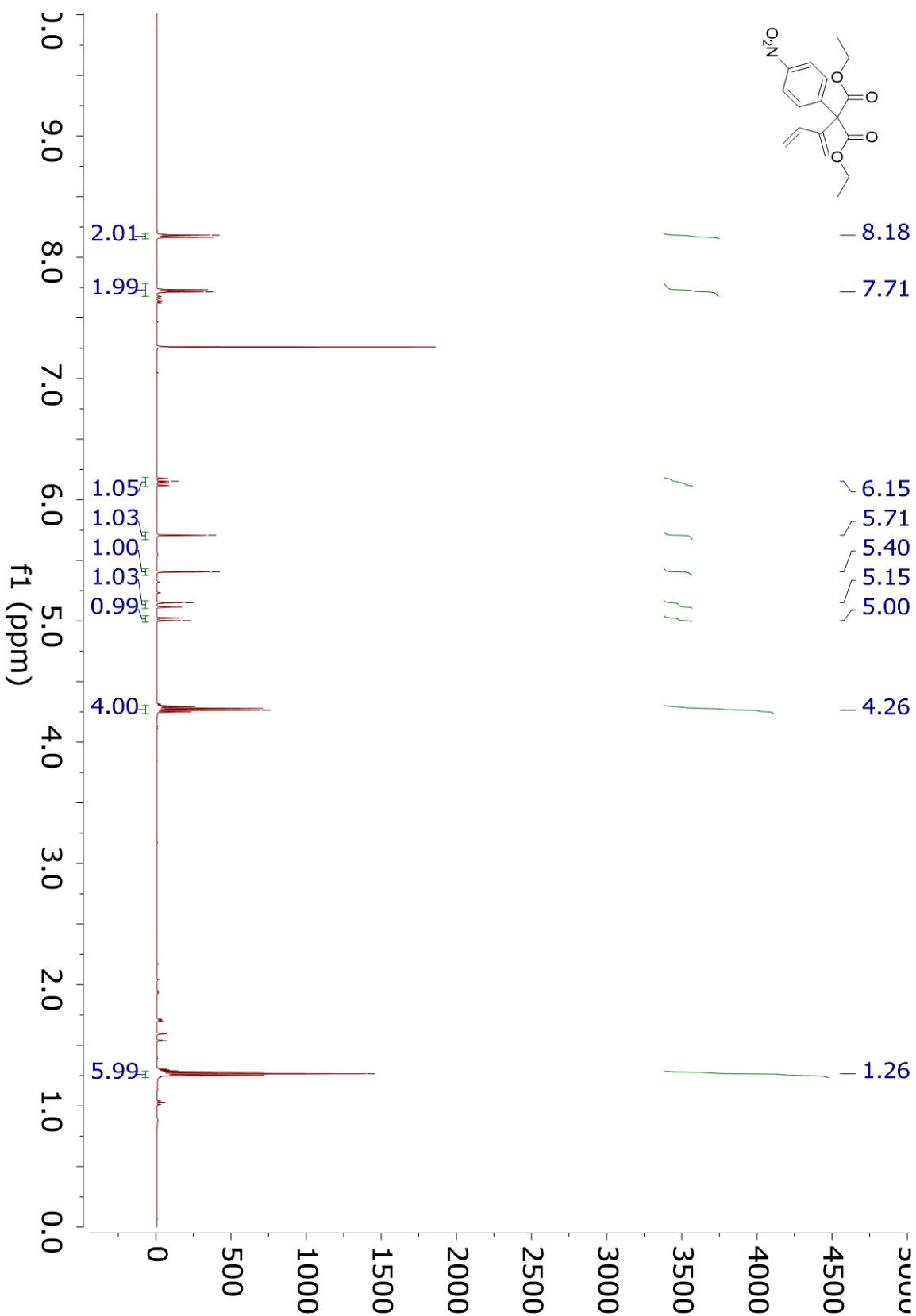
¹H NMR 4.12g



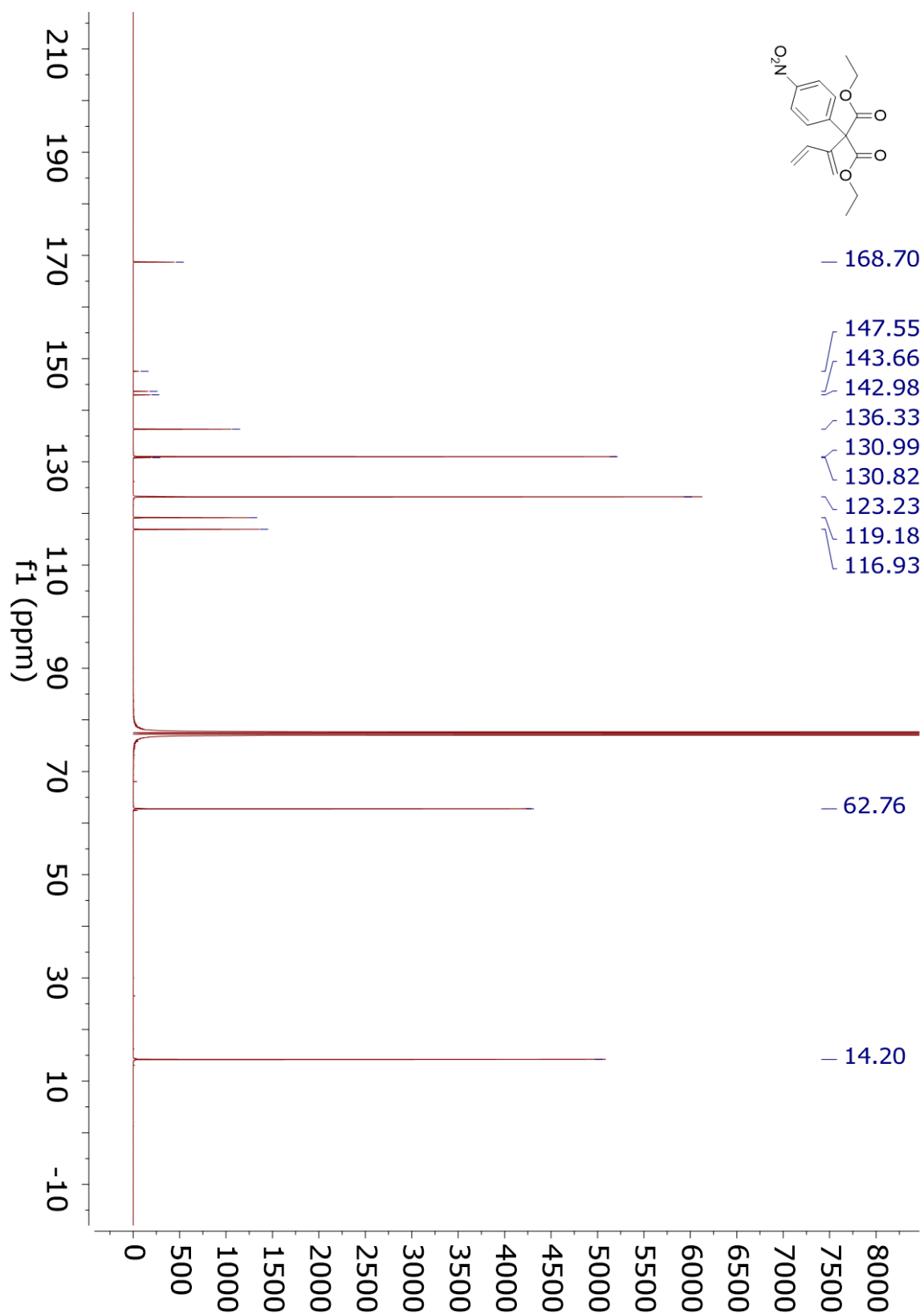
¹³C NMR 4.12g



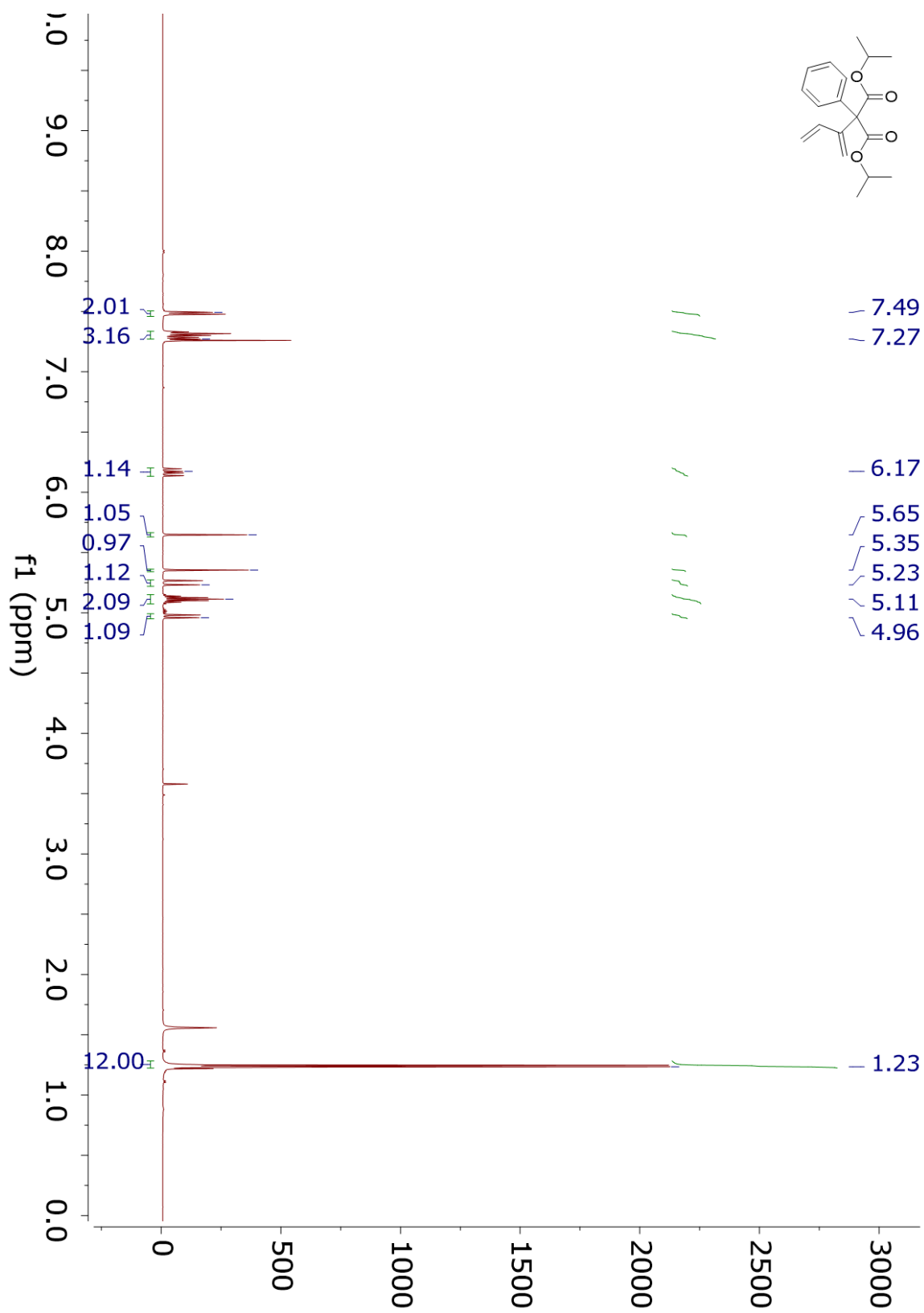
¹H NMR 4.12h



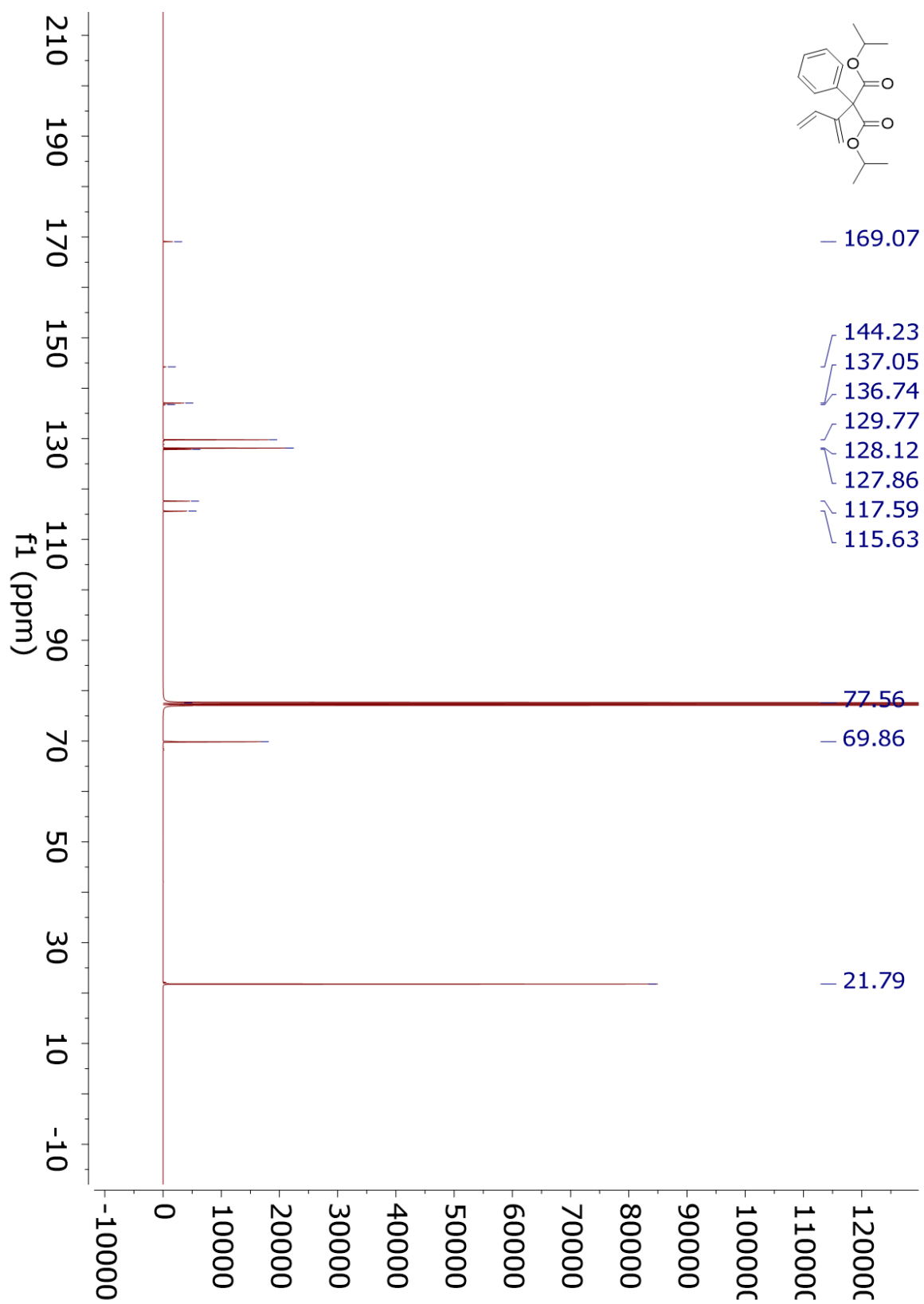
¹³C NMR 4.12h



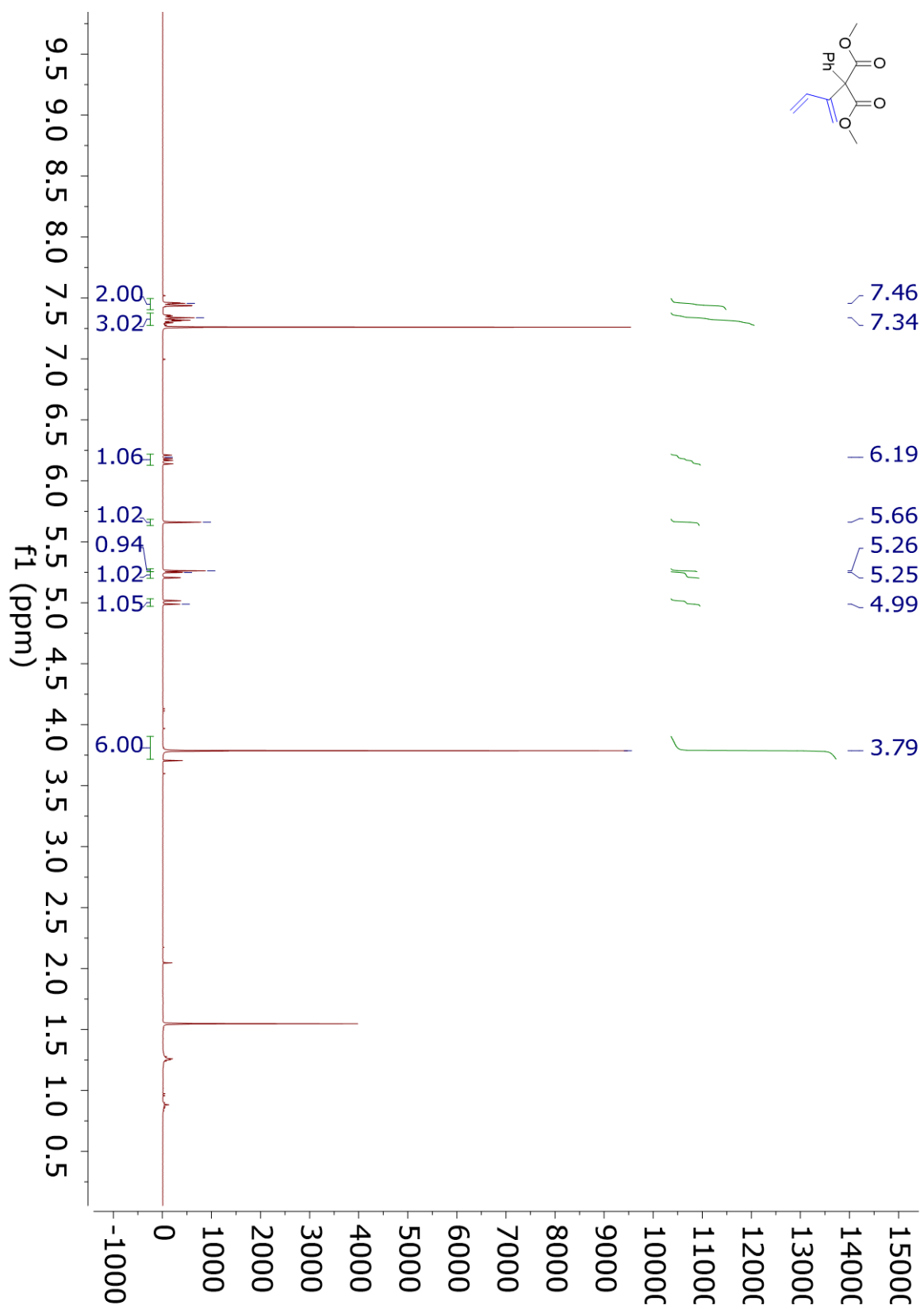
¹H NMR 4.12i



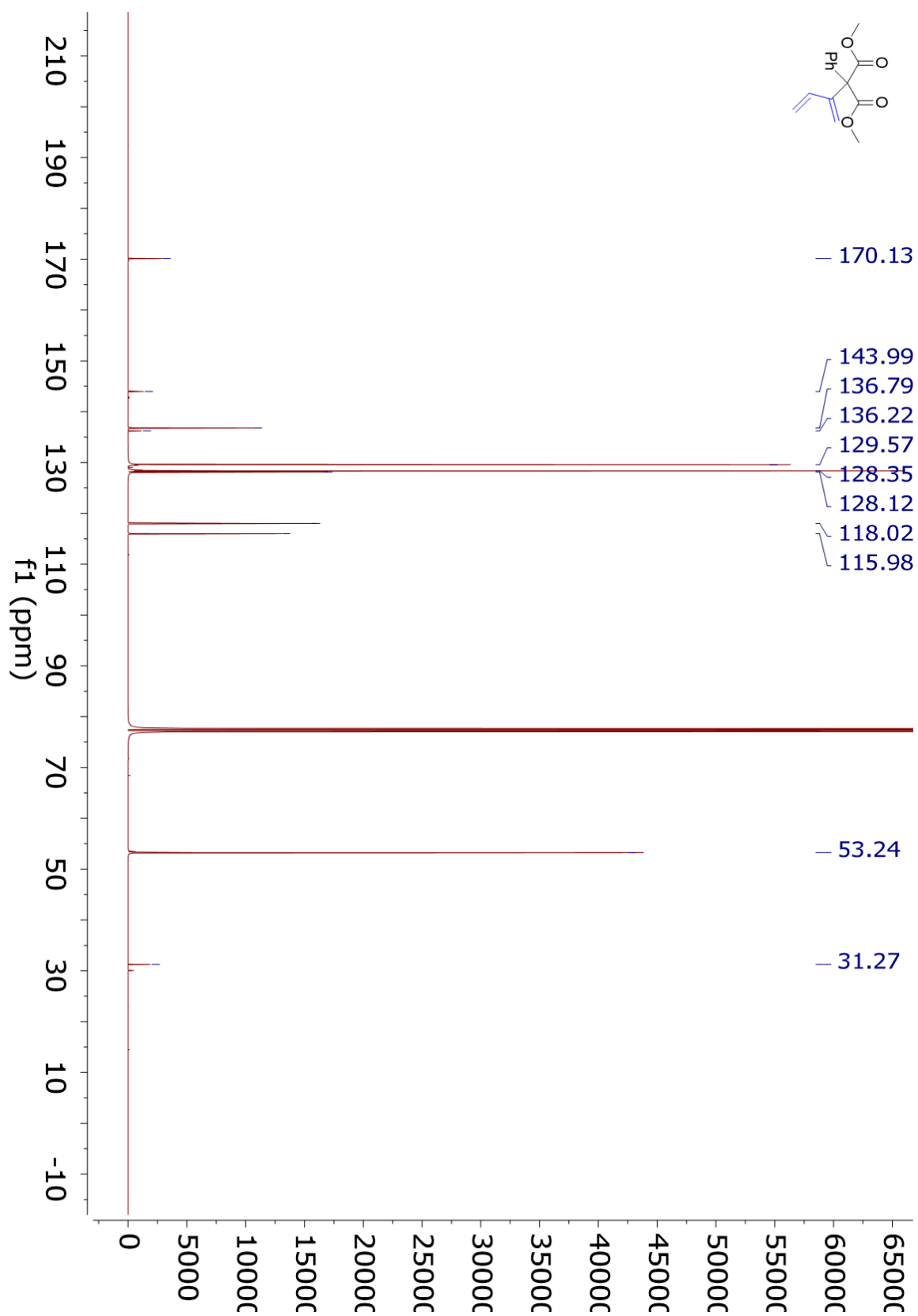
¹³C NMR 4.12i



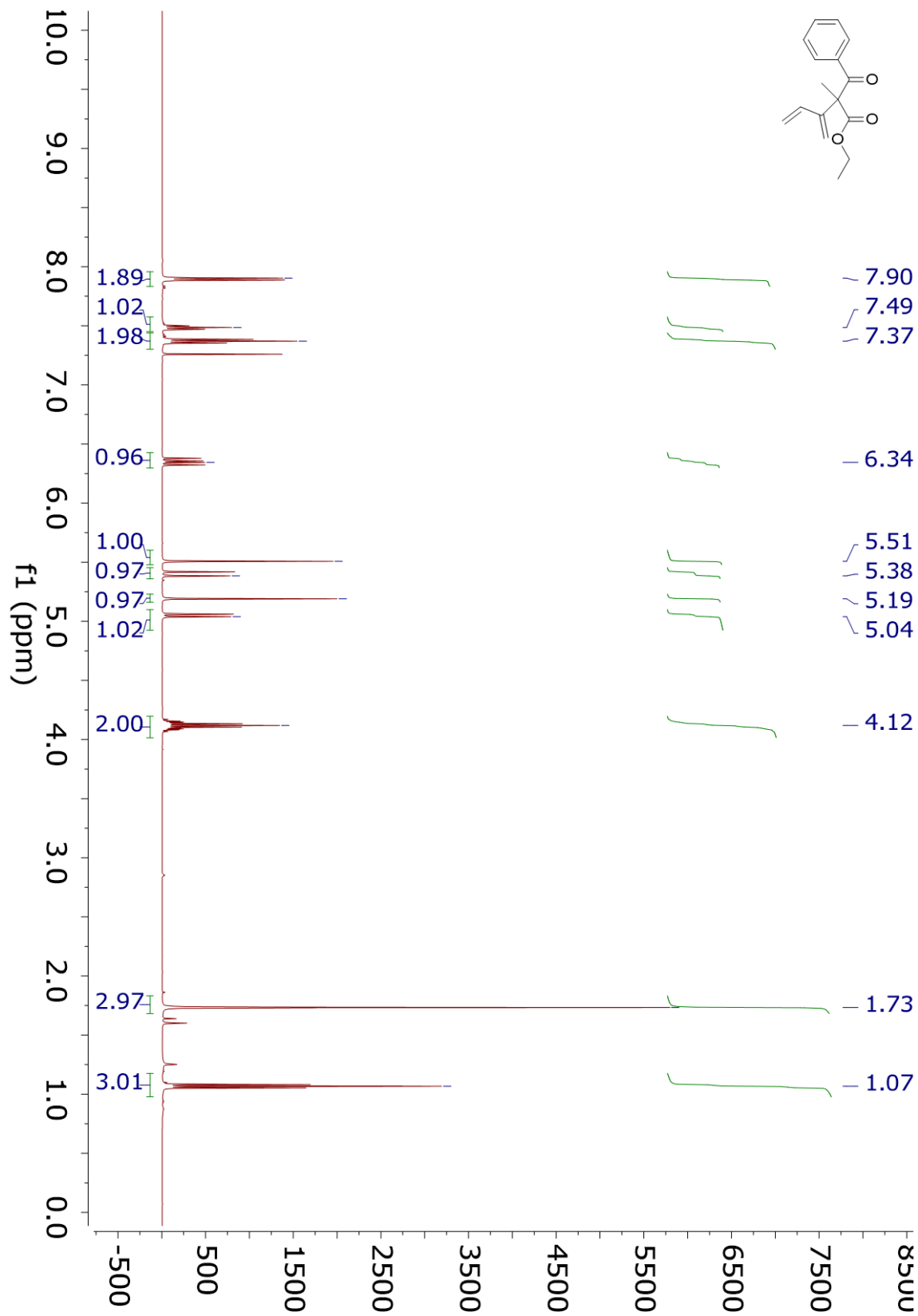
¹H NMR 4.12j



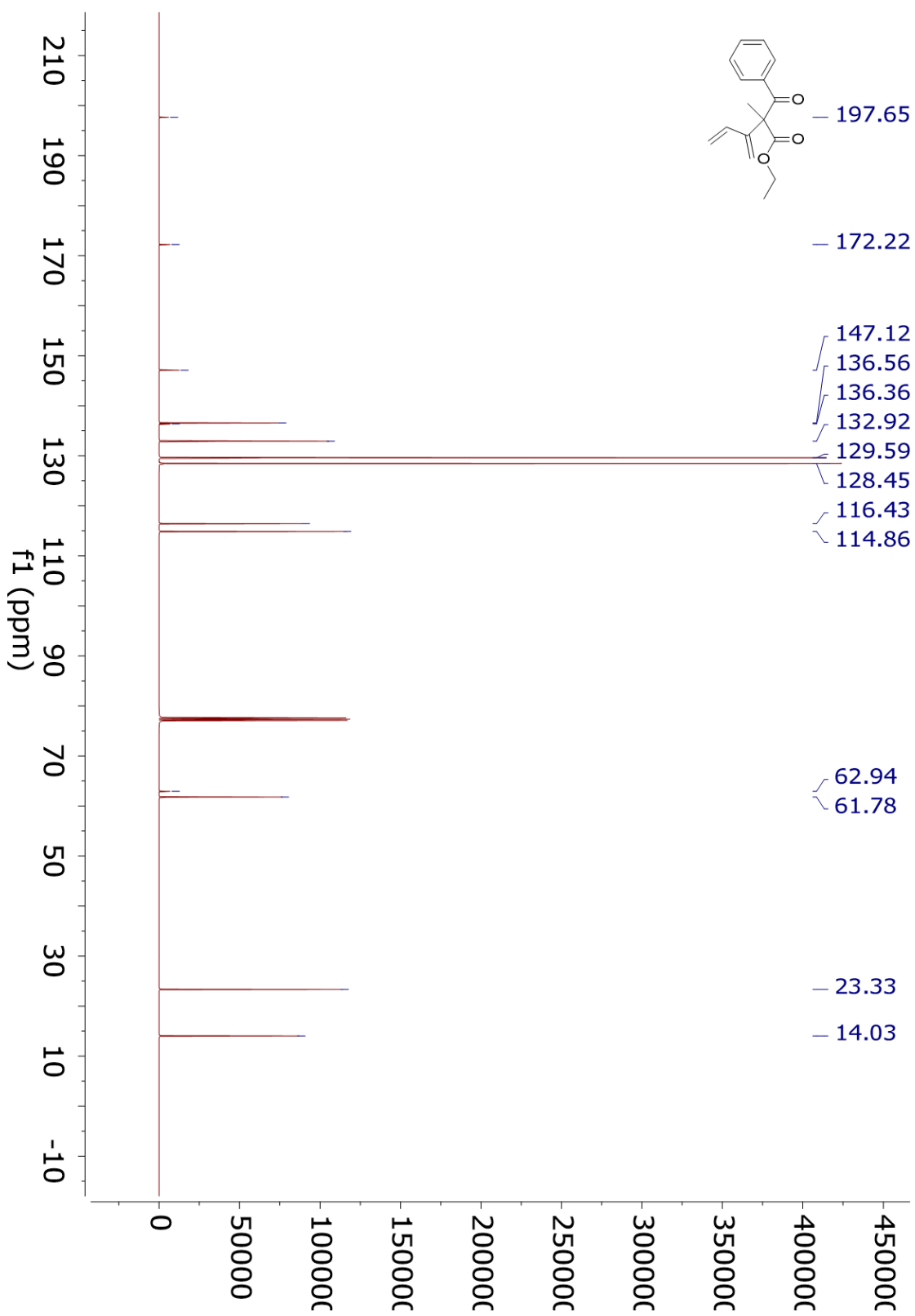
¹³C NMR 4.12j



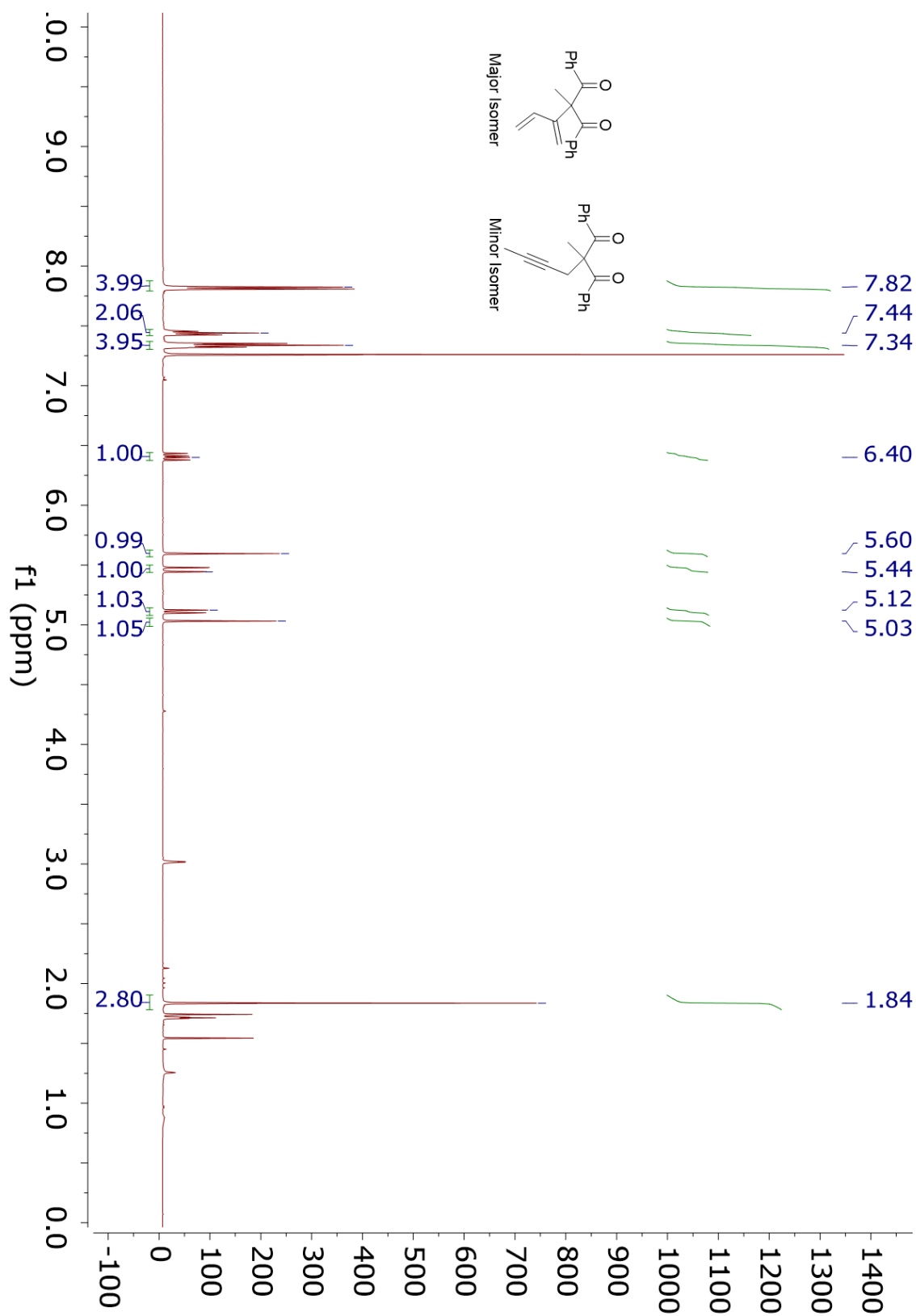
¹H NMR 4.12k



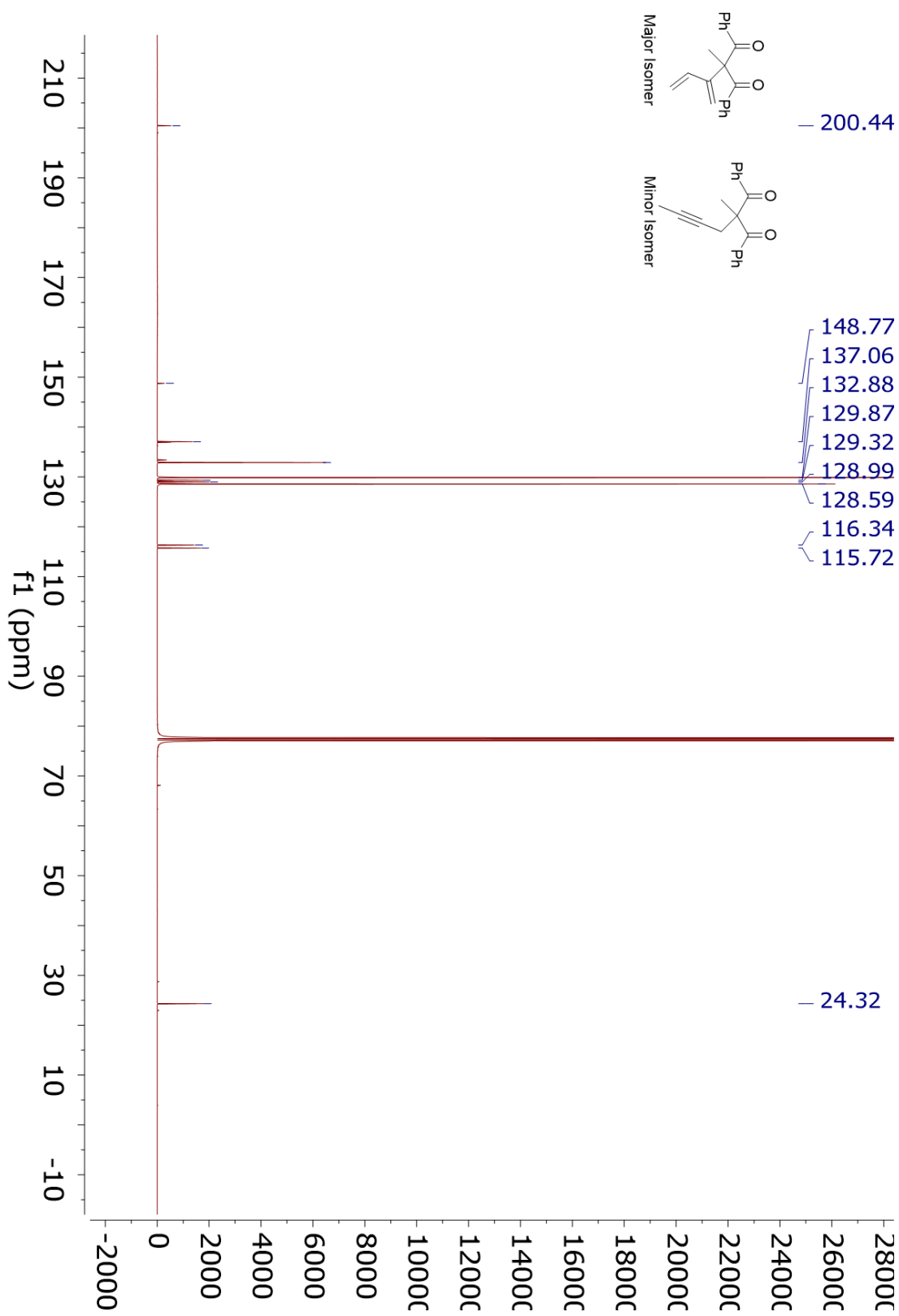
¹³C NMR 4.12k



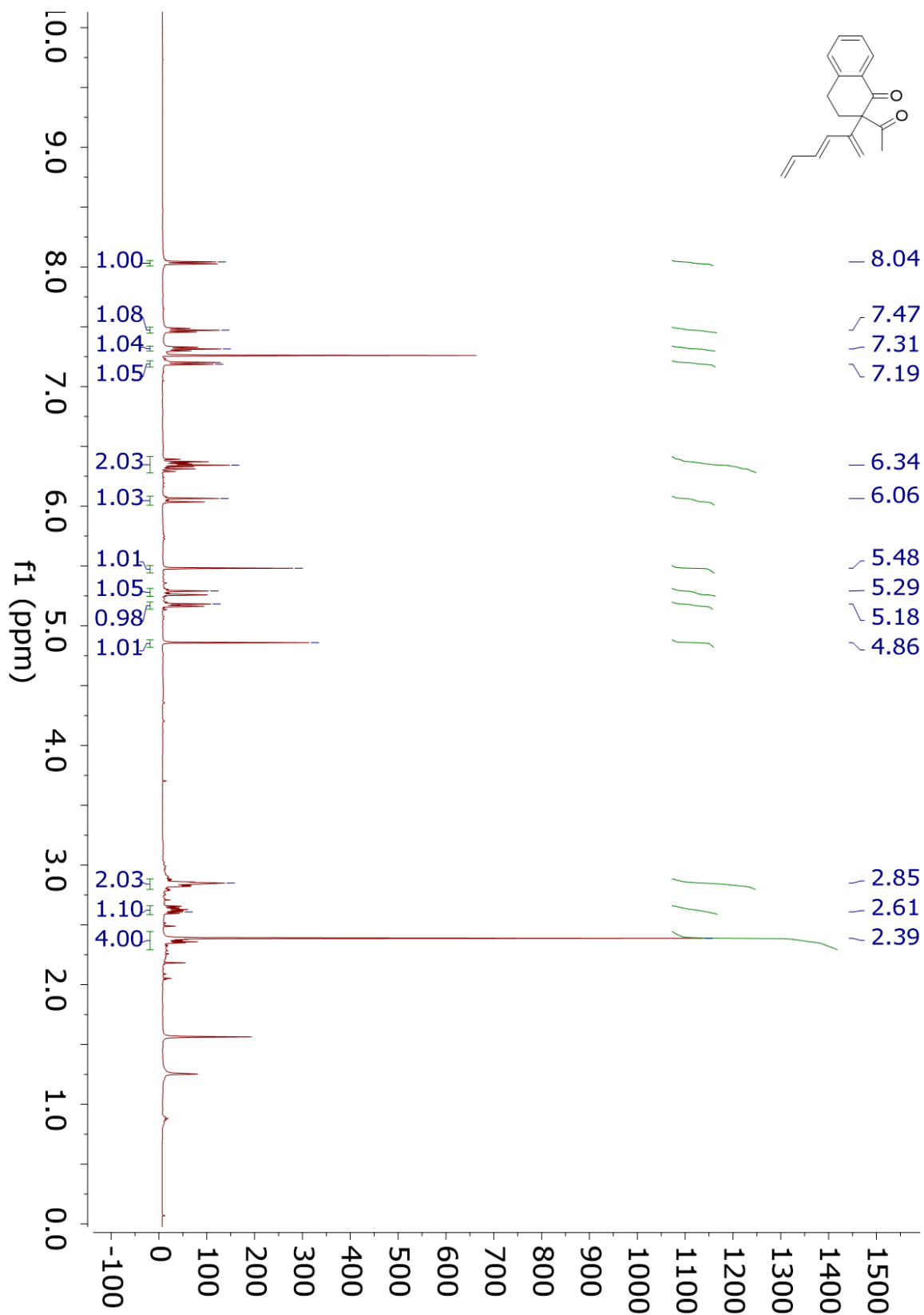
¹H NMR 4.121



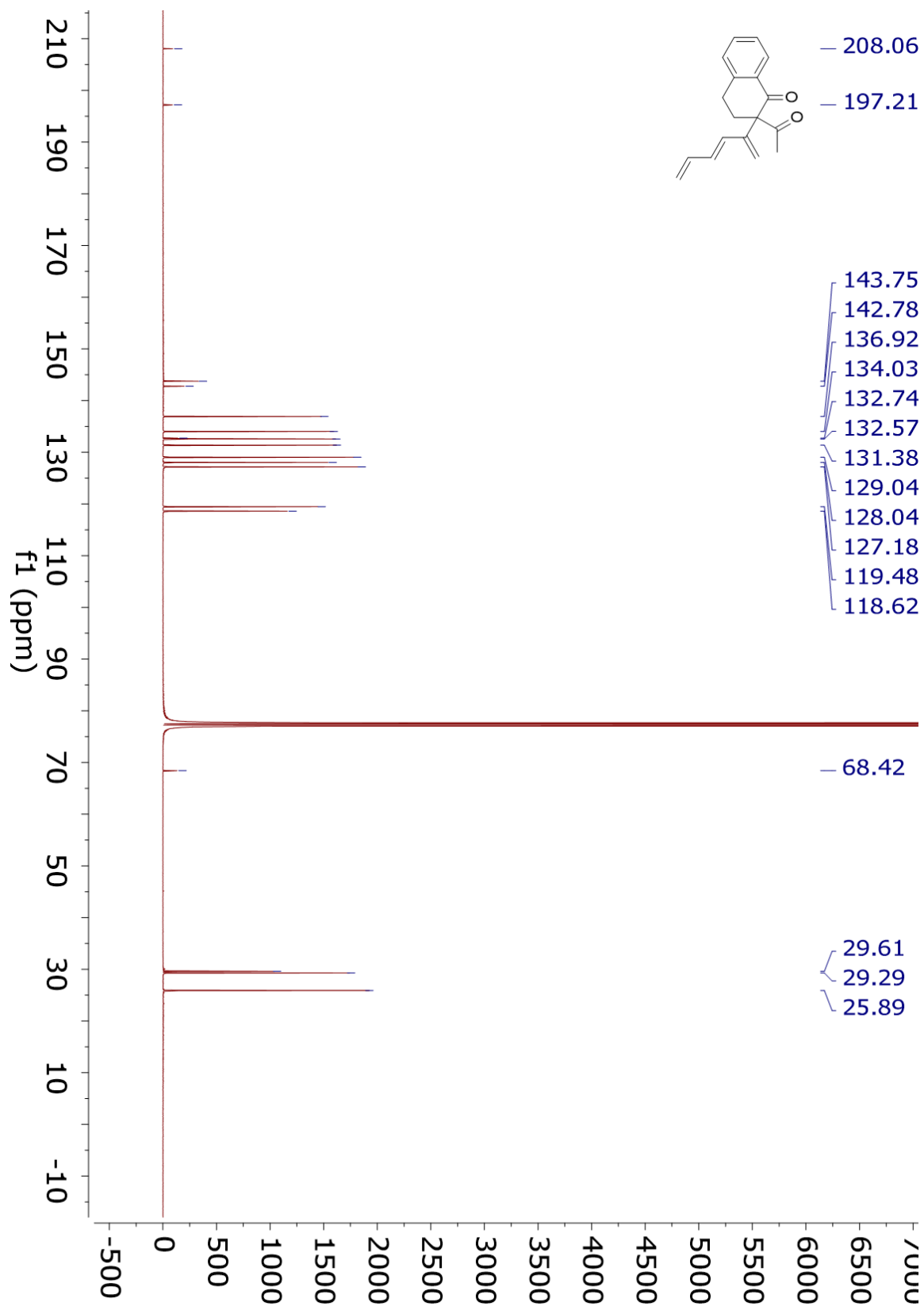
¹³C NMR 4.121



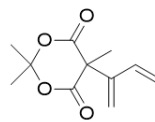
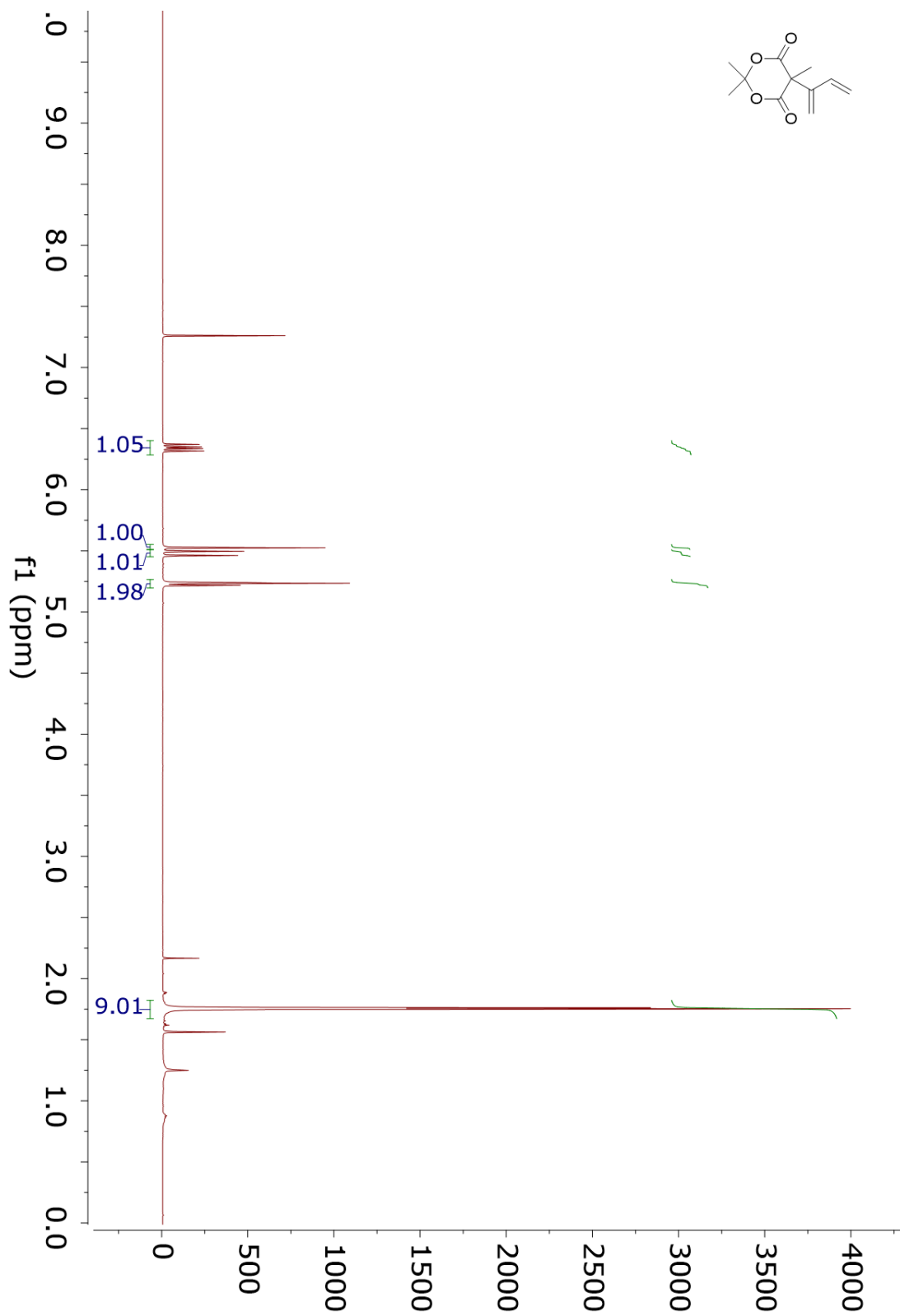
¹H NMR 4.12m



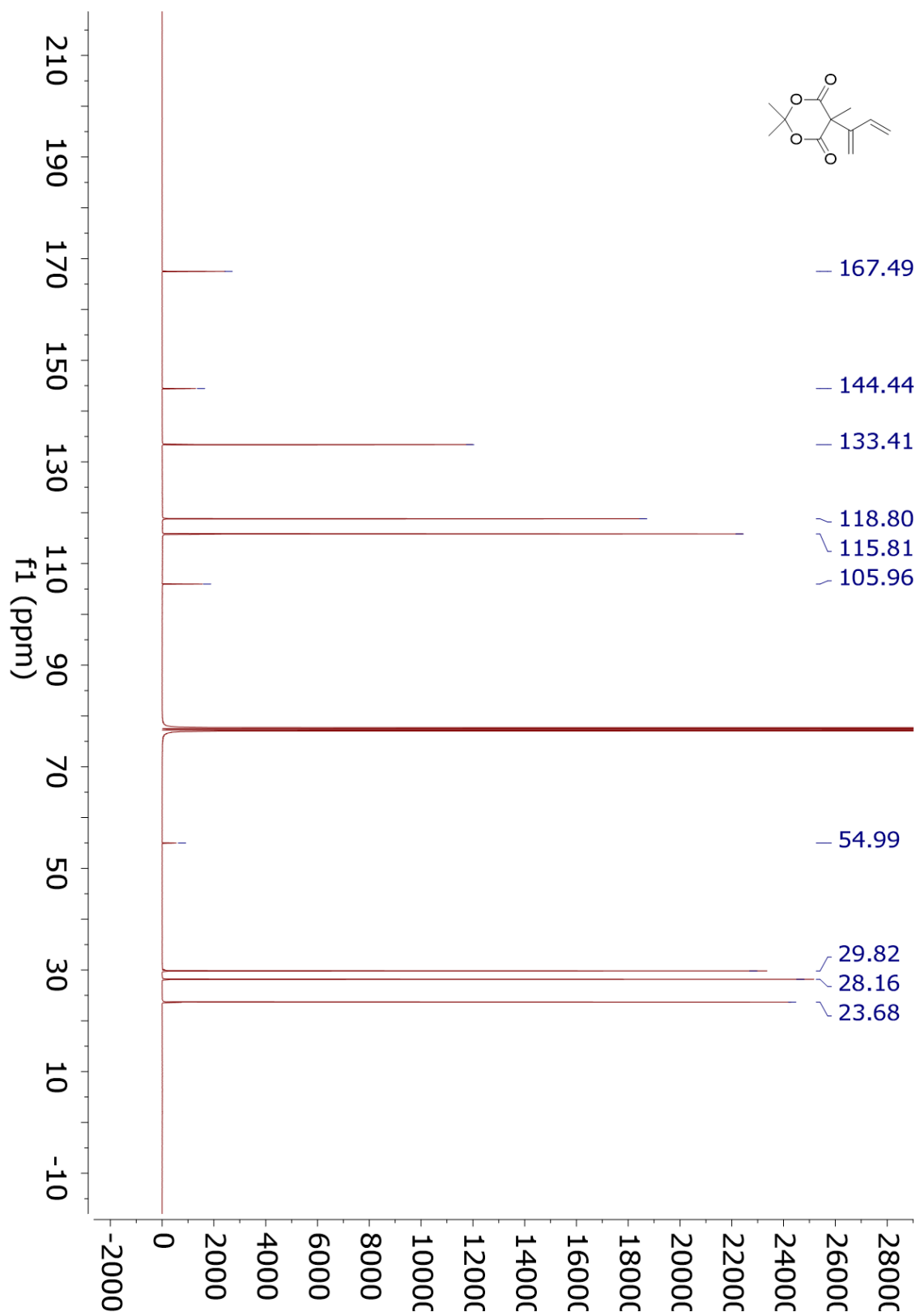
¹³C NMR 4.12m



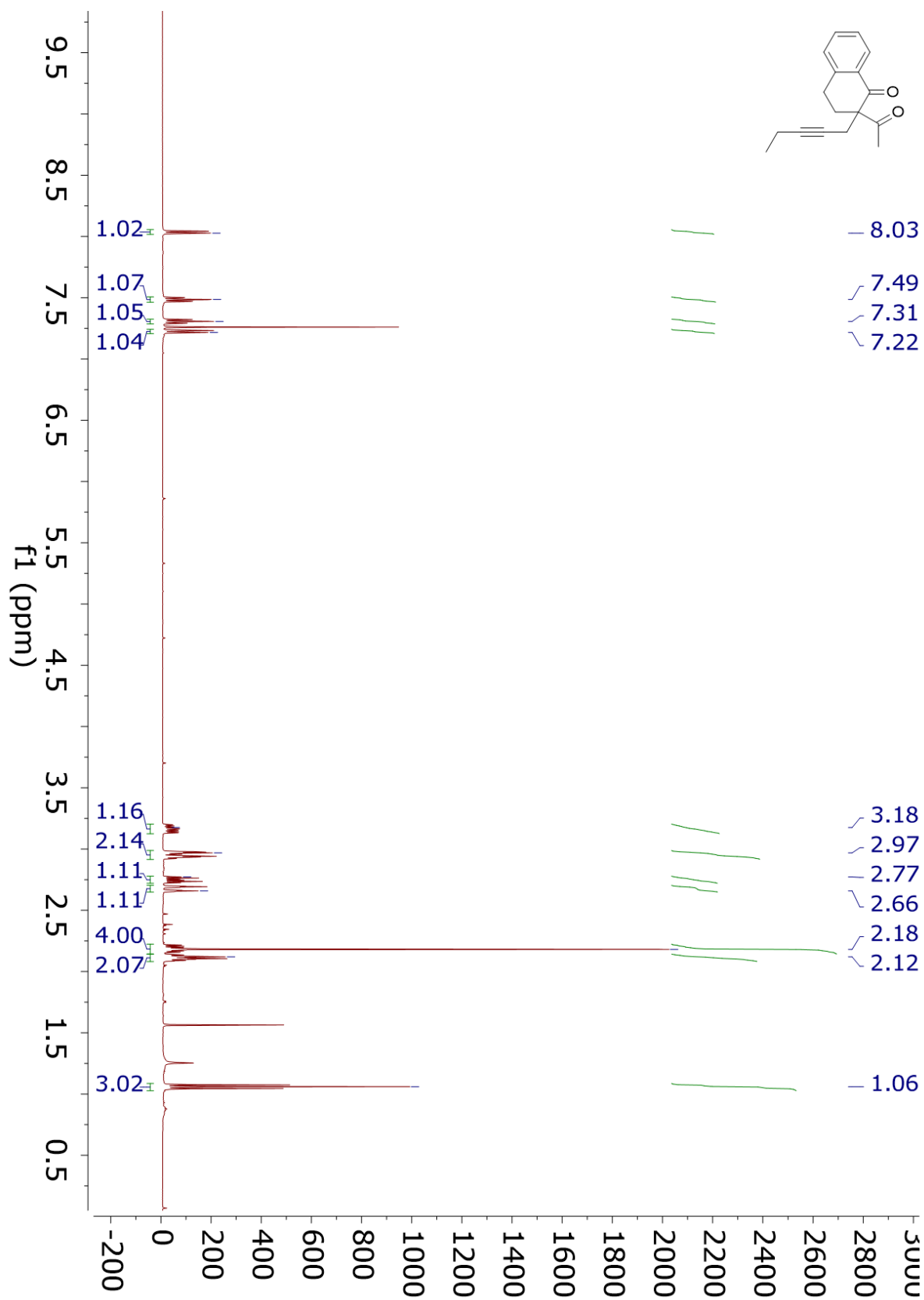
¹H NMR 4.12n



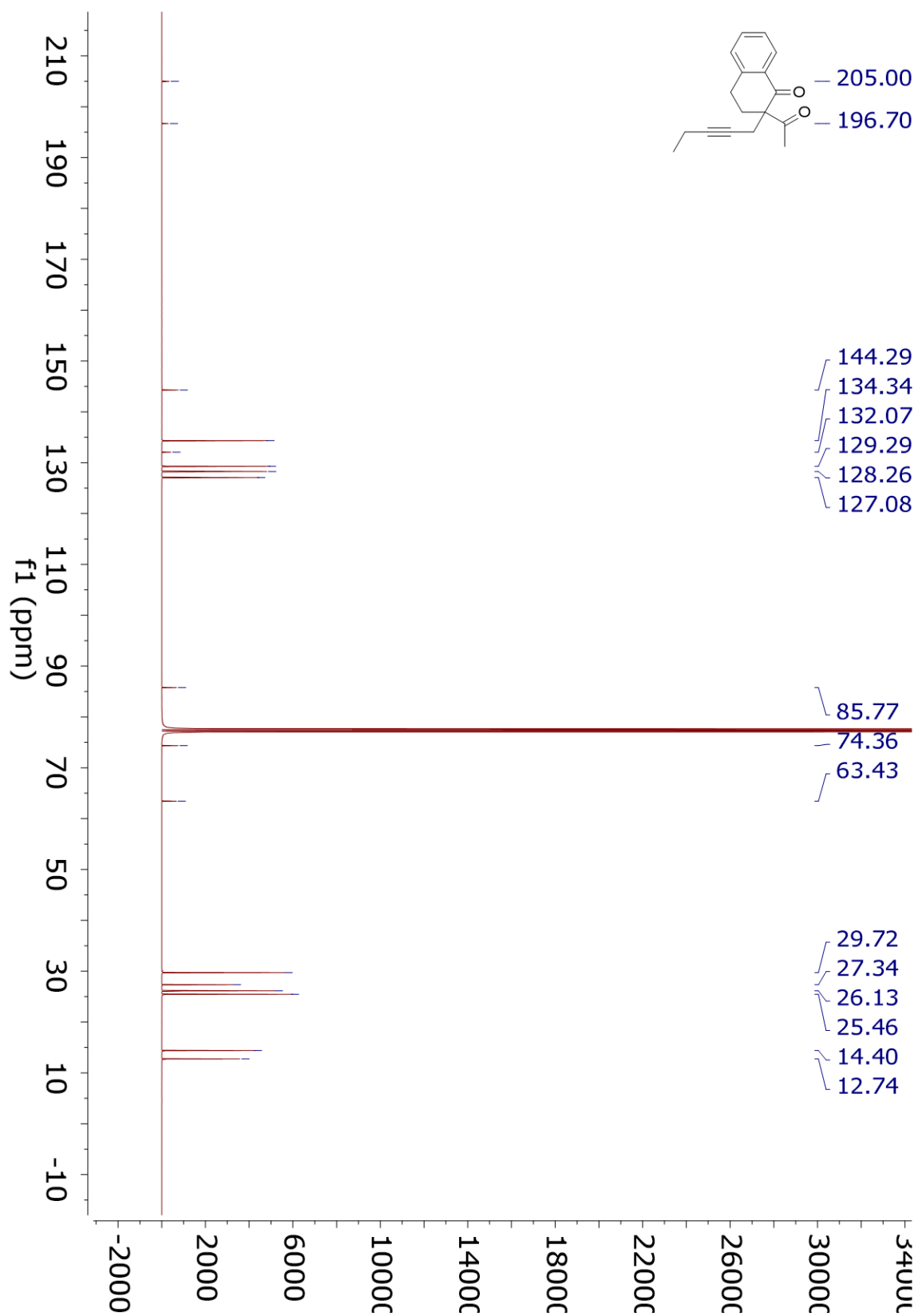
¹³C NMR 4.12n



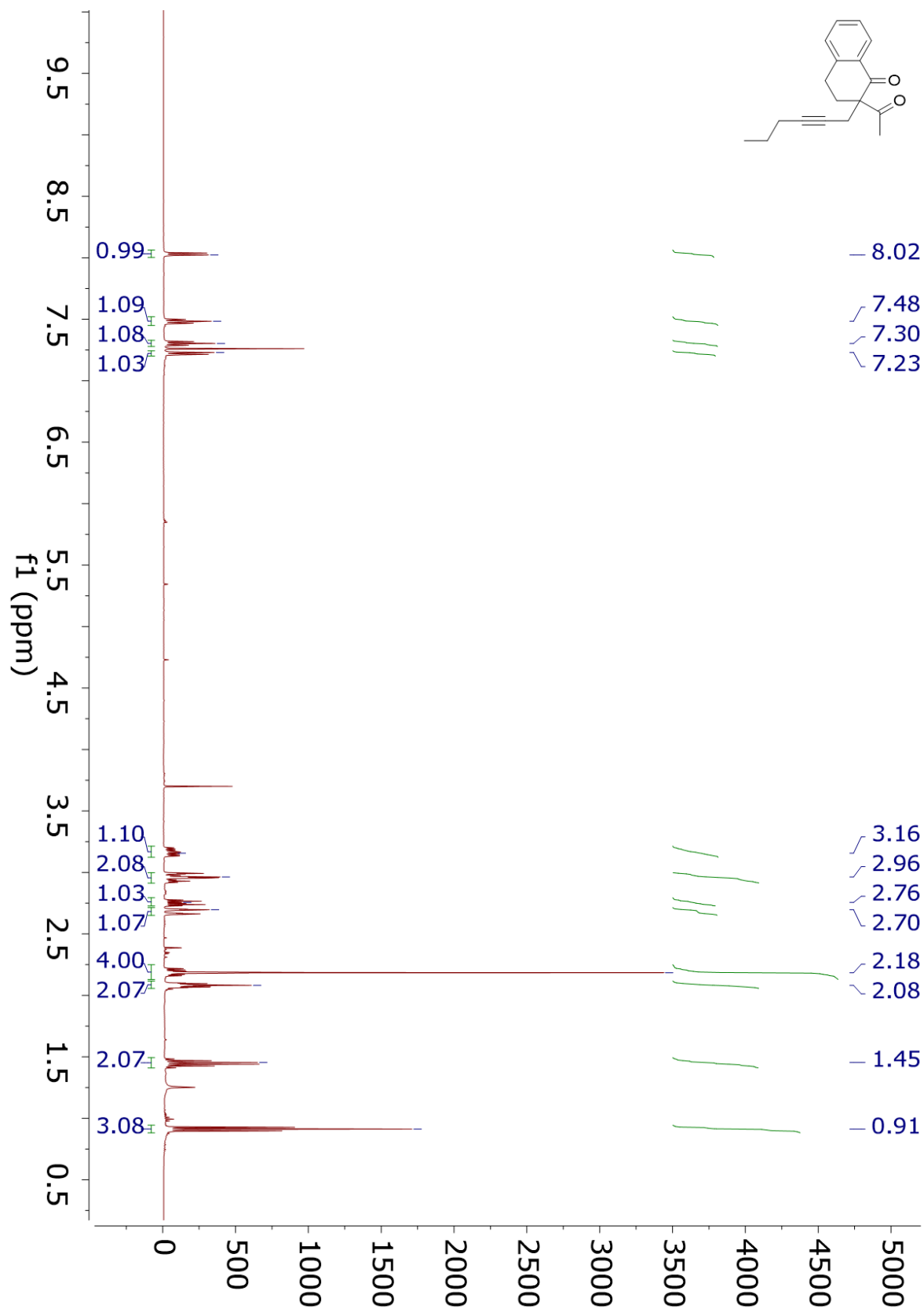
¹H NMR 4.13a



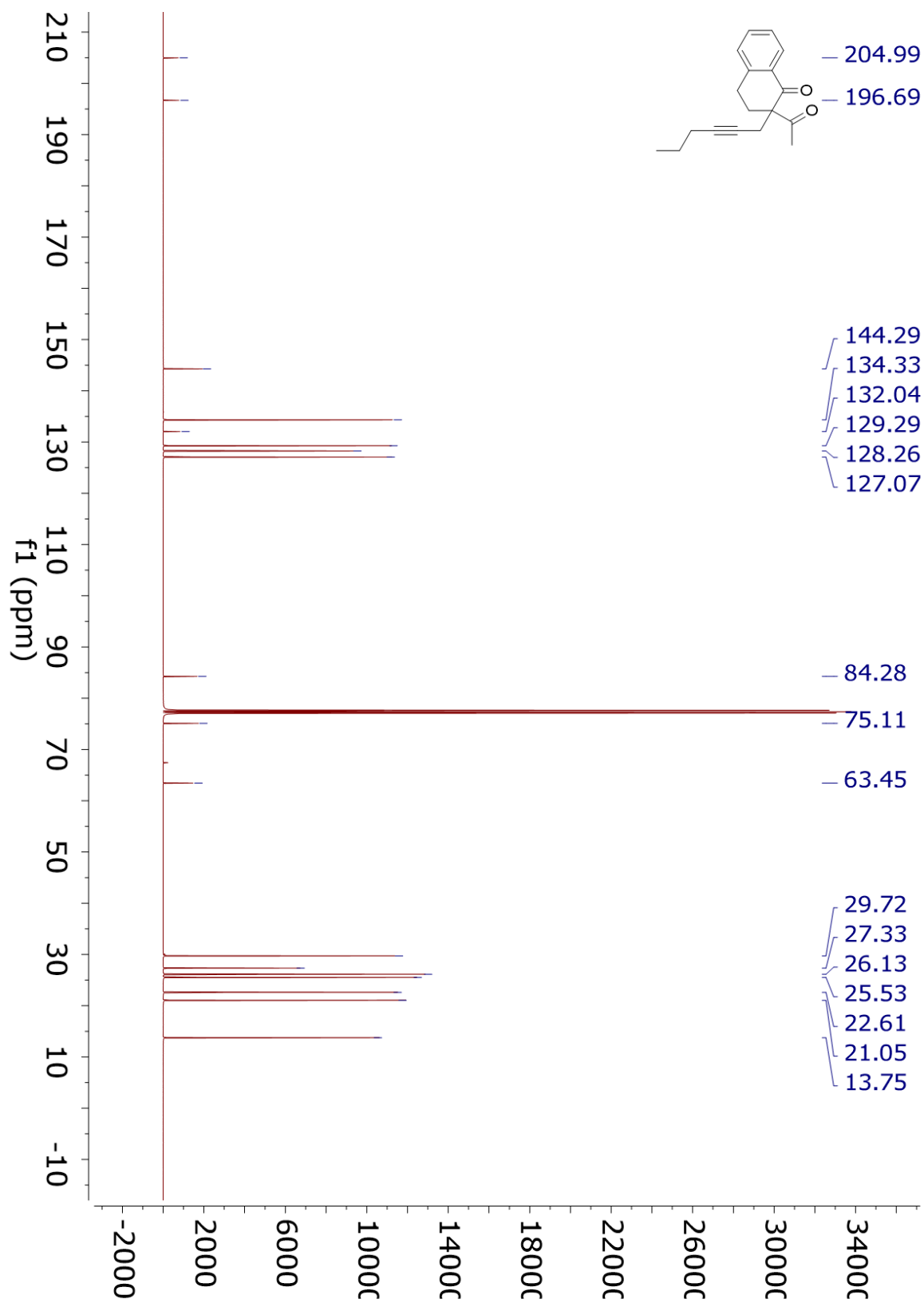
¹³C NMR 4.13a



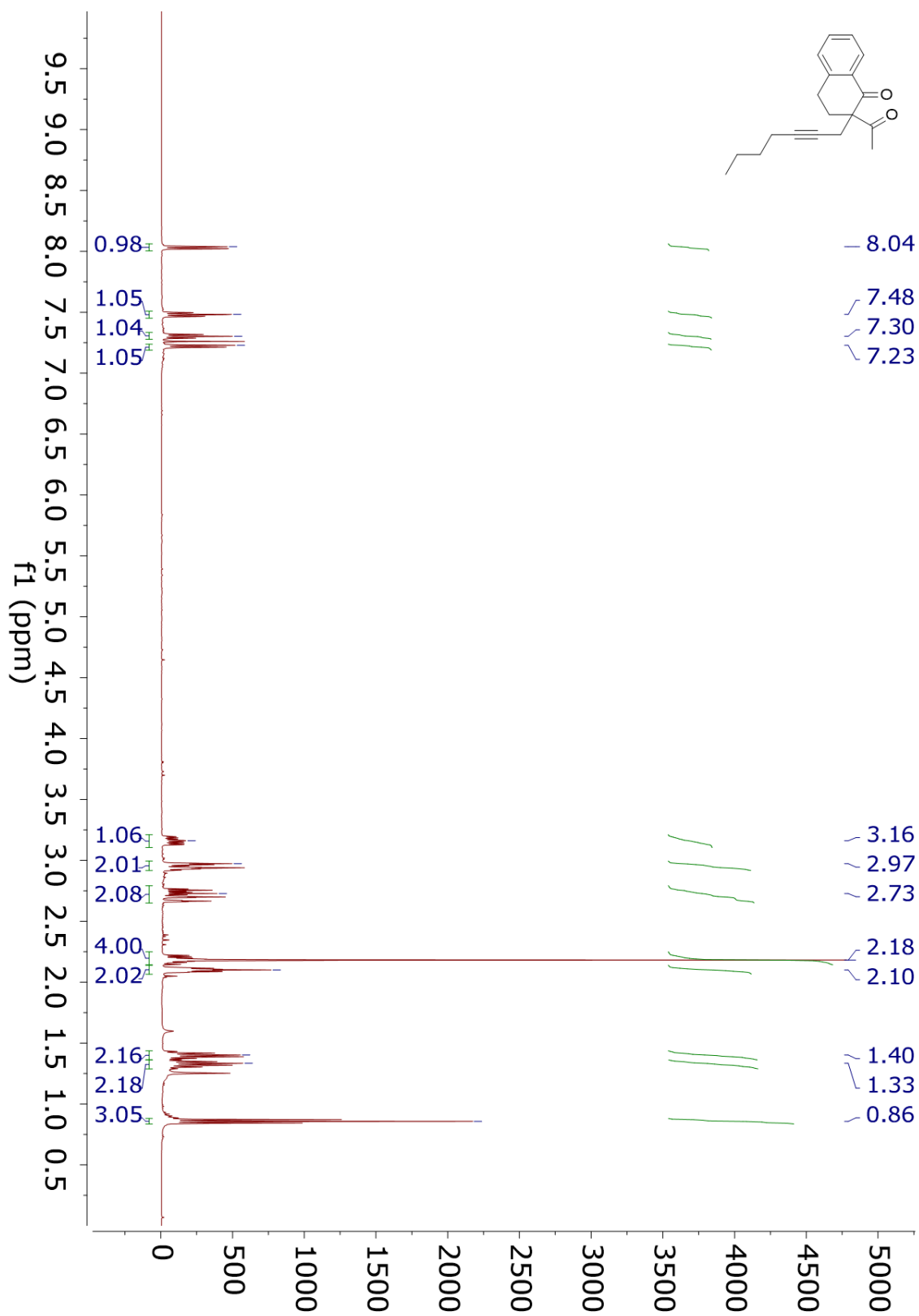
¹H NMR 4.13b



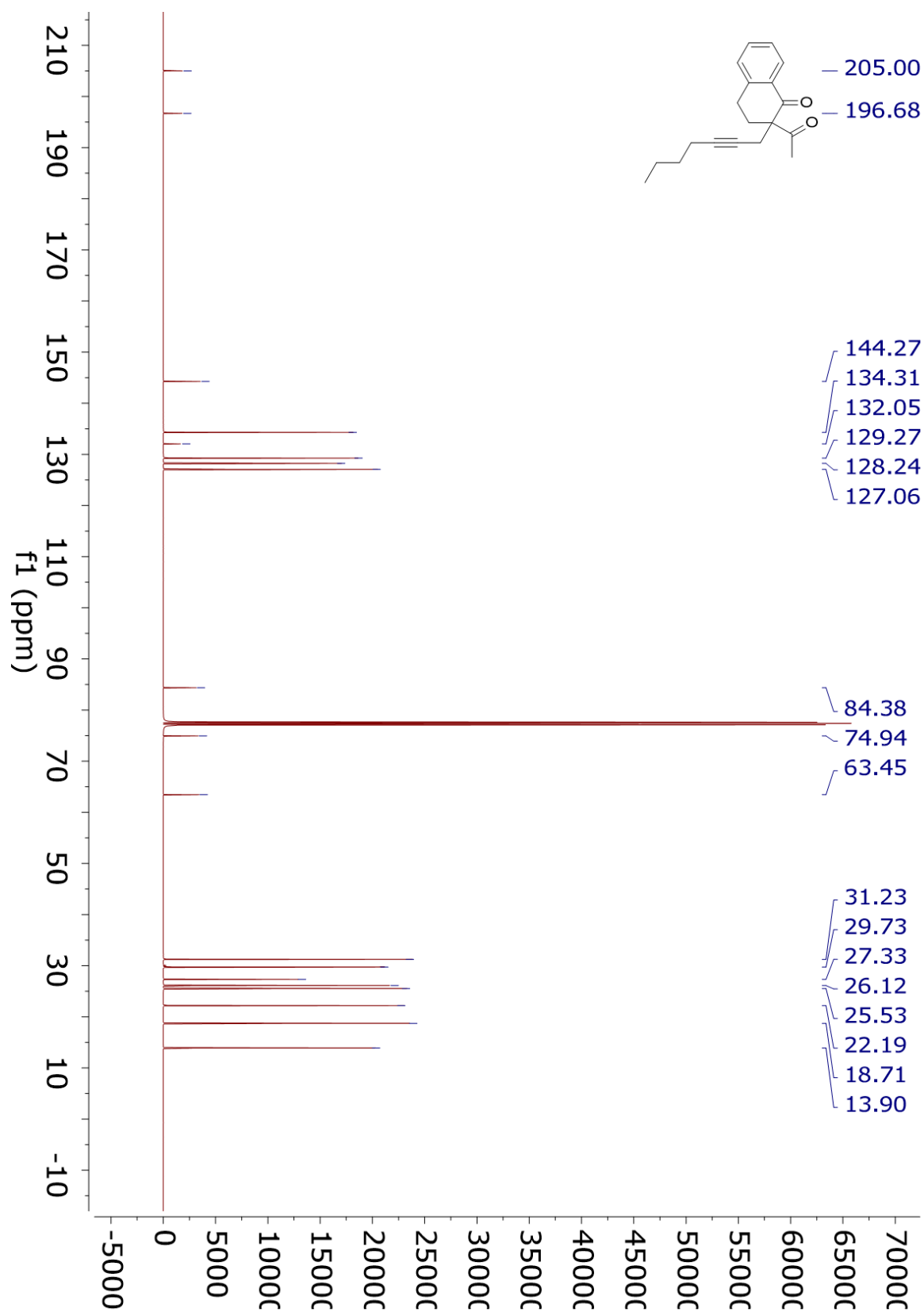
¹³C NMR 4.13b



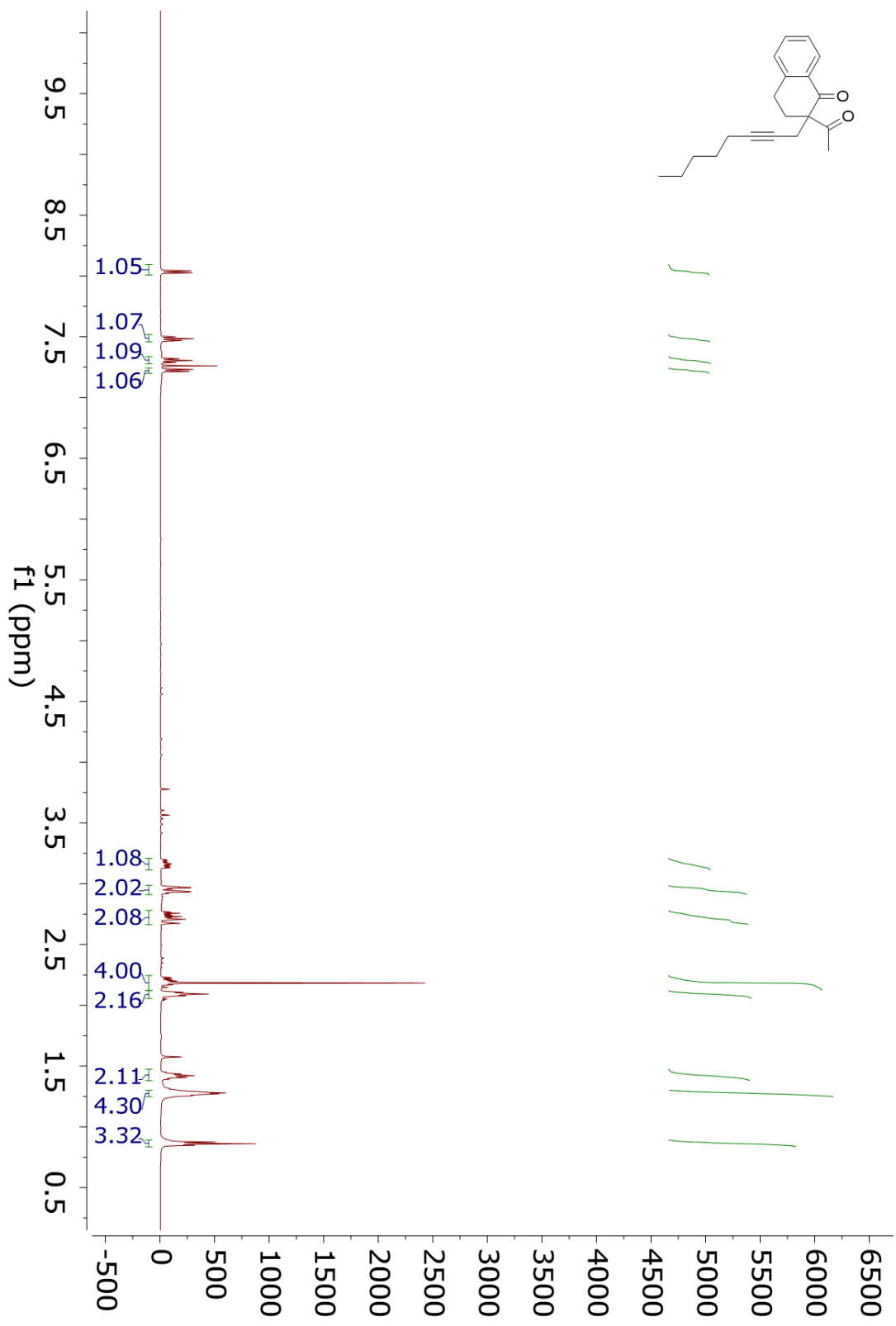
¹H NMR 4.13c



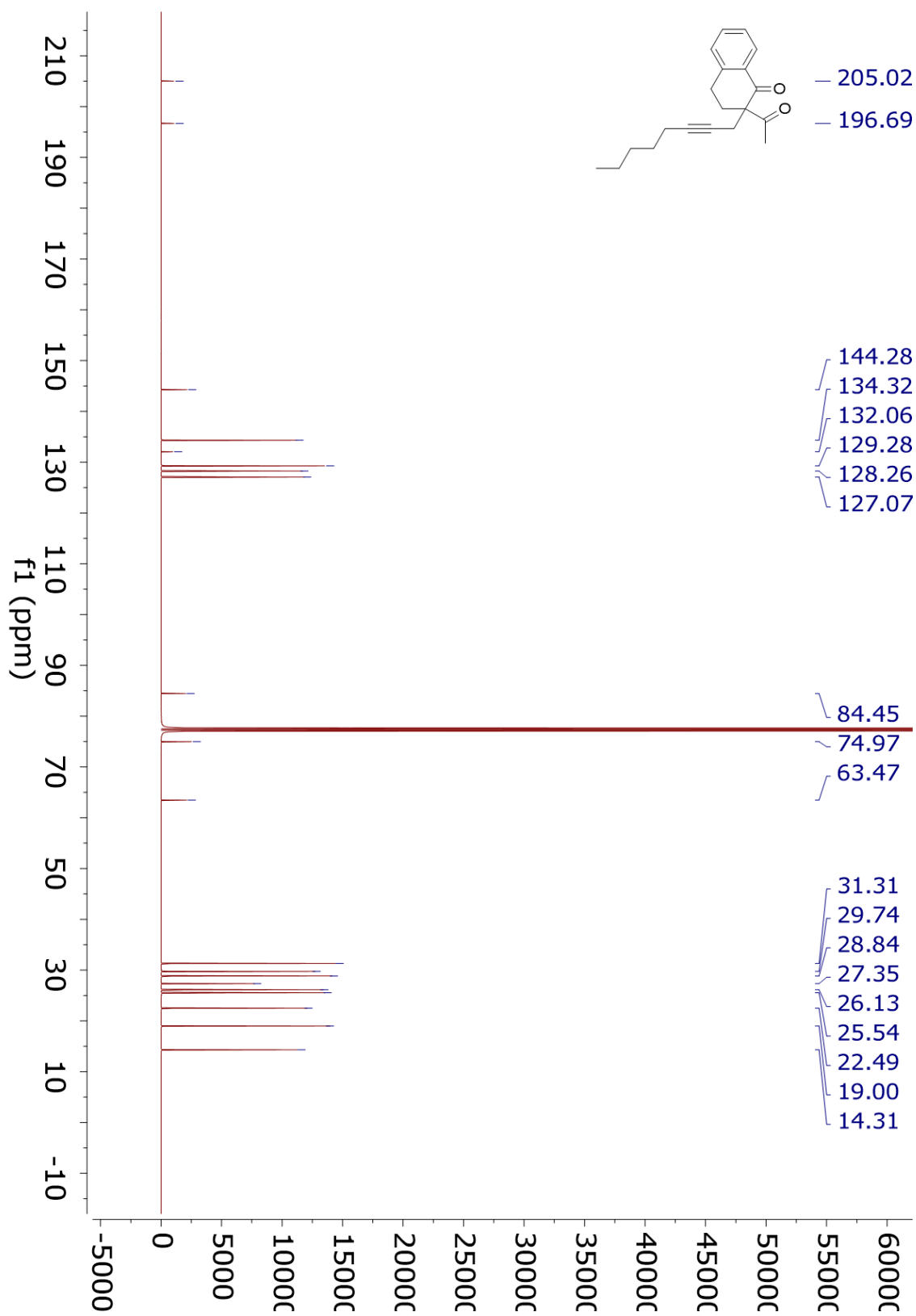
¹³C NMR 4.13c



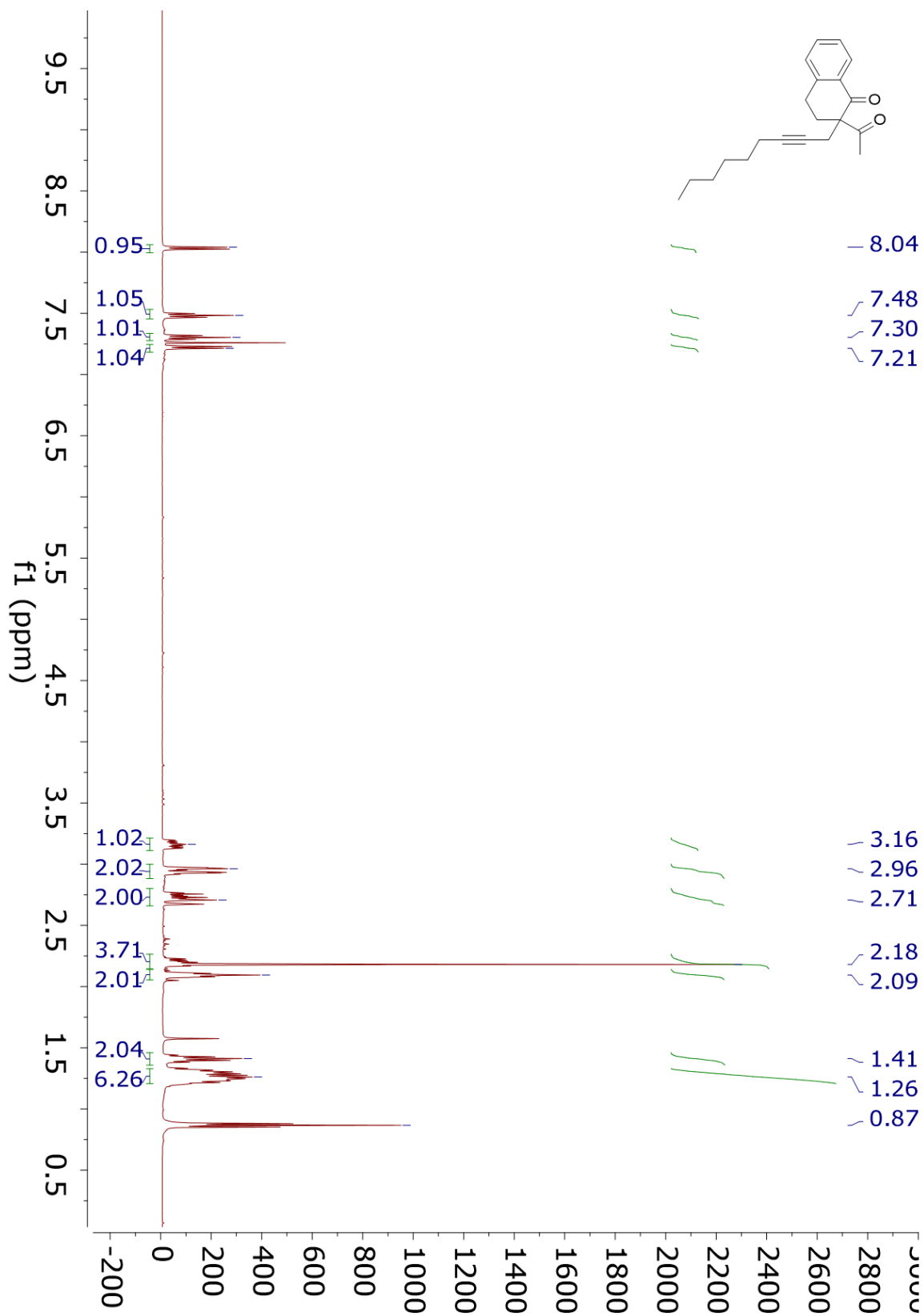
¹H NMR 4.13d



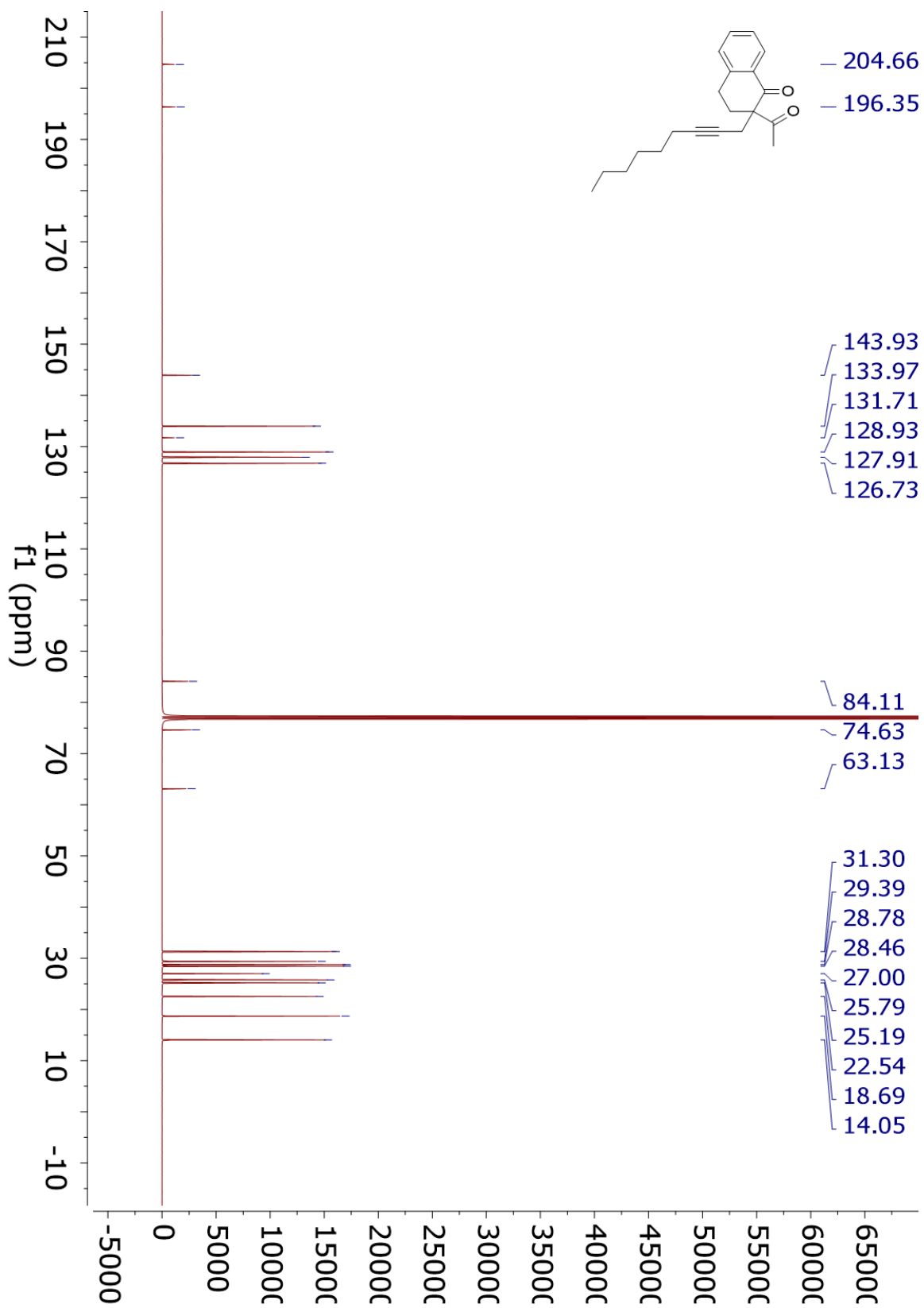
¹³C NMR 4.13d



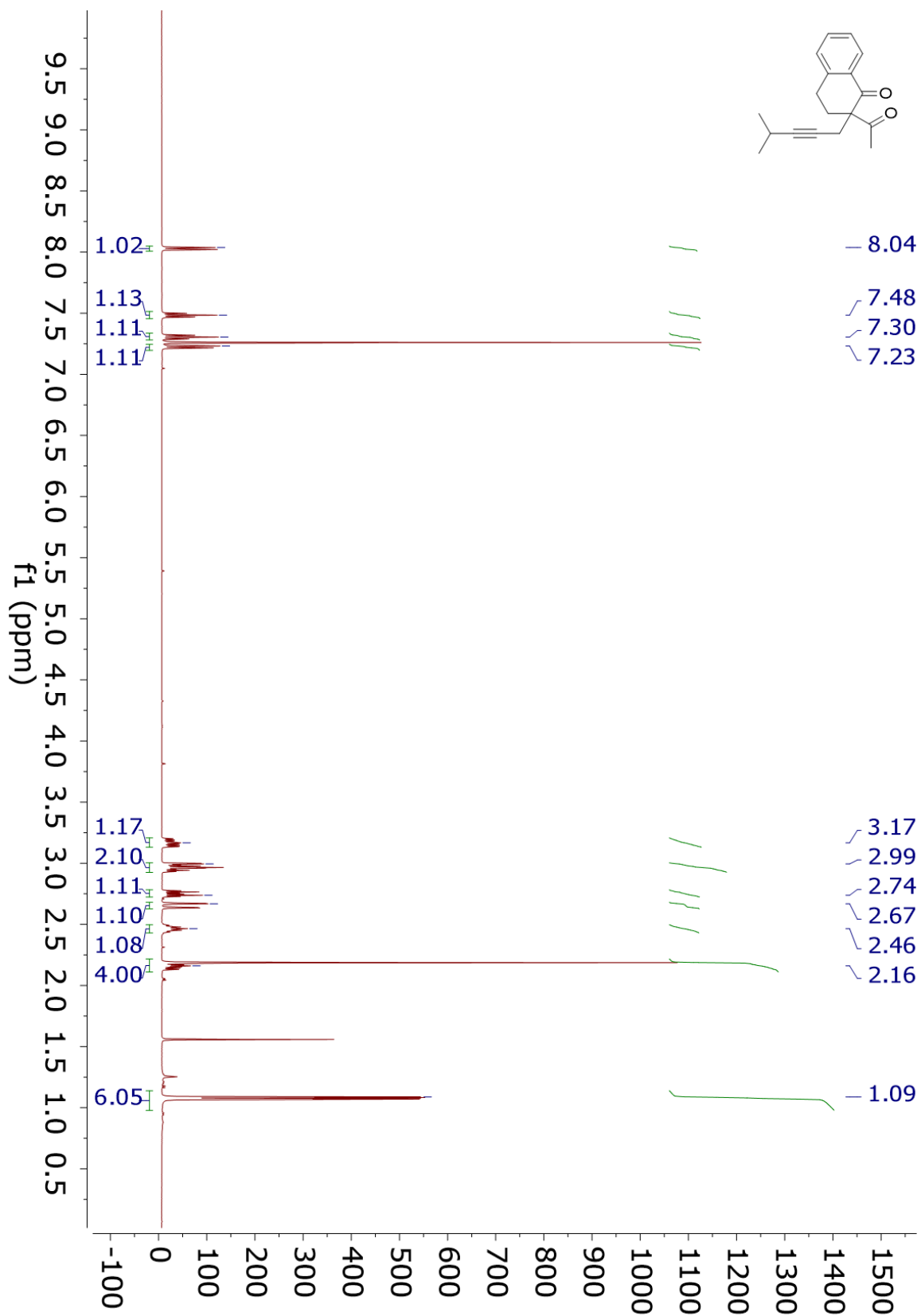
¹H NMR 4.13e



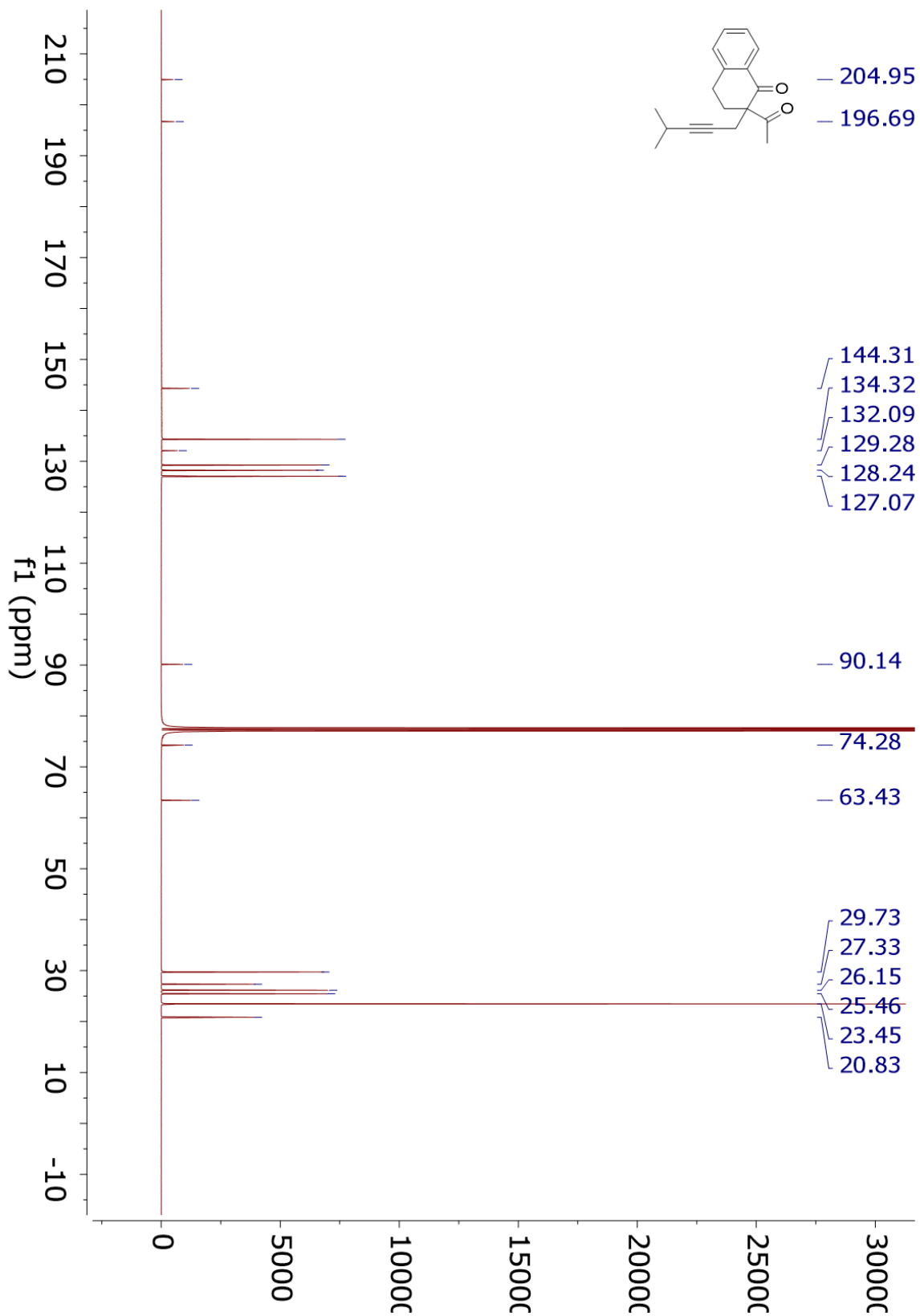
¹³C NMR 4.13e



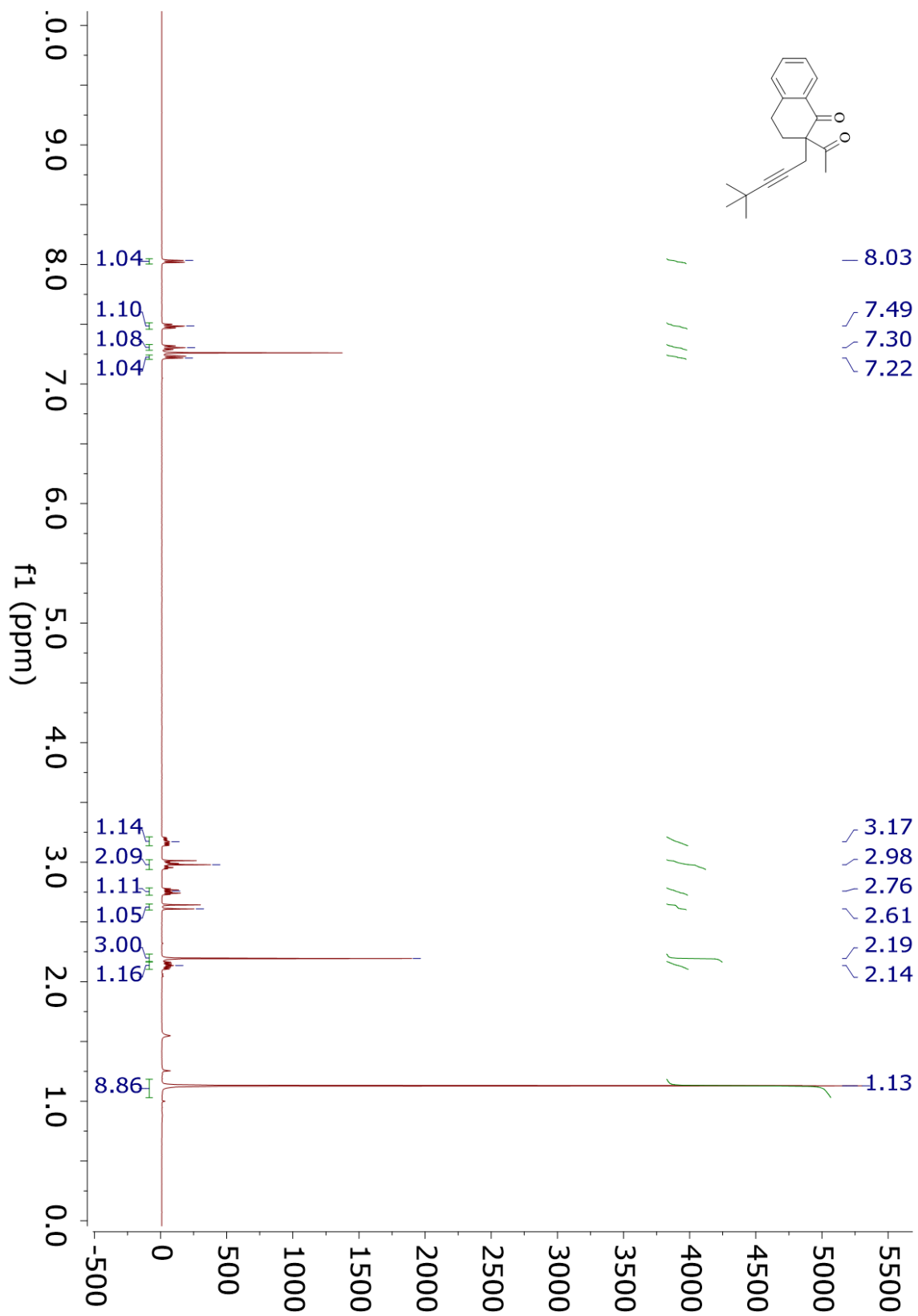
¹H NMR 4.13f



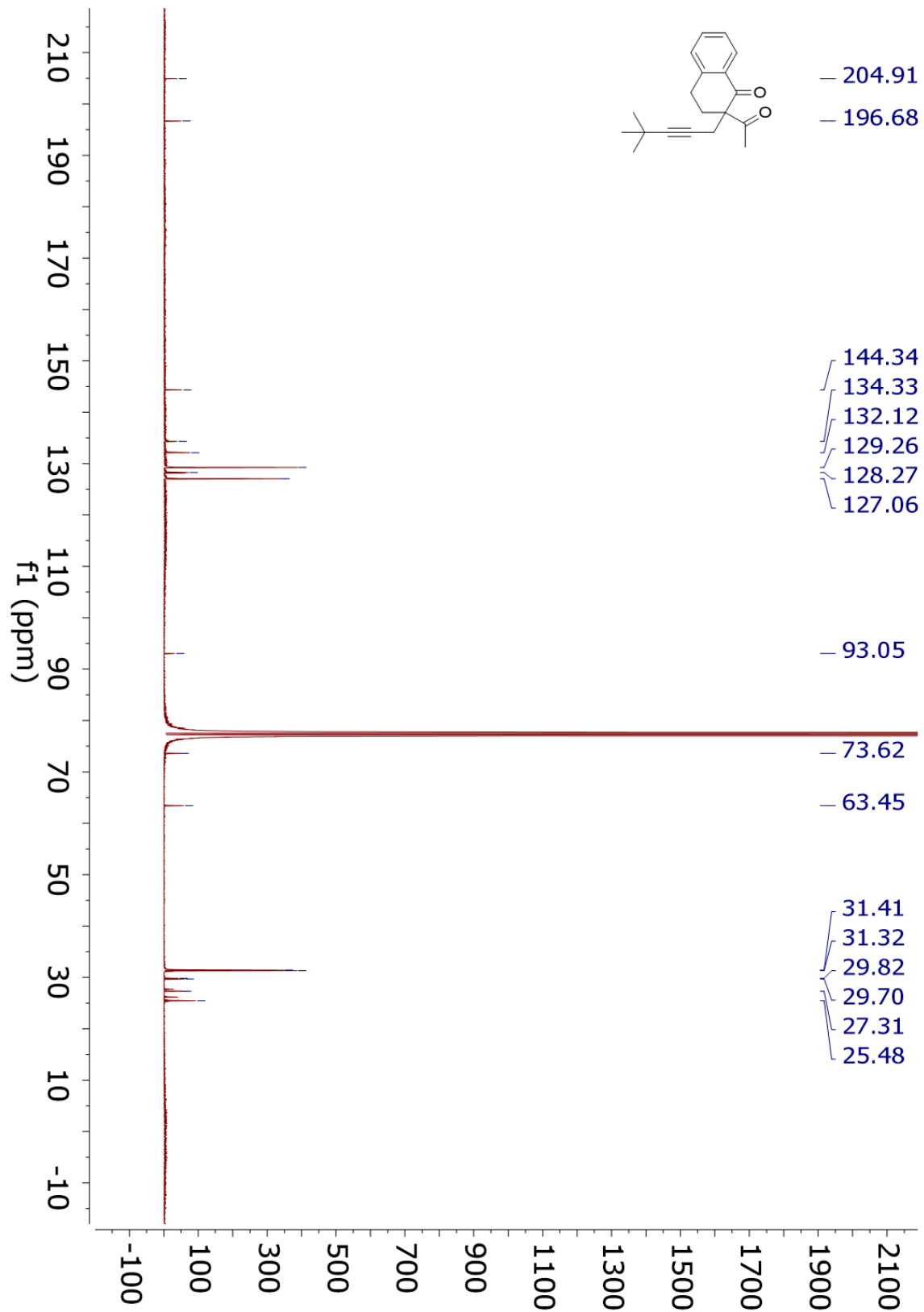
¹³C NMR 4.13f



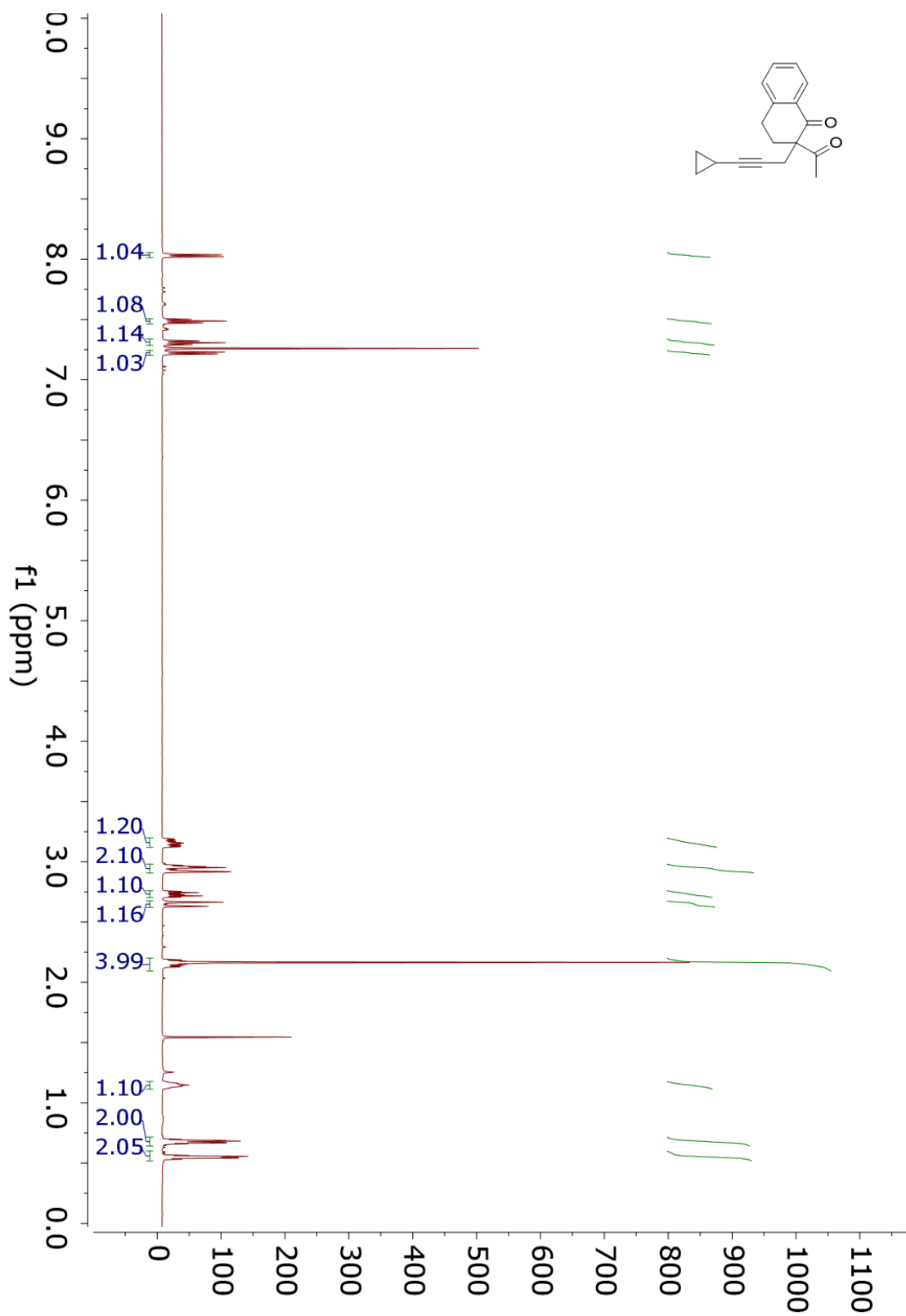
¹H NMR 4.13g



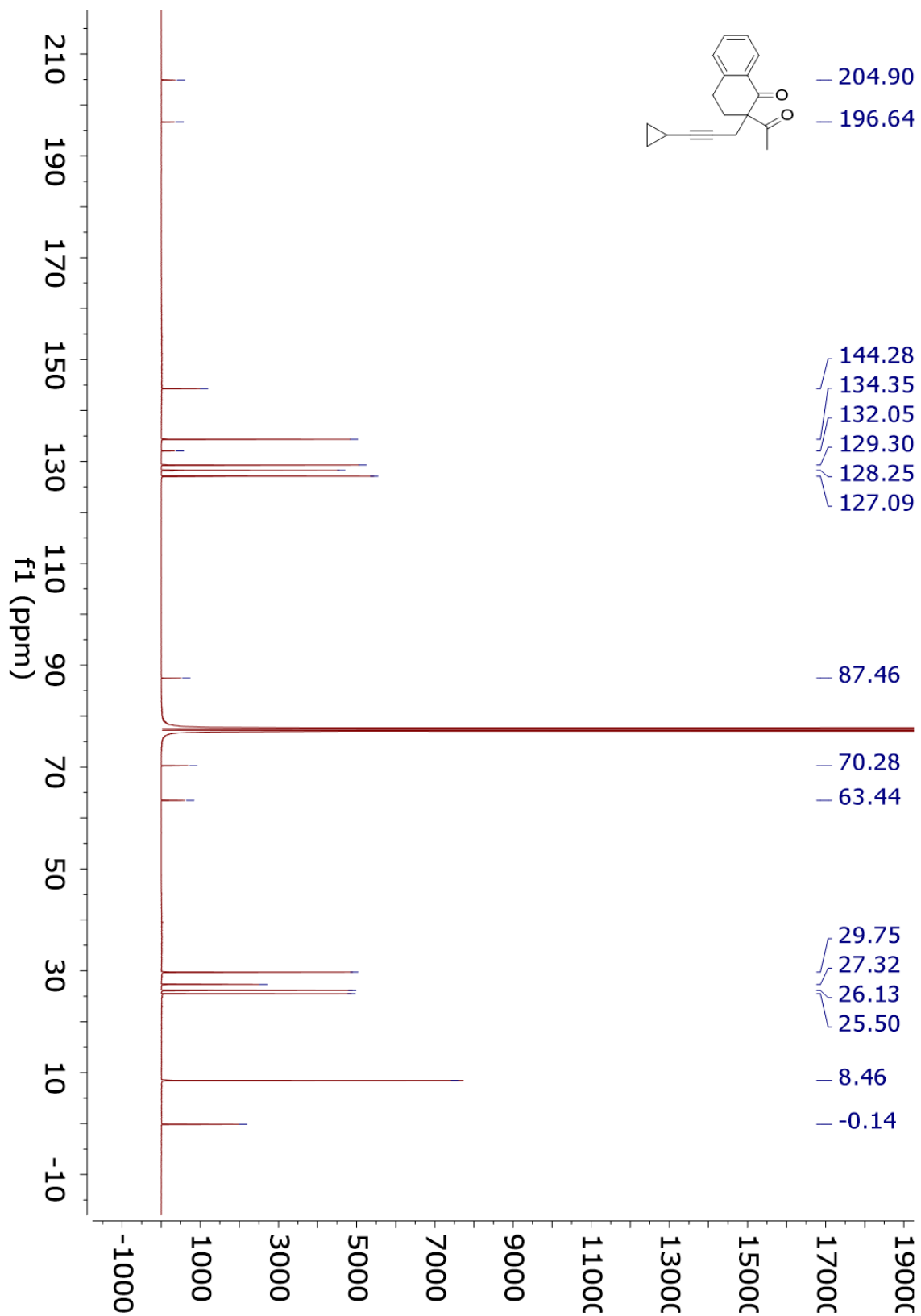
¹³C NMR 4.13g



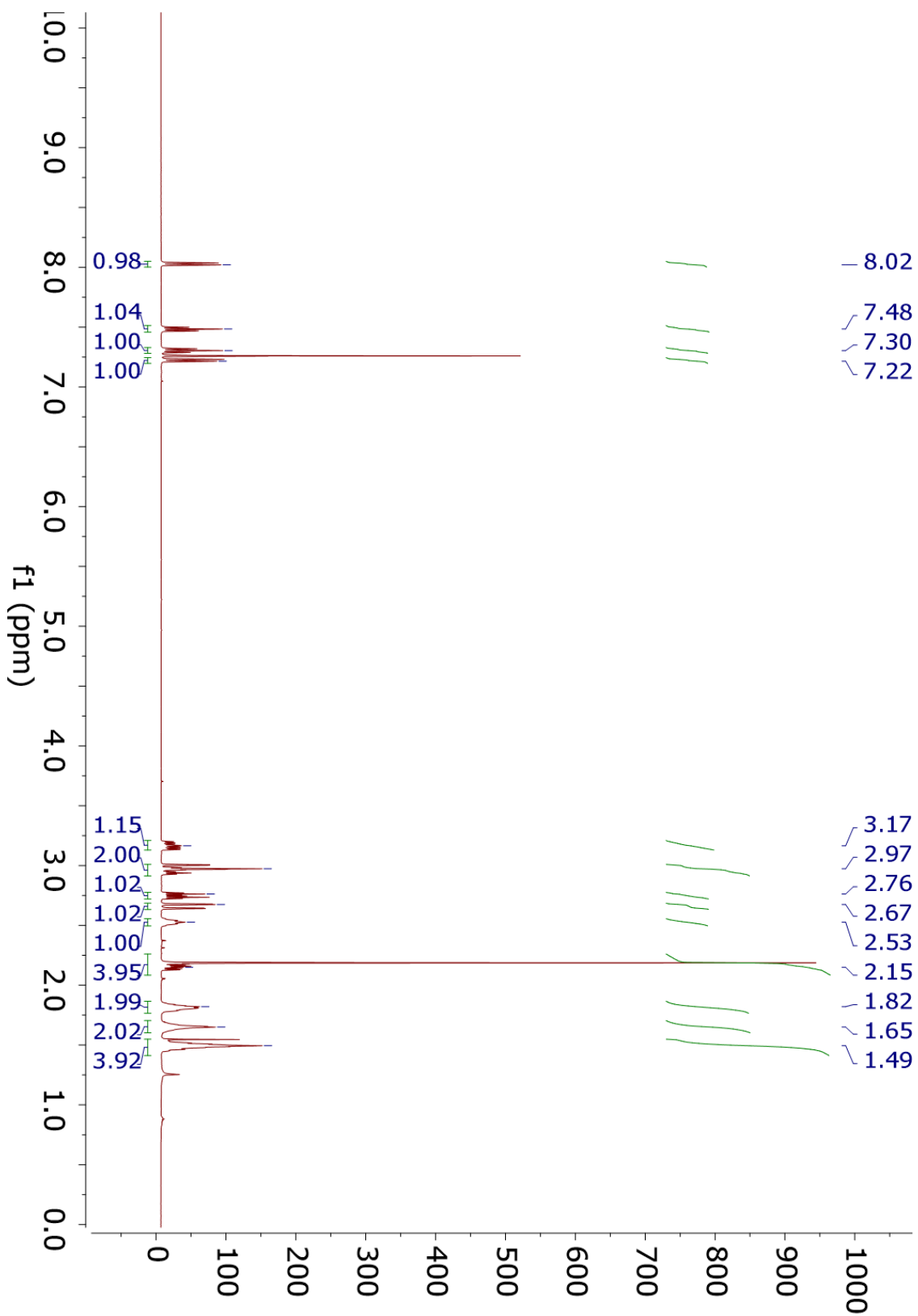
¹H NMR 4.13h



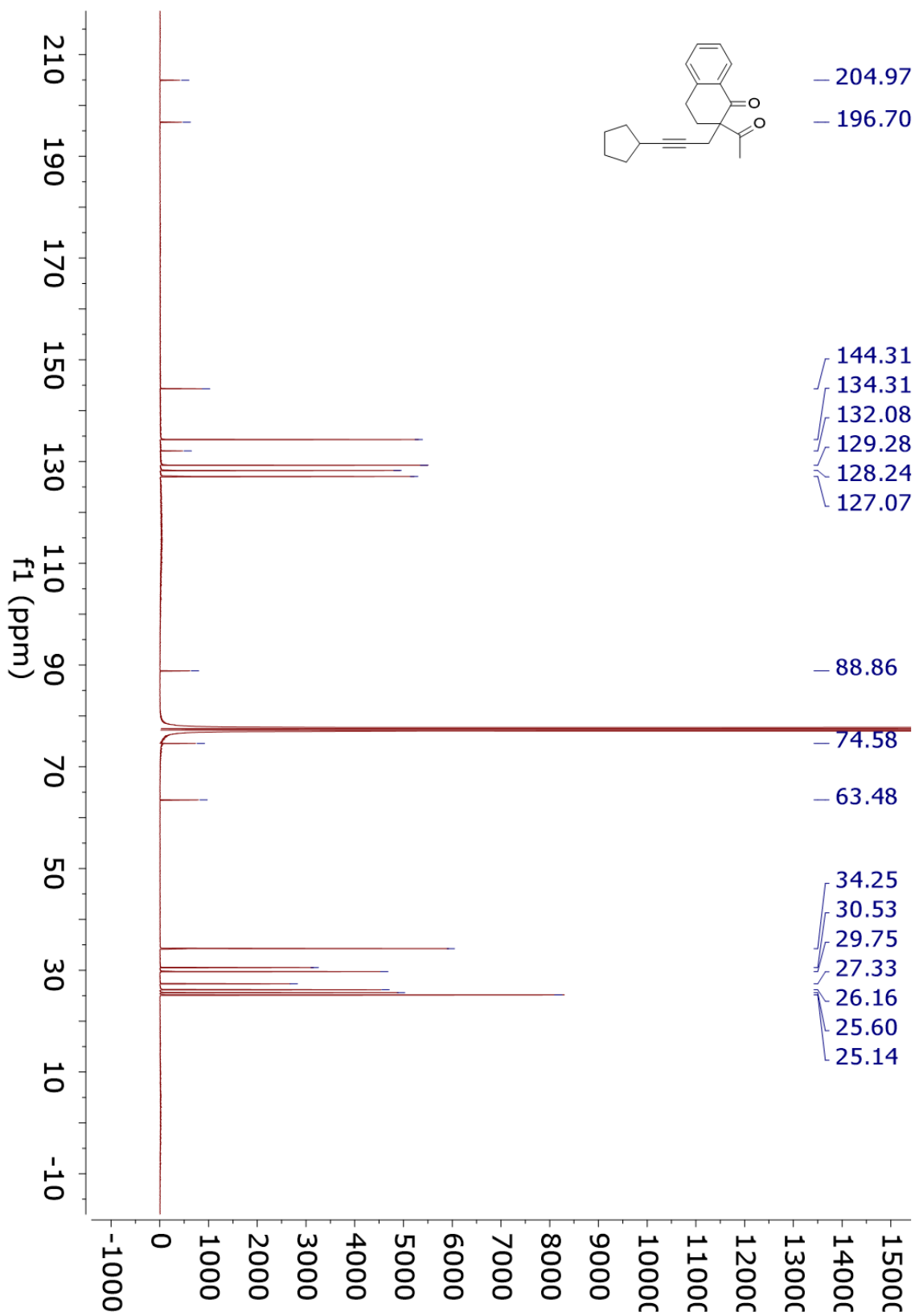
¹³C NMR 4.13h



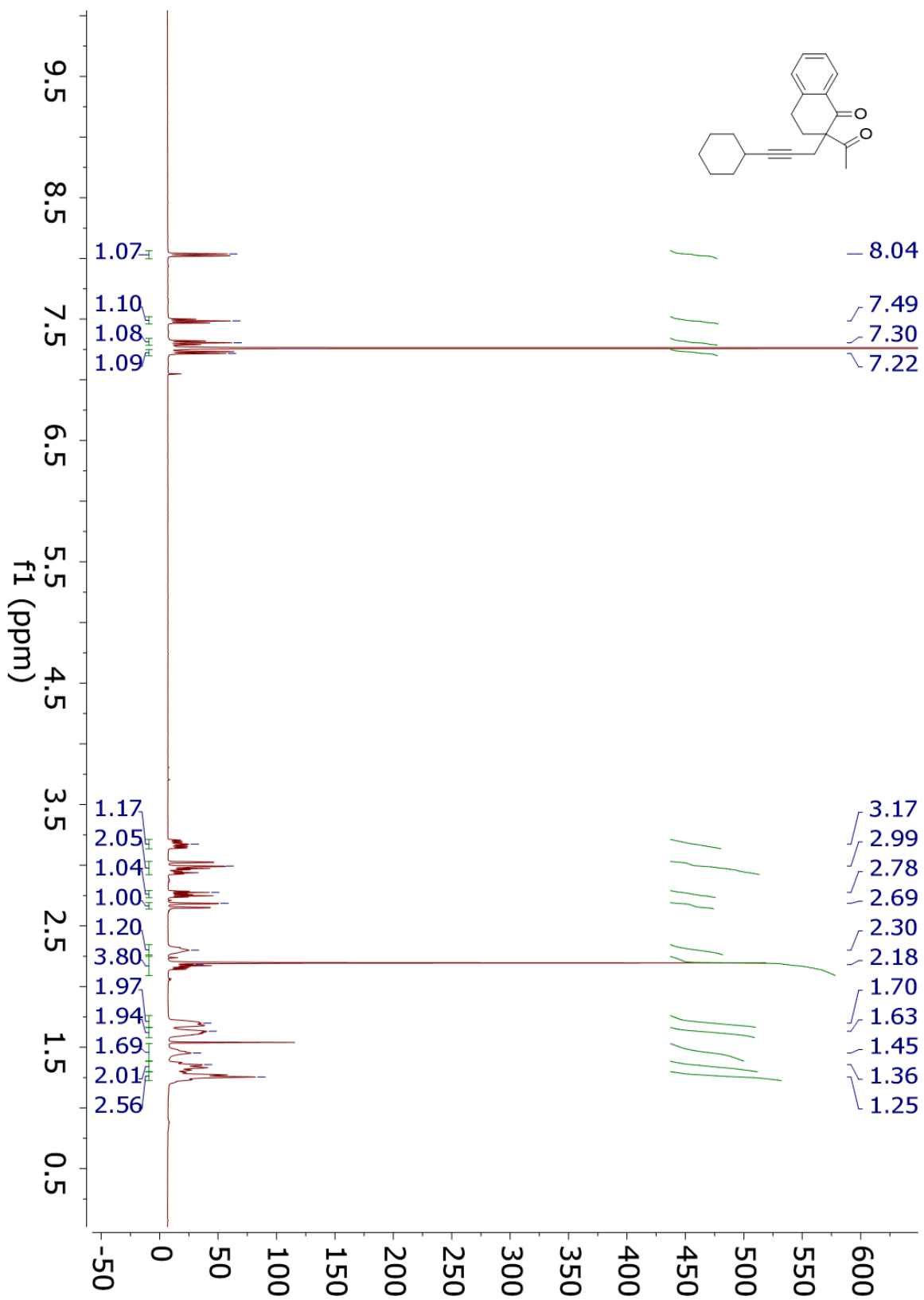
¹H NMR 4.13i



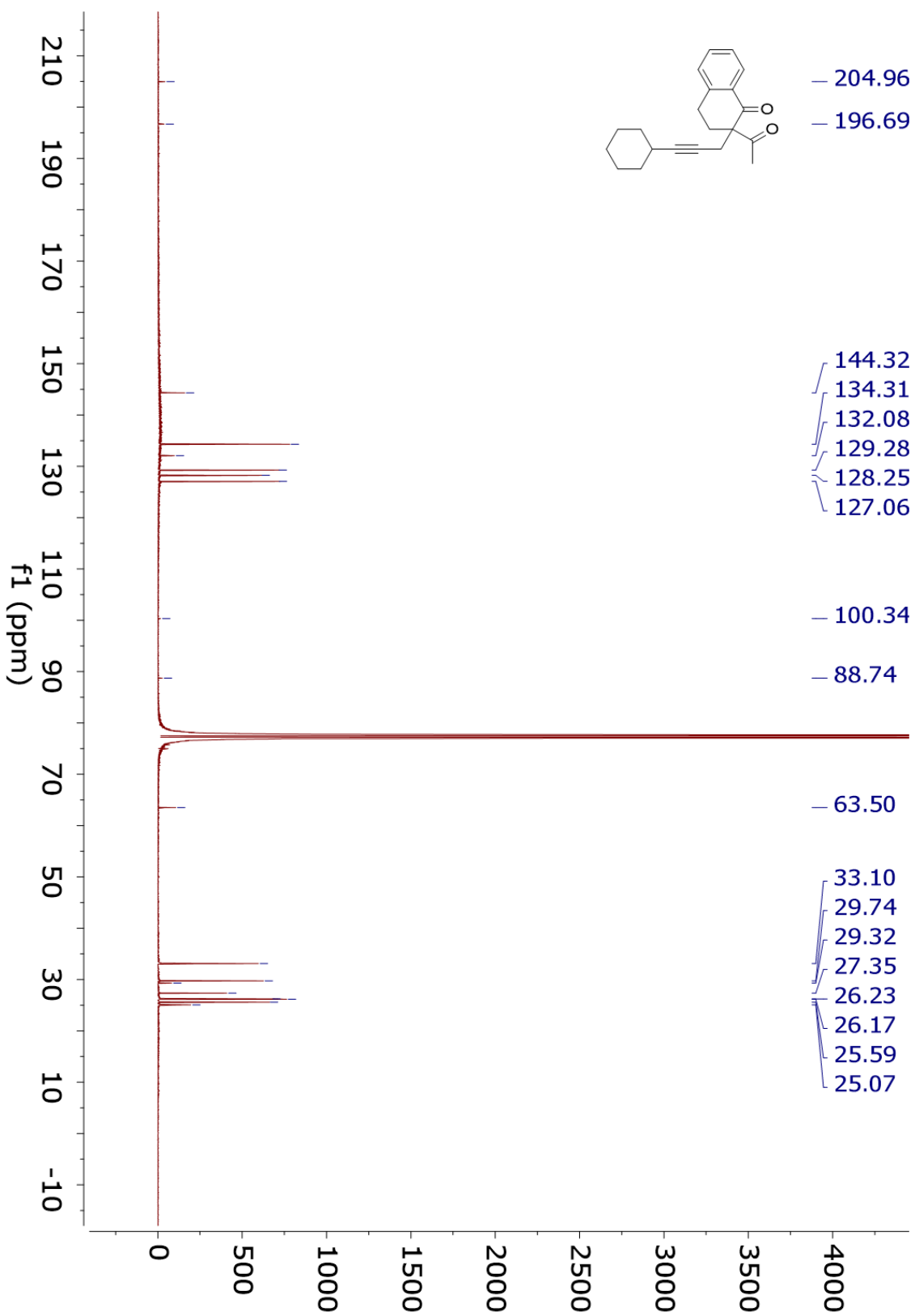
¹³C NMR 4.13i



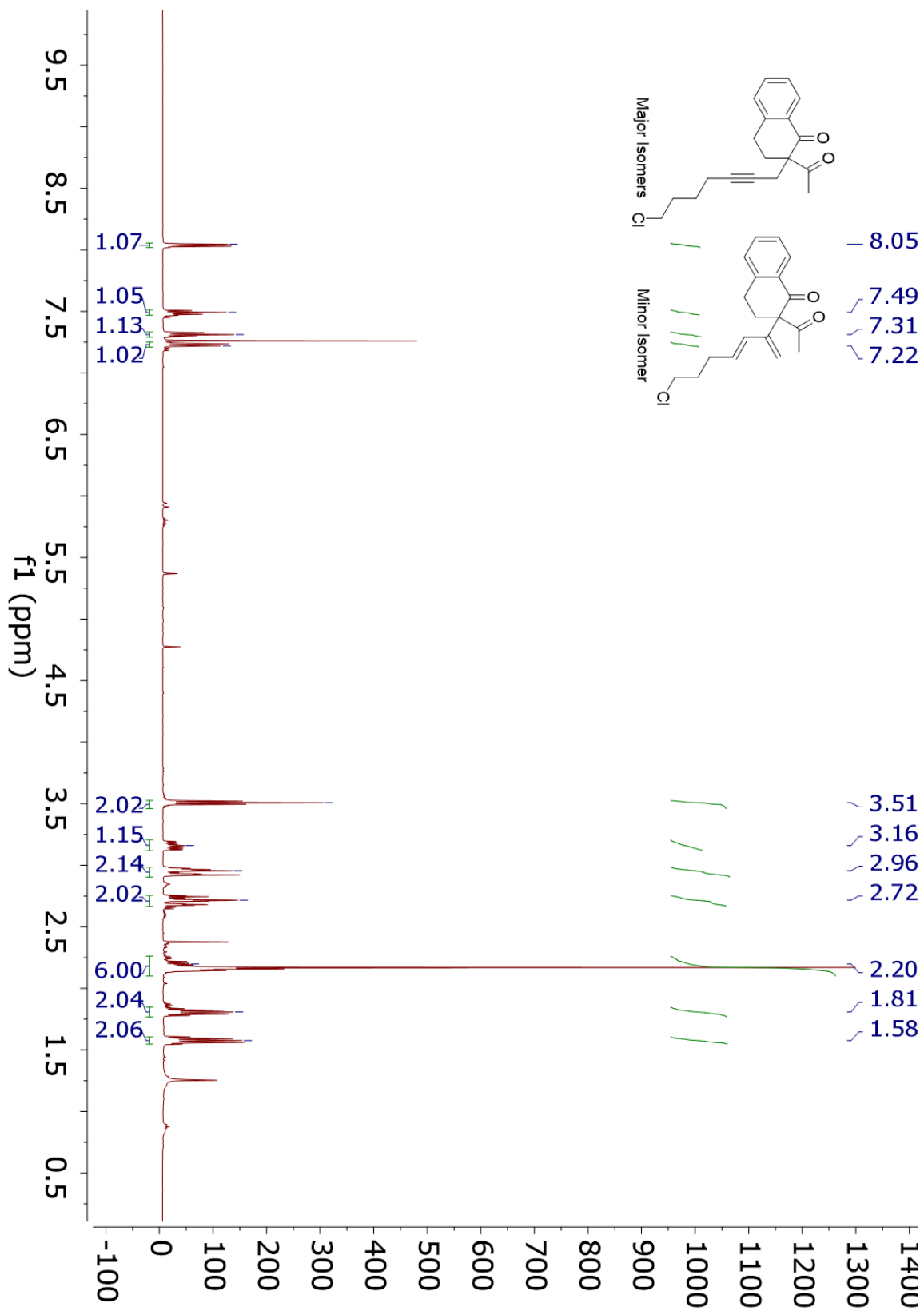
¹H NMR 4.13j



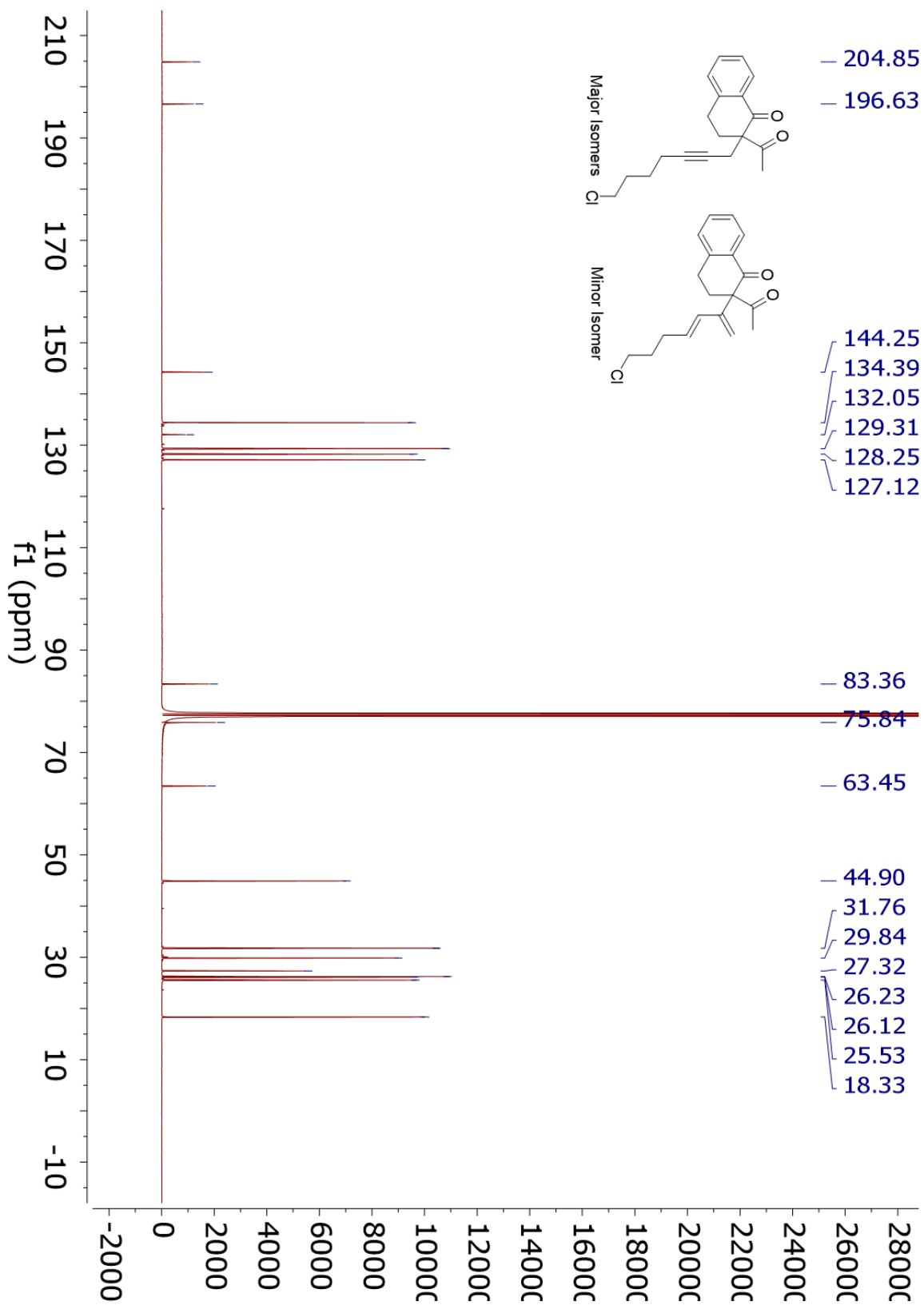
¹³C NMR 4.13j



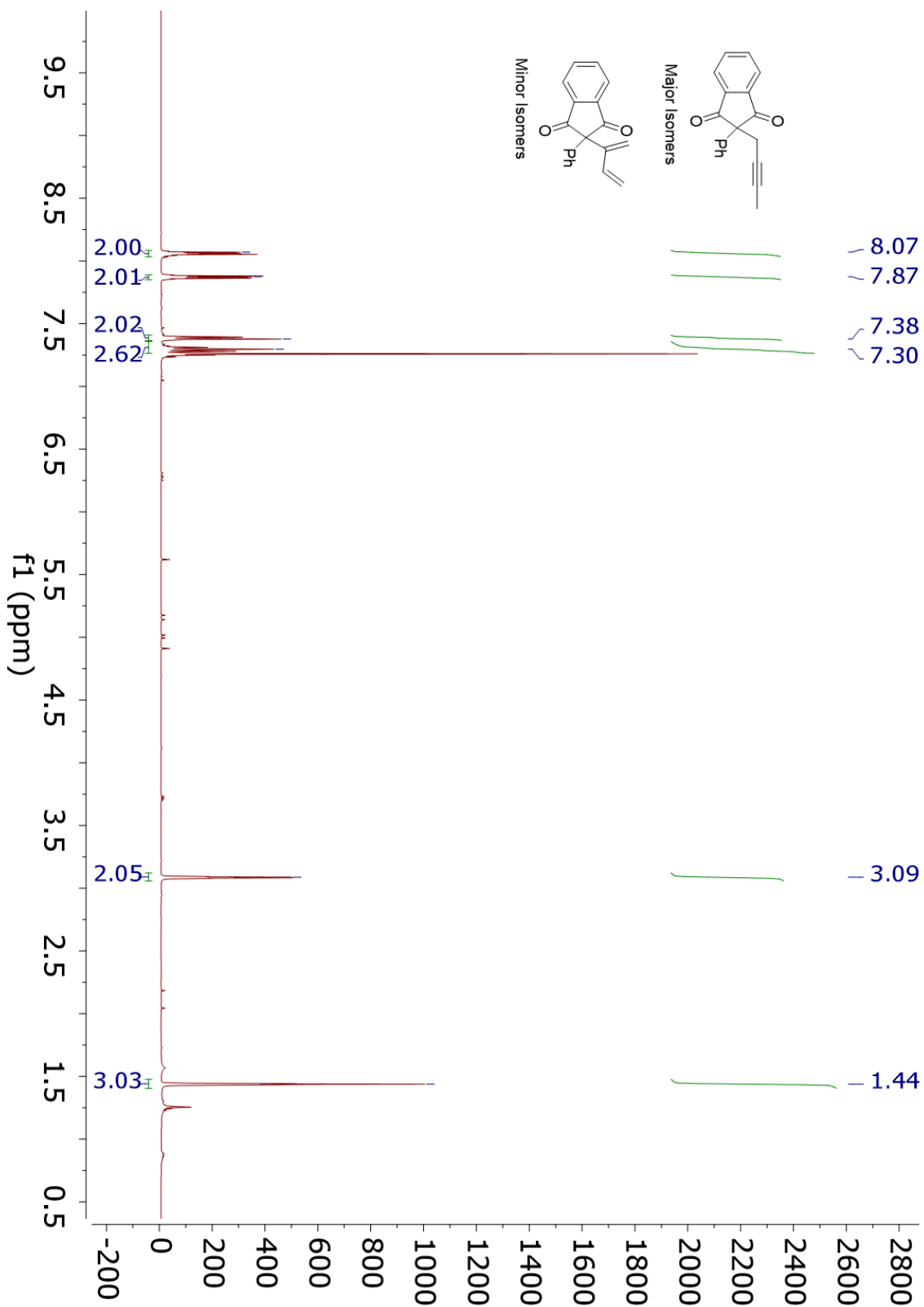
¹H NMR 4.13k



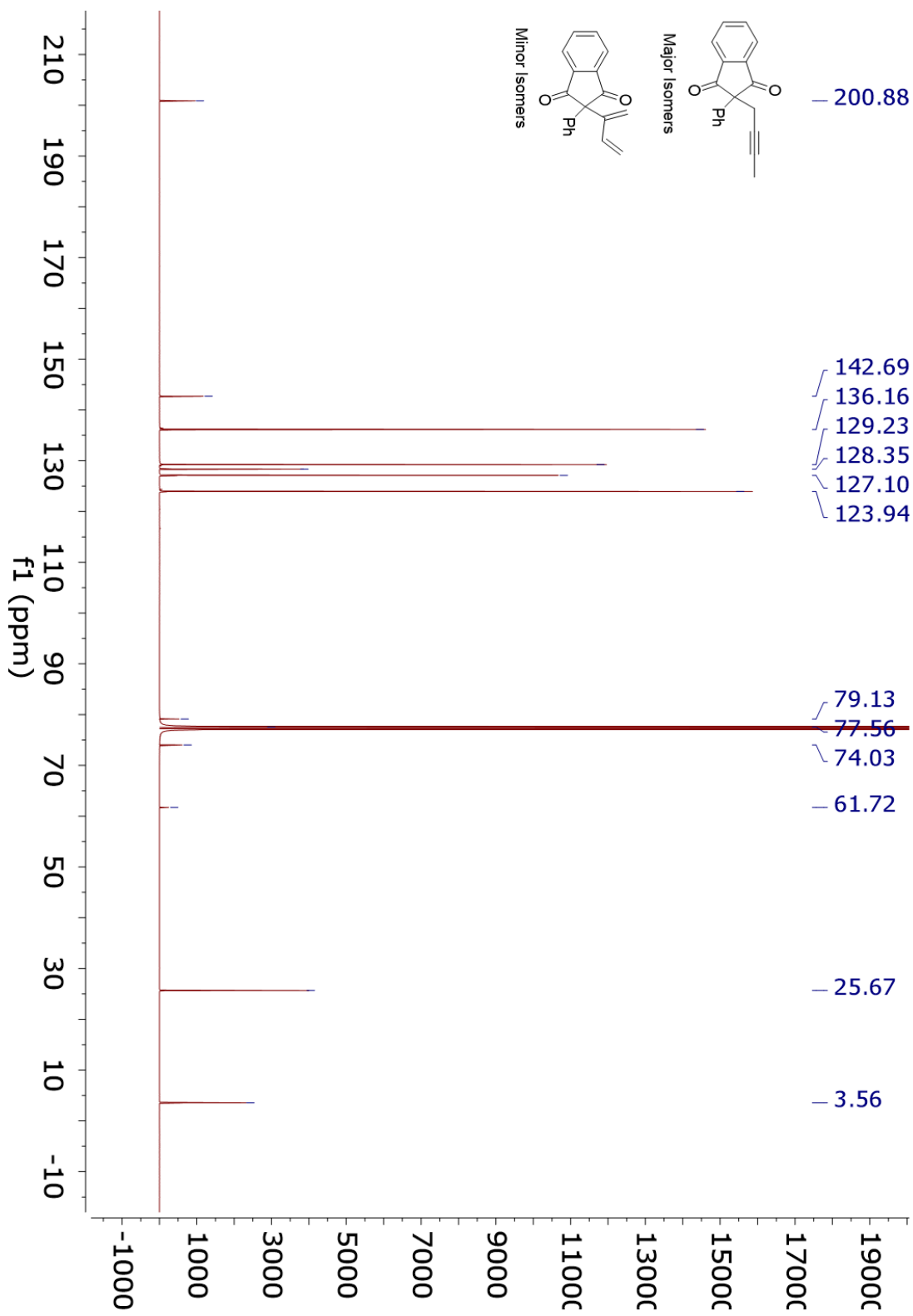
¹³C NMR 4.13k



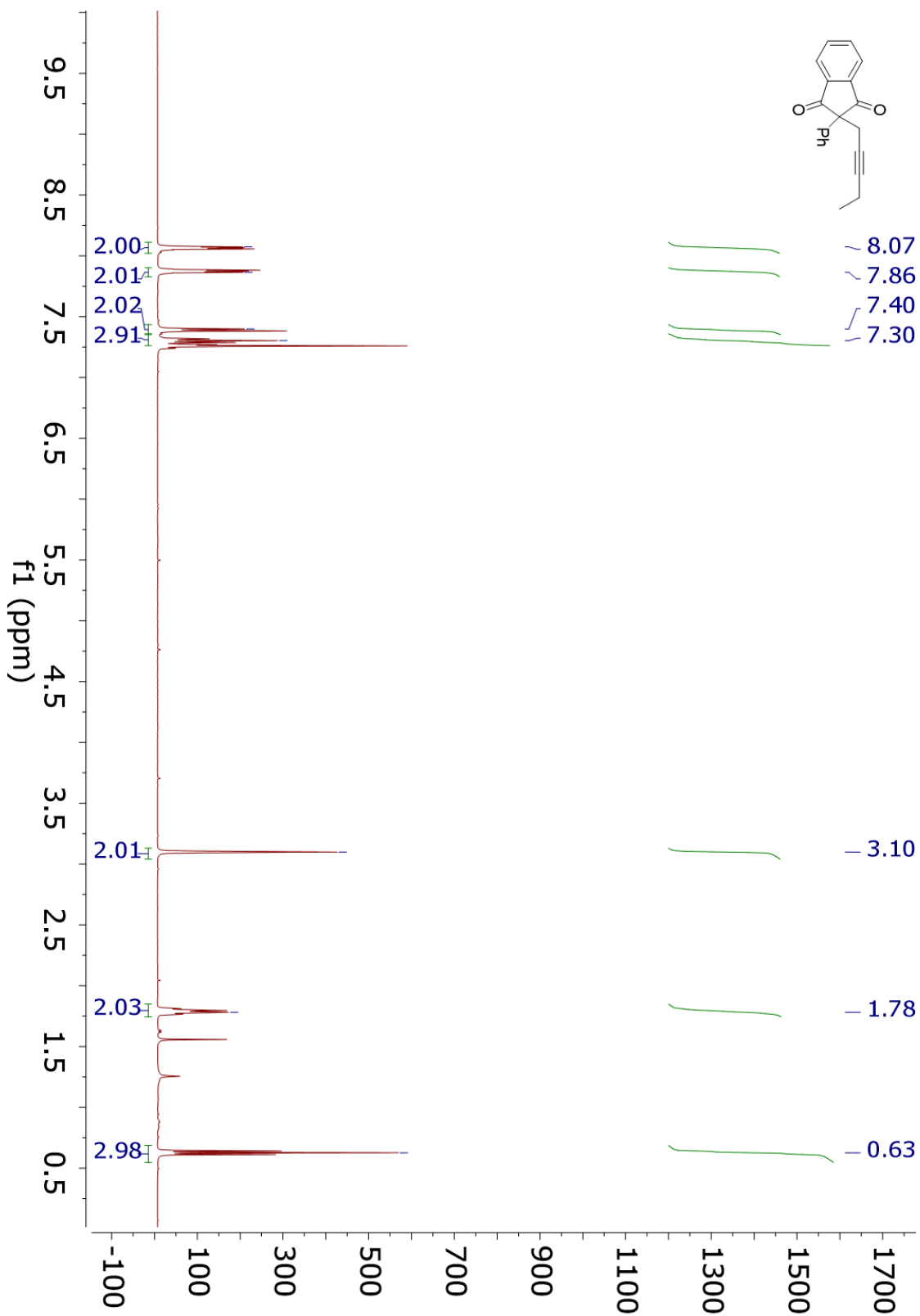
¹H NMR 4.13I



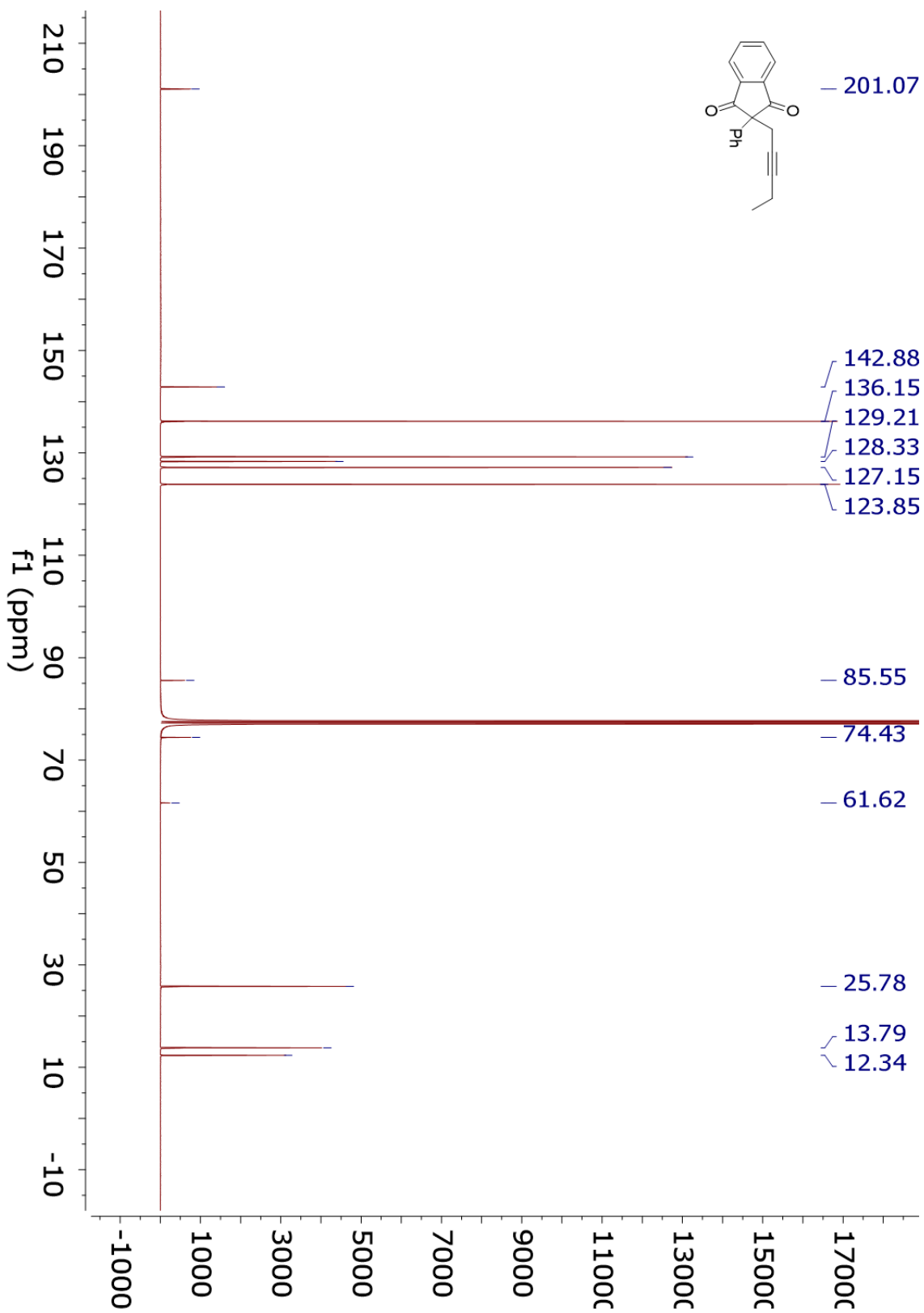
¹³C NMR 4.131



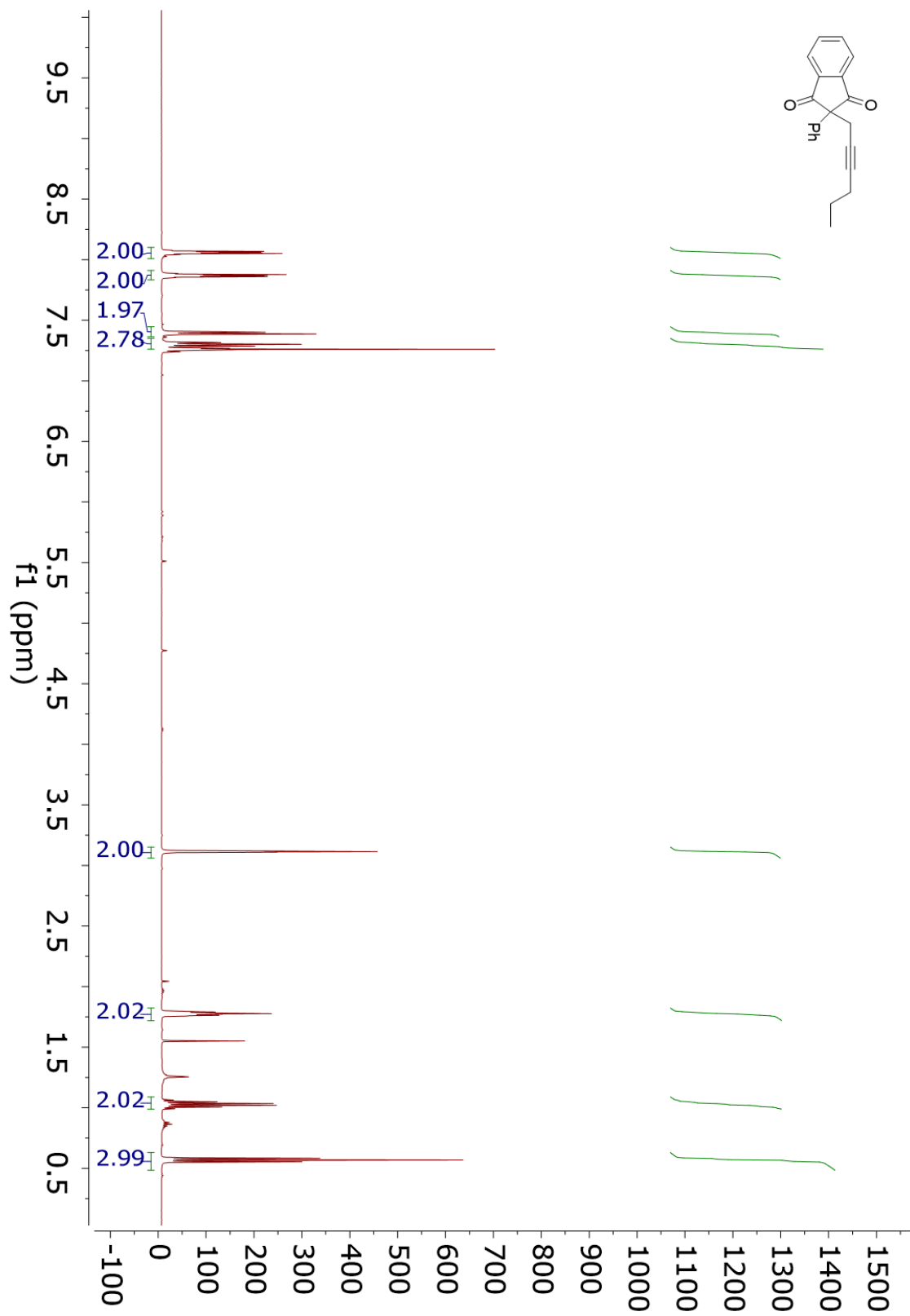
¹H NMR 4.13m



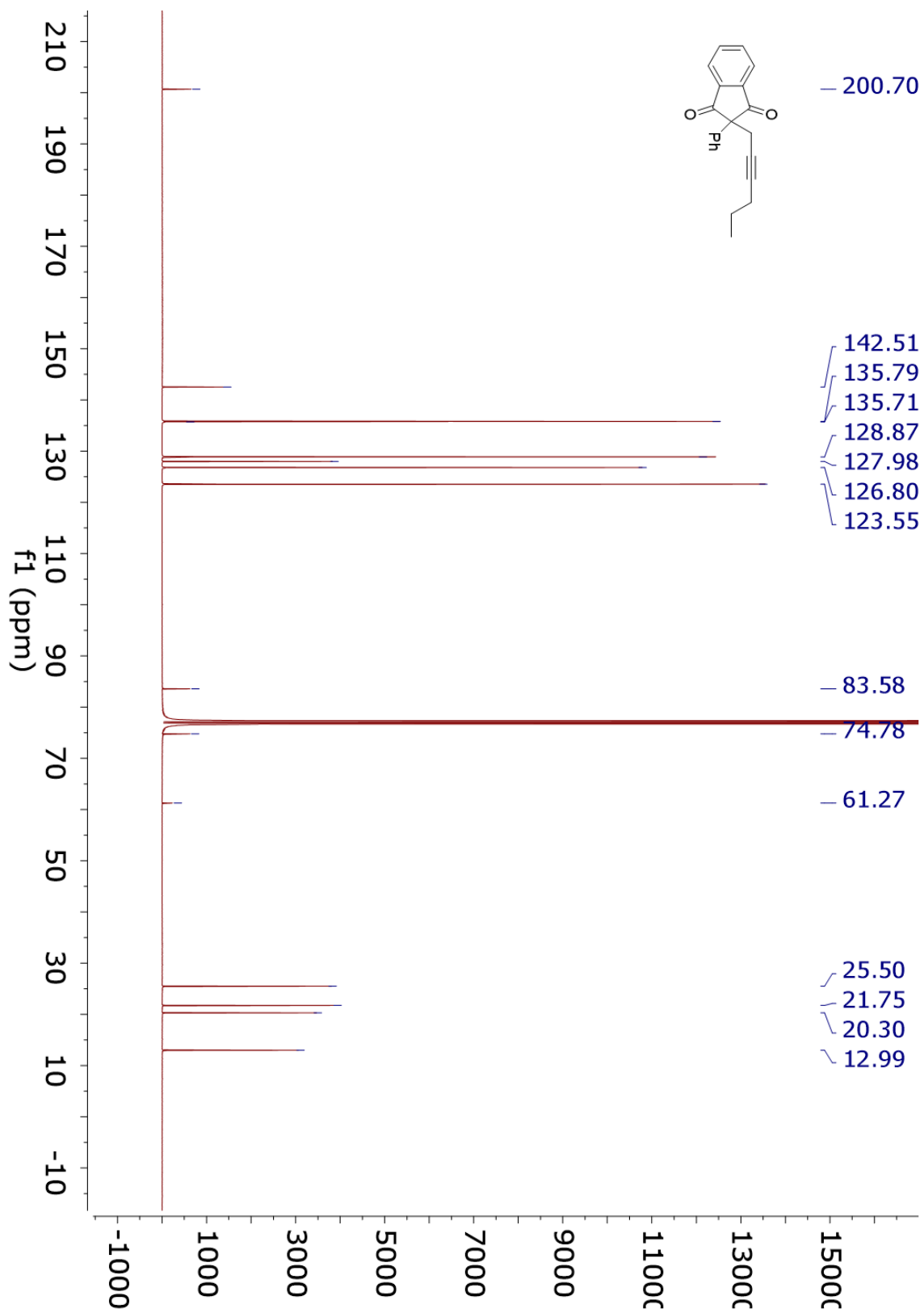
¹³C NMR 4.13m



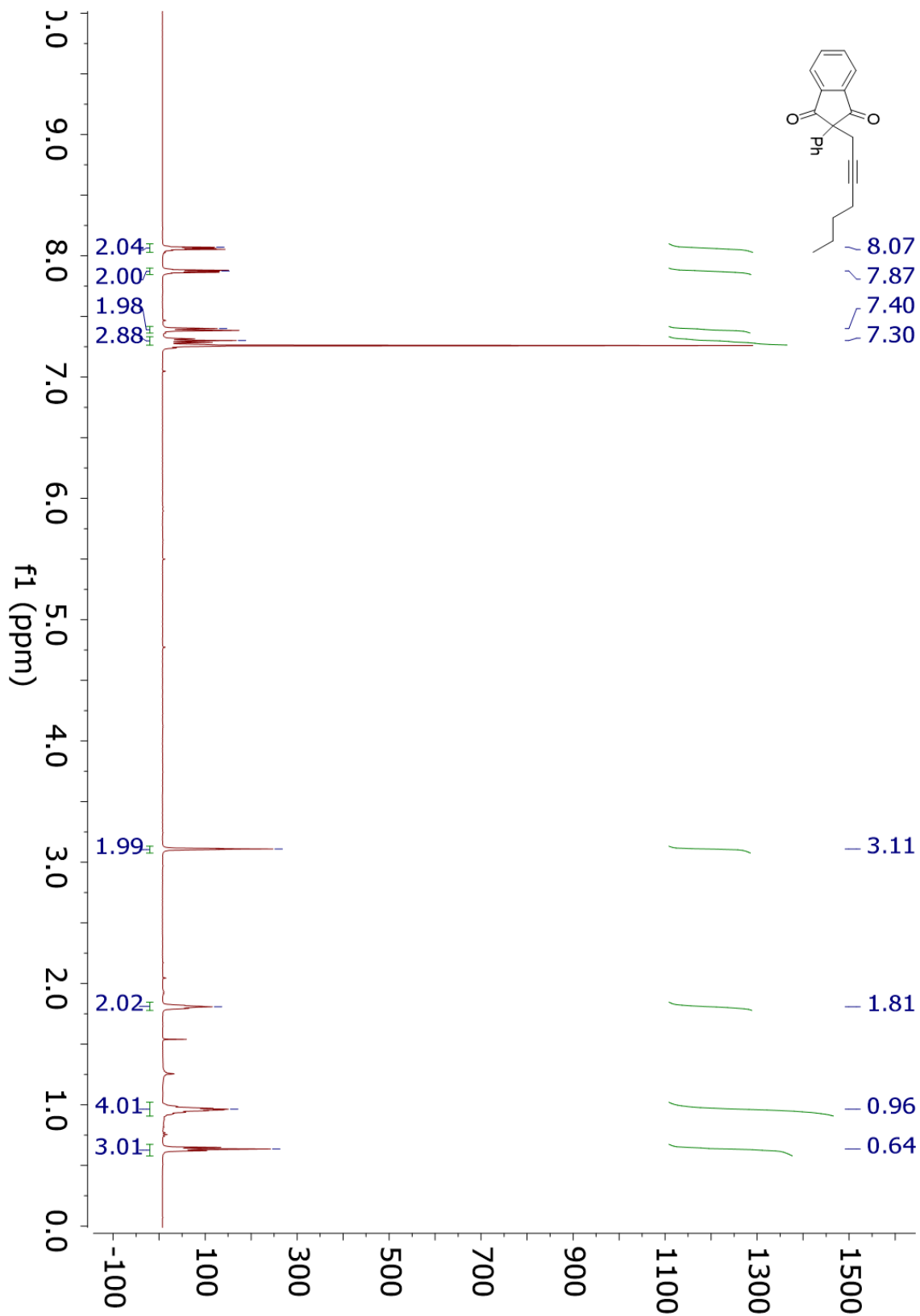
¹H NMR 4.13n



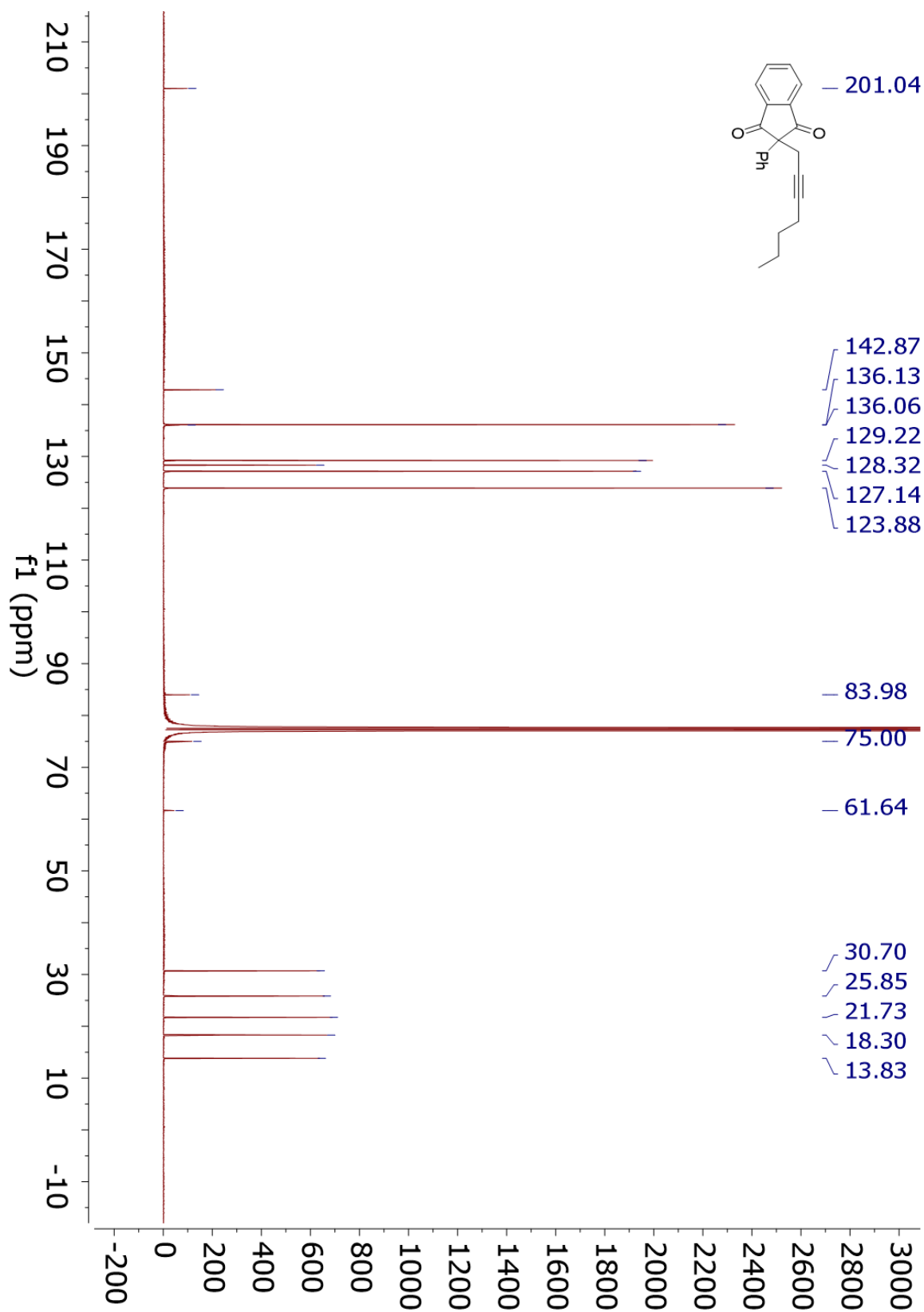
¹³C NMR 4.13n



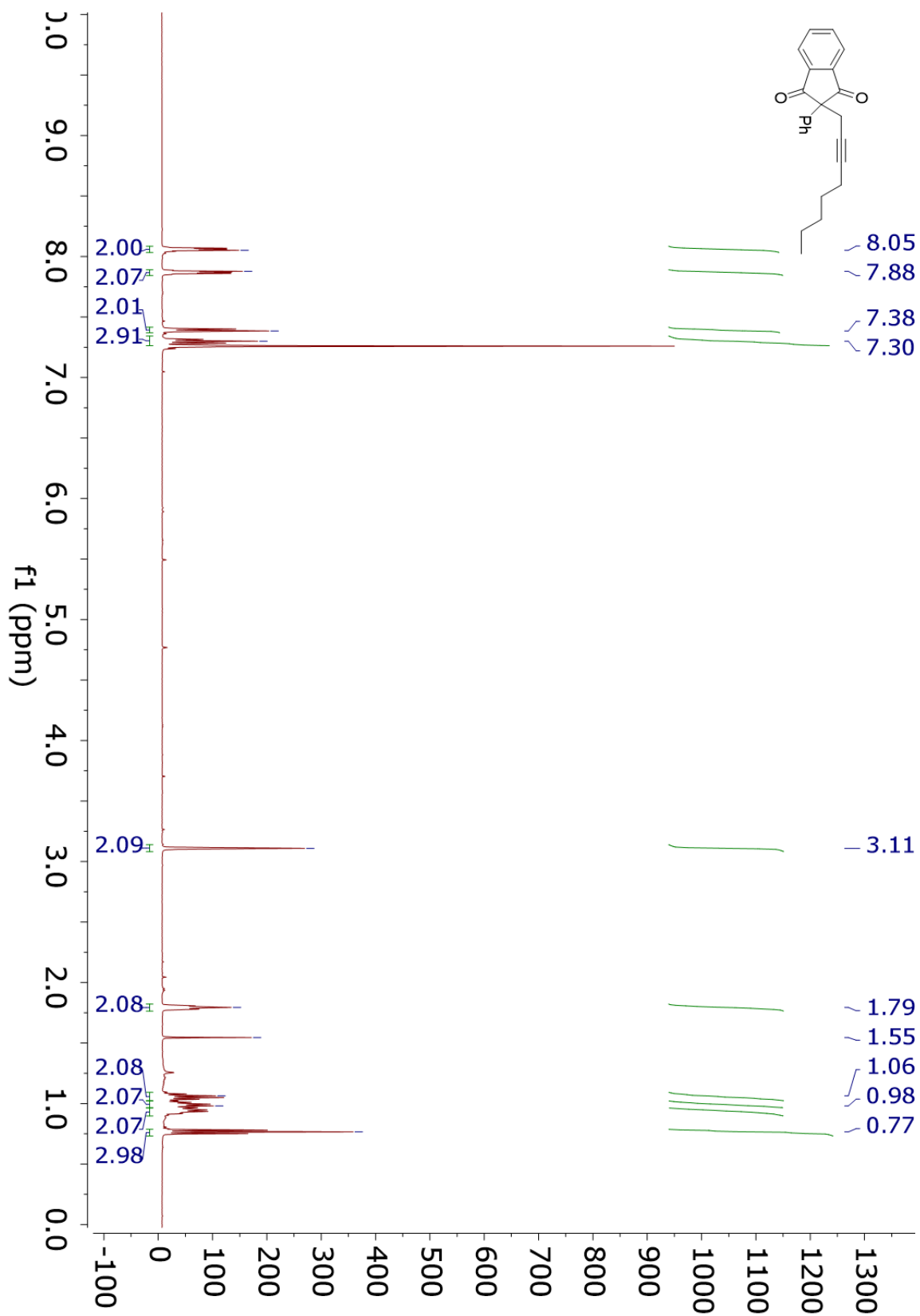
¹H NMR 4.13o



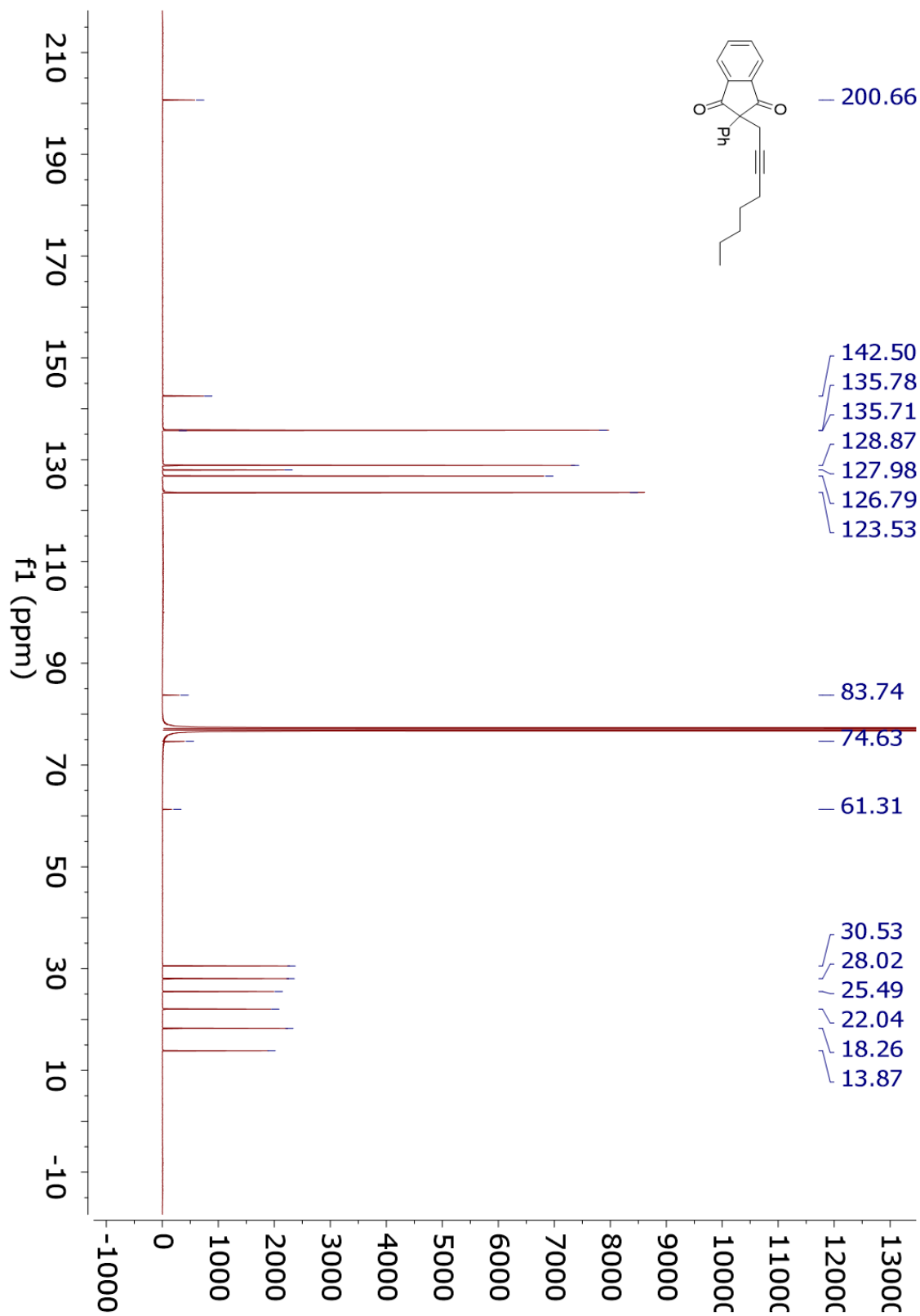
¹³C NMR 4.13o



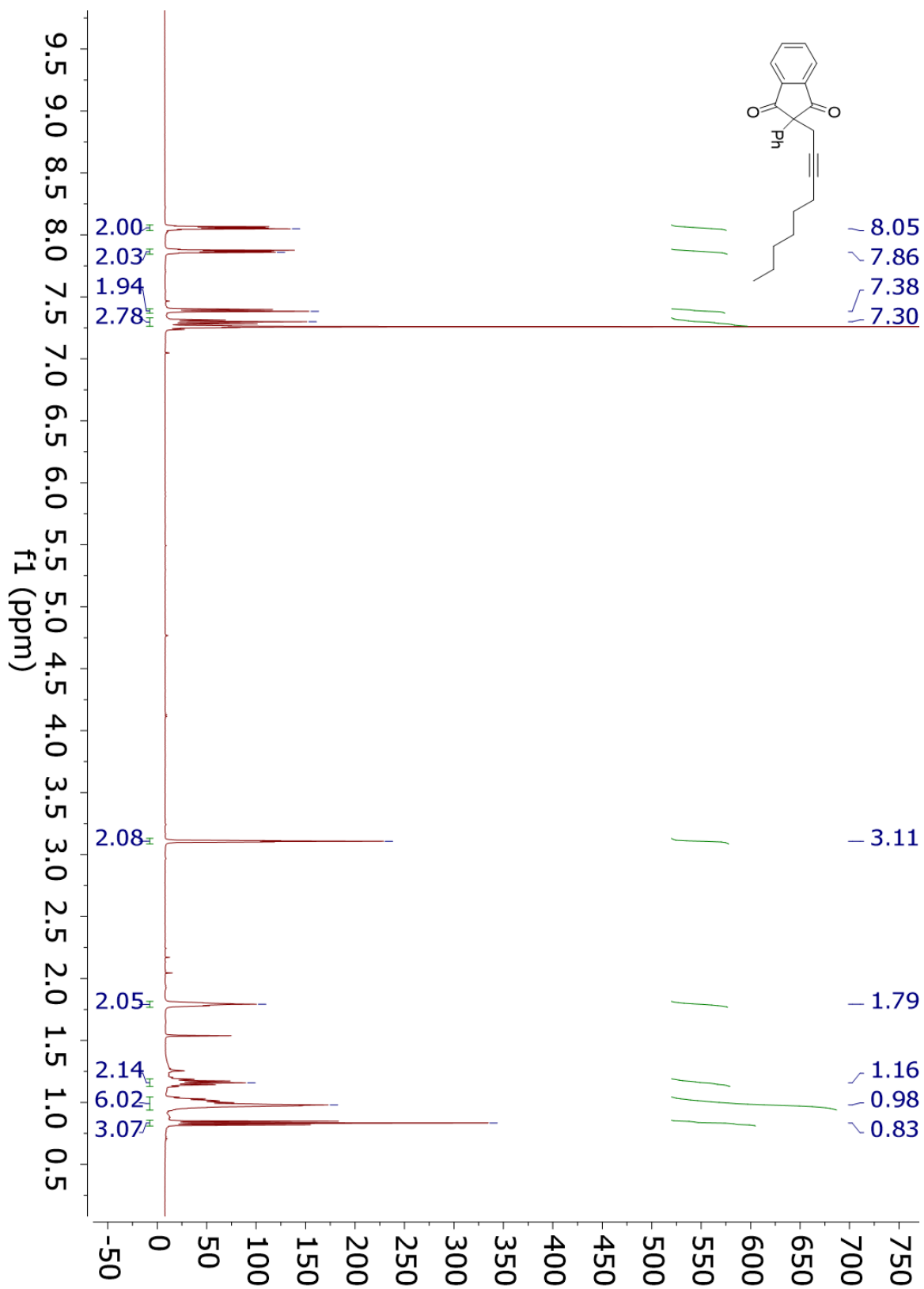
¹H NMR 4.13p



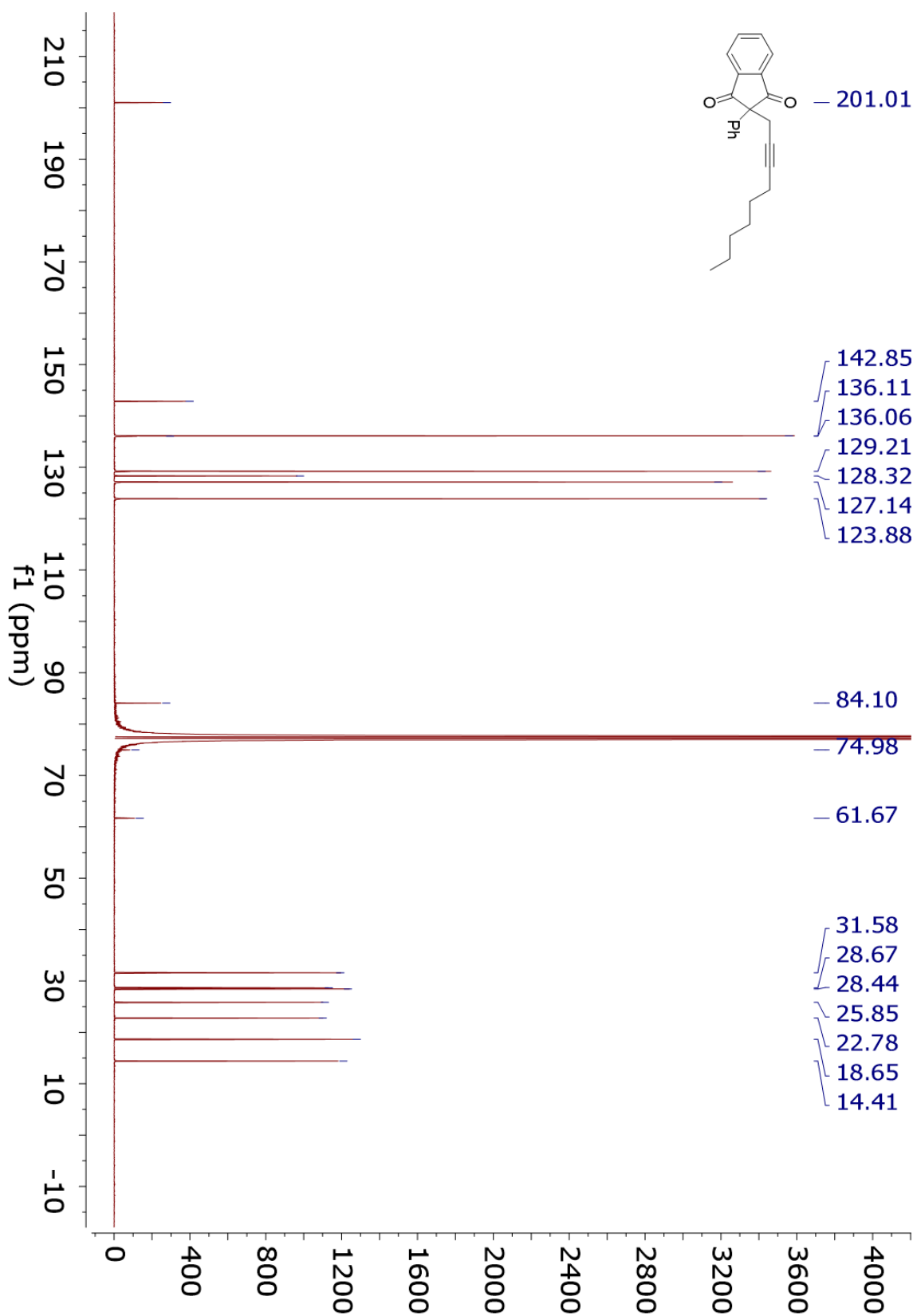
¹³C NMR 4.13p



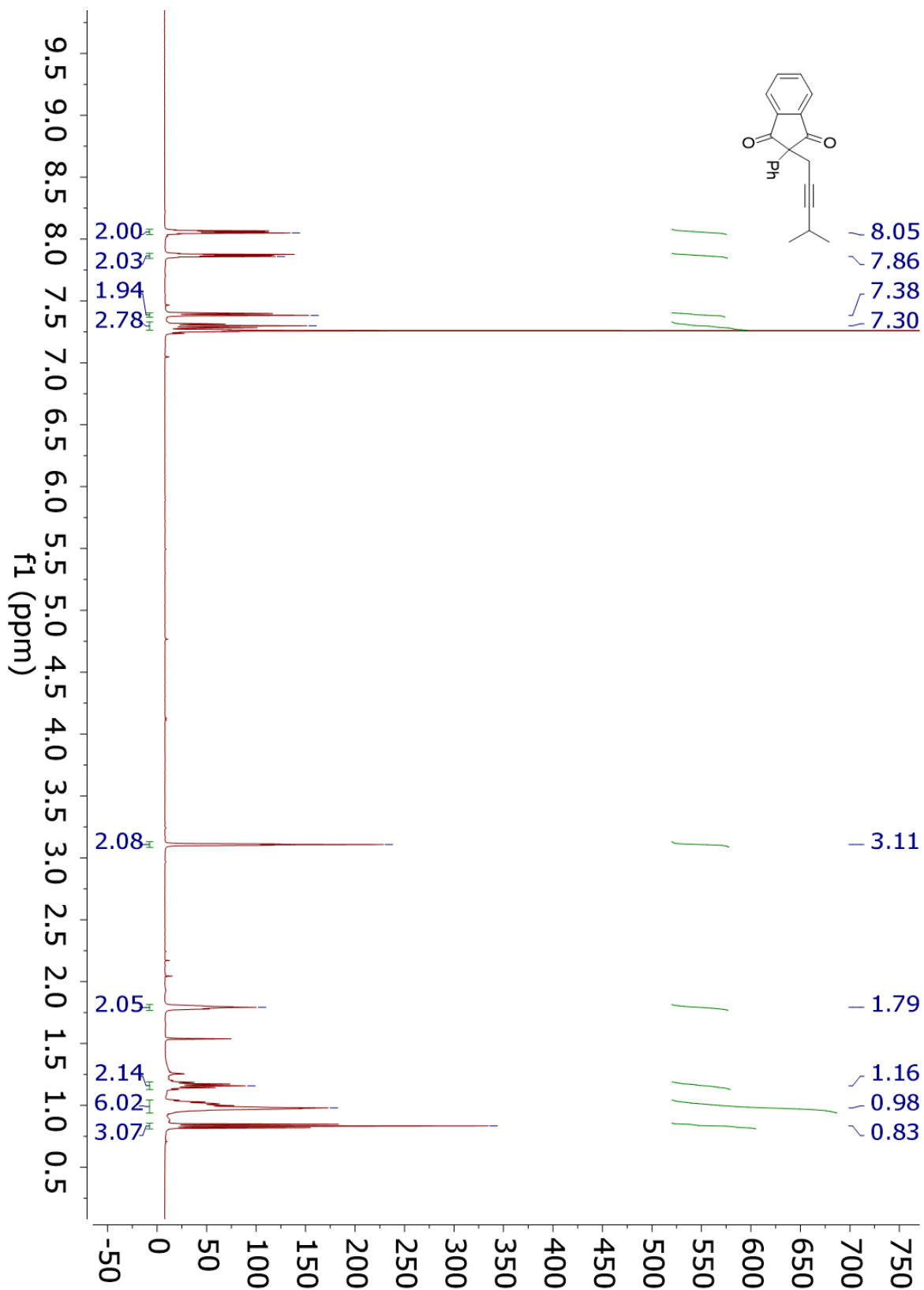
¹H NMR 4.13q



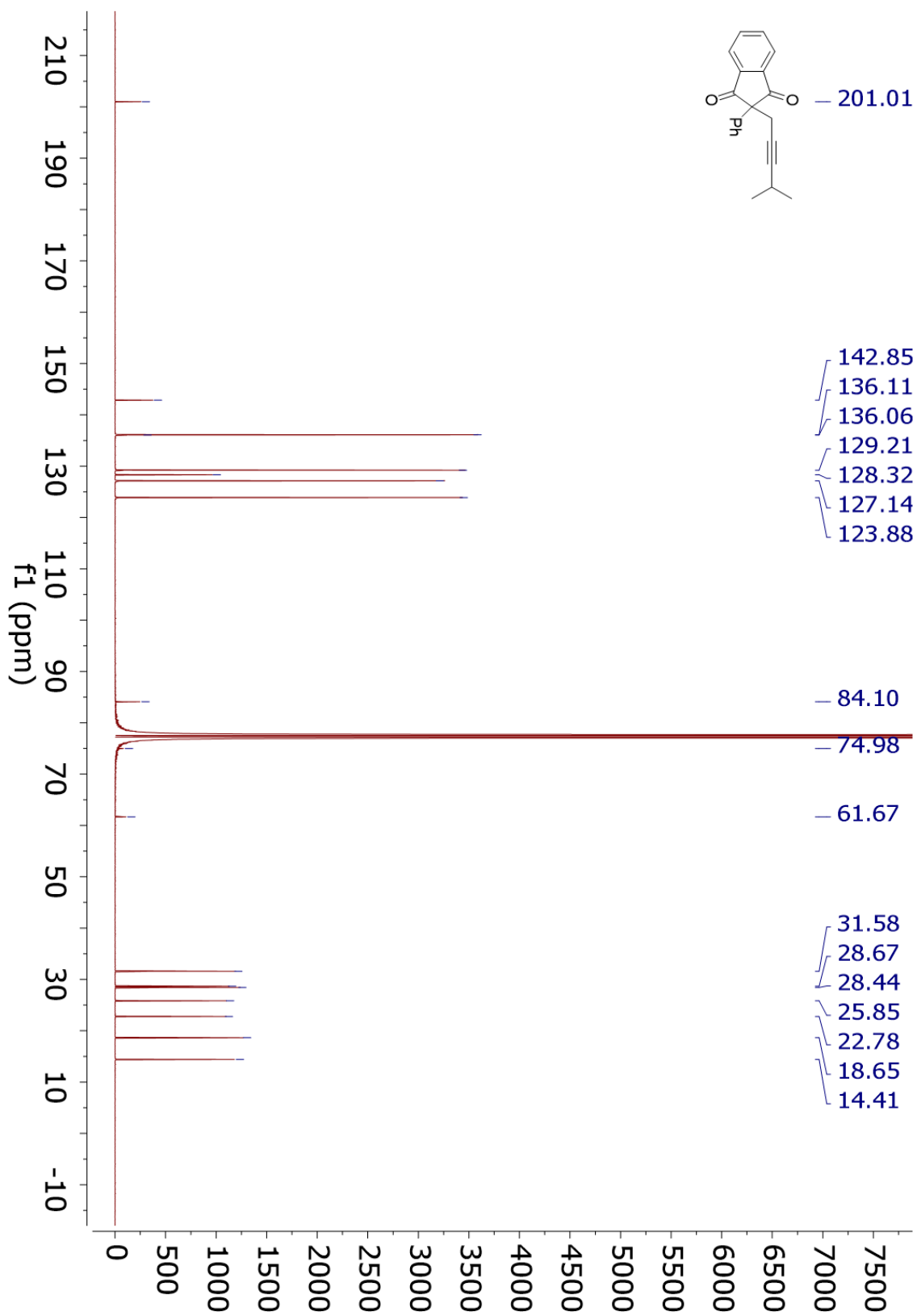
¹³C NMR 4.13q



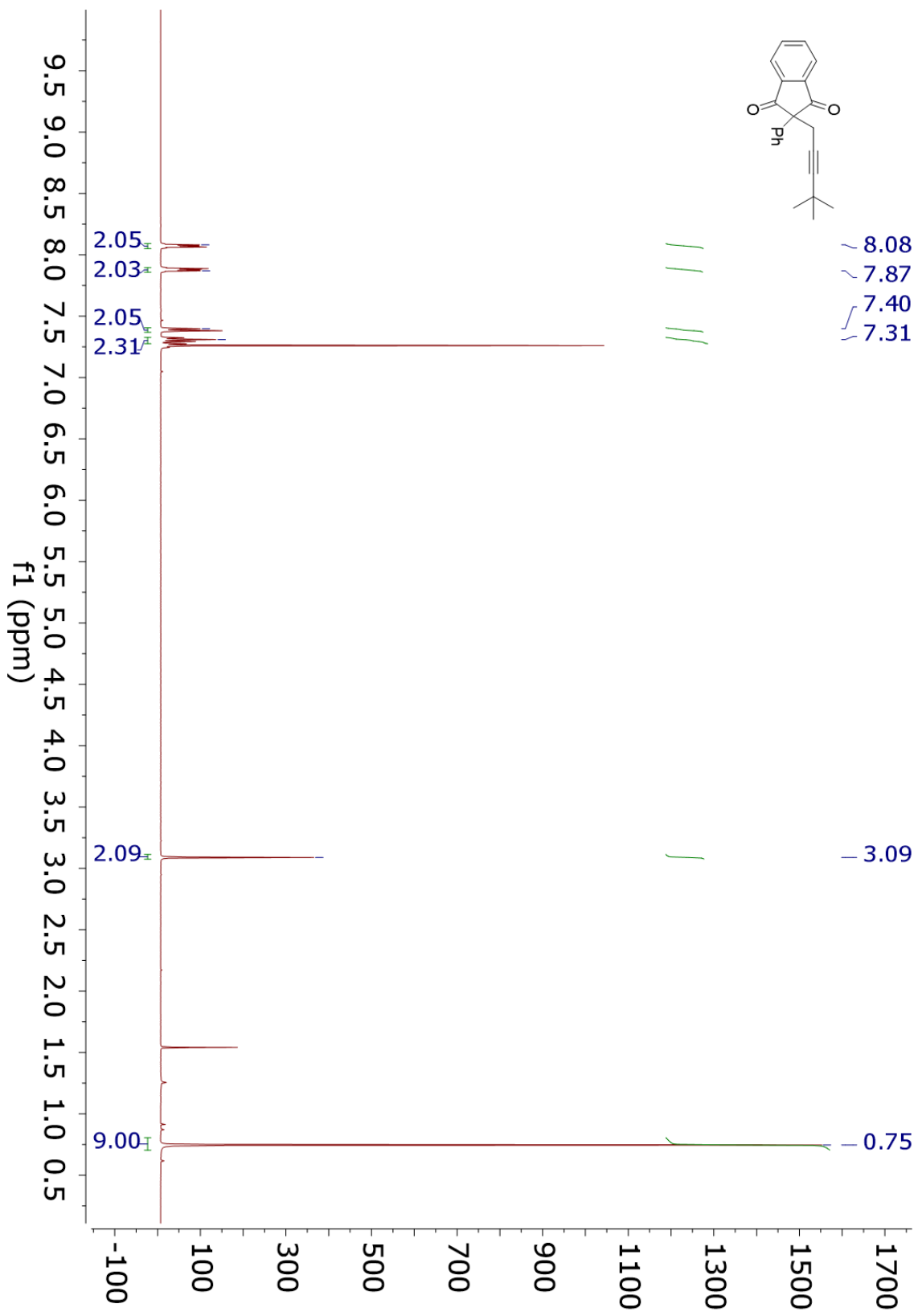
¹H NMR 4.13r



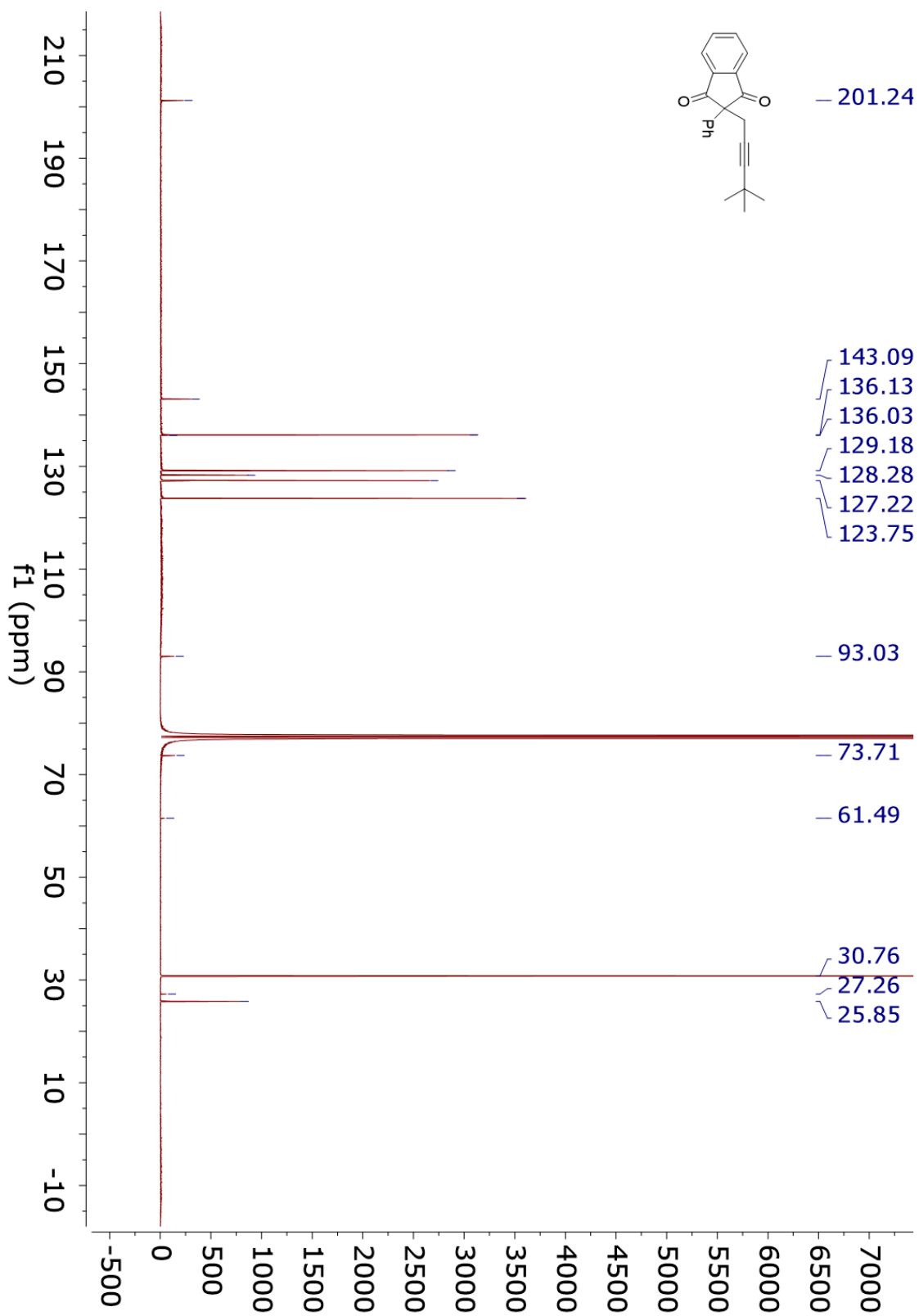
¹³C NMR 4.13r



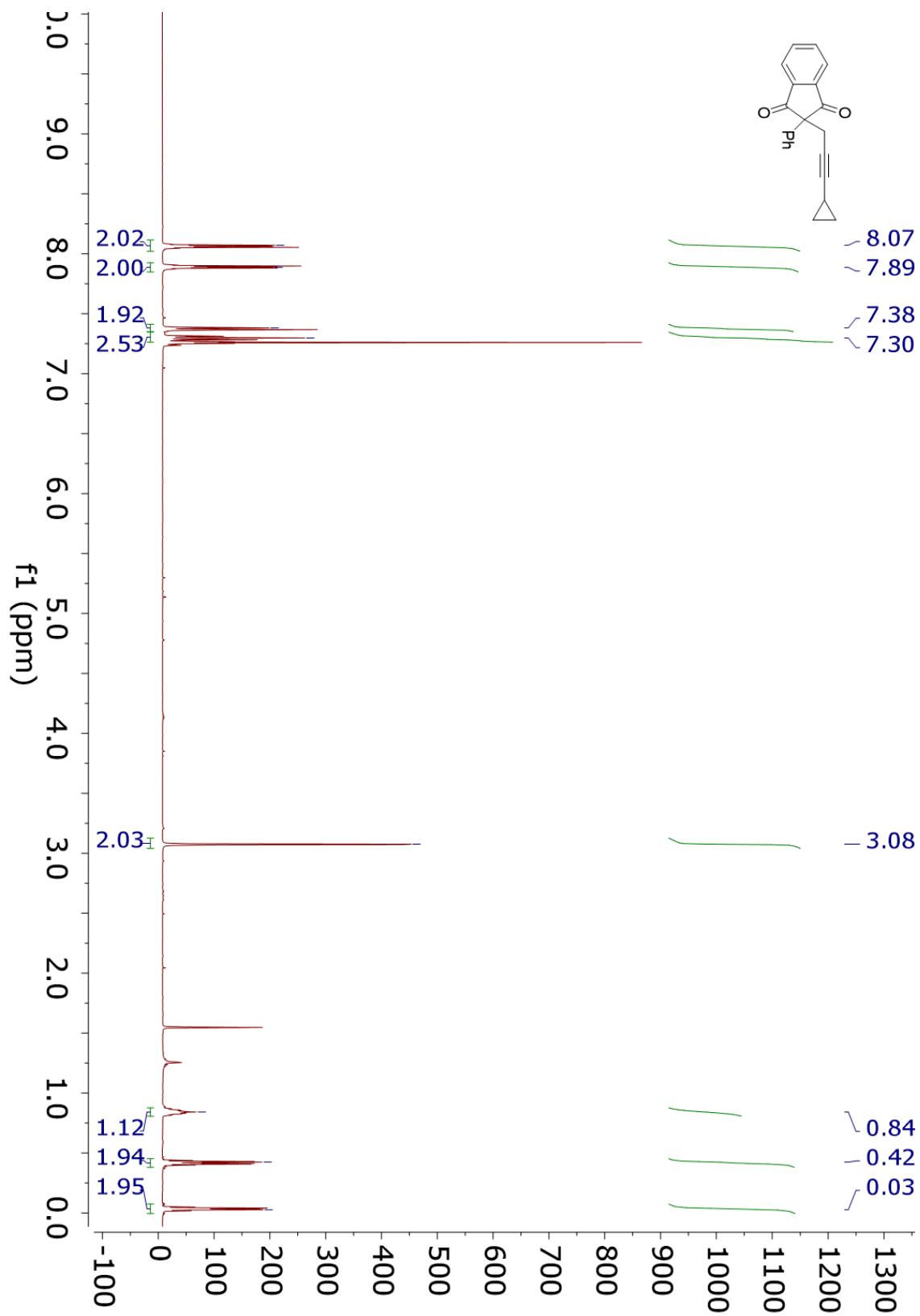
¹H NMR 4.13s



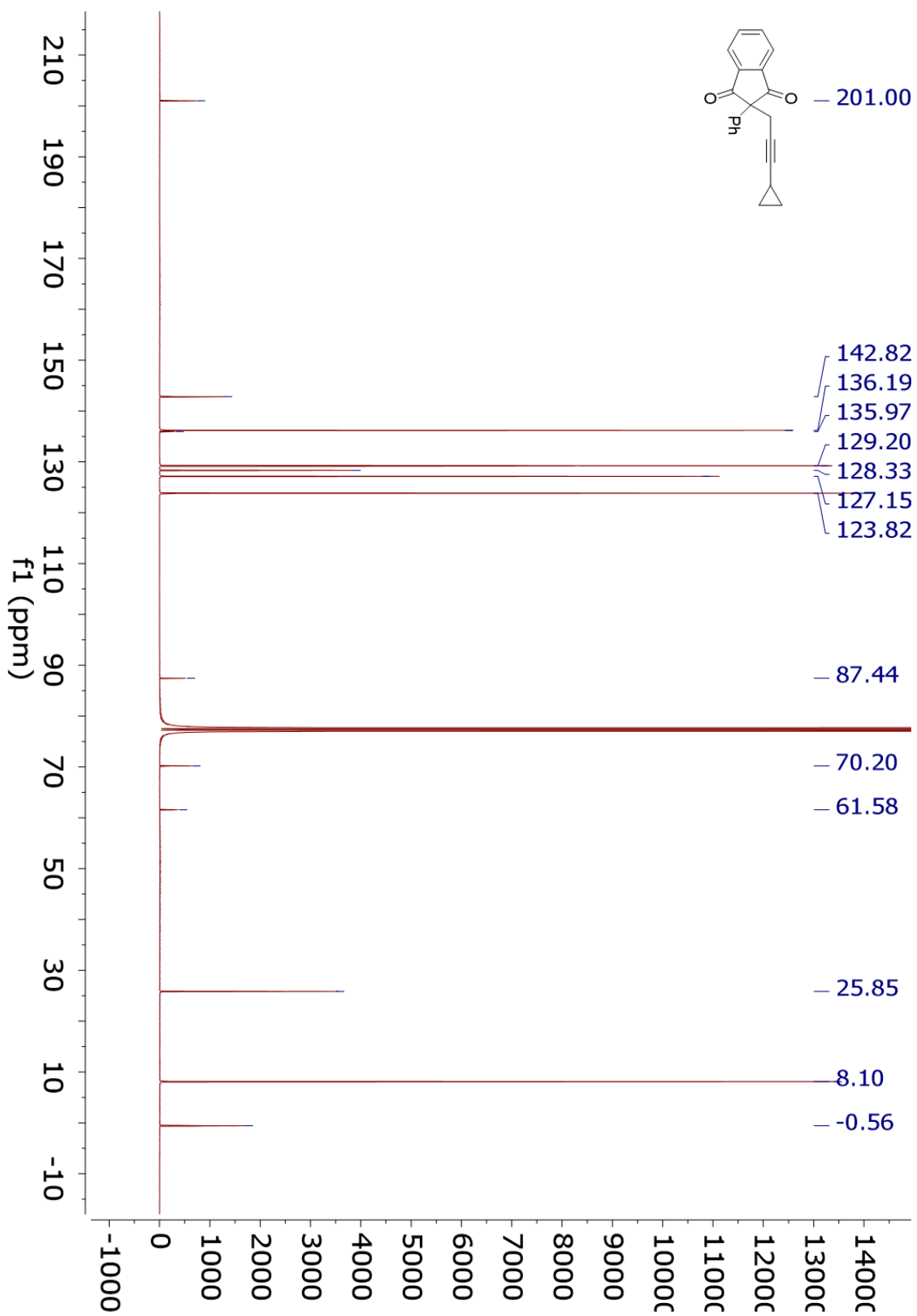
¹³C NMR 4.13s



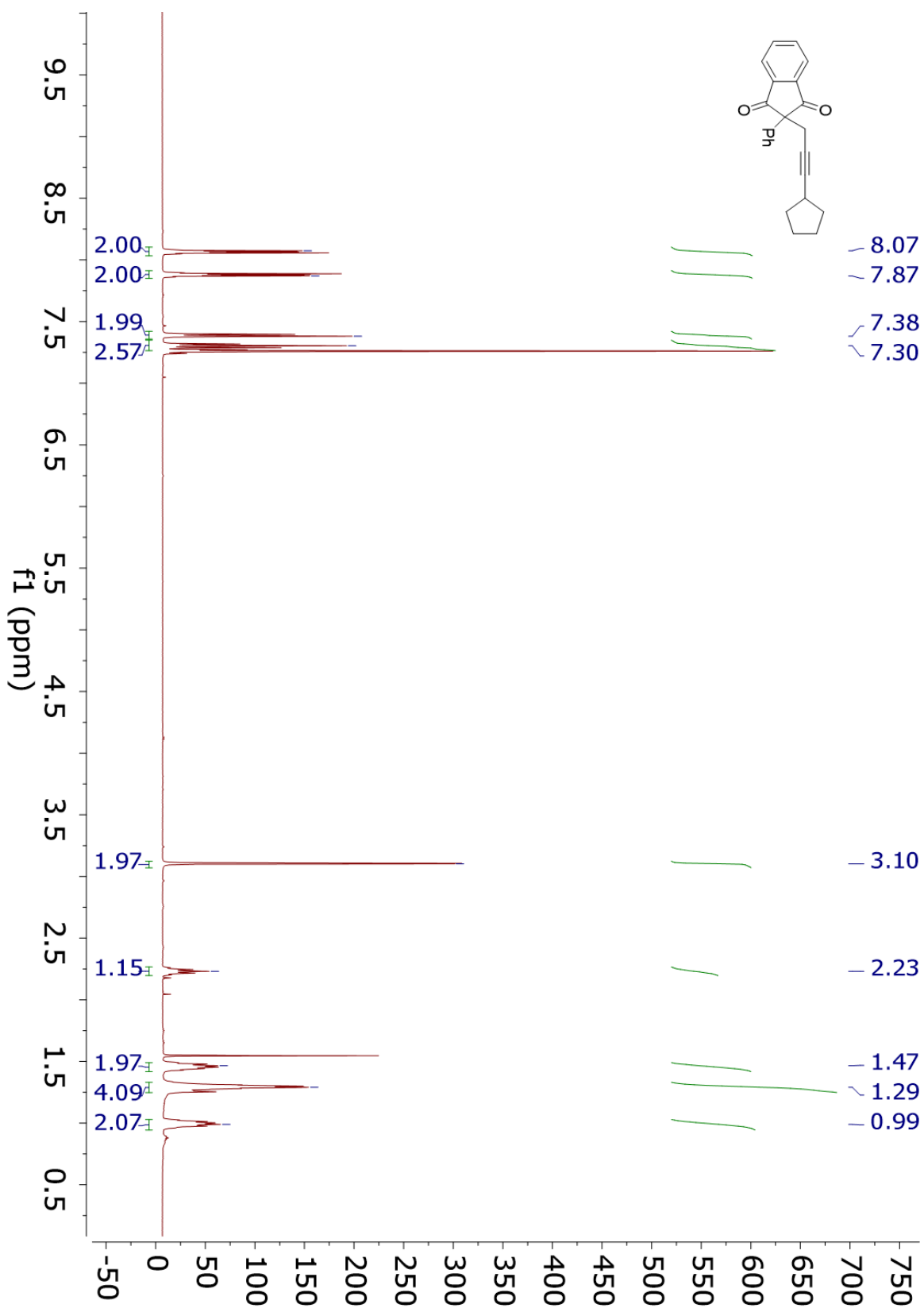
¹H NMR 4.13t



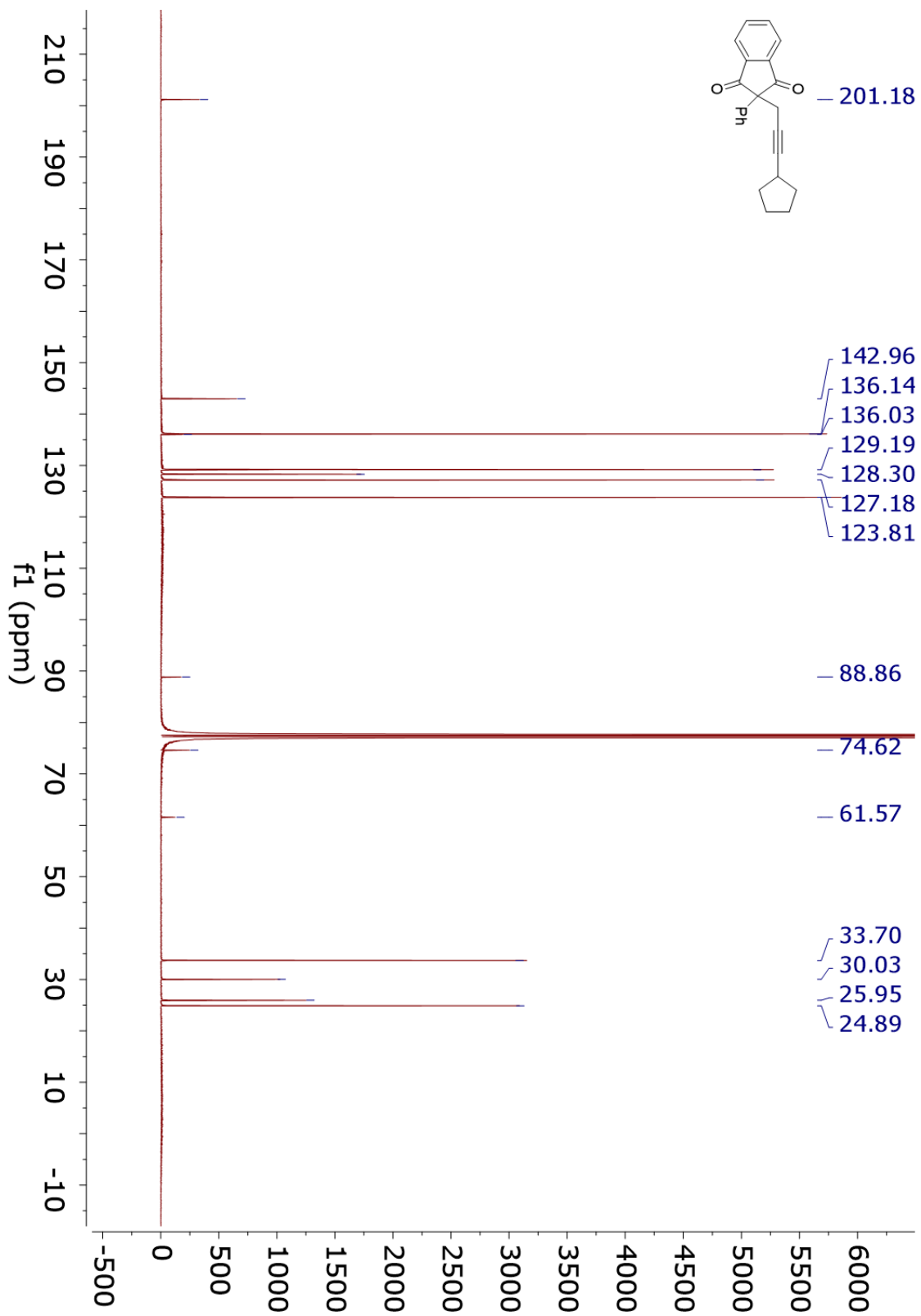
¹³C NMR 4.13t



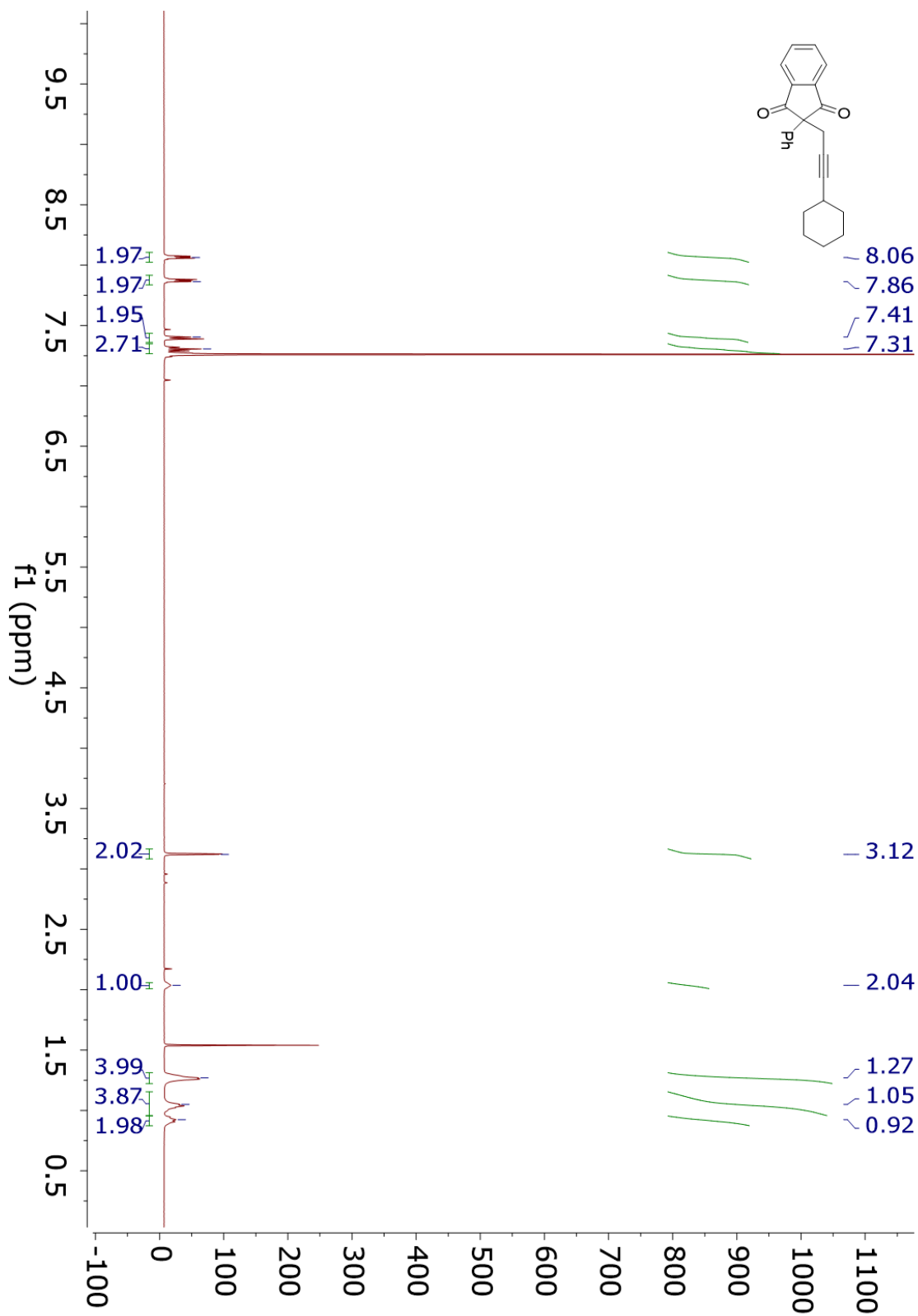
¹H NMR 4.13u



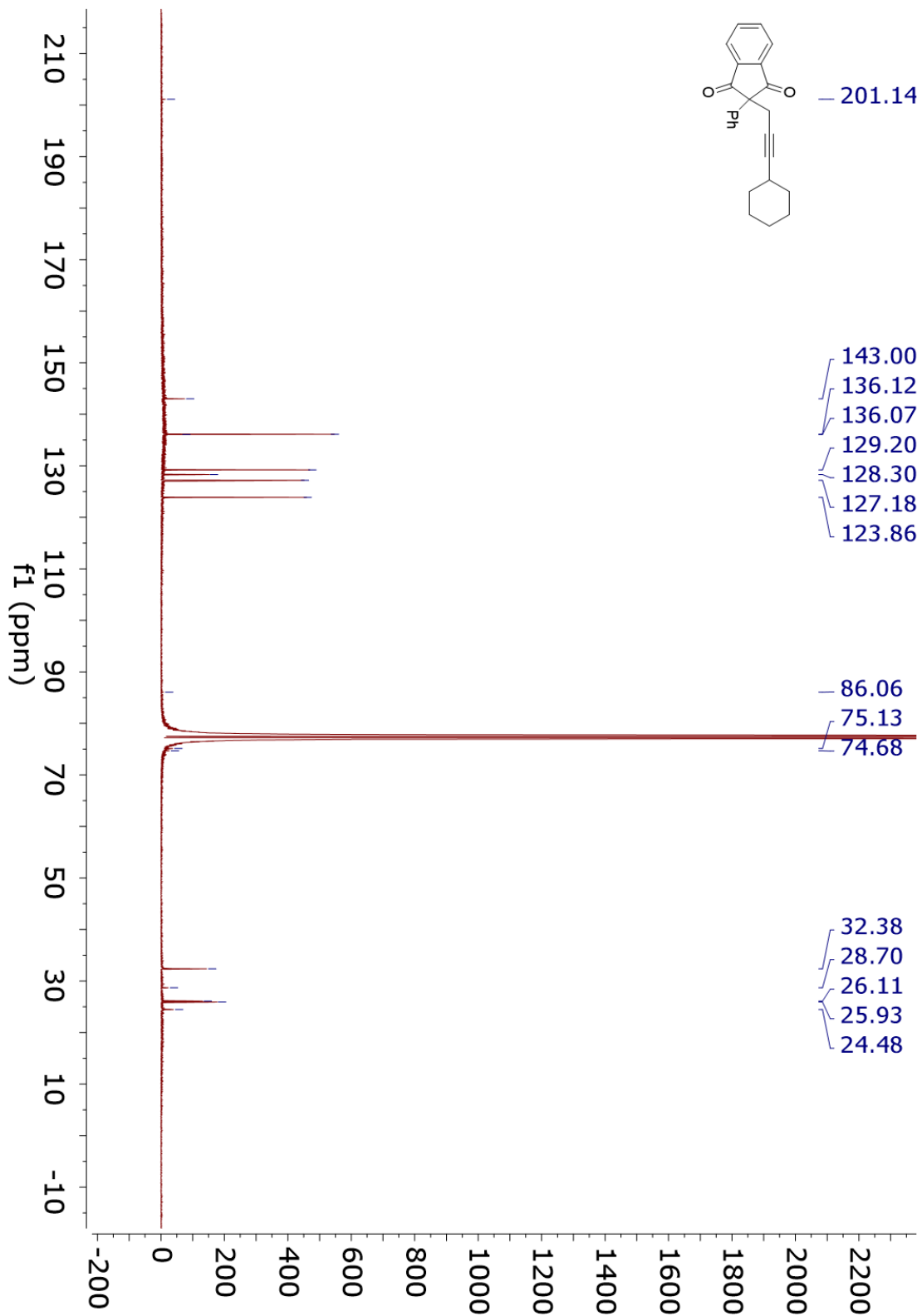
¹³C NMR 4.13u



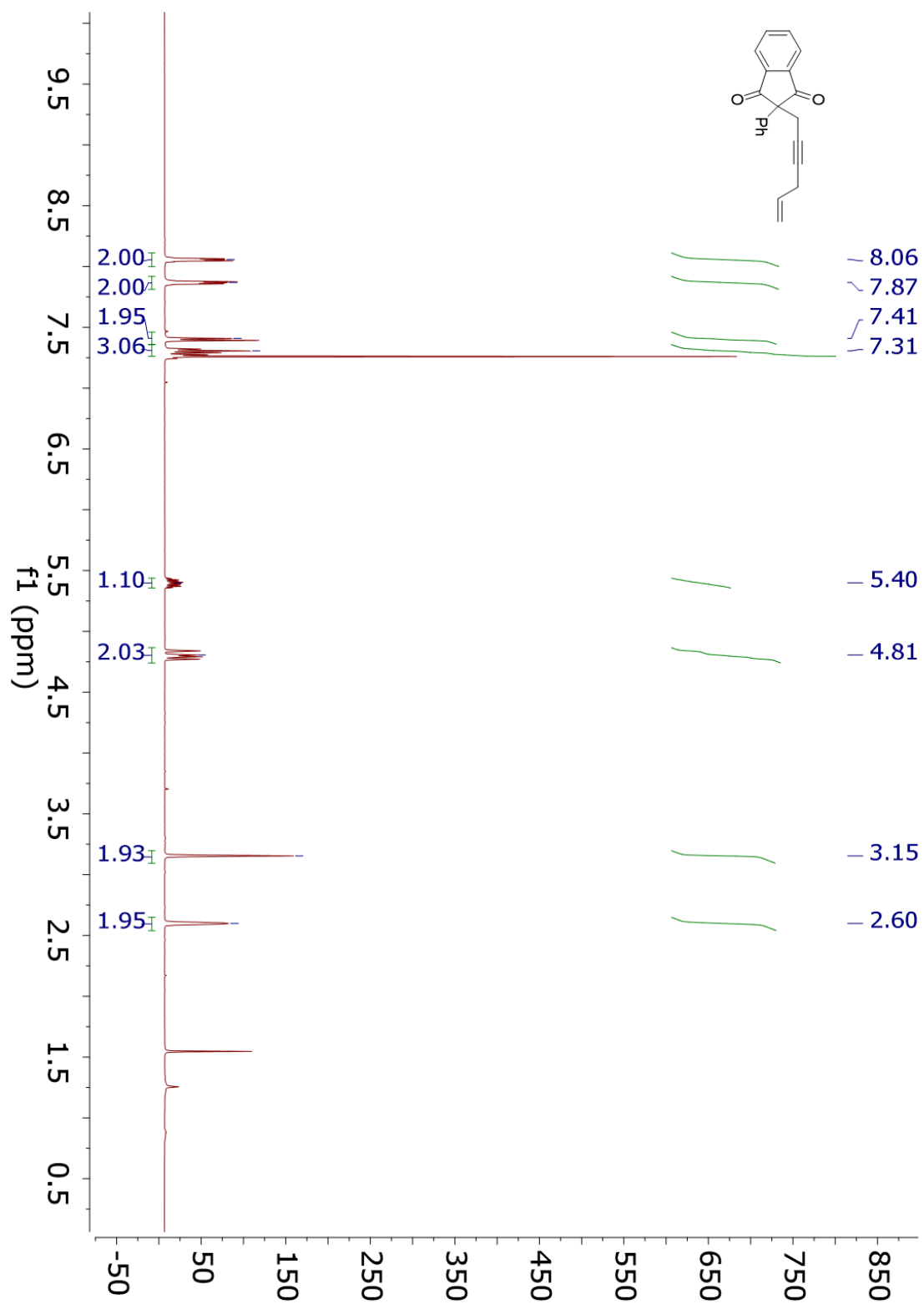
¹H NMR 4.13v



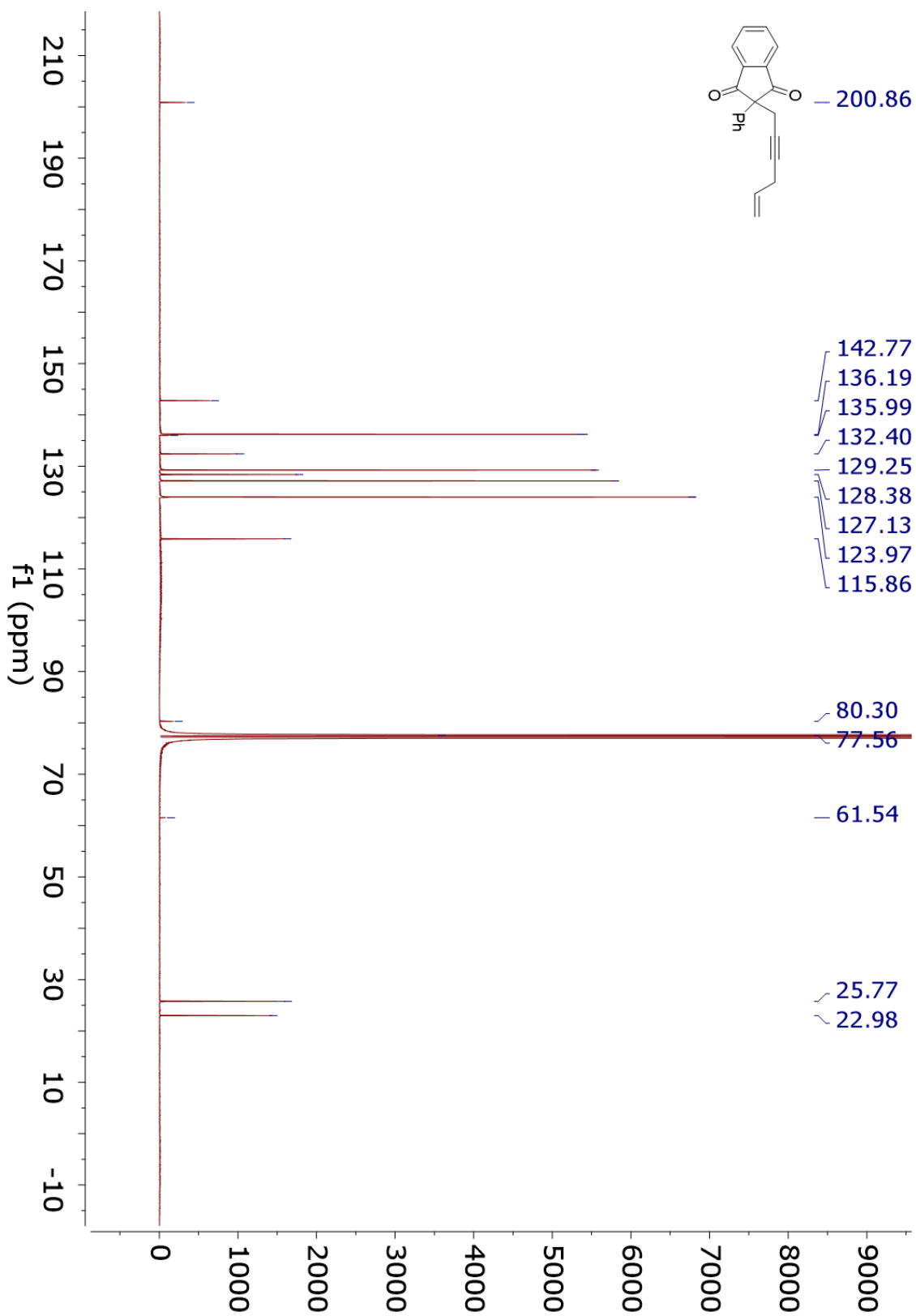
¹³C NMR 4.13v



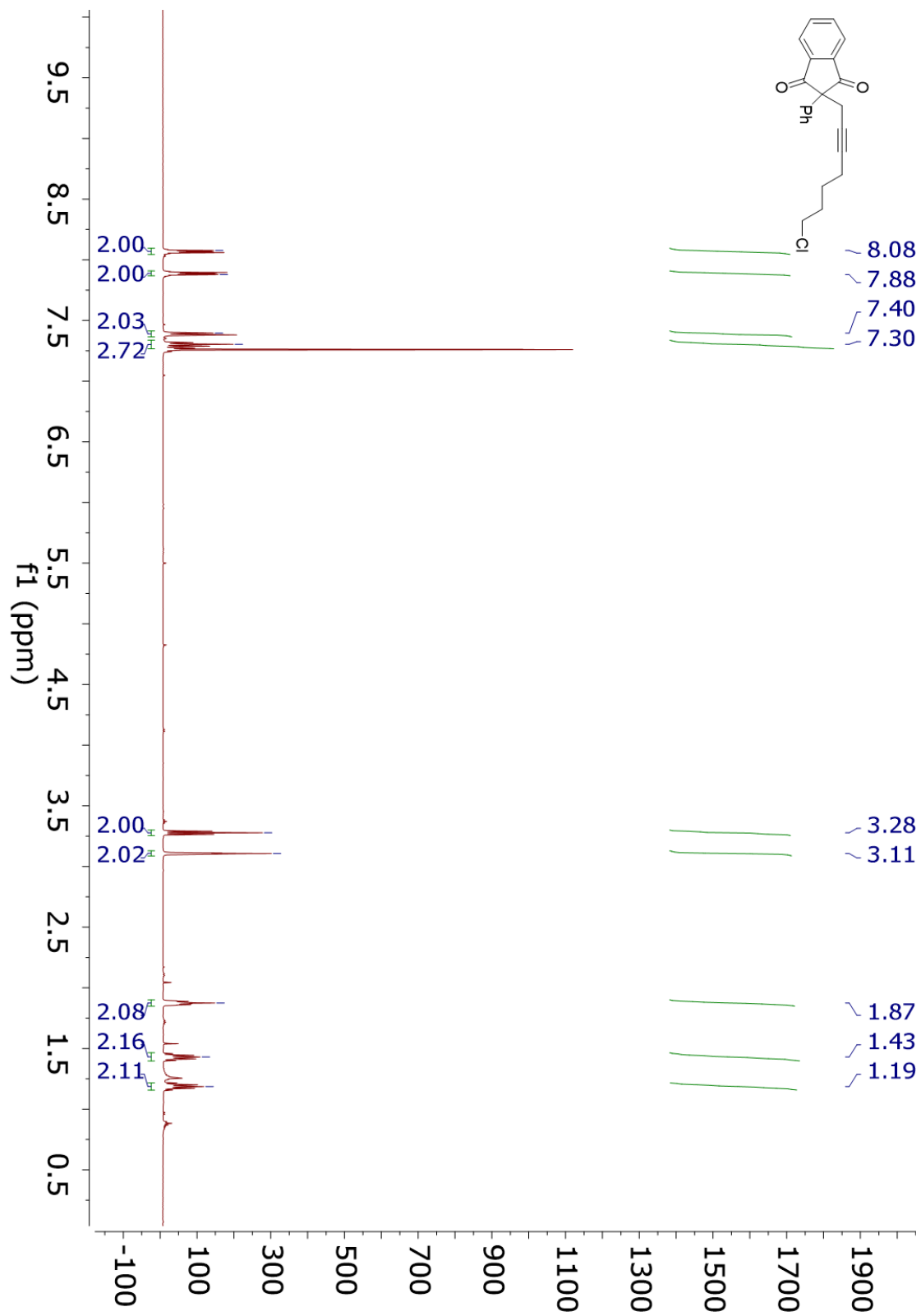
¹H NMR 4.13w



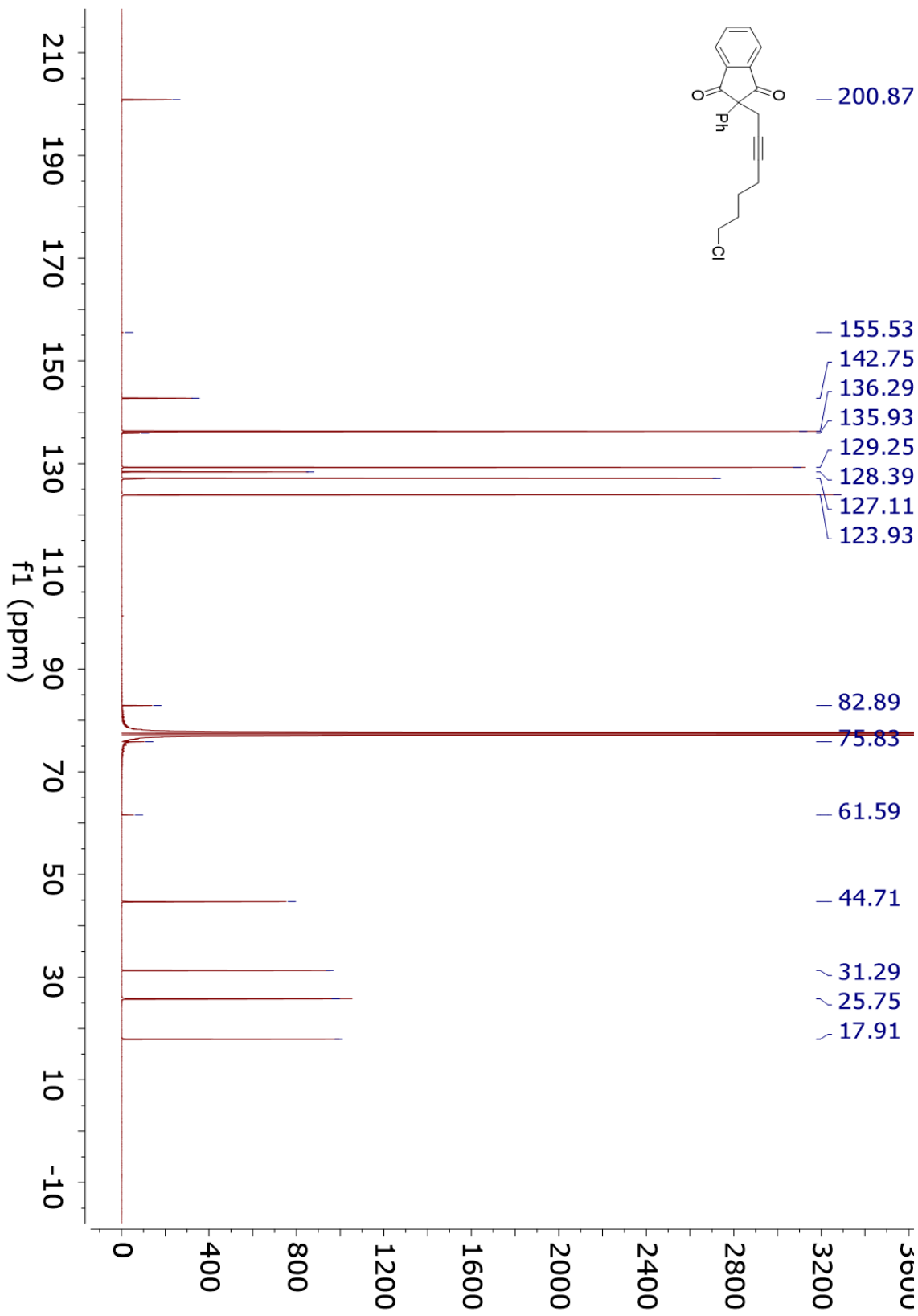
¹³C NMR 4.13w



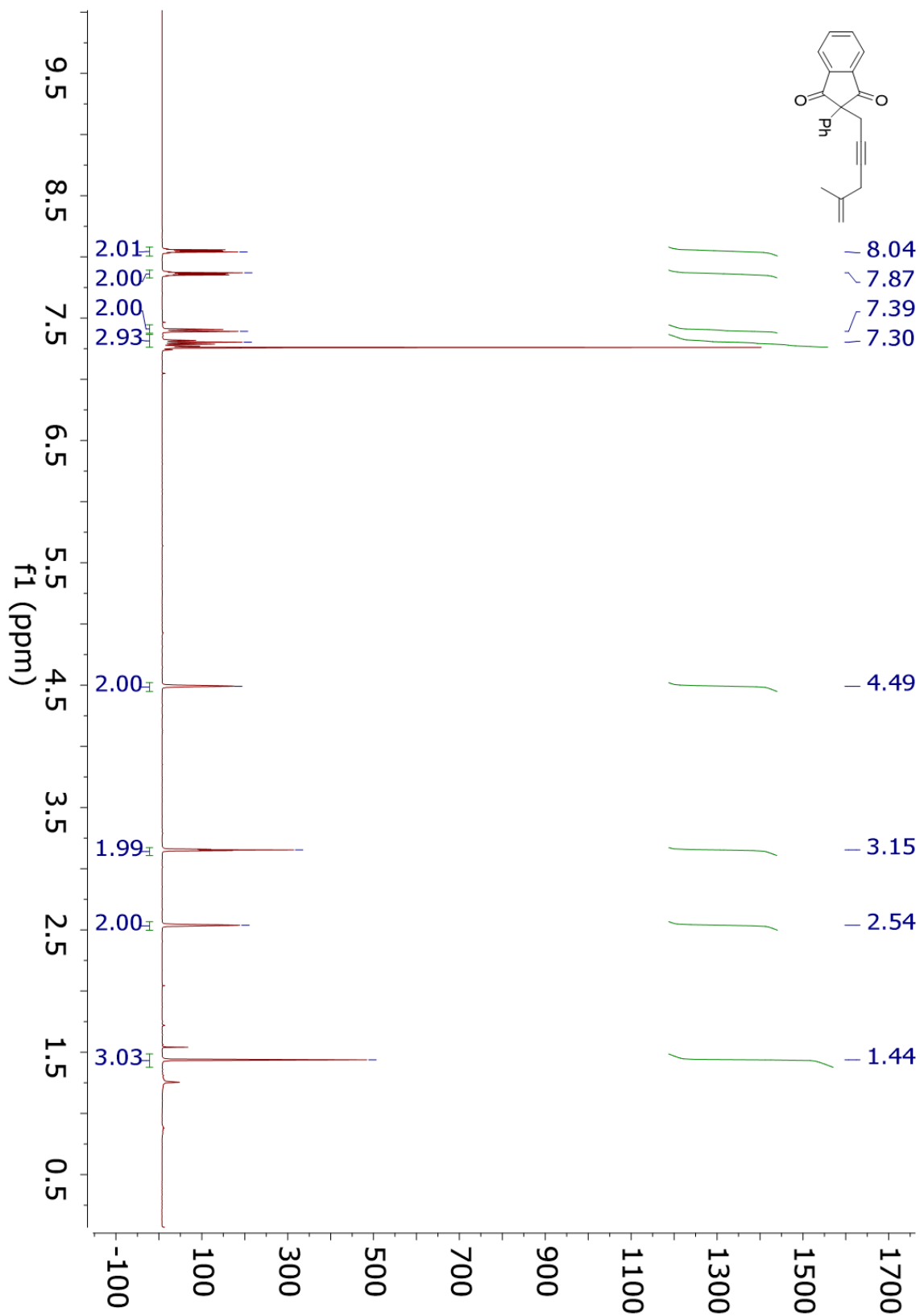
¹H NMR 4.13x



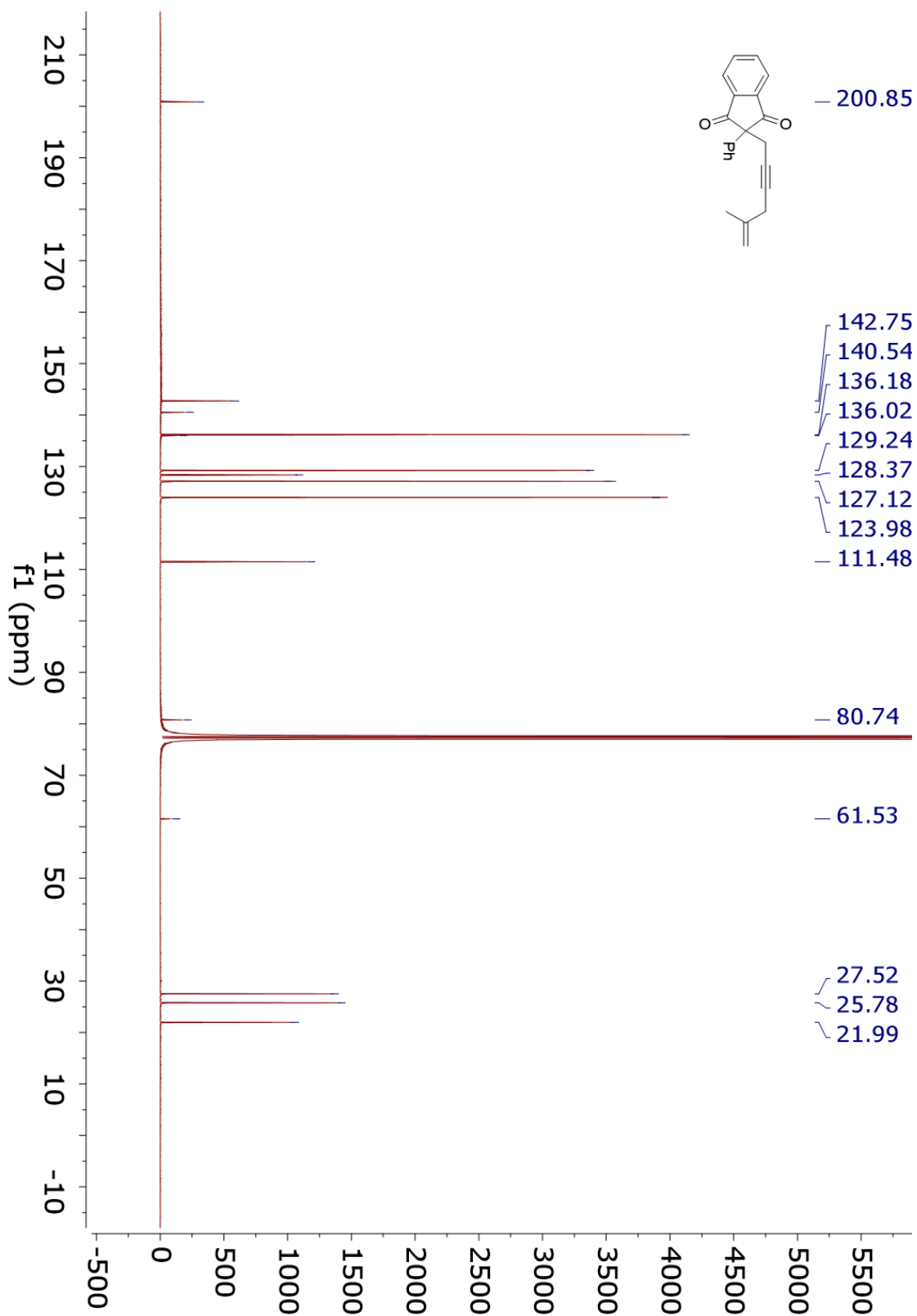
¹³C NMR 4.13x



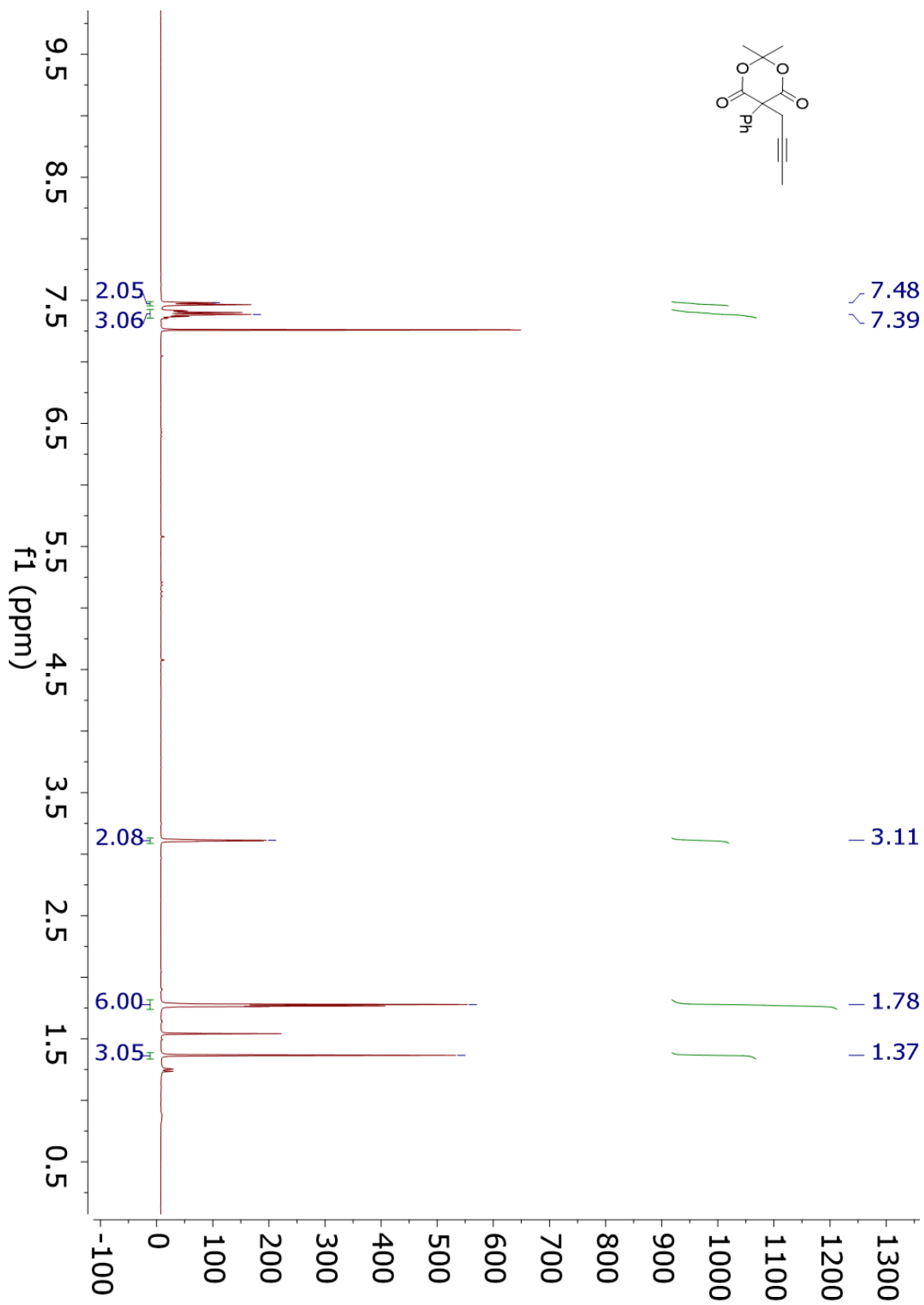
¹H NMR 4.13y



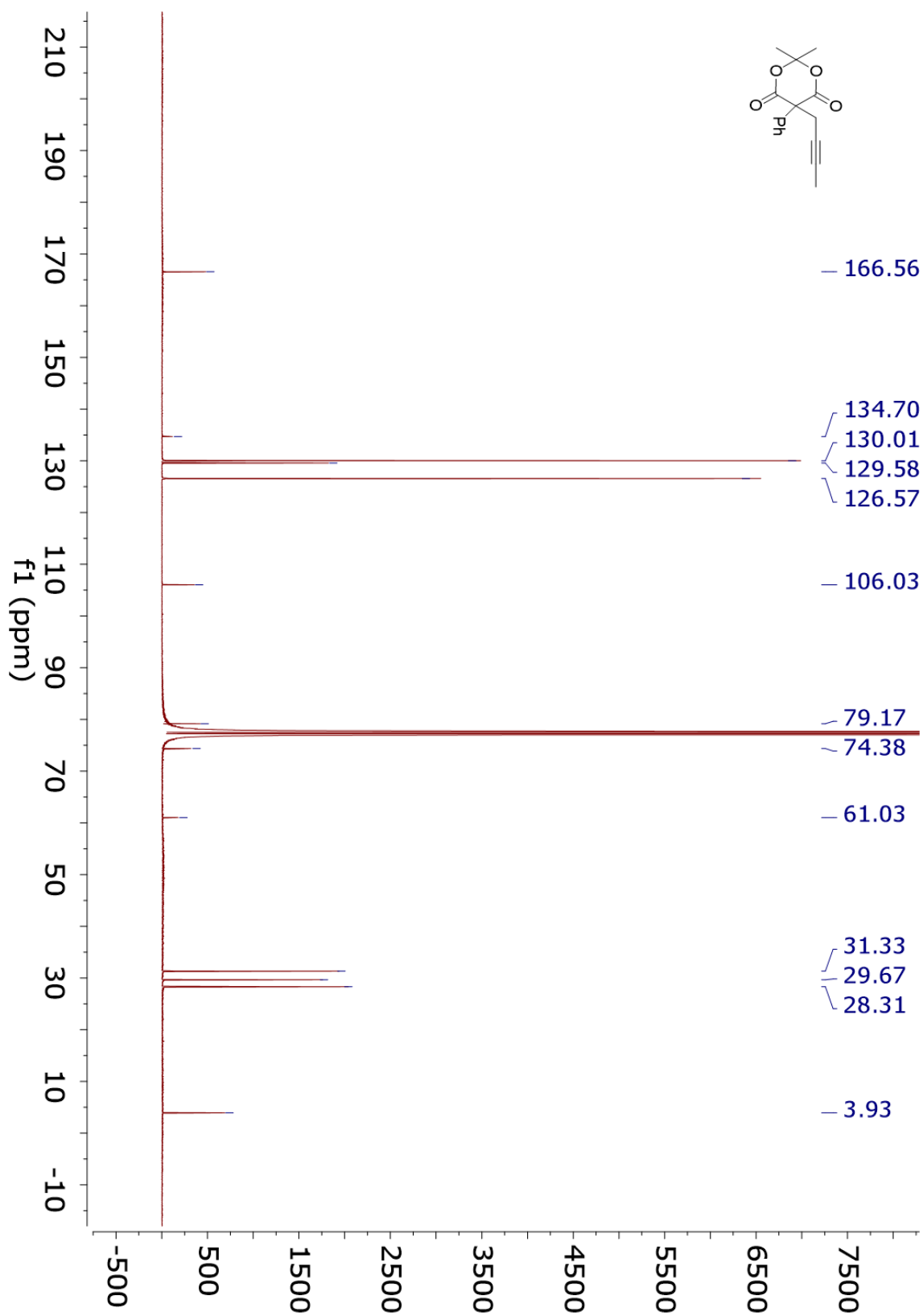
¹³C NMR 4.13y



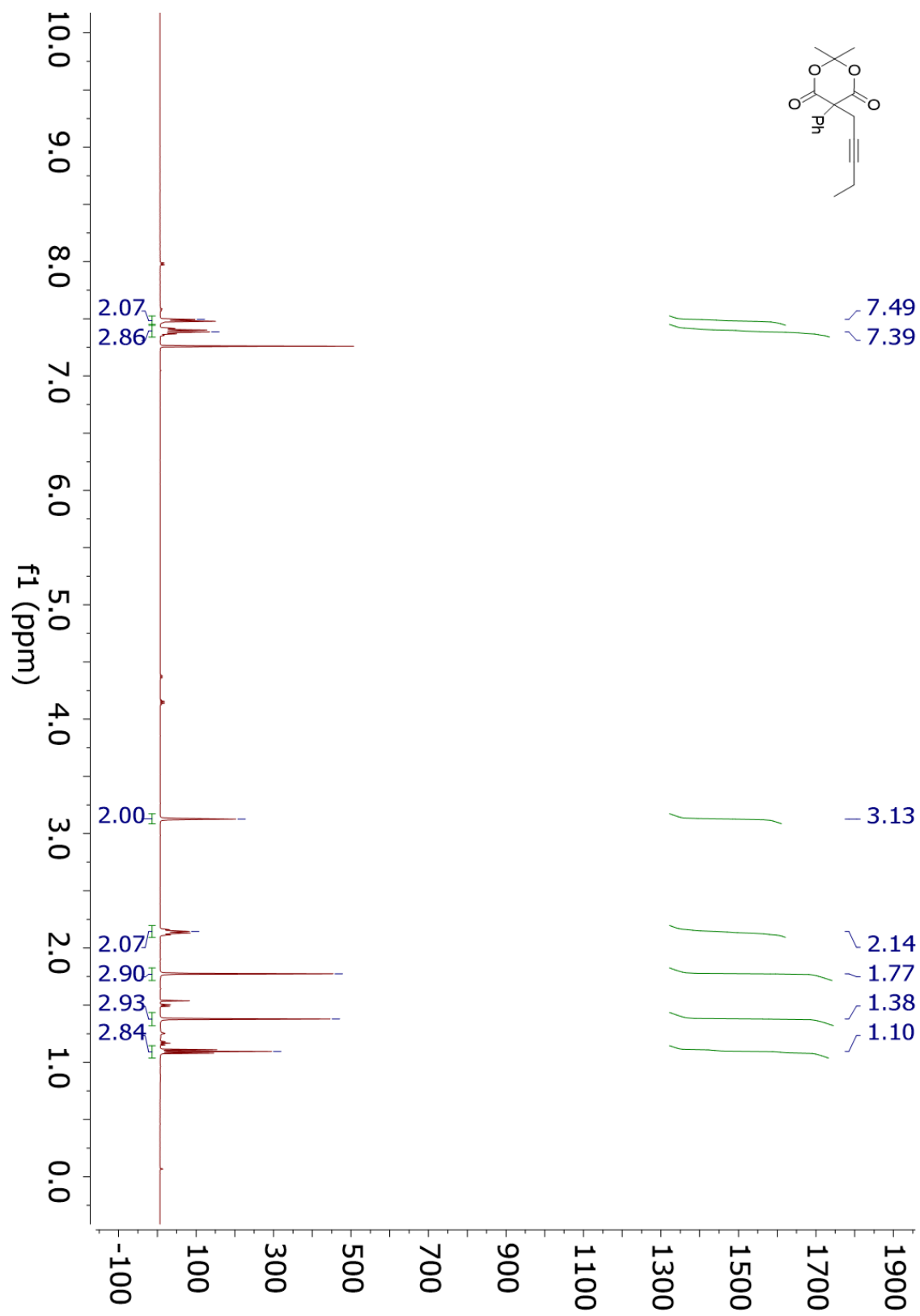
¹H NMR 4.13z



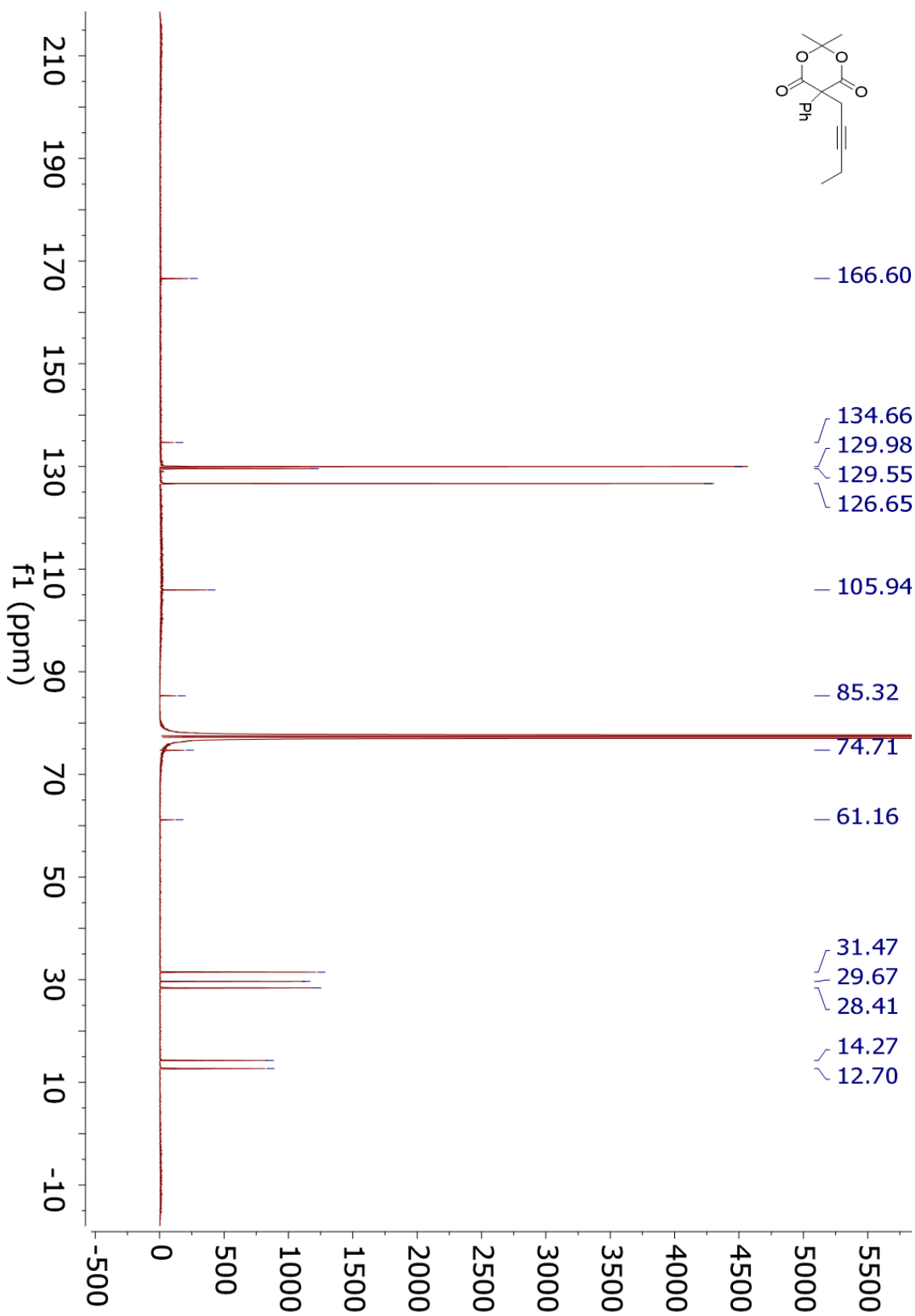
¹³C NMR 4.13z



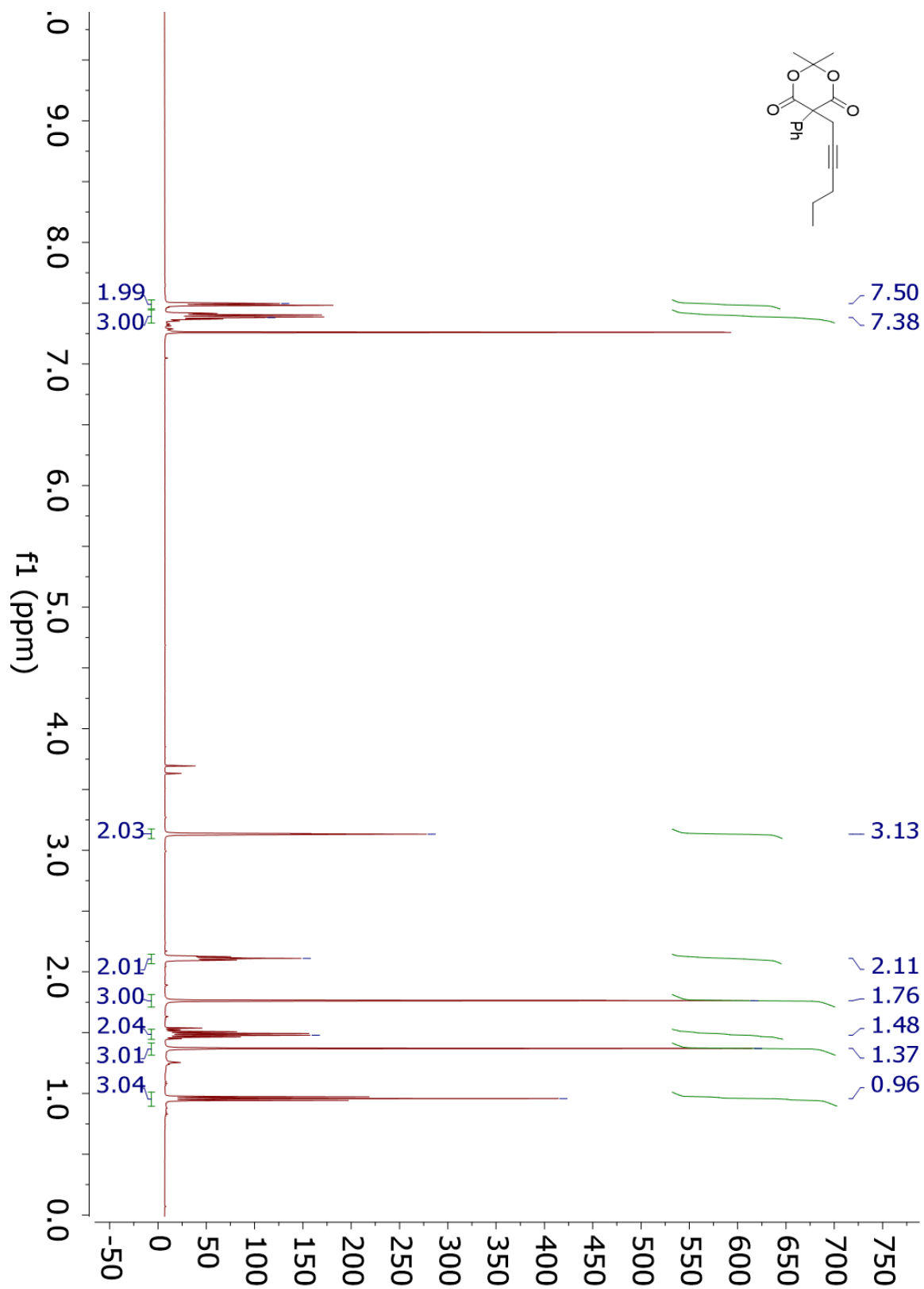
¹H NMR 4.13aa



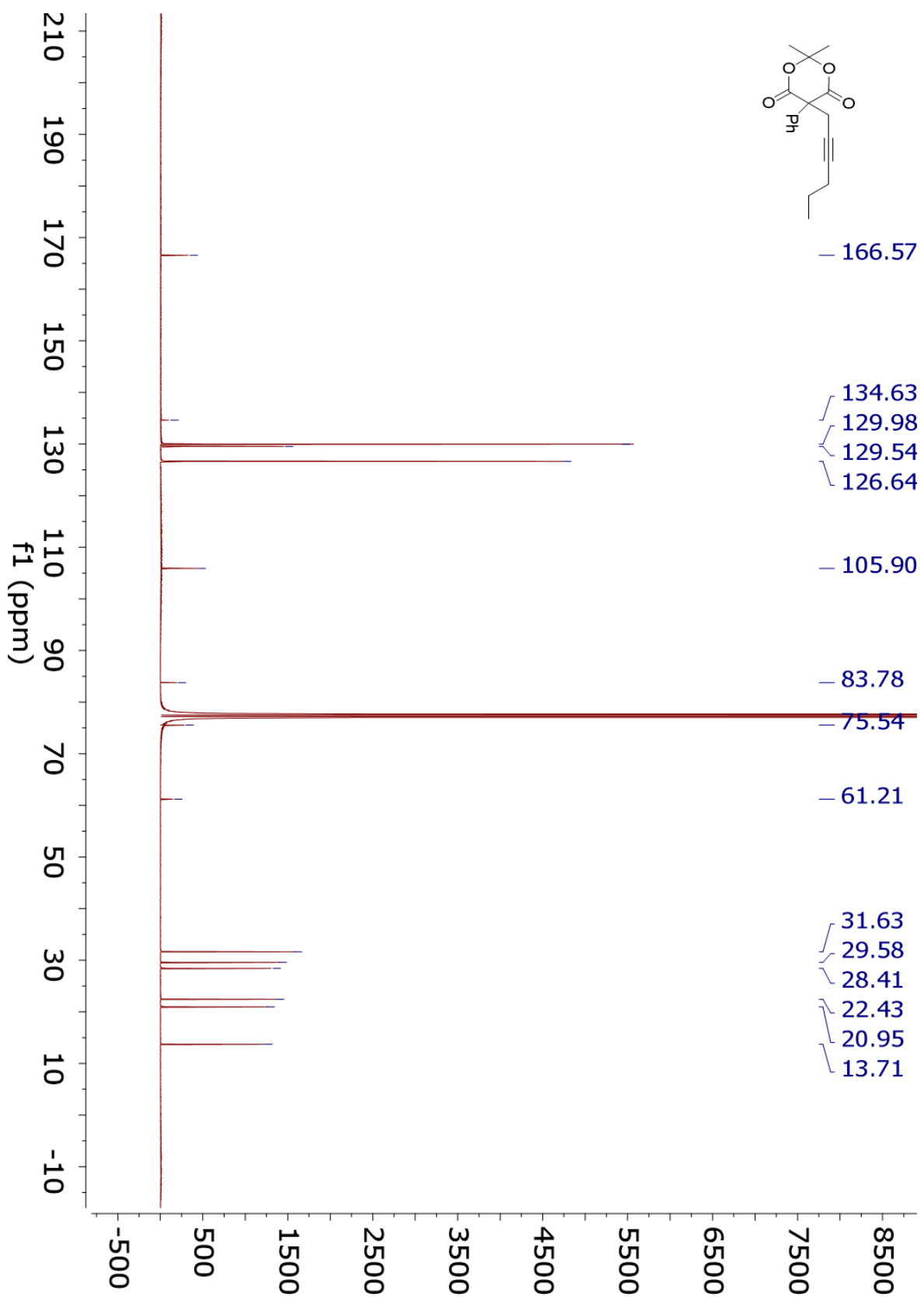
¹³C NMR 4.13aa



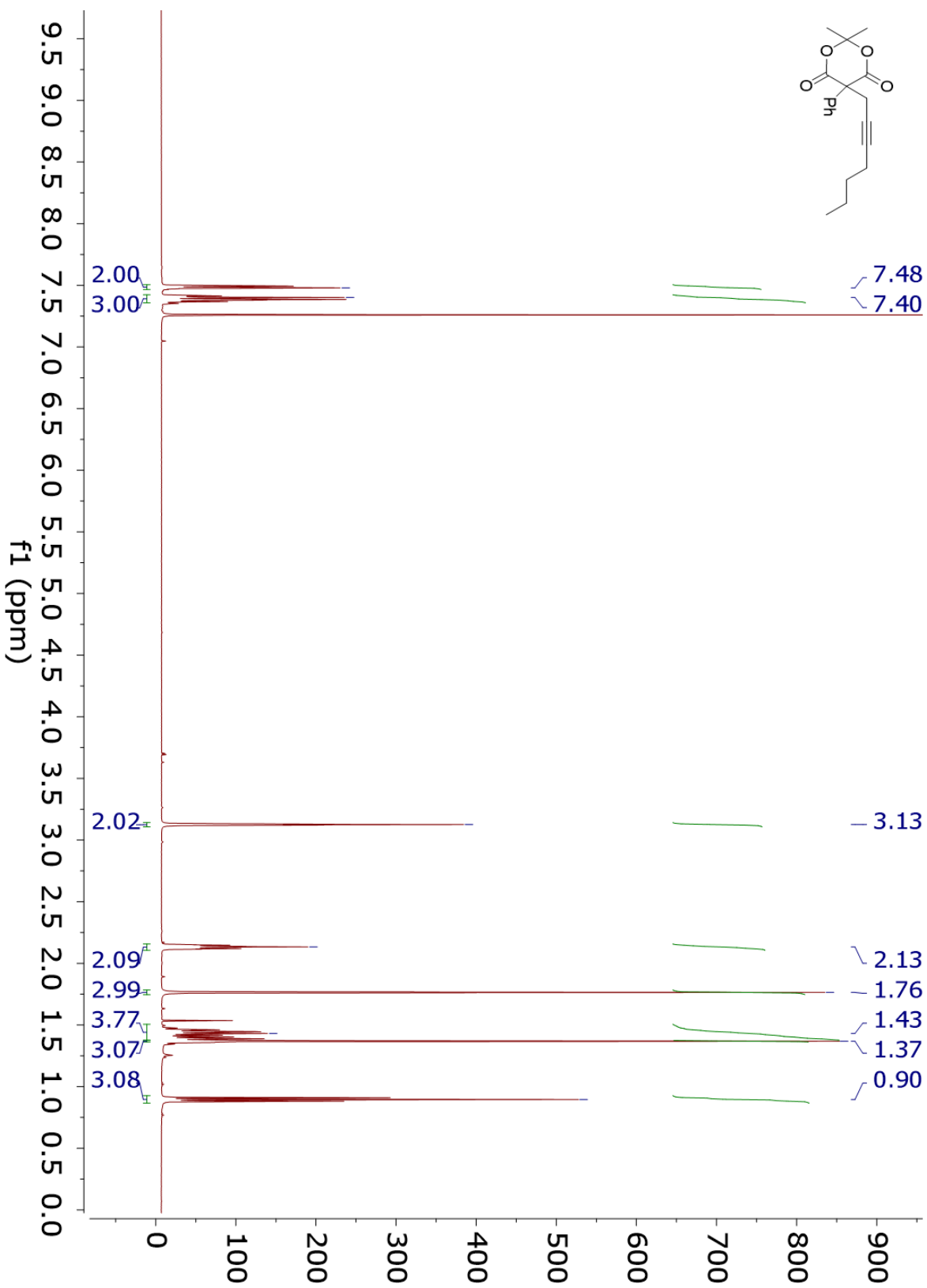
¹H NMR 4.13bb



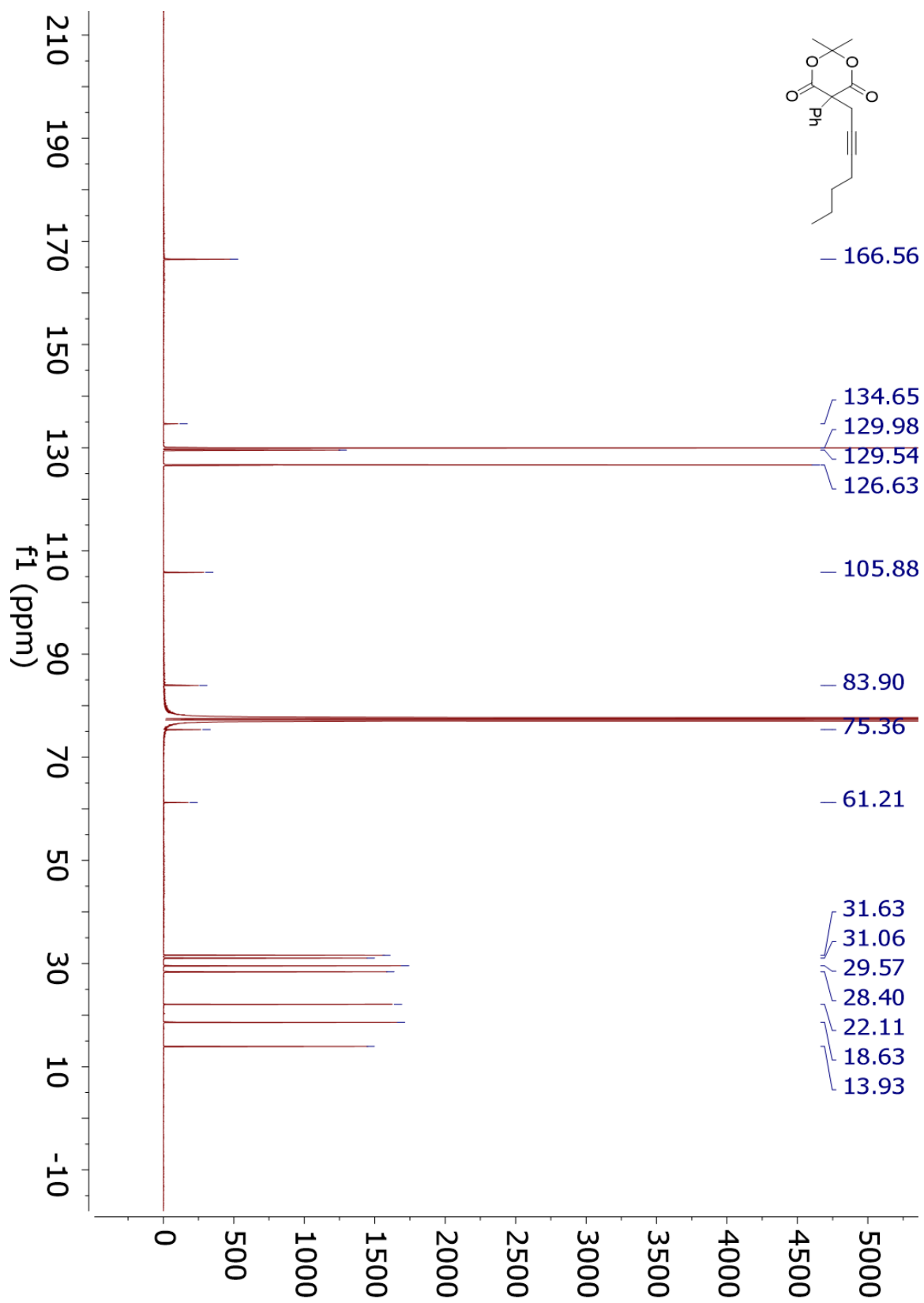
¹³C NMR 4.13bb



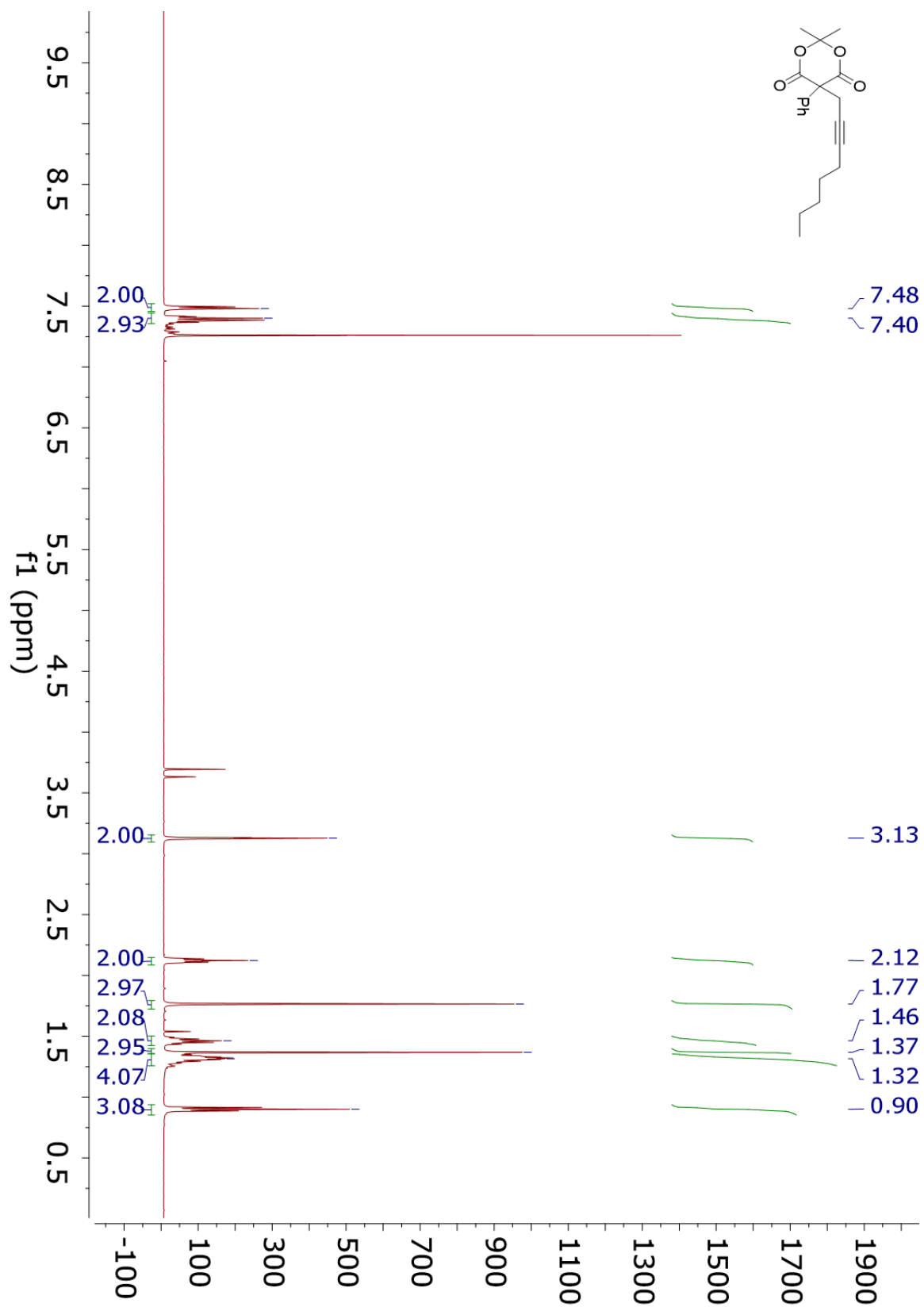
¹H NMR 4.13cc



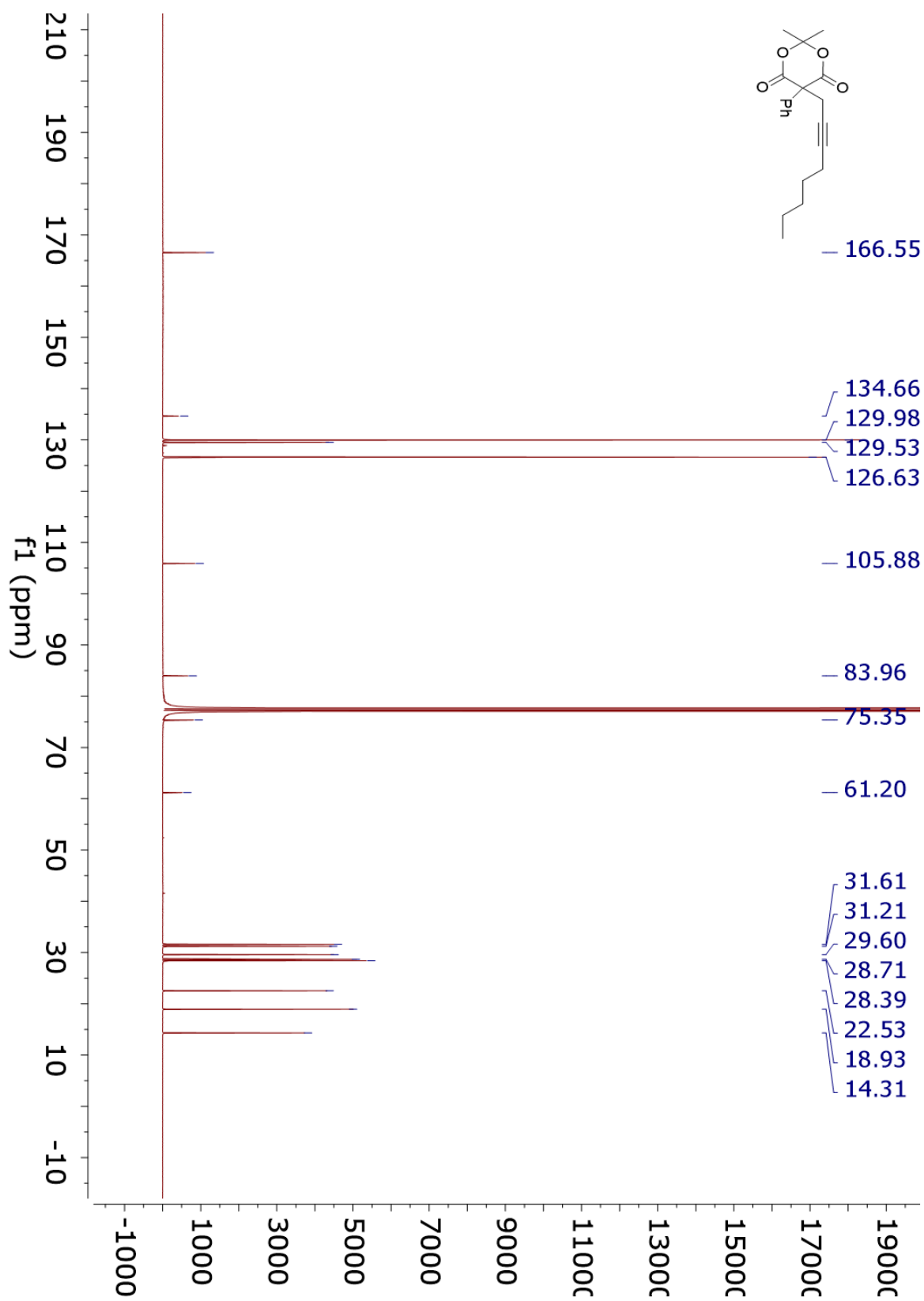
¹³C NMR 4.13cc



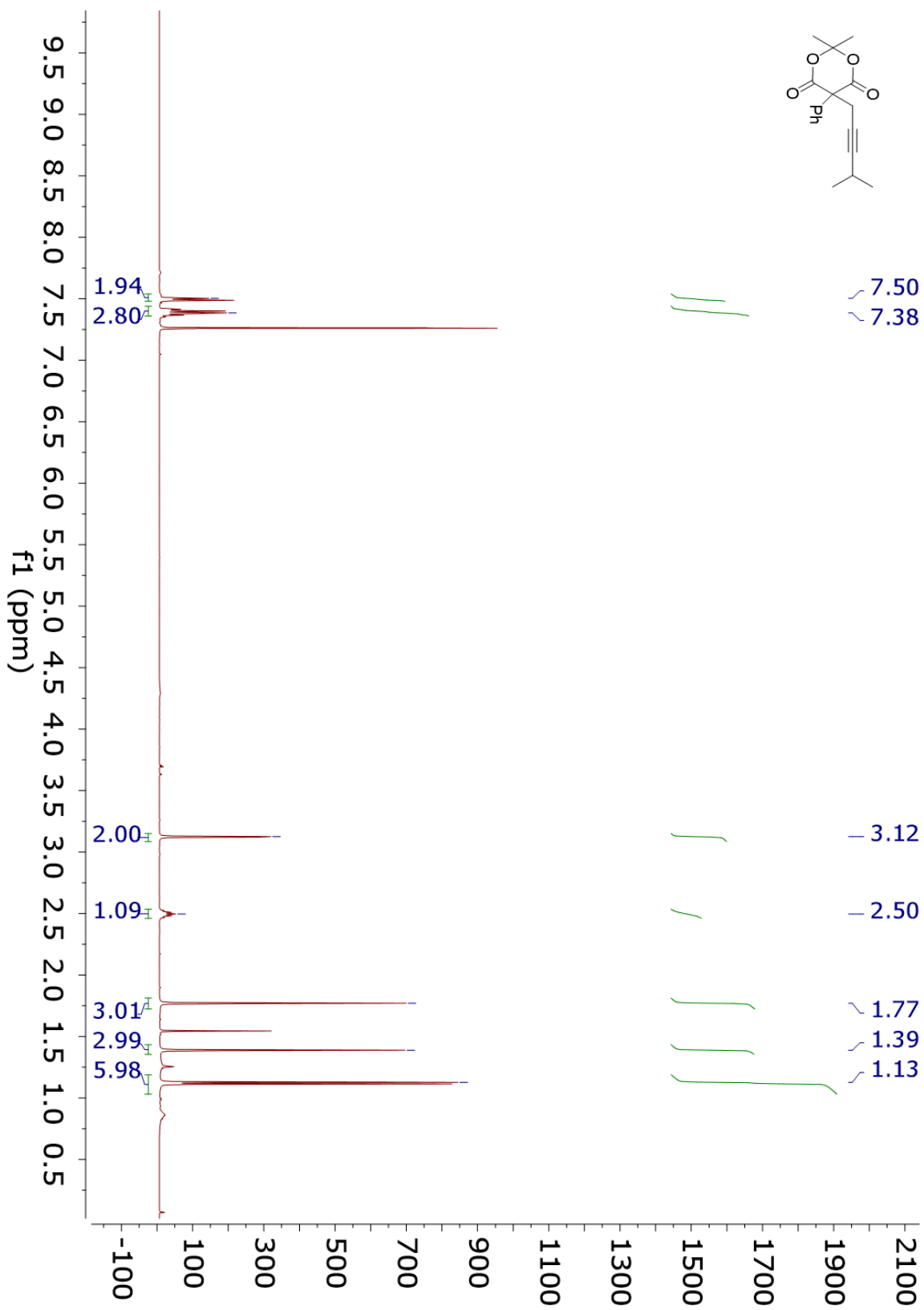
¹H NMR 4.13dd



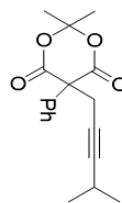
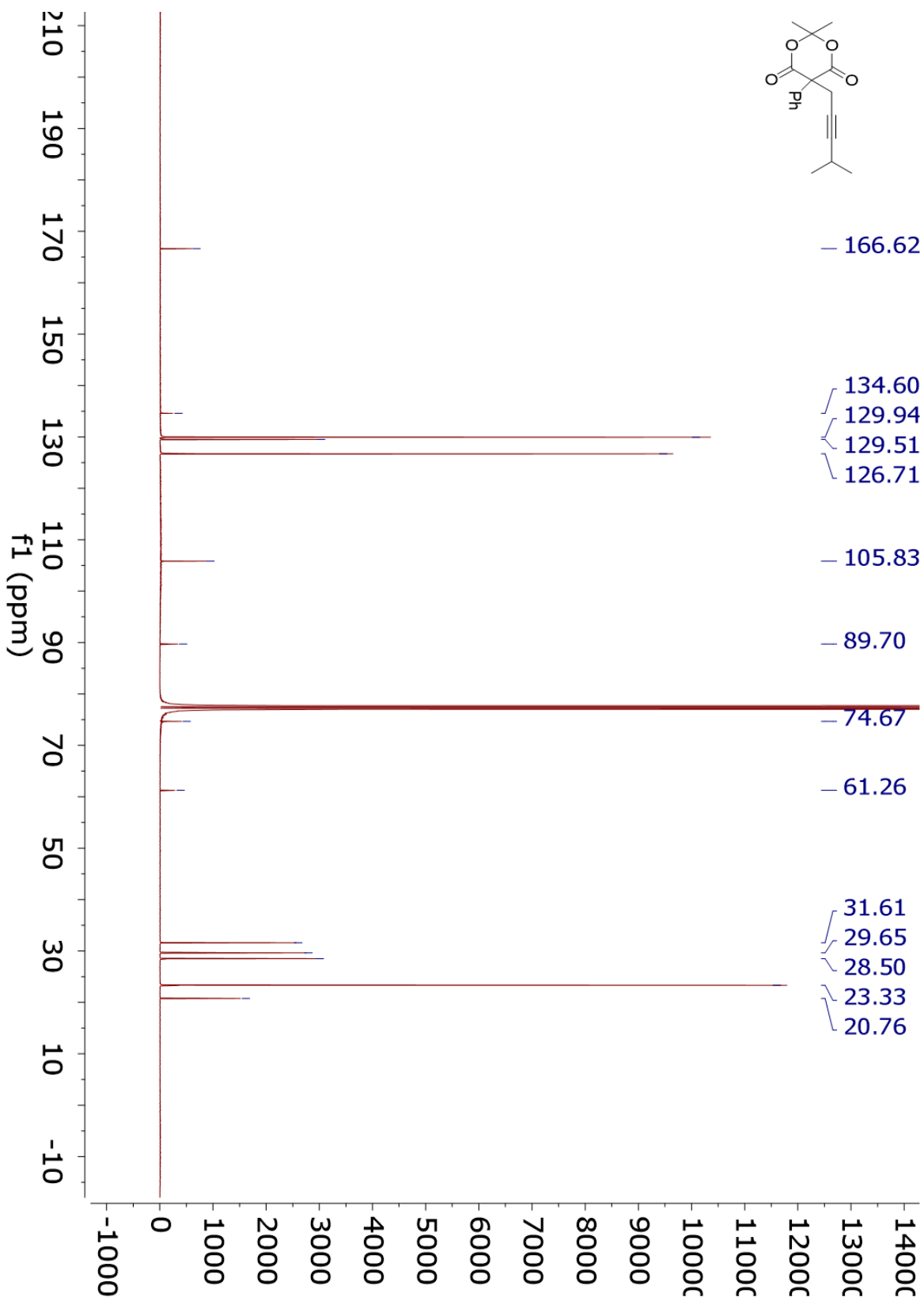
¹³C NMR 4.13dd



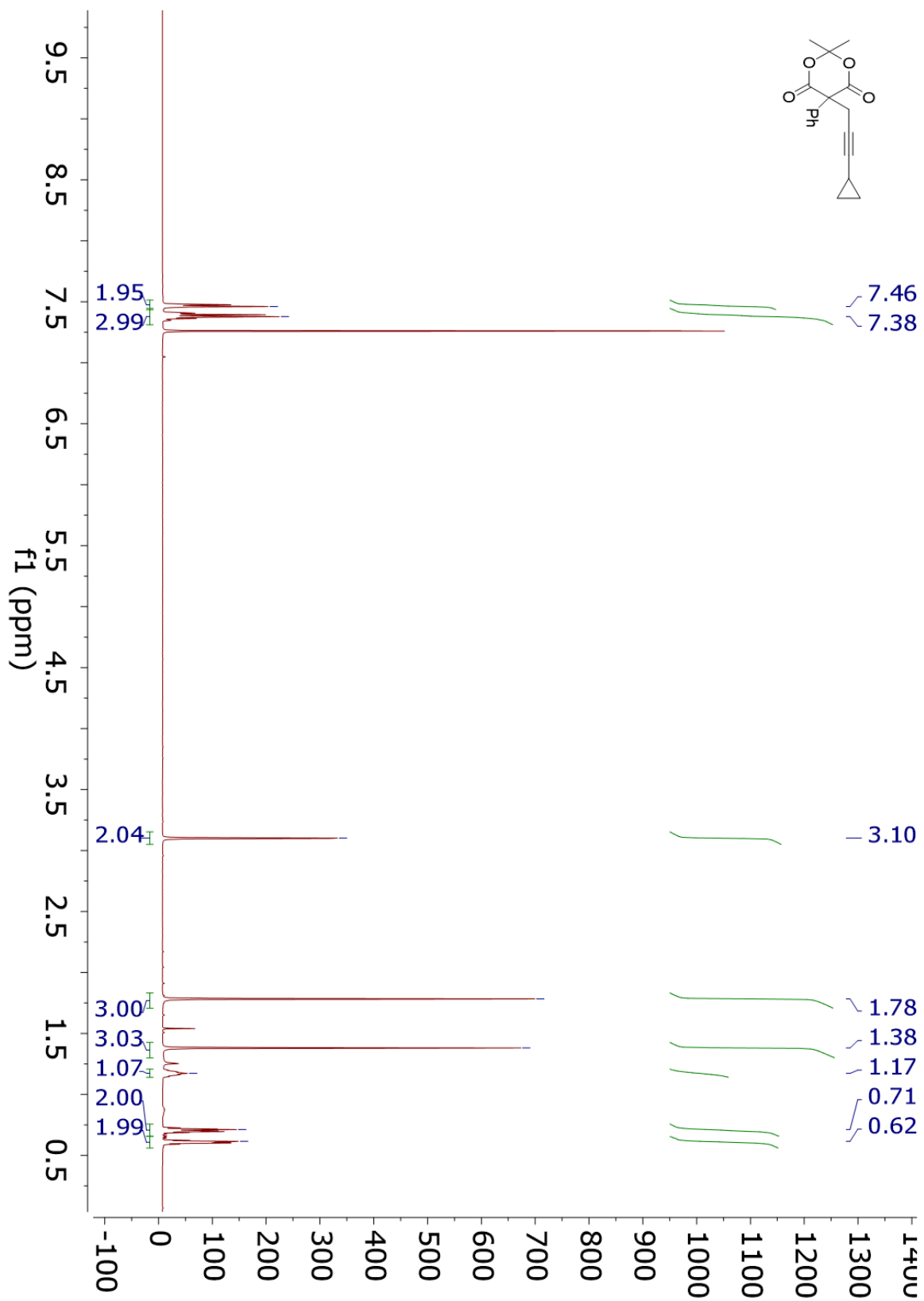
¹H NMR 4.13ee



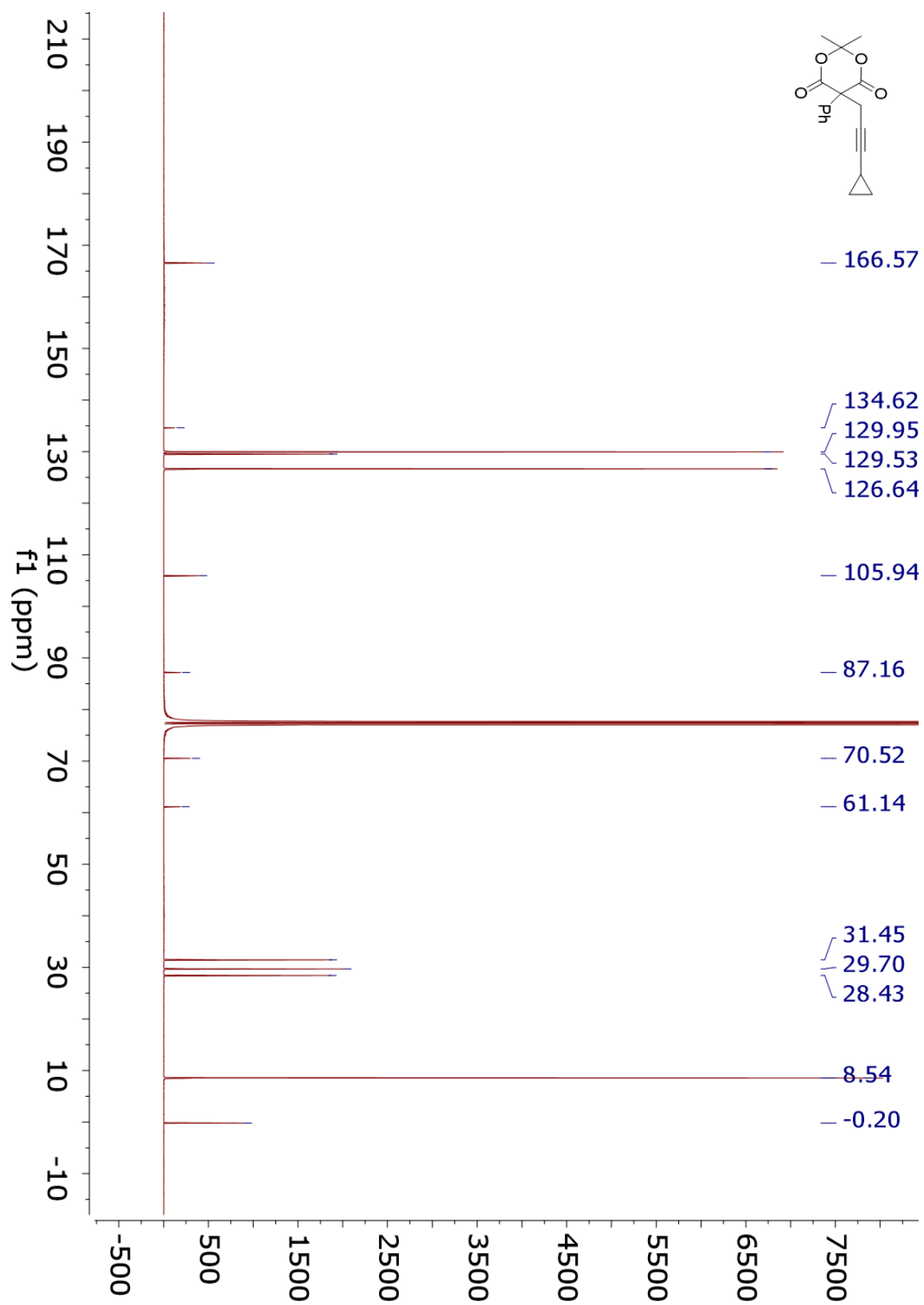
¹³C NMR 4.13ee



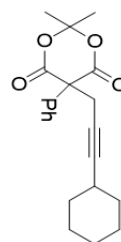
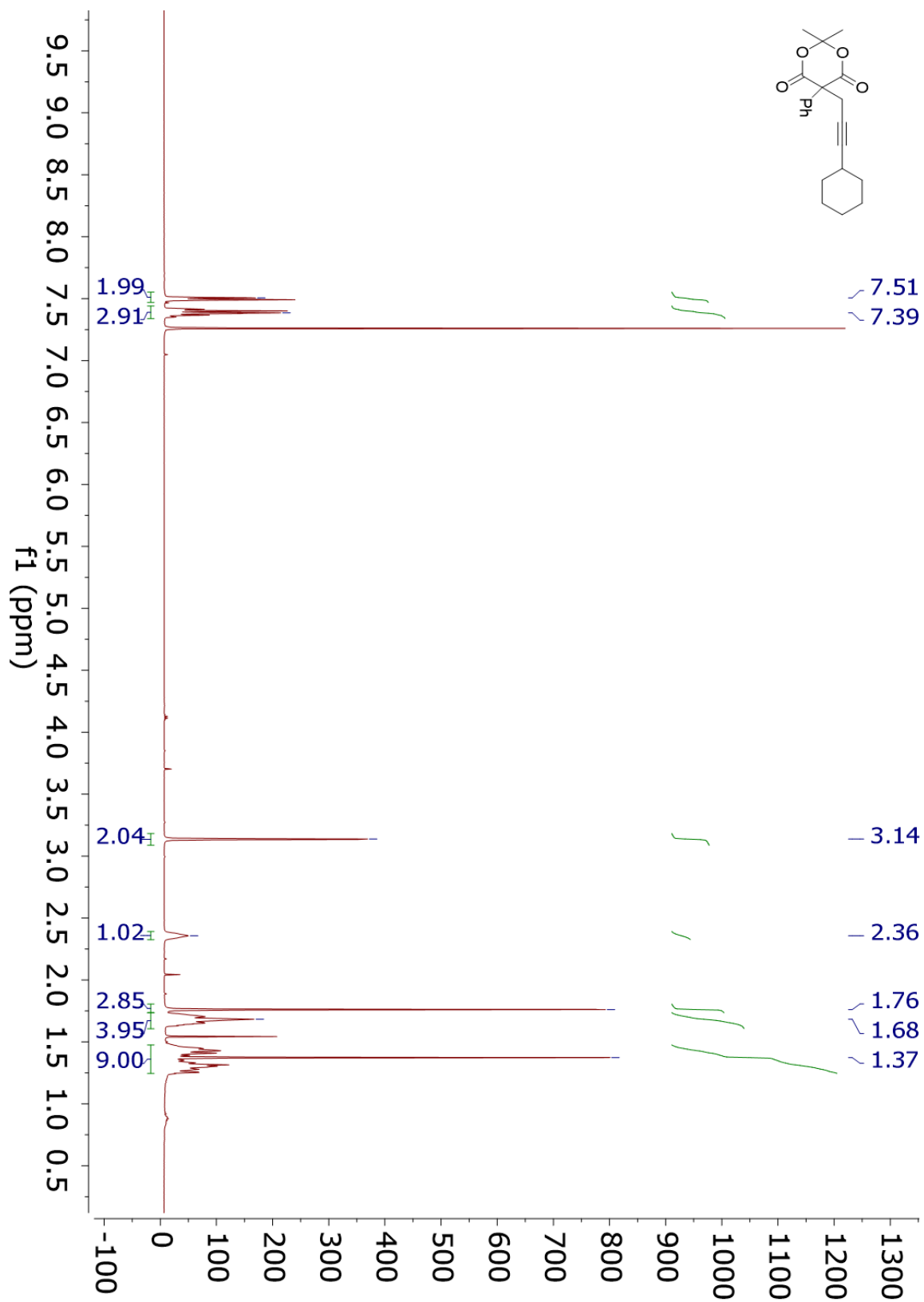
¹H NMR 4.13ff



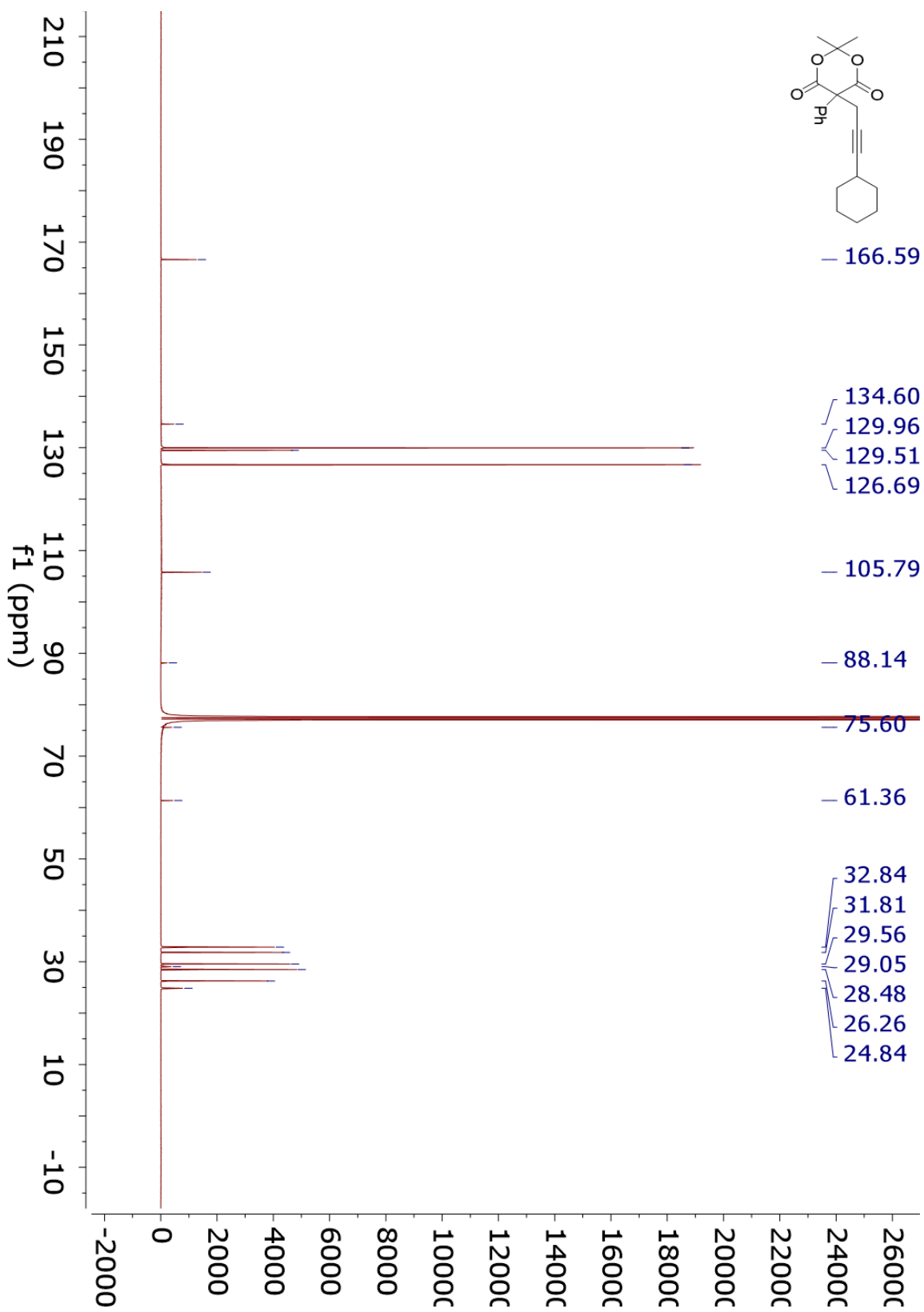
¹³C NMR 4.13ff



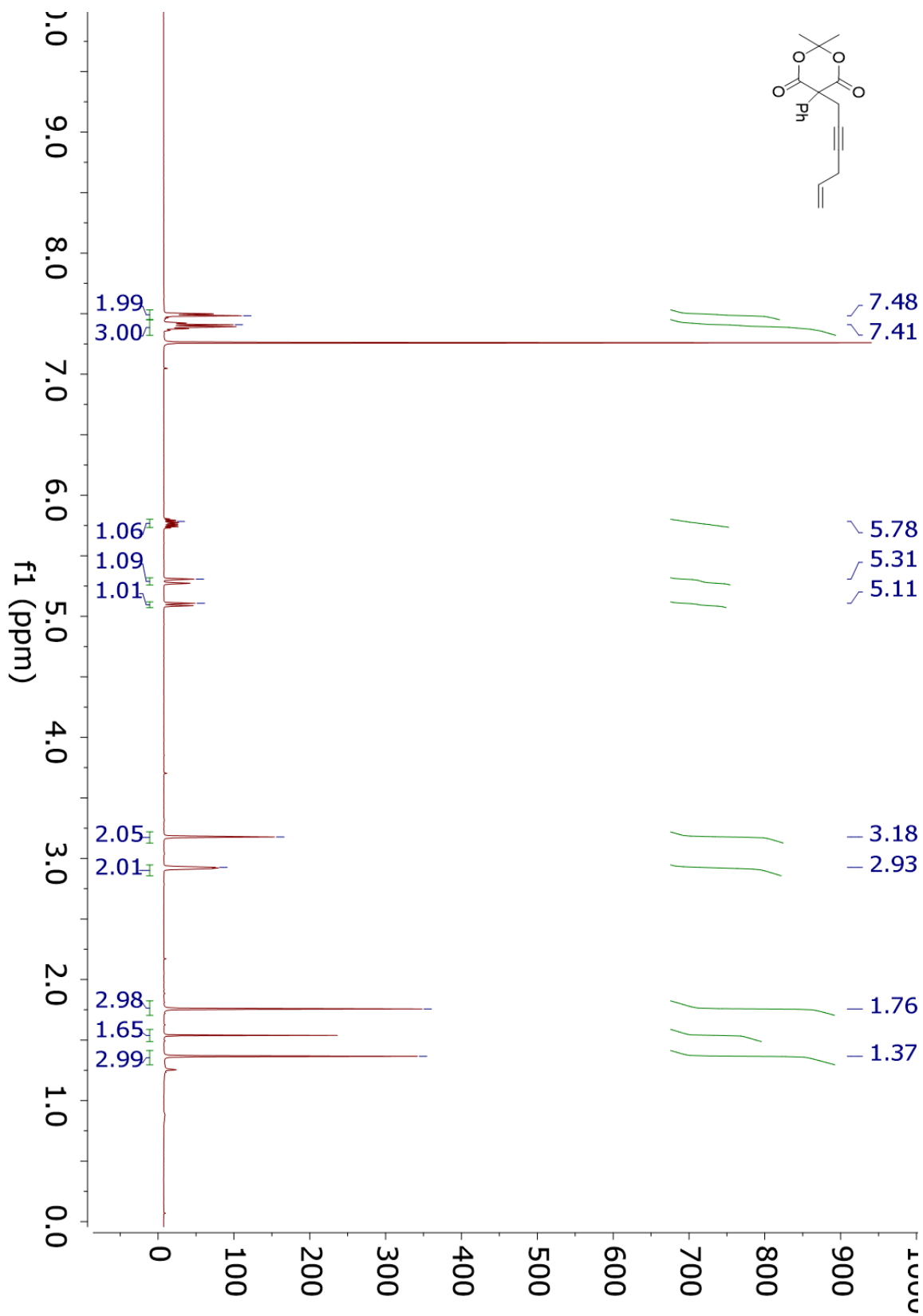
¹H NMR 4.13gg



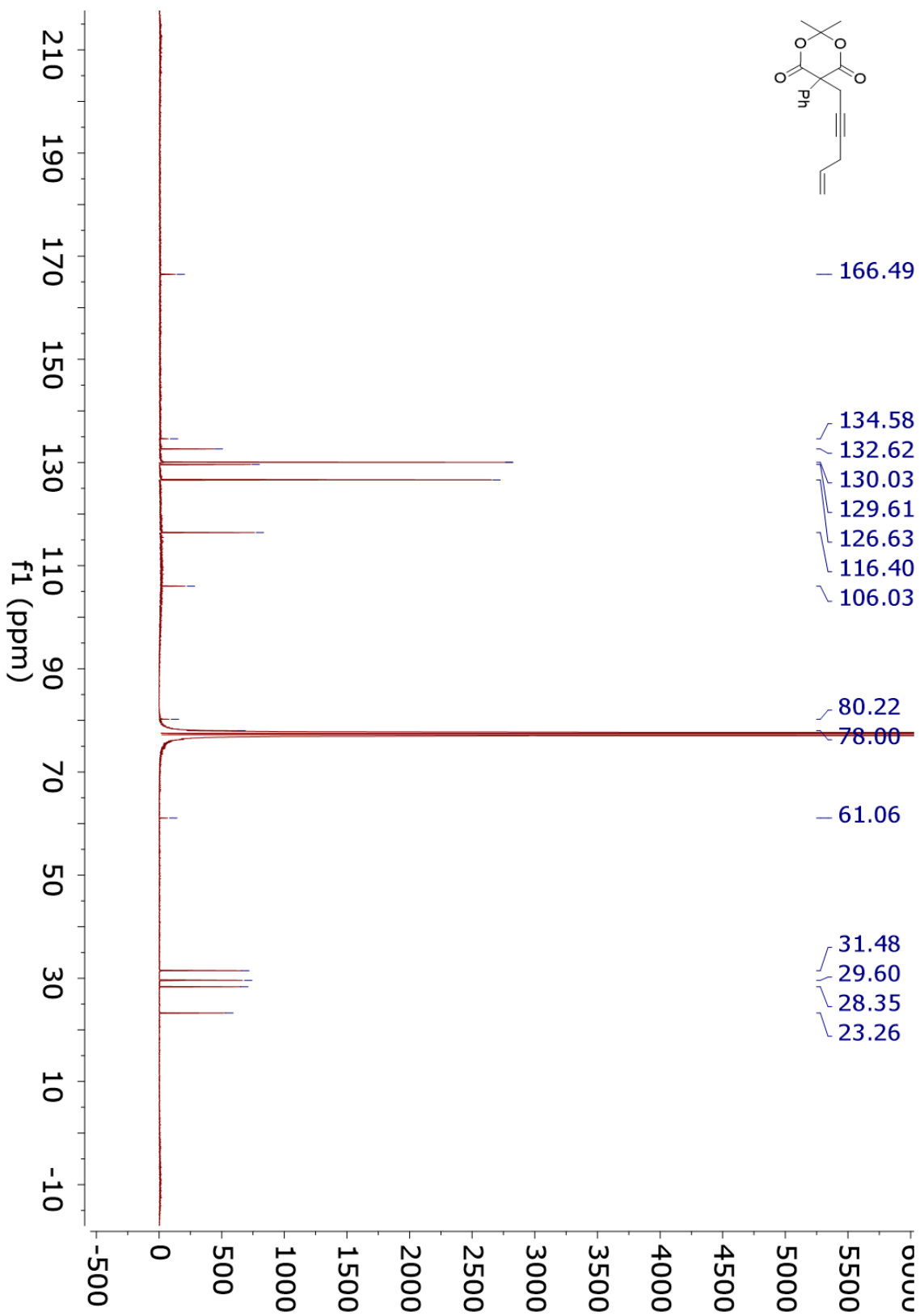
¹³C NMR 4.13gg



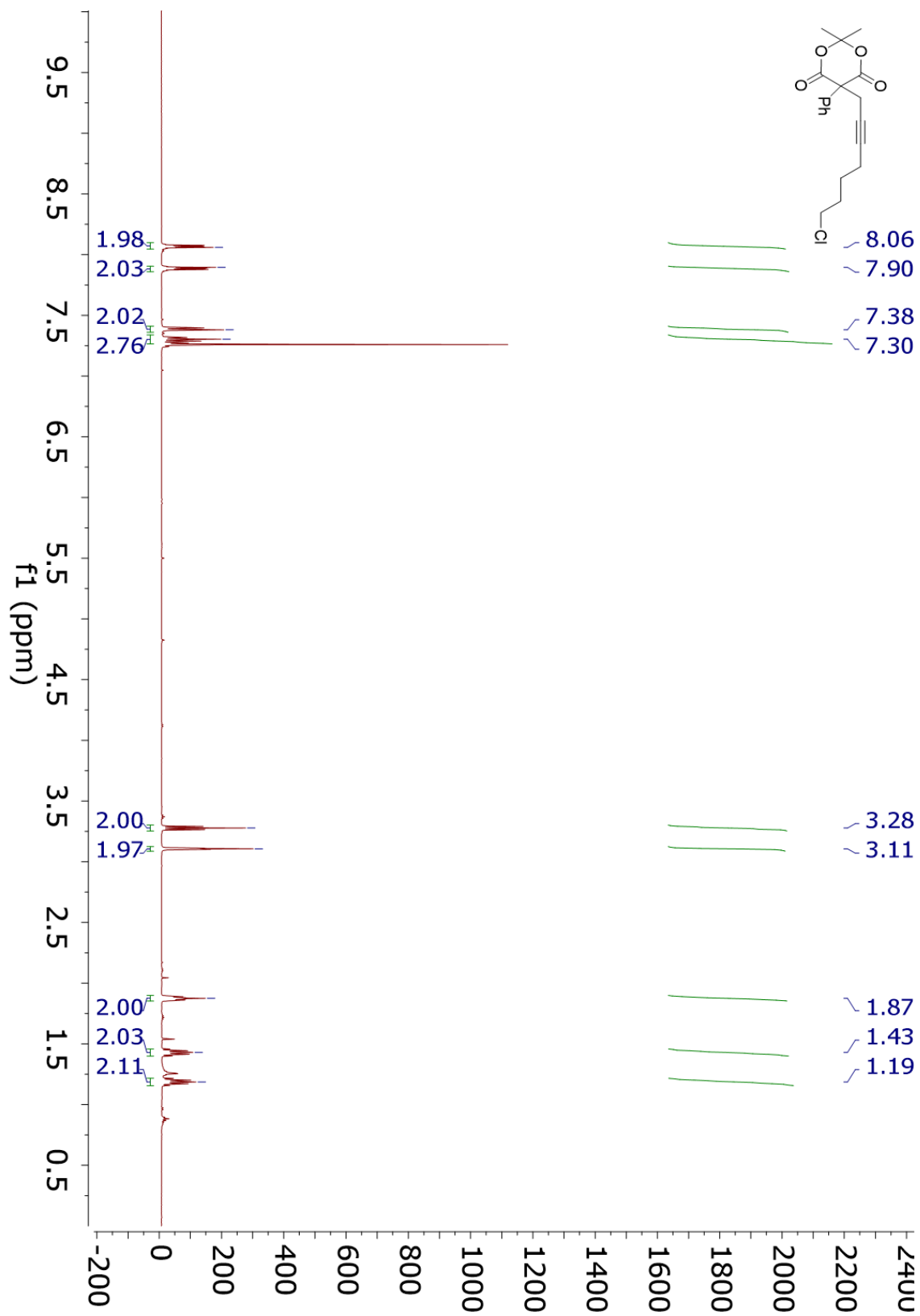
¹H NMR 4.13hh



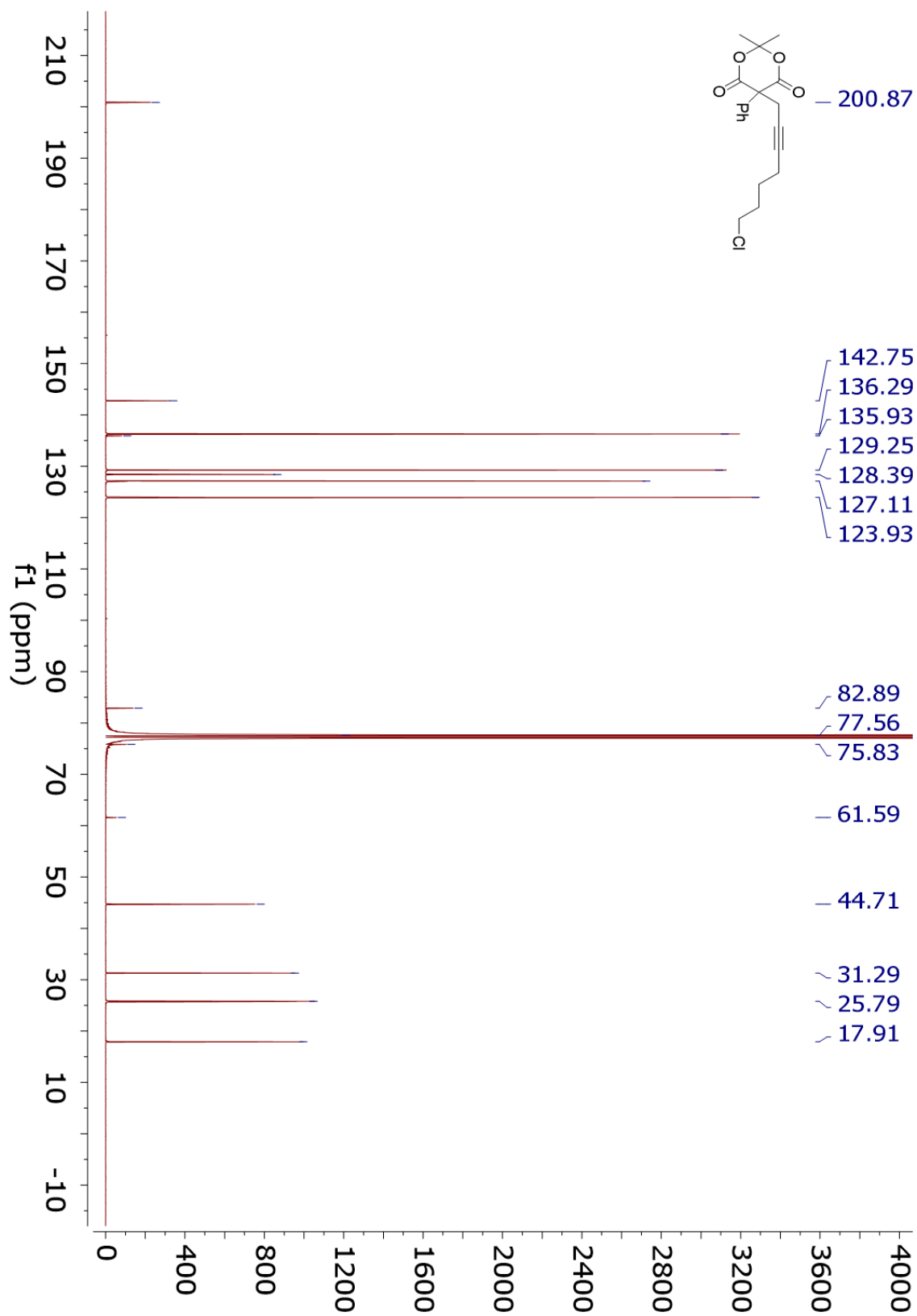
¹³C NMR 4.13hh



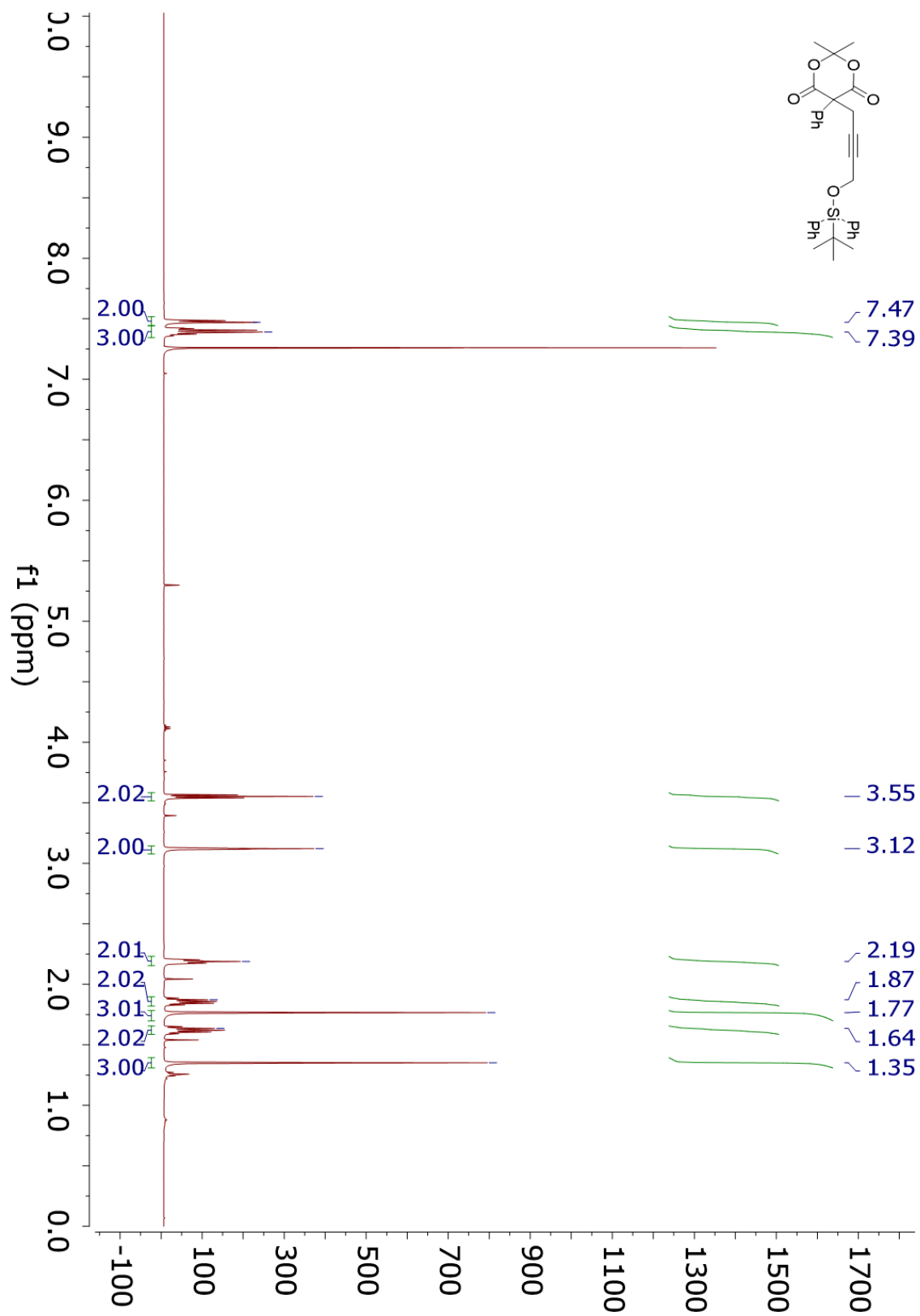
¹H NMR 4.13ii



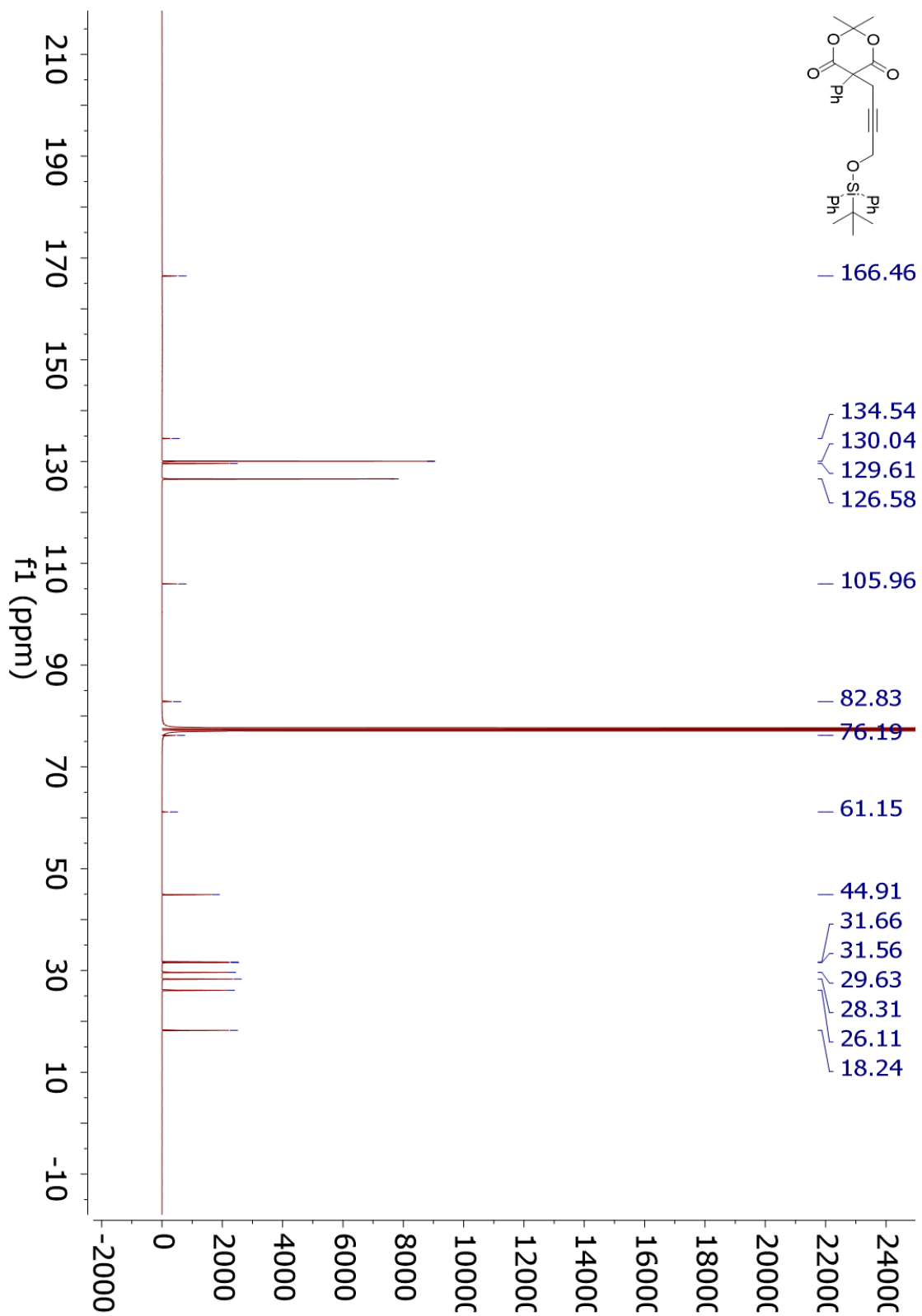
¹³C NMR 4.13ii



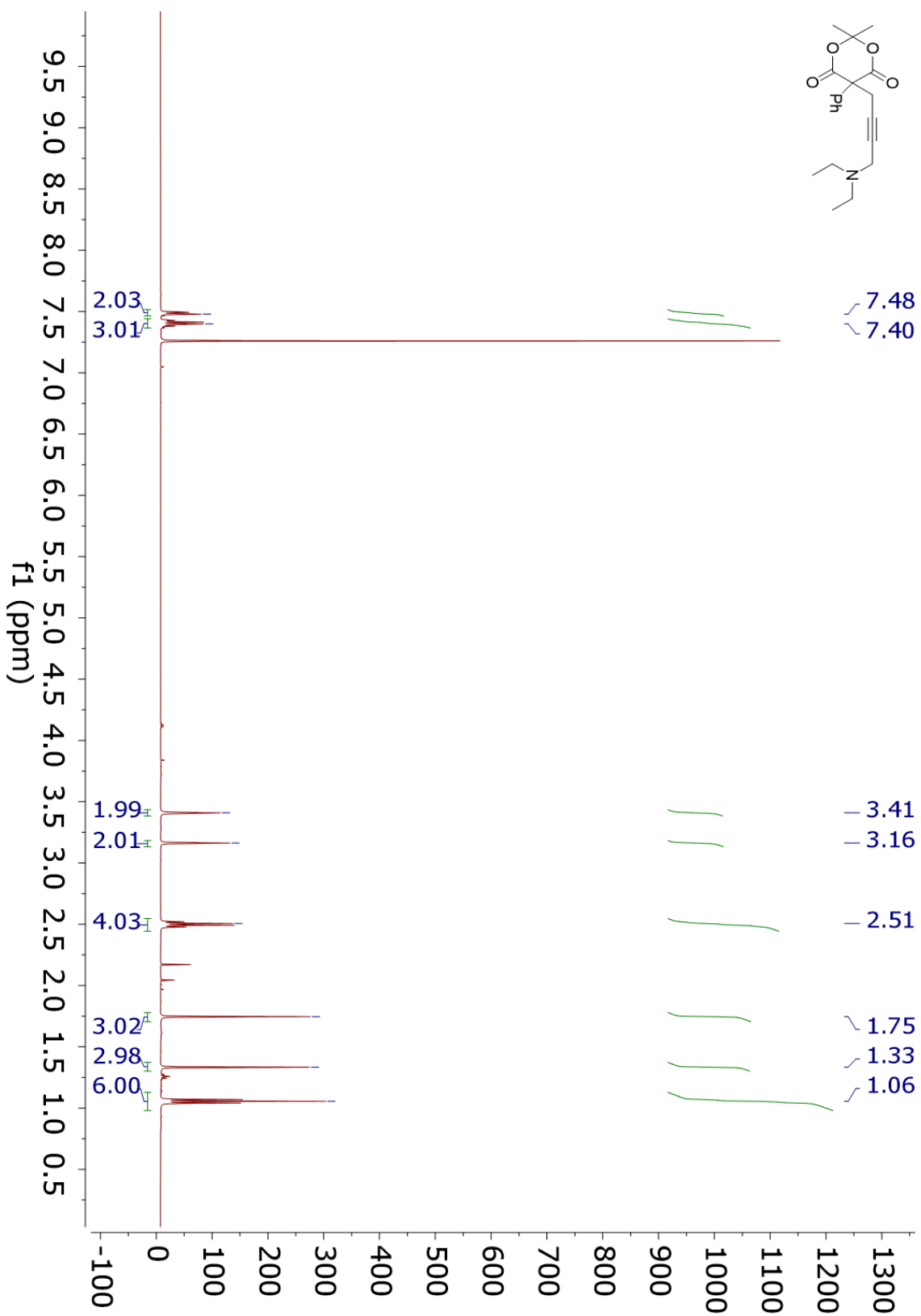
¹H NMR 4.13jj



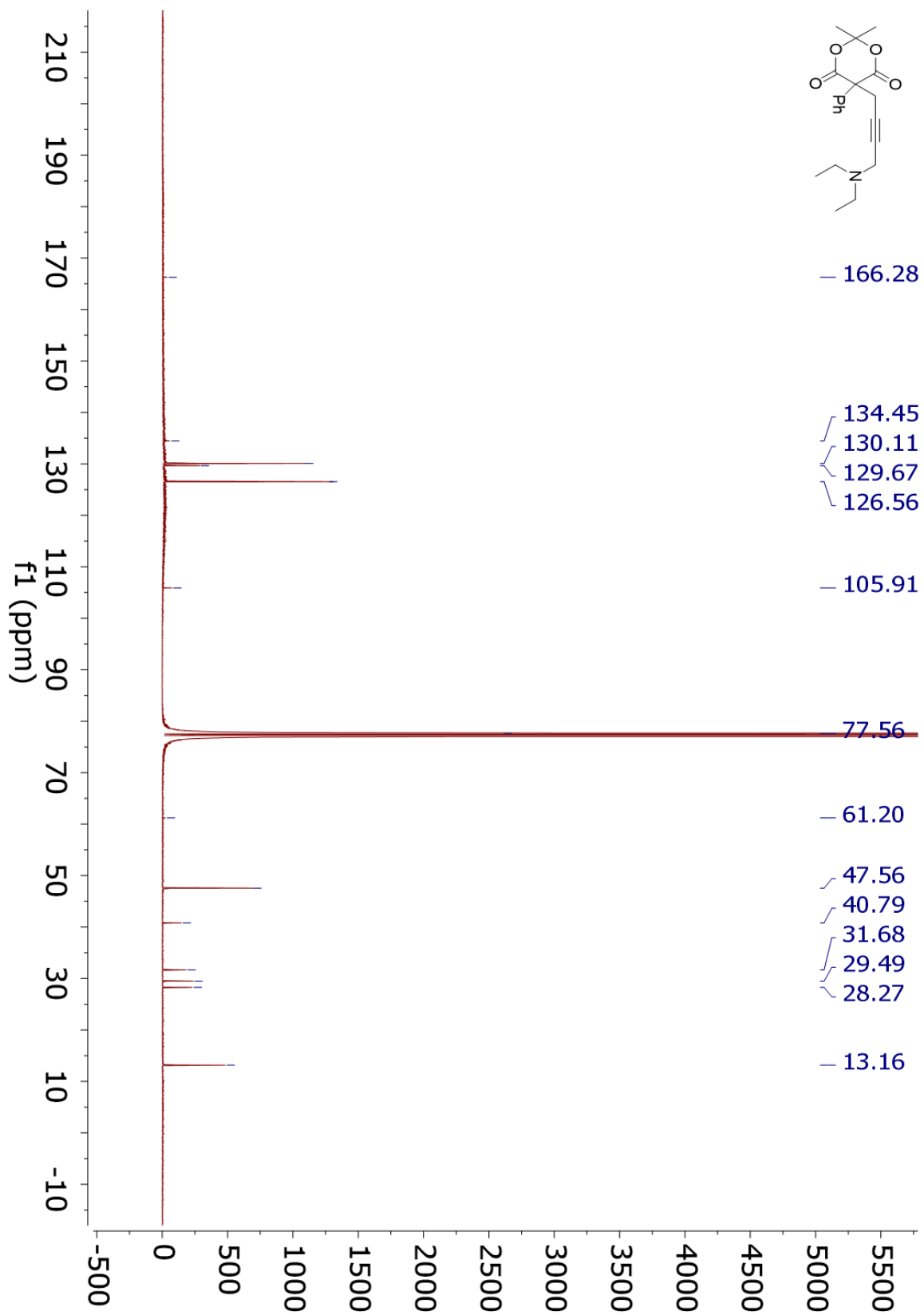
¹³C NMR 4.13jj



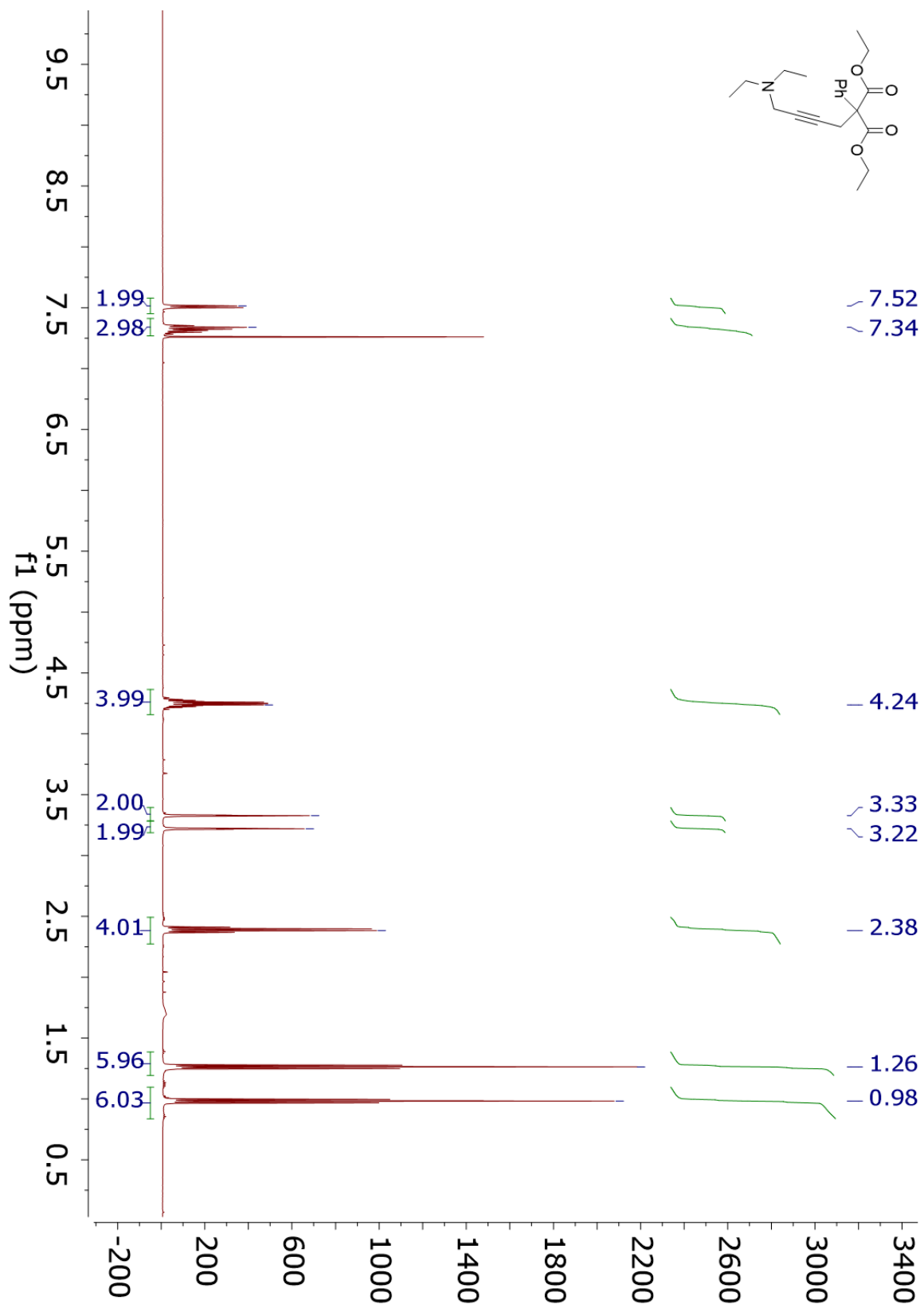
¹H NMR 4.13kk



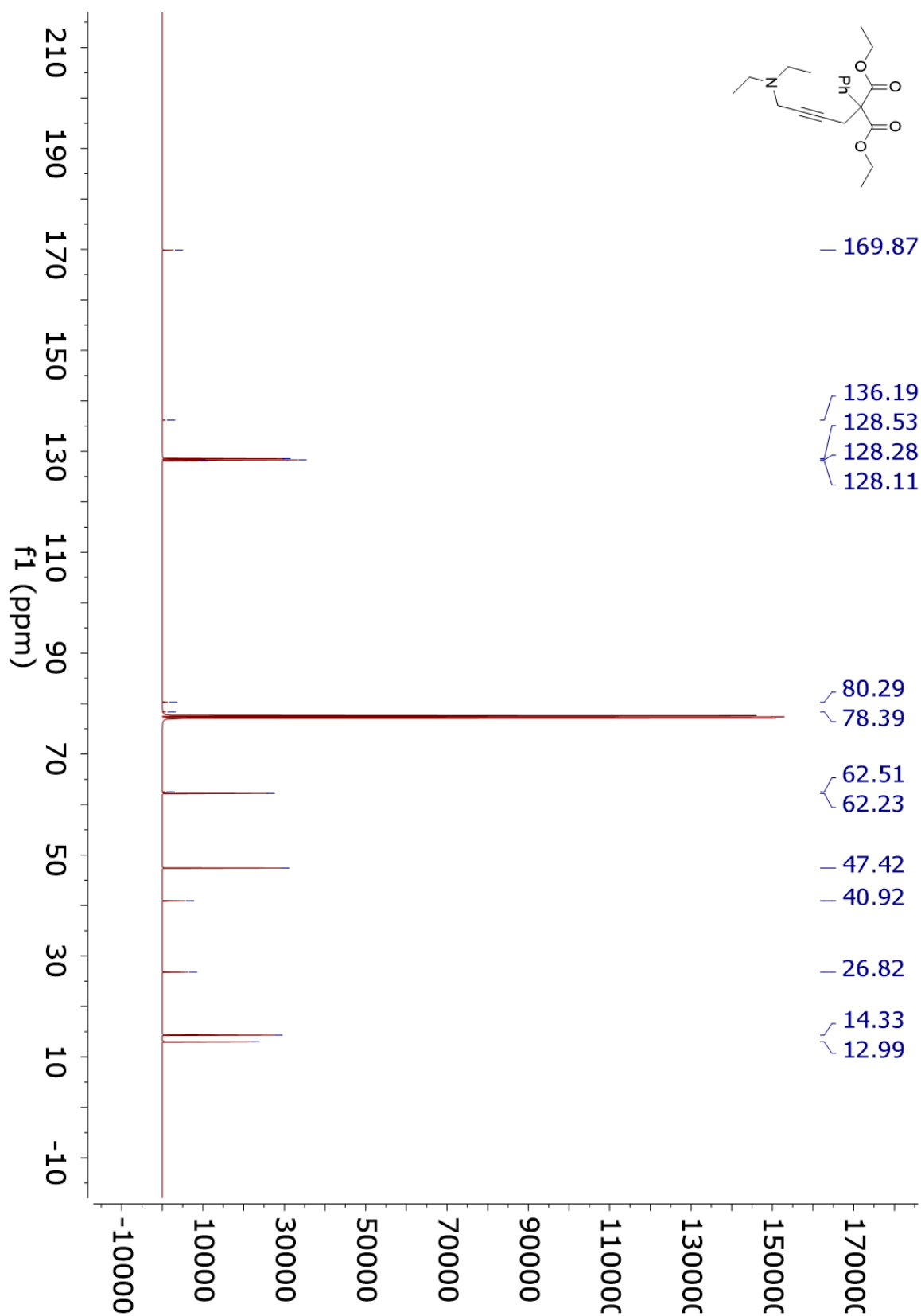
¹³C NMR 4.13kk



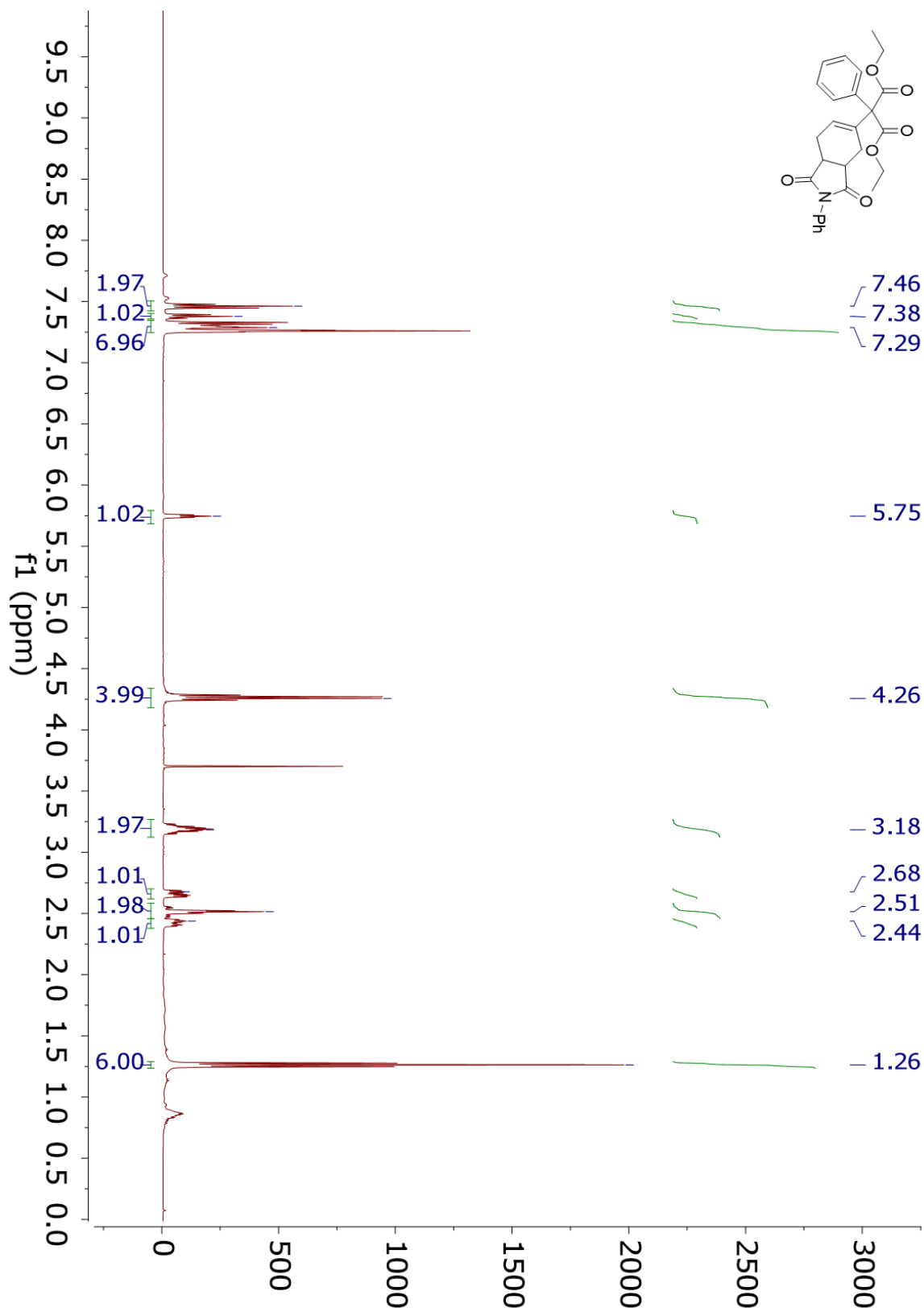
¹H NMR 4.13II



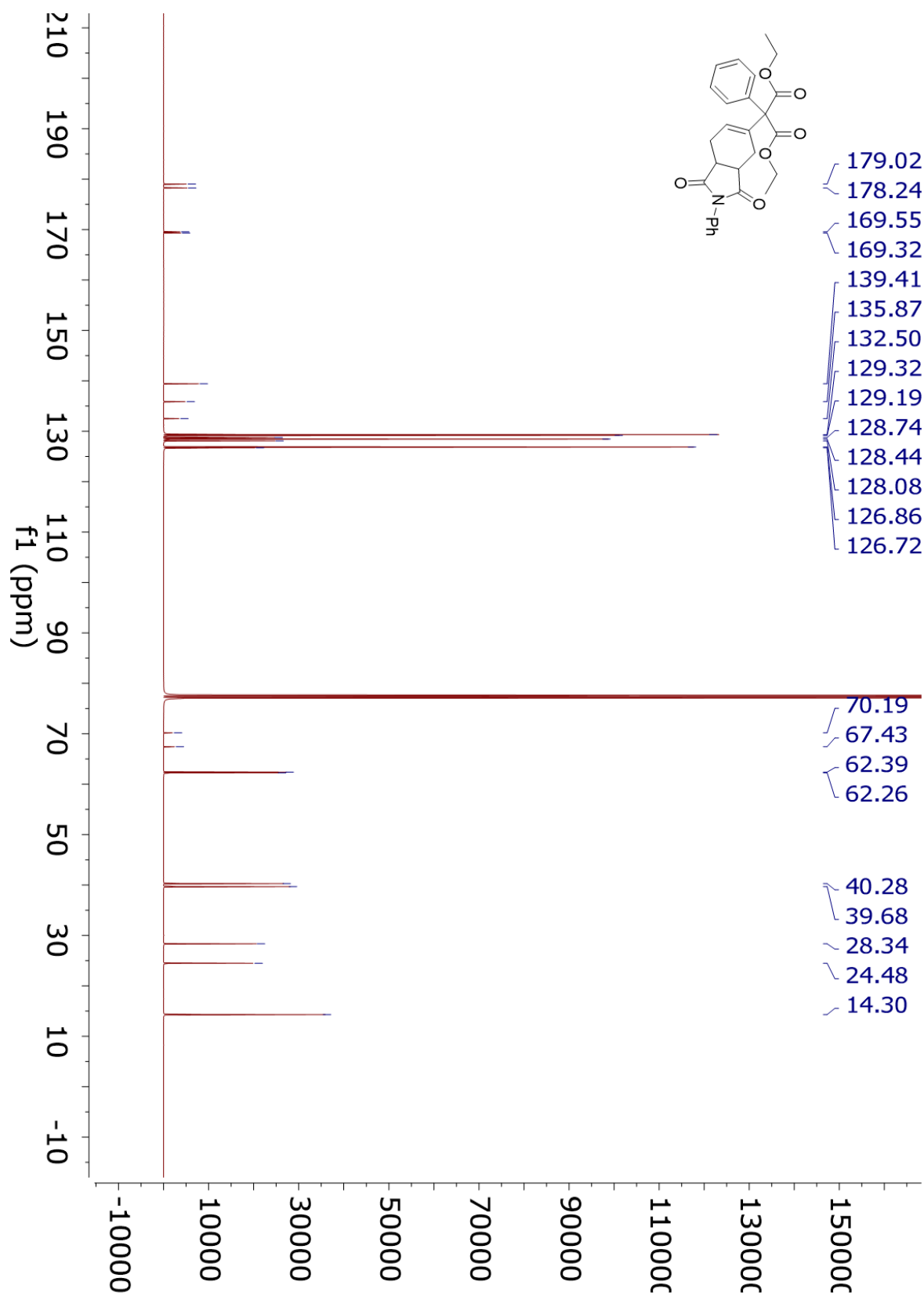
¹³C NMR 4.1311



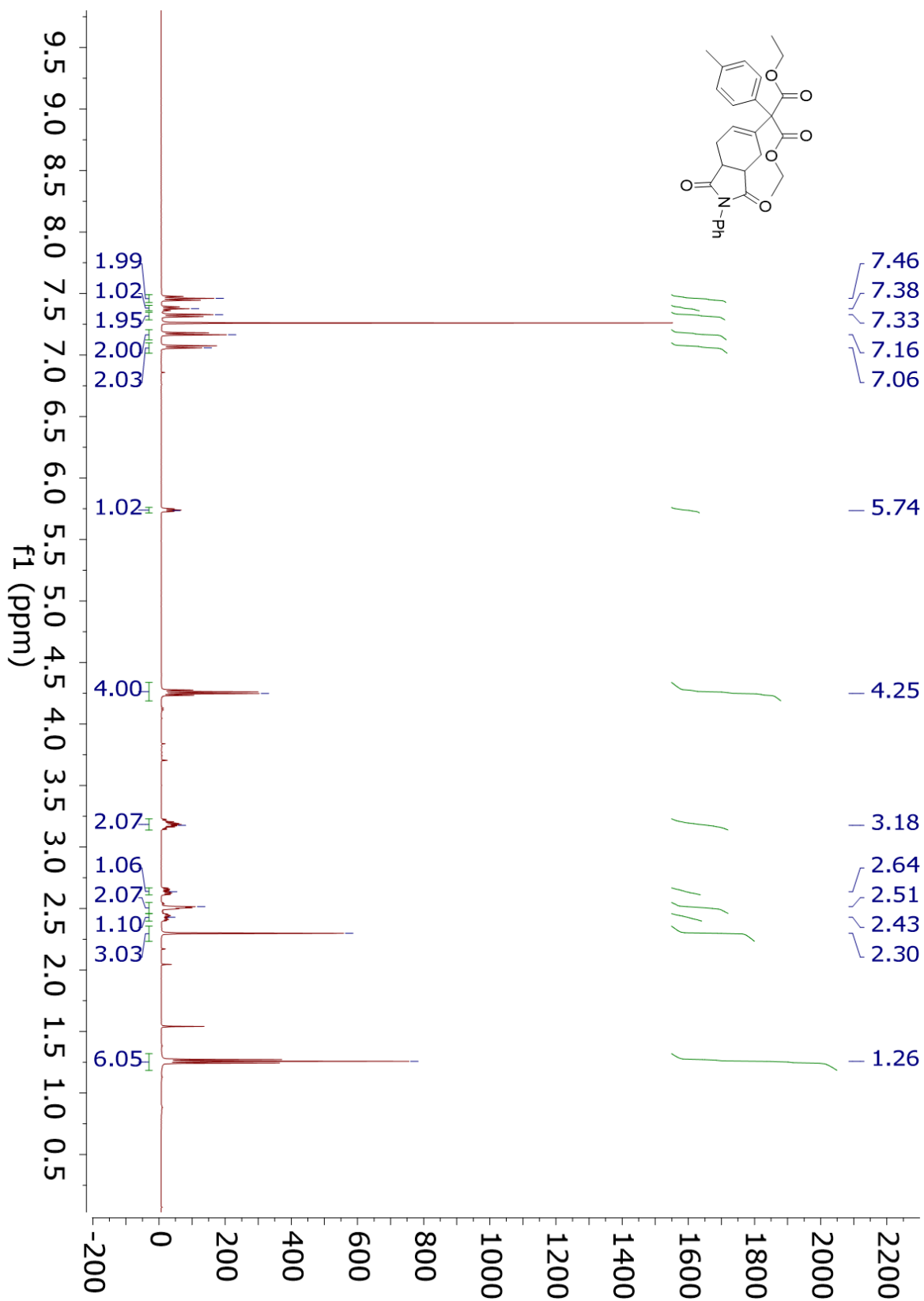
¹H NMR 4.14a



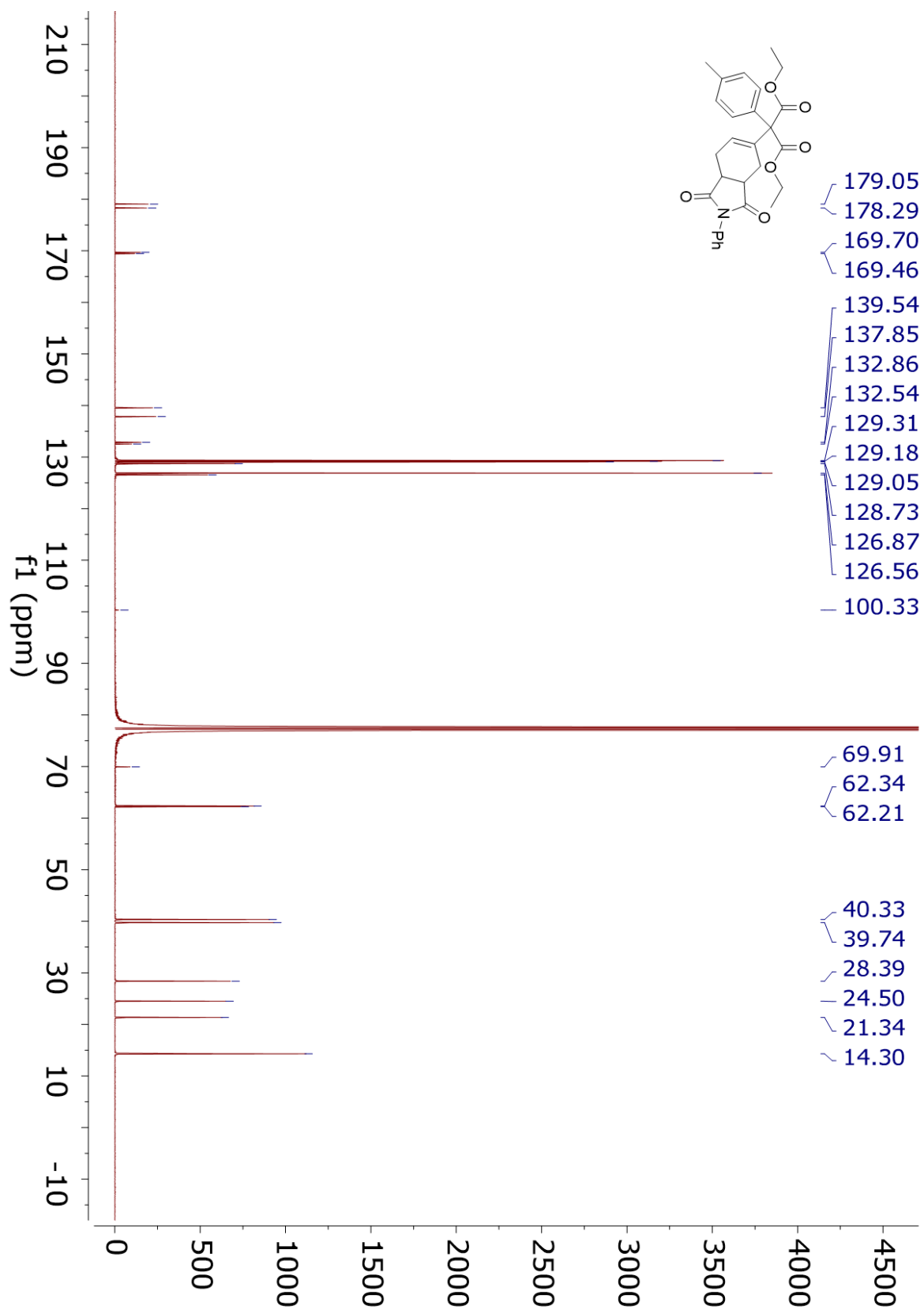
¹³C NMR 4.14a



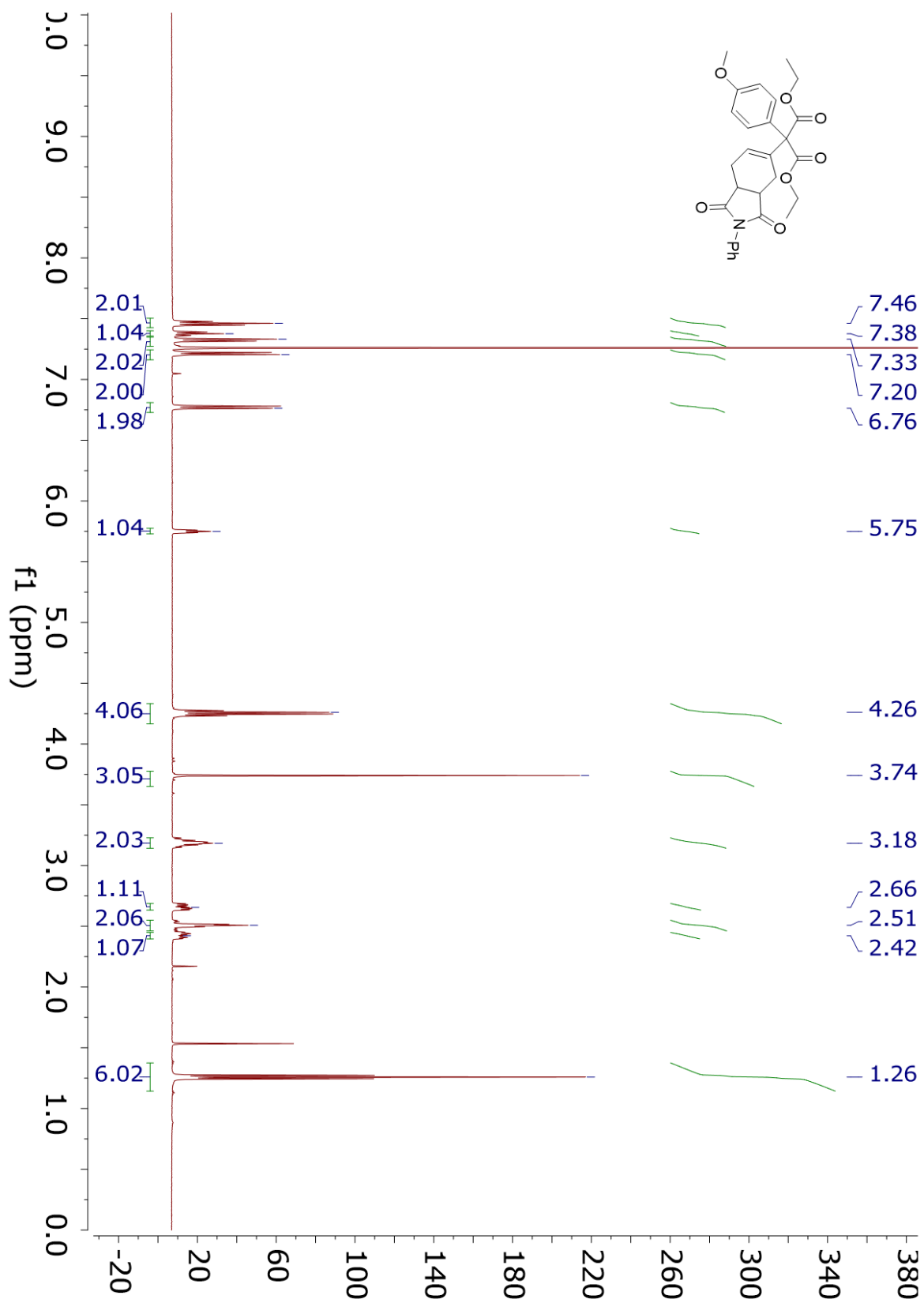
¹H NMR 4.14b



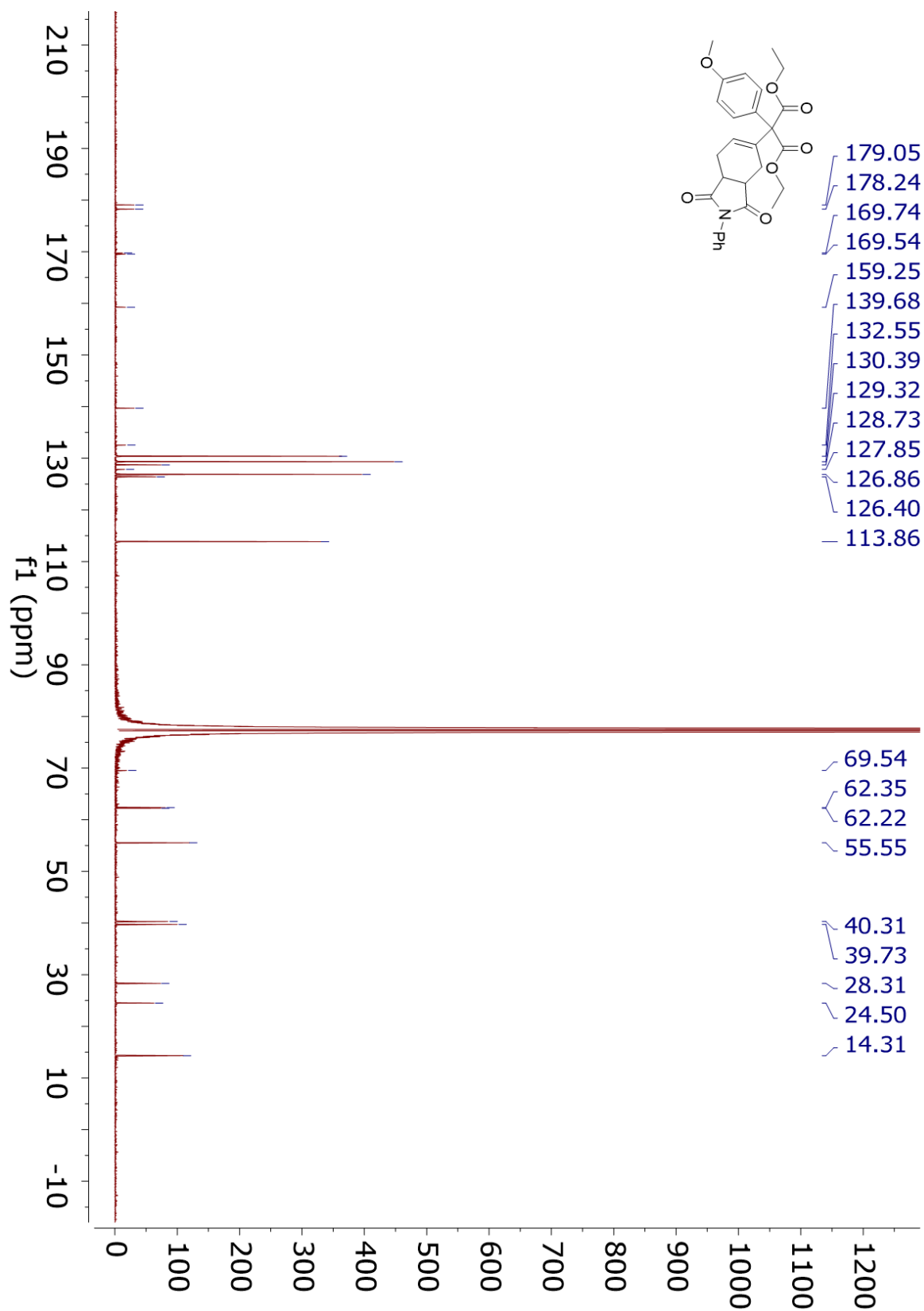
¹³C NMR 4.14b



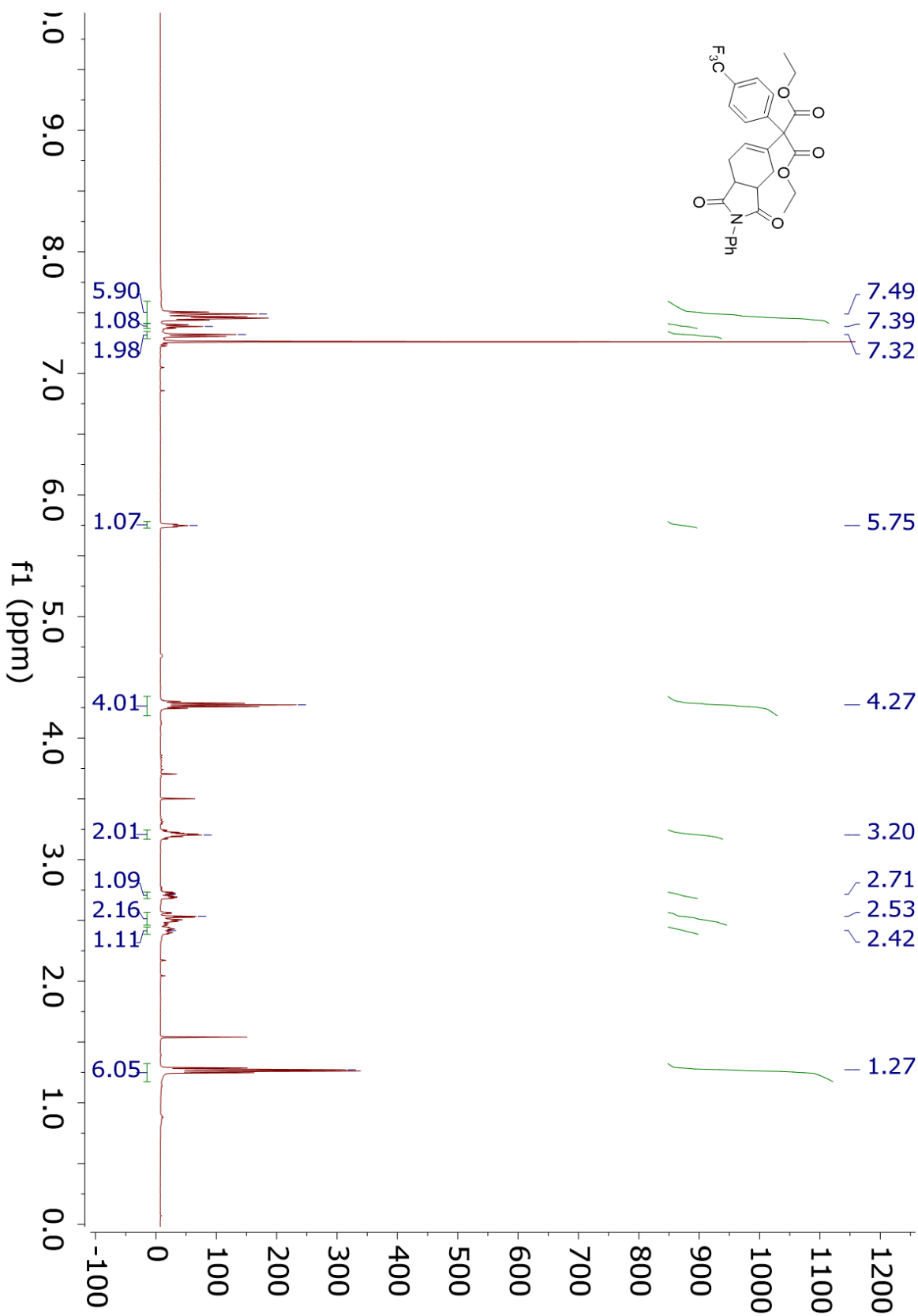
¹H NMR 4.14c



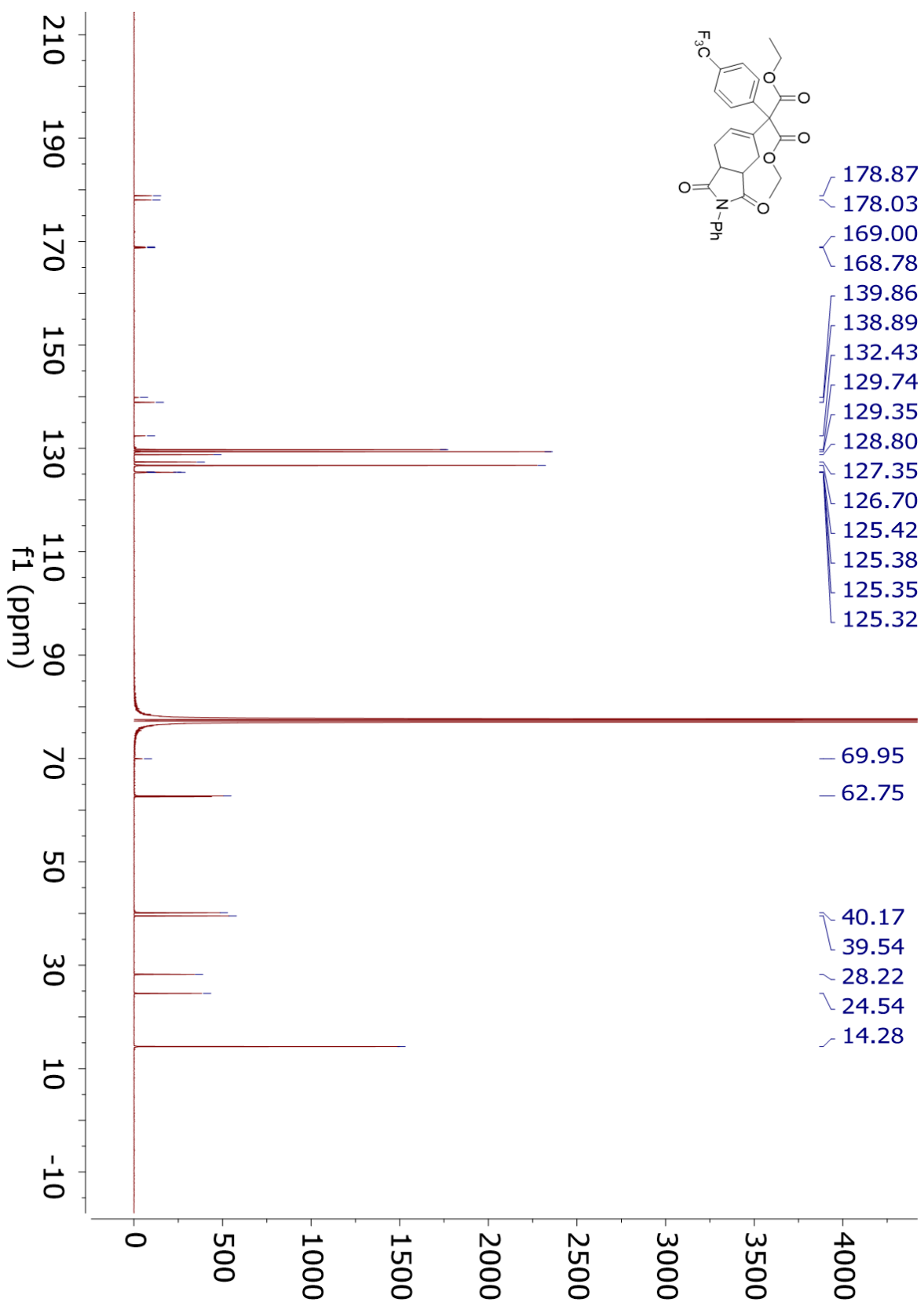
¹³C NMR 4.14c



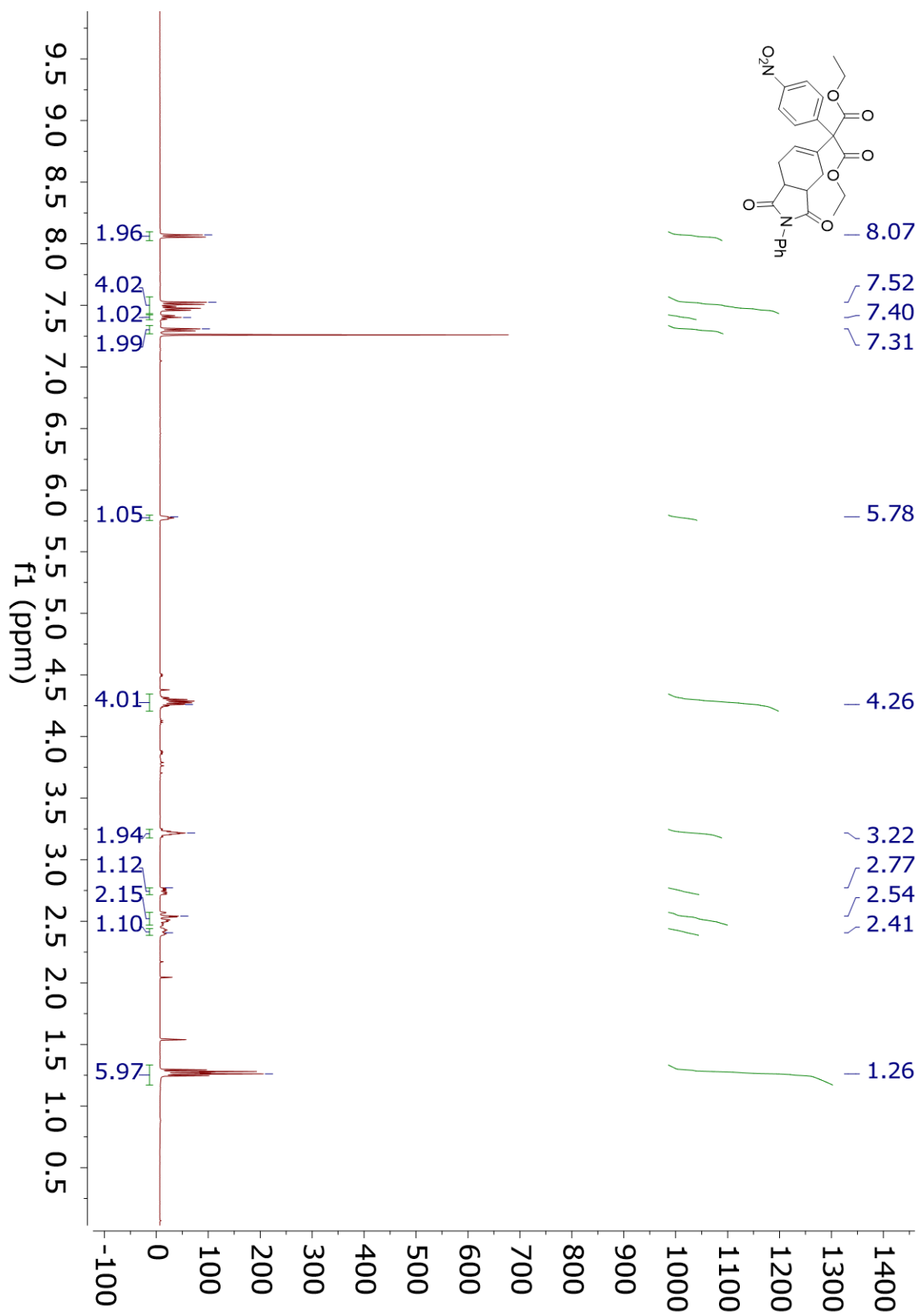
¹H NMR 4.14d



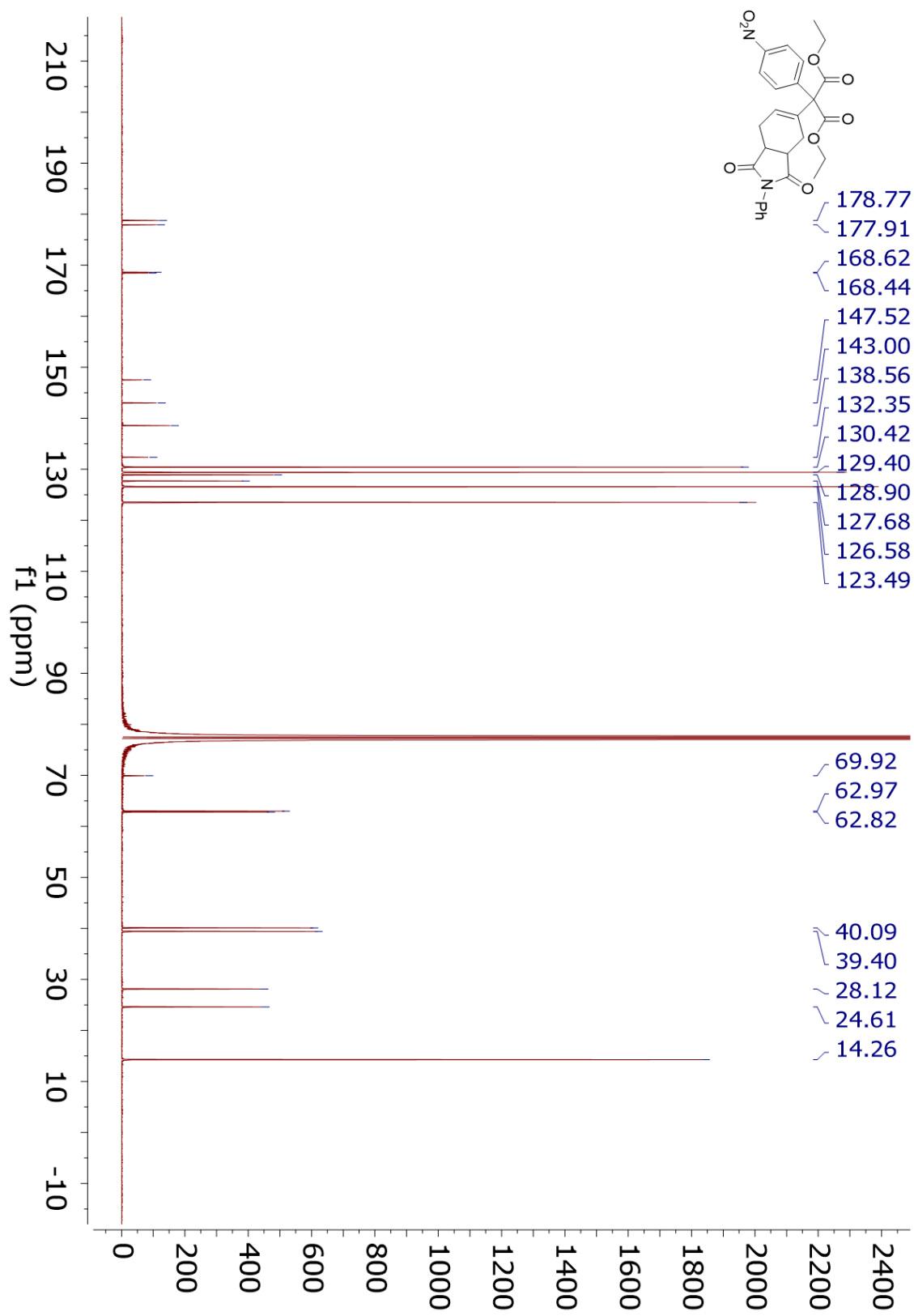
¹³C NMR 4.14d



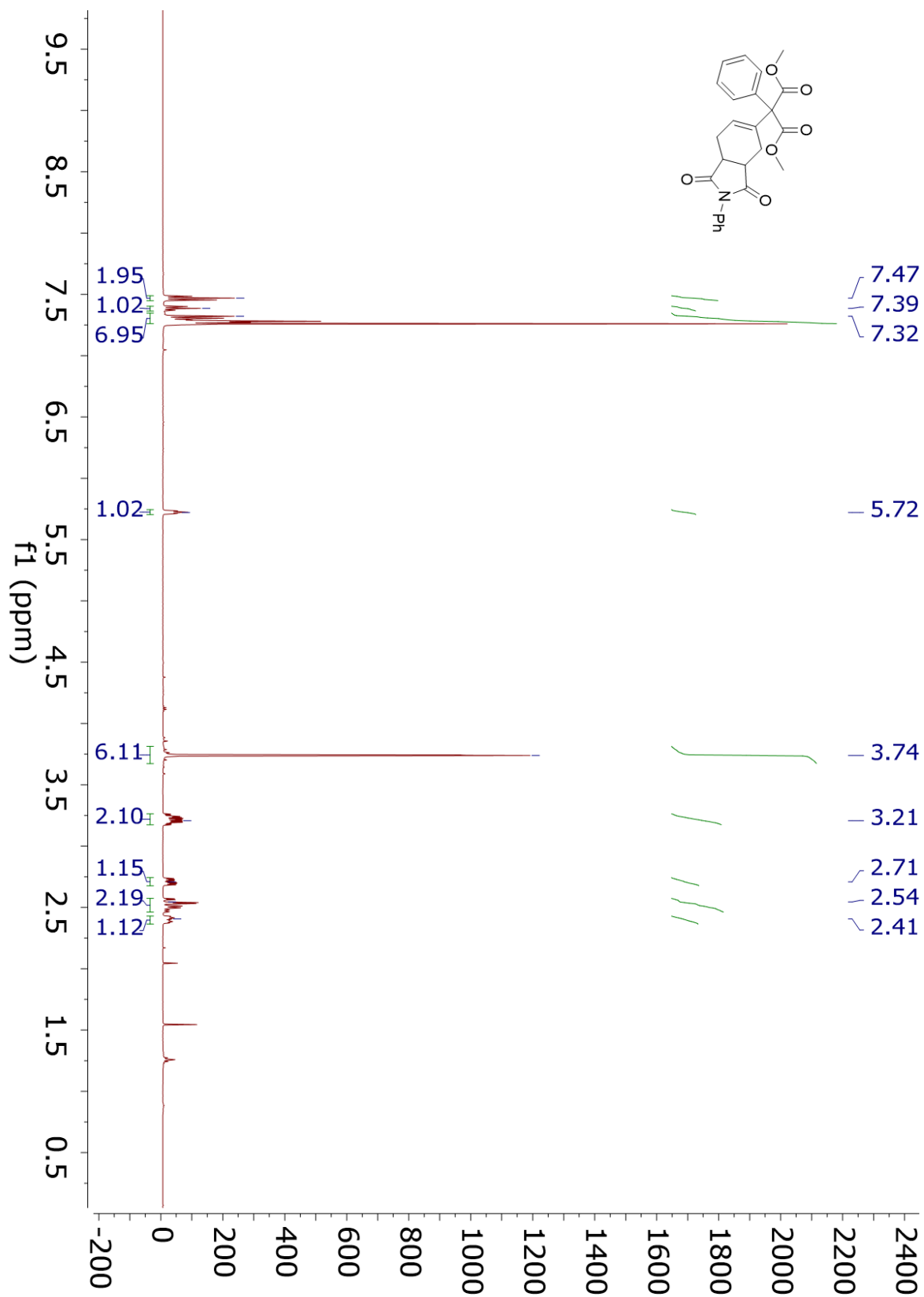
¹H NMR 4.14e



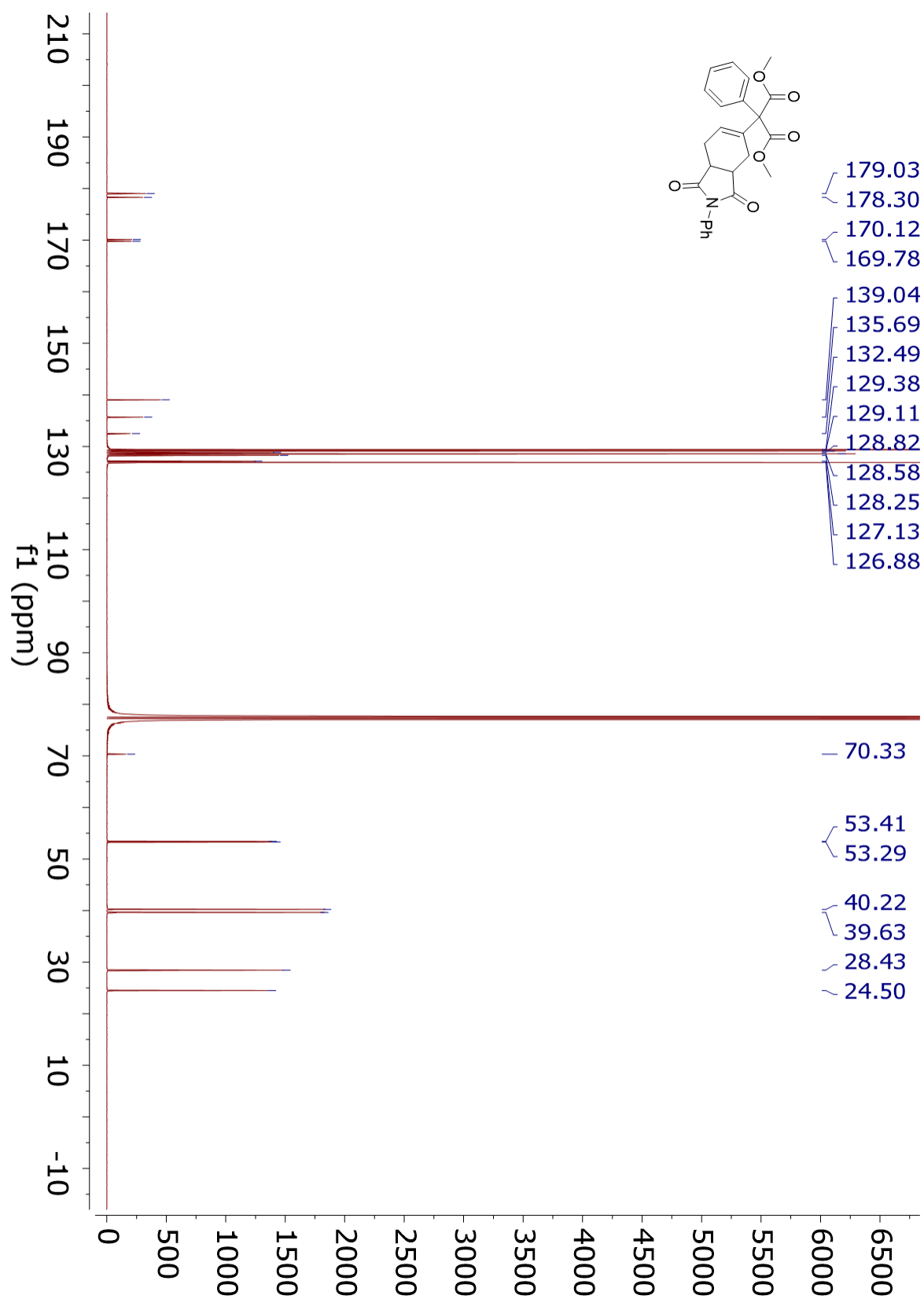
¹³C NMR 4.14e



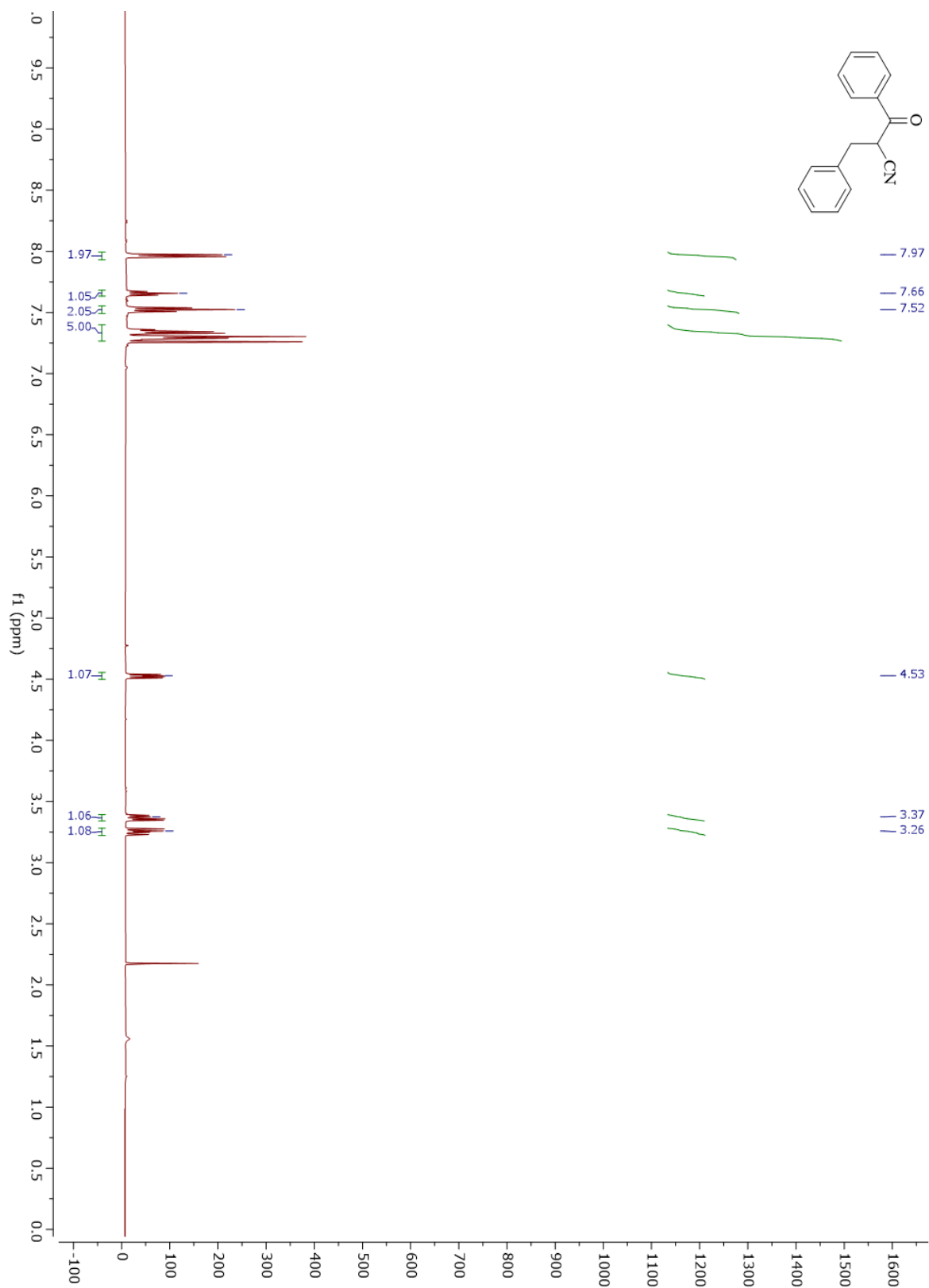
¹H NMR 4.14f



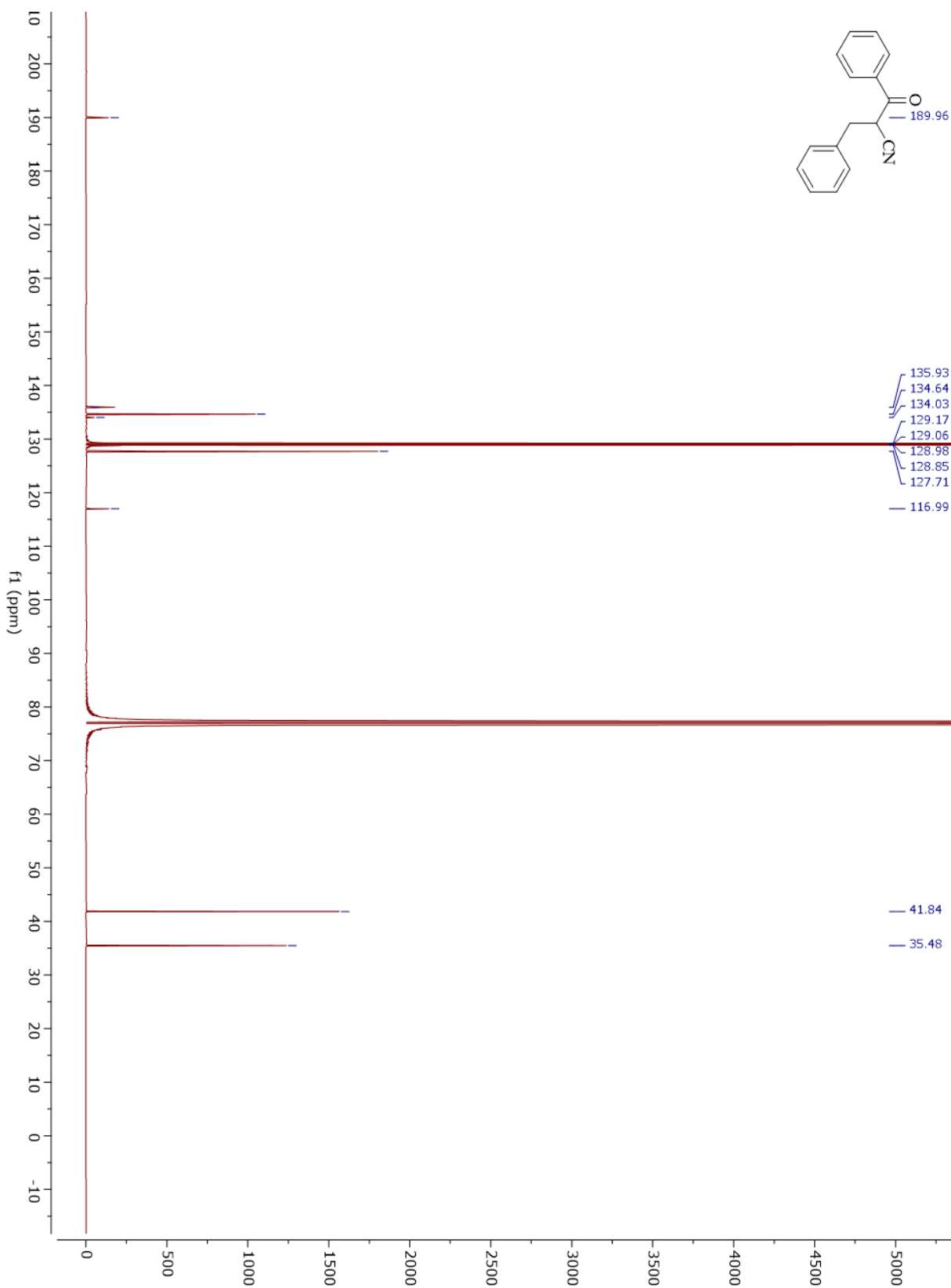
¹³C NMR 4.14f



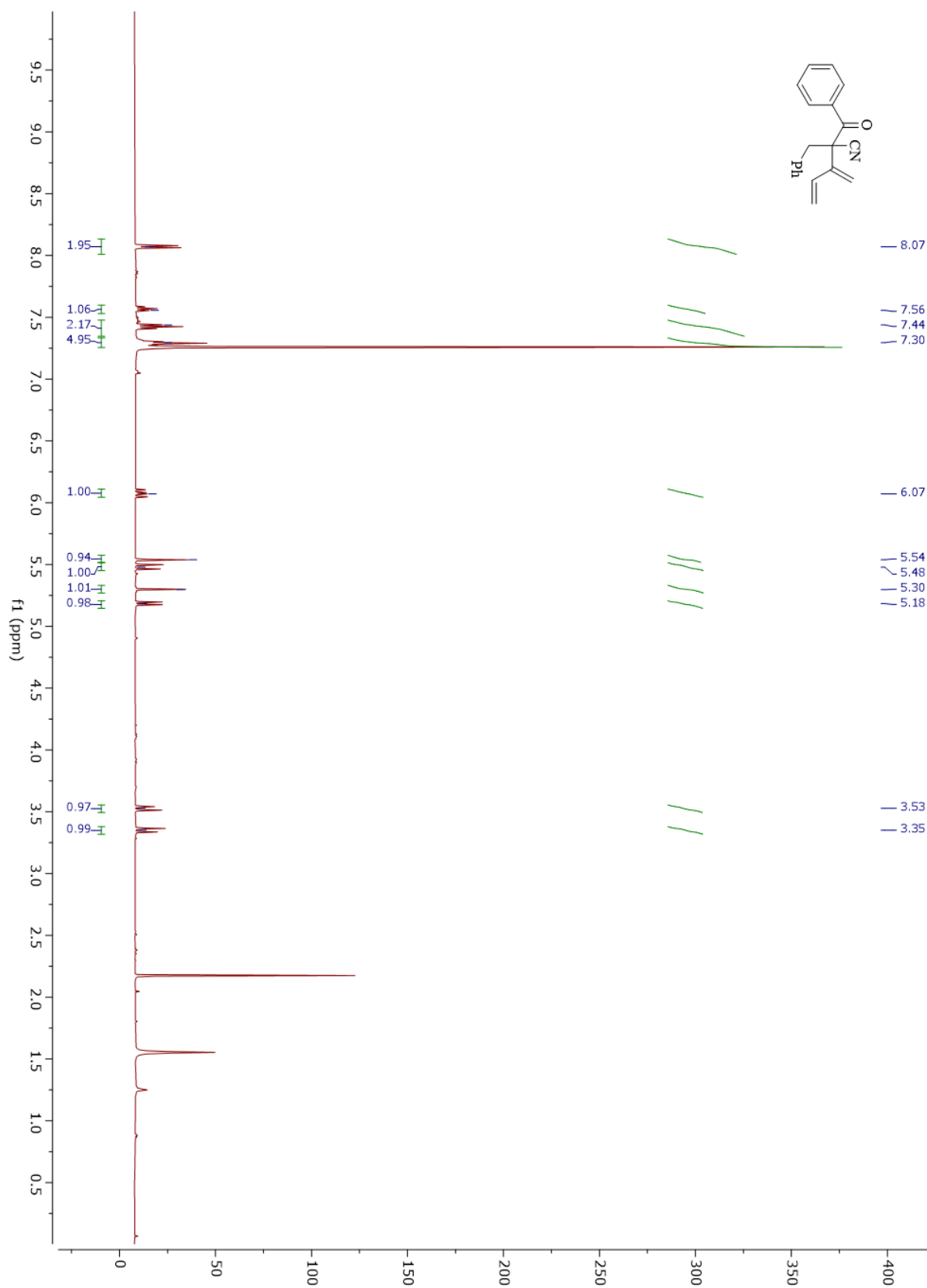
¹H NMR 4.15a



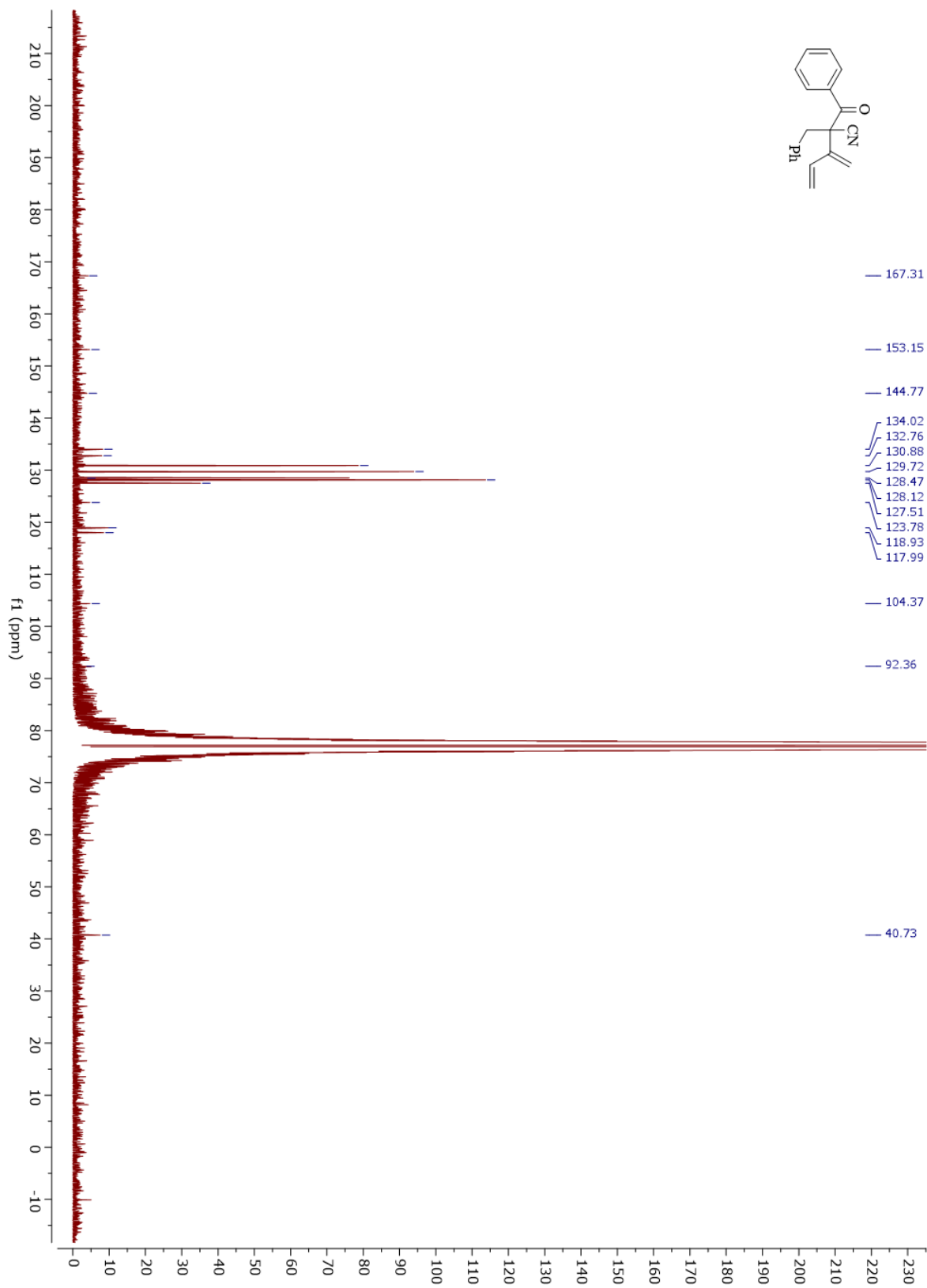
¹³C NMR 4.15a



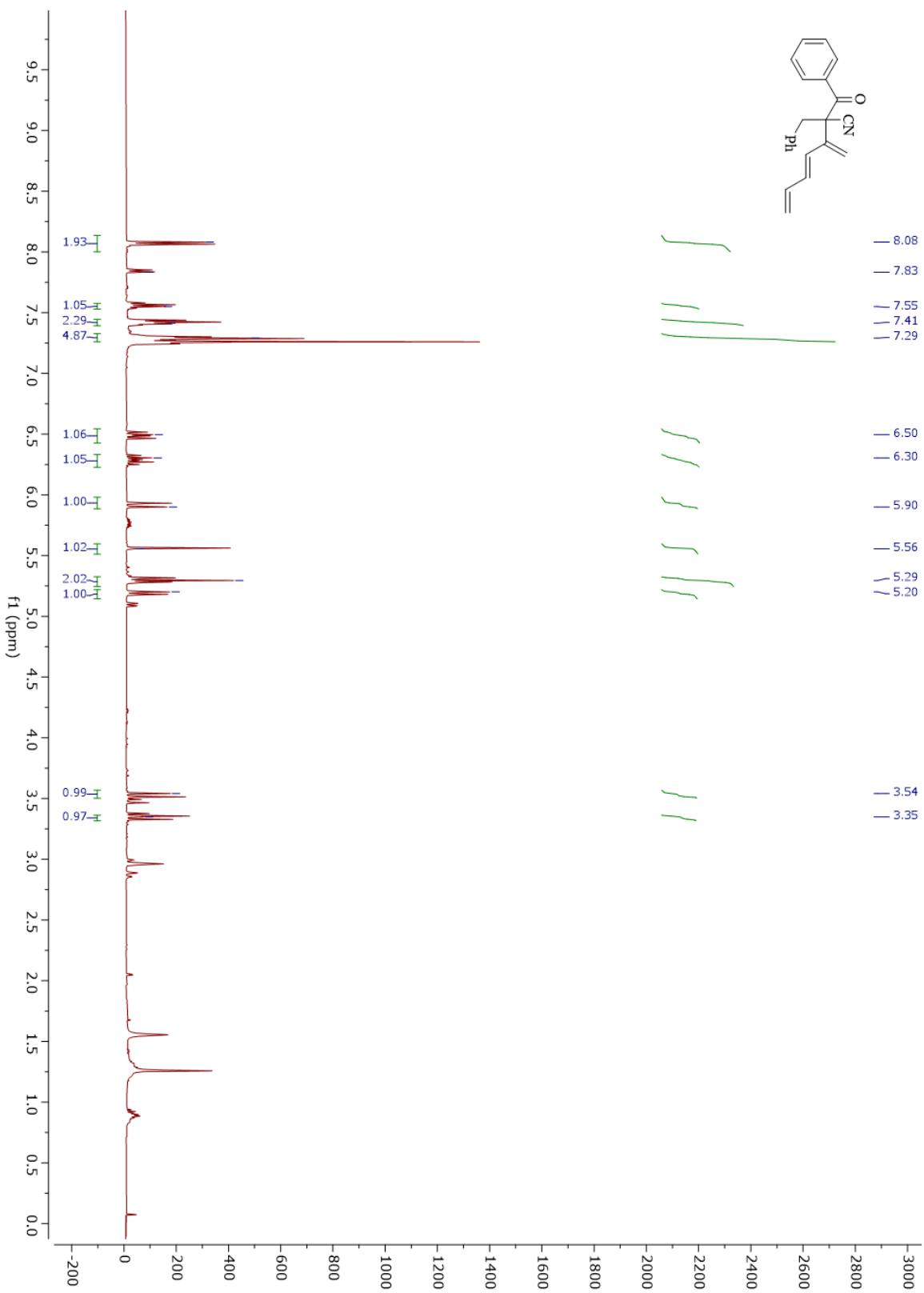
¹H NMR 4.16a



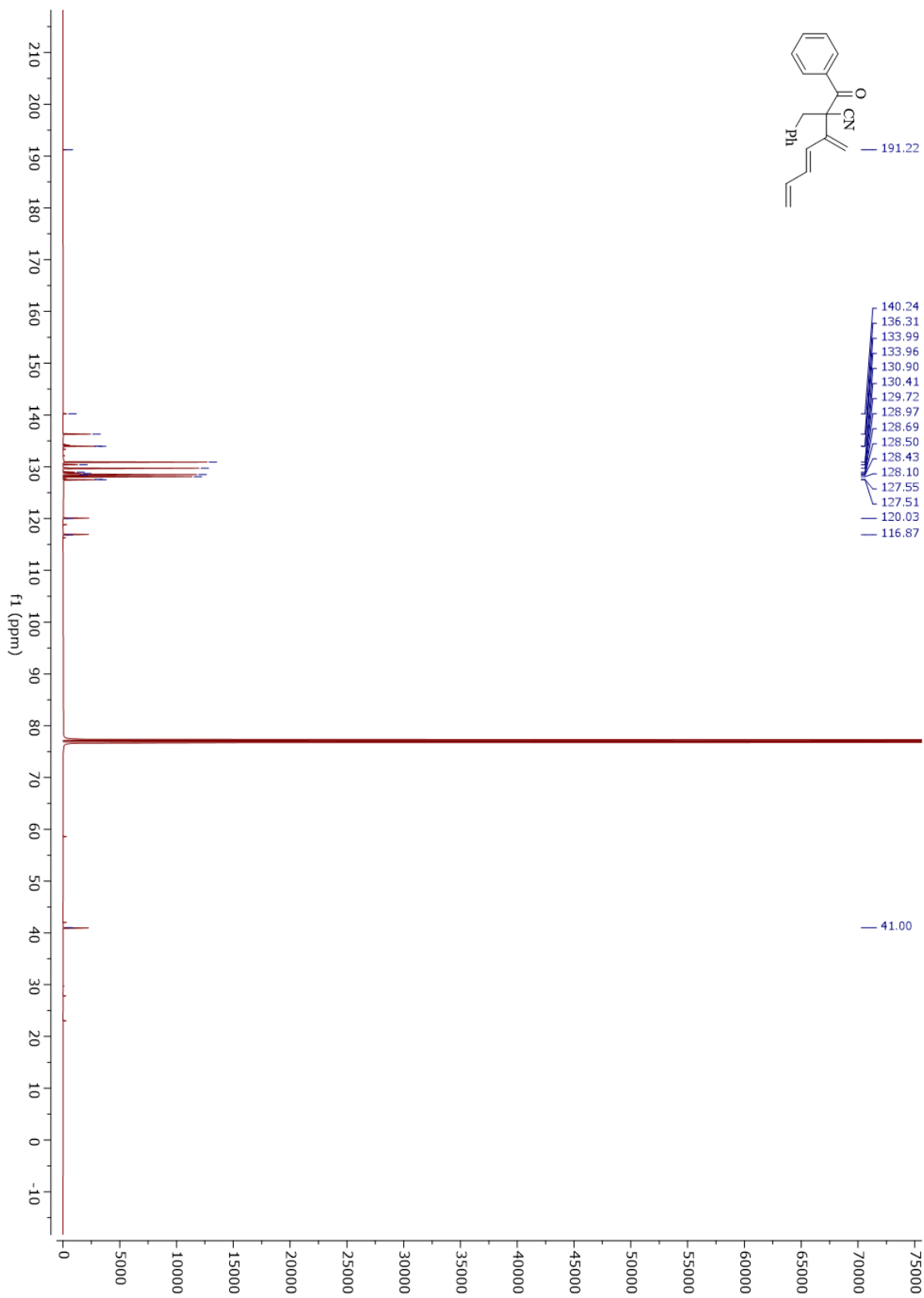
¹³C NMR 4.16a



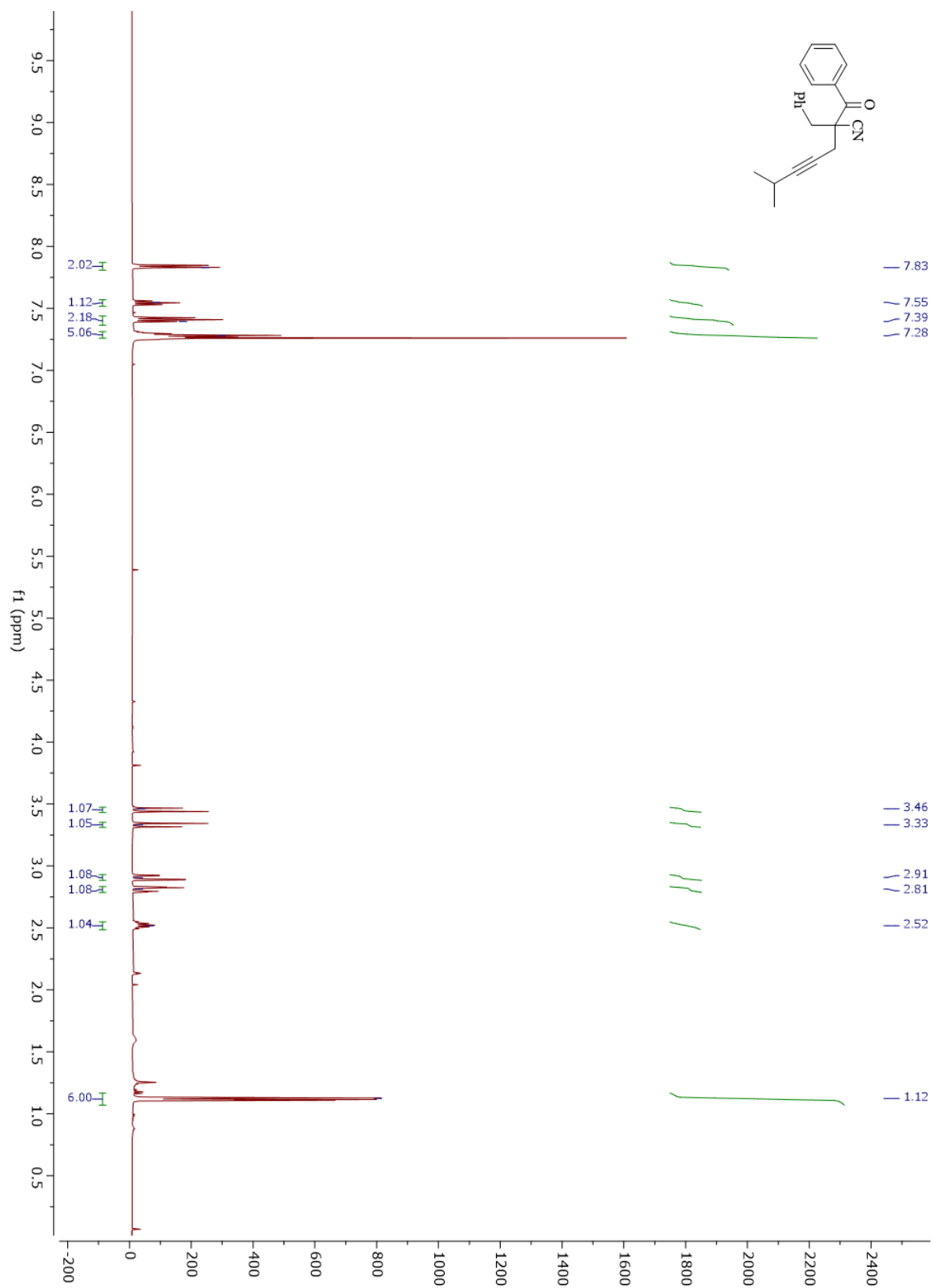
¹H NMR 4.16b



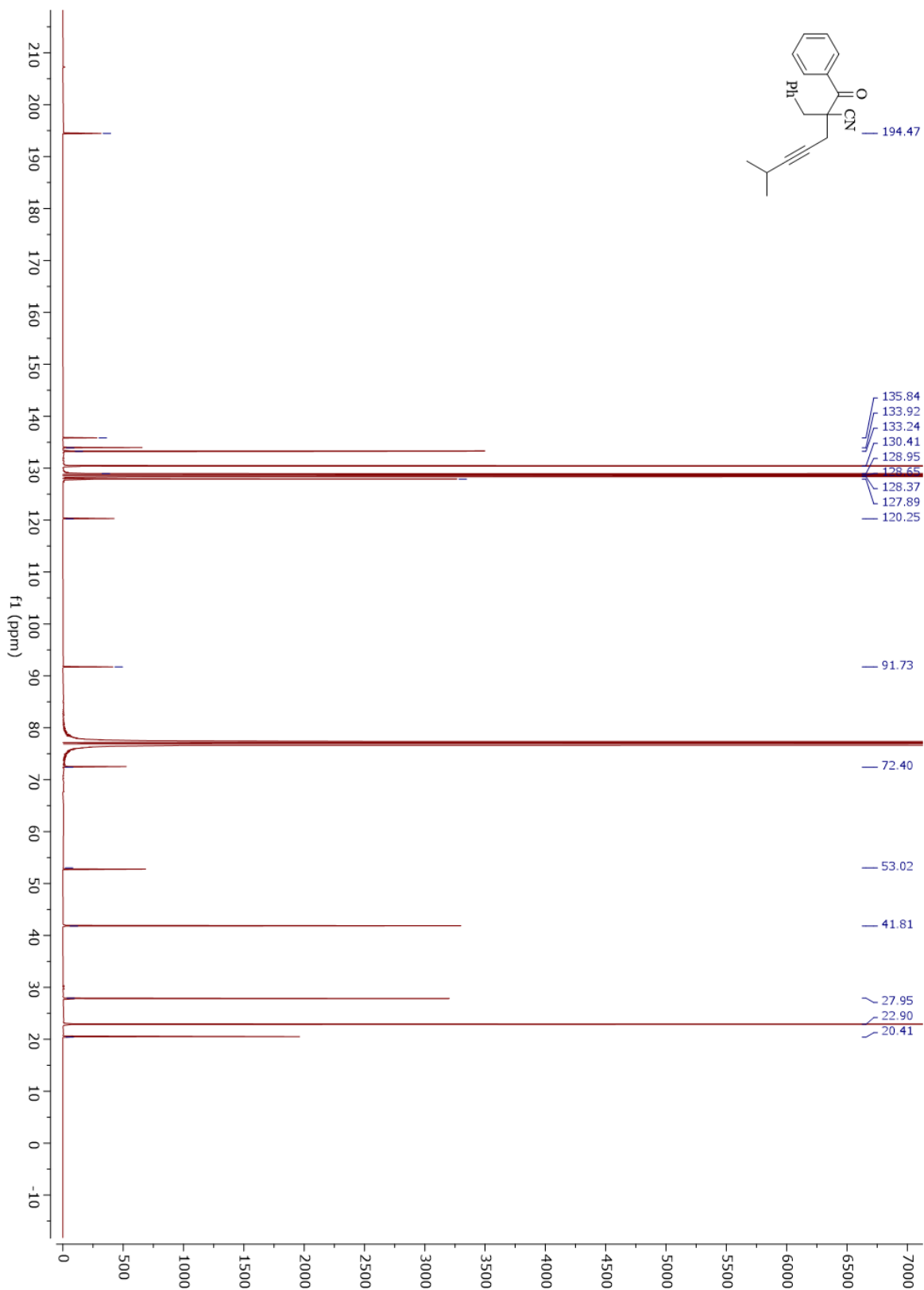
¹³C NMR 4.16b



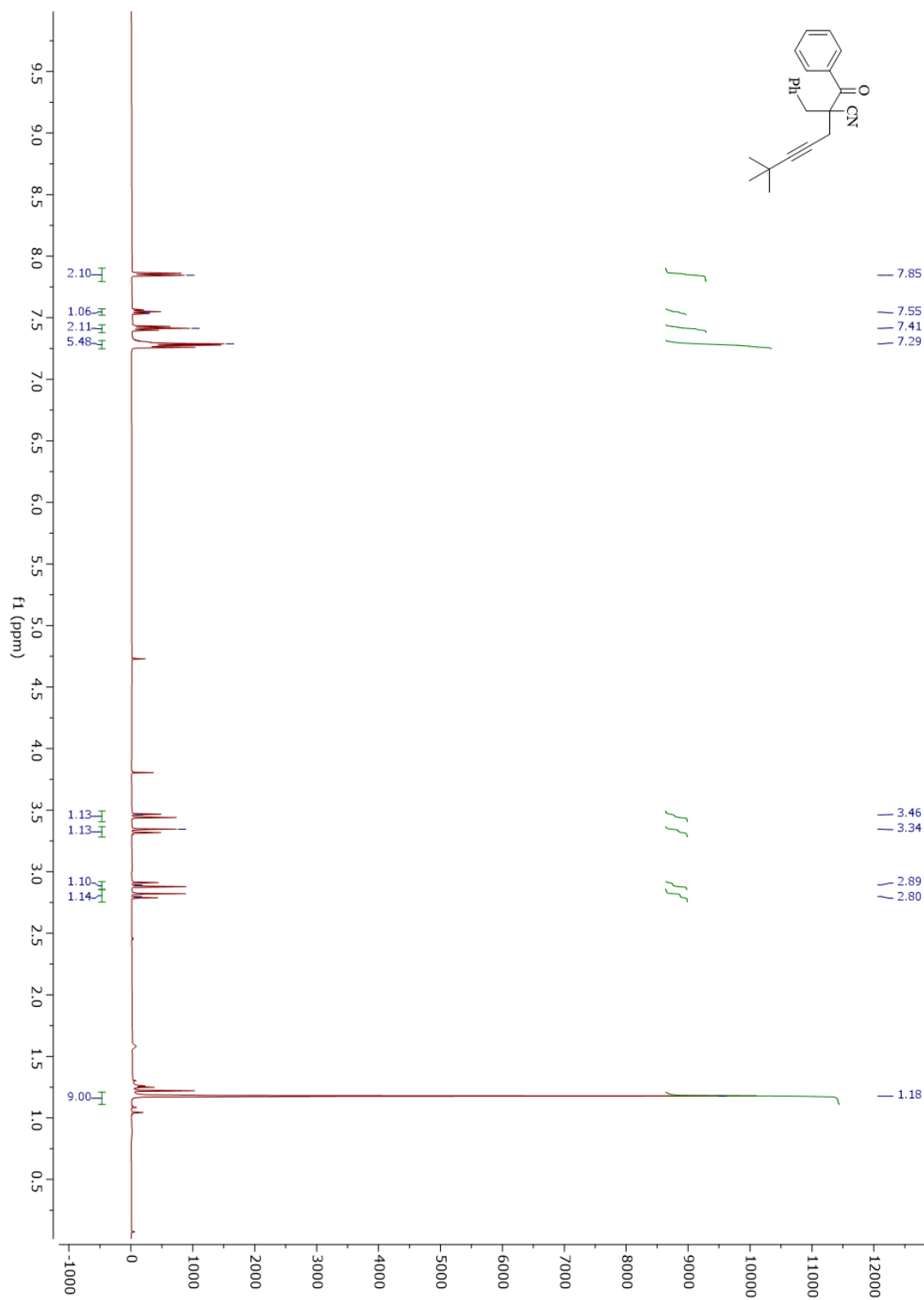
¹H NMR 4.16c



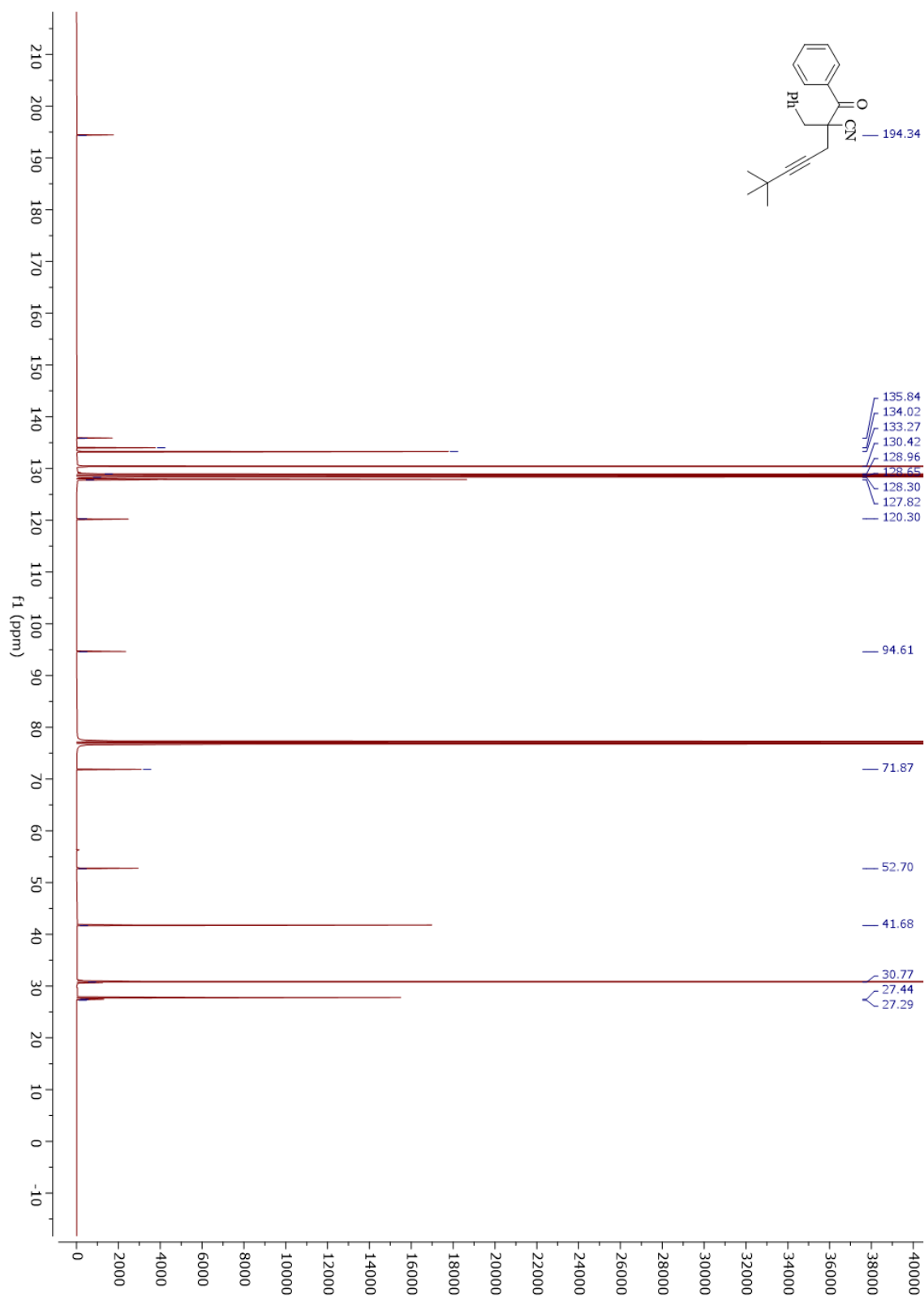
¹³C NMR 4.16c



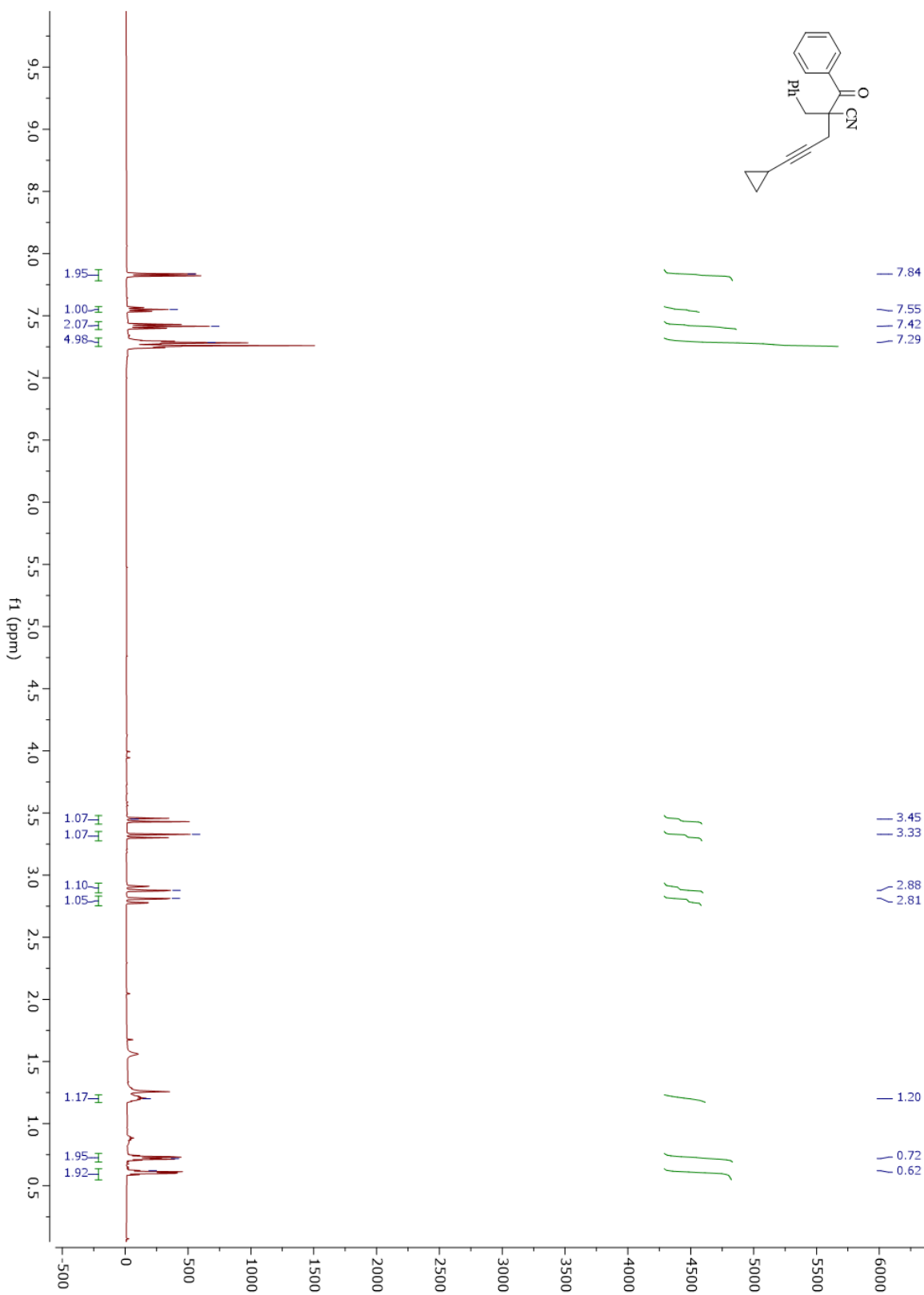
¹H NMR 4.16d



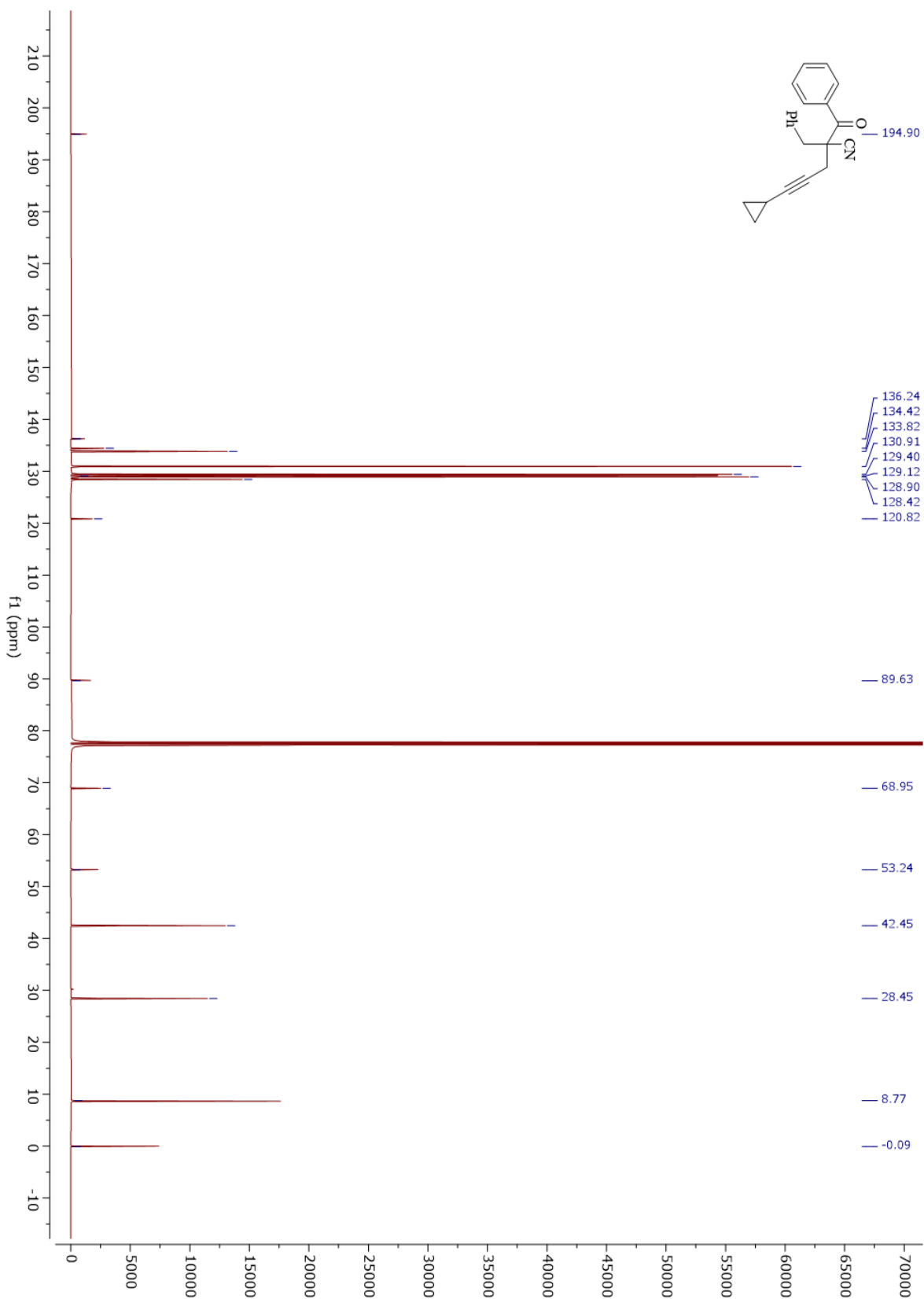
¹³C NMR 4.16d



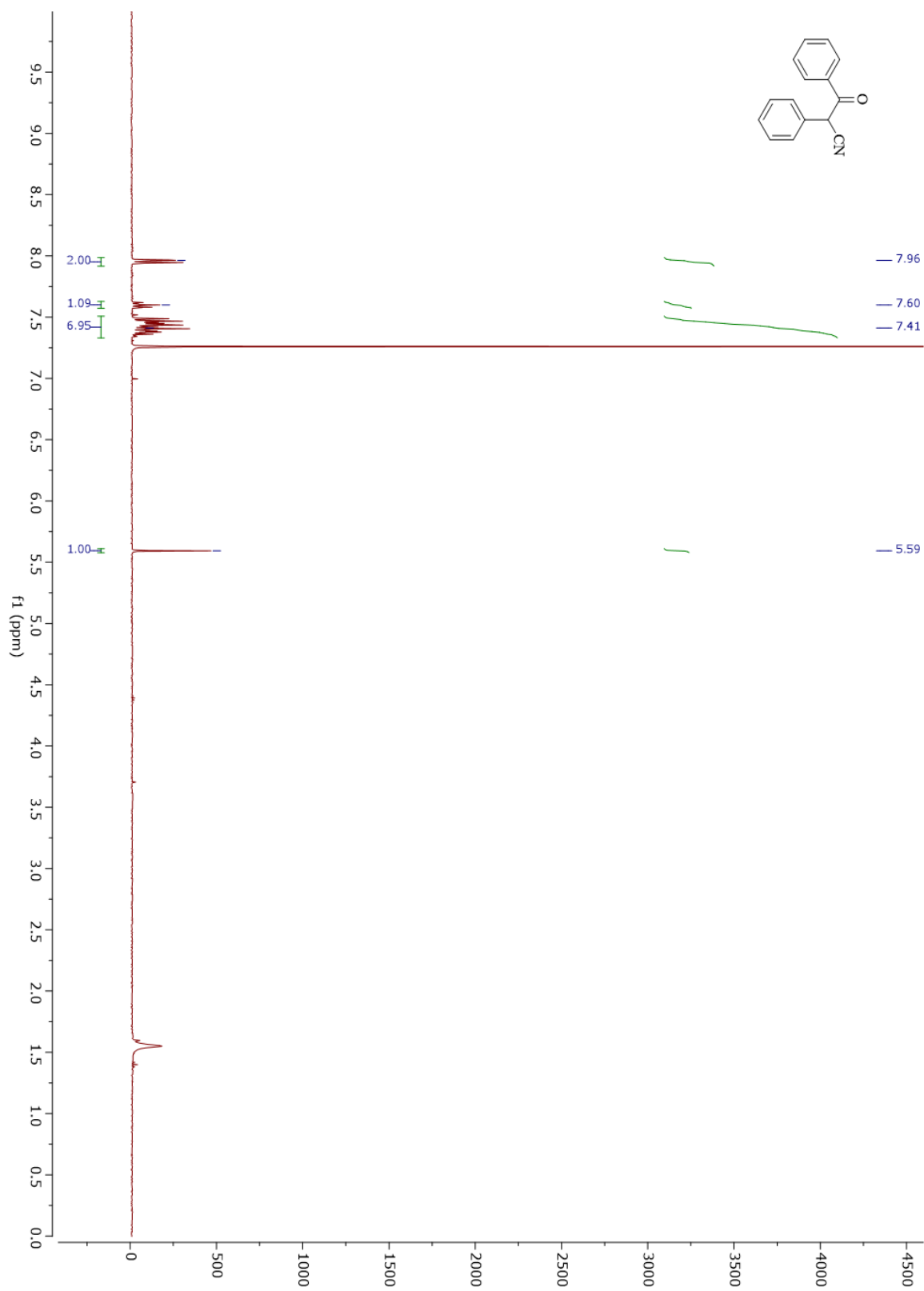
¹H NMR 4.16e



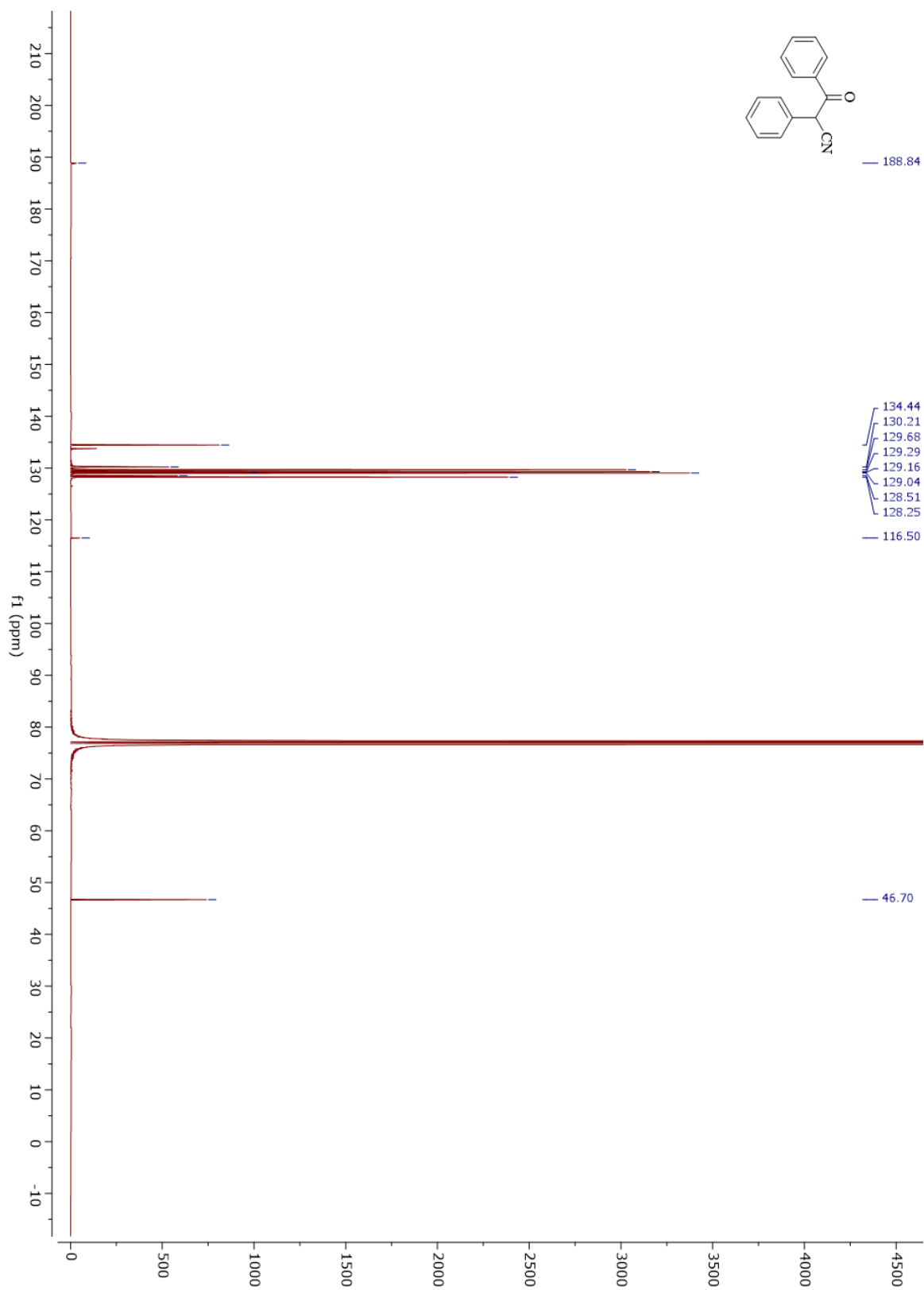
¹³C NMR 4.16e



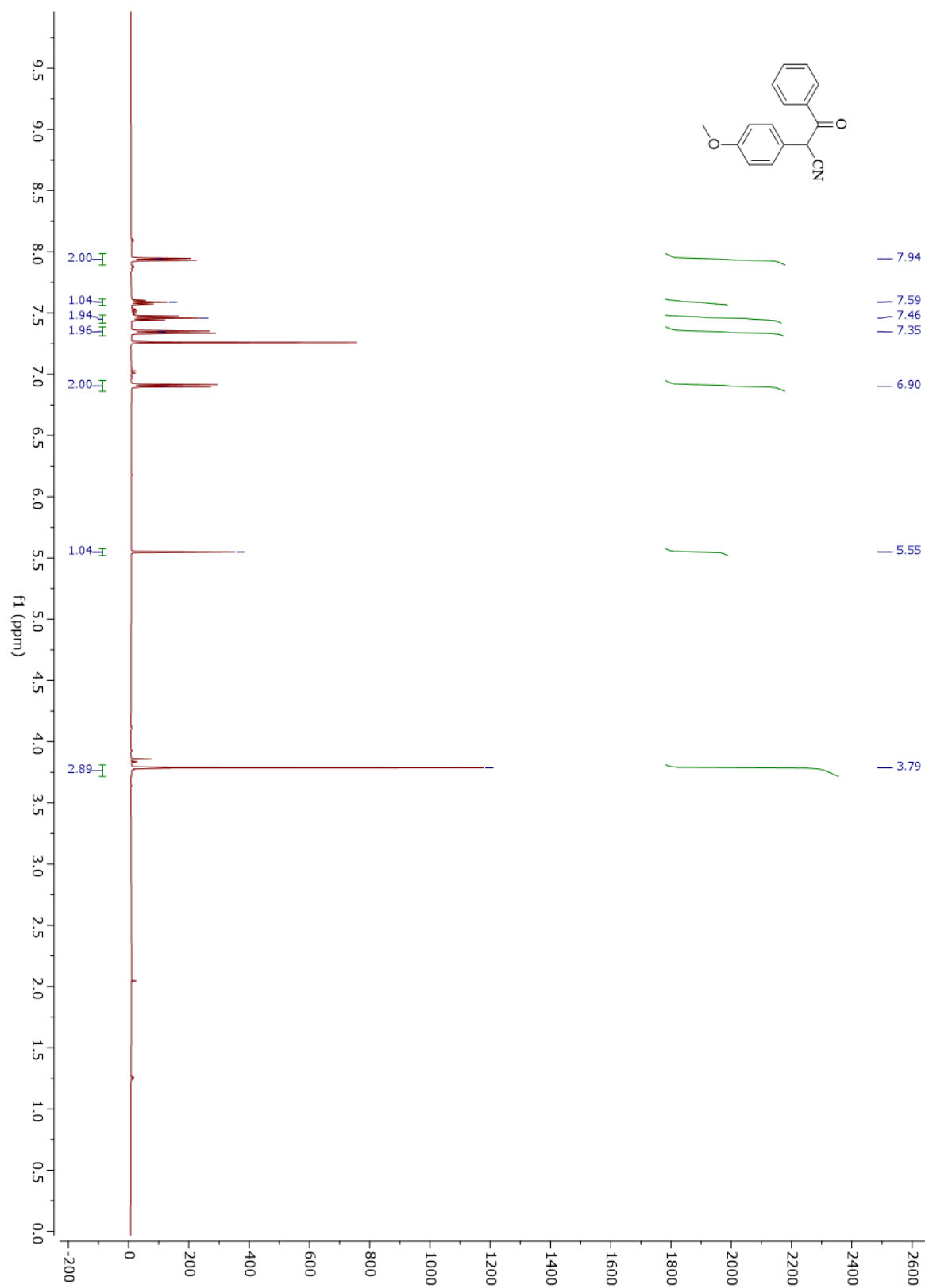
¹H NMR 4.17a



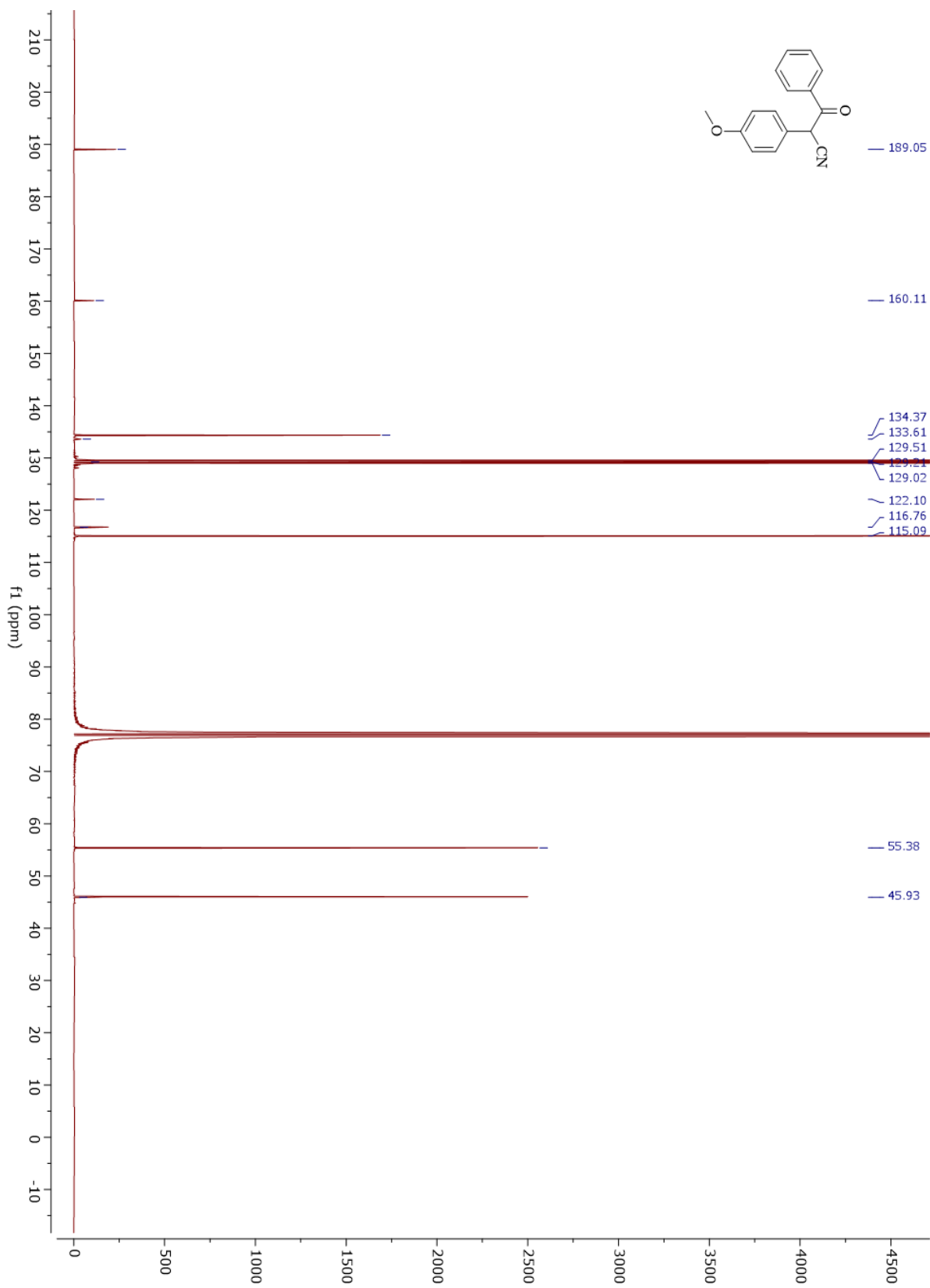
¹³C NMR 4.17a



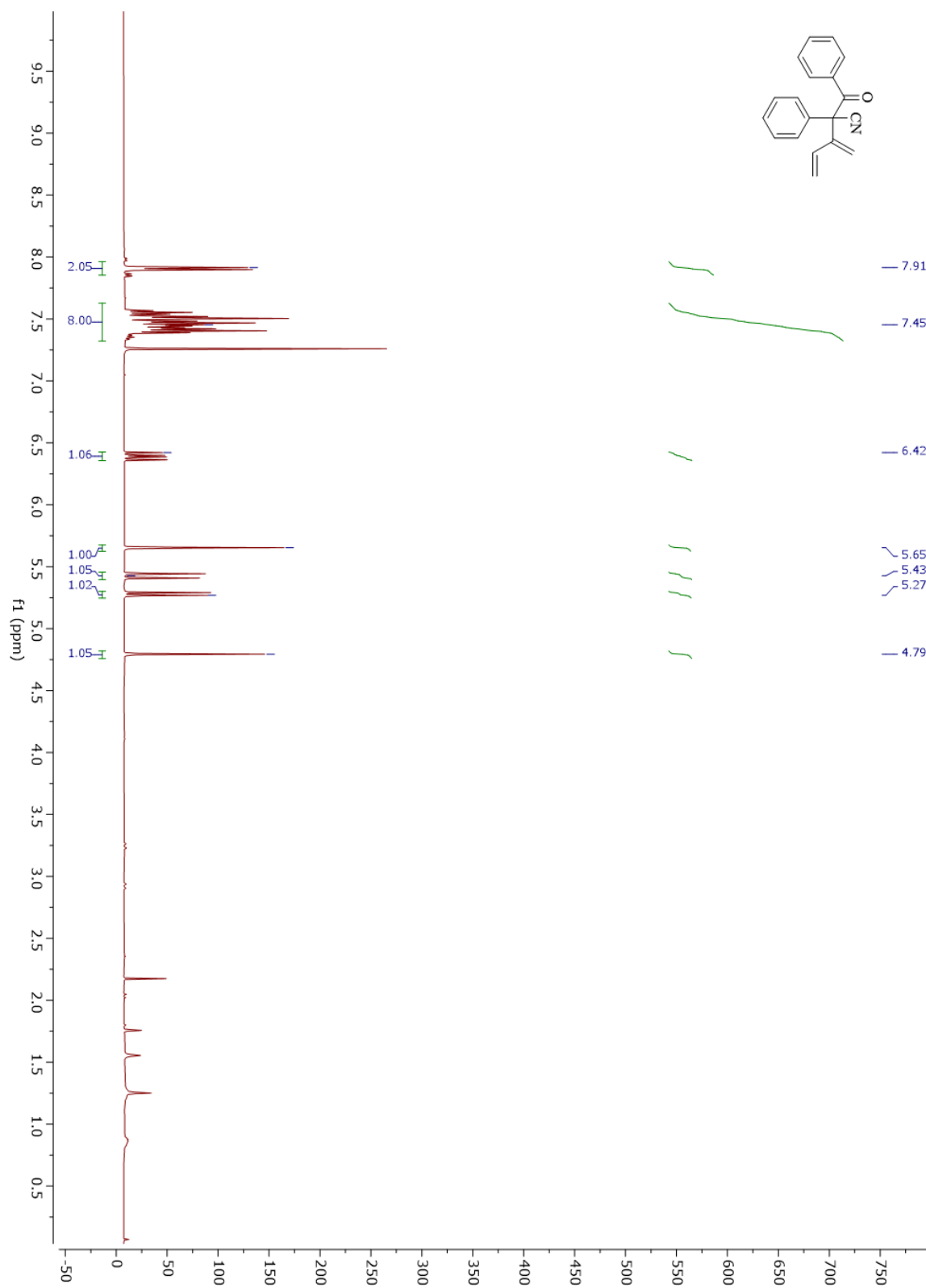
¹H NMR 4.17b



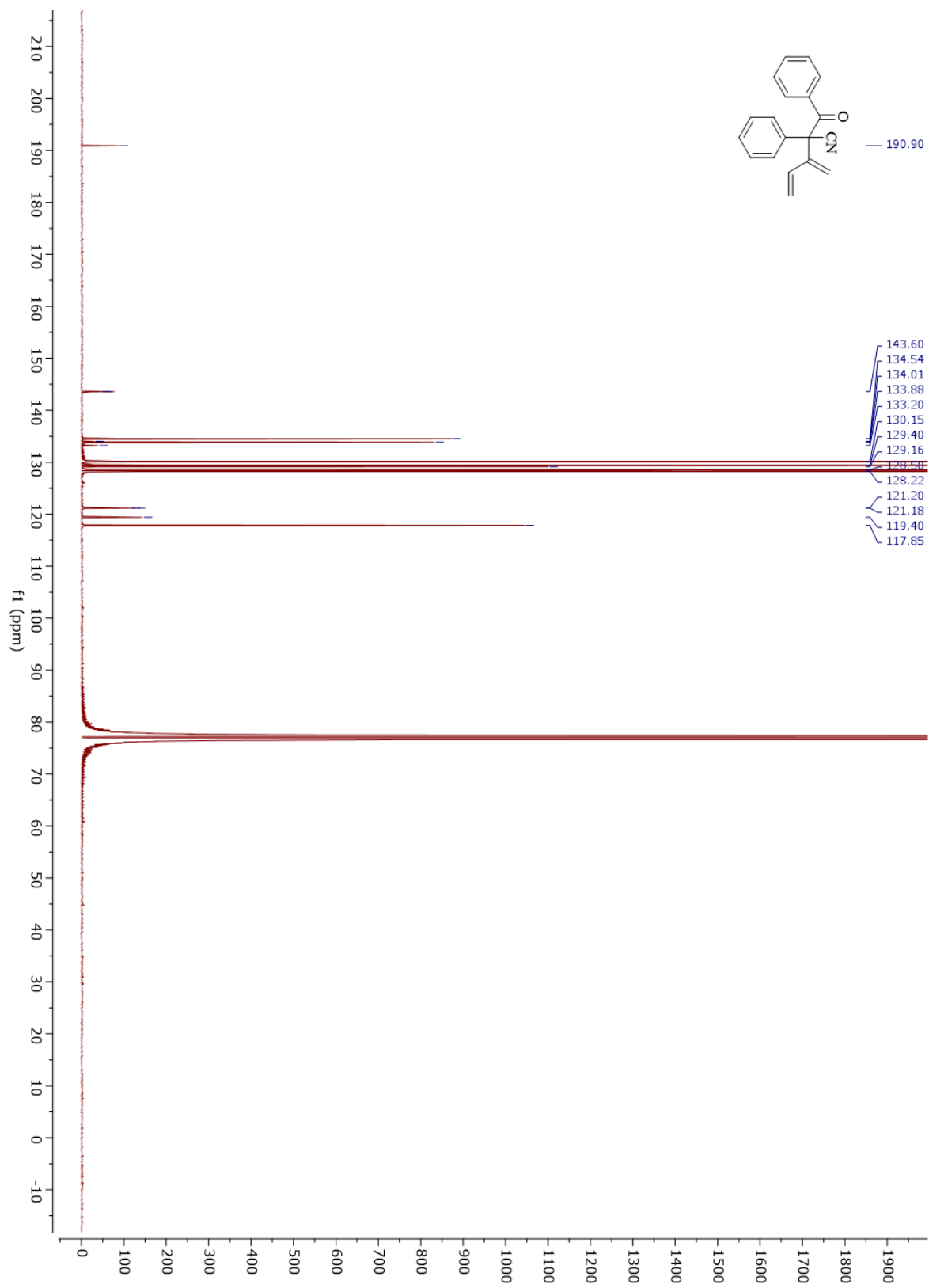
¹³C NMR 4.17b



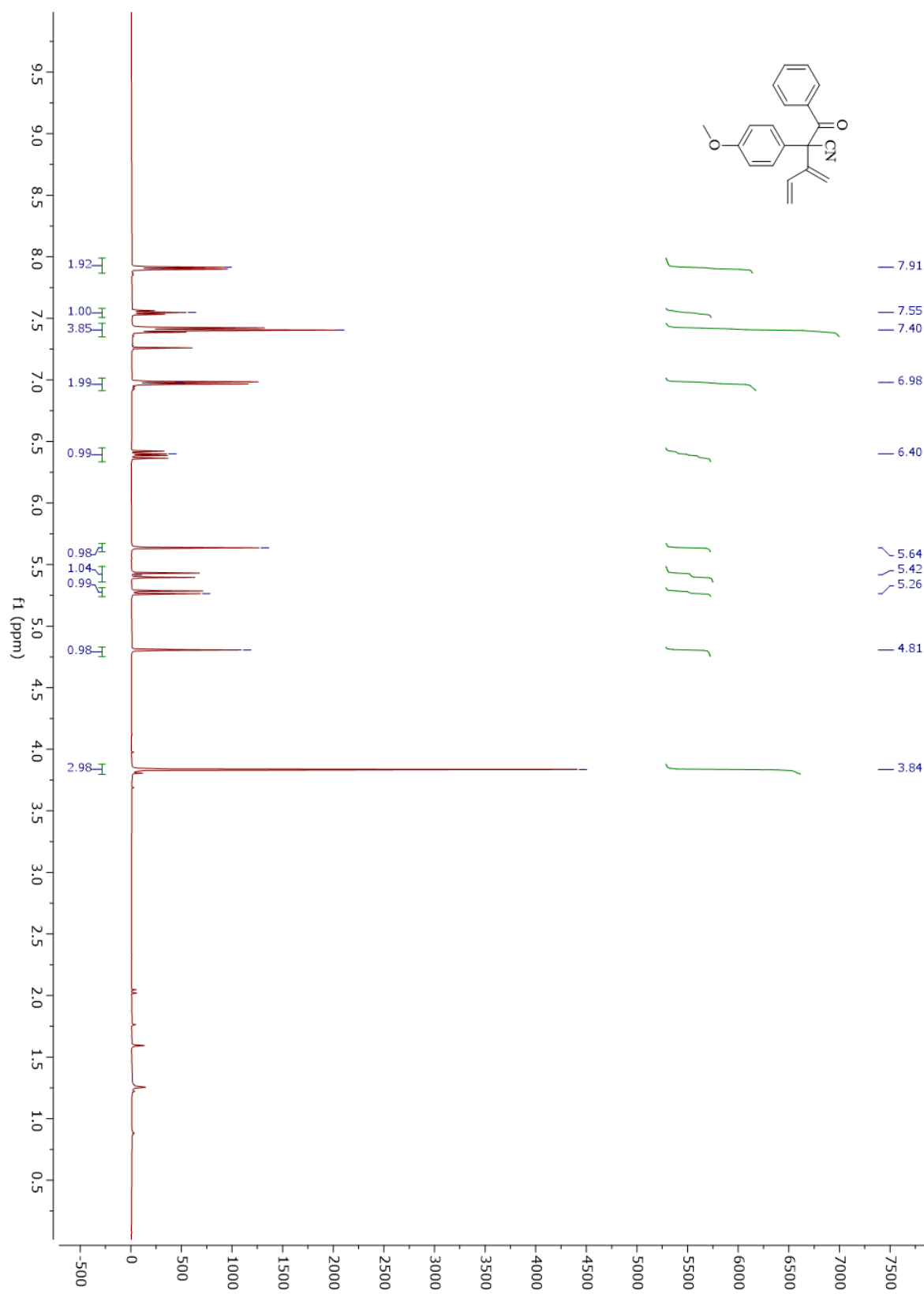
¹H NMR 4.18a



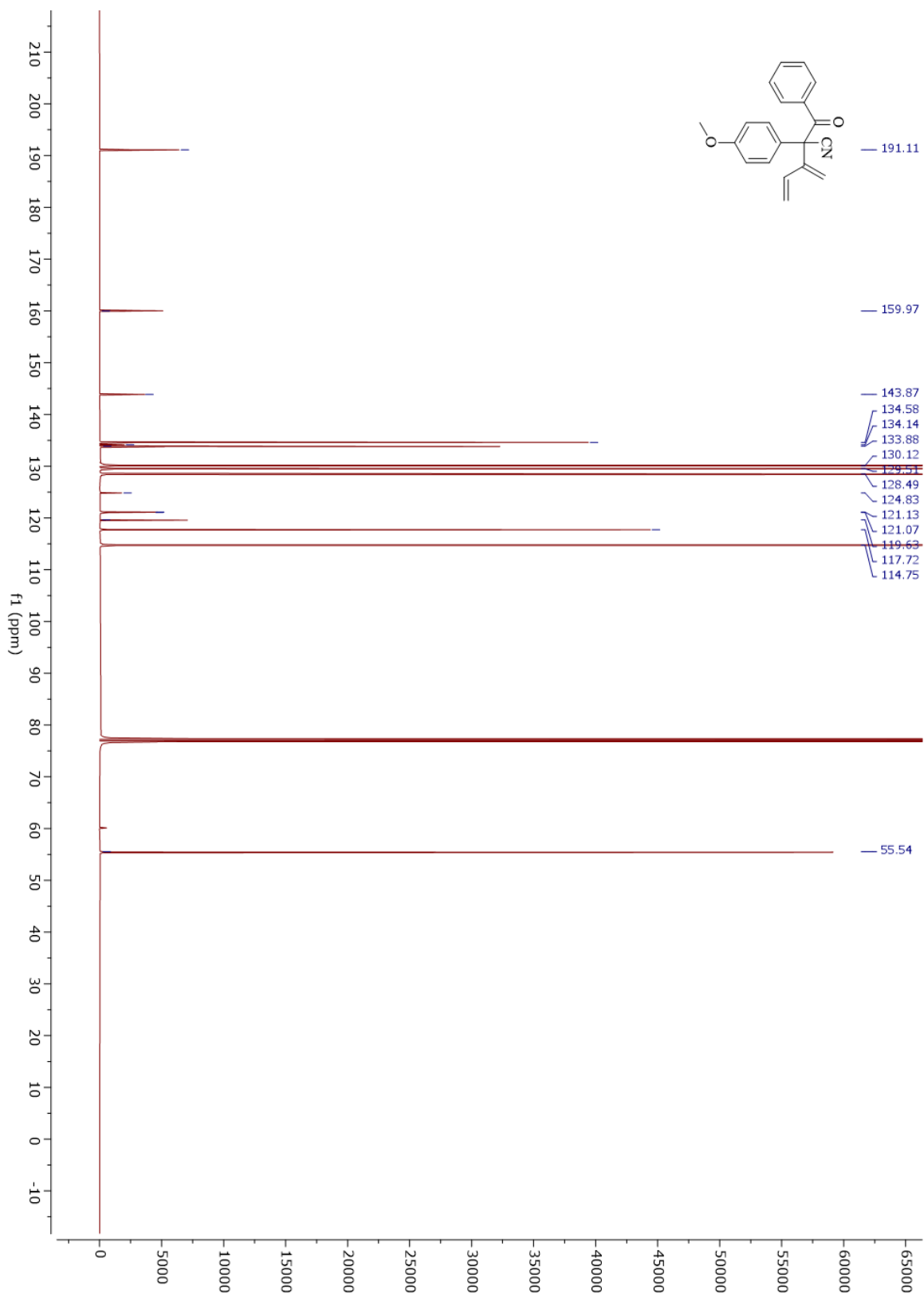
¹³C NMR 4.18a



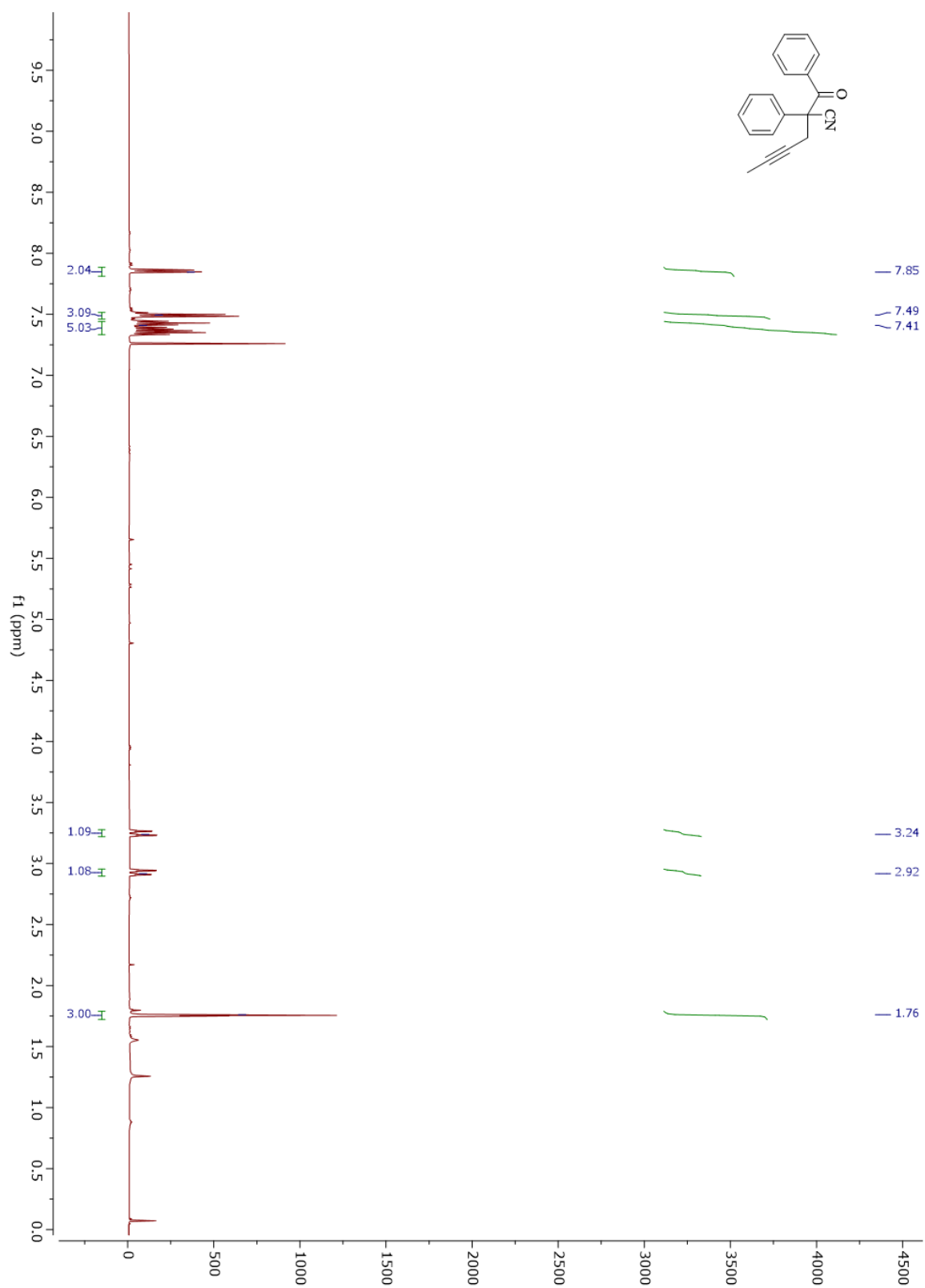
¹H NMR 4.18b



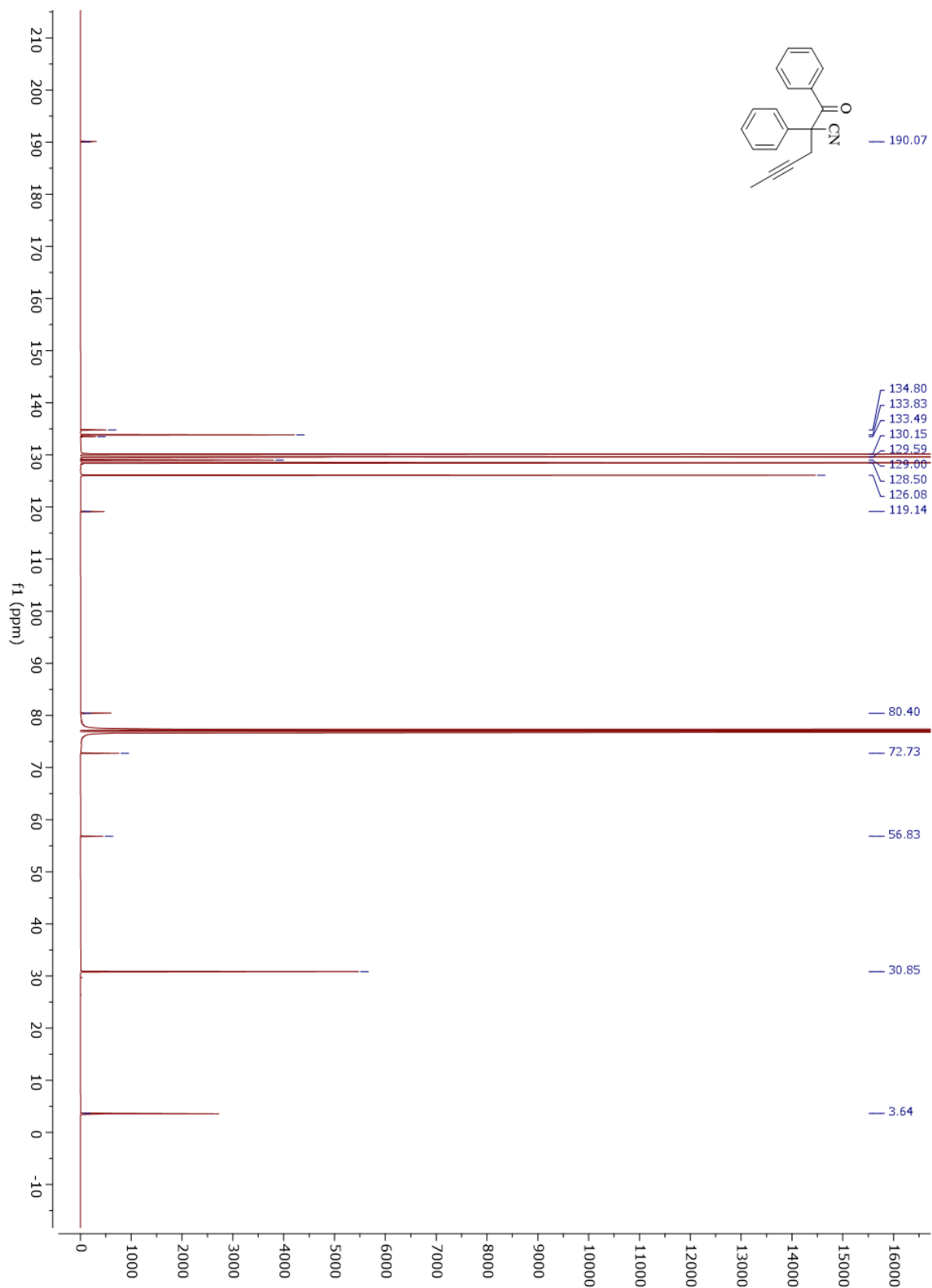
¹³C NMR 4.18b



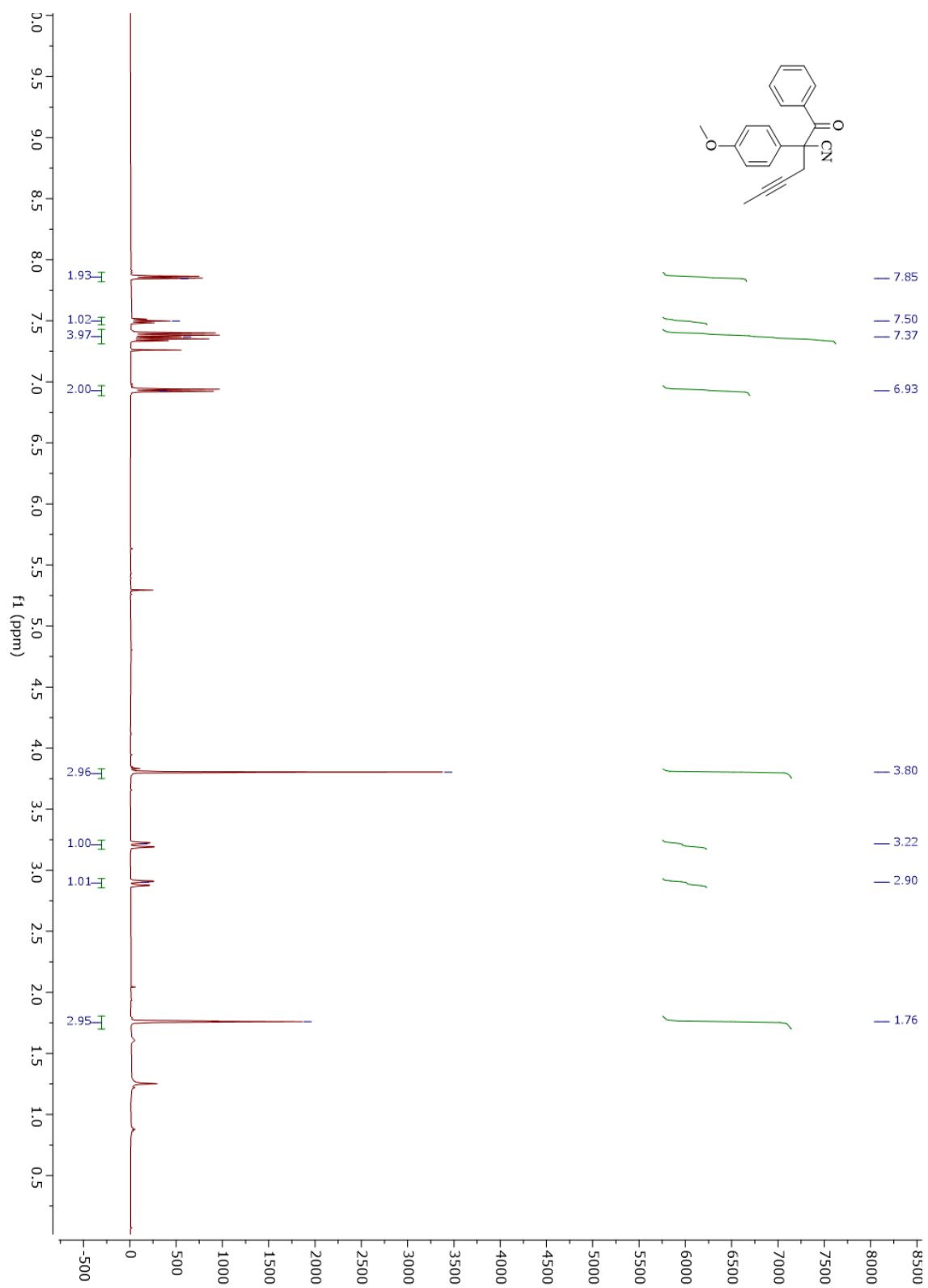
¹H NMR 4.18h



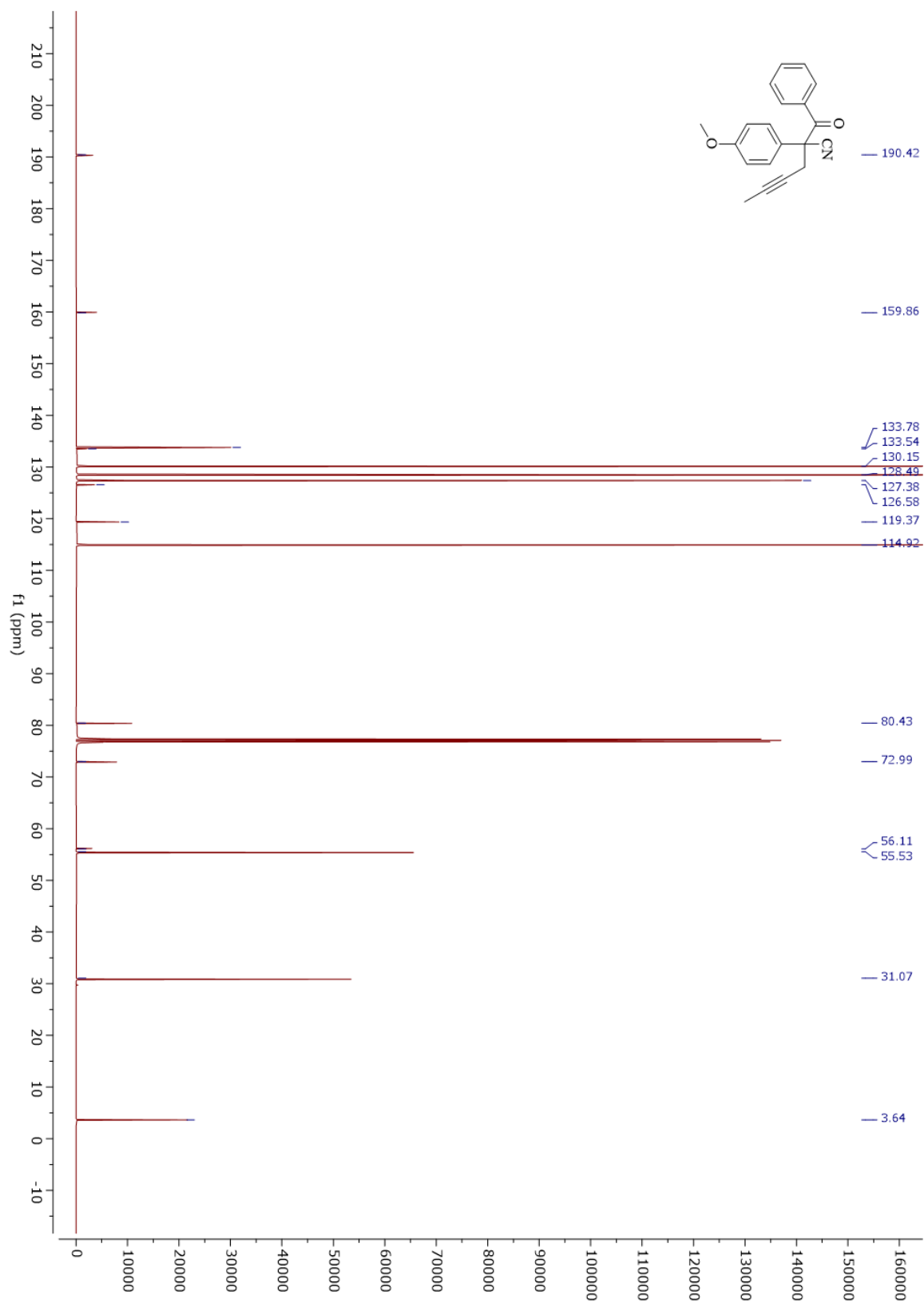
¹³C NMR 4.18h



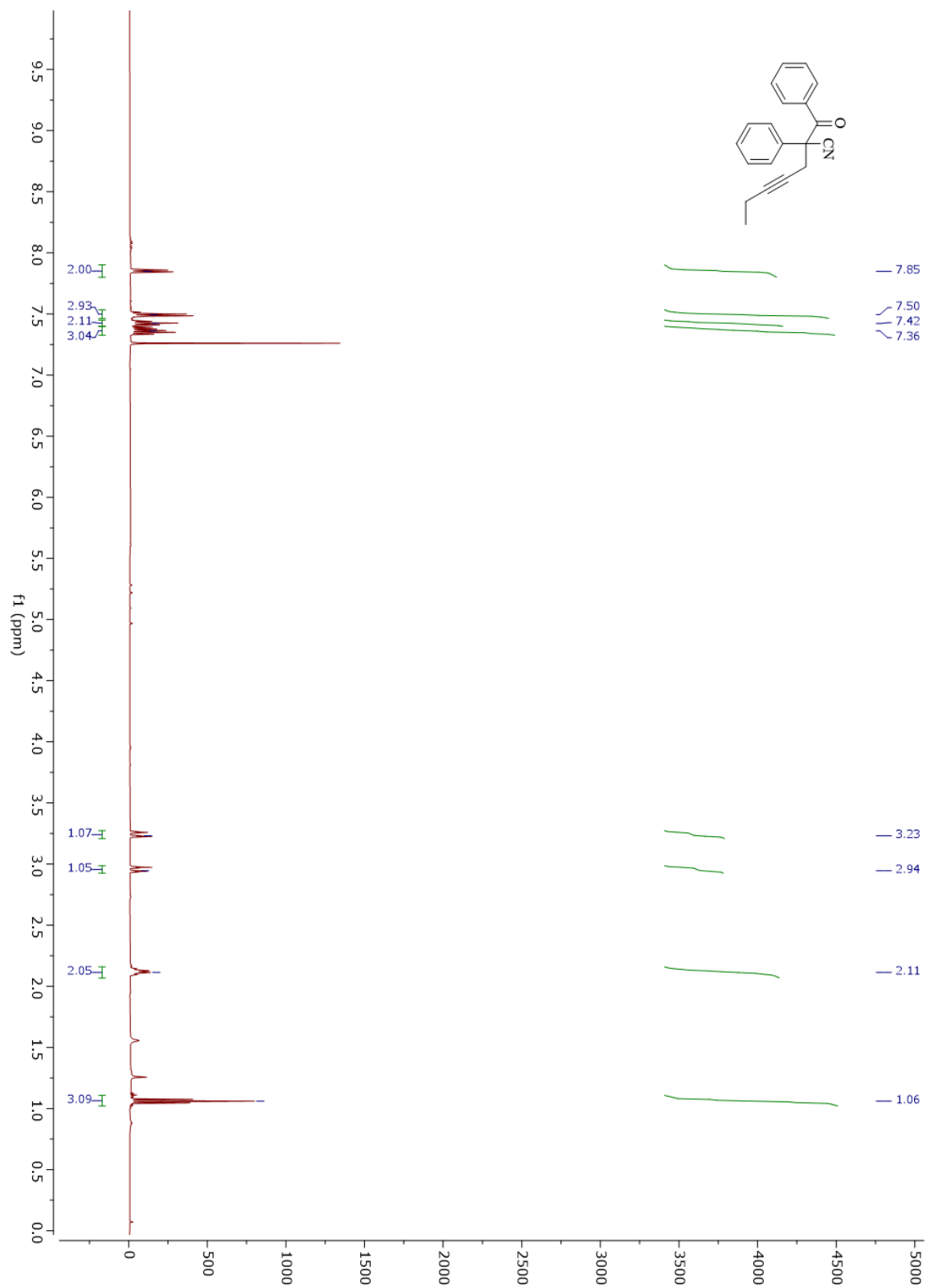
¹H NMR 4.18i



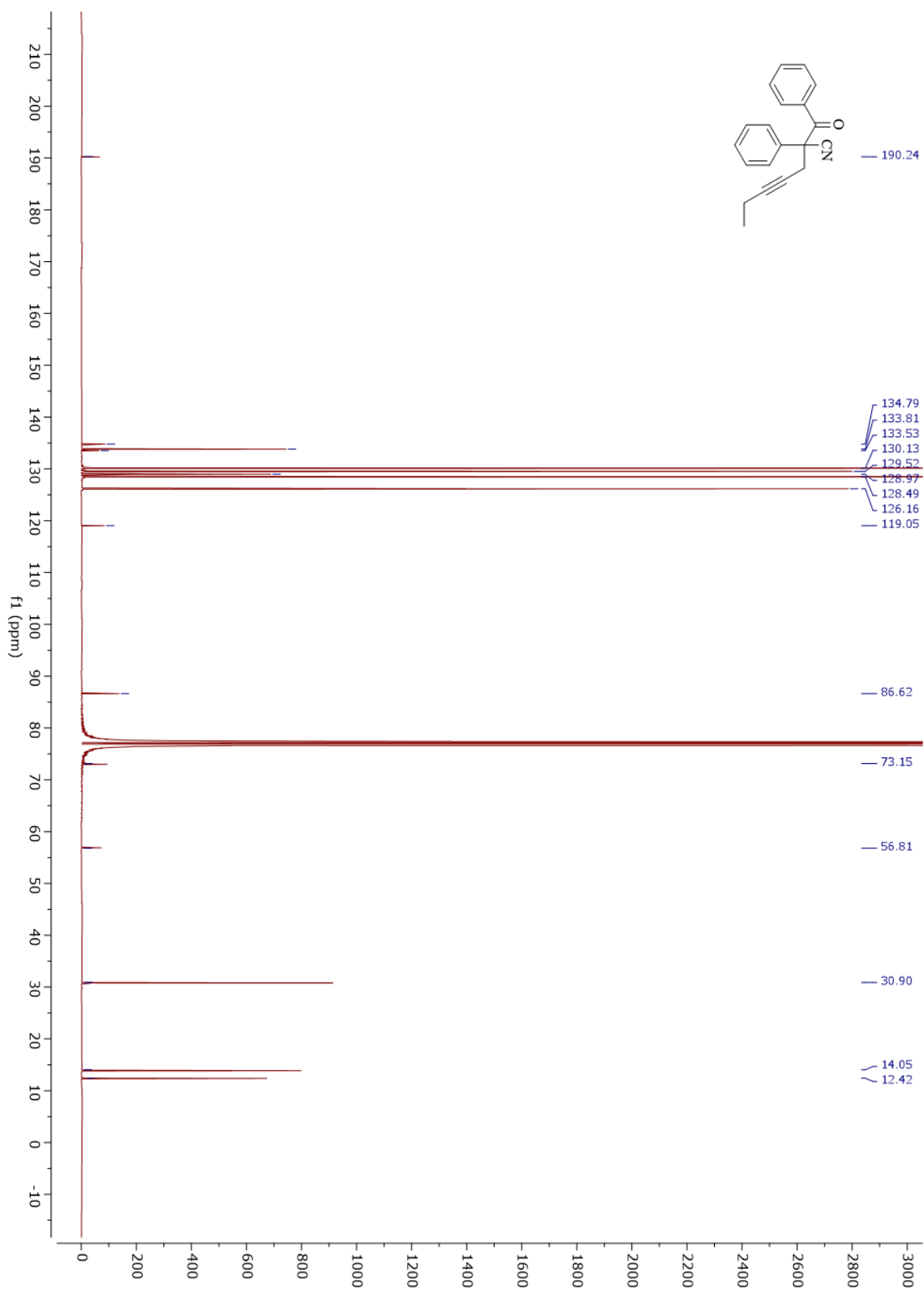
¹³C NMR 4.18i



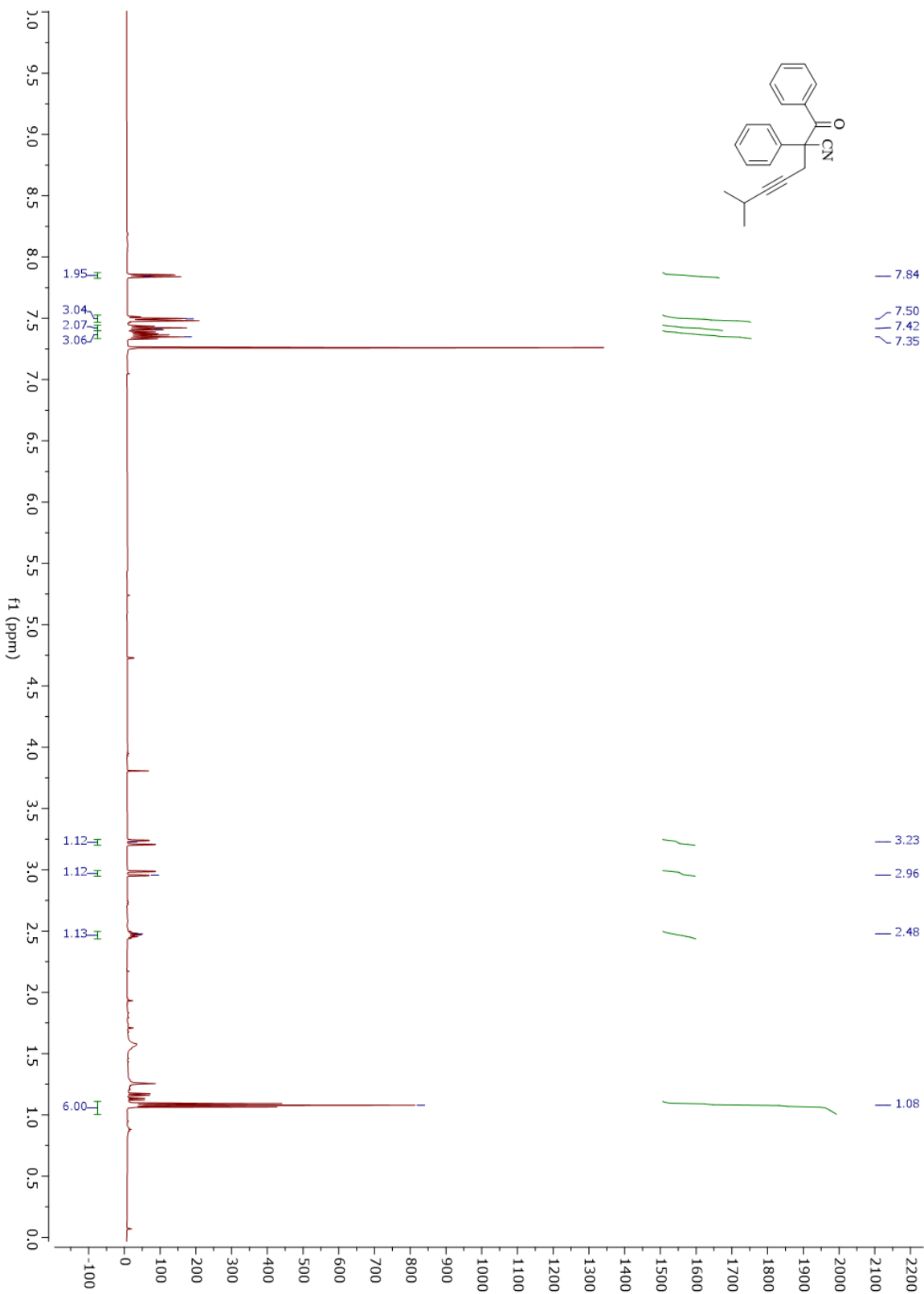
¹H NMR 4.18j



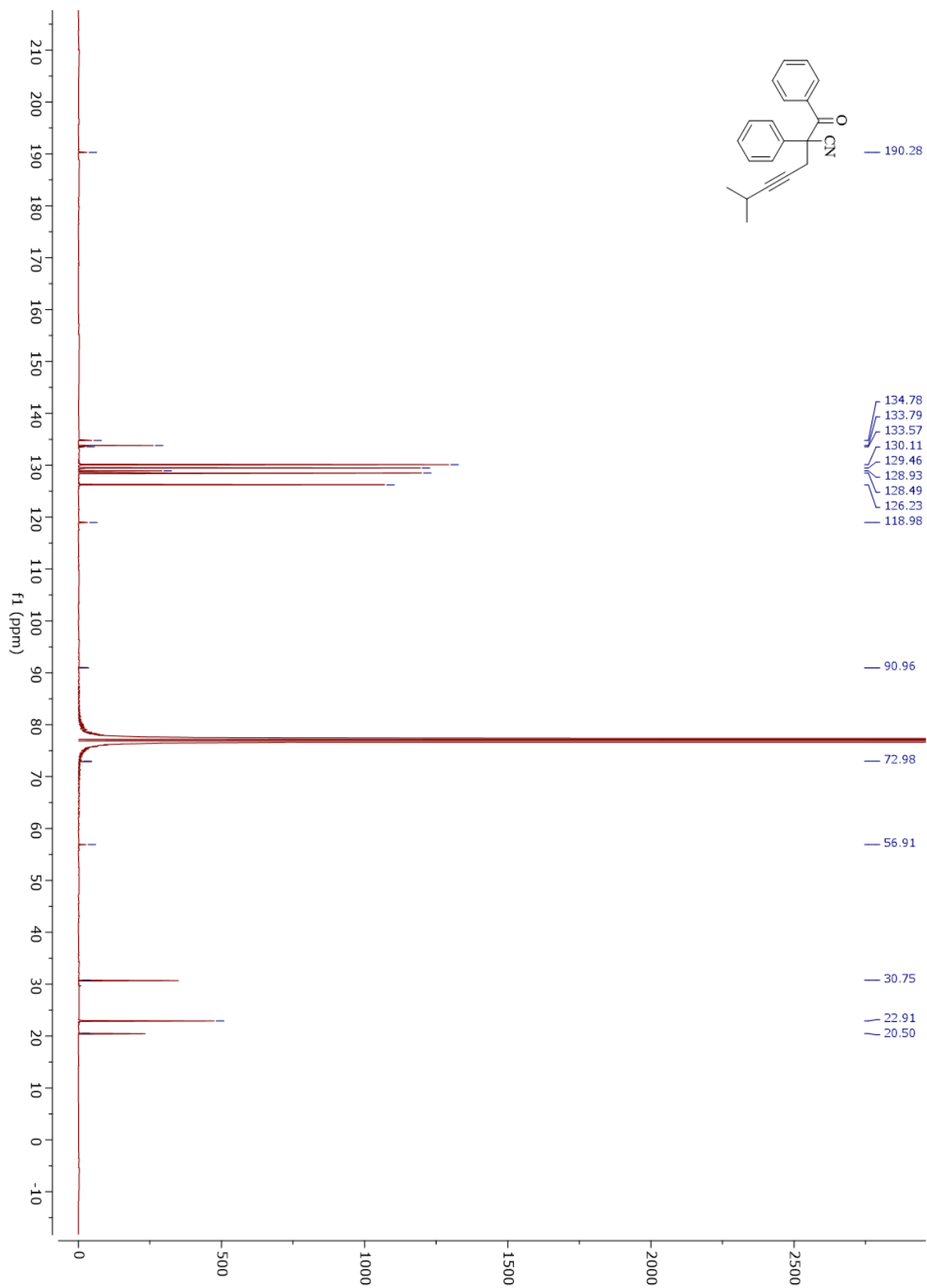
¹³C NMR 4.18j



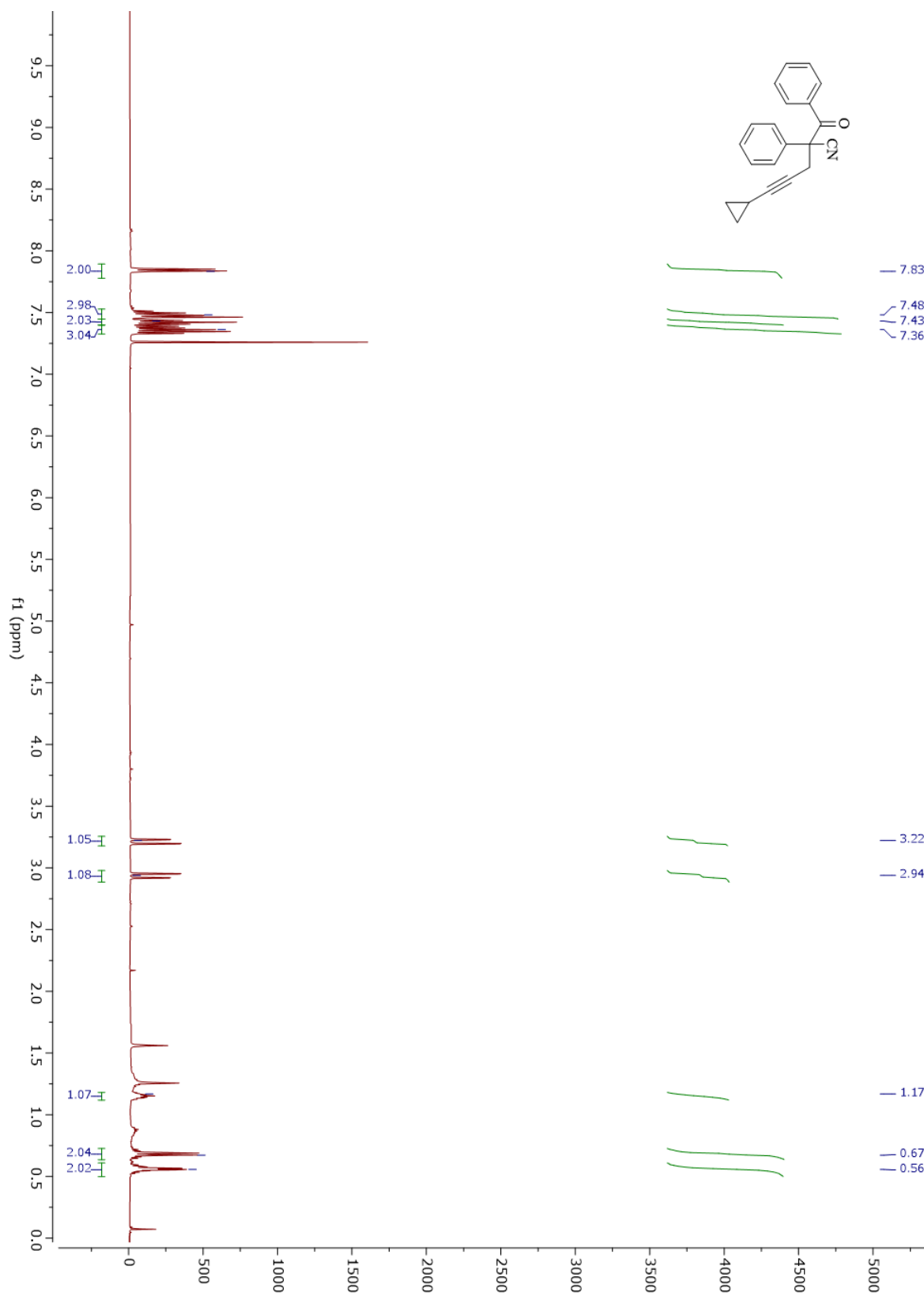
¹H NMR 4.18k



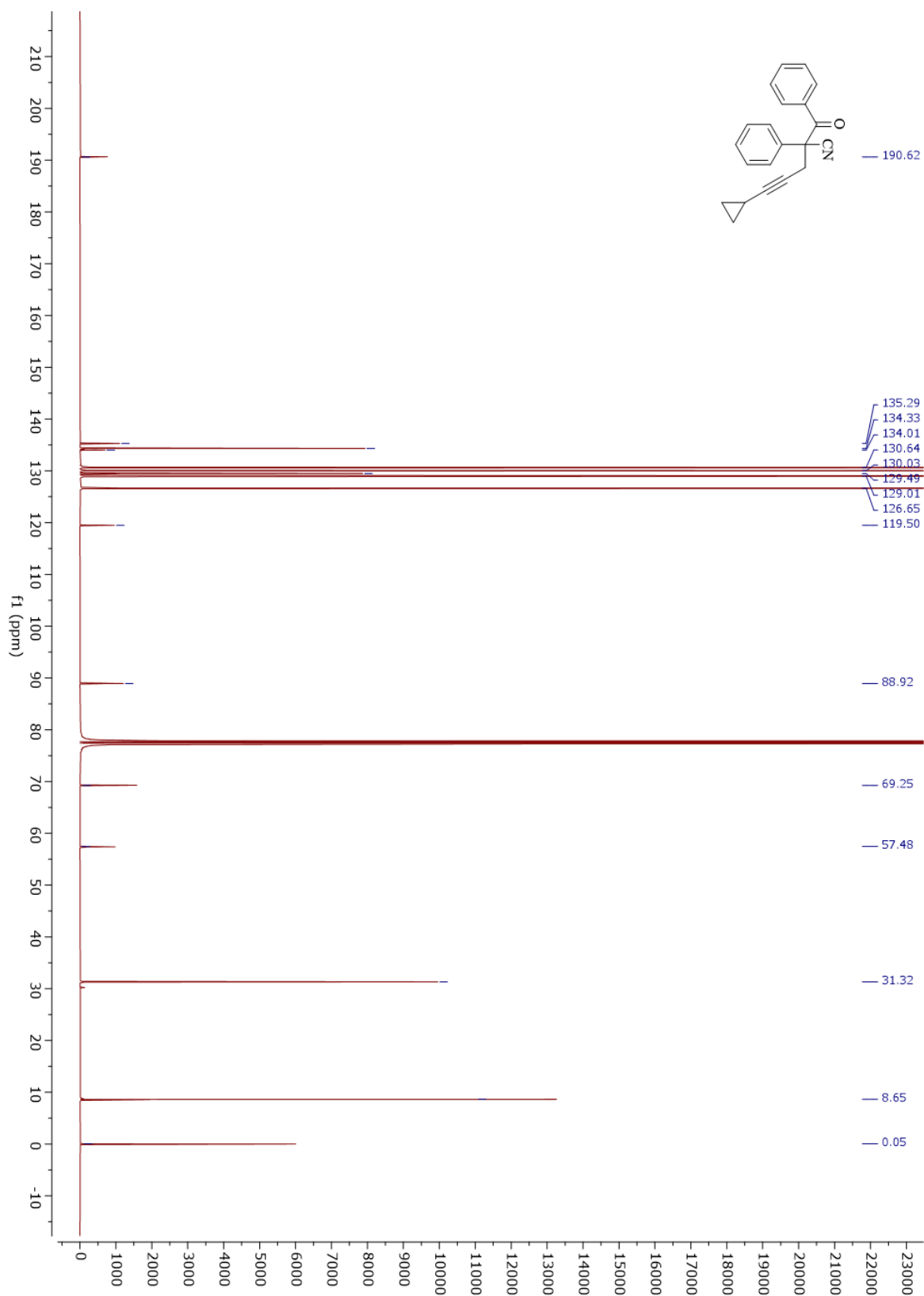
¹³C NMR 4.18k



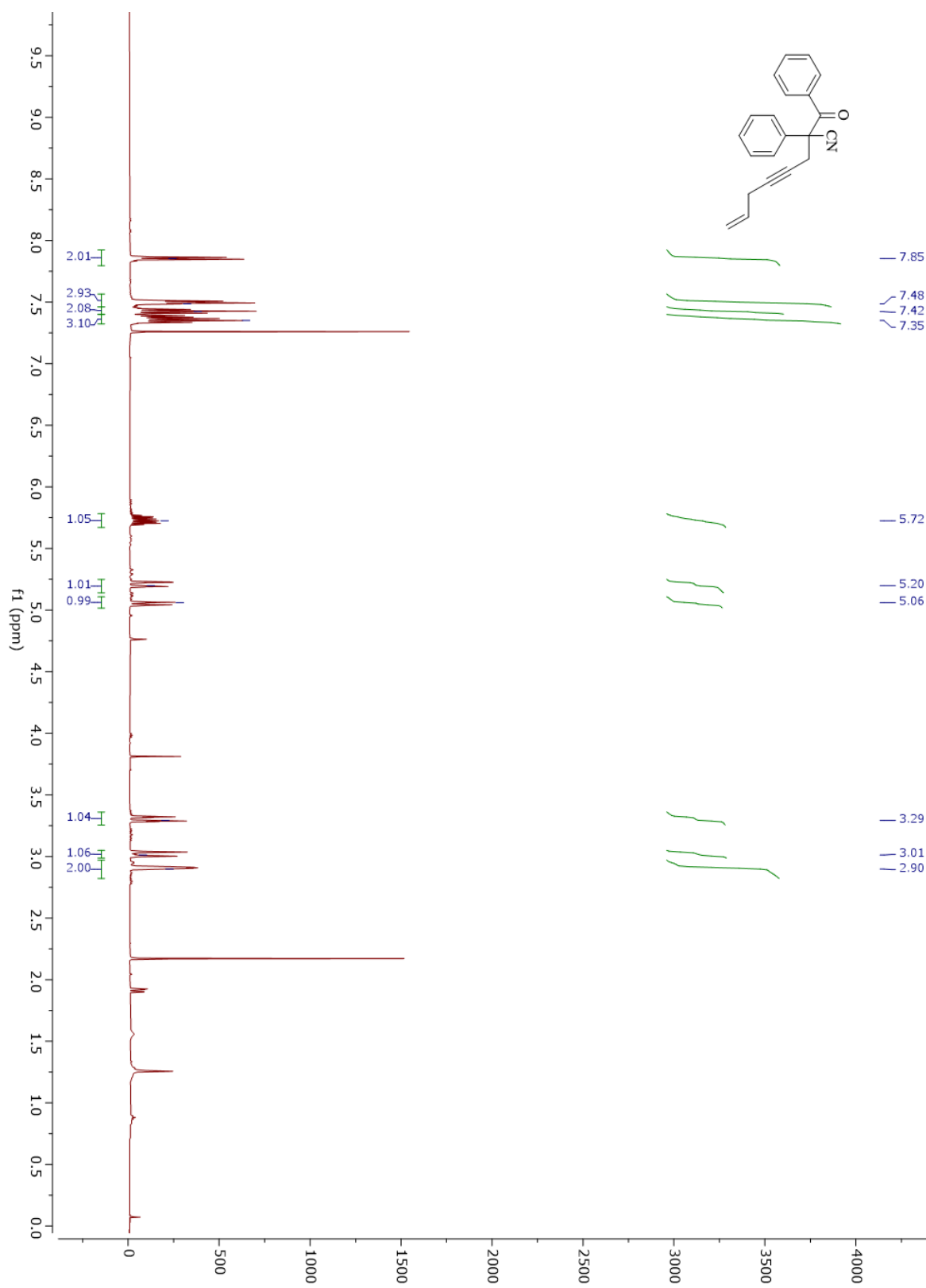
¹H NMR 4.181



¹³C NMR 4.181



¹H NMR 4.18m



¹³C NMR 4.18m

